CHEM 1000: GENERAL CHEMISTRY



LibreTexts™

Northeastern University

This text is disseminated via the Open Education Resource (OER) LibreTexts Project (https://LibreTexts.org) and like the thousands of other texts available within this powerful platform, it is freely available for reading, printing, and "consuming."

The LibreTexts mission is to bring together students, faculty, and scholars in a collaborative effort to provide an accessible, and comprehensive platform that empowers our community to develop, curate, adapt, and adopt openly licensed resources and technologies; through these efforts we can reduce the financial burden born from traditional educational resource costs, ensuring education is more accessible for students and communities worldwide.

Most, but not all, pages in the library have licenses that may allow individuals to make changes, save, and print this book. Carefully consult the applicable license(s) before pursuing such effects. Instructors can adopt existing LibreTexts texts or Remix them to quickly build course-specific resources to meet the needs of their students. Unlike traditional textbooks, LibreTexts' web based origins allow powerful integration of advanced features and new technologies to support learning.



LibreTexts is the adaptable, user-friendly non-profit open education resource platform that educators trust for creating, customizing, and sharing accessible, interactive textbooks, adaptive homework, and ancillary materials. We collaborate with individuals and organizations to champion open education initiatives, support institutional publishing programs, drive curriculum development projects, and more.

The LibreTexts libraries are Powered by NICE CXone Expert and was supported by the Department of Education Open Textbook Pilot Project, the California Education Learning Lab, the UC Davis Office of the Provost, the UC Davis Library, the California State University Affordable Learning Solutions Program, and Merlot. This material is based upon work supported by the National Science Foundation under Grant No. 1246120, 1525057, and 1413739.

Any opinions, findings, and conclusions or recommendations expressed in this material are those of the author(s) and do not necessarily reflect the views of the National Science Foundation nor the US Department of Education.

Have questions or comments? For information about adoptions or adaptions contact info@LibreTexts.org or visit our main website at https://LibreTexts.org.

This text was compiled on 01/12/2026

TABLE OF CONTENTS

Licensing

1: Introduction to Analytical Chemistry

- 1.1: What is Analytical Chemistry?
- 1.2: The Analytical Perspective
- 1.3: Common Analytical Problems
- 1.E: Introduction to Analytical Chemistry (Exercises)
- 1.S: Introduction to Analytical Chemistry (Summary)

2: Basic Tools of Analytical Chemistry

- 2.1: Measurements in Analytical Chemistry
- 2.2: Concentration
- 2.3: Stoichiometric Calculations
- 2.4: Basic Equipment
- 2.5: Preparing Solutions
- 2.6: Spreadsheets and Computational Software
- 2.7: The Laboratory Notebook
- 2.E: Basic Tools of Analytical Chemistry (Exercises)
- 2.S: Basic Tools of Analytical Chemistry (Summary)

3: The Vocabulary of Analytical Chemistry

- 3.1: Analysis, Determination, and Measurement
- 3.2: Techniques, Methods, Procedures, and Protocols
- 3.3: Classifying Analytical Techniques
- 3.4: Selecting an Analytical Method
- 3.5: Developing the Procedure
- 3.6: Protocols
- 3.7: The Importance of Analytical Methodology
- 3.E: The Vocabulary of Analytical Chemistry (Exercises)
- 3.S: The Vocabulary of Analytical Chemistry (Summary)
- Index

4: Evaluating Analytical Data

- 4.1: Characterizing Measurements and Results
- 4.2: Characterizing Experimental Errors
- 4.3: Propagation of Uncertainty
- 4.4: The Distribution of Measurements and Results
- 4.5: Statistical Analysis of Data
- 4.6: Statistical Methods for Normal Distributions
- 4.7: Detection Limits
- 4.8: Using Excel and R to Analyze Data
- 4.E: Evaluating Analytical Data (Exercises)
- 4.S: Evaluating Analytical Data (Summary)

5: Standardizing Analytical Methods

- 5.1: Analytical Standards
- 5.2: Calibrating the Signal
- 5.3: Determining the Sensitivity
- 5.4: Linear Regression and Calibration Curves
- 5.5: Blank Corrections
- 5.6: Using Excel and R for a Regression Analysis
- 5.E: Standardizing Analytical Methods (Exercises)
- 5.S: Standardizing Analytical Methods (Summary)

6: Equilibrium Chemistry

- 6.1: Reversible Reactions and Chemical Equilibria
- 6.2: Thermodynamics and Equilibrium Chemistry
- 6.3: Manipulating Equilibrium Constants
- 6.4: Equilibrium Constants for Chemical Reactions
- 6.5: Le Châtelier's Principle
- 6.6: Ladder Diagrams
- 6.7: Solving Equilibrium Problems
- 6.8: Buffer Solutions
- 6.9: Activity Effects
- 6.10: Using Excel and R to Solve Equilibrium Problems
- 6.11: Some Final Thoughts on Equilibrium Calculations
- 6.E: Equilibrium Chemistry (Exercises)
- 6.S: Equilibrium Chemistry (Summary)

7: Collecting and Preparing Samples

- 7.1: The Importance of Sampling
- 7.2: Designing a Sampling Plan
- 7.3: Implementing the Sampling Plan
- 7.4: Separating the Analyte from Interferents
- 7.5: General Theory of Separation Efficiency
- 7.6: Classifying Separation Techniques
- 7.7: Liquid–Liquid Extractions
- 7.8: Separation Versus Preconcentration
- 7.E: Collecting and Preparing Samples (Exercises)
- 7.S: Collecting and Preparing Samples (Summary)

8: Gravimetric Methods

- 8.1: Overview of Gravimetric Methods
- 8.2: Precipitation Gravimetry
- 8.3: Volatilization Gravimetry
- 8.4: Particulate Gravimetry
- 8.E: Gravimetric Methods (Exercises)
- 8.S: Gravimetric Methods (Summary)

9: Titrimetric Methods

- 9.1: Overview of Titrimetry
- 9.2: Acid–Base Titrations
- 9.3: Complexation Titrations
- 9.4: Redox Titrations
- 9.5: Precipitation Titrations
- 9.E: Titrimetric Methods (Exercises)
- 9.S: Titrimetric Methods (Summary)

10: Spectroscopic Methods

- 10.1: Overview of Spectroscopy
- 10.2: Spectroscopy Based on Absorption
- 10.3: UV/Vis and IR Spectroscopy
- 10.4: Atomic Absorption Spectroscopy
- 10.5: Emission Spectroscopy
- 10.6: Photoluminescence Spectroscopy
- 10.7: Atomic Emission Spectroscopy
- 10.8: Spectroscopy Based on Scattering
- 10.E: Spectroscopic Methods (Exercises)
- 10.S: Spectroscopic Methods (Summary)

11: Electrochemical Methods

- 11.1: Overview of Electrochemistry
- 11.2: Potentiometric Methods
- 11.3: Coulometric Methods
- 11.4: Voltammetric Methods
- 11.E: Electrochemical Methods (Exercises)
- 11.S: Electrochemical Methods (Summary)

12: Chromatographic & Electrophoretic Methods

- 12.1: Overview of Analytical Separations
- 12.2: General Theory of Column Chromatography
- 12.3: Optimizing Chromatographic Separations
- 12.4: Gas Chromatography
- 12.5: High-Performance Liquid Chromatography
- 12.6: Other Forms of Liquid Chromatography
- 12.7: Electrophoresis
- 12.E: Chromatographic and Electrophoretic Methods (Exercises)
- 12.S: Chromatographic and Electrophoretic Methods (Summary)
- Index

13: Kinetic Methods

- 13.1: Kinetic Methods Versus Equilibrium Methods
- 13.2: Chemical Kinetics
- 13.3: Radiochemistry
- 13.4: Flow Injection Analysis
- 13.E: Kinetic Methods (Exercises)

- 13.S: Kinetic Methods (Summary)

14: Developing a Standard Method

- 14.1: Optimizing the Experimental Procedure
- 14.2: Verifying the Method
- 14.3: Validating the Method as a Standard Method
- 14.4: Using Excel and R for an Analysis of Variance
- 14.E: Developing a Standard Method (Exercises)
- 14.S: Developing a Standard Method (Summary)

15: Quality Assurance

- 15.1: The Analytical Perspective—Revisited
- 15.2: Quality Control
- 15.3: Quality Assessment
- 15.4: Evaluating Quality Assurance Data
- 15.E: Quality Assurance (Exercises)

Additional Resources

Index

Glossary

Detailed Licensing

Licensing

*A detailed breakdown of this resource's licensing can be found in **Back Matter/Detailed Licensing**.*

CHAPTER OVERVIEW

1: Introduction to Analytical Chemistry

Chemistry is the study of matter, including its composition and structure, its physical properties, and its reactivity. There are many ways to study chemistry, but, we traditionally divide it into five fields: organic chemistry, inorganic chemistry, biochemistry, physical chemistry, and analytical chemistry. Although this division is historical and, perhaps, arbitrary—as witnessed by current interest in interdisciplinary areas such as bioanalytical chemistry and organometallic chemistry—these five fields remain the simplest division spanning the discipline of chemistry.

Topic hierarchy

1.1: What is Analytical Chemistry?

1.2: The Analytical Perspective

1.3: Common Analytical Problems

1.E: Introduction to Analytical Chemistry (Exercises)

1.S: Introduction to Analytical Chemistry (Summary)

Thumbnail: Several graduated cylinders of various thickness and heights with white side markings in front of a large beaker. They are all filled about halfway with red or blue chemical compounds. The blue ink is showing signs of Brownian motion when dissolving into water. Image used with permission (CC BY-SA 3.0; Horia Varlan from Bucharest, Romania).

Contributors

- David Harvey (DePauw University)

1: Introduction to Analytical Chemistry is shared under a CC BY-NC-SA 4.0 license and was authored, remixed, and/or curated by LibreTexts.

1.1: What is Analytical Chemistry?

1.1: What is Analytical Chemistry?

1.1: What is Analytical Chemistry? is shared under a CC BY-NC-SA 4.0 license and was authored, remixed, and/or curated by LibreTexts.

1.2: The Analytical Perspective

1.2: The Analytical Perspective

1.2: The Analytical Perspective is shared under a CC BY-NC-SA 4.0 license and was authored, remixed, and/or curated by LibreTexts.

1.3: Common Analytical Problems

1.3: Common Analytical Problems

1.3: Common Analytical Problems is shared under a CC BY-NC-SA 4.0 license and was authored, remixed, and/or curated by LibreTexts.

1.E: Introduction to Analytical Chemistry (Exercises)

1. For each of the following problems indicate whether its solution requires a qualitative analysis, a quantitative analysis, a characterization analysis, or a fundamental analysis. More than one type of analysis may be appropriate for some problems.

a. A hazardous-waste disposal site is believed to be leaking contaminants into the local groundwater.
b. An art museum is concerned that a recent acquisition is a forgery.
c. Airport security needs a more reliable method for detecting the presence of explosive materials in luggage.
d. The structure of a newly discovered virus needs to be determined.
e. A new visual indicator is needed for an acid–base titration.
f. A new law requires a method for evaluating whether automobiles are emitting too much carbon monoxide.

2. Read the article "When Machine Tastes Coffee: Instrumental Approach to Predict the Sensory Profile of Espresso Coffee," by several scientists working at the Nestlé Research Center in Lausanne, Switzerland. You will find the article on pages 1574-1581 in Volume 80 of Analytical Chemistry, published in 2008. Write an essay summarizing the nature of the problem and how it was solved. As a guide, refer to Figure 1.3 for a model of the analytical approach to solving problems.

Note

Use this link to access the article's abstract from the journal's web site. If your institution has an on-line subscription you also will be able to download a PDF version of the article.

1.4.3 Solutions to Practice Exercises

Literature Exercise 1.1

What is the analytical problem and why is it important?

A medical diagnoses often relies on the results of a clinical analysis. When visiting a doctor, he or she may ask the nurse to draw a sample of your blood and send it to the lab for analysis. In some cases the result of the analysis is available in 10-15 minutes. What is possible in a developed country, such as the United States, may not be feasible in a country with fewer resources because lab equipment is expensive, and because there may be a shortage of trained personnel to run the tests and to interpret the results. The problem addressed in this paper, therefore, is the development of a reliable device for rapidly and quantitatively performing clinical assays in less than ideal circumstances.

What criteria did the authors consider in designing their experiments?

In considering solutions to this problem, the authors identify seven important criteria for the device: it must be inexpensive; it must operate without the need for much electricity, so that it can be taken to remote sites; it must be adaptable to many types of assays; its operation must not require a highly skilled technician; it must be quantitative; it must be accurate; and it must produce results rapidly.

What is the basic experimental procedure?

The authors describe the development of a paper-based microfluidic device that allows anyone to run an analysis by dipping the device into a sample (synthetic urine, in this case). The sample moves by capillary action into test zones containing reagents that react with specific species (glucose and protein, for this prototype device). The reagents react to produce a color whose intensity is proportional to the species' concentration. Digital pictures of the microfluidic device are taken with a cell phone camera and sent to an off-site physician who analyzes the picture using image editing software and interprets the assay's result. (This is an example of a colorimetric method of analysis. Colorimetric methods are covered in Chapter 10.)

What interferences were considered and how did they overcome them?

In developing this analytical method the authors considered several chemical or physical interferences. One concern was the possibility of non-specific interactions between the paper and the glucose or protein, which could lead to non-uniform image in the test zones. A careful analysis of the distribution of glucose and protein in the text zones showed that this was

not a problem. A second concern was the possible presence in samples of particulate materials that might interfere with the analyses. Paper is a natural filter for particulate materials and the authors found that samples containing dust, sawdust, and pollen did not interfere with the analysis for glucose. Pollen, however, is an interferent for the protein analysis, presumably because it, too, contains protein.

How did the authors calibrate the assay?

To calibrate the device the authors analyzed a series of standard solutions containing known concentrations of glucose and protein. Because an image's intensity depends upon the available light, a standard sample is run with the test samples, which allows a single calibration curve to be used for samples collected under different lighting conditions.

How did the authors validate their experimental method?

The test device contains two test zones for each analyte, allowing for duplicate analyses and providing one level of experimental validation. To further validate the device, the authors completed 12 analyses at each of three known concentrations of glucose and protein, obtaining acceptable accuracy and precision in all cases.

Is there any evidence of repeating steps 2, 3, and 4?

Developing this analytical method required several repetitive paths through steps 2, 3, and 4 of the analytical approach. Examples of this feedback loop include optimizing the shape of the test zones, and evaluating the importance of sample size.

In summary, the authors report the successful development of an inexpensive, portable, and easy-to-use device for running clinical samples in developing countries. Click here to return to the chapter.

Contributors and Attributions

- David Harvey (DePauw University)

1.E: Introduction to Analytical Chemistry (Exercises) is shared under a CC BY-NC-SA 4.0 license and was authored, remixed, and/or curated by LibreTexts.

1.S: Introduction to Analytical Chemistry (Summary)

Analytical chemists work to improve the ability of all chemists to make meaningful measurements. Chemists working in the other traditional areas of chemistry, as well as in interdisciplinary fields such as medicinal chemistry, clinical chemistry, and environmental chemistry, need better tools for analyzing materials. The need to work with smaller samples, with more complex materials, with processes occurring on shorter time scales, and with species present at lower concentrations challenges analytical chemists to improve existing analytical methods and to develop new ones.

Typical problems on which analytical chemists work include qualitative analyses (What is present?), quantitative analyses (How much is present?), characterization analyses (What are the sample's chemical and physical properties?), and fundamental analyses (How does this method work and how can it be improved?).

1.4.1 Key Terms

- characterization analysis
- fundamental analysis
- qualitative analysis
- quantitative analysis

Additional Resources

Gathered here are three types of resources: suggested experiments, mostly from the *Journal of Chemical Education* and *The Chemical Educator*, that provide practical examples of concepts in the textbook; additional readings from the analytical literature that extend and supplement topics covered in the textbook. Although primarily intended for the use of instructors, these resources also will benefit students who wish to pursue a topic at more depth.

The role of analytical chemistry within the broader discipline of chemistry has been discussed by many prominent analytical chemists. Several notable examples are listed here.

- Baiulescu, G. E.; Patroescu, C; Chalmers, R. A. *Education and Teaching in Analytical Chemistry*, Ellis Horwood: Chichester, 1982.
- de Haseth, J. "What is Analytical Chemistry?," *Spectroscopy* **1990**, *5*, 19-21.
- Heiftje, G. M. "The Two Sides of Analytical Chemistry," *Anal. Chem*. **1985**, *57*, 256A-267A.
- Heiftje, G. M. "But is It Analytical Chemistry?," *Am. Lab.* **1993**, October, 53-61.
- Kissinger, P. T. "Analytical Chemistry—What is It? Why Teach It?," *Trends Anal. Chem.* **1992**, *11*, 57-57.
- Laitinen, H. A.; Ewing, G. (eds.) *A History of Analytical Chemistry*, The Division of Analytical Chemistry of the American Chemical Society: Washington, D. C., 1972.
- Laitinen, H. A. "Analytical Chemistry in a Changing World," *Anal. Chem.* **1980**, *52*, 605A-609A.
- Laitinen, H. A. "History of Analytical Chemistry in the U. S. A.," *Talanta*, **1989**, *36*, 1-9.
- McLafferty, F. W. "Analytical Chemistry: Historic and Modern," *Acc. Chem. Res.* **1990**, *23*, 63-64.
- Mottola, H. A. "The Interdisciplinary and Multidisciplinary Nature of Contemporary Analytical Chemistry and its Core Components," *Anal. Chim. Acta* **1991**, *242*, 1-3.
- Noble, D. "From Wet Chemistry to Instrumental Analysis: A Perspective on Analytical Sciences," *Anal. Chem.* **1994**, *66*, 251A-263A.
- Tyson, J. *Analysis: What Analytical Chemists Do*, Royal Society of Chemistry: Cambridge, England 1988.

For additional discussion of clinical assays based on paper-based microfluidic devices, see the following papers.

- Ellerbee, A. K.; Phillips, S. T.; Siegel, A. C.; Mirica, K. A.; Martinez, A. W.; Striehl, P.; Jain, N.; Prentiss, M.; Whitesides, G. M. "Quantifying Colorimetric Assays in Paper-Based Microfluidic Devices by Measuring the Transmission of Light Through Paper," *Anal. Chem.* **2009**, *81*, 8447–8452.
- Martinez, A. W.; Phillips, S. T.; Whitesides, G. M. "Diagnostics for the Developing World: Microfluidic Paper-Based Analytical Devices," *Anal. Chem.* **2010**, *82*, 3–10.

This textbook provides one presentation introducing the discipline of analytical chemistry. There are other textbooks for introductory courses in analytical chemistry and you may find it useful to consult them when you encounter a difficult concept; often a fresh perspective will help crystallize your understanding. The textbooks listed here are excellent resources.

- Enke, C. *The Art and Science of Chemical Analysis*, Wiley: New York.
- Harris, D. *Quantitative Chemical Analysis*, W. H. Freeman and Company: New York.
- Kellner, R.; Mermet, J.-M.; Otto, M.; Valcárcel, M.; Widmer, H. M. *Analytical Chemistry*, Wiley-VCH: Weinheim, Germany.
- Rubinson, J. F.; Rubinson, K. A. *Contemporary Chemical Analysis*, Prentice Hall: Upper Saddle River, NJ.
- Skoog, D. A.; West, D. M.; Holler, F. J. *Fundamentals of Analytical Chemistry*, Saunders: Philadelphia.

To explore the practice of modern analytical chemistry there is no better resource than the primary literature. The following journals publish broadly in the area of analytical chemistry.

- Analytical Chemistry Analytica Chimica Acta Analyst Analytical Bioanalytical Chemistry (ABC)

References

1. Ravey, M. Spectroscopy, 1990, 5(7), 11.
2. de Haseth, J. Spectroscopy, 1990, 5(7), 11.
3. Fresenius. C. R. A System of Instruction in Quantitative Chemical Analysis; John Wiley and Sons: New York, 1881.
4. Kolthoff, I. M.; Sandell, E. B. Textbook of Quantitative Inorganic Analysis, 3rd Ed., The Macmillan Company: New York, 1952.
5. Van Loon, J. C. Analytical Atomic Absorption Spectroscopy, Academic Press: New York, 1980.
6. Murray, R. W. Anal. Chem. 1991, 63, 271A.
7. For several different viewpoints see (a) Beilby, A. L. J. Chem. Educ. 1970, 47, 237-238; (b) Lucchesi, C. A. Am. Lab. 1980, October, 112-119; (c) Atkinson, G. F. J. Chem. Educ. 1982, 59, 201-202; (d) Pardue, H. L.; Woo, J. J. Chem. Educ. 1984, 61, 409-412; (e) Guarnieri, M. J. Chem. Educ. 1988, 65, 201-203, (f) Strobel, H. A. Am. Lab. 1990, October, 17-24.
8. See, for example, the following laboratory texts: (a) Sorum, C. H.; Lagowski, J. J. Introduction to Semimicro Qualitative Analysis, 5th Ed.; Prenctice-Hall: Englewood, NJ, 1977; (b) Shriner, R. L.; Fuson, R. C.; Curtin, D. Y. The Systematic Identification of Organic Compounds, 5th Ed.; John Wiley and Sons: New York, 1964.

Contributors

- David Harvey (DePauw University)

1.S: Introduction to Analytical Chemistry (Summary) is shared under a CC BY-NC-SA 4.0 license and was authored, remixed, and/or curated by LibreTexts.

CHAPTER OVERVIEW

2: Basic Tools of Analytical Chemistry

In the chapters that follow we will explore many aspects of analytical chemistry. In the process we will consider important questions such as “How do we treat experimental data?”, “How do we ensure that our results are accurate?”, “How do we obtain a representative sample?”, and “How do we select an appropriate analytical technique?” Before we look more closely at these and other questions, we will first review some basic tools of importance to analytical chemists.

Topic hierarchy

2.1: Measurements in Analytical Chemistry
2.2: Concentration
2.3: Stoichiometric Calculations
2.4: Basic Equipment
2.5: Preparing Solutions
2.6: Spreadsheets and Computational Software
2.7: The Laboratory Notebook
2.E: Basic Tools of Analytical Chemistry (Exercises)
2.S: Basic Tools of Analytical Chemistry (Summary)

Thumbnail: A Roberval balance. The pivots of the parallelogram understructure makes it insensitive to load positioning away from center, so improves its accuracy, and ease of use. Image used with permission (CC BY-SA 3.0; Nikodem Nijaki)

Contributors

- David Harvey (DePauw University)

2: Basic Tools of Analytical Chemistry is shared under a CC BY-NC-SA 4.0 license and was authored, remixed, and/or curated by LibreTexts.

2.1: Measurements in Analytical Chemistry

2.1: Measurements in Analytical Chemistry

2.1: Measurements in Analytical Chemistry is shared under a CC BY-NC-SA 4.0 license and was authored, remixed, and/or curated by LibreTexts.

2.2: Concentration

2.2: Concentration

2.2: Concentration is shared under a CC BY-NC-SA 4.0 license and was authored, remixed, and/or curated by LibreTexts.

2.3: Stoichiometric Calculations

2.3: Stoichiometric Calculations

2.3: Stoichiometric Calculations is shared under a CC BY-NC-SA 4.0 license and was authored, remixed, and/or curated by LibreTexts.

2.4: Basic Equipment

2.4: Basic Equipment

2.4: Basic Equipment is shared under a CC BY-NC-SA 4.0 license and was authored, remixed, and/or curated by LibreTexts.

2.5: Preparing Solutions

2.5: Preparing Solutions

2.5: Preparing Solutions is shared under a CC BY-NC-SA 4.0 license and was authored, remixed, and/or curated by LibreTexts.

2.6: Spreadsheets and Computational Software

2.6: Spreadsheets and Computational Software

2.6: Spreadsheets and Computational Software is shared under a CC BY-NC-SA 4.0 license and was authored, remixed, and/or curated by LibreTexts.

2.7: The Laboratory Notebook

2.7: The Laboratory Notebook

2.7: The Laboratory Notebook is shared under a CC BY-NC-SA 4.0 license and was authored, remixed, and/or curated by LibreTexts.

2.E: Basic Tools of Analytical Chemistry (Exercises)

1. Indicate how many significant figures are in each of the following numbers.

a. 903
b. 0.903
c. 1.0903
d. 0.0903
e. 0.09030
f. 9.03×10^2

2. Round each of the following to three significant figures.

a. 0.89377
b. 0.89328
c. 0.89350
d. 0.8997
e. 0.08907

3. Round each to the stated number of significant figures.

a. the atomic weight of carbon to 4 significant figures
b. the atomic weight of oxygen to 3 significant figures
c. Avogadro's number to 4 significant figures
d. Faraday's constant to 3 significant figures

4. Report results for the following calculations to the correct number of significant figures.

a. 4.591 + 0.2309 + 67.1 =
b. 313 – 273.15 =
c. 712 × 8.6 =
d. 1.43/0.026 =
e. (8.314 × 298)/96485 =
f. $\log(6.53 \times 10^{-5})$ =
g. $10^{-7.14}$ =
h. $(6.51 \times 10^{-5}) \times (8.14 \times 10^{-9})$ =

5. A 12.1374 g sample of an ore containing Ni and Co was carried through Fresenius' analytical scheme shown in Figure 1.1. At point A the combined mass of Ni and Co was found to be 0.2306 g, while at point B the mass of Co was found to be 0.0813 g. Report the weight percent Ni in the ore to the correct number of significant figures.

6. Figure 1.2 shows an analytical method for the analysis of Ni in ores based on the precipitation of Ni^{2+} using dimethylglyoxime. The formula for the precipitate is $Ni(C_4H_{14}N_4O_4)_2$. Calculate the precipitate's formula weight to the correct number of significant figures.

7. An analyst wishes to add 256 mg of Cl^- to a reaction mixture. How many mL of 0.217 M $BaCl_2$ is this?

8. The concentration of lead in an industrial waste stream is 0.28 ppm. What is its molar concentration?

9. Commercially available concentrated hydrochloric acid is 37.0% w/w HCl. Its density is 1.18 g/mL. Using this information calculate (a) the molarity of concentrated HCl, and (b) the mass and volume (in mL) of solution containing 0.315 moles of HCl.

10. The density of concentrated ammonia, which is 28.0% w/w NH_3, is 0.899 g/mL. What volume of this reagent should be diluted to 1.0×10^3 mL to make a solution that is 0.036 M in NH_3?

11. A 250.0 mL aqueous solution contains 45.1 µg of a pesticide. Express the pesticide's concentration in weight percent, in parts per million, and in parts per billion.

12. A city's water supply is fluoridated by adding NaF. The desired concentration of F^- is 1.6 ppm. How many mg of NaF should be added per gallon of treated water if the water supply already is 0.2 ppm in F^-?

13. What is the pH of a solution for which the concentration of H^+ is 6.92×10^{-6} M? What is the $[H^+]$ in a solution whose pH is 8.923?

14. When using a graduate cylinder, the absolute accuracy with which you can deliver a given volume is ±1% of the cylinder's maximum volume. What are the absolute and relative uncertainties if you deliver 15 mL of a reagent using a 25 mL graduated cylinder? Repeat for a 50 mL graduated cylinder.

15. Calculate the molarity of a potassium dichromate solution prepared by placing 9.67 grams of $K_2Cr_2O_7$ in a 100-mL volumetric flask, dissolving, and diluting to the calibration mark.

16. For each of the following explain how you would prepare 1.0 L of a solution that is 0.10 M in K^+. Repeat for concentrations of 1.0×10^2 ppm K^+ and 1.0% w/v K^+.

a. KCl
b. K_2SO_4
c. $K_3Fe(CN)_6$

17. A series of dilute NaCl solutions are prepared starting with an initial stock solution of 0.100 M NaCl. Solution A is prepared by pipeting 10 mL of the stock solution into a 250-mL volumetric flask and diluting to volume. Solution B is prepared by pipeting 25 mL of solution A into a 100-mL volumetric flask and diluting to volume. Solution C is prepared by pipeting 20 mL of solution B into a 500-mL volumetric flask and diluting to volume. What is the molar concentration of NaCl in solutions A, B and C?

> **Note**
>
> This is an example of a serial dilution, which is a useful method for preparing very dilute solutions of reagents.

18. Calculate the molar concentration of NaCl, to the correct number of significant figures, if 1.917 g of NaCl is placed in a beaker and dissolved in 50 mL of water measured with a graduated cylinder. If this solution is quantitatively transferred to a 250-mL volumetric flask and diluted to volume, what is its concentration to the correct number of significant figures?

19. What is the molar concentration of NO_3^- in a solution prepared by mixing 50.0 mL of 0.050 M KNO_3 with 40.0 mL of 0.075 M $NaNO_3$? What is pNO_3 for the mixture?

20. What is the molar concentration of Cl^- in a solution prepared by mixing 25.0 mL of 0.025 M NaCl with 35.0 mL of 0.050 M $BaCl_2$? What is pCl for the mixture?

21. To determine the concentration of ethanol in cognac a 5.00 mL sample of cognac is diluted to 0.500 L. Analysis of the diluted cognac gives an ethanol concentration of 0.0844 M. What is the molar concentration of ethanol in the undiluted cognac?

2.8.2 Solutions to Practice Exercises

Practice Exercise 2.1

The correct answer to this exercise is 1.9×10^{-2}. To see why this is correct, let's work through the problem in a series of steps. Here is the original problem

$$\frac{0.250 \times (9.93 \times 10^{-3}) - 0.100 \times (1.927 \times 10^{-2})}{9.93 \times 10^{-3} + 1.927 \times 10^{-2}} = \tag{2.E.1}$$

Following the correct order of operations we first complete the two multiplications in the numerator. In each case the answer has three significant figures, although we retain an extra digit, highlighted in red, to avoid round-off errors.

$$\frac{2.482 \times 10^{-3} - 1.927 \times 10^{-3}}{9.93 \times 10^{-3} + 1.927 \times 10^{-2}} = \tag{2.E.2}$$

Completing the subtraction in the numerator leaves us with two significant figures since the last significant digit for each value is in the hundredths place.

$$\frac{0.555 \times 10^{-3}}{9.93 \times 10^{-3} + 1.927 \times 10^{-2}} = \tag{2.E.3}$$

The two values in the denominator have different exponents. Because we are adding together these values, we first rewrite them using a common exponent.

$$\frac{0.555 \times 10^{-3}}{0.993 \times 10^{-2} + 1.927 \times 10^{-2}} = \tag{2.E.4}$$

The sum in the denominator has four significant figures since each value has three decimal places.

$$\frac{0.555 \times 10^{-3}}{2.920 \times 10^{-2}} = \tag{2.E.5}$$

Finally, we complete the division, which leaves us with a result having two significant figures.

$$\frac{0.555 \times 10^{-3}}{2.920 \times 10^{-2}} = 1.9 \times 10^{-2} \tag{2.E.6}$$

Click here to return to the chapter.

Practice Exercise 2.2

The concentrations of the two solutions are

$$\frac{0.50 \text{ mol NaCl}}{\text{L}} \times \frac{58.43 \text{ g NaCl}}{\text{mol NaCl}} \times \frac{10^6 \text{ g}}{\text{g}} \times \frac{1 \text{ L}}{1000 \text{ mL}} = 2.9 \times 10^3 \text{ g/mL} \tag{2.E.7}$$

$$\frac{0.25 \text{ mol SrCl}_2}{\text{L}} \times \frac{158.5 \text{ g SrCl}_2}{\text{mol NaCl}} \times \frac{10^6 \text{ g}}{\text{g}} \times \frac{1 \text{ L}}{1000 \text{ mL}} = 4.0 \times 10^3 \text{ g/mL} \tag{2.E.8}$$

The solution of $SrCl_2$ has the larger concentration when expressed in μg/mL instead of in mol/L.
Click here to return to the chapter.

Practice Exercise 2.3

The concentrations of K^+ and SO_4^{2-} are

$$\frac{1.5 \text{ g } K_2SO_4}{0.500 \text{ L}} \times \frac{1 \text{ mol } K_2SO_4}{174.3 \text{ g } K_2SO_4} \times \frac{2 \text{ mol } K^+}{\text{mol } K_2SO_4} = 3.44 \times 10^{-2} \text{ M } K^+ \tag{2.E.9}$$

$$\frac{1.5 \text{ g } K_2SO_4}{0.500 \text{ L}} \times \frac{1 \text{ mol } K_2SO_4}{174.3 \text{ g } K_2SO_4} \times \frac{1 \text{ mol } SO_4^{2-}}{\text{mol } K_2SO_4} = 1.72 \times 10^{-2} \text{ M } SO_4^{2-} \tag{2.E.10}$$

The pK and pSO_4 values are

$$\text{pK} = -\log(3.44 \times 10^{-2}) = 1.46 \tag{2.E.11}$$

$$\text{pSO}_4 = -\log(1.72 \times 10^{-2}) = 1.76 \tag{2.E.12}$$

Click here to return to the chapter.

Practice Exercise 2.4

First, we find the moles of AgBr

$$0.250 \text{ g AgBr} \times \frac{1 \text{ mol AgBr}}{187.8 \text{ g AgBr}} = 1.331 \times 10^{-3} \tag{2.E.13}$$

and then the moles and volume of $Na_2S_2O_3$

$$1.331 \times 10^{-3} \text{ mol AgBr} \times \frac{2 \text{ mol } Na_2S_2O_3}{\text{mol AgBr}} = 2.662 \times 10^{-3} \tag{2.E.14}$$

$$2.662 \times 10^{-3}\ \text{mol } Na_2S_2O_3 \times \frac{1\ \text{L}}{0.0138\ \text{mol } Na_2S_2O_3} \times \frac{1000\ \text{mL}}{\text{L}} = 193\ \text{mL} \tag{2.E.15}$$

Click here to return to the chapter.

Practice Exercise 2.5

Preparing 500 mL of 0.1250 M $KBrO_3$ requires

$$0.500\ \text{L} \times \frac{0.1250\ \text{mol } KBrO_3}{\text{L}} \times \frac{167.00\ \text{g } KBrO_3}{\text{mol } KBrO_3} = 10.44\ \text{g } KBrO_3 \tag{2.E.16}$$

Because the concentration has four significant figures, we must prepare the solution using volumetric glassware. Place a 10.44 g sample of $KBrO_3$ in a 500-mL volumetric flask and fill part way with water. Swirl to dissolve the $KBrO_3$ and then dilute with water to the flask's calibration mark.

Click here to return to the chapter.

Practice Exercise 2.6

The first solution is a stock solution, which we then dilute to prepare the standard solution. The concentration of Zn^{2+} in the stock solution is

$$\frac{1.004\ \text{g Zn}}{500\ \text{mL}} \times \frac{10^6\ \text{g}}{\text{g}} = 2008\ \text{g/mL} \tag{2.E.17}$$

To find the concentration of the standard solution we use equation 2.3

$$\frac{2008\ \text{g } Zn^{2+}}{\text{mL}} \times 2.000\ \text{mL} = C_{\text{new}} \times 250.0\ \text{mL} \tag{2.E.18}$$

where C_{new} is the standard solution's concentration. Solving gives a concentration of 16.06 μg Zn^{2+}/mL.
Click here to return to the chapter.

Contributors and Attributions

- David Harvey (DePauw University)

2.E: Basic Tools of Analytical Chemistry (Exercises) is shared under a CC BY-NC-SA 4.0 license and was authored, remixed, and/or curated by LibreTexts.

2.S: Basic Tools of Analytical Chemistry (Summary)

2.S: Basic Tools of Analytical Chemistry (Summary)

2.S: Basic Tools of Analytical Chemistry (Summary) is shared under a CC BY-NC-SA 4.0 license and was authored, remixed, and/or curated by LibreTexts.

CHAPTER OVERVIEW

3: The Vocabulary of Analytical Chemistry

If you leaf through an issue of the journal Analytical Chemistry, you will soon discover that the authors and readers share a common vocabulary of analytical terms. You are probably familiar with some of these terms, such as accuracy and precision, but other terms, such as analyte and matrix may be less familiar to you. In order to participate in the community of analytical chemists, you must first understand its vocabulary. The goal of this chapter, therefore, is to introduce you to some important analytical terms. Becoming comfortable with these terms will make the material in the chapters that follow easier to read and understand.

Topic hierarchy

3.1: Analysis, Determination, and Measurement
3.2: Techniques, Methods, Procedures, and Protocols
3.3: Classifying Analytical Techniques
3.4: Selecting an Analytical Method
3.5: Developing the Procedure
3.6: Protocols
3.7: The Importance of Analytical Methodology
3.E: The Vocabulary of Analytical Chemistry (Exercises)
3.S: The Vocabulary of Analytical Chemistry (Summary)
Index

Thumbnail: Colonies of fecal coliform bacteria from a water supply. Source: Susan Boyer. Photo courtesy of ARS–USDA (www.ars.usda.gov). Fecal coliform counts provide a general measure of the presence of pathogenic organisms in a water supply. For drinking water, the current maximum contaminant level (MCL) for total coliforms, including fecal coliforms is less than 1 colony/100 mL. Municipal water departments must regularly test the water supply and must take action if more than 5% of the samples in any month test positive for coliform bacteria.

Contributors

- David Harvey (DePauw University)

3: The Vocabulary of Analytical Chemistry is shared under a CC BY-NC-SA 4.0 license and was authored, remixed, and/or curated by LibreTexts.

CHAPTER OVERVIEW

Front Matter

TitlePage
InfoPage

3: The Vocabulary of Analytical Chemistry

This text is disseminated via the Open Education Resource (OER) LibreTexts Project (https://LibreTexts.org) and like the thousands of other texts available within this powerful platform, it is freely available for reading, printing, and "consuming."

The LibreTexts mission is to bring together students, faculty, and scholars in a collaborative effort to provide an accessible, and comprehensive platform that empowers our community to develop, curate, adapt, and adopt openly licensed resources and technologies; through these efforts we can reduce the financial burden born from traditional educational resource costs, ensuring education is more accessible for students and communities worldwide.

Most, but not all, pages in the library have licenses that may allow individuals to make changes, save, and print this book. Carefully consult the applicable license(s) before pursuing such effects. Instructors can adopt existing LibreTexts texts or Remix them to quickly build course-specific resources to meet the needs of their students. Unlike traditional textbooks, LibreTexts' web based origins allow powerful integration of advanced features and new technologies to support learning.



LibreTexts is the adaptable, user-friendly non-profit open education resource platform that educators trust for creating, customizing, and sharing accessible, interactive textbooks, adaptive homework, and ancillary materials. We collaborate with individuals and organizations to champion open education initiatives, support institutional publishing programs, drive curriculum development projects, and more.

The LibreTexts libraries are Powered by NICE CXone Expert and was supported by the Department of Education Open Textbook Pilot Project, the California Education Learning Lab, the UC Davis Office of the Provost, the UC Davis Library, the California State University Affordable Learning Solutions Program, and Merlot. This material is based upon work supported by the National Science Foundation under Grant No. 1246120, 1525057, and 1413739.

Any opinions, findings, and conclusions or recommendations expressed in this material are those of the author(s) and do not necessarily reflect the views of the National Science Foundation nor the US Department of Education.

Have questions or comments? For information about adoptions or adaptions contact info@LibreTexts.org or visit our main website at https://LibreTexts.org.

This text was compiled on 01/12/2026

3.1: Analysis, Determination, and Measurement

3.1: Analysis, Determination, and Measurement

3.1: Analysis, Determination, and Measurement is shared under a CC BY-NC-SA 4.0 license and was authored, remixed, and/or curated by LibreTexts.

3.2: Techniques, Methods, Procedures, and Protocols

3.2: Techniques, Methods, Procedures, and Protocols

3.2: Techniques, Methods, Procedures, and Protocols is shared under a CC BY-NC-SA 4.0 license and was authored, remixed, and/or curated by LibreTexts.

3.3: Classifying Analytical Techniques

3.3: Classifying Analytical Techniques

3.3: Classifying Analytical Techniques is shared under a CC BY-NC-SA 4.0 license and was authored, remixed, and/or curated by LibreTexts.

3.4: Selecting an Analytical Method

3.4: Selecting an Analytical Method

3.4: Selecting an Analytical Method is shared under a CC BY-NC-SA 4.0 license and was authored, remixed, and/or curated by LibreTexts.

3.5: Developing the Procedure

3.5: Developing the Procedure

3.5: Developing the Procedure is shared under a CC BY-NC-SA 4.0 license and was authored, remixed, and/or curated by LibreTexts.

3.6: Protocols

3.6: Protocols

3.6: Protocols is shared under a CC BY-NC-SA 4.0 license and was authored, remixed, and/or curated by LibreTexts.

3.7: The Importance of Analytical Methodology

3.7: The Importance of Analytical Methodology

3.7: The Importance of Analytical Methodology is shared under a CC BY-NC-SA 4.0 license and was authored, remixed, and/or curated by LibreTexts.

3.E: The Vocabulary of Analytical Chemistry (Exercises)

1. When working with a solid sample, it often is necessary to bring the analyte into solution by digesting the sample with a suitable solvent. Any remaining solid impurities are removed by filtration before continuing with the analysis. In a typical total analysis method, the procedure might read

> After digesting the sample in a beaker, remove any solid impurities by passing the solution containing the analyte through filter paper, collecting the filtrate in a clean Erlenmeyer flask. Rinse the beaker with several small portions of solvent, passing these rinsings through the filter paper and collecting them in the same Erlenmeyer flask. Finally, rinse the filter paper with several portions of solvent, collecting the rinsings in the same Erlenmeyer flask.

For a typical concentration method, however, the procedure might state

> After digesting the sample in a beaker, remove any solid impurities by filtering a portion of the solution containing the analyte. Collect and discard the first several mL of filtrate before collecting a sample of approximately 5 mL for further analysis.

Explain why these two procedures are different.

2. A certain concentration method works best when the analyte's concentration is approximately 10 ppb.

a. If the method requires a sample of 0.5 mL, about what mass of analyte is being measured?
b. If the analyte is present at 10% w/v, how would you prepare the sample for analysis?
c. Repeat for the case where the analyte is present at 10% w/w.
d. Based on your answers to parts (a)–(c), comment on the method's suitability for the determination of a major analyte.

3. An analyst needs to evaluate the potential effect of an interferent, I, on the quantitative analysis for an analyte, A. She begins by measuring the signal for a sample in which the interferent is absent and the analyte is present with a concentration of 15 ppm, obtaining an average signal of 23.3 (arbitrary units). When analyzing a sample in which the analyte is absent and the interferent is present with a concentration of 25 ppm, she obtains an average signal of 13.7.

a. What is the sensitivity for the analyte?
b. What is the sensitivity for the interferent?
c. What is the value of the selectivity coefficient?
d. Is the method more selective for the analyte or the interferent?
e. What is the maximum concentration of interferent relative to that of the analyte (i.e. [interferent]/[analyte]), if the error in the analysis is to be less than 1%?

4. A sample was analyzed to determine the concentration of an analyte. Under the conditions of the analysis the sensitivity is 17.2 ppm^{-1}. What is the analyte's concentration if Stotal is 35.2 and Sreag is 0.6?

5. A method for the analysis of Ca^{2+} in water suffers from an interference in the presence of Zn^{2+}. When the concentration of Ca^{2+} is 50 times greater than that of Zn^{2+}, an analysis for Ca^{2+} gives a relative error of –2.0%. What is the value of the selectivity coefficient for this method?

6. The quantitative analysis for reduced glutathione in blood is complicated by the presence of many potential interferents. In one study, when analyzing a solution of 10 ppb glutathione and 1.5 ppb ascorbic acid, the signal was 5.43 times greater than that obtained for the analysis of 10 ppb glutathione.[12] What is the selectivity coefficient for this analysis? The same study found that when analyzing a solution of 350 ppb methionine and 10 ppb glutathione the signal was 0.906 times less than that obtained for the analysis of 10 ppb glutathione. What is the selectivity coefficient for this analysis? In what way do these interferents behave differently?

7. Oungpipat and Alexander described a method for determining the concentration of glycolic acid (GA) in a variety of samples, including physiological fluids such as urine.[13] In the presence of only GA, the signal is given as

$$S_{samp,1} = k_{GA}C_{GA} \tag{3.E.1}$$

and in the presence of both glycolic acid and ascorbic acid (AA), the signal is

$$S_{samp,2} = k_{GA}C_{GA} + k_{AA}C_{AA} \tag{3.E.2}$$

When the concentration of glycolic acid is 1.0×10^{-4} M and the concentration of ascorbic acid is 1.0×10^{-5} M, the ratio of the two signals was found to be

$$\frac{S_{samp,2}}{S_{samp,1}} = 1.44 \tag{3.E.3}$$

a. Using the ratio of the two signals, determine the value of the selectivity ratio $K_{GA,AA}$.
b. Is the method more selective toward glycolic acid or ascorbic acid?
c. If the concentration of ascorbic acid is 1.0×10^{-5} M, what is the smallest concentration of glycolic acid that can be determined such that the error introduced by failing to account for the signal from ascorbic acid is less than 1%?

8. Ibrahim and co-workers developed a new method for the quantitative analysis of hypoxanthine, a natural compound of some nucleic acids.[14] As part of their study they evaluated the method's selectivity for hypoxanthine in the presence of several possible interferents, including ascorbic acid.

a. When analyzing a solution of 1.12×10^{-6} M hypoxanthine the authors obtained a signal of 7.45×10^{-5} amps. What is the sensitivity for hypoxanthine? You may assume that the signal has been corrected for the method blank.
b. When a solution containing 1.12×10^{-6} M hypoxanthine and 6.5×10^{-5} M ascorbic acid was analyzed a signal of 4.04×10^{-5} amps was obtained. What is the selectivity coefficient for this method?
c. Is the method more selective for hypoxanthine or for ascorbic acid?
d. What is the largest concentration of ascorbic acid that may be present if a concentration of 1.12×10^{-6} M hypoxanthine is to be determined within ±1%?

9. Examine a procedure from *Standard Methods for the Analysis of Waters and Wastewaters* (or another manual of standard analytical methods) and identify the steps taken to compensate for interferences, to calibrate equipment and instruments, to standardize the method and to acquire a representative sample.

3.8.3 Solutions to Practice Exercises

Practice Exercise 3.1

Since the signal for Ag^+ in the presence of Ni^{2+} is given as a relative error, the fact that are not given absolute signals is of no consequence. Instead, we will assign a value of 100 as the signal for 1×10^{-9} M Ag^+. With a relative error of +4.9%, the signal for the solution of 1×10^{-9} M Ag^+ and 1.1×10^{-7} M Ni^{2+} is 104.9. The sensitivity for Ag^+ is determined using the solution that does not contain Ni^{2+}.

$$k_{Ag} = \frac{S_{Ag}}{C_{Ag}} = \frac{100}{1 \times 10^{-9}\ \text{M}} = 1.0 \times 10^{11}\ \text{M}^{-1} \tag{3.E.4}$$

Substituting into equation 3.4 values for k_{Ag}, S_{samp} for the solution containing Ag^+ and Ni^{2+}, and the concentrations of Ag^+ and Ni^{2+}

$$S_{samp} = 104.9 = (1.0 \times 10^{11}\ \text{M}^{-1}) \times (1.0 \times 10^{-9}\ \text{M}) + k_{Ni} \times (1.1 \times 10^{-7}\ \text{M}) \tag{3.E.5}$$

and solving gives k_{Ni} as 4.5×10^7 M^{-1}. The selectivity coefficient is

$$K_{Ag,Ni} = \frac{k_{Ni}}{k_{Ag}} = \frac{4.5 \times 10^7\ \text{M}^{-1}}{1.0 \times 10^{11}\ \text{M}^{-1}} = 4.5 \times 10^{-4} \tag{3.E.6}$$

Click here to return to the chapter.

Practice Exercise 3.2

(a) A negative value for $K_{Ag,Hg}$ means that the presence of Hg^{2+} decreases the signal from Ag^+.
(b) In this case we need to consider an error of –1%, since the effect of Hg^{2+} is to decrease the signal from Ag^+. To achieve this error, the term $K_{A,I} \times C_I$ in equation 3.8 must be less than -1% of C_A; thus

$$K_{Ag,Hg} \times C_{Hg} = -0.01 \times C_{Ag} \tag{3.E.7}$$

Substituting in known values for $K_{Ag,Hg}$ and C_{Ag}, we find that the maximum concentration of Hg^{2+} is 1.0×10^{-8} M.

Click here to return to the chapter.

Contributors and Attributions

- David Harvey (DePauw University)

3.E: The Vocabulary of Analytical Chemistry (Exercises) is shared under a CC BY-NC-SA 4.0 license and was authored, remixed, and/or curated by LibreTexts.

3.S: The Vocabulary of Analytical Chemistry (Summary)

3.S: The Vocabulary of Analytical Chemistry (Summary)

3.S: The Vocabulary of Analytical Chemistry (Summary) is shared under a CC BY-NC-SA 4.0 license and was authored, remixed, and/or curated by LibreTexts.

CHAPTER OVERVIEW

Back Matter

Index

Index

D

dire

CHAPTER OVERVIEW

4: Evaluating Analytical Data

When using an analytical method we make three separate evaluations of experimental error. First, before beginning an analysis we evaluate potential sources of errors to ensure that they will not adversely effect our results. Second, during the analysis we monitor our measurements to ensure that errors remain acceptable. Finally, at the end of the analysis we evaluate the quality of the measurements and results, comparing them to our original design criteria. This chapter provides an introduction to sources of error, to evaluating errors in analytical measurements, and to the statistical analysis of data.

Topic hierarchy

4.1: Characterizing Measurements and Results
4.2: Characterizing Experimental Errors
4.3: Propagation of Uncertainty
4.4: The Distribution of Measurements and Results
4.5: Statistical Analysis of Data
4.6: Statistical Methods for Normal Distributions
4.7: Detection Limits
4.8: Using Excel and R to Analyze Data
4.E: Evaluating Analytical Data (Exercises)
4.S: Evaluating Analytical Data (Summary)

Thumbnail: The blue vertical line segments represent multiple realizations of a confidence interval for the population mean μ, represented as a red horizontal dashed line; note that some confidence intervals do not contain the population mean, as expected. Image used with permission (Public Domain; Tsyplakov) .

Contributors

- David Harvey (DePauw University)

4: Evaluating Analytical Data is shared under a CC BY-NC-SA 4.0 license and was authored, remixed, and/or curated by LibreTexts.

4.1: Characterizing Measurements and Results

4.1: Characterizing Measurements and Results

4.1: Characterizing Measurements and Results is shared under a CC BY-NC-SA 4.0 license and was authored, remixed, and/or curated by LibreTexts.

4.2: Characterizing Experimental Errors

4.2: Characterizing Experimental Errors

4.2: Characterizing Experimental Errors is shared under a CC BY-NC-SA 4.0 license and was authored, remixed, and/or curated by LibreTexts.

4.3: Propagation of Uncertainty

4.3: Propagation of Uncertainty

4.3: Propagation of Uncertainty is shared under a CC BY-NC-SA 4.0 license and was authored, remixed, and/or curated by LibreTexts.

4.4: The Distribution of Measurements and Results

4.4: The Distribution of Measurements and Results

4.4: The Distribution of Measurements and Results is shared under a CC BY-NC-SA 4.0 license and was authored, remixed, and/or curated by LibreTexts.

4.5: Statistical Analysis of Data

4.5: Statistical Analysis of Data

4.5: Statistical Analysis of Data is shared under a CC BY-NC-SA 4.0 license and was authored, remixed, and/or curated by LibreTexts.

4.6: Statistical Methods for Normal Distributions

4.6: Statistical Methods for Normal Distributions

4.6: Statistical Methods for Normal Distributions is shared under a CC BY-NC-SA 4.0 license and was authored, remixed, and/or curated by LibreTexts.

4.7: Detection Limits

4.7: Detection Limits

4.7: Detection Limits is shared under a CC BY-NC-SA 4.0 license and was authored, remixed, and/or curated by LibreTexts.

4.8: Using Excel and R to Analyze Data

4.8: Using Excel and R to Analyze Data

4.8: Using Excel and R to Analyze Data is shared under a CC BY-NC-SA 4.0 license and was authored, remixed, and/or curated by LibreTexts.

4.E: Evaluating Analytical Data (Exercises)

Many of the problems that follow require access to statistical tables. For your convenience, here are hyperlinks to the appendices containing these tables.

Appendix 3: Single-Sided Normal Distribution
Appendix 4: Critical Values for the t-Test
Appendix 5: Critical Values for the F-Test
Appendix 6: Critical Values for Dixon's Q-Test
Appendix 7: Critical Values for Grubb's Test

1. The following masses were recorded for 12 different U.S. quarters (all given in grams):

5.683	5.549	5.548	5.552
5.620	5.536	5.539	5.684
5.551	5.552	5.554	5.632

Report the mean, median, range, standard deviation and variance for this data.

2. A determination of acetaminophen in 10 separate tablets of Excedrin Extra Strength Pain Reliever gives the following results (in mg).[16]

224.3	240.4	246.3	239.4	253.1
261.7	229.4	255.5	235.5	249.7

(a) Report the mean, median, range, standard deviation and variance for this data. (b) Assuming that $\overline{X}$ and s^2 are good approximations for μ and σ^2, and that the population is normally distributed, what percentage of tablets contain more than the standard amount of 250 mg acetaminophen per tablet?

3. Salem and Galan developed a new method for determining the amount of morphine hydrochloride in tablets.[17] An analysis of tablets with different nominal dosages gave the following results (in mg/tablet).

100-mg tablets	60-mg tablets	30-mg tablets	10-mg tablets
99.17	54.21	28.51	9.06
94.31	55.62	26.25	8.83
95.92	57.40	25.92	9.08
94.55	57.51	28.62	
93.83	52.59	24.93	

(a) For each dosage, calculate the mean and standard deviation for the mg of morphine hydrochloride per tablet. (b) For each dosage level, assuming that $\overline{X}$ and s^2 are good approximations for μ and σ^2, and that the population is normally distributed, what percentage of tablets contain more than the nominal amount of morphine hydrochloride per tablet?

4. Daskalakis and co-workers evaluated several procedures for digesting oyster and mussel tissue prior to analyzing them for silver.[18] To evaluate the procedures they spiked samples with known amounts of silver and analyzed the samples to determine the amount of silver, reporting results as the percentage of added silver found in the analysis. A procedure was judged acceptable is the spike recoveries fell within the range 100±15%. The spike recoveries for one method are shown here.

106%	108%	92%	99%
101%	93%	93%	104%

Assuming a normal distribution for the spike recoveries, what is the probability that any single spike recovery will be within the accepted range?

5. The formula weight (FW) of a gas can be determined using the following form of the ideal gas law

$$FW = \frac{gRT}{PV} \tag{4.E.1}$$

where g is the mass in grams, R is the gas constant, T is the temperature in Kelvin, P is the pressure in atmospheres, and V is the volume in liters.

In a typical analysis the following data are obtained (with estimated uncertainties in parentheses)

$$\mathrm{g = 0.118\ g\ (\pm 0.002\ g)} \tag{4.E.2}$$
$$\mathrm{R = 0.082056\ L\ atm\ mol^{-1}\ K^{-1}\ (\pm 0.000001\ L\ atm\ mol^{-1}\ K^{-1})} \tag{4.E.3}$$
$$\mathrm{T = 298.2\ K\ (\pm 0.1\ K)} \tag{4.E.4}$$
$$\mathrm{P = 0.724\ atm\ (\pm 0.005\ atm)} \tag{4.E.5}$$
$$\mathrm{V = 0.250\ L\ (\pm 0.005\ L)} \tag{4.E.6}$$

(a) What is the compound's formula weight and its estimated uncertainty? (b) To which variable(s) should you direct your attention if you wish to improve the uncertainty in the compound's molecular weight?

6. To prepare a standard solution of Mn^{2+} a 0.250 g sample of Mn is dissolved in 10 mL of concentrated HNO_3 (measured with a graduated cylinder). The resulting solution is quantitatively transferred to a 100-mL volumetric flask and diluted to volume with distilled water. A 10 mL aliquot of the solution is pipeted into a 500-mL volumetric flask and diluted to volume. (a) Express the concentration of Mn in mg/L, and estimate its uncertainty using a propagation of uncertainty. (b) Can you improve the concentration's uncertainty by using a pipet to measure the HNO_3, instead of a graduated cylinder?

7. The mass of a hygroscopic compound is measured using the technique of weighing by difference. In this technique the compound is placed in a sealed container and weighed. A portion of the compound is removed, and the container and the remaining material are reweighed. The difference between the two masses gives the sample's mass. A solution of a hygroscopic compound with a gram formula weight of 121.34 g/mol (±0.01 g/mol) was prepared in the following manner. A sample of the compound and its container has a mass of 23.5811 grams. A portion of the compound was transferred to a 100-mL volumetric flask and diluted to volume. The mass of the compound and container after the transfer is 22.1559 grams. Calculate the compound's molarity and estimate its uncertainty by a propagation of uncertainty.

8. Show using a propagation of uncertainty that the standard error of the mean for n determinations is $s / \sqrt{n}$.

9. Beginning with equation 4.17 and equation 4.18, use a propagation of uncertainty to derive equation 4.19.

10. What is the smallest mass that we can measure on an analytical balance that has a tolerance of ±0.1 mg, if the relative error must be less than 0.1%?

11. Which of the following is the best way to dispense 100.0 mL of a reagent: (a) use a 50-mL pipet twice; (b) use a 25-mL pipet four times; or (c) use a 10-mL pipet ten times?

12. You can dilute a solution by a factor of 200 using readily available pipets (1-mL to 100-mL) and volumetric flasks (10-mL to 1000-mL) in either one step, two steps, or three steps. Limiting yourself to the glassware in Table 4.2, determine the proper combination of glassware to accomplish each dilution, and rank them in order of their most probable uncertainties.

13. Explain why changing all values in a data set by a constant amount will change $\overline{X}$ but will have no effect on s.

14. Obtain a sample of a metal from your instructor and determine its density by one or both of the following methods:

Method A: Determine the sample's mass with a balance. Calculate the sample's volume using appropriate linear dimensions.

Method B: Determine the sample's mass with a balance. Calculate the sample's volume by measuring the amount of water that it displaces. This can be done by adding water to a graduated cylinder, reading the volume, adding the sample, and reading the new volume. The difference in volumes is equal to the sample's volume.

Determine the density at least 5 times. (a) Report the mean, the standard deviation, and the 95% confidence interval for your results. (b) Find the accepted value for the metal's density and determine the absolute and relative error for your determination of

the metal's density. (c) Use a propagation of uncertainty to determine the uncertainty for your method of analysis. Is the result of this calculation consistent with your experimental results? If not, suggest some possible reasons for this disagreement.

15. How many carbon atoms must a molecule have if the mean number of ^{13}C atoms per molecule is 1.00? What percentage of such molecules will have no atoms of ^{13}C?

16. In Example 4.10 we determined the probability that a molecule of cholesterol, $C_{27}H_{44}O$, had no atoms of ^{13}C. (a) Calculate the probability that a molecule of cholesterol, has 1 atom of ^{13}C. (b) What is the probability that a molecule of cholesterol will have two or more atoms of ^{13}C?

17. Berglund and Wichardt investigated the quantitative determination of Cr in high-alloy steels using a potentiometric titration of Cr(VI)[19].

Before the titration, samples of the steel were dissolved in acid and the chromium oxidized to Cr(VI) using peroxydisulfate. Shown here are the results (as %w/w Cr) for the analysis of a reference steel.

16.968	16.922	16.840	16.883
16.887	16.977	16.857	16.728

Calculate the mean, the standard deviation, and the 95% confidence interval about the mean. What does this confidence interval mean?

18. Ketkar and co-workers developed an analytical method for determining trace levels of atmospheric gases.[20] An analysis of a sample containing 40.0 parts per thousand (ppt) 2-chloroethylsulfide yielded the following results

43.3	34.8	31.9
37.8	34.4	31.9
42.1	33.6	35.3

(a) Determine whether there is a significant difference between the experimental mean and the expected value at $\alpha = 0.05$. (b) As part of this study a reagent blank was analyzed 12 times, giving a mean of 0.16 ppt and a standard deviation of 1.20 ppt. What are the IUPAC detection limit, the limit of identification, and limit of quantitation for this method assuming $\alpha = 0.05$?

19. To test a spectrophotometer's accuracy a solution of 60.06 ppm $K_2Cr_2O_7$ in 5.0 mM H_2SO_4 is prepared and analyzed. This solution has an expected absorbance of 0.640 at 350.0 nm in a 1.0-cm cell when using 5.0 mM H_2SO_4 as a reagent blank. Several aliquots of the solution produce the following absorbance values.

0.639 0.638 0.640 0.639 0.640 0.639 0.638

Determine whether there is a significant difference between the experimental mean and the expected value at $\alpha = 0.01$.

20. Monna and co-workers used radioactive isotopes to date sediments from lakes and estuaries.[21] To verify this method they analyzed a ^{208}Po standard known to have an activity of 77.5 decays/min, obtaining the following results.

77.09	75.37	72.42	76.84	77.84	76.69
78.03	74.96	77.54	76.09	81.12	75.75

Determine whether there is a significant difference between the mean and the expected value at $\alpha = 0.05$.

21. A 2.6540-g sample of an iron ore, known to be 53.51% w/w Fe, is dissolved in a small portion of concentrated HCl and diluted to volume in a 250-mL volumetric flask. A spectrophotometric determination of the concentration of Fe in this solution yields results of 5840, 5770, 5650, and 5660 ppm. Determine whether there is a significant difference between the experimental mean and the expected value at $\alpha = 0.05$.

22. Horvat and co-workers used atomic absorption spectroscopy to determine the concentration of Hg in coal fly ash.[22] Of particular interest to the authors was developing an appropriate procedure for digesting samples and releasing the Hg for analysis.

As part of their study they tested several reagents for digesting samples. Results obtained using HNO_3 and using a 1 + 3 mixture of HNO_3 and HCl are shown here. All concentrations are given as ng Hg/g sample.

HNO_3 161 165 160 167 166
1+3 HNO_3–HCl 159 145 140 147 143 156

Determine whether there is a significant difference between these methods at $\alpha = 0.05$.

23. Lord Rayleigh, John William Strutt (1842-1919), was one of the most well known scientists of the late nineteenth and early twentieth centuries, publishing over 440 papers and receiving the Nobel Prize in 1904 for the discovery of argon. An important turning point in Rayleigh's discovery of Ar was his experimental measurements of the density of N_2. Rayleigh approached this experiment in two ways: first by taking atmospheric air and removing all O_2 and H_2; and second, by chemically producing N_2 by decomposing nitrogen containing compounds (NO, N_2O, and NH_4NO_3) and again removing all O_2 and H_2. Following are his results for the density of N_2, published in *Proc. Roy. Soc.* **1894**, *LV*, 340 (publication 210) (all values are for grams of gas at an equivalent volume, pressure, and temperature).[23]

Atmospheric	2.310 17	2.309 86	2.310 10	2.310 01
Origin:	2.310 24	2.310 10	2.310 28	2.301 82
Chemical	2.301 43	2.298 90	2.298 16	2.298 89
Origin:	2.298 69	2.299 40	2.298 49	

Explain why this data led Rayleigh to look for, and discover Ar.

24. Gács and Ferraroli reported a method for monitoring the concentration of SO_2 in air.[24] They compared their method to the standard method by analyzing urban air samples collected from a single location. Samples were collected by drawing air through a collection solution for 6 min.

Shown here is a summary of their results with SO_2 concentrations reported in $\mu L/m^3$.

standard	21.62	22.20	24.27	
method:	24.25	23.09	21.02	23.54
new	21.54	20.51	22.31	21.30
method:	24.62	25.72	21.54	

Using an appropriate statistical test determine whether there is any significant difference between the standard method and the new method at $\alpha = 0.05$.

25. One way to check the accuracy of a spectrophotometer is to measure absorbencies for a series of standard dichromate solutions obtained from the National Institute of Standards and Technology. Absorbencies are measured at 257 nm and compared to the

accepted values. The results obtained when testing a newly purchased spectrophotometer are shown here. Determine if the tested spectrophotometer is accurate at $\alpha = 0.05$.

Standard	Measured Absorbance	Expected Absorbance
1	0.2872	0.2871
2	0.5773	0.5760
3	0.8674	0.8677
4	1.1623	1.1608
5	1.4559	1.4565

26. Maskarinec and co-workers investigated the stability of volatile organics in environmental water samples.[25] Of particular interest was establishing proper conditions for maintaining the sample's integrity between its collection and analysis. Two preservatives were investigated—ascorbic acid and sodium bisulfate—and maximum holding times were determined for a number of volatile organics and water matrices. The following table shows results (in days) for the holding time of nine organic compounds in surface water.

	Ascorbic Acid	Sodium Bisulfate
methylene chloride	77	62
carbon disulfide	23	54
trichloroethane	52	51
benzene	62	42
1,1,2-trichloroethane	57	53
1,1,2,2-tetrachlorethane	33	85
tetrachloroethene	41	63
toluene	32	94
chlorobenzene	36	86

Determine whether there is a significant difference in the effectiveness of the two preservatives at $\alpha = 0.10$.

27. Using X-ray diffraction, Karstang and Kvalhein reported a new method for determining the weight percent of kalonite in complex clay minerals using X-ray diffraction.[26] To test the method, nine samples containing known amounts of kalonite were prepared and analyzed. The results (as % w/w kalonite) are shown here.

Actual: 5.0 10.0 20.0 40.0 50.0 60.0 80.0 90.0 95.0
Found: 6.8 11.7 19.8 40.5 53.6 61.7 78.9 91.7 94.7

Evaluate the accuracy of the method at $\alpha = 0.05$.

28. Mizutani, Yabuki and Asai developed an electrochemical method for analyzing *l*-malate.[27] As part of their study they analyzed a series of beverages using both their method and a standard spectrophotometric procedure based on a clinical kit purchased from Boerhinger Scientific. The following table summarizes their results. All values are in ppm.

Sample	Electrode	Spectrophotometric
Apple juice 1	34.0	33.4
Apple juice 2	22.6	28.4
Apple juice 3	29.7	29.5
Apple juice 4	24.9	24.8
Grape juice 1	17.8	18.3
Grape juice 2	14.8	15.4
Mixed fruit juice 1	8.6	8.5
Mixed fruit juice 2	31.4	31.9
White wine 1	10.8	11.5
White wine 2	17.3	17.6
White wine 3	15.7	15.4
White wine 4	18.4	18.3

Determine whether there is a significant difference between the methods at $\alpha = 0.05$.

29. Alexiev and colleagues describe an improved photometric method for determining Fe^{3+} based on its ability to catalyze the oxidation of sulphanilic acid by KIO_4.[28] As part of their study the concentration of Fe^{3+} in human serum samples was determined by the improved method and the standard method. The results, with concentrations in µmol/L, are shown in the following table.

Sample	Improved Method	Standard Method
1	8.25	8.06
2	9.75	8.84
3	9.75	8.36
4	9.75	8.73
5	10.75	13.13
6	11.25	13.65
7	13.88	13.85
8	14.25	13.53

Determine whether there is a significant difference between the two methods at $\alpha = 0.05$.

30. Ten laboratories were asked to determine an analyte's concentration in three standard test samples. Following are the results, in μg/mL.[29]

Laboratory	Sample 1	Sample 2	Sample 3
1	22.6	13.6	16.0
2	23.0	14.2	15.9
3	21.5	13.9	16.9
4	21.9	13.9	16.9
5	21.3	13.5	16.7
6	22.1	13.5	17.4
7	23.1	13.9	17.5
8	21.7	13.5	16.8
9	22.2	12.9	17.2
10	21.7	13.8	16.7

Determine if there are any potential outliers in Sample 1, Sample 2 or Sample 3 at a significance level of $\alpha = 0.05$. Use all three methods—Dixon's *Q*-test, Grubb's test, and Chauvenet's criterion—and compare the results to each other.

31. When copper metal and powdered sulfur are placed in a crucible and ignited, the product is a sulfide with an empirical formula of Cu_xS. The value of x can be determined by weighing the Cu and S before ignition, and finding the mass of Cu_xS when the reaction is complete (any excess sulfur leaves as SO_2). The following table shows the Cu/S ratios from 62 such experiments.

1.764 1.838 1.865 1.866 1.872 1.877
1.890 1.891 1.891 1.897 1.899 1.900
1.906 1.908 1.910 1.911 1.916 1.919
1.920 1.922 1.927 1.931 1.935 1.936
1.936 1.937 1.939 1.939 1.940 1.941
1.941 1.942 1.943 1.948 1.953 1.955
1.957 1.957 1.957 1.959 1.962 1.963
1.963 1.963 1.966 1.968 1.969 1.973
1.975 1.976 1.977 1.981 1.981 1.988
1.993 1.993 1.995 1.995 1.995 2.017
2.029 2.042

(a) Calculate the mean and standard deviation for this data. (b) Construct a histogram for this data. From a visual inspection of your histogram, does the data appear to be normally distributed? (c) In a normally distributed population 68.26% of all members lie within the range $\mu \pm 1\sigma$. What percentage of the data lies within the range $\pm$ 1s? Does this support your answer to the previous question? (d) Assuming that $\overline{X}$ and s^2 are good approximations for μ and σ^2, what percentage of all experimentally determined Cu/S ratios will be greater than 2? How does this compare with the experimental data? Does this support your conclusion about whether the data is normally distributed? (e) It has been reported that this method of preparing copper sulfide results in a non-stoichiometric compound with a Cu/S ratio of less than 2. Determine if the mean value for this data is significantly less than 2 at a significance level of $\alpha = 0.01$.

32. Real-time quantitative PCR is an analytical method for determining trace amounts of DNA. During the analysis, each cycle doubles the amount of DNA. A probe species that fluoresces in the presence of DNA is added to the reaction mixture and the increase in fluorescence is monitored during the cycling. The cycle threshold, C_t, is the cycle when the fluorescence exceeds a

threshold value. The data in the following table shows C_t values for three samples using real-time quantitative PCR.[30] Each sample was analyzed 18 times.

Sample X		Sample Y		Sample Z	
24.24	25.14	24.41	28.06	22.97	23.43
23.97	24.57	27.21	27.77	22.93	23.66
24.44	24.49	27.02	28.74	22.95	28.79
24.79	24.68	26.81	28.35	23.12	23.77
23.92	24.45	26.64	28.80	23.59	23.98
24.53	24.48	27.63	27.99	23.37	23.56
24.95	24.30	28.42	28.21	24.17	22.80
24.76	24.60	25.16	28.00	23.48	23.29
25.18	24.57	28.53	28.21	23.80	23.86

Examine this data statistically and write a brief report on your conclusions. Issues you may wish to address include the presence of outliers in the samples, a summary of the descriptive statistics for each sample, and any evidence for a difference between the samples.

4.9.3 Solutions to Practice Exercises

Practice Exercise 4.1

Mean: To find the mean we sum up the individual measurements and divide by the number of measurements. The sum of the 10 concentrations is 1405. Dividing the sum by 10 gives the mean as 140.5, or 1.40×10^2 mmol/L.

Median: To find the median we arrange the 10 measurements from the smallest concentration to the largest concentration; thus

118 132 137 140 141 143 143 145 149 157

The median for a data set with 10 members is the average of the fifth and sixth values; thus, the median is (141 + 143)/2, or 141 mmol/L.

Range: The range is the difference between the largest value and the smallest value; thus, the range is 157 – 118 = 39 mmol/L.

Standard Deviation: To calculate the standard deviation we first calculate the difference between each measurement and the mean value (140.5), square the resulting differences, and add them together. The differences are

-0.5 2.5 0.5 -3.5 -8.5 16.5 2.5 8.5 -22.5 4.5

and the squared differences are

0.25 6.25 0.25 12.25 72.25 272.25 6.25 72.25 506.25 20.25

The total sum of squares, which is the numerator of equation 4.1, is 968.50. The standard deviation is

$$s = \sqrt{\frac{968.50}{10-1}} = 10.37 \approx 10.4 \qquad (4.E.7)$$

Variance: The variance is the square of the standard deviation, or 108.

Click here to return to the chapter.

Practice Exercise 4.2

The first step is to determine the concentration of Cu^{2+} in the final solution. The mass of copper is

$$74.2991\ \text{g} - 73.3216\ \text{g} = 0.9775\ \text{g Cu} \tag{4.E.8}$$

The 10 mL of HNO_3 used to dissolve the copper does not factor into our calculation. The concentration of Cu^{2+} is

$$\frac{0.9775\ \text{g Cu}}{0.5000\ \text{L}} \times \frac{1.000\ \text{mL}}{250.0\ \text{mL}} \times \frac{10^3\ \text{mg}}{\text{g}} = 7.820\ \text{mg Cu}^{2+}/\text{L} \tag{4.E.9}$$

Having found the concentration of Cu^{2+} we continue on to complete the propagation of uncertainty. The absolute uncertainty in the mass of Cu wire is

$$u_{\text{g Cu}} = \sqrt{(0.0001)^2 + (0.0001)^2} = 0.00014\ \text{g} \tag{4.E.10}$$

The relative uncertainty in the concentration of Cu^{2+} is

$$\frac{u_{\text{mg/L}}}{7.820\ \text{mg/L}} = \sqrt{\left(\frac{0.00014}{0.9775}\right)^2 + \left(\frac{0.20}{500.0}\right)^2 + \left(\frac{0.006}{1.000}\right)^2 + \left(\frac{0.12}{250.0}\right)^2} = 0.00603 \tag{4.E.11}$$

Solving for $u_{\text{mg/L}}$ gives the uncertainty as 0.0472. The concentration and uncertainty for Cu^{2+} is 7.820 mg/L ± 0.047 mg/L.

Click here to return to the chapter.

Practice Exercise 4.3

The first step is to calculate the absorbance, which is

$$A = -\log\frac{P}{P_o} = -\log\frac{1.50 \times 10^2}{3.80 \times 10} = \log(0.3947) = 0.4037 \approx 0.404 \tag{4.E.12}$$

Having found the absorbance we continue on to complete the propagation of uncertainty. First, we find the uncertainty for the ratio P/P_o.

$$\frac{u_{P/P_o}}{P/P_o} = \sqrt{\left(\frac{15}{3.80{\times}10^2}\right)^2 + \left(\frac{15}{1.50{\times}10^2}\right)^2} = 1.075 \times 10^{-2} \tag{4.E.13}$$

Finally, from Table 4.10 the uncertainty in the absorbance is

$$u_A = 0.4343 \times \frac{u_{P/P_o}}{P/P_o} = (0.4343) \times (1.075 \times 10^{-2}) = 4.669 \times 10^{-3} \tag{4.E.14}$$

The absorbance and uncertainty is 0.404 ± 0.005 absorbance units.

Click here to return to the chapter.

Practice Exercise 4.4

An uncertainty of 0.8% is a relative uncertainty in the concentration of 0.008; thus

$$0.008 = \sqrt{\left(\frac{0.028}{23.41}\right)^2 + \left(\frac{u_{k_A}}{0.186}\right)^2} \tag{4.E.15}$$

Squaring both sides of the equation gives

$$6.4 \times 10^{-5} = \left(\frac{0.028}{23.41}\right)^2 + \left(\frac{u_{k_A}}{0.186}\right)^2 \tag{4.E.16}$$

$$6.257 \times 10^{-5} = \left(\frac{u_{k_A}}{0.186}\right)^2 \tag{4.E.17}$$

Sovling for u_{kA} gives its value as $1.47{\times}10^{-3}$, or $\pm 0.0015\ \text{ppm}^{-1}$.

Click here to return to the chapter.

Practice Exercise 4.5

To find the percentage of tablets containing less than 245 mg of aspirin we calculate the deviation, z,

$$z = \frac{245 - 250}{5} = -1.00 \tag{4.E.18}$$

and look up the corresponding probability in Appendix 3A, obtaining a value of 15.87%. To find the percentage of tablets containing less than 240 mg of aspirin we find that

$$z = \frac{240 - 250}{5} = -2.00 \tag{4.E.19}$$

which corresponds to 2.28%. The percentage of tablets containing between 240 and 245 mg of aspiring is 15.87% – 2.28% = 13.59%.

Click here to return to the chapter.

Practice Exercise 4.6

The mean is 249.9 mg aspirin/tablet for this sample of seven tablets. For a 95% confidence interval the value of *z* is 1.96. The confidence interval is

$$249.9 \pm \frac{1.96 \times 5}{\sqrt{7}} = 249.9 \pm 3.7 \approx 250 \text{ mg} \pm 4 \text{ mg} \tag{4.E.20}$$

Click here to return to the chapter.

Practice Exercise 4.7

With 100 pennies, we have 99 degrees of freedom for the mean. Although Table 4.15 does not include a value for *t*(0.05, 99), we can approximate its value using the values for *t*(0.05, 60) and *t*(0.05, 100) and assuming a linear change in its value.

$$t(0.05, 99) = t(0.05, 60) - \frac{39}{40}\{t(0.05, 60) - t(0.05, 100)\} \tag{4.E.21}$$

$$t(0.05, 99) = 200 - \frac{39}{40}\{2.000 - 1.984\} = 1.984 \tag{4.E.22}$$

The 95% confidence interval for the pennies is

$$3.095 \pm \frac{1.9844 \times 0.0346}{\sqrt{100}} = 3.095 \text{ g} \pm 0.007 \text{ g} \tag{4.E.23}$$

From Example 4.15, the 95% confidence intervals for the two samples in Table 4.11 are 3.117 g ± 0.047 g and 3.081 g ± 0.046 g. As expected, the confidence interval for the sample of 100 pennies is much smaller than that for the two smaller samples of pennies. Note, as well, that the confidence interval for the larger sample fits within the confidence intervals for the two smaller samples.

Click here to return to the chapter.

Practice Exercise 4.8

The null hypothesis is $H_0 : \overline{X} = \mu$ and the alternative hypothesis is $H_A : \overline{X} \neq \mu$. The mean and standard deviation for the data are 99.26% and 2.35%, respectively. The value for t_{exp} is

$$t_{exp} = \frac{|100.0 - 99.26|\sqrt{7}}{2.35} = 0.833 \tag{4.E.24}$$

and the critical value for *t*(0.05, 6) is 0.836. Because t_{exp} is less than *t*(0.05, 6) we retain the null hypothesis and have no evidence for a significant difference between $\overline{X}$ and μ.

Click here to return to the chapter.

Practice Exercise 4.9

The standard deviations for Lot 1 is 6.451 mg, and 7.849 mg for Lot 2. The null and alternative hypotheses are

$$H_0 : s^2_{\text{Lot 1}} = s^2_{\text{Lot 2}} \quad H_A : s^2_{\text{Lot 1}} \neq s^2_{\text{Lot 2}} \tag{4.E.25}$$

and the value of F_{exp} is

$$F_{exp} = \frac{(7.849)^2}{(6.451)^2} = 1.480 \tag{4.E.26}$$

The critical value for $F(0.05, 5, 6)$ is 5.988. Because $F_{exp} < F(0.05, 5, 6)$, we retain the null hypothesis. There is no evidence at $\alpha = 0.05$ to suggest that the difference in the variances is significant.

Click here to return to the chapter.

Practice Exercise 4.10

To compare the means for the two lots, we will use an unpaired t-test of the null hypothesis $H_0 : \overline{X}_{\text{Lot 1}} = \overline{X}_{\text{Lot 2}}$ and the alternative hypothesis $H_A : \overline{X}_{\text{Lot 1}} \neq \overline{X}_{\text{Lot 2}}$. Because there is no evidence suggesting a difference in the variances (see Practice Exercise 4.9) we pool the standard deviations, obtaining an s_{pool} of

$$s_{pool} = \sqrt{\frac{(7-1)(6.451)^2 + (6-1)(7.849)^2}{7+6-2}} = 7.121 \tag{4.E.27}$$

The means for the two samples are 249.57 mg for Lot 1 and 249.00 mg for Lot 2. The value for t_{exp} is

$$t_{exp} = \frac{|249.57 - 249.00|}{7.121} \times \sqrt{\frac{7 \times 6}{7+6}} = 0.1439 \tag{4.E.28}$$

The critical value for $t(0.05, 11)$ is 2.204. Because t_{exp} is less than $t(0.05, 11)$, we retain the null hypothesis and find no evidence at $\alpha = 0.05$ for a significant difference between the means for the two lots of aspirin tablets.

Click here to return to the chapter.

Practice Exercise 4.11

Treating as Unpaired Data: The mean and standard deviation for the concentration of Zn^{2+} at the air-water interface are 0.5178 mg/L and 0.1732 mg/L respectively, and the values for the sediment-water interface are 0.4445 mg/L and 0.1418 mg/L. An *F*-test of the variances gives an F_{exp} of 1.493 and an $F(0.05, 5, 5)$ of 7.146. Because F_{exp} is smaller than $F(0.05, 5,5)$ we have no evidence at $\alpha = 0.05$ to suggest that the difference in variances is significant. Pooling the standard deviations gives an s_{pool} of 0.1582 mg/L. An unpaired *t*-test gives t_{exp} as 0.8025. Because t_{exp} is smaller than $t(0.05, 11)$, which is 2.204, we have no evidence that there is a difference in the concentration of Zn^{2+} between the two interfaces.

Treating as Paired Data: To treat as paired data we need to calculate the difference, d_i, between the concentration of Zn^{2+} at the air-water interface and at the sediment-water interface for each location.

$$d_i = ([Zn^{2+}]_{\text{air-water}})_i - ([Zn^{2+}]_{\text{sed-water}})_i \tag{4.E.29}$$

Location	1	2	3	4	5	6
d_i (mg/L)	0.015	0.028	0.067	0.121	0.102	0.107

The mean difference is 0.07333 mg/L with a standard deviation of 0.0441 mg/L. The null hypothesis and alternative hypothesis are

$$H_0 : \overline{d} = 0 \quad H_A : \overline{d} \neq 0 \tag{4.E.30}$$

and the value of t_{exp} is

$$t_{exp} = \frac{|0.07333|\sqrt{6}}{0.04410} = 4.073 \tag{4.E.31}$$

Because t_{exp} is greater than $t(0.05, 5)$, which is 2.571, we reject the null hypothesis and accept the alternative hypothesis that there is a significant difference in the concentration of Zn^{2+} between the air-water interface and the sediment-water interface.

The difference in the concentration of Zn^{2+} between locations is much larger than the difference in the concentration of Zn^{2+} between the interfaces. Because out interest is in studying differences between the interfaces, the larger standard deviation when treating the data as unpaired increases the probability of incorrectly retaining the null hypothesis, a type 2 error.

Click here to return to the chapter.

Practice Exercise 4.12

You will find small differences between the values given here for t_{exp} and F_{exp}, and for those values shown with the worked solutions in the chapter. These differences arise because Excel does not round off the results of intermediate calculations.

The two snapshots of Excel spreadsheets shown in Figure 4.29 provide solutions to these two examples.

Click here to return to the chapter.

Example 4.20

	Analyst A	Analyst B
	86.82	81.01
	87.04	86.15
	86.93	81.73
	87.01	83.19
	86.20	80.27
	87.00	83.94

F-Test Two-Sample for Variances

	Analyst B	*Analyst A*
Mean	82.715	86.8333333
Variance	4.67615	0.10246667
Observations	6	6
df	5	5
F	45.6358165	
P(F<=f) one-tail	0.0003574	
F Critical one-tail	5.05032906	

t-Test: Two-Sample Assuming Unequal Variances

	Analyst A	*Analyst B*
Mean	86.8333333	82.715
Variance	0.10246667	4.67615
Observations	6	6
Hypothesized Mean Difference	0	
df	5	
t Stat	4.6147271	
P(T<=t) one-tail	0.00288143	
t Critical one-tail	2.01504837	
P(T<=t) two-tail	0.00576286	
t Critical two-tail	2.57058183	

Example 4.21

Microbiological	Electrochemical
129.5	132.3
89.6	91.0
76.6	73.6
52.2	58.2
110.8	104.2
50.4	49.9
72.4	82.1
141.4	154.1
75.0	73.4
34.1	38.1
60.3	60.1

t-Test: Paired Two Sample for Means

	Microbiological	*Electrochemical*
Mean	81.11818182	83.36363636
Variance	1148.547636	1243.008545
Observations	11	11
Pearson Correlation	0.987510302	
Hypothesized Mean Difference	0	
df	10	
t Stat	-1.322463865	
P(T<=t) one-tail	0.107730346	
t Critical one-tail	1.812461102	
P(T<=t) two-tail	0.215460691	
t Critical two-tail	2.228138842	

Figure 4.29 Excel's output for the data in Practice Exercise 4.12.

Practice Exercise 4.13

Shown here are copies of R sessions for each problem. You will find small differences between the values given here for t_{exp} and F_{exp}, and for those values shown with the worked solutions in the chapter. These differences arise because R does not round off the results of intermediate calculations.

Example 4.20

```
> AnalystA=c(86.82, 87.04, 86.93, 87.01, 86.20, 87.00)
> AnalystB=c(81.01, 86.15, 81.73, 83.19, 80.27, 83.94)
> var.test(AnalystB, AnalystA)

        F test to compare two variances

data: AnalystB and AnalystA
F = 45.6358, num df = 5, denom df = 5, p-value = 0.0007148
alternative hypothesis: true ratio of variances is not equal to 1
95 percent confidence interval:
6.385863 326.130970
sample estimates:
ratio of variances
45.63582
```

> t.test(AnalystA, AnalystB, var.equal=FALSE)

Welch Two Sample t-test

data: AnalystA and AnalystB
t = 4.6147, df = 5.219, p-value = 0.005177
alternative hypothesis: true difference in means is not equal to 0
95 percent confidence interval:
1.852919 6.383748
sample estimates:
mean of x mean of y
86.83333 82.71500

Example 4.21

> micro=c(129.5, 89.6, 76.6, 52.2, 110.8, 50.4, 72.4, 141.4, 75.0, 34.1, 60.3)
> elect=c(132.3, 91.0, 73.6, 58.2, 104.2, 49.9, 82.1, 154.1, 73.4, 38.1, 60.1)
> t.test(micro,elect,paired=TRUE)

Paired t-test

data: micro and elect
t = -1.3225, df = 10, p-value = 0.2155
alternative hypothesis: true difference in means is not equal to 0
95 percent confidence interval:
-6.028684 1.537775
sample estimates:
mean of the differences
-2.245455

Click here to return to the chapter.

Practice Exercise 4.14

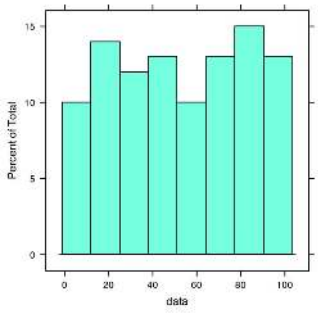
Because we are selecting a random sample of 100 members from a uniform distribution, you will see subtle differences between your plots and the plots shown as part of this answer. Here is a record of my R session and the resulting plots.

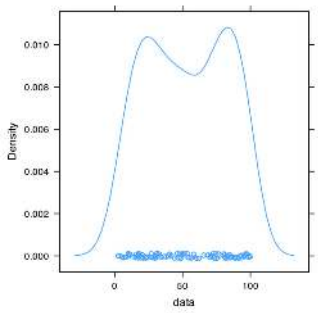
> data=runif(100, min=0, max=0)
> data
[1] 18.928795 80.423589 39.399693 23.757624 30.088554
[6] 76.622174 36.487084 62.186771 81.115515 15.726404
[11] 85.765317 53.994179 7.919424 10.125832 93.153308
[16] 38.079322 70.268597 49.879331 73.115203 99.329723
[21] 48.203305 33.093579 73.410984 75.128703 98.682127
[26] 11.433861 53.337359 81.705906 95.444703 96.843476
[31] 68.251721 40.567993 32.761695 74.635385 70.914957
[36] 96.054750 28.448719 88.580214 95.059215 20.316015
[41] 9.828515 44.172774 99.648405 85.593858 82.745774
[46] 54.963426 65.563743 87.820985 17.791443 26.417481
[51] 72.832037 5.518637 58.231329 10.213343 40.581266
[56] 6.584000 81.261052 48.534478 51.830513 17.214508
[61] 31.232099 60.545307 19.197450 60.485374 50.414960
[66] 88.908862 68.939084 92.515781 72.414388 83.195206
[71] 74.783176 10.643619 41.775788 20.464247 14.547841
[76] 89.887518 56.217573 77.606742 26.956787 29.641171
[81] 97.624246 46.406271 15.906540 23.007485 17.715668

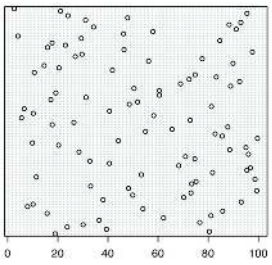
[86] 84.652814 29.379712 4.093279 46.213753 57.963604
[91] 91.160366 34.278918 88.352789 93.004412 31.055807
[96] 47.822329 24.052306 95.498610 21.089686 2.629948
> histogram(data, type="percent")
> densityplot(data)
> dotchart(data)
> bwplot(data)

Figure 4.30 shows the four plots. The histogram divides the data into eight bins, each containing between 10 and 15 members. As we expect for a uniform distribution, the histogram's overall pattern suggests that each outcome is equally probable. In interpreting the kernel density plot it is important to remember that it treats each data point as if it is from a normally distributed population (even though, in this case, the underlying population is uniform). Although the plot appears to suggest that there are two normally distributed populations, the individual results shown at the bottom of the plot provide further evidence for a uniform distribution. The dot chart shows no trend along the *y*-axis, indicating that the individual members of this sample were drawn randomly from the population. The distribution along the *x*-axis also shows no pattern, as expected for a uniform distribution, Finally, the box plot shows no evidence of outliers.

Click here to return to the chapter.







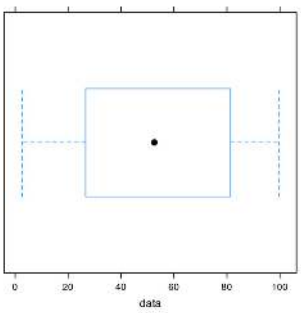


Figure 4.30 Plots generated using R to solve Practice Exercise 4.13.

Contributors and Attributions

- David Harvey (DePauw University)

4.E: Evaluating Analytical Data (Exercises) is shared under a CC BY-NC-SA 4.0 license and was authored, remixed, and/or curated by LibreTexts.

4.S: Evaluating Analytical Data (Summary)

4.S: Evaluating Analytical Data (Summary)

4.S: Evaluating Analytical Data (Summary) is shared under a CC BY-NC-SA 4.0 license and was authored, remixed, and/or curated by LibreTexts.

CHAPTER OVERVIEW

5: Standardizing Analytical Methods

The American Chemical Society's Committee on Environmental Improvement defines standardization as the process of determining the relationship between the signal and the amount of analyte in a sample.[1] In Chapter 3 we defined this relationship as

$$S_{\text{total}} = k_{\text{A}} n_{\text{A}} + S_{\text{reag}} \quad \text{or} \quad S_{\text{total}} = k_{\text{A}} C_{\text{A}} + S_{\text{reag}} \tag{5.1}$$

where S_{total} is the signal, n_A is the moles of analyte, C_A is the analyte's concentration, k_A is the method's sensitivity for the analyte, and S_{reag} is the contribution to S_{total} from sources other than the sample. To standardize a method we must determine values for k_A and S_{reag}. Strategies for accomplishing this are the subject of this chapter.

Topic hierarchy

5.1: Analytical Standards
5.2: Calibrating the Signal
5.3: Determining the Sensitivity
5.4: Linear Regression and Calibration Curves
5.5: Blank Corrections
5.6: Using Excel and R for a Regression Analysis
5.E: Standardizing Analytical Methods (Exercises)
5.S: Standardizing Analytical Methods (Summary)

Thumbnail: Illustration showing the evaluation of a linear regression in which we assume that all uncertainty is the result of indeterminate errors affecting y. The points in blue, y_i, are the original data and the points in red, $\hat{y}_i$, are the predicted values from the regression equation, $\hat{y} = b_0 + b_1 x$. The smaller the total residual error (equation 5.16), the better the fit of the straight-line to the data

Contributors

- David Harvey (DePauw University)

5: Standardizing Analytical Methods is shared under a CC BY-NC-SA 4.0 license and was authored, remixed, and/or curated by LibreTexts.

5.1: Analytical Standards

5.1: Analytical Standards

5.1: Analytical Standards is shared under a CC BY-NC-SA 4.0 license and was authored, remixed, and/or curated by LibreTexts.

5.2: Calibrating the Signal

5.2: Calibrating the Signal

5.2: Calibrating the Signal is shared under a CC BY-NC-SA 4.0 license and was authored, remixed, and/or curated by LibreTexts.

5.3: Determining the Sensitivity

5.3: Determining the Sensitivity

5.3: Determining the Sensitivity is shared under a CC BY-NC-SA 4.0 license and was authored, remixed, and/or curated by LibreTexts.

5.4: Linear Regression and Calibration Curves

5.4: Linear Regression and Calibration Curves

5.4: Linear Regression and Calibration Curves is shared under a CC BY-NC-SA 4.0 license and was authored, remixed, and/or curated by LibreTexts.

5.5: Blank Corrections

5.5: Blank Corrections

5.5: Blank Corrections is shared under a CC BY-NC-SA 4.0 license and was authored, remixed, and/or curated by LibreTexts.

5.6: Using Excel and R for a Regression Analysis

5.6: Using Excel and R for a Regression Analysis

5.6: Using Excel and R for a Regression Analysis is shared under a CC BY-NC-SA 4.0 license and was authored, remixed, and/or curated by LibreTexts.

5.E: Standardizing Analytical Methods (Exercises)

1. Describe how you would use a serial dilution to prepare 100 mL each of a series of standards with concentrations of 1.00×10^{-5}, 1.00×10^{-4}, 1.00×10^{-3}, and 1.00×10^{-2} M from a 0.100 M stock solution. Calculate the uncertainty for each solution using a propagation of uncertainty, and compare to the uncertainty if you were to prepare each solution by a single dilution of the stock solution. You will find tolerances for different types of volumetric glassware and digital pipets in Table 4.2 and Table 4.3. Assume that the uncertainty in the stock solution's molarity is ±0.002.

2. Three replicate determinations of S_{total} for a standard solution that is 10.0 ppm in analyte give values of 0.163, 0.157, and 0.161 (arbitrary units). The signal for the reagent blank is 0.002. Calculate the concentration of analyte in a sample with a signal of 0.118.

3. A 10.00-g sample containing an analyte is transferred to a 250-mL volumetric flask and diluted to volume. When a 10.00 mL aliquot of the resulting solution is diluted to 25.00 mL it gives signal of 0.235 (arbitrary units). A second 10.00-mL portion of the solution is spiked with 10.00 mL of a 1.00-ppm standard solution of the analyte and diluted to 25.00 mL. The signal for the spiked sample is 0.502. Calculate the weight percent of analyte in the original sample.

4. A 50.00 mL sample containing an analyte gives a signal of 11.5 (arbitrary units). A second 50 mL aliquot of the sample, which is spiked with 1.00 mL of a 10.0-ppm standard solution of the analyte, gives a signal of 23.1. What is the analyte's concentration in the original sample?

5. An appropriate standard additions calibration curve based on equation 5.10 places $S_{spike}\times(V_o + V_{std})$ on the *y*-axis and $C_{std}\times V_{std}$ on the *x*-axis. Clearly explain why you can not plot S_{spike} on the *y*-axis and $C_{std}\times[V_{std}/(V_o + V_{std})]$ on the *x*-axis. In addition, derive equations for the slope and *y*-intercept, and explain how you can determine the amount of analyte in a sample from the calibration curve.

6. A standard sample contains 10.0 mg/L of analyte and 15.0 mg/L of internal standard. Analysis of the sample gives signals for the analyte and internal standard of 0.155 and 0.233 (arbitrary units), respectively. Sufficient internal standard is added to a sample to make its concentration 15.0 mg/L Analysis of the sample yields signals for the analyte and internal standard of 0.274 and 0.198, respectively. Report the analyte's concentration in the sample.

7. For each of the pair of calibration curves shown in Figure 5.26, select the calibration curve using the more appropriate set of standards. Briefly explain the reasons for your selections. The scales for the *x*-axis and *y*-axis are the same for each pair.

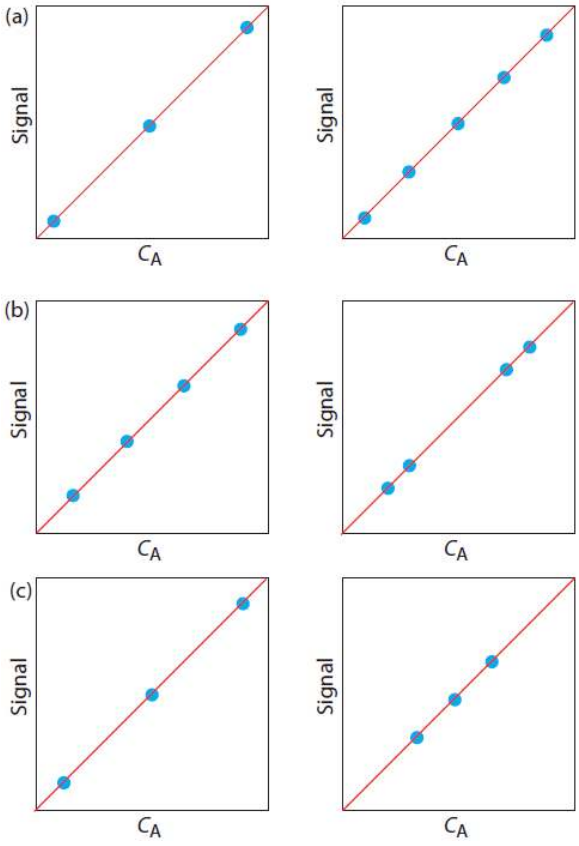


Figure 5.26 Calibration curves to accompany Problem 7.

8. The following data are for a series of external standards of Cd^{2+} buffered to a pH of 4.6.[14]

$[Cd^{2+}]$ (nM)	15.4	30.4	44.9	59.0	72.7	86.0
S_{total}(nA)	4.8	11.4	18.2	25.6	32.3	37.7

(a) Use a linear regression to determine the standardization relationship and report confidence intervals for the slope and the *y*-intercept.

(b) Construct a plot of the residuals and comment on their significance.

At a pH of 3.7 the following data were recorded for the same set of external standards.

$[Cd^{2+}]$ (nM)	15.4	30.4	44.9	59.0	72.7	86.0
S_{total} (nA)	15.0	42.7	58.5	77.0	101	118

(c) How much more or less sensitive is this method at the lower pH?

(d) A single sample is buffered to a pH of 3.7 and analyzed for cadmium, yielding a signal of 66.3. Report the concentration of Cd^{2+} in the sample and its 95% confidence interval.

9. To determine the concentration of analyte in a sample, a standard additions was performed. A 5.00-mL portion of sample was analyzed and then successive 0.10-mL spikes of a 600.0-mg/L standard of the analyte were added, analyzing after each spike. The following table shows the results of this analysis.

V_{spike} (mL)	0.00	0.10	0.20	0.30
S_{total} (arbitrary units)	0.119	0.231	0.339	0.442

Construct an appropriate standard additions calibration curve and use a linear regression analysis to determine the concentration of analyte in the original sample and its 95% confidence interval.

10. Troost and Olavsesn investigated the application of an internal standardization to the quantitative analysis of polynuclear aromatic hydrocarbons.[15] The following results were obtained for the analysis of phenanthrene using isotopically labeled phenanthrene as an internal standard. Each solution was analyzed twice.

C_A/C_{IS}	0.50	1.25	2.00	3.00	4.00
S_A/S_{IS}	0.514 0.522	0.993 1.024	1.486 1.471	2.044 20.80	2.342 2.550

(a) Determine the standardization relationship using a linear regression, and report confidence intervals for the slope and the *y*-intercept. Average the replicate signals for each standard before completing the linear regression analysis.

(b) Based on your results explain why the authors concluded that the internal standardization was inappropriate.

11. In Chapter 4 we used a paired *t*-test to compare two analytical methods used to independently analyze a series of samples of variable composition. An alternative approach is to plot the results for one method versus the results for the other method. If the two methods yield identical results, then the plot should have an expected slope, β_1, of 1.00 and an expected *y*-intercept, β_0, of 0.0. We can use a *t*-test to compare the slope and the *y*-intercept from a linear regression to the expected values. The appropriate test statistic for the *y*-intercept is found by rearranging equation 5.23.

$$t_{exp} = \frac{|\beta_0 - b_0|}{s_{b_0}} = \frac{|b_0|}{s_{b_0}} \tag{5.E.1}$$

Rearranging equation 5.22 gives the test statistic for the slope.

$$t_{exp} = \frac{|\beta_1 - b_1|}{s_{b_1}} = \frac{|1.00 - b_1|}{s_{b_1}} \tag{5.E.2}$$

Reevaluate the data in problem 25 from Chapter 4 using the same significance level as in the original problem.

Note

Although this is a common approach for comparing two analytical methods, it does violate one of the requirements for an unweighted linear regression—that indeterminate errors affect *y* only. Because indeterminate errors affect both analytical methods, the result of unweighted linear regression is biased. More specifically, the regression underestimates the slope, b_1, and overestimates the y-intercept, b_0. We can minimize the effect of this bias by placing the more precise analytical method on the *x*-axis, by using more samples to increase the degrees of freedom, and by using samples that uniformly cover the range of concentrations.

For more information, see Miller, J. C.; Miller, J. N. *Statistics for Analytical Chemistry*, 3rd ed. Ellis Horwood PTR Prentice-Hall: New York, 1993. Alternative approaches are found in Hartman, C.; Smeyers-Verbeke, J.; Penninckx, W.; Massart, D. L. *Anal. Chim. Acta* **1997**, *338*, 19–40, and Zwanziger, H. W.; Sârbu, C. *Anal. Chem.* **1998**, *70*, 1277–1280.

12. Consider the following three data sets, each containing values of y for the same values of x.

	Data Set 1	Data Set 2	Data Set 3
x	y_1	y_2	y_3
10.00	8.04	9.14	7.46
8.00	6.95	8.14	6.77
13.00	7.58	8.74	12.74
9.00	8.81	8.77	7.11
11.00	8.33	9.26	7.81
14.00	9.96	8.10	8.84
6.00	7.24	6.13	6.08
4.00	4.26	3.10	5.39
12.00	10.84	9.13	8.15
7.00	4.82	7.26	6.42
5.00	5.68	4.74	5.73

(a) An unweighted linear regression analysis for the three data sets gives nearly identical results. To three significant figures, each data set has a slope of 0.500 and a y-intercept of 3.00. The standard deviations in the slope and the y-intercept are 0.118 and 1.125 for each data set. All three standard deviations about the regression are 1.24, and all three data regression lines have a correlation coefficients of 0.816. Based on these results for a linear regression analysis, comment on the similarity of the data sets.

(b) Complete a linear regression analysis for each data set and verify that the results from part (a) are correct. Construct a residual plot for each data set. Do these plots change your conclusion from part (a)? Explain.

(c) Plot each data set along with the regression line and comment on your results.

(d) Data set 3 appears to contain an outlier. Remove this apparent outlier and reanalyze the data using a linear regression. Comment on your result.

(e) Briefly comment on the importance of visually examining your data.

13. Fanke and co-workers evaluated a standard additions method for a voltammetric determination of Tl.[16] A summary of their results is tabulated in the following table.

ppm Tl added	Instrument Response (μA)						
0.000	2.53	2.50	2.70	2.63	2.70	2.80	2.52
0.387	8.42	7.96	8.54	8.18	7.70	8.34	7.98
1.851	29.65	28.70	29.05	28.30	29.20	29.95	28.95
5.734	84.8	85.6	86.0	85.2	84.2	86.4	87.8

Use a weighted linear regression to determine the standardization relationship for this data.

5.7.3 Solutions to Practice Exercises

Practice Exercise 5.1

Substituting the sample's absorbance into the calibration equation and solving for C_A give

$$S_{samp} = 0.114 = 29.59\ M^{-1} \times C_A + 0.015 \tag{5.E.3}$$

$$C_A = 3.35 \times 10^{-3}\ M \tag{5.E.4}$$

For the one-point standardization, we first solve for k_A

$$k_A = \frac{S_{std}}{C_{std}} = \frac{0.0931}{3.16 \times 10^{-3}\ M} = 29.46\ M^{-1} \tag{5.E.5}$$

and then use this value of k_A to solve for C_A.

$$C_A = \frac{S_{samp}}{k_A} = \frac{0.114}{29.46\ M^{-1}} = 3.87 \times 10^{-3}\ M \tag{5.E.6}$$

When using multiple standards, the indeterminate errors affecting the signal for one standard are partially compensated for by the indeterminate errors affecting the other standards. The standard selected for the one-point standardization has a signal that is smaller than that predicted by the regression equation, which underestimates k_A and overestimates C_A.

Click here to return to the chapter.

Practice Exercise 5.2

We begin with equation 5.8

$$S_{spike} = k_A \left(C_A \frac{V_o}{V_f} + C_{std} \frac{V_{std}}{V_f} \right) \tag{5.E.7}$$

rewriting it as

$$0 = \frac{k_A C_A V_o}{V_f} + k_A \times \left\{ C_{std} \frac{V_{std}}{V_f} \right\} \tag{5.E.8}$$

which is in the form of the linear equation

$$Y = y\text{-intercept} + \text{slope} \times X \tag{5.E.9}$$

where Y is S_{spike} and X is $C_{std} \times V_{std}/V_f$. The slope of the line, therefore, is k_A, and the y-intercept is $k_A C_A V_o/V_f$. The x-intercept is the value of X when Y is zero, or

$$0 = \frac{k_A C_A V_o}{V_f} + k_A \times \{x\text{-intercept}\} \tag{5.E.10}$$

$$x\text{-intercept} = -\frac{\frac{k_A C_A V_o}{V_f}}{k_A} = -\frac{C_A V_o}{V_f} \tag{5.E.11}$$

Click here to return to the chapter.

Practice Exercise 5.3

Using the calibration equation from Figure 5.7a, we find that the x-intercept is

$$x\text{-intercept} = -\frac{0.1478}{0.0854\ mL^{-1}} = -1.731\ mL \tag{5.E.12}$$

Plugging this into the equation for the x-intercept and solving for C_A gives the concentration of Mn^{2+} as

$$x\text{-intercept} = -3.478\ mL = -\frac{C_A \times 25.00\ mL}{100.6\ mg/L} = 6.96\ mg/L \tag{5.E.13}$$

For Figure 7b, the x-intercept is

$$x\text{-intercept} = -\frac{0.1478}{0.0425\ \text{mL}^{-1}} = -3.478\ \text{mL} \tag{5.E.14}$$

and the concentration of Mn^{2+} is

$$x\text{-intercept} = -3.478\ \text{mL} = -\frac{C_A \times 25.00\ \text{mL}}{50.00\ \text{L}} = 6.96\ \text{mg/L} \tag{5.E.15}$$

Click here to return to the chapter.

Practice Exercise 5.4

We begin by setting up a table to help us organize the calculation.

x_i	y_i	$x_i y_i$	x_i^2
0.000	0.00	0.000	0.000
1.55×10^{-3}	0.050	7.750×10^{-5}	2.403×10^{-6}
3.16×10^{-3}	0.093	2.939×10^{-4}	9.986×10^{-6}
4.74×10^{-3}	0.143	6.778×10^{-4}	2.247×10^{-5}
6.34×10^{-3}	0.188	1.192×10^{-3}	4.020×10^{-5}
7.92×10^{-3}	0.236	1.869×10^{-3}	6.273×10^{-5}

Adding the values in each column gives

$$\sum_i x_i = 2.371 \times 10^{-2} \quad \sum_i y_i = 0.710 \tag{5.E.16}$$

$$\sum_i x_i y_i = 4.110 \times 10^{-3} \quad \sum_i x_i^2 = 1.278 \times 10^{-4} \tag{5.E.17}$$

Substituting these values into equation 5.17 and equation 5.18, we find that the slope and the y-intercept are

$$b_1 = \frac{6 \times (4.110 \times 10^{-3}) - (2.371 \times 10^{-2}) \times (0.710)}{(6 \times 1.378 \times 10^{-4}) - (2.371 \times 10^{-2})^2} = 29.57 \tag{5.E.18}$$

$$b_0 = \frac{0.710 - 29.57 \times (2.371 \times 10^{-2})}{6} = 0.0015 \tag{5.E.19}$$

The regression equation is

$$S_{\text{std}} = 29.57 \times C_{\text{std}} + 0.0015 \tag{5.E.20}$$

To calculate the 95% confidence intervals, we first need to determine the standard deviation about the regression. The following table will help us organize the calculation.

x_i	y_i	$\hat{y}_i$	$(y_i - \hat{y}_i)^2$
0.000	0.00	0.0015	2.250×10^{-6}
1.55×10^{-3}	0.050	0.0473	7.110×10^{-6}
3.16×10^{-3}	0.093	0.0949	3.768×10^{-6}
4.74×10^{-3}	0.143	0.1417	1.791×10^{-6}
6.34×10^{-3}	0.188	0.1890	9.483×10^{-7}
7.92×10^{-3}	0.236	0.2357	9.339×10^{-8}

Adding together the data in the last column gives the numerator of equation 5.19 as 1.596×10^{-5}. The standard deviation about the regression, therefore, is

$$s_r = \sqrt{\frac{1.596 \times 10^{-6}}{6-2}} = 1.997 \times 10^{-3} \tag{5.E.21}$$

Next, we need to calculate the standard deviations for the slope and the *y*-intercept using equation 5.20 and equation 5.21.

$$s_{b_1} = \sqrt{\frac{6 \times (1.997 \times 10^{-3})^2}{6 \times (1.378 \times 10^{-4}) - (2.371 \times 10^{-2})^2}} = 0.3007 \tag{5.E.22}$$

$$s_{b_0} = \sqrt{\frac{(1.997 \times 10^{-3})^2 \times (1.378 \times 10^{-4})}{6 \times (1.378 \times 10^{-4}) - (2.371 \times 10^{-2})^2}} = 1.441 \times 10^{-3} \tag{5.E.23}$$

The 95% confidence intervals are

$$\beta_1 = b_1 \pm ts_{b_1} = 29.57 \pm (2.78 \times 0.3007) = 29.57\ \text{M}^{-1} \pm 0.85\ \text{M}^{-1} \tag{5.E.24}$$

$$\beta_0 = b_0 \pm ts_{b_0} = 0.0015 \pm \{2.78 \times (1.441 \times 10^{-3})\} = 0.0015 \pm 0.0040 \tag{5.E.25}$$

With an average S_{samp} of 0.114, the concentration of analyte, C_{A}, is

$$C_{\text{A}} = \frac{S_{\text{samp}} - b_0}{b_1} = \frac{0.114 - 0.0015}{29.57\ \text{M}^{-1}} = 3.80 \times 10^{-3}\ \text{M} \tag{5.E.26}$$

The standard deviation in C_{A} is

$$s_{C_{\text{A}}} = \frac{1.997 \times 10^{-3}}{29.57} \sqrt{\frac{1}{3} + \frac{1}{6} + \frac{(0.114 - 0.1183)^2}{(29.57)^2 \times (4.408 \times 10^{-5})}} = 4.778 \times 10^{-5} \tag{5.E.27}$$

and the 95% confidence interval is

$$\mu_{C_{\text{A}}} = C_{\text{A}} \pm ts_{C_{\text{A}}} = 3.80 \times 10^{-3} \pm \{2.78 \times (4.778 \times 10^{-5})\} \tag{5.E.28}$$

$$= 3.80 \times 10^{-3}\ \text{M} \pm 0.13 \times 10^{-3}\ \text{M} \tag{5.E.29}$$

Click here to return to the chapter.

Practice Exercise 5.5

To create a residual plot, we need to calculate the residual error for each standard. The following table contains the relevant information.

x_i	y_i	$\hat{y}_i$	$y_i - \hat{y}_i$
0.000	0.00	0.0015	-0.0015
1.55×10^{-3}	0.050	0.0473	0.0027
3.16×10^{-3}	0.093	0.0949	-0.0019
4.74×10^{-3}	0.143	0.1417	0.0013
6.34×10^{-3}	0.188	0.1890	-0.0010
7.92×10^{-3}	0.236	0.2357	0.0003

Figure 5.27 shows a plot of the resulting residual errors is shown here. The residual errors appear random and do not show any significant dependence on the analyte's concentration. Taken together, these observations suggest that our regression model is appropriate.

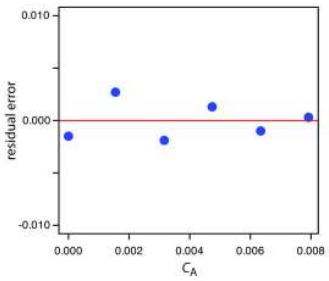


Figure 5.27 Plot of the residual errors for the data in Practice Exercise 5.5.

Click here to return to the chapter.

Practice Exercise 5.6

Begin by entering the data into an Excel spreadsheet, following the format shown in Figure 5.15. Because Excel's Data Analysis tools provide most of the information we need, we will use it here. The resulting output, which is shown in Figure 5.28, contains the slope and the y-intercept, along with their respective 95% confidence intervals. Excel does not provide a function for calculating the uncertainty in the analyte's concentration, C_A, given the signal for a sample, S_{samp}. You must complete these calculations by hand. With an S_{samp}. of 0.114, C_A

$$C_A = \frac{S_{samp} - b_0}{b_1} = \frac{0.114 - 0.0014}{29.59\ M^{-1}} = 3.80 \times 10^{-3}\ M \tag{5.E.30}$$

The standard deviation in C_A is

$$s_{C_A} = \frac{1.996 \times 10^{-3}}{29.59}\sqrt{\frac{1}{3} + \frac{1}{6} + \frac{(0.114 - 0.1183)^2}{(29.59)^2 \times (4.408 \times 10^{-5})}} = 4.772 \times 10^{-5} \tag{5.E.31}$$

and the 95% confidence interval is

$$\mu_{C_A} = C_A \pm t s_{C_A} = 3.80 \times 10^{-3} \pm \{2.78 \times (4.772 \times 10^{-5})\} \tag{5.E.32}$$

$$= 3.80 \times 10^{-3}\ M \pm 0.13 \times 10^{-3}\ M \tag{5.E.33}$$

SUMMARY OUTPUT

Regression Statistics	
Multiple R	0.99979366
R Square	0.99958737
Adjusted R Sq	0.99948421
Standard Erroi	0.00199602
Observations	6

ANOVA

	df	*SS*	*MS*	*F*	*Significance F*
Regression	1	0.0386054	0.0386054	9689.9103	6.3858E-08
Residual	4	1.5936E-05	3.9841E-06		
Total	5	0.03862133			

	Coefficients	*Standard Error*	*t Stat*	*P-value*	*Lower 95%*	*Upper 95%*	*Lower 95.0%*	*Upper 95.0%*
Intercept	0.00139272	0.00144059	0.96677158	0.38840479	-0.00260699	0.00539242	-0.00260699	0.00539242
Cstd	29.5927329	0.30062507	98.437342	6.3858E-08	28.7580639	30.4274019	28.7580639	30.4274019

Figure 5.28 Excel's summary of the regression results for Practice Exercise 5.6.

Click here to return to the chapter.

Practice Exercise 5.7

Figure 5.29 shows an R session for this problem, including loading the *chemCal* package, creating objects to hold the values for C_{std}, S_{std}, and *Ssamp*. Note that for *Ssamp*, we do not have the actual values for the three replicate measurements. In place of the actual measurements, we just enter the average signal three times. This is okay because the calculation depends on the average signal and the number of replicates, and not on the individual measurements.

```
> library("chemCal")
> conc=c(0, 1.55e-3, 3.16e-3, 4.74e-3, 6.34e-3, 7.92e-3)
> signal=c(0, 0.050, 0.093, 0.143, 0.188, 0.236)
> model=lm(signal~conc)
> summary(model)

Call:
lm(formula = signal ~ conc)

Residuals:
      1           2           3           4           5           6
-0.0013927  0.0027385 -0.0019058  0.0013377 -0.0010106  0.0002328

Coefficients:
             Estimate   Std. Error  t value  Pr(>|t|)
(Intercept)  0.001393   0.001441    0.967    0.388
conc         29.592733  0.300625    98.437   6.39e-08 ***
---
Signif. codes:  0 '***' 0.001 '**' 0.01 '*' 0.05 '.' 0.1 ' ' 1

Residual standard error: 0.001996 on 4 degrees of freedom
Multiple R-Squared: 0.9996,   Adjusted R-squared: 0.9995
F-statistic:  9690 on 1 and 4 DF,  p-value: 6.386e-08

> samp=c(0.114, 0.114, 0.114)
> inverse.predict(model,samp,alpha=0.05)
$Prediction
[1] 0.003805234

$`Standard Error`
[1] 4.771723e-05

$Confidence
[1] 0.0001324843

$`Confidence Limits`
[1] 0.003672750 0.003937719
```

Figure 5.29 R session for completing Practice Exercise 5.7.

Click here to return to the chapter.

References

1. ACS Committee on Environmental Improvement "Guidelines for Data Acquisition and Data Quality Evaluation in Environmental Chemistry," *Anal. Chem.* **1980**, *52*, 2242–2249.
2. (a) Smith, B. W.; Parsons, M. L. *J. Chem. Educ*. **1973**, *50*, 679–681; (b) Moody, J. R.; Greenburg, P. R.; Pratt, K. W.; Rains, T. C. *Anal. Chem.* **1988**, *60*, 1203A–1218A.
3. Committee on Analytical Reagents, *Reagent Chemicals*, 8th ed., American Chemical Society: Washington, D. C., 1993.
4. Ebel, S. *Fresenius J. Anal. Chem.* **1992**, *342*, 769.
5. Cardone, M. J.; Palmero, P. J.; Sybrandt, L. B. *Anal. Chem.* **1980**, *52*, 1187–1191.
6. See, for example, Draper, N. R.; Smith, H. Applied Regression Analysis, 3rd ed.; Wiley: New York, 1998.
7. (a) Miller, J. N. *Analyst* **1991**, *116*, 3–14; (b) Sharaf, M. A.; Illman, D. L.; Kowalski, B. R. *Chemometrics*, Wiley-Interscience: New York, 1986, pp. 126-127; (c) Analytical Methods Committee "Uncertainties in concentrations estimated from calibration experiments," AMC Technical Brief, March 2006 (http://www.rsc.org/images/Brief22_tcm18-51117.pdf)
8. Bonate, P. J. *Anal. Chem.* **1993**, *65*, 1367–1372.
9. See, for example, Analytical Methods Committee, "Fitting a linear functional relationship to data with error on both variable," AMC Technical Brief, March, 2002 (http://www.rsc.org/images/brief10_tcm18-25920.pdf).

10. For details about curvilinear regression, see (a) Sharaf, M. A.; Illman, D. L.; Kowalski, B. R. *Chemometrics*, Wiley-Interscience: New York, 1986; (b) Deming, S. N.; Morgan, S. L. *Experimental Design: A Chemometric Approach*, Elsevier: Amsterdam, 1987.
11. Beebe, K. R.; Kowalski, B. R. *Anal. Chem.* **1987**, *59*, 1007A–1017A.
12. Cardone, M. J. *Anal. Chem.* **1986**, *58*, 433–438.
13. Cardone, M. J. *Anal. Chem.* **1986**, *58*, 438–445.
14. Wojciechowski, M.; Balcerzak, J. *Anal. Chim. Acta* **1991**, *249*, 433–445.
15. Troost, J. R.; Olavesen, E. Y. *Anal. Chem.* **1996**, *68*, 708–711.
16. Franke, J. P.; de Zeeuw, R. A.; Hakkert, R. *Anal. Chem.* **1978**, *50*, 1374–1380.

Contributors and Attributions

David Harvey (DePauw University)

5.E: Standardizing Analytical Methods (Exercises) is shared under a CC BY-NC-SA 4.0 license and was authored, remixed, and/or curated by LibreTexts.

5.S: Standardizing Analytical Methods (Summary)

5.S: Standardizing Analytical Methods (Summary)

5.S: Standardizing Analytical Methods (Summary) is shared under a CC BY-NC-SA 4.0 license and was authored, remixed, and/or curated by LibreTexts.

CHAPTER OVERVIEW

6: Equilibrium Chemistry

Regardless of the problem on which an analytical chemist is working, its solution requires a knowledge of chemistry and the ability to apply that knowledge. For example, an analytical chemist studying the effect of pollution on spruce trees needs to know, or know where to find, the chemical differences between *p*-hydroxybenzoic acid and *p*-hydroxyacetophenone, two common phenols found in the needles of spruce trees. Your ability to "think as a chemist" is a product of your experience in the classroom and in the laboratory. The material in this text assumes your familiarity with topics from earlier courses. Because of its importance to analytical chemistry, this chapter provides a review of equilibrium chemistry. Much of the material in this chapter should be familiar to you, although some topics—ladder diagrams and activity, for example—afford you with new ways to look at equilibrium chemistry.

6.1: Reversible Reactions and Chemical Equilibria
6.2: Thermodynamics and Equilibrium Chemistry
6.3: Manipulating Equilibrium Constants
6.4: Equilibrium Constants for Chemical Reactions
6.5: Le Châtelier's Principle
6.6: Ladder Diagrams
6.7: Solving Equilibrium Problems
6.8: Buffer Solutions
6.9: Activity Effects
6.10: Using Excel and R to Solve Equilibrium Problems
6.11: Some Final Thoughts on Equilibrium Calculations
6.E: Equilibrium Chemistry (Exercises)
6.S: Equilibrium Chemistry (Summary)

Thumbnail: *The* $N_2O_{(g)} \rightleftharpoons 2NO_{2(g)}$ *system at Different Temperatures. Nitrogen dioxide (*NO_2*) gas converts to the colorless gas dinitrogen tetroxide (*N_2O_4*) at low temperatures, and converts back to* NO_2 *at higher temperatures. The bottles in this photograph contain equal amounts of gas at different temperatures. Figure used with permission from Wikipedia (CC BY-SA 3.0).*

Contributors

- David Harvey (DePauw University)

6: Equilibrium Chemistry is shared under a CC BY-NC-SA 4.0 license and was authored, remixed, and/or curated by LibreTexts.

6.1: Reversible Reactions and Chemical Equilibria

6.01: Reversible Reactions and Chemical Equilibria

6.1: Reversible Reactions and Chemical Equilibria is shared under a CC BY-NC-SA 4.0 license and was authored, remixed, and/or curated by LibreTexts.

6.2: Thermodynamics and Equilibrium Chemistry

6.02: Thermodynamics and Equilibrium Chemistry

6.2: Thermodynamics and Equilibrium Chemistry is shared under a CC BY-NC-SA 4.0 license and was authored, remixed, and/or curated by LibreTexts.

6.3: Manipulating Equilibrium Constants

6.03: Manipulating Equilibrium Constants

6.3: Manipulating Equilibrium Constants is shared under a CC BY-NC-SA 4.0 license and was authored, remixed, and/or curated by LibreTexts.

6.4: Equilibrium Constants for Chemical Reactions

6.04: Equilibrium Constants for Chemical Reactions

6.4: Equilibrium Constants for Chemical Reactions is shared under a CC BY-NC-SA 4.0 license and was authored, remixed, and/or curated by LibreTexts.

6.5: Le Châtelier’s Principle

6.05: Le Châtelier’s Principle

6.5: Le Châtelier’s Principle is shared under a CC BY-NC-SA 4.0 license and was authored, remixed, and/or curated by LibreTexts.

6.6: Ladder Diagrams

6.06: Ladder Diagrams

6.6: Ladder Diagrams is shared under a CC BY-NC-SA 4.0 license and was authored, remixed, and/or curated by LibreTexts.

6.7: Solving Equilibrium Problems

6.07: Solving Equilibrium Problems

6.7: Solving Equilibrium Problems is shared under a CC BY-NC-SA 4.0 license and was authored, remixed, and/or curated by LibreTexts.

6.8: Buffer Solutions

6.08: Buffer Solutions

6.8: Buffer Solutions is shared under a CC BY-NC-SA 4.0 license and was authored, remixed, and/or curated by LibreTexts.

6.9: Activity Effects

6.09: Activity Effects

6.9: Activity Effects is shared under a CC BY-NC-SA 4.0 license and was authored, remixed, and/or curated by LibreTexts.

6.10: Using Excel and R to Solve Equilibrium Problems

6.10: Using Excel and R to Solve Equilibrium Problems

6.10: Using Excel and R to Solve Equilibrium Problems is shared under a CC BY-NC-SA 4.0 license and was authored, remixed, and/or curated by LibreTexts.

6.11: Some Final Thoughts on Equilibrium Calculations

6.11: Some Final Thoughts on Equilibrium Calculations

6.11: Some Final Thoughts on Equilibrium Calculations is shared under a CC BY-NC-SA 4.0 license and was authored, remixed, and/or curated by LibreTexts.

6.E: Equilibrium Chemistry (Exercises)

Most of the problems that follow require one or more equilibrium constants or standard state potentials. For your convenience, here are hyperlinks to the appendices containing these constants

- Appendix 10: Solubility Products
- Appendix 11: Acid Dissociation Constants
- Appendix 12: Metal-Ligand Formation Constants
- Appendix 13: Standard State Reduction Potentials

1. Write equilibrium constant expressions for the following reactions. What is the value for each reaction's equilibrium constant?

a. $NH_3(aq) + HCl(aq) \leftrightharpoons NH_4^+(aq) + Cl^-(aq)$
b. $PbI_2(s) + S^{2-}(aq) \leftrightharpoons PbS(s) + 2I^-(aq)$
c. $Cd(EDTA)^{2-}(aq) + 4CN^-(aq) \leftrightharpoons Cd(CN)_4^{2-}(aq) + EDTA^{4-}(aq)$
d. $AgCl(s) + 2NH_3(aq) \leftrightharpoons Ag(NH_3)_2^+(aq) + Cl^-(aq)$
e. $BaCO_3(s) + H_3O^+(aq) \leftrightharpoons Ba^{2+}(aq) + H_2CO_3(aq) + H_2O(l)$

2. Using a ladder diagram, explain why the first reaction is favorable and the second reaction is unfavorable.

$$\mathbf{H_3PO_4}(aq) + \mathbf{F^-}(aq) \rightleftharpoons \mathbf{HF}(aq) + \mathbf{H_2PO_4^-}(aq) \tag{6.E.1}$$

$$\mathbf{H_3PO_4}(aq) + \mathbf{2F^-}(aq) \rightleftharpoons \mathbf{2HF}(aq) + \mathbf{HPO_4^{2-}}(aq) \tag{6.E.2}$$

Determine the equilibrium constant for these reactions and verify that they are consistent with your ladder diagram.

3. Calculate the potential for the following redox reaction for a solution in which $[Fe^{3+}]$ = 0.050 M, $[Fe^{2+}]$ = 0.030 M, $[Sn^{2+}]$ = 0.015 M and $[Sn^{4+}]$ = 0.020 M.

$$\mathbf{2Fe^{3+}}(aq) + \mathbf{Sn^{2+}}(aq) \rightleftharpoons \mathbf{Sn^{4+}}(aq) + \mathbf{2Fe^{2+}}(aq) \tag{6.E.3}$$

4. Calculate the standard state potential and the equilibrium constant for each of the following redox reactions. Assume that $[H_3O^+]$ is 1.0 M for acidic solutions, and that $[OH^-]$ is 1.0 M for basic solutions.

a. $MnO_4^-(aq) + H_2SO_3(aq) \leftrightharpoons Mn^{2+}(aq) + SO_4^{2-}$ acidic solution
b. $IO_3^-(aq) + I^-(aq) \leftrightharpoons I_2(s)$ acidic solution
c. $ClO^-(aq) + I^-(aq) \leftrightharpoons IO_3^-(aq) + Cl^-(aq)$ basic solution

> These redox reactions in this problem are not balanced. You will need to balance the reactions before calculating their standard state potentials. Although you may recall how to do this from another course, there is a much easier approach that you can use here. Identify the oxidizing agent and the reducing agent and divide the reaction into two unbalanced half-reactions. Using Appendix 13, find the appropriate balanced half-reactions. Add the two half-reactions together and simplify the stoichiometry to arrive at the balanced redox reaction.
>
> As an example, in (a) the oxidizing agent is MnO_4^- and its unbalanced half-reaction is
>
> $$\mathbf{MnO_4^-}(aq) + \mathbf{5}e^- \rightleftharpoons \mathbf{Mn^{2+}}(aq) \tag{6.E.4}$$
>
> The corresponding balanced half-reaction from Appendix 13 is
>
> $$\mathbf{MnO_4^-}(aq) + \mathbf{8H^+}(aq) + \mathbf{5}e^- \rightleftharpoons \mathbf{Mn^{2+}}(aq) + \mathbf{4H_2O}(l) \tag{6.E.5}$$

5. One analytical method for determining the concentration of sulfur is to oxidize it to SO_4^{2-} and then precipitate it as $BaSO_4$ by adding $BaCl_2$. The mass of the resulting precipitate is proportional to the amount of sulfur in the original sample. The accuracy of this method depends on the solubility of $BaSO_4$, the reaction for which is shown here.

$$\mathbf{BaSO_4}(s) \rightleftharpoons \mathbf{Ba^{2+}}(aq) + \mathbf{SO_4^{2-}}(aq) \tag{6.E.6}$$

How do the following affect the solubility of $BaSO_4$ and, therefore, the accuracy of the analytical method?

a. decreasing the solution's pH
b. adding more $BaCl_2$
c. increasing the volume of the solution by adding H_2O

6. Write a charge balance equation and mass balance equations for the following solutions. Some solutions may have more than one mass balance equation.

a. 0.10 M NaCl
b. 0.10 M HCl
c. 0.10 M HF
d. 0.10 M NaH_2PO_4
e. $MgCO_3$ (saturated solution)
f. 0.10 M $Ag(CN)_2^-$
g. 0.10 M HCl and 0.050 M $NaNO_2$

7. Using the systematic approach to equilibrium problems, calculate the pH of the following solutions. Be sure to state and justify any assumptions you make in solving the problems.

a. 0.050 M $HClO_4$
b. 1.00×10^{-7} M HCl
c. 0.025 M HClO
d. 0.010 M HCOOH
e. 0.050 M $Ba(OH)_2$
f. 0.010 M C_5H_5N

8. Construct ladder diagrams for the following diprotic weak acids (H_2L) and estimate the pH of 0.10 M solutions of H_2L, HL^- and L^{2-}.

a. maleic acid
b. malonic acid
c. succinic acid

9. Using the systematic approach to solving equilibrium problems, calculate the pH of the diprotic weak acid in problem 8. Be sure to state and justify any assumptions you make in solving the problems.

10. Ignoring activity effects, calculate the concentration of Hg_2^{2+} in the following solutions. Be sure to state and justify any assumption you make in solving the problems.

a. a saturated solution of Hg_2Br_2
b. 0.025 M $Hg_2(NO_3)_2$ saturated with Hg_2Br_2
c. 0.050 M NaBr saturated with Hg2Br2

11. The solubility of CaF_2 is controlled by the following two reactions

$$\mathbf{CaF_2}(s) \rightleftharpoons \mathbf{Ca^{2+}}(aq) + \mathbf{2F^-}(aq) \tag{6.E.7}$$

$$\mathbf{HF}(aq) + \mathbf{H_2O}(l) \rightleftharpoons \mathbf{H_3O^+}(aq) + \mathbf{F^-}(aq) \tag{6.E.8}$$

Calculate the solubility of CaF_2 in a solution buffered to a pH of 7.00. Use a ladder diagram to help simplify the calculations. How would your approach to this problem change if the pH is buffered to 2.00? What is the solubility of CaF_2 at this pH? Be sure to state and justify any assumptions you make in solving the problems.

12. Calculate the solubility of $Mg(OH)_2$ in a solution buffered to a pH of 7.00. How does this compare to its solubility in unbuffered deionized water? Be sure to state and justify any assumptions you make in solving the problem.

13. Calculate the solubility of Ag_3PO_4 in a solution buffered to a pH of 7.00. Be sure to state and justify any assumptions you make in solving the problem.

14. Determine the equilibrium composition of saturated solution of AgCl. Assume that the solubility of AgCl is influenced by the following reactions.

$$AgCl(s) \rightleftharpoons Ag^+(aq) + Cl^-(aq) \tag{6.E.9}$$

$$Ag^+(aq) + Cl^-(aq) \rightleftharpoons AgCl(aq) \tag{6.E.10}$$

$$AgCl(aq) + Cl^-(aq) \rightleftharpoons AgCl_2^-(aq) \tag{6.E.11}$$

Be sure to state and justify any assumptions you make in solving the problem.

15. Calculate the ionic strength of the following solutions

a. 0.050 M NaCl
b. 0.025 M $CuCl_2$
c. 0.10 M Na_2SO_4

16. Repeat the calculations in problem 10, this time correcting for the effect of ionic strength. Be sure to state and justify any assumptions you make in solving the problems.

17. Over what pH range do you expect $Ca_3(PO_4)_2$ to have its minimum solubility?

18. Construct ladder diagrams for the following systems, each consisting of two or three equilibria. Using your ladder diagrams, what reactions are likely to occur in each system?

a. HF and H_3PO_4
b. $Ag(CN)_2^-$, $Ni(CN)_4^{2-}$ and $Fe(CN)_6^{3-}$
c. $Cr_2O_7^{2-}/Cr^{3+}$ and Fe^{3+}/Fe^{2+}

19. Calculate the pH of the following acid–base buffers. Be sure to state and justify any assumptions you make in solving the problems.

a. 100 mL of 0.025 M formic acid and 0.015 M sodium formate
b. 50.00 mL of 0.12 M NH_3 and 5.30 mL of 1.0 M HCl
c. 5.00 g of Na_2CO_3 and 5.00 g of $NaHCO_3$ diluted to 100 mL

20. Calculate the pH of the buffers in problem 19 after adding 5.0 mL of 0.10 M HCl. Be sure to state and justify any assumptions you make in solving the problems.

21. Calculate the pH of the buffers in problem 19 after adding 5.0 mL of 0.10 M NaOH. Be sure to state and justify any assumptions you make in solving the problems.

22. Consider the following hypothetical complexation reaction between a metal, M, and a ligand, L

$$M(aq) + L(aq) \rightleftharpoons ML(aq) \tag{6.E.12}$$

with a formation constant of 1.5×10^8. Derive an equation, similar to the Henderson–Hasselbalch equation, relating pM to the concentrations of L and ML. What is the pM for a solution containing 0.010 mol of M and 0.020 mol of L? What is pM be if you add 0.002 mol of M to this solution? Be sure to state and justify any assumptions you make in solving the problem.

23. A redox buffer contains an oxidizing agent and its conjugate reducing agent. Calculate the potential of a solution containing 0.010 mol of Fe^{3+} and 0.015 mol of Fe^{2+}. What is the potential if you add sufficient oxidizing agent to convert 0.002 mol of Fe^{2+} to Fe^{3+}? Be sure to state and justify any assumptions you make in solving the problem.

24. Use either Excel or R to solve the following problems. For these problems, make no simplifying assumptions.
a. the solubility of CaF_2 in deionized water
b. the solubility of AgCl in deionized water (see Problem 14 for the relevant equilibria)
c. the pH of 0.10 M fumaric acid

25. Beginning with the relevant equilibrium reactions, derive equation 6.64 for the rigorous solution to the pH of 0.1 M HF.

6.12.3 Solutions to Practice Exercises

https://chem.libretexts.org/@go/page/70669

Practice Exercise 6.1

The overall reaction is equivalent to

$$\text{Rxn 4} - 2 \times \text{Rxn 1} \tag{6.E.13}$$

Subtracting a reaction is equivalent to adding the reverse reaction; thus, the overall equilibrium constant is

$$K = \frac{K_4}{(K_1)^2} = \frac{5.0}{(0.40)^2} = 31.25 \approx 31 \tag{6.E.14}$$

Click here to return to the chapter.

Practice Exercise 6.2

The K_b for hydrogen oxalate is

$$K_{b,HC_2O_4^-} = \frac{K_w}{K_{a,H_2C_2O_4}} = \frac{1.00 \times 10^{-14}}{5.60 \times 10^{-2}} = 1.79 \times 10^{-13} \tag{6.E.15}$$

and the K_b for oxalate is

$$K_{b,C_2O_4^{2-}} = \frac{K_w}{K_{a,HC_2O_4^-}} = \frac{1.00 \times 10^{-14}}{5.42 \times 10^{-5}} = 1.85 \times 10^{-10} \tag{6.E.16}$$

As we expect, the K_b value for $C_2O_4^{2-}$ is larger than that for $HC_2O_4^-$.

Click here to return to the chapter.

Practice Exercise 6.3

We can write the reaction as a sum of three other reactions. The first reaction is the solubility of AgCl(s), which we characterize by its K_{sp}.

$$AgBr(s) \rightleftharpoons Ag^+(aq) + Br^-(aq) \tag{6.E.17}$$

The remaining two reactions are the stepwise formation of $Ag(S_2O_3)_2^{3-}$, which we characterize by K_1 and K_2.

$$Ag^+(aq) + S_2O_3^{2-}(aq) \rightleftharpoons Ag(S_2O_3)^-(aq) \tag{6.E.18}$$

$$Ag(S_2O_3)^-(aq) + S_2O_3^{2-}(aq) \rightleftharpoons Ag(S_2O_3)_2^{3-}(aq) \tag{6.E.19}$$

Using values for K_{sp}, K_1, and K_2 from Appendix 10 and Appendix 11, we find that the equilibrium constant for our reaction is

$$K = K_{sp} \times K_1 \times K_2 = (5.0 \times 10^{-13})(6.6 \times 10^8)(7.1 \times 10^4) = 23 \tag{6.E.20}$$

Click here to return to the chapter.

Practice Exercise 6.4

The two half-reactions are the oxidation of Fe^{2+} and the reduction of MnO_4^-.

$$Fe^{2+}(aq) \rightleftharpoons Fe^{3+}(aq) + e^- \tag{6.E.21}$$

$$MnO_4^-(aq) + 8H^+(aq) + 5e^- \rightleftharpoons Mn^{2+}(aq) + 4H_2O(l) \tag{6.E.22}$$

From Appendix 13, the standard state reduction potentials for these half-reactions are

$$E^\circ_{Fe^{3+}/Fe^{2+}} = 0.771 \text{ V} \qquad E^\circ_{MnO_4^-/Mn^{2+}} = 1.51 \text{ V} \tag{6.E.23}$$

(a) The standard state potential for the reaction is

$$E^\circ = E^\circ_{MnO_4^-/Mn^{2+}} - E^\circ_{Fe^{3+}/Fe^{2+}} = 1.51 \text{ V} - 0.771 \text{ V} = 0.74 \text{ V} \tag{6.E.24}$$

(b) To calculate the equilibrium constant we substitute appropriate values into equation 6.25.

$$E^\circ = 0.74\ \text{V} = \frac{0.05916}{5}\log K \tag{6.E.25}$$

Solving for K gives its value as

$$\log K = 62.5 \qquad K = 3.2 \times 10^{62} \tag{6.E.26}$$

(c) To calculate the potential under these non-standard state conditions, we make appropriate substitutions into the Nernst equation.

$$E = E^\circ - \frac{RT}{nF}\ln\frac{[\text{Mn}^{2+}][\text{Fe}^{3+}]^5}{[\text{MnO}_4^-][\text{Fe}^{2+}]^5[\text{H}^+]^8} \tag{6.E.27}$$

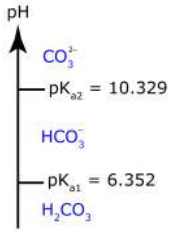
$$E = 0.74 - \frac{0.05916}{5}\log\frac{(0.015)(0.10)^5}{(0.025)(0.50)^5(1\times10^{-7})^8} \tag{6.E.28}$$

$$E = 0.74 - \frac{0.05916}{5}\log\frac{(0.015)(0.10)^5}{(0.025)(0.50)^5(1\times10^{-7})^8} = 0.12\ \text{V} \tag{6.E.29}$$

Click here to return to the chapter.

Practice Exercise 6.5

From Appendix 11, the pK_a values for H_2CO_3 are 6.352 and 10.329. The ladder diagram for H_2CO_3 is shown to the side. The predominate form at a pH of 7.00 is HCO_3^-.



Click here to return to the chapter.

Practice Exercise 6.6

The ladder diagram in Figure 6.5 indicates that the reaction between acetic acid and *p*-nitrophenolate is favorable. Because *p*-nitrophenolate is in excess, we assume that the reaction of acetic acid to acetate is complete. At equilibrium essentially no acetic acid remains and there are 0.040 moles of acetate. Converting acetic acid to acetate consumes 0.040 moles of *p*-nitrophenolate; thus

$$\text{moles } p\text{-nitrophenolate} = 0.090 - 0.040 = 0.050\ \text{mol} \tag{6.E.30}$$

$$\text{moles } p\text{-nitrophenol} = 0.040\ \text{mol} \tag{6.E.31}$$

According to the ladder diagram for this system, the pH is 7.15 when there are equal concentrations of *p*-nitrophenol and *p*-nitrophenolate. Because we have slightly more *p*-nitrophenolate than we have *p*-nitrophenol, the pH is slightly greater than 7.15.

Click here to return to the chapter.

Practice Exercise 6.7

As Hg_2Cl_2 dissolves, two Cl^- are produced for each ion of Hg_2^{2+}. If we assume that x is the change in the molar concentration of Hg_2^{2+}, then the change in the molar concentration of Cl^- is $2x$. The following table helps us keep track of our solution to this problem.

Concentrations	$Hg_2Cl_2(s)$	⇋	$Hg_2^{2+}(aq)$	+	$2Cl^-(aq)$
Initial	solid		0		0
Change	solid		$+x$		$+2x$
Equilibrium	solid		x		$2x$

Substituting the equilibrium concentrations into the K_{sp} expression for Hg_2Cl_2 gives

$$K_{sp} = [\text{Hg}_2^{2+}][\text{Cl}^-]^2 = (x)(2x)^2 = 4x^3 = 1.2\times10^{-18} \tag{6.E.32}$$

$$x = 6.69\times10^{-7} \tag{6.E.33}$$

Substituting x back into the equilibrium expressions for Hg_2^{2+} and Cl^- gives their concentrations as

$$[\text{Hg}_2^{2+}] = x = 6.7\times10^{-7}\ \text{M} \qquad [\text{Cl}^-] = 2x = 1.3\times10^{-6}\ \text{M} \tag{6.E.34}$$

The molar solubility is equal to $[Hg_2^{2+}]$, or 6.7×10^{-7} mol/L.

Click here to return to the chapter.

Practice Exercise 6.8

We begin by setting up a table to help us keep track of the concentrations of Hg_2^{2+} and Cl^- as this system moves toward and reaches equilibrium.

Concentrations	$Hg_2Cl_2(s)$	⇋	$Hg_2^{2+}(aq)$	+	$2Cl^-(aq)$
Initial Change	solid solid		0 $+x$		0.10 $+2x$
Equilibrium	solid		x		$0.10 + 2x$

Substituting the equilibrium concentrations into the K_{sp} expression for Hg_2Cl_2 leaves us with a difficult to solve cubic equation.

$$K_{sp} = [Hg_2^{2+}][Cl^-]^2 = (x)(0.10)^2 = 4x^3 + 0.40x^2 + 0.10x \tag{6.E.35}$$

Let's make an assumption to simplify this problem. Because we expect the value of x to be small, let's assume that

$$[Cl^-] = 0.10 + x \approx 0.10 \text{ M} \tag{6.E.36}$$

This simplifies our problems to

$$K_{sp} = [Hg_2^{2+}][Cl^-]^2 = (x)(0.10)^2 = 0.010x = 1.2 \times 10^{-18} \tag{6.E.37}$$

which gives the value of x as

$$x = 1.2 \times 10^{-16} \text{ M} \tag{6.E.38}$$

The difference between the actual concentration of Cl^-, which is $(0.10 + x)$ M, and our assumption that it is 0.10 M introduces an error of 1.2×10^{-14} %. This is a negligible error. The molar solubility of Hg_2Cl_2 is the same as the concentration of Hg_2^{2+}, or 1.2×10^{-16} M. As expected, the molar solubility in 0.10 M NaCl is less than 6.7×10^{-7} mol/L, which is its solubility in water (see solution to Practice Exercise 6.7).

Click here to return to the chapter.

Practice Exercise 6.9

To help us in determining what ions are in solution, let's write down all the reaction leading to the preparation of the solutions and the equilibria within the solutions. These reactions are the dissolution of two soluble salts

$$KH_2PO_4(s) \rightarrow K^+(aq) + H_2PO_4^-(aq) \tag{6.E.39}$$

$$Na_2HPO_4(s) \rightarrow 2Na^+(aq) + HPO_4^{2-}(aq) \tag{6.E.40}$$

and the acid–base dissociation reactions for $H_2PO_4^-$, HPO_4^{2-}, and H_2O.

$$H_2PO_4^-(aq) + H_2O(l) \rightleftharpoons H_3O^+(aq) + HPO_4^{2-}(aq) \tag{6.E.41}$$

$$H_2PO_4^-(aq) + H_2O(l) \rightleftharpoons OH^-(aq) + H_3PO_4(aq) \tag{6.E.42}$$

$$HPO_4^{2-}(aq) + H_2O(l) \rightleftharpoons H_3O^+(aq) + PO_4^{3-}(aq) \tag{6.E.43}$$

$$2H_2O(l) \rightleftharpoons H_3O^+(aq) + OH^-(aq) \tag{6.E.44}$$

Note that we did not include the base dissociation reaction for HPO_4^{2-} because we already have accounted for its product, $H_2PO_4^-$, in another reaction. The mass balance equations for K^+ and Na^+ are straightforward

$$[K^+] = 0.10 \text{ M} \quad [Na^+] = 0.10 \text{ M} \tag{6.E.45}$$

but the mass balance equation for the phosphate takes a little bit of thought. Both $H_2PO_4^-$ and HPO_4^{2-} produce the same ions in solution. We can, therefore, imagine that the solution initially contains 0.15 M KH_2PO_4, which gives the following mass balance equation.

$$0.15\ \text{M} = [\text{H}_3\text{PO}_4] + [\text{H}_2\text{PO}_4^-] + [\text{HPO}_4^{2-}] + [\text{PO}_4^{3-}] \tag{6.E.46}$$

The charge balance equation is

$$[\text{H}_3\text{O}^+] + [\text{K}^+] + [\text{Na}^+] = [\text{H}_2\text{PO}_4^-] + 2 \times [\text{HPO}_4^{2-}] + 3 \times [\text{PO}_4^{3-}] + [\text{OH}^-] \tag{6.E.47}$$

Click here to return to the chapter.

Practice Exercise 6.10

In determining the pH of 0.050 M NH_3, we need to consider two equilibrium reactions—the base dissociation reaction for NH_3

$$\text{NH}_3(aq) + \text{H}_2\text{O}(l) \rightleftharpoons \text{OH}^-(aq) + \text{NH}_4^+(aq) \tag{6.E.48}$$

and water's dissociation reaction.

$$2\text{H}_2\text{O}(l) \rightleftharpoons \text{H}_3\text{O}^+(aq) + \text{OH}^-(aq) \tag{6.E.49}$$

These two reactions contain four species whose concentrations we need to consider: NH_3, NH_4^+, H_3O^+, and OH^-. We need four equations to solve the problem—these equations are the K_b equation for NH_3

$$K_\text{b} = \frac{[\text{OH}^-][\text{NH}_4^+]}{[\text{NH}_3]} = 1.75 \times 10^{-5} \tag{6.E.50}$$

the K_w equation for H_2O

$$K_\text{w} = [\text{H}_3\text{O}^+][\text{OH}^-] = 1.00 \times 10^{-14} \tag{6.E.51}$$

a mass balance on ammonia

$$C_{\text{NH}_3} = 0.050\ \text{M} = [\text{NH}_3] + [\text{NH}_4^+] \tag{6.E.52}$$

and a charge balance equation

$$[\text{H}_3\text{O}^+] + [\text{NH}_4^+] = [\text{OH}^-] \tag{6.E.53}$$

To solve this problem, we will make two assumptions. Because NH_3 is a base, our first assumption is

$$[\text{OH}^-] >> [\text{H}_3\text{O}^+] \tag{6.E.54}$$

which simplifies the charge balance equation to

$$[\text{NH}_4^+] = [\text{OH}^-] \tag{6.E.55}$$

Because NH_3 is a weak base, our second assumption is

$$[\text{NH}_3] >> [\text{NH}_4^+] \tag{6.E.56}$$

which simplifies the mass balance equation to

$$C_{\text{NH}_3} = 0.050\ \text{M} = [\text{NH}_3] \tag{6.E.57}$$

Substituting the simplified charge balance equation and mass balance equation into the K_b equation leave us with

$$K_\text{b} = \frac{[\text{OH}^-][\text{OH}^-]}{C_{\text{NH}_3}} = \frac{[\text{OH}^-]^2}{C_{\text{NH}_3}} = 1.75 \times 10^{-5} \tag{6.E.58}$$

$$[\text{OH}^-] = \sqrt{K_\text{b} C_{\text{NH}_3}} = \sqrt{(1.75 \times 10^{-5})(0.050)} = 9.35 \times 10^{-4} \tag{6.E.59}$$

Before accepting this answer, we must verify our two assumptions. The first assumption is that the concentration of OH^- is significantly greater than the concentration of H_3O^+. Using K_w, we find that

$$[H_3O^+] = \frac{K_w}{[OH^-]} = \frac{1.00 \times 10^{-14}}{9.35 \times 10^{-4}} = 1.07 \times 10^{-11} \tag{6.E.60}$$

Clearly this assumption is acceptable. Our second assumption is that the concentration of NH_3 is scientifically greater than the concentration of NH_4^+. Using our simplified charge balance equation, we find that

$$[NH_4^+] = [OH^-] = 9.35 \times 10^{-4} \tag{6.E.61}$$

Because the concentration of NH_4^+ is 1.9% of C_{NH3}, our second assumption also is reasonable. Given that $[H_3O^+]$ is 1.07×10^{-11}, the pH is 10.97.

Click here to return to the chapter.

Practice Exercise 6.11

In solving for the pH of 0.10 M alanine, we made the following three assumptions.

$$\text{Assumption One: } [HL] >> [H_2L^+] + [L^-] \tag{6.E.62}$$

$$\text{Assumption Two: } K_{a1}K_w << K_{a1}K_{a2}C_{HL} \tag{6.E.63}$$

$$\text{Assumption Three: } K_{a1} << C_{HL} \tag{6.E.64}$$

The second and third assumptions are easy to check. The value for K_{a1} (4.487×10^{-3}) is 0.45% of C_{HL} (0.10), and $K_{a1} \times K_w$ (4.487×10^{-17}) is 0.074% of $K_{a1} \times K_{a2} \times C_{HL}$ (6.093×10^{-14}). Each assumption introduces an error of less than ±5%.

To test the first assumption, we need to calculate the concentrations of H_2L^+ and L^-, which we accomplish using the equations for K_{a1} and K_{a2}.

$$[H_2L^+] = \frac{[H_3O^+][HL]}{K_{a1}} = \frac{(7.807 \times 10^{-7})(0.10)}{4.487 \times 10^{-3}} = 1.74 \times 10^{-5} \tag{6.E.65}$$

$$[L^-] = \frac{K_{a2}[HL]}{[H_3O^+]} = \frac{(1.358 \times 10^{-10})(0.10)}{7.807 \times 10^{-7}} = 1.74 \times 10^{-5} \tag{6.E.66}$$

Because these concentrations are less than ±5% of C_{HL}, the first assumption also is acceptable.

Click here to return to the chapter.

Practice Exercise 6.12

The acid dissociation constant for $H_2PO_4^-$ is 6.32×10^{-8}, or a pK_a of 7.199. Substituting the initial concentrations of $H_2PO_4^-$ and HPO_4^{2-} into equation 6.60 and solving gives the buffer's pH as

$$\text{pH} = 7.199 + \log \frac{[HPO_4^{2-}]}{[H_2PO_4^-]} = 7.199 + \log \frac{0.050}{0.10} = 6.898 \approx 6.90 \tag{6.E.67}$$

Adding HCl converts a portion of HPO_4^{2-} to $H_2PO_4^-$ as a result of the following reaction

$$HPO_4^{2-}(aq) + H_3O^+(aq) \rightleftharpoons H_2O(l) + H_2PO_4^-(aq) \tag{6.E.68}$$

Because this reaction's equilibrium constant is so large (it is 1.59×10^7), we may treat the reaction as if it goes to completion. The new concentrations of $H_2PO_4^-$ and HPO_4^{2-} are

$$C_{H_2PO_4^-} = \frac{\text{mol } H_2PO_4^- + \text{mol HCl}}{V_{total}} \tag{6.E.69}$$

$$= \frac{(0.10 \text{ M})(010 \text{ L}) + (0.20 \text{ M})(5.0 \times 10^{-3} \text{ L})}{0.10 \text{ L} + 5.0 \times 10^{-3} \text{ L}} = 0.105 \text{ M} \tag{6.E.70}$$

$$C_{HPO_4^{2-}} = \frac{\text{mol } HPO_4^{2-} - \text{mol HCl}}{V_{total}} \tag{6.E.71}$$

$$= \frac{(0.05 \text{ M})(010 \text{ L}) - (0.20 \text{ M})(5.0 \times 10^{-3} \text{ L})}{0.10 \text{ L} + 5.0 \times 10^{-3} \text{ L}} = 0.0381 \text{ M} \tag{6.E.72}$$

Substituting these concentrations into equation 6.60 gives a pH of

$$\text{pH} = 7.199 + \log \frac{[\text{HPO}_4^{2-}]}{[\text{H}_2\text{PO}_4^{-}]} = 7.199 + \log \frac{0.0381}{0.105} = 6.759 \approx 6.76 \tag{6.E.73}$$

As we expect, adding HCl decreases the buffer's pH by a small amount, dropping from 6.90 to 6.76.

Click here to return to the chapter.

Practice Exercise 6.13

We begin by calculating the solution's ionic strength. Because NaCl is a 1:1 ionic salt, the ionic strength is the same as the concentration of NaCl; thus μ = 0.10 M. This assumes, of course, that we can ignore the contributions of Hg_2^{2+} and Cl^- from the solubility of Hg_2Cl_2.

Next we use equation 6.63 to calculate the activity coefficients for Hg_2^{2+} and Cl^-.

$$\log \gamma_{\text{Hg}_2^{2+}} = \frac{-0.51 \times (+2)^2 \times \sqrt{0.10}}{1 + 3.3 \times 0.40 \times \sqrt{0.10}} = -0.455 \tag{6.E.74}$$

$$\gamma_{\text{Hg}_2^{2+}} = 0.351 \tag{6.E.75}$$

$$\log \gamma_{\text{Cl}^-} = \frac{-0.51 \times (-1)^2 \times \sqrt{0.10}}{1 + 3.3 \times 0.3 \times \sqrt{0.10}} = -0.12 \tag{6.E.76}$$

$$\gamma_{\text{Cl}^-} = 0.75 \tag{6.E.77}$$

Defining the equilibrium concentrations of Hg_2^{2+} and Cl^- in terms of the variable *x*

Concentrations	$Hg_2Cl_2(s)$	⇋	$Hg_2^{2+}(aq)$	+	$2Cl^-(aq)$
Initial Change	solid solid		0 +*x*		0.10 +2*x*
Equilibrium	solid		*x*		0.10 + 2*x*

and substituting into the thermodynamic solubility product for Hg_2Cl_2, leave us with

$$K_{sp} = a_{\text{Hg}_2^{2+}} a_{\text{Cl}^-}^2 = \gamma_{\text{Hg}_2^{2+}} [\text{Hg}_2^{2+}] \gamma_{\text{Cl}^-}^2 [\text{Cl}^-]^2 = 1.2 \times 10^{-18} \tag{6.E.78}$$

$$1.2 \times 10^{-18} = (0.351)(x)(0.75)^2(0.10 + x)^2 \tag{6.E.79}$$

Because the value of *x* is likely to be small, let's simplify this equation to

$$1.2 \times 10^{-18} = (0.351)(x)(0.75)^2(0.10)^2 \tag{6.E.80}$$

Solving for *x* gives its value as 6.1×10^{-16}. Because *x* is the concentration of Hg_2^{2+} and 2*x* is the concentration of Cl^-, our decision to ignore their contributions to the ionic strength is reasonable. The molar solubility of Hg_2Cl_2 in 0.10 M NaCl is 6.1×10^{-16} mol/L. In Practice Exercise 6.8, where we ignored ionic strength, we determined that the molar solubility of Hg_2Cl_2 is 1.2×10^{-16} mol/L, a result that is 5× smaller than the its actual value.

Click here to return to the chapter.

Practice Exercise 6.14

To solve this problem, let's set up the following spreadsheet

	A	B
1	pI =	3
2	[I-] =	=10^–b1
3	[Ag+] =	=8.3e–17/b2
4	[Ag(NH3)2+] =	=b2 – b3
5	[NH3] =	=(b4/(b3*1.7e7))^0.5
6	[NH4+] =	=0.10 – b5-2*b4
7	[OH-] =	=1.75e–5*b5/b6
8	[H3O+] =	=1.00e–14/b7
9	error	=b3+b4+b6+b8 – b2 – b7

copying the contents of cells B1-B9 into several additional columns. See our earlier treatment of this problem for the relevant equilibrium reactions and equilibrium constants. The initial guess for pI in cell B1 gives the concentration of I^- in cell B2. Cells B3–B8 calculate the remaining concentrations, using the K_{sp} to obtain $[Ag^+]$, using the mass balance on iodide and silver to obtain $[Ag(NH_3)_2^+]$, using β_2 to calculate $[NH_3]$, using the mass balance on ammonia to find $[NH_4^+]$, using K_b to calculate $[OH^-]$, and using K_w to calculate $[H_3O^+]$. The system's charge balance equation provides a means for determining the calculation's error.

$$[Ag^+] + [Ag(NH_3)_2^+] + [NH_4^+] + [H_3O^+] - [I^-] - [OH^-] = 0 \tag{6.E.81}$$

The largest possible value for pI—corresponding to the smallest concentration of I^- and the lowest possible solubility—occurs for a simple, saturated solution of AgI. When $[Ag^+] = [I^-]$, the concentration of iodide is

$$[I^-] = \sqrt{K_{sp}} = \sqrt{8.3 \times 10^{-17}} = 9.1 \times 10^{-9}\ M \tag{6.E.82}$$

corresponding to a pI of 8.04. Entering initial guesses for pI of 4, 5, 6, 7, and 8 shows that the error changes sign between a pI of 5 and 6. Continuing in this way to narrow down the range for pI, we find that the error function is closest to zero at a pI of 5.42. The concentration of I^- at equilibrium, and the molar solubility of AgI, is 3.8×10^{-6} mol/L, which agrees with our earlier solution to this problem.

Click here to return to the chapter.

Practice Exercise 6.15

To solve this problem, let's use the following function

```
> eval=function(pI){
+ I=10^–pI
+ Ag=8.3e–17/I
+ AgNH3=Ag–I
+ NH3=(AgNH3/(1.7e7*Ag))^0.5
+ NH4=0.10-NH3–2*AgNH3
+ OH=1.75e–5*NH3/NH4
+ H3O=1e–14/OH
+ error=Ag+AgNH3+NH4+H3O–OH–I
+ output=data.frame(pI,error)
+ print(output)
+ }
```

The function accepts an initial guess for pI and calculates the concentrations of species in solution using the definition of pI to calculate $[I^-]$, using the K_{sp} to obtain $[Ag^+]$, using the mass balance on iodide and silver to obtain $[Ag(NH_3)_2^+]$, using β_2 to

calculate [NH_3], using the mass balance on ammonia to find [NH_4^+], using K_b to calculate [OH^-], and using K_w to calculate [H_3O^+]. The system's charge balance equation provides a means for determining the calculation's error.

$$[Ag^+] + [Ag(NH_3)_2^+] + [NH_4^+] + [H_3O^+] - [I^-] - [OH^-] = 0 \tag{6.E.83}$$

The largest possible value for pI—corresponding to the smallest concentration of I^- and the lowest possible solubility—occurs for a simple, saturated solution of AgI. When [Ag^+] = [I^-], the concentration of iodide is

$$[I^-] = \sqrt{K_{sp}} = \sqrt{8.3 \times 10^{-17}} = 9.1 \times 10^{-9}\ M \tag{6.E.84}$$

corresponding to a pI of 8.04. The following session shows the function in action.

```
> pI =c(4, 5, 6, 7, 8)
> eval(pI)
pI error
1 4 -2.56235615
2 5 -0.16620930
3 6 0.07337101
4 7 0.09734824
5 8 0.09989073
> pI =c(5.1, 5.2, 5.3, 5.4, 5.5, 5.6, 5.7, 5.8, 5.9, 6.0)
> eval(pI)
pI error
1 5.1 -0.11144658
2 5.2 -0.06794105
3 5.3 -0.03336475
4 5.4 -0.00568116
5 5.5 0.01571549
6 5.6 0.03308929
7 5.7 0.04685937
8 5.8 0.05779214
9 5.9 0.06647475
10 6.0 0.07337101
> pI =c(5.40, 5.41, 5.42, 5.43, 5.44, 5.45, 5.46, 5.47, 5.48, 5.49, 5.50)
> eval(pI)
pI error
1 5.40 -0.0056811605
2 5.41 -0.0030715484
3 5.42 0.0002310369
4 5.43 -0.0005134898
5 5.44 0.0028281878
6 5.45 0.0052370980
7 5.46 0.0074758181
8 5.47 0.0096260370
9 5.48 0.0117105498
10 5.49 0.0137387291
11 5.50 0.0157154889
```

The error function is closest to zero at a pI of 5.42. The concentration of I^- at equilibrium, and the molar solubility of AgI, is 3.8×10^{-6} mol/L, which agrees with our earlier solution to this problem.

Click here to return to the chapter

References

1. Quilez, J. *Chem. Educ. Res. Pract.* **2004**, *5*, 69–87 (www.uoi.gr/cerp).
2. lthough not specifically on the topic of ladder diagrams as developed in this section, the following sources provide appropriate background information: (a) Runo, J. R.; Peters, D. G. *J. Chem. Educ.* **1993**, *70*, 708–713; (b) Vale, J.; Fernández-Pereira, C.; Alcalde, M. *J. Chem. Educ.* **1993**, *70*, 790–795; (c) Fernández-Pereira, C.; Vale, J. *Chem. Educator* **1996**, *6*, 1–18; (d) Fernández-Pereira, C.; Vale, J.; Alcalde, M. *Chem. Educator* **2003**, *8*, 15–21; (e) Fernández-Pereira, C.; Alcalde, M.; Villegas, R.; Vale, J. J. *Chem. Educ.* **2007**, *84*, 520–525.
3. See, for example, (a) Bower, V. E.; Bates, R. G. *J. Res. Natl. Bur. Stand. (U. S.)* **1955**, *55*, 197–200; (b) Bates, R. G. *Ann. N. Y. Acad. Sci.* **1961**, *92*, 341–356; (c) Bates, R. G. *Determination of pH*, 2nd ed.; Wiley-Interscience: New York, 1973.
4. (a) Lambert, W. J. J. Chem. Educ. 1990, 67, 150–153; (b) http://www.bioinformatics.org/JaMBW/5/4/index.html.
5. Lister, M. W.; Rivington, D. E. *Can. J. Chem.* **1995**, *33*, 1572–1590.
6. Davies, C. W. *Ion Association*, Butterworth: London, 1962.

Contributors and Attributions

David Harvey (DePauw University)

6.E: Equilibrium Chemistry (Exercises) is shared under a CC BY-NC-SA 4.0 license and was authored, remixed, and/or curated by LibreTexts.

6.S: Equilibrium Chemistry (Summary)

6.S: Equilibrium Chemistry (Summary)

6.S: Equilibrium Chemistry (Summary) is shared under a CC BY-NC-SA 4.0 license and was authored, remixed, and/or curated by LibreTexts.

CHAPTER OVERVIEW

7: Collecting and Preparing Samples

When we use an analytical method to solve a problem, there is no guarantee that our results will be accurate or precise. In designing an analytical method we consider potential sources of determinate error and indeterminate error, and take appropriate steps to minimize their effect, such as including reagent blanks and calibrating instruments. Why might a carefully designed analytical method give poor results? One possibility is that we may have failed to account for errors associated with the sample. If we collect the wrong sample, or if we lose analyte while preparing the sample for analysis, then we introduce a determinate source of error. If we fail to collect enough samples, or if we collect samples of the wrong size, then our precision may suffer. In this chapter we consider how collecting samples and preparing them for analysis affects the accuracy and precision of our results.

Topic hierarchy

7.1: The Importance of Sampling
7.2: Designing a Sampling Plan
7.3: Implementing the Sampling Plan
7.4: Separating the Analyte from Interferents
7.5: General Theory of Separation Efficiency
7.6: Classifying Separation Techniques
7.7: Liquid–Liquid Extractions
7.8: Separation Versus Preconcentration
7.E: Collecting and Preparing Samples (Exercises)
7.S: Collecting and Preparing Samples (Summary)

Thumbnail: An example of pipettes and microplates manipulated by an anthropomorphic robot (Andrew Alliance). Image used with permission (Cc BY-SA 3.0; Pzucchel).

Contributors

- David Harvey (DePauw University)

7: Collecting and Preparing Samples is shared under a CC BY-NC-SA 4.0 license and was authored, remixed, and/or curated by LibreTexts.

7.1: The Importance of Sampling

7.1: The Importance of Sampling

7.1: The Importance of Sampling is shared under a CC BY-NC-SA 4.0 license and was authored, remixed, and/or curated by LibreTexts.

7.2: Designing a Sampling Plan

7.2: Designing a Sampling Plan

7.2: Designing a Sampling Plan is shared under a CC BY-NC-SA 4.0 license and was authored, remixed, and/or curated by LibreTexts.

7.3: Implementing the Sampling Plan

7.3: Implementing the Sampling Plan

7.3: Implementing the Sampling Plan is shared under a CC BY-NC-SA 4.0 license and was authored, remixed, and/or curated by LibreTexts.

7.4: Separating the Analyte from Interferents

7.4: Separating the Analyte from Interferents

7.4: Separating the Analyte from Interferents is shared under a CC BY-NC-SA 4.0 license and was authored, remixed, and/or curated by LibreTexts.

7.5: General Theory of Separation Efficiency

7.5: General Theory of Separation Efficiency

7.5: General Theory of Separation Efficiency is shared under a CC BY-NC-SA 4.0 license and was authored, remixed, and/or curated by LibreTexts.

7.6: Classifying Separation Techniques

7.6: Classifying Separation Techniques

7.6: Classifying Separation Techniques is shared under a CC BY-NC-SA 4.0 license and was authored, remixed, and/or curated by LibreTexts.

7.7: Liquid–Liquid Extractions

7.7: Liquid–Liquid Extractions

7.7: Liquid–Liquid Extractions is shared under a CC BY-NC-SA 4.0 license and was authored, remixed, and/or curated by LibreTexts.

7.8: Separation Versus Preconcentration

7.8: Separation Versus Preconcentration

7.8: Separation Versus Preconcentration is shared under a CC BY-NC-SA 4.0 license and was authored, remixed, and/or curated by LibreTexts.

7.E: Collecting and Preparing Samples (Exercises)

1. Because of the risk of lead poisoning, the exposure of children to lead-based paint is a significant public health concern. The first step in the quantitative analysis of lead in dried paint chips is to dissolve the sample. Corl has evaluated several dissolution techniques.[22] In this study, samples of paint were collected and pulverized with a Pyrex mortar and pestle. Replicate portions of the powdered paint were then taken for analysis. The following table shows results for a paint sample and for a standard reference material. Both samples and standards were digested with HNO_3 on a hot plate.

Replicate	% w/w Pb in Sample	% w/w Pb in Standard
1	5.09	11.48
2	6.29	11.62
3	6.64	11.47
4	4.63	11.86

(a) Determine the overall variance, the variance due to the method and the variance due to sampling. (b) What percentage of the overall variance is due to sampling? (c) How might you decrease the variance due to sampling?

2. To analyze a shipment of 100 barrels of an organic solvent, you plan to collect and analyze single samples from ten barrels using a random sampling. From which barrels should you collect samples if the first barrel is given by the 12th entry in the random number table in Appendix 14, with subsequent barrels given by every third entry? Assume that entries in the random number table are arranged by rows.

3. The concentration of dissolved O_2 in a lake shows a daily cycle from the effect of photosynthesis, and a yearly cycle due to seasonal changes in temperature. Suggest an appropriate systematic sampling plan for monitoring the daily change in dissolved O_2. Suggest an appropriate systematic sampling plan for monitoring the yearly change in dissolved O_2.

4. The data in the following table were collected during a preliminary study of the pH of an industrial wastewater stream.

Time (h)	pH	Time (h)	pH
0.5	4.4	9.0	5.7
1.0	4.8	9.5	5.5
1.5	5.2	10.0	6.5
2.0	5.2	10.5	6.0
2.5	5.6	11.0	5.8
3.0	5.4	11.5	6.0
3.5	5.4	12.0	5.6
4.0	4.4	12.5	5.6
4.5	4.8	13.0	5.4
5.0	4.8	13.5	4.9
5.5	4.2	14.0	5.2
6.0	4.2	14.5	4.4
6.5	3.8	15.0	4.0
7.0	4.0	15.5	4.5
7.5	4.0	16.0	4.0
8.0	3.9	16.5	5.0
8.5	4.7	17.0	5.0

Construct a graph of pH as a function of time and suggest an appropriate sampling frequency for a long-term monitoring program.

5. You have been asked to monitor the daily fluctuations in atmospheric ozone in the downtown area of a city to determine if there is relationship between daily traffic patterns and ozone levels. (a) Which of the following sampling plan will you use: random, systematic, judgmental, systematic–judgmental, or stratified? (b) Do you plan to collect and analyze a series of grab samples, or will you form a single composite sample? (c) Will your answers to these questions change if your goal is to determine if the average daily ozone level exceeds a threshold value? If your answer is yes, then what is your new sampling strategy?

6. The distinction between a homogeneous population and a heterogeneous population is important when you are developing a sampling plan. (a) Define homogeneous and heterogeneous. (b) If you collect and analyze a single sample, can you determine if the population is homogeneous or heterogeneous?

7. The sampling of a heterogeneous population is particularly challenging. Explain why you can minimize the sampling variance for a heterogeneous population by increasing the number of samples, but not by increasing the mass of individual samples.

8. Beginning with equation 7.4, derive equation 7.5. Assume that the particles are spherical with a radius of r and a density of d.

9. The sampling constant for the radioisotope ^{24}Na in homogenized human liver has been reported as approximately 35 g.[23] (a) What is the expected relative standard deviation for sampling if you analyze 1.0-g samples? (b) How many 1.0-g samples must you analyze to obtain a maximum sampling error of ±5% at the 95% confidence level?

10. Engels and Ingamells reported the following results for the % w/w K_2O in a mixture of amphibolite and orthoclase.[24]

0.247	0.300	0.236	0.258	0.304	0.330
0.247	0.275	0.212	0.311	0.258	0.187

Each of the 12 samples had a nominal weight of 0.1 g. Determine the approximate value for K_s and the mass of sample needed to achieve a percent relative standard deviation of 2%.

11. The following data has been reported for the determination of KH_2PO_4 in a mixture of KH_2PO_4 and NaCl.[25]

Nominal Mass (g)	Actual Mass (g)	% w/w KH_2PO_4
0.10	0.1039 0.1015 0.1012 0.1010 0.1060 0.0997	0.085 1.078 0.413 1.248 0.654 0.507
0.25	0.2515 0.2465 0.2770 0.2460 0.2485 0.2590	0.847 0.598 0.431 0.842 0.964 1.178
0.50	0.5084 0.4954 0.5286 0.5232 0.4965 0.4995	1.009 0.947 0.618 0.744 0.572 0.709
1.00	1.027 0.987 0.991 0.998 0.997 1.001	0.696 0.843 0.535 0.750 0.711 0.639
2.50	2.496 2.504 2.496 2.496 2.557 2.509	0.766 0.769 0.682 0.609 0.589 0.617

(a) Prepare a graph of % w/w KH_2PO_4 versus the actual sample mass and discuss how this graph is consistent with your understanding of the factors affecting sampling variance. (b) For each nominal mass, calculate the percent relative standard deviation for the analysis. The value of K_s for this analysis has been estimated as 350. For each nominal mass, use this K_s to determine the percent relative standard deviation due to sampling. Considering these calculations, what is your conclusion about the importance of indeterminate sampling errors for this analysis? (c) For each nominal mass, convert the percent relative standard

deviation to an absolute standard deviation. Plot points on your graph corresponding to ±1 absolute standard deviations about the overall average % w/w KH_2PO_4. Draw smooth curves through these two sets of points. Considering these curves, does the sample appear to be homogeneous on the scale at which it is sampled?

12. In this problem you will collect and analyze data in a simulation of the sampling process. Obtain a pack of M&M's (or other similar candy). Collect a sample of five candies and count the number that are red (or any other color of your choice). Report the result of your analysis as % red. Return the candies to the bag, mix thoroughly, and repeat the analysis for a total of 20 determinations. Calculate the mean and the standard deviation for your data. Remove all candies from the bag and determine the true % red for the population. Sampling in this exercise should follow binomial statistics. Calculate the expected mean value and the expected standard deviation, and compare to your experimental results.

13. Determine the error ($\alpha = 0.05$) for the following situations. In each case assume that the variance for a single determination is 0.0025 and that the variance for collecting a single sample is 0.050. (a) Nine samples are collected, each analyzed once. (b) One sample is collected and analyzed nine times. (c) Three samples are collected, each analyzed three times.

14. Which of the sampling schemes in problem 13 is best if you wish to limit the overall error to less than ±0.25, and the cost of collecting a single sample is 1 (arbitrary units), and the cost of analyzing a single sample is 10? Which is the best sampling scheme if the cost of collecting a single sample is 7, and the cost of analyzing a single sample is 3?

15. Maw, Witry, and Emond evaluated a microwave digestion method for Hg against the standard open-vessel digestion method.[26] The standard method requires a 2-h digestion and is operator-intensive. The microwave digestion is complete in approximately 0.5 h and requires little monitoring by the operator. Samples of baghouse dust from air-pollution-control equipment were collected

from a hazardous waste incinerator and digested in triplicate before determining the concentration of Hg in ppm. Results are summarized in the following tables.

ppm Hg Following Microwave Digestion

Sample	Replicate 1	Replicate 2	Replicate 3
1	7.12	7.66	7.17
2	16.1	15.7	15.6
3	4.89	4.62	4.28
4	9.64	9.03	8.44
5	6.76	7.22	7.50
6	6.19	6.61	7.61
7	9.44	9.56	10.7
8	30.8	29.0	26.2

ppm Hg Following Standard Digestion

Sample	Replicate 1	Replicate 2	Replicate 3
1	5.50	5.54	5.40
2	13.1	12.8	13.0
3	5.39	5.12	5.36
4	6.59	6.52	7.20
5	6.20	6.03	5.77
6	6.25	5.65	5.61
7	15.0	13.9	14.0
8	20.4	16.1	20.0

Does the microwave digestion method yields acceptable results in comparison to the standard digestion method?

16. Simpson, Apte, and Batley investigated methods for preserving water samples collected from anoxic (O_2-poor) environments that contain high concentrations of dissolved sulfide.[27] They found that preserving water samples with HNO_3 (a common method for preserving aerobic samples) gave significant negative determinate errors when analyzing for Cu^{2+}. Preserving samples by first adding H_2O_2 and then adding HNO_3, eliminated the determinate error. Explain their observations.

17. In a particular analysis the selectivity coefficient, $K_{A,I}$, is 0.816. When a standard sample with an analyte-to-interferent ratio of 5:1 is carried through the analysis, the error in determining the analyte is +6.3%. (a) Determine the apparent recovery for the analyte if $R_I = 0$. (b) Determine the apparent recovery for the interferent if $R_A = 0$.

18. The amount of Co in an ore is to be determined using a procedure for which Fe in an interferent. To evaluate the procedure's accuracy, a standard sample of ore known to have a Co/Fe ratio of 10.2:1 is analyzed. When pure samples of Co and Fe are taken through the procedure the following calibration relationships are obtained

$$S_{Co} = 0.786 \times m_{Co} \quad (7.E.1)$$

$$S_{Fe} = 0.669 \times m_{Fe} \quad (7.E.2)$$

where S is the signal and m is the mass of Co or Fe. When 278.3 mg of Co are taken through the separation step, 275.9 mg are recovered. Only 3.6 mg of Fe are recovered when a 184.9 mg sample of Fe is carried through the separation step. Calculate (a) the recoveries for Co and Fe; (b) the separation factor; (c) the error if no attempt is made to separate the Co and Fe before the analysis; (d) the error if the separation step is carried out; and (e) the maximum recovery for Fe if the recovery for Co is 1.00, and the maximum allowed error is 0.05%.

19. The amount of calcium in a sample of urine was determined by a method for which magnesium is an interferent. The selectivity coefficient, $K_{Ca,Mg}$, for the method is 0.843. When a sample with a Mg/Ca ratio of 0.50 was carried through the procedure, an error of –3.7% was obtained. The error was +5.5% when using a sample with a Mg/Ca ratio of 2.0. (a) Determine the recoveries for Ca and Mg. (b) What is the expected error for a urine sample in which the Mg/Ca ratio is 10.0?

20. Using the formation constants in Appendix 12, show that F^- is an effective masking agent for preventing a reaction between Al^{3+} and EDTA. Assume that the only significant forms of fluoride and EDTA are F^- and Y^{4-}.

21. Cyanide is frequently used as a masking agent for metal ions. Its effectiveness as a masking agent is better in more basic solutions. Explain the reason for this pH dependency.

22. Explain how an aqueous sample consisting of Cu^{2+}, Sn^{4+}, Pb^{2+}, and Zn^{2+} can be separated into its component parts by adjusting the pH of the solution.

23. A solute, S, has a distribution ratio between water and ether of 7.5. Calculate the extraction efficiency if you extract a 50.0-mL aqueous sample of S using 50.0 mL of ether as: (a) a single portion of 50.0 mL; (b) two portions, each of 25.0 mL; (c) four portions, each of 12.5 mL; and (d) five portions, each of 10.0 mL. Assume that the solute is not involved in any secondary equilibria.

24. What volume of ether is needed to extract 99.9% of the solute in problem 23 when using: (a) 1 extraction; (b) 2 extractions; (c) four extractions; and (d) five extractions.

25. What is the minimum distribution ratio if 99% of the solute in a 50.0-mL sample is to be extracted with a single 50.0-mL portion of an organic solvent? Repeat for the case where two 25.0-mL portions of the organic solvent are used.

26. A weak acid, HA, with a K_a of 1.0×10^{-5} has a partition coefficient, K_D, of 1.2×10^3 between water and an organic solvent. What restriction on the sample's pH is necessary to ensure that 99.9% of the weak acid in a 50.0-mL sample is extracted with a single 50.0-mL portion of the organic solvent?

27. For problem 26, how many extractions are needed if the sample's pH cannot be decreased below 7.0?

28. A weak base, B, with a K_b of 1.0×10^{-3} has a partition coefficient, K_D, of 5.0×10^2 between water and an organic solvent. What restriction on the sample's pH is necessary to ensure that 99.9% of the weak base is in a 50.0-mL sample is extracted with two 25.0-mL portions of the organic solvent?

29. A sample contains a weak acid analyte, HA, and a weak acid interferent, HB. The acid dissociation constants and the partition coefficients for the weak acids are as follows: $K_{a,HA} = 1.0 \times 10^{-3}$, $K_{a,HB} = 1.0 \times 10^{-7}$, $K_{D,HA} = K_{D,HB} = 5.0 \times 10^2$. (a) Calculate the extraction efficiency for HA and HB when a 50.0-mL sample, buffered to a pH of 7.0, is extracted with 50.0 mL of the organic solvent. (b) Which phase is enriched in the analyte? (c) What are the recoveries for the analyte and the interferent in this phase? (d) What is the separation factor? (e) A quantitative analysis is conducted on the phase enriched in analyte. What is the expected relative error if the selectivity coefficient, $K_{HA,HB}$, is 0.500 and the initial ratio of HB/HA is 10.0?

30. The relevant equilibria for the extraction of I_2 from an aqueous solution of KI into an organic phase are shown in Figure 7.32. (a) Is the extraction efficiency for I_2 better at higher or at lower concentrations of I^-? (b) Derive an expression for the distribution ratio for this extraction.

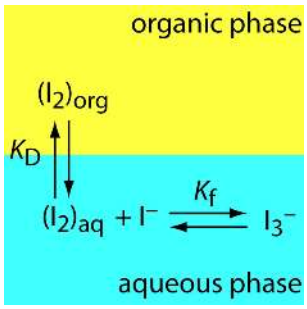


Figure 7.32 Extraction scheme for Problem 7.30.

31. The relevant equilibria for extracting the metal-ligand complex ML_2 from an aqueous solution into an organic phase are shown in Figure 7.31. (a) Derive an expression for the distribution ratio for this extraction. (b) Calculate the extraction efficiency when a 50.0-mL aqueous sample that is 0.15 mM in M^{2+} and 0.12 M in L^- is extracted with 25.0 mL of the organic phase. Assume that K_D is 10.3 and that β_2 is 560.

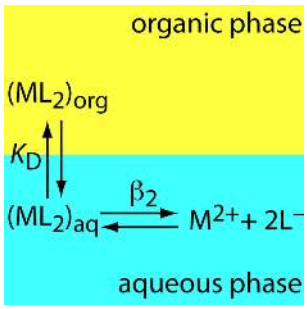


Figure 7.33 Extraction scheme for Problem 7.31.

32. Derive equation 7.32.

33. The following information is available for the extraction of Cu^{2+} by CCl_4 and dithizone: $K_{D,c} = 7 \times 10^4$; $\beta_2 = 5 \times 10^{22}$; $K_{a,HL} = 2 \times 10^{-5}$;$K_{D,HL} = 1.01 \times 10^4$; and $n = 2$. What is the extraction efficiency if a 100-mL sample of an aqueous solution that is 1.0×10^{-7} M Cu^{2+} and 1 M in HCl is extracted with 10 mL of CCl_4 containing 4.0×10^{-4} M dithizone (HL)?

https://chem.libretexts.org/@go/page/70680

34. Cupferron is a ligand whose strong affinity for metal ions makes it useful as a chelating agent in liquid–liquid extractions. The following table provides pH-dependent distribution ratios for the extraction of Hg^{2+}, Pb^{2+}, and Zn^{2+} from an aqueous solution to an organic solvent.

	Distribution Ratio for		
pH	Hg^{2+}	Pb^{2+}	Zn^{2+}
1	3.3	0.0	0.0
2	10.0	0.43	0.0
3	32.3	999	0.0
4	32.3	9999	0.0
5	19.0	9999	0.18
6	4.0	9999	0.33
7	1.0	9999	0.82
8	0.54	9999	1.50
9	0.15	9999	2.57
10	0.05	9999	2.57

(a) Suppose you have a 50.0-mL sample of an aqueous solution containing Hg^{2+}, Pb^{2+}, and Zn^{2+}. Describe how you can effect a separation of these metal ions. (b) Under the conditions of your extraction for Hg^{2+}, what percent of the Hg^{2+} remains in the aqueous phase after three 50.0-mL extractions with the organic solvent? (c) Under the conditions of your extraction for Pb^{2+}, what is the minimum volume of organic solvent needed to extract 99.5% of the Pb^{2+} in a single extraction? (d) Under the conditions of your extraction for Zn^{2+}, how many extractions are needed to remove 99.5% of the Zn^{2+} if each extraction uses 25.0 mL of organic solvent?

7.9.3 Solutions to Practice Exercises

Practice Exercise 7.1

To reduce the overall variance by improving the method's standard deviation requires that

$$s^2 = 5.00\ \text{ppm}^2 = s^2_{\text{samp}} + s^2_{\text{meth}} = (2.1\ \text{ppm})^2 + s^2_{\text{meth}} \tag{7.E.3}$$

Solving for s_{meth} gives its value as 0.768 ppm. Relative to its original value of 1.1 ppm, this is reduction of 3.0×10^1%. To reduce the overall variance by improving the standard deviation for sampling requires that

$$s^2 = 5.00\ \text{ppm}^2 = s^2_{\text{samp}} + s^2_{\text{meth}} = s^2_{\text{samp}} + (1.1\ \text{ppm})^2 \tag{7.E.4}$$

Solving for s_{samp} gives its value as 1.95 ppm. Relative to its original value of 2.1 ppm, this is reduction of 7.1%.

Click here to return to the chapter.

Practice Exercise 7.2

The analytical method's standard deviation is 1.96×10^{-3} g/cm^3 as this is the standard deviation for the analysis of a single sample of the polymer. The sampling variance is

$$s_{samp}^2 = s^2 - s_{meth}^2 = (3.65 \times 10^{-2})^2 - (1.96 \times 10^{-3})^2 = 1.33 \times 10^{-3} \tag{7.E.5}$$

Converting the variance to a standard deviation gives s_{meth} as 3.64×10^{-2} g/cm^3.

Click here to return to the chapter.

Practice Exercise 7.3

To determine the sampling constant, K_s, we need to know the average mass of the samples and the percent relative standard deviation for the concentration of olaquindox in the feed. The average mass for the five samples is 0.95792 g. The average concentration of olaquindox in the samples is 23.14 mg/kg with a standard deviation of 2.200 mg/kg. The percent relative standard deviation, R, is

$$R = \frac{s_{samp}}{\bar{X}} \times 100 = \frac{2.200 \text{ mg/kg}}{23.14 \text{ mg/kg}} \times 100 = 9.507 \approx 9.51 \tag{7.E.6}$$

Solving for K_s gives its value as

$$K_s = mR^2 = (0.95792 \text{ g})(9.507)^2 = 86.58 \text{ g} \approx 86.6 \text{ g} \tag{7.E.7}$$

To obtain a percent relative standard deviation of 5.0%, individual samples need to have a mass of at least

$$m = \frac{K_s}{R^2} = \frac{86.58 \text{ g}}{(5.0)^2} = 3.5 \text{ g} \tag{7.E.8}$$

To reduce the sample's mass from 3.5 g to 1 g, we must change the mass by a factor of

$$\frac{3.5 \text{ g}}{1 \text{ g}} = 3.5\times \tag{7.E.9}$$

If we assume that the sample's particles are spherical, then we must reduce a particle's radius by a factor of

$$r^3 = 3.5\times \tag{7.E.10}$$

$$r = 1.5\times \tag{7.E.11}$$

Click here to return to the chapter.

Practice Exercise 7.4

Because the value of t depends on the number of samples—a result we have yet to calculate—we begin by letting $n_{samp} = \infty$ and using $t(0.05, \infty)$ for the value of t. From Appendix 4, the value for $t(0.05, \infty)$ is 1.960. Our first estimate for n_{samp} is

$$n_{samp} = \frac{t^2 s_{samp}^2}{e^2} = \frac{(1.960)^2(5.0)^2}{(2.5)^2} = 15.4 \approx 15 \tag{7.E.12}$$

Letting $n_{samp} = 15$, the value of $t(0.05, 14)$ from Appendix 4 is 2.145. Recalculating n_{samp} gives

$$n_{samp} = \frac{t^2 s_{samp}^2}{e^2} = \frac{(2.145)^2(5.0)^2}{(2.5)^2} = 18.4 \approx 18 \tag{7.E.13}$$

Letting $n_{samp} = 18$, the value of $t(0.05, 17)$ from Appendix 4 is 2.103. Recalculating n_{samp} gives

$$n_{samp} = \frac{t^2 s_{samp}^2}{e^2} = \frac{(2.103)^2(5.0)^2}{(2.5)^2} = 17.7 \approx 18 \tag{7.E.14}$$

Because two successive calculations give the same value for n_{samp}, we need 18 samples to achieve a sampling error of ±2.5% at the 95% confidence interval.

Click here to return to the chapter.

Practice Exercise 7.5

If we collect a single sample (cost $20), then we can analyze that sample 13 times (cost $650) and stay within our budget. For this scenario, the percent relative error is

$$e = t\sqrt{\frac{s_{\text{samp}}^2}{n_{\text{samp}}} + \frac{s_{\text{meth}}^2}{n_{\text{samp}} n_{\text{rep}}}} = 2.179\sqrt{\frac{0.10}{1} + \frac{0.20}{1 \times 13}} = 0.74 \tag{7.E.15}$$

where t(0.05, 12) is 2.179. Because this percent relative error is larger than ±0.50%, this is not a suitable sampling strategy.

Next, we try two samples (cost $40), analyzing each six times (cost $600). For this scenario, the percent relative error is

$$e = t\sqrt{\frac{s_{\text{samp}}^2}{n_{\text{samp}}} + \frac{s_{\text{meth}}^2}{n_{\text{samp}} n_{\text{rep}}}} = 2.2035\sqrt{\frac{0.10}{2} + \frac{0.20}{2 \times 6}} = 0.57 \tag{7.E.16}$$

where t(0.05, 11) is 2.2035. Because this percent relative error is larger than ±0.50%, this also is not a suitable sampling strategy.

Next we try three samples (cost $60), analyzing each four times (cost $600). For this scenario, the percent relative error is

$$e = t\sqrt{\frac{s_{\text{samp}}^2}{n_{\text{samp}}} + \frac{s_{\text{meth}}^2}{n_{\text{samp}} n_{\text{rep}}}} = 2.2035\sqrt{\frac{0.10}{3} + \frac{0.20}{3 \times 4}} = 0.49 \tag{7.E.17}$$

where t(0.05, 11) is 2.2035. Because both the total cost ($660) and the percent relative error meet our requirements, this is a suitable sampling strategy.

There are other suitable sampling strategies that meet both goals. The strategy requiring the least expense is to collect eight samples, analyzing each once for a total cost of $560 and a percent relative error of ±0.46%. Collecting 10 samples and analyzing each one time, gives a percent relative error of ±0.39% at a cost of $700.

Click here to return to the chapter.

Practice Exercise 7.6

The fluoride ion, F^-, is a suitable masking agent as it binds with Al^{3+} to form the stable AlF_6^{3-} complex, leaving iron in solution.

Click here to return to the chapter.

Practice Exercise 7.7

The relevant reactions and equilibrium constants are

$$\text{Fe}^{2+}(aq) + 3\text{phen}(aq) \rightleftharpoons \text{Fe(phen)}_3^{2+}(aq) \quad \beta_3 = 5 \times 10^{20} \tag{7.E.18}$$

$$\text{Fe}^{3+}(aq) + 3\text{phen}(aq) \rightleftharpoons \text{Fe(phen)}_3^{3+}(aq) \quad \beta_3 = 6 \times 10^{13} \tag{7.E.19}$$

where phen is an abbreviation for 1,10-phenanthroline. Because β_3 is larger for the complex with Fe^{2+} than it is for the complex with Fe^{3+}, 1,10-phenanthroline will bind Fe^{2+} before it binds Fe^{3+}. A ladder diagram for this system (Figure 6.34) suggests that an equilibrium p(phen) between 5.6 and 5.9 will fully complex Fe^{2+} without any significant formation of the $Fe(phen)_3^{3+}$ complex. Adding a stoichiometrically equivalent amount of 1,10-phenanthroline to a solution of Fe^{2+} will be sufficient to mask Fe^{2+} in the presence of Fe^{3+}. Adding a large excess of 1,10-phenanthroline, however, will decrease p(phen) and allow the formation of both metal–ligand complexes.

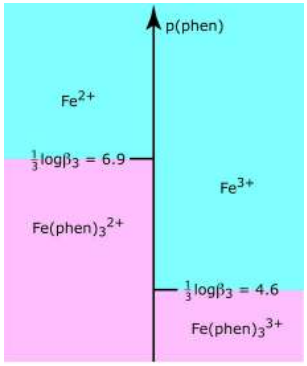


Figure 7.34 Ladder diagram for Practice Exercise 7.7.

Click here to return to the chapter.

Practice Exercise 7.8

(a) The solute's distribution ratio between water and toluene is

$$D = \frac{[S_{org}]}{[S_{aq}]} = \frac{0.889\ \text{g} \times \frac{1\ \text{mol}}{117.3\ \text{g}} \times \frac{1}{0.00500\ \text{L}}}{(1.235\ \text{g} - 0.889\ \text{g}) \times \frac{1\ \text{mol}}{117.3\ \text{g}} \times \frac{1}{0.01000\ \text{L}}} = 5.14 \tag{7.E.20}$$

(b) The fraction of solute remaining in the aqueous phase after one extraction is

$$(q_{aq})_1 = \frac{V_{aq}}{DV_{org} + V_{aq}} = \frac{20.00\ \text{mL}}{(5.14)(10.00\ \text{mL}) + 20.00\ \text{mL}} = 0.280 \tag{7.E.21}$$

The extraction efficiency, therefore, is 72.0%.

(c) To extract 99.9% of the solute requires

$$(Q_{aq})_n = 0.001 = \frac{20.00\ \text{mL}}{(5.14)(10.00\ \text{mL}) + 20.00\ \text{mL}}^{\,n} = 0.280^n \tag{7.E.22}$$

$$\log(0.001) = n\log(0.280) \tag{7.E.23}$$

$$n = 5.4 \tag{7.E.24}$$

a minimum of six extractions.

Click here to return to the chapter.

Practice Exercise 7.9

Because the weak base exists in two forms, only one of which extracts into the organic phase, the partition coefficient, K_D, and the distribution ratio, D, are not identical.

$$K_D = \frac{[B_{org}]}{[B_{aq}]} \tag{7.E.25}$$

$$D = \frac{[B_{org}]_{total}}{[B_{aq}]_{total}} = \frac{[B_{org}]}{[B_{aq}] + [HB^+_{aq}]} \tag{7.E.26}$$

Using the K_b expression for the weak base

$$K_b = \frac{[OH_{aq}^-][HB^+_{aq}]}{[B_{aq}]} \tag{7.E.27}$$

we solve for the concentration of HB^+ and substitute back into the equation for D, obtaining

$$D = \frac{[B_{org}]}{[B_{aq}] + \frac{K_b \times [B_{aq}]}{[OH_{aq}^-]}} = \frac{[B_{org}]}{[B_{aq}]1 + \frac{K_b}{[OH_{aq}^-]}} = \frac{K_D[OH_{aq}^-]}{[OH_{aq}^-] + K_b} \tag{7.E.28}$$

At a pH of 9.0, the $[OH^-]$ is 1×10^{-5} M and the distribution ratio has a value of

$$D = \frac{K_D[OH_{aq}^-]}{[OH_{aq}^-] + K_b} = \frac{(5.00)(1.0 \times 10^{-5})}{1.0 \times 10^{-5} + 1.0 \times 10^{-4}} = 0.455 \tag{7.E.29}$$

After one extraction, the fraction of B remaining in the aqueous phase is

$$(q_{aq})_1 = \frac{25.00\ mL}{(0.455)(50.00\ mL) + 25.00\ mL} = 0.524 \tag{7.E.30}$$

The extraction efficiency, therefore, is 47.6%. At a pH of 9, most of the weak base is present as HB^+, which explains why the overall extraction efficiency is so poor.

Click here to return to the chapter.

Contributors and Attributions

David Harvey (DePauw University)

7.E: Collecting and Preparing Samples (Exercises) is shared under a CC BY-NC-SA 4.0 license and was authored, remixed, and/or curated by LibreTexts.

7.S: Collecting and Preparing Samples (Summary)

7.S: Collecting and Preparing Samples (Summary)

7.S: Collecting and Preparing Samples (Summary) is shared under a CC BY-NC-SA 4.0 license and was authored, remixed, and/or curated by LibreTexts.

CHAPTER OVERVIEW

8: Gravimetric Methods

Gravimetry includes all analytical methods in which the analytical signal is a measurement of mass or a change in mass. When you step on a scale after exercising you are making, in a sense, a gravimetric determination of your mass. Mass is the most fundamental of all analytical measurements, and gravimetry is unquestionably our oldest quantitative analytical technique. The publication in 1540 of Vannoccio Biringuccio's *Pirotechnia* is an early example of applying gravimetry—although not yet known by this name—to the analysis of metals and ores.[1] Although gravimetry no longer is the most important analytical method, it continues to find use in specialized applications.

Topic hierarchy

8.1: Overview of Gravimetric Methods
8.2: Precipitation Gravimetry
8.3: Volatilization Gravimetry
8.4: Particulate Gravimetry
8.E: Gravimetric Methods (Exercises)
8.S: Gravimetric Methods (Summary)

Thumbnails: An analytical balance (Mettler ae-260) that is often used in gravimetric analysis Methods. Image used with permission (Public Domain; US DEA).

Contributors

- David Harvey (DePauw University)

8: Gravimetric Methods is shared under a CC BY-NC-SA 4.0 license and was authored, remixed, and/or curated by LibreTexts.

8.1: Overview of Gravimetric Methods

Before we consider specific gravimetric methods, let's take a moment to develop a broad survey of **gravimetry**. Later, as you read through the descriptions of specific gravimetric methods, this survey will help you focus on their similarities instead of their differences. You will find that it is easier to understand a new analytical method when you can see its relationship to other similar methods.

8.1.1 Using Mass as an Analytical Signal

Suppose you are to determine the total suspended solids in the water released by a sewage-treatment facility. Suspended solids are just that—solid matter that has yet to settle out of its solution matrix. The analysis is easy. After collecting a sample, you pass it through a preweighed filter that retains the suspended solids, and dry the filter and solids to remove any residual moisture. The mass of suspended solids is the difference between the filter's final mass and its original mass. We call this a **direct analysis** because the analyte—the suspended solids in this example—is the species that is weighed.

> **Note**
>
> Method 2540D in *Standard Methods for the Examination of Waters and Wastewaters*, 20th Edition (American Public Health Association, 1998) provides an approved method for determining total suspended solids. The method uses a glass-fiber filter to retain the suspended solids. After filtering the sample, the filter is dried to a constant weight at 103–105°C.

What if our analyte is an aqueous ion, such as Pb^{2+}? Because the analyte is not a solid, we cannot isolate it by filtration. We can still measure the analyte's mass directly if we first convert it into a solid form. If we suspend a pair of Pt electrodes in the sample and apply a sufficiently positive potential between them for a long enough time, we can force the following reaction to completion.

$$\mathrm{Pb^{2+}}(aq) + 4\mathrm{H_2O}(l) \rightleftharpoons \mathrm{PbO_2}(s) + \mathrm{H_2}(g) + 2\mathrm{H_3O^+}(aq) \tag{8.1.1}$$

Oxidizing Pb^{2+} deposits PbO_2 on the Pt anode. If we weigh the anode before and after applying the potential, the change in its mass gives the mass of PbO_2 and, from the reaction's stoichiometry, the amount of Pb^{2+} in the sample. This is a direct analysis because PbO_2 contains the analyte.

Sometimes it is easier to remove the analyte and let a change in mass serve as the analytical signal. Suppose you need to determine a food's moisture content. One approach is to heat a sample of the food to a temperature that vaporizes the water, capturing it in a preweighed absorbent trap. The change in the absorbent's mass provides a direct determination of the amount of water in the sample. An easier approach is to weigh the sample of food before and after heating, using the change in its mass as an indication of the amount of water originally present. We call this an **indirect analysis** because we determine the analyte using a signal that is proportional its disappearance.

> **Note**
>
> Method 925.10 in *Official Methods of Analysis*, 18th Edition (AOAC International, 2007) provides an approved method for determining the moisture content of flour. A preweighed sample is heated for one hour in a 130°C oven and transferred to a desiccator while it cools to room temperature. The loss in mass gives the amount of water in the sample.

The indirect determination of a sample's moisture content is done by difference. The sample's initial mass includes the water, but its final mass does not. We can also determine an analyte indirectly without its ever being weighed. For example, phosphite, PO_3^{3-}, reduces Hg^{2+} to Hg_2^{2+}, which in the presence of Cl^- precipitates as Hg_2Cl_2.

$$\begin{aligned} &2\mathrm{HgCl_2}(aq) + \mathrm{PO_3^{3-}}(aq) + 3\mathrm{H_2O}(l) \\ &\rightleftharpoons \mathrm{Hg_2Cl_2}(s) + 2\mathrm{H_3O^+}(aq) + 2\mathrm{Cl^-}(aq) + 2\mathrm{PO_4^{3-}}(aq) \end{aligned} \tag{8.1.2}$$

If we add $HgCl_2$ in excess, each mole of PO_3^{3-} produces one mole of Hg_2Cl_2. The precipitate's mass, therefore, provides an indirect measurement of the amount of PO_3^{3-} in the original sample.

8.1.2 Types of Gravimetric Methods

The four examples in the previous section illustrate different ways in which the measurement of mass may serve as an analytical signal. When the signal is the mass of a precipitate, we call the method **precipitation gravimetry**. The indirect determination of

PO_3^{3-} by precipitating Hg_2Cl_2 is an example, as is the direct determination of Cl^- by precipitating AgCl.

In **electrogravimetry**, we deposit the analyte as a solid film an electrode in an electrochemical cell. The deposition as PbO_2 at a Pt anode is one example of electrogravimetry. The reduction of Cu^{2+} to Cu at a Pt cathode is another example of electrogravimetry.

> **Note**
>
> We will not consider electrogravimetry in this chapter. See Chapter 11 on electrochemical methods of analysis for a further discussion of electrogravimetry.

When we use thermal or chemical energy to remove a volatile species, we call the method **volatilization gravimetry**. In determining the moisture content of bread, for example, we use thermal energy to vaporize the water in the sample. To determine the amount of carbon in an organic compound, we use the chemical energy of combustion to convert it to CO_2.

Finally, in **particulate gravimetry** we determine the analyte by separating it from the sample's matrix using a filtration or an extraction. The determination of total suspended solids is one example of particulate gravimetry.

8.1.3 Conservation of Mass

An accurate gravimetric analysis requires that the analytical signal—whether it is a mass or a change in mass—be proportional to the amount of analyte in our sample. For all gravimetric methods this proportionality involves a **conservation of mass**. If the method relies on one or more chemical reactions, then the stoichiometry of the reactions must be known. Thus, for the analysis of PO_3^{3-} described earlier, we know that each mole of Hg_2Cl_2 corresponds to a mole of PO_3^{3-} in our sample. If we remove the analyte from its matrix, then the separation must be selective for the analyte. When determining the moisture content in bread, for example, we know that the mass of H_2O in the bread is the difference between the sample's final mass and its initial mass.

> **Note**
>
> We will return to this concept of applying a conservation of mass later in the chapter when we consider specific examples of gravimetric methods.

8.1.4 Why Gravimetry is Important

Except for particulate gravimetry, which is the most trivial form of gravimetry, you probably will not use gravimetry after you complete this course. Why, then, is familiarity with gravimetry still important? The answer is that gravimetry is one of only a small number of **definitive techniques** whose measurements require only base SI units, such as mass or the mole, and defined constants, such as Avogadro's number and the mass of ^{12}C. Ultimately, we must be able to trace the result of an analysis to a definitive technique, such as gravimetry, that we can relate to fundamental physical properties.[2] Although most analysts never use gravimetry to validate their results, they often verifying an analytical method by analyzing a standard reference material whose composition is traceable to a definitive technique.[3]

> **Note**
>
> Other examples of definitive techniques are coulometry and isotope-dilution mass spectrometry. Coulometry is discussed in Chapter 11. Isotope-dilution mass spectrometry is beyond the scope of an introductory textbook; however, you will find some suggested readings in this chapter's Additional Resources.

Contributors

David Harvey (DePauw University)

8.1: Overview of Gravimetric Methods is shared under a CC BY-NC-SA 4.0 license and was authored, remixed, and/or curated by LibreTexts.

8.2: Precipitation Gravimetry

In precipitation gravimetry an insoluble compound forms when we add a precipitating reagent, or **precipitant**, to a solution containing our analyte. In most methods the precipitate is the product of a simple metathesis reaction between the analyte and the precipitant; however, any reaction generating a precipitate can potentially serve as a gravimetric method.

Most precipitation gravimetric methods were developed in the nineteenth century, or earlier, often for the analysis of ores. Figure 1.1 in Chapter 1, for example, illustrates a precipitation gravimetric method for the analysis of nickel in ores.

8.2.1 Theory and Practice

All precipitation gravimetric analysis share two important attributes. First, the precipitate must be of low solubility, of high purity, and of known composition if its mass is to accurately reflect the analyte's mass. Second, the precipitate must be easy to separate from the reaction mixture.

Solubility Considerations

To provide accurate results, a precipitate's solubility must be minimal. The accuracy of a total analysis technique typically is better than ±0.1%, which means that the precipitate must account for at least 99.9% of the analyte. Extending this requirement to 99.99% ensures that the precipitate's solubility does not limit the accuracy of a gravimetric analysis.

> **Note**
>
> A total analysis technique is one in which the analytical signal—mass in this case—is proportional to the absolute amount of analyte in the sample. See Chapter 3 for a discussion of the difference between total analysis techniques and concentration techniques.

We can minimize solubility losses by carefully controlling the conditions under which the precipitate forms. This, in turn, requires that we account for every equilibrium reaction affecting the precipitate's solubility. For example, we can determine Ag^+ gravimetrically by adding NaCl as a precipitant, forming a precipitate of AgCl.

$$Ag^+(aq) + Cl^-(aq) \rightleftharpoons AgCl(s) \tag{8.1}$$

If this is the only reaction we consider, then we predict that the precipitate's solubility, S_{AgCl}, is given by the following equation.

$$S_{AgCl} = [Ag^+] = \frac{K_{sp}}{[Cl^-]} \tag{8.2}$$

Equation 8.2 suggests that we can minimize solubility losses by adding a large excess of Cl^-. In fact, as shown in Figure 8.1, adding a large excess of Cl^- increases the precipitate's solubility.

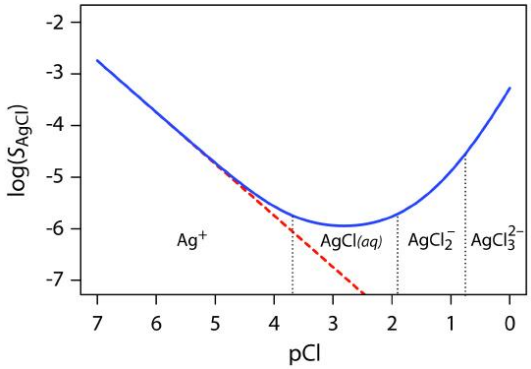


Figure 8.1 Solubility of AgCl as a function of pCl. The dashed red line shows our prediction for S_{AgCl} if we incorrectly assume that only reaction 8.1 and equation 8.2 affect silver chloride's solubility. The solid blue curve is calculated using equation 8.7, which accounts for reaction 8.1 and reactions 8.3–8.5. Because the solubility of AgCl spans several orders of magnitude, S_{AgCl} is displayed on the *y*-axis in logarithmic form.

To understand why the solubility of AgCl is more complicated than the relationship suggested by equation 8.2, we must recognize that Ag^+ also forms a series of soluble silver-chloro metal–ligand complexes.

$$Ag^+(aq) + Cl^-(aq) \rightleftharpoons AgCl(aq) \quad \log K_1 = 3.70 \tag{8.3}$$

$$AgCl(aq) + Cl^-(aq) \rightleftharpoons AgCl_2^-(aq) \quad \log K_2 = 1.92 \tag{8.4}$$

$$AgCl_2^-(aq) + Cl^-(aq) \rightleftharpoons AgCl_3^{2-}(aq) \quad \log K_3 = 0.78 \tag{8.5}$$

The actual solubility of AgCl is the sum of the equilibrium concentrations for all soluble forms of Ag^+, as shown by the following equation.

$$S_{AgCl} = [Ag^+] + [AgCl(aq)] + [AgCl_2^-] + [AgCl_3^{2-}] \tag{8.6}$$

By substituting into equation 8.6 the equilibrium constant expressions for reaction 8.1 and reactions 8.3–8.5, we can define the solubility of AgCl as

$$S_{AgCl} = \frac{K_{sp}}{[Cl^-]} + K_1K_{sp} + K_1K_2K_{sp}[Cl^-] + K_1K_2K_3K_{sp}[Cl^-]^2 \tag{8.7}$$

Note

Problem 1 in the end-of-chapter problems asks you to show that equation 8.7 is correct by completing the derivation.

Equation 8.7 explains the solubility curve for AgCl shown in Figure 8.1. As we add NaCl to a solution of Ag^+, the solubility of AgCl initially decreases because of reaction 8.1. Under these conditions, the final three terms in equation 8.7 are small and equation 8.1 is sufficient to describe AgCl's solubility. At higher concentrations of Cl^-, reaction 8.4 and reaction 8.5 increase the solubility of AgCl. Clearly the equilibrium concentration of chloride is important if we want to determine the concentration of silver by precipitating AgCl. In particular, we must avoid a large excess of chloride.

Note

The predominate silver-chloro complexes for different values of pCl are shown by the ladder diagram along the *x*-axis in Figure 8.1 Note that the increase in solubility begins when the higher-order soluble complexes, $AgCl_2^-$ and $AgCl_3^{2-}$, become the predominate species.

Another important parameter that may affect a precipitate's solubility is pH. For example, a hydroxide precipitates such as $Fe(OH)_3$ is more soluble at lower pH levels where the concentration of OH^- is small. Because fluoride is a weak base, the solubility of calcium fluoride, S_{CaF2}, also is pH-dependent. We can derive an equation for S_{CaF2} by considering the following equilibrium reactions

$$CaF_2(s) \rightleftharpoons Ca^{2+}(aq) + 2F^-(aq) \quad K_{sp} = 3.9 \times 10^{-11} \tag{8.8}$$

$$HF(aq) + H_2O(l) \rightleftharpoons H_3O^+(aq) + F^-(aq) \quad K_a = 6.8 \times 10^{-4} \tag{8.9}$$

and the following equation for the solubility of CaF_2.

$$S_{CaF_2} = [Ca^{2+}] = \frac{1}{2}\{[F^-] + [HF]\} \tag{8.10}$$

Note

Be sure that equation 8.10 makes sense to you. Reaction 8.8 tells us that the dissolution of CaF_2 produces one mole of Ca^{2+} for every two moles of F^-, which explains the term of 1/2 in equation 8.10. Because F^- is a weak base, we need to account for both of its chemical forms in solution, which explains why we include HF.

Substituting the equilibrium constant expressions for reaction 8.8 and reaction 8.9 into equation 8.10 defines the solubility of CaF_2 in terms of the equilibrium concentration of H_3O^+.

$$S_{CaF_2} = [Ca^{2+}] = \left\{\frac{K_{sp}}{4}\left(1 + \frac{[H_3O^+]}{K_a}\right)^2\right\}^{1/3} \tag{8.11}$$

Note

Problem 4 in the end-of-chapter problems asks you to show that equation 8.11 is correct by completing the derivation.

Figure 8.2 shows how pH affects the solubility of CaF_2. Depending on the solution's pH, the predominate form of fluoride is either HF or F^-. When the pH is greater than 4.17, the predominate species is F^- and the solubility of CaF_2 is independent of pH because only reaction 8.8 occurs to an appreciable extent. At more acidic pH levels, the solubility of CaF_2 increases because of the contribution of reaction 8.9.

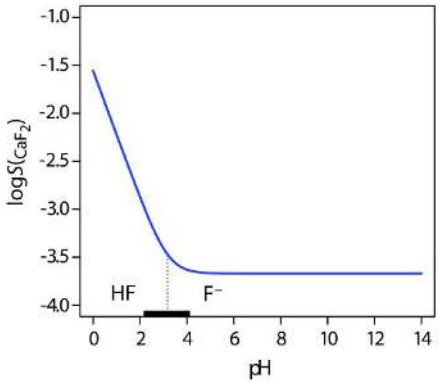


Figure 8.2 Solubility of CaF_2 as a function of pH. The solid blue curve is a plot of equation 8.11. The predominate form of fluoride in solution is shown by the ladder diagram along the *x*-axis, with the black rectangle showing the region where both HF and F^- are important species. Note that the solubility of CaF_2 is independent of pH for pH levels greater than 4.17, and that its solubility increases dramatically at lower pH levels where HF is the predominate species. Because the solubility of CaF_2 spans several orders of magnitude, its solubility is shown in logarithmic form.

When solubility is a concern, it may be possible to decrease solubility by using a non-aqueous solvent. A precipitate's solubility is generally greater in an aqueous solution because of water's ability to stabilize ions through solvation. The poorer solvating ability of non-aqueous solvents, even those which are polar, leads to a smaller solubility product. For example, the K_{sp} of $PbSO_4$ is 2×10^{-8} in H_2O and 2.6×10^{-12} in a 50:50 mixture of H_2O and ethanol.

Practice Exercise 8.1

You can use a ladder diagram to predict the conditions for minimizing a precipitate's solubility. Draw a ladder diagram for oxalic acid, $H_2C_2O_4$, and use it to establish a suitable range of pH values for minimizing the solubility of CaC_2O_4. Relevant equilibrium constants may be found in the appendices.

Click here to review your answer to this exercise.

Avoiding Impurities

In addition to having a low solubility, the precipitate must be free from impurities. Because precipitation usually occurs in a solution that is rich in dissolved solids, the initial precipitate is often impure. We must remove these impurities before determining the precipitate's mass.

The greatest source of impurities is the result of chemical and physical interactions occurring at the precipitate's surface. A precipitate is generally crystalline—even if only on a microscopic scale—with a well-defined lattice of cations and anions. Those cations and anions at the precipitate's surface carry, respectively, a positive or a negative charge because they have incomplete coordination spheres. In a precipitate of AgCl, for example, each silver ion in the precipitate's interior is bound to six chloride ions. A silver ion at the surface, however, is bound to no more than five chloride ions and carries a partial positive charge (Figure 8.3). The presence of these partial charges makes the precipitate's surface an active site for the chemical and physical interactions that produce impurities.

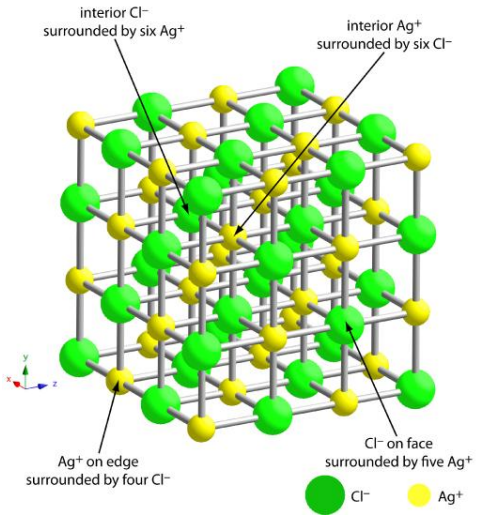


Figure 8.3 Ball-and-stick diagram showing the lattice structure of AgCl. Each silver ion in the lattice's interior binds with six chloride ions, and each chloride ion in the interior binds with six silver ions. Those ions on the lattice's surface or edges bind to fewer than six ions and carry a partial charge. A silver ion on the surface, for example, carries a partial positive charge. These charges make the surface of a precipitate an active site for chemical and physical interactions.

One common impurity is an **inclusion**. A potential interfering ion whose size and charge is similar to a lattice ion, may substitute into the lattice structure, provided that the interferent precipitates with the same crystal structure (Figure 8.4a). The probability of forming an inclusion is greatest when the concentration of the interfering ion is substantially greater than the lattice ion's concentration. An inclusion does not decrease the amount of analyte that precipitates, provided that the precipitant is present in sufficient excess. Thus, the precipitate's mass is always larger than expected.

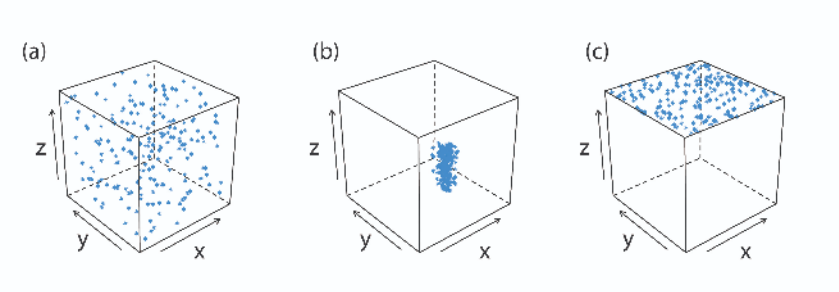


Figure 8.4 Three examples of impurities that may form during precipitation. The cubic frame represents the precipitate and the blue marks are impurities: (a) inclusions, (b) occlusions, and (c) surface adsorbates. Inclusions are randomly distributed throughout the precipitate. Occlusions are localized within the interior of the precipitate and surface adsorbates are localized on the precipitate's exterior. For ease of viewing, in (c) adsorption is shown on only one surface.

An inclusion is difficult to remove since it is chemically part of the precipitate's lattice. The only way to remove an inclusion is through **reprecipitation**. After isolating the precipitate from its supernatant solution, we dissolve it by heating in a small portion of a suitable solvent. We then allow the solution to cool, reforming the precipitate. Because the interferent's concentration is less than that in the original solution, the amount of included material is smaller. We can repeat the process of reprecipitation until the inclusion's mass is insignificant. The loss of analyte during reprecipitation, however, can be a significant source of error.

Note

Suppose that 10% of an interferent forms an inclusion during each precipitation. When we initially form the precipitate, 10% of the original interferent is present as an inclusion. After the first reprecipitation, 10% of the included interferent remains, which is 1% of the original interferent. A second reprecipitation decreases the interferent to 0.1% of the original amount.

Occlusions form when interfering ions become trapped within the growing precipitate. Unlike inclusions, which are randomly dispersed within the precipitate, an occlusion is localized, either along flaws within the precipitate's lattice structure or within aggregates of individual precipitate particles (Figure 8.4b). An occlusion usually increases a precipitate's mass; however, the mass is smaller if the occlusion includes the analyte in a lower molecular weight form than that of the precipitate.

We can minimize occlusions by maintaining the precipitate in equilibrium with its supernatant solution for an extended time. This process is called a **digestion**. During digestion, the dynamic nature of the solubility–precipitation equilibrium, in which the precipitate dissolves and reforms, ensures that the occlusion is reexposed to the supernatant solution. Because the rates of dissolution and reprecipitation are slow, there is less opportunity for forming new occlusions.

After precipitation is complete the surface continues to attract ions from solution (Figure 8.4c). These **surface adsorbates** comprise a third type of impurity. We can minimize surface adsorption by decreasing the precipitate's available surface area. One benefit of digesting a precipitate is that it increases the average particle size. Because the probability of a particle completely dissolving is inversely proportional to its size, during digestion larger particles increase in size at the expense of smaller particles. One consequence of forming a smaller number of larger particles is an overall decrease in the precipitate's surface area. We also can remove surface adsorbates by washing the precipitate, although the potential loss of analyte can not be ignored.

Inclusions, occlusions, and surface adsorbates are examples of **coprecipitates**—otherwise soluble species that form within the precipitate containing the analyte. Another type of impurity is an interferent that forms an independent precipitate under the conditions of the analysis. For example, the precipitation of nickel dimethylglyoxime requires a slightly basic pH. Under these conditions, any Fe^{3+} in the sample precipitates as $Fe(OH)_3$. In addition, because most precipitants are rarely selective toward a single analyte, there is always a risk that the precipitant will react with both the analyte and an interferent.

> **Note**
>
> In addition to forming a precipitate with Ni^{2+}, dimethylglyoxime also forms precipitates with Pd^{2+} and Pt^{2+}. These cations are potential interferents in an analysis for nickel.

We can minimize the formation of additional precipitates by carefully controlling solution conditions. If an interferent forms a precipitate that is less soluble than the analyte's precipitate, we can precipitate the interferent and remove it by filtration, leaving the analyte behind in solution. Alternatively, we can mask the analyte or the interferent to prevent its precipitation.

Both of the above-mentioned approaches are illustrated in Fresenius' analytical method for determining Ni in ores containing Pb^{2+}, Cu^{2+}, and Fe^{3+} (see Figure 1.1 in Chapter 1). Dissolving the ore in the presence of H_2SO_4 selectively precipitates Pb^{2+} as $PbSO_4$. Treating the supernatant with H_2S precipitates the Cu^{2+} as CuS. After removing the CuS by filtration, adding ammonia precipitates Fe^{3+} as $Fe(OH)_3$. Nickel, which forms a soluble amine complex, remains in solution.

Controlling Particle Size

Size matters when it comes to forming a precipitate. Larger particles are easier to filter, and, as noted earlier, a smaller surface area means there is less opportunity for surface adsorbates to form. By carefully controlling the reaction conditions we can significantly increase a precipitate's average particle size.

Precipitation consists of two distinct events: nucleation, the initial formation of smaller stable particles of precipitate, and particle growth. Larger particles form when the rate of particle growth exceeds the rate of nucleation. Understanding the conditions favoring particle growth is important when designing a gravimetric method of analysis.

We define a solute's **relative supersaturation**, *RSS*, as

$$RSS = \frac{Q - S}{S} \tag{8.12}$$

where Q is the solute's actual concentration and S is the solute's concentration at equilibrium.[4] The numerator of equation 8.12, $Q - S$, is a measure of the solute's supersaturation. A solution with a large, positive value of *RSS* has a high rate of nucleation, producing a precipitate with many small particles. When the *RSS* is small, precipitation is more likely to occur by particle growth than by nucleation.

Note

A supersaturated solution is one that contains more dissolved solute than that predicted by equilibrium chemistry. The solution is inherently unstable and precipitates solute to reach its equilibrium position. How quickly this process occurs depends, in part, on the value of *RSS*.

Examining equation 8.12 shows that we can minimize *RSS* by decreasing the solute's concentration, *Q*, or by increasing the precipitate's solubility, *S*. A precipitate's solubility usually increases at higher temperatures, and adjusting pH may affect a precipitate's solubility if it contains an acidic or a basic ion. Temperature and pH, therefore, are useful ways to increase the value of *S*. Conducting the precipitation in a dilute solution of analyte, or adding the precipitant slowly and with vigorous stirring are ways to decrease the value of *Q*.

There are practical limitations to minimizing *RSS*. Some precipitates, such as $Fe(OH)_3$ and PbS, are so insoluble that *S* is very small and a large *RSS* is unavoidable. Such solutes inevitably form small particles. In addition, conditions favoring a small *RSS* may lead to a relatively stable supersaturated solution that requires a long time to fully precipitate. For example, almost a month is required to form a visible precipitate of $BaSO_4$ under conditions in which the initial *RSS* is 5.[5]

A visible precipitate takes longer to form when *RSS* is small both because there is a slow rate of nucleation and because there is a steady decrease in *RSS* as the precipitate forms. One solution to the latter problem is to generate the precipitant in situ as the product of a slow chemical reaction. This maintains the *RSS* at an effectively constant level. Because the precipitate forms under conditions of low *RSS*, initial nucleation produces a small number of particles. As additional precipitant forms, particle growth supersedes nucleation, resulting in larger precipitate particles. This process is called **homogeneous precipitation**.[6]

Two general methods are used for homogeneous precipitation. If the precipitate's solubility is pH-dependent, then we can mix the analyte and the precipitant under conditions where precipitation does not occur, and then increase or decrease the pH by chemically generating OH^- or H_3O^+. For example, the hydrolysis of urea is a source of OH^-.

$$CO(NH_2)_2(aq) + H_2O(l) \rightleftharpoons 2NH_3(aq) + CO_2(g) \quad (8.2.1)$$

$$NH_3(aq) + H_2O(l) \rightleftharpoons OH^-(aq) + NH_4^+(aq) \quad (8.2.2)$$

Because the hydrolysis of urea is temperature-dependent—it is negligible at room temperature—we can use temperature to control the rate of hydrolysis and the rate of precipitate formation. Precipitates of CaC_2O_4, for example, have been produced by this method. After dissolving the sample containing Ca^{2+}, the solution is made acidic with HCl before adding a solution of 5% w/v $(NH_4)_2C_2O_4$. Because the solution is acidic, a precipitate of CaC_2O_4 does not form. The solution is heated to approximately 50°C and urea is added. After several minutes, a precipitate of CaC_2O_4 begins to form, with precipitation reaching completion in about 30 min.

In the second method of homogeneous precipitation, the precipitant is generated by a chemical reaction. For example, Pb^{2+} is precipitated homogeneously as $PbCrO_4$ by using bromate, BrO_3^-, to oxidize Cr^{3+} to CrO_4^{2-}.

$$6\,BrO_3^-(aq) + 10Cr^{3+}(aq) + 22H_2O(l) \rightleftharpoons 3Br_2(aq) + 10CrO_4^{2-}(aq) + 44H^+(aq) \quad (8.2.3)$$

Figure 8.5 shows the result of preparing $PbCrO_4$ by the direct addition of $KCrO_4$ (Beaker A) and by homogenous precipitation (Beaker B). Both beakers contain the same amount of $PbCrO_4$. Because the direct addition of $KCrO_4$ leads to rapid precipitation and the formation of smaller particles, the precipitate remains less settled than the precipitate prepared homogeneously. Note, as well, the difference in the color of the two precipitates.



Figure 8.5 Two precipitates of $PbCrO_4$. In Beaker A, combining 0.1 M $Pb(NO_3)_2$ and 0.1 M K_2CrO_4 forms the precipitate under conditions of high *RSS*. The precipitate forms rapidly and consists of very small particles. In Beaker B, heating a solution of 0.1 M $Pb(NO_3)_2$, 0.1 M $Cr(NO_3)_3$, and 0.1 M $KBrO_3$ slowly oxidizes Cr^{3+} to CrO_4^{2-}, precipitating $PbCrO_4$ under conditions of low *RSS*. The precipitate forms slowly and consists of much larger particles.

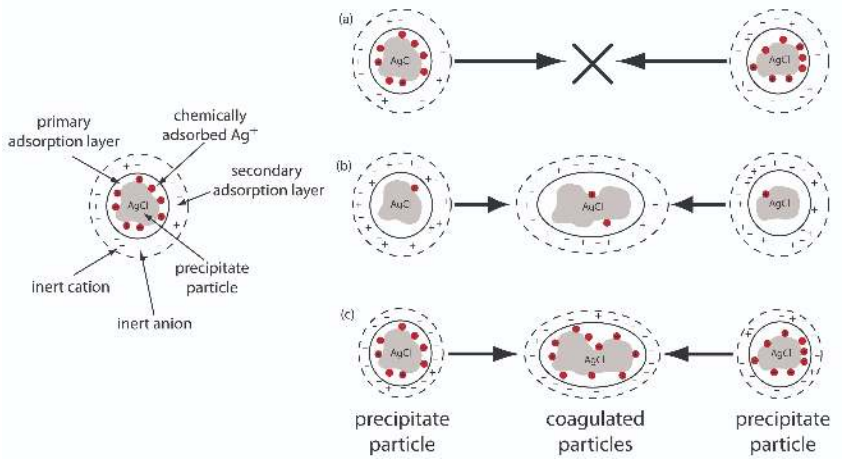
Note

The effect of particle size on color is well-known to geologists, who use a streak test to help identify minerals. The color of a bulk mineral and its color when powdered are often different. Rubbing a mineral across an unglazed porcelain plate leaves behind a small streak of the powdered mineral. Bulk samples of hematite, Fe_2O_3, are black in color, but its streak is a familiar rust-red. Crocite, the mineral $PbCrO_4$, is red-orange in color; its streak is orange-yellow.

A homogeneous precipitation produces large particles of precipitate that are relatively free from impurities. These advantages, however, are offset by requiring more time to produce the precipitate and a tendency for the precipitate to deposit as a thin film on the container's walls. The latter problem is particularly severe for hydroxide precipitates generated using urea.

An additional method for increasing particle size deserves mention. When a precipitate's particles are electrically neutral they tend to coagulate into larger particles that are easier to filter. Surface adsorption of excess lattice ions, however, provides the precipitate's particles with a net positive or a net negative surface charge. Electrostatic repulsion between the particles prevents them from coagulating into larger particles.

Let's use the precipitation of AgCl from a solution of $AgNO_3$ using NaCl as a precipitant to illustrate this effect. Early in the precipitation, when NaCl is the limiting reagent, excess Ag^+ ions chemically adsorb to the AgCl particles, forming a positively charged primary adsorption layer (Figure 8.6a). The solution in contact with this layer contains more inert anions, NO_3^- in this case, than inert cations, Na^+, giving a secondary adsorption layer with a negative charge that balances the primary adsorption layer's positive charge. The solution outside the secondary adsorption layer remains electrically neutral. **Coagulation** cannot occur if the secondary adsorption layer is too thick because the individual particles of AgCl are unable to approach each other closely enough.



https://chem.libretexts.org/@go/page/70684

Figure 8.6 Two methods for coagulating a precipitate of AgCl. (a) Coagulation does not happen due to the electrostatic repulsion between the two positively charged particles. (b) Decreasing the charge within the primary adsorption layer, by adding additional NaCl, decreases the electrostatic repulsion, allowing the particles to coagulate. (c) Adding additional inert ions decreases the thickness of the secondary adsorption layer. Because the particles can approach each other more closely, they are able to coagulate.

We can induce coagulation in three ways: by decreasing the number of chemically adsorbed Ag^+ ions, by increasing the concentration of inert ions, or by heating the solution. As we add additional NaCl, precipitating more of the excess Ag^+, the number of chemically adsorbed silver ions decreases and coagulation occurs (Figure 8.6b). Adding too much NaCl, however, creates a primary adsorption layer of excess Cl^- with a loss of coagulation.

> **Note**
>
> The coagulation and decoagulation of AgCl as we add NaCl to a solution of $AgNO_3$ can serve as an endpoint for a titration. See Chapter 9 for additional details.

A second way to induce coagulation is to add an inert electrolyte, which increases the concentration of ions in the secondary adsorption layer. With more ions available, the thickness of the secondary absorption layer decreases. Particles of precipitate may now approach each other more closely, allowing the precipitate to coagulate. The amount of electrolyte needed to cause spontaneous coagulation is called the critical coagulation concentration.

Heating the solution and precipitate provides a third way to induce coagulation. As the temperature increases, the number of ions in the primary adsorption layer decreases, lowering the precipitate's surface charge. In addition, heating increases the particles' kinetic energy, allowing them to overcome the electrostatic repulsion that prevents coagulation at lower temperatures.

Filtering the Precipitate

After precipitating and digesting the precipitate, we separate it from solution by filtering. The most common filtration method uses filter paper, which is classified according to its speed, its size, and its ash content on ignition. Speed, or how quickly the supernatant passes through the filter paper, is a function of the paper's pore size. A larger pore allows the supernatant to pass more quickly through the filter paper, but does not retain small particles of precipitate. Filter paper is rated as fast (retains particles larger than 20–25 μm), medium–fast (retains particles larger than 16 μm), medium (retains particles larger than 8 μm), and slow (retains particles larger than 2–3 μm). The proper choice of filtering speed is important. If the filtering speed is too fast, we may fail to retain some of the precipitate, causing a negative determinate error. On the other hand, the precipitate may clog the pores if we use a filter paper that is too slow.

> **Note**
>
> A filter paper's size is just its diameter. Filter paper comes in many sizes, including 4.25 cm, 7.0 cm, 11.0 cm, 12.5 cm, 15.0 cm, and 27.0 cm. Choose a size that fits comfortably into your funnel. For a typical 65-mm long-stem funnel, 11.0 cm and 12.5 cm filter paper are good choices.

Because filter paper is hygroscopic, it is not easy to dry it to a constant weight. When accuracy is important, the filter paper is removed before determining the precipitate's mass. After transferring the precipitate and filter paper to a covered crucible, we heat the crucible to a temperature that coverts the paper to $CO_2(g)$ and $H_2O(g)$, a process called **ignition**.

> **Note**
>
> Igniting a poor quality filter paper leaves behind a residue of inorganic ash. For quantitative work, use a low-ash filter paper. This grade of filter paper is pretreated with a mixture of HCl and HF to remove inorganic materials. Quantitative filter paper typically has an ash content of less than 0.010% w/w.

Gravity filtering is accomplished by folding the filter paper into a cone and placing it in a long-stem funnel (Figure 8.7). A seal between the filter cone and the funnel is formed by dampening the paper with water or supernatant, and pressing the paper to the wall of the funnel. When properly prepared, the funnel's stem fills with the supernatant, increasing the rate of filtration.

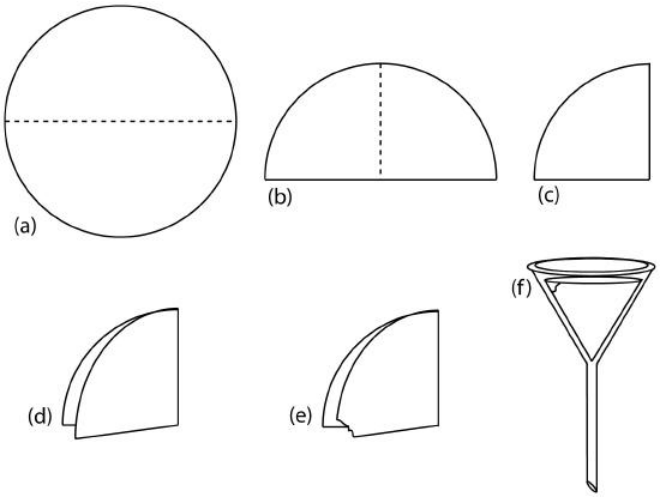


Figure 8.7 Preparing a filter paper cone. The filter paper circle in (a) is folded in half (b), and folded in half again (c). The folded filter paper is parted (d) and a small corner is torn off (e). The filter paper is opened up into a cone and placed in the funnel (f).

The precipitate is transferred to the filter in several steps. The first step is to decant the majority of the **supernatant** through the filter paper without transferring the precipitate (Figure 8.8). This prevents the filter paper from clogging at the beginning of the filtration process. The precipitate is rinsed while it remains in its beaker, with the rinsings decanted through the filter paper. Finally, the precipitate is transferred onto the filter paper using a stream of rinse solution. Any precipitate clinging to the walls of the beaker is transferred using a rubber policeman (a flexible rubber spatula attached to the end of a glass stirring rod).

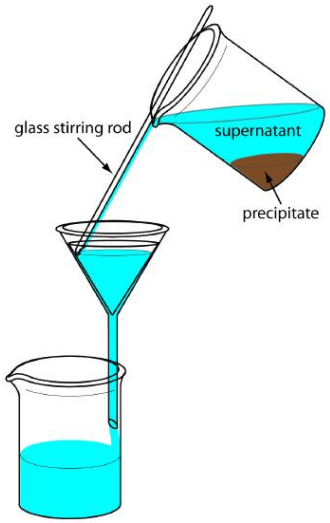


Figure 8.8 Proper procedure for transferring the supernatant to the filter paper cone.

An alternative method for filtering a precipitate is a filtering crucible. The most common is a fritted-glass crucible containing a porous glass disk filter. Fritted-glass crucibles are classified by their porosity: coarse (retaining particles larger than 40–60 μm), medium (retaining particles greater than 10–15 μm), and fine (retaining particles greater than 4–5.5 μm). Another type of filtering crucible is the Gooch crucible, which is a porcelain crucible with a perforated bottom. A glass fiber mat is placed in the crucible to retain the precipitate. For both types of crucibles, the precipitate is transferred in the same manner described earlier for filter paper. Instead of using gravity, the supernatant is drawn through the crucible with the assistance of suction from a vacuum aspirator or pump (Figure 8.9).

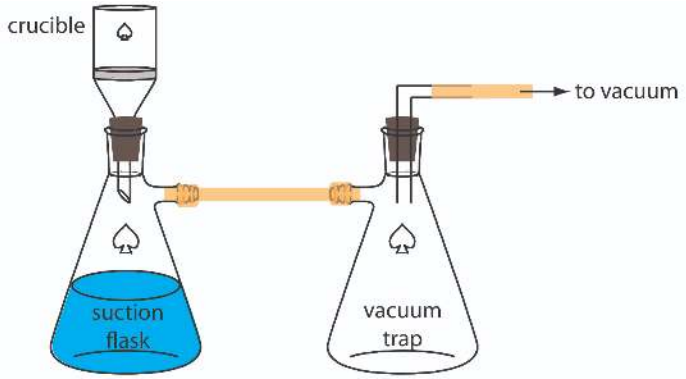


Figure 8.9 Procedure for filtering a precipitate through a filtering crucible. The trap prevents water from an aspirator from back-washing into the suction flask.

Rinsing the Precipitate

Because the supernatant is rich with dissolved inert ions, we must remove any residual traces of supernatant to avoid a positive determinate error without incurring solubility losses. In many cases this simply involves the use of cold solvents or rinse solutions containing organic solvents such as ethanol. The pH of the rinse solution is critical if the precipitate contains an acidic or basic ion. When coagulation plays an important role in determining particle size, adding a volatile inert electrolyte to the rinse solution prevents the precipitate from reverting into smaller particles that might pass through the filter. This process of reverting to smaller particles is called **peptization**. The volatile electrolyte is removed when drying the precipitate.

In general, we can minimize the loss of analyte by using several small portions of rinse solution instead of a single large volume. Testing the used rinse solution for the presence of impurities is another way to guard against over rinsing the precipitate. For example, if Cl^- is a residual ion in the supernatant, we can test for its presence using $AgNO_3$. After collecting a small portion of the rinse solution, we add a few drops of $AgNO_3$ and look for the presence or absence of a precipitate of AgCl. If a precipitate forms, then we know that Cl^- is present and continue to rinse the precipitate. Additional rinsing is not needed if the $AgNO_3$ does not produce a precipitate.

Drying the Precipitate

After separating the precipitate from its supernatant solution, the precipitate is dried to remove residual traces of rinse solution and any volatile impurities. The temperature and method of drying depend on the method of filtration and the precipitate's desired chemical form. Placing the precipitate in a laboratory oven and heating to a temperature of 110°C is sufficient when removing water and other easily volatilized impurities. Higher temperatures require a muffle furnace, a Bunsen burner, or a Meker burner, and are necessary if we need to thermally decompose the precipitate before weighing.

Because filter paper absorbs moisture, we must remove it before weighing the precipitate. This is accomplished by folding the filter paper over the precipitate and transferring both the filter paper and the precipitate to a porcelain or platinum crucible. Gentle heating first dries and then chars the filter paper. Once the paper begins to char, we slowly increase the temperature until all traces of the filter paper are gone and any remaining carbon is oxidized to CO_2.

Fritted-glass crucibles can not withstand high temperatures and must be dried in an oven at temperatures below 200°C. The glass fiber mats used in Gooch crucibles can be heated to a maximum temperature of approximately 500°C.

Composition of the Final Precipitate

For a quantitative application, the final precipitate must have a well-defined composition. Precipitates containing volatile ions or substantial amounts of hydrated water, are usually dried at a temperature that completely removes these volatile species. For example, one standard gravimetric method for the determination of magnesium involves its precipitation as $MgNH_4PO_4 \cdot 6H_2O$. Unfortunately, this precipitate is difficult to dry at lower temperatures without losing an inconsistent amount of hydrated water and ammonia. Instead, the precipitate is dried at temperatures above 1000°C where it decomposes to magnesium pyrophosphate, $Mg_2P_2O_7$.

An additional problem is encountered if the isolated solid is nonstoichiometric. For example, precipitating Mn^{2+} as $Mn(OH)_2$ and heating frequently produces a nonstoichiometric manganese oxide, MnO_x, where *x* varies between one and two. In this case the nonstoichiometric product is the result of forming of a mixture of oxides with different oxidation state of manganese. Other nonstoichiometric compounds form as a result of lattice defects in the crystal structure.[7]

Note

The best way to appreciate the theoretical and practical details discussed in this section is to carefully examine a typical precipitation gravimetric method. Although each method is unique, the determination of Mg^{2+} in water and wastewater by precipitating $MgNH_4PO_4 \cdot 6H_2O$ and isolating $Mg_2P_2O_7$ provides an instructive example of a typical procedure. The description here is based on Method 3500-Mg D in *Standard Methods for the Examination of Water and Wastewater*, 19th Ed., American Public Health Association: Washington, D. C., 1995. With the publication of the 20th Edition in 1998, this method is no longer listed as an approved method.

Representative Method 8.1

Determination of Mg^{2+} in Water and Wastewater

Description of Method

Magnesium is precipitated as $MgNH_4PO_4 \cdot 6H_2O$ using $(NH_4)_2HPO_4$ as the precipitant. The precipitate's solubility in neutral solutions is relatively high (0.0065 g/100 mL in pure water at 10°C), but it is much less soluble in the presence of dilute ammonia (0.0003 g/100 mL in 0.6 M NH_3). Because the precipitant is not selective, a preliminary separation of Mg^{2+} from potential interferents is necessary. Calcium, which is the most significant interferent, is removed by precipitating it as CaC_2O_4. The presence of excess ammonium salts from the precipitant, or the addition of too much ammonia leads to the formation of $Mg(NH_4)_4(PO_4)_2$, which forms $Mg(PO_3)_2$ after drying. The precipitate is isolated by filtering, using a rinse solution of dilute ammonia. After filtering, the precipitate is converted to $Mg_2P_2O_7$ and weighed.

Procedure

Transfer a sample containing no more than 60 mg of Mg^{2+} into a 600-mL beaker. Add 2–3 drops of methyl red indicator, and, if necessary, adjust the volume to 150 mL. Acidify the solution with 6 M HCl and add 10 mL of 30% w/v $(NH_4)_2HPO_4$. After cooling and with constant stirring, add concentrated NH_3 dropwise until the methyl red indicator turns yellow (pH > 6.3). After stirring for 5 min, add 5 mL of concentrated NH_3 and continue stirring for an additional 10 min. Allow the resulting solution and precipitate to stand overnight. Isolate the precipitate by filtering through filter paper, rinsing with 5% v/v NH_3. Dissolve the precipitate in 50 mL of 10% v/v HCl, and precipitate a second time following the same procedure. After filtering, carefully remove the filter paper by charring. Heat the precipitate at 500°C until the residue is white, and then bring the precipitate to constant weight at 1100°C.

Questions

1. Why does the procedure call for a sample containing no more than 60 mg of Mg^{2+}?

A 60-mg portion of Mg^{2+} generates approximately 600 mg of $MgNH_4PO_4 \cdot 6H_2O$. This is a substantial amount of precipitate. A larger quantity of precipitate may be difficult to filter and difficult to adequately rinse free of impurities.

2. Why is the solution acidified with HCl before adding the precipitant?

The HCl ensures that $MgNH_4PO_4 \cdot 6H_2O$ does not immediately precipitate when adding the precipitant. Because PO_4^{3-} is a weak base, the precipitate is soluble in a strongly acidic solution. If the precipitant is added under neutral or basic conditions (high *RSS*) the resulting precipitate consists of smaller, less pure particles. Increasing the pH by adding base allows the precipitate to form under more favorable (low *RSS*) conditions.

3. Why is the acid–base indicator methyl red added to the solution?

The indicator's color change, which occurs at a pH of approximately 6.3, indicates when there is sufficient NH_3 to neutralize the HCl added at the beginning of the procedure. The amount of NH_3 is crucial to this procedure. If we add insufficient NH_3, then the solution is too acidic, which increases the precipitate's solubility and leads to a negative determinate error. If we add too much NH_3, the precipitate may contain traces of $Mg(NH_4)_4(PO_4)_2$, which, on drying, forms $Mg(PO_3)_2$ instead of $Mg_2P_2O_7$. This

increases the mass of the ignited precipitate, giving a positive determinate error. After adding enough NH_3 to neutralize the HCl, we add the additional 5 mL of NH_3 to quantitatively precipitate $MgNH_4PO_4 \cdot 6H_2O$.

4. Explain why forming $Mg(PO_3)_2$ instead of $Mg_2P_2O_7$ increases the precipitate's mass.

Each mole of $Mg_2P_2O_7$ contains two moles of phosphorous and each mole of $Mg(PO_3)_2$ contains only one mole of phosphorous A conservation of mass, therefore, requires that two moles of $Mg(PO_3)_2$ form in place of each mole of $Mg_2P_2O_7$. One mole of $Mg_2P_2O_7$ weighs 222.6 g. Two moles of $Mg(PO_3)_2$ weigh 364.5 g. Any replacement of $Mg_2P_2O_7$ with $Mg(PO_3)_2$ must increase the precipitate's mass.

5. What additional steps, beyond those discussed in questions 2 and 3, help improve the precipitate's purity?

Two additional steps in the procedure help in forming a precipitate that is free of impurities: digestion and reprecipitation.

6. Why is the precipitate rinsed with a solution of 5% v/v NH_3?

This is done for the same reason that precipitation is carried out in an ammonical solution; using dilute ammonia minimizes solubility losses when rinsing the precipitate.

8.2.2 Quantitative Applications

Although no longer a commonly used technique, precipitation gravimetry still provides a reliable means for assessing the accuracy of other methods of analysis, or for verifying the composition of standard reference materials. In this section we review the general application of precipitation gravimetry to the analysis of inorganic and organic compounds.

Inorganic Analysis

Table 8.1 provides a summary of some precipitation gravimetric methods for inorganic cations and anions. Several methods for the homogeneous generation of precipitants are shown in Table 8.2. The majority of inorganic precipitants show poor selectivity for the analyte. Many organic precipitants, however, are selective for one or two inorganic ions. Table 8.3 lists several common organic precipitants.

Precipitation gravimetry continues to be listed as a standard method for the determination of SO_4^{2-} in water and wastewater analysis.[8] Precipitation is carried out using $BaCl_2$ in an acidic solution (adjusted with HCl to a pH of 4.5–5.0) to prevent the possible precipitation of $BaCO_3$ or $Ba_3(PO_4)_2$, and near the solution's boiling point. The precipitate is digested at 80–90°C for at least two hours. Ashless filter paper pulp is added to the precipitate to aid in filtration. After filtering, the precipitate is ignited to constant weight at 800°C. Alternatively, the precipitate is filtered through a fine porosity fritted glass crucible (without adding filter paper pulp), and dried to constant weight at 105°C. This procedure is subject to a variety of errors, including occlusions of $Ba(NO_3)_2$, $BaCl_2$, and alkali sulfates.

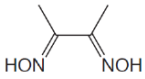
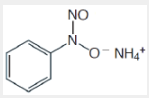
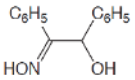
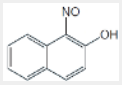
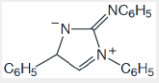
Table 8.1 Selected Precipitation Gravimetric Methods for Inorganic Cations and Anions (Arranged by Precipitant)

Analyte	Precipitant	Precipitate Formed	Precipitate Weighed
Ba^{2+}	$(NH_4)_2CrO_4$	$BaCrO_4$	$BaCrO_4$
Pb^{2+}	K_2CrO_4	$PbCrO_4$	$PbCrO_4$
Ag^{+}	HCl	AgCl	AgCl
Hg_2^{2+}	HCl	Hg_2Cl_2	Hg_2Cl_2
Al^{3+}	NH_3	$Al(OH)_3$	Al_2O_3
Be^{2+}	NH_3	$Be(OH)_2$	BeO
Fe^{3+}	NH_3	$Fe(OH)_3$	Fe_2O_3
Ca^{2+}	$(NH_4)_2C_2O_4$	CaC_2O_4	$CaCO_3$ or CaO
Sb^{3+}	H_2S	Sb_2S_3	Sb_2S_3
As^{3+}	H_2S	As_2S_3	As_2S_3
Hg^{2+}	H_2S	HgS	HgS
Ba^{2+}	H_2SO_4	$BaSO_4$	$BaSO_4$
Pb^{2+}	H_2SO_4	$PbSO_4$	$PbSO_4$
Sr^{2+}	H_2SO_4	$SrSO_4$	$SrSO_4$
Be^{3+}	$(NH_4)_2HPO_4$	NH_4BePO_4	$Be_2P_2O_7$
Mg^{2+}	$(NH_4)_2HPO_4$	NH_4MgPO_4	$Mg_2P_2O_7$
Zn^{2+}	$(NH_4)_2HPO_4$	NH_4ZnPO_4	$Zn_2P_2O_7$
Sr^{2+}	KH_2PO_4	$SrHPO_4$	$Sr_2P_2O_7$
CN^{-}	$AgNO_3$	AgCN	AgCN
I^{-}	$AgNO_3$	AgI	AgI
Br^{-}	$AgNO_3$	AgBr	AgBr
Cl^{-}	$AgNO_3$	AgCl	AgCl
ClO_3^{-}	$FeSO_4$/ $AgNO_3$	AgCl	AgCl
SCN^{-}	SO_2/ $CuSO_4$	CuSCN	CuSCN
SO_4^{2-}	$BaCl_2$	$BaSO_4$	$BaSO_4$

Table 8.2 Reactions for the Homogeneous Preparation of Selected Inorganic Precipitants

Precipitant	Reaction
OH^-	$(NH_2)_2CO(aq) + 3H_2O(l) \leftrightharpoons 2NH_4^+(aq) + CO_2(g) + 2OH^-(aq)$
SO_4^{2-}	$NH_2HSO_3(aq) + 2H_2O(l) \leftrightharpoons NH_4^+(aq) + H_3O^+(aq) + SO_4^{2-}(aq)$
S^{2-}	$CH_3CSNH_2(aq) + H_2O(l) \leftrightharpoons CH_3CONH_2(aq) + H_2S\ (aq)$
IO_3^-	$HOCH_2CH_2OH(aq) + IO_4^-(aq) \leftrightharpoons 2HCHO(aq) + H_2O(l) + IO_3^-(aq)$
PO_4^{3-}	$(CH_3O)_3PO(aq) + 3H_2O(l) \leftrightharpoons 3CH_3OH(aq) + H_3PO_4(aq)$
$C_2O_4^{2-}$	$(C_2H_5)_2C_2O_4(aq) + 2H_2O(l) \leftrightharpoons 2C_2H_5OH(aq) + H_2C_2O_4(aq)$
CO_3^{2-}	$Cl_3CCOOH(aq) + 2OH^-(aq) \leftrightharpoons CHCl_3(aq) + CO_3^{2-}(aq) + H_2O(l)$

Table 8.3 Selected Precipitation Gravimetric Methods for Inorganic Ions Using an Organic Precipitant

Analyte	Precipitant	Structure	Precipitate Formed	Precipitate Weighed
Ni^{2+}	dimethylglyoxime		$Ni(C_4H_7O_2N_2)_2$	$Ni(C_4H_7O_2N_2)_2$
Fe^{3+}	cupferron		$Fe(C_6H_5N_2O_2)_3$	Fe_2O_3
Cu^{2+}	cupron		$CuC_{14}H_{11}O_2N$	$CuC_{14}H_{11}O_2N$
Co^{2+}	1-nitrso-2-napthol		$Co(C_{10}H_6O_2N)_3$	Co or $CoSO_4$
K^+	sodium tetraphenylborate	$Na[B(C_6H_5)_4]$	$K[B(C_6H_5)_4$	$K[B(C_6H_5)_4$
NO_3^-	nitron		$C_{20}H_{16}N_4HNO_3$	$C_{20}H_{16}N_4HNO_3$

Organic Analysis

Several organic functional groups or heteroatoms can be determined using precipitation gravimetric methods. Table 8.4 provides a summary of several representative examples. Note that the procedure for the determination of alkoxy functional groups is an indirect analysis.

Table 8.4: Selected Precipitation Gravimetric Methods for the Analysis of Organic Functional Groups and Heteroatoms

Analyte	Treatment	Precipitant	Precipitate
Organic halides R–X X = Cl, Br, I	Oxidation with HNO_3 in the presence of Ag^+	$AgNO_3$	AgX
Organic halides R–X X = Cl, Br, I	Combustion in O_2 (with a Pt catalyst) in the presence of Ag^+	$AgNO_3$	AgX
Organic sulfur	Oxidation with HNO_3 in the presence of Ba^{2+}	$BaCl_2$	$BaSO_4$
Organic sulfur	Combustion in O_2 (with Pt catalyst) with SO_2 and SO_3 collected in dilute H_2O_2	$BaCl_2$	$BaSO_4$
Alkoxy groups –O–R or –COO–R R = CH_3 or C_2H_5	Reaction with HI to produce RI	$AgNO_3$	AgI

Quantitative Calculations

The stoichiometry of a precipitation reaction provides a mathematical relationship between the analyte and the precipitate. Because a precipitation gravimetric method may involve several chemical reactions before the precipitation reaction, knowing the stoichiometry of the precipitation reaction may not be sufficient. Even if you do not have a complete set of balanced chemical reactions, you can deduce the mathematical relationship between the analyte and the precipitate using a conservation of mass. The following example demonstrates the application of this approach to the direct analysis of a single analyte.

Example 8.1

To determine the amount of magnetite, Fe_3O_4, in an impure ore, a 1.5419-g sample is dissolved in concentrated HCl, giving a mixture of Fe^{2+} and Fe^{3+}. After adding HNO_3 to oxidize Fe^{2+} to Fe^{3+} and diluting with water, Fe^{3+} is precipitated as $Fe(OH)_3$ by adding NH_3. Filtering, rinsing, and igniting the precipitate provides 0.8525 g of pure Fe_2O_3. Calculate the %w/w Fe_3O_4 in the sample.

Solution

A conservation of mass requires that all the iron from the ore is found in the Fe_2O_3. We know there are 2 moles of Fe per mole of Fe_2O_3 (FW = 159.69 g/mol) and 3 moles of Fe per mole of Fe_3O_4 (FW = 231.54 g/mol); thus

$$0.8525 \text{ g } Fe_2O_3 \times \frac{2 \text{ mol Fe}}{159.69 \text{ g } Fe_2O_3} \times \frac{231.54 \text{ g } Fe_3O_4}{3 \text{ mol Fe}} = 0.82405 \text{ g } Fe_3O_4 \tag{8.2.4}$$

The % w/w s Fe_3O_4 in the sample, therefore, is

$$\frac{0.82405 \text{ g } Fe_3O_4}{1.5419 \text{ g sample}} \times 100 = 53.44\% \text{ w/w } Fe_3O_4 \tag{8.2.5}$$

Practice Exercise 8.2

A 0.7336-g sample of an alloy containing copper and zinc is dissolved in 8 M HCl and diluted to 100 mL in a volumetric flask. In one analysis, the zinc in a 25.00-mL portion of the solution is precipitated as $ZnNH_4PO_4$, and subsequently isolated as $Zn_2P_2O_7$, yielding 0.1163 g. The copper in a separate 25.00-mL portion of the solution is treated to precipitate CuSCN, yielding 0.2931 g. Calculate the %w/w Zn and the %w/w Cu in the sample.

Click here to review your answer to this exercise.

In Practice Exercise 8.2 the sample contains two analytes. Because we can selectively precipitate each analyte, finding their respective concentrations is a straightforward stoichiometric calculation. But what if we cannot precipitate the two analytes

separately? To find the concentrations of both analytes, we still need to generate two precipitates, at least one of which must contain both analytes. Although this complicates the calculations, we can still use a conservation of mass to solve the problem.

Example 8.2

A 0.611-g sample of an alloy containing Al and Mg is dissolved and treated to prevent interferences by the alloy's other constituents. Aluminum and magnesium are precipitated using 8-hydroxyquinoline, providing a mixed precipitate of $Al(C_9H_6NO)_3$ and $Mg(C_9H_6NO)_2$ that weighs 7.815 g. Igniting the precipitate converts it to a mixture of Al_2O_3 and MgO that weighs 1.002 g. Calculate the %w/w Al and %w/w Mg in the alloy.

Solution

The masses of the solids provide us with the following two equations.

$$\text{g Al}(C_9H_6NO)_3 + \text{g Mg}(C_9H_6NO)_2 = 7.815 \text{ g} \tag{8.2.6}$$

$$\text{g } Al_2O_3 + \text{g MgO} = 1.002 \text{ g} \tag{8.2.7}$$

With two equations and four unknowns, we need two additional equations to solve the problem. A conservation of mass requires that all the aluminum in $Al(C_9H_6NO)_3$ is found in Al_2O_3; thus

$$\text{g } Al_2O_3 = \text{g Al}(C_9H_6NO)_3 \times \frac{1 \text{ mol Al}}{459.45 \text{ g Al}(C_9H_6NO)_3} \times \frac{101.96 \text{ g } Al_2O_3}{2 \text{ mol } Al_2O_3} \tag{8.2.8}$$

$$\text{g } Al_2O_3 = 0.11096 \times \text{g Al}(C_9H_6NO)_3 \tag{8.2.9}$$

Using the same approach, a conservation of mass for magnesium gives

$$\text{g MgO} = \text{g Mg}(C_9H_6NO)_2 \times \frac{1 \text{ mol Mg}}{312.61 \text{ g Mg}(C_9H_6NO)_2} \times \frac{40.304 \text{ g MgO}}{\text{mol Mg}} \tag{8.2.10}$$

$$\text{g MgO} = 0.12893 \times \text{g Mg}(C_9H_6NO)_2 \tag{8.2.11}$$

Substituting the equations for g MgO and g Al_2O_3 into the equation for the combined weights of MgO and Al_2O_3 leaves us with two equations and two unknowns.

$$\text{g Al}(C_9H_6NO)_3 + \text{g Mg}(C_9H_6NO)_2 = 7.815 \text{ g} \tag{8.2.12}$$

$$0.11096 \times \text{g Al}(C_9H_6NO)_3 + 0.12893 \times \text{g Mg}(C_9H_6NO)_2 = 1.002 \text{ g} \tag{8.2.13}$$

Multiplying the first equation by 0.11096 and subtracting the second equation gives

$$-0.01797 \times \text{g Mg}(C_9H_6NO)_2 = -0.1348 \text{ g} \tag{8.2.14}$$

$$\text{g Mg}(C_9H_6NO)_2 = 7.501 \text{ g} \tag{8.2.15}$$

$$\text{g Al}(C_9H_6NO)_3 = 7.815 \text{ g} - 7.501 \text{ g Mg}(C_9H_6NO)_2 = 0.314 \text{ g} \tag{8.2.16}$$

Now we can finish the problem using the approach from Example 8.1. A conservation of mass requires that all the aluminum and magnesium in the sample of Dow metal is found in the precipitates of $Al(C_9H_6NO)_3$ and the $Mg(C_9H_6NO)_2$. For aluminum, we find that

$$0.314 \text{ g Al}(C_9H_6NO)_3 \times \frac{1 \text{ mol Al}}{459.45 \text{ g Al}(C_9H_6NO)_3} \times \frac{26.982 \text{ g Al}}{\text{mol Al}} = 0.01844 \text{ g Al} \tag{8.2.17}$$

$$\frac{0.01844 \text{ g Al}}{0.611 \text{ g sample}} \times 100 = 3.02\% \text{ w/w Al} \tag{8.2.18}$$

and for magnesium we have

$$7.501 \text{ g Mg}(C_9H_6NO)_2 \times \frac{1 \text{ mol Mg}}{312.61 \text{ g Mg}(C_9H_6NO)_2} \times \frac{24.305 \text{ g Mg}}{\text{mol Mg}} = 0.5832 \text{ g Mg} \tag{8.2.19}$$

$$\frac{0.5832 \text{ g Mg}}{0.611 \text{ g sample}} \times 100 = 95.5\% \text{ w/w Mg} \tag{8.2.20}$$

Practice Exercise 8.3

A sample of a silicate rock weighing 0.8143 g is brought into solution and treated to yield a 0.2692-g mixture of NaCl and KCl. The mixture of chloride salts is subsequently dissolved in a mixture of ethanol and water, and treated with $HClO_4$, precipitating 0.5713 g of $KClO_4$. What is the %w/w Na_2O in the silicate rock?

Click here to review your answer to this exercise.

The previous problems are examples of direct methods of analysis because the precipitate contains the analyte. In an indirect analysis the precipitate forms as a result of a reaction with the analyte, but the analyte is not part of the precipitate. As shown by the following example, despite the additional complexity, we can use conservation principles to organize our calculations.

Example 8.3

An impure sample of Na_3PO_3 weighing 0.1392 g is dissolved in 25 mL of water. A solution containing 50 mL of 3% w/v $HgCl_2$, 20 mL of 10% w/v sodium acetate, and 5 mL of glacial acetic acid is then prepared. Adding the solution of Na_3PO_3 to the solution containing $HgCl_2$, oxidizes PO_3^{3-} to PO_4^{3-}, precipitating Hg_2Cl_2. After digesting, filtering, and rinsing the precipitate, 0.4320 g of Hg_2Cl_2 is obtained. Report the purity of the original sample as % w/w Na_3PO_3.

Solution

This is an example of an indirect analysis because the precipitate, Hg_2Cl_2, does not contain the analyte, Na_3PO_3. Although the stoichiometry of the reaction between Na_3PO_3 and $HgCl_2$ is given earlier in the chapter, let's see how we can solve the problem using conservation principles.

The reaction between Na_3PO_3 and $HgCl_2$ is a redox reaction in which phosphorous increases its oxidation state from +3 in Na_3PO_3 to +5 in Na_3PO_4, and in which mercury decreases its oxidation state from +2 in $HgCl_2$ to +1 in Hg_2Cl_2. A redox reaction must obey a conservation of electrons—all the electrons released by the reducing agent, Na_3PO_3, must be accepted by the oxidizing agent, $HgCl_2$. Knowing this, we write the following stoichiometric conversion factors:

$$\frac{2 \text{ mol } e^-}{\text{mol } Na_3PO_4} \text{ and } \frac{1 \text{ mol } e^-}{\text{mol } HgCl_2} \tag{8.2.21}$$

(Although you can write the balanced reactions for any analysis, applying conservation principles can save you a significant amount of time!)

Now we are ready to solve the problem. First, we use a conservation of mass for mercury to convert the precipitate's mass to the moles of $HgCl_2$.

$$0.4320 \text{ g } Hg_2Cl_2 \times \frac{2 \text{ mol Hg}}{472.09 \text{ g HgCl}} \times \frac{1 \text{ mol } HgCl_2}{\text{mol Hg}} = 1.8302 \times 10^{-3} \text{ mol } HgCl_2 \tag{8.2.22}$$

Next, we use the conservation of electrons to find the mass of Na_3PO_3.

$$1.8302 \times 10^{-3} \text{ mol } HgCl_2 \times \frac{1 \text{ mol } e^-}{\text{mol } HgCl_2} \times \frac{1 \text{ mol } Na_3PO_3}{2 \text{ mol } e^-} \times \frac{147.94 \text{ g } Na_3PO_3}{\text{mol } Na_3PO_3} = 0.13538 \text{ g } Na_3PO_3 \tag{8.2.23}$$

(As you become comfortable with using conservation principles, you will see opportunities for further simplifying problems. For example, a conservation of electrons requires that the electrons released by Na_3PO_3 end up in the product, Hg_2Cl_2, yielding the following stoichiometric conversion factor:

$$\frac{2 \text{ mol } e^-}{\text{mol } Hg_2Cl_2} \tag{8.2.24}$$

This conversion factor provides a direct link between the mass of Hg_2Cl_2 and the mass of Na_3PO_3.)

Finally, we calculate the %w/w Na_3PO_3 in the sample.

$$\frac{0.13538 \text{ g } Na_3PO_3}{0.1392 \text{ g sample}} \times 100 = 97.26\% \text{ w/w } Na_3PO_3 \tag{8.2.25}$$

Practice Exercise 8.4

One approach for determining phosphate, PO_4^{3-}, is to precipitate it as ammonium phosphomolybdate, $(NH_4)_3PO_4 \cdot 12MoO_3$. After isolating the precipitate by filtration, it is dissolved in acid and the molybdate precipitated and weighed as $PbMoO_3$. Suppose we know that our samples contain at least 12.5% Na_3PO_4 and we need to recover a minimum of 0.600 g of $PbMoO_3$? What is the minimum amount of sample needed for each analysis?

Click here to review your answer to this exercise.

8.2.2 Qualitative Applications

A precipitation reaction is a useful method for identifying inorganic and organic analytes. Because a qualitative analysis does not require quantitative measurements, the analytical signal is simply the observation that a precipitate has formed. Although qualitative applications of precipitation gravimetry have been largely replaced by spectroscopic methods of analysis, they continue to find application in spot testing for the presence of specific analytes.[9]

Note

Any of the precipitants listed in Table 8.1, Table 8.3, and Table 8.4 can be used for a qualitative analysis.

8.2.3 Evaluating Precipitation Gravimetry

Scale of Operation

The scale of operation for precipitation gravimetry is limited by the sensitivity of the balance and the availability of sample. To achieve an accuracy of ±0.1% using an analytical balance with a sensitivity of ±0.1 mg, we must isolate at least 100 mg of precipitate. As a consequence, precipitation gravimetry is usually limited to major or minor analytes, in macro or meso samples (see Figure 3.5 in Chapter 3). The analysis of trace level analytes or micro samples usually requires a microanalytical balance.

Accuracy

For a macro sample containing a major analyte, a relative error of 0.1–0.2% is routinely achieved. The principle limitations are solubility losses, impurities in the precipitate, and the loss of precipitate during handling. When it is difficult to obtain a precipitate that is free from impurities, it may be possible to determine an empirical relationship between the precipitate's mass and the mass of the analyte by an appropriate calibration.

Note

Problem 8.27 provides an example of how to determine an analyte's concentration by establishing an empirical relationship between the analyte and the precipitate.

Precision

The relative precision of precipitation gravimetry depends on the sample's size and the precipitate's mass. For a smaller amount of sample or precipitate, a relative precision of 1–2 ppt is routinely obtained. When working with larger amounts of sample or precipitate, the relative precision can be extended to several ppm. Few quantitative techniques can achieve this level of precision.

Sensitivity

For any precipitation gravimetric method we can write the following general equation relating the signal (grams of precipitate) to the absolute amount of analyte in the sample

$$\text{grams precipitate} = k \times \text{grams analyte} \tag{8.13}$$

Note

Equation 8.13 assumes that we have used a suitable blank to correct the signal for any contributions of the reagent to the precipitate's mass.

where k, the method's sensitivity, is determined by the stoichiometry between the precipitate and the analyte. Consider, for example, the determination of Fe as Fe_2O_3. Using a conservation of mass for iron, the precipitate's mass is

$$\text{g Fe}_2\text{O}_3 = \text{g Fe} \times \frac{\text{1 mol Fe}}{\text{AW Fe}} \times \frac{\text{FW Fe}_2\text{O}_3}{\text{2 mol Fe}} \tag{8.2.26}$$

and the value of k is

$$k = \frac{1}{2} \times \frac{\text{FW Fe}_2\text{O}_3}{\text{AW Fe}} \tag{8.14}$$

As we can see from equation 8.14, there are two ways to improve a method's sensitivity. The most obvious way to improve sensitivity is to increase the ratio of the precipitate's molar mass to that of the analyte. In other words, it helps to form a precipitate with the largest possible formula weight. A less obvious way to improve a method's sensitivity is indicated by the term of 1/2 in equation 8.14, which accounts for the stoichiometry between the analyte and precipitate. We can also improve sensitivity by forming a precipitate that contains fewer units of the analyte.

Practice Exercise 8.5

Suppose you wish to determine the amount of iron in a sample. Which of the following compounds—FeO, Fe_2O_3, or Fe_3O_4—provides the greatest sensitivity?

Click here to review your answer to this exercise.

Selectivity

Due to the chemical nature of the precipitation process, precipitants are usually not selective for a single analyte. For example, silver is not a selective precipitant for chloride because it also forms precipitates with bromide and iodide. Interferents are often a serious problem and must be considered if accurate results are to be obtained.

Time, Cost, and Equipment

Precipitation gravimetry is time intensive and rarely practical if you have a large number of samples to analyze. However, because much of the time invested in precipitation gravimetry does not require an analyst's immediate supervision, it may be a practical alternative when working with only a few samples. Equipment needs are few—beakers, filtering devices, ovens or burners, and balances—inexpensive, routinely available in most laboratories, and easy to maintain.

Contributors

David Harvey (DePauw University)

8.2: Precipitation Gravimetry is shared under a CC BY-NC-SA 4.0 license and was authored, remixed, and/or curated by LibreTexts.

8.3: Volatilization Gravimetry

A second approach to gravimetry is to thermally or chemically decompose the sample and measure the resulting change in its mass. Alternatively, we can trap and weigh a volatile decomposition product. Because the release of a volatile species is an essential part of these methods, we classify them collectively as volatilization gravimetric methods of analysis.

8.3.1 Theory and Practice

Whether an analysis is direct or indirect, volatilization gravimetry usually requires that we know the products of the decomposition reaction. This is rarely a problem for organic compounds, which typically decompose to form simple gases such as CO_2, H_2O, and N_2. For an inorganic compound, however, the products often depend on the decomposition temperature.

Thermogravimetry

One method for determining the products of a thermal decomposition is to monitor the sample's mass as a function of temperature, a process called **thermogravimetry**. Figure 8.10 shows a typical thermogram in which each change in mass—each "step" in the thermogram—represents the loss of a volatile product. As shown in Example 8.4, we can use a **thermogram** to identify a compound's decomposition reactions.

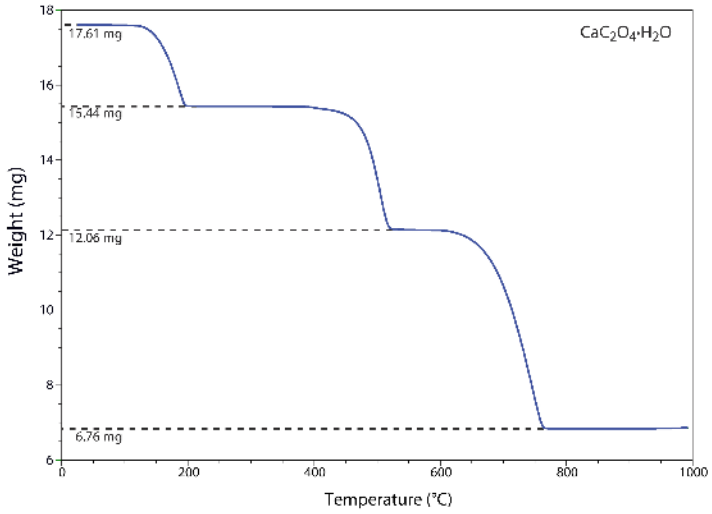


Figure 8.10 Thermogram for $CaC_2O_4 \cdot H_2O$ obtained by heating a sample from room temperature to 1000°C at a rate of 20°C/min. Each change in mass results from the loss of a volatile product. The sample's initial mass and its mass after each loss are shown by the dotted lines. See Example 8.4 for information on interpreting this thermogram.

Example 8.4

The thermogram in Figure 8.10 shows the mass of a sample of calcium oxalate monohydrate, $CaC_2O_4 \cdot H_2O$, as a function of temperature. The original sample weighing 17.61 mg was heated from room temperature to 1000°C at a rate of 20°C per minute. For each step in the thermogram, identify the volatilization product and the solid residue that remains.

Solution

From 100–250°C the sample loses 17.61 mg – 15.44 mg, or 2.17 mg, which is

$$\frac{2.17 \text{ mg}}{17.61 \text{ mg}} \times 100 = 12.3\% \tag{8.3.1}$$

of the sample's original mass. In terms of $CaC_2O_4 \cdot H_2O$, this corresponds to a loss of

$$0.123 \times 146.11 \text{ g/mol} = 18.0 \text{ g/mol} \tag{8.3.2}$$

The product's molar mass and the temperature range for the decomposition, suggest that this is a loss of $H_2O(g)$, leaving a residue of CaC_2O_4.

The loss of 3.38 mg from 350–550°C is a 19.2% decrease in the sample's original mass, or a loss of

$$0.192 \times 146.11 \text{ g/mol} = 28.1 \text{ g/mol} \tag{8.3.3}$$

which is consistent with the loss of $CO(g)$ and a residue of $CaCO_3$.

Finally, the loss of 5.30 mg from 600-800°C is a 30.1% decrease in the sample's original mass, or a loss of

$$0.301 \times 146.11 \text{ g/mol} = 44.0 \text{ g/mol} \tag{8.3.4}$$

This loss in molar mass is consistent with the release of $CO_2(g)$, leaving a final residue of CaO.

Identifying the products of a thermal decomposition provides information that we can use to develop an analytical procedure. For example, the thermogram in Figure 8.10 shows that we must heat a precipitate of $CaC_2O_4 \cdot H_2O$ to a temperature between 250 and 400°C if we wish to isolate and weigh CaC_2O_4. Alternatively, heating the sample to 1000°C allows us to isolate and weigh CaO.

Practice Exercise 8.6

Under the same conditions as Figure 8.10, the thermogram for a 22.16 mg sample of $MgC_2O_4 \cdot H_2O$ shows two steps: a loss of 3.06 mg from 100–250°C and a loss of 12.24 mg from 350–550°C. For each step, identify the volatilization product and the solid residue that remains. Using your results from this exercise and the results from Example 8.4, explain how you can use thermogravimetry to analyze a mixture containing $CaC_2O_4 \cdot H_2O$ and $MgC_2O_4 \cdot H_2O$. You may assume that other components in the sample are inert and thermally stable below 1000°C.

Click here to review your answer to this exercise.

Equipment

Depending on the method of analysis, the equipment for volatilization gravimetry may be simple or complex. In the simplest experimental design, we place the sample in a crucible and decompose it at a fixed temperature using a Bunsen burner, a Meker burner, a laboratory oven, or a muffle furnace. The sample's mass and the mass of the residue are measured using an analytical balance.

Trapping and weighing the volatile products of a thermal decomposition requires specialized equipment. The sample is placed in a closed container and heated. As decomposition occurs, a stream of an inert purge-gas sweeps the volatile products through one or more selective absorbent traps.

In a thermogravimetric analysis, the sample is placed on a small balance pan attached to one arm of an electromagnetic balance (Figure 8.11). The sample is lowered into an electric furnace and the furnace's temperature is increased at a fixed rate of few degrees per minute while continuously monitoring the sample's weight. The instrument usually includes a gas line for purging the volatile decomposition products out of the furnace, and a heat exchanger to dissipate the heat emitted by the furnace.

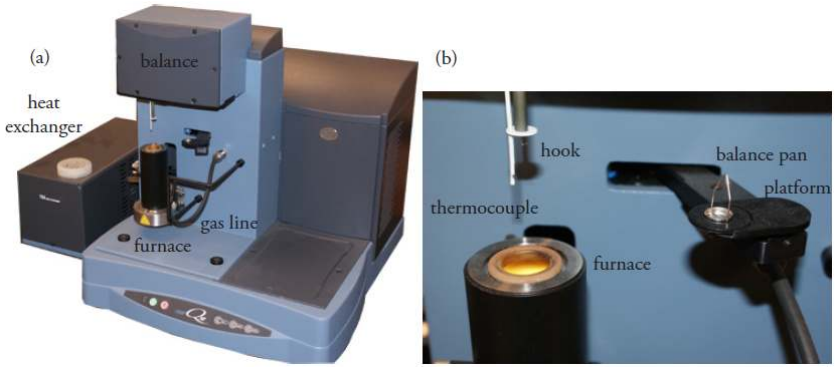


Figure 8.11 (a) Instrumentation for conducting a thermogravimetric analysis. The balance sits on the top of the instrument with the sample suspended below. A gas line supplies an inert gas that sweeps the volatile decomposition products out of the furnace. The heat exchanger dissipates the heat from the furnace to a reservoir of water. (b) Close-up showing the balance pan, which sits on a moving platform, the thermocouple for monitoring temperature, a hook for lowering the sample pan into the furnace, and the opening to the furnace. After placing a small portion of the sample on the balance pan, the platform rotates over the furnace and

transfers the balance pan to a hook that is suspended from the balance. Once the balance pan is in place, the platform rotates back to its initial position. The balance pan and the thermocouple are then lowered into the furnace.

Note

The best way to appreciate the theoretical and practical details discussed in this section is to carefully examine a typical volatilization gravimetric method. Although each method is unique, the determination of Si in ores and alloys by forming volatile SiF_4 provides an instructive example of a typical procedure. The description here is based on a procedure from Young, R. S. *Chemical Analysis in Extractive Metallurgy*, Griffen: London, 1971, pp. 302–304.

Representative Method 8.2

Determination of Si in Ores and Alloys

Description of Method

Silicon is determined by dissolving the sample in acid and dehydrating to precipitate SiO_2. Because a variety of other insoluble oxides also form, the precipitate's mass is not a direct measure of the amount of silicon in the sample. Treating the solid residue with HF results in the formation of volatile SiF_4. The decrease in mass following the loss of SiF_4 provides an indirect measure of the amount of silicon in the original sample.

Procedure

Transfer a sample of between 0.5 and 5.0 g to a platinum crucible along with an excess of Na_2CO_3, and heat until a melt forms. After cooling, dissolve the residue in dilute HCl. Evaporate the solution to dryness on a steam bath and heat the residue, which contains SiO_2 and other solids, for one hour at 110°C. Moisten the residue with HCl and repeat the dehydration. Remove any acid soluble materials from the residue by adding 50 mL of water and 5 mL of concentrated HCl. Bring the solution to a boil and filter through #40 filter paper. (#40 filter paper is a medium speed, ashless filter paper for filtering crystalline solids.) Wash the residue with hot 2% v/v HCl followed by hot water. Evaporate the filtrate to dryness twice and, following the same procedure, treat to remove any acid-soluble materials. Combine the two precipitates, and dry and ignite to a constant weight at 1200°C. After cooling, add 2 drops of 50% v/v H_2SO_4 and 10 mL of HF. Remove the volatile SiF_4 by evaporating to dryness on a hot plate. Finally, bring the residue to constant weight by igniting at 1200°C.

Questions

1. According to the procedure the sample should weigh between 0.5 and 5.0 g. How should you decide upon the amount of sample to use?

In this procedure the critical measurement is the decrease in mass following the volatilization of SiF_4. The reaction responsible for the loss of mass is

$$\mathrm{SiO_2}(s) + 4\mathrm{HF}(aq) \rightarrow \mathrm{SiF_4}(g) + 2\mathrm{H_2O}(l) \qquad (8.3.5)$$

Water and any excess HF are removed during the final ignition, and do not contribute to the change in mass. The loss in mass, therefore, is equivalent to the mass of SiO_2 present after the dehydration step. Every 0.1 g of Si in the original sample results in the loss of 0.21 g of SiO_2.

(Problem 8.31 asks you to verify that this loss of mass is correct.)

How much sample we use depends on what is an acceptable uncertainty when measuring mass. A 0.5-g sample that is 50% w/w in Si, for example, will lose 0.53 g. If we are using a balance that measures mass to the nearest ±0.1 mg, then the relative uncertainty in mass is approximately ±0.02%; this is a reasonable level of uncertainty for a gravimetric analysis. A 0.5 g sample that is only 5% w/w Si experiences a weight loss of only 0.053 g and has a relative uncertainty of ±0.2%. In this case a larger sample is needed.

2. Why are acid-soluble materials removed before treating the dehydrated residue with HF?

Any acid-soluble materials in the sample will react with HF or H_2SO_4. If the products of these reactions are volatile, or if they decompose at 1200°C, then the change in mass is not due solely to the volatilization of SiF_4. As a result, we overestimate the amount of Si in our sample.

3. Why is H_2SO_4 added with the HF?

Many samples containing silicon also contain aluminum and iron, which, when dehydrating the sample, form Al_2O_3 and Fe_2O_3. These oxides are potential interferents because they also form volatile fluorides. In the presence of H_2SO_4, however, aluminum and iron preferentially form non-volatile sulfates. These sulfates eventually decompose back to their respective oxides when we heat the residue to 1200°C. As a result, the change in weight after treating with HF and H_2SO_4 is due only to the loss of SiF_4.

8.3.2 Quantitative Applications

Unlike precipitation gravimetry, which is rarely used as a standard method of analysis, volatilization gravimetric methods continue to play an important role in chemical analysis. Several important examples are discussed below.

Inorganic Analysis

Determining the inorganic ash content of an organic material, such as a polymer, is an example of a direct volatilization gravimetric analysis. After weighing the sample, it is placed in an appropriate crucible and the organic material carefully removed by combustion, leaving behind the inorganic ash. The crucible containing the residue is heated to a constant weight using either a burner or an oven before determining the mass of the inorganic ash.

Another example of volatilization gravimetry is the determination of dissolved solids in natural waters and wastewaters. In this method, a sample of water is transferred to a weighing dish and dried to a constant weight at either 103–105°C or at 180°C. Samples dried at the lower temperature retain some occluded water and lose some carbonate as CO_2. The loss of organic material, however, is minimal. At the higher temperature, the residue is free from occluded water, but the loss of carbonate is greater. In addition, some chloride, nitrate, and organic material is lost through thermal decomposition. In either case, the residue that remains after drying to a constant weight at 500°C is the amount of fixed solids in the sample, and the loss in mass provides an indirect measure of the sample's volatile solids.

Indirect analyses based on the weight of residue remaining after volatilization are commonly used in determining moisture in a variety of products, and in determining silica in waters, wastewaters, and rocks. Moisture is determined by drying a preweighed sample with an infrared lamp or a low temperature oven. The difference between the original weight and the weight after drying equals the mass of water lost.

Organic Analysis

The most important application of volatilization gravimetry is for the elemental analysis of organic materials. During combustion with pure O_2, many elements, such as carbon and hydrogen, are released as gaseous combustion products, such as $CO_2(g)$ and $H_2O(g)$. Passing the combustion products through preweighed tubes containing selective absorbents and measuring the increases in mass provides a direct analysis for the mass of carbon and hydrogen in the organic material.

> **Note**
>
> Instead of measuring mass, modern instruments for completing an elemental analysis use gas chromatography (Chapter 12) or infrared spectroscopy (Chapter 10) to monitor the gaseous decomposition products.

Alkaline metals and earths in organic materials can be determined by adding H_2SO_4 to the sample before combustion. After combustion is complete, the metal remains behind as a solid residue of metal sulfate. Silver, gold, and platinum can be determined by burning the organic sample, leaving a metallic residue of Ag, Au, or Pt. Other metals are determined by adding HNO_3 before combustion, leaving a residue of the metal oxide.

Volatilization gravimetry is also used to determine biomass in waters and wastewaters. Biomass is a water quality index that provides an indication of the total mass of organisms contained within a sample of water. A known volume of the sample is passed through a preweighed 0.45-μm membrane filter or a glass-fiber filter, and dried at 105°C for 24 h. The residue's mass provides a direct measure of biomass. If samples are known to contain a substantial amount of dissolved inorganic solids, the residue can be ignited at 500°C for one hour, volatilizing the biomass. The resulting inorganic residue is wetted with distilled water to rehydrate any clay minerals and dried to a constant weight at 105°C. The difference in mass before and after ignition provides an indirect measure of biomass.

Quantitative Calculations

For some applications, such as determining the amount of inorganic ash in a polymer, a quantitative calculation is straightforward and does not require a balanced chemical reaction. For other applications, however, the relationship between the analyte and the analytical signal depends upon the stoichiometry of any relevant reactions. Once again, a conservation of mass is useful when solving problems.

Example 8.5

A 101.3-mg sample of an organic compound containing chlorine is combusted in pure O_2 and the volatile gases collected in absorbent traps. The trap for CO_2 increases in mass by 167.6 mg and the trap for H_2O shows a 13.7-mg increase. A second sample of 121.8 mg is treated with concentrated HNO_3 producing Cl_2, which subsequently reacts with Ag^+, forming 262.7 mg of AgCl. Determine the compound's composition, as well as its empirical formula.

Solution

A conservation of mass requires that all the carbon in the organic compound must be in the CO_2 produced during combustion; thus

$$167.6 \text{ mg } CO_2 \times \frac{1 \text{ g } CO_2}{1000 \text{ mg } CO_2} \times \frac{1 \text{ mol C}}{44.011 \text{ g } CO_2} \times \frac{12.011 \text{ g C}}{\text{mol C}} \times \frac{1000 \text{ mg C}}{\text{g C}} = 45.74 \text{ mg C} \tag{8.3.6}$$

$$\frac{45.74 \text{ mg C}}{101.3 \text{ mg sample}} \times 100 = 45.15\% \text{ w/w C} \tag{8.3.7}$$

Using the same approach for hydrogen and chlorine, we find that

$$13.7 \text{ mg } H_2O \times \frac{1 \text{ g } H_2O}{1000 \text{ mg } H_2O} \times \frac{2 \text{ mol H}}{18.015 \text{ g } H_2O} \times \frac{1.008 \text{ g H}}{\text{mol H}} \times \frac{1000 \text{ mg H}}{\text{g H}} = 1.533 \text{ mg H} \tag{8.3.8}$$

$$\frac{1.533 \text{ mg H}}{101.3 \text{ mg sample}} \times 100 = 1.51\% \text{ w/w H} \tag{8.3.9}$$

$$262.7 \text{ mg AgCl} \times \frac{1 \text{ g AgCl}}{1000 \text{ mg AgCl}} \times \frac{1 \text{ mol Cl}}{143.32 \text{ g AgCl}} \times \frac{35.453 \text{ g Cl}}{\text{mol Cl}} \times \frac{1000 \text{ mg Cl}}{\text{g Cl}} = 64.98 \text{ mg Cl} \tag{8.3.10}$$

$$\frac{64.98 \text{ mg Cl}}{121.8 \text{ mg sample}} \times 100 = 53.35\% \text{ w/w Cl} \tag{8.3.11}$$

Adding together the weight percents for C, H, and Cl gives a total of 100.01%; thus, the compound contains only these three elements. To determine the compound's empirical formula we note that a gram of sample contains 0.4515 g of C, 0.0151 g of H and 0.5335 g of Cl. Expressing each element in moles gives 0.0376 moles C, 0.0150 moles H and 0.0150 moles Cl. Hydrogen and chlorine are present in a 1:1 molar ratio. The molar ratio of C to moles of H or Cl is

$$\frac{\text{moles C}}{\text{moles H}} = \frac{\text{moles C}}{\text{moles Cl}} = \frac{0.0376}{0.0150} = 2.51 \approx 2.5 \tag{8.3.12}$$

Thus, the simplest, or empirical formula for the compound is $C_5H_2Cl_2$.

In an indirect volatilization gravimetric analysis, the change in the sample's weight is proportional to the amount of analyte. Note that in the following example it is not necessary to apply a conservation of mass to relate the analytical signal to the analyte.

Example 8.6

A sample of slag from a blast furnace is analyzed for SiO_2 by decomposing a 0.5003-g sample with HCl, leaving a residue with a mass of 0.1414 g. After treating with HF and H_2SO_4, and evaporating the volatile SiF_4, a residue with a mass of 0.0183 g remains. Determine the %w/w SiO_2 in the sample.

Solution

In this procedure the difference in the residue's mass before and after volatilizing SiF_4 gives the mass of SiO_2 in the sample; thus the sample contains

$$0.1414\,\text{g} - 0.0183\,\text{g} = 0.1231\,\text{g}\,\text{SiO}_2 \tag{8.3.13}$$

and the %w/w SiO_2 is

$$\frac{0.1231\ \text{g}\ \text{SiO}_2}{0.5003\ \text{g}} \times 100 = 24.61\%\ \text{w/w}\ \text{SiO}_2 \tag{8.3.14}$$

Practice Exercise 8.7

Heating a 0.3317-g mixture of CaC_2O_4 and MgC_2O_4 yields a residue of 0.1794 g at 600°C and a residue of 0.1294 g at 1000°C. Calculate the %w/w CaC_2O_4 in the sample. You may wish to review your answer to Practice Exercise 8.6 as you consider this problem.

Click here to review your answer to this exercise.

Finally, in some quantitative applications we can compare the result for a sample to a similar result obtained using a standard.

Example 8.7

A 26.23-mg sample of MgC_2O_4•H_2O and inert materials is heated to constant weight at 1200°C, leaving a residue weighing 20.98 mg. A sample of pure MgC_2O_4•H_2O, when treated in the same fashion, undergoes a 69.08% change in its mass. Determine the %w/w MgC_2O_4•H_2O in the sample.

Solution

The change in the sample's mass is 5.25 mg, which corresponds to

$$5.25\ \text{mg lost} \times \frac{100.0\ \text{mg}\ \text{MgC}_2\text{O}_4 \cdot \text{H}_2\text{O}}{69.08\ \text{mg lost}} = 7.60\ \text{mg}\ \text{MgC}_2\text{O}_4 \cdot \text{H}_2\text{O} \tag{8.3.15}$$

The %w/w MgC_2O_4•H_2O in the sample is

$$\frac{7.60\ \text{mg}\ \text{MgC}_2\text{O}_4 \cdot \text{H}_2\text{O}}{26.23\ \text{mg sample}} \times 100 = 29.0\%\ \text{w/w}\ \text{MgC}_2\text{O}_4 \cdot \text{H}_2\text{O} \tag{8.3.16}$$

(Alternatively, you can determine that the final product of the decomposition is MgO (see Practice Exercise 8.6) and use a conservation of mass for Mg to arrive at the same answer.)

8.3.3 Evaluating Volatilization Gravimetry

The scale of operation, accuracy, and precision of a gravimetric volatilization method is similar to that described in Section 8B.4 for precipitation gravimetry. The sensitivity of a direct analysis is fixed by the analyte's chemical form following combustion or volatilization. We can improve the sensitivity of an indirect analysis by choosing conditions that give the largest possible change in mass. For example, the thermogram in Figure 8.10 shows us that an indirect analysis for CaC_2O_4•H_2O is more sensitive if we measure the change in mass following ignition at 1000°C than if we ignite the sample at 300°C.

Selectivity is not a problem for a direct analysis if we trap the analyte using a selective absorbent trap. A direct analysis based on the residue's weight following combustion or volatilization is possible if the residue only contains the analyte of interest. As noted earlier, an indirect analysis is only feasible when the change in mass results from the loss of a single volatile product containing the analyte.

Volatilization gravimetric methods are time and labor intensive. Equipment needs are few, except when combustion gases must be trapped, or for a thermogravimetric analysis, when specialized instrumentation is needed.

Contributors

David Harvey (DePauw University)

8.3: Volatilization Gravimetry is shared under a CC BY-NC-SA 4.0 license and was authored, remixed, and/or curated by LibreTexts.

8.4: Particulate Gravimetry

Precipitation and volatilization gravimetric methods require that the analyte, or some other species in the sample, participate in a chemical reaction. In a direct precipitation gravimetric analysis, for example, we convert a soluble analyte into an insoluble form that precipitates from solution. In some situations, however, the analyte is already present as in a particulate form that is easy to separate from its liquid, gas, or solid matrix. When such a separation is possible, we can determine the analyte's mass without relying on a chemical reaction.

> **Note**
>
> A particulate is any tiny portion of matter, whether it is a speck of dust, a globule of fat, or a molecule of ammonia. For particulate gravimetry we simply need a method for collecting the particles and a balance for measuring their mass.

8.4.1 Theory and Practice

There are two methods for separating a particulate analyte from its matrix. The most common method is filtration, in which we separate solid particulates from their gas, liquid, or solid matrix. A second method, which is useful for gas particles, solutes, and solids, is an extraction.

Filtration

To separate solid particulates from their matrix we use gravity or apply suction from a vacuum pump or aspirator to pull the sample through a filter. The type of filter we use depends upon the size of the solid particles and the sample's matrix. Filters for liquid samples are constructed from a variety of materials, including cellulose fibers, glass fibers, cellulose nitrate, and polytetrafluoroethylene (PTFE). Particle retention depends on the size of the filter's pores. Cellulose fiber filter papers range in pore size from 30 μm to 2–3 μm. Glass fiber filters, manufactured using chemically inert borosilicate glass, are available with pore sizes between 2.5 μm and 0.3 μm. Membrane filters, which are made from a variety of materials, including cellulose nitrate and PTFE, are available with pore sizes from 5.0 μm to 0.1 μm.

> **Note**
>
> For additional information, see our earlier discussion in this chapter on filtering precipitates, and the discussion in Chapter 7 of separations based on size.

Solid aerosol particulates are collected using either a single-stage or a multiple-stage filter. In a single-stage system, we pull the gas through a single filter, retaining particles larger than the filter's pore size. When collecting samples from a gas line, we place the filter directly in the line. Atmospheric gases are sampled with a high volume sampler that uses a vacuum pump to pull air through the filter at a rate of approximately 75 m^3/h. In either case, the filtering media for liquid samples also can be used to collect aerosol particulates. In a multiple-stage system, a series of filtering units separates and the particles in two or more size ranges.

The particulates in a solid matrix are separated by size using one or more sieves (Figure 8.12). Sieves are available in a variety of mesh sizes ranging from approximately 25 mm to 40 μm. By stacking sieves of different mesh size, we can isolate particulates into several narrow size ranges. Using the sieves in Figure 8.12, for example, we can separate a solid into particles with diameters >1700 μm, with diameters between 1700 μm and 500 μm, with diameters between 500 μm and 250 μm, and those with a diameter <250 μm.



Figure 8.12 Three sieves with, from left to right, mesh sizes of 1700 μm, 500 μm, and 250 μm. Source: BMK (commons.wikimedia.com).

Extraction

Filtering limits particulate gravimetry to solid analytes that are easily separated from their matrix. We can extend particulate gravimetry to the analysis of gas phase analytes, solutes, and poorly filterable solids by extracting them with a suitable solvent. After the extraction, we evaporate the solvent before determining the analyte's mass. Alternatively, we can determine the analyte indirectly by measuring the change in the sample's mass after extracting the analyte. Solid-phase extractions, such as those described in Chapter 7, also may be used.

> **Note**
>
> For a more detailed review of extractions, see Chapter 7.

Another method for extracting an analyte from its matrix is by adsorption onto a solid substrate, by absorption into a thin polymer or chemical film coated on a solid substrate, or by chemically binding to a suitable receptor that is covalently bound to a solid substrate (Figure 8.13). Adsorption, absorption, and binding occur at the interface between the solution containing the analyte and the substrate's surface, the thin film, or the receptor. Although the amount of extracted analyte is too small to measure using a conventional balance, it can be measured using a quartz crystal microbalance.

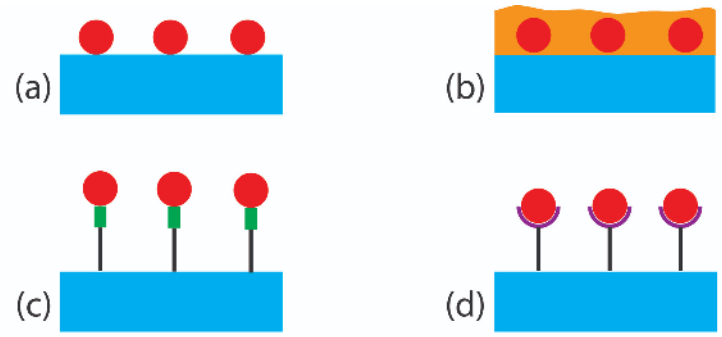


Figure 8.13 Four possible mechanisms for the solid-state extraction of an analyte: (a) adsorption onto a solid substrate; (b) absorption into a thin polymer film or chemical film coated on a solid substrate; (c) metal–ligand complexation in which the ligand is covalently bound to the solid substrate using an organic tether; and (d) antibody–antigen binding in which the receptor is covalently bound to the solid substrate using an organic tether.

The measurement of mass using a **quartz crystal microbalance** takes advantage of the piezoelectric effect.[10] The application of an alternating electrical field across a quartz crystal induces an oscillatory vibrational motion in the crystal. Every quartz crystal vibrates at a characteristic resonant frequency that depends on the crystal's properties, including the mass per unit area of any material coated on the crystal's surface. The change in mass following adsorption, absorption, or binding of the analyte, therefore, can be determined by monitoring the change in the quartz crystal's characteristic resonant frequency. The exact relationship between the change in frequency and mass is determined by a calibration curve.

> **Note**
>
> If you own a wristwatch, there is a good chance that its operation relies on a quartz crystal. The piezoelectric properties of quartz were discovered in 1880 by Paul-Jacques Currie and Pierre Currie. Because the oscillation frequency of a quartz crystal is so precise, it quickly found use in the keeping of time. The first quartz clock was built in 1927 at the Bell Telephone labs, and Seiko introduced the first quartz wristwatches in 1969.

8.4.2 Quantitative Applications

Particulate gravimetry is important in the environmental analysis of water, air, and soil samples. The analysis for suspended solids in water samples, for example, is accomplished by filtering an appropriate volume of a well-mixed sample through a glass fiber filter and drying the filter to constant weight at 103–105°C.

The microbiological testing of water also uses particulate gravimetry. One example is the analysis for coliform bacteria in which an appropriate volume of sample is passed through a sterilized 0.45-μm membrane filter. The filter is placed on a sterilized absorbent pad saturated with a culturing medium and incubated for 22–24 hours at 35 ± 0.5^{o}C. Coliform bacteria are identified by the

presence of individual bacterial colonies that form during the incubation period (Figure 8.14). As with qualitative applications of precipitation gravimetry, the signal in this case is a visual observation rather than a measurement of mass.

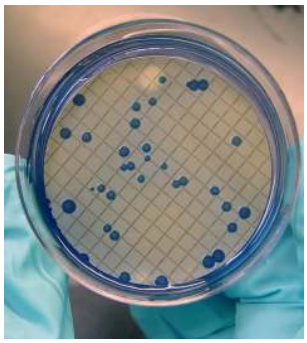


Figure 8.14 Colonies of fecal coliform bacteria from a water supply. Source: Susan Boyer. Photo courtesy of ARS–USDA (www.ars.usda.gov).

Total airborne particulates are determined using a high-volume air sampler equipped with either cellulose fiber or glass fiber filters. Samples from urban environments require approximately 1 h of sampling time, but samples from rural environments require substantially longer times.

Grain size distributions for sediments and soils are used to determine the amount of sand, silt, and clay in a sample. For example, a grain size of 2 mm serves as the boundary between gravel and sand. The grain size for the sand–silt and the silt–clay boundaries are 1/16 mm and 1/256 mm, respectively.

Several standard quantitative analytical methods for agricultural products are based on measuring the sample's mass following a selective solvent extraction. For example, the crude fat content in chocolate can be determined by extracting with ether for 16 hours in a Soxhlet extractor. After the extraction is complete, the ether is allowed to evaporate and the residue is weighed after drying at 100°C. This analysis has also been accomplished indirectly by weighing a sample before and after extracting with supercritical CO_2.

Quartz crystal microbalances equipped with thin film polymer films or chemical coatings have found numerous quantitative applications in environmental analysis. Methods have been reported for the analysis of a variety of gaseous pollutants, including ammonia, hydrogen sulfide, ozone, sulfur dioxide, and mercury. Biochemical particulate gravimetric sensors also have been developed. For example, a piezoelectric immunosensor has been developed that shows a high selectivity for human serum albumin, and is capable of detecting microgram quantities.[11]

Quantitative Calculations

The result of a quantitative analysis by particulate gravimetry is just the ratio, using appropriate units, of the amount of analyte relative to the amount of sample.

Example 8.8

A 200.0-mL sample of water was filtered through a pre-weighed glass fiber filter. After drying to constant weight at 105°C, the filter was found to have increased in mass by 48.2 mg. Determine the sample's total suspended solids.

Solution

A ppm is equivalent to a mg of analyte per liter of solution; thus, the total suspended solids for the sample is

$$\frac{48.2 \text{ mg solids}}{0.2000 \text{ L sample}} = 241 \text{ ppm solids}$$

8.4.3 Evaluating Particulate Gravimetry

The scale of operation and detection limit for particulate gravimetry can be extended beyond that of other gravimetric methods by increasing the size of the sample taken for analysis. This is usually impracticable for other gravimetric methods because of the difficulty of manipulating a larger sample through the individual steps of the analysis. With particulate gravimetry, however, the

part of the sample that is not analyte is removed when filtering or extracting. Consequently, particulate gravimetry is easily extended to the analysis of trace-level analytes.

Except for methods relying on a quartz crystal microbalance, particulate gravimetry uses the same balances as other gravimetric methods, and is capable of achieving similar levels of accuracy and precision. Since particulate gravimetry is defined in terms of the mass of the particle itself, the sensitivity of the analysis is given by the balance's sensitivity. Selectivity, on the other hand, is determined either by the filter's pore size, or by the properties of the extracting phase. Because it requires a single step, particulate gravimetric methods based on filtration generally require less time, labor and capital than other gravimetric methods.

Contributors

David Harvey (DePauw University)

8.4: Particulate Gravimetry is shared under a CC BY-NC-SA 4.0 license and was authored, remixed, and/or curated by LibreTexts.

8.E: Gravimetric Methods (Exercises)

1. Starting with the equilibrium constant expressions for reaction 8.1, and reactions 8.3–8.5, verify that equation 8.7 is correct.

2. Equation 8.7 explains how the solubility of AgCl varies as a function of the equilibrium concentration of Cl^-. Derive a similar equation that describes the solubility of AgCl as a function of the equilibrium concentration of Ag^+. Graph the resulting solubility function and compare it to that shown in Figure 8.1.

3. Construct a solubility diagram for $Zn(OH)_2$ that takes into account the following soluble zinc-hydroxide complexes: $Zn(OH)^+$, $Zn(OH)_3^-$, and $Zn(OH)_4^{2-}$. What is the optimum pH for quantitatively precipitating $Zn(OH)_2$? For your solubility diagram, plot log(*S*) on the *y*-axis and pH on the *x*-axis. See the appendices for relevant equilibrium constants.

4. Starting with equation 8.10, verify that equation 8.11 is correct.

5. For each of the following precipitates, use a ladder diagram to identify the pH range where the precipitates has its lowest solubility? See the appendices for relevant equilibrium constants.

a. CaC_2O_4 b. $PbCrO_4$ c. $BaSO_4$ d. $SrCO_3$ e. ZnS

6. Mixing solutions of 1.5 M KNO_3 and 1.5 M $HClO_4$ produces a white precipitate of $KClO_4$. If permanganate ions are present, an inclusion of $KMnO_4$ is possible. Impure precipitates of $KClO_4$ are purple if an inclusion of $KMnO_4$ is present. Shown below are descriptions of two experiments in which $KClO_4$ is precipitated in the presence of MnO_4^-. Explain why the experiments lead to the different results shown in Figure 8.15.

> **Experiment 1.** Place 1 mL of 1.5 M KNO_3 in a test tube, add 3 drops of 0.1 M $KMnO_4$, and swirl to mix. Add 1 mL of 1.5 M $HClO_4$ dropwise, agitating the solution between drops. Destroy the excess $KMnO_4$ by adding 0.1 M $NaHSO_3$ dropwise. The resulting precipitate of $KClO_4$ has an intense purple color.
>
> **Experiment 2.** Place 1 mL of 1.5 M $HClO_4$ in a test tube, add 3 drops of 0.1 M $KMnO_4$, and swirl to mix. Add 1 mL of 1.5 M KNO_3 dropwise, agitating the solution between drops. Destroy the excess $KMnO_4$ by adding 0.1 M $NaHSO_3$ dropwise. The resulting precipitate of $KClO_4$ has a pale purple in color.



Figure 8.15 Results for the experiments in Problem 8.6. (a) Experiment 1; (b) Experiment 2.

7. Mixing solutions of $Ba(SCN)_2$ and $MgSO_4$ produces a precipitate of $BaSO_4$. Shown below are the descriptions and results for three experiments using different concentrations of $Ba(SCN)_2$ and $MgSO_4$. Explain why these experiments produce different results.

> **Experiment 1.** When equal volumes of 3.5 M $Ba(SCN)_2$ and 3.5 M $MgSO_4$ are mixed, a gelatinous precipitate immediately forms.
>
> **Experiment 2.** When equal volumes of 1.5 M $Ba(SCN)_2$ and 1.5 M $MgSO_4$ are mixed, a curdy precipitate immediately forms. Individual particles of $BaSO_4$ can be seen as points under a magnification of 1500×(a particle size less than 0.2 μm).
>
> **Experiment 3.** When equal volumes of 0.5 mM $Ba(SCN)_2$ and 0.5 mM $MgSO_4$ are mixed, the complete precipitation of $BaSO_4$ requires 2–3 h. Individual crystals of $BaSO_4$ obtain lengths of approximately 5 μm.

8. Aluminum is determined gravimetrically by precipitating $Al(OH)_3$ and isolating Al_2O_3. A sample containing approximately 0.1 grams of Al is dissolved in 200 mL of H_2O, and 5 grams of NH_4Cl and a few drops of methyl red indicator are added (methyl red is red at pH levels below 4 and yellow at pH levels above 6). The solution is heated to boiling and 1:1 NH_3 is added dropwise till the

indicator turns yellow, precipitating $Al(OH)_3$. The precipitate is held at the solution's boiling point for several minutes before filtering and rinsing with a hot solution of 2% w/v NH_4NO_3. The precipitate is then ignited at 1000–1100°C, forming Al_2O_3.

(a) Cite two ways in which this procedure encourages the formation of larger particles of precipitate.

(b) The ignition step must be carried out carefully to ensure the quantitative conversion of $Al(OH)_3$ to Al_2O_3. What is the effect of an incomplete conversion on the %w/w Al?

(c) What is the purpose of adding NH_4Cl and methyl red indicator?

(d) An alternative procedure involves isolating and weighing the precipitate as the 8-hydroxyquinolate, $Al(C_9H_6ON)_3$. Why might this be a more advantageous form of Al for a gravimetric analysis? Are there any disadvantages?

9. Calcium is determined gravimetrically by precipitating $CaC_2O_4 \cdot H_2O$ and isolating $CaCO_3$. After dissolving a sample in 10 mL of water and 15 mL of 6 M HCl, the resulting solution is heated to boiling and a warm solution of excess ammonium oxalate is added. The solution is maintained at 80°C and 6 M NH_3 is added dropwise, with stirring, until the solution is faintly alkaline. The resulting precipitate and solution are removed from the heat and allowed to stand for at least one hour. After testing the solution for completeness of precipitation, the sample is filtered, rinsed with 0.1% w/v ammonium oxalate, and dried at 100–120°C for 1 hour. The precipitate is transferred to a muffle furnace where it is converted to $CaCO_3$ by drying at 500 ± 25°C until constant weight.

(a) Why is the precipitate of $CaC_2O_4 \cdot H_2O$ converted to $CaCO_3$?

(b) In the final step, if the sample is heated at too high of a temperature some $CaCO_3$ may be converted to CaO. What effect would this have on the reported %w/w Ca?

(c) Why is the precipitant, $(NH_4)_2C_2O_4$, added to a hot, acidic solution instead of a cold, alkaline solution?

10. Iron is determined gravimetrically by precipitating as $Fe(OH)_3$ and igniting to Fe_2O_3. After dissolving a sample in 50 mL of H_2O and 10 mL of 6 M HCl, any Fe^{2+} is converted Fe^{3+} by oxidizing with 1–2 mL of concentrated HNO_3. The sample is heated to remove the oxides of nitrogen and the solution is diluted to 200 mL. After bringing the solution to a boil, $Fe(OH)_3$ is precipitated by slowly adding 1:1 NH_3 until the odor of NH_3 is detected. The solution is boiled for an additional minute and the precipitate is allowed to settler. The precipitate is then filtered and rinsed with several portions of hot 1% w/v NH_4NO_3 until no Cl^- is found in the wash water. Finally, the precipitate is ignited to constant weight at 500–550°C and weighed as Fe_2O_3.

(a) If ignition is not carried out under oxidizing conditions (plenty of O_2 present), the final product may contain Fe_3O_4. What effect would this have on the reported %w/w Fe?

(b) The precipitate is washed with a dilute solution of NH_4NO_3. Why is NH_4NO_3 added to the wash water?

(c) Why does the procedure call for adding NH_3 until the odor of ammonia is detected?

(d) Describe how you might test the filtrate for Cl^-.

11. Sinha and Shome described a gravimetric method for molybdenum in which it is precipitated as $MoO_2(C_{13}H_{10}NO_2)_2$ using *n*-benzoylphenylhydroxylamine, $C_{13}H_{11}NO_2$, as a precipitant.[12] The precipitate is weighed after igniting to MoO_3. As part of their study, the authors determined the optimum conditions for the analysis. Samples containing 0.0770 g of Mo were taken through the

procedure while varying the temperature, the amount of precipitant added, and the pH of the solution. The solution volume was held constant at 300 mL for all experiments. A summary of their results are shown in the following table.

Temperature (^oC)	Mass(g) of precipitant	Volume(mL) of 10 M HCl	Mass (g) of MoO_3
30	0.20	0.9	0.0675
30	0.30	0.9	0.1014
30	0.35	0.9	0.1140
30	0.42	0.9	0.1155
30	0.42	0.3	0.1150
30	0.42	18.0	0.1152
30	0.42	48.0	0.1160
30	0.42	75.0	0.1159
50	0.42	0.9	0.1156
75	0.42	0.9	0.1158
80	0.42	0.9	0.1129

Considering these results, discuss the optimum conditions for determining Mo by this method. Express your results for the precipitant as the minimum %w/v in excess, needed to ensure a quantitative precipitation.

12. A sample of an impure iron ore is approximately 55% w/w Fe. The amount of Fe in the sample is to be determined gravimetrically by isolating it as Fe_2O_3. What mass of sample do you need to ensure that you isolate at least 1 g of Fe_2O_3?

13. The concentration of arsenic in an insecticide is determined gravimetrically by precipitating $MgNH_4AsO_4$ and isolating $Mg_2As_2O_7$. Determine the %w/w As_2O_3 in a 1.627-g sample of insecticide if it yields 106.5 mg of $Mg_2As_2O_7$.

14. After preparing a sample of alum, $K_2SO_4•Al_2(SO_4)_3•24H_2O$, a student determined its purity by dissolving a 1.2391-g sample and precipitating the aluminum as $Al(OH)_3$. After filtering, rinsing, and igniting, 0.1357 g of Al_2O_3 is obtained. What is the purity of the alum preparation?

15. To determine the amount of iron in a dietary supplement, a random sample of 15 tablets weighing a total of 20.505 g was ground into a fine powder. A 3.116-g sample was dissolved and treated to precipitate the iron as $Fe(OH)_3$. The precipitate was collected, rinsed, and ignited to a constant weight as Fe_2O_3, yielding 0.355 g. Report the iron content of the dietary supplement as g $FeSO_4•7H_2O$ per tablet.

16. A 1.4639-g sample of limestone was analyzed for Fe, Ca, and Mg. The iron was determined as Fe_2O_3 yielding 0.0357 g. Calcium was isolated as $CaSO_4$, yielding a precipitate of 1.4058 g, and Mg was isolated as 0.0672 g of $Mg_2As_2O_7$. Report the

amount of Fe, Ca, and Mg in the limestone sample as %w/w Fe_2O_3, %w/w CaO, and %w/w MgO.

17. The number of ethoxy groups (CH_3CH_2O–) in an organic compound is determined by the following two reactions.

$$R(CH_2CH_3)_x + xHI \rightarrow R(OH)_x + xCH_3CH_2I \quad (8.E.1)$$

$$CH_3CH_2I + Ag^+ + H_2O \rightarrow AgI(s) + CH_3CH_2OH \quad (8.E.2)$$

A 36.92-mg sample of an organic compound with an approximate molecular weight of 176 was treated in this fashion, yielding 0.1478 g of AgI. How many ethoxy groups are there in each molecule of the compound?

18. A 516.7-mg sample containing a mixture of K_2SO_4 and $(NH_4)_2SO_4$ was dissolved in water and treated with $BaCl_2$, precipitating the SO_4^{2-} as $BaSO_4$. The resulting precipitate was isolated by filtration, rinsed free of impurities, and dried to a constant weight, yielding 863.5 mg of $BaSO_4$. What is the %w/w K_2SO_4 in the sample?

19. The amount of iron and manganese in an alloy can be determined by precipitating the metals with 8-hydroxyquinoline, C_9H_7NO. After weighing the mixed precipitate, the precipitate is dissolved and the amount of 8-hydroxyquinoline determined by another method. In a typical analysis a 127.3-mg sample of an alloy containing iron, manganese, and other metals was dissolved in acid and treated with appropriate masking agents to prevent an interference from other metals. The iron and manganese were precipitated and isolated as $Fe(C_9H_6NO)_3$ and $Mn(C_9H_6NO)_2$, yielding a total mass of 867.8 mg. The amount of 8-hydroxyquinolate in the mixed precipitate was determined to be 5.276 mmol. Calculate the %w/w Fe and %w/w Mn in the alloy.

20. A 0.8612-g sample of a mixture of NaBr, NaI, and $NaNO_3$ was analyzed by adding $AgNO_3$ and precipitating a 1.0186-g mixture of AgBr and AgI. The precipitate was then heated in a stream of Cl_2, converting it to 0.7125 g of AgCl. Calculate the %w/w $NaNO_3$ in the sample.

20. The earliest determinations of elemental atomic weights were accomplished gravimetrically. In determining the atomic weight of manganese, a carefully purified sample of $MnBr_2$ weighing 7.16539 g was dissolved and the Br^- precipitated as AgBr, yielding 12.53112 g. What is the atomic weight for Mn if the atomic weights for Ag and Br are taken to be 107.868 and 79.904, respectively?

22. While working as a laboratory assistant you prepared 0.4 M solutions of $AgNO_3$, $Pb(NO_3)_2$, $BaCl_2$, KI and Na_2SO_4. Unfortunately, you became distracted and forgot to label the solutions before leaving the laboratory. Realizing your error, you label the solutions A–E and perform all possible binary mixings of the five solutions, obtaining the results shown in Figure 8.16 (key: NP means no precipitate formed, W means a white precipitate formed, and Y means a yellow precipitate formed). Identify solutions A–E.

	A	B	C	D	E
A		NP	Y	NP	W
B			Y	W	W
C				NP	NP
D					W

Figure 8.16 Results of the binary mixing of solutions A–E for Problem 8.22.

23. A solid sample has approximately equal amounts of two or more of the following soluble salts: $AgNO_3$, $ZnCl_2$, K_2CO_3, $MgSO_4$, $Ba(C_2H_3O_2)_2$, and NH_4NO_3. A sample of the solid, sufficient to give at least 0.04 moles of any single salt, was added to 100 mL of water, yielding a white precipitate and a clear solution. The precipitate was collected and rinsed with water. When a portion of the precipitate was placed in dilute HNO_3 it completely dissolved, leaving a colorless solution. A second portion of the precipitate was placed in dilute HCl, yielding a precipitate and a clear solution. Finally, the filtrate from the original precipitate was treated with excess NH_3, yielding a white precipitate. Identify the salts that must be present in the sample, the salts that must be absent and the salts for which there is insufficient information to make this determination.[13]

24. Two methods have been proposed for the analysis of sulfur in impure samples of pyrite, FeS_2. Sulfur can be determined in a direct analysis by oxidizing it to SO_4^{2-} and precipitating it as $BaSO_4$. An indirect analysis is possible if the iron is precipitated as

$Fe(OH)_3$ and isolated as Fe_2O_3. Which of these methods will provide a more sensitive determination for sulfur? What other factors should you consider in choosing between these methods?

25. A sample of impure pyrite known to be approximately 90–95% w/w FeS_2 is to be analyzed by oxidizing the sulfur to SO_4^{2-} and precipitating it as $BaSO_4$. How many grams of the sample must you take to form at least 1 g of $BaSO_4$?

26. A series of samples containing any possible combination of KCl, NaCl, and NH_4Cl is to be analyzed by adding $AgNO_3$ and precipitating AgCl. What is the minimum volume of 5% w/v $AgNO_3$ necessary to completely precipitate the chloride in any 0.5-g sample?

27. If a precipitate of known stoichiometry does not form, a gravimetric analysis is still feasible if we can establish experimentally the mole ratio between the analyte and the precipitate. Consider, for example, the precipitation gravimetric analysis of Pb as $PbCrO_4$.[14]

(a) For each gram of Pb, how many grams of $PbCrO_4$ should form?

(b) In a study of this procedure, Grote found that 1.568 g of $PbCrO_4$ formed for each gram of Pb. What is the apparent stoichiometry between Pb and $PbCrO_4$?

(c) Does failing to account for the actual stoichiometry lead to a positive determinate error or a negative determinate error?

28. Determine the uncertainty for the gravimetric analysis described in Example 8.1. The expected accuracy for a gravimetric method is 0.1–0.2%. What additional sources of error might account for the difference between your estimated uncertainty and the expected accuracy?

29. A 38.63-mg sample of potassium ozonide, KO_3, was heated to 70°C for 1 h, undergoing a weight loss of 7.10 mg. A 29.6-mg sample of impure KO_3 experiences a 4.86-mg weight loss when treated under similar condition. What is the %w/w KO_3 in the sample?

30. The water content of an 875.4-mg sample of cheese was determined with a moisture analyzer. What is the %w/w H_2O in the cheese if the final mass was found to be 545.8 mg?

31. Representative Method 8.2 describes a procedure for determining Si in ores and alloys. In this analysis a weight loss of 0.21 g corresponds to 0.1 g of Si. Show that this relationship is correct.

32. The iron in an organometallic compound was determined by treating a 0.4873-g sample with HNO_3 and heating to volatilize the organic material. After ignition, the residue of Fe_2O_3 weighed 0.2091 g.

(a) What is the %w/w Fe in this compound?

(b) The carbon and hydrogen in a second sample of the compound were determined by a combustion analysis. When a 0.5123-g sample was carried through the analysis, 1.2119 g of CO_2 and 0.2482 g of H_2O were collected. What are the %w/w C and %w/w H in this compound and what is the compound's empirical formula?

33. A polymer's ash content is determined by placing a weighed sample in a Pt crucible that has been previously brought to a constant weight. The polymer is melted under gentle heating from a Bunsen burner until the volatile vapor ignites. The polymer is

allowed to burn until only a non-combustible residue remains. The residue is brought to constant weight at 800°C in a muffle furnace. The following data were collected during the analysis of two samples of a polymer resin.

Polymer A	g crucible	g crucible + polymer	g crucible + ash
replicate 1	19.1458	21.2287	19.7717
replicate 2	15.9193	17.9522	16.5310
replicate 3	15.6992	17.6660	16.2909

Polymer B	g crucible	g crucible + polymer	g crucible + ash
replicate 1	19.1457	21.0693	19.7187
replicate 2	15.6991	12.8273	16.3327
replicate 3	15.9196	17.9037	16.5110

(a) For each polymer, determine the mean and the standard deviation for the %w/w ash.

(b) Is there any evidence at $\alpha = 0.05$ for a significant difference between the two polymers? See the appendices for statistical tables.

34. In the presence of water vapor the surface of zirconia, ZrO_2, chemically adsorbs H_2O, forming surface hydroxyls, ZrOH (additional water is physically adsorbed as H_2O). When heated above 200°C, the surface hydroxyls convert to $H_2O(g)$, releasing one molecule of water for every two surface hydroxyls. Below 200°C only physically absorbed water is lost. Nawrocki, et al. used thermogravimetry to determine the density of surface hydroxyls on a sample of zirconia that was heated to 700°C and cooled in a desiccator containing humid N_2.[15] Heating the sample from 200°C to 900°C released 0.006 g of H_2O for every gram of dehydroxylated ZrO_2. Given that the zirconia had a surface area of 33 m^2/g and that one molecule of H_2O forms two surface hydroxyls, calculate the density of surface hydroxyls in $\mu mol/m^2$.

35. The concentration of airborne particulates in an industrial workplace was determined by pulling the air through a single-stage air sampler equipped with a glass-fiber filter. The air was sampled for 20 min at a rate of 75 m^3/h. At the end of the sampling period, the filter's mass was found to have increased by 345.2 mg. What is the concentration of particulates in the air sample in mg/m^3 and mg/L?

36. The fat content of potato chips is determined indirectly by weighing a sample before and after extracting the fat with supercritical CO_2. The following data were obtained for the analysis of potato chips.[16]

Sample Number	Initial Mass (g)	Final Mass (g)
1	1.1661	0.9253
2	1.1723	0.9252
3	1.2525	0.9850
4	1.2280	0.9562
5	1.2837	1.0119

(a) Determine the mean and standard deviation for the %w/w fat.

(b) This sample of potato chips is known to have a fat content of 22.7% w/w. Is there any evidence for a determinate error at $\alpha = 0.05$? See the appendices for statistical tables.

37. Delumyea and McCleary reported results for the %w/w organic material in sediment samples collected at different depths from a cove on the St. Johns River in Jacksonville, FL.[17] After collecting a sediment core, they sectioned it into 2-cm increments. Each increment was treated using the following procedure:

(a) The sediment was placed in 50 mL of deionized water and the resulting slurry filtered through preweighed filter paper;

(b) The filter paper and the sediment were placed in a preweighed evaporating dish and dried to a constant weight in an oven at 110°C;

(c) The evaporating dish containing the filter paper and the sediment were transferred to a muffle furnace where the filter paper and any organic material in the sample were removed by ashing;

(d) Finally, the inorganic residue remaining after ashing was weighed.

Using the following data, determine the %w/w organic material as a function of the average depth for each increment.

	Mass (g) of...		Mass (g) of Filter Paper, Dish, and Sediment...	
Depth (cm)	Filter Paper	Dish	After Drying	After Ashing
0–2	1.590	43.21	52.10	49.49
2–4	1.745	40.62	48.83	46.00
4–6	1.619	41.23	52.86	47.84
6–8	1.611	42.10	50.59	47.13
8–10	1.658	43.62	51.88	47.53
10–12	1.628	43.24	49.45	45.31
12–14	1.633	43.08	47.92	44.20
14–16	1.630	43.96	58.31	55.53
16–18	1.636	43.36	54.37	52.75

38. Yao, et al. recently described a method for the quantitative analysis of thiourea based on its reaction with I_2.[18]

$$CS(NH_2)_2 + 4I_2 + 6H_2O \rightarrow (NH_4)_2SO_4 + 8HI + CO_2 \quad (8.E.3)$$

The procedure calls for placing a 100-µL aqueous sample containing thiourea in a 60-mL separatory funnel and adding 10 mL of a pH 7 buffer and 10 mL of 12 µM I_2 in CCl_4. The contents of the separatory funnel are shaken and the organic and aqueous layers allowed to separate. The organic layer, which contains the excess I_2, is transferred to the surface of a piezoelectric crystal on which a thin layer of Au has been deposited. After allowing the I_2 to adsorb to the Au, the CCl_4 is removed and the crystal's frequency shift, Δf, measured. The following data is reported for a series of thiourea standards.

[thiourea] (M)	Δf(Hz)	[thiourea] (M)	Δf (Hz)
3.00×10^{-7}	74.6	1.50×10^{-6}	327
5.00×10^{-7}	120	2.50×10^{-6}	543
7.00×10^{-7}	159	3.50×10^{-6}	789
9.00×10^{-7}	205	5.00×10^{-6}	1089

(a) Characterize this method with respect to the scale of operation shown in Figure 3.5 of Chapter 3.

(b) Using a regression analysis, determine the relationship between the crystal's frequency shift and the concentration of thiourea.

(c) If a sample containing an unknown amount of thiourea gives a Δf of 176 Hz, what is the molar concentration of thiourea in the sample?

(d) What is the 95% confidence interval for the concentration of thiourea in this sample assuming one replicate? See the appendices for statistical tables.

8.5.3 Solutions to Practice Exercises

Practice Exercise 8.1

The solubility reaction for CaC_2O_4 is

$$CaC_2O_4(s) \rightleftharpoons Ca^{2+}(aq) + C_2O_4^{2-}(aq) \tag{8.E.4}$$

To minimize solubility, the pH needs to be basic enough that oxalate, $C_2O_4^{2-}$, does not react to form $HC_2O_4^-$ or $H_2C_2O_4$. The ladder diagram for oxalic acid, including approximate buffer ranges, is shown in Figure 8.17. Maintaining a pH greater than 5.3 ensures that $C_2O_4^{2-}$ is the only important form of oxalic acid in solution, minimizing the solubility of CaC_2O_4.

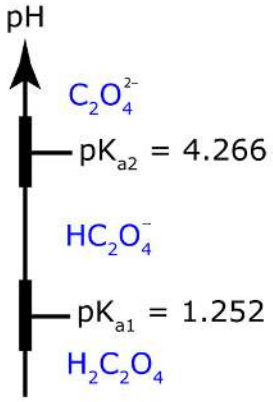


Figure 8.17 pH ladder diagram for oxalic acid, $H_2C_2O_4$.

Click here to return to the chapter.

Practice Exercise 8.2

A conservation of mass requires that all the zinc in the alloy is found in the final product, $Zn_2P_2O_7$. We know that there are 2 moles of Zn per mole of $Zn_2P_2O_7$; thus

$$0.1163 \text{ g } Zn_2P_2O_7 \times \frac{2 \text{ mol Zn}}{304.72 \text{ g } Zn_2P_2O_7} \times \frac{65.39 \text{ g Zn}}{\text{mol Zn}} = 4.991 \times 10^{-2} \text{ g Zn} \tag{8.E.5}$$

This is the mass of Zn in 25% of the sample (a 25.00 mL portion of the 100.0 mL total volume). The %w/w Zn, therefore, is

$$\frac{4.991 \times 10^{-2} \text{ g Zn} \times 4}{0.7336 \text{ g sample}} \times 100 = 27.22\% \text{ w/w Zn} \tag{8.E.6}$$

For copper, we find that

$$0.1163 \text{ g CuSCN} \times \frac{1 \text{ mol Cu}}{121.64 \text{ g CuSCN}} \times \frac{63.55 \text{ g Cu}}{\text{mol Cu}} = 0.1249 \text{ g Cu} \tag{8.E.7}$$

$$\frac{0.1249 \text{ g Cu} \times 4}{0.7336 \text{ g sample}} \times 100 = 67.88\% \text{ w/w Cu} \tag{8.E.8}$$

Click here to return to the chapter.

Practice Exercise 8.3

The masses of the solids provide us with the following equations

$$\text{g NaCl} + \text{g KCl} = 0.2692 \text{ g} \tag{8.E.9}$$

$$(\text{g KClO}_4)_{\text{NaCl}} + (\text{g KClO}_4)_{\text{KCl}} = 0.5713 \text{ g} \tag{8.E.10}$$

where $(\text{g KClO}_4)_{\text{NaCl}}$ and $(\text{g KClO}_4)_{\text{KCl}}$ are the masses of $KClO_4$ from the reaction of $HClO_4$ with NaCl and KCl. With two equations and four unknowns, we need two additional equations to solve the problem. A conservation of mass requires that all the chlorine in NaCl is found in the $(KClO_4)_{NaCl}$; thus

$$(\text{g KClO}_4)_{\text{NaCl}} = \text{g NaCl} \times \frac{1 \text{ mol Cl}}{58.44 \text{ g NaCl}} \times \frac{138.55 \text{ g KClO}_4}{\text{mol Cl}} \tag{8.E.11}$$

$$(\text{g KClO}_4)_{\text{NaCl}} = 2.3708 \times \text{g NaCl} \tag{8.E.12}$$

Using the same approach for KCl gives

$$(\text{g KClO}_4)_{\text{KCl}} = \text{g KCl} \times \frac{1 \text{ mol Cl}}{74.55 \text{ g KCl}} \times \frac{138.55 \text{ g KClO}_4}{\text{mol Cl}} \tag{8.E.13}$$

$$(\text{g KClO}_4)_{\text{KCl}} = 1.8584 \times \text{g KCl} \tag{8.E.14}$$

Substituting the equations for $(\text{g KClO}_4)_{\text{NaCl}}$ and $(\text{g KClO}_4)_{\text{KCl}}$ into the equation for their combined masses leaves us with two equations and two unknowns.

$$\text{g NaCl} + \text{g KCl} = 0.2692 \text{ g} \tag{8.E.15}$$

$$2.3708 \times \text{g NaCl} + 1.8584 \times \text{g KCl} = 0.5713 \text{ g} \tag{8.E.16}$$

Multiplying the first equation by 1.8584 and subtracting the second equation gives

$$-0.5124 \times \text{g NaCl} = -0.07102 \text{ g} \tag{8.E.17}$$

$$\text{g NaCl} = 0.1386 \text{ g} \tag{8.E.18}$$

To report the %w/w Na_2O in the sample, we use a conservation of mass on sodium.

$$0.1386 \text{ g NaCl} \times \frac{1 \text{ mol Na}}{58.44 \text{ g NaCl}} \times \frac{61.98 \text{ g Na}_2\text{O}}{2 \text{ mol Na}} = 0.07350 \text{ g Na}_2\text{O} \tag{8.E.19}$$

$$\frac{0.07350 \text{ g Na}_2\text{O}}{0.8143 \text{ g sample}} \times 100 = 9.026\% \text{ w/w Na}_2\text{O} \tag{8.E.20}$$

Click here to return to the chapter.

Practice Exercise 8.4

To find the mass of $(NH_4)_3PO_4$•$12MoO_3$ producing 0.600 g of $PbMoO_3$, we first use a conservation of mass for molybdenum; thus

$$0.600 \text{ g PbMoO}_3 \times \frac{1 \text{ mol Mo}}{351.14 \text{ g PbMoO}_3} \times \frac{1876.38 \text{ g (NH}_4)_3\text{PO}_4 \cdot 12\text{MoO}_3}{12 \text{ mol Mo}} = 0.2672 \text{ g (NH}_4)_3\text{PO}_4 \cdot 12\text{MoO}_3 \tag{8.E.21}$$

Next, to convert this mass of $(NH_4)_3PO_4$•$12MoO_3$ to a mass of Na_3PO_4, we use a conservation of mass on PO_4^{3-}.

$$0.2672 \text{ g (NH}_4)_3\text{PO}_4 \cdot 12\text{MoO}_3 \times \frac{1 \text{ mol PO}_4^{3-}}{1876.38 \text{ g (NH}_4)_3\text{PO}_4 \cdot 12\text{MoO}_3} \times \frac{163.94 \text{ g Na}_3\text{PO}_4}{\text{mol PO}_4^{3-}} = 0.02335 \text{ g Na}_3\text{PO}_4 \tag{8.E.22}$$

Finally, we convert this mass of Na_3PO_4 to the corresponding mass of sample.

$$0.02335 \text{ g Na}_3\text{PO}_4 \times \frac{100 \text{ g sample}}{12.5 \text{ g Na}_3\text{PO}_4} = 0.187 \text{ g sample} \tag{8.E.23}$$

A sample of 0.187 g is sufficient to guarantee 0.600 g of $PbMoO_3$. If a sample contains more than 12.5% Na_3PO_4, then a 0.187-g sample will produce more than 0.600 g of $PbMoO_3$.

Click here to return to the chapter.

Practice Exercise 8.5

To determine which form has the greatest sensitivity, we use a conservation of mass for iron to find the relationship between the precipitate's mass and the mass of iron.

$$\text{g FeO} = \text{g Fe} \times \frac{\text{1 mol Fe}}{\text{55.85 g Fe}} \times \frac{\text{71.85 g FeO}}{\text{mol Fe}} = 1.286 \times \text{g Fe} \tag{8.E.24}$$

$$\text{g } Fe_2O_3 = \text{g Fe} \times \frac{\text{1 mol Fe}}{\text{55.85 g Fe}} \times \frac{\text{159.70 g } Fe_2O_3}{\text{2 mol Fe}} = 1.430 \times \text{g Fe} \tag{8.E.25}$$

$$\text{g } Fe_3O_4 = \text{g Fe} \times \frac{\text{1 mol Fe}}{\text{55.85 g Fe}} \times \frac{\text{231.55 g } Fe_3O_4}{\text{3 mol Fe}} = 1.382 \times \text{ g Fe} \tag{8.E.26}$$

Of the three choices, the greatest sensitivity is obtained with Fe_2O_3 because it provides the largest value for *k*.

Click here to return to the chapter.

Practice Exercise 8.6

From 100–250°C the sample loses 13.8% of its mass, or a loss of

$$0.138 \times 130.35 \text{ g/mol} = 18.0 \text{ g/mol} \tag{8.E.27}$$

consistent with the loss of $H_2O(g)$, leaving a residue of MgC_2O_4. From 350–550°C the sample loses 55.23% of its original mass, or a loss of

$$0.5523 \times 130.35 \text{ g/mol} = 71.99 \text{ g/mol} \tag{8.E.28}$$

This weight loss is consistent with the simultaneous loss of $CO(g)$ and $CO_2(g)$, leaving a residue of MgO.

We can analyze the mixture by heating a portion of the sample to 300°C, 600°C, and 1000°C, recording the mass at each temperature. The loss of mass between 600°C and 1000°C, Δm_2, is due to the loss of $CO_2(g)$ from the decomposition of $CaCO_3$ to CaO, and is proportional to the mass of $CaC_2O_4 \cdot H_2O$ in the sample.

$$\text{g } CaC_2O_4 \cdot H_2O = \Delta m_2 \times \frac{\text{1 mol } CO_2}{\text{44.01 g } CO_2} \times \frac{\text{146.11 g } CaC_2O_4 \cdot H_2O}{\text{mol } CO_2} \tag{8.E.29}$$

The change in mass between 300°C and 600°C, Δm_1, is due to the loss of $CO(g)$ from $CaC_2O_4 \cdot H_2O$ and the loss of $CO(g)$ and $CO_2(g)$ from $MgC_2O_4 \cdot H_2O$. Because we already know the amount of $CaC_2O_4 \cdot H_2O$ in the sample, we can calculate its contribution to Δm_1.

$$(\Delta m_1)_{Ca} = \text{g } CaC_2O_4 \cdot H_2O \times \frac{\text{1 mol CO}}{\text{146.11 g } CaC_2O_4 \cdot H_2O} \times \frac{\text{28.01 g CO}}{\text{mol CO}} \tag{8.E.30}$$

The change in mass due to the decomposition of $MgC_2O_4 \cdot H_2O$

$$(\Delta m_1)_{Mg} = (\Delta m_1) - (\Delta m_1)_{Ca} \tag{8.E.31}$$

provides the mass of $MgC_2O_4 \cdot H_2O$ in the sample.

$$\text{g } MgC_2O_4 \cdot H_2O = (\Delta m_1)_{Mg} \times \frac{\text{1 mol } (CO + CO_2)}{\text{130.35 g } MgC_2O_4 \cdot H_2O} \times \frac{\text{78.02 g } (CO + CO_2)}{\text{1 mol } (CO + CO_2)} \tag{8.E.32}$$

Click here to return to the chapter.

Practice Exercise 8.7

In Practice Exercise 8.6 we developed an equation for the mass of $CaC_2O_4 \cdot H_2O$ in a mixture of $CaC_2O_4 \cdot H_2O$, $MgC_2O_4 \cdot H_2O$, and inert materials. Adapting this equation to a sample containing CaC_2O_4, CaC_2O, and inert materials is easy; thus

$$\begin{aligned}\text{g } CaC_2O_4 &= (0.1794 \text{ g} - 0.1294 \text{ g}) \times \frac{\text{1 mol } CO_2}{\text{44.01 g } CO_2} \times \frac{\text{128.10 g } CaC_2O_4}{\text{mol } CO_2} \\ &= 0.1455 \text{ g } CaC_2O_4\end{aligned} \tag{8.E.33}$$

The %w/w CaC_2O_4 in the sample is

$$\frac{0.1455 \text{ g } CaC_2O_4}{0.3317 \text{ g sample}} \times 100 = 43.86\% \text{ w/w } CaC_2O_4 \tag{8.E.34}$$

Click here to return to the chapter.

Contributors and Attributions

- David Harvey (DePauw University)

8.E: Gravimetric Methods (Exercises) is shared under a CC BY-NC-SA 4.0 license and was authored, remixed, and/or curated by LibreTexts.

8.S: Gravimetric Methods (Summary)

In a gravimetric analysis, a measurement of mass or a change in mass provides quantitative information about the analyte. The most common form of gravimetry uses a precipitation reaction to generate a product whose mass is proportional to the amount of analyte. In many cases the precipitate includes the analyte; however, an indirect analysis in which the analyte causes the precipitation of another compound also is possible. Precipitation gravimetric procedures must be carefully controlled to produce precipitates that are easy to filter, free from impurities, and of known stoichiometry.

In volatilization gravimetry, thermal or chemical energy decomposes the sample containing the analyte. The mass of residue remaining after decomposition, the mass of volatile products collected with a suitable trap, or a change in mass due to the loss of volatile material are all gravimetric measurements.

When the analyte is already present in a particulate form that is easy to separate from its matrix, then a particulate gravimetric analysis may be feasible. Examples include the determination of dissolved solids and the determination of fat in foods.

8.5.1 Key Terms

coagulation	ignition	quartz crystal microbalance
conservation of mass	inclusion	relative supersaturation
coprecipitate	indirect analysis	reprecipitation
definitive technique	occlusion	supernatant
digestion	particulate gravimetry	surface adsorbate
direct analysis	peptization	thermogram
electrogravimetry	precipitant	thermogravimetry
gravimetry	precipitation gravimetry	volatilization gravimetry
homogeneous precipitation		

References

1. Smith, C. S.; Gnodi, M. T. translation of Biringuccio, V. *Pirotechnia*, MIT Press: Cambridge, MA, 1959.
2. Valacárcel, M.; Ríos, A. *Analyst* **1995**, *120*, 2291–2297.
3. (a) Moody, J. R.; Epstein, M. S. *Spectrochim. Acta* **1991**, *46B*, 1571–1575; (b) Epstein, M. S. *Spectrochim. Acta* **1991**, *46B*, 1583–1591.
4. Von Weimarn, P. P. *Chem. Revs.* **1925**, *2*, 217–242.
5. Bassett, J.; Denney, R. C.; Jeffery, G. H. Mendham. J. *Vogel's Textbook of Quantitative Inorganic Analysis*, Longman: London, 4th Ed., 1981, p. 408.
6. Gordon, L.; Salutsky, M. L.; Willard, H. H. *Precipitation from Homogeneous Solution*, Wiley: NY, 1959.
7. Ward, R., ed., *Non-Stoichiometric Compounds* (*Ad. Chem. Ser. 39*), American Chemical Society: Washington, D. C., 1963.
8. Method 4500-SO_4^{2-} C and Method 4500-SO_4^{2-} D as published in *Standard Methods for the Examination of Waters and Wastewaters*, 20th Ed., American Public Health Association: Washington, D. C., 1998.
9. Jungreis, E. *Spot Test Analysis*; 2nd Ed., Wiley: New York, 1997.
10. (a) Ward, M. D.; Buttry, D. A. *Science* **1990**, *249*, 1000–1007; (b) Grate, J. W.; Martin, S. J. ; White, R. M. *Anal. Chem.* **1993**, *65*, 940A–948A; (c) Grate, J. W.; Martin, S. J. ; White, R. M. *Anal. Chem.* **1993**, *65*, 987A–996A.
11. Muratsugu, M.; Ohta, F.; Miya, Y.; Hosokawa, T.; Kurosawa, S.; Kamo, N.; Ikeda, H. *Anal. Chem.* **1993**, *65*, 2933–2937.
12. Sinha, S. K.; Shome, S. C. *Anal. Chim. Acta* **1960**, *24*, 33–36.
13. Adapted from Sorum, C. H.; Lagowski, J. J. *Introduction to Semimicro Qualitative Analysis*, Prentice-Hall: Englewood Cliffs, N. J., 5th Ed., 1977, p. 285.
14. Grote, F. Z. *Anal. Chem.* **1941**, *122*, 395–398.
15. Nawrocki, J.; Carr, P. W.; Annen, M. J.; Froelicher, S. *Anal. Chim. Acta* **1996**, *327*, 261–266.
16. *Fat Determination by SFE*, ISCO, Inc. Lincoln, NE.
17. Delumyea, R. D.; McCleary, D. L. *J. Chem. Educ.* **1993**, *70*, 172–173.18 Yao, S. F.; He, F. J. Nie, L. H. *Anal. Chim. Acta* **1992**, *268*, 311–314.

Contributors

- David Harvey (DePauw University)

8.S: Gravimetric Methods (Summary) is shared under a CC BY-NC-SA 4.0 license and was authored, remixed, and/or curated by LibreTexts.

CHAPTER OVERVIEW

9: Titrimetric Methods

Titrimetry, in which volume serves as the analytical signal, made its first appearance as an analytical method in the early eighteenth century. Titrimetric methods were not well received by the analytical chemists of that era because they could not duplicate the accuracy and precision of a gravimetric analysis. Not surprisingly, few standard texts from the 1700s and 1800s include titrimetric methods of analysis.

Precipitation gravimetry developed as an analytical method without a general theory of precipitation. An empirical relationship between a precipitate's mass and the mass of analyte—what analytical chemists call a gravimetric factor—was determined experimentally by taking a known mass of analyte through the procedure. Today, we recognize this as an early example of an external standardization. Gravimetric factors were not calculated using the stoichiometry of a precipitation reaction because chemical formulas and atomic weights were not yet available! Unlike gravimetry, the development and acceptance of titrimetry required a deeper understanding of stoichiometry, of thermodynamics, and of chemical equilibria. By the 1900s, the accuracy and precision of titrimetric methods were comparable to that of gravimetric methods, establishing titrimetry as an accepted analytical technique.

Topic hierarchy

9.1: Overview of Titrimetry
9.2: Acid–Base Titrations
9.3: Complexation Titrations
9.4: Redox Titrations
9.5: Precipitation Titrations
9.E: Titrimetric Methods (Exercises)
9.S: Titrimetric Methods (Summary)

Thumbnail: A Winkler titration to determine the concentration of dissolved oxygen in a water sample. The dissolved oxygen has been converted to an equivalent amount of iodine, which is being titrated with thiosulfate using a starch indicator. The blue color in the flask will disappear when all the iodine has been converted to iodide. Image used with permission (CC BY-SA 3.0; Will Woodgate (Cornwall College, UK)).

Contributors

- David Harvey (DePauw University)

9: Titrimetric Methods is shared under a CC BY-NC-SA 4.0 license and was authored, remixed, and/or curated by LibreTexts.

9.1: Overview of Titrimetry

In **titrimetry** we add a reagent, called the **titrant**, to a solution containing another reagent, called the **titrand**, and allow them to react. The type of reaction provides us with a simple way to divide titrimetry into the following four categories: acid–base titrations, in which an acidic or basic titrant reacts with a titrand that is a base or an acid; complexometric titrations based on metal–ligand complexation; redox titrations, in which the titrant is an oxidizing or reducing agent; and precipitation titrations, in which the titrand and titrant form a precipitate.

> **Note**
>
> We are deliberately avoiding the term analyte at this point in our introduction to titrimetry. Although in most titrations the analyte is the titrand, there are circumstances where the analyte is the titrant. When discussing specific methods, we will use the term analyte where appropriate.

Despite the difference in chemistry, all titrations share several common features. Before we consider individual titrimetric methods in greater detail, let's take a moment to consider some of these similarities. As you work through this chapter, this overview will help you focus on similarities between different titrimetric methods. You will find it easier to understand a new analytical method when you can see its relationship to other similar methods.

9.1.1 Equivalence Points and End points

If a titration is to be accurate we must combine stoichiometrically equivalent amount of titrant and titrand. We call this stoichiometric mixture the **equivalence point**. Unlike precipitation gravimetry, where we add the precipitant in excess, an accurate titration requires that we know the exact volume of titrant at the equivalence point, V_{eq}. The product of the titrant's equivalence point volume and its molarity, M_T, is equal to the moles of titrant reacting with the titrand.

$$\text{moles of titrant} = M_T \times V_{eq} \tag{9.1.1}$$

If we know the stoichiometry of the titration reaction, then we can calculate the moles of titrand.

Unfortunately, for most titrations there is no obvious sign when we reach the equivalence point. Instead, we stop adding titrant when at an **end point** of our choosing. Often this end point is a change in the color of a substance, called an **indicator**, that we add to the titrand's solution. The difference between the end point volume and the equivalence point volume is a determinate **titration error**. If the end point and the equivalence point volumes coincide closely, then the titration error is insignificant and it is safely ignored. Clearly, selecting an appropriate end point is critically important.

9.1.2 Volume as a Signal

> **Note**
>
> Instead of measuring the titrant's volume, we may choose to measure its mass. Although we generally can measure mass more precisely than we can measure volume, the simplicity of a volumetric titration makes it the more popular choice.

Almost any chemical reaction can serve as a titrimetric method provided it meets the following four conditions. The first condition is that we must know the stoichiometry between the titrant and the titrand. If this is not the case, then we cannot convert the moles of titrant consumed in reaching the end point to the moles of titrand in our sample. Second, the titration reaction must effectively proceed to completion; that is, the stoichiometric mixing of the titrant and the titrand must result in their reaction. Third, the titration reaction must occur rapidly. If we add the titrant faster than it can react with the titrand, then the end point and the equivalence point will differ significantly. Finally, there must be a suitable method for accurately determining the end point. These are significant limitations and, for this reason, there are several common titration strategies.

> **Note**
>
> Depending on how we are detecting the endpoint, we may stop the titration too early or too late. If the end point is a function of the titrant's concentration, then adding the titrant too quickly leads to an early end point. On the other hand, if the end point is a function of the titrant's concentration, then the end point exceeds the equivalence point.

A simple example of a titration is an analysis for Ag^+ using thiocyanate, SCN^-, as a titrant.

$$Ag^+(aq) + SCN^-(aq) \rightleftharpoons Ag(SCN)(s) \tag{9.1.2}$$

> **Note**
>
> This is an example of a precipitation titration. You will find more information about precipitation titrations in Section 9.5.

This reaction occurs quickly and with a known stoichiometry, satisfying two of our requirements. To indicate the titration's end point, we add a small amount of Fe^{3+} to the analyte's solution before beginning the titration. When the reaction between Ag^+ and SCN^- is complete, formation of the red-colored $Fe(SCN)^{2+}$ complex signals the end point. This is an example of a **direct titration** since the titrant reacts directly with the analyte.

If the titration's reaction is too slow, if a suitable indicator is not available, or if there is no useful direct titration reaction, then an indirect analysis may be possible. Suppose you wish to determine the concentration of formaldehyde, H_2CO, in an aqueous solution. The oxidation of H_2CO by I_3^-

$$H_2CO(aq) + I_3^-(aq) + 3OH^-(aq) \rightleftharpoons HCO_2^-(aq) + 3I^-(aq) + 2H_2O(l) \tag{9.1.3}$$

is a useful reaction, but it is too slow for a titration. If we add a known excess of I_3^- and allow its reaction with H_2CO to go to completion, we can titrate the unreacted I_3^- with thiosulfate, $S_2O_3^{2-}$.

$$I_3^-(aq) + 2S_2O_3^{2-}(aq) \rightleftharpoons S_4O_6^{2-}(aq) + 3I^-(aq) \tag{9.1.4}$$

> **Note**
>
> This is an example of a redox titration. You will find more information about redox titrations in Section 9.4.

The difference between the initial amount of I_3^- and the amount in excess gives us the amount of I_3^- reacting with the formaldehyde. This is an example of a **back titration**.

Calcium ion plays an important role in many environmental systems. A direct analysis for Ca^{2+} might take advantage of its reaction with the ligand ethylenediaminetetraacetic acid (EDTA), which we represent here as Y^{4-}.

$$Ca^{2+}(aq) + Y^{4-}(aq) \rightleftharpoons CaY^{2-}(aq) \tag{9.1.5}$$

Unfortunately, for most samples this titration does not have a useful indicator. Instead, we react the Ca^{2+} with an excess of MgY^{2-}

$$Ca^{2+}(aq) + MgY^{2-}(aq) \rightleftharpoons CaY^{2-}(aq) + Mg^{2+}(aq) \tag{9.1.6}$$

releasing an amount of Mg^{2+} equivalent to the amount of Ca^{2+} in the sample.

> **Note**
>
> MgY^{2-} is the Mg^{2+}–EDTA metal–ligand complex. You can prepare a solution of MgY^{2-} by combining equimolar solutions of Mg^{2+} and EDTA.

Because the titration of Mg^{2+} with EDTA

$$Mg^{2+}(aq) + Y^{4-}(aq) \rightleftharpoons MgY^{2-}(aq) \tag{9.1.7}$$

has a suitable end point, we can complete the analysis.

> **Note**
>
> This is an example of a complexation titration. You will find more information about complexation titrations in Section 9.3.

The amount of EDTA used in the titration provides an indirect measure of the amount of Ca^{2+} in the original sample. Because the species we are titrating was displaced by the analyte, we call this a **displacement titration**.

If a suitable reaction involving the analyte does not exist it may be possible to generate a species that we can titrate. For example, we can determine the sulfur content of coal by using a combustion reaction to convert sulfur to sulfur dioxide

$$S(s) + O_2(g) \rightarrow SO_2(g) \tag{9.1.8}$$

and then convert the SO_2 to sulfuric acid, H_2SO_4, by bubbling it through an aqueous solution of hydrogen peroxide, H_2O_2.

$$SO_2(g) + H_2O_2(aq) \rightarrow H_2SO_4(aq) \tag{9.1.9}$$

Titrating H_2SO_4 with NaOH

$$H_2SO_4(aq) + 2NaOH(aq) \rightleftharpoons 2H_2O(l) + Na_2SO_4(aq) \tag{9.1.10}$$

provides an indirect determination of sulfur.

> **Note**
>
> This is an example of an acid–base titration. You will find more information about acid–base titrations in Section 9.2.

9.1.3 Titration Curves

To find a titration's end point, we need to monitor some property of the reaction that has a well-defined value at the equivalence point. For example, the equivalence point for a titration of HCl with NaOH occurs at a pH of 7.0. A simple method for finding the equivalence point is to continuously monitor the titration mixture's pH using a pH electrode, stopping the titration when we reach a pH of 7.0. Alternatively, we can add an indicator to the titrand's solution that changes color at a pH of 7.0.

> **Note**
>
> Why a pH of 7.0 is the equivalence point for this titration is a topic we will cover in Section 9.2.

Suppose the only available indicator changes color at an end point pH of 6.8. Is the difference between the end point and the equivalence point small enough that we can safely ignore the titration error? To answer this question we need to know how the pH changes during the titration.

A **titration curve** provides us with a visual picture of how a property of the titration reaction changes as we add the titrant to the titrand. The titration curve in Figure 9.1, for example, was obtained by suspending a pH electrode in a solution of 0.100 M HCl (the titrand) and monitoring the pH while adding 0.100 M NaOH (the titrant). A close examination of this titration curve should convince you that an end point pH of 6.8 produces a negligible titration error. Selecting a pH of 11.6 as the end point, however, produces an unacceptably large titration error.

> **Note**
>
> For the titration curve in Figure 9.1, the volume of titrant to reach a pH of 6.8 is 24.99995 mL, a titration error of -2.00×10^{-4}%. Typically, we can only read the volume to the nearest ±0.01 mL, which means this uncertainty is too small to affect our results.
>
> The volume of titrant to reach a pH of 11.6 is 27.07 mL, or a titration error of +8.28%. This is a significant error.

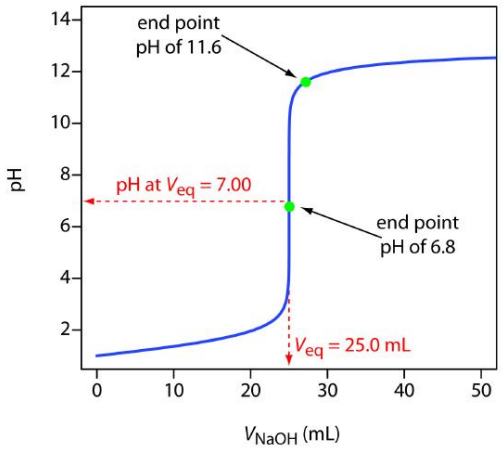


Figure 9.1 Typical acid–base titration curve showing how the titrand's pH changes with the addition of titrant. The titrand is a 25.0 mL solution of 0.100 M HCl and the titrant is 0.100 M NaOH. The titration curve is the solid blue line, and the equivalence point volume (25.0 mL) and pH (7.00) are shown by the dashed red lines. The green dots show two end points. The end point at a pH of 6.8 has a small titration error, and the end point at a pH of 11.6 has a larger titration error.

The titration curve in Figure 9.1 is not unique to an acid–base titration. Any titration curve that follows the change in concentration of a species in the titration reaction (plotted logarithmically) as a function of the titrant's volume has the same general sigmoidal shape. Several additional examples are shown in Figure 9.2.

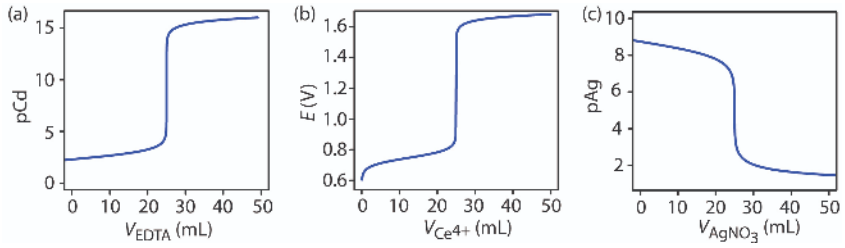


Figure 9.2 Additional examples of titration curves. (a) Complexation titration of 25.0 mL of 1.0 mM Cd^{2+} with 1.0 mM EDTA at a pH of 10. The *y*-axis displays the titrand's equilibrium concentration as pCd. (b) Redox titration of 25.0 mL of 0.050 M Fe^{2+} with 0.050 M Ce^{4+} in 1 M $HClO_4$. The *y*-axis displays the titration mixture's electrochemical potential, *E*, which, through the Nernst equation is a logarithmic function of concentrations. (c) Precipitation titration of 25.0 mL of 0.10 M NaCl with 0.10 M $AgNO_3$. The *y*-axis displays the titrant's equilibrium concentration as pAg.

The titrand's or the titrant's concentration is not the only property we can use when recording a titration curve. Other parameters, such as the temperature or absorbance of the titrand's solution, may provide a useful end point signal. Many acid–base titration reactions, for example, are exothermic. As the titrant and titrand react the temperature of the titrand's solution steadily increases. Once we reach the equivalence point, further additions of titrant do not produce as exothermic a response. Figure 9.3 shows a typical **thermometric titration curve** with the intersection of the two linear segments indicating the equivalence point.

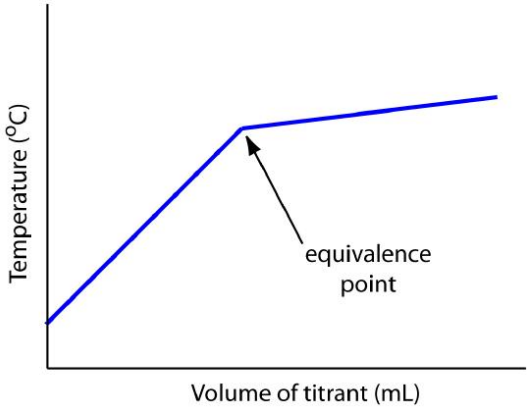


Figure 9.3 Example of a thermometric titration curve showing the location of the equivalence point.

9.1.4 The Buret

The only essential equipment for an acid–base titration is a means for delivering the titrant to the titrand's solution. The most common method for delivering titrant is a **buret** (Figure 9.4). A buret is a long, narrow tube with graduated markings, equipped with a stopcock for dispensing the titrant. The buret's small internal diameter provides a better defined meniscus, making it easier to read the titrant's volume precisely. Burets are available in a variety of sizes and tolerances (Table 9.1), with the choice of buret determined by the needs of the analysis. You can improve a buret's accuracy by calibrating it over several intermediate ranges of volumes using the method described in Chapter 5 for calibrating pipets. Calibrating a buret corrects for variations in the buret's internal diameter.

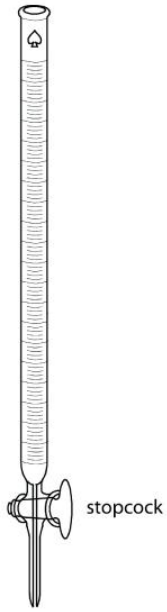


Figure 9.4 Typical volumetric buret. The stopcock is in the open position, allowing the titrant to flow into the titrand's solution. Rotating the stopcock controls the titrant's flow rate.

Table 9.1 Specifications for Volumetric Burets

Volume (mL)	Class	Subdivision (mL)	Tolerance (mL)
5	A B	0.01 0.01	±0.01 ±0.01
10	A B	0.02 0.02	±0.02 ±0.04
25	A B	0.1 0.1	±0.03 ±0.06
50	A B	0.1 0.1	±0.05 ±0.10
100	A B	0.2 0.2	±0.10 ±0.20

A titration can be automated by using a pump to deliver the titrant at a constant flow rate (Figure 9.5). Automated titrations offer the additional advantage of using a microcomputer for data storage and analysis.



Figure 9.5 Typical instrumentation for an automated acid–base titration showing the titrant, the pump, and the titrand. The pH electrode in the titrand's solution is used to monitor the titration's progress. You can see the titration curve in the lower-left quadrant of the computer's display. Modified from: Datamax (commons.wikipedia.org).

Contributors

David Harvey (DePauw University)

9.1: Overview of Titrimetry is shared under a CC BY-NC-SA 4.0 license and was authored, remixed, and/or curated by LibreTexts.

9.2: Acid–Base Titrations

Before 1800, most **acid–base titrations** used H_2SO_4, HCl, or HNO_3 as acidic titrants, and K_2CO_3 or Na_2CO_3 as basic titrants. A titration's end point was determined using litmus as an indicator, which is red in acidic solutions and blue in basic solutions, or by the cessation of CO_2 effervescence when neutralizing CO_3^{2-}. Early examples of acid–base titrimetry include determining the acidity or alkalinity of solutions, and determining the purity of carbonates and alkaline earth oxides.

Three limitations slowed the development of acid–base titrimetry: the lack of a strong base titrant for the analysis of weak acids, the lack of suitable indicators, and the absence of a theory of acid–base reactivity. The introduction, in 1846, of NaOH as a strong base titrant extended acid–base titrimetry to the determination of weak acids. The synthesis of organic dyes provided many new indicators. Phenolphthalein, for example, was first synthesized by Bayer in 1871 and used as an indicator for acid–base titrations in 1877.

Despite the increasing availability of indicators, the absence of a theory of acid–base reactivity made it difficult to select an indicator. The development of equilibrium theory in the late 19th century led to significant improvements in the theoretical understanding of acid–base chemistry, and, in turn, of acid–base titrimetry. Sørenson's establishment of the pH scale in 1909 provided a rigorous means for comparing indicators. The determination of acid–base dissociation constants made it possible to calculate a theoretical titration curve, as outlined by Bjerrum in 1914. For the first time analytical chemists had a rational method for selecting an indicator, establishing acid–base titrimetry as a useful alternative to gravimetry.

9.2.1 Acid–Base Titration Curves

In the overview to this chapter we noted that a titration's end point should coincide with its equivalence point. To understand the relationship between an acid–base titration's end point and its equivalence point we must know how the pH changes during a titration. In this section we will learn how to calculate a titration curve using the equilibrium calculations from Chapter 6. We also will learn how to quickly sketch a good approximation of any acid–base titration curve using a limited number of simple calculations.

Titrating Strong Acids and Strong Bases

For our first titration curve, let's consider the titration of 50.0 mL of 0.100 M HCl using a titrant of 0.200 M NaOH. When a strong base and a strong acid react the only reaction of importance is

$$H_3O^+(aq) + OH^-(aq) \rightarrow 2H_2O(l) \tag{9.1}$$

Note

Although we have not written reaction 9.1 as an equilibrium reaction, it is at equilibrium; however, because its equilibrium constant is large—it is equal to $(K_w)^{-1}$ or 1.00×10^{14}—we can treat reaction 9.1 as though it goes to completion.

Note

Step 1: Calculate the volume of titrant needed to reach the equivalence point.

The first task in constructing the titration curve is to calculate the volume of NaOH needed to reach the equivalence point, V_{eq}. At the equivalence point we know from reaction 9.1 that

$$\text{moles HCl} = \text{moles NaOH} \tag{9.2.1}$$

$$M_a \times V_a = M_b \times V_b \tag{9.2.2}$$

where the subscript 'a' indicates the acid, HCl, and the subscript 'b' indicates the base, NaOH. The volume of NaOH needed to reach the equivalence point is

$$V_{eq} = V_b = \frac{M_a V_a}{M_b} = \frac{(0.100\ \text{M})(50.0\ \text{mL})}{0.200\ \text{M}} = 25.0\ \text{mL} \tag{9.2.3}$$

Note

Step 2: Calculate pH values before the equivalence point by determining the concentration of unreacted titrand.

Before the equivalence point, HCl is present in excess and the pH is determined by the concentration of unreacted HCl. At the start of the titration the solution is 0.100 M in HCl, which, because HCl is a strong acid, means that the pH is

$$\text{pH} = -\log[\text{H}_3\text{O}^+] = -\log[\text{HCl}] = -\log(0.100) = 1.00 \tag{9.2.4}$$

After adding 10.0 mL of NaOH the concentration of excess HCl is

$$[\text{HCl}] = \frac{\text{initial moles HCl} - \text{moles NaOH added}}{\text{total volume}} = \frac{M_\text{a}V_\text{a} - M_\text{b}V_\text{b}}{V_\text{a} + V_\text{b}} \tag{9.2.5}$$

$$= \frac{(0.100\text{ M})(50.0\text{ mL}) - (0.200\text{ M})(10.0\text{ mL})}{50.0\text{ mL} + 10.0\text{ mL}} = 0.0500\text{ M} \tag{9.2.6}$$

and the pH increases to 1.30.

Note

Step 3: The pH at the equivalence point for the titration of a strong acid with a strong base is 7.00.

At the equivalence point the moles of HCl and the moles of NaOH are equal. Since neither the acid nor the base is in excess, the pH is determined by the dissociation of water.

$$K_\text{w} = 1.00 \times 10^{-14} = [\text{H}_3\text{O}^+][\text{OH}^-] = [\text{H}_3\text{O}^+]^2 \tag{9.2.7}$$

$$[\text{H}_3\text{O}^+] = 1.00 \times 10^{-7}\text{ M} \tag{9.2.8}$$

Thus, the pH at the equivalence point is 7.00.

Note

Step 4: Calculate pH values after the equivalence point by determining the concentration of excess titrant.

For volumes of NaOH greater than the equivalence point, the pH is determined by the concentration of excess OH^-. For example, after adding 30.0 mL of titrant the concentration of OH^- is

$$[\text{OH}^-] = \frac{\text{moles NaOH added} - \text{initial moles HCl}}{\text{total volume}} = \frac{M_\text{b}V_\text{b} - M_\text{a}V_\text{a}}{V_\text{a} + V_\text{b}} \tag{9.2.9}$$

$$= \frac{(0.200\text{ M})(30.0\text{ mL}) - (0.100\text{ M})(50.0\text{ mL})}{50.0\text{ mL} + 30.0\text{ mL}} = 0.0125\text{ M} \tag{9.2.10}$$

To find the concentration of H_3O^+ we use the K_w expression

$$[\text{H}_3\text{O}^+] = \frac{K_\text{w}}{[\text{OH}^-]} = \frac{1.00 \times 10^{-14}}{0.0125\text{ M}} = 8.00 \times 10^{-13}\text{ M} \tag{9.2.11}$$

giving a pH of 12.10. Table 9.2 and Figure 9.6 show additional results for this titration curve. You can use this same approach to calculate the titration curve for the titration of a strong base with a strong acid, except the strong base is in excess before the equivalence point and the strong acid is in excess after the equivalence point.

Table 9.2 Titration of 50.0 mL of 0.100 M HCl with 0.200 M NaOH

Volume of NaOH (mL)	pH	Volume of NaOH (mL)	pH
0.00	1.00	26.0	11.42
5.00	1.14	28.0	11.89
10.0	1.30	30.0	12.10
15.0	1.51	35.0	12.37
20.0	1.85	40.0	12.52
22.0	2.08	45.0	12.62
24.0	2.57	50.0	12.70
25.0	7.00		

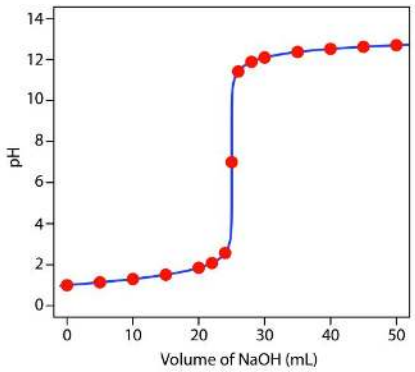


Figure 9.6 Titration curve for the titration of 50.0 mL of 0.100 M HCl with 0.200 M NaOH. The red points correspond to the data in Table 9.2. The blue line shows the complete titration curve.

Practice Exercise 9.1

Construct a titration curve for the titration of 25.0 mL of 0.125 M NaOH with 0.0625 M HCl.

Click here to review your answer to this exercise.

Titrating a Weak Acid with a Strong Base

Note

Step 1: Calculate the volume of titrant needed to reach the equivalence point.

For this example, let's consider the titration of 50.0 mL of 0.100 M acetic acid, CH_3COOH, with 0.200 M NaOH. Again, we start by calculating the volume of NaOH needed to reach the equivalence point; thus

$$\text{moles } CH_3COOH = \text{moles NaOH} \tag{9.2.12}$$

$$M_a \times V_a = M_b \times V_b \tag{9.2.13}$$

$$V_{eq} = V_b = \frac{M_a V_a}{M_b} = \frac{(0.100\text{ M})(50.0\text{ mL})}{0.200\text{ M}} = 25.0\text{ mL} \tag{9.2.14}$$

Note

Step 2: Before adding the titrant, the pH is determined by the titrand, which in this case is a weak acid.

Before adding NaOH the pH is that for a solution of 0.100 M acetic acid. Because acetic acid is a weak acid, we calculate the pH using the method outlined in Chapter 6.

$$CH_3COOH(aq) + H_2O(l) \rightleftharpoons H_3O^+(aq) + CH_3COO^-(aq) \tag{9.2.15}$$

$$K_a = \frac{[H_3O^+][CH_3COO^-]}{[CH_3COOH]} = \frac{(x)(x)}{0.100 - x} = 1.75 \times 10^{-5} \tag{9.2.16}$$

$$x = [H_3O^+] = 1.32 \times 10^{-3}\,M \tag{9.2.17}$$

At the beginning of the titration the pH is 2.88.

Adding NaOH converts a portion of the acetic acid to its conjugate base, CH_3COO^-.

$$CH_3COOH(aq) + OH^-(aq) \rightarrow H_2O(l) + CH_3COO^-(aq) \tag{9.2}$$

Note

Because the equilibrium constant for reaction 9.2 is quite large

$$K = K_a/K_w = 1.75 \times 10^9 \tag{9.2.18}$$

we can treat the reaction as if it goes to completion.

Any solution containing comparable amounts of a weak acid, HA, and its conjugate weak base, A^-, is a buffer. As we learned in Chapter 6, we can calculate the pH of a buffer using the Henderson–Hasselbalch equation.

$$pH = pK_a + \log \frac{[A^-]}{[HA]} \tag{9.2.19}$$

Note

Step 3: Before the equivalence point, the pH is determined by a buffer containing the titrand and its conjugate form.

Before the equivalence point the concentration of unreacted acetic acid is

$$[CH_3COOH] = \frac{\text{initial moles } CH_3COOH - \text{moles NaOH added}}{\text{total volume}} \tag{9.2.20}$$

$$= \frac{M_aV_a - M_bV_b}{V_a + V_b} \tag{9.2.21}$$

and the concentration of acetate is

$$[CH_3COO^-] = \frac{\text{moles NaOH added}}{\text{total volume}} = \frac{M_bV_b}{V_a + V_b} \tag{9.2.22}$$

For example, after adding 10.0 mL of NaOH the concentrations of CH_3COOH and CH_3COO^- are

$$[CH_3COOH] = \frac{(0.100\text{ M})(50.0\text{ mL}) - (0.200\text{ M})(10.0\text{ mL})}{50.0\text{ mL} + 10.0\text{ mL}} \tag{9.2.23}$$

$$= 0.0500\,M \tag{9.2.24}$$

$$[CH_3COO^-] = \frac{(0.200\text{ M})(10.0\text{ mL})}{50.0\text{ mL} + 10.0\text{ mL}} = 0.0333\text{ M} \tag{9.2.25}$$

which gives us a pH of

$$pH = 4.76 + \log \frac{0.0333\text{ M}}{0.0500\text{ M}} = 4.58 \tag{9.2.26}$$

Note

Step 4: The pH at the equivalence point is determined by the titrand's conjugate form, which in this case is a weak base.

At the equivalence point the moles of acetic acid initially present and the moles of NaOH added are identical. Because their reaction effectively proceeds to completion, the predominate ion in solution is CH_3COO^-, which is a weak base. To calculate the pH we first determine the concentration of CH_3COO^-

$$[CH_3COO^-] = \frac{\text{moles NaOH added}}{\text{total volume}} \tag{9.2.27}$$

$$= \frac{(0.200\text{ M})(25.0\text{ mL})}{50.0\text{ mL} + 25.0\text{ mL}} = 0.0667\text{ M} \tag{9.2.28}$$

Note

Alternatively, we can calculate acetate's concentration using the initial moles of acetic acid; thus

$$[\mathrm{CH_3COO^-}] = \frac{\text{initial moles } \mathrm{CH_3COOH}}{\text{total volume}} \tag{9.2.29}$$

$$= \frac{(0.100\ \mathrm{M})(50.0\ \mathrm{mL})}{50.0\ \mathrm{mL} + 25.0\ \mathrm{mL}} \tag{9.2.30}$$

$$= 0.0667\ \mathrm{M} \tag{9.2.31}$$

Next, we calculate the pH of the weak base as shown earlier in Chapter 6.

$$\mathrm{CH_3COO^-}(aq) + \mathrm{H_2O}(l) \rightleftharpoons \mathrm{OH^-}(aq) + \mathrm{CH_3COOH}(aq) \tag{9.2.32}$$

$$K_\mathrm{b} = \frac{[\mathrm{OH^-}][\mathrm{CH_3COOH}]}{[\mathrm{CH_3COO^-}]} = \frac{(x)(x)}{0.0667 - x} = 5.71 \times 10^{-10} \tag{9.2.33}$$

$$x = [\mathrm{OH^-}] = 6.17 \times 10^{-6}\ \mathrm{M} \tag{9.2.34}$$

$$[\mathrm{H_3O^+}] = \frac{K_\mathrm{w}}{[\mathrm{OH^-}]} = \frac{1.00 \times 10^{-14}}{6.17 \times 10^{-6}} = 1.62 \times 10^{-9}\ \mathrm{M} \tag{9.2.35}$$

The pH at the equivalence point is 8.79.

Note

Step 5: Calculate pH values after the equivalence point by determining the concentration of excess titrant.

After the equivalence point, the titrant is in excess and the titration mixture is a dilute solution of NaOH. We can calculate the pH using the same strategy as in the titration of a strong acid with a strong base. For example, after adding 30.0 mL of NaOH the concentration of $\mathrm{OH^-}$ is

$$[\mathrm{OH^-}] = \frac{(0.200\ \mathrm{M})(30.0\ \mathrm{mL}) - (0.100\ \mathrm{M})(50.0\ \mathrm{mL})}{50.0\ \mathrm{mL} + 30.0\ \mathrm{mL}} = 0.0125\ \mathrm{M} \tag{9.2.36}$$

$$[\mathrm{H_3O^+}] = \frac{K_\mathrm{w}}{[\mathrm{OH^-}]} = \frac{1.00 \times 10^{-14}}{0.0125\ \mathrm{M}} = 8.00 \times 10^{-13}\ \mathrm{M} \tag{9.2.37}$$

giving a pH of 12.10. Table 9.3 and Figure 9.7 show additional results for this titration. You can use this same approach to calculate the titration curve for the titration of a weak base with a strong acid, except the initial pH is determined by the weak base, the pH at the equivalence point by its conjugate weak acid, and the pH after the equivalence point by excess strong acid.

Table 9.3 Titration of 50.0 mL of 0.100 M Acetic Acid with 0.200 M NaOH

Volume of NaOH (mL)	pH	Volume of NaOH (mL)	pH
0.00	2.88	26.0	11.42
5.00	4.16	28.0	11.89
10.0	4.58	30.0	12.10
15.0	4.94	35.0	12.37
20.0	5.36	40.0	12.52
22.0	5.63	45.0	12.62
24.0	6.14	50.0	12.70
25.0	8.79		

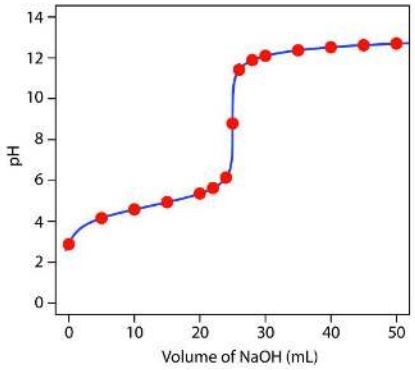


Figure 9.7 Titration curve for the titration of 50.0 mL of 0.100 M CH_3COOH with 0.200 M NaOH. The red points correspond to the data in Table 9.3. The blue line shows the complete titration curve.

Practice Exercise 9.2

Construct a titration curve for the titration of 25.0 mL of 0.125 M NH_3 with 0.0625 M HCl.

Click here to review your answer to this exercise.

We can extend our approach for calculating a weak acid–strong base titration curve to reactions involving multiprotic acids or bases, and mixtures of acids or bases. As the complexity of the titration increases, however, the necessary calculations become more time consuming. Not surprisingly, a variety of algebraic[1] and computer spreadsheet[2] approaches have been described to aid in constructing titration curves.

Sketching An Acid–Base Titration Curve

To evaluate the relationship between a titration's equivalence point and its end point, we need to construct only a reasonable approximation of the exact titration curve. In this section we demonstrate a simple method for sketching an acid–base titration curve. Our goal is to sketch the titration curve quickly, using as few calculations as possible. Let's use the titration of 50.0 mL of 0.100 M CH_3COOH with 0.200 M NaOH to illustrate our approach.

Note

This is the same example that we used in developing the calculations for a weak acid–strong base titration curve. You can review the results of that calculation in Table 9.3 and Figure 9.7.

We begin by calculating the titration's equivalence point volume, which, as we determined earlier, is 25.0 mL. Next we draw our axes, placing pH on the *y*-axis and the titrant's volume on the *x*-axis. To indicate the equivalence point volume, we draw a vertical line corresponding to 25.0 mL of NaOH. Figure 9.8a shows the result of the first step in our sketch.

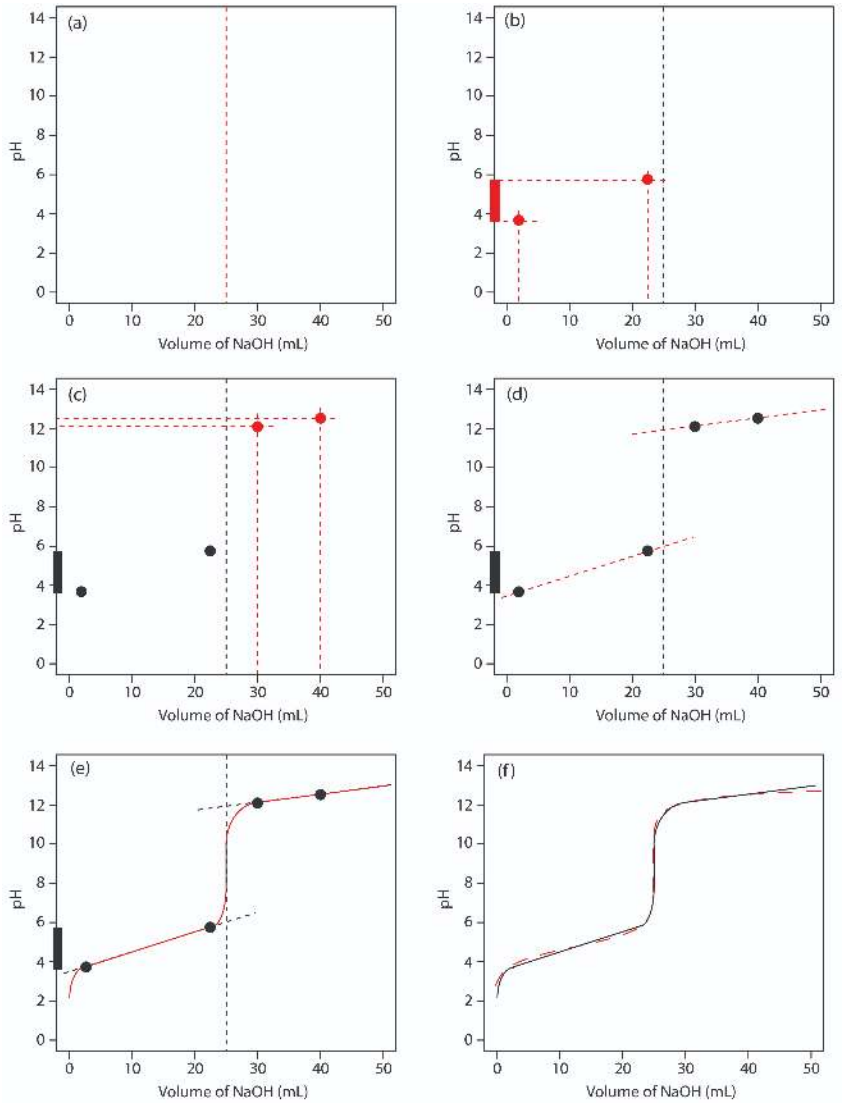


Figure 9.8 Illustrations showing the steps in sketching an approximate titration curve for the titration of 50.0 mL of 0.100 M CH_3COOH with 0.200 M NaOH: (a) locating the equivalence point volume; (b) plotting two points before the equivalence point; (c) plotting two points after the equivalence point; (d) preliminary approximation of titration curve using straight-lines; (e) final approximation of titration curve using a smooth curve; (f) comparison of approximate titration curve (solid black line) and exact titration curve (dashed red line). See the text for additional details.

Before the equivalence point the titration mixture's pH is determined by a buffer of acetic acid, CH_3COOH, and acetate, CH_3COO^-. Although we can easily calculate a buffer's pH using the Henderson–Hasselbalch equation, we can avoid this calculation by making a simple assumption. You may recall from Chapter 6 that a buffer operates over a pH range extending approximately ±1 pH unit on either side of the weak acid's pK_a value. The pH is at the lower end of this range, pH = pK_a – 1, when the weak acid's concentration is 10× greater than that of its conjugate weak base. The buffer reaches its upper pH limit, pH = pK_a + 1, when the weak acid's concentration is 10× smaller than that of its conjugate weak base. When titrating a weak acid or a weak base, the buffer spans a range of volumes from approximately 10% of the equivalence point volume to approximately 90% of the equivalence point volume.

Figure 9.8b shows the second step in our sketch. First, we superimpose acetic acid's ladder diagram on the *y*-axis, including its buffer range, using its pK_a value of 4.76. Next, we add points representing the pH at 10% of the equivalence point volume (a pH of 3.76 at 2.5 mL) and at 90% of the equivalence point volume (a pH of 5.76 at 22.5 mL).

Note

The actual values are 9.09% and 90.9%, but for our purpose, using 10% and 90% is more convenient; that is, after all, one advantage of an approximation! Problem 9.4 in the end-of-chapter problems asks you to verify these percentages.

The third step in sketching our titration curve is to add two points after the equivalence point. The pH after the equivalence point is fixed by the concentration of excess titrant, NaOH. Calculating the pH of a strong base is straightforward, as we have seen earlier. Figure 9.8c shows the pH after adding 30.0 mL and 40.0 mL of NaOH.

Note

See Table 9.3 for the values.

Next, we draw a straight line through each pair of points, extending the lines through the vertical line representing the equivalence point's volume (Figure 9.8d). Finally, we complete our sketch by drawing a smooth curve that connects the three straight-line segments (Figure 9.8e). A comparison of our sketch to the exact titration curve (Figure 9.8f) shows that they are in close agreement.

Practice Exercise 9.3

Sketch a titration curve for the titration of 25.0 mL of 0.125 M NH_3 with 0.0625 M HCl and compare to the result from Practice Exercise 9.2.

Click here to review your answer to this exercise.

As shown by the following example, we can adapt this approach to acid–base titrations, including those involving polyprotic weak acids and bases, or mixtures of weak acids and bases.

Example 9.1

Sketch titration curves for the following two systems: (a) the titration of 50.0 mL of 0.050 M H_2A, a diprotic weak acid with a pK_{a1} of 3 and a pK_{a2} of 7; and (b) the titration of a 50.0 mL mixture containing 0.075 M HA, a weak acid with a pK_a of 3, and 0.025 M HB, a weak acid with a pK_a of 7. For both titrations the titrant is 0.10 M NaOH.

Solution

Figure 9.9a shows the titration curve for H_2A, including the ladder diagram on the *y*-axis, the equivalence points at 25.0 mL and 50.0 mL, two points before each equivalence point, two points after the last equivalence point, and the straight-lines that help in sketching the final curve. Before the first equivalence point the pH is controlled by a buffer consisting of H_2A and HA^-. An HA^-/A^{2-} buffer controls the pH between the two equivalence points. After the second equivalence point the pH reflects the concentration of excess NaOH.

Figure 9.9b shows the titration curve for the mixture of HA and HB. Again, there are two equivalence points. In this case, however, the equivalence points are not equally spaced because the concentration of HA is greater than that for HB. Since HA is the stronger of the two weak acids it reacts first; thus, the pH before the first equivalence point is controlled by a buffer consisting of HA and A^-. Between the two equivalence points the pH reflects the titration of HB and is determined by a buffer consisting of HB and B^-. After the second equivalence point excess NaOH is responsible for the pH.

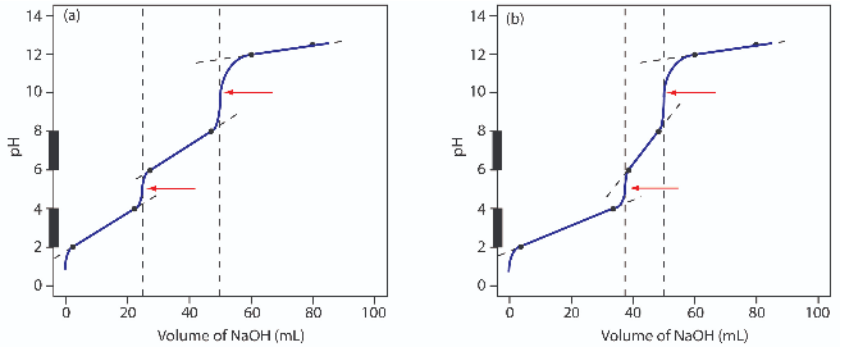


Figure 9.9 Titration curves for Example 9.1. The red arrows show the locations of the equivalence points.

Practice Exercise 9.4

Sketch the titration curve for 50.0 mL of 0.050 M H_2A, a diprotic weak acid with a pK_{a1} of 3 and a pK_{a2} of 4, using 0.100 M NaOH as the titrant. The fact that pK_{a2} falls within the buffer range of pK_{a1} presents a challenge that you will need to consider. Click here to review your answer to this exercise.

9.2.2 Selecting and Evaluating the End point

Earlier we made an important distinction between a titration's end point and its equivalence point. The difference between these two terms is important and deserves repeating. An equivalence point, which occurs when we react stoichiometrically equal amounts of the analyte and the titrant, is a theoretical not an experimental value. A titration's end point is an experimental result, representing our best estimate of the equivalence point. Any difference between an equivalence point and its corresponding end point is a source of determinate error. It is even possible that an equivalence point does not have a useful end point.

Where is The Equivalence Point?

Earlier we learned how to calculate the pH at the equivalence point for the titration of a strong acid with a strong base, and for the titration of a weak acid with a strong base. We also learned to quickly sketch a titration curve with only a minimum of calculations. Can we also locate the equivalence point without performing any calculations. The answer, as you might guess, is often yes!

For most acid–base titrations the inflection point, the point on a titration curve having the greatest slope, very nearly coincides with the equivalence point.[3] The red arrows in Figure 9.9, for example, indicate the equivalence points for the titration curves from Example 9.1. An inflection point actually precedes its corresponding equivalence point by a small amount, with the error approaching 0.1% for weak acids or weak bases with dissociation constants smaller than 10^{-9}, or for very dilute solutions.

The principal limitation to using an inflection point to locate the equivalence point is that the inflection point must be present. For some titrations the inflection point may be missing or difficult to find. Figure 9.10, for example, demonstrates the affect of a weak acid's dissociation constant, K_a, on the shape of titration curve. An inflection point is visible, even if barely so, for acid dissociation constants larger than 10^{-9}, but is missing when K_a is 10^{-11}.

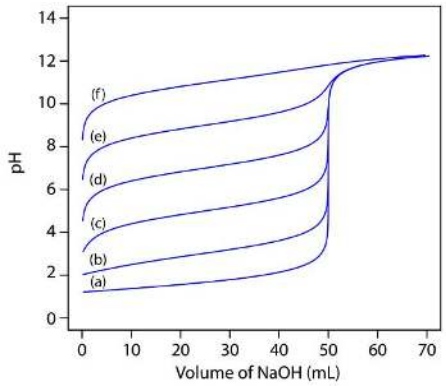


Figure 9.10 Weak acid–strong base titration curves for the titration of 50.0 mL of 0.100 M HA with 0.100 M NaOH. The pK_a values for HA are (a) 1, (b) 3, (c) 5, (d) 7, (e) 9, and (f) 11.

An inflection point also may be missing or difficult to detect if the analyte is a multiprotic weak acid or weak base with successive dissociation constants that are similar in magnitude. To appreciate why this is true let's consider the titration of a diprotic weak acid, H_2A, with NaOH. During the titration the following two reactions occur.

$$H_2A(aq) + OH^-(aq) \rightarrow HA^-(aq) + H_2O(l) \quad (9.3)$$

$$HA^-(aq) + OH^-(aq) \rightarrow A^{2-}(aq) + H_2O(l) \quad (9.4)$$

To see two distinct inflection points, reaction 9.3 must be essentially complete before reaction 9.4 begins.

Figure 9.11 shows titration curves for three diprotic weak acids. The titration curve for maleic acid, for which K_{a1} is approximately 20,000× larger than K_{a2}, has two distinct inflection points. Malonic acid, on the other hand, has acid dissociation constants that differ by a factor of approximately 690. Although malonic acid's titration curve shows two inflection points, the first is not as

distinct as that for maleic acid. Finally, the titration curve for succinic acid, for which the two K_a values differ by a factor of only 27, has only a single inflection point corresponding to the neutralization of $HC_4H_4O_4^-$ to $C_4H_4O_4^{2-}$. In general, we can detect separate inflection points when successive acid dissociation constants differ by a factor of at least 500 (a ΔpK_a of at least 2.7).

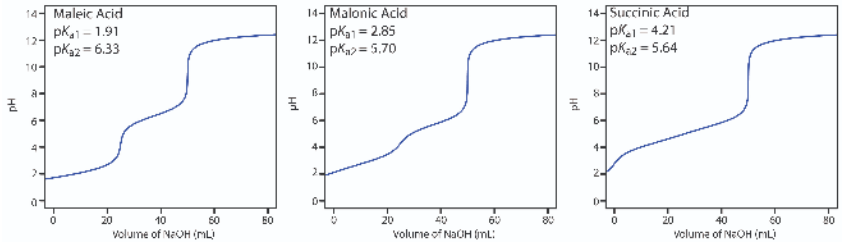


Figure 9.11 Titration curves for the diprotic weak acids maleic acid, malonic acid, and succinic acid. Each titration curve is for 50.0 mL of 0.0500 M weak acid using 0.100 M NaOH. Although each titration curve has equivalence points at 25.0 mL and 50.0 mL of NaOH, the titration curve for succinic acid shows only one inflection point.

Finding the End point with an Indicator

One interesting group of weak acids and weak bases are organic dyes. Because an organic dye has at least one highly colored conjugate acid–base species, its titration results in a change in both pH and color. We can use this change in color to indicate the end point of a titration, provided that it occurs at or near the titration's equivalence point.

Let's use an indicator, HIn, to illustrate how an acid–base indicator works. Because the indicator's acid and base forms have different colors—the weak acid, HIn, is yellow and the weak base, In^-, is red—the color of a solution containing the indicator depends on their relative concentrations. The indicator's acid dissociation reaction

$$\mathrm{HIn}(aq) + \mathrm{H_2O}(l) \rightleftharpoons \mathrm{H_3O^+}(aq) + \mathrm{In^-}(aq) \tag{9.2.38}$$

has an equilibrium constant of

$$K_a = \frac{[\mathrm{H_3O^+}][\mathrm{In^-}]}{[\mathrm{HIn}]} \tag{9.5}$$

Taking the negative log of each side of equation 9.5, and rearranging to solve for pH leaves with a equation

$$\mathrm{pH} = \mathrm{p}K_a + \log \frac{[\mathrm{In^-}]}{[\mathrm{HIn}]} \tag{9.6}$$

relating the solution's pH to the relative concentrations of HIn and In^-.

If we can detect HIn and In^- with equal ease, then the transition from yellow to red (or from red to yellow) reaches its midpoint, which is orange, when their concentrations are equal, or when the pH is equal to the indicator's pK_a. If the indicator's pK_a and the pH at the equivalence point are identical, then titrating until the indicator turns orange is a suitable end point. Unfortunately, we rarely know the exact pH at the equivalence point. In addition, determining when the concentrations of HIn and In^- are equal may be difficult if the indicator's change in color is subtle.

We can establish the range of pHs over which the average analyst observes a change in the indicator's color by making the following assumptions—the indicator's color is yellow if the concentration of HIn is 10× greater than that of In^-, and its color is red if the concentration of HIn is 10× smaller than that of In^-. Substituting these inequalities into equation 9.6

$$\mathrm{pH} = \mathrm{p}K_a + \log \frac{1}{10} = \mathrm{p}K_a - 1 \tag{9.2.39}$$

$$\mathrm{pH} = \mathrm{p}K_a + \log \frac{10}{1} = \mathrm{p}K_a + 1 \tag{9.2.40}$$

shows that the indicator changes color over a pH range extending ±1 unit on either side of its pK_a. As shown in Figure 9.12, the indicator is yellow when the pH is less than $pK_a - 1$, and it is red for pHs greater than $pK_a + 1$. For pHs between $pK_a - 1$ and $pK_a + 1$ the indicator's color passes through various shades of orange. The properties of several common acid–base indicators are shown in Table 9.4.

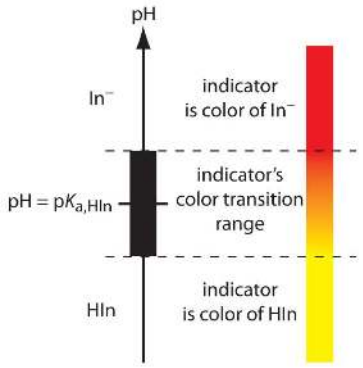


Figure 9.12 Diagram showing the relationship between pH and an indicator's color. The ladder diagram defines pH values where HIn and In^- are the predominate species. The indicator changes color when the pH is between pKa – 1 and pKa + 1.

Table 9.4 Properties of Selected Acid–Base Indicators

Indicator	Acid Color	Base Color	pH Range	pK_a
cresol red	red	yellow	0.2–1.8	–
thymol blue	red	yellow	1.2–2.8	1.7
bromophenol blue	yellow	blue	3.0–4.6	4.1
methyl orange	red	yellow	3.1–4.4	3.7
Congo red	blue	red	3.0–5.0	–
bromocresol green	yellow	blue	3.8–5.4	4.7
methyl red	red	yellow	4.2–6.3	5.0
bromocresol purple	yellow	purple	5.2–6.8	6.1
litmus	red	blue	5.0–8.0	–
bromothymol blue	yellow	blue	6.0–7.6	7.1
phenol red	yellow	blue	6.8–8.4	7.8
cresol red	yellow	red	7.2–8.8	8.2
thymol blue	yellow	red	8.0–9.6	8.9
phenolphthalein	colorless	red	8.3–10.0	9.6
alizarin yellow R	yellow	orange–red	10.1–12.0	–

Note

You may wonder why an indicator's pH range, such as that for phenolphthalein, is not equally distributed around its pK_a value. The explanation is simple. Figure 9.12 presents an idealized view of an indicator in which our sensitivity to the indicator's two colors is equal. For some indicators only the weak acid or the weak base is colored. For other indicators both the weak acid and the weak base are colored, but one form is easier to see. In either case, the indicator's pH range is skewed in the direction of the indicator's less colored form. Thus, phenolphthalein's pH range is skewed in the direction of its colorless form, shifting the pH range to values lower than those suggested by Figure 9.12.

The relatively broad range of pHs over which an indicator changes color places additional limitations on its feasibility for signaling a titration's end point. To minimize a determinate titration error, an indicator's entire pH range must fall within the rapid change in

pH at the equivalence point. For example, in Figure 9.13 we see that phenolphthalein is an appropriate indicator for the titration of 50.0 mL of 0.050 M acetic acid with 0.10 M NaOH. Bromothymol blue, on the other hand, is an inappropriate indicator because its change in color begins before the initial sharp rise in pH, and, as a result, spans a relatively large range of volumes. The early change in color increases the probability of obtaining inaccurate results, while the range of possible end point volumes increases the probability of obtaining imprecise results.

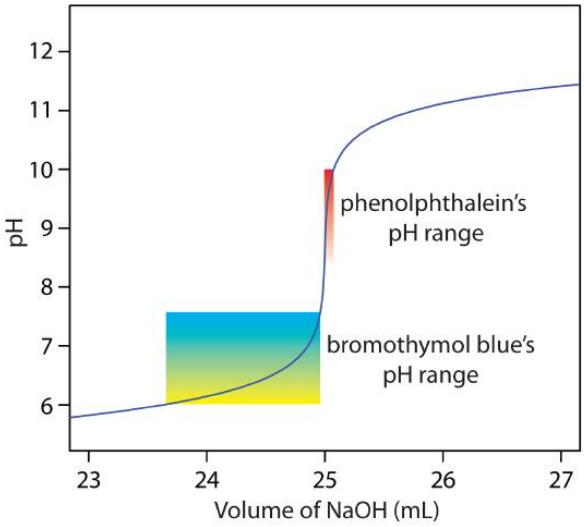


Figure 9.13 Portion of the titration curve for 50.0 mL of 0.050 M CH_3COOH with 0.10 M NaOH, highlighting the region containing the equivalence point. The end point transitions for the indicators phenolphthalein and bromothymol blue are superimposed on the titration curve.

Practice Exercise 9.5

Suggest a suitable indicator for the titration of 25.0 mL of 0.125 M NH_3 with 0.0625 M NaOH. You constructed a titration curve for this titration in Practice Exercise 9.2 and Practice Exercise 9.3.

Click here to review your answer to this exercise.

Finding the End point by Monitoring pH

An alternative approach for locating a titration's end point is to continuously monitor the titration's progress using a sensor whose signal is a function of the analyte's concentration. The result is a plot of the entire titration curve, which we can use to locate the end point with a minimal error.

The obvious sensor for monitoring an acid–base titration is a pH electrode and the result is a **potentiometric titration curve**. (See Chapter 11 for more details about pH electrodes.) For example, Figure 9.14a shows a small portion of the potentiometric titration curve for the titration of 50.0 mL of 0.050 M CH_3COOH with 0.10 M NaOH, focusing on the region containing the equivalence point. The simplest method for finding the end point is to locate the titration curve's inflection point, as shown by the arrow. This is also the least accurate method, particularly if the titration curve has a shallow slope at the equivalence point.

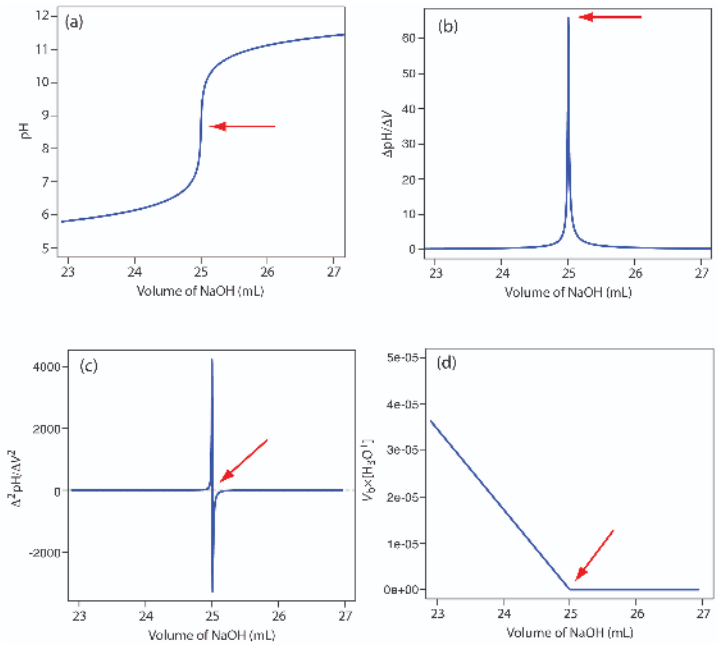


Figure 9.14 Titration curves for the titration of 50.0 mL of 0.050 M CH_3COOH with 0.10 M NaOH: (a) normal titration curve; (b) first derivative titration curve; (c) second derivative titration curve; (d) Gran plot. The red arrow shows the location of the titration's end point.

Another method for locating the end point is to plot the titration curve's first derivative, which gives the titration curve's slope at each point along the *x*-axis. Examine Figure 9.14a and consider how the titration curve's slope changes as we approach, reach, and pass the equivalence point. Because the slope reaches its maximum value at the inflection point, the first derivative shows a spike at the equivalence point (Figure 9.14b).

The second derivative of a titration curve may be more useful than the first derivative because the equivalence point intersects the volume axis. Figure 9.14c shows the resulting titration curve.

Derivative methods are particularly useful when titrating a sample that contains more than one analyte. If we rely on indicators to locate the end points, then we usually must complete separate titrations for each analyte. If we record the titration curve, however, then a single titration is sufficient. The precision with which we can locate the end point also makes derivative methods attractive for an analyte with a poorly defined normal titration curve.

Derivative methods work well only if we record sufficient data during the rapid increase in pH near the equivalence point. This is usually not a problem if we use an automatic titrator, such as that seen earlier in Figure 9.5. Because the pH changes so rapidly near the equivalence point—a change of several pH units with the addition of several drops of titrant is not unusual—a manual titration does not provide enough data for a useful derivative titration curve. A manual titration does contain an abundance of data during the more gently rising portions of the titration curve before and after the equivalence point. This data also contains information about the titration curve's equivalence point.

Note

Suppose we have the following three points on our titration curve:

volume (mL)	pH
23.65	6.00
23.91	6.10
24.13	6.20

Mathematically, we can approximate the first derivative as ΔpH/ΔV, where ΔpH is the change in pH between successive additions of titrant. Using the first two points, the first derivative is

$$\frac{\Delta \text{pH}}{\Delta V} = \frac{6.10 - 6.00}{23.91 - 23.65} = 0.385 \tag{9.2.41}$$

which we assign to the average of the two volumes, or 23.78 mL. For the second and third points, the first derivative is 0.455 and the average volume is 24.02 mL.

volume (mL)	ΔpH/ΔV
23.78	0.385
24.02	0.455

We can approximate the second derivative as Δ(ΔpH/ΔV)/ΔV, or Δ^2pH/ΔV^2. Using the two points from our calculation of the first derivative, the second derivative is

$$\frac{\Delta^2 \text{pH}}{\Delta V^2} = \frac{0.455 - 0.385}{23.78 - 24.02} = 0.292 \tag{9.2.42}$$

Note that calculating the first derivative comes at the expense of losing one piece of information (three points become two points), and calculating the second derivative comes at the expense of losing two pieces of information.

Consider again the titration of acetic acid, CH_3COOH, with NaOH. At any point during the titration acetic acid is in equilibrium with H_3O^+ and CH_3COO^-

$$\text{CH}_3\text{COOH}(aq) + \text{H}_2\text{O}(l) \rightleftharpoons \text{H}_3\text{O}^+(aq) + \text{CH}_3\text{COO}^-(aq) \tag{9.2.43}$$

for which the equilibrium constant is

$$K_\text{a} = \frac{[\text{H}_3\text{O}^+][\text{CH}_3\text{COO}^-]}{[\text{CH}_3\text{COOH}]} \tag{9.2.44}$$

Before the equivalence point the concentrations of CH_3COOH and CH_3COO^- are

$$[\text{CH}_3\text{COOH}] = \frac{\text{initial moles CH}_3\text{COOH} - \text{moles NaOH added}}{\text{total volume}} \tag{9.2.45}$$

$$= \frac{M_\text{a}V_\text{a} - M_\text{b}V_\text{b}}{V_\text{a} + V_\text{b}} \tag{9.2.46}$$

$$[\text{CH}_3\text{COO}^-] = \frac{\text{moles NaOH added}}{\text{total volume}} = \frac{M_\text{b}V_\text{b}}{V_\text{a} + V_\text{b}} \tag{9.2.47}$$

Substituting these equations into the K_a expression and rearranging leaves us with

$$K_\text{a} = \frac{[\text{H}_3\text{O}^+](M_\text{b}V_\text{b})}{M_\text{a}V_\text{a} - M_\text{b}V_\text{b}} \tag{9.2.48}$$

$$K_\text{a}M_\text{a}V_\text{a} - K_\text{a}M_\text{b}V_\text{b} = [\text{H}_3\text{O}^+](M_\text{b}V_\text{b}) \tag{9.2.49}$$

$$\frac{K_\text{a}M_\text{a}V_\text{a}}{M_\text{b}} - K_\text{a}V_\text{b} = [\text{H}_3\text{O}^+] \times V_\text{b} \tag{9.2.50}$$

Finally, recognizing that the equivalence point volume is

$$V_\text{eq} = \frac{M_\text{a}V_\text{a}}{M_\text{b}} \tag{9.2.51}$$

leaves us with the following equation.

$$[\text{H}_3\text{O}^+] \times V_\text{b} = K_\text{a}V_\text{eq} - K_\text{a}V_\text{b} \tag{9.2.52}$$

For volumes of titrant before the equivalence point, a plot of $V_b \times [H_3O^+]$ versus V_b is a straight-line with an x-intercept of V_{eq} and a slope of $-K_a$. Figure 9.14d shows a typical result. This method of data analysis, which converts a portion of a titration curve into a straight-line, is a **Gran plot**.

Finding the End point by Monitoring Tempmperature

The reaction between an acid and a base is exothermic. Heat generated by the reaction is absorbed by the titrand, increasing its temperature. Monitoring the titrand's temperature as we add the titrant provides us with another method for recording a titration curve and identifying the titration's end point (Figure 9.15).

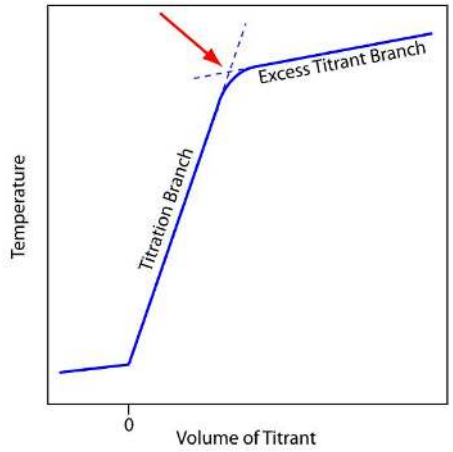


Figure 9.15 Typical thermometric titration curve. The endpoint, shown by the red arrow, is found by extrapolating the titration branch and the excess titration branch.

Before adding titrant, any change in the titrand's temperature is the result of warming or cooling as it equilibrates with the surroundings. Adding titrant initiates the exothermic acid–base reaction, increasing the titrand's temperature. This part of a thermometric titration curve is called the titration branch. The temperature continues to rise with each addition of titrant until we reach the equivalence point. After the equivalence point, any change in temperature is due to the titrant's enthalpy of dilution, and the difference between the temperatures of the titrant and titrand. Ideally, the equivalence point is a distinct intersection of the titration branch and the excess titrant branch. As shown in Figure 9.15, however, a thermometric titration curve usually shows curvature near the equivalence point due to an incomplete neutralization reaction, or to the excessive dilution of the titrand and the titrant during the titration. The latter problem is minimized by using a titrant that is 10–100 times more concentrated than the analyte, although this results in a very small end point volume and a larger relative error. If necessary, the end point is found by extrapolation.

Although not a particularly common method for monitoring acid–base titrations, a thermometric titration has one distinct advantage over the direct or indirect monitoring of pH. As discussed earlier, the use of an indicator or the monitoring of pH is limited by the magnitude of the relevant equilibrium constants. For example, titrating boric acid, H_3BO_3, with NaOH does not provide a sharp end point when monitoring pH because boric acid's K_a of 5.8×10^{-10} is too small (Figure 9.16a). Because boric acid's enthalpy of neutralization is fairly large, –42.7 kJ/mole, however, its thermometric titration curve provides a useful endpoint (Figure 9.16b).

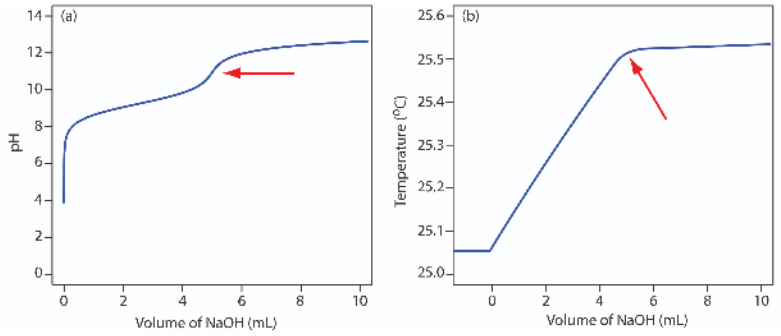


Figure 9.16 Titration curves for the titration of 50.0 mL of 0.050 M H_3BO_3 with 0.50 M NaOH obtained by monitoring (a) pH, and (b) temperature. The red arrows show the end points for the titrations.

9.2.3 Titrations in Nonaqueous Solvents

Thus far we have assumed that the titrant and the titrand are aqueous solutions. Although water is the most common solvent in acid–base titrimetry, switching to a nonaqueous solvent can improve a titration's feasibility.

For an amphoteric solvent, SH, the autoprotolysis constant, K_s, relates the concentration of its protonated form, SH_2^+, to that of its deprotonated form, S^-

$$2SH \rightleftharpoons SH_2^+ + S^- \tag{9.2.53}$$

$$K_s = [SH_2^+][S^-] \tag{9.2.54}$$

and the solvent's pH and pOH are

$$pH = -\log[SH_2^+] \tag{9.2.55}$$

$$pOH = -\log[S^-] \tag{9.2.56}$$

> **Note**
>
> You should recognize that K_w is just specific form of K_s when the solvent is water.

The most important limitation imposed by K_s is the change in pH during a titration. To understand why this is true, let's consider the titration of 50.0 mL of 1.0×10^{-4} M HCl using 1.0×10^{-4} M NaOH. Before the equivalence point, the pH is determined by the untitrated strong acid. For example, when the volume of NaOH is 90% of V_{eq}, the concentration of H_3O^+ is

$$[H_3O^+] = \frac{M_a V_a - M_b V_b}{V_a + V_b} \tag{9.2.57}$$

$$= \frac{(1.0 \times 10^{-4}\ \text{M})(50.0\ \text{mL}) - (1.0 \times 10^{-4}\ \text{M})(45.0\ \text{mL})}{50.0\ \text{mL} + 45.0\ \text{mL}} \tag{9.2.58}$$

$$= 5.3 \times 10^{-6}\ \text{M} \tag{9.2.59}$$

> **Note**
>
> The titration's equivalence point requires 50.0 mL of NaOH; thus, 90% of V_{eq} is 45.0 mL of NaOH.

and the pH is 5.3. When the volume of NaOH is 110% of V_{eq}, the concentration of OH^- is

$$[OH^-] = \frac{M_b V_b - M_a V_a}{V_a + V_b} \tag{9.2.60}$$

$$= \frac{(1.0 \times 10^{-4}\ \text{M})(55.0\ \text{mL}) - (1.0 \times 10^{-4}\ \text{M})(50.0\ \text{mL})}{50.0\ \text{mL} + 55.0\ \text{mL}} \tag{9.2.61}$$

$$= 4.8 \times 10^{-6}\ \text{M} \tag{9.2.62}$$

> **Note**
>
> The titration's equivalence point requires 50.0 mL of NaOH; thus, 110% of V_{eq} is 55.0 mL of NaOH.

and the pOH is 5.3. The titrand's pH is

$$pH = pK_w - pOH = 14 - 5.3 = 8.7 \tag{9.2.63}$$

and the change in the titrand's pH as the titration goes from 90% to 110% of V_{eq} is

$$\Delta pH = 8.7 - 5.3 = 3.4 \tag{9.2.64}$$

If we carry out the same titration in a nonaqueous solvent with a K_s of 1.0×10^{-20}, the pH after adding 45.0 mL of NaOH is still 5.3. However, the pH after adding 55.0 mL of NaOH is

$$pH = pK_s - pOH = 20 - 5.3 = 14.7 \tag{9.2.65}$$

In this case the change in pH

$$\Delta pH = 14.7 - 5.3 = 9.4 \tag{9.2.66}$$

is significantly greater than that obtained when the titration is carried out in water. Figure 9.17 shows the titration curves in both the aqueous and the nonaqueous solvents.

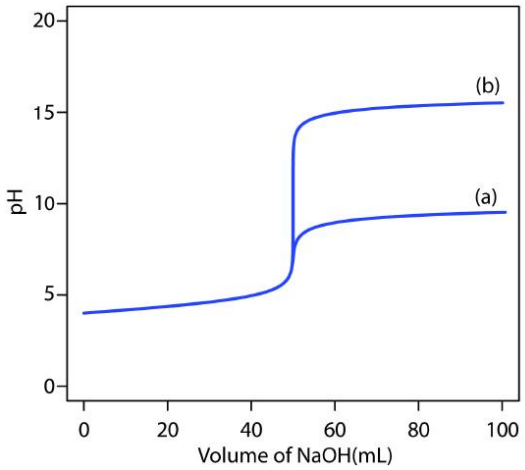


Figure 9.17 Titration curves for 50.0 mL of 1.0×10^{-4} M HCl using 1.0×10^{-4} M NaOH in (a) water, $K_w = 1.0 \times 10^{-14}$, and (b) a nonaqueous solvent, $K_s = 1.0 \times 10^{-20}$.

Another parameter affecting the feasibility of an acid–base titration is the titrand's dissociation constant. Here, too, the solvent plays an important role. The strength of an acid or a base is a relative measure of the ease transferring a proton from the acid to the solvent, or from the solvent to the base. For example, HF, with a K_a of 6.8×10^{-4}, is a better proton donor than CH_3COOH, for which K_a is 1.75×10^{-5}.

The strongest acid that can exist in water is the hydronium ion, H_3O^+. HCl and HNO_3 are strong acids because they are better proton donors than H_3O^+ and essentially donate all their protons to H_2O, **leveling** their acid strength to that of H_3O^+. In a different solvent HCl and HNO_3 may not behave as strong acids.

If we place acetic acid in water the dissociation reaction

$$CH_3COOH(aq) + H_2O(l) \rightleftharpoons H_3O^+(aq) + CH_3COO^-(aq) \tag{9.2.67}$$

does not proceed to a significant extent because CH_3COO^- is a stronger base than H_2O, and H_3O^+ is a stronger acid than CH_3COOH. If we place acetic acid in a solvent, such as ammonia, that is a stronger base than water, then the reaction

$$CH_3COOH + NH_3 \rightleftharpoons NH_4^+ + CH_3COO^- \tag{9.2.68}$$

proceeds to a greater extent. In fact, both HCl and CH_3COOH are strong acids in ammonia.

All other things being equal, the strength of a weak acid increases if we place it in a solvent that is more basic than water, and the strength of a weak base increases if we place it in a solvent that is more acidic than water. In some cases, however, the opposite effect is observed. For example, the pK_b for NH_3 is 4.75 in water and it is 6.40 in the more acidic glacial acetic acid. In contradiction to our expectations, NH_3 is a weaker base in the more acidic solvent. A full description of the solvent's effect on the pK_a of weak acid or the pK_b of a weak base is beyond the scope of this text. You should be aware, however, that a titration that is not feasible in water may be feasible in a different solvent.

Note

The best way to appreciate the theoretical and practical details discussed in this section is to carefully examine a typical acid–base titrimetric method. Although each method is unique, the following description of the determination of protein in bread provides an instructive example of a typical procedure. The description here is based on Method 13.86 as published in *Official Methods of Analysis*, 8th Ed., Association of Official Agricultural Chemists: Washington, D. C., 1955.

Representative Method 9.1

Determination of Protein in Bread

Description of the Method

This method is based on a determination of %w/w nitrogen using the Kjeldahl method. The protein in a sample of bread is oxidized to NH_4^+ using hot concentrated H_2SO_4. After making the solution alkaline, which converts the NH_4^+ to NH_3, the ammonia is distilled into a flask containing a known amount of HCl. The amount of unreacted HCl is determined by a back titration with standard strong base titrant. Because different cereal proteins contain similar amounts of nitrogen, multiplying the experimentally determined %w/w N by a factor of 5.7 gives the %w/w protein in the sample (on average there are 5.7 g protein for every gram of nitrogen).

Procedure

Transfer a 2.0-g sample of bread, which has previously been air-dried and ground into a powder, to a suitable digestion flask, along with 0.7 g of a HgO catalyst, 10 g of K_2SO_4, and 25 mL of concentrated H_2SO_4. Bring the solution to a boil. Continue boiling until the solution turns clear and then boil for at least an additional 30 minutes. After cooling the solution below room temperature, remove the Hg^{2+} catalyst by adding 200 mL of H_2O and 25 mL of 4% w/v K_2S. Add a few Zn granules to serve as boiling stones and 25 g of NaOH. Quickly connect the flask to a distillation apparatus and distill the NH_3 into a collecting flask containing a known amount of standardized HCl. The tip of the condenser must be placed below the surface of the strong acid. After the distillation is complete, titrate the excess strong acid with a standard solution of NaOH using methyl red as an indicator (Figure 9.18).

Questions

1. Oxidizing the protein converts all of its nitrogen to NH_4^+. Why is the amount of nitrogen not determined by titrating the NH_4^+ with a strong base?

There are two reasons for not directly titrating the ammonium ion. First, because NH_4^+ is a very weak acid (its K_a is 5.6×10^{-10}), its titration with NaOH yields a poorly defined end point. Second, even if the end point can be determined with acceptable accuracy and precision, the solution also contains a substantial larger concentration of unreacted H_2SO_4. The presence of two acids that differ greatly in concentration makes for a difficult analysis. If the titrant's concentration is similar to that of H_2SO_4, then the equivalence point volume for the titration of NH_4^+ is too small to measure reliably. On the other hand, if the titrant's concentration is similar to that of NH_4^+, the volume needed to neutralize the H_2SO_4 is unreasonably large.

2. Ammonia is a volatile compound as evidenced by the strong smell of even dilute solutions. This volatility is a potential source of determinate error. Is this determinate error negative or positive?

Any loss of NH_3 is loss of nitrogen and, therefore, a loss of protein. The result is a negative determinate error.

3. Discuss the steps in this procedure that minimize this determinate error.

Three specific steps minimize the loss of ammonia: (1) the solution is cooled below room temperature before adding NaOH; (2) after adding NaOH, the digestion flask is quickly connected to the distillation apparatus; and (3) the condenser's tip is placed below the surface of the HCl to ensure that the NH_3 reacts with the HCl before it can be lost through volatilization.

4. How does K_2S remove Hg^{2+}, and why is its removal important?

Adding sulfide precipitates Hg^{2+} as HgS. This is important because NH_3 forms stable complexes with many metal ions, including Hg^{2+}. Any NH_3 that reacts with Hg^{2+} is not collected during distillation, providing another source of determinate error.

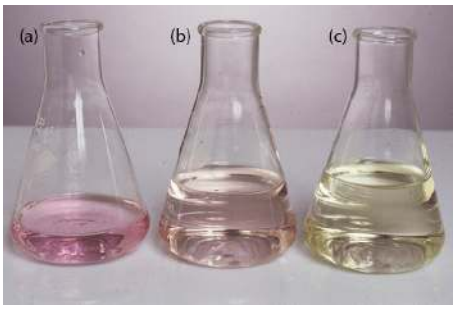


Figure 9.18 Methyl red's endpoint for the titration of a strong acid with a strong base; the indicator is: (a) red prior to the end point; (b) orange at the end point; and (c) yellow after the end point.

9.2.4 Q Quantitative Applications

Although many quantitative applications of acid–base titrimetry have been replaced by other analytical methods, a few important applications continue to be relevant. In this section we review the general application of acid–base titrimetry to the analysis of inorganic and organic compounds, with an emphasis on applications in environmental and clinical analysis. First, however, we discuss the selection and standardization of acidic and basic titrants.

Selecting and Standardizing a Titrant

The most common strong acid titrants are HCl, $HClO_4$, and H_2SO_4. Solutions of these titrants are usually prepared by diluting a commercially available concentrated stock solution. Because the concentrations of concentrated acids are known only approximately, the titrant's concentration is determined by standardizing against one of the primary standard weak bases listed in Table 9.5.

> **Note**
>
> The nominal concentrations of the concentrated stock solutions are 12.1 M HCl, 11.7 M $HClO_4$, and 18.0 M H_2SO_4.

Table 9.5 Selected Primary Standards for Standardizing Strong Acid and Strong Base Titrants

Primary Standard	Standardization of Acidic Titrants Titration Reaction	Comment
Na_2CO_3	$Na_2CO_3 + 2H_3O^+ \rightarrow H_2CO_3 + 2Na^+ + 2H_2O$	a
$(HOCH_2)_3CNH_2$	$(HOCH_2)_3CNH_2 + H_3O^+ \rightarrow (HOCH_2)_3CNH_3^+ + H_2O$	b
$Na_2B_4O_7$	$Na_2B_4O_7 + 2H_3O^+ + 3H_2O \rightarrow 2Na^+ + 4H_3BO_3$	
Primary Standard	Standardization of Basic Titrants Titration Reaction	Comment
$KHC_8H_4O_4$	$KHC_8H_4O_4 + OH^- \rightarrow K^+ + C_8H_4O_4^- + H_2O$	c
C_6H_5COOH	$C_6H_5COOH + OH^- \rightarrow C_6H_5COO^- + H_2O$	d
$KH(IO_3)_2$	$KH(IO_3)_2 + OH^- \rightarrow K^+ + 2IO_3^- + H_2O$	

[a] The end point for this titration is improved by titrating to the second equivalence point, boiling the solution to expel CO_2, and retitrating to the second equivalence point. The reaction in this case is
$Na_2CO_3 + 2H_3O^+ \rightarrow CO_2 + 2Na^+ + 3K^+$

[b] *Tris*-(hydroxymethyl)aminomethane often goes by the shorter name of TRIS or THAM.

[c] Potassium hydrogen phthalate often goes by the shorter name of KHP.

[d] Because it is not very soluble in water, dissolve benzoic acid in a small amount of ethanol before diluting with water.

The most common strong base titrant is NaOH. Sodium hydroxide is available both as an impure solid and as an approximately 50% w/v solution. Solutions of NaOH may be standardized against any of the primary weak acid standards listed in Table 9.5.

Using NaOH as a titrant is complicated by potential contamination from the following reaction between CO_2 and OH^-.

$$CO_2(aq) + 2OH^-(aq) \rightarrow CO_3^{2-}(aq) + H_2O(l) \tag{9.7}$$

Note

Any solution in contact with the atmosphere contains a small amount of $CO_2(aq)$ from the equilibrium

$$CO_2(g) \rightleftharpoons CO_2(aq) \tag{9.2.69}$$

During the titration, NaOH reacts with both the titrand and CO_2, increasing the volume of NaOH needed to reach the titration's end point. This is not a problem if end point pH is less than 6. Below this pH the CO_3^{2-} from reaction 9.7 reacts with H_3O^+ to form carbonic acid.

$$CO_3^{2-}(aq) + 2H_3O^+(aq) \rightarrow H_2CO_3(aq) + 2H_2O(l) \tag{9.8}$$

Combining reaction 9.7 and reaction 9.8 gives an overall reaction that does not include OH^-.

$$CO_2(aq) + H_2O(l) \rightarrow H_2CO_3(aq) \tag{9.2.70}$$

Under these conditions the presence of CO_2 does not affect the quantity of OH^- used in the titration and is not a source of determinate error.

If the end point pH is between 6 and 10, however, the neutralization of CO_3^{2-} requires one proton

$$CO_3^{2-}(aq) + H_3O^+(aq) \rightarrow HCO_3^-(aq) + H_2O(l) \tag{9.2.71}$$

and the net reaction between CO_2 and OH^- is

$$CO_2(aq) + OH^-(aq) \rightarrow HCO_3^-(aq) \tag{9.2.72}$$

Under these conditions some OH^- is consumed in neutralizing CO_2, resulting in a determinate error. We can avoid the determinate error if we use the same end point pH in both the standardization of NaOH and the analysis of our analyte, although this often is not practical.

Solid NaOH is always contaminated with carbonate due to its contact with the atmosphere, and can not be used to prepare a carbonate-free solution of NaOH. Solutions of carbonate-free NaOH can be prepared from 50% w/v NaOH because Na_2CO_3 is insoluble in concentrated NaOH. When CO_2 is absorbed, Na_2CO_3 precipitates and settles to the bottom of the container, allowing access to the carbonate-free NaOH. When preparing a solution of NaOH, be sure to use water that is free from dissolved CO_2. Briefly boiling the water expels CO_2, and after cooling, it may be used to prepare carbonate-free solutions of NaOH. A solution of carbonate-free NaOH is relatively stable f we limit its contact with the atmosphere. Standard solutions of sodium hydroxide should not be stored in glass bottles as NaOH reacts with glass to form silicate; instead, store such solutions in polyethylene bottles.

Inorganic Analysis

Acid–base titrimetry is a standard method for the quantitative analysis of many inorganic acids and bases. A standard solution of NaOH can be used to determine the concentration of inorganic acids, such as H_3PO_4 or H_3AsO_4, and inorganic bases, such as Na_2CO_3 can be analyzed using a standard solution of HCl.

An inorganic acid or base that is too weak to be analyzed by an aqueous acid–base titration can be analyzed by adjusting the solvent, or by an indirect analysis. For example, when analyzing boric acid, H_3BO_3, by titrating with NaOH, accuracy is limited by boric acid's small acid dissociation constant of 5.8×10^{-10}. (Figure 9.16a shows a typical result for the titration of H_3BO_3 with NaOH.) Boric acid's K_a value increases to 1.5×10^{-4} in the presence of mannitol, because it forms a complex with the borate ion. The result is a sharper end point and a more accurate titration. Similarly, the analysis of ammonium salts is limited by the small

acid dissociation constant of 5.7×10^{-10} for NH_4^+. In this case, we can convert NH_4^+ to NH_3 by neutralizing with strong base. The NH_3, for which K_b is 1.58×10^{-5}, is then removed by distillation and titrated with HCl.

We can analyze a neutral inorganic analyte if we can first convert it into an acid or base. For example, we can determine the concentration of NO_3^- by reducing it to NH_3 in a strongly alkaline solution using Devarda's alloy, a mixture of 50% w/w Cu, 45% w/w Al, and 5% w/w Zn.

$$3NO_3^-(aq) + 8Al(s) + 5OH^-(aq) + 2H_2O(l) \rightarrow 8AlO_2^-(aq) + 3NH_3(aq) \quad (9.2.73)$$

The NH_3 is removed by distillation and titrated with HCl. Alternatively, we can titrate NO_3^- as a weak base by placing it in an acidic nonaqueous solvent such as anhydrous acetic acid and using $HClO_4$ as a titrant.

Acid–base titrimetry continues to be listed as a standard method for the determination of alkalinity, acidity, and free CO_2 in waters and wastewaters. **Alkalinity** is a measure of a sample's capacity to neutralize acids. The most important sources of alkalinity are OH^-, HCO_3^-, and CO_3^{2-}, although other weak bases, such as phosphate, may contribute to the overall alkalinity. Total alkalinity is determined by titrating to a fixed end point pH of 4.5 (or to the bromocresol green end point) using a standard solution of HCl or H_2SO_4. Results are reported as mg $CaCO_3$/L.

> **Note**
>
> Although a variety of strong bases and weak bases may contribute to a sample's alkalinity, a single titration cannot distinguish between the possible sources. Reporting the total alkalinity as if $CaCO_3$ is the only source provides a means for comparing the acid-neutralizing capacities of different samples.

When the sources of alkalinity are limited to OH^-, HCO_3^-, and CO_3^{2-}, separate titrations to a pH of 4.5 (or the bromocresol green end point) and a pH of 8.3 (or the phenolphthalein end point) allow us to determine which species are present and their respective concentrations. Titration curves for OH^-, HCO_3^-, and CO_3^{2-} are shown in Figure 9.19. For a solution containing only OH^- alkalinity, the volumes of strong acid needed to reach the two end points are identical (Figure 9.19a). When the only source of alkalinity is CO_3^{2-}, the volume of strong acid needed to reach the end point at a pH of 4.5 is exactly twice that needed to reach the end point at a pH of 8.3 (Figure 9.19b). If a solution contains only HCO_3^- alkalinity, the volume of strong acid needed to reach the end point at a pH of 8.3 is zero, but that for the pH 4.5 end point is greater than zero (Figure 9.19c).

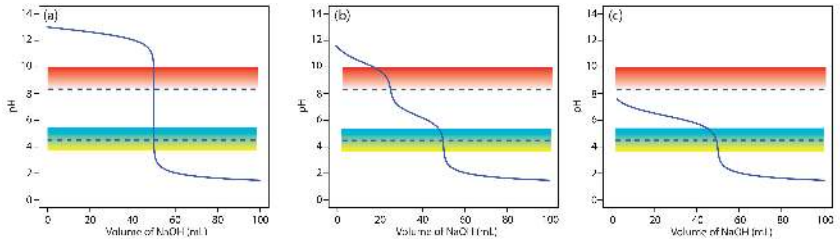


Figure 9.19 Titration curves for 50.0 mL of (a) 0.10 M NaOH, (b) 0.050 M Na_2CO_3, and (c) 0.10 M $NaHCO_3$ using 0.10 M HCl. The dashed lines indicate the fixed pH end points of 8.3 and 4.5. The color gradients show the phenolphthalein (red → colorless) and bromocresol green (blue → green) endpoints. When titrating to the phenolphthalein endpoint, the titration continues until the last trace of red is lost.

Mixtures of OH^- and CO_3^{2-}, or of HCO_3^- and CO_3^{2-} also are possible. Consider, for example, a mixture of OH^- and CO_3^{2-}. The volume of strong acid to titrate OH^- is the same whether we titrate to a pH of 8.3 or a pH of 4.5. Titrating CO_3^{2-} to a pH of 4.5, however, requires twice as much strong acid as titrating to a pH of 8.3. Consequently, when titrating a mixture of these two ions, the volume of strong acid to reach a pH of 4.5 is less than twice that to reach a pH of 8.3. For a mixture of HCO_3^- and CO_3^{2-} the volume of strong acid to reach a pH of 4.5 is more than twice that to reach a pH of 8.3. Table 9.6 summarizes the relationship between the sources of alkalinity and the volumes of titrant needed to reach the two end points.

Table 9.6 Relationship Between End Point Volumes and Sources of Alkalinity

Source of Alkalinity	Relationship Between End Point Volumes
OH^-	$V_{pH\ 4.5} = V_{pH\ 8.3}$
CO_3^{2-}	$V_{pH\ 4.5} = 2 \times V_{pH\ 8.3}$
HCO_3^-	$V_{pH\ 4.5} > 0$; $V_{pH\ 8.3} = 0$
OH^- and CO_3^{2-}	$V_{pH\ 4.5} < 2 \times V_{pH\ 8.3}$
CO_3^{2-} and HCO_3^-	$V_{pH\ 4.5} > 2 \times V_{pH\ 8.3}$

Acidity is a measure of a water sample's capacity for neutralizing base, and is conveniently divided into strong acid and weak acid acidity. Strong acid acidity, from inorganic acids such as HCl, HNO_3, and H_2SO_4, is common in industrial effluents and acid mine drainage. Weak acid acidity is usually dominated by the formation of H_2CO_3 from dissolved CO_2, but also includes contributions from hydrolyzable metal ions such as Fe^{3+}, Al^{3+}, and Mn^{2+}. In addition, weak acid acidity may include a contribution from organic acids.

Acidity is determined by titrating with a standard solution of NaOH to fixed pH of 3.7 (or the bromothymol blue end point) and a fixed pH 8.3 (or the phenolphthalein end point). Titrating to a pH of 3.7 provides a measure of strong acid acidity, and titrating to a pH of 8.3 provides a measure of total acidity. Weak acid acidity is the difference between the total and strong acid acidities. Results are expressed as the amount of $CaCO_3$ that can be neutralized by the sample's acidity. (As is the case with alkalinity, acidity is reported as mg $CaCO_3$/L.) An alternative approach for determining strong acid and weak acid acidity is to obtain a potentiometric titration curve and use a Gran plot to determine the two equivalence points. This approach has been used, for example, to determine the forms of acidity in atmospheric aerosols.[4]

Water in contact with either the atmosphere, or with carbonate-bearing sediments contains free CO_2 that exists in equilibrium with $CO_2(g)$ and aqueous H_2CO_3, HCO_3^-, and CO_3^{2-}. (Free CO_2 is the same thing as $CO_2(aq)$.) The concentration of free CO_2 is determined by titrating with a standard solution of NaOH to the phenolphthalein end point, or to a pH of 8.3, with results reported as mg CO_2/L. This analysis is essentially the same as that for the determination of total acidity, and can only be applied to water samples that do not contain strong acid acidity.

Organic Analysis

Acid–base titrimetry continues to have a small, but important role for the analysis of organic compounds in pharmaceutical, biochemical, agricultural, and environmental laboratories. Perhaps the most widely employed acid–base titration is the **Kjeldahl analysis** for organic nitrogen. Examples of analytes determined by a Kjeldahl analysis include caffeine and saccharin in pharmaceutical products, proteins in foods, and the analysis of nitrogen in fertilizers, sludges, and sediments. Any nitrogen present in a –3 oxidation state is quantitatively oxidized to NH_4^+. Because some aromatic heterocyclic compounds, such as pyridine, are difficult to oxidize, a catalyst is used to ensure a quantitative oxidation. Nitrogen in other oxidation states, such as nitro and azo nitrogens, may be oxidized to N_2, resulting in a negative determinate error. Including a reducing agent, such as salicylic acid, converts this nitrogen to a –3 oxidation state, eliminating this source of error. Table 9.7 provides additional examples in which an element is quantitative converted into a titratable acid or base.

> **Note**
>
> See Representative Method 9.1 for one application of a Kjeldahl analysis.

Table 9.7 Selected Elemental Analyses Based on an Acid–Base Titration

Element	Convert to...	Reaction Producing Titratable Acid or Base[a]	Titration Details
N	$NH_3(g)$	$NH_3(g) + \mathbf{HCl}(aq) \rightarrow NH_4^+(aq) + Cl^-(aq)$	add HCl in excess and back titrate with NaOH
S	$SO_2(g)$	$SO_2(g) + H_2O_2(aq) \rightarrow \mathbf{H_2SO_4}(aq)$	titrate H_2SO_4 with NaOH
C	$CO_2(g)$	$CO_2(g) + \mathbf{Ba(OH)_2}(aq) \rightarrow BaCO_3(s) + H_2O(l)$	add excess $Ba(OH)_2$ and back titrate with HCl
Cl	$\mathbf{HCl}(g)$	—	titrate HCl with NaOH
F	$SiF_4(g)$	$3SiF_4(aq) + 2H_2O(l) \rightarrow 2\mathbf{H_2SiF_6}(aq) + SiO_2(s)$	titrate H_2SiF_4 with NaOH

[a] The species that is titrated is shown in bold.

Several organic functional groups are weak acids or weak bases. Carboxylic (–COOH), sulfonic ($–SO_3H$) and phenolic ($–C_6H_5OH$) functional groups are weak acids that can be successfully titrated in either aqueous or nonaqueous solvents. Sodium hydroxide is the titrant of choice for aqueous solutions. Nonaqueous titrations are often carried out in a basic solvent, such as ethylenediamine, using tetrabutylammonium hydroxide, $(C_4H_9)_4NOH$, as the titrant. Aliphatic and aromatic amines are weak bases that can be titrated using HCl in aqueous solution, or $HClO_4$ in glacial acetic acid. Other functional groups can be analyzed indirectly following a reaction that produces or consumes an acid or base. Typical examples are shown in Table 9.8.

Table 9.8 Selected Acid–Base Titrimetric Procedures for Organic Functional Groups Based on the Production or Consumption of Acid or Base

Functional Group	Reaction Producing Titratable Acid or Base[a]	Titration Details
ester	$RCOOR'(aq) + \mathbf{OH^-}(aq) \rightarrow RCOO^-(aq) + HOR'(aq)$	titrate OH^- with HCl
carbonyl	$R_2C{=}O(aq) + NH_2OHiHCl(aq) \rightarrow R_2C{=}NOH(aq) + \mathbf{HCl}(aq) + H_2O(l)$	titrate HCl with NaOH
alcohol[b]	[1] $(CH_3CO)_2O + ROH \rightarrow CH_3COOR + \mathbf{CH_3COOH}$ [2] $(CH_3CO)_2O + H_2O \rightarrow 2\mathbf{CH_3COOH}$	titrate CH_3COOH with NaOH; a blank titration of acetic anhydride,$(CH_3CO)_2O$, corrects for the contribution of reaction [2]

[a] The species that is titrated is shown in **bold**.

[b] The acetylation reaction [1] is carried out in pyridine to prevent the hydrolysis of acetic by water. After the acetylation reaction is complete, water is added to covert any unreacted acetic anhydride to acetic acid [2].

Many pharmaceutical compounds are weak acids or bases that can be analyzed by an aqueous or nonaqueous acid–base titration; examples include salicylic acid, phenobarbital, caffeine, and sulfanilamide. Amino acids and proteins can be analyzed in glacial acetic acid using $HClO_4$ as the titrant. For example, a procedure for determining the amount of nutritionally available protein uses an acid–base titration of lysine residues.[5]

Quantitative Calculations

The quantitative relationship between the titrand and the titrant is determined by the stoichiometry of the titration reaction. If the titrand is polyprotic, then we must know to which equivalence point we are titrating. The following example illustrates how we can use a ladder diagram to determine a titration reaction's stoichiometry.

Example 9.2

A 50.00 mL sample of a citrus drink requires 17.62 mL of 0.04166 M NaOH to reach the phenolphthalein end point. Express the sample's acidity as grams of citric acid, $C_6H_8O_7$, per 100 mL.

Solution

Because citric acid is a triprotic weak acid, we must first determine if the phenolphthalein end point corresponds to the first, second, or third equivalence point. Citric acid's ladder diagram is shown in Figure 9.20a. Based on this ladder diagram, the first equivalence point is between a pH of 3.13 and a pH of 4.76, the second equivalence point is between a pH of 4.76 and a pH of 6.40, and the third equivalence point is greater than a pH of 6.40. Because phenolphthalein's end point pH is 8.3–10.0 (see Table 9.4), the titration proceeds to the third equivalence point and the titration reaction is

$$C_6H_8O_7(aq) + 3OH^-(aq) \rightarrow C_6H_5O_7^{3-}(aq) + 3H_2O(l) \tag{9.2.74}$$

In reaching the equivalence point, each mole of citric acid consumes three moles of NaOH; thus

$$0.04166 \text{ M NaOH} \times 0.01762 \text{ L NaOH} = 7.3405 \times 10^{-5} \text{ moles NaOH} \tag{9.2.75}$$

$$7.3405 \times 10^{-5} \text{ mol NaOH} \times \frac{1 \text{ mol } C_6H_8O_7}{3 \text{ mol NaOH}} = 2.4468 \times 10^{-4} \text{ mol } C_6H_8O_7 \tag{9.2.76}$$

$$2.4468 \times 10^{-4} \text{ mol } C_6H_8O_7 \times \frac{192.13 \text{ g } C_6H_8O_7}{\text{mol } C_6H_8O_7} = 0.04701 \text{ g } C_6H_8O_7 \tag{9.2.77}$$

Because this is the amount of citric acid in a 50.00 mL sample, the concentration of citric acid in the citrus drink is 0.09402 g/100 mL. The complete titration curve is shown in Figure 9.20b.

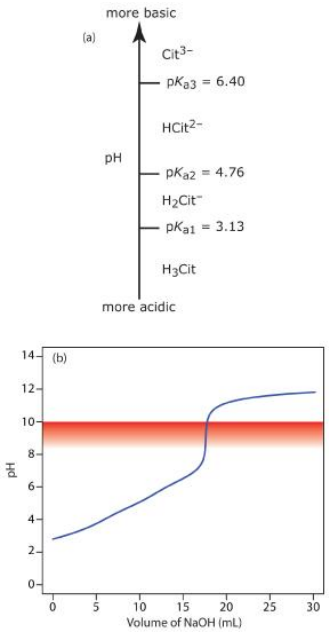


Figure 9.20 (a) Ladder diagram for citric acid; (b) Titration curve for the sample in Example 9.2 showing phenolphthalein's pH transition region.

Practice Exercise 9.6

Your company recently received a shipment of salicylic acid, $C_7H_6O_3$, to be used in the production of acetylsalicylic acid (aspirin). The shipment can be accepted only if the salicylic acid is more than 99% pure. To evaluate the shipment's purity, a 0.4208-g sample is dissolved in water and titrated to the phenolphthalein end point, requiring 21.92 mL of 0.1354 M NaOH. Report the shipment's purity as %w/w $C_7H_6O_3$. Salicylic acid is a diprotic weak acid with pK_a values of 2.97 and 13.74.

Click here to review your answer to this exercise.

In an indirect analysis the analyte participates in one or more preliminary reactions, one of which produces or consumes acid or base. Despite the additional complexity, the calculations are straightforward.

Example 9.3

The purity of a pharmaceutical preparation of sulfanilamide, $C_6H_4N_2O_2S$, is determined by oxidizing sulfur to SO_2 and bubbling it through H_2O_2 to produce H_2SO_4. The acid is titrated to the bromothymol blue end point with a standard solution of NaOH. Calculate the purity of the preparation given that a 0.5136-g sample requires 48.13 mL of 0.1251 M NaOH.

Solution

The bromothymol blue end point has a pH range of 6.0–7.6. Sulfuric acid is a diprotic acid, with a pK_{a2} of 1.99 (the first K_a value is very large and the acid dissociation reaction goes to completion, which is why H_2SO_4 is a strong acid). The titration, therefore, proceeds to the second equivalence point and the titration reaction is

$$H_2SO_4(aq) + 2OH^-(aq) \rightarrow 2H_2O(l) + SO_4^{2-}(aq) \tag{9.2.78}$$

Using the titration results, there are

$$0.1251\ \text{M NaOH} \times 0.04813\ \text{L NaOH} = 6.021 \times 10^{-3}\ \text{mol NaOH} \tag{9.2.79}$$

$$6.021 \times 10^{-3}\ \text{mol NaOH} \times \frac{1\ \text{mol } H_2SO_4}{2\ \text{mol NaOH}} = 3.010 \times 10^{-3}\ \text{mol } H_2SO_4 \tag{9.2.80}$$

produced by bubbling SO_2 through H_2O_2. Because all the sulfur in H_2SO_4 comes from the sulfanilamide, we can use a conservation of mass to determine the amount of sulfanilamide in the sample.

$$3.010 \times 10^{-3}\ \text{mol } H_2SO_4 \times \frac{1\ \text{mol S}}{\text{mol } H_2SO_4} \times \frac{1\ \text{mol } C_6H_4N_2O_2S}{\text{mol S}} \times \frac{168.18\ \text{g } C_6H_4N_2O_2S}{\text{mol } C_6H_4N_2O_2S} \tag{9.2.81}$$

$$= 0.5062\ \text{g } C_6H_4N_2O_2S \tag{9.2.82}$$

$$\frac{0.5062\ \text{g } C_6H_4N_2O_2S}{0.5136\ \text{g sample}} \times 100 = 98.56\%\ \text{w/w } C_6H_4N_2O_2S \tag{9.2.83}$$

Practice Exercise 9.7

The concentration of NO_2 in air can be determined by passing the sample through a solution of H_2O_2, which oxidizes NO_2 to HNO_3, and titrating the HNO_3 with NaOH. What is the concentration of NO_2, in mg/L, if a 5.0 L sample of air requires 9.14 mL of 0.01012 M NaOH to reach the methyl red end point

Click here to review your answer to this exercise.

Example 9.4

The amount of protein in a sample of cheese is determined by a Kjeldahl analysis for nitrogen. After digesting a 0.9814-g sample of cheese, the nitrogen is oxidized to NH_4^+, converted to NH_3 with NaOH, and distilled into a collection flask containing 50.00 mL of 0.1047 M HCl. The excess HCl is back titrated with 0.1183 M NaOH, requiring 22.84 mL to reach the bromothymol blue end point. Report the %w/w protein in the cheese assuming that there are 6.38 grams of protein for every gram of nitrogen in most dairy products.

(For a back titration we must consider two acid–base reactions. Again, the calculations are straightforward.)

Solution

The HCl in the collection flask reacts with two bases

$$HCl(aq) + NH_3(aq) \rightarrow NH_4^+(aq) + Cl^-(aq) \tag{9.2.84}$$

$$HCl(aq) + OH^-(aq) \rightarrow H_2O(l) + Cl^-(aq) \tag{9.2.85}$$

The collection flask originally contains

$$0.1047 \text{ M HCl} \times 0.05000 \text{ L HCl} = 5.235 \times 10^{-3} \text{ mol HCl} \tag{9.2.86}$$

of which

$$0.1183 \text{ M NaOH} \times 0.02284 \text{ L NaOH} \times \frac{1 \text{ mol HCl}}{\text{mol NaOH}} = 2.702 \times 10^{-3} \text{ mol HCl} \tag{9.2.87}$$

react with NaOH. The difference between the total moles of HCl and the moles of HCl reacting with NaOH

$$5.235 \times 10^{-3} \text{ mol HCl} - 2.702 \times 10^{-3} \text{ mol HCl} = 2.533 \times 10^{-3} \text{ mol HCl} \tag{9.2.88}$$

is the moles of HCl reacting with NH_3. Because all the nitrogen in NH_3 comes from the sample of cheese, we use a conservation of mass to determine the grams of nitrogen in the sample.

$$2.533 \times 10^{-3} \text{ mol HCl} \times \frac{1 \text{ mol NH}_3}{\text{mol HCl}} \times \frac{14.01 \text{ g N}}{\text{mol NH}_3} = 0.03549 \text{ g N} \tag{9.2.89}$$

The mass of protein, therefore, is

$$0.03549 \text{ g N} \times \frac{6.38 \text{ g protein}}{\text{g N}} = 0.2264 \text{ g protein} \tag{9.2.90}$$

and the % w/w protein is

$$\frac{0.2264 \text{ g protein}}{0.9814 \text{ g sample}} \times 100 = 23.1 \tag{9.2.91}$$

Practice Exercise 9.8

Limestone consists mainly of $CaCO_3$, with traces of iron oxides and other metal oxides. To determine the purity of a limestone, a 0.5413-g sample is dissolved using 10.00 mL of 1.396 M HCl. After heating to expel CO_2, the excess HCl was titrated to the phenolphthalein end point, requiring 39.96 mL of 0.1004 M NaOH. Report the sample's purity as %w/w $CaCO_3$.

Click here to review your answer to this exercise.

Earlier we noted that we can use an acid–base titration to analyze a mixture of acids or bases by titrating to more than one equivalence point. The concentration of each analyte is determined by accounting for its contribution to each equivalence point.

Example 9.5

The alkalinity of natural waters is usually controlled by OH^-, HCO_3^-, and CO_3^{2-}, which may be present singularly or in combination. Titrating a 100.0-mL sample to a pH of 8.3 requires 18.67 mL of a 0.02812 M HCl. A second 100.0-mL aliquot requires 48.12 mL of the same titrant to reach a pH of 4.5. Identify the sources of alkalinity and their concentrations in milligrams per liter.

Solution

Because the volume of titrant to reach a pH of 4.5 is more than twice that needed to reach a pH of 8.3, we know, from Table 9.6, that the sample's alkalinity is controlled by CO_3^{2-} and HCO_3^-. Titrating to a pH of 8.3 neutralizes CO_3^{2-} to HCO_3^-

$$CO_3^{2-}(aq) + HCl(aq) \rightarrow HCO_3^-(aq) + Cl^-(aq) \tag{9.2.92}$$

but there is no reaction between the titrant and HCO_3^- (see Figure 9.19). The concentration of CO_3^{2-} in the sample, therefore, is

$$0.02812 \text{ M HCl} \times 0.01867 \text{ L HCl} \times \frac{1 \text{ mol CO}_3^{2-}}{\text{mol HCl}} = 5.250 \times 10^{-4} \text{ mol CO}_3^{2-} \tag{9.2.93}$$

$$\frac{5.250 \times 10^{-4} \text{ mol CO}_3^{2-}}{0.1000 \text{ L}} \times \frac{60.01 \text{ g CO}_3^{2-}}{\text{mol CO}_3^{2-}} \times \frac{1000 \text{ mg}}{\text{g}} = 315.1 \text{ mg/L} \tag{9.2.94}$$

Titrating to a pH of 4.5 neutralizes CO_3^{2-} to H_2CO_3, and HCO_3^- to H_2CO_3 (see Figures 9.19).

$$CO_3^{2-}(aq) + 2HCl(aq) \rightarrow H_2CO_3(aq) + 2Cl^-(aq) \tag{9.2.95}$$

$$HCO_3^-(aq) + HCl(aq) \rightarrow H_2CO_3(aq) + 2Cl^-(aq) \tag{9.2.96}$$

Because we know how many moles of CO_3^{2-} are in the sample, we can calculate the volume of HCl it consumes.

$$5.250 \times 10^{-4}\ \text{mol}\ CO_3^{2-} \times \frac{2\ \text{mol HCl}}{\text{mol}\ CO_3^{2-}} \times \frac{1\ \text{L HCl}}{0.02812\ \text{mol HCl}} \times \frac{1000\ \text{mL}}{\text{L}} = 37.34\ \text{mL} \tag{9.2.97}$$

This leaves 48.12 mL - 37.34 mL, or 10.78 mL of HCl to react with HCO_3^-. The amount of HCO_3^- in the sample is

$$0.02812\ \text{M HCl} \times 0.01078\ \text{L HCl} \times \frac{1\ \text{mol}\ HCO_3^-}{\text{mol HCl}} = 3.031 \times 10^{-4}\ \text{mol}\ HCO_3^- \tag{9.2.98}$$

$$\frac{3.031 \times 10^{-4}\ \text{mol}\ HCO_3^-}{0.1000\ \text{L}} \times \frac{61.02\ \text{g}\ HCO_3^-}{\text{mol}\ HCO_3^-} \times \frac{1000\ \text{mg}}{\text{g}} = 185.0\ \text{mg/L} \tag{9.2.99}$$

Practice Exercise 9.9

Samples containing the monoprotic weak acids 2–methylanilinium chloride ($C_7H_{10}NCl$, pK_a = 4.447) and 3–nitrophenol ($C_6H_5NO_3$, pK_a = 8.39) can be analyzed by titrating with NaOH. A 2.006-g sample requires 19.65 mL of 0.200 M NaOH to reach the bromocresol purple end point and 48.41 mL of 0.200 M NaOH to reach the phenolphthalein end point. Report the %w/w of each compound in the sample.

Click here to review your answer to this exercise.

9.2.5 Qualitative Applications

Example 9.5 shows how we can use an acid–base titration to assign the forms of alkalinity in waters. We can easily extend this approach to other systems. For example, by titrating with either a strong acid or a strong base to the methyl orange and phenolphthalein end points we can determine the composition of solutions containing one or two of the following species: H_3PO_4, $H_2PO_4^-$, HPO_4^{2-}, PO_4^{3-}, HCl, and NaOH. As outlined in Table 9.9, each species or mixture of species has a unique relationship between the volumes of titrant needed to reach these two end points.

Table 9.9 Relationship Between End Point Volumes for Mixtures of Phosphate Species with HCl and NaOH

Solution Composition	Relationship Between End Point Volumes with Strong Base Titrant[a]	Relationship Between End Point Volumes With Strong Acid Titrant[a]
H_3PO_4	$V_{PH} = 2 \times V_{MO}$	—[b]
$H_2PO_4^-$	$V_{PH} > 0$; $V_{MO} = 0$	—
HPO_4^{2-}	—	$V_{MO} > 0$; $V_{PH} = 0$
PO_4^{3-}	—	$V_{MO} = 2 \times V_{PH}$
HCl	$V_{PH} = V_{MO}$	—
NaOH	—	$V_{MO} = V_{PH}$
HCl and H_3PO_4	$V_{PH} < 2 \times V_{MO}$	—
H_3PO_4 and $H_2PO_4^-$	$V_{PH} > 2 \times V_{MO}$	—
$H_2PO_4^-$ and HPO_4^{2-}	$V_{PH} > 0$; $V_{MO} = 0$	$V_{MO} > 0$; $V_{PH} = 0$
HPO_4^{2-} and PO_4^{3-}	—	$V_{MO} > 2 \times V_{PH}$
PO_4^{3-} and NaOH	—	$V_{MO} < 2 \times V_{PH}$

[a] V_{PH} and V_{MO} are, respectively, the volume of titrant at the phenolphthalein and methyl orange end points.
[b] When no information is provided, the volume of titrant to each end point is zero.

9.2.6 Characterization Applications

An acid–base titration can be use to characterize the chemical and physical properties of matter. Two useful characterization applications are the determination of a compound's equivalent weight and its acid or its base dissociation constant.

Equivalent Weights

Suppose we titrate a sample containing an impure weak acid to a well-defined end point using a monoprotic strong base as the titrant. If we assume that the titration involves the transfer of *n* protons, then the moles of titrant needed to reach the end point is

$$\text{moles titrant} = \frac{n \text{ moles titrant}}{\text{moles analyte}} \times \text{moles analyte} \tag{9.2.100}$$

If we know the analyte's identity, we can use this equation to determine the amount of analyte in the sample

$$\text{grams analyte} = \text{moles titrant} \times \frac{1 \text{ mole analyte}}{n \text{ moles titrant}} \times \text{FW analyte} \tag{9.2.101}$$

where FW is the analyte's formula weight.

But what if we do not know the analyte's identify? If we can titrate a pure sample of the analyte, we can obtain some useful information that may help in establishing its identity. Because we do not know the number of protons being titrated, we let $n = 1$ and replace the analyte's formula weight with its equivalent weight (EW)

$$\text{grams analyte} = \text{moles titrant} \times \frac{1 \text{ equivalent analyte}}{1 \text{ moles titrant}} \times \text{EW analyte} \tag{9.2.102}$$

where

$$\text{FW} = n \times \text{EW} \tag{9.2.103}$$

Example 9.6

A 0.2521-g sample of an unknown weak acid is titrated with 0.1005 M NaOH, requiring 42.68 mL to reach the phenolphthalein end point. Determine the compound's equivalent weight. Which of the following compounds is most likely to be the unknown weak acid?

ascorbic acid	$C_8H_8O_6$	FW = 176.1	monoprotic
malonic acid	$C_3H_4O_4$	FW = 104.1	diprotic
succinic acid	$C_4H_6O_4$	FW = 118.1	diprotic
citric acid	$C_6H_8O_7$	FW = 192.1	triprotic

Solution

The moles of NaOH needed to reach the end point is

$$0.1005 \text{ M NaOH} \times 0.04268 \text{ L NaOH} = 4.289 \times 10^{-3} \text{ mol NaOH} \tag{9.2.104}$$

which gives the analyte's equivalent weight as

$$EW = \frac{\text{g analyte}}{\text{equiv. analyte}} = \frac{0.2521 \text{ g}}{4.289 \times 10^{-3} \text{ equiv.}} = 58.78 \text{ g/equivalent} \tag{9.2.105}$$

The possible formula weights for the weak acid are

$$n = 1: \ \text{FW} = \text{EW} = 58.78 \text{ g/equivalent} \tag{9.2.106}$$

$$n = 2: \ \text{FW} = 2 \times \text{EW} = 117.6 \text{ g/equivalent} \tag{9.2.107}$$

$$n = 3: \ \text{FW} = 3 \times \text{EW} = 176.3 \text{ g/equivalent} \tag{9.2.108}$$

If the analyte is a monoprotic weak acid, then its formula weight is 58.78 g/mol, eliminating ascorbic acid as a possibility. If it is a diprotic weak acid, then the analyte's formula weight is either 58.78 g/mol or 117.6 g/mol, depending on whether the titration

is to the first or second equivalence point. Succinic acid, with a formula weight of 118.1 g/mole is a possibility, but malonic acid is not. If the analyte is a triprotic weak acid, then its formula weight is 58.78 g/mol, 117.6 g/mol, or 176.3 g/mol. None of these values is close to the formula weight for citric acid, eliminating it as a possibility. Only succinic acid provides a possible match.

Practice Exercise 9.10

Figure 9.21 shows the potentiometric titration curve for the titration of a 0.500-g sample an unknown weak acid. The titrant is 0.1032 M NaOH. What is the weak acid's equivalent weight?

Click here to review your answer to this exercise.

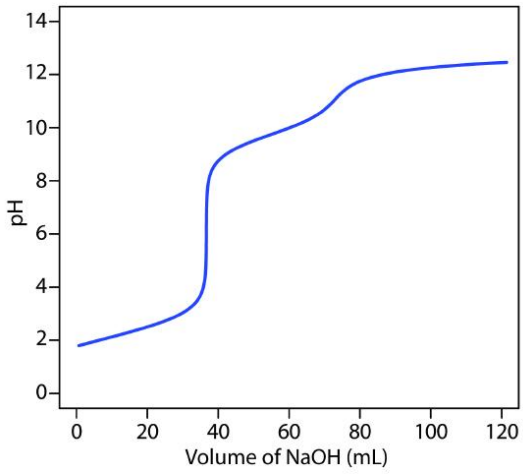


Figure 9.21 Titration curve for Practice Exercise 9.10.

Equilibrium Constants

Another application of acid–base titrimetry is the determination of equilibrium constants. Consider, for example, a solution of acetic acid, CH_3COOH, for which the dissociation constant is

$$K_a = \frac{[H_3O^+][CH_3COO^-]}{[CH_3COOH]} \tag{9.2.109}$$

When the concentrations of CH_3COOH and CH_3COO^- are equal, the K_a expression reduces to $K_a = [H_3O^+]$, or pH = pK_a. If we titrate a solution of acetic acid with NaOH, the pH equals the pK_a when the volume of NaOH is approximately $\frac{1}{2}V_{eq}$. As shown in Figure 9.22, a potentiometric titration curve provides a reasonable estimate of acetic acid's pK_a.

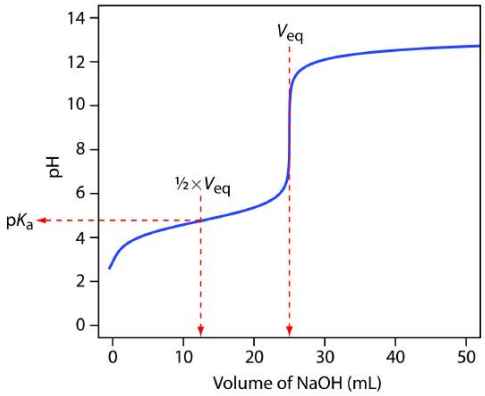


Figure 9.22 Estimating acetic acid's pK_a using its potentiometric titration curve.

This method provides a reasonable estimate of a weak acid's pK_a if the acid is neither too strong nor too weak. These limitations are easily to appreciate if we consider two limiting cases. For the first case let's assume that the weak acid, HA, is more than 50% dissociated before the titration begins (a relatively large K_a value). The concentration of HA before the equivalence point is always

less than the concentration of A^-, and there is no point on the titration curve where [HA] = [A^-]. At the other extreme, if the acid is too weak, less than 50% of the weak acid reacts with the titrant at the equivalence point. In this case the concentration of HA before the equivalence point is always greater than that of A^-. Determining the pK_a by the half-equivalence point method overestimates its value if the acid is too strong and underestimates its value if the acid is too weak.

Practice Exercise 9.11

Use the potentiometric titration curve in Figure 9.21 to estimate the pK_a values for the weak acid in Practice Exercise 9.10.

Click here to review your answer to this exercise.

A second approach for determining a weak acid's pK_a is to use a Gran plot. For example, earlier in this chapter we derived the following equation for the titration of a weak acid with a strong base.

$$[H_3O^+] \times V_b = K_a V_{eq} - K_a V_b \tag{9.2.110}$$

A plot of $[H_3O^+] \times V_b$ versus V_b, for volumes less than the equivalence point, yields a straight line with a slope of $-K_a$. Other linearizations have been developed which use the entire titration curve, or that require no assumptions.[6] This approach to determining acidity constants has been used to study the acid–base properties of humic acids, which are naturally occurring, large molecular weight organic acids with multiple acidic sites. In one study a humic acid was found to have six titratable sites, three of which were identified as carboxylic acids, two of which were believed to be secondary or tertiary amines, and one of which was identified as a phenolic group.[7]

9.2.7 Evaluation of Acid–Base Titrimetry

Scale of Operation

In an acid–base titration the volume of titrant needed to reach the equivalence point is proportional to the moles of titrand. Because the pH of the titrand or the titrant is a function of its concentration, however, the change in pH at the equivalence point—and thus the feasibility of an acid–base titration—depends on their respective concentrations. Figure 9.23, for example, shows a series of titration curves for the titration of several concentrations of HCl with equimolar solutions NaOH. For titrand and titrant concentrations smaller than 10^{-3} M, the change in pH at the end point may be too small to provide accurate and precise results.

Note

Acid–base titrimetry is an example of a total analysis technique in which the signal is proportional to the absolute amount of analyte. See Chapter 3 for a discussion of the difference between total analysis techniques and concentration techniques.

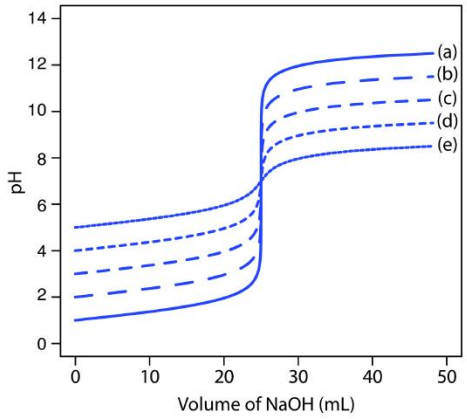


Figure 9.23 Titration curves for 25.0 mL of (a) 10^{-1} M HCl, (b) 10^{-2} M HCl, (c) 10^{-3} M HCl, (d) 10^{-4} M HCl, and (e) 10^{-5} M HCl. In each case the titrant is an equimolar solution of NaOH.

A minimum concentration of 10^{-3} M places limits on the smallest amount of analyte that we can successfully analyze. For example, suppose our analyte has a formula weight of 120 g/mol. To successfully monitor the titration's end point using an indicator or with a pH probe, the titrand needs an initial volume of approximately 25 mL. If we assume that the analyte's formula weight is 120

g/mol, then each sample must contain at least 3 mg of analyte. For this reason, acid–base titrations are generally limited to major and minor analytes (see Figure 3.6 in Chapter 3). We can extend the analysis of gases to trace analytes by pulling a large volume of the gas through a suitable collection solution.

One goal of analytical chemistry is to extend analyses to smaller samples. Here we describe two interesting approaches to titrating μL and pL samples. In one experimental design (Figure 9.24), samples of 20–100 μL were held by capillary action between a flat-surface pH electrode and a stainless steel sample stage.[8] The titrant was added by using the oscillations of a piezoelectric ceramic device to move an angled glass rod in and out of a tube connected to a reservoir containing the titrant. Each time the glass tube was withdrawn an approximately 2 nL microdroplet of titrant was released. The microdroplets were allowed to fall onto the sample, with mixing accomplished by spinning the sample stage at 120 rpm. A total of 450 microdroplets, with a combined volume of 0.81–0.84 μL, was dispensed between each pH measurement. In this fashion a titration curve was constructed. This method was used to titrate solutions of 0.1 M HCl and 0.1 M CH_3COOH with 0.1 M NaOH. Absolute errors ranged from a minimum of +0.1% to a maximum of –4.1%, with relative standard deviations from 0.15% to 4.7%. Sample as small as 20 μL were successfully titrated.

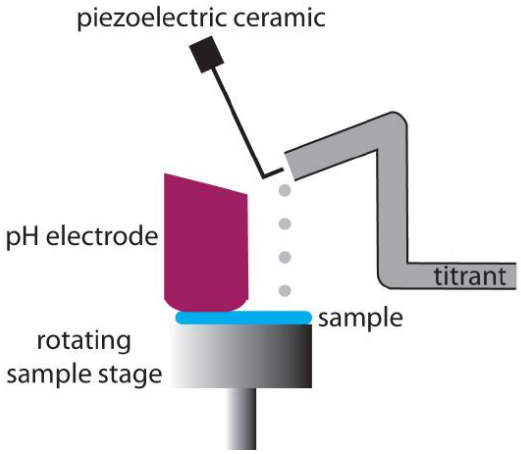


Figure 9.24 Experimental design for a microdroplet titration apparatus.

Another approach carries out the acid–base titration in a single drop of solution.[9] The titrant is delivered using a microburet fashioned from a glass capillary micropipet (Figure 9.25). The microburet has a 1-2 μm tip filled with an agar gel membrane. The tip of the microburet is placed within a drop of the sample solution, which is suspended in heptane, and the titrant is allowed to diffuse into the sample. The titration's progress is monitored using an acid–base indicator, and the time needed to reach the end point is measured. The rate of the titrant's diffusion from the microburet is determined by a prior calibration. Once calibrated the end point time can be converted to an end point volume. Samples usually consisted of picoliter volumes (10^{-12} liters), with the smallest sample being 0.7 pL. The precision of the titrations was usually about 2%.

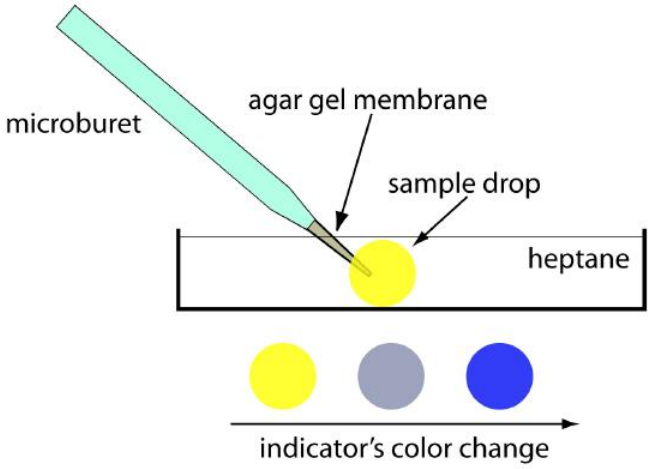


Figure 9.25 Experimental set-up for a diffusional microtitration. The indicator is a mixture of bromothymol blue and bromocresol purple.

Titrations conducted with microliter or picoliter sample volumes require a smaller absolute amount of analyte. For example, diffusional titrations have been successfully conducted on as little as 29 femtomoles (10^{-15} moles) of nitric acid. Nevertheless, the analyte must still be present in the sample at a major or minor level for the titration to be performed accurately and precisely.

Accuracy

When working with a macro–major or a macro–minor sample, an acid–base titration can achieve a relative error of 0.1–0.2%. The principal limitation to accuracy is the difference between the end point and the equivalence point.

> **Note**
>
> See Figure 3.5 in Chapter 3 to review the characteristics of macro–major and macro–minor samples.

Precision

An acid–base titration's relative precision depends primarily on the precision with which we can measure the end point volume and the precision in detecting the end point. Under optimum conditions, an acid–base titration has a relative precision of 0.1–0.2%. We can improve the relative precision by using the largest possible buret and ensuring that we use most of its capacity in reaching the end point. A smaller volume buret is a better choice when using costly reagents, when waste disposal is a concern, or when the titration must be completed quickly to avoid competing chemical reactions. Automatic titrators are particularly useful for titrations requiring small volumes of titrant because they provide significantly better precision (typically about ±0.05% of the buret's volume).

The precision of detecting the end point depends on how it is measured and the slope of the titration curve at the end point. With an indicator the precision of the end point signal is usually ±0.03–0.10 mL. Potentiometric end points usually are more precise.

Sensitivity

For an acid–base titration we can write the following general analytical equation relating the titrant's volume to the absolute amount of titrand

$$\text{volume of titrant} = k \times \text{moles of titrand} \tag{9.2.111}$$

where k, the sensitivity, is determined by the stoichiometry between the titrand and the titrant. Consider, for example, the determination of sulfurous acid, H_2SO_3, by titrating with NaOH to the first equivalence point

$$H_2SO_3(aq) + OH^-(aq) \rightarrow H_2O(l) + HSO_3^-(aq) \tag{9.2.112}$$

At the equivalence point the relationship between the moles of NaOH and the moles of H_2SO_3 is

$$\text{mol NaOH} = \text{mol } H_2SO_3 \tag{9.2.113}$$

Substituting the titrant's molarity and volume for the moles of NaOH and rearranging

$$M_{NaOH} \times V_{NaOH} = \text{ mol } H_2SO_3 \tag{9.2.114}$$

$$V_{NaOH} = \frac{1}{M_{NaOH}} \times \text{mol } H_2SO_3 \tag{9.2.115}$$

we find that k is

$$k = \frac{1}{M_{NaOH}} \tag{9.2.116}$$

There are two ways in which we can improve a titration's sensitivity. The first, and most obvious, is to decrease the titrant's concentration because it is inversely proportional to the sensitivity, k.

The second approach, which only applies if the titrand is multiprotic, is to titrate to a later equivalence point. If we titrate H_2SO_3 to the second equivalence point

$$H_2SO_3(aq) + 2OH^-(aq) \rightarrow 2H_2O(l) + SO_3^{2-}(aq) \tag{9.2.117}$$

then each mole of H_2SO_3 consumes two moles of NaOH

$$\text{mol NaOH} = 2 \times \text{mol } H_2SO_3 \tag{9.2.118}$$

and the sensitivity becomes

$$k = \frac{2}{M_{NaOH}} \tag{9.2.119}$$

In practice, however, any improvement in sensitivity is offset by a decrease in the end point's precision if the larger volume of titrant requires us to refill the buret. Consequently, standard acid–base titrimetric procedures are written to ensure that titrations require 60–100% of the buret's volume.

Selectivity

Acid–base titrants are not selective. A strong base titrant, for example, reacts with all acids in a sample, regardless of their individual strengths. If the titrand contains an analyte and an interferent, then selectivity depends on their relative acid strengths. Two limiting situations must be considered.

If the analyte is a stronger acid than the interferent, then the titrant will react with the analyte before it begins reacting with the interferent. The feasibility of the analysis depends on whether the titrant's reaction with the interferent affects the accurate location of the analyte's equivalence point. If the acid dissociation constants are substantially different, the end point for the analyte can be accurately determined. Conversely, if the acid dissociation constants for the analyte and interferent are similar, then an accurate end point for the analyte may not be found. In the latter case a quantitative analysis for the analyte is not possible.

In the second limiting situation the analyte is a weaker acid than the interferent. In this case the volume of titrant needed to reach the analyte's equivalence point is determined by the concentration of both the analyte and the interferent. To account for the interferent's contribution to the end point, an end point for the interferent must be present. Again, if the acid dissociation constants for the analyte and interferent are significantly different, then the analyte's determination is possible. If the acid dissociation constants are similar, however, there is only a single equivalence point and the analyte's and interferent's contributions to the equivalence point volume can not be separated.

Time, Cost, and Equipment

Acid–base titrations require less time than most gravimetric procedures, but more time than many instrumental methods of analysis, particularly when analyzing many samples. With an automatic titrator, however, concerns about analysis time are less significant. When performing a titration manually our equipment needs—a buret and, perhaps, a pH meter—are few in number, inexpensive, routinely available, and easy to maintain. Automatic titrators are available for between $3000 and $10 000.

Contributors

David Harvey (DePauw University)

9.2: Acid–Base Titrations is shared under a CC BY-NC-SA 4.0 license and was authored, remixed, and/or curated by LibreTexts.

9.3: Complexation Titrations

The earliest examples of metal–ligand **complexation titrations** are Liebig's determinations, in the 1850s, of cyanide and chloride using, respectively, Ag^+ and Hg^{2+} as the titrant. Practical analytical applications of complexation titrimetry were slow to develop because many metals and ligands form a series of metal–ligand complexes. Liebig's titration of CN^- with Ag^+ was successful because they form a single, stable complex of $Ag(CN)_2^-$, giving a single, easily identified end point. Other metal–ligand complexes, such as CdI_4^{2-}, are not analytically useful because they form a series of metal–ligand complexes (CdI^+, $CdI_2(aq)$, CdI_3^- and CdI_4^{2-}) that produce a sequence of poorly defined end points.

> **Note**
>
> Recall that an acid–base titration curve for a diprotic weak acid has a single end point if its two K_a values are not sufficiently different. See Figure 9.11 for an example.

In 1945, Schwarzenbach introduced aminocarboxylic acids as multidentate ligands. The most widely used of these new ligands—ethylenediaminetetraacetic acid, or EDTA—forms strong 1:1 complexes with many metal ions. The availability of a ligand that gives a single, easily identified end point made complexation titrimetry a practical analytical method.

9.3.1 Chemistry and Properties of EDTA

Ethylenediaminetetraacetic acid, or EDTA, is an aminocarboxylic acid. EDTA, which is shown in Figure 9.26a in its fully deprotonated form, is a Lewis acid with six binding sites—four negatively charged carboxylate groups and two tertiary amino groups—that can donate six pairs of electrons to a metal ion. The resulting metal–ligand complex, in which EDTA forms a cage-like structure around the metal ion (Figure 9.26b), is very stable. The actual number of coordination sites depends on the size of the metal ion, however, all metal–EDTA complexes have a 1:1 stoichiometry.

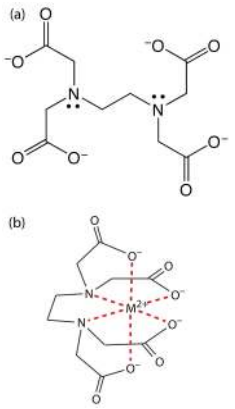


Figure 9.26 Structures of (a) EDTA, in its fully deprotonated form, and (b) in a six-coordinate metal–EDTA complex with a divalent metal ion.

Metal–ED TA Formation Constants

To illustrate the formation of a metal–EDTA complex, let's consider the reaction between Cd^{2+} and EDTA

$$Cd^{2+}(aq) + Y^{4-}(aq) \rightleftharpoons CdY^{2-}(aq) \tag{9.9}$$

where Y^{4-} is a shorthand notation for the fully deprotonated form of EDTA shown in Figure 9.26a. Because the reaction's formation constant

$$K_f = \frac{[CdY^{2-}]}{[Cd^{2+}][Y^{4-}]} = 2.9 \times 10^{16} \tag{9.10}$$

is large, its equilibrium position lies far to the right. Formation constants for other metal–EDTA complexes are found in Table E4.

EDTA is a Weak Acid

In addition to its properties as a ligand, EDTA is also a weak acid. The fully protonated form of EDTA, H_6Y^{2+}, is a hexaprotic weak acid with successive pK_a values of

$pK_{a1} = 0.0$	$pK_{a2} = 1.5$	$pK_{a3} = 2.0$
$pK_{a4} = 2.66$	$pK_{a5} = 6.16$	$pK_{a6} = 10.24$

The first four values are for the carboxylic acid protons and the last two values are for the ammonium protons. Figure 9.27 shows a ladder diagram for EDTA. The specific form of EDTA in reaction 9.9 is the predominate species only at pH levels greater than 10.17.

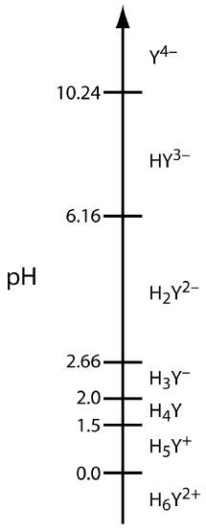


Figure 9.27 Ladder diagram for EDTA.

Conditional Metal–Ligand Formation Constants

The formation constant for CdY^{2-} in equation 9.10 assumes that EDTA is present as Y^{4-}. Because EDTA has many forms, when we prepare a solution of EDTA we know it total concentration, C_{EDTA}, not the concentration of a specific form, such as Y^{4-}. To use equation 9.10, we need to rewrite it in terms of C_{EDTA}.

At any pH a mass balance on EDTA requires that its total concentration equal the combined concentrations of each of its forms.

$$C_{EDTA} = [H_6Y^{2+}] + [H_5Y^{+}] + [H_4Y] + [H_3Y^{-}] + [H_2Y^{2-}] + [HY^{3-}] + [Y^{4-}] \quad (9.3.1)$$

To correct the formation constant for EDTA's acid–base properties we need to calculate the fraction, $\alpha_{Y^{4-}}$, of EDTA present as Y^{4-}.

$$\alpha_{Y^{4-}} \frac{[Y^{4-}]}{C_{EDTA}} \quad (9.11)$$

Table 9.10 Values of $\alpha_{Y^{4-}}$ for Selected pH Levels

pH	$\alpha_{Y^{4-}}$	pH	$\alpha_{Y^{4-}}$
1	1.9×10^{-18}	8	5.6×10^{-3}
2	3.4×10^{-14}	9	5.4×10^{-2}
3	2.6×10^{-11}	10	0.37
4	3.8×10^{-9}	11	0.85
5	3.7×10^{-7}	12	0.98
6	2.4×10^{-5}	13	1.00
7	5.0×10^{-4}	14	1.00

Note

Problem 9.42 from the end of chapter problems asks you to verify the values in Table 9.10 by deriving an equation for $\alpha_{Y^{4-}}$.

Table 9.10 provides values of $\alpha_{Y^{4-}}$ for selected pH levels. Solving equation 9.11 for $[Y^{4-}]$ and substituting into equation 9.10 for the CdY^{2-} formation constant

$$K_f = \frac{[CdY^{2-}]}{[Cd^{2+}]\alpha_{Y^{4-}} C_{EDTA}} \tag{9.3.2}$$

and rearranging gives

$$K_f' = K_f \times \alpha_{Y^{4-}} = \frac{[CdY^{2-}]}{[Cd^{2+}]C_{EDTA}} \tag{9.12}$$

where K_f' is a pH-dependent **conditional formation constant**. As shown in Table 9.11, the conditional formation constant for CdY^{2-} becomes smaller and the complex becomes less stable at more acidic pHs.

Table 9.11 Conditional Formation Constants for CdY^{2-}

pH	K_f'	pH	K_f'
1	5.5×10^{-2}	8	1.6×10^{14}
2	1.0×10^{3}	9	1.6×10^{15}
3	7.7×10^{5}	10	1.1×10^{16}
4	1.1×10^{8}	11	2.5×10^{16}
5	1.1×10^{10}	12	2.9×10^{16}
6	6.8×10^{11}	13	2.9×10^{16}
7	1.5×10^{13}	14	2.9×10^{16}

EDTA Competes With Other Ligands

To maintain a constant pH during a complexation titration we usually add a buffering agent. If one of the buffer's components is a ligand that binds Cd^{2+}, then EDTA must compete with the ligand for Cd^{2+}. For example, an NH_4^+/NH_3 buffer includes NH_3, which forms several stable Cd^{2+}–NH_3 complexes. Because EDTA forms a stronger complex with Cd^{2+} it will displace NH_3, but the stability of the Cd^{2+}–EDTA complex decreases.

We can account for the effect of an **auxiliary complexing agent**, such as NH_3, in the same way we accounted for the effect of pH. Before adding EDTA, the mass balance on Cd^{2+}, C_{Cd}, is

$$C_{Cd} = [Cd^{2+}] + [Cd(NH_3)^{2+}] + [Cd(NH_3)_2^{2+}] + [Cd(NH_3)_3^{2+}] + [Cd(NH_3)_4^{2+}] \tag{9.3.3}$$

and the fraction of uncomplexed Cd^{2+}, $\alpha_{Cd^{2+}}$, is

$$\alpha_{Cd^{2+}} = \frac{[Cd^{2+}]}{C_{Cd}} \tag{9.13}$$

Note

The value of $\alpha_{Cd^{2+}}$ depends on the concentration of NH_3. Contrast this with $\alpha_{Y^{4-}}$, which depends on pH.

Solving equation 9.13 for $[Cd^{2+}]$ and substituting into equation 9.12 gives

$$K_f' = K_f \times \alpha_{Y^{4-}} = \frac{[CdY^{2-}]}{\alpha_{Cd^{2+}} C_{Cd} C_{EDTA}} \tag{9.3.4}$$

Because the concentration of NH_3 in a buffer is essentially constant, we can rewrite this equation

$$K_f'' = K_f \times \alpha_{Y^{4-}} \times \alpha_{Cd^{2+}} = \frac{[CdY^{2-}]}{C_{Cd} C_{EDTA}} \tag{9.14}$$

to give a conditional formation constant, K_f'', that accounts for both pH and the auxiliary complexing agent's concentration. Table 9.12 provides values of $\alpha_{M^{2+}}$ for several metal ion when NH_3 is the complexing agent.

Table 9.12 Values of $\alpha_{M^{2+}}$ for Selected Concentrations of Ammonia

$[NH_3]$(M)	$\alpha_{Ca^{2+}}$	$\alpha_{Cd^{2+}}$	$\alpha_{Co^{2+}}$	$\alpha_{Cu^{2+}}$	$\alpha_{Mg^{2+}}$	$\alpha_{Ni^{2+}}$	$\alpha_{Zn^{2+}}$
1	5.50×10^{-1}	6.09×10^{-8}	1.00×10^{-6}	3.79×10^{-14}	1.76×10^{-1}	9.20×10^{-10}	3.95×10^{-10}
0.5	7.36×10^{-1}	1.05×10^{-6}	2.22×10^{-5}	6.86×10^{-13}	4.13×10^{-1}	3.44×10^{-8}	6.27×10^{-9}
0.1	9.39×10^{-1}	3.51×10^{-4}	6.64×10^{-3}	4.63×10^{-10}	8.48×10^{-1}	5.12×10^{-5}	3.68×10^{-6}
0.05	9.69×10^{-1}	2.72×10^{-3}	3.54×10^{-2}	7.17×10^{-9}	9.22×10^{-1}	6.37×10^{-4}	5.45×10^{-5}
0.01	9.94×10^{-1}	8.81×10^{-2}	3.55×10^{-1}	3.22×10^{-6}	9.84×10^{-1}	4.32×10^{-2}	1.82×10^{-2}
0.005	9.97×10^{-1}	2.27×10^{-1}	5.68×10^{-1}	3.62×10^{-5}	9.92×10^{-1}	1.36×10^{-1}	1.27×10^{-1}
0.001	9.99×10^{-1}	6.09×10^{-1}	8.84×10^{-1}	4.15×10^{-3}	9.98×10^{-1}	5.76×10^{-1}	7.48×10^{-1}

9.3.2 Complexometric EDTA Titration Curves

Now that we know something about EDTA's chemical properties, we are ready to evaluate its usefulness as a titrant. To do so we need to know the shape of a complexometric EDTA titration curve. In section 9B we learned that an acid–base titration curve shows how the titrand's pH changes as we add titrant. The analogous result for a complexation titration shows the change in pM, where M is the metal ion, as a function of the volume of EDTA. In this section we will learn how to calculate a titration curve using the equilibrium calculations from Chapter 6. We also will learn how to quickly sketch a good approximation of any complexation titration curve using a limited number of simple calculations.

Calculating the Titration Curve

Let's calculate the titration curve for 50.0 mL of 5.00×10^{-3} M Cd^{2+} using a titrant of 0.0100 M EDTA. Furthermore, let's assume that the titrand is buffered to a pH of 10 with a buffer that is 0.0100 M in NH_3.

Note

Step 1: Calculate the conditional formation constant for the metal–EDTA complex.

Because the pH is 10, some of the EDTA is present in forms other than Y^{4-}. In addition, EDTA must compete with NH_3 for the Cd^{2+}. To evaluate the titration curve, therefore, we first need to calculate the conditional formation constant for CdY^{2-}. From Table 9.10 and Table 9.11 we find that $\alpha_{Y^{4-}}$ is 0.35 at a pH of 10, and that $\alpha_{Cd^{2+}}$ is 0.0881 when the concentration of NH_3 is 0.0100 M. Using these values, the conditional formation constant is

$$K_f'' = K_f \times \alpha_{Y^{4-}} \times \alpha_{Cd^{2+}} = (2.9 \times 10^{16})(0.37)(0.0881) = 9.5 \times 10^{14} \tag{9.3.5}$$

Because K_f'' is so large, we can treat the titration reaction

$$Cd^{2+}(aq) + Y^{4-}(aq) \rightarrow CdY^{2-}(aq) \tag{9.3.6}$$

as if it proceeds to completion.

Note

Step 2: Calculate the volume of EDTA needed to reach the equivalence point.

The next task in calculating the titration curve is to determine the volume of EDTA needed to reach the equivalence point. At the equivalence point we know that

$$\text{moles EDTA} = \text{moles } Cd^{2+} \tag{9.3.7}$$

$$M_{EDTA} \times V_{EDTA} = M_{Cd} \times V_{Cd} \tag{9.3.8}$$

Substituting in known values, we find that it requires

$$V_{eq} = V_{EDTA} = \frac{M_{Cd}V_{Cd}}{M_{EDTA}} = \frac{(5.00 \times 10^{-3}\ \text{M})(50.0\ \text{mL})}{0.0100\ \text{M}} = 25.0\ \text{mL} \tag{9.3.9}$$

of EDTA to reach the equivalence point.

Note

Step 3: Calculate pM values before the equivalence point by determining the concentration of unreacted metal ions.

Before the equivalence point, Cd^{2+} is present in excess and pCd is determined by the concentration of unreacted Cd^{2+}. Because not all the unreacted Cd^{2+} is free—some is complexed with NH_3—we must account for the presence of NH_3. For example, after adding 5.0 mL of EDTA, the total concentration of Cd^{2+} is

$$C_{Cd} = \frac{\text{initial moles } Cd^{2+} - \text{moles EDTA added}}{\text{total volume}} = \frac{M_{Cd}V_{Cd} - M_{EDTA}V_{EDTA}}{V_{Cd} + V_{EDTA}} \tag{9.3.10}$$

$$= \frac{(5.00 \times 10^{-3}\ \text{M})(50.0\ \text{mL}) - (0.0100\ \text{M})(5.0\ \text{mL})}{50.0\ \text{mL} + 5.0\ \text{mL}} = 3.64 \times 10^{-3}\ \text{M} \tag{9.3.11}$$

To calculate the concentration of free Cd^{2+} we use equation 9.13

$$[Cd^{2+}] = \alpha_{Cd^{2+}} \times C_{Cd} = (0.0881)(3.64 \times 10^{-4}\ \text{M}) = 3.21 \times 10^{-4}\ \text{M} \tag{9.3.12}$$

which gives a pCd of

$$\text{pCd} = -\log[Cd^{2+}] = -\log(3.21 \times 10^{-4}) = 3.49 \tag{9.3.13}$$

Note

Step 4: Calculate pM at the equivalence point using the conditional formation constant.

At the equivalence point all the Cd^{2+} initially in the titrand is now present as CdY^{2-}. The concentration of Cd^{2+}, therefore, is determined by the dissociation of the CdY^{2-} complex. First, we calculate the concentration of CdY^{2-}.

$$[CdY^{2-}] = \frac{\text{initial moles } Cd^{2+}}{\text{total volume}} = \frac{M_{Cd}V_{Cd}}{V_{Cd} + V_{EDTA}} \tag{9.3.14}$$

$$= \frac{(5.00 \times 10^{-3}\ \text{M})(50.0\ \text{mL})}{50.0\ \text{mL} + 25.0\ \text{mL}} = 3.33 \times 10^{-3}\ \text{M} \tag{9.3.15}$$

Next, we solve for the concentration of Cd^{2+} in equilibrium with CdY^{2-}.

$$K_f'' = \frac{[CdY^{2-}]}{C_{Cd}C_{EDTA}} = \frac{3.33 \times 10^{-3} - x}{(x)(x)} = 9.5 \times 10^{14} \tag{9.3.16}$$

$$x = C_{Cd} = 1.9 \times 10^{-9}\ \text{M} \tag{9.3.17}$$

Note

At the equivalence point the initial moles of Cd^{2+} and the moles of EDTA added are equal. The total concentrations of Cd^{2+}, C_{Cd}, and the total concentration of EDTA, C_{EDTA}, are equal.

Once again, to find the concentration of uncomplexed Cd^{2+} we must account for the presence of NH_3; thus

$$[Cd^{2+}] = \alpha_{Cd^{2+}} \times C_{Cd} = (0.0881)(1.9 \times 10^{-9}\ \text{M}) = 1.70 \times 10^{-10}\ \text{M} \tag{9.3.18}$$

and pCd is 9.77 at the equivalence point.

Note

Step 5: Calculate pM after the equivalence point using the conditional formation constant.

After the equivalence point, EDTA is in excess and the concentration of Cd^{2+} is determined by the dissociation of the CdY^{2-} complex. First, we calculate the concentrations of CdY^{2-} and of unreacted EDTA. For example, after adding 30.0 mL of EDTA

$$[CdY^{2-}] = \frac{\text{initial moles } Cd^{2+}}{\text{total volume}} = \frac{M_{Cd}V_{Cd}}{V_{Cd} + V_{EDTA}} \tag{9.3.19}$$

$$= \frac{(5.00 \times 10^{-3}\ \text{M})(50.0\ \text{mL})}{50.0\ \text{mL} + 30.0\ \text{mL}} = 3.13 \times 10^{-3}\ \text{M} \tag{9.3.20}$$

$$C_{EDTA} = \frac{M_{EDTA}V_{EDTA} - M_{Cd}V_{Cd}}{V_{Cd} + V_{EDTA}} \tag{9.3.21}$$

$$= \frac{(0.0100\ \text{M})(30.0\ \text{mL}) - (5.00 \times 10^{-3}\ \text{M})(50.0\ \text{mL})}{50.0\ \text{mL} + 30.0\ \text{mL}} \tag{9.3.22}$$

$$= 6.25 \times 10^{-4}\ \text{M} \tag{9.3.23}$$

Substituting into equation 9.14 and solving for $[Cd^{2+}]$ gives

$$\frac{[CdY^{2-}]}{C_{Cd}C_{EDTA}} = \frac{3.13 \times 10^{-3}\ \text{M}}{C_{Cd}(6.25 \times 10^{-4}\ \text{M})} = 9.5 \times 10^{14} \tag{9.3.24}$$

$$C_{Cd} = 5.4 \times 10^{-15}\ \text{M} \tag{9.3.25}$$

$$[Cd^{2+}] = \alpha_{Cd^{2+}} \times C_{Cd} = (0.0881)(5.4 \times 10^{-15}\ \text{M}) = 4.8 \times 10^{-16}\ \text{M} \tag{9.3.26}$$

a pCd of 15.32. Table 9.13 and Figure 9.28 show additional results for this titration.

Note

After the equilibrium point we know the equilibrium concentrations of CdY^{2-} and EDTA. We can solve for the equilibrium concentration of C_{Cd} using K_f'' and then calculate $[Cd^{2+}]$ using $\alpha_{Cd^{2+}}$. Because we use the same conditional formation constant, K_f'', for all calculations, this is the approach shown here.

There is a second method for calculating $[Cd^{2+}]$ after the equivalence point. Because the calculation uses only $[CdY^{2-}]$ and C_{EDTA}, we can use K_f' instead of K_f''; thus

$$\frac{[CdY^{2-}]}{[Cd^{2+}]C_{EDTA}} = \alpha_{Y^{4-}} \times K_f \tag{9.3.27}$$

$$\frac{3.13 \times 10^{-3}\ \text{M}}{[Cd^{2+}](6.25 \times 10^{-4}\ \text{M})} = (0.37)(2.9 \times 10^{16}) \tag{9.3.28}$$

Solving gives $[Cd^{2+}] = 4.7 \times 10^{-16}$ M and a pCd of 15.33. We will use this approach when learning how to sketch a complexometric titration curve.

Table 9.13 Titration of 50.0 mL of 5.00×10^{-3} M Cd^{2+} with 0.0100 M EDTA at a pH of 10 and in the Presence of 0.0100 M NH_3

Volume of EDTA (mL)	pCd	Volume of EDTA (mL)	pCd
0.00	3.36	27.0	14.95
5.00	3.49	30.0	15.33
10.0	3.66	35.0	15.61
15.0	3.87	40.0	15.76
20.0	4.20	45.0	15.86
23.0	4.62	50.0	15.94

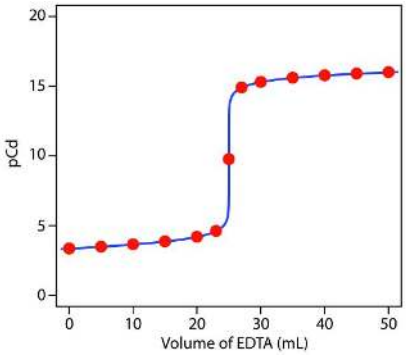


Figure 9.28 Titration curve for the titration of 50.0 mL of 5.00×10^{-3} M Cd^{2+} with 0.0100 M EDTA at a pH of 10 and in the presence of 0.0100 M NH_3. The red points correspond to the data in Table 9.13. The blue line shows the complete titration curve.

Practice Exercise 9.12

Calculate titration curves for the titration of 50.0 mL of 5.00×10^{-3} M Cd^{2+} with 0.0100 M EDTA (a) at a pH of 10 and (b) at a pH of 7. Neither titration includes an auxiliary complexing agent. Compare your results with Figure 9.28 and comment on the effect of pH and of NH_3 on the titration of Cd^{2+} with EDTA.

Click here to review your answer to this exercise.

Sketching an EDTA Titration Curve

To evaluate the relationship between a titration's equivalence point and its end point, we need to construct only a reasonable approximation of the exact titration curve. In this section we demonstrate a simple method for sketching a complexation titration curve. Our goal is to sketch the titration curve quickly, using as few calculations as possible. Let's use the titration of 50.0 mL of 5.00×10^{-3} M Cd^{2+} with 0.0100 M EDTA in the presence of 0.0100 M NH_3 to illustrate our approach.

Note

This is the same example that we used in developing the calculations for a complexation titration curve. You can review the results of that calculation in Table 9.13 and Figure 9.28.

We begin by calculating the titration's equivalence point volume, which, as we determined earlier, is 25.0 mL. Next, we draw our axes, placing pCd on the *y*-axis and the titrant's volume on the *x*-axis. To indicate the equivalence point's volume, we draw a vertical line corresponding to 25.0 mL of EDTA. Figure 9.29a shows the result of the first step in our sketch.

Before the equivalence point, Cd^{2+} is present in excess and pCd is determined by the concentration of unreacted Cd^{2+}. Because not all the unreacted Cd^{2+} is free—some is complexed with NH_3—we must account for the presence of NH_3. The calculations are straightforward, as we saw earlier. Figure 9.29b shows the pCd after adding 5.00 mL and 10.0 mL of EDTA.

Note

See Table 9.13 for the values.

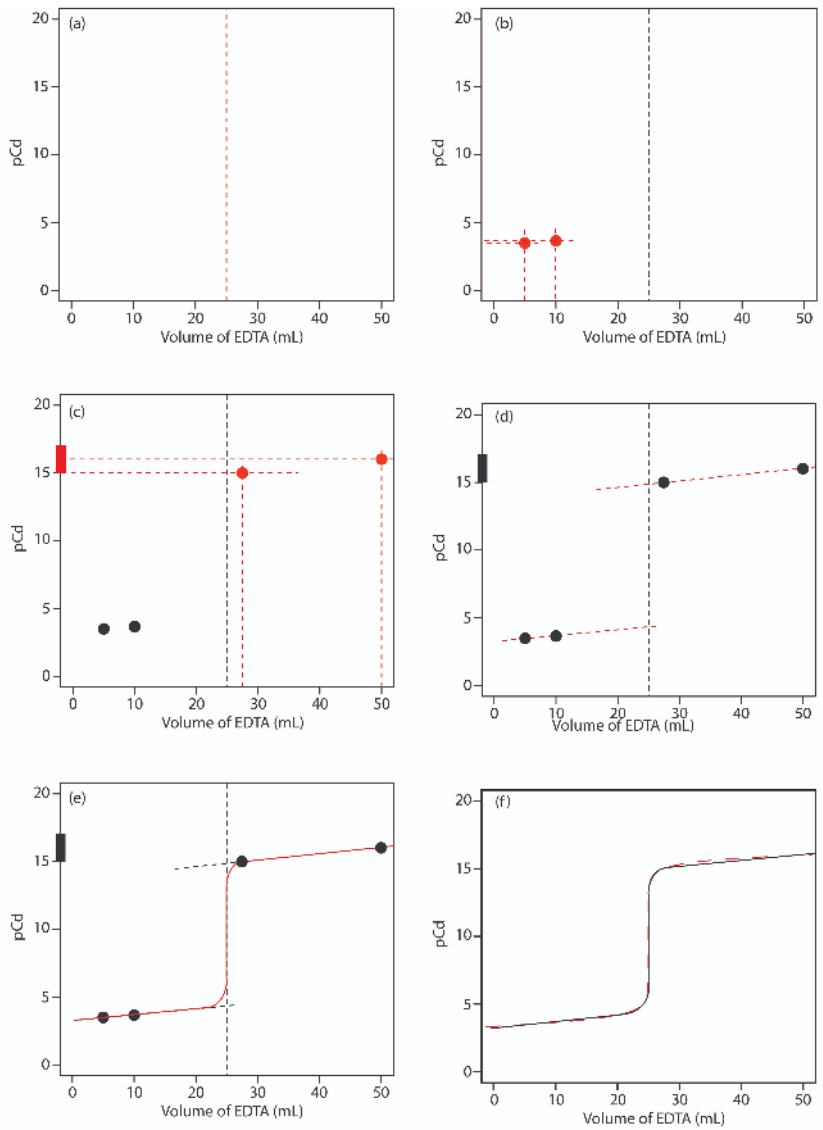


Figure 9.29 Illustrations showing the steps in sketching an approximate titration curve for the titration of 50.0 mL of 5.00×10^{-3} M Cd^{2+} with 0.0100 M EDTA in the presence of 0.0100 M NH_3: (a) locating the equivalence point volume; (b) plotting two points before the equivalence point; (c) plotting two points after the equivalence point; (d) preliminary approximation of titration curve using straight-lines; (e) final approximation of titration curve using a smooth curve; (f) comparison of approximate titration curve (solid black line) and exact titration curve (dashed red line). See the text for additional details.

The third step in sketching our titration curve is to add two points after the equivalence point. Here the concentration of Cd^{2+} is controlled by the dissociation of the Cd^{2+}–EDTA complex. Beginning with the conditional formation constant

$$K_f' = \frac{[CdY^{2-}]}{[Cd^{2+}]C_{EDTA}} = \alpha_{Y^{4-}} \times K_f = (0.37)(2.9 \times 10^{16}) = 1.1 \times 10^{16} \tag{9.3.29}$$

we take the log of each side and rearrange, arriving at

$$\log K_f' = -\log[Cd^{2+}] + \log \frac{[CdY^{2-}]}{C_{EDTA}} \tag{9.3.30}$$

$$pCd = \log K_f' + \log \frac{C_{EDTA}}{[CdY^{2-}]} \tag{9.3.31}$$

> **Note**
>
> See the final side comment in the previous section for an explanation of why we are ignoring the effect of NH_3 on the concentration of Cd^{2+}.

Note that after the equivalence point, the titrand's solution is a metal–ligand complexation buffer, with pCd determined by C_{EDTA} and $[CdY^{2-}]$. The buffer is at its lower limit of pCd = $\log K_f' - 1$ when

$$\frac{C_{EDTA}}{[CdY^{2-}]} = \frac{\text{moles EDTA added} - \text{initial moles } Cd^{2+}}{\text{initial moles } Cd^{2+}} = \frac{1}{10} \tag{9.3.32}$$

Making appropriate substitutions and solving, we find that

$$\frac{M_{EDTA}V_{EDTA} - M_{Cd}V_{Cd}}{M_{Cd}V_{Cd}} = \frac{1}{10} \tag{9.3.33}$$

$$M_{EDTA}V_{EDTA} - M_{Cd}V_{Cd} = 0.1 \times M_{Cd}V_{Cd} \tag{9.3.34}$$

$$V_{EDTA} = \frac{1.1 \times M_{Cd}V_{Cd}}{M_{EDTA}} = 1.1 \times V_{eq} \tag{9.3.35}$$

Thus, when the titration reaches 110% of the equivalence point volume, pCd is $\log K_f' - 1$. A similar calculation should convince you that pCd = $\log K_f'$ when the volume of EDTA is $2 \times V_{eq}$.

> **Note**
>
> Our derivation here is general and applies to any complexation titration using EDTA as a titrant.

Figure 9.29c shows the third step in our sketch. First, we add a ladder diagram for the CdY^{2-} complex, including its buffer range, using its $\log K_f'$ value of 16.04. Next, we add points representing pCd at 110% of V_{eq} (a pCd of 15.04 at 27.5 mL) and at 200% of V_{eq} (a pCd of 16.04 at 50.0 mL).

Next, we draw a straight line through each pair of points, extending the line through the vertical line representing the equivalence point's volume (Figure 9.29d). Finally, we complete our sketch by drawing a smooth curve that connects the three straight-line segments (Figure 9.29e). A comparison of our sketch to the exact titration curve (Figure 9.29f) shows that they are in close agreement.

> **Practice Exercise 9.13**
>
> Sketch titration curves for the titration of 50.0 mL of 5.00×10^{-3} M Cd^{2+} with 0.0100 M EDTA (a) at a pH of 10 and (b) at a pH of 7. Compare your sketches to the calculated titration curves from Practice Exercise 9.12.
>
> Click here to review your answer to this exercise.

9.3.3 Selecting and Evaluating the End point

The equivalence point of a complexation titration occurs when we react stoichiometrically equivalent amounts of titrand and titrant. As is the case with acid–base titrations, we estimate the equivalence point of a complexation titration using an experimental end point. A variety of methods are available for locating the end point, including indicators and sensors that respond to a change in the solution conditions.

Finding the End point with an Indicator

Most indicators for complexation titrations are organic dyes—known as **metallochromic indicators**—that form stable complexes with metal ions. The indicator, In^{m-}, is added to the titrand's solution where it forms a stable complex with the metal ion, MIn^{n-}. As we add EDTA it reacts first with free metal ions, and then displaces the indicator from MIn^{n-}.

$$MIn^{n-} + Y^{4-} \rightarrow MY^{2-} + In^{m-} \tag{9.3.36}$$

If MIn^{n-} and In^{m-} have different colors, then the change in color signals the end point.

The accuracy of an indicator's end point depends on the strength of the metal–indicator complex relative to that of the metal–EDTA complex. If the metal–indicator complex is too strong, the change in color occurs after the equivalence point. If the metal–indicator complex is too weak, however, the end point occurs before we reach the equivalence point.

Most metallochromic indicators also are weak acids. One consequence of this is that the conditional formation constant for the metal–indicator complex depends on the titrand's pH. This provides some control over an indicator's titration error because we can adjust the strength of a metal–indicator complex by adjusted the pH at which we carry out the titration. Unfortunately, because the indicator is a weak acid, the color of the uncomplexed indicator also changes with pH. Figure 9.30, for example, shows the color of the indicator calmagite as a function of pH and pMg, where H_2In^-, HIn^{2-}, and In^{3-} are different forms of the uncomplexed indicator, and $MgIn^-$ is the Mg^{2+}–calmagite complex. Because the color of calmagite's metal–indicator complex is red, its use as a metallochromic indicator has a practical pH range of approximately 8.5–11 where the uncomplexed indicator, HIn^{2-}, has a blue color.

Note

Figure 9.30 is essentially a two-variable ladder diagram. The solid lines are equivalent to a step on a conventional ladder diagram, indicating conditions where two (or three) species are equal in concentration.

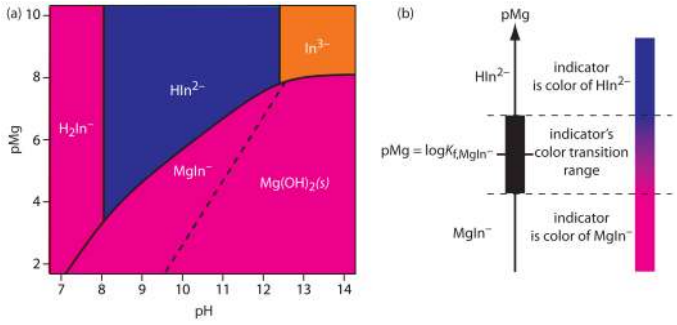


Figure 9.30 (a) Predominance diagram for the metallochromic indicator calmagite showing the most important form and color of calmagite as a function of pH and pMg, where H_2In^-, HIn^{2-}, and In^{3-} are uncomplexed forms of calmagite, and $MgIn^-$ is its complex with Mg^{2+}. Conditions to the right of the dashed line, where Mg^{2+} precipitates as $Mg(OH)_2$, are not analytically useful for a complexation titration. A red to blue end point is possible if we maintain the titrand's pH in the range 8.5–11. (b) Diagram showing the relationship between the concentration of Mg^{2+} (as pMg) and the indicator's color. The ladder diagram defines pMg values where $MgIn^-$ and HIn^- are predominate species. The indicator changes color when pMg is between $\log K_f - 1$ and $\log K_f + 1$.

Table 9.14 provides examples of metallochromic indicators and the metal ions and pH conditions for which they are useful. Even if a suitable indicator does not exist, it is often possible to complete an EDTA titration by introducing a small amount of a secondary metal–EDTA complex, if the secondary metal ion forms a stronger complex with the indicator and a weaker complex with EDTA than the analyte. For example, calmagite gives poor end points when titrating Ca^{2+} with EDTA. Adding a small amount of Mg^{2+}–EDTA to the titrand gives a sharper end point. Because Ca^{2+} forms a stronger complex with EDTA, it displaces Mg^{2+}, which then forms the red-colored Mg^{2+}–calmagite complex. At the titration's end point, EDTA displaces Mg^{2+} from the Mg^{2+}–calmagite complex, signaling the end point by the presence of the uncomplexed indicator's blue form.

Table 9.14 Selected Metallochromic Indicators

Indicator	pH Range	Metal Ions[a]
calmagite	8.5–11	Ba, *Ca*, Mg, Zn
eriochrome Black T	7.5–10.5	Ba, *Ca*, Mg, Zn
eriochrome Blue Black R	8–12	*Ca*, Mg, Zn, Cu
murexide	6–13	Ca, Ni, Cu
PAN	2–11	Cd, Cu, Zn
salicylic acid	2–3	Fe

[a] metal ions in *italic* font have poor end points

Finding the End point by Monitoring Absorbance

> **Note**
>
> Two other methods for finding the end point of a complexation titration are a thermometric titration, in which we monitor the titrand's temperature as we add the titrant, and a potentiometric titration in which we use an ion selective electrode to monitor the metal ion's concentration as we add the titrant. The experimental approach is essentially identical to that described earlier for an acid–base titration, to which you may refer.
>
> See Chapter 11 for more details about ion selective electrodes.

An important limitation when using an indicator is that we must be able to see the indicator's change in color at the end point. This may be difficult if the solution is already colored. For example, when titrating Cu^{2+} with EDTA, ammonia is used to adjust the titrand's pH. The intensely colored $Cu(NH_3)_4^{2+}$ complex obscures the indicator's color, making an accurate determination of the end point difficult. Other absorbing species present within the sample matrix may also interfere. This is often a problem when analyzing clinical samples, such as blood, or environmental samples, such as natural waters.

If at least one species in a complexation titration absorbs electromagnetic radiation, we can identify the end point by monitoring the titrand's absorbance at a carefully selected wavelength. For example, we can identify the end point for a titration of Cu^{2+} with EDTA, in the presence of NH_3 by monitoring the titrand's absorbance at a wavelength of 745 nm, where the $Cu(NH_3)_4^{2+}$ complex absorbs strongly. At the beginning of the titration the absorbance is at a maximum. As we add EDTA, however, the reaction

$$\mathrm{Cu(NH_3)_4^{2+}}(aq) + \mathrm{Y^{4-}}(aq) \rightarrow \mathrm{CuY^{2-}}(aq) + 4\mathrm{NH_3}(aq) \tag{9.3.37}$$

decreases the concentration of $Cu(NH_3)_4^{2+}$ and decreases the absorbance until we reach the equivalence point. After the equivalence point the absorbance remains essentially unchanged. The resulting **spectrophotometric titration curve** is shown in Figure 9.31a. Note that the titration curve's *y*-axis is not the actual absorbance, A, but a corrected absorbance, A_{corr}

$$A_{corr} = A \times \frac{V_{EDTA} + V_{Cu}}{V_{Cu}} \tag{9.3.38}$$

where V_{EDTA} and V_{Cu} are, respectively, the volumes of EDTA and Cu. Correcting the absorbance for the titrand's dilution ensures that the spectrophotometric titration curve consists of linear segments that we can extrapolate to find the end point. Other common spectrophotometric titration curves are shown in Figures 9.31b-f.

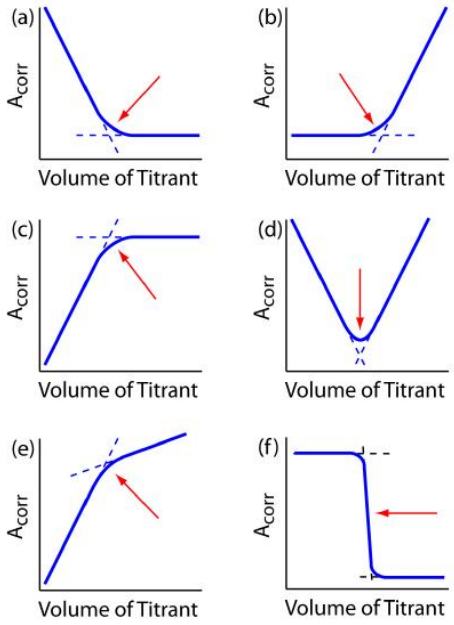


Figure 9.31 Examples of spectrophotometric titration curves: (a) only the titrand absorbs; (b) only the titrant absorbs; (c) only the product of the titration reaction absorbs; (d) both the titrand and the titrant absorb; (e) both the titration reaction's product and the titrant absorb; (f) only the indicator absorbs. The red arrows indicate the end points for each titration curve.

Note

The best way to appreciate the theoretical and practical details discussed in this section is to carefully examine a typical complexation titrimetric method. Although each method is unique, the following description of the determination of the hardness of water provides an instructive example of a typical procedure. The description here is based on Method 2340C as published in *Standard Methods for the Examination of Water and Wastewater*, 20th Ed., American Public Health Association: Washington, D. C., 1998.

Representative Method 9.2

Determination of Hardness of Water and Wastewater

Description of the Method

The operational definition of water hardness is the total concentration of cations in a sample capable of forming insoluble complexes with soap. Although most divalent and trivalent metal ions contribute to hardness, the most important are Ca^{2+} and Mg^{2+}. Hardness is determined by titrating with EDTA at a buffered pH of 10. Calmagite is used as an indicator. Hardness is reported as mg $CaCO_3$/L.

Procedure

Select a volume of sample requiring less than 15 mL of titrant to keep the analysis time under 5 minutes and, if necessary, dilute the sample to 50 mL with distilled water. Adjust the sample's pH by adding 1–2 mL of a pH 10 buffer containing a small amount of Mg^{2+}–EDTA. Add 1–2 drops of indicator and titrate with a standard solution of EDTA until the red-to-blue end point is reached (Figure 9.32).

Questions

1. Why is the sample buffered to a pH of 10? What problems might you expect at a higher pH or a lower pH?

Of the cations contributing to hardness, Mg^{2+} forms the weakest complex with EDTA and is the last cation to be titrated. Calmagite is a useful indicator because it gives a distinct end point when titrating Mg^{2+}. Because of calmagite's acid–base properties, the range of pMg values over which the indicator changes color is pH–dependent (Figure 9.30). Figure 9.33 shows the titration curve for a 50-mL solution of 10^{-3} M Mg^{2+} with 10^{-2} M EDTA at pHs of 9, 10, and 11. Superimposed on each titration curve is the range of conditions for which the average analyst will observe the end point. At a pH of 9 an early end point is possible, leading to a negative determinate error. A late end point and a positive determinate error are possible if we use a pH of 11.

2. Why is a small amount of the Mg^{2+}–EDTA complex added to the buffer?

The titration's end point is signaled by the indicator calmagite. The indicator's end point with Mg^{2+} is distinct, but its change in color when titrating Ca^{2+} does not provide a good end point. If the sample does not contain any Mg^{2+} as a source of hardness, then the titration's end point is poorly defined, leading to inaccurate and imprecise results.

Adding a small amount of Mg^{2+}–EDTA to the buffer ensures that the titrand includes at least some Mg^{2+}. Because Ca^{2+} forms a stronger complex with EDTA, it displaces Mg^{2+} from the Mg^{2+}–EDTA complex, freeing the Mg^{2+} to bind with the indicator. This displacement is stoichiometric, so the total concentration of hardness cations remains unchanged. The displacement by EDTA of Mg^{2+} from the Mg^{2+}–indicator complex signals the titration's end point.

3. Why does the procedure specify that the titration take no longer than 5 minutes?

A time limitation suggests that there is a kinetically controlled interference, possibly arising from a competing chemical reaction. In this case the interference is the possible precipitation of $CaCO_3$ at a pH of 10.

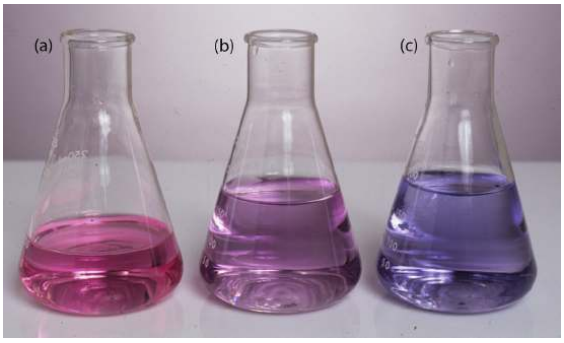


Figure 9.32 End point for the titration of hardness with EDTA using calmagite as an indicator; the indicator is: (a) red prior to the end point due to the presence of the Mg^{2+}–indicator complex; (b) purple at the titration's end point; and (c) blue after the end point due to the presence of uncomplexed indicator.

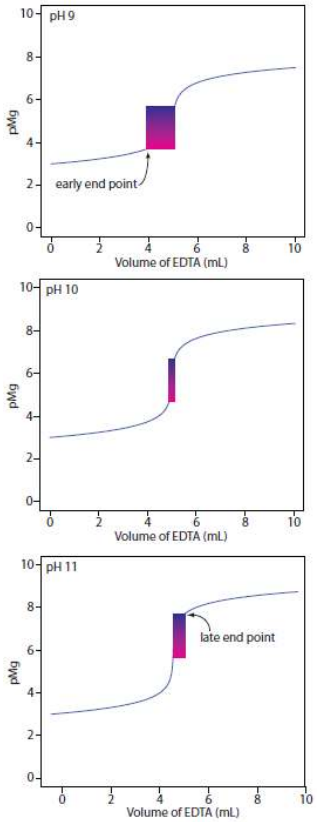


Figure 9.33 Titration curves for 50 mL of 10^{-3} M Mg^{2+} with 10^{-3} M EDTA at pHs 9, 10, and 11 using calmagite as an indicator. The range of pMg and volume of EDTA over which the indicator changes color is shown for each titration curve.

9.3.4 Quantitative Applications

Although many quantitative applications of complexation titrimetry have been replaced by other analytical methods, a few important applications continue to be relevant. In the section we review the general application of complexation titrimetry with an emphasis on applications from the analysis of water and wastewater. First, however, we discuss the selection and standardization of complexation titrants.

Selection and Standardization of Titrants

EDTA is a versatile titrant that can be used to analyze virtually all metal ions. Although EDTA is the usual titrant when the titrand is a metal ion, it cannot be used to titrate anions. In the later case, Ag^{+} or Hg^{2+} are suitable titrants.

Solutions of EDTA are prepared from its soluble disodium salt, $Na_2H_2Y•2H_2O$ and standardized by titrating against a solution made from the primary standard $CaCO_3$. Solutions of Ag^+ and Hg^{2+} are prepared using $AgNO_3$ and $Hg(NO_3)_2$, both of which are secondary standards. Standardization is accomplished by titrating against a solution prepared from primary standard grade NaCl.

Inorganic Analysis

Complexation titrimetry continues to be listed as a standard method for the determination of hardness, Ca^{2+}, CN^-, and Cl^- in waters and wastewaters. The evaluation of hardness was described earlier in Representative Method 9.2. The determination of Ca^{2+} is complicated by the presence of Mg^{2+}, which also reacts with EDTA. To prevent an interference the pH is adjusted to 12–13, precipitating Mg^{2+} as $Mg(OH)_2$. Titrating with EDTA using murexide or Eriochrome Blue Black R as the indicator gives the concentration of Ca^{2+}.

Cyanide is determined at concentrations greater than 1 mg/L by making the sample alkaline with NaOH and titrating with a standard solution of $AgNO_3$, forming the soluble $Ag(CN)_2^-$ complex. The end point is determined using *p*-dimethylaminobenzalrhodamine as an indicator, with the solution turning from a yellow to a salmon color in the presence of excess Ag^+.

Chloride is determined by titrating with $Hg(NO_3)_2$, forming $HgCl_2(aq)$. The sample is acidified to a pH of 2.3–3.8 and diphenylcarbazone, which forms a colored complex with excess Hg^{2+}, serves as the indicator. A pH indicator—xylene cyanol FF—is added to ensure that the pH is within the desired range. The initial solution is a greenish blue, and the titration is carried out to a purple end point.

Quantitative Calculations

The quantitative relationship between the titrand and the titrant is determined by the stoichiometry of the titration reaction. For a titration using EDTA, the stoichiometry is always 1:1.

Example 9.7

The concentration of a solution of EDTA was determined by standardizing against a solution of Ca^{2+} prepared using a primary standard of $CaCO_3$. A 0.4071-g sample of $CaCO_3$ was transferred to a 500-mL volumetric flask, dissolved using a minimum of 6 M HCl, and diluted to volume. After transferring a 50.00-mL portion of this solution to a 250-mL Erlenmeyer flask, the pH was adjusted by adding 5 mL of a pH 10 NH_3–NH_4Cl buffer containing a small amount of Mg^{2+}–EDTA. After adding calmagite as an indicator, the solution was titrated with the EDTA, requiring 42.63 mL to reach the end point. Report the molar concentration of EDTA in the titrant.

(Note that in this example, the analyte is the titrant.)

Solution

The primary standard of Ca^{2+} has a concentration of

$$\frac{0.4071\ \text{g}\ CaCO_3}{0.5000\ \text{L}} \times \frac{1\ \text{mol}\ Ca^{2+}}{100.09\ \text{g}\ CaCO_3} = 8.135 \times 10^{-3}\ \text{M}\ Ca^{2+} \tag{9.3.39}$$

The moles of Ca^{2+} in the titrand is

$$8.135 \times 10^{-3}\ \text{M}\ Ca^{2+} \times 0.05000\ \text{L}\ Ca^{2+} = 4.068 \times 10^{-4}\ \text{mol}\ Ca^{2+} \tag{9.3.40}$$

which means that 4.068×10^{-4} moles of EDTA are used in the titration. The molarity of EDTA in the titrant is

$$\frac{4.068 \times 10^{-4}\ \text{mol EDTA}}{0.04263\ \text{L EDTA}} = 9.543 \times 10^{-3}\ \text{M EDTA} \tag{9.3.41}$$

Practice Exercise 9.14

A 100.0-mL sample is analyzed for hardness using the procedure outlined in Representative Method 9.2, requiring 23.63 mL of 0.0109 M EDTA. Report the sample's hardness as mg $CaCO_3$/L.

Click here to review your answer to this exercise.

As shown in the following example, we can easily extended this calculation to complexation reactions using other titrants.

Example 9.8

The concentration of Cl^- in a 100.0-mL sample of water from a freshwater aquifer was tested for the encroachment of sea water by titrating with 0.0516 M $Hg(NO_3)_2$. The sample was acidified and titrated to the diphenylcarbazone end point, requiring 6.18 mL of the titrant. Report the concentration of Cl^-, in mg/L, in the aquifer.

Solution

The reaction between Cl^- and Hg^{2+} produces a metal–ligand complex of $HgCl_2(aq)$. Each mole of Hg^{2+} reacts with 2 moles of Cl^-; thus

$$\frac{0.0516 \text{ mol } Hg(NO_3)_2}{\text{L}} \times 0.00618 \text{ L } Hg(NO_3)_2 \times \frac{2 \text{ mol } Cl^-}{\text{mol } Hg(NO_3)_2} \times \frac{35.453 \text{ g } Cl^-}{\text{mol } Cl^-} = 0.0226 \text{ g } Cl^- \quad (9.3.42)$$

are in the sample. The concentration of Cl^- in the sample is

$$\frac{0.0226 \text{ g } Cl^-}{0.1000 \text{ L}} \times \frac{1000 \text{ mg}}{\text{g}} = 226 \text{ mg/L} \quad (9.3.43)$$

Practice Exercise 9.15

A 0.4482-g sample of impure NaCN is titrated with 0.1018 M $AgNO_3$, requiring 39.68 mL to reach the end point. Report the purity of the sample as %w/w NaCN.

Click here to review your answer to this exercise.

Finally, complex titrations involving multiple analytes or back titrations are possible.

Example 9.9

An alloy of chromel containing Ni, Fe, and Cr was analyzed by a complexation titration using EDTA as the titrant. A 0.7176-g sample of the alloy was dissolved in HNO_3 and diluted to 250 mL in a volumetric flask. A 50.00-mL aliquot of the sample, treated with pyrophosphate to mask the Fe and Cr, required 26.14 mL of 0.05831 M EDTA to reach the murexide end point. A second 50.00-mL aliquot was treated with hexamethylenetetramine to mask the Cr. Titrating with 0.05831 M EDTA required 35.43 mL to reach the murexide end point. Finally, a third 50.00-mL aliquot was treated with 50.00 mL of 0.05831 M EDTA, and back titrated to the murexide end point with 6.21 mL of 0.06316 M Cu^{2+}. Report the weight percents of Ni, Fe, and Cr in the alloy.

Solution

The stoichiometry between EDTA and each metal ion is 1:1. For each of the three titrations, therefore, we can easily equate the moles of EDTA to the moles of metal ions that are titrated.

Titration 1: moles Ni = moles EDTA

Titration 2: moles Ni + moles Fe = moles EDTA

Titration 3: moles Ni + moles Fe + moles Cr + moles Cu = moles EDTA

We can use the first titration to determine the moles of Ni in our 50.00-mL portion of the dissolved alloy. The titration uses

$$\frac{0.05831 \text{ mol EDTA}}{\text{L}} \times 0.02614 \text{ L EDTA} = 1.524 \times 10^{-3} \text{ mol EDTA} \quad (9.3.44)$$

which means the sample contains 1.524×10^{-3} mol Ni.

Having determined the moles of EDTA reacting with Ni, we can use the second titration to determine the amount of Fe in the sample. The second titration uses

$$\frac{0.05831 \text{ mol EDTA}}{\text{L}} \times 0.03543 \text{ L EDTA} = 2.066 \times 10^{-3} \text{ mol EDTA} \quad (9.3.45)$$

of which 1.524×10^{-3} mol are used to titrate Ni. This leaves 5.42×10^{-4} mol of EDTA to react with Fe; thus, the sample contains 5.42×10^{-4} mol of Fe.

Finally, we can use the third titration to determine the amount of Cr in the alloy. The third titration uses

$$\frac{0.05831 \text{ mol EDTA}}{\text{L}} \times 0.05000 \text{ L EDTA} = 2.916 \times 10^{-3} \text{ mol EDTA} \tag{9.3.46}$$

of which 1.524×10^{-3} mol are used to titrate Ni and 5.42×10^{-4} mol are used to titrate Fe. This leaves 8.50×10^{-4} mol of EDTA to react with Cu and Cr. The amount of EDTA reacting with Cu is

$$\frac{0.06316 \text{ mol } Cu^{2+}}{\text{L}} \times 0.00621 \text{ L } Cu^{2+} \times \frac{1 \text{ mol EDTA}}{\text{mol } Cu^{2+}} = 3.92 \times 10^{-4} \text{ mol EDTA} \tag{9.3.47}$$

leaving 4.58×10^{-4} mol of EDTA to react with Cr. The sample, therefore, contains 4.58×10^{-4} mol of Cr.

Having determined the moles of Ni, Fe, and Cr in a 50.00-mL portion of the dissolved alloy, we can calculate the %w/w of each analyte in the alloy.

$$\frac{1.524 \times 10^{-3} \text{ mol Ni}}{50.00 \text{ mL}} \times 250.0 \text{ mL} \times \frac{58.69 \text{ g Ni}}{\text{mol Ni}} = 0.4472 \text{ g Ni} \tag{9.3.48}$$

$$\frac{0.4472 \text{ g Ni}}{0.7176 \text{ g sample}} \times 100 = 62.32\% \text{ w/w Ni} \tag{9.3.49}$$

$$\frac{5.42 \times 10^{-4} \text{ mol Fe}}{50.00 \text{ mL}} \times 250.0 \text{ mL} \times \frac{55.847 \text{ g Fe}}{\text{mol Fe}} = 0.151 \text{ g Fe} \tag{9.3.50}$$

$$\frac{0.151 \text{ g Fe}}{0.7176 \text{ g sample}} \times 100 = 21.0\% \text{ w/w Fe} \tag{9.3.51}$$

$$\frac{4.58 \times 10^{-4} \text{ mol Cr}}{50.00 \text{ mL}} \times 250.0 \text{ mL} \times \frac{51.996 \text{ g Cr}}{\text{mol Cr}} = 0.119 \text{ g Cr} \tag{9.3.52}$$

$$\frac{0.119 \text{ g Cr}}{0.7176 \text{ g sample}} \times 100 = 16.6\% \text{ w/w Fe} \tag{9.3.53}$$

Practice Exercise 9.16

A indirect complexation titration with EDTA can be used to determine the concentration of sulfate, SO_4^{2-}, in a sample. A 0.1557-g sample is dissolved in water, any sulfate present is precipitated as $BaSO_4$ by adding $Ba(NO_3)_2$. After filtering and rinsing the precipitate, it is dissolved in 25.00 mL of 0.02011 M EDTA. The excess EDTA is then titrated with 0.01113 M Mg^{2+}, requiring 4.23 mL to reach the end point. Calculate the %w/w Na_2SO_4 in the sample.

Click here to review your answer to this exercise.

9.3.5 Evaluation of Complexation Titrimetry

The scale of operations, accuracy, precision, sensitivity, time, and cost of a complexation titration are similar to those described earlier for acid–base titrations. Complexation titrations, however, are more selective. Although EDTA forms strong complexes with most metal ion, by carefully controlling the titrand's pH we can analyze samples containing two or more analytes. The reason we can use pH to provide selectivity is shown in Figure 9.34a. A titration of Ca^{2+} at a pH of 9 gives a distinct break in the titration curve because the conditional formation constant for CaY^{2-} of 2.6×10^9 is large enough to ensure that the reaction of Ca^{2+} and EDTA goes to completion. At a pH of 3, however, the conditional formation constant of 1.23 is so small that very little Ca^{2+} reacts with the EDTA.

Suppose we need to analyze a mixture of Ni^{2+} and Ca^{2+}. Both analytes react with EDTA, but their conditional formation constants differ significantly. If we adjust the pH to 3 we can titrate Ni^{2+} with EDTA without titrating Ca^{2+} (Figure 9.34b). When the titration is complete, we adjust the titrand's pH to 9 and titrate the Ca^{2+} with EDTA.

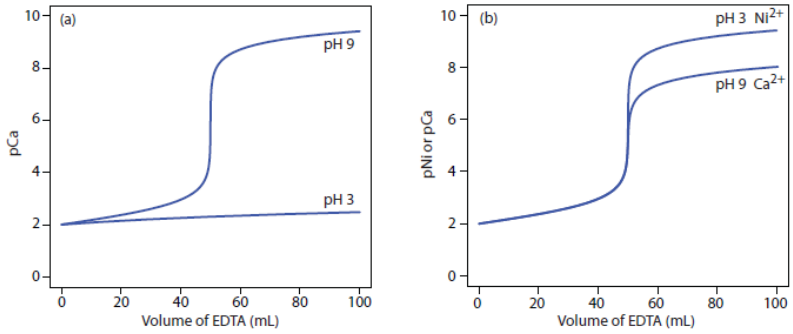


Figure 9.34 Titration curves illustrating how we can use the titrand's pH to control EDTA's selectivity. (a) Titration of 50.0 mL of 0.010 M Ca^{2+} at a pH of 3 and a pH of 9 using 0.010 M EDTA. At a pH of 3 the CaY^{2-} complex is too weak to successfully titrate. (b) Titration of a 50.0 mL mixture of 0.010 M Ca^{2+} and 0.010 M Ni^{2+} at a pH of 3 and a pH of 9 using 0.010 M EDTA. At a pH of 3 EDTA reacts only with Ni^{2+}. When the titration is complete, raising the pH to 9 allows for the titration of Ca^{2+}.

A spectrophotometric titration is a particularly useful approach for analyzing a mixture of analytes. For example, as shown in Figure 9.35, we can determine the concentration of a two metal ions if there is a difference between the absorbance of the two metal-ligand complexes.

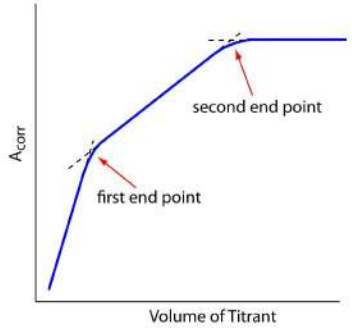


Figure 9.35 Spectrophotometric titration curve for the complexation titration of a mixture of two analytes. The red arrows indicate the end points for each analyte.

Contributors

David Harvey (DePauw University)

9.3: Complexation Titrations is shared under a CC BY-NC-SA 4.0 license and was authored, remixed, and/or curated by LibreTexts.

9.4: Redox Titrations

Analytical titrations using redox reactions were introduced shortly after the development of acid–base titrimetry. The earliest **Redox titration** took advantage of the oxidizing power of chlorine. In 1787, Claude Berthollet introduced a method for the quantitative analysis of chlorine water (a mixture of Cl_2, HCl, and HOCl) based on its ability to oxidize indigo, a dye that is colorless in its oxidized state. In 1814, Joseph Gay-Lussac developed a similar method for determining chlorine in bleaching powder. In both methods the end point is a change in color. Before the equivalence point the solution is colorless due to the oxidation of indigo. After the equivalence point, however, unreacted indigo imparts a permanent color to the solution.

The number of redox titrimetric methods increased in the mid-1800s with the introduction of MnO_4^-, $Cr_2O_7^{2-}$, and I_2 as oxidizing titrants, and of Fe^{2+} and $S_2O_3^{2-}$ as reducing titrants. Even with the availability of these new titrants, redox titrimetry was slow to develop due to the lack of suitable indicators. A titrant can serve as its own indicator if its oxidized and reduced forms differ significantly in color. For example, the intensely purple MnO_4^- ion serves as its own indicator since its reduced form, Mn^{2+}, is almost colorless. Other titrants require a separate indicator. The first such indicator, diphenylamine, was introduced in the 1920s. Other redox indicators soon followed, increasing the applicability of redox titrimetry.

9.4.1 Redox Titration Curves

To evaluate a redox titration we need to know the shape of its titration curve. In an acid–base titration or a complexation titration, the titration curve shows how the concentration of H_3O^+ (as pH) or M^{n+} (as pM) changes as we add titrant. For a redox titration it is convenient to monitor the titration reaction's potential instead of the concentration of one species.

You may recall from Chapter 6 that the Nernst equation relates a solution's potential to the concentrations of reactants and products participating in the redox reaction. Consider, for example, a titration in which a titrand in a reduced state, A_{red}, reacts with a titrant in an oxidized state, B_{ox}.

$$A_{red} + B_{ox} \rightleftharpoons B_{red} + A_{ox} \tag{9.4.1}$$

where A_{ox} is the titrand's oxidized form, and B_{red} is the titrant's reduced form. The reaction's potential, E_{rxn}, is the difference between the reduction potentials for each half-reaction.

$$E_{rxn} = E_{B_{ox}/B_{red}} - E_{A_{ox}/A_{red}} \tag{9.4.2}$$

After each addition of titrant the reaction between the titrand and the titrant reaches a state of equilibrium. Because the potential at equilibrium is zero, the titrand's and the titrant's reduction potentials are identical.

$$E_{B_{ox}/B_{red}} = E_{A_{ox}/A_{red}} \tag{9.4.3}$$

This is an important observation because we can use either half-reaction to monitor the titration's progress.

Before the equivalence point the titration mixture consists of appreciable quantities of the titrand's oxidized and reduced forms. The concentration of unreacted titrant, however, is very small. The potential, therefore, is easier to calculate if we use the Nernst equation for the titrand's half-reaction

$$E_{rxn} = E^o_{A_{ox}/A_{red}} - \frac{RT}{nF} \ln \frac{[A_{red}]}{[A_{ox}]} \tag{9.4.4}$$

> **Note**
>
> Although the Nernst equation is written in terms of the half-reaction's standard state potential, a matrix-dependent **formal potential** often is used in its place. See Appendix 13 for the standard state potentials and formal potentials for selected half-reactions.

After the equivalence point it is easier to calculate the potential using the Nernst equation for the titrant's half-reaction.

$$E_{rxn} = E^o_{B_{ox}/B_{red}} - \frac{RT}{nF} \ln \frac{[B_{red}]}{[B_{ox}]} \tag{9.4.5}$$

Calculating the Titration Curve

Let's calculate the titration curve for the titration of 50.0 mL of 0.100 M Fe^{2+} with 0.100 M Ce^{4+} in a matrix of 1 M $HClO_4$. The reaction in this case is

$$Fe^{2+}(aq) + Ce^{4+}(aq) \rightleftharpoons Ce^{3+}(aq) + Fe^{3+}(aq) \tag{9.15}$$

Note

In 1 M $HClO_4$, the formal potential for the reduction of Fe^{3+} to Fe^{2+} is +0.767 V, and the formal potential for the reduction of Ce^{4+} to Ce^{3+} is +1.70 V.

Because the equilibrium constant for reaction 9.15 is very large—it is approximately 6×10^{15}—we may assume that the analyte and titrant react completely.

Note

Step 1: Calculate the volume of titrant needed to reach the equivalence point.

The first task is to calculate the volume of Ce^{4+} needed to reach the titration's equivalence point. From the reaction's stoichiometry we know that

$$\text{moles } Fe^{2+} = \text{moles } Ce^{4+} \tag{9.4.6}$$

$$M_{Fe} \times V_{Fe} = M_{Ce} \times V_{Ce} \tag{9.4.7}$$

Solving for the volume of Ce^{4+} gives the equivalence point volume as

$$V_{eq} = V_{Ce} = \frac{M_{Fe}V_{Fe}}{M_{Ce}} = \frac{(0.100\text{ M})(50.0\text{ mL})}{(0.100\text{ M})} = 50.0\text{ mL} \tag{9.4.8}$$

Note

Step 2: Calculate the potential before the equivalence point by determining the concentrations of the titrand's oxidized and reduced forms, and using the Nernst equation for the titrand's reduction half-reaction.

Before the equivalence point, the concentration of unreacted Fe^{2+} and the concentration of Fe^{3+} are easy to calculate. For this reason we find the potential using the Nernst equation for the Fe^{3+}/Fe^{2+} half-reaction.

$$E = E^o_{Fe^{3+}/Fe^{2+}} - \frac{RT}{nF}\log\frac{[Fe^{2+}]}{[Fe^{3+}]} = +0.767\text{V} - 0.05916\log\frac{[Fe^{2+}]}{[Fe^{3+}]} \tag{9.16}$$

For example, the concentrations of Fe^{2+} and Fe^{3+} after adding 10.0 mL of titrant are

$$[Fe^{2+}] = \frac{\text{initial moles } Fe^{2+} - \text{moles } Ce^{4+} \text{ added}}{\text{total volume}} = \frac{M_{Fe}V_{Fe} - M_{Ce}V_{Ce}}{V_{Fe} + V_{Ce}} \tag{9.4.9}$$

$$= \frac{(0.100\text{ M})(50.0\text{ mL}) - (0.100\text{ M})(10.0\text{ mL})}{50.0\text{ mL} + 10.0\text{ mL}} = 6.67 \times 10^{-2}\text{ M} \tag{9.4.10}$$

$$[Fe^{3+}] = \frac{\text{moles } Ce^{4+} \text{ added}}{\text{total volume}} = \frac{M_{Ce}V_{Ce}}{V_{Fe} + V_{Ce}} \tag{9.4.11}$$

$$= \frac{(0.100\text{ M})(10.0\text{ mL})}{50.0\text{ mL} + 10.0\text{ mL}} = 1.67 \times 10^{-2}\text{ M} \tag{9.4.12}$$

Substituting these concentrations into equation 9.16 gives a potential of

$$E = +0.767\text{ V} - 0.05916\log\frac{6.67 \times 10^{-2}\text{ M}}{1.67 \times 10^{-2}\text{ M}} = +0.731\text{ V} \tag{9.4.13}$$

Note

Step 3: Calculate the potential after the equivalence point by determining the concentrations of the titrant's oxidized and reduced forms, and using the Nernst equation for the titrant's reduction half-reaction.

After the equivalence point, the concentration of Ce^{3+} and the concentration of excess Ce^{4+} are easy to calculate. For this reason we find the potential using the Nernst equation for the Ce^{4+}/Ce^{3+} half-reaction.

$$E = E^o_{Ce^{4+}/Ce^{3+}} - \frac{RT}{nF}\log\frac{[Ce^{3+}]}{[Ce^{4+}]} = +1.70\text{ V} - 0.05916\log\frac{[Ce^{3+}]}{[Ce^{4+}]} \tag{9.17}$$

For example, after adding 60.0 mL of titrant, the concentrations of Ce^{3+} and Ce^{4+} are

$$[Ce^{3+}] = \frac{\text{initial moles } Fe^{2+}}{\text{total volume}} = \frac{M_{Fe}V_{Fe}}{V_{Fe}+V_{Ce}} \tag{9.4.14}$$

$$= \frac{(0.100\text{ M})(50.0\text{ mL})}{50.0\text{ mL} + 60.0\text{ mL}} = 4.55\times10^{-3}\text{ M} \tag{9.4.15}$$

$$[Ce^{4+}] = \frac{\text{moles } Ce^{4+}\text{ added} - \text{initial moles } Fe^{2+}}{\text{total volume}} = \frac{M_{Ce}V_{Ce} - M_{Fe}V_{Fe}}{V_{Fe}+V_{Ce}} \tag{9.4.16}$$

$$= \frac{(0.100\text{ M})(60.0\text{ mL}) - (0.100\text{ M})(50.0\text{ mL})}{50.0\text{ mL} + 60.0\text{ mL}} = 9.09\times10^{-3}\text{ M} \tag{9.4.17}$$

Substituting these concentrations into equation 9.17 gives a potential of

$$E = +1.70\text{ V} - 0.05916\log\frac{4.55\times10^{-2}\text{ M}}{9.09\times10^{-3}\text{ M}} = +1.66\text{ V} \tag{9.4.18}$$

Note

Step 4: Calculate the potential at the equivalence point.

At the titration's equivalence point, the potential, E_{eq}, in equation 9.16 and equation 9.17 are identical. Adding the equations together to gives

$$2E_{eq} = E^o_{Fe^{3+}/Fe^{2+}} + E^o_{Ce^{4+}/Ce^{3+}} - 0.05916\log\frac{[Fe^{2+}][Ce^{3+}]}{[Fe^{3+}][Ce^{4+}]} \tag{9.4.19}$$

Because $[Fe^{2+}] = [Ce^{4+}]$ and $[Ce^{3+}] = [Fe^{3+}]$ at the equivalence point, the log term has a value of zero and the equivalence point's potential is

$$E_{eq} = \frac{E^o_{Fe^{3+}/Fe^{2+}} + E^o_{Ce^{4+}/Ce^{3+}}}{2} = \frac{0.767\text{ V} + 1.70\text{ V}}{2} = 1.23\text{ V} \tag{9.4.20}$$

Additional results for this titration curve are shown in Table 9.15 and Figure 9.36.

Table 9.15 Data for the Titration of 50.0 mL of 0.100 M Fe^{2+} with 0.100 M Ce^{4+}

Volume of Ce^{4+} (mL)	E (V)	Volume Ce^{4+} (mL)	E (V)
10.0	0.731	60.0	1.66
20.0	0.757	70.0	1.68
30.0	0.777	80.0	1.69
40.0	0.803	90.0	1.69
50.0	1.23	100.0	1.70

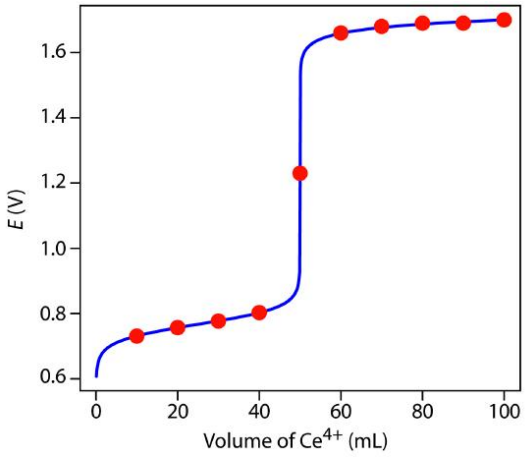


Figure 9.36 Titration curve for the titration of 50.0 mL of 0.100 M Fe^{2+} with 0.100 M Ce^{4+}. The red points correspond to the data in Table 9.15. The blue line shows the complete titration curve.

Practice Exercise 9.17

Calculate the titration curve for the titration of 50.0 mL of 0.0500 M Sn^{2+} with 0.100 M Tl^{3+}. Both the titrand and the titrant are 1.0 M in HCl. The titration reaction is

$$Sn^{2+}(aq) + Tl^{3+}(aq) \rightarrow Sn^{4+}(aq) + Tl^{+}(aq) \tag{9.4.21}$$

Click here to review your answer to this exercise.

Sketching a Redox Titration Curve

To evaluate the relationship between a titration's equivalence point and its end point we need to construct only a reasonable approximation of the exact titration curve. In this section we demonstrate a simple method for sketching a redox titration curve. Our goal is to sketch the titration curve quickly, using as few calculations as possible. Let's use the titration of 50.0 mL of 0.100 M Fe^{2+} with 0.100 M Ce^{4+} in a matrix of 1 M $HClO_4$.

Note

This is the same example that we used in developing the calculations for a redox titration curve. You can review the results of that calculation in Table 9.15 and Figure 9.36.

We begin by calculating the titration's equivalence point volume, which, as we determined earlier, is 50.0 mL. Next, we draw our axes, placing the potential, *E*, on the *y*-axis and the titrant's volume on the *x*-axis. To indicate the equivalence point's volume, we draw a vertical line corresponding to 50.0 mL of Ce^{4+}. Figure 9.37a shows the result of the first step in our sketch.

Before the equivalence point, the potential is determined by a redox buffer of Fe^{2+} and Fe^{3+}. Although we can easily calculate the potential using the Nernst equation, we can avoid this calculation by making a simple assumption. You may recall from Chapter 6 that a redox buffer operates over a range of potentials that extends approximately ±(0.05916/*n*) unit on either side of $E^{o}_{Fe^{3+}/Fe^{2+}}$. The potential is at the buffer's lower limit

$$E = E^{o}_{Fe^{3+}/Fe^{2+}} - 0.05916 \tag{9.4.22}$$

when the concentration of Fe^{2+} is 10× greater than that of Fe^{3+}. The buffer reaches its upper potential

$$E = E^{o}_{Fe^{3+}/Fe^{2+}} + 0.05916 \tag{9.4.23}$$

when the concentration of Fe^{2+} is 10× smaller than that of Fe^{3+}. The redox buffer spans a range of volumes from approximately 10% of the equivalence point volume to approximately 90% of the equivalence point volume.

Figure 9.37b shows the second step in our sketch. First, we superimpose a ladder diagram for Fe^{2+} on the *y*-axis, using its $E^{o}_{Fe^{3+}/Fe^{2+}}$ value of 0.767 V and including the buffer's range of potentials. Next, we add points representing the pH at 10% of the equivalence

point volume (a potential of 0.708 V at 5.0 mL) and at 90% of the equivalence point volume (a potential of 0.826 V at 45.0 mL).

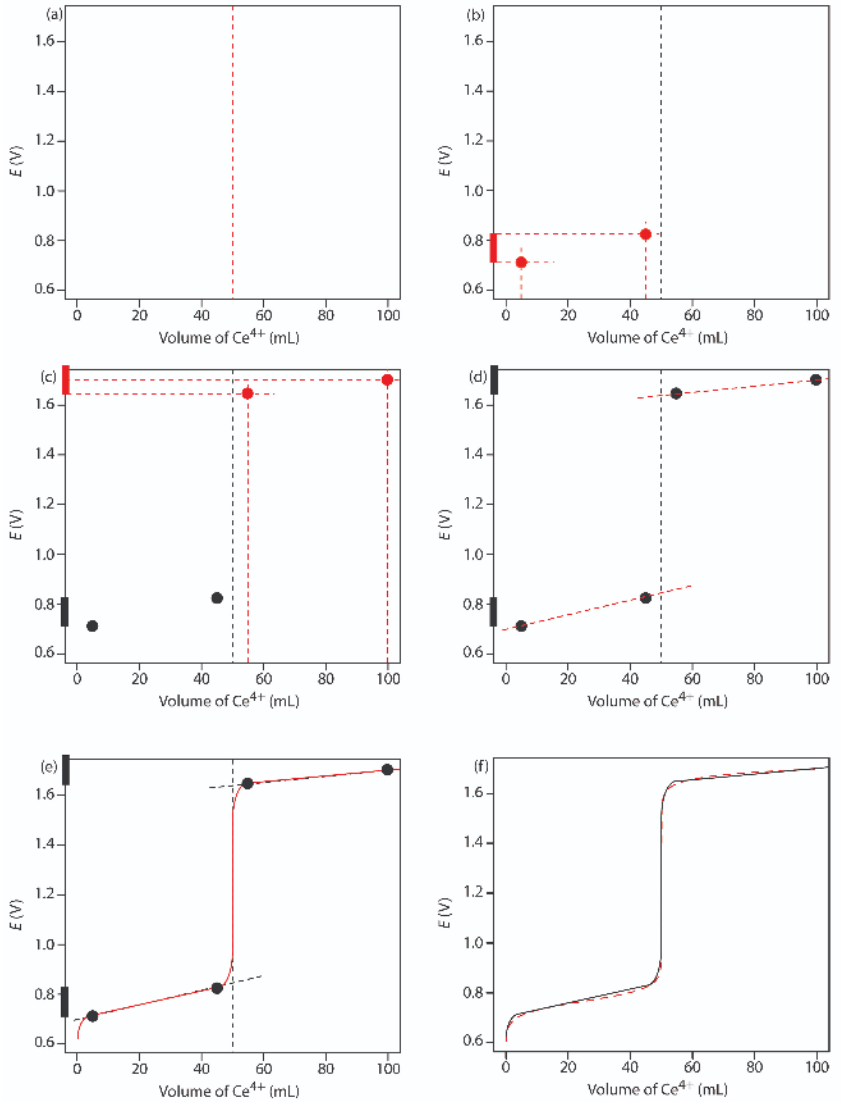
> **Note**
>
> We used a similar approach when sketching the acid–base titration curve for the titration of acetic acid with NaOH.

The third step in sketching our titration curve is to add two points after the equivalence point. Here the potential is controlled by a redox buffer of Ce^{3+} and Ce^{4+}. The redox buffer is at its lower limit of $E = E^{o}_{Ce^{4+}/Ce^{3+}} - 0.05916$ when the titrant reaches 110% of the equivalence point volume and the potential is $E^{o}_{Ce^{4+}/Ce^{3+}}$ when the volume of Ce^{4+} is $2 \times V_{eq}$.

Figure 9.37c shows the third step in our sketch. First, we add a ladder diagram for Ce^{4+}, including its buffer range, using its $E^{o}_{Ce^{4+}/Ce^{3+}}$ value of 1.70 V. Next, we add points representing the potential at 110% of V_{eq} (a value of 1.66 V at 55.0 mL) and at 200% of V_{eq} (a value of 1.70 V at 100.0 mL).

> **Note**
>
> We used a similar approach when sketching the complexation titration curve for the titration of Mg^{2+} with EDTA.

Next, we draw a straight line through each pair of points, extending the line through the vertical line representing the equivalence point's volume (Figure 9.37d). Finally, we complete our sketch by drawing a smooth curve that connects the three straight-line segments (Figure 9.37e). A comparison of our sketch to the exact titration curve (Figure 9.37f) shows that they are in close agreement.



https://chem.libretexts.org/@go/page/70693

Figure 9.37 Illustrations showing the steps in sketching an approximate titration curve for the titration of 50.0 mL of 0.100 M Fe^{2+} with 0.100 M Ce^{4+} in 1 M $HClO_4$: (a) locating the equivalence point volume; (b) plotting two points before the equivalence point; (c) plotting two points after the equivalence point; (d) preliminary approximation of titration curve using straight-lines; (e) final approximation of titration curve using a smooth curve; (f) comparison of approximate titration curve (solid black line) and exact titration curve (dashed red line). See the text for additional details.

Practice Exercise 9.18

Sketch the titration curve for the titration of 50.0 mL of 0.0500 M Sn^{4+} with 0.100 M Tl^{+}. Both the titrand and the titrant are 1.0 M in HCl. The titration reaction is

$$Sn^{2+}(aq) + Tl^{3+}(aq) \rightarrow Sn^{4+}(aq) + Tl^{+}(aq) \tag{9.4.24}$$

Compare your sketch to your calculated titration curve from Practice Exercise 9.17.

Click here to review your answer to this exercise.

9.4.2 Selecting and Evaluating the End point

A redox titration's equivalence point occurs when we react stoichiometrically equivalent amounts of titrand and titrant. As is the case with acid–base and complexation titrations, we estimate the equivalence point of a complexation titration using an experimental end point. A variety of methods are available for locating the end point, including indicators and sensors that respond to a change in the solution conditions.

Where is the Equivalence Point?

For an acid–base titration or a complexometric titration the equivalence point is almost identical to the inflection point on the steeping rising part of the titration curve. If you look back at Figure 9.7 and Figure 9.28, you will see that the inflection point is in the middle of this steep rise in the titration curve, which makes it relatively easy to find the equivalence point when you sketch these titration curves. We call this a **symmetric equivalence point**. If the stoichiometry of a redox titration is symmetric—one mole of titrant reacts with each mole of titrand—then the equivalence point is symmetric. If the titration reaction's stoichiometry is not 1:1, then the equivalence point is closer to the top or to bottom of the titration curve's sharp rise. In this case we have an **asymmetric equivalence point**.

Example 9.10

Derive a general equation for the equivalence point's potential when titrating Fe^{2+} with MnO_4^-.

$$5Fe^{2+}(aq) + MnO_4^-(aq) + 8H^+(aq) \rightarrow 5Fe^{3+}(aq) + Mn^{2+}(aq) + 4H_2O \tag{9.4.25}$$

(We often use H^+ instead of H_3O^+ when writing a redox reaction.)

Solution

The half-reactions for Fe^{2+} and MnO_4^- are

$$Fe^{2+}(aq) \rightarrow Fe^{3+}(aq) + e^- \tag{9.4.26}$$

$$MnO_4^-(aq) + 8H^+(aq) + 5e^- \rightarrow Mn^{2+}(aq) + 4H_2O(l) \tag{9.4.27}$$

for which the Nernst equations are

$$E = E^o_{Fe^{3+}/Fe^{2+}} - 0.05916 \log \frac{[Fe^{2+}]}{[Fe^{3+}]} \tag{9.4.28}$$

$$E = E^o_{MnO_4^-/Mn^{2+}} - \frac{0.05916}{5} \log \frac{[Mn^{2+}]}{[MnO_4^-][H^+]^8} \tag{9.4.29}$$

Before adding these two equations together we must multiply the second equation by 5 so that we can combine the log terms; thus

$$6E = E^o_{Fe^{3+}/Fe^{2+}} + 5E^o_{MnO_4^-/Mn^{2+}} - 0.05916 \log \frac{[Fe^{2+}][Mn^{2+}]}{[Fe^{3+}][MnO_4^-][H^+]^8} \quad (9.4.30)$$

At the equivalence point we know that

$$[Fe^{2+}] = 5 \times [MnO_4^-] \quad (9.4.31)$$

$$[Fe^{3+}] = 5 \times [Mn^{2+}] \quad (9.4.32)$$

Substituting these equalities into the previous equation and rearranging gives us a general equation for the potential at the equivalence point.

$$6E_{eq} = E^o_{Fe^{3+}/Fe^{2+}} + 5E^o_{MnO_4^-/Mn^{2+}} - 0.05916 \log \frac{5[MnO_4^-][Mn^{2+}]}{5[Mn^{2+}][MnO_4^-][H^+]^8} \quad (9.4.33)$$

$$E_{eq} = \frac{E^o_{Fe^{3+}/Fe^{2+}} + 5E^o_{MnO_4^-/Mn^{2+}}}{6} - \frac{0.05916}{6} \log \frac{1}{[H^+]^8} \quad (9.4.34)$$

$$E_{eq} = \frac{E^o_{Fe^{3+}/Fe^{2+}} + 5E^o_{MnO_4^-/Mn^{2+}}}{6} + \frac{0.05916 \times 8}{6} \log[H^+] \quad (9.4.35)$$

$$E_{eq} = \frac{E^o_{Fe^{3+}/Fe^{2+}} + 5E^o_{MnO_4^-/Mn^{2+}}}{6} - 0.07888pH \quad (9.4.36)$$

Our equation for the equivalence point has two terms. The first term is a weighted average of the titrand's and the titrant's standard state potentials, in which the weighting factors are the number of electrons in their respective half-reactions. (Instead of standard state potentials, you can use formal potentials.) The second term shows that E_{eq} for this titration is pH-dependent. At a pH of 1 (in H_2SO_4), for example, the equivalence point has a potential of

$$E_{eq} = \frac{0.768 + 5 \times 1.51}{6} - 0.07888 \times 1 = 1.31 \text{ V} \quad (9.4.37)$$

Figure 9.38 shows a typical titration curve for titration of Fe^{2+} with MnO_4^-. Note that the titration's equivalence point is asymmetrical.

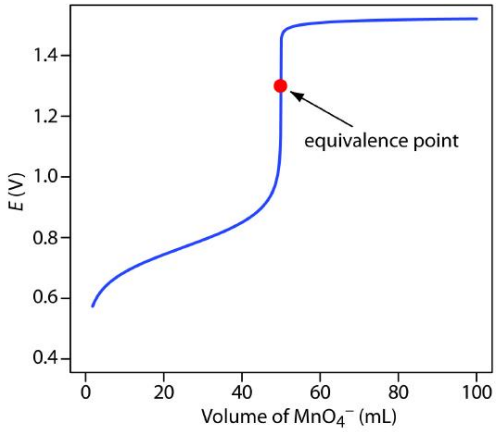


Figure 9.38 Titration curve for the titration of 50.0 mL of 0.100 M Fe^{2+} with 0.0200 M MnO_4^- at a fixed pH of 1 (using H_2SO_4). The equivalence point is shown by the red dot.

Exercise 9.19

Derive a general equation for the equivalence point's potential for the titration of U^{4+} with Ce^{4+}. The unbalanced reaction is

$$Ce^{4+}(aq) + U^{4+}(aq) \rightarrow UO_2^{2+}(aq) + Ce^{3+}(aq) \quad (9.4.38)$$

What is the equivalence point's potential if the pH is 1?

Click here to review your answer to this exercise.

Finding the End point with an Indicator

Three types of indicators are used to signal a redox titration's end point. The oxidized and reduced forms of some titrants, such as MnO_4^-, have different colors. A solution of MnO_4^- is intensely purple. In an acidic solution, however, permanganate's reduced form, Mn^{2+}, is nearly colorless. When using MnO_4^- as a titrant, the titrand's solution remains colorless until the equivalence point. The first drop of excess MnO_4^- produces a permanent tinge of purple, signaling the end point.

Some indicators form a colored compound with a specific oxidized or reduced form of the titrant or the titrand. Starch, for example, forms a dark blue complex with I_3^-. We can use this distinct color to signal the presence of excess I_3^- as a titrant—a change in color from colorless to blue—or the completion of a reaction consuming I_3^- as the titrand—a change in color from blue to colorless. Another example of a specific indicator is thiocyanate, SCN^-, which forms a soluble red-colored complex of $Fe(SCN)^{2+}$ with Fe^{3+}.

The most important class of indicators are substances that do not participate in the redox titration, but whose oxidized and reduced forms differ in color. When we add a **redox indicator** to the titrand, the indicator imparts a color that depends on the solution's potential. As the solution's potential changes with the addition of titrant, the indicator changes oxidation state and changes color, signaling the end point.

To understand the relationship between potential and an indicator's color, consider its reduction half-reaction

$$\mathrm{In_{ox}} + ne^- \rightleftharpoons \mathrm{In_{red}} \tag{9.4.39}$$

where In_{ox} and In_{red} are, respectively, the indicator's oxidized and reduced forms.

Note

For simplicity, In_{ox} and In_{red} are shown without specific charges. Because there is a change in oxidation state, In_{ox} and In_{red} cannot both be neutral.

The Nernst equation for this half-reaction is

$$E = E^o_{\mathrm{In_{ox}/In_{red}}} - \frac{0.05916}{n} \log \frac{[\mathrm{In_{red}}]}{[\mathrm{In_{ox}}]} \tag{9.4.40}$$

As shown in Figure 9.39, if we assume that the indicator's color changes from that of In_{ox} to that of In_{red} when the ratio $[In_{red}]/[In_{ox}]$ changes from 0.1 to 10, then the end point occurs when the solution's potential is within the range

$$E = E^o_{\mathrm{In_{ox}/In_{red}}} \pm \frac{0.05916}{n} \tag{9.4.41}$$

Note

This is the same approach we took in considering acid–base indicators and complexation indicators.

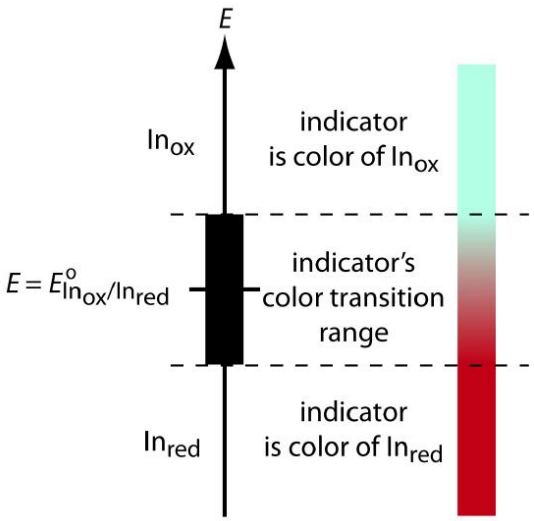


Figure 9.39 Diagram showing the relationship between E and an indicator's color. The ladder diagram defines potentials where In_{red} and In_{ox} are the predominate species. The indicator changes color when E is within the range

$$E = E^{o}_{Inox/Inred} \pm 0.05916/n$$

A partial list of redox indicators is shown in Table 9.16. Examples of appropriate and inappropriate indicators for the titration of Fe^{2+} with Ce^{4+} are shown in Figure 9.40.

Table 9.16 Selected Examples of Redox Indicators

Indicator	Color of In_{ox}	Color of In_{red}	$E^{o}_{Inox/Inred}$
indigo tetrasulfate	blue	colorless	0.36
methylene blue	blue	colorless	0.53
diphenylamine	violet	colorless	0.75
diphenylamine sulfonic acid	red-violet	colorless	0.85
tris(2,2´-bipyridine)iron	pale blue	red	1.120
ferroin	pale blue	red	1.147
tris(5-nitro-1,10-phenanthroline)iron	pale blue	red-violet	1.25

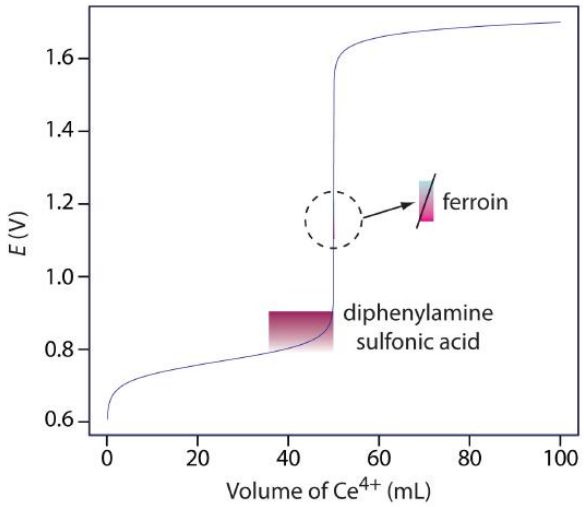


Figure 9.40 Titration curve for the titration of 50.0 mL of 0.100 M Fe^{2+} with 0.100 M Ce^{4+}. The end point transitions for the indicators diphenylamine sulfonic acid and ferroin are superimposed on the titration curve. Because the transition for ferroin is too small to see on the scale of the *x*-axis—it requires only 1–2 drops of titrant—the color change is expanded to the right.

Other Methods for Finding the End point

Another method for locating a redox titration's end point is a potentiometric titration in which we monitor the change in potential while adding the titrant to the titrand. The end point is found by visually examining the titration curve. The simplest experimental design for a potentiometric titration consists of a Pt indicator electrode whose potential is governed by the titrand's or titrant's redox half-reaction, and a reference electrode that has a fixed potential. A further discussion of potentiometry is found in Chapter 11. Other methods for locating the titration's end point include thermometric titrations and spectrophotometric titrations.

Note

The best way to appreciate the theoretical and practical details discussed in this section is to carefully examine a typical redox titrimetric method. Although each method is unique, the following description of the determination of the total chlorine residual in water provides an instructive example of a typical procedure. The description here is based on Method 4500-Cl B as published in *Standard Methods for the Examination of Water and Wastewater*, 20th Ed., American Public Health Association: Washington, D. C., 1998.

Representative Method 9.3

Determination of Total Chlorine Residual

Description of the Method

The chlorination of public water supplies produces several chlorine-containing species, the combined concentration of which is called the total chlorine residual. Chlorine may be present in a variety of states, including the free residual chlorine, consisting of Cl_2, HOCl and OCl^-, and the combined chlorine residual, consisting of NH_2Cl, $NHCl_2$, and NCl_3. The total chlorine residual is determined by using the oxidizing power of chlorine to convert I^- to I_3^-. The amount of I_3^- formed is then determined by titrating with $Na_2S_2O_3$ using starch as an indicator. Regardless of its form, the total chlorine residual is reported as if Cl_2 is the only source of chlorine, and is reported as mg Cl/L.

Procedure

Select a volume of sample requiring less than 20 mL of $Na_2S_2O_3$ to reach the end point. Using glacial acetic acid, acidify the sample to a pH of 3–4, and add about 1 gram of KI. Titrate with $Na_2S_2O_3$ until the yellow color of I_3^- begins to disappear. Add 1 mL of a starch indicator solution and continue titrating until the blue color of the starch–I_3^- complex disappears (Figure 9.41). Use a blank titration to correct the volume of titrant needed to reach the end point for reagent impurities.

Questions

1. Is this an example of a direct or an indirect analysis?

This is an indirect analysis because the chlorine-containing species do not react with the titrant. Instead, the total chlorine residual oxidizes I^- to I_3^-, and the amount of I_3^- is determined by titrating with $Na_2S_2O_3$.

2. Why does the procedure rely on an indirect analysis instead of directly titrating the chlorine-containing species using KI as a titrant?

Because the total chlorine residual consists of six different species, a titration with I^- does not have a single, well-defined equivalence point. By converting the chlorine residual to an equivalent amount of I_3^-, the indirect titration with $Na_2S_2O_3$ has a single, useful equivalence point.

Even if the total chlorine residual is from a single species, such as HOCl, a direct titration with KI is impractical. Because the product of the titration, I_3^-, imparts a yellow color, the titrand's color would change with each addition of titrant, making it difficult to find a suitable indicator.

3. Both oxidizing and reducing agents can interfere with this analysis. Explain the effect of each type of interferent has on the total chlorine residual.

An interferent that is an oxidizing agent converts additional I^- to I_3^-. Because this extra I_3^- requires an additional volume of $Na_2S_2O_3$ to reach the end point, we overestimate the total chlorine residual. If the interferent is a reducing agent, it reduces back to I^- some of the I_3^- produced by the reaction between the total chlorine residual and iodide. As a result. we underestimate the total chlorine residual.



Figure 9.41 Endpoint for the determination of the total chlorine residual. (a) Acidifying the sample and adding KI forms a brown solution of I_3^-. (b) Titrating with $Na_2S_2O_3$ converts I_3^- to I^- with the solution fading to a pale yellow color as we approach the end point. (c) Adding starch forms the deep purple starch–I_3^- complex. (d) As the titration continues, the end point is a sharp transition from a purple to a colorless solution. The change in color from (c) to (d) typically takes 1–2 drops of titrant.

9.4.3 Quantitative Applications

Although many quantitative applications of redox titrimetry have been replaced by other analytical methods, a few important applications continue to be relevant. In this section we review the general application of redox titrimetry with an emphasis on environmental, pharmaceutical, and industrial applications. We begin, however, with a brief discussion of selecting and characterizing redox titrants, and methods for controlling the titrand's oxidation state.

Adjusting the Titrand's Oxidation State

If a redox titration is to be used in a quantitative analysis, the titrand must initially be present in a single oxidation state. For example, iron can be determined by a redox titration in which Ce^{4+} oxidizes Fe^{2+} to Fe^{3+}. Depending on the sample and the method of sample preparation, iron may initially be present in both the +2 and +3 oxidation states. Before titrating, we must reduce any Fe^{3+} to Fe^{2+}. This type of pretreatment can be accomplished using an auxiliary reducing agent or oxidizing agent.

A metal that is easy to oxidize—such as Zn, Al, and Ag—can serve as an **auxiliary reducing agent**. The metal, as a coiled wire or powder, is added to the sample where it reduces the titrand. Because any unreacted auxiliary reducing agent will react with the titrant, it must be removed before beginning the titration. This can be accomplished by simply removing the coiled wire, or by filtering.

An alternative method for using an auxiliary reducing agent is to immobilize it in a column. To prepare a reduction column an aqueous slurry of the finally divided metal is packed in a glass tube equipped with a porous plug at the bottom. The sample is placed at the top of the column and moves through the column under the influence of gravity or vacuum suction. The length of the reduction column and the flow rate are selected to ensure the analyte's complete reduction.

Two common reduction columns are used. In the **Jones reductor** the column is filled with amalgamated zinc, Zn(Hg), prepared by briefly placing Zn granules in a solution of $HgCl_2$. Oxidation of zinc

$$\mathbf{Zn(Hg)}(s) \rightarrow \mathbf{Zn^{2+}}(aq) + \mathbf{Hg}(l) + 2e^- \tag{9.4.42}$$

provides the electrons for reducing the titrand. In the **Walden reductor** the column is filled with granular Ag metal. The solution containing the titrand is acidified with HCl and passed through the column where the oxidation of silver

$$\mathbf{Ag}(s) + \mathbf{Cl^-}(aq) \rightarrow \mathbf{AgCl}(s) + e^- \tag{9.4.43}$$

provides the necessary electrons for reducing the titrand. Table 9.17 provides a summary of several applications of reduction columns.

Table 9.17 Examples of Reactions For Reducing a Titrand's Oxidation State Using a Reduction Column

Oxidized Titrand	Walden Reductor	Jones Reductor
Cr^{3+}	—	$Cr^{3+}(aq) + e^- \rightarrow Cr^{2+}(aq)$
Cu^{2+}	$Cu^{2+}(aq) + e^- \rightarrow Cu^{+}(aq)$	$Cu^{2+}(aq) + 2e^- \rightarrow Cr(s)$
Fe^{3+}	$Fe^{3+}(aq) + e^- \rightarrow Fe^{2+}(aq)$	$Fe^{3+}(aq) + e^- \rightarrow Fe^{2+}(aq)$
TiO^{2+}	—	$TiO^{2+}(aq) + 2H^{+}(aq) + e^- \rightarrow Ti^{3+}(aq) + H_2O(l)$
MoO_2^{2+}	$MoO_2^{2+}(aq) + e^- \rightarrow MoO_2^{+}(aq)$	$MoO_2^{2+}(aq) + 4H^{+}(aq) + 3e^- \rightarrow Mo^{3+}(aq) + 2H_2O(l)$
VO_2^{+}	$VO_2^{+}(aq) + 2H^{+}(aq) + e^- \rightarrow VO^{2+}(aq) + H_2O(l)$	$VO_2^{+}(aq) + 4H^{+}(aq) + 3e^- \rightarrow V^{2+}(aq) + 2H_2O(l)$

Several reagents are commonly used as **auxiliary oxidizing agents**, including ammonium peroxydisulfate, $(NH_4)_2S_2O_8$, and hydrogen peroxide, H_2O_2. Peroxydisulfate is a powerful oxidizing agent

$$\mathbf{S_2O_8^{2-}}(aq) + 2e^- \rightarrow 2\mathbf{SO_4^{2-}}(aq) \tag{9.4.44}$$

capable of oxidizing Mn^{2+} to MnO_4^-, Cr^{3+} to $Cr_2O_7^{2-}$, and Ce^{3+} to Ce^{4+}. Excess peroxydisulfate is easily destroyed by briefly boiling the solution. The reduction of hydrogen peroxide in acidic solution

$$\mathbf{H_2O_2}(aq) + 2\mathbf{H^+}(aq) + 2e^- \rightarrow 2\mathbf{H_2O}(l) \tag{9.4.45}$$

provides another method for oxidizing a titrand. Excess H_2O_2 is destroyed by briefly boiling the solution.

Selecting and Standardizing a Titrant

If it is to be used quantitatively, the titrant's concentration must remain stable during the analysis. Because a titrant in a reduced state is susceptible to air oxidation, most redox titrations use an oxidizing agent as the titrant. There are several common oxidizing titrants, including MnO_4^-, Ce^{4+}, $Cr_2O_7^{2-}$, and I_3^-. Which titrant is used often depends on how easy it is to oxidize the titrand. A titrand that is a weak reducing agent needs a strong oxidizing titrant if the titration reaction is to have a suitable end point.

The two strongest oxidizing titrants are MnO_4^- and Ce^{4+}, for which the reduction half-reactions are

$$\mathbf{MnO_4^-}(aq) + 8\mathbf{H^+}(aq) + 5e^- \rightleftharpoons \mathbf{Mn^{2+}}(aq) + 4\mathbf{H_2O}(l) \tag{9.4.46}$$

$$\mathbf{Ce^{4+}}(aq) + e^- \rightleftharpoons \mathbf{Ce^{3+}}(aq) \tag{9.4.47}$$

Solutions of Ce4+ usually are prepared from the primary standard cerium ammonium nitrate, Ce(NO3)4•2NH4NO3, in 1 M H2SO4. When prepared using a reagent grade material, such as Ce(OH)4, the solution is standardized against a primary standard reducing agent such as Na2C2O4 or Fe2+ (prepared using iron wire) using ferroin as an indicator. Despite its availability as a primary standard and its ease of preparation, Ce4+ is not as frequently used as MnO4– because it is more expensive.

Note

The standardization reactions are

$$Ce^{4+}(aq) + Fe^{2+}(aq) \rightarrow Ce^{3+}(aq) + Fe^{3+}(aq) \quad (9.4.48)$$

$$2Ce^{4+}(aq) + H_2C_2O_4(aq) \rightarrow 2Ce^{3+}(aq) + 2CO_2(g) + 2H^+(aq) \quad (9.4.49)$$

Solutions of MnO_4^- are prepared from $KMnO_4$, which is not available as a primary standard. Aqueous solutions of permanganate are thermodynamically unstable due to its ability to oxidize water.

$$4\,MnO_4^-(aq) + 2H_2O(l) \rightleftharpoons 4MnO_2(s) + 3O_2(g) + 4OH^-(aq) \quad (9.4.50)$$

This reaction is catalyzed by the presence of MnO_2, Mn^{2+}, heat, light, and the presence of acids and bases. A moderately stable solution of permanganate can be prepared by boiling it for an hour and filtering through a sintered glass filter to remove any solid MnO_2 that precipitates. Standardization is accomplished against a primary standard reducing agent such as $Na_2C_2O_4$ or Fe^{2+} (prepared using iron wire), with the pink color of excess MnO_4^- signaling the end point. A solution of MnO_4^- prepared in this fashion is stable for 1–2 weeks, although the standardization should be rechecked periodically.

Note

The standardization reactions are

$$MnO_4^-(aq) + 5Fe^{2+}(aq) + 8H^+(aq) \rightarrow Mn^{2+}(aq) + 5Fe^{3+}(aq) + 4H_2O(l) \quad (9.4.51)$$

$$2\,MnO_4^-(aq) + 5H_2C_2O_4(aq) + 6H^+(aq) \rightarrow 2Mn^{2+}(aq) + 10CO_2(g) + 8H_2O(l) \quad (9.4.52)$$

Potassium dichromate is a relatively strong oxidizing agent whose principal advantages are its availability as a primary standard and the long term stability of its solutions. It is not, however, as strong an oxidizing agent as MnO_4^- or Ce^{4+}, which makes it less useful when the titrand is a weak reducing agent. Its reduction half-reaction is

$$Cr_2O_7^{2-}(aq) + 14H^+(aq) + 6e^- \rightleftharpoons 2Cr^{3+}(aq) + 7H_2O(l) \quad (9.4.53)$$

Although a solution of $Cr_2O_7^{2-}$ is orange and a solution of Cr^{3+} is green, neither color is intense enough to serve as a useful indicator. Diphenylamine sulfonic acid, whose oxidized form is red-violet and reduced form is colorless, gives a very distinct end point signal with $Cr_2O_7^{2-}$.

Iodine is another important oxidizing titrant. Because it is a weaker oxidizing agent than MnO_4^-, Ce^{4+}, and $Cr_2O_7^{2-}$, it is useful only when the titrand is a stronger reducing agent. This apparent limitation, however, makes I_2 a more selective titrant for the analysis of a strong reducing agent in the presence of a weaker reducing agent. The reduction half-reaction for I_2 is

$$I_2(aq) + 2e^- \rightleftharpoons 2I^-(aq) \quad (9.4.54)$$

Because iodine is not very soluble in water, solutions are prepared by adding an excess of I^-. The complexation reaction

$$I_2(aq) + I^-(aq) \rightleftharpoons I_3^-(aq) \quad (9.4.55)$$

increases the solubility of I_2 by forming the more soluble triiodide ion, I_3^-. Even though iodine is present as I_3^- instead of I_2, the number of electrons in the reduction half-reaction is unaffected.

$$I_3^-(aq) + 2e^- \rightleftharpoons 3I^-(aq) \quad (9.4.56)$$

Solutions of I_3^- are normally standardized against $Na_2S_2O_3$ using starch as a specific indicator for I_3^-.

Note

The standardization reaction is

$$I_3^-(aq) + 2S_2O_3^{2-}(aq) \rightarrow 3I^-(aq) + 2S_4O_6^{2-}(aq) \quad (9.4.57)$$

An oxidizing titrant such as MnO_4^-, Ce^{4+}, $Cr_2O_7^{2-}$, and I_3^-, is used when the titrand is in a reduced state. If the titrand is in an oxidized state, we can first reduce it with an auxiliary reducing agent and then complete the titration using an oxidizing titrant. Alternatively, we can titrate it using a reducing titrant. Iodide is a relatively strong reducing agent that could serve as a reducing titrant except that a solution of I– is susceptible to the air-oxidation of I^- to I_3^-.

$$3I^-(aq) \rightleftharpoons I_3^-(aq) + 2e^- \quad (9.4.58)$$

Note

A freshly prepared solution of KI is clear, but after a few days it may show a faint yellow coloring due to the presence of I_3^-.

Instead, adding an excess of KI reduces the titrand, releasing a stoichiometric amount of I_3^-. The amount of I_3^- produced is then determined by a back titration using thiosulfate, $S_2O_3^{2-}$, as a reducing titrant.

$$2S_2O_3^{2-}(aq) \rightleftharpoons 2S_4O_6^{2-}(aq) + 2e^- \quad (9.4.59)$$

Solutions of $S_2O_3^{2-}$ are prepared using $Na_2S_2O_3 \cdot 5H_2O$, and must be standardized before use. Standardization is accomplished by dissolving a carefully weighed portion of the primary standard KIO_3 in an acidic solution containing an excess of KI. The reaction between IO_3^- and I^-

$$IO_3^-(aq) + 8I^-(aq) + 6H^+(aq) \rightarrow 3\,I_3^-(aq) + 3H_2O(l) \quad (9.4.60)$$

liberates a stoichiometric amount of I_3^-. By titrating this I_3^- with thiosulfate, using starch as a visual indicator, we can determine the concentration of $S_2O_3^{2-}$ in the titrant.

Note

The standardization titration is

$$I_3^-(aq) + 2S_2O_3^{2-}(aq) \rightarrow 3I^-(aq) + 2S_4O_6^{2-}(aq) \quad (9.4.61)$$

which is the same reaction used to standardize solutions of I_3^-. This approach to standardizing solutions of $S_2O_3^{2-}$. is similar to the determination of the total chlorine residual outlined in Representative Method 9.3.

Although thiosulfate is one of the few reducing titrants that is not readily oxidized by contact with air, it is subject to a slow decomposition to bisulfite and elemental sulfur. If used over a period of several weeks, a solution of thiosulfate should be restandardized periodically. Several forms of bacteria are able to metabolize thiosulfate, which also can lead to a change in its concentration. This problem can be minimized by adding a preservative such as HgI_2 to the solution.

Another useful reducing titrant is ferrous ammonium sulfate, $Fe(NH_4)_2(SO_4)_2 \cdot 6H_2O$, in which iron is present in the +2 oxidation state. A solution of Fe^{2+} is susceptible to air-oxidation, but when prepared in 0.5 M H_2SO_4 it remains stable for as long as a month. Periodic restandardization with $K_2Cr_2O_7$ is advisable. The titrant can be used to directly titrate the titrand by oxidizing Fe^{2+} to Fe^{3+}. Alternatively, ferrous ammonium sulfate is added to the titrand in excess and the quantity of Fe^{3+} produced determined by back titrating with a standard solution of Ce^{4+} or $Cr_2O_7^{2-}$.

Inorganic Analysis

One of the most important applications of redox titrimetry is evaluating the chlorination of public water supplies. Representative Method 9.3, for example, describes an approach for determining the total chlorine residual by using the oxidizing power of chlorine to oxidize I^- to I_3^-. The amount of I_3^- is determined by back titrating with $S_2O_3^{2-}$.

The efficiency of chlorination depends on the form of the chlorinating species. There are two contributions to the total chlorine residual—the free chlorine residual and the combined chlorine residual. The free chlorine residual includes forms of chlorine that are available for disinfecting the water supply. Examples of species contributing to the free chlorine residual include Cl_2, HOCl and OCl^-. The combined chlorine residual includes those species in which chlorine is in its reduced form and, therefore, no longer capable of providing disinfection. Species contributing to the combined chlorine residual are NH_2Cl, $NHCl_2$ and NCl_3.

When a sample of iodide-free chlorinated water is mixed with an excess of the indicator *N*,*N*-diethyl-*p*-phenylenediamine (DPD), the free chlorine oxidizes a stoichiometric portion of DPD to its red-colored form. The oxidized DPD is then back titrated to its colorless form using ferrous ammonium sulfate as the titrant. The volume of titrant is proportional to the free residual chlorine.

Having determined the free chlorine residual in the water sample, a small amount of KI is added, catalyzing the reduction monochloramine, NH_2Cl, and oxidizing a portion of the DPD back to its red-colored form. Titrating the oxidized DPD with ferrous ammonium sulfate yields the amount of NH_2Cl in the sample. The amount of dichloramine and trichloramine are determined in a similar fashion.

The methods described above for determining the total, free, or combined chlorine residual also are used to establish a water supply's chlorine demand. Chlorine demand is defined as the quantity of chlorine needed to completely react with any substance that can be oxidized by chlorine, while also maintaining the desired chlorine residual. It is determined by adding progressively greater amounts of chlorine to a set of samples drawn from the water supply and determining the total, free, or combined chlorine residual.

Another important example of redox titrimetry, which finds applications in both public health and environmental analyses is the determination of dissolved oxygen. In natural waters, such as lakes and rivers, the level of dissolved O_2 is important for two reasons: it is the most readily available oxidant for the biological oxidation of inorganic and organic pollutants; and it is necessary for the support of aquatic life. In a wastewater treatment plant dissolved O_2 is essential for the aerobic oxidation of waste materials. If the concentration of dissolved O_2 falls below a critical value, aerobic bacteria are replaced by anaerobic bacteria, and the oxidation of organic waste produces undesirable gases, such as CH_4 and H_2S.

One standard method for determining the dissolved O_2 content of natural waters and wastewaters is the Winkler method. A sample of water is collected without exposing it to the atmosphere, which might change the concentration of dissolved O_2. The sample is first treated with a solution of $MnSO_4$, and then with a solution of NaOH and KI. Under these alkaline conditions the dissolved oxygen oxidizes Mn^{2+} to MnO_2.

$$2Mn^{2+}(aq) + 4OH^-(aq) + O_2(g) \rightarrow 2MnO_2(s) + 2H_2O(l) \tag{9.4.62}$$

After the reaction is complete, the solution is acidified with H_2SO_4. Under the now acidic conditions I^- is oxidized to I_3^- by MnO_2.

$$MnO_2(s) + 3I^-(aq) + 4H^+(aq) \rightarrow Mn^{2+} + I_3^-(aq) + 2H_2O(l) \tag{9.4.63}$$

The amount of I_3^- formed is determined by titrating with $S_2O_3^{2-}$ using starch as an indicator. The Winkler method is subject to a variety of interferences, and several modifications to the original procedure have been proposed. For example, NO_2^- interferes because it can reduce I_3^- to I^- under acidic conditions. This interference is eliminated by adding sodium azide, NaN_3, reducing NO_2^- to N_2. Other reducing agents, such as Fe^{2+}, are eliminated by pretreating the sample with $KMnO_4$, and destroying the excess permanganate with $K_2C_2O_4$.

Another important example of redox titrimetry is the determination of water in nonaqueous solvents. The titrant for this analysis is known as the Karl Fischer reagent and consists of a mixture of iodine, sulfur dioxide, pyridine, and methanol. Because the concentration of pyridine is sufficiently large, I_2 and SO_2 react with pyridine (py) to form the complexes py•I_2 and py•SO_2. When added to a sample containing water, I_2 is reduced to I^- and SO_2 is oxidized to SO_3.

$$py \bullet I_2 + py \bullet SO_2 + py + H_2O \rightarrow 2py \bullet HI + py \bullet SO_3 \tag{9.4.64}$$

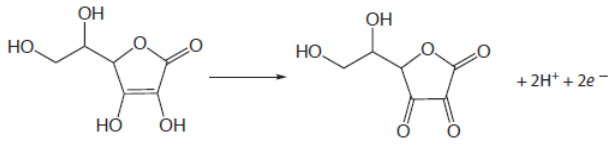
Methanol is included to prevent the further reaction of py•SO_3 with water. The titration's end point is signaled when the solution changes from the product's yellow color to the brown color of the Karl Fischer reagent.

Organic Analysis

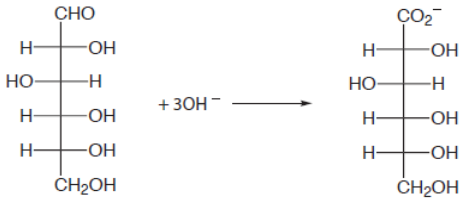
Redox titrimetry also is used for the analysis of organic analytes. One important example is the determination of the chemical oxygen demand (COD) of natural waters and wastewaters. The COD provides a measure of the quantity of oxygen necessary to completely oxidize all the organic matter in a sample to CO_2 and H_2O. Because no attempt is made to correct for organic matter that can not be decomposed biologically, or for slow decomposition kinetics, the COD always overestimates a sample's true oxygen demand. The determination of COD is particularly important in managing industrial wastewater treatment facilities where it is used to monitor the release of organic-rich wastes into municipal sewer systems or the environment.

A sample's COD is determined by refluxing it in the presence of excess $K_2Cr_2O_7$, which serves as the oxidizing agent. The solution is acidified with H_2SO_4 using Ag_2SO_4 to catalyze the oxidation of low molecular weight fatty acids. Mercuric sulfate, $HgSO_4$, is added to complex any chloride that is present, preventing the precipitation of the Ag^+ catalyst as AgCl. Under these conditions, the efficiency for oxidizing organic matter is 95–100%. After refluxing for two hours, the solution is cooled to room temperature and the excess $Cr_2O_7^{2-}$ is determined by back titrating using ferrous ammonium sulfate as the titrant and ferroin as the indicator. Because it is difficult to completely remove all traces of organic matter from the reagents, a blank titration must be performed. The difference in the amount of ferrous ammonium sulfate needed to titrate the sample and the blank is proportional to the COD.

Iodine has been used as an oxidizing titrant for a number of compounds of pharmaceutical interest. Earlier we noted that the reaction of $S_2O_3^{2-}$ with I_3^- produces the tetrathionate ion, $S_4O_6^{2-}$. The tetrathionate ion is actually a dimer consisting of two thiosulfate ions connected through a disulfide (–S–S–) linkage. In the same fashion, I_3^- can be used to titrate mercaptans of the general formula RSH, forming the dimer RSSR as a product. The amino acid cysteine also can be titrated with I_3^-. The product of this titration is cystine, which is a dimer of cysteine. Triiodide also can be used for the analysis of ascorbic acid (vitamin C) by oxidizing the enediol functional group to an alpha diketone



and for the analysis of reducing sugars, such as glucose, by oxidizing the aldehyde functional group to a carboxylate ion in a basic solution.



An organic compound containing a hydroxyl, a carbonyl, or an amine functional group adjacent to an hydoxyl or a carbonyl group can be oxidized using metaperiodate, IO_4^-, as an oxidizing titrant.

$$IO_4^-(aq) + H_2O(l) + 2e^- \rightleftharpoons IO_3^-(aq) + 2OH^-(aq) \tag{9.4.65}$$

A two-electron oxidation cleaves the C–C bond between the two functional groups, with hydroxyl groups being oxidized to aldehydes or ketones, carbonyl functional groups being oxidized to carboxylic acids, and amines being oxidized to an aldehyde and an amine (ammonia if a primary amine). The analysis is conducted by adding a known excess of IO_4^- to the solution containing the analyte, and allowing the oxidation to take place for approximately one hour at room temperature. When the oxidation is complete, an excess of KI is added, which converts any unreacted IO_4^- to IO_3^- and I_3^-.

$$IO_4^-(aq) + 3I^-(aq) + H_2O(l) \rightarrow IO_3^-(aq) + I_3^-(aq) + 2OH^-(aq) \tag{9.4.66}$$

The I_3^- is then determined by titrating with $S_2O_3^{2-}$ using starch as an indicator.

Quantitative Calculations

The quantitative relationship between the titrand and the titrant is determined by the stoichiometry of the titration reaction. If you are unsure of the balanced reaction, you can deduce the stoichiometry by remembering that the electrons in a redox reaction must be conserved.

Example 9.11

The amount of Fe in a 0.4891-g sample of an ore was determined by titrating with $K_2Cr_2O_7$. After dissolving the sample in HCl, the iron was brought into the +2 oxidation state using a Jones reductor. Titration to the diphenylamine sulfonic acid end point required 36.92 mL of 0.02153 M $K_2Cr_2O_7$. Report the ore's iron content as %w/w Fe_2O_3.

(Although we can deduce the stoichiometry between the titrant and the titrand without balancing the titration reaction, the balanced reaction

$$\begin{aligned} &K_2Cr_2O_7(aq) + 6Fe^{2+}(aq) + 14H^+(aq) \\ &\rightarrow 2Cr^{3+}(aq) + 2K^+(aq) + 6Fe^{3+}(aq) + 7H_2O(l) \end{aligned} \quad (9.4.67)$$

does provide useful information. For example, the presence of H^+ reminds us that the reaction^fs feasibility is pH-dependent.)

Solution

Because we have not been provided with the titration reaction, let's use a conservation of electrons to deduce the stoichiometry. During the titration the analyte is oxidized from Fe^{2+} to Fe^{3+}, and the titrant is reduced from $Cr_2O_7^{2-}$ to Cr^{3+}. Oxidizing Fe^{2+} to Fe^{3+} requires only a single electron. Reducing $Cr_2O_7^{2-}$, in which each chromium is in the +6 oxidation state, to Cr^{3+} requires three electrons per chromium, for a total of six electrons. A conservation of electrons for the titration, therefore, requires that each mole of $K_2Cr_2O_7$ reacts with six moles of Fe^{2+}.

The moles of $K_2Cr_2O_7$ used in reaching the end point is

$$(0.02153\ \text{M}\ K_2Cr_2O_7) \times (0.03692\ \text{L}\ K_2Cr_2O_7) = 7.949 \times 10^{-4}\ \text{mol}\ K_2Cr_2O_7 \quad (9.4.68)$$

which means that the sample contains

$$7.949 \times 10^{-4}\ \text{mol}\ K_2Cr_2O_7 \times \frac{6\ \text{mol}\ Fe^{2+}}{\text{mol}\ K_2Cr_2O_7} = 4.769 \times 10^{-3}\ \text{mol}\ Fe^{2+} \quad (9.4.69)$$

Thus, the %w/w Fe_2O_3 in the sample of ore is

$$4.769 \times 10^{-3}\ \text{mol}\ Fe^{2+} \times \frac{1\ \text{mol}\ Fe_2O_3}{2\ \text{mol}\ Fe^{2+}} \times \frac{159.69\ \text{g}\ Fe_2O_3}{\text{mol}\ Fe_2O_3} = 0.3808\ \text{g}\ Fe_2O_3 \quad (9.4.70)$$

$$\frac{0.3808\ \text{g}\ Fe_2O_3}{0.4891\ \text{g sample}} \times 100 = 77.86\%\ \text{w/w}\ Fe_2O_3 \quad (9.4.71)$$

Practice Exercise 9.20

The purity of a sample of sodium oxalate, $Na_2C_2O_4$, is determined by titrating with a standard solution of $KMnO_4$. If a 0.5116-g sample requires 35.62 mL of 0.0400 M $KMnO_4$ to reach the titration's end point, what is the %w/w $Na_2C_2O_4$ in the sample.

Click here to review your answer to this exercise.

As shown in the following two examples, we can easily extend this approach to an analysis that requires an indirect analysis or a back titration.

Example 9.12

A 25.00-mL sample of a liquid bleach was diluted to 1000 mL in a volumetric flask. A 25-mL portion of the diluted sample was transferred by pipet into an Erlenmeyer flask containing an excess of KI, reducing the OCl^- to Cl^-, and producing I_3^-. The liberated I_3^- was determined by titrating with 0.09892 M $Na_2S_2O_3$, requiring 8.96 mL to reach the starch indicator end point. Report the %w/v NaOCl in the sample of bleach.

Solution

To determine the stoichiometry between the analyte, NaOCl, and the titrant, $Na_2S_2O_3$, we need to consider both the reaction between OCl^- and I^-, and the titration of I_3^- with $Na_2S_2O_3$.

First, in reducing OCl^- to Cl^-, the oxidation state of chlorine changes from +1 to –1, requiring two electrons. The oxidation of three I^- to form I_3^- releases two electrons as the oxidation state of each iodine changes from –1 in I^- to –⅓ in I_3^-. A conservation of electrons, therefore, requires that each mole of OCl^- produces one mole of I_3^-.

Second, in the titration reaction, I_3^-. is reduced to I^- and $S_2O_3^{2-}$ is oxidized to $S_4O_6^{2-}$. Reducing I_3^- to $3I^-$ requires two elections as each iodine changes from an oxidation state of –⅓ to –1. In oxidizing $S_2O_3^{2-}$ to $S_4O_6^{2-}$, each sulfur changes its oxidation state from +2 to +2.5, releasing one electron for each $S_2O_3^{2-}$. A conservation of electrons, therefore, requires that each mole of I_3^- reacts with two moles of $S_2O_3^{2-}$.

Finally, because each mole of OCl^- produces one mole of I_3^-, and each mole of I_3^- reacts with two moles of $S_2O_3^{2-}$, we know that every mole of NaOCl in the sample ultimately results in the consumption of two moles of $Na_2S_2O_3$.

The balanced reactions for this analysis are:

$$OCl^-(aq) + 3I^-(aq) + 2H^+(aq) \rightarrow I_3^-(aq) + Cl^-(aq) + H_2O(l) \tag{9.4.72}$$

$$I_3^-(aq) + 2S_2O_3^{2-}(aq) \rightarrow S_4O_6^{2-}(aq) + 3I^-(aq) \tag{9.4.73}$$

The moles of $Na_2S_2O_3$ used in reaching the titration's end point is

$$(0.09892\ M\ Na_2S_2O_3) \times (0.00896\ L\ Na_2S_2O_3) = 8.86 \times 10^{-4}\ mol\ Na_2S_2O_3 \tag{9.4.74}$$

which means the sample contains

$$8.86 \times 10^{-4}\ mol\ Na_2S_2O_3 \times \frac{1\ mol\ NaOCl}{2\ mol\ Na_2S_2O_3} \times \frac{74.44\ g\ NaOCl}{mol\ NaOCl} = 0.03299\ g\ NaOCl \tag{9.4.75}$$

Thus, the %w/v NaOCl in the diluted sample is

$$\frac{0.03299\ g\ NaOCl}{25.00\ mL} \times 100 = 1.32\%\ w/v\ NaOCl \tag{9.4.76}$$

Because the bleach was diluted by a factor of 40 (25 mL to 1000 mL), the concentration of NaOCl in the bleach is 5.28% (w/v).

Example 9.13

The amount of ascorbic acid, $C_6H_8O_6$, in orange juice was determined by oxidizing the ascorbic acid to dehydroascorbic acid, $C_6H_6O_6$, with a known amount of I_3^-, and back titrating the excess I_3^- with $Na_2S_2O_3$. A 5.00-mL sample of filtered orange juice was treated with 50.00 mL of 0.01023 M I_3^-. After the oxidation was complete, 13.82 mL of 0.07203 M $Na_2S_2O_3$ was needed to reach the starch indicator end point. Report the concentration ascorbic acid in mg/100 mL.

Solution

For a back titration we need to determine the stoichiometry between I_3^- and the analyte, $C_6H_8O_6$, and between I_3^- and the titrant, $Na_2S_2O_3$. The later is easy because we know from Example 9.12 that each mole of I_3^- reacts with two moles of $Na_2S_2O_3$.

The balanced reactions for this analysis are:

$$C_6H_8O_6(aq) + I_3^-(aq) \rightarrow 3I^-(aq) + C_6H_6O_6(aq) + 2H^+(aq) \tag{9.4.77}$$

$$I_3^-(aq) + 2S_2O_3^{2-}(aq) \rightarrow S_4O_6^{2-}(aq) + 3I^-(aq) \tag{9.4.78}$$

In oxidizing ascorbic acid to dehydroascorbic acid, the oxidation state of carbon changes from +⅔ in $C_6H_8O_6$ to +1 in $C_6H_6O_6$. Each carbon releases ⅓ of an electron, or a total of two electrons per ascorbic acid. As we learned in Example 9.12, reducing I_3^- requires two electrons; thus, a conservation of electrons requires that each mole of ascorbic acid consumes one mole of I_3^-.

The total moles of I_3^- reacting with $C_6H_8O_6$ and with $Na_2S_2O_3$ is

$$(0.01023\ M\ I_3^-) \times (0.05000\ L\ I_3^-) = 5.115 \times 10^{-4}\ mol\ I_3^- \tag{9.4.79}$$

The back titration consumes

$$0.01382\ L\ Na_2S_2O_3 \times \frac{0.07203\ mol\ Na_2S_2O_3}{L\ Na_2S_2O_3} \times \frac{1\ mol\ I_3^-}{2\ mol\ Na_2S_2O_3} = 4.977 \times 10^{-4}\ mol\ I_3^- \tag{9.4.80}$$

Subtracting the moles of I_3^- reacting with $Na_2S_2O_3$ from the total moles of I_3^- gives the moles reacting with ascorbic acid.

$$5.115 \times 10^{-4}\ mol\ I_3^- - 4.977 \times 10^{-4}\ mol\ I_3^- = 1.38 \times 10^{-5}\ mol\ I_3^- \tag{9.4.81}$$

The grams of ascorbic acid in the 5.00-mL sample of orange juice is

$$1.38 \times 10^{-5} \text{ mol } I_3^- \times \frac{1 \text{ mol } C_6H_8O_6}{\text{mol } I_3^-} \times \frac{176.13 \text{ g } C_6H_8O_6}{\text{mol } C_6H_8O_6} = 2.43 \times 10^{-3} \text{ g } C_6H_8O_6 \quad (9.4.82)$$

There are 2.43 mg of ascorbic acid in the 5.00-mL sample, or 48.6 mg per 100 mL of orange juice.

Practice Exercise 9.21

A quantitative analysis for ethanol, C_2H_6O, can be accomplished by a redox back titration. Ethanol is oxidized to acetic acid, $C_2H_4O_2$, using excess dichromate, $Cr_2O_7^{2-}$, which is reduced to Cr^{3+}. The excess dichromate is titrated with Fe^{2+}, giving Cr^{3+} and Fe^{3+} as products. In a typical analysis, a 5.00-mL sample of a brandy is diluted to 500 mL in a volumetric flask. A 10.00-mL sample is taken and the ethanol is removed by distillation and collected in 50.00 mL of an acidified solution of 0.0200 M $K_2Cr_2O_7$. A back titration of the unreacted $Cr_2O_7^{2-}$ requires 21.48 mL of 0.1014 M Fe^{2+}. Calculate the %w/v ethanol in the brandy.

Click here to review your answer to this exercise.

9.4.4 Evaluation of Redox Titrimetry

The scale of operations, accuracy, precision, sensitivity, time, and cost of a redox titration are similar to those described earlier in this chapter for acid–base or a complexation titration. As with acid–base titrations, we can extend a redox titration to the analysis of a mixture of analytes if there is a significant difference in their oxidation or reduction potentials. Figure 9.42 shows an example of the titration curve for a mixture of Fe^{2+} and Sn^{2+} using Ce^{4+} as the titrant. A titration of a mixture of analytes is possible if their standard state potentials or formal potentials differ by at least 200 mV.

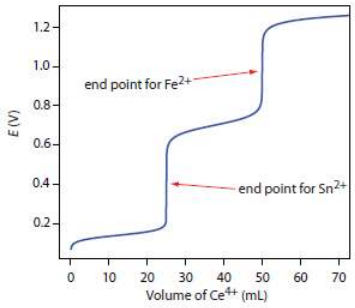


Figure 9.42 Titration curve for the titration of 50.0 mL of 0.0125 M Sn^{2+} and 0.0250 M Fe^{2+} with 0.050 M Ce^{4+}. Both the titrand and the titrant are 1M in HCl.

Contributors

David Harvey (DePauw University)

9.4: Redox Titrations is shared under a CC BY-NC-SA 4.0 license and was authored, remixed, and/or curated by LibreTexts.

9.5: Precipitation Titrations

Thus far we have examined titrimetric methods based on acid–base, complexation, and redox reactions. A reaction in which the analyte and titrant form an insoluble precipitate also can serve as the basis for a titration. We call this type of titration a **precipitation titration**.

One of the earliest precipitation titrations—developed at the end of the eighteenth century—was the analysis of K_2CO_3 and K_2SO_4 in potash. Calcium nitrate, $Ca(NO_3)_2$, was used as the titrant, forming a precipitate of $CaCO_3$ and $CaSO_4$. The titration's end point was signaled by noting when the addition of titrant ceased to generate additional precipitate. The importance of precipitation titrimetry as an analytical method reached its zenith in the nineteenth century when several methods were developed for determining Ag^+ and halide ions.

9.5.1 Titration Curves

A precipitation titration curve follows the change in either the titrand's or the titrant's concentration as a function of the titrant's volume. As we have done with other titrations, we first show how to calculate the titration curve and then demonstrate how we can quickly sketch a reasonable approximation of the titration curve.

Calculating the Titration Curve

Let's calculate the titration curve for the titration of 50.0 mL of 0.0500 M NaCl with 0.100 M $AgNO_3$. The reaction in this case is

$$Ag^+(aq) + Cl^-(aq) \rightleftharpoons AgCl(s) \tag{9.5.1}$$

Because the reaction's equilibrium constant is so large

$$K = (K_{sp})^{-1} = (1.8 \times 10^{-10})^{-1} = 5.6 \times 10^9 \tag{9.5.2}$$

we may assume that Ag^+ and Cl^- react completely.

> **Note**
>
> Step 1: Calculate the volume of $AgNO_3$ needed to reach the equivalence point.

By now you are familiar with our approach to calculating a titration curve. The first task is to calculate the volume of Ag^+ needed to reach the equivalence point. The stoichiometry of the reaction requires that

$$\text{moles } Ag^+ = \text{moles } Cl^- \tag{9.5.3}$$

$$M_{Ag} \times V_{Ag} = M_{Cl} \times V_{Cl} \tag{9.5.4}$$

Solving for the volume of Ag^+

$$V_{eq} = V_{Ag} = \frac{M_{Cl}V_{Cl}}{M_{Ag}} = \frac{(0.0500\text{ M})(50.0\text{ mL})}{(0.100\text{ M})} = 25.0\text{ mL} \tag{9.5.5}$$

shows that we need 25.0 mL of Ag+ to reach the equivalence point.

> **Note**
>
> Step 2: Calculate pCl before the equivalence point by determining the concentration of unreacted NaCl.

Before the equivalence point the titrand, Cl^-, is in excess. The concentration of unreacted Cl^- after adding 10.0 mL of Ag^+, for example, is

$$[Cl^-] = \frac{\text{initial moles } Cl^- - \text{moles } Ag^+ \text{ added}}{\text{total volume}} = \frac{M_{Cl}V_{Cl} - M_{Ag}V_{Ag}}{V_{Cl} + V_{Ag}} \tag{9.5.6}$$

$$= \frac{(0.0500\text{ M})(50.0\text{ mL}) - (0.100\text{ M})(10.0\text{ mL})}{50.0\text{ mL} + 10.0\text{ mL}} = 2.50 \times 10^{-2}\text{ M} \tag{9.5.7}$$

which corresponds to a pCl of 1.60.

Note

Step 3: Calculate pCl at the equivalence point using the K_{sp} for AgCl to calculate the concentration of Cl^-.

At the titration's equivalence point, we know that the concentrations of Ag^+ and Cl^- are equal. To calculate the concentration of Cl^- we use the K_{sp} expression for AgCl; thus

$$K_{sp} = [Ag^+][Cl^-] = (x)(x) = 1.8 \times 10^{-10} \tag{9.5.8}$$

Solving for x gives $[Cl^-]$ as 1.3×10^{-5} M, or a pCl of 4.89.

Note

Step 4: Calculate pCl after the equivalence point by first calculating the concentration of excess $AgNO_3$ and then calculating the concentration of Cl^- using the K_{sp} for AgCl.

After the equivalence point, the titrant is in excess. We first calculate the concentration of excess Ag^+ and then use the K_{sp} expression to calculate the concentration of Cl^-. For example, after adding 35.0 mL of titrant

$$[Ag^+] = \frac{\text{moles } Ag^+ \text{ added} - \text{initial moles } Cl^-}{\text{total volume}} = \frac{M_{Ag}V_{Ag} - M_{Cl}V_{Cl}}{V_{Cl} + V_{Ag}} \tag{9.5.9}$$

$$= \frac{(0.100 \text{ M})(35.0 \text{ mL}) - (0.0500 \text{ M})(50.0 \text{ mL})}{50.0 \text{ mL} + 35.0 \text{ mL}} = 1.18 \times 10^{-2} \text{ M} \tag{9.5.10}$$

$$[Cl^-] = \frac{K_{sp}}{[Ag^+]} = \frac{1.8 \times 10^{-10}}{1.18 \times 10^{-2}} = 1.5 \times 10^{-8} \text{ M} \tag{9.5.11}$$

or a pCl of 7.81. Additional results for the titration curve are shown in Table 9.18 and Figure 9.43.

Table 9.18: Titration of 50.0 mL of 0.0500 M NaCl with 0.100 M $AgNO_3$

Volume of $AgNO_3$ (mL)	pCl	Volume of $AgNO_3$ (mL)	pCl
0.00	1.30	30.0	7.54
5.00	1.44	35.0	7.82
10.0	1.60	40.0	7.97
15.0	1.81	45.0	8.07
20.0	2.15	50.0	8.14
25.0	4.89		

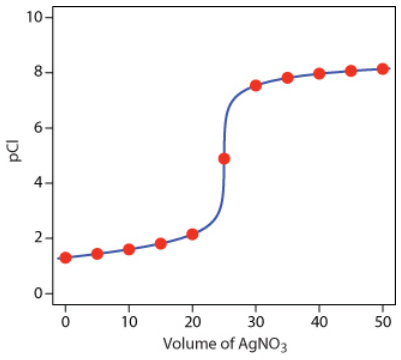


Figure 9.43 *Titration curve for the titration of 50.0 mL of 0.0500 M NaCl with 0.100 M $AgNO_3$. The red points corresponds to the data in Table 9.18. The blue line shows the complete titration curve.*

Practice Exercise 9.22

When calculating a precipitation titration curve, you can choose to follow the change in the titrant's concentration or the change in the titrand's concentration. Calculate the titration curve for the titration of 50.0 mL of 0.0500 M $AgNO_3$ with 0.100 M NaCl as pAg versus V_{NaCl}, and as pCl versus V_{NaCl}.

Click here to review your answer to this exercise.

Sketching the Titration Curve

To evaluate the relationship between a titration's equivalence point and its end point we need to construct only a reasonable approximation of the exact titration curve. In this section we demonstrate a simple method for sketching a precipitation titration curve. Our goal is to sketch the titration curve quickly, using as few calculations as possible. Let's use the titration of 50.0 mL of 0.0500 M NaCl with 0.100 M $AgNO_3$.

Note

This is the same example that we used in developing the calculations for a precipitation titration curve. You can review the results of that calculation in Table 9.18 and Figure 9.43.

We begin by calculating the titration's equivalence point volume, which, as we determined earlier, is 25.0 mL. Next we draw our axes, placing pCl on the *y*-axis and the titrant's volume on the *x*-axis. To indicate the equivalence point's volume, we draw a vertical line corresponding to 25.0 mL of $AgNO_3$. Figure 9.44a shows the result of this first step in our sketch.

Before the equivalence point, Cl^- is present in excess and pCl is determined by the concentration of unreacted Cl^-. As we learned earlier, the calculations are straightforward. Figure 9.44b shows pCl after adding 10.0 mL and 20.0 mL of $AgNO_3$.

Note

See Table 9.18 for the values.

After the equivalence point, Ag^+ is in excess and the concentration of Cl^- is determined by the solubility of AgCl. Again, the calculations are straightforward. Figure 4.43c shows pCl after adding 30.0 mL and 40.0 mL of $AgNO_3$.

Note

See Table 9.18 for the values.

Next, we draw a straight line through each pair of points, extending them through the vertical line representing the equivalence point's volume (Figure 9.44d). Finally, we complete our sketch by drawing a smooth curve that connects the three straight-line segments (Figure 9.44e). A comparison of our sketch to the exact titration curve (Figure 9.44f) shows that they are in close agreement.

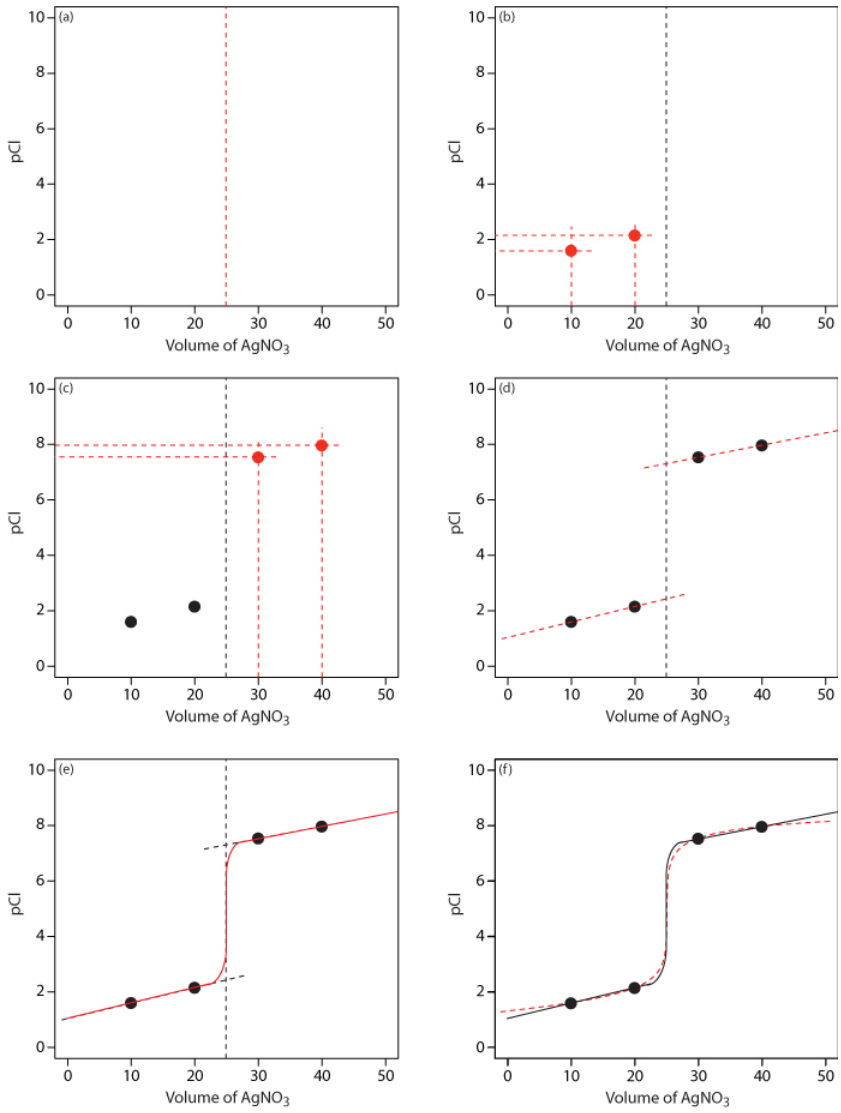


Figure 9.44 Illustrations showing the steps in sketching an approximate titration curve for the titration of 50.0 mL of 0.0500 M NaCl with 0.100 M $AgNO_3$: (a) locating the equivalence point volume; (b) plotting two points before the equivalence point; (c) plotting two points after the equivalence point; (d) preliminary approximation of titration curve using straight-lines; (e) final approximation of titration curve using a smooth curve; (f) comparison of approximate titration curve (solid black line) and exact titration curve (dashed red line). See the text for additional details. A better fit is possible if the two points before the equivalence point are further apart—for example, 0 mL and 20 mL— and the two points after the equivalence point are further apart.

9.5.2 Selecting and Evaluating the End point

At the beginning of this section we noted that the first precipitation titration used the cessation of precipitation to signal the end point. At best, this is a cumbersome method for detecting a titration's end point. Before precipitation titrimetry became practical, better methods for identifying the end point were necessary.

Finding the End point With an Indicator

There are three general types of indicators for precipitation titrations, each of which changes color at or near the titration's equivalence point. The first type of indicator is a species that forms a precipitate with the titrant. In the **Mohr method** for Cl^- using Ag^+ as a titrant, for example, a small amount of K_2CrO_4 is added to the titrand's solution. The titration's end point is the formation of a reddish-brown precipitate of Ag_2CrO_4.

> **Note**
>
> The Mohr method was first published in 1855 by Karl Friedrich Mohr.

Because CrO_4^{2-} imparts a yellow color to the solution, which might obscure the end point, only a small amount of K_2CrO_4 is added. As a result, the end point is always later than the equivalence point. To compensate for this positive determinate error, an analyte-free reagent blank is analyzed to determine the volume of titrant needed to affect a change in the indicator's color. Subtracting the end point for the reagent blank from the titrand's end point gives the titration's end point. Because CrO_4^{2-} is a weak base, the titrand's solution is made slightly alkaline. If the pH is too acidic, chromate is present as $HCrO_4^-$ instead of CrO_4^{2-}, and the Ag_2CrO_4 end point is delayed. The pH also must be less than 10 to avoid the precipitation of silver hydroxide.

A second type of indicator uses a species that forms a colored complex with the titrant or the titrand. In the **Volhard method** for Ag^+ using KSCN as the titrant, for example, a small amount of Fe^{3+} is added to the titrand's solution. The titration's end point is the formation of the reddish-colored $Fe(SCN)^{2+}$ complex. The titration must be carried out in an acidic solution to prevent the precipitation of Fe^{3+} as $Fe(OH)_3$.

> *The Volhard method was first published in 1874 by Jacob Volhard.*

The third type of end point uses a species that changes color when it adsorbs to the precipitate. In the **Fajans method** for Cl^- using Ag^+ as a titrant, for example, the anionic dye dichlorofluoroscein is added to the titrand's solution. Before the end point, the precipitate of AgCl has a negative surface charge due to the adsorption of excess Cl^-. Because dichlorofluoroscein also carries a negative charge, it is repelled by the precipitate and remains in solution where it has a greenish-yellow color. After the end point, the surface of the precipitate carries a positive surface charge due to the adsorption of excess Ag^+. Dichlorofluoroscein now adsorbs to the precipitate's surface where its color is pink. This change in the indicator's color signals the end point.

> *The Fajans method was first published in the 1920s by Kasimir Fajans.*

Finding the End point Potentiometrically

Another method for locating the end point is a potentiometric titration in which we monitor the change in the titrant's or the titrand's concentration using an ion-selective electrode. The end point is found by visually examining the titration curve. A further discussion of potentiometry is found in Chapter 11.

9.5.3 Quantitative Applications

Although precipitation titrimetry is rarely listed as a standard method of analysis, it may still be useful as a secondary analytical method for verifying other analytical methods. Most precipitation titrations use Ag^+ as either the titrand or the titration. A titration in which Ag^+ is the titrant is called an **argentometric titration**. Table 9.19 provides a list of several typical precipitation titrations.

Table 9.19: Representative Examples of Precipitation Titrations

Titrand	Titrant[a]	End Point[b]
AsO_4^{3-}	$AgNO_3$, KSCN	Volhard
Br^-	$AgNO_3$ $AgNO_3$, KSCN	Mohr or Fajans Volhard
Cl^-	$AgNO_3$ $AgNO_3$, KSCN	Mohr or Fajans Volhard*
CO_3^{2-}	$AgNO_3$, KSCN	Volhard*
$C_2O_4^{2-}$	$AgNO_3$, KSCN	Volhard*
CrO_4^{2-}	$AgNO_3$, KSCN	Volhard*
I^-	$AgNO_3$ $AgNO_3$, KSCN	Fajans Volhard
PO_4^{3-}	$AgNO_3$, KSCN	Volhard*
S^{2-}	$AgNO_3$, KSCN	Volhard*
SCN^-	$AgNO_3$, KSCN	Volhard*

[a] When two reagents are listed, the analysis is by a back titration. The first reagent is added in excess and the second reagent used to back titrate the excess.

[b] For those Volhard methods identified with an asterisk (*) the precipitated silver salt must be removed before carrying out the back titration.

Quantitative Calculations

The quantitative relationship between the titrand and the titrant is determined by the stoichiometry of the titration reaction. If you are unsure of the balanced reaction, you can deduce the stoichiometry from the precipitate's formula. For example, in forming a precipitate of Ag_2CrO_4, each mole of CrO_4^{2-} reacts with two moles of Ag^+.

Example 9.14

A mixture containing only KCl and NaBr is analyzed by the Mohr method. A 0.3172-g sample is dissolved in 50 mL of water and titrated to the Ag_2CrO_4 end point, requiring 36.85 mL of 0.1120 M $AgNO_3$. A blank titration requires 0.71 mL of titrant to reach the same end point. Report the %w/w KCl in the sample.

Solution

To find the moles of titrant reacting with the sample, we first need to correct for the reagent blank; thus

$$V_{Ag} = 36.85\ \text{mL} - 0.71\ \text{mL} = 36.14\ \text{mL} \tag{9.5.12}$$

$$(0.1120\ \text{M}\ AgNO_3) \times (0.03614\ \text{L}\ AgNO_3) = 4.048 \times 10^{-3}\ \text{mol}\ AgNO_3 \tag{9.5.13}$$

Titrating with $AgNO_3$ produces a precipitate of AgCl and AgBr. In forming the precipitates, each mole of KCl consumes one mole of $AgNO_3$ and each mole of NaBr consumes one mole of $AgNO_3$; thus

$$\text{moles KCl} + \text{moles NaBr} = 4.048 \times 10^{-3} \tag{9.5.14}$$

We are interested in finding the mass of KCl, so let's rewrite this equation in terms of mass. We know that

$$\text{moles KCl} = \frac{\text{g KCl}}{74.551\ \text{g KCl/mol KCl}} \tag{9.5.15}$$

$$\text{moles NaBr} = \frac{\text{g NaBr}}{102.89\ \text{g NaBr/mol NaBr}} \tag{9.5.16}$$

which we substitute back into the previous equation

$$\frac{\text{g KCl}}{74.551\ \text{g KCl/mol KCl}} + \frac{\text{g NaBr}}{102.89\ \text{g NaBr/mol NaBr}} = 4.048 \times 10^{-3} \tag{9.5.17}$$

Because this equation has two unknowns—g KCl and g NaBr—we need another equation that includes both unknowns. A simple equation takes advantage of the fact that the sample contains only KCl and NaBr; thus,

$$\text{g NaBr} = 0.3172\ \text{g} - \text{g KCl} \tag{9.5.18}$$

$$\frac{\text{g KCl}}{74.551\ \text{g KCl/mol KCl}} + \frac{0.3172\ \text{g} - \text{g KCl}}{102.89\ \text{g NaBr/mol NaBr}} = 4.048 \times 10^{-3} \tag{9.5.19}$$

$$1.341 \times 10^{-2}(\text{g KCl}) + 3.083 \times 10^{-3} - 9.719 \times 10^{-3}(\text{g KCl}) = 4.048 \times 10^{-3} \tag{9.5.20}$$

$$3.69 \times 10^{-3}(\text{g KCl}) = 9.65 \times 10^{-4} \tag{9.5.21}$$

The sample contains 0.262 g of KCl and the %w/w KCl in the sample is

$$\frac{0.262\ \text{g KCl}}{0.3172\ \text{g sample}} \times 100 = 82.6 \tag{9.5.22}$$

The analysis for I^- using the Volhard method requires a back titration. A typical calculation is shown in the following example.

Example 9.15

The %w/w I^- in a 0.6712-g sample was determined by a Volhard titration. After adding 50.00 mL of 0.05619 M $AgNO_3$ and allowing the precipitate to form, the remaining silver was back titrated with 0.05322 M KSCN, requiring 35.14 mL to reach the end point. Report the %w/w I^- in the sample.

Solution

There are two precipitates in this analysis: $AgNO_3$ and I^- form a precipitate of AgI, and $AgNO_3$ and KSCN form a precipitate of AgSCN. Each mole of I^- consumes one mole of $AgNO_3$, and each mole of KSCN consumes one mole of $AgNO_3$; thus

$$\text{moles } AgNO_3 = \text{moles } I^- + \text{moles KSCN} \tag{9.5.23}$$

Solving for the moles of I^- we find

$$\text{moles } I^- = \text{moles } AgNO_3 - \text{moles KSCN} \tag{9.5.24}$$

$$\text{moles } I^- = M_{Ag} \times V_{Ag} - M_{KSCN} \times V_{KSCN} \tag{9.5.25}$$

$$\begin{aligned}\text{moles } I^- = {} & (0.05619\ \text{M } AgNO_3) \times (0.05000\ \text{L } AgNO_3) \\ & - (0.05322\ \text{M KSCN}) \times (0.03514\ \text{L KSCN})\end{aligned} \tag{9.5.26}$$

that there are 9.393×10^{-4} moles of I^- in the sample. The %w/w I^- in the sample is

$$\frac{(9.393 \times 10^{-4}\ \text{mol } I^-) \times 126.9\ \text{g } I^-/\text{mol } I^-}{0.6712\ \text{g sample}} \times 100 = 17.76\%\ \text{w/w } I^- \tag{9.5.27}$$

Practice Exercise 9.23

A 1.963-g sample of an alloy is dissolved in HNO_3 and diluted to volume in a 100-mL volumetric flask. Titrating a 25.00-mL portion with 0.1078 M KSCN requires 27.19 mL to reach the end point. Calculate the %w/w Ag in the alloy.

Click here to review your answer to this exercise.

9.5.4 Evaluation of Precipitation Titrimetry

The scale of operations, accuracy, precision, sensitivity, time, and cost of a precipitation titration is similar to those described elsewhere in this chapter for acid–base, complexation, and redox titrations. Precipitation titrations also can be extended to the analysis of mixtures provided that there is a significant difference in the solubilities of the precipitates. Figure 9.45 shows an example of a titration curve for a mixture of I^- and Cl^- using Ag^+ as a titrant.

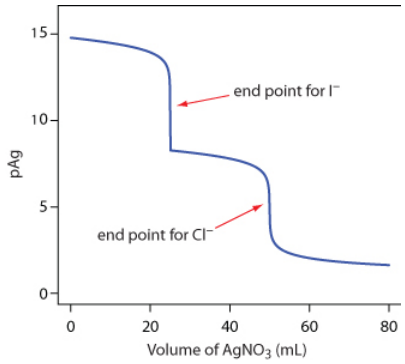


Figure 9.45 Titration curve for the titration of a 50.0 mL mixture of 0.0500 M I^- and 0.0500 M Cl^- using 0.100 M Ag^+ as a titrant. The red arrows show the end points. Note that the end point for I^- is earlier than the end point for Cl^- because AgI is less soluble than AgCl.

Contributors

- David Harvey (DePauw University)

9.5: Precipitation Titrations is shared under a CC BY-NC-SA 4.0 license and was authored, remixed, and/or curated by LibreTexts.

9.E: Titrimetric Methods (Exercises)

Some of the problems that follow require one or more equilibrium constants or standard state potentials. For your convenience, here are hyperlinks to the appendices containing these constants.

Appendix 10: Solubility Products
Appendix 11: Acid Dissociation Constants
Appendix 12: Metal-Ligand Formation Constants
Appendix 13: Standard State Reduction Potentials

1. Calculate or sketch titration curves for the following acid–base titrations.

a. 25.0 mL of 0.100 M NaOH with 0.0500 M HCl
b. 50.0 mL of 0.0500 M HCOOH with 0.100 M NaOH
c. 50.0 mL of 0.100 M NH_3 with 0.100 M HCl
d. 50.0 mL of 0.0500 M ethylenediamine with 0.100 M HCl
e. 50.0 mL of 0.0400 M citric acid with 0.120 M NaOH
f. 50.0 mL of 0.0400 M H_3PO_4 with 0.120 M NaOH

2. Locate the equivalence point for each titration curve in problem 1. What is the stoichiometric relationship between the moles of acid and the moles of base at each of these equivalence points?

3. Suggest an appropriate visual indicator for each of the titrations in problem 1.

4. In sketching the titration curve for a weak acid we approximate the pH at 10% of the equivalence point volume as $pK_a - 1$, and the pH at 90% of the equivalence point volume as $pK_a + 1$. Show that these assumptions are reasonable.

5. Tartaric acid, $H_2C_4H_4O_6$, is a diprotic weak acid with a pK_{a1} of 3.0 and a pK_{a2} of 4.4. Suppose you have a sample of impure tartaric acid (purity > 80%), and that you plan to determine its purity by titrating with a solution of 0.1 M NaOH using an indicator to signal the end point. Describe how you will carry out the analysis, paying particular attention to how much sample to use, the desired pH range for the indicator, and how you will calculate the %w/w tartaric acid.

6. The following data for the titration of a monoprotic weak acid with a strong base were collected using an automatic titrator. Prepare normal, first derivative, second derivative, and Gran plot titration curves for this data, and locate the equivalence point for each.

Volume of NaOH (ml)	pH	Volume of NaOH (mL)	pH
0.25	3.0	49.95	7.8
0.86	3.2	49.97	8.0
1.63	3.4	49.98	8.2
2.72	3.6	49.99	8.4
4.29	3.8	50.00	8.7
6.54	4.0	50.01	9.1
9.67	4.2	50.02	9.4
13.79	4.4	50.04	9.6
18.83	4.6	50.06	9.8
24.47	4.8	50.10	10.0
30.15	5.0	50.16	10.2
35.33	5.2	50.25	10.4
39.62	5.4	50.40	10.6
42.91	5.6	50.63	10.8
45.28	5.8	51.01	11.0
46.91	6.0	51.61	11.2
48.01	6.2	52.58	11.4
48.72	6.4	54.15	11.6
49.19	6.6	56.73	11.8
49.48	6.8	61.11	12.0
49.67	7.0	68.83	12.2
49.79	7.2	83.54	12.4
49.78	7.4	116.14	12.6
49.92	7.6		

7. Schwartz published the following simulated data for the titration of a 1.02×10^{-4} M solution of a monoprotic weak acid (pK_a = 8.16) with 1.004×10^{-3} M NaOH.[10] The simulation assumes that a 50-mL pipet is used to transfer a portion of the weak acid solution to the titration vessel. A calibration of the pipet shows that it delivers a volume of only 49.94 mL. Prepare normal, first derivative, second derivative, and Gran plot titration curves for this data, and determine the equivalence point for each. How do

these equivalence points compare to the expected equivalence point? Comment on the utility of each titration curve for the analysis of very dilute solutions of very weak acids.

mL of NaOH	pH	mL of NaOH	pH
0.03	6.212	4.79	8.858
0.09	6.504	4.99	8.926
0.29	6.936	5.21	8.994
0.72	7.367	5.41	9.056
1.06	7.567	5.61	9.118
1.32	7.685	5.85	9.180
1.53	7.776	6.05	9.231
1.76	7.863	6.28	9.283
1.97	7.938	6.47	9.327
2.18	8.009	6.71	9.374
2.38	8.077	6.92	9.414
2.60	8.146	7.15	9.451
2.79	8.208	7.36	9.484
3.01	8.273	7.56	9.514
3.41	8.332	7.79	9.545
3.60	8.458	8.21	9.572
3.80	8.521	8.44	9.599
3.99	8.584	8.64	9.645
4.18	8.650	8.84	9.666
4.40	8.720	9.07	9.688
4.57	8.784	9.27	9.706

8. Calculate or sketch the titration curve for a 50.0 mL solution of a 0.100 M monoprotic weak acid (pK_a = 8) with 0.1 M strong base in a nonaqueous solvent with $K_s = 10^{-20}$. You may assume that the change in solvent does not affect the weak acid's pK_a. Compare your titration curve to the titration curve when water is the solvent.

9. The titration of a mixture of *p*-nitrophenol (pK_a = 7.0) and *m*-nitrophenol (pK_a = 8.3) can be followed spectrophotometrically. Neither acid absorbs at a wavelength of 545 nm, but their respective conjugate bases do absorb at this wavelength. The *m*-nitrophenolate ion has a greater absorbance than an equimolar solution of the *p*-nitrophenolate ion. Sketch the spectrophotometric titration curve for a 50.00-mL mixture consisting of 0.0500 M *p*-nitrophenol and 0.0500 M *m*-nitrophenol with 0.100 M NaOH. Compare your result to the expected potentiometric titration curves.

10. The quantitative analysis for aniline ($C_6H_5NH_2$, $K_b = 3.94 \times 10^{-10}$) can be carried out by an acid–base titration using glacial acetic acid as the solvent and $HClO_4$ as the titrant. A known volume of sample containing 3–4 mmol of aniline is transferred to a 250-mL Erlenmeyer flask and diluted to approximately 75 mL with glacial acetic acid. Two drops of a methyl violet indicator are added, and the solution is titrated with previously standardized 0.1000 M $HClO_4$ (prepared in glacial acetic acid using anhydrous $HClO_4$) until the end point is reached. Results are reported as parts per million aniline.

(a) Explain why this titration is conducted using glacial acetic acid as the solvent instead of water.

(b) One problem with using glacial acetic acid as solvent is its relatively high coefficient of thermal expansion of 0.11%/°C. For example, 100.00 mL of glacial acetic acid at 25°C occupies 100.22 mL at 27°C. What is the effect on the reported concentration of aniline if the standardization of $HClO_4$ is conducted at a temperature that is lower than that for the analysis of the unknown?

(c) The procedure calls for a sample containing 3–4 mmoles of aniline. Why is this requirement necessary?

11. Using a ladder diagram, explain why the presence of dissolved CO_2 leads to a determinate error for the standardization of NaOH if the end point's pH falls between 6–10, but no determinate error if the end point's pH is less than 6.

12. A water sample's acidity is determined by titrating to fixed end point pHs of 3.7 and 8.3, with the former providing a measure of the concentration of strong acid, and the later a measure of the combined concentrations of strong acid and weak acid. Sketch a titration curve for a mixture of 0.10 M HCl and 0.10 M H_2CO_3 with 0.20 M strong base, and use it to justify the choice of these end points.

13. Ethylenediaminetetraacetic acid, H_4Y, is a weak acid with successive acid dissociation constants of 0.010, 2.19×10^{-3}, 6.92×10^{-7}, and 5.75×10^{-11}. Figure 9.46 shows a titration curve for H_4Y with NaOH. What is the stoichiometric relationship between H_4Y and NaOH at the equivalence point marked with the red arrow?

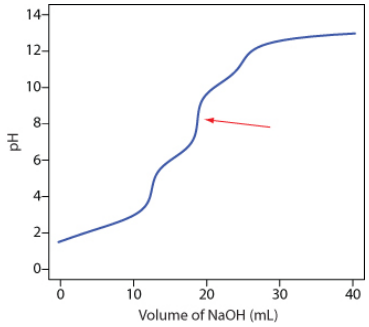


Figure 9.46 Titration curve for Problem 9.13.

14. A Gran plot method has been described for the quantitative analysis of a mixture consisting of a strong acid and a monoprotic weak acid.[11] A 50.00-mL mixture of HCl and CH_3COOH is transferred to an Erlenmeyer flask and titrated by using a digital pipet to add successive 1.00-mL aliquots of 0.09186 M NaOH. The progress of the titration is monitored by recording the pH after each

addition of titrant. Using the two papers listed in the footnote as a reference, prepare a Gran plot for the following data, and determine the concentrations of HCl and CH_3COOH.

Volume of NaOH (mL)	pH	Volume of NaOH (mL)	pH	Volume of NaOH (mL)	pH
1.00	1.83	24.00	4.45	47.00	12.14
2.00	1.86	25.00	4.53	48.00	12.17
3.00	1.89	26.00	4.61	49.00	12.20
4.00	1.92	27.00	4.69	50.00	12.23
5.00	1.95	28.00	4.76	51.00	12.26
6.00	1.99	29.00	4.84	52.00	12.28
7.00	2.03	30.00	4.93	53.00	12.30
8.00	2.10	31.00	5.02	54.00	12.32
9.00	2.18	32.00	5.13	55.00	12.34
10.00	2.31	33.00	5.23	56.00	12.36
11.00	2.51	34.00	5.37	57.00	12.38
12.00	2.81	35.00	5.52	58.00	12.39
13.00	3.16	36.00	5.75	59.00	12.40
14.00	3.36	37.00	6.14	60.00	12.42
15.00	3.54	38.00	10.30	61.00	12.43
16.00	3.69	39.00	11.31	62.00	12.44
17.00	3.81	40.00	11.58	63.00	12.45
18.00	3.93	41.00	11.74	64.00	12.47
19.00	4.02	42.00	11.85	65.00	12.48
20.00	4.14	43.00	11.93	66.00	12.49
21.00	4.22	44.00	12.00	67.00	12.50
22.00	4.30	45.00	12.05	68.00	12.51
23.00	4.38	46.00	12.10	69.00	12.52

15. Explain why it is not possible for a sample of water to simultaneously have OH^- and HCO_3^- as sources of alkalinity.

https://chem.libretexts.org/@go/page/70695

16. For each of the following, determine the sources of alkalinity (OH^-, HCO_3^-, CO_3^{2-}) and their respective concentrations in parts per million. In each case a 25.00-mL sample is titrated with 0.1198 M HCl to the bromocresol green and the phenolphthalein end points.

	Volume of HCl (mL) to the phenolphthalein end point	Volume of HCl (mL) to the bromocresol green end point
a	21.36	21.38
b	5.67	21.13
c	0.00	14.28
d	17.12	34.26
e	21.36	25.69

17. A sample may contain any of the following: HCl, NaOH, H_3PO_4, $H_2PO_4^-$, HPO_4^{2-}, or PO_4^{3-}. The composition of a sample is determined by titrating a 25.00-mL portion with 0.1198 M HCl or 0.1198 M NaOH to the phenolphthalein and the methyl orange end points. For each of the following, determine which species are present in the sample, and their respective molar concentrations.

	Titrant	Phenolphthalein end point volume (mL)	methyl orange end point volume (mL)
a	HCl	11.54	35.29
b	NaOH	19.79	9.89
c	HCl	22.76	22.78
d	NaOH	39.42	17.48

18. The protein in a 1.2846-g sample of an oat cereal is determined by a Kjeldahl analysis. The sample is digested with H_2SO_4, the resulting solution made basic with NaOH, and the NH_3 distilled into 50.00 mL of 0.09552 M HCl. The excess HCl is back titrated using 37.84 mL of 0.05992 M NaOH. Given that the proteins in grains average 17.54% w/w N, report the %w/w protein in the sample.

19. The concentration of SO_2 in air is determined by bubbling a sample of air through a trap containing H_2O_2. Oxidation of SO_2 by H_2O_2 results in the formation of H_2SO_4, which is then determined by titrating with NaOH. In a typical analysis, a sample of air was passed through the peroxide trap at a rate of 12.5 L/min for 60 min and required 10.08 mL of 0.0244 M NaOH to reach the phenolphthalein end point. Calculate the μL/L SO_2 in the sample of air. The density of SO_2 at the temperature of the air sample is 2.86 mg/mL.

20. The concentration of CO_2 in air is determined by an indirect acid–base titration. A sample of air is bubbled through a solution containing an excess of $Ba(OH)_2$, precipitating $BaCO_3$. The excess $Ba(OH)_2$ is back titrated with HCl. In a typical analysis a 3.5-L sample of air was bubbled through 50.00 mL of 0.0200 M $Ba(OH)_2$. Back titrating with 0.0316 M HCl required 38.58 mL to reach

the end point. Determine the ppm CO_2 in the sample of air given that the density of CO_2 at the temperature of the sample is 1.98 g/L.

21. The purity of a synthetic preparation of methylethyl ketone, C_3H_8O, is determined by reacting it with hydroxylamine hydrochloride, liberating HCl (see reaction in Table 9.8). In a typical analysis a 3.00-mL sample was diluted to 50.00 mL and treated with an excess of hydroxylamine hydrochloride. The liberated HCl was titrated with 0.9989 M NaOH, requiring 32.68 mL to reach the end point. Report the percent purity of the sample given that the density of methylethyl ketone is 0.805 g/mL.

22. Animal fats and vegetable oils are triesters formed from the reaction between glycerol (1,2,3-propanetriol) and three long-chain fatty acids. One of the methods used to characterize a fat or an oil is a determination of its saponification number. When treated with boiling aqueous KOH, an ester saponifies into the parent alcohol and fatty acids (as carboxylate ions). The saponification number is the number of milligrams of KOH required to saponify 1.000 gram of the fat or the oil. In a typical analysis a 2.085-g sample of butter is added to 25.00 mL of 0.5131 M KOH. After saponification is complete the excess KOH is back titrated with 10.26 mL of 0.5000 M HCl. What is the saponification number for this sample of butter?

23. A 250.0-mg sample of an organic weak acid is dissolved in an appropriate solvent and titrated with 0.0556 M NaOH, requiring 32.58 mL to reach the end point. Determine the compound's equivalent weight.

24. Figure 9.47 shows a potentiometric titration curve for a 0.4300-g sample of a purified amino acid that was dissolved in 50.00 mL of water and titrated with 0.1036 M NaOH. Identify the amino acid from the possibilities listed in the following table.

amino acid	formula weight (g/mol)	K_a
alanine	89.1	1.36×10^{-10}
glycine	75.1	1.67×10^{-10}
methionine	149.2	8.9×10^{-10}
taurine	125.2	1.8×10^{-9}
asparagine	150	1.9×10^{-9}
leucine	131.2	1.79×10^{-10}
phenylalanine	166.2	4.9×10^{-10}
valine	117.2	1.91×10^{-10}

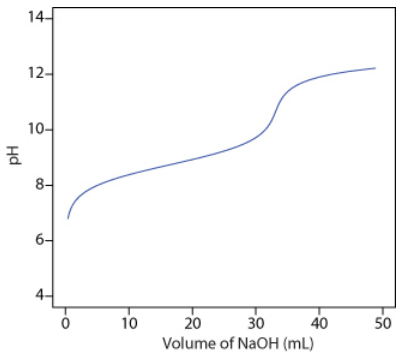


Figure 9.47 Titration curve for Problem 9.24.

25. Using its titration curve, determine the acid dissociation constant for the weak acid in problem 9.6.

26. Where in the scale of operations do the microtitration techniques discussed in section 9B.7 belong?

27. An acid–base titration may be used to determine an analyte's gram equivalent weight, but it can not be used to determine its gram formula weight. Explain why.

28. Commercial washing soda is approximately 30–40% w/w Na_2CO_3. One procedure for the quantitative analysis of washing soda contains the following instructions:

> Transfer an approximately 4-g sample of the washing soda to a 250-mL volumetric flask. Dissolve the sample in about 100 mL of H_2O and then dilute to the mark. Using a pipet, transfer a 25-mL aliquot of this solution to a 125-mL Erlenmeyer flask, and add 25-mL of H_2O and 2 drops of bromocresol green indicator. Titrate the sample with 0.1 M HCl to the indicator's end point.

What modifications, if any, are necessary if you want to adapt this procedure to evaluate the purity of commercial Na_2CO_3 that is >98% pure?

29. A variety of systematic and random errors are possible when standardizing a solution of NaOH against the primary weak acid standard potassium hydrogen phthalate (KHP). Identify, with justification, whether the following are systematic or random sources of error, or if they have no effect. If the error is systematic, then indicate whether the experimentally determined molarity for NaOH is too high or too low. The standardization reaction is

$$C_8H_5O_4^-(aq) + OH^-(aq) \rightarrow C_8H_4O_4^{2-}(aq) + H_2O(l) \tag{9.E.1}$$

(a) The balance used to weigh KHP is not properly calibrated and always reads 0.15 g too low.

(b) The indicator for the titration changes color between a pH of 3–4.

(c) An air bubble, which is lodged in the buret's tip at the beginning of the analysis, dislodges during the titration.

(d) Samples of KHP are weighed into separate Erlenmeyer flasks, but the balance is only tarred with the first flask.

(e) The KHP is not dried before it was used.

(f) The NaOH is not dried before it was used.

(g) The procedure states that the sample of KHP should be dissolved in 25 mL of water, but it is accidentally dissolved in 35 mL of water.

30. The concentration of *o*-phthalic acid in an organic solvent, such as *n*-butanol, is determined by an acid–base titration using aqueous NaOH as the titrant. As the titrant is added, the *o*-phthalic acid is extracted into the aqueous solution where it reacts with the titrant. The titrant must be added slowly to allow sufficient time for the extraction to take place.

(a) What type of error do you expect if the titration is carried out too quickly?

(b) Propose an alternative acid–base titrimetric method that allows for a more rapid determination of the concentration of *o*-phthalic acid in *n*-butanol.

31. Calculate or sketch titration curves for 50.00 mL of 0.0500 Mg^{2+} with 0.0500 M EDTA at a pH of 7 and 10. Locate the equivalence point for each titration curve.

32. Calculate or sketch titration curves for 25.0 mL of 0.0500 M Cu^{2+} with 0.025 M EDTA at a pH of 10, and in the presence of 10^{-3} M and 10^{-1} M NH_3. Locate the equivalence point for each titration curve.

33. Sketch the spectrophotometric titration curve for the titration of a mixture of 5.00×10^{-3} M Bi^{3+} and 5.00×10^{-3} M Cu^{2+} with 0.0100 M EDTA. Assume that only the Cu^{2+}–EDTA complex absorbs at the selected wavelength.

34. The EDTA titration of mixtures of Ca^{2+} and Mg^{2+} can be followed thermometrically because the formation of the Ca^{2+}–EDTA complex is exothermic and the formation of the Mg^{2+}–EDTA complex is endothermic. Sketch the thermometric titration curve for a mixture of 5.00×10^{-3} M Ca^{2+} and 5.00×10^{-3} M Mg^{2+} with 0.0100 M EDTA. The heats of formation for CaY^{2-} and MgY^{2-} are, respectively, –23.9 kJ/mole and 23.0 kJ/mole.

35. EDTA is one member of a class of aminocarboxylate ligands that form very stable 1:1 complexes with metal ions. The following table provides logK_f values for the complexes of six such ligands with Ca^{2+} and Mg^{2+}. Which ligand is the best choice for the direct titration of Ca^{2+} in the presence of Mg^{2+}?

		Mg^{2+}	Ca^{2+}
EDTA	ethylenediaminetetraacetic acid	8.7	10.7
HEDTA	N-hydroxyethylenediaminetriacetic acid	7.0	8.0
EEDTA	ethyletherdiaminetetraacetic acid	8.3	10.0
DGTA	ethyleneglycol-bis(β-aminoethylether)-N,N´-tetraacetic acid	5.4	10.9
DTPA	diethylenetriaminepentaacetic acid	9.0	10.7
CyDTA	cyclohexanediaminetetraacetic acid	10.3	12.3

36. The amount of calcium in physiological fluids can be determined by a complexometric titration with EDTA. In one such analysis a 0.100-mL sample of a blood serum was made basic by adding 2 drops of NaOH and titrated with 0.00119 M EDTA, requiring 0.268 mL to reach the end point. Report the concentration of calcium in the sample as milligrams Ca per 100 mL.

37. After removing the membranes from an eggshell, the shell is dried and its mass recorded as 5.613 g. The eggshell is transferred to a 250-mL beaker and dissolved in 25 mL of 6 M HCl. After filtering, the solution containing the dissolved eggshell is diluted to 250 mL in a volumetric flask. A 10.00-mL aliquot is placed in a 125-mL Erlenmeyer flask and buffered to a pH of 10. Titrating with 0.04988 M EDTA requires 44.11 mL to reach the end point. Determine the amount of calcium in the eggshell as %w/w $CaCO_3$.

38. The concentration of cyanide, CN^-, in a copper electroplating bath can be determined by a complexometric titration with Ag^+, forming the soluble $Ag(CN)_2^-$ complex. In a typical analysis a 5.00-mL sample from an electroplating bath is transferred to a 250-mL Erlenmeyer flask, and treated with 100 mL of H_2O, 5 mL of 20% w/v NaOH and 5 mL of 10% w/v KI. The sample is titrated with 0.1012 M $AgNO_3$, requiring 27.36 mL to reach the end point as signaled by the formation of a yellow precipitate of AgI. Report the concentration of cyanide as parts per million of NaCN.

39. Before the introduction of EDTA most complexation titrations used Ag^+ or CN^- as the titrant. The analysis for Cd^{2+}, for example, was accomplished indirectly by adding an excess of KCN to form $Cd(CN)_4^{2-}$, and back titrating the excess CN^- with Ag^+, forming $Ag(CN)_2^-$. In one such analysis a 0.3000-g sample of an ore was dissolved and treated with 20.00 mL of 0.5000 M KCN. The excess CN^- required 13.98 mL of 0.1518 M $AgNO_3$ to reach the end point. Determine the %w/w Cd in the ore.

40. Solutions containing both Fe^{3+} and Al^{3+} can be selectively analyzed for Fe^{3+} by buffering to a pH of 2 and titrating with EDTA. The pH of the solution is then raised to 5 and an excess of EDTA added, resulting in the formation of the Al^{3+}–EDTA complex. The excess EDTA is back-titrated using a standard solution of Fe^{3+}, providing an indirect analysis for Al^{3+}.

(a) At a pH of 2, verify that the formation of the Fe^{3+}–EDTA complex is favorable, and that the formation of the Al^{3+}–EDTA complex is not favorable.

(b) A 50.00-mL aliquot of a sample containing Fe^{3+} and Al^{3+} is transferred to a 250-mL Erlenmeyer flask and buffered to a pH of 2. A small amount of salicylic acid is added, forming the soluble red-colored Fe^{3+}–salicylic acid complex. The solution is titrated with 0.05002 M EDTA, requiring 24.82 mL to reach the end point as signaled by the disappearance of the Fe^{3+}–salicylic acid complex's red color. The solution is buffered to a pH of 5 and 50.00 mL of 0.05002 M EDTA is added. After ensuring that the formation of the Al^{3+}–EDTA complex is complete, the excess EDTA was back titrated with 0.04109 M Fe^{3+}, requiring 17.84 mL to reach the end point as signaled by the reappearance of the red-colored Fe^{3+}–salicylic acid complex. Report the molar concentrations of Fe^{3+} and Al^{3+} in the sample.

41. Prada and colleagues described an indirect method for determining sulfate in natural samples, such as seawater and industrial effluents.[12] The method consists of three steps: precipitating the sulfate as $PbSO_4$; dissolving the $PbSO_4$ in an ammonical solution

of excess EDTA to form the soluble PbY^{2-} complex; and titrating the excess EDTA with a standard solution of Mg^{2+}. The following reactions and equilibrium constants are known

$PbSO_4(s) \rightleftharpoons Pb^{2+}(aq) + SO_4^{2-}(aq)$	$K_{sp} = 1.6 \times 10^{-8}$
$Pb^{2+}(aq) + Y^{4-}(aq) \rightleftharpoons PbY^{2-}(aq)$	$K_f = 1.1 \times 10^{18}$
$Mg^{2+}(aq) + Y^{4-}(aq) \rightleftharpoons MgY^{2-}(aq)$	$K_f = 4.9 \times 10^{8}$
$Zn^{2+}(aq) + Y^{4-}(aq) \rightleftharpoons ZnY^{2-}(aq)$	$K_f = 3.2 \times 10^{16}$

(a) Verify that a precipitate of $PbSO_4$ dissolves in a solution of Y^{4-}.

(b) Sporek proposed a similar method using Zn^{2+} as a titrant and found that the accuracy was frequently poor.[13] One explanation is that Zn^{2+} might react with the PbY^{2-}complex, forming ZnY^{2-}. Show that this might be a problem when using Zn^{2+} as a titrant, but that it is not a problem when using Mg^{2+} as a titrant. Would such a displacement of Pb^{2+} by Zn^{2+} lead to the reporting of too much or too little sulfate?

(c) In a typical analysis, a 25.00-mL sample of an industrial effluent was carried through the procedure using 50.00 mL of 0.05000 M EDTA. Titrating the excess EDTA required 12.42 mL of 0.1000 M Mg^{2+}. Report the molar concentration of SO_4^{2-} in the sample of effluent.

42. Table 9.10 provides values for the fraction of EDTA present as Y^{4-}, $\alpha_{Y^{4-}}$. Values of $\alpha_{Y^{4-}}$ are calculated using the equation

$$\alpha_{Y^{4-}} = \frac{[Y^{4-}]}{C_{EDTA}} \tag{9.E.2}$$

where $[Y^{4-}]$ is the concentration of the fully deprotonated EDTA and C_{EDTA} is the total concentration of EDTA in all of its forms

$$C_{EDTA} = [H_6Y^{2+}] + [H_5Y^{+}] + [H_4Y] + [H_3Y^{-}] + [H_2Y^{2-}] + [HY^{3-}] + [Y^{4-}] \tag{9.E.3}$$

Using the following equilibria

$H_6Y^{2+}(aq) + H_2O(l) \rightleftharpoons H_3O^{+}(aq) + H_5Y^{+}(aq)$	K_{a1}
$H_5Y^{+}(aq) + H_2O(l) \rightleftharpoons H_3O^{+}(aq) + H_4Y(aq)$	K_{a2}
$H_4Y(aq) + H_2O(l) \rightleftharpoons H_3O^{+}(aq) + H_3Y^{-}(aq)$	K_{a3}
$H_3Y^{-}(aq) + H_2O(l) \rightleftharpoons H_3O^{+}(aq) + H_2Y^{2-}(aq)$	K_{a4}
$H_2Y^{2-}(aq) + H_2O(l) \rightleftharpoons H_3O^{+}(aq) + HY^{3-}(aq)$	K_{a5}
$HY^{3-}(aq) + H_2O(l) \rightleftharpoons H_3O^{+}(aq) + Y^{4-}(aq)$	K_{a6}

show that

$$\alpha_{Y^{4-}} = \frac{K_{a1}K_{a2}K_{a3}K_{a4}K_{a5}K_{a6}}{d} \tag{9.E.4}$$

where

$$d = [H^+]^6 + [H^+]^5K_{a1} + [H^+]^4K_{a1}K_{a2} + [H^+]^3K_{a1}K_{a2}K_{a3} + \tag{9.E.5}$$

$$[H^+]^2K_{a1}K_{a2}K_{a3}K_{a4} + [H^+]^1K_{a1}K_{a2}K_{a3}K_{a4}K_{a5} + K_{a1}K_{a2}K_{a3}K_{a4}K_{a5}K_{a6} \tag{9.E.6}$$

43. Calculate or sketch titration curves for the following (unbalanced) redox titration reactions at 25ºC. Assume the analyte is initially present at a concentration of 0.0100 M and that a 25.0-mL sample is taken for analysis. The titrant, which is the underlined species in each reaction, is 0.0100 M.

(a) $V^{2+}(aq) + \underline{Ce^{4+}}(aq) \rightarrow V^{3+}(aq) + Ce^{3}+(aq)$
(b) $Ti^{2+}(aq) + \underline{Fe^{3+}}(aq) \rightarrow Ti^{3+}(aq) + Fe^{2+}(aq)$
(c) $Fe^{2+}(aq) + \underline{MnO_4^{-}}(aq) \rightarrow Fe^{3+}(aq) + Mn^{2+}(aq)$ (at pH = 1)

44. What is the equivalence point for each titration in problem 43?

45. Suggest an appropriate indicator for each titration in problem 43.

46. The iron content of an ore can be determined by a redox titration using $K_2Cr_2O_7$ as the titrant. A sample of the ore is dissolved in concentrated HCl using Sn^{2+} to speed its dissolution by reducing Fe^{3+} to Fe^{2+}. After the sample is dissolved, Fe^{2+} and any excess Sn^{2+} are oxidized to Fe^{3+} and Sn^{4+} using MnO_4^-. The iron is then carefully reduced to Fe^{2+} by adding a 2–3 drop excess of Sn^{2+}. A solution of $HgCl_2$ is added and, if a white precipitate of Hg_2Cl_2 forms, the analysis is continued by titrating with $K_2Cr_2O_7$. The sample is discarded without completing the analysis if a precipitate of Hg_2Cl_2 does not form, or if a gray precipitate (due to Hg) forms.

(a) Explain why the analysis is not completed if a white precipitate of Hg_2Cl_2 forms, or if a gray precipitate forms.

(b) Is a determinate error introduced if the analyst forgets to add Sn^{2+} in the step where the iron ore is dissolved?

(c) Is a determinate error introduced if the iron is not quantitatively oxidized back to Fe^{3+} by the MnO_4^-?

47. The amount of Cr^{3+} in an inorganic salt can be determined by a redox titration. A portion of sample containing approximately 0.25 g of Cr^{3+} is accurately weighed and dissolved in 50 mL of H_2O. The Cr^{3+} is oxidized to $Cr_2O_7^{2-}$ by adding 20 mL of 0.1 M $AgNO_3$, which serves as a catalyst, and 50 mL of 10%w/v $(NH_4)_2S_2O_8$, which serves as the oxidizing agent. After the reaction is complete the resulting solution is boiled for 20 minutes to destroy the excess $S_2O_8^{2-}$, cooled to room temperature, and diluted to 250 mL in a volumetric flask. A 50-mL portion of the resulting solution is transferred to an Erlenmeyer flask, treated with 50 mL of a standard solution of Fe^{2+}, and acidified with 200 mL of 1 M H_2SO_4, reducing the $Cr_2O_7^{2-}$ to Cr^{3+}. The excess Fe^{2+} is then determined by a back titration with a standard solution of $K_2Cr_2O_7$ using an appropriate indicator. The results are reported as %w/w Cr^{3+}.

(a) There are several places in the procedure where a reagent's volume is specified (see underlined text). Which of these measurements must be made using a volumetric pipet?

(b) Excess peroxydisulfate, $S_2O_8^{2-}$ is destroyed by boiling the solution. What is the effect on the reported %w/w Cr^{3+} if some of the $S_2O_8^{2-}$ is not destroyed during this step?

(c) Solutions of Fe^{2+} undergo slow air oxidation to Fe^{3+}. What is the effect on the reported %w/w Cr^{3+} if the standard solution of Fe^{2+} is inadvertently allowed to be partially oxidized?

48. The exact concentration of H_2O_2 in a solution that is nominally 6% w/v H_2O_2 can be determined by a redox titration with MnO_4^-. A 25-mL aliquot of the sample is transferred to a 250-mL volumetric flask and diluted to volume with distilled water. A 25-mL aliquot of the diluted sample is added to an Erlenmeyer flask, diluted with 200 mL of distilled water, and acidified with 20 mL of 25% v/v H_2SO_4. The resulting solution is titrated with a standard solution of $KMnO_4$ until a faint pink color persists for 30 s. The results are reported as %w/v H_2O_2.

(a) Many commercially available solutions of H_2O_2 contain an inorganic or organic stabilizer to prevent the autodecomposition of the peroxide to H_2O and O_2. What effect does the presence of this stabilizer have on the reported %w/v H_2O_2 if it also reacts with MnO_4^-?

(b) Laboratory distilled water often contains traces of dissolved organic material that may react with MnO_4^-. Describe a simple method to correct for this potential interference.

(c) What modifications to the procedure, if any, are need if the sample has a nominal concentration of 30% w/v H_2O_2.

49. The amount of iron in a meteorite was determined by a redox titration using $KMnO_4$ as the titrant. A 0.4185-g sample was dissolved in acid and the liberated Fe^{3+} quantitatively reduced to Fe^{2+} using a Walden reductor. Titrating with 0.02500 M $KMnO_4$ requires 41.27 mL to reach the end point. Determine the %w/w Fe_2O_3 in the sample of meteorite.

50. Under basic conditions, MnO_4^- can be used as a titrant for the analysis of Mn^{2+}, with both the analyte and the titrant forming MnO_2. In the analysis of a mineral sample for manganese, a 0.5165-g sample is dissolved and the manganese reduced to Mn^{2+}. The solution is made basic and titrated with 0.03358 M $KMnO_4$, requiring 34.88 mL to reach the end point. Calculate the %w/w Mn in the mineral sample.

51. The amount of uranium in an ore can be determined by a redox back titration. The analysis is accomplished by dissolving the ore in sulfuric acid and reducing the resulting UO_2^{2+} to U^{4+} with a Walden reductor. The resulting solution is treated with an excess of Fe^{3+}, forming Fe^{2+} and U^{6+}. The Fe^{2+} is titrated with a standard solution of $K_2Cr_2O_7$. In a typical analysis a 0.315-g sample of ore is passed through the Walden reductor and treated with 50.00 mL of 0.0125 M Fe^{3+}. Back titrating with 0.00987 M $K_2Cr_2O_7$ requires 10.52 mL. What is the %w/w U in the sample?

52. The thickness of the chromium plate on an auto fender was determined by dissolving a 30.0-cm^2 section in acid, and oxidizing the liberated Cr^{3+} to $Cr_2O_7^{2-}$ with peroxydisulfate. After removing the excess peroxydisulfate by boiling, 500.0 mg of $Fe(NH_4)_2(SO_4)_2 \cdot 6H_2O$ was added, reducing the $Cr_2O_7^{2-}$ to Cr^{3+}. The excess Fe^{2+} was back titrated, requiring 18.29 mL of 0.00389 M $K_2Cr_2O_7$ to reach the end point. Determine the average thickness of the chromium plate given that the density of Cr is 7.20 g/cm^3.

53. The concentration of CO in air can be determined by passing a known volume of air through a tube containing I_2O_5, forming CO_2 and I_2. The I_2 is removed from the tube by distilling it into a solution containing an excess of KI, producing I_3^-. The I_3^- is titrated with a standard solution of $Na_2S_2O_3$. In a typical analysis a 4.79-L sample of air was sampled as described here, requiring 7.17 mL of 0.00329 M $Na_2S_2O_3$ to reach the end point. If the air has a density of 1.23×10^{-3} g/mL, determine the parts per million CO in the air.

54. The level of dissolved oxygen in a water sample can be determined by the Winkler method. In a typical analysis a 100.0-mL sample is made basic and treated with a solution of $MnSO_4$, resulting in the formation of MnO_2. An excess of KI is added and the solution is acidified, resulting in the formation of Mn^{2+} and I_2. The liberated I_2 is titrated with a solution of 0.00870 M $Na_2S_2O_3$, requiring 8.90 mL to reach the starch indicator end point. Calculate the concentration of dissolved oxygen as parts per million O_2.

55. The analysis for Cl^- using the Volhard method requires a back titration. A known amount of $AgNO_3$ is added, precipitating AgCl. The unreacted Ag^+ is determined by back titrating with KSCN. There is a complication, however, because AgCl is more soluble than AgSCN.

(a) Why do the relative solubilities of AgCl and AgSCN lead to a titration error?

(b) Is the resulting titration error a positive or a negative determinate error?

(c) How might you modify the procedure to prevent this eliminate this source of determinate error?

(d) Will this source of determinate error be of concern when using the Volhard method to determine Br^-?

56. Voncina and co-workers suggest that a precipitation titration can be monitored by measuring pH as a function of the volume of titrant if the titrant is a weak base.[14] For example, when titrating Pb^{2+} with CrO_4^{2-} the solution containing the analyte is initially acidified to a pH of 3.50 using HNO_3. Before the equivalence point the concentration of CrO_4^{2-} is controlled by the solubility product of $PbCrO_4$. After the equivalence point the concentration of CrO_4^{2-} is determined by the amount of excess titrant. Considering the reactions controlling the concentration of CrO_4^{2-}, sketch the expected titration curve of pH versus volume of titrant.

57. Calculate or sketch the titration curve for the titration of 50.0 mL of 0.0250 M KI with 0.0500 M $AgNO_3$. Prepare separate titration curve using pAg and pI on the *y*-axis.

58. Calculate or sketch the titration curve for the titration of 25.0 mL mixture of 0.0500 M KI and 0.0500 M KSCN with 0.0500 M $AgNO_3$.

59. A 0.5131-g sample containing KBr is dissolved in 50 mL of distilled water. Titrating with 0.04614 M $AgNO_3$ requires 25.13 mL to reach the Mohr end point. A blank titration requires 0.65 mL to reach the same end point. Report the %w/w KBr in the sample.

60. A 0.1093-g sample of impure Na_2CO_3 was analyzed by the Volhard method. After adding 50.00 mL of 0.06911 M $AgNO_3$, the sample was back titrated with 0.05781 M KSCN, requiring 27.36 mL to reach the end point. Report the purity of the Na_2CO_3 sample.

61. A 0.1036-g sample containing only $BaCl_2$ and NaCl is dissolved in 50 mL of distilled water. Titrating with 0.07916 M $AgNO_3$ requires 19.46 mL to reach the Fajans end point. Report the %w/w $BaCl_2$ in the sample.

9.6.3 Solutions to Practice Exercises

Practice Exercise 9.1

The volume of HCl needed to reach the equivalence point is

$$V_{eq} = V_a = \frac{M_b V_b}{M_a} = \frac{(0.125\ \text{M})(25.0\ \text{mL})}{0.0625\ \text{M}} = 50.0\ \text{mL} \tag{9.E.7}$$

Before the equivalence point, NaOH is present in excess and the pH is determined by the concentration of unreacted OH^-. For example, after adding 10.0 mL of HCl

$$[OH^-] = \frac{(0.125\ \text{M})(25.0\ \text{mL}) - (0.0625\ \text{M})(10.0\ \text{mL})}{25.0\ \text{mL} + 10.0\ \text{mL}} = 0.0714\ \text{M} \tag{9.E.8}$$

$$[H_3O^+] = \frac{K_w}{[OH^-]} = \frac{1.0 \times 10^{-14}}{0.0714\ \text{M}} = 1.40 \times 10^{-13}\ \text{M} \tag{9.E.9}$$

the pH is 12.85.

For the titration of a strong base with a strong acid the pH at the equivalence point is 7.00.

For volumes of HCl greater than the equivalence point, the pH is determined by the concentration of excess HCl. For example, after adding 70.0 mL of titrant the concentration of HCl is

$$[HCl] = \frac{(0.0625\ \text{M})(70.0\ \text{mL}) - (0.125\ \text{M})(25.0\ \text{mL})}{70.0\ \text{mL} + 25.0\ \text{mL}} = 0.0132\ \text{M} \tag{9.E.10}$$

giving a pH of 1.88. Some additional results are shown here.

Volume of HCl (mL)	pH	Volume of HCl (mL)	pH
0	13.10	60	2.13
10	12.85	70	1.88
20	12.62	80	1.75
30	12.36	90	1.66
40	11.98	100	1.60
50	7.00		

Click here to return to the chapter.

Practice Exercise 9.2

The volume of HCl needed to reach the equivalence point is

$$V_{eq} = V_a = \frac{M_b V_b}{M_a} = \frac{(0.125\ \text{M})(25.0\ \text{mL})}{0.0625\ \text{M}} = 50.0\ \text{mL} \tag{9.E.11}$$

Before adding HCl the pH is that for a solution of 0.100 M NH_3.

$$K_b = \frac{[OH^-][NH_4^+]}{[NH_3]} = \frac{(x)(x)}{0.125 - x} = 1.75 \times 10^{-5} \tag{9.E.12}$$

$$x = [OH^-] = 1.47 \times 10^{-3}\ \text{M} \tag{9.E.13}$$

The pH at the beginning of the titration, therefore, is 11.17.

Before the equivalence point the pH is determined by an NH_3/NH_4^+ buffer. For example, after adding 10.0 mL of HCl

$$[NH_3] = \frac{(0.125\ \text{M})(25.0\ \text{mL}) - (0.0625\ \text{M})(10.0\ \text{mL})}{25.0\ \text{mL} + 10.0\ \text{mL}} = 0.0714\ \text{M} \tag{9.E.14}$$

$$[NH_4^+] = \frac{(0.0625\ M)(10.0\ mL)}{25.0\ mL + 10.0\ mL} = 0.0179\ M \tag{9.E.15}$$

$$pH = 9.244 + \log \frac{0.0714\ M}{0.0179\ M} = 9.84 \tag{9.E.16}$$

At the equivalence point the predominate ion in solution is NH_4^+. To calculate the pH we first determine the concentration of NH_4^+

$$[NH_4^+] = \frac{(0.125\ M)(25.0\ mL)}{25.0\ mL + 50.0\ mL} = 0.0417\ M \tag{9.E.17}$$

and then calculate the pH

$$K_a = \frac{[H_3O^+][NH_3]}{[NH_4^+]} = \frac{(x)(x)}{0.0417 - x} = 5.70 \times 10^{-10} \tag{9.E.18}$$

$$x = [H_3O^+] = 4.88 \times 10^{-6}\ M \tag{9.E.19}$$

obtaining a value of 5.31.

After the equivalence point, the pH is determined by the excess HCl. For example, after adding 70.0 mL of HCl

$$[HCl] = \frac{(0.0625\ M)(70.0\ mL) - (0.125\ M)(25.0\ mL)}{25.0\ mL + 70.0\ mL} = 0.0132\ M \tag{9.E.20}$$

and the pH is 1.88. Some additional results are shown here.

Volume of HCl (mL)	pH	Volume of HCl (mL)	pH
0	11.17	60	2.13
10	9.84	70	1.88
20	9.42	80	1.75
30	9.07	90	1.66
40	8.64	100	1.60
50	5.31		

Click here to return to the chapter.

Practice Exercise 9.3

Figure 9.48 shows a sketch of the titration curve. The two points before the equivalence point (V_{HCl} = 5 mL, pH = 10.24 and V_{HCl} = 45 mL, pH = 8.24) are plotted using the pK_a of 9.244 for NH_4^+. The two points after the equivalence point (V_{HCl} = 60 mL, pH = 2.13 and V_{HCl} = 80 mL, pH = 1.75) are from the answer to Practice Exercise 9.2.

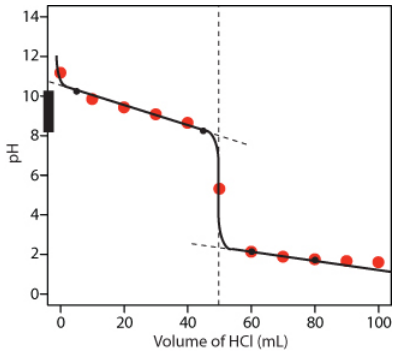


Figure 9.48 Titration curve for Practice Exercise 9.3. The black dots and curve are the approximate sketch of the titration curve. The points in red are the calculations from Practice Exercise 9.2.

Click here to return to the chapter.

Practice Exercise 9.4

Figure 9.49 shows a sketch of the titration curve. The titration curve has two equivalence points, one at 25.0 mL ($H_2A \rightarrow HA^-$) and one at 50.0 mL ($HA^- \rightarrow A^{2-}$). In sketching the curve, we plot two points before the first equivalence point using the pK_a of 3 for H_2A

$$V_{HCl} = 2.5 \text{ mL, pH} = 2 \text{ and } V_{HCl} = 22.5 \text{ mL, pH} = 4 \tag{9.E.21}$$

two points between the equivalence points using the pK_a of 5 for HA^-

$$V_{HCl} = 27.5 \text{ mL, pH} = 3, \text{ and } V_{HCl} = 47.5 \text{ mL, pH} = 5 \tag{9.E.22}$$

and two points after the second equivalence point

$$V_{HCl} = 70 \text{ mL, pH} = 12.22 \text{ and } V_{HCl} = 90 \text{ mL, pH} = 12.46 \tag{9.E.23}$$

Drawing a smooth curve through these points presents us with the following dilemma—the pH appears to increase as the titrant's volume approaches the first equivalence point and then appears to decrease as it passes through the first equivalence point. This is, of course, absurd; as we add NaOH the pH cannot decrease. Instead, we model the titration curve before the second equivalence point by drawing a straight line from the first point (V_{HCl} = 2.5 mL, pH = 2) to the fourth (V_{HCl} = 47.5 mL, pH = 5), ignoring the second and third points. The results is a reasonable approximation of the exact titration curve.

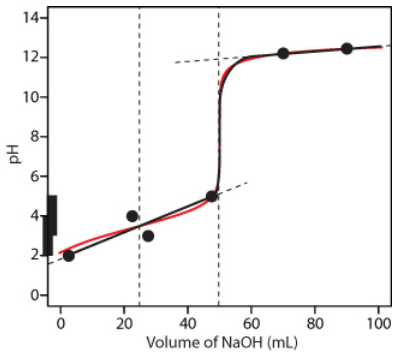


Figure 9.49 Titration curve for Practice Exercise 9.4. The black points and curve are the approximate titration curve, and the red curve is the exact titration curve.

Click here to return to the chapter.

Practice Exercise 9.5

The pH at the equivalence point is 5.31 (see Practice Exercise 9.2) and the sharp part of the titration curve extends from a pH of approximately 7 to a pH of approximately 4. Of the indicators in Table 9.4, methyl red is the best choice because its pK_a value of 5.0 is closest to the equivalence point's pH and because the pH range of 4.2–6.3 for its change in color will not produce a significant titration error.

Click here to return to the chapter.

Practice Exercise 9.6

Because salicylic acid is a diprotic weak acid, we must first determine to which equivalence point it is being titrated. Using salicylic acid's pK_a values as a guide, the pH at the first equivalence point is between a pH of 2.97 and 13.74, and the second equivalence points is at a pH greater than 13.74. From Table 9.4, phenolphthalein's end point falls in the pH range 8.3–10.0. The titration, therefore, is to the first equivalence point for which the moles of NaOH equal the moles of salicylic acid; thus

$$\frac{0.1354 \text{ mol NaOH}}{\text{L}} \times 0.02192 \text{ L} = 2.968 \times 10^{-3} \text{ mol NaOH} \tag{9.E.24}$$

$$2.968 \times 10^{-3} \text{ mol NaOH} \times \frac{1 \text{ mol } C_7H_6O_3}{\text{mol NaOH}} \times \frac{138.12 \text{ g } C_7H_6O_3}{\text{mol } C_7H_6O_3} = 0.4099 \text{ g } C_7H_6O_3 \tag{9.E.25}$$

$$\frac{0.4099 \text{ g } C_7H_6O_3}{0.4208 \text{ g sample}} \times 100 = 97.41\% \text{ w/w } C_7H_6O_3 \tag{9.E.26}$$

Because the purity of the sample is less than 99%, we reject the shipment.

Click here to return to the chapter.

Practice Exercise 9.7

The moles of HNO_3 produced by pulling the air sample through the solution of H_2O_2 is

$$\frac{0.01012 \text{ mol NaOH}}{\text{L}} \times 0.00914 \text{ L} \times \frac{1 \text{ mol } HNO_3}{\text{mol NaOH}} = 9.25 \times 10^{-5} \text{ mol } HNO_3 \tag{9.E.27}$$

A conservation of mass on nitrogen requires that each mole of NO_2 in the sample of air produces one mole of HNO_3; thus, the mass of NO_2 in the sample is

$$9.25 \times 10^{-5} \text{ mol } HNO_3 \times \frac{1 \text{ mol } NO_2}{\text{mol } HNO_3} \times \frac{46.01 \text{ g } NO_2}{\text{mol } NO_2} = 4.26 \times 10^{-3} \text{ g } NO_2 \tag{9.E.28}$$

and the concentration of NO_2 is

$$\frac{4.26 \times 10^{-3} \text{ g } NO_2}{5 \text{ L air}} \times \frac{1000 \text{ mg}}{\text{g}} = 0.852 \text{ mg } NO_2\text{/L air} \tag{9.E.29}$$

Click here to return to the chapter.

Practice Exercise 9.8

The total moles of HCl used in this analysis is

$$\frac{1.396 \text{ mol NaOH}}{\text{L}} \times 0.01000 \text{ L} = 1.396 \times 10^{-2} \text{ mol HCl} \tag{9.E.30}$$

Of this,

$$\frac{0.1004 \text{ mol NaOH}}{\text{L}} \times 0.03996 \text{ L} \times \frac{1 \text{ mol HCl}}{\text{mol NaOH}} = 4.012 \times 10^{-3} \text{ mol HCl} \tag{9.E.31}$$

are consumed in the back titration with NaOH, which means that

$$1.396 \times 10^{-2} \text{ mol HCl} - 4.012 \times 10^{-3} \text{ mol HCl} = 9.95 \times 10^{-3} \text{ mol HCl} \tag{9.E.32}$$

react with the $CaCO_3$. Because CO_3^{2-} is dibasic, each mole of $CaCO_3$ consumes two moles of HCl; thus

$$9.95 \times 10^{-3} \text{ mol HCl} \times \frac{1 \text{ mol } CaCO_3}{2 \text{ mol HCl}} \times \frac{100.09 \text{ g } CaCO_3}{\text{mol } CaCO_3} = 0.498 \text{ g } CaCO_3 \tag{9.E.33}$$

$$\frac{0.498 \text{ g } CaCO_3}{0.5143 \text{ g sample}} \times 100 = 96.8\% \text{ w/w } CaCO_3 \tag{9.E.34}$$

Click here to return to the chapter.

Practice Exercise 9.9

Of the two analytes, 2-methylanilinium is the stronger acid and is the first to react with the titrant. Titrating to the bromocresol purple end point, therefore, provides information about the amount of 2-methylanilinium in the sample.

$$\frac{0.200 \text{ mol NaOH}}{\text{L}} \times 0.01965 \text{ L} \times \frac{1 \text{ mol } C_7H_{10}NCl}{\text{mol NaOH}} \times \frac{143.61 \text{ g } C_7H_{10}NCl}{\text{mol } C_7H_{10}NCl} = 0.564 \text{ g } C_7H_{10}NCl \tag{9.E.35}$$

$$\frac{0.564 \text{ g } C_7H_{10}NCl}{2.006 \text{ g sample}} \times 100 = 28.1\% \text{ w/w } C_7H_{10}NCl \tag{9.E.36}$$

Titrating from the bromocresol purple end point to the phenolphthalein end point, a total of 48.41 mL – 19.65 mL, or 28.76 mL, gives the amount of NaOH reacting with 3-nitrophenol. The amount of 3-nitrophenol in the sample, therefore, is

$$\frac{0.200 \text{ mol NaOH}}{\text{L}} \times 0.02876 \text{ L} \times \frac{1 \text{ mol } C_6H_5NO_3}{\text{mol NaOH}} \times \frac{139.11 \text{ g } C_6H_5NO_3}{\text{mol } C_6H_5NO_3} = 0.800 \text{ g } C_6H_5NO_3 \tag{9.E.37}$$

$$\frac{0.800 \text{ g } C_6H_5NO_3}{2.006 \text{ g sample}} \times 100 = 38.8\% \text{ w/w } C_6H_5NO_3 \tag{9.E.38}$$

Click here to return to the chapter.

Practice Exercise 9.10

The first of the two visible end points is approximately 37 mL of NaOH. The analyte's equivalent weight, therefore, is

$$\frac{0.1032 \text{ mol NaOH}}{\text{L}} \times 0.037 \text{ L} \times \frac{1 \text{ equivalent}}{\text{mol NaOH}} = 3.8 \times 10^{-3} \text{ equivalents} \tag{9.E.39}$$

$$EW = \frac{0.5000 \text{ g}}{3.8 \times 10^{-3} \text{ equivalents}} = 1.3 \times 10^{2} \text{ g/equivalent} \tag{9.E.40}$$

Click here to return to the chapter.

Practice Exercise 9.11

At ½V_{eq}, or approximately 18.5 mL, the pH is approximately 2.2; thus, we estimate that the analyte's pK_a is 2.2.

Click here to return to the chapter.

Practice Exercise 9.12

Let's begin with the calculations at a pH of 10. At a pH of 10 some of the EDTA is present in forms other than Y^{4-}. To evaluate the titration curve, therefore, we need the conditional formation constant for CdY^{2-}, which, from Table 9.11 is $K_f' = 1.1 \times 10^{16}$. Note that the conditional formation constant is larger in the absence of an auxiliary complexing agent.

The titration's equivalence point requires

$$V_{eq} = V_{EDTA} = \frac{M_{Cd}V_{Cd}}{M_{EDTA}} = \frac{(5.00 \times 10^{-3} \text{ M})(50.0 \text{ mL})}{0.0100 \text{ M}} = 25.0 \text{ mL} \tag{9.E.41}$$

of EDTA.

Before the equivalence point, Cd^{2+} is present in excess and pCd is determined by the concentration of unreacted Cd^{2+}. For example, after adding 5.00 mL of EDTA, the total concentration of Cd^{2+} is

$$[Cd^{2+}] = \frac{(5.00 \times 10^{-3} \text{ M})(50.0 \text{ mL}) - (0.0100 \text{ M})(5.00 \text{ mL})}{50.0 \text{ mL} + 5.00 \text{ mL}} \tag{9.E.42}$$

$$= 3.64 \times 10^{-3} \text{ M} \tag{9.E.43}$$

which gives a pCd of 2.43.

At the equivalence point all the Cd^{2+} initially in the titrand is now present as CdY^{2-}. The concentration of Cd^{2+}, therefore, is determined by the dissociation of the CdY^{2-} complex. First, we calculate the concentration of CdY^{2-}.

$$[CdY^{2-}] = \frac{(5.00 \times 10^{-3} \text{ M})(50.0 \text{ mL})}{50.0 \text{ mL} + 25.0 \text{ mL}} = 3.33 \times 10^{-3} \text{ M} \tag{9.E.44}$$

Next, we solve for the concentration of Cd^{2+} in equilibrium with CdY^{2-}.

$$K_f' = \frac{[CdY^{2-}]}{[Cd^{2+}]C_{EDTA}} = \frac{3.33 \times 10^{-3} - x}{(x)(x)} = 1.1 \times 10^{16} \tag{9.E.45}$$

Solving gives $[Cd^{2+}]$ as 5.50×10^{-10} M, or a pCd of 9.26 at the equivalence point.

After the equivalence point, EDTA is in excess and the concentration of Cd^{2+} is determined by the dissociation of the CdY^{2-} complex. First, we calculate the concentrations of CdY^{2-} and of unreacted EDTA. For example, after adding 30.0 mL of EDTA

$$[CdY^{2-}] = \frac{(5.00 \times 10^{-3}\ M)(50.0\ mL)}{50.0\ mL + 30.0\ mL} = 3.13 \times 10^{-3}\ M \tag{9.E.46}$$

$$C_{EDTA} = \frac{(0.0100\ M)(30.0\ mL) - (5.00 \times 10^{-3}\ M)(50.0\ mL)}{50.0\ mL + 30.0\ mL} \tag{9.E.47}$$

$$= 6.25 \times 10^{-4}\ M \tag{9.E.48}$$

Substituting into the equation for the conditional formation constant and solving for $[Cd^{2+}]$ gives

$$\frac{3.13 \times 10^{-3}\ M}{[Cd^{2+}](6.25 \times 10^{-4}\ M)} = 1.1 \times 10^{16} \tag{9.E.49}$$

$[Cd^{2+}]$ as 4.55×10^{-16} M, or a pCd of 15.34.

The calculations at a pH of 7 are identical, except the conditional formation constant for CdY^{2-} is 1.5×10^{13} instead of 1.1×10^{16}. The following table summarizes results for these two titrations as well as the results from Table 9.13 for the titration of Cd^{2+} at a pH of 10 in the presence of 0.0100 M NH_3 as an auxiliary complexing agent.

Volume of EDTA (mL)	pCd at pH 10	pCd at pH 10 w/ 0.0100 M NH_3	pCd at pH 7
0	2.30	3.36	2.30
5.00	2.43	3.49	2.43
10.0	2.60	3.66	2.60
15.0	2.81	3.87	2.81
20.0	3.15	4.20	3.15
23.0	3.56	4.62	3.56
25.0	9.26	9.77	7.83
27.0	14.94	14.95	12.08
30.0	15.34	15.33	12.48
35.0	15.61	15.61	12.78
40.0	15.76	15.76	12.95
45.0	15.86	15.86	13.08
50.0	15.94	15.94	13.18

Examining these results allows us to draw several conclusions. First, in the absence of an auxiliary complexing agent the titration curve before the equivalence point is independent of pH (compare columns 2 and 4). Second, for any pH, the titration curve after the equivalence point is the same regardless of whether or not an auxiliary complexing agent is present (compare columns 2 and 3). Third, the largest change in pH through the equivalence point occurs at higher pHs and in the absence of an auxiliary complexing agent. For example, from 23.0 mL to 27.0 mL of EDTA the change in pCd is 11.38 at a pH of 10, 10.33 at a pH of 10 and in the presence of 0.0100 M NH_3, and 8.52 at a pH of 7.

Click here to return to the chapter.

Practice Exercise 9.13

Figure 9.50 shows a sketch of the titration curves. The two points before the equivalence point (V_{EDTA} = 5 mL, pCd = 2.43 and V_{EDTA} = 15 mL, pCd = 2.81) are the same for both pHs and are taken from the results of Practice Exercise 9.12. The two points

after the equivalence point for a pH of 7 (V_{EDTA} = 27.5 mL, pCd = 12.2 and V_{EDTA} = 50 mL, pCd = 13.2) are plotted using the logK_f' of 13.2 for CdY^{2-}. The two points after the equivalence point for a pH of 10 (V_{EDTA} = 27.5 mL, pCd = 15.0 and V_{EDTA} = 50 mL, pCd = 16.0) are plotted using the logK_f' of 16.0 for CdY^{2-}.

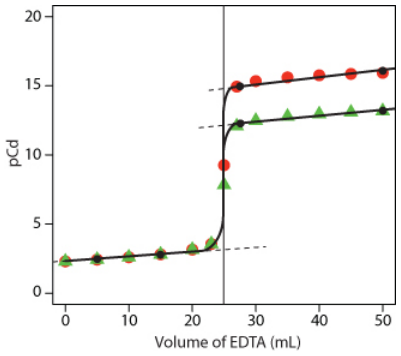


Figure 9.50 Titration curve for Practice Exercise 9.13. The black dots and curve are the approximate sketches of the two titration curves. The points in red are the calculations from Practice Exercise 9.12 for a pH of 10, and the points in green are the calculations from Practice Exercise 9.12 for a pH of 7.

Click here to return to the chapter.

Practice Exercise 9.14

In an analysis for hardness we treat the sample as if Ca^{2+} is the only metal ion reacting with EDTA. The grams of Ca^{2+} in the sample, therefore, is

$$\frac{0.0109 \text{ mol EDTA}}{\text{L}} \times 0.02363 \text{ L} \times \frac{1 \text{ mol } Ca^{2+}}{\text{mol EDTA}} = 2.58 \times 10^{-4} \text{ mol } Ca^{2+} \tag{9.E.50}$$

$$2.58 \times 10^{-4} \text{ mol } Ca^{2+} \times \frac{1 \text{ mol } CaCO_3}{\text{mol } Ca^{2+}} \times \frac{100.09 \text{ g } CaCO_3}{\text{mol } CaCO_3} = 0.0258 \text{ g } CaCO_3 \tag{9.E.51}$$

and the sample's hardness is

$$\frac{0.0258 \text{ g } CaCO_3}{0.1000 \text{ L}} \times \frac{1000 \text{ mg}}{\text{g}} = 258 \text{ mg } CaCO_3/\text{L} \tag{9.E.52}$$

Click here to return to the chapter.

Practice Exercise 9.15

The titration of CN^- with Ag^+ produces a metal-ligand complex of $Ag(CN)_2^{2-}$; thus, each mole of $AgNO_3$ reacts with two moles of NaCN. The grams of NaCN in the sample is

$$\frac{0.1018 \text{ mol } AgNO_3}{\text{L}} \times 0.03968 \text{ L} \times \frac{2 \text{ mol NaCN}}{\text{mol } AgNO_3} \times \frac{49.01 \text{ g NaCN}}{\text{mol NaCN}} = 0.3959 \text{ g NaCN} \tag{9.E.53}$$

and the purity of the sample is

$$\frac{0.3959 \text{ g NaCN}}{0.4482 \text{ g sample}} \times 100 = 88.33\% \text{ w/w NaCN} \tag{9.E.54}$$

Click here to return to the chapter.

Practice Exercise 9.16

The total moles of EDTA used in this analysis is

$$\frac{0.02011 \text{ mol EDTA}}{\text{L}} \times 0.02500 \text{ L} = 5.028 \times 10^{-4} \text{ mol EDTA} \tag{9.E.55}$$

Of this,

$$\frac{0.01113 \text{ mol } Mg^{2+}}{\text{L}} \times 0.00423 \text{ L} \times \frac{1 \text{ mol EDTA}}{\text{mol } Mg^{2+}} = 4.708 \times 10^{-5} \text{ mol EDTA} \tag{9.E.56}$$

are consumed in the back titration with Mg^{2+}, which means that

$$5.028 \times 10^{-4} \text{ mol EDTA} - 4.708 \times 10^{-5} \text{ mol EDTA} = 4.557 \times 10^{-4} \text{ mol EDTA} \tag{9.E.57}$$

react with the $BaSO_4$. Each mole of $BaSO_4$ reacts with one mole of EDTA; thus

$$4.557 \times 10^{-4} \text{ mol EDTA} \times \frac{1 \text{ mol } BaSO_4}{\text{mol EDTA}} \times \frac{1 \text{ mol } Na_2SO_4}{\text{mol } BaSO_4} \times \frac{142.04 \text{ g } Na_2SO_4}{\text{mol } Na_2SO_4} = 0.06473 \text{ g } Na_2SO_4 \tag{9.E.58}$$

$$\frac{0.06473 \text{ g } Na_2SO_4}{0.1557 \text{ g sample}} \times 100 = 41.23\% \text{ w/w } Na_2SO_4 \tag{9.E.59}$$

Click here to return to the chapter.

Practice Exercise 9.17

The volume of Tl^{3+} needed to reach the equivalence point is

$$V_{eq} = V_{Tl} = \frac{M_{Sn} V_{Sn}}{M_{Tl}} = \frac{(0.050 \text{ M})(50.0 \text{ mL})}{0.100 \text{ M}} = 25.0 \text{ mL} \tag{9.E.60}$$

Before the equivalence point, the concentration of unreacted Sn^{2+} and the concentration of Sn^{4+} are easy to calculate. For this reason we find the potential using the Nernst equation for the Sn^{4+}/Sn^{2+} half-reaction.For example, the concentrations of Sn^{2+} and Sn^{4+} after adding 10.0 mL of titrant are

$$[Sn^{2+}] = \frac{(0.050 \text{ M})(50.0 \text{ mL}) - (0.100 \text{ M})(10.0 \text{ mL})}{50.0 \text{ mL} + 10.0 \text{ mL}} = 0.0250 \text{ M} \tag{9.E.61}$$

$$[Sn^{4+}] = \frac{(0.100 \text{ M})(10.0 \text{ mL})}{50.0 \text{ mL} + 10.0 \text{ mL}} = 0.0167 \text{ M} \tag{9.E.62}$$

and the potential is

$$E = +0.139 \text{ V} - \frac{0.05916}{2} \log \frac{0.0250 \text{ M}}{0.0167 \text{ M}} = +0.134 \text{ V} \tag{9.E.63}$$

After the equivalence point, the concentration of Tl^{+} and the concentration of excess Tl^{3+} are easy to calculate. For this reason we find the potential using the Nernst equation for the Tl^{3+}/Tl^{+} half-reaction. For example, after adding 40.0 mL of titrant, the concentrations of Tl^{+} and Tl^{3+} are

$$[Tl^{+}] = \frac{(0.0500 \text{ M})(50.0 \text{ mL})}{50.0 \text{ mL} + 40.0 \text{ mL}} = 0.0278 \text{ M} \tag{9.E.64}$$

$$[Tl^{3+}] = \frac{(0.100 \text{ M})(40.0 \text{ mL}) - (0.0500 \text{ M})(50.0 \text{ mL})}{50.0 \text{ mL} + 40.0 \text{ mL}} = 0.0167 \text{ M} \tag{9.E.65}$$

and the potential is

$$E = +0.77 \text{ V} - \frac{0.05916}{2} \log \frac{0.0278 \text{ M}}{0.0167 \text{ M}} = +0.76 \text{ V} \tag{9.E.66}$$

At the titration's equivalence point, the potential, E_{eq}, potential is

$$E_{eq} = \frac{0.139 \text{ V} + 0.77 \text{ V}}{2} = 0.45 \text{ V} \tag{9.E.67}$$

Some additional results are shown here.

Volume of Tl^{3+} (mL)	E (V)	Volume of Tl^{3+} (mL)	E (V)
5	0.121	30	0.75
10	0.134	35	0.75
15	0.144	40	0.76
20	0.157	45	0.76
25	0.45	50	0.76

Click here to return to the chapter.

Practice Exercise 9.18

Figure 9.51 shows a sketch of the titration curve. The two points before the equivalence point

$$V_{Tl} = 2.5 \text{ mL},\ E = +0.109 \text{ V and } V_{Tl} = 22.5 \text{ mL},\ E = +0.169 \text{ V} \tag{9.E.68}$$

are plotted using the redox buffer for Sn^{4+}/Sn^{2+}, which spans a potential range of +0.139 ± 0.5916/2. The two points after the equivalence point

$$V_{Tl} = 27.5 \text{ mL},\ E = +0.74 \text{ V and } V_{EDTA} = 50 \text{ mL},\ E = +0.77 \text{ V} \tag{9.E.69}$$

are plotted using the redox buffer for Tl^{3+}/Tl^{+}, which spans the potential range of +0.139 ± 0.5916/2.

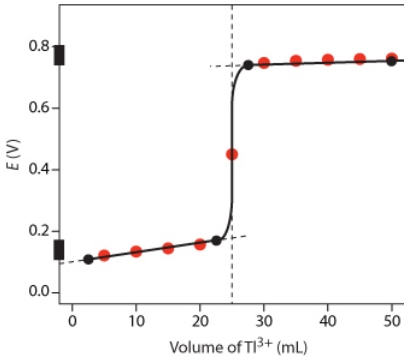


Figure 9.51 Titration curve for Practice Exercise 9.18. The black dots and curve are the approximate sketch of the titration curve. The points in red are the calculations from Practice Exercise 9.17.

Click here to return to the chapter.

Practice Exercise 9.19

The two half reactions are

$$Ce^{4+}(aq) + e^{-} \rightarrow Ce^{3+}(aq) \tag{9.E.70}$$

$$U^{4+}(aq) + 2H_2O \rightarrow UO_2^{2+}(aq) + 4H^{+}(aq) + 2e^{-} \tag{9.E.71}$$

for which the Nernst equations are

$$E = E^{\circ}_{Ce^{4+}/Ce^{3+}} - \frac{0.05916}{1} \log \frac{[Ce^{3+}]}{[Ce^{4+}]} \tag{9.E.72}$$

$$E = E^{\circ}_{UO_2^{2+}/U^{4+}} - \frac{0.05916}{2} \log \frac{[U^{4+}]}{[UO_2^{2+}][H^{+}]^4} \tag{9.E.73}$$

Before adding these two equations together we must multiply the second equation by 2 so that we can combine the log terms; thus

$$3E = E^\circ_{Ce^{4+}/Ce^{3+}} + 2E^\circ_{UO_2^{2+}/U^{4+}} - 0.05916 \log \frac{[Ce^{3+}][U^{4+}]}{[Ce^{4+}][UO_2^{2+}][H^+]^4} \tag{9.E.74}$$

At the equivalence point we know that

$$[Ce^{3+}] = 2 \times [UO_2^{2+}] \tag{9.E.75}$$

$$[Ce^{4+}] = 2 \times [U^{4+}] \tag{9.E.76}$$

Substituting these equalities into the previous equation and rearranging gives us a general equation for the potential at the equivalence point.

$$3E = E^\circ_{Ce^{4+}/Ce^{3+}} + 2E^\circ_{UO_2^{2+}/U^{4+}} - 0.05916 \log \frac{2[UO_2^{2+}][U^{4+}]}{2[U^{4+}][UO_2^{2+}][H^+]^4} \tag{9.E.77}$$

$$E = \frac{E^\circ_{Ce^{4+}/Ce^{3+}} + 2E^\circ_{UO_2^{2+}/U^{4+}}}{3} - \frac{0.05916}{3} \log \frac{1}{[H^+]^4} \tag{9.E.78}$$

$$E = \frac{E^\circ_{Ce^{4+}/Ce^{3+}} + 2E^\circ_{UO_2^{2+}/U^{4+}}}{3} + \frac{0.05916 \times 4}{3} \log[H^+] \tag{9.E.79}$$

$$E = \frac{E^\circ_{Ce^{4+}/Ce^{3+}} + 2E^\circ_{UO_2^{2+}/U^{4+}}}{3} - 0.07888 \text{ pH} \tag{9.E.80}$$

At a pH of 1 the equivalence point has a potential of

$$E_{eq} = \frac{1.72 + 2 \times 0.327}{3} - 0.07888 \times 1 = 0.712 \text{ V} \tag{9.E.81}$$

Click here to return to the chapter.

Practice Exercise 9.20

Because we have not been provided with a balanced reaction, let's use a conservation of electrons to deduce the stoichiometry. Oxidizing $C_2O_4^{2-}$, in which each carbon has a +3 oxidation state, to CO_2, in which carbon has an oxidation state of +4, requires one electron per carbon, or a total of two electrons for each mole of $C_2O_4^{2-}$. Reducing MnO_4^-, in which each manganese is in the +7 oxidation state, to Mn^{2+} requires five electrons. A conservation of electrons for the titration, therefore, requires that two moles of $KMnO_4$ (10 moles of e^-) reacts with five moles of $Na_2C_2O_4$ (10 moles of e^-).

The moles of $KMnO_4$ used in reaching the end point is

$$(0.0400 \text{ M } KMnO_4) \times (0.03562 \text{ L } KMnO_4) = 1.42 \times 10^{-3} \text{ mol } KMnO_4 \tag{9.E.82}$$

which means that the sample contains

$$1.42 \times 10^{-3} \text{ mol } KMnO_4 \times \frac{5 \text{ mol } Na_2C_2O_4}{2 \text{ mol } KMnO_4} = 3.55 \times 10^{-3} \text{ mol } Na_2C_2O_4 \tag{9.E.83}$$

Thus, the %w/w $Na_2C_2O_4$ in the sample of ore is

$$3.55 \times 10^{-3} \text{ mol } Na_2C_2O_4 \times \frac{134.00 \text{ g } Na_2C_2O_4}{\text{mol } Na_2C_2O_4} = 0.476 \text{ g } Na_2C_2O_4 \tag{9.E.84}$$

$$\frac{0.476 \text{ g } Na_2C_2O_4}{0.5116 \text{ g sample}} \times 100 = 93.0\% \text{ w/w } Na_2C_2O_4 \tag{9.E.85}$$

Click here to return to the chapter.

Practice Exercise 9.21

For a back titration we need to determine the stoichiometry between $Cr_2O_7^{2-}$ and the analyte, C_2H_6O, and between $Cr_2O_7^{2-}$ and the titrant, Fe^{2+}. In oxidizing ethanol to acetic acid, the oxidation state of carbon changes from –2 in C_2H_6O to 0 in $C_2H_4O_2$. Each carbon releases two electrons, or a total of four electrons per C_2H_6O. In reducing $Cr_2O_7^{2-}$, in which each chromium has an oxidation state of +6, to Cr^{3+}, each chromium loses three electrons, for a total of six electrons per $Cr_2O_7^{2-}$. Oxidation of Fe^{2+} to

Fe^{3+} requires one electron. A conservation of electrons requires that each mole of $K_2Cr_2O_7$ (6 moles of e^-) reacts with six moles of Fe^{2+} (6 moles of e^-), and that four moles of $K_2Cr_2O_7$ (24 moles of e^-) react with six moles of C_2H_6O (24 moles of e^-).

The total moles of $K_2Cr_2O_7$ reacting with C_2H_6O and with Fe^{2+} is

$$(0.0200\ \text{M}\ \text{K}_2\text{Cr}_2\text{O}_7) \times (0.05000\ \text{L}\ \text{I}_3^-) = 1.00 \times 10^{-3}\ \text{mol}\ \text{K}_2\text{Cr}_2\text{O}_7 \tag{9.E.86}$$

The back titration with Fe^{2+} consumes

$$0.02148\ \text{L}\ \text{Fe}^{2+} \times \frac{0.1014\ \text{mol}\ \text{Fe}^{2+}}{\text{L}\ \text{Fe}^{2+}} \times \frac{1\ \text{mol}\ \text{K}_2\text{Cr}_2\text{O}_7}{6\ \text{mol}\ \text{Fe}^{2+}} = 3.63 \times 10^{-4}\ \text{mol}\ \text{K}_2\text{Cr}_2\text{O}_7 \tag{9.E.87}$$

Subtracting the moles of $K_2Cr_2O_7$ reacting with Fe^{2+} from the total moles of $K_2Cr_2O_7$ gives the moles reacting with the analyte.

$$1.00 \times 10^{-3}\ \text{K}_2\text{Cr}_2\text{O}_7 - 3.63 \times 10^{-4}\ \text{mol}\ \text{K}_2\text{Cr}_2\text{O}_7 = 6.37 \times 10^{-4}\ \text{mol}\ \text{K}_2\text{Cr}_2\text{O}_7 \tag{9.E.88}$$

The grams of ethanol in the 10.00-mL sample of diluted brandy is

$$6.37 \times 10^{-4}\ \text{mol}\ \text{K}_2\text{Cr}_2\text{O}_7 \times \frac{6\ \text{mol}\ \text{C}_2\text{H}_6\text{O}}{4\ \text{mol}\ \text{K}_2\text{Cr}_2\text{O}_7} \times \frac{46.50\ \text{g}\ \text{C}_2\text{H}_6\text{O}}{\text{mol}\ \text{C}_2\text{H}_6\text{O}} = 0.0444\ \text{g}\ \text{C}_2\text{H}_6\text{O} \tag{9.E.89}$$

The %w/v C_2H_6O in the brandy is

$$\frac{0.0444\ \text{g}\ \text{C}_2\text{H}_6\text{O}}{10.00\ \text{mL dilute brandy}} \times \frac{500.0\ \text{mL dilute brandy}}{5.00\ \text{mL brandy}} \times 100 = 44.4\%\ \text{w/v}\ \text{C}_2\text{H}_6\text{O} \tag{9.E.90}$$

Click here to return to the chapter.

Practice Exercise 9.22

The first task is to calculate the volume of NaCl needed to reach the equivalence point; thus

$$V_{eq} = V_{NaCl} = \frac{M_{Ag}V_{Ag}}{M_{NaCl}} = \frac{(0.0500\ \text{M})(50.0\ \text{mL})}{(0.100\ \text{M})} = 25.0\ \text{mL} \tag{9.E.91}$$

Before the equivalence point the titrand, Ag^+, is in excess. The concentration of unreacted Ag^+ after adding 10.0 mL of NaCl, for example, is

$$[\text{Ag}^+] = \frac{(0.0500\ \text{M})(50.0\ \text{mL}) - (0.100\ \text{M})(10.0\ \text{mL})}{50.0\ \text{mL} + 10.0\ \text{mL}} = 2.50 \times 10^{-2}\ \text{M} \tag{9.E.92}$$

which corresponds to a pAg of 1.60. To find the concentration of Cl^- we use the K_{sp} for AgCl; thus

$$[\text{Cl}^-] = \frac{K_{sp}}{[\text{Ag}^+]} = \frac{1.8 \times 10^{-10}}{2.50 \times 10^{-2}} = 7.2 \times 10^{-9}\ \text{M} \tag{9.E.93}$$

or a pCl of 8.14.

At the titration's equivalence point, we know that the concentrations of Ag^+ and Cl^- are equal. To calculate their concentrations we use the K_{sp} expression for AgCl; thus

$$K_{sp} = [\text{Ag}^+][\text{Cl}^-] = (x)(x) = 1.8 \times 10^{-10} \tag{9.E.94}$$

Solving for x gives a concentration of Ag^+ and the concentration of Cl^- as 1.3×10^{-5} M, or a pAg and a pCl of 4.89.

After the equivalence point, the titrant is in excess. For example, after adding 35.0 mL of titrant

$$[\text{Cl}^-] = \frac{(0.100\ \text{M})(35.0\ \text{mL}) - (0.0500\ \text{M})(50.0\ \text{mL})}{50.0\ \text{mL} + 35.0\ \text{mL}} = 1.18 \times 10^{-2}\ \text{M} \tag{9.E.95}$$

or a pCl of 1.93. To find the concentration of Ag^+ we use the K_{sp} for AgCl; thus

$$[\text{Ag}^+] = \frac{K_{sp}}{[\text{Cl}^-]} = \frac{1.8 \times 10^{-10}}{1.18 \times 10^{-2}} = 1.5 \times 10^{-8}\ \text{M} \tag{9.E.96}$$

or a pAg of 7.82. The following table summarizes additional results for this titration.

Volume of NaCl (mL)	pAg	pCl
0	1.30	–
5.00	1.44	8.31
10.0	1.60	8.14
15.0	1.81	7.93
20.0	2.15	7.60
25.0	4.89	4.89
30.0	7.54	2.20
35.0	7.82	1.93
40.0	7.97	1.78
45.0	8.07	1.68
50.0	8.14	1.60

Click here to return to the chapter.

Practice Exercise 9.23

The titration uses

$$\frac{0.1078\ \text{M KSCN}}{\text{L}} \times 0.02719\ \text{L} = 2.931 \times 10^{-3}\ \text{mol KSCN} \tag{9.E.97}$$

The stoichiometry between SCN^- and Ag^+ is 1:1; thus, there are

$$2.931 \times 10^{-3}\ \text{mol Ag}^+ \times \frac{107.87\ \text{g Ag}}{\text{mol Ag}} = 0.3162\ \text{g Ag} \tag{9.E.98}$$

in the 25.00 mL sample. Because this represents ¼ of the total solution, there are 0.3162 × 4 or 1.265 g Ag in the alloy. The %w/w Ag in the alloy is

$$\frac{1.265\ \text{g Ag}}{1.963\ \text{g sample}} \times 100 = 64.44\%\ \text{w/w Ag} \tag{9.E.99}$$

Click here to return to the chapter.

Contributors and Attributions

David Harvey (DePauw University)

9.E: Titrimetric Methods (Exercises) is shared under a CC BY-NC-SA 4.0 license and was authored, remixed, and/or curated by LibreTexts.

9.S: Titrimetric Methods (Summary)

In a titrimetric method of analysis, the volume of titrant reacting stoichiometrically with a titrand provides quantitative information about the amount of analyte in a sample. The volume of titrant corresponding to this stoichiometric reaction is called the equivalence point. Experimentally we determine the titration's end point using an indicator that changes color near the equivalence point. Alternatively, we can locate the end point by continuously monitoring a property of the titrand's solution—absorbance, potential, and temperature are typical examples—that changes as the titration progresses. In either case, an accurate result requires that the end point closely match the equivalence point. Knowing the shape of a titration curve is critical to evaluating the feasibility of a titrimetric method.

Many titrations are direct, in which the analyte participates in the titration as the titrand or the titrant. Other titration strategies may be used when a direct reaction between the analyte and titrant is not feasible. In a back titration a reagent is added in excess to a solution containing the analyte. When the reaction between the reagent and the analyte is complete, the amount of excess reagent is determined by a titration. In a displacement titration the analyte displaces a reagent, usually from a complex, and the amount of displaced reagent is determined by an appropriate titration.

Titrimetric methods have been developed using acid–base, complexation, redox, and precipitation reactions. Acid–base titrations use a strong acid or a strong base as a titrant. The most common titrant for a complexation titration is EDTA. Because of their stability against air oxidation, most redox titrations use an oxidizing agent as a titrant. Titrations with reducing agents also are possible. Precipitation titrations often involve Ag^+ as either the analyte or titrant.

9.6.1 Key Terms

acid–base titration	displacement titration	precipitation titration
acidity	end point	redox indicator
alkalinity	equivalence point	redox titration
argentometric titration	Fajans method	spectrophotometric titration
asymmetric equivalence point	formal potential	symmetric equivalence point
auxiliary complexing agent	Gran plot	thermometric titration
auxiliary oxidizing agent	indicator	titrand
auxiliary reducing agent	Jones reductor	titrant
back titration	Kjeldahl analysis	titration curve
buret	leveling	titration error
complexation titration	metallochromic indicator	titrimetry
conditional formation constant	Mohr method	Volhard method
direct titration	potentiometric titration	Walden reductor

<

References

1. (a) Willis, C. J. *J. Chem. Educ.* **1981**, *58*, 659–663; (b) Nakagawa, K. *J. Chem. Educ.* **1990**, *67*, 673–676; (c) Gordus, A. A. *J. Chem. Educ.* **1991**, *68*, 759–761; (d) de Levie, R. *J. Chem. Educ.* **1993**, *70*, 209–217; (e) Chaston, S. *J. Chem. Educ.* **1993**, *70*, 878–880; (f) de Levie, R. *Anal. Chem.* **1996**, *68*, 585–590.
2. (a) Currie, J. O.; Whiteley, R. V. *J. Chem. Educ.* **1991**, *68*, 923–926; (b) Breneman, G. L.; Parker, O. J. *J. Chem. Educ.* **1992**, *69*, 46–47; (c) Carter, D. R.; Frye, M. S.; Mattson, W. A. *J. Chem. Educ.* **1993**, *70*, 67–71; (d) Freiser, H. *Concepts and Calculations in Analytical Chemistry*, CRC Press: Boca Raton, 1992.
3. Meites, L.; Goldman, J. A. *Anal. Chim. Acta* **1963**, *29*, 472–479.
4. Ferek, R. J.; Lazrus, A. L.; Haagenson, P. L.; Winchester, J. W. *Environ. Sci. Technol.* **1983**, *17*, 315–324.
5. (a) Molnár-Perl, I.; Pintée-Szakács, M. *Anal. Chim. Acta* **1987**, *202*, 159–166; (b) Barbosa, J.; Bosch, E.; Cortina, J. L.; Rosés, M. *Anal. Chim. Acta* **1992**, *256*, 177–181.
6. (a) Gonzalez, A. G.; Asuero, A. G. *Anal. Chim. Acta* **1992**, *256*, 29–33; (b) Papanastasiou, G.; Ziogas, I.; Kokkindis, G. *Anal. Chim. Acta* **1993**, *277*, 119–135.
7. Alexio, L. M.; Godinho, O. E. S.; da Costa, W. F. *Anal. Chim. Acta* **1992**, *257*, 35–39.

8. Steele, A.; Hieftje, G. M. *Anal. Chem.* **1984**, *56*, 2884–2888.
9. (a) Gratzl, M.; Yi, C. *Anal. Chem.* **1993**, *65*, 2085–2088; (b) Yi, C.; Gratzl, M. *Anal. Chem.* **1994**, *66*, 1976–1982; (c) Hui, K. Y.; Gratzl, M. *Anal. Chem.* **1997**, *69*, 695–698; (d) Yi, C.; Huang, D.; Gratzl, M. *Anal. Chem.* **1996**, *68*, 1580–1584; (e) Xie, H.; Gratzl, M. *Anal. Chem.* **1996**, *68*, 3665–3669.
10. Schwartz, L. M. *J. Chem. Educ.* **1992**, *69*, 879–883.
11. (a) Boiani, J. A. *J. Chem. Educ.* **1986**, *63*, 724–726; (b) Castillo, C. A.; Jaramillo, A. *J. Chem. Educ.* **1989**, *66*, 341.
12. Prada, S.; Guekezian, M.; Suarez-Iha, M. E. V. *Anal. Chim. Acta* **1996**, *329*, 197–202.
13. Sporek, K. F. *Anal. Chem.* **1958**, *30*, 1030–1032.
14. Vončina, D. B.; Dobčnik, D.; Gomišček, S. *Anal. Chim. Acta* **1992**, *263*, 147–153.

Contributors

David Harvey (DePauw University)

9.S: Titrimetric Methods (Summary) is shared under a CC BY-NC-SA 4.0 license and was authored, remixed, and/or curated by LibreTexts.

CHAPTER OVERVIEW

10: Spectroscopic Methods

An early example of a colorimetric analysis is Nessler's method for ammonia, which was introduced in 1856. Nessler found that adding an alkaline solution of HgI_2 and KI to a dilute solution of ammonia produces a yellow to reddish brown colloid, with the colloid's color depending on the concentration of ammonia. By visually comparing the color of a sample to the colors of a series of standards, Nessler was able to determine the concentration of ammonia.

Colorimetry, in which a sample absorbs visible light, is one example of a spectroscopic method of analysis. At the end of the nineteenth century, spectroscopy was limited to the absorption, emission, and scattering of visible, ultraviolet, and infrared electromagnetic radiation. Since its introduction, spectroscopy has expanded to include other forms of electromagnetic radiation—such as X-rays, microwaves, and radio waves—and other energetic particles—such as electrons and ions.

Topic hierarchy

10.1: Overview of Spectroscopy
10.2: Spectroscopy Based on Absorption
10.3: UV/Vis and IR Spectroscopy
10.4: Atomic Absorption Spectroscopy
10.5: Emission Spectroscopy
10.6: Photoluminescence Spectroscopy
10.7: Atomic Emission Spectroscopy
10.8: Spectroscopy Based on Scattering
10.E: Spectroscopic Methods (Exercises)
10.S: Spectroscopic Methods (Summary)

Contributors

- David Harvey (DePauw University)

10: Spectroscopic Methods is shared under a CC BY-NC-SA 4.0 license and was authored, remixed, and/or curated by LibreTexts.

10.1: Overview of Spectroscopy

The focus of this chapter is on the interaction of ultraviolet, visible, and infrared radiation with matter. Because these techniques use optical materials to disperse and focus the radiation, they often are identified as optical spectroscopies. For convenience we will use the simpler term **spectroscopy** in place of optical spectroscopy; however, you should understand that we are considering only a limited part of a much broader area of analytical techniques.

Despite the difference in instrumentation, all spectroscopic techniques share several common features. Before we consider individual examples in greater detail, let's take a moment to consider some of these similarities. As you work through the chapter, this overview will help you focus on similarities between different spectroscopic methods of analysis. You will find it easier to understand a new analytical method when you can see its relationship to other similar methods.

10.1.1 What is Electromagnetic Radiation

Electromagnetic radiation—light—is a form of energy whose behavior is described by the properties of both waves and particles. Some properties of electromagnetic radiation, such as its refraction when it passes from one medium to another (Figure 10.1.1), are explained best by describing light as a wave. Other properties, such as absorption and emission, are better described by treating light as a particle. The exact nature of electromagnetic radiation remains unclear, as it has since the development of quantum mechanics in the first quarter of the 20th century.[1] Nevertheless, the dual models of wave and particle behavior provide a useful description for electromagnetic radiation.



***Figure* 10.1.1:** *The Golden Gate bridge as seen through rain drops. Refraction of light by the rain drops produces the distorted images. Source: Mila Zinkova (commons.wikipedia.org).*

Wave Properties of Electromagnetic Radiation

Electromagnetic radiation consists of oscillating electric and magnetic fields that propagate through space along a linear path and with a constant velocity. In a vacuum electromagnetic radiation travels at the speed of light, c, which is 2.997 92 × 10^8 m/s. When electromagnetic radiation moves through a medium other than a vacuum its velocity, v, is less than the speed of light in a vacuum. The difference between v and c is sufficiently small (<0.1%) that the speed of light to three significant figures, 3.00 × 10^8 m/s, is accurate enough for most purposes.

The oscillations in the electric and magnetic fields are perpendicular to each other, and to the direction of the wave's propagation. Figure 10.1.2 shows an example of plane-polarized electromagnetic radiation, consisting of a single oscillating electric field and a single oscillating magnetic field.

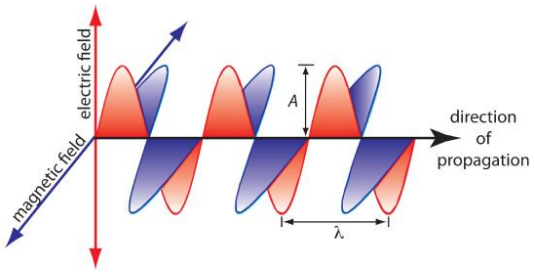


Figure 10.1.2: Plane-polarized electromagnetic radiation showing the oscillating electric field in red and the oscillating magnetic field in blue. The radiation's amplitude, A, and its wavelength, λ, are shown. Normally, electromagnetic radiation is unpolarized, with oscillating electric and magnetic fields present in all possible planes perpendicular to the direction of propagation.

An electromagnetic wave is characterized by several fundamental properties, including its velocity, amplitude, frequency, phase angle, polarization, and direction of propagation.[2] For example, the amplitude of the oscillating electric field at any point along the propagating wave is

$$A_t = A_e \sin(2\pi\nu t + \Phi) \tag{10.1.1}$$

where A_t is the magnitude of the electric field at time t, A_e is the electric field's maximum **amplitude**, ν is the wave's **frequency**—the number of oscillations in the electric field per unit time—and Φ is a **phase angle**, which accounts for the fact that A_t need not have a value of zero at t = 0. The identical equation for the magnetic field is

$$A_t = A_m \sin(2\pi\nu t + \Phi) \tag{10.1.2}$$

where A_m is the magnetic field's maximum amplitude.

Other properties also are useful for characterizing the wave behavior of electromagnetic radiation. The **wavelength**, λ, is defined as the distance between successive maxima (see Figure **10.1.2**). For ultraviolet and visible electromagnetic radiation the wavelength is usually expressed in nanometers (1 nm = 10^{-9} m), and for infrared radiation it is given in microns (1 μm = 10^{-6} m). The relationship between wavelength and frequency is

$$\lambda = \frac{c}{\nu} \tag{10.1.3}$$

Note

When electromagnetic radiation moves between different media—for example, when it moves from air into water—its frequency, ν, remains constant. Because its velocity depends upon the medium in which it is traveling, the electromagnetic radiation's wavelength, λ, changes. If we replace the speed of light in a vacuum, c, with its speed in the medium, v, then the wavelength is

$$\lambda = \frac{v}{\nu} \tag{10.1.4}$$

This change in wavelength as light passes between two media explains the refraction of electromagnetic radiation shown in Figure **10.1.1**.

Another unit useful unit is the **wavenumber**, $\bar{\nu}$, which is the reciprocal of wavelength

$$\bar{\nu} = \frac{1}{\lambda} \tag{10.1.5}$$

Wavenumbers are frequently used to characterize infrared radiation, with the units given in cm^{-1}.

Example 10.1.1

In 1817, Josef Fraunhofer studied the spectrum of solar radiation, observing a continuous spectrum with numerous dark lines. Fraunhofer labeled the most prominent of the dark lines with letters. In 1859, Gustav Kirchhoff showed that the D line in the sun's spectrum was due to the absorption of solar radiation by sodium atoms. The wavelength of the sodium D line is 589 nm. What are the frequency and the wavenumber for this line?

Solution

The frequency and wavenumber of the sodium D line are

$$\nu = \frac{c}{\lambda} = \frac{3.00 \times 10^8 \text{ m/s}}{589 \times 10^{-9} \text{ m}} = 5.09 \times 10^{14} \text{ s}^{-1} \tag{10.1.6}$$

$$\bar{\nu} = \frac{1}{\lambda} = \frac{1}{589 \times 10^{-9} \text{ m}} \times \frac{1 \text{ m}}{100 \text{ cm}} = 1.70 \times 10^4 \text{ cm}^{-1} \tag{10.1.7}$$

Exercise 10.1

Another historically important series of spectral lines is the Balmer series of emission lines form hydrogen. One of the lines has a wavelength of 656.3 nm. What are the frequency and the wavenumber for this line?

Click here to review your answer to this exercise.

Particle Properties of Electromagnetic Radiation

When matter absorbs electromagnetic radiation it undergoes a change in energy. The interaction between matter and electromagnetic radiation is easiest to understand if we assume that radiation consists of a beam of energetic particles called photons. When a **photon** is absorbed by a sample it is "destroyed," and its energy acquired by the sample.[3] The energy of a photon, in joules, is related to its frequency, wavelength, and wavenumber by the following equalities

$$E = h\nu = \frac{hc}{\lambda} = hc\bar{\nu} \tag{10.1.8}$$

where h is Planck's constant, which has a value of 6.626×10^{-34} J·s.

Example 10.1.2

What is the energy of a photon from the sodium D line at 589 nm?

Solution

The photon's energy is

$$E = \frac{hc}{\lambda} = \frac{(6.626 \times 10^{-34}\ \text{J} \cdot \text{s})(3.00 \times 10^{8}\ \text{m/s})}{589 \times 10^{-9}\ \text{m}} = 3.37 \times 10^{-19}\ \text{J} \tag{10.1.9}$$

Exercise 10.2

What is the energy of a photon for the Balmer line at a wavelength of 656.3 nm?

Click here to review your answer to this exercise.

The Electromagnetic Spectrum

The frequency and wavelength of electromagnetic radiation vary over many orders of magnitude. For convenience, we divide electromagnetic radiation into different regions—the **electromagnetic spectrum**—based on the type of atomic or molecular transition that gives rise to the absorption or emission of photons (Figure **10.1.3**). The boundaries between the regions of the electromagnetic spectrum are not rigid, and overlap between spectral regions is possible.

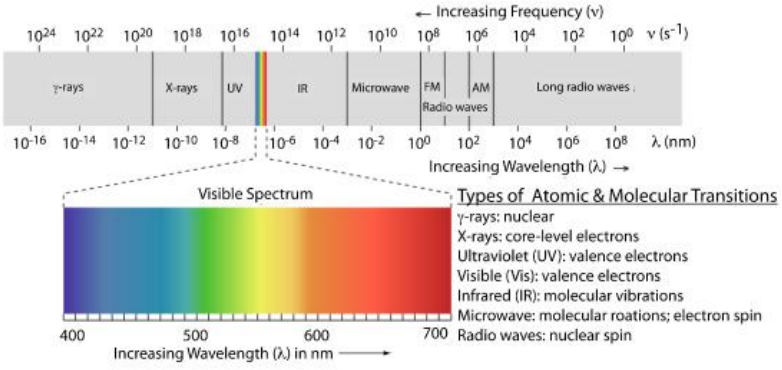


Figure* 10.1.3*: *The electromagnetic spectrum showing the boundaries between different regions and the type of atomic or molecular transition responsible for the change in energy. The colored inset shows the visible spectrum. Source: modified from Zedh (www.commons.wikipedia.org).*

10.1.2 Photons as a Signal Source

In the previous section we defined several characteristic properties of electromagnetic radiation, including its energy, velocity, amplitude, frequency, phase angle, polarization, and direction of propagation. A spectroscopic measurement is possible only if the photon's interaction with the sample leads to a change in one or more of these characteristic properties. We can divide spectroscopy

into two broad classes of techniques. In one class of techniques there is a transfer of energy between the photon and the sample. Table **10.1.1** provides a list of several representative examples.

Table* 10.1.1: Examples of Spectroscopic Techniques Involving an Exchange of Energy Between a Photon and the Sample*

Type of Energy Transfer	Region of Electromagnetic Spectrum	Spectroscopic Technique[a]
absorption	γ-ray	Mossbauer spectroscopy
	X-ray	X-ray absorption spectroscopy
	UV/Vis	*UV/Vis spectroscopy* *atomic absorption spectroscopy*
	IR	*infrared spectroscopy* raman spectroscopy
	Microwave	microwave spectroscopy
	Radio wave	electron spin resonance spectroscopy nuclear magnetic resonance spectroscopy
emission (thermal excitation)	UV/Vis	*atomic emission spectroscopy*
photoluminescence	X-ray	X-ray fluorescence
	UV/Vis	*fluorescence spectroscopy* *phosphorescence spectroscopy* atomic fluorescence spectroscopy
chemiluminescence	UV/Vis	chemiluminescence spectroscopy

[a] Techniques discussed in this text are shown in *italics*.

In absorption spectroscopy a photon is absorbed by an atom or molecule, which undergoes a transition from a lower-energy state to a higher-energy, or excited state (Figure **10.1.4**). The type of transition depends on the photon's energy. The electromagnetic spectrum in Figure **10.1.3**, for example, shows that absorbing a photon of visible light promotes one of the atom's or molecule's valence electrons to a higher-energy level. When an molecule absorbs infrared radiation, on the other hand, one of its chemical bonds experiences a change in vibrational energy.

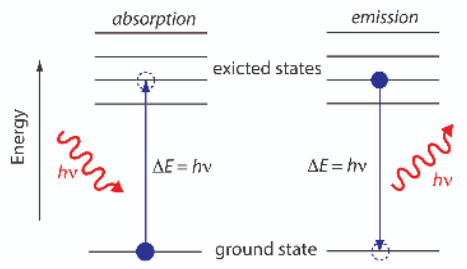


Figure* 10.1.4: Simplified energy diagram showing the absorption and emission of a photon by an atom or a molecule. When a photon of energy hν strikes the atom or molecule, absorption may occur if the difference in energy, ΔE, between the ground state and the excited state is equal to the photon's energy. An atom or molecule in an excited state may emit a photon and return to the ground state. The photon's energy, hν, equals the difference in energy, ΔE, between the two states.*

When it absorbs electromagnetic radiation the number of photons passing through a sample decreases. The measurement of this decrease in photons, which we call **absorbance**, is a useful analytical signal. Note that the each of the energy levels in Figure **10.1.4** has a well-defined value because they are quantized. Absorption occurs only when the photon's energy, *h*ν, matches the difference in energy, Δ*E*, between two energy levels. A plot of absorbance as a function of the photon's energy is called an **absorbance spectrum**. Figure **10.1.5**, for example, shows the absorbance spectrum of cranberry juice.

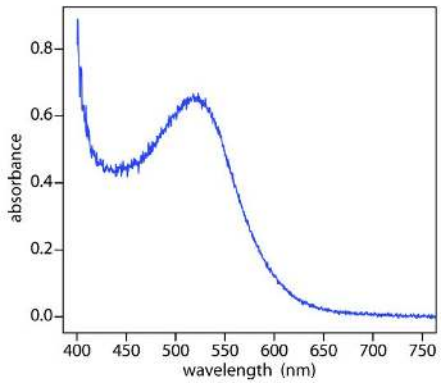


Figure* 10.1.5*: *Visible absorbance spectrum for cranberry juice. The anthocyanin dyes in cranberry juice absorb visible light with blue, green, and yellow wavelengths (see Figure* **10.1.3***). As a result, the juice appears red.*

When an atom or molecule in an excited state returns to a lower energy state, the excess energy often is released as a photon, a process we call **emission** (Figure **10.1.4**). There are several ways in which an atom or molecule may end up in an excited state, including thermal energy, absorption of a photon, or by a chemical reaction. Emission following the absorption of a photon is also called **photoluminescence**, and that following a chemical reaction is called **chemiluminescence**. A typical emission spectrum is shown in Figure **10.1.6**.

> **Note**
>
> Molecules also can release energy in the form of heat. We will return to this point later in the chapter.

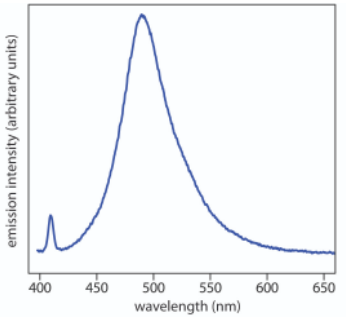


Figure* 10.1.6*: *Photoluminescence spectrum of the dye coumarin 343, which is incorporated in a reverse micelle suspended in cyclohexanol. The dye's absorbance spectrum (not shown) has a broad peak around 400 nm. The sharp peak at 409 nm is from the laser source used to excite coumarin 343. The broad band centered at approximately 500 nm is the dye's emission band. Because the dye absorbs blue light, a solution of coumarin 343 appears yellow in the absence of photoluminescence. Its photoluminescent emission is blue-green. Source: data from Bridget Gourley, Department of Chemistry & Biochemistry, DePauw University).*

In the second broad class of spectroscopic techniques, the electromagnetic radiation undergoes a change in amplitude, phase angle, polarization, or direction of propagation as a result of its refraction, reflection, scattering, diffraction, or dispersion by the sample. Several representative spectroscopic techniques are listed in Table **10.1.2**.

Table* 10.1.2: Examples of Spectroscopic Techniques That Do Not Involve an Exchange of Energy Between a Photon and the Sample*

Region of Electromagnetic Spectrum	Type of Interaction	Spectroscopic Technique[a]
X-ray	diffraction	X-ray diffraction
UV/Vis	refraction	refractometry
	scattering	*nephelometry* *turbidimetry*
	dispersion	optical rotary dispersion

[a] Techniques discussed in this text are shown in *italics*.

10.1.3 Basic Components of Spectroscopic Instruments

The spectroscopic techniques in Table **10.1.1** and Table **10.1.2** use instruments that share several common basic components, including a source of energy, a means for isolating a narrow range of wavelengths, a detector for measuring the signal, and a signal processor that displays the signal in a form convenient for the analyst. In this section we introduce these basic components. Specific instrument designs are considered in later sections.

> **Note**
>
> You will find a more detailed treatment of these components in the additional resources for this chapter.

Sources of Energy

All forms of spectroscopy require a source of energy. In absorption and scattering spectroscopy this energy is supplied by photons. Emission and photoluminescence spectroscopy use thermal, radiant (photon), or chemical energy to promote the analyte to a suitable excited state.

Sources of Electromagnetic Radiation. A source of electromagnetic radiation must provide an output that is both intense and stable. Sources of electromagnetic radiation are classified as either continuum or line sources. A **continuum source** emits radiation over a broad range of wavelengths, with a relatively smooth variation in intensity (Figure **10.1.7**). A **line source**, on the other hand, emits radiation at selected wavelengths (Figure **10.1.8**). Table **10.1.3** provides a list of the most common sources of electromagnetic radiation.

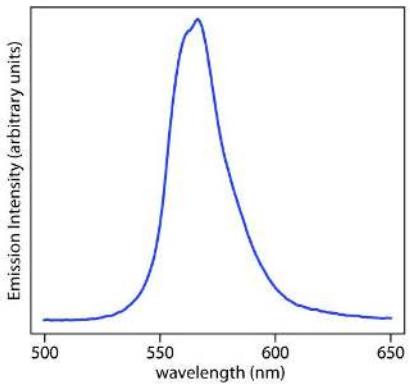


Figure* 10.1.7*: *Spectrum showing the emission from a green LED, which provides continuous emission over a wavelength range of approximately 530–640 nm.*

https://chem.libretexts.org/@go/page/70698

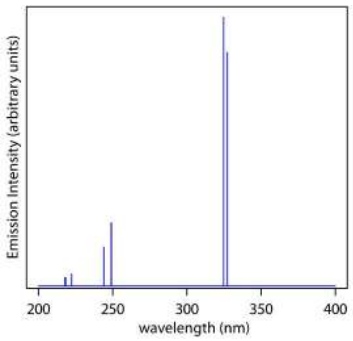


Figure 10.1.8 Emission spectrum from a Cu hollow cathode lamp. This spectrum consists of seven distinct emission lines (the first two differ by only 0.4 nm and are not resolved in this spectrum). Each emission line has a width of approximately 0.01 nm at ½ of its maximum intensity.

Table **10.1.3***: Common Sources of Electromagnetic Radiation*

Source	Wavelength Region	Useful for...
H_2 and D_2 lamp	continuum source from 160–380 nm	molecular absorption
tungsten lamp	continuum source from 320–2400 nm	molecular absorption
Xe arc lamp	continuum source from 200–1000 nm	molecular fluorescence
nernst glower	continuum source from 0.4–20 μm	molecular absorption
globar	continuum source from 1–40 μm	molecular absorption
nichrome wire	continuum source from 0.75–20 μm	molecular absorption
hollow cathode lamp	line source in UV/Visible	atomic absorption
Hg vapor lamp	line source in UV/Visible	molecular fluorescence
laser	line source in UV/Visible/IR	atomic and molecular absorption, fluorescence, and scattering

Sources of Thermal Energy. The most common sources of thermal energy are flames and plasmas. Flames sources use the combustion of a fuel and an oxidant to achieve temperatures of 2000–3400 K. Plasmas, which are hot, ionized gases, provide temperatures of 6000–10 000 K.

Chemical Sources of Energy. Exothermic reactions also may serve as a source of energy. In chemiluminescence the analyte is raised to a higher-energy state by means of a chemical reaction, emitting characteristic radiation when it returns to a lower-energy state. When the chemical reaction results from a biological or enzymatic reaction, the emission of radiation is called bioluminescence. Commercially available “light sticks” and the flash of light from a firefly are examples of chemiluminescence and bioluminescence.

Wavelength Selection

In Nessler’s original colorimetric method for ammonia, described at the beginning of the chapter, the sample and several standard solutions of ammonia are placed in separate tall, flat-bottomed tubes. As shown in Figure **10.1.9**, after adding the reagents and allowing the color to develop, the analyst evaluates the color by passing natural, ambient light through the bottom of the tubes and looking down through the solutions. By matching the sample’s color to that of a standard, the analyst is able to determine the concentration of ammonia in the sample.

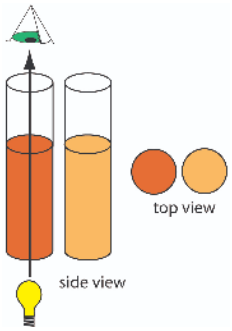


Figure 10.1.9 Nessler's original method for comparing the color of two solutions. Natural light passes upwards through the samples and standards and the analyst views the solutions by looking down toward the light source. The top view, shown on the right, is what the analyst sees. To determine the analyte's concentration, the analyst exchanges standards until the two colors match.

In Figure 10.1.9 every wavelength of light from the source passes through the sample. If there is only one absorbing species, this is not a problem. If two components in the sample absorbs different wavelengths of light, then a quantitative analysis using Nessler's original method becomes impossible. Ideally we want to select a wavelength that only the analyte absorbs. Unfortunately, we can not isolate a single wavelength of radiation from a continuum source. As shown in Figure 10.1.10, a wavelength selector passes a narrow band of radiation characterized by a **nominal wavelength**, an **effective bandwidth** and a maximum throughput of radiation. The effective bandwidth is defined as the width of the radiation at half of its maximum throughput.

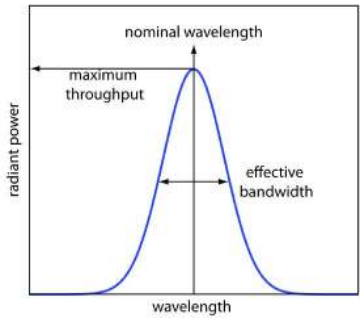


Figure 10.1.10 Radiation exiting a wavelength selector showing the band's nominal wavelength and its effective bandwidth.

The ideal wavelength selector has a high throughput of radiation and a narrow effective bandwidth. A high throughput is desirable because more photons pass through the wavelength selector, giving a stronger signal with less background noise. A narrow effective bandwidth provides a higher **resolution**, with spectral features separated by more than twice the effective bandwidth being resolved. As shown in Figure 10.1.11, these two features of a wavelength selector generally are in opposition. Conditions favoring a higher throughput of radiation usually provide less resolution. Decreasing the effective bandwidth improves resolution, but at the cost of a noisier signal.[4] For a qualitative analysis, resolution is usually more important than noise, and a smaller effective bandwidth is desirable. In a quantitative analysis less noise is usually desirable.

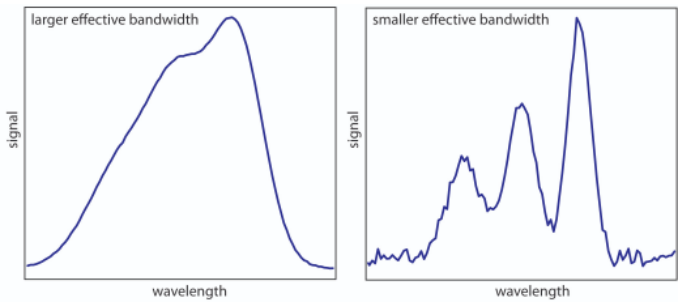


Figure 10.1.11: *Example showing the effect of the wavelength selector's effective bandwidth on resolution and noise. The spectrum with the smaller effective bandwidth has a better resolution, allowing us to see the presence of three peaks, but at the expense of a*

noisier signal. The spectrum with the larger effective bandwidth has less noise, but at the expense of less resolution between the three peaks.

Wavelength Selection Using Filters. The simplest method for isolating a narrow band of radiation is to use an absorption or interference **filter**. Absorption filters work by selectively absorbing radiation from a narrow region of the electromagnetic spectrum. Interference filters use constructive and destructive interference to isolate a narrow range of wavelengths. A simple example of an absorption filter is a piece of colored glass. A purple filter, for example, removes the complementary color green from 500–560 nm. Commercially available absorption filters provide effective bandwidths of 30–250 nm, although the throughput may be only 10% of the source's emission intensity at the low end of this range. Interference filters are more expensive than absorption filters, but have narrower effective bandwidths, typically 10–20 nm, with maximum throughputs of at least 40%.

Wavelength Selection Using Monochromators. A filter has one significant limitation—because a filter has a fixed nominal wavelength, if you need to make measurements at two different wavelengths, then you need to use two different filters. A **monochromator** is an alternative method for selecting a narrow band of radiation that also allows us to continuously adjust the band's nominal wavelength.

The construction of a typical monochromator is shown in Figure **10.1.1**2. Radiation from the source enters the monochromator through an entrance slit. The radiation is collected by a collimating mirror, which reflects a parallel beam of radiation to a diffraction grating. The diffraction grating is an optically reflecting surface with a large number of parallel grooves (see insert to Figure **10.1.1**2). The diffraction grating disperses the radiation and a second mirror focuses the radiation onto a planar surface containing an exit slit. In some monochromators a prism is used in place of the diffraction grating.

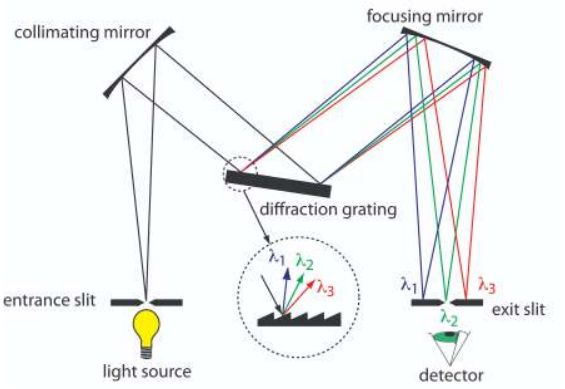


Figure 10.1.12 Schematic diagram of a monochromator that uses a diffraction grating to disperse the radiation.

Radiation exits the monochromator and passes to the detector. As shown in Figure **10.1.1**2, a monochromator converts a **polychromatic** source of radiation at the entrance slit to a **monochromatic** source of finite effective bandwidth at the exit slit. The choice of which wavelength exits the monochromator is determined by rotating the diffraction grating. A narrower exit slit provides a smaller effective bandwidth and better resolution, but allows a smaller throughput of radiation.

Note

- Polychromatic means many colored. Polychromatic radiation contains many different wavelengths of light.
- Monochromatic means one color, or one wavelength. Although the light exiting a monochromator is not strictly of a single wavelength, its narrow effective bandwidth allows us to think of it as monochromatic.

Monochromators are classified as either fixed-wavelength or scanning. In a fixed-wavelength monochromator we select the wavelength by manually rotating the grating. Normally a fixed-wavelength monochromator is used for a quantitative analysis where measurements are made at one or two wavelengths. A scanning monochromator includes a drive mechanism that continuously rotates the grating, allowing successive wavelengths to exit from the monochromator. Scanning monochromators are used to acquire spectra, and, when operated in a fixed-wavelength mode, for a quantitative analysis.

Interferometers. An **interferometer** provides an alternative approach for wavelength selection. Instead of filtering or dispersing the electromagnetic radiation, an interferometer allows source radiation of all wavelengths to reach the detector simultaneously (Figure **10.1.1**3). Radiation from the source is focused on a beam splitter that reflects half of the radiation to a fixed mirror and

transmits the other half to a movable mirror. The radiation recombines at the beam splitter, where constructive and destructive interference determines, for each wavelength, the intensity of light reaching the detector. As the moving mirror changes position, the wavelengths of light experiencing maximum constructive interference and maximum destructive interference also changes. The signal at the detector shows intensity as a function of the moving mirror's position, expressed in units of distance or time. The result is called an **interferogram**, or a time domain spectrum. The time domain spectrum is converted mathematically, by a process called a Fourier transform, to a spectrum (also called a frequency domain spectrum) showing intensity as a function of the radiation's energy.

> **Note**
>
> The mathematical details of the Fourier transform are beyond the level of this textbook. You can consult the chapter's additional resources for additional information.

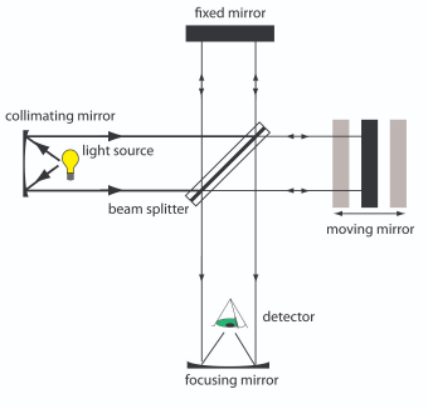


***Figure* 10.1.13** *Schematic diagram of an interferometers.*

In comparison to a monochromator, an interferometer has two significant advantages. The first advantage, which is termed **Jacquinot's advantage**, is the higher throughput of source radiation. Because an interferometer does not use slits and has fewer optical components from which radiation can be scattered and lost, the throughput of radiation reaching the detector is 80–200× greater than that for a monochromator. The result is less noise. The second advantage, which is called **Fellgett's advantage**, is a savings in the time needed to obtain a spectrum. Because the detector monitors all frequencies simultaneously, an entire spectrum takes approximately one second to record, as compared to 10–15 minutes with a scanning monochromator.

Detectors

In Nessler's original method for determining ammonia (Figure **10.1.9**) the analyst's eye serves as the detector, matching the sample's color to that of a standard. The human eye, of course, has a poor range—responding only to visible light—nor is it particularly sensitive or accurate. Modern detectors use a sensitive **transducer** to convert a signal consisting of photons into an easily measured electrical signal. Ideally the detector's signal, S, is a linear function of the electromagnetic radiation's power, P,

$$S = kP + D \tag{10.1.10}$$

where k is the detector's sensitivity, and D is the detector's **dark current**, or the background current when we prevent the source's radiation from reaching the detector.

> **Note**
>
> Transducer is a general term that refers to any device that converts a chemical or physical property into an easily measured electrical signal. The retina in your eye, for example, is a transducer that converts photons into an electrical nerve impulse.

There are two broad classes of spectroscopic transducers: thermal transducers and photon transducers. Table **10.1.4** provides several representative examples of each class of transducers.

Table **10.1.4***: Examples of Transducers for Spectroscopy*

Transducer	Class	Wavelength Range	Output Signal
phototube	photon	200–1000 nm	current
photomultiplier	photon	110–1000 nm	current
Si photodiode	photon	250–1100 nm	current
photoconductor	photon	750–6000 nm	change in resistance
photovoltaic cell	photon	400–5000 nm	current or voltage
thermocouple	thermal	0.8–40 μm	voltage
thermistor	thermal	0.8–40 μm	change in resistance
pneumatic	thermal	0.8–1000 μm	membrane displacement
pyroelectric	thermal	0.3–1000 μm	current

Photon Transducers. Phototubes and photomultipliers contain a photosensitive surface that absorbs radiation in the ultraviolet, visible, or near IR, producing an electrical current proportional to the number of photons reaching the transducer (Figure **10.1.14**). Other photon detectors use a semiconductor as the photosensitive surface. When the semiconductor absorbs photons, valence electrons move to the semiconductor's conduction band, producing a measurable current. One advantage of the Si photodiode is that it is easy to miniaturize. Groups of photodiodes may be gathered together in a linear array containing from 64–4096 individual photodiodes. With a width of 25 μm per diode, for example, a linear array of 2048 photodiodes requires only 51.2 mm of linear space. By placing a **photodiode array** along the monochromator's focal plane, it is possible to monitor simultaneously an entire range of wavelengths.

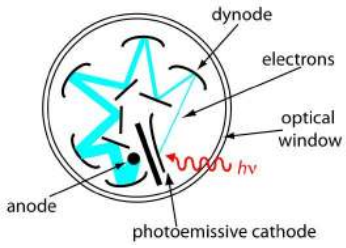


Figure* 10.1.14*: *Schematic of a photomultiplier. A photon strikes the photoemissive cathode producing electrons, which accelerate toward a positively charged dynode. Collision of these electrons with the dynode generates additional electrons, which accelerate toward the next dynode. A total of 10^6–10^7 electrons per photon eventually reach the anode, generating an electrical current.*

Thermal Transducers. Infrared photons do not have enough energy to produce a measurable current with a photon transducer. A thermal transducer, therefore, is used for infrared spectroscopy. The absorption of infrared photons by a thermal transducer increases its temperature, changing one or more of its characteristic properties. A pneumatic transducer, for example, is a small tube of xenon gas with an IR transparent window at one end and a flexible membrane at the other end. Photons enter the tube and are absorbed by a blackened surface, increasing the temperature of the gas. As the temperature inside the tube fluctuates, the gas

expands and contracts and the flexible membrane moves in and out. Monitoring the membrane's displacement produces an electrical signal.

Signal Processors

A transducer's electrical signal is sent to a **signal processor** where it is displayed in a form that is more convenient for the analyst. Examples of signal processors include analog or digital meters, recorders, and computers equipped with digital acquisition boards. A signal processor also is used to calibrate the detector's response, to amplify the transducer's signal, to remove noise by filtering, or to mathematically transform the signal.

> **Note**
>
> If the retina in your eye is a transducer, then your brain is a signal processor.

Contributors

David Harvey (DePauw University)

10.1: Overview of Spectroscopy is shared under a CC BY-NC-SA 4.0 license and was authored, remixed, and/or curated by LibreTexts.

10.2: Spectroscopy Based on Absorption

In absorption spectroscopy a beam of electromagnetic radiation passes through a sample. Much of the radiation passes through the sample without a loss in intensity. At selected wavelengths, however, the radiation's intensity is attenuated. This process of attenuation is called absorption.

10.2.1 Absorbance Spectra

There are two general requirements for an analyte's absorption of electromagnetic radiation. First, there must be a mechanism by which the radiation's electric field or magnetic field interacts with the analyte. For ultraviolet and visible radiation, absorption of a photon changes the energy of the analyte's valence electrons. A bond's vibrational energy is altered by the absorption of infrared radiation. (Figure 10.3 provides a list of the types of atomic and molecular transitions associated with different types of electromagnetic radiation.)

The second requirement is that the photon's energy, $h\nu$, must exactly equal the difference in energy, ΔE, between two of the analyte's quantized energy states. Figure 10.4 shows a simplified view of a photon's absorption, which is useful because it emphasizes that the photon's energy must match the difference in energy between a lower-energy state and a higher-energy state. What is missing, however, is information about what types of energy states are involved, which transitions between energy states are likely to occur, and the appearance of the resulting spectrum.

We can use the energy level diagram in Figure 10.15 to explain an absorbance spectrum. The lines labeled E_0 and E_1 represent the analyte's ground (lowest) electronic state and its first electronic excited state. Superimposed on each electronic energy level is a series of lines representing vibrational energy levels.

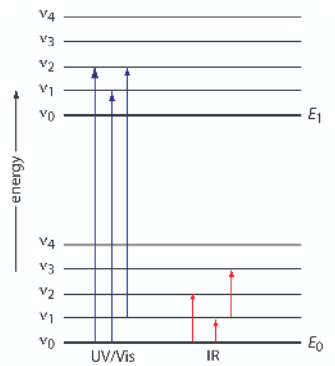


Figure 10.15 Diagram showing two electronic energy levels (E_0 and E_1), each with five vibrational energy levels (ν_0–ν_4). Absorption of ultraviolet and visible radiation leads to a change in the analyte's electronic energy levels and, possibly, a change in vibrational energy as well. A change in vibrational energy without a change in electronic energy levels occurs with the absorption of infrared radiation.

Infrared Spectra for Molecules and Polyatomic Ions

The energy of infrared radiation produces a change in a molecule's or a polyatomic ion's vibrational energy, but is not sufficient to effect a change in its electronic energy. As shown in Figure 10.15, vibrational energy levels are quantized; that is, a molecule may have only certain, discrete vibrational energies. The energy for an allowed vibrational mode, E_ν, is

$$E_\nu = \upsilon + \frac{1}{2}h\nu_0 \qquad (10.2.1)$$

where υ is the vibrational quantum number, which has values of 0, 1, 2, …, and ν_0 is the bond's fundamental vibrational frequency. The value of ν_0, which is determined by the bond's strength and by the mass at each end of the bond, is a characteristic property of a bond. For example, a carbon-carbon single bond (C–C) absorbs infrared radiation at a lower energy than a carbon-carbon double bond (C=C) because a single bond is weaker than a double bond.

At room temperature most molecules are in their ground vibrational state ($\upsilon = 0$). A transition from the ground vibrational state to the first vibrational excited state ($\upsilon = 1$) requires absorption of a photon with an energy of $h\nu_0$. Transitions in which $\Delta\upsilon$ is ±1 give

rise to the fundamental absorption lines. Weaker absorption lines, called overtones, result from transitions in which Δv is ±2 or ±3. The number of possible normal vibrational modes for a linear molecule is $3N - 5$, and for a non-linear molecule is $3N - 6$, where N is the number of atoms in the molecule. Not surprisingly, infrared spectra often show a considerable number of absorption bands. Even a relatively simple molecule, such as ethanol (C_2H_6O), for example, has $3 \times 9 - 6$, or 21 possible normal modes of vibration, although not all of these vibrational modes give rise to an absorption. The IR spectrum for ethanol is shown in Figure 10.16.

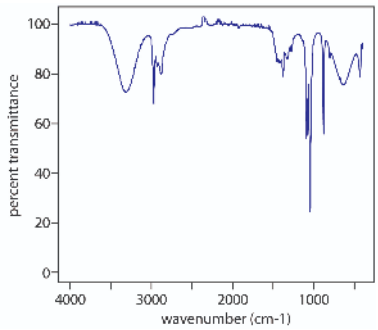


Figure 10.16 Infrared spectrum of ethanol.

Example: Methane

Why does a non-linear molecule have $3N - 6$ vibrational modes? Consider a molecule of methane, CH_4. Each of the five atoms in methane can move in one of three directions (x, y, and z) for a total of $5 \times 3 = 15$ different ways in which the molecule can move. A molecule can move in three ways: it can move from one place to another, what we call translational motion; it can rotate around an axis; and its bonds can stretch and bend, what we call vibrational motion.

Because the entire molecule can move in the x, y, and z directions, three of methane's 15 different motions are translational. In addition, the molecule can rotate about its x, y, and z axes, accounting for three additional forms of motion. This leaves $15 - 3 - 3 = 9$ vibrational modes.

A linear molecule, such as CO_2, has $3N - 5$ vibrational modes because it can rotate around only two axes.

UV/Vis Spectra for Molecules and Ions

The valence electrons in organic molecules and polyatomic ions, such as CO_3^{2-}, occupy quantized sigma bonding, σ, pi bonding, π, and non-bonding, n, molecular orbitals (MOs). Unoccupied sigma antibonding, σ*, and pi antibonding, π*, molecular orbitals are slightly higher in energy. Because the difference in energy between the highest-energy occupied MOs and the lowest-energy unoccupied MOs corresponds to ultraviolet and visible radiation, absorption of a photon is possible.

Four types of transitions between quantized energy levels account for most molecular UV/Vis spectra. Table 10.5 lists the approximate wavelength ranges for these transitions, as well as a partial list of bonds, functional groups, or molecules responsible for these transitions. Of these transitions, the most important are $n \rightarrow \pi^*$ and $\pi \rightarrow \pi^*$ because they involve important functional groups that are characteristic of many analytes and because the wavelengths are easily accessible. The bonds and functional groups that give rise to the absorption of ultraviolet and visible radiation are called **chromophores**.

Table 10.5 Electronic Transitions Involving n, σ, and π Molecular Orbitals

Transition	Wavelength Range	Examples
$\sigma \rightarrow \sigma^*$	<200 nm	C–C, C–H
$n \rightarrow \sigma^*$	160–260 nm	H_2O, CH_3OH, CH_3Cl
$\pi \rightarrow \pi^*$	200–500 nm	C=C, C=O, C=N, C^≡C
$n \rightarrow \pi^*$	250–600 nm	C=O, C=N, N=N, N=O

Many transition metal ions, such as Cu^{2+} and Co^{2+}, form colorful solutions because the metal ion absorbs visible light. The transitions giving rise to this absorption are valence electrons in the metal ion^fs d−orbitals. For a free metal ion, the five d−orbitals

are of equal energy. In the presence of a complexing ligand or solvent molecule, however, the *d*−orbitals split into two or more groups that differ in energy and with a magnitude that can be quantified by crystal field theory. For example, in an octahedral complex of $Cu(H_2O)_6^{2+}$ the six water molecules perturb the *d*−orbitals into two groups, as shown in Figure 10.17. The resulting *d*−*d* transitions for transition metal ions are relatively weak.

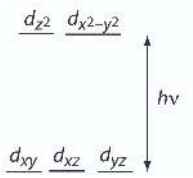


Figure 10.17 Splitting of the *d*-orbitals in an octahedral field.

A more important source of UV/Vis absorption for inorganic metal–ligand complexes is charge transfer, in which absorption of a photon produces an excited state in which there is transfer of an electron from the metal, *M*, to the ligand, *L*.

$$M—L + h\nu \rightarrow (M^+—L^-)^* \tag{10.2.2}$$

Charge-transfer absorption is important because it produces very large absorbances. One important example of a charge-transfer complex is that of *o*-phenanthroline with Fe^{2+}, the UV/Vis spectrum for which is shown in Figure 10.18. Charge-transfer absorption in which an electron moves from the ligand to the metal also is possible.

> **Note**
>
> Why is a larger absorbance desirable? An analytical method is more sensitive if a smaller concentration of analyte gives a larger signal.

Comparing the IR spectrum in Figure 10.16 to the UV/Vis spectrum in Figure 10.18 shows us that UV/Vis absorption bands are often significantly broader than those for IR absorption. We can use Figure 10.15 to explain why this is true. When a species absorbs UV/Vis radiation, the transition between electronic energy levels may also include a transition between vibrational energy levels. The result is a number of closely spaced absorption bands that merge together to form a single broad absorption band.

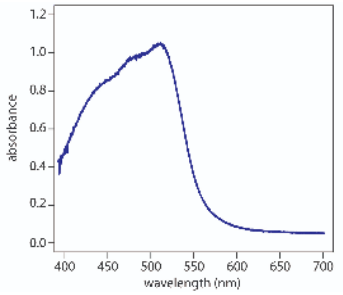


Figure 10.18 UV/Vis spectrum for the metal–ligand complex $Fe(phen)_3^{2+}$, where phen is the ligand *o*-phenanthroline.

UV/Vis Spectra for Atoms

The energy of ultraviolet and visible electromagnetic radiation is sufficient to cause a change in an atom's valence electron configuration. Sodium, for example, has a single valence electron in its 3*s* atomic orbital. As shown in Figure 10.19, unoccupied, higher energy atomic orbitals also exist.

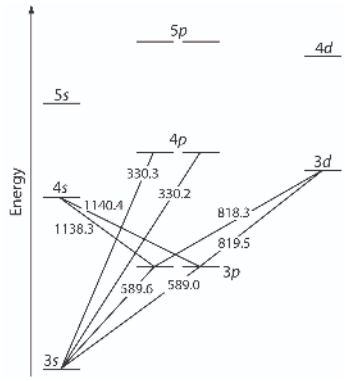


Figure 10.19 Valence shell energy level diagram for sodium. The wavelengths (in wavenumbers) corresponding to several transitions are shown.

The valence shell energy level diagram in Figure 10.19 might strike you as odd because it shows that the 3*p* orbitals are split into two groups of slightly different energy. The reasons for this splitting are unimportant in the context of our treatment of atomic absorption. For further information about the reasons for this splitting, consult the chapter's additional resources.

Absorption of a photon is accompanied by the excitation of an electron from a lower-energy atomic orbital to an orbital of higher energy. Not all possible transitions between atomic orbitals are allowed. For sodium the only allowed transitions are those in which there is a change of ±1 in the orbital quantum number (l); thus transitions from $s \rightarrow p$ orbitals are allowed, and transitions from $s \rightarrow d$ orbitals are forbidden.

The atomic absorption spectrum for Na is shown in Figure 10.20, and is typical of that found for most atoms. The most obvious feature of this spectrum is that it consists of a small number of discrete absorption lines corresponding to transitions between the ground state (the 3*s* atomic orbital) and the 3*p* and 4*p* atomic orbitals. Absorption from excited states, such as the $3p \rightarrow 4s$ and the $3p \rightarrow 3d$ transitions included in Figure 10.19, are too weak to detect. Because an excited state's lifetime is short—typically an excited state atom takes 10^{-7} to 10^{-8} s to return to a lower energy state—an atom in the exited state is likely to return to the ground state before it has an opportunity to absorb a photon.

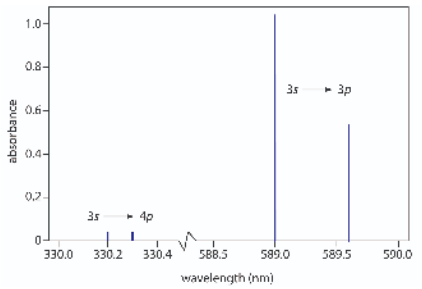


Figure 10.20 Atomic absorption spectrum for sodium. Note that the scale on the *x*-axis includes a break.

Another feature of the atomic absorption spectrum in Figure 10.20 is the narrow width of the absorption lines, which is a consequence of the fixed difference in energy between the ground and excited states. Natural line widths for atomic absorption, which are governed by the uncertainty principle, are approximately 10^{-5} nm. Other contributions to broadening increase this line width to approximately 10^{-3} nm.

10.2.2 Transmittance and Absorbance

As light passes through a sample, its power decreases as some of it is absorbed. This attenuation of radiation is described quantitatively by two separate, but related terms: transmittance and absorbance. As shown in Figure 10.21a, **transmittance** is the ratio of the source radiation's power exiting the sample, P_T, to that incident on the sample, P_0.

$$T = \frac{P_T}{P_0} \tag{10.1}$$

Multiplying the transmittance by 100 gives the percent transmittance, %T, which varies between 100% (no absorption) and 0% (complete absorption). All methods of detecting photons—including the human eye and modern photoelectric transducers—measure the transmittance of electromagnetic radiation.

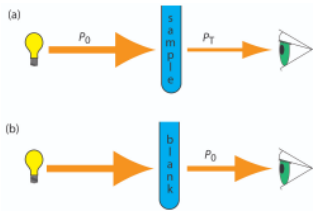


Figure 10.21 *(a) Schematic diagram showing the attenuation of radiation passing through a sample; P_0 is the radiant power from the source and P_T is the radiant power transmitted by the sample. (b) Schematic diagram showing how we redefine P_0 as the radiant power transmitted by the blank. Redefining P_0 in this way corrects the transmittance in (a) for the loss of radiation due to scattering, reflection, or absorption by the sample's container and absorption by the sample's matrix.*

Equation 10.1 does not distinguish between different mechanisms that prevent a photon emitted by the source from reaching the detector. In addition to absorption by the analyte, several additional phenomena contribute to the attenuation of radiation, including reflection and absorption by the sample's container, absorption by other components in the sample's matrix, and the scattering of radiation. To compensate for this loss of the radiation's power, we use a method blank. As shown in Figure 10.21b, we redefine P_0 as the power exiting the method blank.

An alternative method for expressing the attenuation of electromagnetic radiation is absorbance, A, which we define as

$$A = -\log T = -\log \frac{P_T}{P_0} \tag{10.2}$$

Absorbance is the more common unit for expressing the attenuation of radiation because it is a linear function of the analyte's concentration. We will show that this is true in Section 10.2.3.

Example 10.3

A sample has a percent transmittance of 50%. What is its absorbance?

SOLUTION

A percent transmittance of 50.0% is the same as a transmittance of 0.500 Substituting into equation 10.2 gives

$$A = -\log T = -\log(0.500) = 0.301 \tag{10.2.3}$$

Exercise 10.3

What is the %T for a sample if its absorbance is 1.27?

Click here to review your answer to this exercise.

Equation 10.1 has an important consequence for atomic absorption. As we saw in Figure 10.20, atomic absorption lines are very narrow. Even with a high quality monochromator, the effective bandwidth for a continuum source is 100–1000× greater than the width of an atomic absorption line. As a result, little of the radiation from a continuum source is absorbed ($P_0 \approx P_T$), and the measured absorbance is effectively zero. For this reason, atomic absorption requires a line source instead of a continuum source.

10.2.3 Absorbance and Concentration: Beer's Law

When monochromatic electromagnetic radiation passes through an infinitesimally thin layer of sample of thickness dx, it experiences a decrease in its power of dP (Figure 10.22). The fractional decrease in power is proportional to the sample's thickness and the analyte's concentration, C; thus]

$$-\frac{dP}{P} = \alpha C dx \tag{10.3}$$

where P is the power incident on the thin layer of sample, and α is a proportionality constant. Integrating the left side of equation 10.3 over the entire sample

$$-\int_{P_o}^{P_T} \frac{dP}{P} = \alpha C \int_o^b dx \tag{10.2.4}$$

$$\ln \frac{P_0}{P_T} = \alpha b C \tag{10.2.5}$$

converting from $\ln$ to $\log_{10}$, and substituting in equation 10.2, gives

$$A = abC \tag{10.4}$$

where a is the analyte's **absorptivity** with units of cm^{-1} $conc^{-1}$. If we express the concentration using molarity, then we replace a with the **molar absorptivity**, ε, which has units of cm^{-1} M^{-1}.

$$A = \epsilon b C \tag{10.5}$$

The absorptivity and molar absorptivity are proportional to the probability that the analyte absorbs a photon of a given energy. As a result, values for both a and ε depend on the wavelength of the absorbed photon.

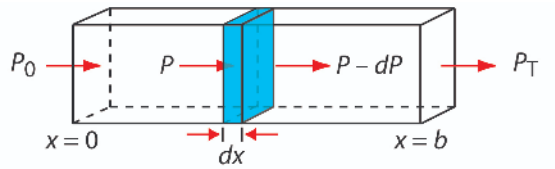


Figure 10.22 Factors used in deriving the Beer-Lambert law.

Example 10.4

A 5.00×10^{-4} M solution of an analyte is placed in a sample cell with a pathlength of 1.00 cm. When measured at a wavelength of 490 nm, the solution's absorbance is 0.338. What is the analyte's molar absorptivity at this wavelength?

SOLUTION

Solving equation 10.5 for ε and making appropriate substitutions gives

$$\epsilon = \frac{A}{bC} = \frac{0.338}{(1.00\ \text{cm})(5.00 \times 10^{-4}\ \text{M})} = 676\ \text{cm}^{-1}\ \text{M}^{-1} \tag{10.2.6}$$

Exercise 10.4

A solution of the analyte from Example 10.4 has an absorbance of 0.228 in a 1.00-cm sample cell. What is the analyte's concentration?

Click here to review your answer to this exercise.

Equation 10.4 and equation 10.5, which establish the linear relationship between absorbance and concentration, are known as the Beer-Lambert law, or more commonly, as **Beer's law**. Calibration curves based on Beer's law are common in quantitative analyses.

10.2.4 Beer's Law and Multicomponent Samples

We can extend Beer's law to a sample containing several absorbing components. If there are no interactions between the components, the individual absorbances, A_i, are additive. For a two-component mixture of analyte's X and Y, the total absorbance, A_{tot}, is

$$A_{tot} = A_X + A_Y = \epsilon_X b C_X + \epsilon_Y b C_Y \tag{10.2.7}$$

Generalizing, the absorbance for a mixture of n components, A_{mix}, is

$$A_{mix} = \sum_{i=0}^{n} A_i = \sum_{i=1}^{n} \varepsilon_i b C_i \tag{10.6}$$

10.2.5 Limitations to Beer's Law

Beer's law suggests that a calibration curve is a straight line with a *y*-intercept of zero and a slope of *ab* or ε*b*. In many cases a calibration curve deviates from this ideal behavior (Figure 10.23). Deviations from linearity are divided into three categories: fundamental, chemical, and instrumental.

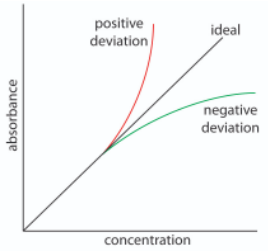


Figure 10.23 Calibration curves showing positive and negative deviations from the ideal Beer's law calibration curve, which is a straight line.

Fundamental Limitations to Beer's Law

Beer's law is a limiting law that is valid only for low concentrations of analyte. There are two contributions to this fundamental limitation to Beer's law.

1. At higher concentrations the individual particles of analyte no longer behave independently of each other. The resulting interaction between particles of analyte may change the analyte's absorptivity.
2. A second contribution is that the analyte's absorptivity depends on the sample's refractive index. Because the refractive index varies with the analyte's concentration, the values of *a* and ε may change. For sufficiently low concentrations of analyte, the refractive index is essentially constant and the calibration curve is linear.

Chemical Limitations to Beer's Law

A chemical deviation from Beer's law may occur if the analyte is involved in an equilibrium reaction. Consider, as an example, an analysis for the weak acid, HA. To construct a Beer's law calibration curve we prepare a series of standards—each containing a known total concentration of HA—and measure each standard's absorbance at the same wavelength. Because HA is a weak acid, it is in equilibrium with its conjugate weak base, A^-.

$$\mathrm{HA}_{(aq)} + \mathrm{H_2O}_{(l)} \rightleftharpoons \mathrm{H_3O^+}_{(aq)} + \mathrm{A^-}_{(aq)} \tag{10.2.8}$$

If both HA and A^- absorb at the chosen wavelength, then Beer's law is

$$A = \epsilon_{\mathrm{HA}} b C_{\mathrm{HA}} + \epsilon_{\mathrm{A}} b C_{\mathrm{A}} \tag{10.7}$$

where C_{HA} and C_A are the equilibrium concentrations of HA and A^-. Because the weak acid's total concentration, C_{total}, is

$$C_{\mathrm{total}} = C_{\mathrm{HA}} + C_{\mathrm{A}} \tag{10.2.9}$$

the concentrations of HA and A^- can be written as

$$C_{\mathrm{HA}} = \alpha_{\mathrm{HA}} C_{\mathrm{total}} \tag{10.8}$$

$$C_{\mathrm{A}} = (1 - \alpha_{\mathrm{HA}}) C_{\mathrm{total}} \tag{10.9}$$

where α_{HA} is the fraction of weak acid present as HA. Substituting equation 10.8 and equation 10.9 into equation 10.7 and rearranging, gives

$$A = (\epsilon_{\mathrm{HA}} \alpha_{\mathrm{HA}} + \epsilon_{\mathrm{A}} - \epsilon_{\mathrm{A}} \alpha_{\mathrm{HA}}) b C_{\mathrm{total}} \tag{10.10}$$

To obtain a linear Beer's law calibration curve, one of two conditions must be met. If α_{HA} and α_A have the same value at the chosen wavelength, then equation 10.10 simplifies to

$$A = \epsilon_{\mathrm{A}} b C_{\mathrm{total}} \tag{10.2.10}$$

Alternatively, if α_{HA} has the same value for all standards, then each term within the parentheses of equation 10.10 is constant—which we replace with *k*—and a linear calibration curve is obtained at any wavelength.

$$A = kbC_{total} \tag{10.2.11}$$

Because HA is a weak acid, the value of α_{HA} varies with pH. To hold α_{HA} constant we buffer each standard to the same pH. Depending on the relative values of $\alpha_{HA}$and α_A, the calibration curve has a positive or a negative deviation from Beer's law if we do not buffer the standards to the same pH.

Note

For a monoprotic weak acid, the equation for α_{HA} is

$$\alpha_{HA} = \frac{[H_3O^+]}{[H_3O^+] + K_a} \tag{10.2.12}$$

Problem 10.6 in the end of chapter problems asks you to explore this chemical limitation to Beer's law.

Instrumental Limitations to Beer's Law

There are two principal instrumental limitations to Beer's law. The first limitation is that Beer's law assumes that the radiation reaching the sample is of a single wavelength—that is, that the radiation is purely monochromatic. As shown in Figure 10.10, however, even the best wavelength selector passes radiation with a small, but finite effective bandwidth. Polychromatic radiation always gives a negative deviation from Beer's law, but the effect is smaller if the value of ε is essentially constant over the wavelength range passed by the wavelength selector. For this reason, as shown in Figure 10.24, it is better to make absorbance measurements at the top of a broad absorption peak. In addition, the deviation from Beer's law is less serious if the source's effective bandwidth is less than one-tenth of the natural bandwidth of the absorbing species.[5] When measurements must be made on a slope, linearity is improved by using a narrower effective bandwidth.

Note

Another reason for measuring absorbance at the top of an absorbance peak is that it provides for a more sensitive analysis. Note that the green calibration curve in Figure 10.24 has a steeper slope—a greater sensitivity—than the red calibration curve. Problem 10.7 in the end of chapter problems ask you to explore the effect of polychromatic radiation on the linearity of Beer's law.

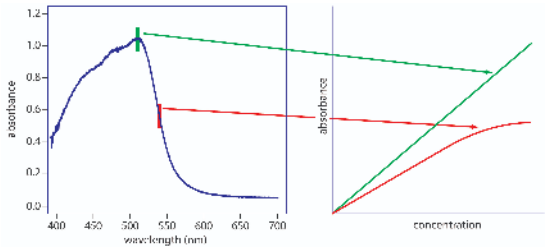


Figure 10.24 Effect of the choice of wavelength on the linearity of a Beer's law calibration curve.

Stray radiation is the second contribution to instrumental deviations from Beer's law. Stray radiation arises from imperfections in the wavelength selector that allow light to enter the instrument and reach the detector without passing through the sample. Stray radiation adds an additional contribution, P_{stray}, to the radiant power reaching the detector; thus

$$A = -\log\left(\frac{P_T + P_{stray}}{P_0 + P_{stray}}\right) \tag{10.2.13}$$

For a small concentration of analyte, P_{stray} is significantly smaller than P_0 and P_T, and the absorbance is unaffected by the stray radiation. At a higher concentration of analyte, however, less light passes through the sample and P_T and P_{stray} may be similar in magnitude. This results is an absorbance that is smaller than expected, and a negative deviation from Beer's law.

Note

Problem 10.8 in the end of chapter problems ask you to explore the effect of stray radiation on the linearity of Beer's law.

Contributors

David Harvey (DePauw University)

10.2: Spectroscopy Based on Absorption is shared under a CC BY-NC-SA 4.0 license and was authored, remixed, and/or curated by LibreTexts.

10.3: UV/Vis and IR Spectroscopy

In Figure 10.9 we examined Nessler's original method for matching the color of a sample to the color of a standard. Matching the colors was a labor intensive process for the analyst. Not surprisingly, spectroscopic methods of analysis were slow to develop. The 1930s and 1940s saw the introduction of photoelectric transducers for ultraviolet and visible radiation, and thermocouples for infrared radiation. As a result, modern instrumentation for absorption spectroscopy became routinely available in the 1940s—progress has been rapid ever since.

10.3.1 Instrumentation

Frequently an analyst must select—from among several instruments of different design—the one instrument best suited for a particular analysis. In this section we examine several different instruments for molecular absorption spectroscopy, emphasizing their advantages and limitations. Methods of sample introduction are also covered in this section.

Instrument Designs for Molecular UV/Vis Absorption

Filter Photometer. The simplest instrument for molecular UV/Vis absorption is a **filter photometer** (Figure 10.25), which uses an absorption or interference filter to isolate a band of radiation. The filter is placed between the source and the sample to prevent the sample from decomposing when exposed to higher energy radiation. A filter photometer has a single optical path between the source and detector, and is called a **single-beam** instrument. The instrument is calibrated to 0% T while using a shutter to block the source radiation from the detector. After opening the shutter, the instrument is calibrated to 100% T using an appropriate blank. The blank is then replaced with the sample and its transmittance measured. Because the source's incident power and the sensitivity of the detector vary with wavelength, the photometer must be recalibrated whenever the filter is changed. Photometers have the advantage of being relatively inexpensive, rugged, and easy to maintain. Another advantage of a photometer is its portability, making it easy to take into the field. Disadvantages of a photometer include the inability to record an absorption spectrum and the source's relatively large effective bandwidth, which limits the calibration curve's linearity.

> **Note**
>
> The percent transmittance varies between 0% and 100%. As we learned in Figure 10.21, we use a blank to determine P_0, which corresponds to 100% T. Even in the absence of light the detector records a signal. Closing the shutter allows us to assign 0% T to this signal. Together, setting 0% T and 100% T calibrates the instrument. The amount of light passing through a sample produces a signal that is greater than or equal to that for 0% T and smaller than or equal to that for 100%T.

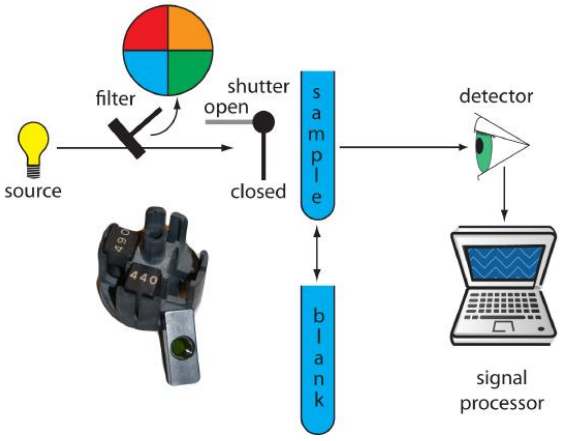


Figure 10.25 Schematic diagram of a filter photometer. The analyst either inserts a removable filter or the filters are placed in a carousel, an example of which is shown in the photographic inset. The analyst selects a filter by rotating it into place.

Single-Beam Spectrophotometer. An instrument that uses a monochromator for wavelength selection is called a **spectrophotometer**. The simplest spectrophotometer is a single-beam instrument equipped with a fixed-wavelength monochromator (Figure 10.26). Single-beam spectrophotometers are calibrated and used in the same manner as a photometer. One example of a single-beam spectrophotometer is Thermo Scientific's Spectronic 20D+, which is shown in the photographic insert to

Figure 10.26. The Spectronic 20D+ has a range of 340–625 nm (950 nm when using a red-sensitive detector), and a fixed effective bandwidth of 20 nm. Battery-operated, hand-held single-beam spectrophotometers are available, which are easy to transport into the field. Other single-beam spectrophotometers also are available with effective bandwidths of 2–8 nm. Fixed wavelength single-beam spectrophotometers are not practical for recording spectra because manually adjusting the wavelength and recalibrating the spectrophotometer is awkward and time-consuming. The accuracy of a single-beam spectrophotometer is limited by the stability of its source and detector over time.

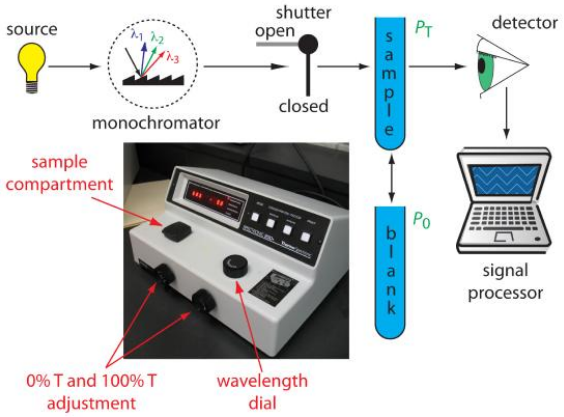


Figure 10.26 Schematic diagram of a fixed-wavelength single-beam spectrophotometer. The photographic inset shows a typical instrument. The shutter remains closed until the sample or blank is placed in the sample compartment. The analyst manually selects the wavelength by adjusting the wavelength dial. Inset photo modified from: Adi (www.commons.wikipedia.org).

Double-Beam Spectrophotometer. The limitations of fixed-wavelength, single-beam spectrophotometers are minimized by using a **double-beam** spectrophotometer (Figure 10.27). A chopper controls the radiation's path, alternating it between the sample, the blank, and a shutter. The signal processor uses the chopper's known speed of rotation to resolve the signal reaching the detector into the transmission of the blank, P_0, and the sample, P_T. By including an opaque surface as a shutter, it is possible to continuously adjust 0% T. The effective bandwidth of a double-beam spectrophotometer is controlled by adjusting the monochromator's entrance and exit slits. Effective bandwidths of 0.2–3.0 nm are common. A scanning monochromator allows for the automated recording of spectra. Double-beam instruments are more versatile than single-beam instruments, being useful for both quantitative and qualitative analyses, but also are more expensive.

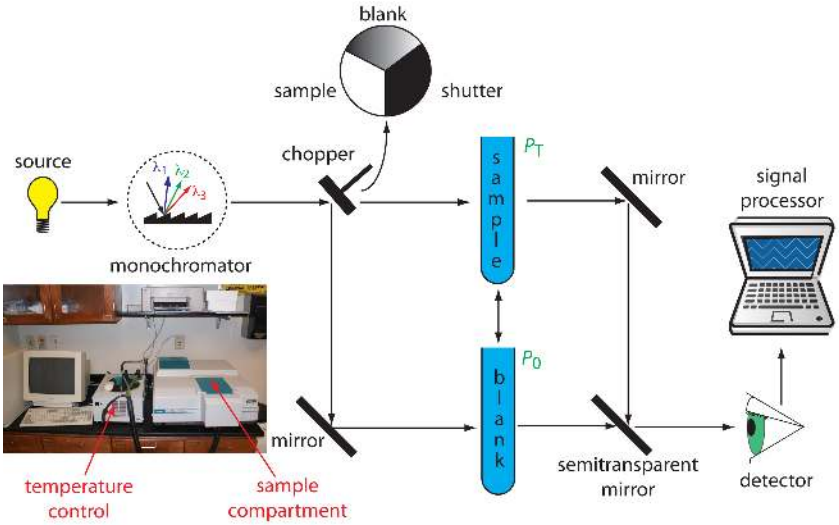


Figure 10.27 Schematic diagram of a scanning, double-beam spectrophotometer. A chopper directs the source's radiation, using a transparent window to pass radiation to the sample and a mirror to reflect radiation to the blank. The chopper's opaque surface serves as a shutter, which allows for a constant adjustment of the spectrophotometer's 0% T. The photographic insert shows a typical instrument. The unit in the middle of the photo is a temperature control unit that allows the sample to be heated or cooled.

Diode Array Spectrometer. An instrument with a single detector can monitor only one wavelength at a time. If we replace a single photomultiplier with many photodiodes, we can use the resulting array of detectors to record an entire spectrum simultaneously in as little as 0.1 s. In a diode array spectrometer the source radiation passes through the sample and is dispersed by a grating (Figure 10.28). The photodiode array is situated at the grating's focal plane, with each diode recording the radiant power over a narrow range of wavelengths. Because we replace a full monochromator with just a grating, a diode array spectrometer is small and compact.

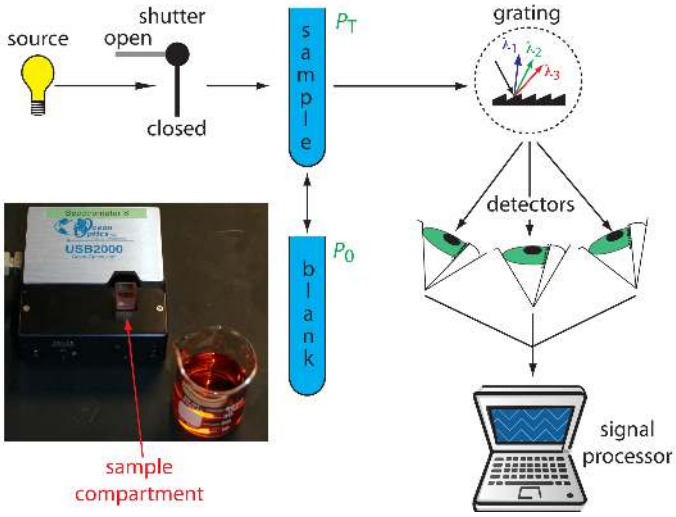


Figure 10.28 Schematic diagram of a diode array spectrophotometer. The photographic insert shows a typical instrument. Note that the 50-mL beaker provides a sense of scale.

One advantage of a diode array spectrometer is the speed of data acquisition, which allows to collect several spectra for a single sample. Individual spectra are added and averaged to obtain the final spectrum. This **signal averaging** improves a spectrum's signal-to-noise ratio. If we add together n spectra, the sum of the signal at any point, x, increases as nS_x, where S_x is the signal. The noise at any point, N_x, is a random event, which increases as $\sqrt{n}N_x$ when we add together n spectra. The **signal-to-noise ratio** (S/N) after n scans is

$$\frac{S}{N} = \frac{nS_x}{\sqrt{n}N_x} = \sqrt{n}\frac{S_x n}{N_x} \tag{10.3.1}$$

where S_x/N_x is the signal-to-noise ratio for a single scan. The impact of signal averaging is shown in Figure 10.29. The first spectrum shows the signal for a single scan, which consists of a single, noisy peak. Signal averaging using 4 scans and 16 scans decreases the noise and improves the signal-to-noise ratio. One disadvantage of a photodiode array is that the effective bandwidth per diode is roughly an order of magnitude larger than that for a high quality monochromator.

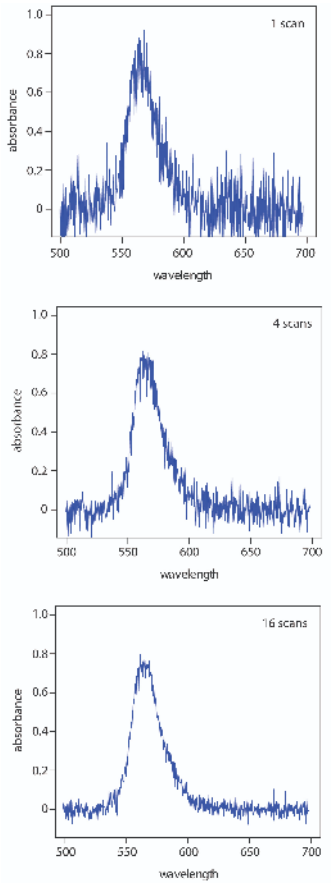


Figure 10.29 Effect of signal averaging on a spectrum's signal-to-noise ratio. From top to bottom: spectrum for a single scan; average spectrum after four scans; and average spectrum after adding 16 scans.

Sample Cells. The sample compartment provides a light-tight environment that limits the addition of stray radiation. Samples are normally in the liquid or solution state, and are placed in cells constructed with UV/Vis transparent materials, such as quartz, glass, and plastic (Figure 10.30). A quartz or fused-silica cell is required when working at a wavelength <300 nm where other materials show a significant absorption. The most common pathlength is 1 cm (10 mm), although cells with shorter (as little as 0.1 cm) and longer pathlengths (up to 10 cm) are available. Longer pathlength cells are useful when analyzing a very dilute solution, or for gas samples. The highest quality cells allow the radiation to strike a flat surface at a 90º angle, minimizing the loss of radiation to reflection. A test tube is often used as a sample cell with simple, single-beam instruments, although differences in the cell's pathlength and optical properties add an additional source of error to the analysis.



Figure 10.30 Examples of sample cells for UV/Vis spectroscopy. From left to right (with path lengths in parentheses): rectangular plastic cuvette (10.0 mm), rectangular quartz cuvette (5.000 mm), rectangular quartz cuvette (1.000 mm), cylindrical quartz cuvette (10.00 mm), cylindrical quartz cuvette (100.0 mm). Cells often are available as a matched pair, which is important when using a double-beam instrument.

If we need to monitor an analyte's concentration over time, it may not be possible to physically remove samples for analysis. This is often the case, for example, when monitoring industrial production lines or waste lines, when monitoring a patient's blood, or when monitoring environmental systems. With a **fiber-optic probe** we can analyze samples in situ. An example of a remote sensing fiber-optic probe is shown in Figure 10.31. The probe consists of two bundles of fiber-optic cable. One bundle transmits radiation from the source to the probe's tip, which is designed to allow the sample to flow through the sample cell. Radiation from the source passes through the solution and is reflected back by a mirror. The second bundle of fiber-optic cable transmits the nonabsorbed radiation to the wavelength selector. Another design replaces the flow cell shown in Figure 10.31 with a membrane containing a reagent that reacts with the analyte. When the analyte diffuses across the membrane it reacts with the reagent, producing a product that absorbs UV or visible radiation. The nonabsorbed radiation from the source is reflected or scattered back to the detector. Fiber optic probes that show chemical selectivity are called optrodes.[6]

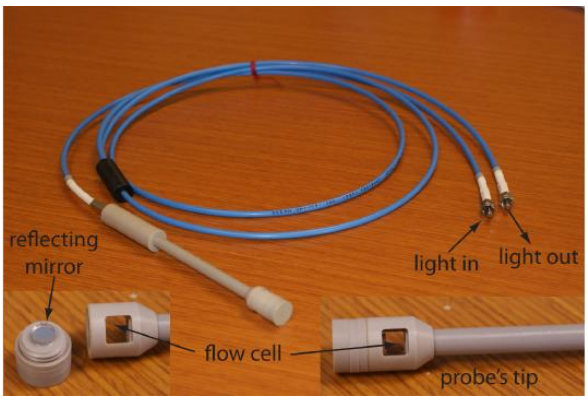


Figure 10.31 Example of a fiber-optic probe. The inset photographs provide a close-up look at the probe's flow cell and the reflecting mirror.

Instrument Designs for Infrared Absorption

Filter Photometer. The simplest instrument for IR absorption spectroscopy is a filter photometer similar to that shown in Figure 10.25 for UV/Vis absorption. These instruments have the advantage of portability, and typically are used as dedicated analyzers for gases such as HCN and CO.

Double-beam spectrophotometer. Infrared instruments using a monochromator for wavelength selection use double-beam optics similar to that shown in Figure 10.27. Double-beam optics are preferred over single-beam optics because the sources and detectors for infrared radiation are less stable than those for UV/Vis radiation. In addition, it is easier to correct for the absorption of infrared radiation by atmospheric CO_2 and H_2O vapor when using double-beam optics. Resolutions of 1–3 cm^{-1} are typical for most instruments.

Fourier transform spectrometer. In a Fourier transform infrared spectrometer, or FT–IR, the monochromator is replaced with an interferometer (Figure 10.13). Because an FT-IR includes only a single optical path, it is necessary to collect a separate spectrum to compensate for the absorbance of atmospheric CO_2 and H_2O vapor. This is done by collecting a background spectrum without the sample and storing the result in the instrument's computer memory. The background spectrum is removed from the sample's spectrum by ratioing the two signals. In comparison to other instrument designs, an FT–IR provides for rapid data acquisition, allowing an enhancement in signal-to-noise ratio through signal-averaging.

Sample Cells. Infrared spectroscopy is routinely used to analyze gas, liquid, and solid samples. Sample cells are made from materials, such as NaCl and KBr, that are transparent to infrared radiation. Gases are analyzed using a cell with a pathlength of approximately 10 cm. Longer pathlengths are obtained by using mirrors to pass the beam of radiation through the sample several times.

A liquid samples may be analyzed using a variety of different sample cells (Figure 10.32). For non-volatile liquids a suitable sample can be prepared by placing a drop of the liquid between two NaCl plates, forming a thin film that typically is less than 0.01 mm thick. Volatile liquids must be placed in a sealed cell to prevent their evaporation.

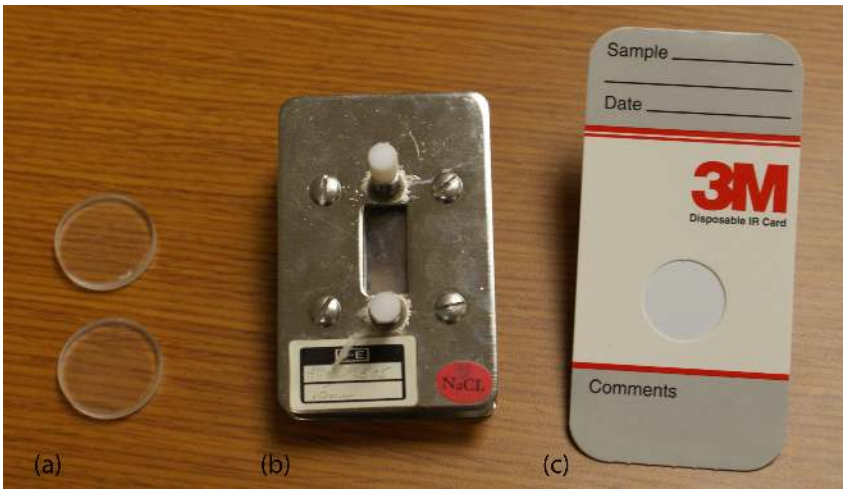


Figure 10.32 Three examples of IR sample cells: (a) NaCl salts plates; (b) fixed pathlength (0.5 mm) sample cell with NaCl windows; (c) disposable card with a polyethylene window that is IR transparent with the exception of strong absorption bands at 2918 cm^{-1} and 2849 cm^{-1}.

The analysis of solution samples is limited by the solvent's IR absorbing properties, with CCl_4, CS_2, and $CHCl_3$ being the most common solvents. Solutions are placed in cells containing two NaCl windows separated by a Teflon spacer. By changing the Teflon spacer, pathlengths from 0.015–1.0 mm can be obtained.

Transparent solid samples can be analyzed directly by placing them in the IR beam. Most solid samples, however, are opaque, and must be dispersed in a more transparent medium before recording the IR spectrum. If a suitable solvent is available, then the solid can be analyzed by preparing a solution and analyzing as described above. When a suitable solvent is not available, solid samples may be analyzed by preparing a mull of the finely powdered sample with a suitable oil. Alternatively, the powdered sample can be mixed with KBr and pressed into an optically transparent pellet.

The analysis of an aqueous sample is complicated by the solubility of the NaCl cell window in water. One approach to obtaining infrared spectra on aqueous solutions is to use **attenuated total reflectance** instead of transmission. Figure 10.33 shows a diagram of a typical attenuated total reflectance (ATR) FT–IR instrument. The ATR cell consists of a high refractive index material, such as ZnSe or diamond, sandwiched between a low refractive index substrate and a lower refractive index sample. Radiation from the source enters the ATR crystal where it undergoes a series of total internal reflections before exiting the crystal. During each reflection the radiation penetrates into the sample to a depth of a few microns. The result is a selective attenuation of the radiation at those wavelengths where the sample absorbs. ATR spectra are similar, but not identical, to those obtained by measuring the transmission of radiation.

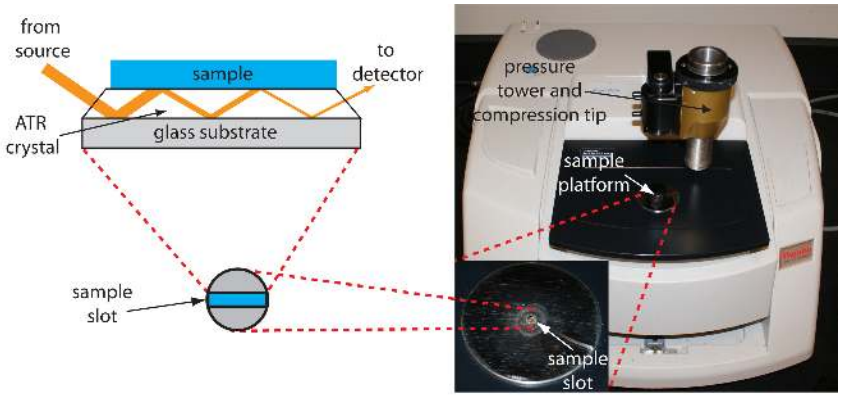


Figure 10.33 FT-IR spectrometer equipped with a diamond ATR sample cell. The inserts show a close-up photo of the sample platform, a sketch of the ATR's sample slot, and a schematic showing how the source's radiation interacts with the sample. The pressure tower is used to ensure the contact of solid samples with the ATR crystal.

Solid samples also can be analyzed using an ATR sample cell. After placing the solid in the sample slot, a compression tip ensures that it is in contact with the ATR crystal. Examples of solids that have been analyzed by ATR include polymers, fibers, fabrics, powders, and biological tissue samples. Another reflectance method is diffuse reflectance, in which radiation is reflected from a rough surface, such as a powder. Powdered samples are mixed with a non-absorbing material, such as powdered KBr, and the reflected light is collected and analyzed. As with ATR, the resulting spectrum is similar to that obtained by conventional transmission methods.

> **Note**
>
> Further details about these, and other methods for preparing solids for infrared analysis can be found in this chapter's additional resources.

10.3.2 Quantitative Applications

The determination of an analyte's concentration based on its absorption of ultraviolet or visible radiation is one of the most frequently encountered quantitative analytical methods. One reason for its popularity is that many organic and inorganic compounds have strong absorption bands in the UV/Vis region of the electromagnetic spectrum. In addition, if an analyte does not absorb UV/Vis radiation—or if its absorbance is too weak—we often can react it with another species that is strongly absorbing. For example, a dilute solution of Fe^{2+} does not absorb visible light. Reacting Fe^{2+} with *o*-phenanthroline, however, forms an orange–red complex of $Fe(phen)_3^{2+}$ that has a strong, broad absorbance band near 500 nm. An additional advantage to UV/Vis absorption is that in most cases it is relatively easy to adjust experimental and instrumental conditions so that Beer's law is obeyed.

> **Note**
>
> Figure 10.18 shows the visible spectrum for $Fe(phen)_3^{2+}$.

A quantitative analysis based on the absorption of infrared radiation, although important, is less frequently encountered than those for UV/Vis absorption. One reason is the greater tendency for instrumental deviations from Beer's law when using infrared radiation. Because an infrared absorption band is relatively narrow, any deviation due to the lack of monochromatic radiation is more pronounced. In addition, infrared sources are less intense than UV/Vis sources, making stray radiation more of a problem. Differences in pathlength for samples and standards when using thin liquid films or KBr pellets are a problem, although an internal standard can be used to correct for any difference in pathlength. Finally, establishing a 100% T ($A = 0$) baseline is often difficult because the optical properties of NaCl sample cells may change significantly with wavelength due to contamination and degradation. We can minimize this problem by measuring absorbance relative to a baseline established for the absorption band. Figure 10.34 shows how this is accomplished.

> **Note**
>
> Another approach is to use a cell with a fixed pathlength, such as that shown in Figure 10.32b.

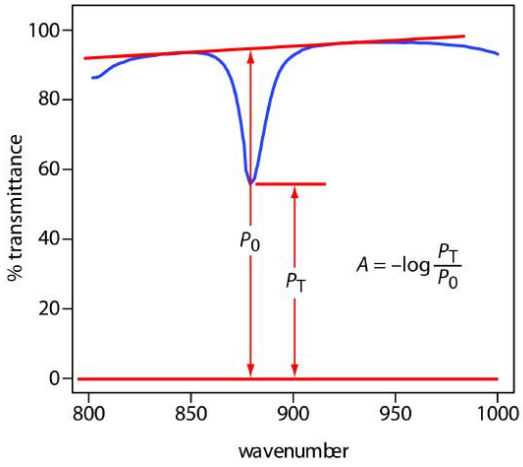


Figure 10.34 Method for determining absorbance from an IR spectrum.

Environmental Applications

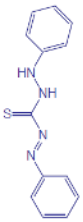
The analysis of waters and wastewaters often relies on the absorption of ultraviolet and visible radiation. Many of these methods are outlined in Table 10.6. Several of these methods are described here in more detail.

Table 10.6 Examples of the Molecular UV/Vis Analysis of Waters and Wastewaters

Analyte	Method	λ (nm)
	Trace Metals	
aluminum	react with Eriochrome cyanide R dye at pH6; forms red to pink complex	535
arsenic	reduce to AsH_3 using Zn and react with silver diethyldithiocarbamate; forms red complex	535
cadmium	extract into $CHCl_3$ containing dithizone from a sample made basic with NaOH; forms pink to red complex	518
chromium	oxidize to Cr(VI) and react with diphenylcarbazide; forms red-violet product	540
copper	react with neocuprine in neutral to slightly acid solution and extract into $CHCl_3/CH_3OH$; forms yellow complex	457
iron	reduce to Fe^{2+} and react with *o*-phenanthroline; forms orange-red complex	510
lead	extract into $CHCl_3$ containing dithizone from sample made basic with NH_3/NH_4^+ buffer; forms cherry red complex	510
manganese	oxidize to MnO_4^- with persulfate; forms purple solution	525
mercury	extract into $CHCl_3$ containing dithizone from acidic sample; forms orange complex	492
zinc	react with zincon at pH 9; forms blue complex	620
	Inorganic Nonmetals	
ammonia	reaction with hypochlorite and phenol using a manganous salt catalyst; forms blue indophenol as product	630
cyanide	react with chloroamine-T to form CNCl and then with a pyridine-barbituric acid; forms a red-blue dye	578

Analyte	Method	λ (nm)
fluoride	react with red Zr-SPADNS lake; formation of ZrF_6^{2-} decreases color of the red lake	570
chlorine (residual)	react with leuco crystal violet; forms blue product	592
nitrate	react with Cd to form NO_2^- and then react with sulfanilamide and *N*-(1-napthyl)-ethylenediamine; forms red azo dye	543
phosphate	react with ammonium molybdate and then reduce with $SnCl_2$; forms molybdenum blue	690
Organics		
phenol	react with 4-aminoantipyrine and $K_3Fe(CN)_6$; forms yellow antipyrine dye	460
anionic surfactant	react with cationic methylene blue dye and extract into $CHCl_3$; forms blue ion pair	652

Although the quantitative analysis of metals in waters and wastewaters is accomplished primarily by atomic absorption or atomic emission spectroscopy, many metals also can be analyzed following the formation of a colored metal–ligand complex. One advantage to these spectroscopic methods is that they are easily adapted to the analysis of samples in the field using a filter photometer. One ligand that is used in the analysis of several metals is diphenylthiocarbazone, also known as dithizone. Dithizone is not soluble in water, but when a solution of dithizone in $CHCl_3$ is shaken with an aqueous solution containing an appropriate metal ion, a colored metal–dithizonate complex forms that is soluble in $CHCl_3$. The selectivity of dithizone is controlled by adjusting the sample's pH. For example, Cd^{2+} is extracted from solutions that are made strongly basic with NaOH, Pb^{2+} from solutions that are made basic with an NH_3/NH_4^+ buffer, and Hg^{2+} from solutions that are slightly acidic.



Note

Atomic absorption is the subject of Section 10.4 and atomic emission is the subject of Section 10.7.

The structure of dithizone is shown to the right. See Chapter 7 for a discussion of extracting metal ions using dithizone.

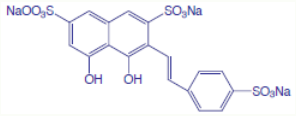
When chlorine is added to water the portion available for disinfection is called the chlorine residual. There are two forms of chlorine residual. The free chlorine residual includes Cl_2, HOCl, and OCl^-. The combined chlorine residual, which forms from the reaction of NH_3 with HOCl, consists of monochloramine, NH_2Cl, dichloramine, $NHCl_2$, and trichloramine, NCl_3. Because the free chlorine residual is more efficient at disinfection, there is an interest in methods that can distinguish between the different forms of the total chlorine residual. One such method is the leuco crystal violet method. The free residual chlorine is determined by adding

leuco crystal violet to the sample, which instantaneously oxidizes to give a blue colored compound that is monitored at 592 nm. Completing the analysis in less than five minutes prevents a possible interference from the combined chlorine residual. The total chlorine residual (free + combined) is determined by reacting a separate sample with iodide, which reacts with both chlorine residuals to form HOI. When the reaction is complete, leuco crystal violet is added and oxidized by HOI, giving the same blue colored product. The combined chlorine residual is determined by difference.

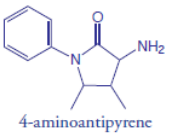
> **Note**
>
> In Chapter 9 we explored how the total chlorine residual can be determined by a redox titration; see Representative Method 9.3 for further details. The method described here allows us to divide the total chlorine residual into its component parts.

The concentration of fluoride in drinking water may be determined indirectly by its ability to form a complex with zirconium. In the presence of the dye SPADNS, solutions of zirconium form a red colored compound, called a lake, that absorbs at 570 nm. When fluoride is added, the formation of the stable ZrF_6^{2-} complex causes a portion of the lake to dissociate, decreasing the absorbance. A plot of absorbance versus the concentration of fluoride, therefore, has a negative slope.

> **Note**
>
> SPADNS, which is shown below, is an abbreviation for the sodium salt of 2-(4-sulfophenylazo)-1,8-dihydroxy-3,6-napthalenedisulfonic acid, which is a mouthful to say.



Spectroscopic methods also are used to determine organic constituents in water. For example, the combined concentrations of phenol, and ortho- and meta- substituted phenols are determined by using steam distillation to separate the phenols from nonvolatile impurities. The distillate reacts with 4-aminoantipyrine at pH 7.9 ± 0.1 in the presence of $K_3Fe(CN)_6$, forming a yellow colored antipyrine dye. After extracting the dye into $CHCl_3$, its absorbance is monitored at 460 nm. A calibration curve is prepared using only the unsubstituted phenol, C_6H_5OH. Because the molar absorptivity of substituted phenols are generally less than that for phenol, the reported concentration represents the minimum concentration of phenolic compounds.



Molecular absorption also can be used for the analysis of environmentally significant airborne pollutants. In many cases the analysis is carried out by collecting the sample in water, converting the analyte to an aqueous form that can be analyzed by methods such as those described in Table 10.6. For example, the concentration of NO_2 can be determined by oxidizing NO_2 to NO_3^-. The concentration of NO_3^- is then determined by first reducing it to NO_2^- with Cd, and then reacting NO_2^- with sulfanilamide and *N*-(1-naphthyl)-ethylenediamine to form a red azo dye. Another important application is the analysis for SO_2, which is determined by collecting the sample in an aqueous solution of $HgCl_4^{2-}$ where it reacts to form $Hg(SO_3)_2^{2-}$. Addition of *p*-rosaniline and formaldehyde produces a purple complex that is monitored at 569 nm. Infrared absorption is useful for the analysis of organic vapors, including HCN, SO_2, nitrobenzene, methyl mercaptan, and vinyl chloride. Frequently, these analyses are accomplished using portable, dedicated infrared photometers.



Clinical Applications

The analysis of clinical samples is often complicated by the complexity of the sample matrix, which may contribute a significant background absorption at the desired wavelength. The determination of serum barbiturates provides one example of how this problem is overcome. The barbiturates are first extracted from a sample of serum with $CHCl_3$ and then extracted from the $CHCl_3$ into 0.45 M NaOH (pH ≈ 13). The absorbance of the aqueous extract is measured at 260 nm, and includes contributions from the barbiturates as well as other components extracted from the serum sample. The pH of the sample is then lowered to approximately 10 by adding NH_4Cl and the absorbance remeasured. Because the barbiturates do not absorb at this pH, we can use the absorbance at pH 10, $A_{\text{pH 10}}$, to correct the absorbance at pH 13, $A_{\text{pH 13}}$

$$A_{\text{barb}} = A_{\text{pH 13}} - \frac{V_{\text{samp}} + V_{\text{NH}_4\text{Cl}}}{V_{\text{samp}}} \times A_{\text{pH 10}} \qquad (10.3.2)$$

where A_{barb} is the absorbance due to the serum barbiturates, and V_{samp} and V_{NH4Cl} are the volumes of sample and NH_4Cl, respectively. Table 10.7 provides a summary of several other methods for analyzing clinical samples.

Table 10.7 Examples of the Molecular UV/Vis Analysis of Clinical Samples

Analyte	Method	λ (nm)
total serum protein	react with NaOH and Cu^{2+}; forms blue-violet complex	540
serum cholesterol	react with Fe^{3+} in presence of isopropanol, acetic acid, and H_2SO_4; forms blue-violet complex	540
uric acid	react with phosphotungstic acid; forms tungsten blue	710
serum barbiturates	extract into $CHCl_3$ to isolate from interferents and then extract into 0.45 M NaOH	260
glucose	react with *o*-toludine at 100°C; forms blue-green complex	630
protein-bound iodine	decompose protein to release iodide, which catalyzes redox reaction between Ce^{3+} and As^{3+}; forms yellow colored Ce^{4+}	420

Industrial Analysis

UV/Vis molecular absorption is used for the analysis of a diverse array of industrial samples including pharmaceuticals, food, paint, glass, and metals. In many cases the methods are similar to those described in Table 10.6 and Table 10.7. For example, the amount of iron in food can be determined by bringing the iron into solution and analyzing using the *o*-phenanthroline method listed in Table 10.6.

Many pharmaceutical compounds contain chromophores that make them suitable for analysis by UV/Vis absorption. Products that have been analyzed in this fashion include antibiotics, hormones, vitamins, and analgesics. One example of the use of UV absorption is in determining the purity of aspirin tablets, for which the active ingredient is acetylsalicylic acid. Salicylic acid, which is produced by the hydrolysis of acetylsalicylic acid, is an undesirable impurity in aspirin tablets, and should not be present at more than 0.01% w/w. Samples can be screened for unacceptable levels of salicylic acid by monitoring the absorbance at a wavelength of 312 nm. Acetylsalicylic acid absorbs at 280 nm, but absorbs poorly at 312 nm. Conditions for preparing the sample are chosen such that an absorbance of greater than 0.02 signifies an unacceptable level of salicylic acid.

Forensic Applications

UV/Vis molecular absorption is routinely used for the analysis of narcotics and for drug testing. One interesting forensic application is the determination of blood alcohol using the Breathalyzer test. In this test a 52.5-mL breath sample is bubbled through an acidified solution of $K_2Cr_2O_7$, which oxidizes ethanol to acetic acid. The concentration of ethanol in the breath sample is determined by the decrease in absorbance at 440 nm where the dichromate ion absorbs. A blood alcohol content of 0.10%, which is above the legal limit, corresponds to 0.025 mg of ethanol in the breath sample.

Developing a Quantitative Method for a Single Component

In developing a quantitative analytical method, the conditions under which Beer's law is obeyed must be established. First, the most appropriate wavelength for the analysis is determined from an absorption spectrum. In most cases the best wavelength corresponds to an absorption maximum because it provides greater sensitivity and is less susceptible to instrumental limitations. Second, if an instrument with adjustable slits is being used, then an appropriate slit width needs to be chosen. The absorption spectrum also aids in selecting a slit width. Usually we set the slits to be as wide as possible because this increases the throughput of source radiation, while also being narrow enough to avoid instrumental limitations to Beer's law. Finally, a calibration curve is constructed to determine the range of concentrations for which Beer's law is valid. Additional considerations that are important in any quantitative method are the effect of potential interferents and establishing an appropriate blank.

Note

The best way to appreciate the theoretical and practical details discussed in this section is to carefully examine a typical analytical method. Although each method is unique, the following description of the determination of iron in water and

wastewater provides an instructive example of a typical procedure. The description here is based on Method 3500- Fe B as published in *Standard Methods for the Examination of Water and Wastewater*, 20th Ed., American Public Health Association: Washington, D. C., 1998.

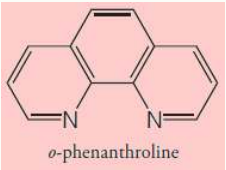
Representative Method 10.1

Determination of Iron in Water and Wastewater

Description of Method

Iron in the +2 oxidation state reacts with *o*-phenanthroline to form the orange-red $Fe(phen)_3^{2+}$ complex. The intensity of the complex's color is independent of solution acidity between a pH of 3 and 9. Because the complex forms more rapidly at lower pH levels, the reaction is usually carried out within a pH range of 3.0–3.5. Any iron present in the +3 oxidation state is reduced with hydroxylamine before adding *o*-phenanthroline. The most important interferents are strong oxidizing agents, polyphosphates, and metal ions such as Cu^{2+}, Zn^{2+}, Ni^{2+}, and Cd^{2+}. An interference from oxidizing agents is minimized by adding an excess of hydroxylamine, and an interference from polyphosphate is minimized by boiling the sample in the presence of acid. The absorbance of samples and standards are measured at a wavelength of 510 nm using a 1-cm cell (longer pathlength cells also may be used). Beer's law is obeyed for concentrations of within the range of 0.2–4.0 mg Fe/L.

(Figure 10.18 shows the visible spectrum for $Fe(phen)_3^{2+}$.)



o-phenanthroline

Procedure

For samples containing less than 2 mg Fe/L, directly transfer a 50-mL portion to a 125-mL Erlenmeyer flask. Samples containing more than 2 mg Fe/L must be diluted before acquiring the 50-mL portion. Add 2 mL of concentrated HCl and 1 mL of hydroxylamine to the sample. Heat the solution to boiling and continue boiling until the solution's volume is reduced to between 15 and 20 mL. After cooling to room temperature, transfer the solution to a 50-mL volumetric flask, add 10 mL of an ammonium acetate buffer, 2 mL of a 1000 ppm solution of *o*-phenanthroline, and dilute to volume. Allow 10–15 minutes for color development before measuring the absorbance, using distilled water to set 100% T. Calibration standards, including a blank, are prepared by the same procedure using a stock solution containing a known concentration of Fe^{2+}.

Questions

1. Explain why strong oxidizing agents are interferents, and why an excess of hydroxylamine prevents the interference.

A strong oxidizing agent oxidizes some Fe^{2+} to Fe^{3+}. Because $Fe(phen)_3^{3+}$ does not absorb as strongly as $Fe(phen)_3^{2+}$, the absorbance decreases, producing a negative determinate error. The excess hydroxylamine reacts with the oxidizing agents, removing them from the solution.

2. The color of the complex is stable between pH levels of 3 and 9. What are some possible complications at more acidic or more basic pH's?

Because *o*-phenanthroline is a weak base, its conditional formation constant for $Fe(phen)_3^{2+}$ is less favorable at more acidic pH levels, where *o*-phenanthroline is protonated. The result is a decrease in absorbance and a less sensitive analytical method.

(In Chapter 9 we saw the same effect of pH on the complexation reactions between EDTA and metal ions.)

When the pH is greater than 9, competition between OH^- and *o*-phenanthroline for Fe^{2+} also decreased the absorbance. In addition, if the pH is sufficiently basic there is a risk that the iron will precipitate as $Fe(OH)_2$.

3. Cadmium is an interferent because it forms a precipitate with *o*-phenanthroline. What effect would the formation of precipitate have on the determination of iron?

Because *o*-phenanthroline is present in large excess (2000 µg of *o*-phenanthroline for 100 µg of Fe^{2+}), it is not likely that the interference is due to an insufficient amount of *o*-phenanthroline being available to react with the Fe^{2+}. The presence of a precipitate in the sample cell results in the scattering of radiation, which causes an apparent increase in absorbance. Because the measured absorbance increases, the reported concentration is too high.

(Although scattering is a problem here, it can serve as the basis of a useful analytical method. See Section 10.8 for further details.)

4. Even high quality ammonium acetate contains a significant amount of iron. Why is this source of iron not a problem?

Because all samples and standards are prepared using the same volume of ammonium acetate buffer, the contribution of this source of iron is accounted for by the calibration curve's reagent blank.

Quantitative Analysis for a Single Analyte

To determine the concentration of a an analyte we measure its absorbance and apply Beer's law using any of the standardization methods described in Chapter 5. The most common methods are a normal calibration curve using external standards and the method of standard additions. A single point standardization is also possible, although we must first verify that Beer's law holds for the concentration of analyte in the samples and the standard.

Example 10.5

The determination of Fe in an industrial waste stream was carried out by the *o*-phenanthroline described in Representative Method 10.1. Using the data in the following table, determine the mg Fe/L in the waste stream.

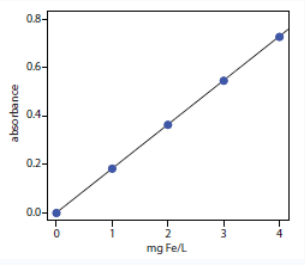
mg Fe/L	absorbance
0.00	0.000
1.00	0.183
2.00	0.364
3.00	0.546
4.00	0.727
sample	0.269

Solution

Linear regression of absorbance versus the concentration of Fe in the standards gives a calibration curve with the following equation.

$$A = 0.0006 + 0.1817 \times (\text{mg Fe/L}) \qquad (10.3.3)$$

Substituting the sample's absorbance into the calibration expression gives the concentration of Fe in the waste stream as 1.48 mg Fe/L.



https://chem.libretexts.org/@go/page/70700

Practice Exercise 10.5

The concentration of Cu^{2+} in a sample can be determined by reacting it with the ligand cuprizone and measuring its absorbance at 606 nm in a 1.00-cm cell. When a 5.00-mL sample is treated with cuprizone and diluted to 10.00 mL, the resulting solution has an absorbance of 0.118. A second 5.00-mL sample is mixed with 1.00 mL of a 20.00 mg/L standard of Cu^{2+}, treated with cuprizone and diluted to 10.00 mL, giving an absorbance of 0.162. Report the mg Cu^{2+}/L in the sample.

Click here to review your answer to this exercise.

Quantitative Analysis of Mixtures

Suppose we need to determine the concentration of two analytes, X and Y, in a sample. If each analyte has a wavelength where the other analyte does not absorb, then we can proceed using the approach in Example 10.5. Unfortunately, UV/Vis absorption bands are so broad that it frequently is not possible to find suitable wavelengths. Because Beer's law is additive the mixture's absorbance, A_{mix}, is

$$(A_{mix})_{\lambda 1} = (\varepsilon_X)_{\lambda 1} b C_X + (\varepsilon_Y)_{\lambda 1} b C_Y \tag{10.11}$$

where λ1 is the wavelength at which we measure the absorbance. Because equation 10.11 includes terms for the concentration of both X and Y, the absorbance at one wavelength does not provide enough information to determine either C_X or C_Y. If we measure the absorbance at a second wavelength

$$(A_{mix})_{\lambda 2} = (\varepsilon_X)_{\lambda 2} b C_X + (\varepsilon_Y)_{\lambda 2} b C_Y \tag{10.12}$$

then C_X and C_Y can be determined by solving simultaneously equation10.11 and equation 10.12. Of course, we also must determine the value for ε_X and ε_Y at each wavelength. For a mixture of *n* components, we must measure the absorbance at *n* different wavelengths.

Example 10.6

The concentrations of Fe^{3+} and Cu^{2+} in a mixture can be determined following their reaction with hexacyanoruthenate (II), $Ru(CN)_6^{4-}$, which forms a purple-blue complex with Fe^{3+} (λ_{max} = 550 nm) and a pale-green complex with Cu^{2+} (λ_{max} = 396 nm).[7] The molar absorptivities (M^{-1} cm^{-1}) for the metal complexes at the two wavelengths are summarized in the following table.

	ε_{550}	ε_{396}
Fe^{3+}	9970	84
Cu^{2+}	34	856

When a sample containing Fe^{3+} and Cu^{2+} is analyzed in a cell with a pathlength of 1.00 cm, the absorbance at 550 nm is 0.183 and the absorbance at 396 nm is 0.109. What are the molar concentrations of Fe^{3+} and Cu^{2+} in the sample?

Solution

Substituting known values into equations 10.11 and 10.12 gives

$$A_{550} = 0.183 = 9970 C_{Fe} + 34 C_{Cu} \tag{10.3.4}$$

$$A_{396} = 0.109 = 84 C_{Fe} + 856 C_{Cu} \tag{10.3.5}$$

To determine C_{Fe} and C_{Cu} we solve the first equation for C_{Cu}

$$C_{Cu} = \frac{0.183 - 9970 C_{Fe}}{34} \tag{10.3.6}$$

and substitute the result into the second equation.

$$0.109 = 84 C_{Fe} + 856 \times \frac{0.183 - 9970 C_{Fe}}{34} = 4.607 - (2.51 \times 10^5) C_{Fe} \tag{10.3.7}$$

Solving for C_{Fe} gives the concentration of Fe^{3+} as 1.79×10^{-5} M. Substituting this concentration back into the equation for the mixture's absorbance at 396 nm gives the concentration of Cu^{2+} as 1.26×10^{-4} M.

(Another approach is to multiply the first equation by 856/34 giving

$$4.607 = 251009C_{Fe} + 856C_{Cu} \quad (10.3.8)$$

Subtracting the second equation from this equation

$$\begin{aligned} 4.607 &= 251009C_{Fe} + 856C_{Cu} && (10.3.9)\\ -0.109 &= 84C_{Fe} + 856C_{Cu} && (10.3.10)\\ \hline 4.498 &= 250925C_{Fe} && (10.3.11) \end{aligned}$$

we find that C_{Fe} is 1.79×10^{-5}. Having determined C_{Fe} we can substitute back into one of the other equations to solve for C_{Cu}, which is 1.26×10^{-5}.)

Practice Exercise 10.6

The absorbance spectra for Cr^{3+} and Co^{2+} overlap significantly. To determine the concentration of these analytes in a mixture, its absorbance was measured at 400 nm and at 505 nm, yielding values of 0.336 and 0.187, respectively. The individual molar absorptivities (M^{-1} cm^{-1}) are

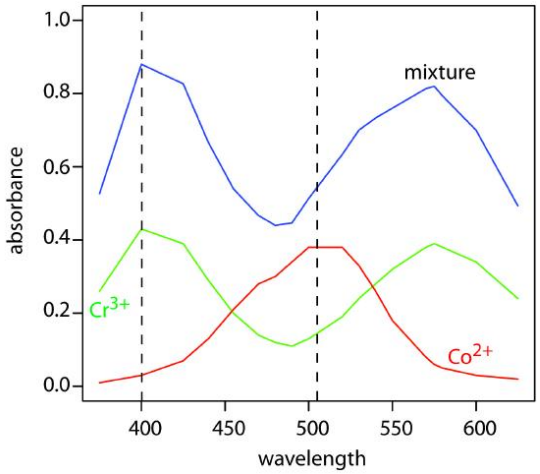
	ε_{400}	ε_{505}
Cr^{3+}	15.2	0.533
Co^{2+}	5.60	5.07

Click here to review your answer to this exercise.

To obtain results with good accuracy and precision the two wavelengths should be selected so that $\varepsilon_X > \varepsilon_Y$ at one wavelength and $\varepsilon_X < \varepsilon_Y$ at the other wavelength. It is easy to appreciate why this is true. Because the absorbance at each wavelength is dominated by one analyte, any uncertainty in the concentration of the other analyte has less of an impact. Figure 10.35 shows that the choice of wavelengths for Practice Exercise 10.6 are reasonable. When the choice of wavelengths is not obvious, one method for locating the optimum wavelengths is to plot $\varepsilon_X/\varepsilon_Y$ as function of wavelength, and determine the wavelengths where $\varepsilon_X/\varepsilon_Y$ reaches maximum and minimum values.[8]

Note

For example, in Example 10.6 the molar absorptivity for Fe^{3+} at 550 nm is 119× that for Cu^{2+}, and the molar absorptivity for Cu^{2+} at 396 nm is 10.2× that for Fe^{3+}.



https://chem.libretexts.org/@go/page/70700

Figure 10.35 Visible absorption spectra for 0.0250 M Cr^{3+}, 0.0750 M Co^{2+}, and for a mixture of Cr^{3+} and Co^{2+}. The two wavelengths used for analyzing the mixture of Cr^{3+} and Co^{2+} are shown by the dashed lines. The data for the two standard solutions are from reference 7.

When the analyte's spectra overlap severely, such that $\varepsilon_X \approx \varepsilon_Y$ at all wavelength, other computational methods may provide better accuracy and precision. In a multiwavelength linear regression analysis, for example, a mixture's absorbance is compared to that for a set of standard solutions at several wavelengths.[9] If A_{SX} and A_{SY} are the absorbance values for standard solutions of components X and Y at any wavelength, then

$$A_{SX} = \varepsilon_X b C_{SX} \tag{10.13}$$

$$A_{SY} = \varepsilon_Y b C_{SY} \tag{10.14}$$

where C_{SX} and C_{SY} are the known concentrations of X and Y in the standard solutions. Solving equation 10.13 and equation 10.14 for ε_X and ε_Y, substituting into equation 10.11, and rearranging, gives

$$\frac{A_{mix}}{A_{SX}} = \frac{C_X}{C_{SX}} + \frac{C_Y}{C_{SY}} \times \frac{A_{SY}}{A_{SX}} \tag{10.3.12}$$

To determine C_X and C_Y the mixture's absorbance and the absorbances of the standard solutions are measured at several wavelengths. Graphing A_{mix}/A_{SX} versus A_{SY}/A_{SX} gives a straight line with a slope of C_Y/C_{SY} and a *y*-intercept of C_X/C_{SX}. This approach is particularly helpful when it is not possible to find wavelengths where $\varepsilon_X > \varepsilon_Y$ and $\varepsilon_X < \varepsilon_Y$.

Note

The approach outlined here for a multiwavelength linear regression uses a single standard solution for each analyte. A more rigorous approach uses multiple standards for each analyte. The math behind the analysis of this data—what we call a multiple linear regression—is beyond the level of this text. For more details about multiple linear regression see Brereton, R. G. *Chemometrics: Data Analysis for the Laboratory and Chemical Plant*, Wiley: Chichester, England, 2003.

Example 10.7

Figure 10.35 shows visible absorbance spectra for a standard solution of 0.0250 M Cr^{3+}, a standard solution of 0.0750 M Co^{2+}, and a mixture containing unknown concentrations of each ion. The data for these spectra are shown here.[10]

λ (nm)	A_{Cr}	A_{Co}	A_{mix}	λ (nm)	A_{Cr}	A_{Co}	A_{mix}
375	0.26	0.01	0.53	520	0.19	0.38	0.63
400	0.43	0.03	0.88	530	0.24	0.33	0.70
425	0.39	0.07	0.83	540	0.28	0.26	0.73
440	0.29	0.13	0.67	550	0.32	0.18	0.76
455	0.20	0.21	0.54	570	0.38	0.08	0.81
470	0.14	0.28	0.47	575	0.39	0.06	0.82
480	0.12	0.30	0.44	580	0.38	0.05	0.79
490	0.11	0.34	0.45	600	0.34	0.03	0.70
500	0.13	0.38	0.51	625	0.24	0.02	0.49

Use a multiwavelength regression analysis to determine the composition of the unknown.

Solution

First we need to calculate values for A_{mix}/A_{SX} and for A_{SY}/A_{SX}. Let's define X as Co^{2+} and Y as Cr^{3+}. For example, at a wavelength of 375 nm A_{mix}/A_{SX} is 0.53/0.01, or 53 and A_{SY}/A_{SX} is 0.26/0.01, or 26. Completing the calculation for all

wavelengths and graphing A_{mix}/A_{SX} versus A_{SY}/A_{SX}gives the result shown in Figure 10.36. Fitting a straight-line to the data gives a regression model of

$$\frac{A_{mix}}{A_{SX}} = 0.636 + 2.01 \times \frac{A_{SY}}{A_{SX}} \tag{10.3.13}$$

Using the *y*-intercept, the concentration of Co^{2+} is

$$\frac{C_X}{C_{SX}} = \frac{C_{Co}}{0.0750\ M} = 0.636 \tag{10.3.14}$$

or C_{Co} = 0.048 M, and using the slope the concentration of Cr^{3+} is

$$\frac{C_Y}{C_{SY}} = \frac{C_{Cr}}{0.0250\ M} = 2.01 \tag{10.3.15}$$

or C_{Cr} = 0.050 M.

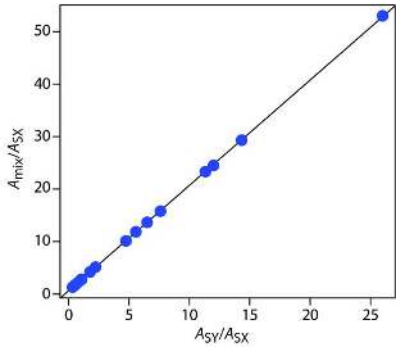


Figure 10.36 Multiwavelength linear regression analysis for the data in Example 10.7.

Practice Exercise 10.7

A mixture of MnO_4^- and $Cr_2O_7^{2-}$, and standards of 0.10 mM $KMnO_4$ and of 0.10 mM $K_2Cr_2O_7$ gives the results shown in the following table. Determine the composition of the mixture. The data for this problem is from Blanco, M. C.; Iturriaga, H.; Maspoch, S.; Tarin, P. *J. Chem. Educ.* **1989**, *66*, 178–180.

λ (nm)	A_{Mn}	A_{Cr}	A_{mix}
266	0.042	0.410	0.766
288	0.082	0.283	0.571
320	0.168	0.158	0.422
350	0.125	0.318	0.672
360	0.056	0.181	0.366

(There are many additional ways to analyze mixtures spectrophotometrically, including generalized standard additions, H-point standard additions, principal component regression to name a few. Consult the chapter's additional resources for further information.)

Click here to review your answer to this exercise.

10.3.3 Qualitative Applications

As discussed earlier in Section 10.2.1, ultraviolet, visible, and infrared absorption bands result from the absorption of electromagnetic radiation by specific valence electrons or bonds. The energy at which the absorption occurs, and its intensity is determined by the chemical environment of the absorbing moiety. For example, benzene has several ultraviolet absorption bands

due to π → π* transitions. The position and intensity of two of these bands, 203.5 nm (ε = 7400 M^{-1} cm^{-1}) and 254 nm (ε = 204 M^{-1} cm^{-1}), are sensitive to substitution. For benzoic acid, in which a carboxylic acid group replaces one of the aromatic hydrogens, the two bands shift to 230 nm (ε = 11 600 M^{-1} cm^{-1}) and 273 nm (ε = 970 M^{-1} cm^{-1}). A variety of rules have been developed to aid in correlating UV/Vis absorption bands to chemical structure. Similar correlations have been developed for infrared absorption bands. For example a carbonyl's C=O stretch is sensitive to adjacent functional groups, occurring at 1650 cm^{-1} for acids, 1700 cm^{-1} for ketones, and 1800 cm^{-1} for acid chlorides. The interpretation of UV/Vis and IR spectra receives adequate coverage elsewhere in the chemistry curriculum, notably in organic chemistry, and is not considered further in this text.

With the availability of computerized data acquisition and storage it is possible to build digital libraries of standard reference spectra. The identity of an a unknown compound can often be determined by comparing its spectrum against a library of reference spectra, a process is known as **spectral searching**. Comparisons are made using an algorithm that calculates the cumulative difference between the sample's spectrum and a reference spectrum. For example, one simple algorithm uses the following equation

$$D = \sum_{i=1}^{n} |(A_{sample})_i - (A_{reference})_i| \tag{10.3.16}$$

where D is the cumulative difference, A_{sample} is the sample's absorbance at wavelength or wavenumber i, $A_{\text{reference}}$ is the absorbance of the reference compound at the same wavelength or wavenumber, and n is the number of digitized points in the spectra. The cumulative difference is calculated for each reference spectrum. The reference compound with the smallest value of D provides the closest match to the unknown compound. The accuracy of spectral searching is limited by the number and type of compounds included in the library, and by the effect of the sample's matrix on the spectrum.

Another advantage of computerized data acquisition is the ability to subtract one spectrum from another. When coupled with spectral searching it may be possible, by repeatedly searching and subtracting reference spectra, to determine the identity of several components in a sample without the need of a prior separation step. An example is shown in Figure 10.37 in which the composition of a two-component mixture is determined by successive searching and subtraction. Figure 10.37a shows the spectrum of the mixture. A search of the spectral library selects cocaine · HCl (Figure 10.37b) as a likely component of the mixture. Subtracting the reference spectrum for cocaine · HCl from the mixture's spectrum leaves a result (Figure 10.37c) that closely matches mannitol's reference spectrum (Figure 10.37d). Subtracting the reference spectrum for leaves only a small residual signal (Figure 10.37e).

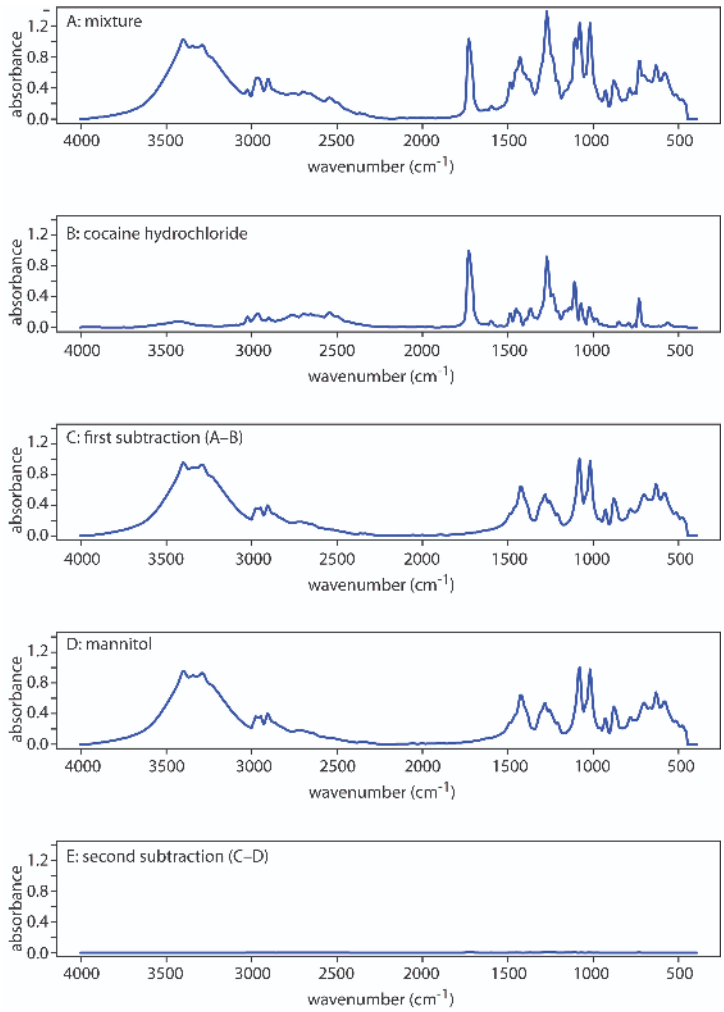


Figure 10.37 Identifying the components of a mixture by spectral searching and subtracting. (a) IR spectrum of the mixture; (b) Reference IR spectrum of cocaine · HCl; (c) Result of subtracting the spectrum of cocaine · HCl from the mixture's spectrum; (d) Reference IR spectrum of mannitol; and (e) The residual spectrum after removing mannitol's contribution to the mixture's spectrum.

> **Note**
>
> IR spectra traditionally are displayed using percent transmittance, %T, along the *y*-axis (for example, see Figure 10.16). Because absorbance—not percent transmittance—is a linear function of concentration, spectral searching and spectral subtraction, is easier to do when displaying absorbance on the *y*-axis.

10.3.4 Characterization Applications

Molecular absorption, particularly in the UV/Vis range, has been used for a variety of different characterization studies, including determining the stoichiometry of metal–ligand complexes and determining equilibrium constants. Both of these examples are examined in this section.

Stoichiometry of a Metal-Ligand Complex

We can determine the stoichiometry of a metal–ligand complexation reaction

$$\mathrm{M} + y\mathrm{L} \rightleftharpoons \mathrm{ML}_y \tag{10.3.17}$$

using one of three methods: the method of continuous variations, the mole-ratio method, and the slope-ratio method. Of these approaches, the **method of continuous variations**, also called Job's method, is the most popular. In this method a series of

solutions is prepared such that the total moles of metal and ligand, n_{total}, in each solution is the same. If $(n_M)_i$ and $(n_L)_i$ are, respectively, the moles of metal and ligand in solution i, then

$$n_{total} = (n_M)_i + (n_L)_i \tag{10.3.18}$$

The relative amount of ligand and metal in each solution is expressed as the mole fraction of ligand, $(X_L)_i$, and the mole fraction of metal, $(X_M)_i$,

$$(X_L)_i = \frac{(n_L)_i}{n_{total}} \tag{10.3.19}$$

$$(X_M)_i = 1 - \frac{(n_L)_i}{n_{total}} = \frac{(n_M)_i}{n_{total}} \tag{10.3.20}$$

The concentration of the metal–ligand complex in any solution is determined by the limiting reagent, with the greatest concentration occurring when the metal and the ligand are mixed stoichiometrically. If we monitor the complexation reaction at a wavelength where only the metal–ligand complex absorbs, a graph of absorbance versus the mole fraction of ligand will have two linear branches—one when the ligand is the limiting reagent and a second when the metal is the limiting reagent. The intersection of these two branches represents a stoichiometric mixing of the metal and the ligand. We can use the mole fraction of ligand at the intersection to determine the value of y for the metal–ligand complex ML_y.

$$y = \frac{n_L}{n_M} = \frac{X_L}{X_M} = \frac{X_L}{1 - X_L} \tag{10.3.21}$$

Note

You also can plot the data as absorbance versus the mole fraction of metal. In this case, y is equal to $(1–X_M)/X_M$.

Example 10.8

To determine the formula for the complex between Fe^{2+} and *o*-phenanthroline, a series of solutions is prepared in which the total concentration of metal and ligand is held constant at 3.15×10^{-4} M. The absorbance of each solution is measured at a wavelength of 510 nm. Using the following data, determine the formula for the complex.

X_L	absorbance	X_L	absorbance
0.000	0.000	0.600	0.693
0.100	0.116	0.700	0.809
0.200	0.231	0.800	0.693
0.300	0.347	0.900	0.347
0.400	0.462	1.000	0.000
0.500	0.578		

(To prepare the solutions for this example I first prepared a solution of 3.15×10^{-4} M Fe^{2+} and a solution of 3.15×10^{-4} M *o*-phenanthroline. Because the two stock solutions are of equal concentration, diluting a portion of one solution with the other solution gives a mixture in which the combined concentration of *o*-phenanthroline and Fe^{2+} is 3.15×10^{-4} M. If each solution has the same volume, then each solution contains the same total moles of metal and ligand.)

Solution

A plot of absorbance versus the mole fraction of ligand is shown in Figure 10.38. To find the maximum absorbance, we extrapolate the two linear portions of the plot. The two lines intersect at a mole fraction of ligand of 0.75. Solving for y gives

$$y = \frac{X_L}{1–X_L} = \frac{0.75}{1–0.75} = 3 \tag{10.3.22}$$

The formula for the metal–ligand complex is Fe(*o*-phenanthroline)$_3^{2+}$.

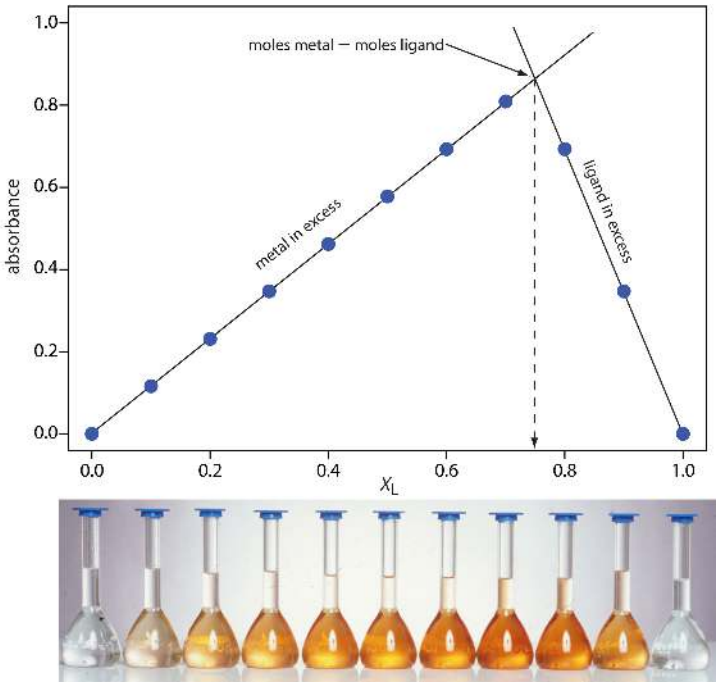


Figure 10.38 Continuous variations plot for Example 10.8. The photo shows the solutions used in gathering the data. Each solution is displayed directly below its corresponding point on the continuous variations plot.

Practice Exercise 10.8

Use the continuous variations data in the following table to determine the formula for the complex between Fe^{2+} and SCN^-. The data for this problem is adapted from Meloun, M.; Havel, J.; Högfeldt, E. *Computation of Solution Equilibria*, Ellis Horwood: Chichester, England, 1988, p. 236.

X_L	absorbance	X_L	absorbance	X_L	absorbance	X_L	absorbance
0.0200	0.068	0.2951	0.670	0.5811	0.790	0.8923	0.325
0.0870	0.262	0.3887	0.767	0.6860	0.701	0.9787	0.071
0.1792	0.471	0.4964	0.807	0.7885	0.540		

Click here to review your answer to this exercise.

Several precautions are necessary when using the method of continuous variations. First, the metal and the ligand must form only one metal–ligand complex. To determine if this condition is true, plots of absorbance versus X_L are constructed at several different wavelengths and for several different values of n_{total}. If the maximum absorbance does not occur at the same value of X_L for each set of conditions, then more than one metal–ligand complex must be present. A second precaution is that the metal–ligand complex's absorbance must obey Beer's law. Third, if the metal–ligand complex's formation constant is relatively small, a plot of absorbance versus X_L may show significant curvature. In this case it is often difficult to determine the stoichiometry by extrapolation. Finally, because the stability of a metal–ligand complex may be influenced by solution conditions, the composition of the solutions must be carefully controlled. When the ligand is a weak base, for example, the solutions must be buffered to the same pH.

In the **mole-ratio method** the amount of one reactant, usually the moles of metal, is held constant, while the amount of the other reactant is varied. The absorbance is monitored at a wavelength where the metal–ligand complex absorbs. A plot of absorbance as a function of the ligand-to-metal mole ratio, n_L/n_M, has two linear branches, which intersect at a mole–ratio corresponding to the

complex's formula. Figure 10.39a shows a mole-ratio plot for the formation of a 1:1 complex in which the absorbance is monitored at a wavelength where only the complex absorbs. Figure 10.39b shows a mole-ratio plot for a 1:2 complex in which all three species—the metal, the ligand, and the complex—absorb at the selected wavelength. Unlike the method of continuous variations, the mole-ratio method can be used for complexation reactions that occur in a stepwise fashion if there is a difference in the molar absorptivities of the metal–ligand complexes, and if the formation constants are sufficiently different. A typical mole-ratio plot for the step-wise formation of ML and ML_2 is shown in Figure 10.39c.

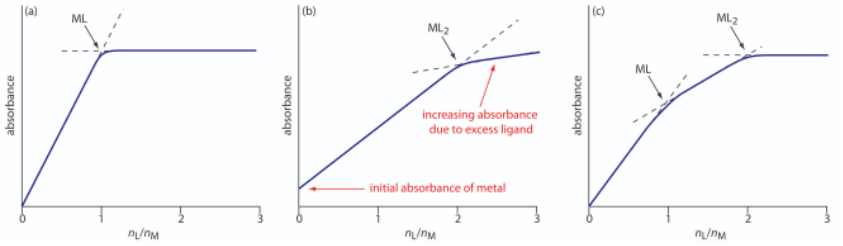


Figure 10.39 Mole-ratio plots for: (a) a 1:1 metal–ligand complex in which only the complex absorbs; (b) a 1:2 metal–ligand complex in which the metal, the ligand, and the complex absorb; and (c) the stepwise formation of a 1:1 and a 1:2 metal–ligand complex.

In both the method of continuous variations and the mole-ratio method we determine the complex's stoichiometry by extrapolating absorbance data from conditions in which there is a linear relationship between absorbance and the relative amounts of metal and ligand. If a metal–ligand complex is very weak, a plot of absorbance versus X_L or n_L/n_M may be so curved that it is impossible to determine the stoichiometry by extrapolation. In this case the slope-ratio may be used.

In the **slope-ratio method** two sets of solutions are prepared. The first set of solutions contains a constant amount of metal and a variable amount of ligand, chosen such that the total concentration of metal, C_M, is much larger than the total concentration of ligand, C_L. Under these conditions we may assume that essentially all the ligand reacts in forming the metal–ligand complex. The concentration of the complex, which has the general form M_xL_y, is

$$[M_xL_y] = \frac{C_L}{y} \tag{10.3.23}$$

If we monitor the absorbance at a wavelength where only M_xL_y absorbs, then

$$A = \varepsilon b[M_xL_y] = \frac{\varepsilon b C_L}{y} \tag{10.3.24}$$

and a plot of absorbance versus C_L is linear with a slope, s_L, of

$$s_L = \frac{\varepsilon b}{y} \tag{10.3.25}$$

A second set of solutions is prepared with a fixed concentration of ligand that is much greater than a variable concentration of metal; thus

$$[M_xL_y] = \frac{C_M}{x} \tag{10.3.26}$$

$$A = \varepsilon b[M_xL_y] = \frac{\varepsilon b C_M}{x} \tag{10.3.27}$$

$$s_M = \frac{\varepsilon b}{x} \tag{10.3.28}$$

A ratio of the slopes provides the relative values of x and y.

$$\frac{s_M}{s_L} = \frac{\varepsilon b/x}{\varepsilon b/y} = \frac{y}{x} \tag{10.3.29}$$

An important assumption in the slope-ratio method is that the complexation reaction continues to completion in the presence of a sufficiently large excess of metal or ligand. The slope-ratio method also is limited to systems in which only a single complex is

formed and for which Beer's law is obeyed.

Determination of Equilibrium Constants

Another important application of molecular absorption spectroscopy is the determination of equilibrium constants. Let's consider, as a simple example, an acid–base reaction of the general form

$$\mathrm{HIn}(aq) + \mathrm{H_2O}(l) \leftrightharpoons \mathrm{H_3O^+}(aq) + \mathrm{In^-}(aq) \tag{10.3.30}$$

where HIn and In^- are the conjugate weak acid and weak base forms of an acid–base indicator. The equilibrium constant for this reaction is

$$K_a = \frac{[\mathrm{H_3O^+}][\mathrm{In^-}]}{[\mathrm{HIn}]} \tag{10.3.31}$$

To determine the equilibrium constant's value, we prepare a solution in which the reaction is in a state of equilibrium and determine the equilibrium concentration of H_3O^+, HIn, and In^-. The concentration of H_3O^+ is easy to determine by simply measuring the solution's pH. To determine the concentration of HIn and In^- we can measure the solution's absorbance.

If both HIn and In^- absorb at the selected wavelength, then, from equation 10.6, we know that

$$A = \varepsilon_{\mathrm{HIn}} b[\mathrm{HIn}] + \varepsilon_{\mathrm{In}} b[\mathrm{In^-}] \tag{10.15}$$

where ε_{HIn} and ε_{In} are the molar absorptivities for HIn and In^-. The total concentration of indicator, C, is given by a mass balance equation

$$C = [\mathrm{HIn}] + [\mathrm{In^-}] \tag{10.16}$$

Solving equation 10.16 for [HIn] and substituting into equation 10.15 gives

$$A = \varepsilon_{\mathrm{HIn}} b(C - [\mathrm{In^-}]) + \varepsilon_{\mathrm{In}} b[\mathrm{In^-}] \tag{10.3.32}$$

which we simplify to

$$A = \varepsilon_{\mathrm{HIn}} bC - \varepsilon_{\mathrm{HIn}} b[\mathrm{In^-}] + \varepsilon_{\mathrm{In}} b[\mathrm{In^-}] \tag{10.3.33}$$

$$A = A_{\mathrm{HIn}} + b[\mathrm{In^-}](\varepsilon_{\mathrm{In}} - \varepsilon_{\mathrm{HIn}}) \tag{10.17}$$

where A_{HIn}, which is equal to $\varepsilon_{HIn}bC$, is the absorbance when the pH is acidic enough that essentially all the indicator is present as HIn. Solving equation 10.17 for the concentration of In^- gives

$$[\mathrm{In^-}] = \frac{A - A_{\mathrm{HIn}}}{b(\varepsilon_{\mathrm{In}} - \varepsilon_{\mathrm{HIn}})} \tag{10.18}$$

Proceeding in the same fashion, we can derive a similar equation for the concentration of HIn

$$[\mathrm{HIn}] = \frac{A_{\mathrm{In}} - A}{b(\varepsilon_{\mathrm{In}} - \varepsilon_{\mathrm{HIn}})} \tag{10.19}$$

where A_{In}, which is equal to $\varepsilon_{In}bC$, is the absorbance when the pH is basic enough that only In^- contributes to the absorbance. Substituting equation 10.18 and equation 10.19 into the equilibrium constant expression for HIn gives

$$K_a = [\mathrm{H_3O^+}]\frac{A - A_{\mathrm{HIn}}}{A_{\mathrm{In}} - A} \tag{10.20}$$

We can use equation 10.20 to determine the value of K_a in one of two ways. The simplest approach is to prepare three solutions, each of which contains the same amount, C, of indicator. The pH of one solution is made sufficiently acidic such that [HIn] >> [In^-]. The absorbance of this solution gives A_{HIn}. The value of A_{In} is determined by adjusting the pH of the second solution such that [In^-] >> [HIn]. Finally, the pH of the third solution is adjusted to an intermediate value, and the pH and absorbance, A, recorded. The value of K_a is calculated using equation 10.20.

Example 10.9

The acidity constant for an acid–base indicator is determined by preparing three solutions, each of which has a total indicator concentration of 5.00×10^{-5} M. The first solution is made strongly acidic with HCl and has an absorbance of 0.250. The second solution was made strongly basic and has an absorbance of 1.40. The pH of the third solution is 2.91 and has an absorbance of 0.662. What is the value of K_a for the indicator?

Solution

The value of K_a is determined by making appropriate substitutions into 10.20; thus

$$K_a = (1.23 \times 10^{-3}) \times \frac{0.662 - 0.250}{1.40 - 0.662} = 6.87 \times 10^{-4} \tag{10.3.34}$$

Practice Exercise 10.9

To determine the K_a of a merocyanine dye, the absorbance of a solution of 3.5×10^{-4} M dye was measured at a pH of 2.00, a pH of 6.00, and a pH of 12.00, yielding absorbances of 0.000, 0.225, and 0.680, respectively. What is the value of K_a for this dye? The data for this problem is adapted from Lu, H.; Rutan, S. C. *Anal. Chem.*, **1996**, *68*, 1381–1386.

Click here to review your answer to this exercise.

A second approach for determining K_a is to prepare a series of solutions, each containing the same amount of indicator. Two solutions are used to determine values for A_{HIn} and A_{In}. Taking the log of both sides of equation 10.20 and rearranging leave us with the following equation.

$$\log \frac{A - A_{HIn}}{A_{In} - A} = \text{pH} - \text{p}K_a \tag{10.21}$$

A plot of $\log[(A - A_{HIn})/(A_{In} - A)]$ versus pH is a straight-line with a slope of +1 and a *y*-intercept of $-\text{p}K_a$.

Practice Exercise 10.10

To determine the K_a of the indicator bromothymol blue, the absorbance of a series of solutions containing the same concentration of the indicator was measured at pH levels of 3.35, 3.65, 3.94, 4.30, and 4.64, yielding absorbances of 0.170, 0.287, 0.411, 0.562, and 0.670, respectively. Acidifying the first solution to a pH of 2 changes its absorbance to 0.006, and adjusting the pH of the last solution to 12 changes its absorbance to 0.818. What is the value of K_a for this day? The data for this problem is from Patterson, G. S. *J. Chem. Educ.*, **1999**, *76*, 395–398.

Click here to review your answer to this exercise.

In developing these approaches for determining K_a we considered a relatively simple system in which the absorbance of HIn and In^- are easy to measure and for which it is easy to determine the concentration of H_3O^+. In addition to acid–base reactions, we can adapt these approaches to any reaction of the general form

$$X(aq) + Y(aq) \leftrightharpoons Z(aq) \tag{10.3.35}$$

including metal–ligand complexation reactions and redox reactions, provided that we can determine spectrophotometrically the concentration of the product, Z, and one of the reactants, and that the concentration of the other reactant can be measured by another method. With appropriate modifications, more complicated systems, in which one or more of these parameters can not be measured, also can be treated.[11]

10.3.5 Evaluation of UV/Vis and IR Spectroscopy

Scale of Operation

Molecular UV/Vis absorption is routinely used for the analysis of trace analytes in macro and meso samples. Major and minor analytes can be determined by diluting the sample before analysis, while concentrating a sample may allow for the analysis of ultratrace analytes. The scale of operations for infrared absorption is generally poorer than that for UV/Vis absorption.

> **Note**
>
> See Figure 3.5 to review the meaning of macro and meso for describing samples, and the meaning of major, minor, and ultratrace for describing analytes.

Accuracy

Under normal conditions a relative error of 1–5% is easy to obtained with UV/Vis absorption. Accuracy is usually limited by the quality of the blank. Examples of the type of problems that may be encountered include the presence of particulates in a sample that scatter radiation and interferents that react with analytical reagents. In the latter case the interferent may react to form an absorbing species, giving rise to a positive determinate error. Interferents also may prevent the analyte from reacting, leading to a negative determinate error. With care, it may be possible to improve the accuracy of an analysis by as much as an order of magnitude.

Precision

In absorption spectroscopy, precision is limited by indeterminate errors—primarily instrumental noise—introduced when measuring absorbance. Precision is generally worse for low absorbances where $P_0 \approx P_T$, and for high absorbances when P_T approaches 0. We might expect, therefore, that precision will vary with transmittance.

We can derive an expression between precision and transmittance by applying the propagation of uncertainty as described in Chapter 4. To do so we rewrite Beer's law as

$$C = -\frac{1}{\varepsilon b}\log T \tag{10.22}$$

Table 4.10 in Chapter 4 helps us in completing the propagation of uncertainty for equation 10.22, giving the absolute uncertainty in the concentration, s_C, as

$$s_C = -\frac{0.4343}{\varepsilon b} \times \frac{s_T}{T} \tag{10.23}$$

where s_T is the absolute uncertainty in the transmittance. Dividing equation 10.23 by equation 10.22 gives the relative uncertainty in concentration, s_C/C, as

$$\frac{s_C}{C} = \frac{0.4343 s_T}{T \log T} \tag{10.3.36}$$

If we know the absolute uncertainty in transmittance, we can determine the relative uncertainty in concentration for any transmittance.

Determining the relative uncertainty in concentration is complicated because s_T may be a function of the transmittance. As shown in Table 10.8, three categories of indeterminate instrumental error have been observed.[12] A constant s_T is observed for the uncertainty associated with reading %T on a meter's analog or digital scale. Typical values are ±0.2–0.3% (a k_1 of ±0.002–0.003) for an analog scale, and ±0.001% a (k_1 of ±0.000 01) for a digital scale. A constant s_T also is observed for the thermal transducers used in infrared spectrophotometers. The effect of a constant s_T on the relative uncertainty in concentration is shown by curve A in Figure 10.40. Note that the relative uncertainty is very large for both high and low absorbances, reaching a minimum when the absorbance is 0.4343. This source of indeterminate error is important for infrared spectrophotometers and for inexpensive UV/Vis spectrophotometers. To obtain a relative uncertainty in concentration of ±1–2%, the absorbance must be kept within the range 0.1–1.

Table 10.8 Effect of Indeterminate Errors on Relative Uncertainty in Concentration

Category	Sources of Indeterminate Error	Relative Uncertainty in Concentration
$s_T = k_1$	%T readout resolution noise in thermal detectors	$\frac{s_C}{C} = \frac{0.4343 k_1}{T \log T}$
$s_T = k_2\sqrt{T^2 + T}$	noise in photon detectors	$\frac{s_C}{C} = \frac{0.4343 k_2}{\log T}\sqrt{1 + \frac{1}{T}}$
$s_T = k_3 T$	positioning of sample cell fluctuations in source intensity	$\frac{s_C}{C} = \frac{0.4343 k_3}{\log T}$

Values of s_T are a complex function of transmittance when indeterminate errors are dominated by the noise associated with photon detectors. Curve B in Figure 10.40 shows that the relative uncertainty in concentration is very large for low absorbances, but is less at higher absorbances. Although the relative uncertainty reaches a minimum when the absorbance is 0.963, there is little change in the relative uncertainty for absorbances within the range 0.5–2. This source of indeterminate error generally limits the precision of high quality UV/Vis spectrophotometers for mid-to-high absorbances.

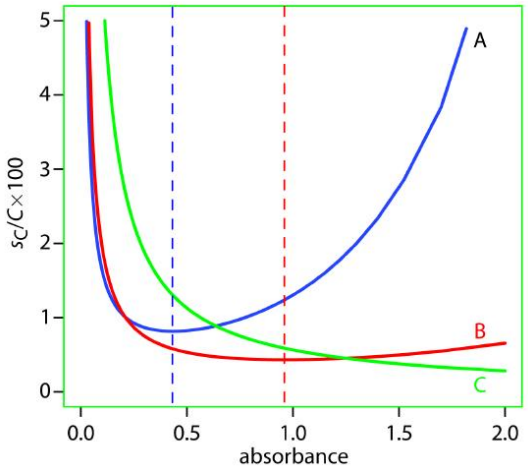


Figure 10.40 Percent relative uncertainty in concentration as a function of absorbance for the categories of indeterminate errors in Table 10.8. A: k_1 = ±0.0030; B: k_2 = ±0.0030; C:k_3 = ±0.0130. The dashed lines correspond to the minimum uncertainty for curve A (absorbance of 0.4343) and for curve B (absorbance of 0.963).

Finally, the value of s_T is directly proportional to transmittance for indeterminate errors resulting from fluctuations in the source's intensity and from uncertainty in positioning the sample within the spectrometer. The latter is particularly important because the optical properties of any sample cell are not uniform. As a result, repositioning the sample cell may lead to a change in the intensity of transmitted radiation. As shown by curve C in Figure 10.40, the effect is only important at low absorbances. This source of indeterminate errors is usually the limiting factor for high quality UV/Vis spectrophotometers when the absorbance is relatively small.

When the relative uncertainty in concentration is limited by the %T readout resolution, the precision of the analysis can be improved by redefining 100% T and 0% T. Normally 100% T is established using a blank and 0% T is established while preventing the source's radiation from reaching the detector. If the absorbance is too high, precision can be improved by resetting 100% T using a standard solution of the analyte whose concentration is less than that of the sample (Figure 10.41a). For a sample whose absorbance is too low, precision can be improved by redefining 0% T using a standard solution of the analyte whose concentration is greater than that of the analyte (Figure 10.41b). In this case a calibration curve is required because a linear relationship between absorbance and concentration no longer exists. Precision can be further increased by combining these two methods (Figure 10.41c). Again, a calibration curve is necessary since the relationship between absorbance and concentration is no longer linear.

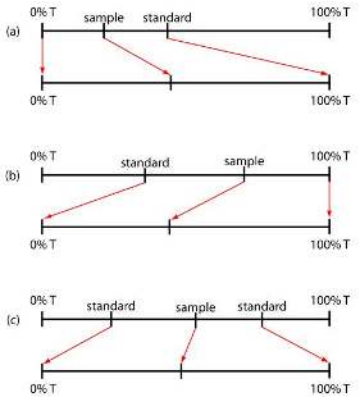


Figure 10.41 Methods for improving the precision of absorption methods: (a) high-absorbance method; (b) low-absorbance method; (c) maximum precision method.

Sensitivity

The sensitivity of a molecular absorption method, which is the slope of a Beer's law calibration curve, is the product of the analyte's absorptivity and the pathlength of the sample cell (εb). You can improve a method's sensitivity by selecting a wavelength where absorbance is at a maximum or by increasing the pathlength.

> **Note**
>
> See Figure 10.24 for an example of how the choice of wavelength affects a calibration curve's sensitivity.

Selectivity

Selectivity is rarely a problem in molecular absorption spectrophotometry. In many cases it is possible to find a wavelength where only the analyte absorbs. When two or more species do contribute to the measured absorbance, a multicomponent analysis is still possible, as shown in Example 10.6 and Example 10.7.

Time, Cost, and Equipment

The analysis of a sample by molecular absorption spectroscopy is relatively rapid, although additional time may be required if we need to chemically convert a nonabsorbing analyte into an absorbing form. The cost of UV/Vis instrumentation ranges from several hundred dollars for a simple filter photometer, to more than $50,000 for a computer controlled high resolution, double-beam instrument equipped with variable slits, and operating over an extended range of wavelengths. Fourier transform infrared spectrometers can be obtained for as little as $15,000–$20,000, although more expensive models are available.

Contributors

David Harvey (DePauw University)

10.3: UV/Vis and IR Spectroscopy is shared under a CC BY-NC-SA 4.0 license and was authored, remixed, and/or curated by LibreTexts.

10.4: Atomic Absorption Spectroscopy

Guystav Kirchoff and Robert Bunsen first used atomic absorption spectroscopy—along with atomic emission—in 1859 and 1860 as a means for identify atoms in flames and hot gases. Although atomic emission continued to develop as an analytical technique, progress in atomic absorption languished for almost a century. Modern atomic absorption spectroscopy has its beginnings in 1955 as a result of the independent work of A. C. Walsh and C. T. J. Alkemade.[13] Commercial instruments were in place by the early 1960s, and the importance of atomic absorption as an analytical technique was soon evident.

10.4.1 Instrumentation

Atomic absorption spectrophotometers use the same single-beam or double-beam optics described earlier for molecular absorption spectrophotometers (see Figure 10.26 and Figure 10.27). There is, however, an important additional need in atomic absorption spectroscopy—we must covert the analyte into free atoms. In most cases our analyte is in solution form. If our sample is a solid, then we must bring it into solution before the analysis. When analyzing a lake sediment for Cu, Zn, and Fe, for example, we bring the analytes into solution as Cu^{2+}, Zn^{2+}, and Fe^{3+} by extracting them with a suitable reagent. For this reason, only the introduction of solution samples is considered in this text.

> **Note**
>
> What reagent we choose to use depends on our research goals. If we need to know the total amount of metal in the sediment, then we might use a microwave digestion using a mixture of concentrated acids, such as HNO_3, HCl, and HF. This destroys the sediment's matrix and brings everything into solution. On the other hand, if our interest is biologically available metals, we might extract the sample under milder conditions, such as a dilute solution of HCl or CH_3COOH at room temperature.

Atomization

The process of converting an analyte to a free gaseous atom is called **atomization**. Converting an aqueous analyte into a free atom requires that we strip away the solvent, volatilize the analytes, and, if necessary, dissociate the analyte into free atoms. Desolvating an aqueous solution of $CuCl_2$, for example, leaves us with solid particulates of $CuCl_2$. Converting the particulate $CuCl_2$ to gas phases atoms of Cu and Cl requires thermal energy.

$$\mathrm{CuCl_{2(aq)} \rightarrow CuCl_{2(s)} \rightarrow Cu_{(g)} + 2\,Cl_{(g)}} \tag{10.4.1}$$

There are two common atomization methods: flame atomization and electrothermal atomization, although a few elements are atomized using other methods.

Flame Atomizer

Figure 10.42 shows a typical flame atomization assembly with close-up views of several key components. In the unit shown here, the aqueous sample is drawn into the assembly by passing a high-pressure stream of compressed air past the end of a capillary tube immersed in the sample. When the sample exits the nebulizer it strikes a glass impact bead, converting it into a fine aerosol mist within the spray chamber. The aerosol mist is swept through the spray chamber by the combustion gases—compressed air and acetylene in this case—to the burner head where the flame's thermal energy desolvates the aerosol mist to a dry aerosol of small, solid particles. The flame's thermal energy then volatilizes the particles, producing a vapor consisting of molecular species, ionic species, and free atoms.

> **Note**
>
> Compressed air is one of the two gases whose combustion produces the flame.

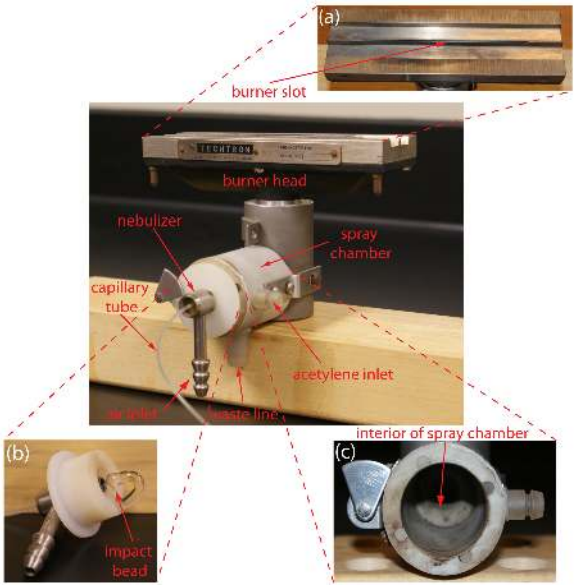


Figure 10.42 *Flame atomization assembly with expanded views of (a) the burner head showing the burner slot where the flame is located; (b) the nebulizer's impact bead; and (c) the interior of the spray chamber. Although the unit shown here is from an older instrument, the basic components of a modern flame AA spectrometer are the same.*

Burner. The slot burner in Figure 10.42a provides a long optical pathlength and a stable flame. Because absorbance increases linearly with the path length, a long path length provides greater sensitivity. A stable flame minimizes uncertainty due to fluctuations in the flame.

The burner is mounted on an adjustable stage that allows the entire assembly to move horizontally and vertically. Horizontal adjustments ensure that the flame is aligned with the instrument's optical path. Vertical adjustments adjust the height within the flame from which absorbance is monitored. This is important because two competing processes affect the concentration of free atoms in the flame. The more time the analyte spends in the flame the greater the atomization efficiency; thus, the production of free atoms increases with height. On the other hand, a longer residence time allows more opportunity for the free atoms to combine with oxygen to form a molecular oxide. For an easily oxidized metal, such as Cr, the concentration of free atoms is greatest just above the burner head. For metals, such as Ag, which are difficult to oxidize, the concentration of free atoms increases steadily with height (Figure 10.43). Other atoms show concentration profiles that maximize at a characteristic height.

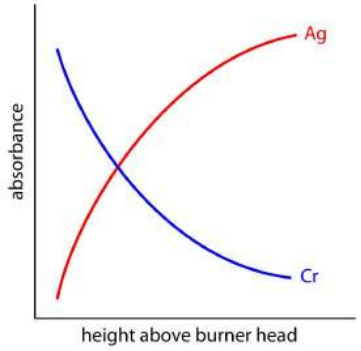


Figure 10.43 *Absorbance versus height profiles for Ag and Cr in flame atomic absorption spectroscopy.*

Flame. The flame's temperature, which affects the efficiency of atomization, depends on the fuel–oxidant mixture, several examples of which are listed in Table 10.9. Of these, the air–acetylene and the nitrous oxide–acetylene flames are the most popular. Normally the fuel and oxidant are mixed in an approximately stoichiometric ratio; however, a fuel-rich mixture may be necessary for easily oxidized analytes.

Table 10.9 *Fuels and Oxidants Used for Flame Combustion*

fuel	oxidant	temperature range (°C)
natural gas	air	1700–1900
hydrogen	air	2000–2100
acetylene	air	2100–2400
acetylene	nitrous oxide	2600–2800
acetylene	oxygen	3050–3150

Figure 10.44 shows a cross-section through the flame, looking down the source radiation's optical path. The primary combustion zone is usually rich in gas combustion products that emit radiation, limiting is usefulness for atomic absorption. The interzonal region generally is rich in free atoms and provides the best location for measuring atomic absorption. The hottest part of the flame is typically 2–3 cm above the primary combustion zone. As atoms approach the flame's secondary combustion zone, the decrease in temperature allows for formation of stable molecular species.

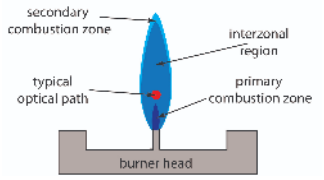


Figure 10.44 *Profile of typical flame using a slot burner. The relative size of each zone depends on many factors, including the choice of fuel and oxidant, and their relative proportions.*

Sample Introduction. The most common means for introducing samples into a flame atomizer is a continuous aspiration in which the sample flows through the burner while we monitor the absorbance. Continuous aspiration is sample intensive, typically requiring from 2–5 mL of sample.

Flame microsampling allows us to introduce a discrete sample of fixed volume, and is useful when we have a limited amount of sample or when the sample's matrix is incompatible with the flame atomizer. For example, continuously aspirating a sample that has a high concentration of dissolved solids—sea water, for example, comes to mind—may build-up a solid deposit on the burner head that obstructs the flame and that lowers the absorbance. Flame microsampling is accomplished using a micropipet to place 50–250 µL of sample in a Teflon funnel connected to the nebulizer, or by dipping the nebulizer tubing into the sample for a short time. Dip sampling is usually accomplished with an automatic sampler. The signal for flame microsampling is a transitory peak whose height or area is proportional to the amount of analyte that is injected.

Advantages and Disadvantages of Flame Atomization. The principal advantage of flame atomization is the reproducibility with which the sample is introduced into the spectrophotometer. A significant disadvantage to flame atomizers is that the efficiency of atomization may be quite poor. There are two reasons for poor atomization efficiency. First, the majority of the aerosol droplets produced during nebulization are too large to be carried to the flame by the combustion gases. Consequently, as much as 95% of the sample never reaches the flame. A second reason for poor atomization efficiency is that the large volume of combustion gases significantly dilutes the sample. Together, these contributions to the efficiency of atomization reduce sensitivity because the analyte's concentration in the flame may be a factor of 2.5×10^{-6} less than that in solution.[14] This is the reason for the waste line shown at the bottom of the spray chamber in Figure 10.42.

Electrothermal Atomizers

A significant improvement in sensitivity is achieved by using the resistive heating of a graphite tube in place of a flame. A typical electrothermal atomizer, also known as a **graphite furnace**, consists of a cylindrical graphite tube approximately 1–3 cm in length and 3–8 mm in diameter. As shown in Figure 10.45, the graphite tube is housed in an sealed assembly that has optically transparent windows at each end. A continuous stream of an inert gas is passed through the furnace, protecting the graphite tube from oxidation and removing the gaseous products produced during atomization. A power supply is used to pass a current through the graphite tube, resulting in resistive heating.

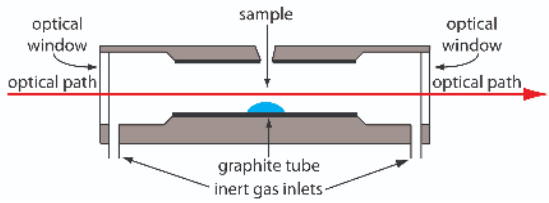


***Figure 10.45**: Diagram showing a cross-section of an electrothermal analyzer.*

Samples of between 5–50 μL are injected into the graphite tube through a small hole at the top of the tube. Atomization is achieved in three stages. In the first stage the sample is dried to a solid residue using a current that raises the temperature of the graphite tube to about 110°C. In the second stage, which is called ashing, the temperature is increased to between 350–1200°C. At these temperatures any organic material in the sample is converted to CO_2 and H_2O, and volatile inorganic materials are vaporized. These gases are removed by the inert gas flow. In the final stage the sample is atomized by rapidly increasing the temperature to between 2000–3000°C. The result is a transient absorbance peak whose height or area is proportional to the absolute amount of analyte injected into the graphite tube. Together, the three stages take approximately 45–90 s, with most of this time used for drying and ashing the sample.

Electrothermal atomization provides a significant improvement in sensitivity by trapping the gaseous analyte in the small volume within the graphite tube. The analyte's concentration in the resulting vapor phase may be as much as 1000× greater than in a flame atomization.[15] This improvement in sensitivity—and the resulting improvement in detection limits—is offset by a significant decrease in precision. Atomization efficiency is strongly influenced by the sample's contact with the graphite tube, which is difficult to control reproducibly.

Miscellaneous Atomization Methods

A few elements may be atomized by a chemical reaction that produces a volatile product. Elements such as As, Se, Sb, Bi, Ge, Sn, Te, and Pb, for example, form volatile hydrides when reacted with $NaBH_4$ in acid. An inert gas carries the volatile hydrides to either a flame or to a heated quartz observation tube situated in the optical path. Mercury is determined by the cold-vapor method in which it is reduced to elemental mercury with $SnCl_2$. The volatile Hg is carried by an inert gas to an unheated observation tube situated in the instrument's optical path.

10.4.2 Quantitative Applications

Atomic absorption is widely used for the analysis of trace metals in a variety of sample matrices. Using Zn as an example, atomic absorption methods have been developed for its determination in samples as diverse as water and wastewater, air, blood, urine, muscle tissue, hair, milk, breakfast cereals, shampoos, alloys, industrial plating baths, gasoline, oil, sediments, and rocks.

Developing a quantitative atomic absorption method requires several considerations, including choosing a method of atomization, selecting the wavelength and slit width, preparing the sample for analysis, minimizing spectral and chemical interferences, and selecting a method of standardization. Each of these topics is considered in this section.

Developing a Quantitative Method

Flame or Electrothermal Atomization? The most important factor in choosing a method of atomization is the analyte's concentration. Because of its greater sensitivity, it takes less analyte to achieve a given absorbance when using electrothermal atomization. Table 10.10, which compares the amount of analyte needed to achieve an absorbance of 0.20 when using flame atomization and electrothermal atomization, is useful when selecting an atomization method. For example, flame atomization is the method of choice if our samples contain 1–10 mg Zn^{2+}/L, but electrothermal atomization is the best choice for samples containing 1–10 μg Zn^{2+}/L.

***Table 10.10:** Concentration of Analyte Yielding an Absorbance of 0.20*

	Concentration (mg/L)[a]

element	flame atomization	electrothermal atomization
Ag	1.5	0.0035
Al	40	0.015
As	40[b]	0.050
Ca	0.8	0.003
Cd	0.6	0.001
Co	2.5	0.021
Cr	2.5	0.0075
Cu	1.5	0.012
Fe	2.5	0.006
Hg	70[b]	0.52
Mg	0.15	0.00075
Mn	1	0.003
Na	0.3	0.00023
Ni	2	0.024
Pb	5	0.080
Pt	70	0.29
Sn	50[b]	0.023
Zn	0.3	0.00071

[a] Source: Varian Cookbook, SpectraAA Software Version 4.00 Pro.

[b] As: 10 mg/L by hydride vaporization; Hg: 11.5 mg/L by cold-vapor; and Sn:18 mg/L by hydride vaporization

Selecting the Wavelength and Slit Width. The source for atomic absorption is a hollow cathode lamp consisting of a cathode and anode enclosed within a glass tube filled with a low pressure of Ne or Ar (Figure 10.46). Applying a potential across the electrodes ionizes the filler gas. The positively charged gas ions collide with the negatively charged cathode, sputtering atoms from the cathode's surface. Some of the sputtered atoms are in the excited state and emit radiation characteristic of the metal(s) from which the cathode was manufactured. By fashioning the cathode from the metallic analyte, a hollow cathode lamp provides emission lines that correspond to the analyte's absorption spectrum.

Note

Because atomic absorption lines are narrow, we need to use a line source instead of a continuum source (compare, for example, Figure 10.18 with Figure 10.20). The effective bandwidth when using a continuum source is roughly 1000^× larger than an atomic absorption line; thus, $P_T \approx P_0$, $\%T \approx 100$, and $A \approx 0$. Because a hollow cathode lamp is a line source, P_T and P_0 have different values giving a $\%T < 100$ and $A > 0$.

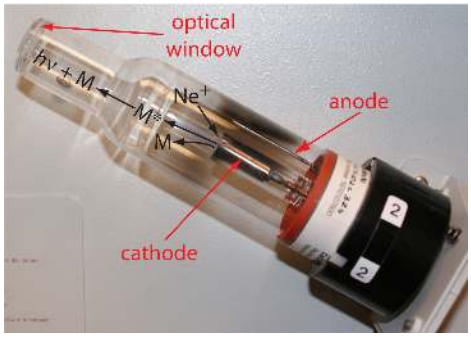


Figure 10.46: *Photo of a typical multielemental hollow cathode lamp. The cathode in this lamp is fashioned from an alloy containing Co, Cr, Cu, Fe, Mn, and Ni, and is surrounded by a glass shield to isolate it from the anode. The lamp is filled with Ne gas. Also shown is the process leading to atomic emission. See the text for an explanation.*

Each element in a hollow cathode lamp provides several atomic emission lines that we can use for atomic absorption. Usually the wavelength that provides the best sensitivity is the one we choose to use, although a less sensitive wavelength may be more appropriate for a larger concentration of analyte. For the Cr hollow cathode lamp in Table 10.11, for example, the best sensitivity is obtained using a wavelength of 357.9 nm.

Another consideration is the intensity of the emission line. If several emission lines meet our need for sensitivity, we may wish to use the emission line with the largest relative P_0 because there is less uncertainty in measuring P_0 and P_T. When analyzing samples containing ≈10 mg Cr/L, for example, the first three wavelengths in Table 10.11 provide an appropriate sensitivity. The wavelengths of 425.5 nm and 429.0 nm, however, have a greater P_0 and will provide less uncertainty in the measured absorbance.

Table 10.11 *Atomic Emission Lines for a Cr Hollow Cathode Lamp*

wavelength (nm)	slit width (nm)	mg Cr/L giving A = 0.20	P_0 (relative)
357.9	0.2	2.5	40
425.4	0.2	12	85
429.0	0.5	20	100
520.5	0.2	1500	15
520.8	0.2	500	20

The emission spectrum from a hollow cathode lamp includes, besides emission lines for the analyte, additional emission lines for impurities present in the metallic cathode and from the filler gas. These additional lines are a source of stray radiation that leads to an instrumental deviation from Beer's law. The monochromator's slit width is set as wide as possible, improving the throughput of radiation, while, at the same time, being narrow enough to eliminate the stray radiation.

Preparing the Sample. Flame and electrothermal atomization require that the sample be in solution. Solid samples are brought into solution by dissolving in an appropriate solvent. If the sample is not soluble it may be digested, either on a hot-plate or by microwave, using HNO_3, H_2SO_4, or $HClO_4$. Alternatively, we can extract the analyte using a Soxhlet extractor. Liquid samples may be analyzed directly or extracted if the matrix is incompatible with the method of atomization. A serum sample, for instance, is difficult to aspirate when using flame atomization and may produce an unacceptably high background absorbance when using electrothermal atomization. A liquid–liquid extraction using an organic solvent and a chelating agent is frequently used to concentrate analytes. Dilute solutions of Cd^{2+}, Co^{2+}, Cu^{2+}, Fe^{3+}, Pb^{2+}, Ni^{2+}, and Zn^{2+}, for example, can be concentrated by extracting with a solution of ammonium pyrrolidine dithiocarbamate in methyl isobutyl ketone.See Chapter 7 to review different methods for preparing samples for analysis.

Minimizing Spectral Interference. A spectral interference occurs when an analyte's absorption line overlaps with an interferent's absorption line or band. Because they are so narrow, the overlap of two atomic absorption lines is seldom a problem. On the other hand, a molecule's broad absorption band or the scattering of source radiation is a potentially serious spectral interference.

An important consideration when using a flame as an atomization source is its effect on the measured absorbance. Among the products of combustion are molecular species that exhibit broad absorption bands and particulates that scatter radiation from the source. If we fail to compensate for these spectral interference, then the intensity of transmitted radiation decreases. The result is an apparent increase in the sample's absorbance. Fortunately, absorption and scattering of radiation by the flame are corrected by analyzing a blank.

Spectral interferences also occur when components of the sample's matrix other than the analyte react to form molecular species, such as oxides and hydroxides. The resulting absorption and scattering constitutes the sample's background and may present a significant problem, particularly at wavelengths below 300 nm where the scattering of radiation becomes more important. If we know the composition of the sample's matrix, then we can prepare our samples using an identical matrix. In this case the background absorption is the same for both the samples and standards. Alternatively, if the background is due to a known matrix component, then we can add that component in excess to all samples and standards so that the contribution of the naturally occurring interferent is insignificant. Finally, many interferences due to the sample's matrix can be eliminated by increasing the atomization temperature. For example, by switching to a higher temperature flame it may be possible to prevent the formation of interfering oxides and hydroxides.

If the identity of the matrix interference is unknown, or if it is not possible to adjust the flame or furnace conditions to eliminate the interference, then we must find another method to compensate for the background interference. Several methods have been developed to compensate for matrix interferences, and most atomic absorption spectrophotometers include one or more of these methods.

One of the most common methods for **background correction** is to use a continuum source, such as a D_2 lamp. Because a D_2 lamp is a continuum source, absorbance of its radiation by the analyte's narrow absorption line is negligible. Only the background, therefore, absorbs radiation from the D_2 lamp. Both the analyte and the background, on the other hand, absorb the hollow cathode's radiation. Subtracting the absorbance for the D_2 lamp from that for the hollow cathode lamp gives a corrected absorbance that compensates for the background interference. Although this method of background correction may be quite effective, it does assume that the background absorbance is constant over the range of wavelengths passed by the monochromator. If this is not true, subtracting the two absorbances may underestimate or overestimate the background.

> **Note**
>
> Other methods of background correction have been developed, including Zeeman effect background correction and Smith–Hieftje background correction, both of which are included in some commercially available atomic absorption spectrophotometers. Consult the chapter's additional resources for additional information.

Minimizing Chemical Interferences. The quantitative analysis of some elements is complicated by chemical interferences occurring during atomization. The two most common chemical interferences are the formation of nonvolatile compounds containing the analyte and ionization of the analyte.

One example of the formation of nonvolatile compounds is the effect of PO_4^{3-} or Al^{3+} on the flame atomic absorption analysis of Ca^{2+}. In one study, for example, adding 100 ppm Al^{3+} to a solution of 5 ppm Ca^{2+} decreased the calcium ion's absorbance from 0.50 to 0.14, while adding 500 ppm PO_4^{3-} to a similar solution of Ca^{2+} decreased the absorbance from 0.50 to 0.38. These interferences were attributed to the formation of nonvolatile particles of $Ca_3(PO_4)_2$ and an Al–Ca–O oxide.[16]

When using flame atomization, we can minimize the formation of nonvolatile compounds by increasing the flame's temperature, either by changing the fuel-to-oxidant ratio or by switching to a different combination of fuel and oxidant. Another approach is to add a releasing agent or a protecting agent to the samples. A **releasing agent** is a species that reacts with the interferent, releasing the analyte during atomization. Adding Sr^{2+} or La^{3+} to solutions of Ca^{2+}, for example, minimizes the effect of PO_4^{3-} and Al^{3+} by reacting in place of the analyte. Thus, adding 2000 ppm $SrCl_2$ to the Ca^{2+}/PO_4^{3-} and Ca^{2+}/Al^{3+} mixtures described in the previous paragraph increased the absorbance to 0.48. A **protecting agent** reacts with the analyte to form a stable volatile complex. Adding 1% w/w EDTA to the Ca^{2+}/PO_4^{3-} solution described in the previous paragraph increased the absorbance to 0.52.

Ionization interferences occur when thermal energy from the flame or the electrothermal atomizer is sufficient to ionize the analyte

$$M_{(g)} \overset{\Delta}{\rightleftharpoons} M^+_{(g)} + e^- \tag{10.24}$$

where M is the analyte. Because the absorption spectra for M and M^+ are different, the position of the equilibrium in reaction 10.24 affects absorbance at wavelengths where M absorbs. To limit ionization we add a high concentration of an **ionization suppressor**, which is simply a species that ionizes more easily than the analyte. If the concentration of the ionization suppressor is sufficient, then the increased concentration of electrons in the flame pushes reaction 10.24 to the left, preventing the analyte's ionization. Potassium and cesium are frequently used as an ionization suppressor because of their low ionization energy.

Standardizing the Method. Because Beer's law also applies to atomic absorption, we might expect atomic absorption calibration curves to be linear. In practice, however, most atomic absorption calibration curves are nonlinear, or linear for only a limited range of concentrations. Nonlinearity in atomic absorption is a consequence of instrumental limitations, including stray radiation from the hollow cathode lamp and the variation in molar absorptivity across the absorption line. Accurate quantitative work, therefore, often requires a suitable means for computing the calibration curve from a set of standards.

Note

Most instruments include several different algorithms for computing the calibration curve. The instrument in my lab, for example, includes five algorithms. Three of the algorithms fit absorbance data using linear, quadratic, or cubic polynomial functions of the analyte's concentration. It also includes two algorithms that fit the concentrations of the standards to quadratic functions of the absorbance.

When possible, a quantitative analysis is best conducted using external standards. Unfortunately, matrix interferences are a frequent problem, particularly when using electrothermal atomization. For this reason the method of standard additions is often used. One limitation to this method of standardization, however, is the requirement that there be a linear relationship between absorbance and concentration.

Note

The best way to appreciate the theoretical and practical details discussed in this section is to carefully examine a typical analytical method. Although each method is unique, the following description of the determination of Cu and Zn in biological tissues provides an instructive example of a typical procedure. The description here is based on Bhattacharya, S. K.; Goodwin, T. G.; Crawford, A. J. *Anal. Lett.* **1984**, *17*, 1567–1593, and Crawford, A. J.; Bhattacharya, S. K. Varian Instruments at Work, Number AA–46, April 1985.

Representative Method 10.2

Determination of Cu and Zn in Tissue Samples

Description of Method

Copper and zinc are isolated from tissue samples by digesting the sample with HNO_3 after first removing any fatty tissue. The concentration of copper and zinc in the supernatant are determined by atomic absorption using an air-acetylene flame.

Procedure

Tissue samples are obtained by a muscle needle biopsy and dried for 24–30 h at 105°C to remove all traces of moisture. The fatty tissue in the dried samples is removed by extracting overnight with anhydrous ether. After removing the ether, the sample is dried to obtain the fat-free dry tissue weight (FFDT). The sample is digested at 68°C for 20–24 h using 3 mL of 0.75 M HNO_3. After centrifuging at 2500 rpm for 10 minutes, the supernatant is transferred to a 5-mL volumetric flask. The digestion is repeated two more times, for 2–4 hours each, using 0.9-mL aliquots of 0.75 M HNO_3. These supernatants are added to the 5-mL volumetric flask, which is diluted to volume with 0.75 M HNO_3. The concentrations of Cu and Zn in the diluted supernatant are determined by flame atomic absorption spectroscopy using an air-acetylene flame and external standards. Copper is analyzed at a wavelength of 324.8 nm with a slit width of 0.5 nm, and zinc is analyzed at 213.9 nm with a slit width of 1.0 nm. Background correction using a D_2 lamp is necessary for zinc. Results are reported as mg of Cu or Zn per gram of FFDT.

Questions

1. Describe the appropriate matrix for the external standards and for the blank?

The matrix for the standards and the blank should match the matrix of the samples; thus, an appropriate matrix is 0.75 M HNO_3. Any interferences from other components of the sample matrix are minimized by background correction.

2. Why is a background correction necessary for the analysis of Zn, but not for the analysis of Cu?

Background correction compensates for background absorption and scattering due to interferents in the sample. Such interferences are most severe when using a wavelength less than 300 nm. This is the case for Zn, but not for Cu.

3. A Cu hollow cathode lamp has several emission lines. Explain why this method uses the line at 324.8 nm.

wavelength (nm)	slit width (nm)	mg Cu/L for A = 0.20	P_0 (relative)
217.9	0.2	15	3
218.2	0.2	15	3
222.6	0.2	60	5
244.2	0.2	400	15
249.2	0.5	200	24
324.8	0.5	1.5	100
327.4	0.5	3	87

With 1.5 mg Cu/L giving an absorbance of 0.20, the emission line at 324.8 nm has the best sensitivity. In addition, it is the most intense emission line, which decreases the uncertainty in the measured absorbance.

Example 10.10

To evaluate the method described in Representative Method 10.2, a series of external standard is prepared and analyzed, providing the results shown here.[17]

µg Cu/mL	absorbance	µg Cu/mL	absorbance
0.000	0.000	0.500	0.033
0.100	0.006	0.600	0.039
0.200	0.013	0.700	0.046
0.300	0.020	1.000	0.066
0.400	0.026		

A bovine liver standard reference material was used to evaluate the method's accuracy. After drying and extracting the sample, a 11.23-mg FFDT tissue sample gives an absorbance of 0.023. Report the amount of copper in the sample as µg Cu/g FFDT.

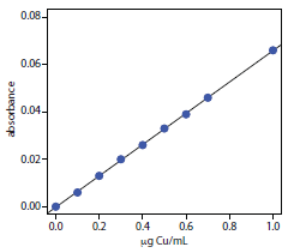
Solution

Linear regression of absorbance versus the concentration of Cu in the standards gives a calibration curve with the following equation.

$$A = -0.0002 + 0.0661 \times \frac{\text{g Cu}}{\text{mL}} \tag{10.4.2}$$

Substituting the sample's absorbance into the calibration equation gives the concentration of copper as 0.351 µg/mL. The concentration of copper in the tissue sample, therefore, is

$$\frac{\frac{0.351\ \text{g Cu}}{\text{mL}} \times 5.000\ \text{mL}}{0.01123\ \text{g sample}} = 156\ \text{g Cu/g FFDT} \tag{10.4.3}$$



10.4.3 - Evaluation of Atomic Absorption Spectroscopy

Scale of Operation

Atomic absorption spectroscopy is ideally suited for the analysis of trace and ultratrace analytes, particularly when using electrothermal atomization. For minor and major analyte, sample can be diluted before the analysis. Most analyses use a macro or a meso sample. The small volume requirement for electrothermal atomization or flame microsampling, however, makes practical the analysis micro and ultramicro samples.

> **Note**
>
> See Figure 3.5 to review the meaning of macro and meso for describing samples, and the meaning of major, minor, and ultratrace for describing analytes.

Accuracy

If spectral and chemical interferences are minimized, an accuracy of 0.5–5% is routinely attainable. When the calibration curve is nonlinear, accuracy may be improved by using a pair of standards whose absorbances closely bracket the sample's absorbance and assuming that the change in absorbance is linear over this limited concentration range. Determinate errors for electrothermal atomization are often greater than that obtained with flame atomization due to more serious matrix interferences.

Precision

For absorbance values greater than 0.1–0.2, the relative standard deviation for atomic absorption is 0.3–1% for flame atomization and 1–5% for electrothermal atomization. The principle limitation is the variation in the concentration of free analyte atoms resulting from variations in the rate of aspiration, nebulization, and atomization when using a flame atomizer, and the consistency of injecting samples when using electrothermal atomization.

Sensitivity

The sensitivity of a flame atomic absorption analysis is influenced strongly by the flame's composition and by the position in the flame from which we monitor the absorbance. Normally the sensitivity of an analysis is optimized by aspirating a standard solution of the analyte and adjusting operating conditions, such as the fuel-to-oxidant ratio, the nebulizer flow rate, and the height of the burner, to give the greatest absorbance. With electrothermal atomization, sensitivity is influenced by the drying and ashing stages that precede atomization. The temperature and time used for each stage must be optimized for each type of sample.

> **Note**
>
> See Chapter 14 for several strategies for optimizing experiments.

Sensitivity is also influenced by the sample's matrix. We have already noted, for example, that sensitivity can be decreased by chemical interferences. An increase in sensitivity may be realized by adding a low molecular weight alcohol, ester, or ketone to the solution, or by using an organic solvent.

Selectivity

Due to the narrow width of absorption lines, atomic absorption provides excellent selectivity. Atomic absorption can be used for the analysis of over 60 elements at concentrations at or below the level of μg/L.

Time, Cost, and Equipment

The analysis time when using flame atomization is short, with sample throughputs of 250–350 determinations per hour when using a fully automated system. Electrothermal atomization requires substantially more time per analysis, with maximum sample throughputs of 20–30 determinations per hour. The cost of a new instrument ranges from between $10,000–$50,000 for flame atomization, and from $18,000–$70,000 for electrothermal atomization. The more expensive instruments in each price range include double-beam optics, automatic samplers, and can be programmed for multielemental analysis by allowing the wavelength and hollow cathode lamp to be changed automatically.

Contributors

David Harvey (DePauw University)

10.4: Atomic Absorption Spectroscopy is shared under a CC BY-NC-SA 4.0 license and was authored, remixed, and/or curated by LibreTexts.

10.5: Emission Spectroscopy

An analyte in an excited state possesses an energy, E_2, that is greater than its energy when it is in a lower energy state, E_1. When the analyte returns to its lower energy state—a process we call **relaxation**—the excess energy, ΔE

$$\Delta E = E_2 - E_1 \tag{10.5.1}$$

must be released. Figure 10.4 shows a simplified picture of this process.

The amount of time the analyte spends in the excited state—its **lifetime**—is short, typically 10^{-5}–10^{-9} s for electronic excited states and 10^{-15} s for vibrational excited states. Relaxation of an analyte's excited-state, A*, occurs through several mechanisms, including collisions with other species in the sample, by photochemical reactions, and by the emission of photons. In the first process, which is called vibrational relaxation, or nonradiative relaxation, the excess energy is released as heat.

$$\mathrm{A^* \rightarrow A + heat} \tag{10.5.2}$$

Relaxation by a photochemical reaction may involve a decomposition reaction

$$\mathrm{A^* \rightarrow X + Y} \tag{10.5.3}$$

or a reaction between A* and another species

$$\mathrm{A^* + Z \rightarrow X + Y} \tag{10.5.4}$$

In both cases the excess energy is used up in the chemical reaction or released as heat.

In the third mechanism, the excess energy is released as a photon of electromagnetic radiation.

$$\mathrm{A^* \rightarrow A} + h\nu \tag{10.5.5}$$

The release of a photon following thermal excitation is called emission and that following the absorption of a photon is called photoluminescence. In chemiluminescence and bioluminescence, excitation results from a chemical or biochemical reaction, respectively. Spectroscopic methods based on photoluminescence are the subject of the next section and atomic emission is covered in Section 10.7.

Contributors

- David Harvey (DePauw University)

10.5: Emission Spectroscopy is shared under a CC BY-NC-SA 4.0 license and was authored, remixed, and/or curated by LibreTexts.

10.6: Photoluminescence Spectroscopy

Photoluminescence is divided into two categories: fluorescence and phosphorescence. A pair of electrons occupying the same electronic ground state have opposite spins and are said to be in a singlet spin state (Figure 10.47a). When an analyte absorbs an ultraviolet or visible photon, one of its valence electrons moves from the ground state to an excited state with a conservation of the electron's spin (Figure 10.47b). Emission of a photon from the **singlet excited state** to the singlet ground state—or between any two energy levels with the same spin—is called **fluorescence**. The probability of fluorescence is very high and the average lifetime of an electron in the excited state is only 10^{-5}–10^{-8} s. Fluorescence, therefore, decays rapidly once the source of excitation is removed.

In some cases an electron in a singlet excited state is transformed to a **triplet excited state** (Figure 10.47c) in which its spin is no longer paired with the ground state. Emission between a triplet excited state and a singlet ground state—or between any two energy levels that differ in their respective spin states–is called **phosphorescence**. Because the average lifetime for phosphorescence ranges from 10^{-4}–10^{4} s, phosphorescence may continue for some time after removing the excitation source.

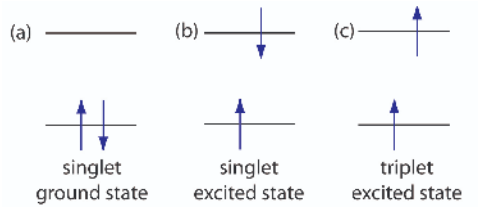


Figure 10.47 Electron configurations for (a) a singlet ground state; (b) a singlet excited state; and (c) a triplet excited state.

The use of molecular fluorescence for qualitative analysis and semi-quantitative analysis can be traced to the early to mid 1800s, with more accurate quantitative methods appearing in the 1920s. Instrumentation for fluorescence spectroscopy using a filter or a monochromator for wavelength selection appeared in, respectively, the 1930s and 1950s. Although the discovery of phosphorescence preceded that of fluorescence by almost 200 years, qualitative and quantitative applications of molecular phosphorescence did not receive much attention until after the development of fluorescence instrumentation.

10.6.1 Fluorescence and Phosphorescence Spectra

To appreciate the origin of fluorescence and phosphorescence we must consider what happens to a molecule following the absorption of a photon. Let's assume that the molecule initially occupies the lowest vibrational energy level of its electronic ground state, which is a singlet state labeled S_0 in Figure 10.48. Absorption of a photon excites the molecule to one of several vibrational energy levels in the first excited electronic state, S_1, or the second electronic excited state, S_2, both of which are singlet states. Relaxation to the ground state occurs by a number of mechanisms, some involving the emission of photons and others occurring without emitting photons. These relaxation mechanisms are shown in Figure 10.48. The most likely relaxation pathway is the one with the shortest lifetime for the excited state.

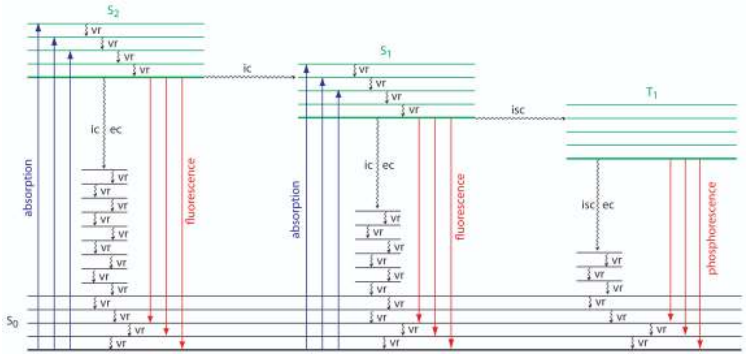


Figure 10.48 Energy level diagram for a molecule showing pathways for the deactivation of an excited state: ***vr*** is vibrational relaxation; ***ic*** is internal conversion; ***ec*** is external conversion; and ***isc*** is an intersystem crossing. The lowest vibrational energy for

each electronic state is indicated by the thicker line. The electronic ground state is shown in black and the three electronic excited states are shown in green. The absorption, fluorescence, and phosphorescence of photons also are shown.

Radiationless Deactivation

When a molecule relaxes without emitting a photon we call the process **radiationless deactivation**. One example of radiationless deactivation is **vibrational relaxation**, in which a molecule in an excited vibrational energy level loses energy by moving to a lower vibrational energy level in the same electronic state. Vibrational relaxation is very rapid, with an average lifetime of $<10^{-12}$ s. Because vibrational relaxation is so efficient, a molecule in one of its excited state's higher vibrational energy levels quickly returns to the excited state's lowest vibrational energy level.

Another form of radiationless deactivation is an **internal conversion** in which a molecule in the ground vibrational level of an excited state passes directly into a higher vibrational energy level of a lower energy electronic state of the same spin state. By a combination of internal conversions and vibrational relaxations, a molecule in an excited electronic state may return to the ground electronic state without emitting a photon. A related form of radiationless deactivation is an **external conversion** in which excess energy is transferred to the solvent or to another component of the sample's matrix.

A final form of radiationless deactivation is an **intersystem crossing** in which a molecule in the ground vibrational energy level of an excited electronic state passes into a higher vibrational energy level of a lower energy electronic state with a different spin state. For example, an intersystem crossing is shown in Figure 10.48 between a singlet excited state, S_1, and a triplet excited state, T_1.

> **Note**
>
> Let's use Figure 10.48 to illustrate how a molecule can relax back to its ground state without emitting a photon. Suppose our molecule is in the highest vibrational energy level of the second electronic excited state. After a series of vibrational relaxations brings the molecule to the lowest vibrational energy level of S_2, it undergoes an internal conversion into a higher vibrational energy level of the first excited electronic state. Vibrational relaxations bring the molecule to the lowest vibrational energy level of S_1. Following an internal conversion into a higher vibrational energy level of the ground state, the molecule continues to undergo vibrational relaxation until it reaches the lowest vibrational energy level of S_0.

Relaxation by Fluorescence

Fluorescence occurs when a molecule in an excited state's lowest vibrational energy level returns to a lower energy electronic state by emitting a photon. Because molecules return to their ground state by the fastest mechanism, fluorescence is observed only if it is a more efficient means of relaxation than a combination of internal conversions and vibrational relaxations.

A quantitative expression of fluorescence efficiency is the **fluorescent quantum yield**, Φ_f, which is the fraction of excited state molecules returning to the ground state by fluorescence. Fluorescent quantum yields range from 1, when every molecule in an excited state undergoes fluorescence, to 0 when fluorescence does not occur.

The intensity of fluorescence, I_f, is proportional to the amount of radiation absorbed by the sample, $P_0 - P_T$, and the fluorescent quantum yield

$$I_f = k\Phi_f(P_0 - P_T) \tag{10.25}$$

where k is a constant accounting for the efficiency of collecting and detecting the fluorescent emission. From Beer's law we know that

$$\frac{P_T}{P_0} = 10^{-\varepsilon bC} \tag{10.26}$$

where C is the concentration of the fluorescing species. Solving equation 10.26 for P_T and substituting into equation 10.25 gives, after simplifying

$$I_f = k\Phi_f P_0(1 - 10^{-\varepsilon bC}) \tag{10.27}$$

When $\varepsilon bC < 0.01$, which often is the case when concentration is small, equation 10.27 simplifies to

$$I_f = 2.303k\Phi_f\varepsilon bCP_0 = k'P_0 \tag{10.28}$$

where k' is a collection of constants. The intensity of fluorescent emission, therefore, increases with an increase in the quantum efficiency, the source^fs incident power, and the molar absorptivity and the concentration of the fluorescing species.

Fluorescence is generally observed when the molecule's lowest energy absorption is a $\pi \rightarrow \pi^*$ transition, although some $n \rightarrow \pi^*$ transitions show weak fluorescence. Most unsubstituted, nonheterocyclic aromatic compounds have favorable fluorescence quantum yields, although substitutions on the aromatic ring can significantly effect Φ_f. For example, the presence of an electron-withdrawing group, such as $–NO_2$, decreases Φ_f, while adding an electron-donating group, such as –OH, increases Φ_f. Fluorescence also increases for aromatic ring systems and for aromatic molecules with rigid planar structures. Figure 10.49 shows the fluorescence of quinine under a UV lamp.



Figure 10.49 Tonic water, which contains quinine, is fluorescent when placed under a UV lamp. Source: Splarka (commons.wikipedia.org).

A molecule's fluorescent quantum yield is also influenced by external variables, such as temperature and solvent. Increasing the temperature generally decreases Φ_f because more frequent collisions between the molecule and the solvent increases external conversion. A decrease in the solvent's viscosity decreases Φ_f for similar reasons. For an analyte with acidic or basic functional groups, a change in pH may change the analyte's structure and its fluorescent properties.

As shown in Figure 10.48, fluorescence may return the molecule to any of several vibrational energy levels in the ground electronic state. Fluorescence, therefore, occurs over a range of wavelengths. Because the change in energy for fluorescent emission is generally less than that for absorption, a molecule's fluorescence spectrum is shifted to higher wavelengths than its absorption spectrum.

Relaxation by Phosphorescence

A molecule in a triplet electronic excited state's lowest vibrational energy level normally relaxes to the ground state by an intersystem crossing to a singlet state or by an external conversion. Phosphorescence occurs when the molecule relaxes by emitting a photon. As shown in Figure 10.48, phosphorescence occurs over a range of wavelengths, all of which are at lower energies than the molecule's absorption band. The intensity of phosphorescence, I_p, is given by an equation similar to equation 10.28 for fluorescence

$$I_p = 2.303k\Phi_p\varepsilon bCP_0 = k'P_0 \tag{10.29}$$

where Φ_p is the **phosphorescent quantum yield**.

Phosphorescence is most favorable for molecules with $n \rightarrow \pi^*$ transitions, which have a higher probability for an intersystem crossing than $\pi \rightarrow \pi^*$ transitions. For example, phosphorescence is observed with aromatic molecules containing carbonyl groups or heteroatoms. Aromatic compounds containing halide atoms also have a higher efficiency for phosphorescence. In general, an increase in phosphorescence corresponds to a decrease in fluorescence.

Because the average lifetime for phosphorescence is very long, ranging from 10^{-4}–10^{4} s, the phosphorescent quantum yield is usually quite small. An improvement in Φ_p is realized by decreasing the efficiency of external conversion. This may be accomplished in several ways, including lowering the temperature, using a more viscous solvent, depositing the sample on a solid substrate, or trapping the molecule in solution. Figure 10.50 shows an example of phosphorescence.

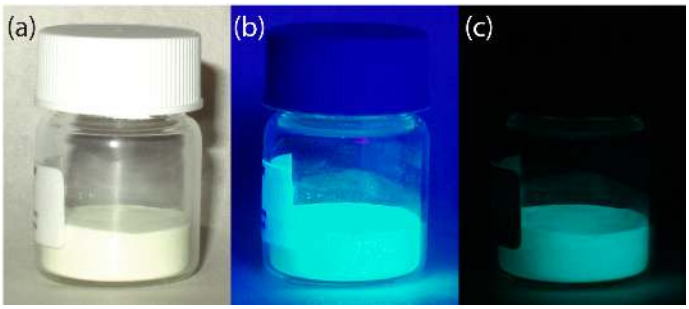


Figure 10.50 An europium doped strontium silicate-aluminum oxide powder under (a) natural light, (b) a long-wave UV lamp, and (c) in total darkness. The photo taken in total darkness shows the phosphorescent emission. Source: modified from Splarka (commons.wikipedia.org).

Excitation versus Emission Spectra

Photoluminescence spectra are recorded by measuring the intensity of emitted radiation as a function of either the excitation wavelength or the emission wavelength. An **excitation spectrum** is obtained by monitoring emission at a fixed wavelength while varying the excitation wavelength. When corrected for variations in the source's intensity and the detector's response, a sample's excitation spectrum is nearly identical to its absorbance spectrum. The excitation spectrum provides a convenient means for selecting the best excitation wavelength for a quantitative or qualitative analysis.

In an **emission spectrum** a fixed wavelength is used to excite the sample and the intensity of emitted radiation is monitored as function of wavelength. Although a molecule has only a single excitation spectrum, it has two emission spectra, one for fluorescence and one for phosphorescence. Figure 10.51 shows the UV absorption spectrum and the UV fluorescence emission spectrum for tyrosine.

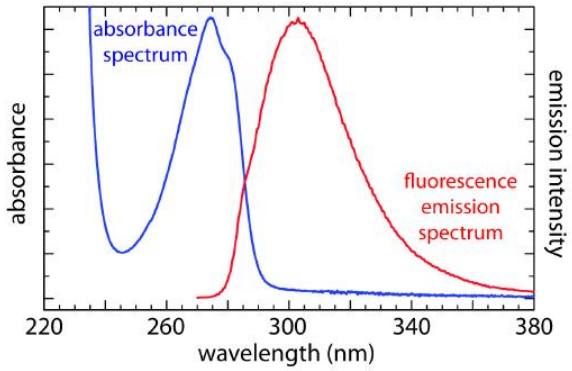


Figure 10.51 Absorbance spectrum and fluorescence emission spectrum for tyrosine in a pH 7, 0.1 M phosphate buffer. The emission spectrum uses an excitation wavelength of 260 nm. Source: modified from Mark Somoza (commons.wikipedia.org).

10.6.2 Instrumentation

The basic instrumental needs for monitoring fluorescence and phosphorescence—a source of radiation, a means of selecting a narrow band of radiation, and a detector—are the same as those for absorption spectroscopy. The unique demands of both techniques, however, require some modifications to the instrument designs seen earlier in Figure 10.25 (filter photometer), Figure 10.26 (single-beam spectrophotometer), Figure 10.27 (double-beam spectrophotometer), and Figure 10.28 (diode array spectrometer). The most important difference is the detector cannot be placed directly across from the source. Figure 10.52 shows

why this is the case. If we place the detector along the source's axis it will receive both the transmitted source radiation, P_T, and the fluorescent, I_f, or phosphorescent, I_p, radiation. Instead, we rotate the director and place it at 90° to the source.

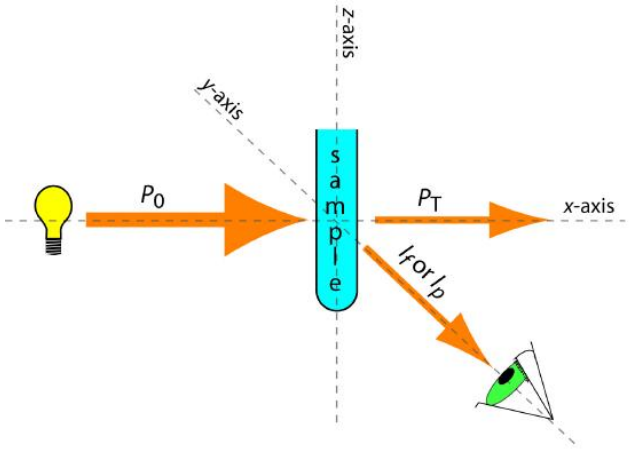


Figure 10.52 Schematic diagram showing the orientation of the source and the detector when measuring fluorescence and phosphorescence. Contrast this to Figure 10.21, which shows the orientation for absorption spectroscopy.

Instruments for Measuring Fluorescence

Figure 10.53 shows the basic design of an instrument for measuring fluorescence, which includes two wavelength selectors, one for selecting an excitation wavelength from the source and one for selecting the emission wavelength from the sample. In a **fluorimeter** the excitation and emission wavelengths are selected using absorption or interference filters. The excitation source for a fluorimeter is usually a low-pressure Hg vapor lamp that provides intense emission lines distributed throughout the ultraviolet and visible region (254, 312, 365, 405, 436, 546, 577, 691, and 773 nm). When a monochromator is used to select the excitation and emission wavelengths, the instrument is called a **spectrofluorimeter**. With a monochromator the excitation source is usually high-pressure Xe arc lamp, which has a continuous emission spectrum. Either instrumental design is appropriate for quantitative work, although only a spectrofluorimeter can be used to record an excitation or emission spectrum.

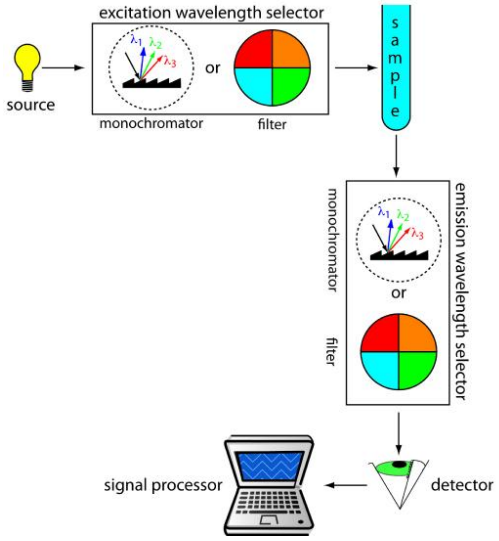


Figure 10.53 Schematic diagram for measuring fluorescence showing the placement of the wavelength selectors for excitation and emission. When a filter is used the instrument is called a fluorimeter, and when a monochromator is used the instrument is called a spectrofluorimeter.

The sample cells for molecular fluorescence are similar to those for molecular absorption. Remote sensing with fiber optic probes also can be adapted for use with either a fluorimeter or spectrofluorimeter. An analyte that is fluorescent can be monitored directly.

For analytes that are not fluorescent, a suitable fluorescent probe molecule can be incorporated into the tip of the fiber optic probe. The analyte's reaction with the probe molecule leads to an increase or decrease in fluorescence.

Instruments for Measuring Phosphorescence

Instrumentation for molecular phosphorescence must discriminate between phosphorescence and fluorescence. Because the lifetime for fluorescence is shorter than that for phosphorescence, discrimination is easily achieved by incorporating a delay between exciting the sample and measuring phosphorescent emission. Figure 10.54 shows how two out-of-phase choppers can be use to block emission from reaching the detector when the sample is being excited, and to prevent source radiation from reaching the sample while we are measuring the phosphorescent emission.

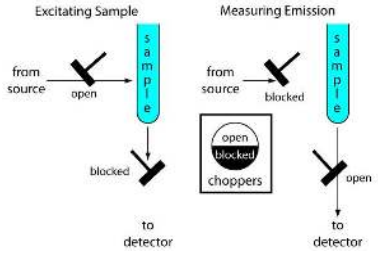


Figure 10.54 Schematic diagram showing how choppers are used to prevent fluorescent emission from interfering with the measurement of phosphorescent emission.

Because phosphorescence is such a slow process, we must prevent the excited state from relaxing by external conversion. Traditionally, this has been accomplished by dissolving the sample in a suitable organic solvent, usually a mixture of ethanol, isopentane, and diethylether. The resulting solution is frozen at liquid-N_2 temperatures, forming an optically clear solid. The solid matrix minimizes external conversion due to collisions between the analyte and the solvent. External conversion also is minimized by immobilizing the sample on a solid substrate, making possible room temperature measurements. One approach is to place a drop of the solution containing the analyte on a small disc of filter paper. After drying the sample under a heat lamp, the sample is placed in the spectrofluorimeter for analysis. Other solid surfaces that have been used include silica gel, alumina, sodium acetate, and sucrose. This approach is particularly useful for the analysis of thin layer chromatography plates.

10.6.3 Quantitative Applications

Molecular fluorescence and, to a lesser extent, phosphorescence have been used for the direct or indirect quantitative analysis of analytes in a variety of matrices. A direct quantitative analysis is possible when the analyte's fluorescent or phosphorescent quantum yield is favorable. When the analyte is not fluorescent or phosphorescent, or if the quantum yield is unfavorable, then an indirect analysis may be feasible. One approach is to react the analyte with a reagent to form a product with fluorescent or phosphorescent properties. Another approach is to measure a decrease in fluorescence or phosphorescence when the analyte is added to a solution containing a fluorescent or phosphorescent probe molecule. A decrease in emission is observed when the reaction between the analyte and the probe molecule enhances radiationless deactivation, or produces a nonemittng product. The application of fluorescence and phosphorescence to inorganic and organic analytes are considered in this section.

Inorganic Analytes

Except for a few metal ions, most notably UO_2^+, most inorganic ions are not sufficiently fluorescent for a direct analysis. Many metal ions may be determined indirectly by reacting with an organic ligand to form a fluorescent, or less commonly, a phosphorescent metal–ligand complex. One example is the reaction of Al^{3+} with the sodium salt of 2, 4, 3′-trihydroxyazobenzene-5′-sulfonic acid—also known as alizarin garnet R—which forms a fluorescent metal–ligand complex (Figure 10.55). The analysis is carried out using an excitation wavelength of 470 nm, monitoring fluorescence at 500 nm. Table 10.12 provides additional examples of chelating reagents that form fluorescent metal–ligand complexes with metal ions. A few inorganic nonmetals are determined by their ability to decrease, or quench, the fluorescence of another species. One example is the analysis for F– based on its ability to quench the fluorescence of the Al^{3+}–alizarin garnet R complex.

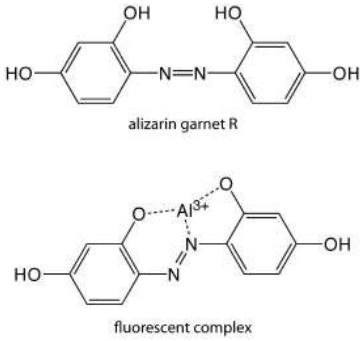


Figure 10.55 Structure of alizarin garnet R and its metal–ligand complex with Al^{3+}.

Table 10.12 Chelating Agents for the Fluorescence Analysis of Metal Ions

chelating agent	metal ions
8-hydroxyquinoline	Al^{3+}, Be^{2+}, Zn^{2+}, Li^{+}, Mg^{2+} (and others)
flavonal	Zr^{2+}, Sn^{4+}
benzoin	$B_4O_7^{2-}$, Zn^{2+}
2ˆ', 3, 4ˆ', 5, 7-pentahydroxyflavone	Be^{2+}
2-(*o*-hydroxyphenyl) benzoxazole	Cd^{2+}

Organic Analytes

As noted earlier, organic compounds containing aromatic rings generally are fluorescent and aromatic heterocycles are often phosphorescent. As shown in Table 10.13, several important biochemical, pharmaceutical, and environmental compounds may be analyzed quantitatively by fluorimetry or phosphorimetry. If an organic analyte is not naturally fluorescent or phosphorescent, it may be possible to incorporate it into a chemical reaction that produces a fluorescent or phosphorescent product. For example, the enzyme creatine phosphokinase can be determined by using it to catalyze the formation of creatine from phosphocreatine. Reacting the creatine with ninhydrin produces a fluorescent product of unknown structure.

Table 10.13 Examples of Naturally Photoluminescent Organic Analytes

class	compounds (F = fluorescence; P = phosphorescence)
aromatic amino acids	phenylalanine (F) tyrosine (F) tryptophan (F, P)
vitamins	vitamin A (F) vitamin B2 (F) vitamin B6 (F) vitamin B12 (F) vitamin E (F) folic acid (F)
catecholamines	dopamine (F) norepinephrine (F)
pharmaceuticals and drugs	quinine (F) salicylic acid (F, P) morphine (F) barbiturates (F) LSD (F) codeine (P) caffeine (P) sulfanilamide (P)
environmental pollutants	pyrene (F) benzo[a]pyrene (F) organothiophosphorous pesticides (F) carbamate insecticides (F) DDT (P)

Standardizing the Method

From equation 10.28 and equation 10.29 we know that the intensity of fluorescent or phosphorescent emission is a linear function of the analyte's concentration provided that the sample's absorbance of source radiation ($A = \varepsilon bC$) is less than approximately 0.01. Calibration curves often are linear over four to six orders of magnitude for fluorescence and over two to four orders of magnitude for phosphorescence. For higher concentrations of analyte the calibration curve becomes nonlinear because the assumptions leading to equation 10.28 and equation 10.29 no longer apply. Nonlinearity may be observed for small concentrations of analyte due to the presence of fluorescent or phosphorescent contaminants. As discussed earlier, quantum efficiency is sensitive to temperature and sample matrix, both of which must be controlled when using external standards. In addition, emission intensity depends on the molar absorptivity of the photoluminescent species, which is sensitive to the sample matrix.

Note

The best way to appreciate the theoretical and practical details discussed in this section is to carefully examine a typical analytical method. Although each method is unique, the following description of the determination of quinine in urine provides an instructive example of a typical procedure. The description here is based on Mule, S. J.; Hushin, P. L. *Anal. Chem.* **1971**, *43*, 708–711, and O'Reilly, J. E.; *J. Chem. Educ.* **1975**, *52*, 610–612.

Representative Method 10.3

Determination of Quinine in Urine

Description of Method

Quinine is an alkaloid used in treating malaria. It is a strongly fluorescent compound in dilute solutions of H_2SO_4 ($\Phi_f = 0.55$). Quinine's excitation spectrum has absorption bands at 250 nm and 350 nm and its emission spectrum has a single emission band

at 450 nm. Quinine is rapidly excreted from the body in urine and is easily determined by measuring its fluorescence following its extraction from the urine sample.

(Figure 10.49 shows the fluorescence of the quinine in tonic water.)

Procedure

Transfer a 2.00-mL sample of urine to a 15-mL test tube and adjust its pH to between 9 and 10 using 3.7 M NaOH. Add 4 mL of a 3:1 (v/v) mixture of chloroform and isopropanol and shake the contents of the test tube for one minute. Allow the organic and the aqueous (urine) layers to separate and transfer the organic phase to a clean test tube. Add 2.00 mL of 0.05 M H_2SO_4 to the organic phase and shake the contents for one minute. Allow the organic and the aqueous layers to separate and transfer the aqueous phase to the sample cell. Measure the fluorescent emission at 450 nm using an excitation wavelength of 350 nm. Determine the concentration of quinine in the urine sample using a calibration curve prepared with a set of external standards in 0.05 M H_2SO_4, prepared from a 100.0 ppm solution of quinine in 0.05 M H_2SO_4. Use distilled water as a blank.

Questions

1. Chloride ion quenches the intensity of quinine's fluorescent emission. For example, in the presence of 100 ppm NaCl (61 ppm Cl^-) quinine's emission intensity is only 83% of its emission intensity in the absence of chloride. The presence of 1000 ppm NaCl (610 ppm Cl^-) further reduces quinine's fluorescent emission to less than 30% of its emission intensity in the absence of chloride. The concentration of chloride in urine typically ranges from 4600–6700 ppm Cl^-. Explain how this procedure prevents an interference from chloride.

The procedure uses two extractions. In the first of these extractions, quinine is separated from urine by extracting it into a mixture of chloroform and isopropanol, leaving the chloride behind in the original sample.

2. Samples of urine may contain small amounts of other fluorescent compounds, which interfere with the analysis if they are carried through the two extractions. Explain how you can modify the procedure to take this into account?

One approach is to prepare a blank using a sample of urine known to be free of quinine. Subtracting the blank's fluorescent signal from the measured fluorescence from urine samples corrects for the interfering compounds.

3. The fluorescent emission for quinine at 450 nm can be induced using an excitation frequency of either 250 nm or 350 nm. The fluorescent quantum efficiency is the same for either excitation wavelength. Quinine's absorption spectrum shows that ε_{250} is greater than ε_{350}. Given that quinine has a stronger absorbance at 250 nm, explain why its fluorescent emission intensity is greater when using 350 nm as the excitation wavelength.

From equation 10.28 we know that I_f is a function of the following terms: k, Φ_f, P_0, ε, b, and C. We know that Φ_f, b, and C are the same for both excitation wavelengths and that ε is larger for a wavelength of 250 nm; we can, therefore, ignore these terms. The greater emission intensity when using an excitation wavelength of 350 nm must be due to a larger value for P_0 or k. In fact, P_0 at 350 nm for a high-pressure Xe arc lamp is about 170% of that at 250 nm. In addition, the sensitivity of a typical photomultiplier detector (which contributes to the value of k) at 350 nm is about 140% of that at 250 nm.

Example 10.11

To evaluate the method described in Representative Method 10.3, a series of external standard was prepared and analyzed, providing the results shown in the following table. All fluorescent intensities were corrected using a blank prepared from a

quinine-free sample of urine. The fluorescent intensities are normalized by setting I_f for the highest concentration standard to 100.

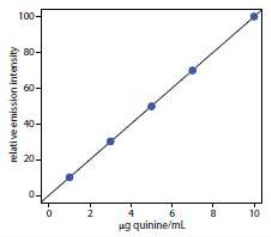
[quinine] (µg/mL)	I_f
1.00	10.11
3.00	30.20
5.00	49.84
7.00	69.89
10.00	100.0

After ingesting 10.0 mg of quinine, a volunteer provided a urine sample 24-h later. Analysis of the urine sample gives an relative emission intensity of 28.16. Report the concentration of quinine in the sample in mg/L and the percent recovery for the ingested quinine.

Solution

Linear regression of the relative emission intensity versus the concentration of quinine in the standards gives a calibration curve with the following equation.

$$I_f = 0.124 + 9.978 \times \frac{\text{g quinine}}{\text{mL}} \tag{10.6.1}$$



Substituting the sample's relative emission intensity into the calibration equation gives the concentration of quinine as 2.81 µg/mL. Because the volume of urine taken, 2.00 mL, is the same as the volume of 0.05 M H_2SO_4 used in extracting quinine, the concentration of quinine in the urine also is 2.81 µg/mL. The recovery of the ingested quinine is

$$\frac{\frac{2.81\text{ g}}{\text{ml urine}} \times 2.00\text{ mL urine} \times \frac{1\text{ mg}}{1000\text{ g}}}{10.0\text{ mg quinine ingested}} \times 100 = 0.0562\% \tag{10.6.2}$$

(It can take up 10–11 days for the body to completely excrete quinine.)

10.6.4 Evaluation of Photoluminescence Spectroscopy

Scale of Operation

Photoluminescence spectroscopy is used for the routine analysis of trace and ultratrace analytes in macro and meso samples. Detection limits for fluorescence spectroscopy are strongly influenced by the analyte's quantum yield. For an analyte with $\Phi_f > 0.5$, a picomolar detection limit is possible when using a high quality spectrofluorimeter. For example, the detection limit for quinine sulfate, for which Φ_f is 0.55, is generally between 1 part per billion and 1 part per trillion. Detection limits for phosphorescence are somewhat higher, with typical values in the nanomolar range for low-temperature phosphorimetry, and in the micromolar range for room-temperature phosphorimetry using a solid substrate.

Note

See Figure 3.5 to review the meaning of macro and meso for describing samples, and the meaning of major, minor, and ultratrace for describing analytes.

Accuracy

The accuracy of a fluorescence method is generally between 1–5% when spectral and chemical interferences are insignificant. Accuracy is limited by the same types of problems affecting other optical spectroscopic methods. In addition, accuracy is affected by interferences influencing the fluorescent quantum yield. The accuracy of phosphorescence is somewhat greater than that for fluorescence.

Precision

The relative standard deviation for fluorescence is usually between 0.5–2% when the analyte's concentration is well above its detection limit. Precision is usually limited by the stability of the excitation source. The precision for phosphorescence is often limited by reproducibility in preparing samples for analysis, with relative standard deviations of 5–10% being common.

Sensitivity

From equation 10.28 and equation 10.29 we know that the sensitivity of a fluorescent or phosphorescent method is influenced by a number of parameters. The importance of quantum yield and the effect of temperature and solution composition on Φ_f and Φ_p already have been considered. Besides quantum yield, the sensitivity of an analysis can be improved by using an excitation source that has a greater emission intensity, P_0, at the desired wavelength, and by selecting an excitation wavelength that has a greater absorbance. Another approach for improving sensitivity is to increase the volume in the sample from which emission is monitored. Figure 10.56 shows how rotating a monochromator's slits from their usual vertical orientation to a horizontal orientation increases the sampling volume. The result can increase the emission from the sample by 5–30×.

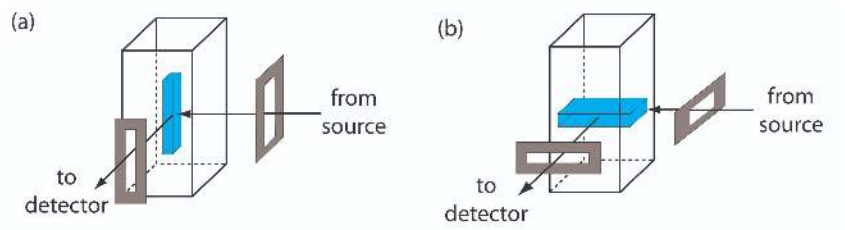


Figure 10.56 Use of slit orientation to change the volume from which fluorescence is measured: (a) vertical slit orientation; (b) horizontal slit orientation. Suppose the slit's dimensions are 0.1 mm × 3 mm. In (a) the dimensions of the sampling volume are 0.1 mm × 0.1mm × 3 mm, or 0.03 mm^3. For (b) the dimensions of the sampling volume are 0.1 mm × 3 mm × 3 mm, or 0.9 mm^3, a 30-fold increase in the sampling volume.

Selectivity

The selectivity of fluorescence and phosphorescence is superior to that of absorption spectrophotometry for two reasons: first, not every compound that absorbs radiation is fluorescent or phosphorescent; and, second, selectivity between an analyte and an interferent is possible if there is a difference in either their excitation or their emission spectra. The total emission intensity is a linear sum of that from each fluorescent or phosphorescent species. The analysis of a sample containing *n* components, therefore, can be accomplished by measuring the total emission intensity at *n* wavelengths.

Time, Cost, and Equipment

As with other optical spectroscopic methods, fluorescent and phosphorescent methods provide a rapid means for analyzing samples and are capable of automation. Fluorimeters are relatively inexpensive, ranging from several hundred to several thousand dollars, and often are satisfactory for quantitative work. Spectrofluorimeters are more expensive, with models often exceeding $50,000.

Contributors

David Harvey (DePauw University)

10.6: Photoluminescence Spectroscopy is shared under a CC BY-NC-SA 4.0 license and was authored, remixed, and/or curated by LibreTexts.

10.7: Atomic Emission Spectroscopy

The focus of this section is on the emission of ultraviolet and visible radiation following the thermal excitation of atoms. Atomic emission spectroscopy has a long history. Qualitative applications based on the color of flames were used in the smelting of ores as early as 1550 and were more fully developed around 1830 with the observation of atomic spectra generated by flame emission and spark emission.[18] Quantitative applications based on the atomic emission from electric sparks were developed by Lockyer in the early 1870 and quantitative applications based on flame emission were pioneered by Lundegardh in 1930. Atomic emission based on emission from a plasma was introduced in 1964.

10.7.1 Atomic Emission Spectra

Atomic emission occurs when a valence electron in a higher energy atomic orbital returns to a lower energy atomic orbital. Figure 10.57 shows a portion of the energy level diagram for sodium, which consists of a series of discrete lines at wavelengths corresponding to the difference in energy between two atomic orbitals.

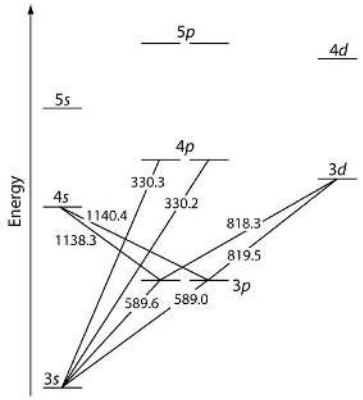


Figure 10.57 Valence shell energy level diagram for sodium. The wavelengths corresponding to several transitions are shown. Note that this is the same energy level diagram as Figure 10.19.

The intensity of an atomic emission line, I_e, is proportional to the number of atoms, N^*, populating the excited state,

$$I_e = kN^* \tag{10.30}$$

where k is a constant accounting for the efficiency of the transition. If a system of atoms is in thermal equilibrium, the population of excited state i is related to the total concentration of atoms, N, by the Boltzmann distribution. For many elements at temperatures of less than 5000 K the Boltzmann distribution is approximated as

$$N^* = N\left(\frac{g_i}{g_0}\right)e^{-E_i/kT} \tag{10.31}$$

where g_i and g_0 are statistical factors that account for the number of equivalent energy levels for the excited state and the ground state, E_i is the energy of the excited state relative to a ground state energy, E_0, of 0, k is Boltzmann's constant (1.3807×10^{-23} J/K), and T is the temperature in kelvin. From equation 10.31 we expect that excited states with lower energies have larger populations and more intense emission lines. We also expect emission intensity to increase with temperature.

10.7.2 Equipment

An atomic emission spectrometer is similar in design to the instrumentation for atomic absorption. In fact, it is easy to adapt most flame atomic absorption spectrometers for atomic emission by turning off the hollow cathode lamp and monitoring the difference in the emission intensity when aspirating the sample and when aspirating a blank. Many atomic emission spectrometers, however, are dedicated instruments designed to take advantage of features unique to atomic emission, including the use of plasmas, arcs, sparks, and lasers as atomization and excitation sources, and an enhanced capability for multielemental analysis.

Atomization and Excitation

Atomic emission requires a means for converting a solid, liquid, or solution analyte into a free gaseous atom. The same source of thermal energy usually serves as the excitation source. The most common methods are flames and plasmas, both of which are useful for liquid or solution samples. Solid samples may be analyzed by dissolving in a solvent and using a flame or plasma atomizer.

Flame Sources

Atomization and excitation in flame atomic emission is accomplished using the same nebulization and spray chamber assembly used in atomic absorption (Figure 10.42). The burner head consists of single or multiple slots, or a Meker style burner. Older atomic emission instruments often used a total consumption burner in which the sample is drawn through a capillary tube and injected directly into the flame.

Plasma Sources

A **plasma** is a hot, partially ionized gas that contains an abundant concentration of cations and electrons. The plasmas used in atomic emission are formed by ionizing a flowing stream of argon gas, producing argon ions and electrons. A plasma's high temperature results from resistive heating as the electrons and argon ions move through the gas. Because plasmas operate at much higher temperatures than flames, they provide better atomization and a higher population of excited states.

A schematic diagram of the inductively coupled plasma source (ICP) is shown in Figure 10.58. The ICP torch consists of three concentric quartz tubes, surrounded at the top by a radio-frequency induction coil. The sample is mixed with a stream of Ar using a nebulizer, and is carried to the plasma through the torch's central capillary tube. Plasma formation is initiated by a spark from a Tesla coil. An alternating radio-frequency current in the induction coils creates a fluctuating magnetic field that induces the argon ions and the electrons to move in a circular path. The resulting collisions with the abundant unionized gas give rise to resistive heating, providing temperatures as high as 10 000 K at the base of the plasma, and between 6000 and 8000 K at a height of 15–20 mm above the coil, where emission is usually measured. At these high temperatures the outer quartz tube must be thermally isolated from the plasma. This is accomplished by the tangential flow of argon shown in the schematic diagram.

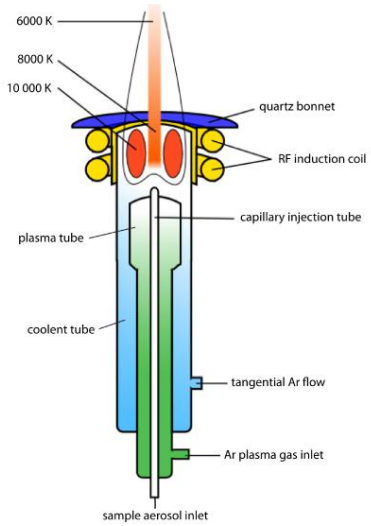


Figure 10.58 Schematic diagram of an inductively coupled plasma torch. Source: modified from Xvlun (commons.wikipedia.org).

Multielemental Analysis

Atomic emission spectroscopy is ideally suited for multielemental analysis because all analytes in a sample are excited simultaneously. If the instrument includes a scanning monochromator, we can program it to move rapidly to an analyte's desired wavelength, pause to record its emission intensity, and then move to the next analyte's wavelength. This sequential analysis allows for a sampling rate of 3–4 analytes per minute.

Another approach to a multielemental analysis is to use a multichannel instrument that allows us to simultaneously monitor many analytes. A simple design for a multichannel spectrometer couples a monochromator with multiple detectors that can be positioned

in a semicircular array around the monochromator at positions corresponding to the wavelengths for the analytes (Figure 10.59).

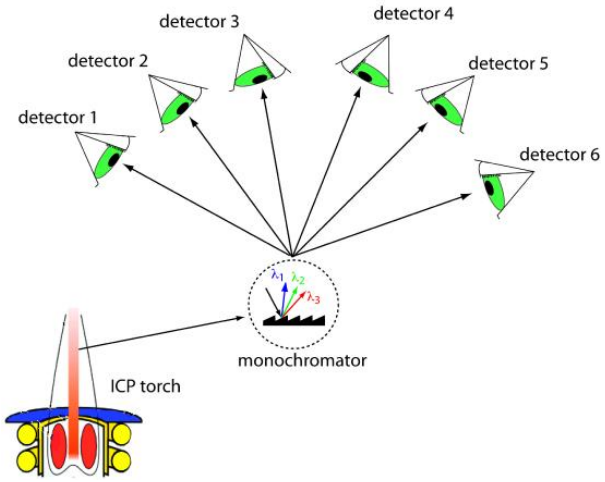


Figure 10.59 Schematic diagram of a multichannel atomic emission spectrometer for the simultaneous analysis of several elements. The ICP torch is modified from Xvlun (commons.wikipedia.org). Instruments may contain as many as 48–60 detectors.

10.7.3 Quantitative Applications

Atomic emission is widely used for the analysis of trace metals in a variety of sample matrices. The development of a quantitative atomic emission method requires several considerations, including choosing a source for atomization and excitation, selecting a wavelength and slit width, preparing the sample for analysis, minimizing spectral and chemical interferences, and selecting a method of standardization.

Choice of Atomization and Excitation Source

Except for the alkali metals, detection limits when using an ICP are significantly better than those obtained with flame emission (Table 10.14). Plasmas also are subject to fewer spectral and chemical interferences. For these reasons a plasma emission source is usually the better choice.

Table 10.14 Detection Limits for Atomic Emission[a]

	detection limit in μg/mL

	detection limit in μg/mL	
element	flame emission	ICP
Ag	2	0.2
Al	3	0.2
As	2000	2
Ca	0.1	0.0001
Cd	300	0.07
Co	5	0.1
Cr	1	0.08
Fe	10	0.09
Hg	150	1
K	0.01	30
Li	0.001	0.02
Mg	1	0.003
Mn	1	0.01
Na	0.01	0.1
Ni	10	0.2
Pb	0.2	1
Pt	2000	0.9
Sn	100	3
Zn	1000	0.1

[a] Source: Parsons, M. L.; Major, S.; Forster, A. R.; App. Spectrosc. 1983, 37, 411–418.

Selecting the Wavelength and Slit Width

The choice of wavelength is dictated by the need for sensitivity and the need to avoid interferences from the emission lines of other constituents in the sample. Because an analyte's atomic emission spectrum has an abundance of emission lines—particularly when using a high temperature plasma source—it is inevitable that there will be some overlap between emission lines. For example, an analysis for Ni using the atomic emission line at 349.30 nm is complicated by the atomic emission line for Fe at 349.06 nm. Narrower slit widths provide better resolution, but at the cost of less radiation reaching the detector. The easiest approach to selecting a wavelength is to record the sample's emission spectrum and look for an emission line that provides an intense signal and is resolved from other emission lines.

Preparing the Sample

Flame and plasma sources are best suited for samples in solution and liquid form. Although a solid sample can be analyzed by directly inserting it into the flame or plasma, they usually are first brought into solution by digestion or extraction.

Minimizing Spectral Interferences

The most important spectral interference is broad, background emission from the flame or plasma and emission bands from molecular species. This background emission is particularly severe for flames because the temperature is insufficient to break down

refractory compounds, such as oxides and hydroxides. Background corrections for flame emission are made by scanning over the emission line and drawing a baseline (Figure 10.60). Because a plasma's temperature is much higher, a background interference due to molecular emission is less of a problem. Although emission from the plasma's core is strong, it is insignificant at a height of 10–30 mm above the core where measurements normally are made.

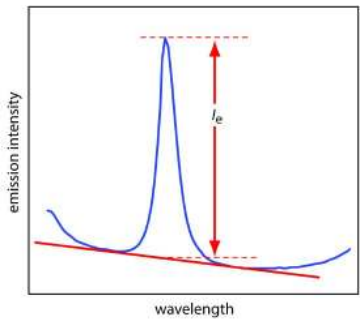


Figure 10.60 Method for correcting an analyte's emission for the flame's background emission.

Minimizing Chemical Interferences

Flame emission is subject to the same types of chemical interferences as atomic absorption. These interferences are minimized by adjusting the flame's composition and adding protecting agents, releasing agents, or ionization suppressors. An additional chemical interference results from **self-absorption**. Because the flame's temperature is greatest at its center, the concentration of analyte atoms in an excited state is greater at the flame's center than at its outer edges. If an excited state atom in the flame's center emits a photon while returning to its ground state, then a ground state atom in the cooler, outer regions of the flame may absorb the photon, decreasing the emission intensity. For higher concentrations of analyte self-absorption may invert the center of the emission band (Figure 10.61).

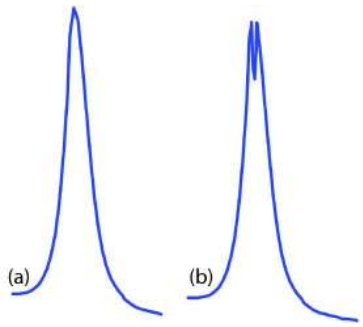


Figure 10.61 Atomic emission lines for (a) a low concentration of analyte, and (b) a high concentration of analyte showing the effect of self-absorption.

Chemical interferences with plasma sources generally are not significant because the plasma's higher temperature limits the formation of nonvolatile species. For example, PO_4^{3-} is a significant interferent when analyzing samples for Ca^{2+} by flame emission, but has a negligible effect when using a plasma source. In addition, the high concentration of electrons from the ionization of argon minimizes ionization interferences.

Standardizing the Method

From equation 10.30 we know that emission intensity is proportional to the population of the analyte's excited state, N^*. If the flame or plasma is in thermal equilibrium, then the excited state population is proportional to the analyte's total population, N, through the Boltzmann distribution (equation 10.31).

A calibration curve for flame emission is usually linear over two to three orders of magnitude, with ionization limiting linearity when the analyte's concentrations is small and self-absorption limiting linearity for higher concentrations of analyte. When using a plasma, which suffers from fewer chemical interferences, the calibration curve often is linear over four to five orders of magnitude and is not affected significantly by changes in the matrix of the standards.

Emission intensity may be affected significantly by many parameters, including the temperature of the excitation source and the efficiency of atomization. An increase in temperature of 10 K, for example, produces a 4% increase in the fraction of Na atoms occupying the 3p excited state. This is potentially significant uncertainty that may limit the use of external standards. The method of internal standards can be used when variations in source parameters are difficult to control. To compensate for changes in the temperature of the excitation source, the internal standard is selected so that its emission line is close to the analyte's emission line. In addition, the internal standard should be subject to the same chemical interferences to compensate for changes in atomization efficiency. To accurately compensate for these errors the analyte and internal standard emission lines must be monitored simultaneously.

Note

The best way to appreciate the theoretical and practical details discussed in this section is to carefully examine a typical analytical method. Although each method is unique, the following description of the determination of sodium in salt substitutes provides an instructive example of a typical procedure. The description here is based on Goodney, D. E. *J. Chem. Educ.* **1982**, *59*, 875–876.

Representative Method 10.4

Determination of Sodium in a Salt Substitute

Description of Method

Salt substitutes, which are used in place of table salt for individuals on low–sodium diets, replaces NaCl with KCl. Depending on the brand, fumaric acid, calcium hydrogen phosphate, or potassium tartrate also may be present. Although intended to be sodium-free, salt substitutes contain small amounts of NaCl as an impurity. Typically, the concentration of sodium in a salt substitute is about 100 μg/g The exact concentration of sodium is easily determined by flame atomic emission. Because it is difficult to match the matrix of the standards to that of the sample, the analysis is accomplished by the method of standard additions.

Procedure

A sample is prepared by placing an approximately 10-g portion of the salt substitute in 10 mL of 3 M HCl and 100 mL of distilled water. After the sample has dissolved, it is transferred to a 250-mL volumetric flask and diluted to volume with distilled water. A series of standard additions is prepared by placing 25-mL portions of the diluted sample into separate 50-mL volumetric flasks, spiking each with a known amount of an approximately 10 mg/L standard solution of Na^+, and diluting to volume. After zeroing the instrument with an appropriate blank, the instrument is optimized at a wavelength of 589.0 nm while aspirating a standard solution of Na^+. The emission intensity is measured for each of the standard addition samples and the concentration of sodium in the salt substitute is reported in μg/g.

Questions

1. Potassium ionizes more easily than sodium. What problem might this present if you use external standards prepared from a stock solution of 10 mg Na/L instead of using a set of standard additions?

Because potassium is present at a much higher concentration than sodium, its ionization suppresses the ionization of sodium. Normally suppressing ionization is a good thing because it increases emission intensity. In this case, however, the difference between the matrix of the standards and the sample's matrix means that the sodium in a standard experiences more ionization than an equivalent amount of sodium in a sample. The result is a determinate error.

2. One way to avoid a determinate error when using external standards is to match the matrix of the standards to that of the sample. We could, for example, prepare external standards using reagent grade KCl to match the matrix to that of the sample. Why is this not a good idea for this analysis?

Sodium is a common contaminant, which is found in many chemicals. Reagent grade KCl, for example, may contain 40–50 μg Na/g. This is a significant source of sodium, given that the salt substitute contains approximately 100 μg Na/g.

3. Suppose you decide to use an external standardization. Given the answer to the previous questions, is the result of your analysis likely to underestimate or overestimate the amount of sodium in the salt substitute?

The solid black line in Figure 10.62 shows the ideal calibration curve assuming that we match the matrix of the standards to the sample's matrix, and that we do so without adding an additional sodium. If we prepare the external standards without adding KCl, the emission for each standard decreases due to increased ionization. This is shown by the lower of the two dashed red lines. Preparing the standards by adding reagent grade KCl increases the concentration of sodium due to its contamination. Because we underestimate the actual concentration of sodium in the standards, the resulting calibration curve is shown by the other dashed red line. In both cases, the sample's emission results in our overestimating the concentration of sodium in the sample.

4. One problem with analyzing salt samples is their tendency to clog the aspirator and burner assembly. What effect does this have on the analysis?

Clogging the aspirator and burner assembly decreases the rate of aspiration, which decreases the analyte's concentration in the flame. The result is a decrease in the emission intensity and a negative determinate error.

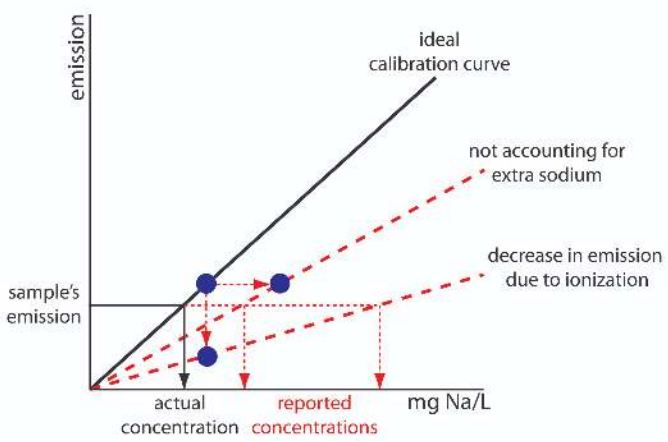


Figure 10.62 External standards calibration curves for the flame atomic emission analysis of Na in a salt substitute. The solid black line shows the ideal calibration curve assuming matrix matching of samples and standards with pure KCl. The lower of the two dashed red lines shows the effect of failing to add KCl to the external standards, which decreases emission. The other dashed red line shows the effect of using KCl that is contaminated with NaCl, which causes us to underestimate the concentration of Na in the standards. In both cases, the result is a positive determinate error in the analysis of samples.

Example 10.12

To evaluate the method described in Representative Method 10.4, a series of standard additions is prepared using a 10.0077-g sample of a salt substitute. The results of a flame atomic emission analysis of the standards is shown here.[19]

added Na (µg/mL)	I_e (arb. units)
0.000	1.79
0.420	2.63
1.051	3.54
2.102	4.94
3.153	6.18

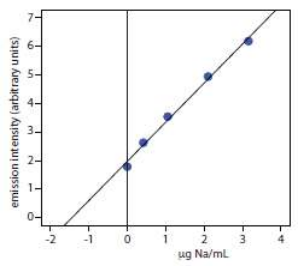
What is the concentration of sodium, in µg/g, in the salt substitute.

(See Section 5C.3 in Chapter 5 to review the method of standard additions.)

Solution

Linear regression of emission intensity versus the concentration of added Na gives a standard additions calibration curve with the following equation.

$$I_e = 1.97 + 1.37 \times \frac{\text{g Na}}{\text{mL}} \tag{10.7.1}$$



The concentration of sodium in the sample is equal to the absolute value of the calibration curve's *x*-intercept. Substituting zero for the emission intensity and solving for sodium's concentration gives a result of 1.44 μg Na/mL. The concentration of sodium in the salt substitute is

$$\frac{\frac{1.44\ \text{g Na}}{\text{mL}} \times \frac{50.00\ \text{mL}}{25.00\ \text{mL}} \times 250.0\ \text{mL}}{10.0077\ \text{g sample}} = 71.9\ \text{g Na/g} \tag{10.7.2}$$

10.7.4 Evaluation of Atomic Emission Spectroscopy

Scale of Operation

The scale of operations for atomic emission is ideal for the direct analysis of trace and ultratrace analytes in macro and meso samples. With appropriate dilutions, atomic emission also can be applied to major and minor analytes.

Note

See Figure 3.5 to review the meaning of macro and meso for describing samples, and the meaning of major, minor, and ultratrace for describing analytes.

Accuracy

When spectral and chemical interferences are insignificant, atomic emission is capable of producing quantitative results with accuracies of between 1–5%. Accuracy frequently is limited by chemical interferences. Because the higher temperature of a plasma source gives rise to more emission lines, the accuracy of using plasma emission often is limited by stray radiation from overlapping emission lines.

Precision

For samples and standards in which the analyte's concentration exceeds the detection limit by at least a factor of 50, the relative standard deviation for both flame and plasma emission is about 1–5%. Perhaps the most important factor affecting precision is the stability of the flame's or the plasma's temperature. For example, in a 2500 K flame a temperature fluctuation of ±2.5 K gives a relative standard deviation of 1% in emission intensity. Significant improvements in precision may be realized when using internal standards.

Sensitivity

Sensitivity is strongly influenced by the temperature of the excitation source and the composition of the sample matrix. Sensitivity is optimized by aspirating a standard solution of analyte and maximizing the emission by adjusting the flame's composition and the height from which we monitor the emission. Chemical interferences, when present, decrease the sensitivity of the analysis. The sensitivity of plasma emission is less affected by the sample matrix. In some cases a calibration curve prepared using standards in a matrix of distilled water can be used for samples with more complex matrices.

Selectivity

The selectivity of atomic emission is similar to that of atomic absorption. Atomic emission has the further advantage of rapid sequential or simultaneous analysis.

Time, Cost, and Equipment

Sample throughput with atomic emission is very rapid when using automated systems capable of multielemental analysis. For example, sampling rates of 3000 determinations per hour have been achieved using a multichannel ICP, and 300 determinations per hour with a sequential ICP. Flame emission is often accomplished using an atomic absorption spectrometer, which typically costs between $10,000–$50,000. Sequential ICP's range in price from $55,000–$150,000, while an ICP capable of simultaneous multielemental analysis costs between $80,000–$200,000. Combination ICP's that are capable of both sequential and simultaneous analysis range in price from $150,000–$300,000. The cost of Ar, which is consumed in significant quantities, can not be overlooked when considering the expense of operating an ICP.

Contributors

David Harvey (DePauw University)

10.7: Atomic Emission Spectroscopy is shared under a CC BY-NC-SA 4.0 license and was authored, remixed, and/or curated by LibreTexts.

10.8: Spectroscopy Based on Scattering

The blue color of the sky during the day and the red color of the sun at sunset result from the scattering of light by small particles of dust, molecules of water, and other gases in the atmosphere. The efficiency of a photon's scattering depends on its wavelength. We see the sky as blue during the day because violet and blue light scatter to a greater extent than other, longer wavelengths of light. For the same reason, the sun appears red at sunset because red light is less efficiently scattered and is more likely to pass through the atmosphere than other wavelengths of light. The scattering of radiation has been studied since the late 1800s, with applications beginning soon thereafter. The earliest quantitative applications of scattering, which date from the early 1900s, used the elastic scattering of light by colloidal suspensions to determine the concentration of colloidal particles.

10.8.1 Origin of Scattering

If we send a focused, monochromatic beam of radiation with a wavelength λ through a medium of particles with dimensions <1.5λ, the radiation scatters in all directions. For example, visible radiation of 500 nm is scattered by particles as large as 750 nm in the longest dimension. Two general categories of scattering are recognized. In elastic scattering, radiation is first absorbed by the particles and then emitted without undergoing change in the radiation's energy. When the radiation emerges with a change in energy, the scattering is said to be inelastic. Only elastic scattering is considered in this text.

Elastic scattering is divided into two types: Rayleigh, or small-particle scattering, and large-particle scattering. Rayleigh scattering occurs when the scattering particle's largest dimension is less than 5% of the radiation's wavelength. The intensity of the scattered radiation is proportional to its frequency to the fourth power, ν^4—accounting for the greater scattering of blue light than red light—and is symmetrically distributed (Figure 10.63a). For larger particles, scattering increases in the forward direction and decreases in the backwards direction as the result of constructive and destructive interferences (Figure 10.63b).

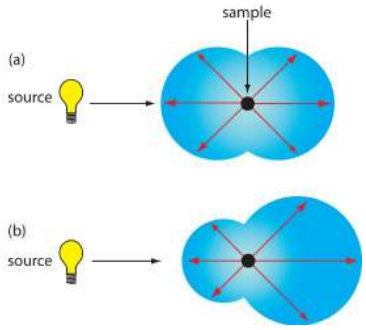


Figure 10.63 Distribution of radiation for (a) Rayleigh, or small-particle scattering, and (b) large-particle scattering.

10.8.2 Turbidimetry and Nephelometry

Turbidimetry and nephelometry are two techniques based on the elastic scattering of radiation by a suspension of colloidal particles. In **turbidimetry** the detector is placed in line with the source and the decrease in the radiation's transmitted power is measured. In **nephelometry** scattered radiation is measured at an angle of 90º to the source. The similarity of turbidimetry to absorbance and of nephelometry to fluorescence is evident in the instrumental designs shown in Figure 10.64. In fact, turbidity can be measured using a UV/Vis spectrophotometer and a spectrofluorimeter is suitable for nephelometry.

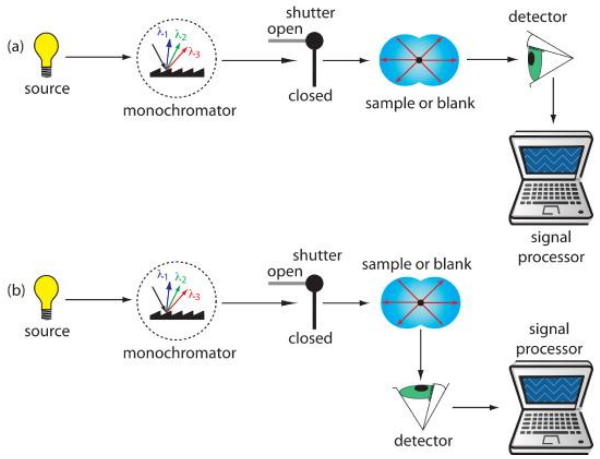


Figure 10.64 Schematic diagrams for (a) a turbimeter, and (b) a nephelometer.

Turbidimetry or Nephelometry?

When developing a scattering method the choice of using turbidimetry or nephelometry is determined by two factors. The most important consideration is the intensity of the scattered radiation relative to the intensity of the source's radiation. If the solution contains a small concentration of scattering particles the intensity of the transmitted radiation, I_T, is approximately the same as the intensity of the source's radiation, I_0. As we learned earlier in the section on molecular absorption, there is substantial uncertainty in determining a small difference between two intense signals. For this reason, nephelometry is a more appropriate choice for samples containing few scattering particles. Turbidimetry is a better choice when the sample contains a high concentration of scattering particles.

A second consideration in choosing between turbidimetry and nephelometry is the size of the scattering particles. For nephelometry, the intensity of scattered radiation at 90° increases when the particles are small and Rayleigh scattering is in effect. For larger particles, as shown in Figure 10.63, the intensity of scattering is diminished at 90°. When using an ultraviolet or visible source of radiation, the optimum particle size is 0.1–1 μm. The size of the scattering particles is less important for turbidimetry where the signal is the relative decrease in transmitted radiation. In fact, turbidimetric measurements are still feasible even when the size of the scattering particles results in an increase in reflection and refraction, although a linear relationship between the signal and the concentration of scattering particles may no longer hold.

Determining Concentration by Turbidimetry

In turbidimetry, the measured transmittance, T, is the ratio of the intensity of source radiation transmitted by the sample, I_T, to the intensity of source radiation transmitted by a blank, I_0.

$$T = \frac{I_T}{I_0} \tag{10.8.1}$$

The relationship between transmittance and the concentration of the scattering particles is similar to that given by Beer's law:

$$-\log T = k\,b\,C \tag{10.32}$$

where

- C is the concentration of the scattering particles in mass per unit volume (w/v),
- b is the pathlength, and
- k is a constant that depends on several factors, including the size and shape of the scattering particles and the wavelength of the source radiation.

As with Beer's law, equation 10.32 may show appreciable deviations from linearity. The exact relationship is established by a calibration curve prepared using a series of standards containing known concentrations of analyte.

Determining Concentration by Nephelometry

In nephelometry the relationship between the intensity of scattered radiation, I_S, and the concentration of scattering particles is

$$I_S = k_S I_0 C \tag{10.33}$$

where k_S is an empirical constant for the system and I_0 is the source radiation's intensity. The value of k_S is determined from a calibration curve prepared using a series of standards containing known concentrations of analyte.

Selecting a Wavelength for the Incident Radiation

The choice of wavelength is based primarily on the need to minimize potential interferences. For turbidimetry, where the incident radiation is transmitted through the sample, a monochromator or filter allow us to avoid wavelengths that are absorbed by the sample. For nephelometry, the absorption of incident radiation is not a problem unless it induces fluorescence from the sample. With a nonfluorescent sample there is no need for wavelength selection, and a source of white light may be used as the incident radiation. For both techniques, other considerations in choosing a wavelength including the effect of wavelength on scattering intensity, the transducer's sensitivity, and the source's intensity. For example, many common photon transducers are more sensitive to radiation at 400 nm than at 600 nm.

Preparing the Sample for Analysis

Although equation 10.32 and equation 10.33 relate scattering to the concentration of scattering particles, the intensity of scattered radiation is also influenced by the particle's size and shape. Samples containing the same number of scattering particles may show significantly different values for -log$T$ or I_S, depending on the average diameter of the particles. For a quantitative analysis, therefore, it is necessary to maintain a uniform distribution of particle sizes throughout the sample and between samples and standards.

Most turbidimetric and nephelometric methods rely on precipitation to form the scattering particles. As we learned in Chapter 8, the properties of a precipitate are determined by the conditions under which it forms. To maintain a reproducible distribution of particle sizes between samples and standards, it is necessary to control parameters such as the concentration of reagents, the order of adding reagents, the pH and temperature, the agitation or stirring rate, the ionic strength, and the time between the precipitate's initial formation and the measurement of transmittance or scattering. In many cases a surface-active agent—such as glycerol, gelatin, or dextrin—is added to stabilize the precipitate in a colloidal state and to prevent the coagulation of the particles.

Applications

Turbidimetry and nephelometry are widely used to determine the clarity of water, beverages, and food products. For example, a nephelometric determination of the turbidity of water compares the sample's scattering to the scattering of a set of standards. The primary standard for measuring turbidity is formazin, which is an easily prepared, stable polymer suspension (Figure 10.65).[20] Formazin prepared by mixing a 1 g/100 mL solution of hydrazine sulfate, $N_2H_4 \cdot H_2SO_4$, with a 10 g/100 mL solution of hexamethylenetetramine produces a suspension that is defined as 4000 nephelometric turbidity units (NTU). A set of standards with NTUs between 0 and 40 is prepared and used to construct a calibration curve. This method is readily adapted to the analysis of the clarity of orange juice, beer, and maple syrup.

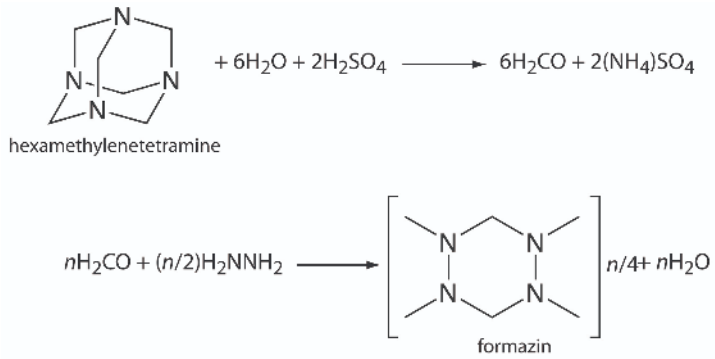


Figure 10.65 Scheme for preparing formazin for use as a turbidity standard.

A number of inorganic cations and anions can be determined by precipitating them under well-defined conditions and measuring the transmittance or scattering of radiation from the precipitated particles. The transmittance or scattering, as given by equation 10.32 or equation 10.33 is proportional to the concentration of the scattering particles, which, in turn, is related by the stoichiometry of the precipitation reaction to the analyte's concentration. Examples of analytes that have been determined in this way are listed in Table 10.15.

Table 10.15 Examples of Analytes Determined by Turbidimetry or Nephelometry

analyte	precipitant	precipitate
Ag^+	NaCl	AgCl
Ca^{2+}	$Na_2C_2O_4$	CaC_2O_4
Cl^-	$AgNO_3$	AgCl
CN^-	$AgNO_3$	AgCN
CO_3^{2-}	$BaCl_2$	$BaCO_3$
F^-	$CaCl_2$	CaF_2
SO_4^{2-}	$BaCl_2$	$BaSO_4$

Note

The best way to appreciate the theoretical and practical details discussed in this section is to carefully examine a typical analytical method. Although each method is unique, the following description of the determination of sulfate in water provides an instructive example of a typical procedure. The description here is based on Method 4500–SO_4^{2-}–C in *Standard Methods for the Analysis of Water and Wastewater*, American Public Health Association: Washington, D. C. 20th Ed., 1998.

Representative Method 10.5

Turbidimetric Determination of Sulfate in Water

Description of Method

Adding $BaCl_2$ to an acidified sample precipitates SO_4^{2-} as $BaSO_4$. The concentration of SO_4^{2-} may be determined either by turbidimetry or by nephelometry using an incident source of radiation of 420 nm. External standards containing know concentrations of SO_4^{2-} are used to standardize the method.

Procedure

Transfer a 100-mL sample to a 250-mL Erlenmeyer flask along with 20.00 mL of a buffer. For samples containing >10 mg SO_4^{2-}/L, the buffer contains 30 g of $MgCl_2 \cdot 6H_2O$, 5 g of $CH_3COONa \cdot 3H_2O$, 1.0 g of KNO_3, and 20 mL of glacial CH_3COOH per liter. The buffer for samples containing <10 mg SO_4^{2-}/L is the same except for the addition of 0.111 g of Na_2SO_4 per L.

Place the sample and the buffer on a magnetic stirrer operated at the same speed for all samples and standards. Add a spoonful of 20–30 mesh $BaCl_2$, using a measuring spoon with a capacity of 0.2–0.3 mL, to precipitate the SO_4^{2-} as $BaSO_4$. Begin timing when the $BaCl_2$ is added and stir the suspension for 60 ± 2 s. Measure the transmittance or scattering intensity 5.0± 0.5 min after the end of stirring.

Prepare a calibration curve over the range 0–40 mg SO_4^{2-}/L by diluting a 100-mg SO_4^{2-}/L standard. Treat the standards using the procedure described above for the sample. Prepare a calibration curve and use it to determine the amount of sulfate in the sample.

Questions

1. What is the purpose of the buffer?

If the precipitate's particles are too small, I_T may be too small to measure reliably. Because rapid precipitation favors the formation of microcrystalline particles of $BaSO_4$, we use conditions that favor precipitate growth over nucleation. The buffer's

high ionic strength and its acidity favors precipitate growth and prevents the formation of microcrystalline $BaSO_4$.

2. Why is it important to use the same stirring rate and time for the samples and standards?

How fast and how long we stir the sample after adding $BaCl_2$ influence the size of the precipitate's particles.

3. Many natural waters have a slight color due to the presence of humic and fulvic acids, and may contain suspended matter (Figure 10.66). Explain why these might interfere with the analysis for sulfate. For each interferent, suggest a method for minimizing its effect on the analysis.

Suspended matter in the sample contributes to the scattering, resulting in a positive determinate error. We can eliminate this interference by filtering the sample prior to its analysis. A sample that is colored may absorb some of the source's radiation, leading to a positive determinate error. We can compensate for this interference by taking a sample through the analysis without adding $BaCl_2$. Because no precipitate forms, we can use the transmittance of this sample blank to correct for the interference.

4. Why is Na_2SO_4 added to the buffer for samples containing <10 mg SO_4^{2-}/L?

The uncertainty in a calibration curve is smallest near its center. If a sample has a high concentration of SO_4^{2-}, we can dilute it so that its concentration falls near the middle of the calibration curve. For a sample with a small concentration of SO_4^{2-}, the buffer increases the concentration of sulfate by

$$\frac{0.111\text{ g }Na_2SO_4}{\text{L}} \times \frac{96.06\text{ g }SO_4^{2-}}{142.04\text{ g }Na_2SO_4} \times \frac{1000\text{ mg}}{\text{g}} \times \frac{20.00\text{ mL}}{250.0\text{ mL}} = \frac{6.00\text{ mg }SO_4^{2-}}{\text{L}} \qquad (10.8.2)$$

After using the calibration curve to determine the amount of sulfate in the sample, subtracting 6.00 mg SO_4^{2-}/L corrects the result.



Figure 10.66 Waterfall on the River Swale in Richmond, England. The river, which flows out of the moors in the Yorkshire Dales, is brown in color as the result of organic matter that leaches from the peat found in the moors.

Example 10.13

To evaluate the method described in Representative Method 10.5, a series of external standard was prepared and analyzed, providing the results shown in the following table.

mg SO_4^{2-}/L	transmittance
0.00	1.00
10.00	0.646
20.00	0.417
30.00	0.269
40.00	0.174

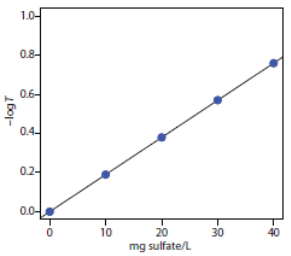
Analysis of a 100.0-mL sample of a surface water gives a transmittance of 0.538. What is the concentration of sulfate in the sample?

Solution

Linear regression of -log$T$ versus concentration of SO_4^{2-} gives a standardization equation of

$$-\log T = -1.04 \times 10^{-5} + 0.0190 \times \frac{\text{mg } SO_4^{2-}}{\text{L}} \quad (10.8.3)$$

Substituting the sample's transmittance into the calibration curve's equation gives the concentration of sulfate in sample as 14.2 mg SO_4^{2-}/L.



Contributors

David Harvey (DePauw University)

10.8: Spectroscopy Based on Scattering is shared under a CC BY-NC-SA 4.0 license and was authored, remixed, and/or curated by LibreTexts.

10.E: Spectroscopic Methods (Exercises)

1. Provide the missing information in the following table.

wavelength (m)	frequency (s^{-1})	wavenumber (cm^{-1})	energy (J)
4.50×10^{-9}			
	1.33×10^{15}		
		3215	
			7.20×10^{-19}

2. Provide the missing information in the following table.

[analyte] (M)	absorbance	%T	molar absorptivity (M^{-1} cm^{-1})	pathlength (cm)
1.40×10^{-4}			1120	1.00
	0.563		750	1.00
2.56×10^{-4}	0.225		440	
1.55×10^{-3}	0.167			5.00
		33.3	565	1.00
4.35×10^{-3}		21.2	1550	
1.20×10^{-4}		81.3		10.00

3. A solution's transmittance is 35.0%. What is the transmittance if you dilute 25.0 mL of the solution to 50.0 mL?

4. A solution's transmittance is 85.0% when measured in a cell with a pathlength of 1.00 cm. What is the %T if you increase the pathlength to 10.00 cm?

5. The accuracy of a spectrophotometer can be evaluated by preparing a solution of 60.06 ppm $K_2Cr_2O_7$ in 0.0050 M H_2SO_4, and measuring its absorbance at a wavelength of 350 nm in a cell with a pathlength of 1.00 cm. The absorbance should be 0.640. What is the molar absorptivity of $K_2Cr_2O_7$ at this wavelength?

6. A chemical deviation to Beer's law may occur if the concentration of an absorbing species is affected by the position of an equilibrium reaction. Consider a weak acid, HA, for which K_a is 2×10^{-5}. Construct Beer's law calibration curves of absorbance versus the total concentration of weak acid (C_{total} = [HA] + [A^-]), using values for C_{total} of 1×10^{-5}, 3×10^{-5}, 5×10^{-5}, 9×10^{-5}, 11×10^{-5}, and 13×10^{-5} M for the following sets of conditions:

(a) $\varepsilon_{HA} = \varepsilon_{A^-} = 2000\ M^{-1}\ cm^{-1}$; unbuffered solution.

(b) $\varepsilon_{HA} = 2000\ M^{-1}\ cm^{-1}$ and $\varepsilon_{A^-} = 500\ M^{-1}\ cm^{-1}$; unbuffered solution.

(c) $\varepsilon_{HA} = 2000\ M^{-1}\ cm^{-1}$ and $\varepsilon_{A^-} = 500\ M^{-1}\ cm^{-1}$; solution is buffered to a pH of 4.5.

Assume a constant pathlength of 1.00 cm for all samples.

7. One instrumental limitation to Beer's law is the effect of polychromatic radiation. Consider a line source that emits radiation at two wavelengths, λ′ and λ″. When treated separately, the absorbances at these wavelengths, A′ and A″, are

$$A' = -\log \frac{P_T'}{P_0'} = \varepsilon' bC \tag{10.E.1}$$

$$A'' = -\log \frac{P_T''}{P_0''} = \varepsilon'' bC \tag{10.E.2}$$

If both wavelengths are measured simultaneously the absorbance is

$$A = -\log \frac{(P_T' + P_T'')}{(P_0' + P_0'')} \tag{10.E.3}$$

(a) Show that if the molar absorptivity at λ′ and λ″ are the same (ε′ = ε″ = ε), the absorbance is equivalent to

$$A = \varepsilon bC \tag{10.E.4}$$

(b) Construct Beer's law calibration curves over the concentration range of zero to 1×10^{-4} M using ε′ = 1000 and ε″ = 1000, and ε′ = 1000 and ε″ = 100. Assume a value of 1.00 cm for the pathlength. Explain the difference between the two curves.

8. A second instrumental limitation to Beer's law is stray radiation. The following data were obtained using a cell with a pathlength of 1.00 cm when stray light is insignificant ($P_{stray} = 0$).

[analyte] (mM)	absorbance
0.00	0.00
2.00	0.40
4.00	0.80
6.00	1.20
8.00	1.60
10.00	2.00

Calculate the absorbance of each solution when P_{stray} is 5% of P_0, and plot Beer's law calibration curves for both sets of data. Explain any differences between the two curves. (*Hint*: Assume that P_0 is 100).

9. In the process of performing a spectrophotometric determination of Fe, an analyst prepares a calibration curve using a single-beam spectrophotometer similar to that shown in Figure 10.26. After preparing the calibration curve, the analyst drops and breaks the cuvette. The analyst acquires a new cuvette, measures the absorbance of his sample, and determines the %w/w Fe in the sample. Will the change in cuvette lead to a determinate error in the analysis? Explain.

10. The spectrophotometric methods for determining Mn in steel and for determining glucose use a chemical reaction to produce a colored species whose absorbance we can monitor. In the analysis of Mn in steel, colorless Mn^{2+} is oxidized to give the purple MnO_4^- ion. To analyze for glucose, which is colorless, we react it with a yellow colored solution of the $Fe(CN)_6^{3-}$, forming the colorless $Fe(CN)_6^{4-}$ ion. The directions for the analysis of Mn do not specify precise reaction conditions, and samples and standards may be treated separately. The conditions for the analysis of glucose, however, require that the samples and standards be treated simultaneously at exactly the same temperature and for exactly the same length of time. Explain why these two experimental procedures are so different.

11. One method for the analysis of Fe^{3+}, which can be used with a variety of sample matrices, is to form the highly colored Fe^{3+}–thioglycolic acid complex. The complex absorbs strongly at 535 nm. Standardizing the method is accomplished using external standards. A 10.00 ppm Fe^{3+} working standard is prepared by transferring a 10-mL aliquot of a 100.0 ppm stock solution of Fe^{3+} to a 100-mL volumetric flask and diluting to volume. Calibration standards of 1.00, 2.00, 3.00, 4.00, and 5.00 ppm are prepared by transferring appropriate amounts of the 10.0 ppm working solution into separate 50-mL volumetric flasks, each containing 5 mL of

thioglycolic acid, 2 mL of 20% w/v ammonium citrate, and 5 mL of 0.22 M NH_3. After diluting to volume and mixing, the absorbances of the external standards are measured against an appropriate blank. Samples are prepared for analysis by taking a portion known to contain approximately 0.1 g of Fe^{3+}, dissolving in a minimum amount of HNO_3, and diluting to volume in a 1-L volumetric flask. A 1.00-mL aliquot of this solution is transferred to a 50-mL volumetric flask, along with 5 mL of thioglycolic acid, 2 mL of 20% w/v ammonium citrate, and 5 mL of 0.22 M NH_3 and diluted to volume. The absorbance of this solution is used to determine the concentration of Fe^{3+} in the sample.

(a) What is an appropriate blank for this procedure?

(b) Ammonium citrate is added to prevent the precipitation of Al^{3+}. What is the effect on the reported concentration of iron in the sample if there is a trace impurity of Fe^{3+} in the ammonium citrate?

(c) Why does the procedure specify that the sample contain approximately 0.1 g of Fe^{3+}?

(d) Unbeknownst to the analyst, the 100-mL volumetric flask used to prepare the 10.00 ppm working standard of Fe^{3+} has a volume that is significantly smaller than 100.0 mL. What effect will this have on the reported concentration of iron in the sample?

12. A spectrophotometric method for the analysis of iron has a linear calibration curve for standards of 0.00, 5.00, 10.00, 15.00, and 20.00 mg Fe/L. An iron ore sample that is 40–60% w/w is to be analyzed by this method. An approximately 0.5-g sample is taken, dissolved in a minimum of concentrated HCl, and diluted to 1 L in a volumetric flask using distilled water. A 5.00 mL aliquot is removed with a pipet. To what volume—10, 25, 50, 100, 250, 500, or 1000 mL—should it be diluted to minimize the uncertainty in the analysis? Explain.

13. Lozano-Calero and colleagues describe a method for the quantitative analysis of phosphorous in cola beverages based on the formation of the intensely blue-colored phosphomolybdate complex, $(NH_4)_3[PO_4(MoO_3)_{12}]$.[21] The complex is formed by adding $(NH_4)_6Mo_7O_{24}$ to the sample in the presence of a reducing agent, such as ascorbic acid. The concentration of the complex is determined spectrophotometrically at a wavelength of 830 nm, using a normal calibration curve as a method of standardization.

In a typical analysis, a set of standard solutions containing known amounts of phosphorous was prepared by placing appropriate volumes of a 4.00 ppm solution of P_2O_5 in a 5-mL volumetric flask, adding 2 mL of an ascorbic acid reducing solution, and diluting to volume with distilled water. Cola beverages were prepared for analysis by pouring a sample into a beaker and allowing it to stand for 24 h to expel the dissolved CO_2. A 2.50-mL sample of the degassed sample was transferred to a 50-mL volumetric flask and diluted to volume. A 250-µL aliquot of the diluted sample was then transferred to a 5-mL volumetric flask, treated with 2 mL of the ascorbic acid reducing solution, and diluted to volume with distilled water.

(a) The authors note that this method can be applied only to noncolored cola beverages. Explain why this is true.

(b) How might you modify this method so that it could be applied to any cola beverage?

(c) Why is it necessary to remove the dissolved gases?

(d) Suggest an appropriate blank for this method?

(e) The author's report a calibration curve of

$$A = -0.02 + 0.72 \times \text{ppm } P_2O_5 \tag{10.E.5}$$

A sample of Crystal Pepsi, analyzed as described above, yields an absorbance of 0.565. What is the concentration of phosphorous, reported as ppm P, in the original sample of Crystal Pepsi?

Note

Crystal Pepsi was a colorless, caffeine-free soda produced by PepsiCo. It was available in the United States from 1992 to 1993.

14. EDTA forms colored complexes with a variety of metal ions that may serve as the basis for a quantitative spectrophotometric method of analysis. The molar absorptivities of the EDTA complexes of Cu^{2+}, Co^{2+}, and Ni^{2+} at three wavelengths are summarized in the following table (all values of ε are in M^{-1} cm^{-1}).

metal	$\varepsilon_{462.9}$	$\varepsilon_{732.0}$	$\varepsilon_{378.7}$
Co^{2+}	15.8	2.11	3.11
Cu^{2+}	2.32	95.2	7.73
Ni^{2+}	1.79	3.03	13.5

Using this information determine the following:

(a) The concentration of Cu^{2+} in a solution that has an absorbance of 0.338 at a wavelength of 732.0 nm.

(b) The concentrations of Cu^{2+} and Co^{2+} in a solution that has an absorbance of 0.453 at a wavelength of 732.0 nm and 0.107 at a wavelength of 462.9 nm.

(c) The concentrations of Cu^{2+}, Co^{2+}, and Ni^{2+} in a sample that has an absorbance of 0.423 at a wavelength of 732.0 nm, 0.184 at a wavelength of 462.9 nm, and 0.291 at a wavelength of 378.7 nm.

The pathlength, *b*, is 1.00 cm for all measurements.

15. The concentration of phenol in a water sample is determined by separating the phenol from non-volatile impurities by steam distillation, followed by reacting with 4-aminoantipyrine and $K_3Fe(CN)_6$ at pH 7.9 to form a colored antipyrine dye. A phenol standard with a concentration of 4.00 ppm has an absorbance of 0.424 at a wavelength of 460 nm using a 1.00 cm cell. A water sample is steam distilled and a 50.00-mL aliquot of the distillate is placed in a 100-mL volumetric flask and diluted to volume with distilled water. The absorbance of this solution is found to be 0.394. What is the concentration of phenol (in parts per million) in the water sample?

16. Saito describes a quantitative spectrophotometric procedure for iron based on a solid-phase extraction using bathophenanthroline in a poly(vinyl chloride) membrane.[22] In the absence of Fe^{2+} the membrane is colorless, but when immersed in a solution of Fe^{2+} and I^-, the membrane develops a red color as a result of the formation of an Fe^{2+}–bathophenanthroline complex. A calibration curve determined using a set of external standards with known concentrations of Fe^{2+} gave a standardization relationship of

$$A = (8.60 \times 10^3\ M^{-1}) \times [Fe^{2+}] \qquad (10.E.6)$$

What is the concentration of iron, in mg Fe/L, for a sample with an absorbance of 0.100?

17. In the DPD colorimetric method for the free chlorine residual, which is reported as mg Cl_2/L, the oxidizing power of free chlorine converts the colorless amine N,N-diethyl-*p*-phenylenediamine to a colored dye that absorbs strongly over the wavelength range of 440–580 nm. Analysis of a set of calibration standards gave the following results.

mg Cl_2/L	absorbance
0.00	0.000
0.50	0.270
1.00	0.543
1.50	0.813
2.00	1.084

A sample from a public water supply is analyzed to determine the free chlorine residual, giving an absorbance of 0.113. What is the free chlorine residual for the sample in mg Cl_2/L?

18. Lin and Brown described a quantitative method for methanol based on its effect on the visible spectrum of methylene blue.[23] In the absence of methanol, the visible spectrum for methylene blue shows two prominent absorption bands centered at approximately 610 nm and 660 nm, corresponding to the monomer and dimer, respectively. In the presence of methanol, the intensity of the dimer's absorption band decreases, while that of the monomer increases. For concentrations of methanol between 0 and 30% v/v, the ratio of the absorbance at 663 nm, A_{663}, to that at 610 nm, A_{610}, is a linear function of the amount of methanol. Using the following standardization data, determine the %v/v methanol in a sample for which A_{610} is 0.75 and A_{663} is 1.07.

%v/v methanol	A_{663}/A_{610}
0.0	1.21
5.0	1.29
10.0	1.42
15.0	1.52
20.0	1.62
25.0	1.74
30.0	1.84

19. The concentration of the barbiturate barbital in a blood sample was determined by extracting 3.00 mL of blood with 15 mL of $CHCl_3$. The chloroform, which now contains the barbital, is extracted with 10.0 mL of 0.45 M NaOH (pH ≈ 13). A 3.00-mL sample of the aqueous extract is placed in a 1.00-cm cell and an absorbance of 0.115 is measured. The pH of the sample in the absorption cell is then adjusted to approximately 10 by adding 0.5 mL of 16% w/v NH_4Cl, giving an absorbance of 0.023. When 3.00 mL of a standard barbital solution with a concentration of 3 mg/100 mL is taken through the same procedure, the absorbance at pH 13 is 0.295 and the absorbance at a pH of 10 is 0.002. Report the mg barbital/100 mL in the sample.

20. Jones and Thatcher developed a spectrophotometric method for analyzing analgesic tablets containing aspirin, phenacetin, and caffeine.[24] The sample is dissolved in $CHCl_3$ and extracted with an aqueous solution of $NaHCO_3$ to remove the aspirin. After the extraction is complete, the chloroform is transferred to a 250-mL volumetric flask and diluted to volume with $CHCl_3$. A 2.00-mL portion of this solution is diluted to volume in a 200-mL volumetric flask with $CHCl_3$. The absorbance of the final solution is measured at wavelengths of 250 nm and 275 nm, at which the absorptivities, in $ppm^{-1}\ cm^{-1}$, for caffeine and phenacetin are

	a_{250}	a_{275}
caffeine	0.0131	0.0485
phenacetin	0.0702	0.0159

Aspirin is determined by neutralizing the $NaHCO_3$ in the aqueous solution and extracting the aspirin into $CHCl_3$. The combined extracts are diluted to 500 mL in a volumetric flask. A 20.00-mL portion of the solution is placed in a 100-mL volumetric flask and diluted to volume with $CHCl_3$. The absorbance of this solution is measured at 277 nm, where the absorptivity of aspirin is 0.00682 $ppm^{-1}\ cm^{-1}$. An analgesic tablet treated by this procedure is found to have absorbances of 0.466 at 250 nm, 0.164 at 275 nm, and 0.600 at 277 nm when using a cell with a 1.00 cm pathlength. Report the milligrams of aspirin, caffeine, and phenacetin in the analgesic tablet.

21. The concentration of SO_2 in a sample of air was determined by the *p*-rosaniline method. The SO_2 was collected in a 10.00-mL solution of $HgCl_4^{2-}$, where it reacts to form $Hg(SO_3)_2^{2-}$, by pulling the air through the solution for 75 min at a rate of 1.6 L/min. After adding *p*-rosaniline and formaldehyde, the colored solution was diluted to 25 mL in a volumetric flask. The absorbance was measured at 569 nm in a 1-cm cell, yielding a value of 0.485. A standard sample was prepared by substituting a 1.00-mL sample of a standard solution containing the equivalent of 15.00 ppm SO_2 for the air sample. The absorbance of the standard was found to be 0.181. Report the concentration of SO_2 in the air in mg SO_2/L. The density of air is 1.18 g/liter.

22. Seaholtz and colleagues described a method for the quantitative analysis of CO in automobile exhaust based on the measurement of infrared radiation at 2170 cm^{-1}.[25] A calibration curve was prepared by filling a 10-cm IR gas cell with a known pressure of CO and measuring the absorbance using an FT-IR. The standardization relationship was found to be

$$A = -1.1 \times 10^{-4} + (9.9 \times 10^{-4}) \times P_{CO} \quad (10.E.7)$$

Samples were prepared by using a vacuum manifold to fill the gas cell. After measuring the total pressure, the absorbance of the sample at 2170 cm^{-1} was measured. Results are reported as %CO (P_{CO}/P_{total}). The analysis of five exhaust samples from a 1973 coupe give the following results.

P_{total} (torr)	absorbance
595	0.1146
354	0.0642
332	0.0591
233	0.0412
143	0.0254

Determine the %CO for each sample, and report the mean value and the 95% confidence interval.

23. Figure 10.32 shows an example of a disposable IR sample card made using a thin sheet of polyethylene. To prepare an analyte for analysis, it is dissolved in a suitable solvent and a portion of the sample placed on the IR card. After the solvent evaporates, leaving the analyte behind as a thin film, the sample's IR spectrum is obtained. Because the thickness of the polyethylene film is not uniform, the primary application of IR cards is for a qualitative analysis. Zhao and Malinowski reported how an internal standardization with KSCN can be used for a quantitative IR analysis of polystyrene.[26] Polystyrene was monitored at 1494 cm^{-1} and KSCN at 2064 cm^{-1}. Standard solutions were prepared by placing weighed portions of polystyrene in a 10-mL volumetric flask and diluting to volume with a solution of 10 g/L KSCN in methyl isobutyl ketone. A typical set of results is shown here.

g polystyrene	0.1609	0.3290	0.4842	0.6402	0.8006
A_{1494}	0.0452	0.1138	0.1820	0.3275	0.3195
A_{2064}	0.1948	0.2274	0.2525	0.3580	0.2703

When a 0.8006-g sample of a poly(styrene/maleic anhydride) copolymer was analyzed, the following results were obtained.

replicate	A_{1494}	A_{2064}
1	0.2729	0.3582
2	0.2074	0.2820
3	0.2785	0.3642

What is the %w/w polystyrene in the copolymer? Given that the reported %w/w polystyrene is 67%, is there any evidence for a determinate error at $\alpha = 0.05$?

24. The following table lists molar absorptivities for the Arsenazo complexes of copper and barium.[27] Suggest appropriate wavelengths for analyzing mixtures of copper and barium using their Arsenzao complexes.

wavelength (nm)	ε_{Cu} (M^{-1} cm^{-1})	ε_{Ba} (M^{-1} cm^{-1})
595	11900	7100
600	15500	7200
607	18300	7400
611	19300	6900
614	19300	7000
620	17800	7100
626	16300	8400
635	10900	9900
641	7500	10500
645	5300	10000
650	3500	8600
655	2200	6600
658	1900	6500
665	1500	3900
670	1500	2800
680	1800	1500

25. Blanco and colleagues report several applications of multiwavelength linear regression analysis for the simultaneous determination of two-component mixtures.[9] For each of the following, determine the molar concentration of each analyte in the mixture.

(a) Titanium and vanadium were determined by forming complexes with H_2O_2. Results for a mixture of Ti(IV) and V(V) and for standards of 63.1 ppm Ti(IV) and 96.4 ppm V(V) are listed in the following table.

	absorbance		
wavelength (nm)	Ti(V) standard	V(V) standard	mixture
390	0.895	0.326	0.651
430	0.884	0.497	0.743
450	0.694	0.528	0.665
470	0.481	0.512	0.547
510	0.173	0.374	0.314

(b) Copper and zinc were determined by forming colored complexes with 2-pyridyl-azo-resorcinol (PAR). The absorbances for PAR, a mixture of Cu^{2+} and Zn^{2+}, and standards of 1.00 ppm Cu^{2+} and 1.00 ppm Zn^{2+} are listed in the following table. Note that you must correct the absorbances for the metal for the contribution from PAR.

	absorbance			
wavelength (nm)	PAR	Cu standard	Zn standard	mixture
480	0.211	0.698	0.971	0.656
496	0.137	0.732	1.018	0.668
510	0.100	0.732	0.891	0.627
526	0.072	0.602	0.672	0.498
540	0.056	0.387	0.306	0.290

26. The stoichiometry of a metal–ligand complex, ML_n, was determined by the method of continuous variations. A series of solutions was prepared in which the combined concentrations of M and L were held constant at 5.15×10^{-4} M. The absorbances of these solutions were measured at a wavelength where only the metal–ligand complex absorbs. Using the following data, determine the formula of the metal–ligand complex.

mole fraction M	mole fraction L	absorbance
1.0	0.0	0.001
0.9	0.1	0.126
0.8	0.2	0.260
0.7	0.3	0.389
0.6	0.4	0.515
0.5	0.5	0.642
0.4	0.6	0.775
0.3	0.7	0.771
0.2	0.8	0.513
0.1	0.9	0.253
0.0	1.0	0.000

27. The stoichiometry of a metal–ligand complex, ML_n, was determined by the mole-ratio method. A series of solutions was prepared in which the concentration of metal was held constant at 3.65×10^{-4} M, and the ligand's concentration was varied from 1×10^{-4} M to 1×10^{-3} M. Using the following data, determine the stoichiometry of the metal-ligand complex.

[ligand] (M)	absorbance
1.0×10^{-4}	0.122
2.0×10^{-4}	0.251
3.0×10^{-4}	0.376
4.0×10^{-4}	0.496
5.0×10^{-4}	0.625
6.0×10^{-4}	0.752
7.0×10^{-4}	0.873
8.0×10^{-4}	0.937
9.0×10^{-4}	0.962
1.0×10^{-3}	1.002

28. The stoichiometry of a metal–ligand complex, ML_n, was determined by the slope-ratio method. Two sets of solutions were prepared. For the first set of solutions the concentration of the metal was held constant at 0.010 M and the concentration of the ligand was varied. When the absorbance of these solutions was measured at a wavelength where only the metal–ligand complex absorbs, the following data were obtained.

[ligand] (M)	absorbance
1.0×10^{-5}	0.012
2.0×10^{-5}	0.029
3.0×10^{-5}	0.042
4.0×10^{-5}	0.055
5.0×10^{-5}	0.069

For the second set of solutions the concentration of the ligand was held constant at 0.010 M, and the concentration of the metal was varied, yielding the following absorbances.

[metal] (M)	absorbance
1.0×10^{-5}	0.040
2.0×10^{-5}	0.085
3.0×10^{-5}	0.125
4.0×10^{-5}	0.162
5.0×10^{-5}	0.206

Using this data, determine the stoichiometry of the metal-ligand complex.

29. Kawakami and Igarashi developed a spectrophotometric method for nitrite based on its reaction with 5, 10, 15, 20-tetrakis(4-aminophenyl)porphrine (TAPP). As part of their study they investigated the stoichiometry of the reaction between TAPP and NO_2^-.

The following data are derived from a figure in their paper.[28]

[TAPP] (M)	$[NO_2^-]$ (M)	absorbance
8.0×10^{-7}	1.6×10^{-7}	0.227
8.0×10^{-7}	3.2×10^{-7}	0.192
8.0×10^{-7}	4.8×10^{-7}	0.158
8.0×10^{-7}	8.0×10^{-7}	0.126
8.0×10^{-7}	1.6×10^{-6}	0.065
8.0×10^{-7}	2.4×10^{-6}	0.047
8.0×10^{-7}	3.2×10^{-6}	0.042
8.0×10^{-7}	4.0×10^{-6}	0.042

What is the stoichiometry of the reaction?

30. The equilibrium constant for an acid–base indicator is determined by preparing three solutions, each of which has a total indicator concentration of 1.35×10^{-5} M. The pH of the first solution is adjusted until it is acidic enough to ensure that only the acid form of the indicator is present, yielding an absorbance of 0.673. The absorbance of the second solution, whose pH is adjusted to give only the base form of the indicator, is 0.118. The pH of the third solution is adjusted to 4.17 and has an absorbance of 0.439. What is the acidity constant for the acid–base indicator?

31. The acidity constant for an organic weak acid was determined by measuring its absorbance as a function of pH while maintaining a constant total concentration of the acid. Using the data in the following table, determine the acidity constant for the organic weak acid.

pH	absorbance
1.53	0.010
2.20	0.010
3.66	0.035
4.11	0.072
4.35	0.103
4.75	0.169
4.88	0.193
5.09	0.227
5.69	0.288
7.20	0.317
7.78	0.317

32. Suppose you need to prepare a set of calibration standards for the spectrophotometric analysis of an analyte that has a molar absorptivity of 1138 M^{-1} cm^{-1} at a wavelength of 625 nm. To maintain an acceptable precision for the analysis, the %T for the standards should be between 15% and 85%.

(a) What is the concentration of the most concentrated and the least concentrated standard you should prepare, assuming a 1.00-cm sample cell.

(b) Explain how you will analyze samples with concentrations that are 10 μM, 0.1 mM, and 1.0 mM in the analyte.

33. When using a spectrophotometer whose precision is limited by the uncertainty of reading %T, the analysis of highly absorbing solutions can lead to an unacceptable level of indeterminate errors. Consider the analysis of a sample for which the molar absorptivity is 1.0×10^4 M^{-1} cm^{-1} and the pathlength is 1.00 cm.

(a) What is the relative uncertainty in concentration for an analyte whose concentration is 2.0×10^{-4} M if s_T is ±0.002?

(b) What is the relative uncertainty in the concentration if the spectrophotometer is calibrated using a blank consisting of a 1.0×10^{-4} M solution of the analyte?

34. Hobbins reported the following calibration data for the flame atomic absorption analysis for phosphorous.[29]

mg P / L	absorbance
2130	0.048
4260	0.110
6400	0.173
8530	0.230

To determine the purity of a sample of Na_2HPO_4, a 2.469-g sample is dissolved and diluted to volume in a 100-mL volumetric flask. Analysis of the resulting solution gives an absorbance of 0.135. What is the purity of the Na_2HPO_4?

35. Bonert and Pohl reported results for the atomic absorption analysis of several metals in the caustic suspensions produced during the manufacture of soda by the ammonia-soda process.[30]

(a) The concentration of Cu was determined by acidifying a 200-mL sample of the caustic solution with 20 mL of concentrated HNO_3, adding 1 mL of 27% w/v H_2O_2, and boiling for 30 min. The resulting solution was diluted to 500 mL, filtered, and analyzed by flame atomic absorption using matrix matched standards. The results for a typical analysis are shown in the following table.

solution	mg Cu / L	absorbance
blank	0.000	0.007
standard 1	0.200	0.014
standard 2	0.500	0.036
standard 3	1.000	0.072
standard 4	2.000	0.146
sample		0.027

Determine the concentration of Cu in the caustic suspension.

(b) The determination of Cr was accomplished by acidifying a 200-mL sample of the caustic solution with 20 mL of concentrated HNO_3, adding 0.2 g of Na_2SO_3 and boiling for 30 min. The Cr was isolated from the sample by adding 20 mL of NH_3, producing a precipitate that includes the chromium as well as other oxides. The precipitate was isolated by filtration, washed, and transferred to a beaker. After acidifying with 10 mL of HNO_3, the solution was evaporated to dryness. The residue was redissolved in a combination of HNO_3 and HCl and evaporated to dryness. Finally, the residue was dissolved in 5 mL of HCl, filtered, diluted to

volume in a 50-mL volumetric flask, and analyzed by atomic absorption using the method of standard additions. The atomic absorption results are summarized in the following table.

sample	mg Cr_{added} / L	absorbance
blank		0.001
sample		0.045
standard addition 1	0.200	0.083
standard addition 2	0.500	0.118
standard addition 3	1.000	0.192

Report the concentration of Cr in the caustic suspension.

36. Quigley and Vernon report results for the determination of trace metals in seawater using a graphite furnace atomic absorption spectrophotometer and the method of standard additions.[31] The trace metals were first separated from their complex, high-salt matrix by coprecipitating with Fe^{3+}. In a typical analysis a 5.00-mL portion of 2000 ppm Fe^{3+} was added to 1.00 L of seawater. The pH was adjusted to 9 using NH_4OH, and the precipitate of $Fe(OH)_3$ allowed to stand overnight. After isolating and rinsing the precipitate, the $Fe(OH)_3$ and coprecipitated metals were dissolved in 2 mL of concentrated HNO_3 and diluted to volume in a 50-mL volumetric flask. To analyze for Mn^{2+}, a 1.00-mL sample of this solution was diluted to 100 mL in a volumetric flask. The following samples were injected into the graphite furnace and analyzed.

sample	absorbance
2.5-µL sample + 2.5 µL of 0 ppb Mn^{2+}	0.223
2.5-µL sample + 2.5 µL of 2.5 ppb Mn^{2+}	0.294
2.5-µL sample + 2.5 µL of 5.0 ppb Mn^{2+}	0.361

Report the parts per billion Mn^{2+} in the sample of seawater.

37. The concentration of Na in plant materials may be determined by flame atomic emission. The material to be analyzed is prepared by grinding, homogenizing, and drying at 103°C. A sample of approximately 4 g is transferred to a quartz crucible and heated on a hot plate to char the organic material. The sample is heated in a muffle furnace at 550°C for several hours. After cooling to room temperature the residue is dissolved by adding 2 mL of 1:1 HNO_3 and evaporated to dryness. The residue is redissolved in 10 mL of 1:9 HNO_3, filtered and diluted to 50 mL in a volumetric flask. The following data were obtained during a typical analysis for the concentration of Na in a 4.0264-g sample of oat bran.

sample	mg Na / L	emission (arbitrary units)
blank	0.00	0.0
standard 1	2.00	90.3
standard 2	4.00	181
standard 3	6.00	272
standard 4	8.00	363
standard 5	10.00	448
sample		238

Determine the mg Na/L in the sample of oat bran.

38. Gluodenis describes the use of ICP atomic emission to analyze samples of brass for Pb and Ni.[32] The analysis for Pb uses external standards prepared from brass samples containing known amounts of lead. Results are shown in the following table.

%w/w Pb	emission intensity
0.000	4.29×10^4
0.0100	1.87×10^5
0.0200	3.20×10^5
0.0650	1.28×10^6
0.350	6.22×10^6
0.700	1.26×10^7
1.04	1.77×10^7
2.24	3.88×10^7
3.15	5.61×10^7
9.25	1.64×10^8

What is the %w/w Pb in a sample of brass that gives an emission intensity of 9.25×10^4?

The analysis for Ni uses an internal standard. Results for a typical calibration are show in the following table.

% w/w Ni	emission intensity ratio
0.000	0.00267
0.0140	0.00154
0.0330	0.00312
0.130	0.120
0.280	0.246
0.280	0.247
0.560	0.533
1.30	1.20
4.82	4.44

What is the %w/w Ni in a sample for which the ratio of emission intensity is 1.10×10^{-3}?

39. Yan and colleagues developed a method for the analysis of iron based its formation of a fluorescent metal–ligand complex with the ligand 5-(4-methylphenylazo)-8-aminoquinoline.[33] In the presence of the surfactant cetyltrimethyl ammonium bromide the analysis is carried out using an excitation wavelength of 316 nm with emission monitored at 528 nm. Standardization with external standards gives the following calibration curve.

$$I_f = -0.03 + 1.594 \times \frac{\text{mg Fe}^{3+}}{\text{L}} \tag{10.E.8}$$

A 0.5113-g sample of dry dog food was ashed to remove organic materials, and the residue dissolved in a small amount of HCl and diluted to volume in a 50-mL volumetric flask. Analysis of the resulting solution gave a fluorescent emission intensity of 5.72. Determine the mg Fe/L in the sample of dog food.

40. A solution of 5.00×10^{-5} M 1,3-dihydroxynaphthelene in 2 M NaOH has a fluorescence intensity of 4.85 at a wavelength of 459 nm. What is the concentration of 1,3-dihydroxynaphthelene in a solution with a fluorescence intensity of 3.74 under identical conditions?

41. The following data was recorded for the phosphorescence intensity for several standard solutions of benzo[a]pyrene.

[benzo[a]pyrene] (M)	emission intensity
0	0.00
1.00×10^{-5}	0.98
3.00×10^{-5}	3.22
6.00×10^{-5}	6.25
1.00×10^{-4}	10.21

What is the concentration of benzo[a]pyrene in a sample yielding a phosphorescent emission intensity of 4.97?

42. The concentration of acetylsalicylic acid, $C_9H_8O_4$, in aspirin tablets can be determined by hydrolyzing to the salicylate ion, $C_7H_5O_2^-$, and determining the concentration of the salicylate ion spectrofluorometrically. A stock standard solution is prepared by weighing 0.0774 g of salicylic acid, $C_7H_6O_2$, into a 1-L volumetric flask and diluting to volume with distilled water. A set of calibration standards is prepared by pipeting 0, 2.00, 4.00, 6.00, 8.00, and 10.00 mL of the stock solution into separate 100-mL volumetric flasks containing 2.00 mL of 4 M NaOH and diluting to volume with distilled water. The fluorescence of the calibration standards was measured at an emission wavelength of 400 nm using an excitation wavelength of 310 nm; results are listed in the following table.

mL of stock solution	emission intensity
0.00	0.00
2.00	3.02
4.00	5.98
6.00	9.18
8.00	12.13
10.00	14.96

Several aspirin tablets are ground to a fine powder in a mortar and pestle. A 0.1013-g portion of the powder is placed in a 1-L volumetric flask and diluted to volume with distilled water. A portion of this solution is filtered to remove insoluble binders and a 10.00-mL aliquot transferred to a 100-mL volumetric flask containing 2.00 mL of 4 M NaOH. After diluting to volume the fluorescence of the resulting solution is found to be 8.69. What is the %w/w acetylsalicylic acid in the aspirin tablets?

43. Selenium (IV) in natural waters can be determined by complexing with ammonium pyrrolidine dithiocarbamate and extracting into $CHCl_3$. This step serves to concentrate the Se(IV) and to separate it from Se(VI). The Se(IV) is then extracted back into an aqueous matrix using HNO_3. After complexing with 2,3-diaminonaphthalene, the complex is extracted into cyclohexane. Fluorescence is measured at 520 nm following its excitation at 380 nm. Calibration is achieved by adding known amounts of

Se(IV) to the water sample before beginning the analysis. Given the following results what is the concentration of Se(IV) in the sample.

[Se(IV)] added (nM)	emission intensity
0.00	323
2.00	597
4.00	862
6.00	1123

44. Fibrinogen is a protein that is produced by the liver and found in human plasma. Its concentration in plasma is clinically important. Many of the analytical methods used to determine the concentration of fibrinogen in plasma are based on light scattering following its precipitation. For example, da Silva and colleagues describe a method in which fibrinogen precipitates in the presence of ammonium sulfate in a guanidine hydrochloride buffer.[34] Light scattering is measured nephelometrically at a wavelength of 340 nm. Analysis of a set of external calibration standards gives the following calibration equation

$$I_s = -4.66 + 9907.63 \times C \tag{10.E.9}$$

where I_s is the intensity of scattered light and C is the concentration of fibrinogen in g/L. A 9.00-mL sample of plasma was collected from a patient and mixed with 1.00 mL of an anticoagulating agent. A 1.00-mL aliquot of this solution was then diluted to 250 mL in a volumetric flask. Analysis of the resulting solution gave a scattering intensity of 44.70. What is the concentration of fibrinogen, in gram per liter, in the plasma sample?

10.9.3 Solutions to Practice Exercises

Practice Exercise 10.1

The frequency and wavenumber for the line are

$$\nu = \frac{c}{\lambda} = \frac{3.00 \times 10^8 \text{ m/s}}{656.3 \times 10^{-9} \text{ m}} = 4.57 \times 10^{14} \text{ s}^{-1} \tag{10.E.10}$$

$$\bar{\nu} = \frac{1}{\lambda} = \frac{1}{656.3 \times 10^{-9} \text{ m}} \times \frac{1 \text{ m}}{100 \text{ cm}} = 1.524 \times 10^4 \text{ cm}^{-1} \tag{10.E.11}$$

Click here to return to the chapter.

Practice Exercise 10.2

The photon's energy is

$$E = \frac{hc}{\lambda} = \frac{(6.626 \times 10^{-34} \text{ J} \cdot \text{s})(3.00 \times 10^8 \text{ m/s})}{656.3 \times 10^{-9} \text{ m}} = 3.03 \times 10^{-19} \text{ J} \tag{10.E.12}$$

Click here to return to the chapter.

Practice Exercise 10.3

To find the transmittance, T, we begin by noting that

$$A = 1.27 = -\log T \tag{10.E.13}$$

Solving for T

$$-1.27 = \log T \tag{10.E.14}$$

$$10^{-1.27} = T \tag{10.E.15}$$

gives a transmittance of 0.054, or a %T of 5.4%.

Click here to return to the chapter.

Practice Exercise 10.4

Making appropriate substitutions into Beer's law

$$A = 0.228 = \varepsilon b C = (676\ \text{M}^{-1}\ \text{cm}^{-1})(1\ \text{cm})C \tag{10.E.16}$$

and solving for C gives a concentration of 3.37×10^{-4} M.

Click here to return to the chapter.

Practice Exercise 10.5

For this standard addition we can write the following equations relating absorbance to the concentration of Cu^{2+} in the sample. First, for the sample, we have

$$0.118 = \varepsilon b C_{\text{Cu}} \tag{10.E.17}$$

and for the standard addition we have

$$0.162 = \varepsilon b \left(C_{\text{Cu}} + \frac{20.00\ \text{mg Cu}}{\text{L}} \times \frac{1.00\ \text{mL}}{10.00\ \text{mL}} \right) \tag{10.E.18}$$

The value of εb is the same in both equation. Solving each equation for εb and equating

$$\frac{0.162}{C_{\text{Cu}} + \frac{20.00\ \text{mg Cu}}{\text{L}} \times \frac{1.00\ \text{mL}}{10.00\ \text{mL}}} = \frac{0.118}{C_{\text{Cu}}} \tag{10.E.19}$$

leaves us with an equation in which C_{Cu} is the only variable. Solving for C_{Cu} gives its value as

$$\frac{0.162}{C_{\text{Cu}} + 2.00\ \text{mg Cu/L}} = \frac{0.118}{C_{\text{Cu}}} \tag{10.E.20}$$

$$0.162 C_{\text{Cu}} = 0.118 C_{\text{Cu}} + 0.236\ \text{mg Cu/L} \tag{10.E.21}$$

$$0.044 C_{\text{Cu}} = 0.236\ \text{mg Cu/L} \tag{10.E.22}$$

$$C_{\text{Cu}} = 5.4\ \text{mg Cu/L} \tag{10.E.23}$$

Click here to return to the chapter.

Practice Exercise 10.6

Substituting into equation 10.11 and equation 10.12 gives

$$A_{400} = 0.336 = 15.2 C_{\text{Cr}} + 5.60 C_{\text{Co}} \tag{10.E.24}$$

$$A_{505} = 0.187 = 0.533 C_{\text{Cr}} + 5.07 C_{\text{Co}} \tag{10.E.25}$$

To determine C_{Cr} and C_{Co} we solve the first equation for C_{Co}

$$C_{\text{Co}} = \frac{0.336 - 15.2 C_{\text{Cr}}}{5.60} \tag{10.E.26}$$

and substitute the result into the second equation.

$$0.187 = 0.533 C_{\text{Cr}} + 5.07 \times \frac{0.336 - 15.2 C_{\text{Cr}}}{5.60} = 0.3042 - 13.23 C_{\text{Cr}} \tag{10.E.27}$$

Solving for C_{Cr} gives the concentration of Cr^{3+} as 8.86×10^{-3} M. Substituting this concentration back into the equation for the mixture's absorbance at 400 nm gives the concentration of Co^{2+} as 3.60×10^{-2} M.

Click here to return to the chapter.

Practice Exercise 10.7

Letting X represent MnO_4^- and Y represent $Cr_2O_7^{2-}$, we plot the equation

$$\frac{A_{mix}}{A_{SX}} = \frac{C_X}{C_{SX}} + \frac{C_Y}{C_{SY}} \times \frac{A_{SY}}{A_{SX}} \tag{10.E.28}$$

placing A_{mix}/A_{SX} on the *y*-axis and A_{SY}/A_{SX} on the *x*-axis. For example, at a wavelength of 266 nm the value of A_{mix}/A_{SX} is 0.766/0.042, or 18.2, and the value of A_{SY}/A_{SX} is 0.410/0.042, or 9.76. Completing the calculations for all wavelengths and plotting the data gives the result shown in Figure 10.67. Fitting a straight-line to the data gives a regression model of

$$\frac{A_{mix}}{A_{SX}} = 0.8147 + 1.7839 \times \frac{A_{SY}}{A_{SX}} \tag{10.E.29}$$

Using the *y*-intercept, the concentration of MnO_4^- is

$$\frac{C_X}{C_{SX}} = \frac{[MnO_4^-]}{1.0 \times 10^{-4}\ M\ \ MnO_4^-} = 0.8147 \tag{10.E.30}$$

or 8.15×10^{-5} M MnO_4^-, and using the slope, the concentration of $Cr_2O_7^{2-}$ is

$$\frac{C_Y}{C_{SY}} = \frac{[Cr_2O_7^{2-}]}{1.0 \times 10^{-4}\ M\ \ Cr_2O_7^{2-}} = 1.7839 \tag{10.E.31}$$

or 1.78×10^{-4} M $Cr_2O_7^{2-}$.

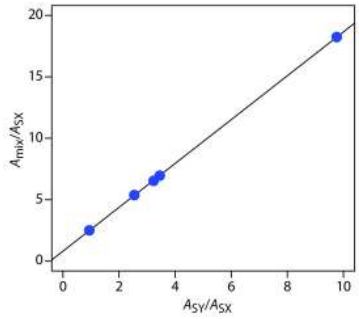


Figure 10.67 Multiwavelength linear regression analysis for the data in Practice Exercise 10.7.

Click here to return to the chapter.

Practice Exercise 10.8

Figure 10.68 shows a continuous variations plot for the data in this exercise. Although the individual data points show substantial curvature—enough curvature that there is little point in trying to draw linear branches for excess metal and excess ligand—the maximum absorbance clearly occurs at an X_L of approximately 0.5. The complex's stoichiometry, therefore, is $Fe(SCN)^{2+}$.

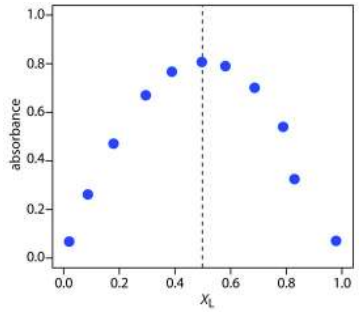


Figure 10.68 Continuous variations plot for the data in Practice Exercise 10.8.

Click here to return to the chapter.

Practice Exercise 10.9

The value of K_a is

$$K_a = (1.00 \times 10^{-6}) \times \frac{0.225 - 0.000}{0.680 - 0.225} = 4.95 \times 10^{-7} \tag{10.E.32}$$

Click here to return to the chapter.

Practice Exercise 10.10

To determineK_a we use equation 10.21, plotting $\log[(A - A_{HIn}) / (A_{In} - A)]$ versus pH, as shown in Figure 10.69. Fitting a straight-line to the data gives a regression model of

$$\log \frac{A - A_{HIn}}{A_{In} - A} = -3.80 + 0.962\text{pH} \tag{10.E.33}$$

The y-intercept is $-pK_a$; thus, the pK_a is 3.80 and the K_a is 1.58×10^{-4}.

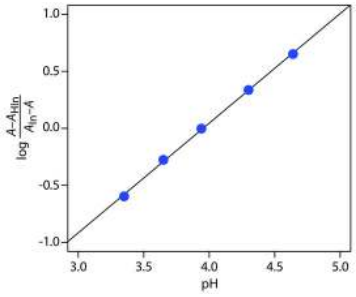


Figure 10.69 Determining the pKa of bromothymol blue using the data in Practice Exercise 10.10.

Click here to return to the chapter.

Contributors and Attributions

David Harvey (DePauw University)

10.E: Spectroscopic Methods (Exercises) is shared under a CC BY-NC-SA 4.0 license and was authored, remixed, and/or curated by LibreTexts.

10.S: Spectroscopic Methods (Summary)

The spectrophotometric methods of analysis covered in this chapter include those based on the absorption, emission, or scattering of electromagnetic radiation. When a molecule absorbs UV/Vis radiation it undergoes a change in its valence shell configuration. A change in vibrational energy results from the absorption of IR radiation. Experimentally we measure the fraction of radiation transmitted, T, by the sample. Instrumentation for measuring absorption requires a source of electromagnetic radiation, a means for selecting a wavelength, and a detector for measuring transmittance. Beer's law relates absorbance to both transmittance and to the concentration of the absorbing species ($A = -\log T = \varepsilon bC$).

In atomic absorption we measure the absorption of radiation by gas phase atoms. Samples are atomized using thermal energy from either a flame or a graphite furnace. Because the width of an atom's absorption band is so narrow, the continuum sources common for molecular absorption can not be used. Instead, a hollow cathode lamp provides the necessary line source of radiation. Atomic absorption suffers from a number of spectral and chemical interferences. The absorption or scattering of radiation from the sample's matrix are important spectral interferences that may be minimized by background correction. Chemical interferences include the formation of nonvolatile forms of the analyte and ionization of the analyte. The former interference is minimized by using a releasing agent or a protecting agent, and an ionization suppressor helps minimize the latter interference.

When a molecule absorbs radiation it moves from a lower energy state to a higher energy state. In returning to the lower energy state the molecule may emit radiation. This process is called photoluminescence. One form of photoluminescence is fluorescence in which the analyte emits a photon without undergoing a change in its spin state. In phosphorescence, emission occurs with a change in the analyte's spin state. For low concentrations of analyte, both fluorescent and phosphorescent emission intensities are a linear function of the analyte's concentration. Thermally excited atoms also emit radiation, forming the basis for atomic emission spectroscopy. Thermal excitation is achieved using either a flame or a plasma.

Spectroscopic measurements may also involve the scattering of light by a particulate form of the analyte. In turbidimetry, the decrease in the radiation's transmission through the sample is measured and related to the analyte's concentration through an equation similar to Beer's law. In nephelometry we measure the intensity of scattered radiation, which varies linearly with the analyte's concentration.

10.9.1 Key Terms

absorbance
absorbance spectrum
absorptivity
amplitude
attenuated total reflectance
atomization
background correction
Beer's law
chemiluminescence
chromophore
continuum source
dark current
double-beam
effective bandwidth
electromagnetic radiation
electromagnetic spectrum
emission
emission spectrum
excitation spectrum
external conversion
Fellgett's advantage
fiber-optic probe
filter
filter photometer
fluorescence
fluorescent quantum yield
fluorimeter
frequency
graphite furnace
interferogram
interferometer
internal conversion
intersystem crossing
ionization suppressor
Jacquinot's advantage
lifetime
line source
method of continuous variations
molar absorptivity
mole-ratio method
monochromatic
monochromator
nephelometry
nominal wavelength
phase angle
phosphorescence
phosphorescent quantum yield
photodiode array
photoluminescence
photon
plasma
polychromatic
protecting agent
radiationless deactivation
relaxation
releasing agent
resolution
self-absorption
signal averaging
signal processor
signal-to-noise ratio
single-beam
singlet excited state
slope-ratio method
spectral searching
spectrofluorimeter
spectrophotometer
spectroscopy
stray radiation
transducer
transmittance
triplet excited state
turbidimetry
vibrational relaxation
wavelength
wavenumber

References

1. Home, D.; Gribbin, J. *New Scientist* 1991, 2 Nov. 30–33.
2. Ball, D. W. *Spectroscopy* **1994**, *9(5)*, 24–25.
3. Ball, D. W. *Spectroscopy* **1994**, *9(6)* 20–21.
4. Jiang, S.; Parker, G. A. *Am. Lab.* **1981**, October, 38–43.
5. (a) Strong, F. C., III *Anal. Chem.* **1984**, *56*, 16A–34A; Gilbert, D. D. *J. Chem. Educ.* **1991**, *68*, A278–A281.
6. (a) Seitz, W. R. *Anal. Chem.* **1984**, *56*, 16A–34A; (b) Angel, S. M. *Spectroscopy* **1987**, *2(2)*, 38–48.
7. DiTusa, M. R.; Schlit, A. A. *J. Chem. Educ.* **1985**, *62*, 541–542.
8. Mehra, M. C.; Rioux, J. *J. Chem. Educ.* **1982**, *59*, 688–689.
9. Blanco, M.; Iturriaga, H.; Maspoch, S.; Tarin, P. *J. Chem. Educ.* **1989**, *66*, 178–180.
10. The data for the two standards are from Brewer, S. *Solving Problems in Analytical Chemistry*, John Wiley & Sons: New York, 1980.
11. Ramette, R. W. *Chemical Equilibrium and Analysis*, Addison-Wesley: Reading, MA, 1981, Chapter 13.
12. Rothman, L. D.; Crouch, S. R.; Ingle, J. D. Jr. *Anal. Chem.* **1975**, *47*, 1226–1233.
13. (a) Walsh, A. *Anal. Chem.* **1991**, *63*, 933A–941A; (b) Koirtyohann, S. R. *Anal. Chem.* **1991**, *63*, 1024A–1031A; (c) Slavin, W. *Anal. Chem.* **1991**, *63*, 1033A–1038A.
14. Ingle, J. D.; Crouch, S. R. *Spectrochemical Analysis*, Prentice-Hall: Englewood Cliffs, NJ, 1988; p. 275.
15. Parsons, M. L.; Major, S.; Forster, A. R. *Appl. Spectrosc.* **1983**, *37*, 411–418.
16. Hosking, J. W.; Snell, N. B.; Sturman, B. T. *J. Chem. Educ.* **1977**, *54*, 128–130.
17. Crawford, A. J.; Bhattacharya, S. K. "Microanalysis of Copper and Zinc in Biopsy-Sized Tissue Specimens by Atomic Absorption Spectroscopy Using a Stoichiometric Air-Acetylene Flame," Varian Instruments at Work, Number AA–46, April 1985.
18. Dawson, J. B. *J. Anal. At. Spectrosc.* **1991**, *6*, 93–98.

19. Goodney, D. E. *J. Chem. Educ.* **1982**, *59*, 875–876
20. Hach, C. C.; Bryant, M. “Turbidity Standards,” Technical Information Series, Booklet No. 12, Hach Company: Loveland, CO, 1995.
21. Lozano-Calero, D.; Martín-Palomeque, P.; Madueño-Loriguillo, S. *J. Chem. Educ.* **1996**, *73*, 1173–1174.
22. Saito, T. *Anal. Chim. Acta* **1992**, *268*, 351–355.
23. Lin, J.; Brown, C. W. *Spectroscopy* **1995**, *10(5)*, 48–51.
24. Jones, M.; Thatcher, R. L. *Anal. Chem.* **1951**, *23*, 957–960.
25. Seaholtz, M. B.; Pence, L. E.; Moe, O. A. Jr. *J. Chem. Educ.* **1988**, *65*, 820–823.
26. Zhao, Z.; Malinowski, E. R. *Spectroscopy* **1996**, *11(7)*, 44–49.
27. Grossman, O.; Turanov, A. N. *Anal. Chim. Acta* **1992**, *257*, 195–202.
28. Kawakami, T.; Igarashi, S. *Anal. Chim. Acta* **1996**, *33*, 175–180.
29. Hobbins, W. B. “Direct Determination of Phosphorous in Aqueous Matricies by Atomic Absorption,” Varian Instruments at Work, Number AA-19, February 1982.
30. Bonert, K.; Pohl, B. “The Determination of Cd, Cr, Cu, Ni, and Pb in Concentrated CaCl2/NaCl solutions by AAS,” AA Instruments at Work (Varian) Number 98, November, 1990.
31. Quigley, M. N.; Vernon, F. *J. Chem. Educ.* **1996**, *73*, 671–673.
32. Gluodenis, T. J. Jr. *Am. Lab.* November 1998, 245–275.
33. Yan, G.; Shi, G.; Liu, Y. *Anal. Chim. Acta* **1992**, *264*, 121–124.
34. da Silva, M. P.; Fernandez-Romero, J. M.; Luque de Castro, M. D. *Anal. Chim. Acta* **1996**, *327*, 101–106.

Contributors

David Harvey (DePauw University)

10.S: Spectroscopic Methods (Summary) is shared under a CC BY-NC-SA 4.0 license and was authored, remixed, and/or curated by LibreTexts.

CHAPTER OVERVIEW

11: Electrochemical Methods

In Chapter 10 we examined several spectroscopic techniques that take advantage of the interaction between electromagnetic radiation and matter. In this chapter we turn our attention to electrochemical techniques in which the potential, current, or charge in an electrochemical cell serves as the analytical signal.

Although there are only three basic electrochemical signals, there are a many possible experimental designs—too many, in fact, to cover adequately in an introductory textbook. The simplest division of electrochemical techniques is between bulk techniques, in which we measure a property of the solution in the electrochemical cell, and interfacial techniques, in which the potential, charge, or current depends on the species present at the interface between an electrode and the solution in which it sits. The measurement of a solution's conductivity, which is proportional to the total concentration of dissolved ions, is one example of a bulk electrochemical technique. A determination of pH using a pH electrode is an example of an interfacial electrochemical technique. Only interfacial electrochemical methods receive further consideration in this chapter.

Topic hierarchy

11.1: Overview of Electrochemistry
11.2: Potentiometric Methods
11.3: Coulometric Methods
11.4: Voltammetric Methods
11.E: Electrochemical Methods (Exercises)
11.S: Electrochemical Methods (Summary)

Thumbnail:Comparison of the current response of a platinum disc electrode in 1 M sulfuric acid given by linear sweep voltammetry and staircase voltammetry methods. Image used with permission (CC BY-SA 3.0; Earth-Rare).

Contributors

- David Harvey (DePauw University)

11: Electrochemical Methods is shared under a CC BY-NC-SA 4.0 license and was authored, remixed, and/or curated by LibreTexts.

11.1: Overview of Electrochemistry

The focus of this chapter is on analytical techniques that use a measurement of potential, charge, or current to determine an analyte's concentration or to characterize an analyte's chemical reactivity. Collectively we call this area of analytical chemistry **electrochemistry** because its originated from the study of the movement of electrons in an oxidation–reduction reaction.

Despite the difference in instrumentation, all electrochemical techniques share several common features. Before we consider individual examples in greater detail, let's take a moment to consider some of these similarities. As you work through the chapter, this overview will help you focus on similarities between different electrochemical methods of analysis. You will find it easier to understand a new analytical method when you can see its relationship to other similar methods.

11.1.1 Five Important Concepts

To understand electrochemistry we need to appreciate five important and interrelated concepts:

1. the electrode's potential determines the analyte's form at the electrode's surface;
2. the concentration of analyte at the electrode's surface may not be the same as its concentration in bulk solution;
3. in addition to an oxidation–reduction reaction, the analyte may participate in other reactions;
4. current is a measure of the rate of the analyte's oxidation or reduction; and
5. we cannot simultaneously control current and potential.

The Electrode's Potential Determines the Analyte's Form

In Chapter 6 we introduced the ladder diagram as a tool for predicting how a change in solution conditions affects the position of an equilibrium reaction. For an oxidation–reduction reaction, the potential determines the reaction's position. Figure 11.1, for example, shows a ladder diagram for the Fe^{3+}/Fe^{2+} and the Sn^{4+}/Sn^{2+} equilibria. If we place an electrode in a solution of Fe^{3+} and Sn^{4+} and adjust its potential to +0.500 V, Fe^{3+} reduces to Fe^{2+}, but Sn^{4+} remains unchanged.

> **Note**
>
> You may wish to review the earlier treatment of oxidation–reduction reactions in Section 6.4.4 and the development of ladder diagrams for oxidation–reduction reactions in Section 6.6.3.

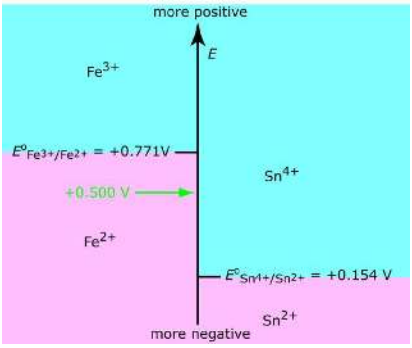


Figure 11.1 Redox ladder diagram for Fe^{3+}/Fe^{2+} and for Sn^{4+}/ Sn^{2+} redox couples. The areas in blue show the potential range where the oxidized forms are the predominate species; the reduced forms are the predominate species in the areas shown in pink. Note that a more positive potential favors the oxidized forms. At a potential of +0.500 V (green arrow) Fe^{3+} reduces to Fe^{2+}, but Sn^{4+} remains unchanged.

Interfacial Concentrations May Not Equal Bulk Concentrations

In Chapter 6 we introduced the Nernst equation, which provides a mathematical relationship between the electrode's potential and the concentrations of an analyte's oxidized and reduced forms in solution. For example, the Nernst equation for Fe^{3+} and Fe^{2+} is

$$E = E^o - \frac{RT}{nF}\log\frac{[Fe^{2+}]}{[Fe^{3+}]} = E^o - \frac{0.05916}{1}\log\frac{[Fe^{2+}]}{[Fe^{3+}]} \quad (11.1)$$

where E is the electrode's potential and E^o is the standard-state reduction potential for the reaction $Fe^{3+} \leftrightharpoons Fe^{2+} + e^-$. Because it is the potential of the electrode that determines the analyte's form at the electrode's surface, the concentration terms in equation 11.1 are those at the electrode's surface, not the concentrations in bulk solution.

This distinction between surface concentrations and bulk concentrations is important. Suppose we place an electrode in a solution of Fe^{3+} and fix its potential at 1.00 V. From the ladder diagram in Figure 11.1, we know that Fe^{3+} is stable at this potential and, as shown in Figure 11.2a, the concentration of Fe^{3+} remains the same at all distances from the electrode's surface. If we change the electrode's potential to +0.500 V, the concentration of Fe^{3+} at the electrode's surface decreases to approximately zero. As shown in Figure 11.2b, the concentration of Fe^{3+} increases as we move away from the electrode's surface until it equals the concentration of Fe^{3+} in bulk solution. The resulting concentration gradient causes additional Fe^{3+} from the bulk solution to diffuse to the electrode's surface.

> **Note**
>
> We call the solution containing this concentration gradient in Fe^{3+} the diffusion layer. We will have more to say about this in Section 11.4.2.

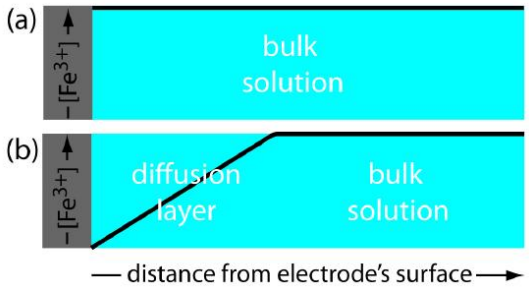


Figure 11.2 Concentration of Fe^{3+} as a function of distance from the electrode's surface at (a) E = +1.00 V and (b) E = +0.500 V. The electrode is shown in gray and the solution in blue.

The Analyte May Participate in Other Reactions

Figure 11.2 shows how the electrode's potential affects the concentration of Fe^{3+}, and how the concentration of Fe^{3+} varies as a function of distance from the electrode's surface. The reduction of Fe^{3+} to Fe^{2+}, which is governed by equation 11.1, may not be the only reaction affecting the concentration of Fe^{3+} in bulk solution or at the electrode's surface. The adsorption of Fe^{3+} at the electrode's surface or the formation of a metal–ligand complex in bulk solution, such as $Fe(OH)^{2+}$, also affects the concentration of Fe^{3+}.

Current is a Measure of Rate

The reduction of Fe^{3+} to Fe^{2+} consumes an electron, which is drawn from the electrode. The oxidation of another species, perhaps the solvent, at a second electrode serves as the source of this electron. The flow of electrons between the electrodes provides a measurable current. Because the reduction of Fe^{3+} to Fe^{2+} consumes one electron, the flow of electrons between the electrodes—in other words, the current—is a measure of the rate of the reduction reaction. One important consequence of this observation is that the current is zero when the reaction $Fe^{3+} \leftrightharpoons Fe^{2+} + e^-$ is at equilibrium.

> **Note**
>
> The rate of the reaction
>
> $$Fe^{3+} \leftrightharpoons Fe^{2+} + e^- \qquad (11.1.1)$$
>
> is the change in the concentration of Fe^{3+} as a function of time.

We Cannot Simultaneously Control Both Current and Potential

If a solution of Fe^{3+} and Fe^{2+} is at equilibrium, the current is zero and the potential is given by equation 11.1. If we change the potential away from its equilibrium position, current flows as the system moves toward its new equilibrium position. Although the initial current is quite large, it decreases over time reaching zero when the reaction reaches equilibrium. The current, therefore,

changes in response to the applied potential. Alternatively, we can pass a fixed current through the electrochemical cell, forcing the reduction of Fe^{3+} to Fe^{2+}. Because the concentrations of Fe^{3+} and Fe^{2+} are constantly changing, the potential, as given by equation 11.1, also changes over time. In short, if we choose to control the potential, then we must accept the resulting current, and we must accept the resulting potential if we choose to control the current.

11.1.2 Controlling and Measuring Current and Potential

Electrochemical measurements are made in an electrochemical cell consisting of two or more electrodes and the electronic circuitry for controlling and measuring the current and the potential. In this section we introduce the basic components of electrochemical instrumentation.

The simplest electrochemical cell uses two electrodes. The potential of one electrode is sensitive to the analyte's concentration, and is called the **working electrode** or the **indicator electrode**. The second electrode, which we call the **counter electrode**, completes the electrical circuit and provides a reference potential against which we measure the working electrode's potential. Ideally the counter electrode's potential remains constant so that we can assign to the working electrode any change in the overall cell potential. If the counter electrode's potential is not constant, we replace it with two electrodes: a **reference electrode** whose potential remains constant and an **auxiliary electrode** that completes the electrical circuit.

Because we cannot simultaneously control the current and the potential, there are only three basic experimental designs: (1) we can measure the potential when the current is zero, (2) we can measure the potential while controlling the current, and (3) we can measure the current while controlling the potential. Each of these experimental designs relies on **Ohm's law**, which states that a current, i, passing through an electrical circuit of resistance, R, generates a potential, E.

$$E = iR \tag{11.1.2}$$

Each of these experimental designs uses a different type of instrument. To help us understand how we can control and measure current and potential, ***we will describe these instruments as if the analyst is operating them manually***. To do so the analyst observes a change in the current or the potential and manually adjusts the instrument's settings to maintain the desired experimental conditions. It is important to understand that modern electrochemical instruments provide an automated, electronic means for controlling and measuring current and potential, and that they do so by using very different electronic circuitry.

> **Note**
>
> For further information about electrochemical instrumentation, see this chapter's additional resources.

Potentiometers

To measure the potential of an electrochemical cell under a condition of zero current we use a **potentiometer**. Figure 11.3 shows a schematic diagram for a manual potentiometer, consisting of a power supply, an electrochemical cell with a working electrode and a counter electrode, an ammeter for measuring the current passing through the electrochemical cell, an adjustable, slide-wire resistor, and a tap key for closing the circuit through the electrochemical cell. Using Ohm's law, the current in the upper half of the circuit is

$$i_{up} = \frac{E_{PS}}{R_{ab}} \tag{11.1.3}$$

where E_{PS} is the power supply's potential, and R_{ab} is the resistance between points a and b of the slide-wire resistor. In a similar manner, the current in the lower half of the circuit is

$$i_{low} = \frac{E_{cell}}{R_{cb}} \tag{11.1.4}$$

where E_{cell} is the potential difference between the working electrode and the counter electrode, and R_{cb} is the resistance between the points c and b of the slide-wire resistor. When $i_{up} = i_{low} = 0$, no current flows through the ammeter and the potential of the electrochemical cell is

$$E_{cell} = \frac{R_{cb}}{R_{ab}} \times E_{PS} \tag{11.2}$$

To determine E_{cell} we momentarily press the tap key and observe the current at the ammeter. If the current is not zero, we adjust the slide wire resistor and remeasure the current, continuing this process until the current is zero. When the current is zero, we use equation 11.2 to calculate E_{cell}.

Using the tap key to momentarily close the circuit containing the electrochemical cell, minimizes the current passing through the cell and limits the change in the composition of the electrochemical cell. For example, passing a current of 10^{-9} A through the electrochemical cell for 1 s changes the concentrations of species in the cell by approximately 10^{-14} moles. Modern potentiometers use operational amplifiers to create a high-impedance voltmeter capable of measuring the potential while drawing a current of less than 10^{-9} A.

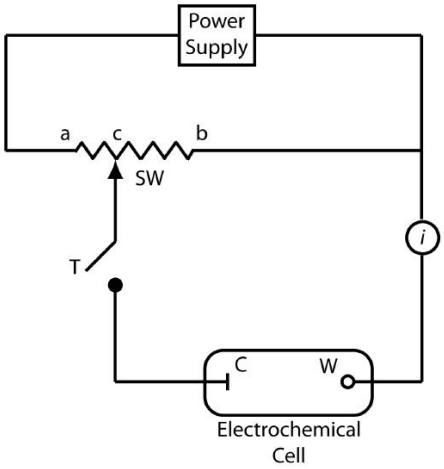


Figure 11.3 Schematic diagram of a manual potentiometer: C is the counter electrode; W is the working electrode; SW is a slide-wire resistor; T is a tap key and *i* is an ammeter for measuring current.

Galvanostats

A **galvanostat** allows us to control the current flowing through an electrochemical cell. A schematic diagram of a constant-current galvanostat is shown in Figure 11.4. The current flowing from the power supply through the working electrode is

$$i = \frac{E_{PS}}{R + R_{cell}} \tag{11.1.5}$$

where E_{PS} is the potential of the power supply, R is the resistance of the resistor, and R_{cell} is the resistance of the electrochemical cell. If $R >> R_{cell}$, then the current between the auxiliary and working electrodes is

$$i = \frac{E_{PS}}{R} \approx \text{constant} \tag{11.1.6}$$

To monitor the potential of the working electrode, which changes as the composition of the electrochemical cell changes, we can include an optional reference electrode and a high-impedance potentiometer.

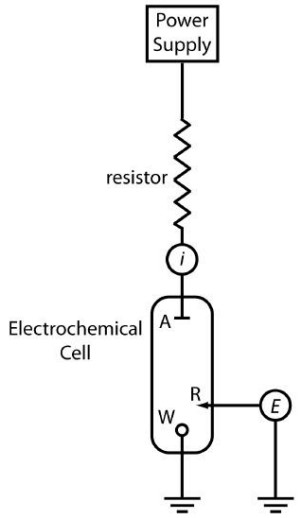


Figure 11.4 Schematic diagram of a galvanostat: A is the auxiliary electrode; W is the working electrode; R is an optional reference electrode, *E* is a high-impedance potentiometer, and *i* is an ammeter. The working electrode and the optional reference electrode are connected to a ground.

Potentiostats

A **potentiostat** allows us to control the potential of the working electrode. Figure 11.5 shows a schematic diagram for a manual potentiostat. The potential of the working electrode is measured relative to a constant-potential reference electrode that is connected to the working electrode through a high-impedance potentiometer. To set the working electrode's potential we adjust the slide wire resistor, which is connected to the auxiliary electrode. If the working electrode's potential begins to drift, we can adjust the slide wire resistor to return the potential to its initial value. The current flowing between the auxiliary electrode and the working electrode is measured with an ammeter. Modern potentiostats include waveform generators that allow us to apply a time-dependent potential profile, such as a series of potential pulses, to the working electrode.

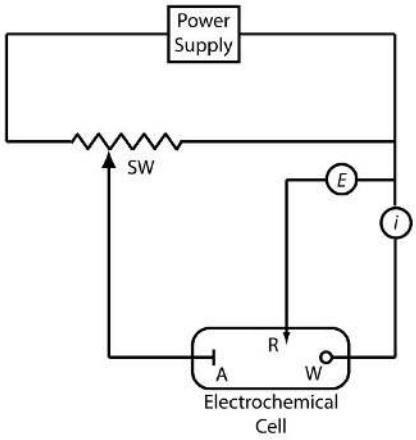


Figure 11.5 Schematic diagram for a manual potentiostat: W is the working electrode; A is the auxiliary electrode; R is the reference electrode; SW is a slide-wire resistor, *E* is a high-impendance potentiometer; and *i* is an ammeter.

11.1.3 Interfacial Electrochemical Techniques

Because this chapter focuses on interfacial electrochemical techniques, let's classify them into several categories. Figure 11.6 provides one version of a family tree highlighting the experimental conditions, the analytical signal, and the corresponding electrochemical techniques. Among the experimental conditions under our control are the potential or the current, and whether we stir the analyte's solution.

At the first level, we divide interfacial electrochemical techniques into static techniques and dynamic techniques. In a static technique we do not allow current to pass through the analyte's solution. Potentiometry, in which we measure the potential of an electrochemical cell under static conditions, is one of the most important quantitative electrochemical methods, and is discussed in detail in section 11.2.

Dynamic techniques, in which we allow current to flow through the analyte's solution, comprise the largest group of interfacial electrochemical techniques. Coulometry, in which we measure current as a function of time, is covered in Section 11.3. Amperometry and voltammetry, in which we measure current as a function of a fixed or variable potential, is the subject of Section 11.4.

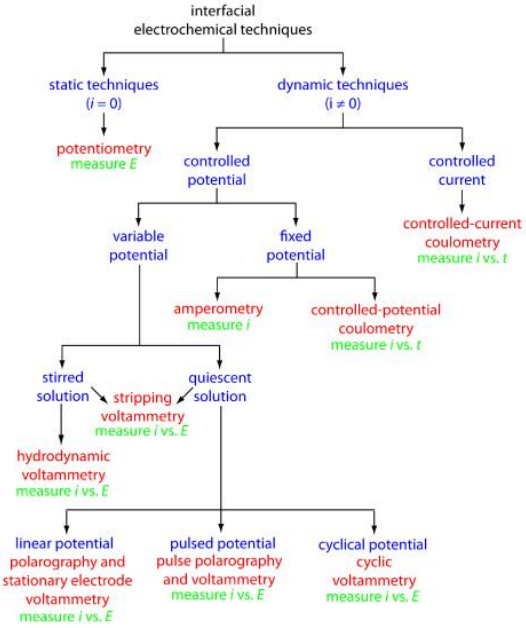


Figure 11.6 Family tree highlighting a number of interfacial electrochemical techniques. The specific techniques are shown in red, the experimental conditions are shown in blue, and the analytical signals are shown in green.

The material in this section—particularly the five important concepts—draws upon a vision for understanding electrochemistry outlined by Larry Faulkner in the article "Understanding Electrochemistry: Some Distinctive Concepts," *J. Chem. Educ.* **1983**, *60*, 262–264. See also, Kissinger, P. T.; Bott, A. W. "Electrochemistry for the Non-Electrochemist," *Current Separations*, **2002**, *20:2*, 51–53.

Contributors

David Harvey (DePauw University)

11.1: Overview of Electrochemistry is shared under a CC BY-NC-SA 4.0 license and was authored, remixed, and/or curated by LibreTexts.

11.2: Potentiometric Methods

In potentiometry we measure the potential of an electrochemical cell under static conditions. Because no current—or only a negligible current—flows through the electrochemical cell, its composition remains unchanged. For this reason, potentiometry is a useful quantitative method. The first quantitative potentiometric applications appeared soon after the formulation, in 1889, of the Nernst equation, which relates an electrochemical cell's potential to the concentration of electroactive species in the cell.[1]

Potentiometry initially was restricted to redox equilibria at metallic electrodes, limiting its application to a few ions. In 1906, Cremer discovered that the potential difference across a thin glass membrane is a function of pH when opposite sides of the membrane are in contact with solutions containing different concentrations of H_3O^+. This discovery led to the development of the glass pH electrode in 1909. Other types of membranes also yield useful potentials. For example, in 1937 Kolthoff and Sanders showed that a pellet of AgCl can be used to determine the concentration of Ag^+. Electrodes based on membrane potentials are called ion-selective electrodes, and their continued development extends potentiometry to a diverse array of analytes.

11.2.1 Potentiometric Measurements

As shown in Figure 11.3, we use a potentiometer to determine the difference between the potential of two electrodes. The potential of one electrode—the working or indicator electrode—responds to the analyte's activity, and the other electrode—the counter or reference electrode—has a known, fixed potential. In this section we introduce the conventions for describing potentiometric electrochemical cells, and the relationship between the measured potential and the analyte's activity.

Note

In Chapter 6 we noted that the equilibrium position of a chemical reaction is a function of the activities of the reactants and products, not their concentrations. To be correct, we should write the Nernst equation, such as equation 11.1, in terms of activities. So why didn't we use activities in Chapter 9 when we calculated redox titration curves? There are two reasons for that choice. First, concentrations are always easier to calculate than activities. Second, in a redox titration we determine the analyte's concentration from the titration's end point, not from the potential at the end point. The only reasons for calculating a titration curve is to evaluate its feasibility and to help in selecting a useful indicator. In most cases, the error we introduce by assuming that concentration and activity are identical is too small to be a significant concern.

In potentiometry we cannot ignore the difference between activity and concentration. Later in this section we will consider how we can design a potentiometric method so that we can ignore the difference between activity and concentration.

See Chapter 6.9 to review our earlier discussion of activity and concentration.

Potentiometric Electrochemical Cells

A schematic diagram of a typical potentiometric electrochemical cell is shown in Figure 11.7. The electrochemical cell consists of two half-cells, each containing an electrode immersed in a solution of ions whose activities determine the electrode's potential. A **salt bridge** containing an inert electrolyte, such as KCl, connects the two half-cells. The ends of the salt bridge are fixed with porous frits, allowing the electrolyte's ions to move freely between the half-cells and the salt bridge. This movement of ions in the salt bridge completes the electrical circuit.

By convention, we identify the electrode on the left as the anode and assign to it the oxidation reaction; thus

$$\mathrm{Zn}(s) \leftrightharpoons \mathrm{Zn}^{2+}(aq) + 2e^- \tag{11.2.1}$$

The electrode on the right is the **cathode**, where the reduction reaction occurs.

$$\mathrm{Ag}^+(aq) + e^- \leftrightharpoons \mathrm{Ag}(s) \tag{11.2.2}$$

Note

The reason for separating the electrodes is to prevent the oxidation and reduction reactions from occurring at one of the electrodes. For example, if we place a strip of Zn metal in a solution of $AgNO_3$, the reduction of Ag^+ to Ag occurs on the surface of the Zn at the same time as a potion of the Zn metal oxidizes to Zn^{2+}. Because the transfer of electrons from Zn to Ag^+ occurs at the electrode's surface, we can not pass them through the potentiometer.

The potential of the electrochemical cell in Figure 11.7 is for the reaction

$$\mathrm{Zn}(s) + 2\,\mathrm{Ag}^+(aq) \leftrightharpoons 2\,\mathrm{Ag}(s) + \mathrm{Zn}^{2+}(aq) \tag{11.2.3}$$

We also define potentiometric electrochemical cells such that the cathode is the indicator electrode and the anode is the reference electrode.

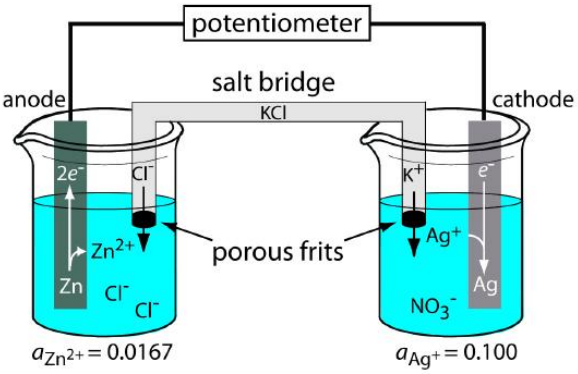


Figure 11.7 Example of a potentiometric electrochemical cell. The activities of Zn^{2+} and Ag^+ are shown below the two half-cells.

Shorthand Notation for Electrochemical Cells

Although Figure 11.7 provides a useful picture of an electrochemical cell, it is not a convenient representation. (Imagine having to draw a picture of each electrochemical cell you are using!) A more useful way to describe an electrochemical cell is a shorthand notation that uses symbols to identify different phases and that lists the composition of each phase. We use a vertical slash (|) to identify a boundary between two phases where a potential develops, and a comma (,) to separate species in the same phase or to identify a boundary between two phases where no potential develops. Shorthand cell notations begin with the anode and continue to the cathode. For example, we describe the electrochemical cell in Figure 11.7 using the following shorthand notation.

$$\mathrm{Zn}(s)\;|\,\mathrm{ZnCl_2}(aq, a_{\mathrm{Zn^{2+}}} = 0.0167)\,||\,\mathrm{AgNO_3}(aq, a_{\mathrm{Ag^+}} = 0.100)\,|\,\mathrm{Ag} \tag{11.2.4}$$

The double vertical slash (||) indicates the salt bridge, the contents of which we usually do not list. Note that a double vertical slash implies that there is a potential difference between the salt bridge and each half-cell.

Example 11.1

What are the anodic, cathodic, and overall reactions responsible for the potential of the electrochemical cell in Figure 11.8? Write the shorthand notation for the electrochemical cell.

Solution

The oxidation of Ag to Ag^+ occurs at the anode, which is the left half-cell. Because the solution contains a source of Cl^-, the anodic reaction is

$$\mathrm{Ag}(s) + \mathrm{Cl}^-(aq) \leftrightharpoons \mathrm{AgCl}(s) + e^- \tag{11.2.5}$$

The cathodic reaction, which is the right half-cell, is the reduction of Fe^{3+} to Fe^{2+}.

$$\mathrm{Fe}^{3+}(aq) + e^- \leftrightharpoons \mathrm{Fe}^{2+}(aq) \tag{11.2.6}$$

The overall cell reaction, therefore, is

$$\mathrm{Ag}(s) + \mathrm{Fe}^{3+}(aq) + \mathrm{Cl}^-(aq) \leftrightharpoons \mathrm{AgCl}(s) + \mathrm{Fe}^{2+}(aq) \tag{11.2.7}$$

The electrochemical cell's shorthand notation is

$$\begin{gathered}\mathrm{Ag}(s)\;|\,\mathrm{HCl}(aq,\, a_{\mathrm{Cl^-}} = 0.100),\ \mathrm{AgCl(sat'd)}\,| \\ |\,\mathrm{FeCl_2}(aq,\, a_{\mathrm{Fe^{2+}}} = 0.0100),\ \mathrm{FeCl_3}(aq,\, a_{\mathrm{Fe^{3+}}} = 0.0500)\,|\,\mathrm{Pt}(s)\end{gathered} \tag{11.2.8}$$

Note that the Pt cathode is an inert electrode that carries electrons to the reduction half-reaction. The electrode itself does not undergo reduction.

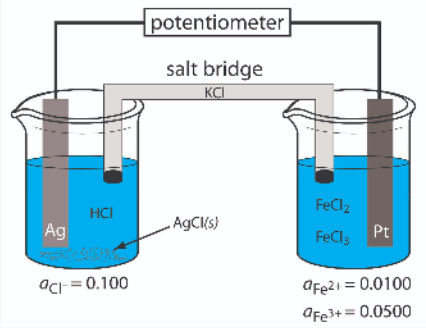


Figure 11.8 Potentiometric electrochemical cell for Example 11.1.

Exercise 11.1

Write the reactions occurring at the anode and the cathode for the potentiometric electrochemical cell with the following shorthand notation.

$$\mathrm{Pt}(s)\,|\,\mathrm{H_2}(g),\,\mathrm{H^+}(aq)\,||\,\mathrm{Cu^{2+}}(aq)\,|\,\mathrm{Cu}(s) \tag{11.2.9}$$

Click here to review your answer to this exercise.

Potential and Activity—The Nernst Equation

The potential of a potentiometric electrochemical cell is

$$E_{\text{cell}} = E_{\text{c}} - E_{\text{a}} \tag{11.3}$$

where E_{c} and E_{a} are reduction potentials for the redox reactions at the cathode and the anode. The reduction potentials are given by the Nernst equation

$$E = E^\circ - \frac{RT}{nF}\ln Q \tag{11.2.10}$$

where E^{o} is the standard-state reduction potential, R is the gas constant, T is the temperature in Kelvins, n is the number of electrons in the redox reaction, F is Faraday's constant, and Q is the reaction quotient. At a temperature of 298 K (25°C) the Nernst equation is

$$E = E^\circ - \frac{0.05916}{n}\log Q \tag{11.4}$$

where E is given in volts.

Note

See Section 6.4.4 for a review of the Nernst equation.

Using equation 11.4, the potential of the anode and cathode in Figure 11.7 are

$$E_{\text{a}} = E^\circ_{\text{Zn}^{2+}/\text{Zn}} - \frac{0.05916}{2}\log\frac{1}{a_{\text{Zn}^{2+}}} \tag{11.2.11}$$

$$E_{\text{c}} = E^\circ_{\text{Ag}^{+}/\text{Ag}} - \frac{0.05916}{1}\log\frac{1}{a_{\text{Ag}^{+}}} \tag{11.2.12}$$

Note

Even though an oxidation reaction is taking place at the anode, we define the anode's potential in terms of the corresponding reduction reaction and the standard-state reduction potential. See Section 6.4.4 for a review of using the Nernst equation in calculations.

Substituting $E_{\text{c}}$and E_{a} into equation 11.3, along with the activities of Zn^{2+} and Ag^{+} and the standard-state reduction potentials gives an E_{cell} of

$$E_{\text{cell}} = \left(E^{\circ}_{Ag^+/Ag} - \frac{0.05916}{1}\log\frac{1}{a_{Ag^+}}\right) - \left(E^{\circ}_{Zn^{2+}/Zn} - \frac{0.05916}{2}\log\frac{1}{a_{Zn^{2+}}}\right) \tag{11.2.13}$$

$$= \left(0.7996\text{ V} - 0.05916\log\frac{1}{0.100}\right) - \left(-0.7618 - \frac{0.05916}{2}\log\frac{1}{0.0167}\right) \tag{11.2.14}$$

$$= +1.555\text{ V} \tag{11.2.15}$$

Note

You will find values for the standard-state reduction potential in Appendix 13.

Example 11.2

What is the potential of the electrochemical cell shown in Example 11.1?

SOLUTION

Substituting E_c and E_a into equation 11.3, along with the concentrations of Fe^{3+}, Fe^{2+}, and Cl^- and the standard-state reduction potentials gives

$$E_{\text{cell}} = \left(E^{\circ}_{Fe^{3+}/Fe^{2+}} - \frac{0.05916}{1}\log\frac{a_{Fe^{2+}}}{a_{Fe^{3+}}}\right) - \left(E^{\circ}_{AgCl/Ag} - \frac{0.05916}{1}\log a_{Cl^-}\right) \tag{11.2.16}$$

$$= \left(0.771\text{ V} - 0.05916\log\frac{0.0100}{0.0500}\right) - (0.2223 - 0.05916\log(0.100)) \tag{11.2.17}$$

$$= +0.531\text{ V} \tag{11.2.18}$$

Exercise 11.2

What is the potential for the electrochemical cell in Practice Exercise 11.1 if the activity of H^+ in the anodic half-cell is 0.100, the fugacity of H_2 in the anodic half-cell is 0.500, and the activity of Cu^{2+} in the cathodic half-cell is 0.0500? Fugacity is the equivalent term for the activity of a gas.

Click here to review your answer to this exercise.

In potentiometry, we assign the reference electrode to the anodic half-cell and assign the indicator electrode to the cathodic half-cell. Thus, if the potential of the cell in Figure 11.7 is +1.50 V and the activity of Zn^{2+} is 0.0167, then we can solve the following equation for a_{Ag^+}

$$+1.50\text{ V} = \left(E^{\circ}_{Ag^+/Ag} - \frac{0.05916}{1}\log\frac{1}{a_{Ag^+}}\right) - \left(E^{\circ}_{Zn^{2+}/Zn} - \frac{0.05916}{2}\log\frac{1}{a_{Zn^{2+}}}\right) \tag{11.2.19}$$

$$= \left(+0.7996\text{ V} - 0.05916\log\frac{1}{a_{Ag^+}}\right) - \left(-0.7618 - \frac{0.05916}{2}\log\frac{1}{0.0167}\right) \tag{11.2.20}$$

obtaining an activity of 0.0118.

Example 11.3

What is the activity of Fe^{3+} in an electrochemical cell similar to that in Example 11.1 if the activity of Cl^- in the left-hand cell is 1.0, the activity of Fe^{2+} in the right-hand cell is 0.015, and E_{cell} is +0.546 V?

Solution

Making appropriate substitutions into equation 11.3

$$+0.546\text{ V} = \left(+0.771\text{ V} - 0.05916\log\frac{0.0151}{a_{Fe^{3+}}}\right) - (+0.2223 - 0.05916\log(1.0)) \tag{11.2.21}$$

and solving for $a_{Fe^{3+}}$ gives its activity as 0.0136.

Exercise 11.3

What is the activity of Cu^{2+} in the electrochemical cell in Practice Exercise 11.1 if the activity of H^+ in the anodic half-cell is 1.00 with a fugacity of 1.00 for H_2, and an E_{cell} of +0.257 V?

Click here to review your answer to this exercise.

Despite the apparent ease of determining an analyte's activity using the Nernst equation, there are several problems with this approach. One problem is that standard-state potentials are temperature-dependent, and the values in reference tables usually are for a temperature of 25°C. We can overcome this problem by maintaining the electrochemical cell at 25°C or by measuring the standard-state potential at the desired temperature.

> **Note**
>
> The standard-state reduction potentials in Appendix 13, for example, are for 25°C.

Another problem is that standard-sate reduction potentials may show significant matrix effects. For example, the standard-state reduction potential for the Fe^{3+}/Fe^{2+} redox couple is +0.735 V in 1 M $HClO_4$, +0.70 V in 1 M HCl, and +0.53 V in 10 M HCl. The difference in potential for equimolar solutions of HCl and $HClO_4$ is the result of a difference in the activity coefficients for Fe^{3+} and Fe^{2+} in these two media. The shift toward a more negative potential with an increase in the concentration of HCl is the result of chloride's ability to form a stronger complex with Fe^{3+} than with Fe^{2+}. We can minimize this problem by replacing the standardstate potential with a matrix-dependent formal potential. Most tables of standard-state potentials, including those in Appendix 13, include selected formal potentials.

A more serious problem is the presence of additional potentials in the electrochemical cell not included in equation 11.3. In writing the shorthand notation for an electrochemical cell we use a double slash (||) to indicate the salt bridge, suggesting a potential exists at the interface between each end of the salt bridge and the solution in which it is immersed. The origin of this potential is discussed in the following section.

Junction Potentials

A **junction potential** develops at the interface between two ionic solution if there difference in the concentration and mobility of the ions. Consider, for example, a porous membrane separating solutions of 0.1 M HCl and 0.01 M HCl (Figure 11.9a). Because the concentration of HCl on the membrane's left side is greater than that on the right side of the membrane, H^+ and Cl^- diffuse in the direction of the arrows. The mobility of H^+, however, is greater than that for Cl^-, as shown by the difference in the lengths of their respective arrows. Because of this difference in mobility, the solution on the right side of the membrane has an excess of H^+ and a positive charge (Figure 11.9b). Simultaneously, the solution on the membrane's left side develops a negative charge because there is an excess concentration of Cl^-. We call this difference in potential across the membrane a junction potential, which we represent as E_j.

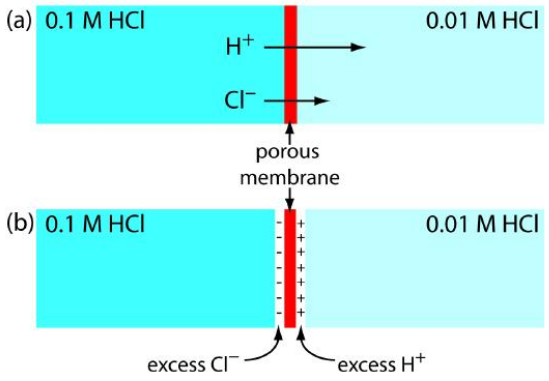


Figure 11.9 *Origin of the junction potential between a solution of 0.1 M HCl and a solution of 0.01 M HCl.*

The magnitude of the junction potential depends upon the concentration of ions on the two sides of the interface, and may be as large as 30–40 mV. For example, a junction potential of 33.09 mV has been measured at the interface between solutions of 0.1 M HCl and 0.1 M NaCl.[2] The magnitude of a salt bridge's junction potential is minimized by using a salt, such as KCl, for which the mobilities of the cation and anion are approximately equal. We can also minimize the magnitude of the junction potential by incorporating a high concentration of the salt in the salt bridge. For this reason salt bridges are frequently constructed using solutions that are saturated with KCl. Nevertheless, a small junction potential, generally of unknown magnitude, is always present.

When we measure the potential of an electrochemical cell the junction potential also contributes to E_{cell}; thus, we rewrite equation 11.3

$$E_{cell} = E_c - E_a + E_j \tag{11.2.22}$$

to include its contribution. If we do not know the junction potential's actual value—which is the usual situation—then we cannot directly calculate the analyte's concentration using the Nernst equation. Quantitative analytical work is possible, however, if we use one of the standardization methods discussed in Chapter 5.3.

> **Note**
>
> These standardization methods are external standards, the method of standard additions, and internal standards. We will return to this point later in this section.

11.2.2 Reference Electrodes

In a potentiometric electrochemical cell one half-cell provides a known reference potential and the potential of the other half-cell indicates the analyte's concentration. By convention, the reference electrode is the anode; thus, the short hand notation for a potentiometric electrochemical cell is

$$\text{reference} \,||\, \text{indicator} \tag{11.2.23}$$

and the cell potential is

$$E_{cell} = E_{ind} - E_{ref} + E_j \tag{11.2.24}$$

The ideal reference electrode provides a stable, known potential so that any change in *E*cell is attributed to analyte's effect on the potential of the indicator electrode. In addition, the ideal reference electrode should be easy to make and to use. Three common reference electrodes are discussed in this section.

Standard Hydrogen Electrode

Although we rarely use the **standard hydrogen electrode** (SHE) for routine analytical work, it is the reference electrode used to establish standard-state potentials for other half-reactions. The SHE consists of a Pt electrode immersed in a solution in which the activity of hydrogen ion is 1.00 and in which the fugacity of $H_2(g)$ is 1.00 (Figure 11.10). A conventional salt bridge connects the SHE to the indicator half-cell. The short hand notation for the standard hydrogen electrode is

$$\text{Pt}(s),\ \text{H}_2(g,\ f_{\text{H}_2} = 1.00)\ |\ \text{H}^+(aq,\ a_{\text{H}^+} = 1.00)\ ||\ \tag{11.2.25}$$

and the standard-state potential for the reaction

$$\text{H}^+(aq) + e^- \rightleftharpoons \frac{1}{2}\text{H}_2(g) \tag{11.2.26}$$

is, by definition, 0.00 V at all temperatures. Despite its importance as the fundamental reference electrode against which we measure all other potentials, the SHE is rarely used because it is difficult to prepare and inconvenient to use.

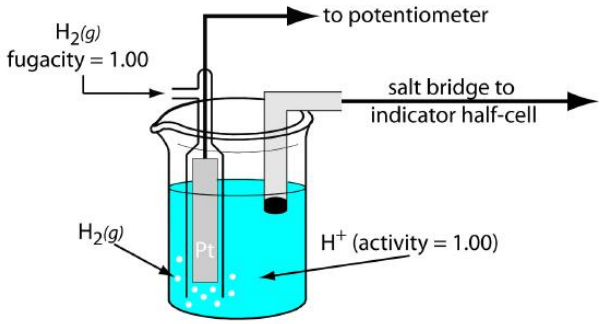


Figure 11.10 Schematic diagram showing the standard hydrogen electrode.

Calomel Electrodes

> **Note**
>
> Calomel is the common name for the compound Hg_2Cl_2.

Calomel reference electrodes are based on the following redox couple between Hg_2Cl_2 and Hg

$$Hg_2Cl_2(s) + 2e^- \leftrightharpoons 2\,Hg(l) + 2\,Cl^-(aq) \tag{11.2.27}$$

for which the Nernst equation is

$$E = E^\circ_{Hg_2Cl_2/Hg} - \frac{0.05916}{2}\log\,(a_{Cl^-})^2 = +0.268\text{ V} - \frac{0.05916}{2}\log\,(a_{Cl^-})^2 \tag{11.2.28}$$

The potential of a calomel electrode, therefore, is determined by the activity of Cl^- in equilibrium with Hg and Hg_2Cl_2.

As shown in Figure 11.11, in a **saturated calomel electrode** (SCE) the concentration of Cl^- is determined by the solubility of KCl. The electrode consists of an inner tube packed with a paste of Hg, Hg_2Cl_2, and KCl, situated within a second tube containing a saturated solution of KCl. A small hole connects the two tubes and a porous wick serves as a salt bridge to the solution in which the SCE is immersed. A stopper in the outer tube provides an opening for adding addition saturated KCl. The short hand notation for this cell is

$$Hg(l)\;|\,Hg_2Cl_2(s),\,KCl(aq,\,\text{sat'd})\,||\tag{11.2.29}$$

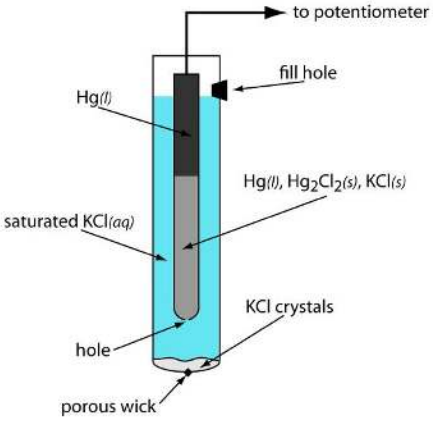


Figure 11.11 Schematic diagram showing the saturated calomel electrode.

Because the concentration of Cl^- is fixed by the solubility of KCl, the potential of an SCE remains constant even if we lose some of the solution to evaporation. A significant disadvantage of the SCE is that the solubility of KCl is sensitive to a change in temperature. At higher temperatures the solubility of KCl increases and the electrode's potential decreases. For example, the potential of the SCE is +0.2444 V at 25°C and +0.2376 V at 35°C. The potential of a calomel electrode containing an unsaturated solution of KCl is less temperature dependent, but its potential changes if the concentration, and thus the activity of Cl^-, increases due to evaporation.

> **Note**
>
> The potential of a calomel electrode is +0.280 V when the concentration of KCl is 1.00 M and +0.336 V when the concentration of KCl is 0.100 M. If the activity of Cl^- is 1.00, the potential is +0.2682 V.

Silver/Silver Chloride Electrodes

Another common reference electrode is the **silver/silver chloride electrode**, which is based on the following redox couple between AgCl and Ag.

$$AgCl(s) + e^- \leftrightharpoons Ag(s) + Cl^-(aq) \tag{11.2.30}$$

As is the case for the calomel electrode, the activity of Cl^- determines the potential of the Ag/AgCl electrode; thus

$$E = E^{\circ}_{\text{AgCl/Ag}} - 0.05916 \log a_{\text{Cl}^-} = +0.2223 \text{ V} - 0.05916 \log a_{\text{Cl}^-} \tag{11.2.31}$$

When prepared using a saturated solution of KCl, the potential of a Ag/AgCl electrode is +0.197 V at 25°C. Another common Ag/AgCl electrode uses a solution of 3.5 M KCl and has a potential of +0.205 V at 25°C.

> **Note**
>
> As you might expect, the potential of a Ag/AgCl electrode using a saturated solution of KCl is more sensitive to a change in temperature than an electrode using an unsaturated solution of KCl.

A typical Ag/AgCl electrode is shown in Figure 11.12 and consists of a silver wire, the end of which is coated with a thin film of AgCl, immersed in a solution containing the desired concentration of KCl. A porous plug serves as the salt bridge. The electrode's short hand notation is

$$\text{Ag}(s) \,|\, \text{AgCl}(s), \text{KCl}(aq, a_{\text{Cl}^-} = x) \,||\, \tag{11.2.32}$$

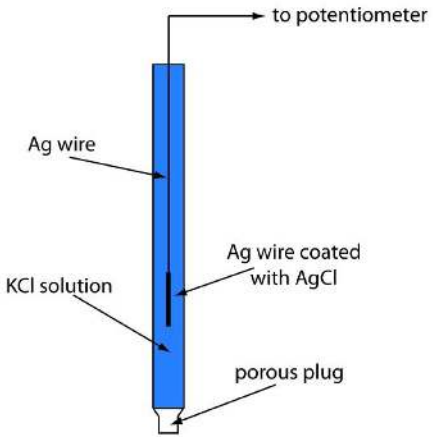


Figure 11.12 Schematic diagram showing a Ag/AgCl electrode. Because the electrode does not contain solid KCl, this is an example of an unsaturated Ag/AgCl electrode.

Converting Potentials Between Reference Electrodes

The standard state reduction potentials in most tables are reported relative to the standard hydrogen electrode's potential of +0.00 V. Because we rarely use the SHE as a reference electrode, we need to be able to convert an indicator electrode's potential to its equivalent value when using a different reference electrode. As shown in the following example, this is easy to do.

> **Example 11.4**
>
> The potential for an Fe^{3+}/Fe^{2+} half-cell is +0.750 V relative to the standard hydrogen electrode. What is its potential when using a saturated calomel electrode or a saturated silver/silver chloride electrode?
>
> ***Solution***
>
> When using a standard hydrogen electrode the potential of the electrochemical cell is
>
> $$E_{\text{cell}} = E_{\text{Fe}^{3+}/\text{Fe}^{2+}} - E_{\text{SHE}} = 0.750 \text{ V} - 0.000 \text{ V} = +0.750 \text{ V} \tag{11.2.33}$$
>
> We can use the same equation to calculate the potential when using a saturated calomel electrode
>
> $$E_{\text{cell}} = E_{\text{Fe}^{3+}/\text{Fe}^{2+}} - E_{\text{SCE}} = 0.750 \text{ V} - 0.2444 \text{ V} = +0.506 \text{ V} \tag{11.2.34}$$
>
> or a saturated silver/silver chloride electrode
>
> $$E_{\text{cell}} = E_{\text{Fe}^{3+}/\text{Fe}^{2+}} - E_{\text{Ag/AgCl}} = 0.750 \text{ V} - 0.197 \text{ V} = +0.553 \text{ V} \tag{11.2.35}$$
>
> Figure 11.13 provides a pictorial representation of the relationship between these different potentials.

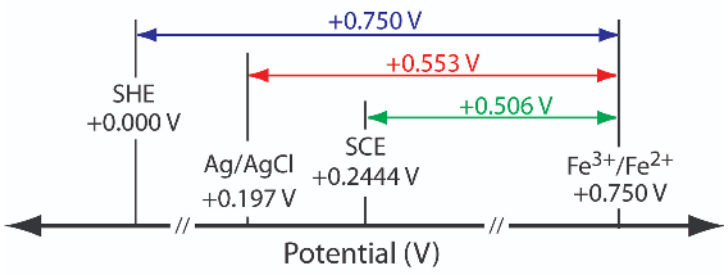


Figure 11.13 Relationship between the potential of an Fe^{3+}/Fe^{2+} half-cell relative to the reference electrodes in Example 11.4. The potential relative to a standard hydrogen electrode is shown in blue, the potential relative to a saturated silver/silver chloride electrode is shown in red, and the potential relative to a saturated calomel electrode is shown in green.

Practice Exercise 11.4

The potential of a UO_2^{+}/U^{4+} half-cell is –0.0190 V relative to a saturated calomel electrode. What is its potential when using a saturated silver/silver chloride electrode or a standard hydrogen electrode?

Click here to review your answer to this exercise.

11.2.3 Metallic Indicator Electrodes

In potentiometry the potential of the indicator electrode is proportional to the analyte's activity. Two classes of indicator electrodes are used in potentiometry: metallic electrodes, which are the subject of this section, and ion-selective electrodes, which are covered in the next section.

Electrodes of the First Kind

If we place a copper electrode in a solution containing Cu^{2+}, the electrode's potential due to the reaction

$$Cu^{2+}(aq) + 2e^- \leftrightharpoons Cu(aq) \tag{11.2.36}$$

is determined by the activity of Cu^{2+}.

$$E = E^\circ_{Cu^{2+}/Cu} - \frac{0.05916}{2}\log\frac{1}{a_{Cu^{2+}}} = +0.3419\,V - \frac{0.05916}{2}\log\frac{1}{a_{Cu^{2+}}} \tag{11.2.37}$$

If copper is the indicator electrode in a potentiometric electrochemical cell that also includes a saturated calomel reference electrode

$$SCE \,||\, Cu^{2+}(aq,\, a_{Cu^{2+}} = x)\,|\,Cu(s) \tag{11.2.38}$$

then we can use the cell potential to determine an unknown activity of Cu^{2+} in the indicator electrode's half-cell

$$E_{cell} = E_{ind} - E_{SCE} + E_j = +0.3419\,V - \frac{0.05916}{2}\log\frac{1}{a_{Cu^{2+}}} - 0.2444\,V + E_j \tag{11.2.39}$$

An indicator electrode in which a metal is in contact with a solution containing its ion is called an **electrode of the first kind**. In general, if a metal, M, is in a solution of M^{n+}, the cell potential is

$$E_{cell} = K - \frac{0.05916}{n}\log\frac{1}{a_{Mn^+}} = K + \frac{0.05916}{n}\log a_{Mn^+} \tag{11.2.40}$$

where K is a constant that includes the standard-state potential for the M^{n+}/M redox couple, the potential of the reference electrode, and the junction potential. For a variety of reasons—including the slow kinetics of electron transfer at the metal–solution interface, the formation of metal oxides on the electrode's surface, and interfering reactions—electrodes of the first kind are limited to the following metals: Ag, Bi, Cd, Cu, Hg, Pb, Sn, Tl, and Zn.

Note

Many of these electrodes, such as Zn, cannot be used in acidic solutions because they are easily oxidized by H^+.

$$\mathrm{Zn}(s) + 2\,\mathrm{H^+}(aq) \leftrightharpoons \mathrm{H_2}(g) + \mathrm{Zn^{2+}}(aq) \tag{11.2.41}$$

Electrodes of the Second Kind

The potential of an electrode of the first kind responds to the activity of M^{n+}. We also can use this electrode to determine the activity of another species if it is in equilibrium with M^{n+}. For example, the potential of a Ag electrode in a solution of Ag^+ is

$$E = E^\circ_{\mathrm{Ag^+/Ag}} - 0.05916 \log \frac{1}{a_{\mathrm{Ag^+}}} = +0.7996\ \mathrm{V} - 0.05916 \log \frac{1}{a_{\mathrm{Ag^+}}} \tag{11.5}$$

If we saturate the indicator electrode's half-cell with AgI, the solubility reaction

$$\mathrm{AgI}(s) \leftrightharpoons \mathrm{Ag^+}(aq) + \mathrm{I^-}(aq) \tag{11.2.42}$$

determines the concentration of Ag^+; thus

$$a_{\mathrm{Ag^+}} = \frac{K_{\mathrm{sp,AgI}}}{a_{\mathrm{I^-}}} \tag{11.6}$$

where $K_{\mathrm{sp,\,AgI}}$ is the solubility product for AgI. Substituting equation 11.6 into equation 11.5

$$E_{\mathrm{cell}} = +0.7996\ \mathrm{V} - 0.05916 \log \frac{a_{\mathrm{I^-}}}{K_{\mathrm{sp,AgI}}} \tag{11.2.43}$$

we find that the potential of the silver electrode is a function of the activity of I^-. If we incorporate this electrode into a potentiometric electrochemical cell with a saturated calomel electrode

$$\mathrm{SCE} \,||\, \mathrm{AgI}(s), \mathrm{I^-}(aq, a_{\mathrm{I^-}} = x) \,|\, \mathrm{Ag}(s) \tag{11.2.44}$$

the cell potential is

$$E_{\mathrm{cell}} = K - 0.05916 \log a_{\mathrm{I^-}} \tag{11.2.45}$$

where K is a constant that includes the standard-state potential for the Ag^+/Ag redox couple, the solubility product for AgI, the reference electrode's potential, and the junction potential.

If an electrode of the first kind responds to the activity of an ion that is in equilibrium with M^{n+}, we call it an **electrode of the second kind**. Two common electrodes of the second kind are the calomel and the silver/silver chloride reference electrodes.

> **Note**
>
> In an electrode of the second kind we link together a redox reaction and another reaction, such as a solubility reaction. You might wonder if we can link together more than two reactions. The short answer is yes. An electrode of the third kind, for example, links together a redox reaction and two other reactions. We will not consider such electrodes in this text.

Redox Electrodes

An electrode of the first kind or second kind develops a potential as the result of a redox reaction involving a metallic electrode. An electrode also can serve as a source of electrons or as a sink for electrons in an unrelated redox reaction, in which case we call it a **redox electrode**. The Pt cathode in Figure 11.8 and Example 11.1 is a redox electrode because its potential is determined by the activity of Fe^{2+} and Fe^{3+} in the indicator half-cell. Note that a redox electrode's potential often responds to the activity of more than one ion, which can limit its usefulness for direct potentiometry.

11.2.4 Membrane Electrodes

If metals are the only useful materials for constructing indicator electrodes, then there would be few useful applications of potentiometry. In 1901 Fritz Haber discovered that there is a change in potential across a glass membrane when its two sides are in solutions of different acidity. The existence of this **membrane potential** led to the development of a whole new class of indicator electrodes called **ion-selective electrodes** (ISEs). In addition to the glass pH electrode, ion-selective electrodes are available for a wide range of ions. It also is possible to construct a membrane electrode for a neutral analyte by using a chemical reaction to generate an ion that can be monitored with an ion-selective electrode. The development of new membrane electrodes continues to be an active area of research.

Membrane Potentials

Figure 11.14 shows a typical potentiometric electrochemical cell equipped with an ion-selective electrode. The short hand notation for this cell is

$$\text{reference(sample)} \;||\; [\text{A}]_{\text{samp}}(aq,\, a_{\text{A}} = x) \;|\; [\text{A}]_{\text{int}}(aq,\, a_{\text{A}} = y) \;||\; \text{reference(internal)} \tag{11.2.46}$$

where the ion-selective membrane is shown by the vertical slash separating the two solutions containing analyte—the sample solution and the ion-selective electrode's internal solution. The electrochemical cell includes two reference electrodes: one immersed in the ion-selective electrode's internal solution and one in the sample. The cell potential, therefore, is

$$E_{\text{cell}} = E_{\text{ref(int)}} - E_{\text{ref(samp)}} + E_{\text{mem}} + E_{\text{j}} \tag{11.7}$$

where E_{mem} is the potential across the membrane. Because the junction potential and the potential of the two reference electrodes are constant, any change in E_{cell} is a result of a change in the membrane's potential.

The analyte's interaction with the membrane generates a membrane potential if there is a difference in its activity on the membrane's two sides.

> **Note**
>
> For now we simply note that a difference in the analyte's activity results in a membrane potential. As we consider different types of ion-selective electrodes, we will explore more specifically the source of the membrane potential.

Current is carried through the membrane by the movement of either the analyte or an ion already present in the membrane's matrix. The membrane potential is given by the following Nernst-like equation

$$E_{\text{mem}} = E_{\text{asym}} - \frac{RT}{zF} \ln \frac{(a_{\text{A}})_{\text{int}}}{(a_{\text{A}})_{\text{samp}}} \tag{11.8}$$

where $(a_{\text{A}})_{\text{samp}}$ is the analyte's concentration in the sample, $(a_{\text{A}})_{\text{int}}$ is the concentration of analyte in the ion-selective electrode's internal solution, and z is the analyte's charge. Ideally, E_{mem} is zero when $(a_{\text{A}})_{\text{int}}$ = $(a_{\text{A}})_{\text{samp}}$. The term E_{asym}, which is an **asymmetry potential**,accounts for the fact that E_{mem} is usually not zero under these conditions.

> **Note**
>
> E_{asym} in equation 11.8 is similar to E^{o} in equation 11.1.

Substituting equation 11.8 into equation 11.7, assuming a temperature of 25°C, and rearranging gives

$$E_{\text{cell}} = K + \frac{0.05916}{z} \log (a_{\text{A}})_{\text{samp}} \tag{11.9}$$

where K is a constant that includes the potentials of the two reference electrodes, the junction potentials, the asymmetry potential, and the analyte's activity in the internal solution. Equation 11.9 is a general equation and applies to all types of ion-selective electrodes.

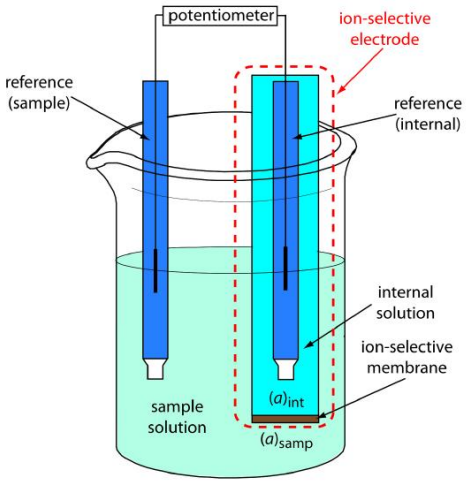


Figure 11.14 Schematic diagram showing a typical potentiometric cell with an ion-selective electrode. The ion-selective electrode's membrane separates the sample, which contains the analyte at an activity of $(a_A)_{samp}$, from an internal solution containing the analyte with an activity of $(a_A)_{int}$.

Selectivity of Membranes

A membrane potential results from a chemical interaction between the analyte and active sites on the membrane's surface. Because the signal depends on a chemical process, most membranes are not selective toward a single analyte. Instead, the membrane potential is proportional to the concentration of each ion that interacts with the membrane's active sites. We can rewrite equation 11.9 to include the contribution of an interferent, I, to the potential

$$E_{cell} = K + \frac{0.05916}{z_A} \log \left\{ a_A + K_{A,I}(a_I)^{z_A/z_I} \right\} \tag{11.2.47}$$

where z_A and z_I are the charges of the analyte and the interferent, and $K_{A,I}$ is a **selectivity coefficient** accounting for the relative response of the interferent. The selectivity coefficient is defined as

$$K_{A,I} = \frac{(a_A)_e}{(a_I)_e^{z_A/z_I}} \tag{11.10}$$

where $(a_A)_e$ and $(a_I)_e$ are the activities of analyte and interferent yielding identical cell potentials. When the selectivity coefficient is 1.00 the membrane responds equally to the analyte and the interferent. A membrane shows good selectivity for the analyte when $K_{A,I}$ is significantly less than 1.00.

> **Note**
>
> See Chapter 3.4.4 for an additional discussion of selectivity.

Selectivity coefficients for most commercially available ion-selective electrodes are provided by the manufacturer. If the selectivity coefficient is not known, it is easy to determine its value experimentally by preparing a series of solutions, each containing the same activity of interferent, $(a_I)_{add}$, but a different activity of analyte. As shown in Figure 11.15, a plot of cell potential versus the log of the analyte's activity has two distinct linear regions. When the analyte's activity is significantly larger than $K_{A,I} \times (a_I)_{add}$, the potential is a linear function of $\log(a_A)$, as given by equation 11.9. If $K_{A,I} \times (a_I)_{add}$ is significantly larger than the analyte's activity, however, the cell potential remains constant. The activity of analyte and interferent at the intersection of these two linear regions is used to calculate $K_{A,I}$.

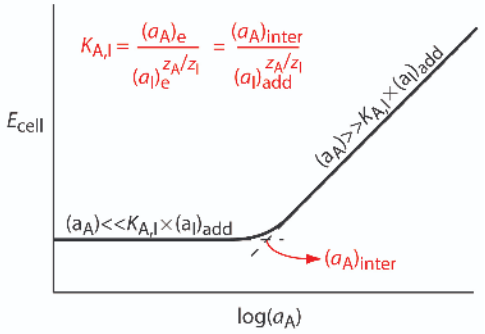


Figure 11.15 *Diagram showing the experimental determination of an ion-selective electrode's selectivity for an analyte. The activity of analyte corresponding to the intersection of the two linear portions of the curve, $(a_A)_{inter}$, produces a cell potential identical to that of the interferent. The equation for the selectivity coefficient, $K_{A,I}$, is shown in red.*

Example 11.5

Sokalski and co-workers described a method for preparing ion-selective electrodes with significantly improved selectivities.[3] For example, a conventional Pb^{2+} ISE has a $\log K_{Pb^{2+}/Mg^{2+}}$ of –3.6. If the potential for a solution in which the activity of Pb^{2+} is 4.1×10^{-12} is identical to that for a solution in which the activity of Mg^{2+} is 0.01025, what is the value of $\log K_{Pb^{2+}/Mg^{2+}}$?

Solution

Making appropriate substitutions into equation 11.10, we find that

$$K_{Pb^{2+}/Mg^{2+}} = \frac{(a_A)_e}{(a_I)_e^{z_A/z_I}} = \frac{4.1\times10^{-12}}{(0.01025)^{2+/2+}} = 4.0\times10^{-10} \qquad (11.2.48)$$

The value of $\log K_{Pb^{2+}/Mg^{2+}}$, therefore, is –9.40.

Exercise 11.5

A ion-selective electrode for NO_2^- has $\log K_{A,I}$ values of –3.1 for F^-, –4.1 for SO_4^{2-}, –1.2 for I^-, and –3.3 for NO_3^-. Which ion is the most serious interferent and for what activity of this interferent is the potential equivalent to a solution in which the activity of NO_2^- is 2.75×10^{-4}?

Click here to review your answer to this exercise

Glass Ion-Selective Electrodes

The first commercial **glass electrodes** were manufactured using Corning 015, a glass with a composition that is approximately 22% Na_2O, 6% CaO and 72% SiO_2. When immersed in an aqueous solution for several hours, the outer approximately 10 nm of the membrane's surface becomes hydrated, resulting in the formation of negatively charged sites, —SiO^-. Sodium ions, Na^+, serve as counter ions. Because H^+ binds more strongly to —SiO^- than does Na^+, they displace the sodium ions

$$H^+ + -SiO-\,Na^+ \leftrightharpoons -SiO-\,H^+ + Na^+ \qquad (11.2.49)$$

giving rise to the membrane's selectivity for H^+. The transport of charge across the membrane is carried by the Na^+ ions. The potential of a glass electrode using Corning 015 obeys the equation

$$E_{cell} = K + 0.05916 \log a_{H^+} \qquad (11.11)$$

over a pH range of approximately 0.5 to 9. At more basic pH levels the glass membrane is more responsive to other cations, such as Na^+ and K^+.

Example 11.6

For a Corning 015 glass membrane the selectivity coefficient K_{H^+/Na^+} is $\approx 10^{-11}$. What is the expected error when measuring the pH of a solution in which the activity of H^+ is 2×10^{-13} and the activity of Na^+ is 0.05?

Solution

A solution in which the actual activity of H^+, $(a_{H^+})_{act}$, is 2×10^{-13} has a pH of 12.7. (pH = –log(a_{H^+})) Because the electrode responds to both H^+ and Na^+, the apparent activity of H^+, $(a_{H^+})_{app}$, is

$$(a_{H^+})_{app} = (a_{H^+})_{act} + (K_{H^+/Na^+} \times a_{Na^+}) \quad (11.2.50)$$

$$= 2 \times 10^{-13} + (10^{-11} \times 0.05) \quad (11.2.51)$$

$$= 7 \times 10^{-13}\ M \quad (11.2.52)$$

The apparent activity of H^+ is equivalent to a pH of 12.2, an error of –0.5 pH units.

Replacing Na_2O and CaO with Li_2O and BaO extends the useful pH range of glass membrane electrodes to pH levels greater than 12.

Glass membrane pH electrodes are often available in a combination form that includes both the indicator electrode and the reference electrode. The use of a single electrode greatly simplifies the measurement of pH. An example of a typical combination electrode is shown in Figure 11.16.

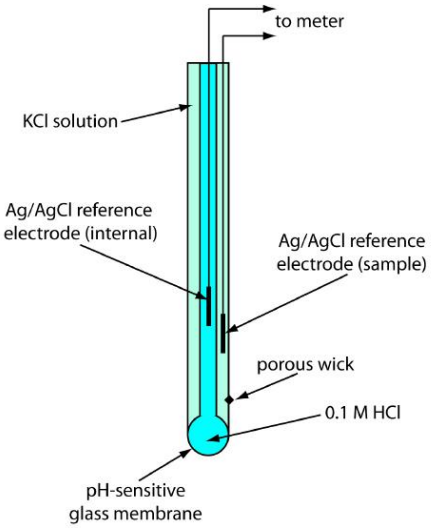


Figure 11.16 Schematic diagram showing a combination glass electrode for measuring pH. The indicator electrode consists of a pH-sensitive glass membrane and an internal Ag/AgCl reference electrode in a solution of 0.1 M HCl. The sample's reference electrode is a Ag/AgCl electrode in a solution of KCl (which may be saturated with KCl or contain a fixed concentration of KCl). A porous wick serves as a salt bridge between the sample and its reference electrode.

The observation that the Corning 015 glass membrane responds to ions other than H^+ (see Example 11.6) led to the development of glass membranes with a greater selectivity for other cations. For example, a glass membrane with a composition of 11% Na_2O, 18% Al_2O_3, and 71% SiO_2 is used as an ion-selective electrode for Na^+. Other glass ion-selective electrodes have been developed for the analysis of Li^+, K^+, Rb^+, Cs^+, NH_4^+, Ag^+, and Tl^+. Table 11.1 provides several examples.

Because the typical thickness of an ion-selective electrode's glass membrane is about 50 μm, they must be handled carefully to avoid cracks or breakage. Glass electrodes usually are stored in a solution of a suitable storage buffer recommended by the manufacturer, which ensures that the membrane's outer surface is fully hydrated. If your glass electrode does dry out, you must recondition it by soaking for several hours in a solution containing the analyte. The composition of a glass membrane changes over time, affecting the electrode's performance. The average lifetime for a typical glass electrode is several years.

Table 11.1 Representative Examples of Glass Membrane Ion-Selective Electrodes for Analytes Other than H

analyte	membrane composition	selectivity coefficients[a]
Na^+	11% Na_2O, 18% Al_2O_3,71% SiO_2	$K_{Na^+/H^+} = 1000$ $K_{Na^+/K^+} = 0.001$ $K_{Na^+/Li^+} = 0.001$
Li^+	15% Li_2O, 25% Al_2O_3, 60% SiO_2	$K_{Li^+/Na^+} = 0.3$ $K_{Li^+/K^+} = 0.001$
K^+	27% Na_2O, 5% Al_2O_3, 68% SiO_2	$K_{K^+/Na^+} = 0.05$

[a] Selectivity coefficients are approximate; values found experimentally may vary substantially from the listed values. See Cammann, K. *Working With Ion-Selective Electrodes*, Springer-Verlag: Berlin, 1977.

Solid-State Ion-Selective Electrodes

A **solid-state ion-selective electrode** uses a membrane consisting of either a polycrystalline inorganic salt or a single crystal of an inorganic salt. We can fashion a polycrystalline solid-state ion-selective electrode by sealing a 1–2 mm thick pellet of Ag_2S—or a mixture of Ag_2S and a second silver salt or another metal sulfide—into the end of a nonconducting plastic cylinder, filling the cylinder with an internal solution containing the analyte, and placing a reference electrode into the internal solution. Figure 11.17 shows a typical design.

> **Note**
>
> The NaCl in a salt shaker is an example of polycrystalline material because it consists of many small crystals of sodium chloride. The NaCl salt plates shown in Figure 10.32a, on the other hand, are an example of a single crystal of sodium chloride.

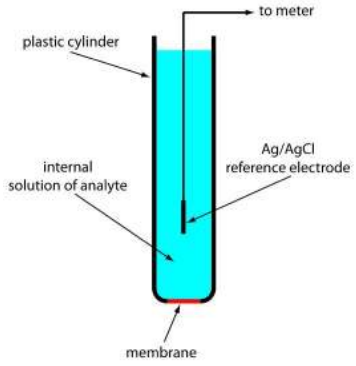


Figure 11.17 Schematic diagram of a solid-state electrode. The internal solution contains a solution of analyte of fixed activity.

The membrane potential for a Ag_2S pellet develops as the result of a difference in the extent of the solubility reaction

$$Ag_2S(s) \leftrightharpoons 2\,Ag^+(aq) + S^{2-}(aq) \tag{11.2.53}$$

on the membrane's two sides, with charge carried across the membrane by Ag^+ ions. When we use the electrode to monitor the activity of Ag^+, the cell potential is

$$E_{cell} = K + 0.05916 \log a_{Ag^+} \tag{11.2.54}$$

The membrane also responds to the activity of S^{2-}, with a cell potential of

$$E_{cell} = K - \frac{0.05916}{2} \log a_{S^{2-}} \tag{11.2.55}$$

If we combine an insoluble silver salt, such as AgCl, with the Ag_2S, then the membrane potential also responds to the concentration of Cl^-, with a cell potential of

$$E_{cell} = K - 0.05916 \log a_{Cl^-} \tag{11.2.56}$$

By mixing Ag_2S with CdS, CuS, or PbS, we can make an ion-selective electrode that responds to the activity of Cd^{2+}, Cu^{2+}, or Pb^{2+}. In this case the cell potential is

$$E_{cell} = K + \frac{0.05916}{2} \log a_{M^{2+}} \tag{11.2.57}$$

where $a_{M^{2+}}$ is the activity of the metal ion.

Table 11.2 provides examples of polycrystalline, Ag_2S-based solid-state ion-selective electrodes. The selectivity of these ion-selective electrodes is determined by the relative solubility of the compounds. A Cl^- ISE using a Ag_2S/AgCl membrane is more selective for Br^- ($K_{Cl^-/Br^-} = 10^2$) and for I^- ($K_{Cl^-/I^-} = 10^6$) because AgBr and AgI are less soluble than AgCl. If the activity of Br^- is sufficiently high, AgCl at the membrane/solution interface is replaced by AgBr and the electrode's response to Cl^- decreases substantially. Most of the polycrystalline ion-selective electrodes listed in Table 11.2 can be used over an extended range of pH levels. The equilibrium between S^{2-} and HS^- limits the analysis for S^{2-} to a pH range of 13–14.

Table 11.2 Representative Examples of Polycrystalline Solid-State Ion-Selective Electrodes

analyte	membrane composition	selectivity coefficients[a]
Ag^+	Ag_2S	$K_{Ag^+/Cu^{2+}} = 10^{-6}$ $K_{Ag^+/Pb^{2+}} = 10^{-10}$ Hg^{2+} interferes
Cd^{2+}	CdS/Ag_2S	$K_{Cd^{2+}/Fe^{2+}} = 200$ $K_{Cd^{2+}/Pb^{2+}} = 6$ Ag^+, Hg^{2+}, and Cu^{2+} must be absent
Cu^{2+}	CuS/Ag_2S	$K_{Cu^{2+}/Fe^{3+}} = 10$ $K_{Cd^{2+}/Cu^+} = 1$ Ag^+ and Hg^{2+} must be absent
Pb^{2+}	PbS/Ag_2S	$K_{Pb^{2+}/Fe^{3+}} = 1$ $K_{Pb^{2+}/Cd^{2+}} = 1$ Ag^+, Hg^{2+}, and Cu^{2+} must be absent
Br^-	$AgBr/Ag_2S$	$K_{Br^-/I^-} = 5000$ $K_{Br^-/Cl^-} = 0.005$ $K_{Br^-/OH^-} = 10^{-5}$ S^{2-} must be absent
Cl^-	$AgCl/Ag_2S$	$K_{Cl^-/I^-} = 10^6$ $K_{Cl^-/Br^-} = 100$ $K_{Cl^-/OH^-} = 0.01$ S^{2-}must be absent
I^-	AgI/Ag_2S	$K_{I^-/S^{2-}} = 30$ $K_{I^-/Br^-} = 10^{-4}$ $K_{I^-/Cl^-} = 10^{-6}$ $K_{I^-/OH^-} = 10^{-7}$
SCN^-	$AgSCN/Ag_2S$	$K_{SCN^-/I^-} = 10^3$ $K_{SCN^-/Br^-} = 100$ $K_{SCN^-/Cl^-} = 0.1$ $K_{SCN^-/OH^-} = 0.01$ S^{2-} must be absent
S^{2-}	Ag_2S	Hg^{2+} interferes

[a] Selectivity coefficients are approximate; values found experimentally may vary substantially from the listed values. See Cammann, K. *Working With Ion-Selective Electrodes*, Springer-Verlag: Berlin, 1977.

The membrane of a F^- ion-selective electrode is fashioned from a single crystal of LaF_3, which is usually doped with a small amount of $EuF_2$to enhance the membrane's conductivity. Because EuF_2 provides only two F^-ions—compared to the three F^- ions in LaF_3—each EuF_2 produces a vacancy in the crystal's lattice. Fluoride ions pass through the membrane by moving into adjacent vacancies. As shown in Figure 11.17, the LaF_3membrane is sealed into the end of a non-conducting plastic cylinder, which contains a standard solution of F^-, typically 0.1 M NaF, and a Ag/AgCl reference electrode.

The membrane potential for a F^- ISE results from a difference in the solubility of LaF_3 on opposite sides of the membrane, with the potential given by

$$E_{cell} = K - 0.05916 \log a_{F^-} \quad (11.2.58)$$

One advantage of the F^- ion-selective electrode is its freedom from interference. The only significant exception is OH^- (K_{F^-/OH^-} = 0.1), which imposes a maximum pH limit for a successful analysis.

Example 11.7

What is the maximum pH that we can tolerate if we wish to analyze a solution in which the activity of F^- is 1×10^{-5} and if the error is to be less than 1%?

Solution

In the presence of OH^- the cell potential is

$$E_{cell} = K - 0.05916 \log \left\{ a_{F^-} + K_{F^-/OH^-} \times a_{OH^-} \right\} \quad (11.2.59)$$

To achieve an error of less than 1%, the term $K_{F^-/OH^-} \times a_{OH^-}$ must be less than 1% of a_{F^-}; thus

$$K_{F^-/OH^-} \times a_{OH^-} \leq 0.01 \times a_{F^-} \quad (11.2.60)$$

$$0.10 \times a_{OH^-} \leq 0.01 \times (1 \times 10^{-5}) \quad (11.2.61)$$

Solving for a_{OH^-} gives its maximum allowable activity as 1×10^{-6}, which corresponds to a pH of less than 8.

Practice Exercise 11.6

Suppose you wish to use the nitrite-selective electrode in Practice Exercise 11.5 to measure the activity of NO_2^-. If the activity of NO_2^- is 2.2×10^{-4}, what is the maximum pH you can tolerate if the error due to OH^- is to be less than 10%? The selectivity coefficient for OH^-, K_{NO2^-/OH^-}, is 630. Do you expect the electrode to have a lower pH limit? Clearly explain your answer.

Click here to review your answer to this exercise.

Below a pH of 4 the predominate form of fluoride in solution is HF, which does not contribute to the membrane potential. For this reason, an analysis for fluoride must be carried out at a pH greater than 4.

Unlike a glass membrane ion-selective electrodes, a solid-state ISE does not need to be conditioned before it is used, and it may be stored dry. The surface of the electrode is subject to poisoning, as described above for a Cl^- ISE in contact with an excessive concentration of Br^-. If an electrode is poisoned, it can be returned to its original condition by sanding and polishing the crystalline membrane.

Note

Poisoning simply means that the surface has been chemically modified, such as AgBr forming on the surface of a AgCl membrane.

Liquid-Based Ion-Selective Electrodes

Another class of ion-selective electrodes uses a hydrophobic membrane containing a liquid organic complexing agent that reacts selectively with the analyte. Three types of organic complexing agents have been used: cation exchangers, anion exchangers, and neutral ionophores. A membrane potential exists if the analyte's activity is different on the two sides of the membrane. Current is carried through the membrane by the analyte.

Note

An **ionophore** is a ligand whose exterior is hydrophobic and whose interior is hydrophilic. The crown ether shown here



is one example of an neutral ionophore.

One example of a **liquid-based ion-selective electrode** is that for Ca^{2+}, which uses a porous plastic membrane saturated with the cation exchanger di-(*n*-decyl) phosphate. As shown in Figure 11.18, the membrane is placed at the end of a non-conducting cylindrical tube, and is in contact with two reservoirs. The outer reservoir contains di-(*n*-decyl) phosphate in di-*n*-octylphenylphosphonate, which soaks into the porous membrane. The inner reservoir contains a standard aqueous solution of Ca^{2+} and a Ag/AgCl reference electrode. Calcium ion-selective electrodes are also available in which the di-(*n*-decyl) phosphate is immobilized in a polyvinyl chloride (PVC) membrane, eliminating the need for the outer reservoir containing di-(*n*-decyl) phosphate.

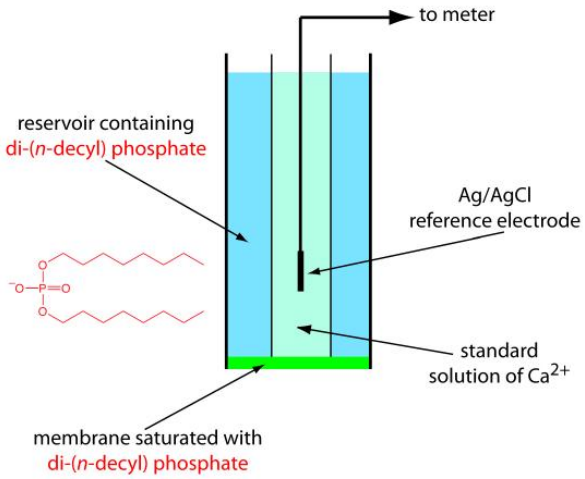


Figure 11.18 Schematic diagram showing a liquid- based ion-selective electrode for Ca^{2+}. The structure of the cation exchanger, di-(*n*-decyl) phosphate, is shown in red.

The membrane potential for the Ca^{2+} ISE develops as the result of a difference in the extent of the complexation reaction

$$Ca^{2+}(aq) + 2\,(C_{10}H_{21}O)_2PO_2^-(mem) \leftrightharpoons Ca[(C_{10}H_{21}O)_2PO_2]_2(mem) \tag{11.2.62}$$

on the two sides of the membrane, where (*mem*) indicates a species that is present in the membrane. The cell potential for the Ca^{2+} ion-selective electrode is

$$E_{cell} = K + \frac{0.05916}{2}\log a_{Ca^{2+}} \tag{11.2.63}$$

The selectivity of this electrode for Ca^{2+} is very good, with only Zn^{2+} showing greater selectivity.

Table 11.3 lists the properties of several liquid-based ion-selective electrodes. An electrode using a liquid reservoir can be stored in a dilute solution of analyte and needs no additional conditioning before use. The lifetime of an electrode with a PVC membrane, however, is proportional to its exposure to aqueous solutions. For this reason these electrodes are best stored by covering the membrane with a cap along with a small amount of wetted gauze to maintain a humid environment. Before using the electrode it is conditioned in a solution of analyte for 30–60 minutes.

Table 11.3 Representative Examples of Liquid-Based Ion-Selective Electrodes

analyte	membrane composition	selectivity coefficients[a]
Ca^{2+}	di-(*n*-decyl) phosphate in PVC	$K_{Ca^{2+}/Zn^{2+}}$ = 1–5 $K_{Ca^{2+}/Al^{3+}}$ = 0.90 $K_{Ca^{2+}/Mn^{2+}}$ = 0.38 $K_{Ca^{2+}/Cu^{2+}}$ = 0.070 $K_{Ca^{2+}/Mg^{2+}}$ = 0.032
K^+	valinomycin in PVC	K_{K^+/Rb^+} = 1.9 K_{K^+/Cs^+} = 0.38 K_{K^+/Li^+} = 10^{-4} K_{K^+/Na^+} = 10^{-5}
Li^+	ETH 149 in PVC	K_{Li^+/H^+} = 1 K_{Li^+/Na^+} = 0.05 K_{Li^+/K^+} = 0.007
NH_4^+	nonactin and monactin in PVC	K_{NH4^+/K^+} = 0.12 K_{NH4^+/H^+} = 0.016 K_{NH4^+/Li^+} = 0.0042 K_{NH4^+/Na^+} = 0.002
ClO_4^-	$Fe(o\text{-phen})_3^{3+}$ in *p*-nitrocymene with porous membrane	K_{ClO4^-/OH^-} = 1 K_{ClO4^-/I^-} = 0.012 $K_{ClO4^-/NO3^-}$ = 0.0015 K_{ClO4^-/Br^-} = 5.6×10^{-4} K_{ClO4^-/Cl^-} = 2.2×10^{-4}
NO_3^-	tetradodecyl ammonium nitrate in PVC	K_{NO3^-/Cl^-} = 0.006 K_{NO3^-/F^-} = 9×10^{-4}

[a] Selectivity coefficients are approximate; values found experimentally may vary substantially from the listed values. See Cammann, K. *Working With Ion-Selective Electrodes*, Springer-Verlag: Berlin, 1977.

Gas-Sensing Electrodes

A number of membrane electrodes respond to the concentration of a dissolved gas. The basic design of a **gas-sensing electrode** is shown in Figure 11.19, consisting of a thin membrane that separates the sample from an inner solution containing an ion-selective electrode. The membrane is permeable to the gaseous analyte, but impermeable to nonvolatile components in the sample's matrix. The gaseous analyte passes through the membrane where it reacts with the inner solution, producing a species whose concentration is monitored by the ion-selective electrode. For example, in a CO_2 electrode, CO_2 diffuses across the membrane where it reacts in the inner solution to produce H_3O^+.

$$\mathrm{CO_2}(aq) + 2\,\mathrm{H_2O}(l) \leftrightharpoons \mathrm{HCO_3^-}(aq) + \mathrm{H_3O^+}(aq) \tag{11.12}$$

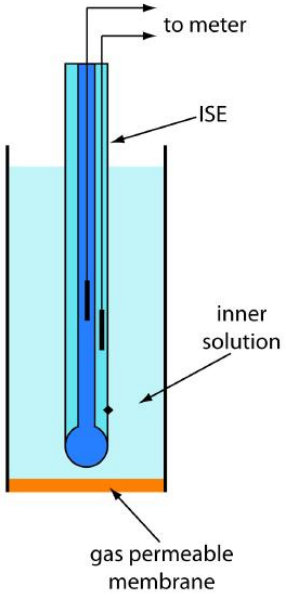


Figure 11.19 Schematic diagram of a gas-sensing membrane electrode.

The change in the activity of H_3O^+ in the inner solution is monitored with a pH electrode, for which the cell potential is given by equation 11.11. To find the relationship between the activity of H_3O^+ in the inner solution and the activity CO_2 in the inner solution we rearrange the equilibrium constant expression for reaction 11.10; thus

$$a_{H_3O^+} = K_a \times \frac{a_{CO_2}}{a_{HCO_3^-}} \tag{11.13}$$

where K_a is the equilibrium constant. If the activity of HCO_3^- in the internal solution is sufficiently large, then its activity is not affected by the small amount of CO_2 that passes through the membrane. Substituting equation 11.13 into equation 11.11 gives

$$E_{cell} = K' + 0.05916 \log a_{CO_2} \tag{11.2.64}$$

where K′ is a constant that includes the constant for the pH electrode, the equilibrium constant for reaction 11.12 and the activity of HCO_3^- in the inner solution.

Table 11.4 lists the properties of several gas-sensing electrodes. The composition of the inner solution changes with use, and both the inner solution and the membrane must be replaced periodically. Gas-sensing electrodes are stored in a solution similar to the internal solution to minimize their exposure to atmospheric gases.

Table 11.4 Representative Examples of Gas-Sensing Electrodes

analyte	inner solution	reaction in inner solution	ion-selective electrode
CO_2	10 mM $NaHCO_3$ 10 mM NaCl	$CO_2(aq) + 2\,H_2O(l) \leftrightharpoons HCO_3^-(aq) + H_3O^+(aq)$	glass pH ISE
HCN	10 mM $KAg(CN)_2$	$HCN(aq) + H_2O(l) \leftrightharpoons CN^-(aq) + H_3O^+(aq)$	Ag_2S solid-state ISE
HF	1 M H_3O^+	$HF(aq) + H_2O(l) \leftrightharpoons F^-(aq) + H_3O^+(aq)$	F^- solid-state ISE
H_2S	pH 5 citrate buffer	$H_2S(aq) + H_2O(l) \leftrightharpoons HS^-(aq) + H_3O^+(aq)$	Ag_2S solid-state ISE
NH_3	10 mM NH_4Cl 0.1 M KNO_3	$NH_3(aq) + H_2O(l) \leftrightharpoons NH_4^+(aq) + OH^-(aq)$	glass pH ISE
NO_2	20 mM $NaNO_2$ 0.1 M KNO_3	$2\,NO_2(aq) + 3\,H_2O(l) \leftrightharpoons NO_3^-(aq) + NO_2^-(aq) + 2\,H_3O^+(aq)$	glass pH ISE
SO_2	1 mM $NaHSO_3$ pH 5	$SO_2(aq) + 2\,H_2O(l) \leftrightharpoons HSO_3^-(aq) + H_3O^+(aq)$	glass pH ISE

Source: Cammann, K. *Working With Ion-Selective Electrodes*, Springer-Verlag: Berlin, 1977.

Potentiometric Biosensors

The approach for developing gas-sensing electrodes can be modified to create potentiometric electrodes that respond to a biochemically important species. The most common class of potentiometric biosensors are **enzyme electrodes**, in which we trap or immobilize an enzyme at the surface of a potentiometric electrode. The analyte's reaction with the enzyme produces a product whose concentration is monitored by the potentiometric electrode. Potentiometric biosensors have also been designed around other biologically active species, including antibodies, bacterial particles, tissues, and hormone receptors.

One example of an enzyme electrode is the urea electrode, which is based on the catalytic hydrolysis of urea by urease

$$CO(NH_2)_2(aq) + 2\,H_2O(l) \leftrightharpoons 2\,NH_4^+(aq) + CO_3^{2-}(aq) \tag{11.2.65}$$

Figure 11.20 shows one version of the urea electrode, which modifies a gas-sensing NH_3 electrode by adding a dialysis membrane that traps a pH 7.0 buffered solution of urease between the dialysis membrane and the gas permeable membrane.[4] (An NH_3 electrode, as shown in Table 11.4, uses a gas-permeable membrane and a glass pH electrode. The NH_3 diffuses across the membrane where it changes the pH of the internal solution.) When immersed in the sample, urea diffuses through the dialysis membrane where it reacts with the enzyme urease to form the ammonium ion, NH_4^+, which is in equilibrium with NH_3.

$$NH_4^+(aq) + H_2O(l) \leftrightharpoons H_3O^+(aq) + NH_3(aq) \tag{11.2.66}$$

The NH_3, in turn, diffuses through the gas permeable membrane where a pH electrode measures the resulting change in pH. The response of the electrode to the concentration of urea is given by

$$E_{cell} = K - (0.05916) \log a_{urea} \tag{11.14}$$

> **Note**
>
> Problem 11.7 asks you to show that equation 11.14 is correct.

https://chem.libretexts.org/@go/page/70710

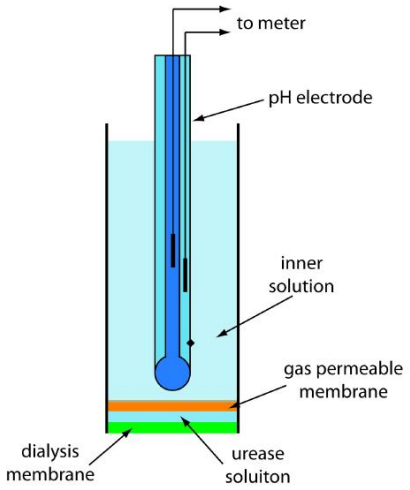


Figure 11.20 Schematic diagram showing an enzyme-based potentiometric biosensor for urea. A solution of the enzyme urease is trapped between a dialysis membrane and a gas permeable membrane. Urea diffuses across the dialysis membrane and reacts with urease, producing NH_3 that diffuses across the gas permeable membrane. The resulting change in the internal solution's pH is measured with the pH electrode.

Another version of the urea electrode (Figure 11.21) immobilizes the enzyme urease in a polymer membrane formed directly on the tip of a glass pH electrode.[5] In this case the response of the electrode is

$$\mathrm{pH} = K a_{\mathrm{urea}} \tag{11.15}$$

> **Note**
>
> Problem 11.8 asks you to explain the difference between equation 11.14 and equation 11.15.

Few potentiometric biosensors are commercially available. As shown in Figure 11.20 and Figure 11.21, however, it is possible to convert an ionselective electrode or a gas-sensing electrode into a biosensor. Several representative examples are described in Table 11.5, and additional examples can be found in this chapter's additional resources.

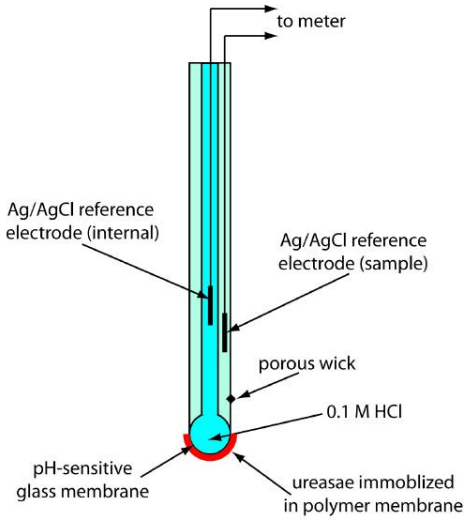


Figure 11.21 Schematic diagram of an enzyme-based potentiometric biosensor for urea in which urease is immobilized in a polymer membrane coated onto the pH-sensitive glass membrane of a pH electrode.

Table 11.5 Representative Examples of Potentiometric Biosensors

analyte	biologically active phase[b]	substance determined
5′-adenosinemonophosphate (5′-AMP)	AMP-deaminase (E)	NH_3
L-arginine	arginine and urease (E)	NH_3
asparagine	asparaginase (E)	NH_4^+
L-cysteine	*Proteus morganii* (B)	H_2S
L-glutamate	yellow squash (T)	CO_2
L-glutamine	*Sarcina flava* (B)	NH_3
oxalate	oxalate decarboxylas (E)	CO_2
penicillin	pencillinase (E)	H_3O^+
L-phenylalanine	L-amino acid oxidase / horseradish peroxidase (E)	I^-
sugars	bacteria from dental plaque (B)	H_3O^+
urea	urease (E)	NH_3 or H_3O^+

[a] Source: Complied from Cammann, K. *Working With Ion-Selective Electrodes*, Springer-Verlag: Berlin, 1977 and Lunte, C. E.; Heineman, W. R. "Electrochemical techniques in Bioanalysis," in Steckham, E. ed. *Topics in Current Chemistry*, Vol. 143, Springer-Verlag: Berlin, 1988, p.8.

[b] Abbreviations: E = enzyme; B = bacterial particle; T = tissue.

11.2.5 Quantitative Applications

The potentiometric determination of an analyte's concentration is one of the most common quantitative analytical techniques. Perhaps the most frequent analytical measurement is the determination of a solution's pH, a measurement we will consider in more detail later in this section. Other areas where potentiometry is important are clinical chemistry, environmental chemistry, and potentiometric titrations. Before considering representative applications, however, we need to examine more closely the relationship between cell potential and the analyte's concentration and methods for standardizing potentiometric measurements.

Activity and Concentration

The Nernst equation relates the cell potential to the analyte's activity. For example, the Nernst equation for a metallic electrode of the first kind is

$$E_{\text{cell}} = K + \frac{0.05916}{n} \log a_{M^{n+}} \tag{11.16}$$

where $a_{M^{n+}}$ is the activity of the metal ion. When we use a potentiometric electrode, however, our goal is to determine the analyte's concentration. As we learned in Chapter 6, an ion's activity is the product of its concentration, $[M^{n+}]$, and a matrix-dependent activity coefficient, $\gamma_{M^{n+}}$.

$$a_{M^{n+}} = [M^{n+}]\gamma_{M^{n+}} \tag{11.17}$$

Substituting equation 11.17 into equation 11.16 and rearranging, gives

$$E_{\text{cell}} = K + \frac{0.05916}{n} \log \gamma_{M^{n+}} + \frac{0.05916}{n} \log [M^{n+}] \tag{11.18}$$

We can solve equation 11.18 for the metal ion's concentration if we know the value for its activity coefficient. Unfortunately, if we do not know the exact ionic composition of the sample's matrix—which is the usual situation—then we cannot calculate the value of $\gamma_{M^{n+}}$. There is a solution to this dilemma. If we design our system so that the standards and the samples have an identical matrix, then the value of $\gamma_{M^{n+}}$ remains constant and equation 11.18 simplifies to

$$E_{cell} = K' + \frac{0.05916}{n} \log[M^{n+}] \quad (11.2.67)$$

where K^′ includes the activity coefficient.

Quantitative Analysis using External Standards

Before determining the concentration of analyte in a sample it is necessary to standardize the electrode. If the electrode's response obeys the Nernst equation, then we only need to determine the constant K using a single external standard. Because a small deviation from the ideal slope of $\pm RT/nF$ or $\pm RT/zF$ is not unexpected, we usually choose to use two or more external standards.

> **Note**
>
> To review the use of external standards, see Section 5.3.2.

In the absence of interferents, a calibration curve of E_{cell} versus $\log a_A$, where A is the analyte, is a straight line. A plot of E_{cell} versus log[A], however, may show curvature at higher concentrations of analyte as a result of a matrix-dependent change in the analyte's activity coefficient. To maintain a consistent matrix we can add a high concentration of inert electrolyte to all samples and standards. If the concentration of added electrolyte is sufficient, the difference between the sample's matrix and that of the standards does not affect the ionic strength and the activity coefficient remains essentially constant. The inert electrolyte that we add to the sample and standards is called a **total ionic strength adjustment buffer** (TISAB).

> **Example 11.8**
>
> The concentration of Ca^{2+} in a water sample is determined using the method of external standards. The ionic strength of the samples and the standards was maintained at a nearly constant level by making each solution 0.5 M in KNO_3. The measured cell potentials for the external standards are shown in the following table.

$[Ca^{2+}]$ (M)	E_{cell} (V)
1.00×10^{-5}	–0.125
5.00×10^{-5}	–0.103
1.00×10^{-4}	–0.093
5.00×10^{-4}	–0.072
1.00×10^{-3}	–0.065
5.00×10^{-3}	–0.043
1.00×10^{-2}	–0.033

What is the concentration of Ca^{2+} in a water sample if its cell potential is found to be –0.084 V?

Solution

Linear regression gives the calibration curve shown in Figure 11.22, with an equation of

$$E_{cell} = 0.027 + 0.0303 \log[Ca^{2+}] \quad (11.2.68)$$

Substituting the sample's cell potential gives the concentration of Ca^{2+} as 2.17×10^{-4} M. Note that the slope of the calibration curve, which is 0.0303, is slightly larger than its ideal value of 0.05916/2 = 0.02958; this is not unusual and is one reason for using multiple standards.

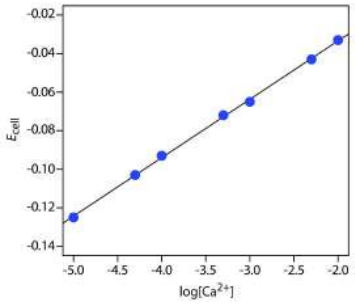


Figure 11.22 Calibration curve for the data in Example 11.8.

Quantitative Analysis using the Method of Standard Additions

Another approach to calibrating a potentiometric electrode is the method of standard additions. First, we transfer a sample with a volume of V_A and an analyte concentration of C_A into a beaker and measure the potential, $(E_{cell})_A$. Next, we make a standard addition by adding to the sample a small volume, V_{std}, of a standard containing a known concentration of analyte, C_{std}, and measure the potential, $(E_{cell})_{std}$. If V_{std} is significantly smaller than V_A, then we can safely ignore the change in the sample's matrix and assume that analyte's activity coefficient is constant. Example 11.9 demonstrates how we can use a one-point standard addition to determine the concentration of analyte in a sample.

Note

To review the method of standard additions, see Section 5.3.3.

Example 11.9

The concentration of Ca^{2+} in a sample of sea water is determined using a Ca ion-selective electrode and a one-point standard addition. A 10.00-mL sample is transferred to a 100-mL volumetric flask and diluted to volume. A 50.00-mL aliquot of the sample is placed in a beaker with the Ca ISE and a reference electrode, and the potential is measured as –0.05290 V. After adding a 1.00-mL aliquot of a 5.00×10^{-2} M standard solution of Ca^{2+} the potential is –0.04417 V. What is the concentration of Ca^{2+} in the sample of sea water?

Solution

To begin, we write the Nernst equation before and after adding the standard addition. The cell potential for the sample is

$$(E_{cell})_A = K + \frac{0.05916}{2} \log C_A \tag{11.2.69}$$

and that following the standard addition is

$$(E_{cell})_{std} = K + \frac{0.05916}{2} \log \left\{ \frac{V_A}{V_{tot}} C_A + \frac{V_{std}}{V_{tot}} C_{std} \right\} \tag{11.2.70}$$

where V_{tot} is the total volume (V_A + V_{std}) after the standard addition. Subtracting the first equation from the second equation gives

$$\begin{aligned} \Delta E_{cell} &= (E_{cell})_{std} - (E_{cell})_A \\ &= \frac{0.05916}{2} \log \left\{ \frac{V_A}{V_{tot}} C_A + \frac{V_{std}}{V_{tot}} C_{std} \right\} - \frac{0.05916}{2} \log C_A \end{aligned} \tag{11.2.71}$$

Rearranging this equation leaves us with

$$\frac{2\Delta E_{cell}}{0.05916} = \log \left\{ \frac{V_A}{V_{tot}} + \frac{V_{std} C_{std}}{V_{tot} C_A} \right\} \tag{11.2.72}$$

Substituting known values for ΔE, V_A, V_{std}, V_{tot} and C_{std},

$$\begin{aligned} \frac{2 \times \{-0.04471 - (-0.05290)\}}{0.05916} \\ = \log \left\{ \frac{50.00\ \text{mL}}{51.00\ \text{mL}} + \frac{(1.00\ \text{mL}) \times (5.00 \times 10^{-2}\ \text{M})}{(51.00\ \text{mL}) \times C_A} \right\} \end{aligned} \tag{11.2.73}$$

$$0.2951 = \log \left\{ 0.9804 + \frac{9.804 \times 10^{-4}}{C_A} \right\} \tag{11.2.74}$$

and taking the inverse log of both sides gives

$$1.973 = 0.9804 + \frac{9.804 \times 10^{-4}}{C_A} \tag{11.2.75}$$

Finally, solving for C_A gives the concentration of Ca^{2+} as 9.88×10^{-4} M. Because we diluted the original sample of seawater by a factor of 10, the concentration of Ca^{2+} in the seawater sample is 9.88×10^{-3} M.

Free Ions Versus Complexed Ions

Most potentiometric electrodes are selective toward the free, uncomplexed form of the analyte, and do not respond to any of the analyte's complexed forms. This selectivity provides potentiometric electrodes with a significant advantage over other quantitative methods of analysis if we need to determine the concentration of free ions. For example, calcium is present in urine both as free Ca^{2+} ions and as protein-bound Ca^{2+} ions. If we analyze a urine sample using atomic absorption spectroscopy, the signal is proportional to the total concentration of Ca^{2+} because both free and bound calcium are atomized. Analyzing urine with a Ca^{2+} ISE, however, gives a signal that is a function of only free Ca^{2+} ions because the protein-bound Ca^{2+} can not interact with the electrode's membrane.

Note

The best way to appreciate the theoretical and practical details discussed in this section is to carefully examine a typical analytical method. Although each method is unique, the following description of the determination of F^- in toothpaste provides an instructive example of a typical procedure. The description here is based on Kennedy, J. H. *Analytical Chemistry—Practice*, Harcourt Brace Jaovanovich: San Diego, 1984, p. 117–118.

Representative Method 11.1

Determination of Fluoride in Toothpaste

Description of the Method

The concentration of fluoride in toothpastes containing soluble F^- may be determined with a F^- ion-selective electrode using a calibration curve prepared with external standards. Although the F^- ISE is very selective (only OH^- with a K_{F^-/OH^-} of 0.1 is a significant interferent), Fe^{3+} and Al^{3+} interfere with the analysis because they form soluble fluoride complexes that do not interact with the ion-selective electrode's membrane. This interference is minimized by reacting any Fe^{3+} and Al^{3+} with a suitable complexing agent.

Procedure

(Problem 11.14 provides some actual data for the determination of fluoride in toothpaste.)

Prepare 1 L of a standard solution of 1.00% w/v SnF_2 and transfer it to a plastic bottle for storage. Using this solution, prepare 100 mL each of standards containing 0.32%, 0.36%, 0.40%, 0.44% and 0.48% w/v SnF_2, adding 400 mg of malic acid to each solution as a stabilizer. Transfer the standards to plastic bottles for storage. Prepare a total ionic strength adjustment buffer (TISAB) by mixing 500 mL of water, 57 mL of glacial acetic acid, 58 g of NaCl, and 4 g of disodium DCTA (*trans*-1,2-cyclohexanetetraacetic acid) in a 1-L beaker, stirring until dissolved. Cool the beaker in a water bath and add 5 M NaOH until the pH is between 5–5.5. Transfer the contents of the beaker to a 1-L volumetric flask and dilute to volume. Prepare each external standard by placing approximately 1 g of a fluoride-free toothpaste, 30 mL of distilled water, and 1.00 mL of standard into a 50-mL plastic beaker and mix vigorously for two min with a stir bar. Quantitatively transfer the resulting suspension to a 100-mL volumetric flask along with 50 mL of TISAB and dilute to volume with distilled water. Store the entire external standard in a 250-mL plastic beaker until your are ready to measure the potential. Prepare toothpaste samples by obtaining an approximately 1-g portion and treating in the same manner as the standards. Measure the cell potential for the external standards and the samples using a F^- ion-selective electrode and an appropriate reference electrode. When measuring the potential, stir solution and allow two to three minutes to reach a stable potential. Report the concentration of F^- in the toothpaste %w/w SnF_2.

Questions

1. The total ionic strength adjustment buffer serves several purposes in this procedure. Identify these purposes.

The composition of the TISAB has three purposes:

(a) The high concentration of NaCl (the final solutions are approximately 1 M NaCl) ensures that the ionic strength of each external standard and each sample is essentially identical. Because the activity coefficient for fluoride is the same in all solutions, we can write the Nernst equation in terms of fluoride's concentration instead of its activity.

(b) The combination of glacial acetic acid and NaOH creates an acetic acid/acetate buffer of pH 5–5.5. As shown in Figure 11.23, the pH of this buffer is high enough to ensure that the predominate form of fluoride is F^- instead of HF. This pH also is sufficiently acidic that it avoids an interference from OH^- (see Example 11.8).

(c) DCTA is added as a complexing agent for Fe^{3+} or Al^{3+}, preventing the formation of FeF_6^{3-} or AlF_6^{3-}.

2. Why is a fluoride-free toothpaste added to the standard solutions?

Adding a fluoride-free toothpaste protects against any unaccounted for matrix effects that might influence the ion-selective electrode's response. This assumes, of course, that the matrices of the two toothpastes are otherwise similar.

3. The procedure specifies that the standards and the sample should be stored in plastic containers. Why is it a bad idea to store the solutions in glass containers?

The fluoride ion is capable of reacting with glass to form SiF_4.

4. Suppose that your calibration curve has a slope of –57.98 mV for each 10-fold change in the concentration of F^-. The ideal slope from the Nernst equation is –59.16 mV per 10-fold change in concentration. What effect does this have on the quantitative analysis for fluoride in toothpaste?

No effect at all! This is why we prepare a calibration curve using multiple standards.

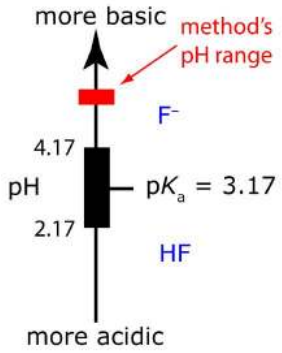


Figure 11.23 Ladder diagram for HF/F^-. Maintaining a pH greater than 4.2 ensures that the only significant form of fluoride is F^-.

Measurement of pH

With the availability of inexpensive glass pH electrodes and pH meters, the determination of pH is one of the most frequent quantitative analytical measurements. The potentiometric determination of pH, however, is not without complications, several of which we discuss in this section.

One complication is confusion over the meaning of pH.[6] The conventional definition of pH in most general chemistry textbooks is

$$\mathrm{pH} = \log[\mathrm{H^+}] \tag{11.19}$$

As we now know, pH actually is a measure of the activity of H^+.

$$\mathrm{pH} = \log a_{\mathrm{H^+}} \tag{11.20}$$

Equation 11.19 only approximates the true pH. If we calculate the pH of 0.1 M HCl using equation 11.19, we obtain a value of 1.00; the solution's actual pH, as defined by equation 11.20, is 1.1.[7] The activity and the concentration of H^+ are not the same in 0.1 M HCl because the activity coefficient for H^+ is not 1.00 in this matrix. Figure 11.24 shows a more colorful demonstration of the difference between activity and concentration.

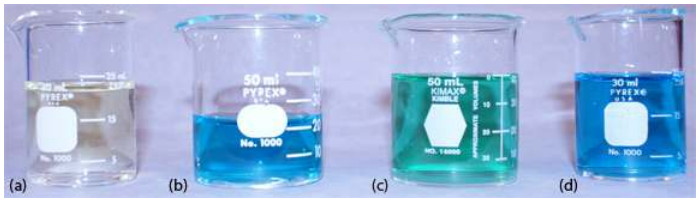


Figure 11.24 *A demonstration of the difference between activity and concentration using the indicator methyl green. The indicator is yellow in its acid form (beaker a: 1.0 M HCl) and is blue in its base form (beaker d: H_2O). In 10 mM HCl the indicator is in its base form (beaker b: 20 mL of 10 mM HCl with 3 drops of methyl green). Adding 20 mL of 5 M LiCl to this solution shifts the indicator's color to green (beaker c). Although the concentration of HCl has been cut in half, the activity of H^+ has increased.*

Note

The demonstration shown here is adapted from McCarty, C. G.; Vitz, E. "pH Paradoxes: Demonstrating That It Is Not True That pH ≡ –log[H^+]," *J. Chem. Educ.* **2006**, *83*, 752–757. This paper provides several additional demonstrations that illustrate the difference between concentration and activity.

A second complication in measuring pH is the uncertainty in the relationship between potential and activity. For a glass membrane electrode, the cell potential, $(E_{cell})_A$, for a solution of unknown pH is

$$(E_{cell})_A = K - \frac{RT}{F}\ln\frac{1}{a_{H^+}} = K - \frac{2.303RT}{F}pH_A \tag{11.21}$$

where K includes the potential of the reference electrode, the asymmetry potential of the glass membrane, and any junction potentials in the electrochemical cell. All the contributions to K are subject to uncertainty, and may change from day to day, as well as between electrodes. For this reason, before using a pH electrode we calibrate it using a standard buffer of known pH. The cell potential for the standard, $(E_{cell})_{std}$, is

$$(E_{cell})_{std} = K - \frac{2.303RT}{F}pH_{std} \tag{11.22}$$

where pH_{std} is the standard's pH. Subtracting equation 11.22 from equation 11.21 and solving for pH_A gives

$$pH_A = pH_{std} - \frac{\{(E_{cell})_A - (E_{cell})_{std}\}F}{2.303RT} \tag{11.23}$$

which is the operational definition of pH adopted by the International Union of Pure and Applied Chemistry.[8]

Note

The equations in this section assume that the pH electrode is the cathode in a potentiometric cell. In this case an increase in pH corresponds to a decrease in the cell potential. Many pH meters are designed with the pH electrode as the anode, resulting in an increase in the cell potential for higher pH values. The operational definition of pH in this case is

$$pH_A = pH_{std} + \frac{\{(E_{cell})_A - (E_{cell})_{std}\}F}{2.303RT} \tag{11.2.76}$$

The difference between this equation and equation 11.23 does not affect the operation of a pH meter.

Calibrating a pH electrode presents a third complication because we need a standard with an accurately known activity for H^+. Table 11.6 provides pH values for several primary standard buffer solutions accepted by the National Institute of Standards and Technology.

To standardize a pH electrode using two buffers, choose one near a pH of 7 and one that is more acidic or basic depending on your sample's expected pH. Rinse your pH electrode in deionized water, blot it dry with a laboratory wipe, and place it in the buffer with a pH closest to 7. Swirl the pH electrode and allow it to equilibrate until you obtain a stable reading. Adjust the "Standardize" or "Calibrate" knob until the meter displays the correct pH. Rinse and dry the electrode, and place it in the second buffer. After the electrode equilibrates, adjust the "Slope" or "Temperature" knob until the meter displays the correct pH.

Some pH meters can compensate for changes in temperature. To use this feature, place a temperature probe in the sample and connect it to the pH meter. Adjust the "Temperature" knob to the solution's temperature and calibrate the pH meter using the "Calibrate" and "Slope" controls. As you are using the pH electrode, the pH meter compensates for any change in the sample's temperature by adjusting the slope of the calibration assuming a Nernstian response of $2.303RT/F$.

Table 11.6 pH Values for Selected NIST Primary Standard Buffers

temp (°C)	saturated (at 25°C) $KHC_4H_4O_7$ (tartrate)	0.05 m $KH_2C_6H_5O_7$ (citrate)	0.05 m $KHC_8H_4O_4$ (phthalate)	0.025 m KH_2PO_4, 0.025m Na_2HPO_4	0.008695 m KH_2PO_4, 0.03043 m Na_2HPO_4	0.01 m $Na_4B_4O_7$	0.025 m $NaHCO_3$, 0.025 m Na_2CO_3
0	—	3.863	4.003	6.984	7.534	9.464	10.317
5	—	3.840	3.999	6.951	7.500	9.395	10.245
10	—	3.820	3.998	6.923	7.472	9.332	10.179
15	—	3.802	3.999	6.900	7.448	9.276	10.118
20	—	3.788	4.002	6.881	7.429	9.225	10.062
25	3.557	3.776	4.008	6.865	7.413	9.180	10.012
30	3.552	3.766	4.015	6.854	7.400	9.139	9.966
35	3.549	3.759	4.024	6.844	7.389	9.012	9.925
40	3.547	3.753	4.035	6.838	7.380	9.068	9.889
45	3/547	3.750	4.047	6.834	7.373	9.038	9.856
50	3.549	3.749	4.060	6.833	7.367	9.011	9.828

Source: Values taken from Bates, R. G. *Determination of pH: Theory and Practice*, 2nd ed. Wiley: New York, 1973. See also Buck, R. P., et. al. “Measurement of pH. Definition, Standards, and Procedures,” *Pure. Appl. Chem.* **2002**, *74*, 2169–2200.

Clinical Applications

Because of their selectivity for analytes in complex matricies, ion-selective electrodes are important sensors for clinical samples. The most common analytes are electrolytes, such as Na^+, K^+, Ca^{2+}, H^+, and Cl^-, and dissolved gases such as CO_2. For extracellular fluids, such as blood and urine, the analysis can be made in vitro. An situ analysis, however, requires a much smaller electrode that can be inserted directly into a cell. Liquid-based membrane microelectrodes with tip diameters smaller than 1 μm are constructed by heating and drawing out a hard-glass capillary tube with an initial diameter of approximately 1–2 mm (Figure 11.25). The microelectrode’s tip is made hydrophobic by dipping into a solution of dichlorodimethyl silane, and an inner solution appropriate for the analyte and a Ag/AgCl wire reference electrode are placed within the microelectrode. The microelectrode is then dipped into a solution of the liquid complexing agent, with a small volume of the liquid complexing agent being retained within the tip by capillary action. Potentiometric microelectrodes have been developed for a number of clinically important analytes, including H^+, K^+, Na^+, Ca^{2+}, Cl^-, and I^-.[9]

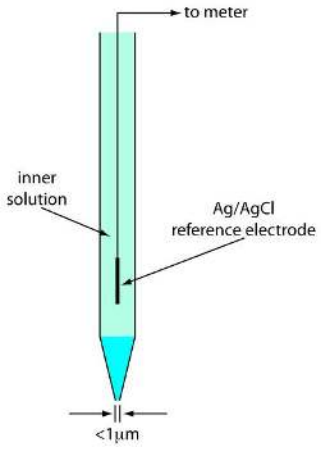


Figure 11.25 Schematic diagram of a liquid-based ion-selective microelectrode.

Environmental Applications

Although ion-selective electrodes are used in environmental analysis, their application is not as widespread as in clinical analysis. Although standard potentiometric methods are available for the analysis of CN^-, F^-, NH_3, and NO_3^- in water and wastewater, other analytical methods generally provide better detection limits. One potential advantage of an ion-selective electrode is the ability to incorporate it into a flow cell for the continuous monitoring of wastewater streams.

Potentiometric Titrations

One method for determining the equivalence point of an acid–base titration is to use a pH electrode to monitor the change in pH during the titration. A potentiometric determination of the equivalence point is possible for acid–base, complexation, redox, and precipitation titrations, as well as for titrations in aqueous and nonaqueous solvents. Acid–base, complexation, and precipitation potentiometric titrations are usually monitored with an ion-selective electrode selective for the analyte, although an electrode selective for the titrant or a reaction product also can be used. A redox electrode, such as a Pt wire, and a reference electrode are used for potentiometric redox titrations. More details about potentiometric titrations are found in Chapter 9.

11.2.6 Evaluation

Scale of Operation

The working range for most ion-selective electrodes is from a maximum concentration of 0.1–1 M to a minimum concentration of 10^{-5}–10^{-11} M.[10] This broad working range extends from major analytes to ultratrace analytes, and is significantly greater than many other analytical techniques. To use a conventional ion-selective electrode we need a minimum sample volume of several mL (a macro sample). Microelectrodes, such as the one shown in Figure 11.25, may be used with ultramicro samples, although the sample must be of sufficient size to be representative of the original sample.

> **Note**
>
> See Figure 3.5 to review the meaning of major and ultratrace analytes, and the meaning of macro and ultramicro samples.

Accuracy

The accuracy of a potentiometric analysis is limited by the error in measuring E_{cell}. Several factors contribute to this measurement error, including the contribution to the potential from interfering ions, the finite current passing through the cell while measuring the potential, differences between the analyte's activity coefficient in the samples and the standard solutions, and junction potentials. We can limit the effect of interfering ions by including a separation step before the potentiometric analysis. Modern high impedance potentiometers minimize the amount of current passing through the electrochemical cell. Finally, we can minimize the errors due to activity coefficients and junction potentials by matching the matrix of the standards to that of the sample. Even in the best circumstances, however, we may observe a difference of approximately ±1 mV for samples with equal concentrations of analyte.

We can evaluate the effect of uncertainty on the accuracy of a potentiometric measurement by using a propagation of uncertainty. For a membrane ion-selective electrode the general expression for potential is

$$E_{\text{cell}} = K + \frac{RT}{zF}\ln[\text{A}] \tag{11.2.77}$$

where z is the analyte's charge . From Table 4.10 in Chapter 4, the uncertainty in the cell potential, ΔE_{cell} is

$$\Delta E_{\text{cell}} = \frac{RT}{zF} \times \frac{\Delta[\text{A}]}{[\text{A}]} \tag{11.2.78}$$

Rearranging and multiplying through by 100 gives the percent relative error in concentration as

$$\%\ \text{relative error} = \frac{\Delta[\text{A}]}{[\text{A}]} \times 100 = \frac{\Delta E_{\text{cell}}}{RT/zF} \times 100 \tag{11.24}$$

The relative error in concentration, therefore, is a function of the measurement error, ΔE_{cell}, and the analyte's charge . Table 11.7 provides representative values for ions with charges of ±1 and ±2 at a temperature of 25°C. Accuracies of 1–5% for monovalent ions and 2–10% for divalent ions are typical. Although equation 11.24 applies to membrane electrodes, we can use if for a metallic electrode by replacing z with n.

Precision

Precision in potentiometry is limited by variations in temperature and the sensitivity of the potentiometer. Under most conditions—and when using a simple, general-purpose potentiometer—we can measure the potential with a repeatability of ±0.1 mV. Using Table 11.7, this corresponds to an uncertainty of ±0.4% for monovalent analytes and ±0.8% for divalent analytes. The reproducibility of potentiometric measurements is about a factor of ten poorer.

Table 11.7 Relationship Between The Uncertainty in Measuring E_{cell} and the Relative Error in the Analyte's Concentration

	% relative error in concentration	
ΔE_{cell} (±mV)	z = ±1	z = ±2
0.1	±0.4	±0.8
0.5	±1.9	±3.9
1.0	±3.9	±7.8
1.5	±5.8	±11.1
2.0	±7.8	±15.6

Sensitivity

The sensitivity of a potentiometric analysis is determined by the term RT/nF or RT/zF in the Nernst equation. Sensitivity is best for smaller values of n or z.

Selectivity

As described earlier, most ion-selective electrodes respond to more than one analyte; the selectivity for the analyte, however, is often significantly greater than for the interfering ions. The manufacturer of an ion-selective usually provides an ISE's selectivity coefficients, which allows the analyst to determine whether a potentiometric analysis is feasible for a given sample.

Time, Cost, and Equipment

In comparison to other techniques, potentiometry provides a rapid, relatively low-cost means for analyzing samples. The limiting factor when analyzing a large number of samples is the need to rinse the electrode between samples. The use of inexpensive, disposable ion-selective electrodes can increase a lab's sample throughput. Figure 11.26 shows one example of a disposable ISE for Ag^+.[11] Commercial instruments for measuring pH or potential are available in a variety of price ranges, and includes portable models for use in the field.

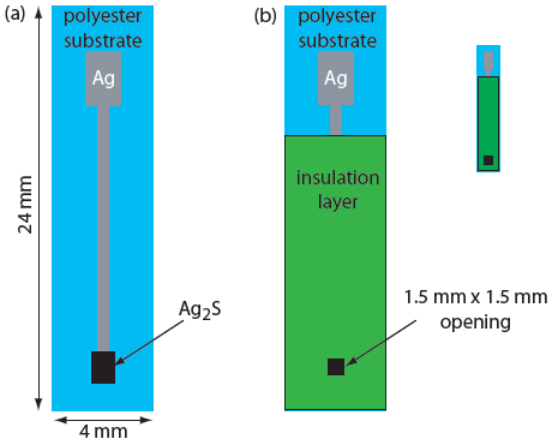


Figure 11.26 Schematic diagram of a disposable ion-selective electrode created by screen-printing. In (a) a thin film of conducting silver is printed on a polyester substrate and a film of Ag_2S overlaid near the bottom. In (b) an insulation layer with a small opening is layered on top, exposing a portion of the Ag_2S membrane that can be immersed in the sample. The top of the polyester substrate remains uncoated, allowing the electrode to be connected to a potentiometer through the Ag film. The small inset shows the electrode's actual size.

Contributors

David Harvey (DePauw University)

11.2: Potentiometric Methods is shared under a CC BY-NC-SA 4.0 license and was authored, remixed, and/or curated by LibreTexts.

11.3: Coulometric Methods

In a potentiometric method of analysis we determine an analyte's concentration by measuring the potential of an electrochemical cell under static conditions. Dynamic techniques, in which current passes through the electrochemical cell, also are important electrochemical methods of analysis. In this section we consider coulometry. Voltammetry and amperometry are covered in section 11D.

Coulometry is based on an exhaustive electrolysis of the analyte. By exhaustive we mean that the analyte is completely oxidized or reduced at the working electrode or that it reacts completely with a reagent generated at the working electrode. There are two forms of coulometry: **controlled-potential coulometry**, in which we apply a constant potential to the electrochemical cell, and **controlled-current coulometry**, in which we pass a constant current through the electrochemical cell.

During an electrolysis, the total charge, Q, in coulombs, passing through the electrochemical cell is proportional to the absolute amount of analyte by **Faraday's law**

$$Q = nFN_A \tag{11.25}$$

where n is the number of electrons per mole of analyte, F is Faraday's constant (96487 C mol^{-1}), and N_A is the moles of analyte. A coulomb is equivalent to an A·sec; thus, when passing a constant current, i, the total charge is

$$Q = it_e \tag{11.26}$$

where t_e is the electrolysis time. If the current varies with time, as it does in controlled-potential coulometry, then the total charge is

$$Q = \int_o^{t_e} i(t)\, dt \tag{11.27}$$

In coulometry, we monitor current as a function of time and use either equation 11.26 or equation 11.27 to calculate Q. Knowing the total charge, we then use equation 11.25 to determine the moles of analyte. To obtain an accurate value for N_A, all the current must be used to oxidize or reduce the analyte. In other words, coulometry requires 100% current efficiency—or an accurately measured current efficiency established using a standard—a factor that we must be consider when designing a coulometric method of analysis.

> **Note**
>
> **Current efficiency** is the percentage of current that actually leads to the analyte's oxidation or reduction.

11.3.1 Controlled-Potential Coulometry

The easiest way to ensure 100% current efficiency is to hold the working electrode at a constant potential, chosen so that the analyte reacts completely without simultaneously oxidizing or reducing an interfering species. As electrolysis progresses the analyte's concentration decreases, as does the current. The resulting current-versus-time profile for controlled-potential coulometry is shown in Figure 11.27. Integrating the area under the curve (equation 11.27) from $t = 0$ to $t = t_e$ gives the total charge. In this section we consider the experimental parameters and instrumentation needed to develop a controlled-potential coulometric method of analysis.

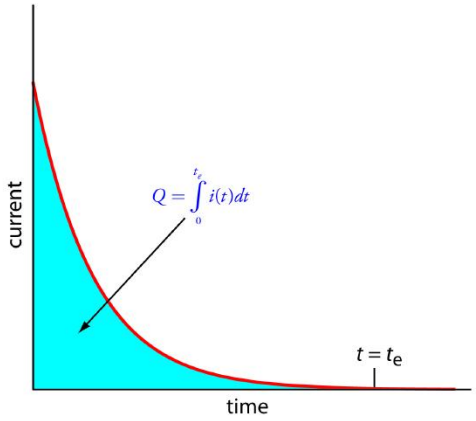


Figure 11.27 Current versus time for a controlled-potential coulometric analysis. The measured current is shown by the red curve. The integrated area under the curve, shown in blue, is the total charge.

Selecting a Constant Potential

To see how an appropriate potential for the working electrode is selected, let's develop a constant-potential coulometric method for Cu^{2+} based on its reduction to copper metal at a Pt working electrode.

$$Cu^{2+}(aq) + 2e^- \leftrightharpoons Cu(s) \tag{11.28}$$

Figure 11.28 shows a ladder diagram for an aqueous solution of Cu^{2+}. From the ladder diagram we know that reaction 11.28 is favored when the working electrode's potential is more negative than +0.342 V versus the standard hydrogen electrode. To ensure a 100% current efficiency, however, the potential must be sufficiently more positive than +0.000 V so that the reduction of H_3O^+ to H_2 does not contribute significantly to the total current flowing through the electrochemical cell.

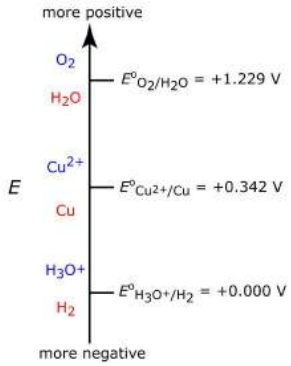


Figure 11.28 Ladder diagram for an aqueous solution of Cu^{2+} showing steps for the reductions of O_2 to H_2O, of Cu^{2+} to Cu, and of H_3O^+ to H_2. For each step, the oxidized species is in blue and the reduced species is in red.

We can use the Nernst equation for reaction 11.28 to estimate the minimum potential for quantitatively reducing Cu^{2+}.

$$E = E^\circ_{Cu^{2+}/Cu} - \frac{0.05916}{2} \log \frac{1}{[Cu^{2+}]} \tag{11.29}$$

> **Note**
>
> So why are we using the concentration of Cu^{2+} in equation 11.29 instead of its activity? In potentiometry we write the Nernst equation using activity because we use E_{cell} to determine the amount of analyte in the sample. Here we are using the Nernst equation to design the analysis. The amount of analyte is given by the total charge, not the applied potential.

If we define a quantitative electrolysis as one in which we reduce 99.99% of Cu^{2+} to Cu, then the concentration of Cu^{2+} at t_e is

$$[Cu^{2+}]_{t_e} = 0.0001 \times [Cu^{2+}]_0 \tag{11.30}$$

where $[Cu^{2+}]_0$ is the initial concentration of Cu^{2+} in the sample. Substituting equation 11.30 into equation 11.29 allows us to calculate the desired potential.

$$E = E^\circ_{Cu^{2+}/Cu} - \frac{0.05916}{2}\log\frac{1}{0.0001 \times [Cu^{2+}]_0} \tag{11.3.1}$$

If the initial concentration of Cu^{2+} is 1.00×10^{-4} M, for example, then the working electrode's potential must be more negative than +0.105 V to quantitatively reduce Cu^{2+} to Cu. Note that at this potential H_3O^+ is not reduced to H_2, maintaining 100% current efficiency.

> **Note**
>
> Many controlled-potential coulometric methods for Cu^{2+} use a potential that is negative relative to the standard hydrogen electrode—see, for example, Rechnitz, G. A. *Controlled-Potential Analysis*, Macmillan: New York, 1963, p.49.
>
> Based on the ladder diagram in Figure 11.28 you might expect that applying a potential <0.000 V will partially reduce H_3O^+ to H_2, resulting in a current efficiency that is less than 100%. The reason we can use such a negative potential is that the reaction rate for the reduction of H_3O^+ to H_2 at is very slow at a Pt electrode. This results in a significant **overpotential**—the need to apply a more positive or a more negative potential than predicted by thermodynamics—that shifts E^o for the H_3O^+/H_2 redox couple to a more negative value.

Minimizing Electrolysis Time

In controlled-potential coulometry, as shown in Figure 11.27, the current decreases over time. As a result, the rate of electrolysis—recall from Section 11A that current is a measure of rate—becomes slower and an exhaustive electrolysis of the analyte may require a long time. Because time is an important consideration when choosing and designing analytical methods, we need to consider the factors affecting the analysis time.

We can approximate the change in current as a function of time in Figure 11.27 by an exponential decay; thus, the current at time t is

$$i = i_0 e^{-kt} \tag{11.31}$$

where i_0 is the current at $t = 0$ and k is a rate constant that is directly proportional to the area of the working electrode and the rate of stirring, and that is inversely proportional to the volume of solution. (Problem11.16 asks you to explain why a larger surface area, a faster stirring rate, and a smaller volume leads to a shorter analysis time.) For an exhaustive electrolysis in which we oxidize or reduce 99.99% of the analyte, the current at the end of the analysis, t_e, is

$$i \leq 0.0001 \times i_0 \tag{11.32}$$

Substituting equation 11.32 into equation 11.31 and solving for t_e gives the minimum time for an exhaustive electrolysis as

$$t_e = -\frac{1}{k} \times \ln(0.0001) = \frac{9.21}{k} \tag{11.3.2}$$

From this equation we see that a larger value for k reduces the analysis time. For this reason we usually carry out a controlled-potential coulometric analysis in a small volume electrochemical cell, using an electrode with a large surface area, and with a high stirring rate. A quantitative electrolysis typically requires approximately 30–60 min, although shorter or longer times are possible.

Instrumentation

A three-electrode potentiostat is used to set the potential in controlled-potential coulometry. The working electrodes is usually one of two types: a cylindrical Pt electrode manufactured from platinum-gauze (Figure 11.29), or a Hg pool electrode. The large overpotential for the reduction of H_3O^+ at Hg makes it the electrode of choice for an analyte requiring a negative potential. For example, a potential more negative than –1 V versus the SHE is feasible at a Hg electrode—but not at a Pt electrode—even in a very acidic solution. Because mercury is easily oxidized, it is less useful if we need to maintain a potential that is positive with respect to the SHE. Platinum is the working electrode of choice when we need to apply a positive potential.

Note

Figure 11.5 shows an example of a manual three-electrode potentiostat. Although a modern potentiostat uses very different circuitry, you can use Figure 11.5 and the accompanying discussion to understand how we can use the three electrodes to set the potential and monitor the current.



Figure 11.29 Example of a cylindrical Pt-gauze electrode for controlled-potential coulometry. The electrode shown here has a diameter of 13 mm and a height of 48 mm, and is fashioned using Pt wire with a diameter of approximately 0.15 mm. The electrode's surface has 360 openings/cm^2 and a total surface area of approximately 40 cm^2.

The auxiliary electrode, which is often a Pt wire, is separated by a salt bridge from the analytical solution. This is necessary to prevent the electrolysis products generated at the auxiliary electrode from reacting with the analyte and interfering in the analysis. A saturated calomel or Ag/AgCl electrode serves as the reference electrode.

The other essential instrumental need for controlled-potential coulometry is a means for determining the total charge. One method is to monitor the current as a function of time and determine the area under the curve, as shown in Figure 11.27. Modern instruments use electronic integration to monitor charge as a function of time. The total charge at the end of the electrolysis is read directly from a digital readout.

Electrogravimetry

If the product of controlled-potential coulometry forms a deposit on the working electrode, then we can use the change in the electrode's mass as the analytical signal. For example, in we apply a potential that reduces Cu^{2+} to Cu at a Pt working electrode, the difference in the electrode's mass before and after electrolysis is a direct measurement of the amount of copper in the sample. We call an analytical technique that uses mass as a signal a gravimetric technique; thus, we call this **electrogravimetry**.

Note

For a review of other gravimetric techniques, see Chapter 8.

11.3.2 Controlled-Current Coulometry

A second approach to coulometry is to use a constant current in place of a constant potential, which produces the current-versus-time profile shown in Figure 11.30. Controlled-current coulometry has two advantages over controlled-potential coulometry. First, the analysis time is shorter because the current does not decrease over time. A typical analysis time for controlled-current coulometry is less than 10 min, compared to approximately 30–60 min for controlled-potential coulometry. Second, because the total charge is simply the product of current and time (equation 11.26), there is no need to integrate the current-time curve in Figure 11.30.

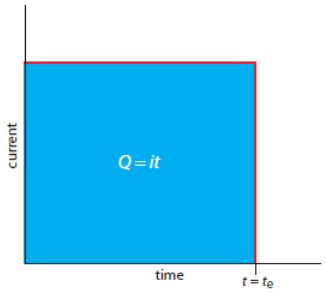


Figure 11.30 Current versus time for a controlled-current coulometric analysis. The measured current is shown by the red curve. The integrated area under the curve, shown in blue, is the total charge.

Using a constant current presents us with two important experimental problems. First, during electrolysis the analyte's concentration—and, therefore, the current due to the its oxidation or reduction—continuously decreases (see Figure 11.27). To maintain a constant current we must allow the potential to change until another oxidation reaction or reduction reaction occurs at the working electrode. Unless we design the system carefully, this secondary reaction decreases the current efficiency to less than 100%. The second problem is that we need a method for determining when the analyte's electrolysis is complete. As shown in Figure 11.27, in a controlled-potential coulometric analysis we know that electrolysis is complete when the current reaches zero, or when it reaches a constant background or residual current. In a controlled-current coulometric analysis, however, current continues to flow even when the analyte's electrolysis is complete. A suitable method for determining the reaction's endpoint, t_e, is needed.

Maintaining Current Efficiency

To illustrate why a change in the working electrode's potential may result in a current efficiency <100%, let's consider the coulometric analysis for Fe^{2+} based on its oxidation to Fe^{3+} at a Pt working electrode in 1 M H_2SO_4.

$$Fe^{2+}(aq) \leftrightharpoons Fe^{3+}(aq) + e^- \tag{11.3.3}$$

Figure 11.31 shows the ladder diagram for this system. At the beginning, the potential of the working electrode remains nearly constant at a level near its initial value. As the concentration of Fe^{2+} decreases, the working electrode's potential shifts toward more positive values until the oxidation of H_2O begins.

$$2\,H_2O(l) \leftrightharpoons O_2(g) + 4\,H^+(aq) + 4e^- \tag{11.3.4}$$

Because a portion of the total current comes from the oxidation of H_2O, the current efficiency for the analysis is less than 100% and we cannot use equation 11.25 to determine the amount of Fe^{2+} in the sample.

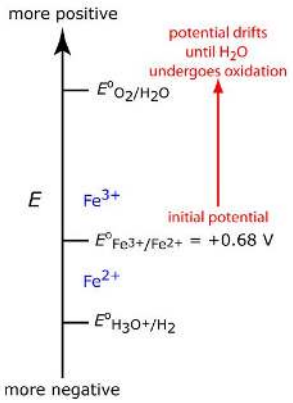


Figure 11.31 Ladder diagram for the constant-current coulometric analysis of Fe^{2+}. The red arrow and text shows how the potential drifts to more positive values, decreasing the current efficiency.

Although we cannot prevent the potential from drifting until another species undergoes oxidation, we can maintain a 100% current efficiency if the product of that oxidation reacts both rapidly and quantitatively with the remaining Fe^{2+}. To accomplish this we can

add an excess of Ce^{3+} to the analytical solution. As shown in Figure 11.32, when the potential of the working electrode shifts to a more positive potential Ce^{3+} eventually begins to oxidize.

$$Ce^{3+}(aq) \leftrightharpoons Ce^{4+}(aq) + e^- \tag{11.33}$$

The Ce^{4+} that forms at the working electrode rapidly mixes with the solution where it reacts with any available Fe^{2+}.

$$Ce^{4+}(aq) + Fe^{2+}(aq) \leftrightharpoons Ce^{3+}(aq) + Fe^{3+}(aq) \tag{11.34}$$

Combining reaction 11.33 and reaction 11.34 shows that the net reaction is the oxidation of Fe^{2+} to Fe^{3+}

$$Fe^{2+}(aq) \leftrightharpoons Fe^{3+}(aq) + e^- \tag{11.3.5}$$

maintaining a current efficiency of 100%. A species, such as Ce^{3+}, which is used to maintain 100% current efficiency, is called a **mediator**.

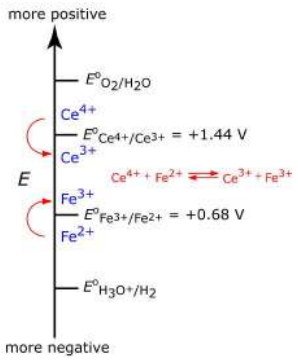


***Figure 11.32**: Ladder diagram for the constant-current coulometric analysis of Fe^{2+} in the presence of a Ce^{3+} mediator. As the potential drifts to more positive values, we eventually reach a potential where Ce^{3+} undergoes oxidation. Because Ce^{4+}, the product of the oxidation of Ce^{3+}, reacts with Fe^{2+}, we maintain current efficiency.*

Endpoint Determination

Adding a mediator solves the problem of maintaining 100% current efficiency, but it does not solve the problem of determining when the analyte's electrolysis is complete. Using our same example, when the oxidation of Fe^{2+} is complete current continues to flow from the oxidation of Ce^{3+}, and, eventually, the oxidation of H_2O. What we need is a signal that tells us when there is no more Fe^{2+} in solution.

For our purposes, it is convenient to treat a controlled-current coulometric analysis as a reaction between the analyte, Fe^{2+}, and the mediator, Ce^{3+}, as shown by reaction 11.34. This reaction is identical to a redox titration; thus, we can use the end points for a redox titration—visual indicators and potentiometric or conductometric measurements—to signal the end of a controlled-current coulometric analysis. For example, ferroin provides a useful visual endpoint for the Ce^{3+} mediated coulometric analysis for Fe^{2+}, changing color from red to blue when the electrolysis of Fe^{2+} is complete.

> **Note**
>
> Reaction 11.34 is the same reaction we used in Chapter 9 to develop our understanding of redox titrimetry.
>
> See Figure 9.40 for the titration curve and for ferroin's color change.

Instrumentation

Controlled-current coulometry normally is carried out using a two-electrode galvanostat, consisting of a working electrode and a counter electrode. The working electrode—often a simple Pt electrode—is also called the generator electrode since it is where the mediator reacts to generate the species that reacts with the analyte. If necessary, the counter electrode is isolated from the analytical solution by a salt bridge or porous frit to prevent its electrolysis products from reacting with the analyte. Alternatively, we can generate the oxidizing agent or the reducing agent externally, and allow it to flow into the analytical solution. Figure 11.33 shows one simple method for accomplishing this. A solution containing the mediator flows into a small-volume electrochemical cell, with the products exiting through separate tubes. Depending upon the analyte, the oxidizing agent or the reducing reagent is selectively

delivered to the analytical solution. For example, we can generate Ce^{4+} using an aqueous solution of Ce^{3+}, directing the Ce^{4+} that forms at the anode into our sample.

> **Note**
>
> Figure 11.4 shows an example of a manual galvanostat. Although a modern galvanostat uses very different circuitry, you can use Figure 11.4 and the accompanying discussion to understand how we can use the working electrode and the counter electrode to control the current. Figure 11.4 includes an optional reference electrode, but its presence or absence is not important if we are not interested in monitoring the working electrode's potential.

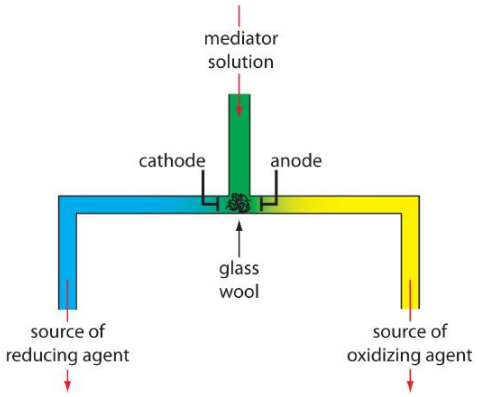


Figure 11.33 One example of a device for the external generation of oxidizing agents and reducing agents for controlled-current coulometry. A solution containing the mediator flows into a small-volume electrochemical cell. The resulting oxidation products, which form at the anode, flow to the right and may serve as an oxidizing agent. Reduction at the cathode generates a reducing agent.

There are two other crucial needs for controlled-current coulometry: an accurate clock for measuring the electrolysis time, t_e, and a switch for starting and stopping the electrolysis. An analog clock can record time to the nearest ±0.01 s, but the need to frequently stop and start the electrolysis as we approach the endpoint may result in an overall uncertainty of ±0.1 s. A digital clock allows for a more accurate measurement of time, with an overall uncertainty of ±1 ms being possible. The switch must control both the current and the clock, so that we can make an accurate determination of the electrolysis time.

Coulometric Titrations

A controlled-current coulometric method is sometimes called a **coulometric titration** because of its similarity to a conventional titration. For example, in the controlled-current coulometric analysis for Fe^{2+} using a Ce^{3+} mediator, the oxidation of Fe^{2+} by Ce^{4+} (reaction 11.34) is identical to the reaction in a redox titration (reaction 9.15).

There are other similarities between controlled-current coulometry and titrimetry. If we combine equation 11.25 and equation 11.26 and solve for the moles of analyte, N_A, we obtain the following equation.

$$N_A = \frac{i}{nF} \times t_e \tag{11.35}$$

Compare equation 11.35 to the relationship between the moles of analyte, N_A, and the moles of titrant, N_T, in a titration

$$N_A = N_T = M_T \times V_T \tag{11.3.6}$$

where M_T and V_T are the titrant's molarity and the volume of titrant at the end point. In constant-current coulometry, the current source is equivalent to the titrant and the value of that current is analogous to the titrant's molarity. Electrolysis time is analogous to the volume of titrant, and t_e is equivalent to the a titration's end point. Finally, the switch for starting and stopping the electrolysis serves the same function as a buret's stopcock.

> **Note**
>
> For simplicity, we are assuming that the stoichiometry between the analyte and titrant is 1:1. The assumption, however, is not important and does not effect our observation of the similarity between controlled-current coulometry and a titration.

11.3.3 Quantitative Applications

Coulometry is used for the quantitative analysis of both inorganic and organic analytes. Examples of controlled-potential and controlled-current coulometric methods are discussed in the following two sections.

Controlled-Potential Coulometry

The majority of controlled-potential coulometric analyses involve the determination of inorganic cations and anions, including trace metals and halides ions. Table 11.8 summarizes several of these methods.

Table 11.8 Representative Controlled-Potential Coulometric Analyses for Inorganic Ions

analyte	electrolytic reaction[a]	electrode
antimony	$Sb(III) + 3e^- \leftrightharpoons Sb$	Pt
arsenic	$As(III) \leftrightharpoons As(V) + 2e^-$	Pt
cadmium	$Cd(II) + 2e^- \leftrightharpoons Cd$	Pt or Hg
cobalt	$Co(II) + 2e^- \leftrightharpoons Co$	Pt or Hg
copper	$Cu(II) + 2e^- \leftrightharpoons Cu$	Pt or Hg
halides (X^-)	$Ag + X^- \leftrightharpoons AgX + e^-$	Ag
iron	$Fe(II) \leftrightharpoons Fe(III) + e^-$	Pt
lead	$Pb(II) + 2e^- \leftrightharpoons Pb$	Pt or Hg
nickel	$Ni(II) + 2e^- \leftrightharpoons Ni$	Pt or Hg
plutonium	$Pu(III) \leftrightharpoons Pu(IV) + e^-$	Pt
silver	$Ag(I) + e^- \leftrightharpoons Ag$	Pt
tin	$Sn(II) + 2e^- \leftrightharpoons Sn$	Pt
uranium	$U(VI) + 2e^- \leftrightharpoons U(IV)$	Pt or Hg
zinc	$Zn(II) + 2e^- \leftrightharpoons Zn$	Pt or Hg

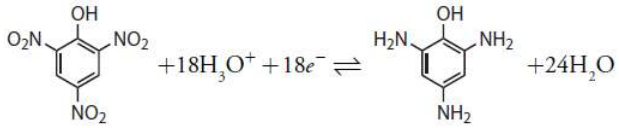
Source: Rechnitz, G. A. *Controlled-Potential Analysis*, Macmillan: New York, 1963.

[a] Electrolytic reactions are written in terms of the change in the analyte's oxidation state. The actual species in solution depends on the analyte.

The ability to control selectivity by carefully adjusting the working electrode's potential makes controlled-potential coulometry particularly useful for the analysis of alloys. For example, we can determine the composition of an alloy containing Ag, Bi, Cd, and Sb by dissolving the sample and placing it in a matrix of 0.2 M H_2SO_4 along with a Pt working electrode and a Pt counter electrode. If we apply a constant potential of +0.40 V versus the SCE, Ag(I) deposits on the electrode as Ag and the other metal ions remain in solution. When electrolysis is complete, we use the total charge to determine the amount of silver in the alloy. By shifting the working electrode's potential to –0.08 V versus the SCE, we deposit Bi on the working electrode. When the

coulometric analysis for bismuth is complete, we determine antimony by shifting the working electrode's potential to –0.33 V versus the SCE, depositing Sb. Finally, we determine cadmium following its electrodeposition on the working electrode at a potential of –0.80 V versus the SCE.

We also can use controlled-potential coulometry for the quantitative analysis of organic compounds, although the number of applications is significantly less than that for inorganic analytes. One example is the six-electron reduction of a nitro group, $–NO_2$, to a primary amine, $–NH_2$, at a mercury electrode. Solutions of picric acid—also known as 2,4,6-trinitrophenol, or TNP, a close relative of TNT—can be analyzed by reducing it to triaminophenol.



Another example is the successive reduction of trichloroacetate to dichloroacetate, and of dichloroacetate to monochloroacetate

$$Cl_3CCOO^-(aq) + H_3O^+(aq) + 2e^- \leftrightharpoons Cl_2HCCOO^-(aq) + Cl^-(aq) + H_2O(l) \quad (11.3.7)$$

$$Cl_2HCCOO^-(aq) + H_3O^+(aq) + 2e^- \leftrightharpoons ClH_2CCOO^-(aq) + Cl^-(aq) + H_2O(l) \quad (11.3.8)$$

We can analyze a mixture of trichloroacetate and dichloroacetate by selecting an initial potential at which only the more easily reduced trichloroacetate reacts. When its electrolysis is complete, we can reduce dichloroacetate by adjusting the potential to a more negative potential. The total charge for the first electrolysis gives the amount of trichloroacetate, and the difference in total charge between the first electrolysis and the second electrolysis gives the amount of dichloroacetate.

Controlled-Current Coulometry (Coulometric Titrations)

The use of a mediator makes a coulometric titration a more versatile analytical technique than controlled-potential coulometry. For example, the direct oxidation or reduction of a protein at a working electrode is difficult if the protein's active redox site lies deep within its structure. A coulometric titration of the protein is possible, however, if we use the oxidation or reduction of a mediator to produce a solution species that reacts with the protein. Table 11.9 summarizes several controlled-current coulometric methods based on a redox reaction using a mediator.

Table 11.9 Representative Examples of Coulometric Redox Titrations

mediator	electrochemically generated reagent and reaction	representative application[a]
Ag^+	Ag^{2+}: $Ag^+ \leftrightharpoons Ag^{2+} + e^-$	$\underline{H_2C_2O_4(aq)} + 2\,Ag^{2+}(aq) + 2\,H_2O(l) \leftrightharpoons 2\,CO_2(g) + 2\,Ag^+(aq) + 2\,H_3O^+(aq)$
Br^-	Br_2: $2Br^- \leftrightharpoons Br_2 + 2e^-$	$\underline{H_2S(aq)} + Br_2(aq) + 2\,H_2O(l) \leftrightharpoons S(s) + 2\,Br^-(aq) + 2\,H_3O^+(aq)$
Ce^{3+}	Ce^{4+}: $Ce^{3+} \leftrightharpoons Ce^{4+} + e^-$	$\underline{Fe(CN)_6^{4-}(aq)} + Ce^{4+}(aq) \leftrightharpoons Fe(CN)_6^{3-}(aq) + Ce^{3+}(aq)$
Cl^-	Cl_2: $2Cl^- \leftrightharpoons Cl_2 + 2e^-$	$\underline{Ti(I)(aq)} + Cl_2(aq) \leftrightharpoons Ti(III)(aq) + 2\,Cl^-(aq)$
Fe^{3+}	Fe^{2+}: $Fe^{3+} + e^- \leftrightharpoons Fe^{2+}$	$\underline{Cr_2O_7^{2-}(aq)} + 6\,Fe^{2+}(aq) + 14\,H_3O^+(aq) \leftrightharpoons 2\,Cr^{3+}(aq) + 6\,Fe^{3+}(aq) + 21\,H_2O(l)$
I^-	I_3^-: $3\,I^- \leftrightharpoons I_3^- + 2e^-$	$\underline{2\,S_2O_3^{2-}(aq)} + I_3^-(aq) \leftrightharpoons 2\,S_4O_6^{2-}(aq) + 3\,I^-(aq)$
Mn^{2+}	Mn^{3+}: $Mn^{2+} \leftrightharpoons Mn^{3+} + e^-$	$\underline{As(III)(aq)} + 2\,Mn^{3+}(aq) \leftrightharpoons As(V)(aq) + 2\,Mn^{2+}(aq)$

[a] The analyte is the underlined species in each reaction.

For an analyte that is not easily oxidized or reduced, we can complete a coulometric titration by coupling a mediator's oxidation or reduction to an acid–base, precipitation, or complexation reaction involving the analyte. For example, if we use H_2O as a mediator, we can generate H_3O^+ at the anode

$$6\,H_2O(l) \rightleftharpoons 4\,H_3O^+(aq) + O_2(g) + 4e^- \tag{11.3.9}$$

and generate OH^- at the cathode.

$$2\,H_2O(l) + 2e^- \rightleftharpoons 2\,OH^-(aq) + H_2(g) \tag{11.3.10}$$

If we carry out the oxidation or reduction of H_2O using the generator cell in Figure 11.33, then we can selectively dispense H_3O^+ or OH^- into a solution containing the analyte. The resulting reaction is identical to that in an acid–base titration. Coulometric acid–base titrations have been used for the analysis of strong and weak acids and bases, in both aqueous and non-aqueous matrices. Table 11.10 summarizes several examples of coulometric titrations involving acid–base, complexation, and precipitation reactions.

Table 11.10 Representative Coulometric Titrations Using Acid–Base, Complexation, and Precipitation Reactions

type of reaction	mediator	electrochemically generated reagent and reaction	representative application[a]
acid–base	H_2O H_2O	H_3O^+: $6H_2O \rightleftharpoons 4H_3O^+ + O_2 + 4e^-$ OH^-: $2H_2O + 2e^- \rightleftharpoons 2OH^- + H_2$	$OH^-(aq) + H_3O^+(aq) \rightleftharpoons 2\,H_2O(l)$ $H_3O^+(aq) + OH^-(aq) \rightleftharpoons 2\,H_2O(l)$
complexation	$HgNH_3Y^{2-}$ Y = EDTA	HY^{3-}: $HgNH_3Y^{2-} + NH_4^+ + 2e^- \rightleftharpoons HY^{3-} + Hg + 2NH_3$	$Ca^{2+}(aq) + HY^{3-}(aq) + H_2O(l) \rightleftharpoons CaY^{2-}(aq) + H_3O^+(aq)$
precipitation	Ag Hg $Fe(CN)_6^{3-}$	Ag^+: $Ag \rightleftharpoons Ag^+ + e^-$ Hg_2^{2+}: $2Hg \rightleftharpoons Hg_2^{2+} + 2e^-$ $Fe(CN)_6^{4-}$: $Fe(CN)_6^{3-} + e^- \rightleftharpoons Fe(CN)_6^{4-}$	$I^-(aq) + Ag^+(aq) \rightleftharpoons AgI(s)$ $2Cl^-(aq) + Hg_2^{2+}(aq) \rightleftharpoons Hg_2Cl_2(s)$ $3Zn^{2+}(aq) + K^+(aq) + Fe(CN)_6^{4-}(aq) \rightleftharpoons K_2Zn_3[Fe(CN)_6]_2(s)$

In comparison to a conventional titration, a coulometric titration has two important advantages. The first advantage is that electrochemically generating a titrant allows us to use an unstable reagent. Although we cannot easily prepare and store a solution of a highly reactive reagent, such as Ag^{2+} or Mn^{3+}, we can generate them electrochemically and use them in a coulometric titration. Second, because it is relatively easy to measure a small quantity of charge, we can use a coulometric titration to determine an analyte whose concentration is too small for a conventional titration.

Quantitative Calculations

The absolute amount of analyte in a coulometric analysis is determined by applying Faraday's law (equation 11.25), with the total charge given by equation 11.26 or equation 11.27. Example 11.10 shows the calculations for a typical coulometric analysis.

Example 11.10

To determine the purity of a sample of $Na_2S_2O_3$, a sample is titrated coulometrically using I^- as a mediator and I_3^- as the titrant. A sample weighing 0.1342 g is transferred to a 100-mL volumetric flask and diluted to volume with distilled water. A 10.00-mL portion is transferred to an electrochemical cell along with 25 mL of 1 M KI, 75 mL of a pH 7.0 phosphate buffer, and several drops of a starch indicator solution. Electrolysis at a constant current of 36.45 mA requires 221.8 s to reach the starch indicator endpoint. Determine the sample's purity.

Solution

As shown in Table 11.9, the coulometric titration of $S_2O_3^{2-}$ with I_3^- is

$$2\,S_2O_3^{2-}(aq) + 3\,I_3^-(aq) \rightleftharpoons S_4O_6^{2-}(aq) + 3\,I^-(aq) \tag{11.3.11}$$

The oxidation of $S_2O_3^{2-}$ to $S_4O_6^{2-}$ requires one electron per $S_2O_3^{2-}$ (n = 1). Combining equation 11.25 and equation 11.26, and solving for the moles and grams of $Na_2S_2O_3$ gives

$$N_A = \frac{it_e}{nF} = \frac{(0.03645\ \text{A})(221.8\ \text{s})}{\left(\frac{1\ \text{mol e}^-}{\text{mol Na}_2\text{S}_2\text{O}_3}\right)\left(\frac{96487\ \text{C}}{\text{mol } e^-}\right)} = 8.379 \times 10^{-5}\ \text{mol Na}_2\text{S}_2\text{O}_3 \quad (11.3.12)$$

$$8.379 \times 10^{-5}\ \text{mol Na}_2\text{S}_2\text{O}_3 \times \frac{158.1\ \text{g Na}_2\text{S}_2\text{O}_3}{\text{mol Na}_2\text{S}_2\text{O}_3} = 0.01325\ \text{g Na}_2\text{S}_2\text{O}_3 \quad (11.3.13)$$

This is the amount of $Na_2S_2O_3$ in a 10.00-mL portion of a 100-mL sample; thus, there are 0.1325 grams of $Na_2S_2O_3$ in the original sample. The sample's purity, therefore, is

$$\frac{0.01325\ \text{g Na}_2\text{S}_2\text{O}_3}{0.1342\ \text{g sample}} \times 100 = 98.73\%\ \text{w/w Na}_2\text{S}_2\text{O}_3 \quad (11.3.14)$$

Note that in using equation 11.25 and equation 11.26, it does not matter whether $S_2O_3^{2-}$ is oxidized at the working electrode or is oxidized by I_3^-.

Exercise 11.7

To analyze a brass alloy, a 0.442-g sample is dissolved in acid and diluted to volume in a 500-mL volumetric flask. Electrolysis of a 10.00-mL sample at –0.3 V versus a SCE reduces Cu^{2+} to Cu, requiring a total charge of 16.11 C. Adjusting the potential to –0.6 V versus a SCE and completing the electrolysis requires 0.442 C to reduce Pb^{2+} to Pb. Report the %w/w Cu and Pb in the alloy.

Click here to review your answer to this exercise.

The best way to appreciate the theoretical and practical details discussed in this section is to carefully examine a typical analytical method. Although each method is unique, the following description of the determination of $Cr_2O_7^{2-}$ provides an instructive example of a typical procedure. The description here is based on Bassett, J.; Denney, R. C.; Jeffery, G. H.; Mendham, J. *Vogel's Textbook of Quantitative Inorganic Analysis*, Longman: London, 1978, p. 559–560.

Representative Method 11.2

Determination of Dichromate by a Coulometric Redox Titration

Description of the Method

The concentration of $Cr_2O_7^{2-}$ in a sample is determined by a coulometric redox titration using Fe^{3+} as a mediator and electrogenerated Fe^{2+} as the titrant. The endpoint of the titration is determined potentiometrically.

Procedure

The electrochemical cell consists of a Pt working electrode and a Pt counter electrode placed in separate cells connected by a porous glass disk. Fill the counter electrode's cell with 0.2 M Na_2SO_4, keeping the level above that of the solution in the working electrode's cell. Connect a platinum electrode and a tungsten electrode to a potentiometer so that you can measure the working electrode's potential during the analysis. Prepare a mediator solution of approximately 0.3 M $NH_4Fe(SO_4)_2$. Add 5.00 mL of sample, 2 mL of 9 M H_2SO_4, and 10–25 mL of the mediator solution to the working electrode's cell, and add distilled water as needed to cover the electrodes. Bubble pure N_2 through the solution for 15 min to remove any O_2 that might be present. Maintain the flow of N_2 during the electrolysis, turning if off momentarily when measuring the potential. Stir the solution using a magnetic stir bar. Adjust the current to 15–50 mA and begin the titration. Periodically stop the titration and measure the potential. Construct a titration curve of potential versus time and determine the time needed to reach the equivalence point.

Questions

1. Is the platinum working electrode the cathode or the anode?

Reduction of Fe^{3+} to Fe^{2+} occurs at the working electrode, making it the cathode in this electrochemical cell.

2. Why is it necessary to remove dissolved oxygen by bubbling N_2 through the solution?

Any dissolved O_2 will oxidize Fe^{2+} back to Fe^{3+}, as shown by the following reaction.

$$4\,Fe^{2+}(aq) + O_2(aq) + 4\,H_3O^+(aq) \rightleftharpoons 4\,Fe^{3+}(aq) + 6\,H_2O(l) \quad (11.3.15)$$

To maintain current efficiency, all the Fe^{2+} must react with $Cr_2O_7^{2-}$. The reaction of Fe^{2+} with O_2 means that more of the Fe^{3+} mediator is needed, increasing the time to reach the titration's endpoint. As a result, we report the presence of too much $Cr_2O_7^{2-}$.

3. What effect is there if the $NH_4Fe(SO_4)_2$ is contaminated with trace amounts of Fe^{2+}? How can you compensate for this source of Fe^{2+}?

There are two sources of Fe^{2+}: that generated from the mediator and that present as an impurity. Because the total amount of Fe^{2+} reacting with $Cr_2O_7^{2-}$ remains unchanged, less Fe^{2+} must be generated from the mediator. This decreases the time needed to reach the titration's end point. Because the apparent current efficiency is greater than 100%, and the reported concentration of $Cr_2O_7^{2-}$ is too small. We can remove trace amount of Fe^{2+} from the mediator solution by adding H_2O_2 and heating at 50–70°C until the evolution of O_2 ceases, converting the Fe^{2+} to Fe^{3+}. Alternatively, we can complete a blank titration to correct for any impurities of Fe^{2+} in the mediator.

4. Why is the level of solution in the counter electrode's cell maintained above the solution level in the working electrode's cell?

This prevents the solution containing the analyte from entering the counter electrode's cell. The oxidation of H_2O at the counter electrode produces O_2, which can react with the Fe^{2+} generated at the working electrode or the Cr^{3+} resulting from the reaction of Fe^{2+} and $Cr_2O_7^{2-}$. In either case, the result is a positive determinate error.

11.3.4 Characterization Applications

One useful application of coulometry is determining the number of electrons involved in a redox reaction. To make the determination, we complete a controlled-potential coulometric analysis using a known amount of a pure compound. The total charge at the end of the electrolysis is used to determine the value of *n* using Faraday's law (equation 11.25).

Example 11.11

A 0.3619-g sample of tetrachloropicolinic acid, $C_6HNO_2Cl_4$, is dissolved in distilled water, transferred to a 1000-mL volumetric flask, and diluted to volume. An exhaustive controlled-potential electrolysis of a 10.00-mL portion of this solution at a spongy silver cathode requires 5.374 C of charge. What is the value of *n* for this reduction reaction?

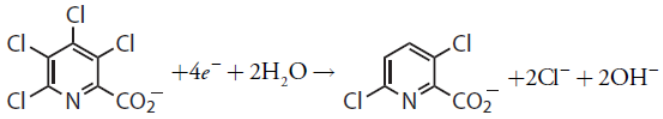
Solution

The 10.00-mL portion of sample contains 3.619 mg, or 1.39×10^{-5} mol of tetrachloropicolinic acid. Solving equation 11.25 for *n* and making appropriate substitutions gives

$$n = \frac{Q}{FN_A} = \frac{5.274\ \text{C}}{(96478\ \text{C/mol}\ e^-)(1.39 \times 10^{-5}\ \text{mol}\ C_6HNO_2Cl_4)} \quad (11.3.16)$$

$$= 4.01\ \text{mol}\ e^-/\text{mol}\ C_6HNO_2Cl_4 \quad (11.3.17)$$

Thus, reducing a molecule of tetrachloropicolinic acid requires four electrons. The overall reaction, which results in the selective formation of 3,6-dichloropicolinic acid, is



11.3.5 Evaluation

Scale of Operation

A coulometric method of analysis can be used to analyze a small absolute amount of an analyte. In controlled-current coulometry, for example, the moles of analyte consumed during an exhaustive electrolysis is given by equation 11.35. An electrolysis using a constant current of 100 μA for 100 s, for example, consumes only 1×10^{-7} mol of analyte if $n = 1$. For an analyte with a molecular weight of 100 g/mol, 1×10^{-7} mol of analyte corresponds to only 10 μg. The concentration of analyte in the electrochemical cell,

however, must be sufficient to allow an accurate determination of the endpoint. When using a visual end point, the smallest concentration of analyte that can be determined by a coulometric titration is approximately 10^{-4} M. As is the case for a conventional titration, a coulometric titration using a visual end point is limited to major and minor analytes. A coulometric titration to a preset potentiometric endpoint is feasible even if the analyte's concentration is as small as 10^{-7} M, extending the analysis to trace analytes.[12]

> **Note**
>
> See Figure 3.5 to review the meaning of major, minor, and and trace analytes.

Accuracy

When using controlled-current coulometry accuracy is determined by the current efficiency, by the accuracy with which we can measure current and time, and by the accuracy of the end point. The maximum measurement errors for current and time are about ±0.01% and ±0.1%, respectively. The maximum end point error for a coulometric titration is at least as good as that for a conventional titration, and is often better when using small quantities of reagents. Together, these measurement errors suggest that an accuracy of 0.1%–0.3% is feasible. The limiting factor in many analyses, therefore, is current efficiency. A current efficiency of greater than 99.5% is fairly routine, and it often exceeds 99.9%.

In controlled-potential coulometry, accuracy is determined by current efficiency and by the determination of charge. If the sample is free of interferents that are easier to oxidize or reduce than the analyte, a current efficiency of greater than 99.9% is routine. When an interferent is present, it can often be eliminated by applying a potential where the exhaustive electrolysis of the interferents is possible without the simultaneous electrolysis of the analyte. Once the interferent has been removed the potential can be switched to a level where electrolysis of the analyte is feasible. The limiting factor in the accuracy of many controlled-potential coulometric methods of analysis is the determination of charge. With electronic integrators the total charge can be determined with an accuracy of better than 0.5%.

If we cannot obtain an acceptable current efficiency, an electrogravimetic analysis may be possible if the analyte—and only the analyte—forms a solid deposit on the working electrode. In this case the working electrode is weighed before beginning the electrolysis and reweighed when the electrolysis is complete. The difference in the electrode's weight gives the analyte's mass.

Precision

Precision is determined by the uncertainties in measuring current, time, and the endpoint in controlled-current coulometry or of charge in controlled-potential coulometry. Precisions of ±0.1–0.3% are routinely obtained in coulometric titrations, and precisions of ±0.5% are typical for controlled-potential coulometry.

Sensitivity

For a coulometric method of analysis the calibration sensitivity is equivalent to nF in equation 11.25. In general, a coulometric method is more sensitive if the analyte's oxidation or reduction involves a larger value of n.

Selectivity

Selectivity in controlled-potential and controlled-current coulometry is improved by carefully adjusting solution conditions and by properly selecting the electrolysis potential. In controlled-potential coulometry, the potential is fixed by the potentiostat, and in controlled-current coulometry the potential is determined by the redox reaction with the mediator. In either case, the ability to control the electrolysis potential affords some measure of selectivity. By adjusting pH or adding a complexing agent, it may be possible to shift the potential at which an analyte or interferent undergoes oxidation or reduction. For example, the standard-state reduction potential for Zn^{2+} is –0.762 V versus the SHE. If we add a solution of NH_3, forming $Zn(NH_3)_4^2$, the standard state potential shifts to –1.04 V. This provides an additional means for controlling selectivity when an analyte and interferent undergo electrolysis at similar potentials.

Time, Cost, and Equipment

Controlled-potential coulometry is a relatively time consuming analysis, with a typical analysis requiring 30–60 min. Coulometric titrations, on the other hand, require only a few minutes, and are easily adapted for automated analysis. Commercial

instrumentation for both controlled-potential and controlled-current coulometry is available, and is relatively inexpensive. Low cost potentiostats and constant-current sources are available for approximately $1000.

Contributors

David Harvey (DePauw University)

11.3: Coulometric Methods is shared under a CC BY-NC-SA 4.0 license and was authored, remixed, and/or curated by LibreTexts.

11.4: Voltammetric Methods

In **voltammetry** we apply a time-dependent potential to an electrochemical cell and measure the resulting current as a function of that potential. We call the resulting plot of current versus applied potential a **voltammogram**, and it is the electrochemical equivalent of a spectrum in spectroscopy, providing quantitative and qualitative information about the species involved in the oxidation or reduction reaction.[13] The earliest voltammetric technique is polarography, developed by Jaroslav Heyrovsky in the early 1920s—an achievement for which he was awarded the Nobel Prize in Chemistry in 1959. Since then, many different forms of voltammetry have been developed, a few of which are highlighted in Figure 11.6. Before examining these techniques and their applications in more detail, we must first consider the basic experimental design for voltammetry and the factors influencing the shape of the resulting voltammogram.

11.4.1 Voltammetric Measurements

Although early voltammetric methods used only two electrodes, a modern voltammeter makes use of a three-electrode potentiostat, such as that shown in Figure 11.5. In voltammetry we apply a time-dependent potential excitation signal to the working electrode—changing its potential relative to the fixed potential of the reference electrode—and measure the current that flows between the working and auxiliary electrodes. The auxiliary electrode is generally a platinum wire, and the reference electrode is usually a SCE or a Ag/AgCl electrode.

> **Note**
>
> Figure 11.5 shows an example of a manual three-electrode potentiostat. Although a modern potentiostat uses very different circuitry, you can use Figure 11.5 and the accompanying discussion to understand how we can control the potential of working electrode and measure the resulting current.
>
> Later in the chapter we will examine several different potential excitation signals, but if you want to sneak a peak, see Figure 11.44, Figure 11.45, Figure 11.46, and Figure 11.47.

For the working electrode we can choose among several different materials, including mercury, platinum, gold, silver, and carbon. The earliest voltammetric techniques, including polarography, used a mercury working electrode. Because mercury is a liquid, the working electrode is often a drop suspended from the end of a capillary tube. In the **hanging mercury drop electrode**, or HMDE, we extrude the drop of Hg by rotating a micrometer screw that pushes the mercury from a reservoir through a narrow capillary tube (Figure 11.34a).

In the **dropping mercury electrode**, or DME, mercury drops form at the end of the capillary tube as a result of gravity (Figure 11.34b). Unlike the HMDE, the mercury drop of a DME grows continuously—as mercury flows from the reservoir under the influence of gravity—and has a finite lifetime of several seconds. At the end of its lifetime the mercury drop is dislodged, either manually or on its own, and replaced by a new drop.

The **static mercury drop electrode**, or SMDE, uses a solenoid driven plunger to control the flow of mercury (Figure 11.34c). Activation of the solenoid momentarily lifts the plunger, allowing mercury to flow through the capillary and forming a single, hanging Hg drop. Repeatedly activating the solenoid produces a series of Hg drops. In this way the SMDE may be used as either a HMDE or a DME.

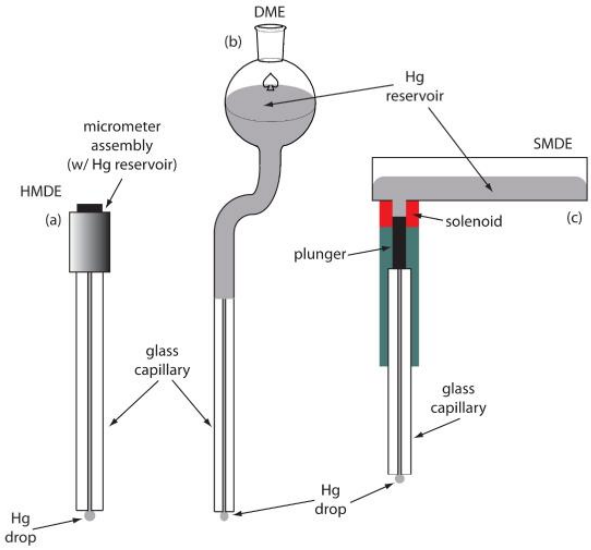


Figure 11.34 Three examples of mercury electrodes: (a) hanging mercury drop electrode, or HMDE; (b) dropping mercury electrode, or DME; and (c) static mercury drop electrode, or SMDE.

There is one additional type of mercury electrode: the **mercury film electrode**. A solid electrode—typically carbon, platinum, or gold—is placed in a solution of Hg^{2+} and held at a potential where the reduction of Hg^{2+} to Hg is favorable, forming a thin mercury film on the solid electrode's surface.

> **Note**
>
> Figure 11.36 shows a typical solid electrode.

Mercury has several advantages as a working electrode. Perhaps the most important advantage is its high overpotential for the reduction of H_3O^+ to H_2, which makes accessible potentials as negative as –1 V versus the SCE in acidic solutions and –2 V versus the SCE in basic solutions (Figure 11.35). A species such as Zn^{2+}, which is difficult to reduce at other electrodes without simultaneously reducing H_3O^+, is easily reduced at a mercury working electrode. Other advantages include the ability of metals to dissolve in mercury—resulting in the formation of an **amalgam**—and the ability to easily renew the surface of the electrode by extruding a new drop. One limitation to using mercury as a working electrode is the ease with which it is oxidized. Depending on the solvent, a mercury electrode can not be used at potentials more positive than approximately –0.3 V to +0.4 V versus the SCE.

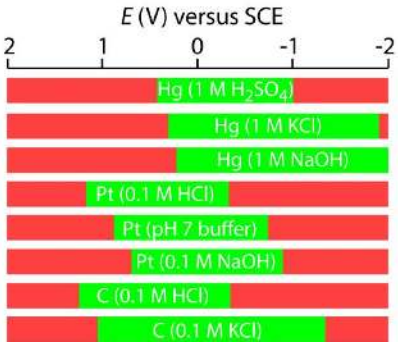


Figure 11.35 Approximate potential windows for mercury, platinum, and carbon (graphite) electrodes in acidic, neutral, and basic aqueous solvents. The useful potential windows are shown in green; potentials in red result in the oxidation or reduction of the solvent or the electrode. Complied from Adams, R. N. *Electrochemistry at Solid Electrodes*, Marcel Dekker, Inc.: New York, 1969 and Bard, A. J.; Faulkner, L. R. *Electrochemical Methods*, John Wiley & Sons: New York, 1980.

Solid electrodes constructed using platinum, gold, silver, or carbon may be used over a range of potentials, including potentials that are negative and positive with respect to the SCE (Figure 11.35). For example, the potential window for a Pt electrode extends from approximately +1.2 V to –0.2 V versus the SCE in acidic solutions, and from +0.7 V to –1 V versus the SCE in basic solutions. A

solid electrode can replace a mercury electrode for many voltammetric analyses that require negative potentials, and is the electrode of choice at more positive potentials. Except for the carbon paste electrode, a solid electrode is fashioned into a disk and sealed into the end of an inert support with an electrical lead (Figure 11.36). The carbon paste electrode is made by filling the cavity at the end of the inert support with a paste consisting of carbon particles and a viscous oil. Solid electrodes are not without problems, the most important of which is the ease with which the electrode's surface is altered by the adsorption of a solution species or by the formation of an oxide layer. For this reason a solid electrode needs frequent reconditioning, either by applying an appropriate potential or by polishing.

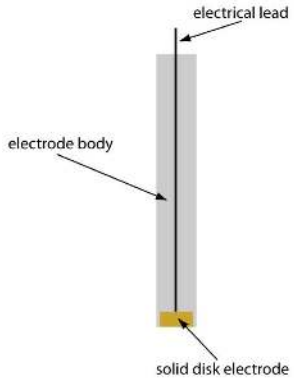


Figure 11.36 Schematic showing a solid electrode. The electrode is fashioned into a disk and sealed in the end of an inert polymer support along with an electrical lead.

A typical arrangement for a voltammetric electrochemical cell is shown in Figure 11.37. In addition to the working electrode, the reference electrode, and the auxiliary electrode, the cell also includes a N_2-purge line for removing dissolved O_2, and an optional stir bar. Electrochemical cells are available in a variety of sizes, allowing the analysis of solution volumes ranging from more than 100 mL to as small as 50 μL.

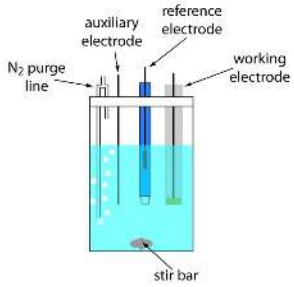


Figure 11.37 Typical electrochemical cell for voltammetry.

11.4.2 Current in Voltammetry

When we oxidize an analyte at the working electrode, the resulting electrons pass through the potentiostat to the auxiliary electrode, reducing the solvent or some other component of the solution matrix. If we reduce the analyte at the working electrode, the current flows from the auxiliary electrode to the cathode. In either case, the current from redox reactions at the working electrode and the auxiliary electrodes is called a **faradaic current**. In this section we consider the factors affecting the magnitude of the faradaic current, as well as the sources of any non-faradaic currents.

Sign Conventions

Because the reaction of interest occurs at the working electrode, we describe the faradaic current using this reaction. A faradaic current due to the analyte's reduction is a **cathodic current**, and its sign is positive. An **anodic current** is due to an oxidation reaction at the working electrode, and its sign is negative.

Influence of Applied Potential on the Faradaic Current

As an example, let's consider the faradaic current when we reduce $Fe(CN)_6^{3-}$ to $Fe(CN)_6^{4-}$ at the working electrode. The relationship between the concentrations of $Fe(CN)_6^{3-}$, the concentration of $Fe(CN)_6^{4-}$, and the potential is given by the Nernst equation

$$E = +0.356\ \text{V} - 0.05916 \log \frac{[Fe(CN)_6^{4-}]_{x=0}}{[Fe(CN)_6^{3-}]_{x=0}} \tag{11.4.1}$$

where +0.356 V is the standard-state potential for the $Fe(CN)_6^{3-}/Fe(CN)_6^{4-}$ redox couple, and x = 0 indicates that the concentrations of $Fe(CN)_6^{3-}$ and $Fe(CN)_6^{4-}$ are those at the surface of the working electrode. We use surface concentrations instead of bulk concentrations because the equilibrium position for the redox reaction

$$Fe(CN)_6^{3-}(aq) + e^- \leftrightharpoons Fe(CN)_6^{4-}(aq) \tag{11.4.2}$$

is established at the electrode's surface.

Let's assume we have a solution for which the initial concentration of $Fe(CN)_6^{3-}$ is 1.0 mM, and in which $Fe(CN)_6^{4-}$ is absent. Figure 11.38 shows the ladder diagram for this solution. If we apply a potential of +0.530 V to the working electrode, the concentrations of $Fe(CN)_6^{3-}$ and $Fe(CN)_6^{4-}$ at the surface of the electrode are unaffected, and no faradaic current is observed (see Figure 11.38). If we switch the potential to +0.356 V some of the $Fe(CN)_6^{3-}$ at the electrode's surface reduces to $Fe(CN)_6^{4-}$ until we reach a condition where

$$[Fe(CN)_6^{3-}]_{x=0} = [Fe(CN)_6^{4-}]_{x=0} = 0.50\ \text{mM} \tag{11.4.3}$$

> **Note**
>
> This is the first of the five important principles of electrochemistry outlined in Section 11.1: the electrode's potential determines the analyte's form at the electrode's surface.

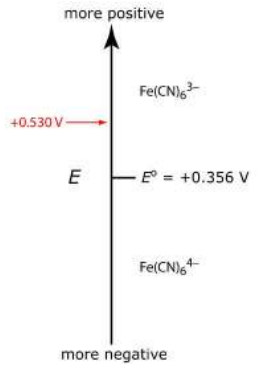


Figure 11.38 Ladder diagram for the $Fe(CN)_6^{3-}/Fe(CN)_6^{4-}$ redox half-reaction.

If this is all that happens after we apply the potential, then there would be a brief surge of faradaic current that quickly returns to zero—not the most interesting of results. Although the concentrations of $Fe(CN)_6^{3-}$ and $Fe(CN)_6^{4-}$ at the electrode surface are 0.50 mM, their concentrations in bulk solution remains unchanged. Because of this difference in concentration, there is a concentration gradient between the solution at the electrode's surface and the bulk solution. This concentration gradient creates a driving force that transports $Fe(CN)_6^{4-}$ away from the electrode and that transports $Fe(CN)_6^{3-}$ to the electrode (Figure 11.39). As the $Fe(CN)_6^{3-}$ arrives at the electrode it, too, is reduced to $Fe(CN)_6^{4-}$. A faradaic current continues to flow until there is no difference between the concentrations of $Fe(CN)_6^{3-}$ and $Fe(CN)_6^{4-}$ at the electrode and their concentrations in bulk solution.

> **Note**
>
> This is the second of the five important principles of electrochemistry outlined in Section 11.1: the analyte's concentration at the electrode may not be the same as its concentration in bulk solution.

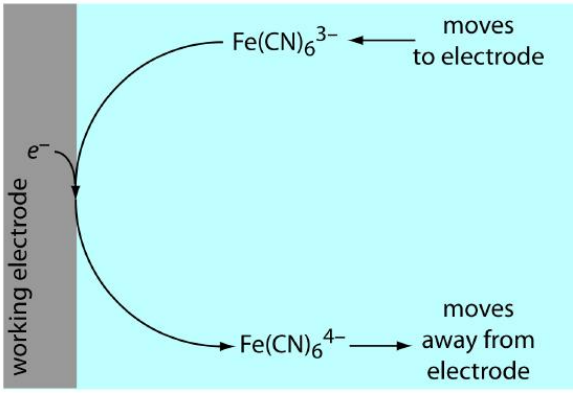


Figure 11.39 Schematic showing the transport of $Fe(CN)_6^{4-}$ away from the electrode's surface and the transport of $Fe(CN)_6^{3-}$ toward the electrode's surface following the reduction of $Fe(CN)_6^{3-}$ to $Fe(CN)_6^{4-}$.

Although the potential at the working electrode determines if a faradaic current flows, the magnitude of the current is determined by the rate of the resulting oxidation or reduction reaction. Two factors contribute to the rate of the electrochemical reaction: the rate at which the reactants and products are transported to and from the electrode—what we call **mass transport**—and the rate at which electrons pass between the electrode and the reactants and products in solution.

> **Note**
>
> This is the fourth of the five important principles of electrochemistry outlined in Section 11.1: current is a measure of rate.

Influence of Mass Transport on the Faradaic Current

There are three modes of mass transport that affect the rate at which reactants and products move toward or away from the electrode surface: diffusion, migration, and convection. **Diffusion** occurs whenever the concentration of an ion or molecule at the surface of the electrode is different from that in bulk solution. If we apply a potential sufficient to completely reduce $Fe(CN)_6^{3-}$ at the electrode surface, the result is a concentration gradient similar to that shown in Figure 11.40. The region of solution over which diffusion occurs is the **diffusion layer**. In the absence of other modes of mass transport, the width of the diffusion layer, δ, increases with time as the $Fe(CN)_6^{3-}$ must diffuse from increasingly greater distances.

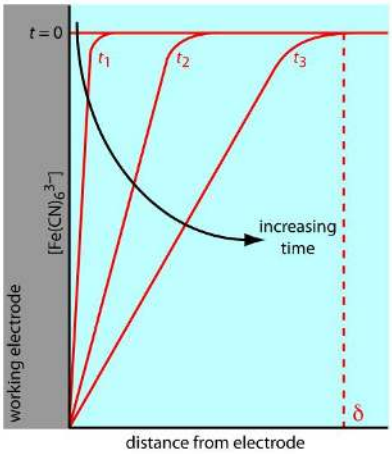


Figure 11.40 Concentration gradients (in red) for $Fe(CN)_6^{3-}$ following the application of a potential that completely reduces it to $Fe(CN)_6^{4-}$. Before applying the potential ($t = 0$) the concentration of $Fe(CN)_6^{3-}$ is the same at all distances from the electrode's surface. After applying the potential, its concentration at the electrode's surface decreases to zero and $Fe(CN)_6^{3-}$ diffuses to the electrode from bulk solution. The longer we apply the potential, the greater the distance over which diffusion occurs. The dashed red line shows the extent of the diffusion layer at time t_3. These profiles assume that convection and migration do not significantly contribute to the mass transport of $Fe(CN)_6^{3-}$.

Convection occurs when we mechanically mix the solution, carrying reactants toward the electrode and removing products from the electrode. The most common form of convection is stirring the solution with a stir bar. Other methods that have been used include rotating the electrode and incorporating the electrode into a flow-cell.

The final mode of mass transport is **migration**, which occurs when a charged particle in solution is attracted to or repelled from an electrode that carries a surface charge. If the electrode carries a positive charge, for example, an anion will move toward the electrode and a cation will move toward the bulk solution. Unlike diffusion and convection, migration only affects the mass transport of charged particles.

The movement of material to and from the electrode surface is a complex function of all three modes of mass transport. In the limit where diffusion is the only significant form of mass transport, the current in a voltammetric cell is equal to

$$i = \frac{nFAD(C_{\text{bulk}} - C_{x=0})}{\delta} \tag{11.36}$$

where n the number of electrons in the redox reaction, F is Faraday's constant, A is the area of the electrode, D is the diffusion coefficient for the species reacting at the electrode, C_{bulk} and $C_{\text{x=0}}$ are its concentrations in bulk solution and at the electrode surface, and δ is the thickness of the diffusion layer.

For equation 11.36 to be valid, convection and migration must not interfere with the formation of a diffusion layer. We can eliminate migration by adding a high concentration of an inert supporting electrolyte. Because ions of similar charge are equally attracted to or repelled from the surface of the electrode, each has an equal probability of undergoing migration. A large excess of an inert electrolyte ensures that few reactants or products experience migration. Although it is easy to eliminate convection by not stirring the solution, there are experimental designs where we cannot avoid convection, either because we must stir the solution or because we are using electrochemical flow cell. Fortunately, as shown in Figure 11.41, the dynamics of a fluid moving past an electrode results in a small diffusion layer—typically 1–10 μm in thickness—in which the rate of mass transport by convection drops to zero.

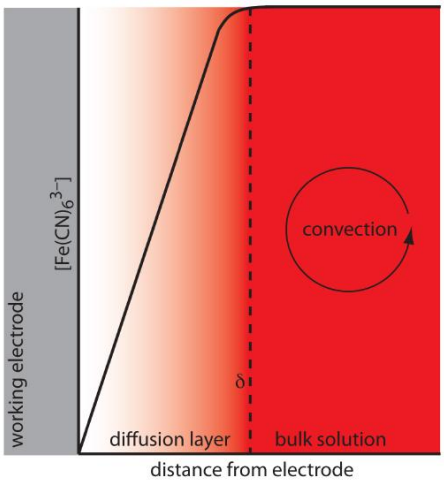


Figure 11.41 Concentration gradient for $Fe(CN)_6^{3-}$ when stirring the solution. Diffusion is the only significant form of mass transport close to the electrode's surface. At distances greater than δ, convection is the only significant form of mass transport, maintaining a homogeneous solution in which the concentration of $Fe(CN)_6^{3-}$ at d is the same as its concentration in bulk solution.

Effect of Electron Transfer Kinetics on the Faradaic Current

The rate of mass transport is one factor influencing the current in voltammetry. The ease with which electrons move between the electrode and the species reacting at the electrode also affects the current. When electron transfer kinetics are fast, the redox reaction is at equilibrium. Under these conditions the redox reaction is **electrochemically reversible** and the Nernst equation applies. If the electron transfer kinetics are sufficiently slow, the concentration of reactants and products at the electrode surface—and thus the magnitude of the faradaic current—are not what is predicted by the Nernst equation. In this case the system is **electrochemically irreversible**.

Charing Currents

In addition to current resulting from redox reactions—what we call faradaic current—the current in an electrochemical cell includes other, nonfaradaic sources. Suppose the charge on an electrode is zero and that we suddenly change its potential so that the electrode's surface acquires a positive charge. Cations near the electrode's surface respond to this positive charge by migrating away from the electrode; anions, on the other hand, migrate toward the electrode. This migration of ions occurs until the electrode's positive surface charge and the negative charge of the solution near the electrode are equal. Because the movement of ions and the movement of electrons are indistinguishable, the result is a small, short-lived **nonfaradaic current** that we call the **charging current**. Every time we change the electrode's potential, a transient charging current flows.

> **Note**
>
> The migration of ions in response to the electrode's surface charge leads to the formation of a structured electrode-solution interface that we call the **electrical double layer**, or EDL. When we change an electrode's potential, the charging current is the result of a restructuring of the EDL. The exact structure of the electrical double layer is not important in the context of this text, but you can consult this chapter's additional resources for additional information.

Residual Current

Even in the absence of analyte, a small, measurable current flows through an electrochemical cell. This **residual current** has two components: a faradaic current due to the oxidation or reduction of trace impurities and the charging current. Methods for discriminating between the analyte's faradaic current and the residual current are discussed later in this chapter.

11.4.3 Shape of Voltammograms

The shape of a voltammogram is determined by several experimental factors, the most important of which are how we measure the current and whether convection is included as a means of mass transport. As shown in Figure 11.42, despite an abundance of different voltammetric techniques, several of which are discussed in this chapter, there are only three common shapes for voltammograms.

For the voltammogram in Figure 11.42a, the current increases from a background residual current to a **limiting current**, i_l. Because the faradaic current is inversely proportional to δ (equation 11.36), a limiting current can only occur if the thickness of the diffusion layer remains constant because we are stirring the solution (see Figure 11.41). In the absence of convection the diffusion layer increases with time (see Figure 11.40). As shown in Figure 11.42b, the resulting voltammogram has a **peak current** instead of a limiting current.

For the voltammograms in Figures 11.42a and 11.42b, we measure the current as a function of the applied potential. We also can monitor the change in current, Δ_i, following a change in potential. The resulting voltammogram, shown in Figure 11.42c, also has a peak current.

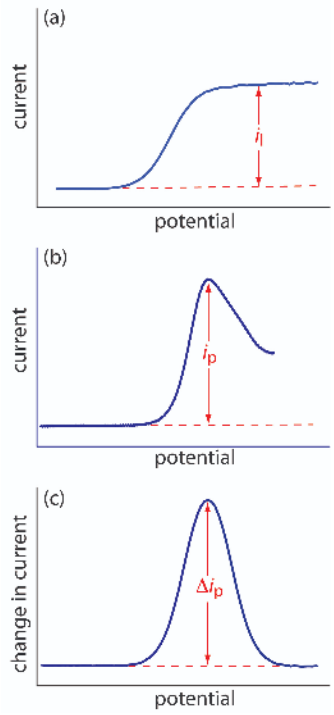


Figure 11.42 The three common shapes for voltammograms. The dashed red line shows the residual current.

11.4.4 Quantitative and Qualitative Aspects of Voltammetry

Earlier we described a voltammogram as the electrochemical equivalent of a spectrum in spectroscopy. In this section we consider how we can extract quantitative and qualitative information from a voltammogram. For simplicity we will limit our treatment to voltammograms similar to Figure 11.42a.

Determining Concentration

Let's assume that the redox reaction at the working electrode is

$$\mathrm{O} + ne^- \leftrightharpoons \mathrm{R} \tag{11.37}$$

where O is the analyte's oxidized form and R is its reduced form. Let's also assume that only O is present in bulk solution and that we are stirring the solution. When we apply a potential causing the reduction of O to R, the current depends on the rate at which O diffuses through the fixed diffusion layer shown in Figure 11.41. Using equation 11.36, the current, i, is

$$i = K_\mathrm{O}([\mathrm{O}]_\mathrm{bulk} - [\mathrm{O}]_{x=0}) \tag{11.38}$$

where K_O is a constant equal to $nFAD_\mathrm{O}/\delta$. When we reach the limiting current, i_l, the concentration of O at the electrode surface is zero and equation 11.38 simplifies to

$$i_l = K_\mathrm{O}[\mathrm{O}]_\mathrm{bulk} \tag{11.39}$$

Equation 11.39 shows us that the limiting current is a linear function of the concentration of O in bulk solution. To determine the value of K_O we can use any of the standardization methods covered in Chapter 5. Equations similar to equation 11.39 can be developed for the voltammograms shown in Figure 11.42b and Figure 11.42c.

Determining the Standard-state Potential

To extract the standard-state potential from a voltammogram, we need to rewrite the Nernst equation for reaction 11.37

$$E = E^\circ_{\mathrm{O/R}} - \frac{0.05916}{n} \log \frac{[\mathrm{R}]_{x=0}}{[\mathrm{O}]_{x=0}} \tag{11.40}$$

in terms of current instead of the concentrations of O and R. We will do this in several steps. First, we substitute equation 11.39 into equation 11.38 and rearrange to give

$$[\mathrm{O}]_{x=0} = \frac{i_l - i}{K_\mathrm{O}} \tag{11.41}$$

Next, we derive a similar equation for $[\mathrm{R}]_{x=0}$, by noting that

$$i = K_\mathrm{R}([\mathrm{R}]_{x=0} - [\mathrm{R}]_\mathrm{bulk}) \tag{11.4.4}$$

Because the concentration of $[\mathrm{R}]_\mathrm{bulk}$ is zero—remember our assumption that the initial solution contains only O—we can simplify this equation

$$i = K_\mathrm{R}[\mathrm{R}]_{x=0} \tag{11.4.5}$$

and solve for $[\mathrm{R}]_{x=0}$.

$$[\mathrm{R}]_{x=0} = \frac{i}{K_\mathrm{R}} \tag{11.42}$$

Now we are ready to finish our derivation. Substituting equation 11.42 and equation 11.41 into equation 11.40 and rearranging leaves us with

$$E = E^\circ_{\mathrm{O/R}} - \frac{0.05916}{n}\log\frac{K_\mathrm{O}}{K_\mathrm{R}} - \frac{0.05916}{n}\log\frac{i}{i_l - i} \tag{11.43}$$

When the current, i, is half of the limiting current, i_l,

$$i = 0.5 \times i_l \tag{11.4.6}$$

we can simplify equation 11.43 to

$$E_{1/2} = E^\circ_{\mathrm{O/R}} - \frac{0.05916}{n}\log\frac{K_\mathrm{O}}{K_\mathrm{R}} \tag{11.44}$$

where $E_{1/2}$ is the half-wave potential (Figure 11.43). If K_O is approximately equal to K_R, which is often the case, then the half-wave potential is equal to the standard-state potential. Note that equation 11.44 is valid only if the redox reaction is electrochemically reversible. We also can use a voltammogram with a peak potential to determine a redox reaction's standard-state potential.

Note

$$\log\frac{i}{i_l - i} = \log\frac{0.5 \times i_l}{i_l - 0.5 \times i_l} = \log\frac{0.5 \times i_l}{0.5 \times i_l} = \log(1) = 0 \tag{11.4.7}$$

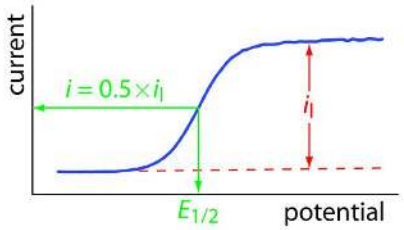


Figure 11.43 Determination of the limiting current, i_l, and the half-wave potential, $E_{1/2}$, for the voltammogram in Figure 11.42a.

11.4.5 Voltammetric Techniques

In voltammetry there are three important experimental parameters under our control: how we change the potential we apply to the working electrode, when we choose to measure the current, and whether we choose to stir the solution. Not surprisingly, there are many different voltammetric techniques. In this section we consider several important examples.

Polarography

The first important voltammetric technique to be developed—**polarography**—uses the dropping mercury electrode shown in Figure 11.34b as the working electrode. As shown in Figure 11.44, the current flowing through the electrochemical cell is measured while applying a linear potential ramp.

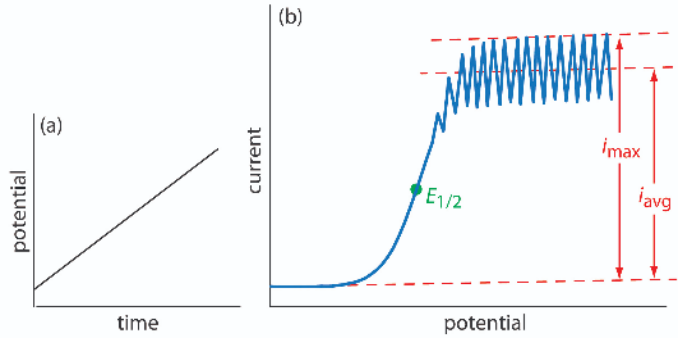


Figure 11.44 Details of normal polarography: (a) the linear potential-excitation signal, and (b) the resulting voltammogram.

Although polarography takes place in an unstirred solution, we obtain a limiting current instead of a peak current. When a Hg drop separates from the glass capillary and falls to the bottom of the electrochemical cell, it mixes the solution. Each new Hg drop, therefore, grows into a solution whose composition is identical to the bulk solution. The oscillations in the current are a result of the Hg drop's growth, which leads to a time-dependent change in the area of the working electrode. The limiting current—which is also called the diffusion current—is measured using either the maximum current, i_{max}, or from the average current, i_{avg}. The relationship between the analyte's concentration, C_A, and the limiting current is given by the Ilkovic equation

$$(i_l)_{max} = 706nD^{1/2}m^{2/3}t^{1/6}C_A = K_{max}C_A \quad (11.4.8)$$

$$(i_l)_{avg} = 607nD^{1/2}m^{2/3}t^{1/6}C_A = K_{avg}C_A \quad (11.4.9)$$

where n is the number of electrons in the redox reaction, D is the analyte's diffusion coefficient, m is the flow rate of the Hg, t is the drop's lifetime and K_{max} and K_{avg} are constants. The half-wave potential, $E_{1/2}$, provides qualitative information about the redox reaction.

> **Note**
>
> See Appendix 15 for a list of selected polarographic half-wave potentials.

Normal polarography has been replaced by various forms of **pulse polarography**, several examples of which are shown in Figure 11.45.[14] Normal pulse polarography (Figure 11.45a), for example, uses a series of potential pulses characterized by a cycle of time of τ, a pulse-time of t_p, a pulse potential of ΔE_p, and a change in potential per cycle of ΔE_s. Typical experimental conditions for normal pulse polarography are τ ≈ 1 s, t_p ≈ 50 ms, and ΔE_s ≈ 2 mV. The initial value of ΔE_p is ≈ 2 mV, and it increases by ≈ 2 mV with each pulse. The current is sampled at the end of each potential pulse for approximately 17 ms before returning the potential to its initial value. The shape of the resulting voltammogram is similar to Figure 11.44, but without the current oscillations. Because we apply the potential for only a small portion of the drop's lifetime, there is less time for the analyte to undergo oxidation or reduction and a smaller diffusion layer. As a result, the faradaic current in normal pulse polarography is greater than in the polarography, resulting in better sensitivity and smaller detection limits.

In differential pulse polarography (Figure 11.45b) the current is measured twice per cycle: for approximately 17 ms before applying the pulse and for approximately 17 ms at the end of the cycle. The difference in the two currents gives rise to the peak-shaped voltammogram. Typical experimental conditions for differential pulse polarography are τ ≈ 1 s, t_p ≈ 50 ms, ΔE_p ≈ 50 mV, and ΔE_s ≈ 2 mV.

> **Note**
>
> The voltammogram for differential pulse polarography is approximately the first derivative of the voltammogram for normal pulse polarography. To see why this is the case, note that the change in current over a fixed change in potential, $\Delta i/\Delta E$,

approximates the slope of the voltammogram for normal pulse polarography. You may recall that the first derivative of a function returns the slope of the function at each point. The first derivative of a sigmoidal function is a peak-shaped function.

Other forms of pulse polarography include staircase polarography (Figure 11.45c) and square-wave polarography (Figure 11.45d). One advantage of square-wave polarography is that we can make τ very small—perhaps as small as 5 ms, compared to 1 s for other pulse polarographies—which can significantly decrease analysis time. For example, suppose we need to scan a potential range of 400 mV. If we use normal pulse polarography with a ΔE_s of 2 mV/cycle and a τ of 1 s/cycle, then we need 200 s to complete the scan. If we use square-wave polarography with a ΔE_s of 2 mV/cycle and a τ of 5 ms/cycle, we can complete the scan in 1 s. At this rate, we can acquire a complete voltammogram using a single drop of Hg!

Polarography is used extensively for the analysis of metal ions and inorganic anions, such as IO_3^- and NO_3^-. We also can use polarography to study organic compounds with easily reducible or oxidizable functional groups, such as carbonyls, carboxylic acids, and carbon-carbon double bonds.

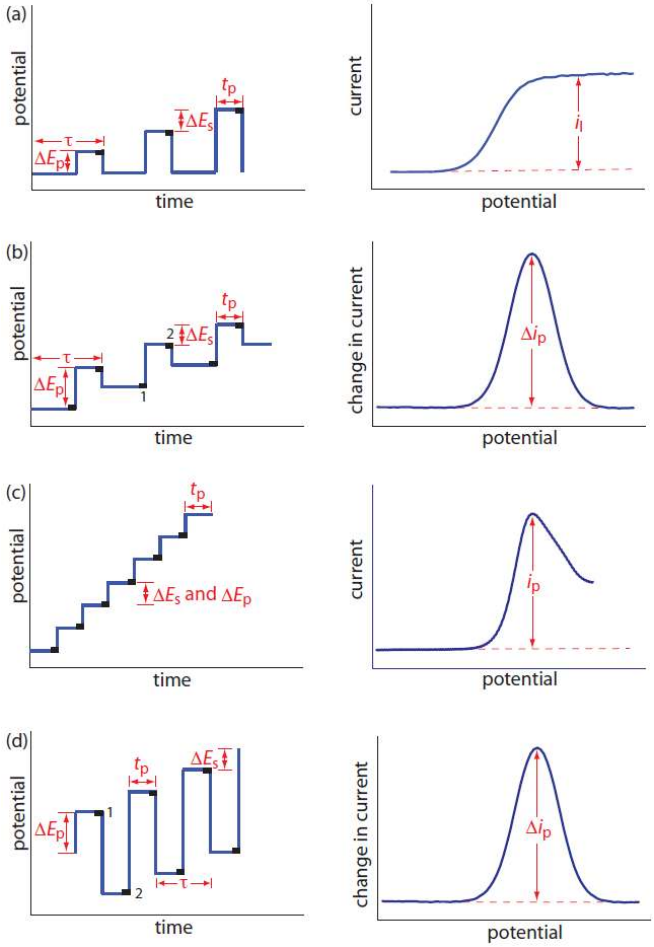


Figure 11.45 Potential-excitation signals and voltammograms for (a) normal pulse polarography, (b) differential pulse polarography, (c) staircase polarography, and (d) square-wave polarography. The current is sampled at the time intervals shown by the black rectangles. When measuring a change in current, Δ*i*, the current at point 1 is subtracted from the current at point 2. The symbols in the diagrams are as follows: τ is the cycle time; ΔE_p is a fixed or variable pulse potential; ΔE_s is the fixed change in potential per cycle, and t_p is the pulse time.

Hydrodynamic Voltammetry

In polarography we obtain a limiting current because as each drop of mercury mixes the solution as it falls to the bottom of the electrochemical cell. If we replace the DME with a solid electrode (see Figure 11.36) we can still obtain a limiting current if we

mechanically stir the solution during the analysis, either using a stir bar or by rotating the electrode. We call this approach **hydrodynamic voltammetry**.

Hydrodynamic voltammetry uses the same potential profiles as in polarography, such as a linear scan (Figure 11.44) or a differential pulse (Figure 11.45b). The resulting voltammograms are identical to those for polarography, except for the lack of current oscillations from the growth of the mercury drops. Because hydrodynamic voltammetry is not limited to Hg electrodes, it is useful for analytes that undergo oxidation or reduction at more positive potentials.

Stripping Voltammetry

Another important voltammetric technique is **stripping voltammetry**, which consists of three related techniques: anodic stripping voltammetry, cathodic stripping voltammetry, and adsorptive stripping voltammetry. Because anodic stripping voltammetry is the more widely used of these techniques, we will consider it in greatest detail.

Anodic stripping voltammetry consists of two steps (Figure 11.46). The first step is a controlled potential electrolysis in which we hold the working electrode—usually a hanging mercury drop or a mercury film electrode—at a cathodic potential sufficient to deposit the metal ion on the electrode. For example, when analyzing Cu^{2+} the deposition reaction is

$$Cu^{2+}(aq) + 2e^- \leftrightharpoons Cu(Hg) \tag{11.4.10}$$

where Cu(Hg) indicates that the copper is amalgamated with the mercury. This step essentially serves as a means of concentrating the analyte by transferring it from the larger volume of the solution to the smaller volume of the electrode. During most of the electrolysis we stir the solution to increase the rate of deposition. Near the end of the deposition time we stop the stirring—eliminating convection as a mode of mass transport—and allow the solution to become quiescent. Typical deposition times are 1–30 min are common, with analytes at lower concentrations requiring longer times.

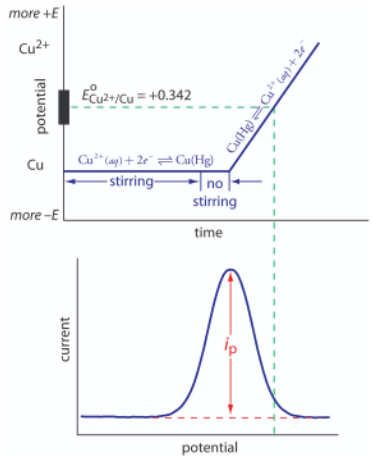


Figure 11.46 Potential-excitation signal and voltammogram for anodic stripping voltammetry at a hanging mercury drop electrode or a mercury film electrode.

In the second step, we scan the potential anodically—that is, toward a more positive potential. When the working electrode's potential is sufficiently positive, the analyte is stripped from the electrode, returning to solution in its oxidized form.

$$Cu(Hg) \rightleftharpoons Cu^{2+}{}_{(aq)} + 2e^- \tag{11.4.11}$$

Monitoring the current during the stripping step gives the peak-shaped voltammogram, as shown in Figure 11.46. The peak current is proportional to the analyte's concentration in the solution. Because we are concentrating the analyte in the electrode, detection limits are much smaller than other electrochemical techniques. An improvement of three orders of magnitude—the equivalent of parts per billion instead of parts per million—is fairly routine.

Anodic stripping voltammetry is very sensitive to experimental conditions, which we must carefully control if our results are to be accurate and precise. Key variables include the area of the mercury film or the size of the hanging Hg drop, the deposition time, the rest time, the rate of stirring, and the scan rate during the stripping step. Anodic stripping voltammetry is particularly useful for metals that form amalgams with mercury, several examples of which are listed in Table 11.11.

Table 11.11 Representative Examples of Analytes Determined by Stripping Voltammetry

anodic stripping voltammetry	cathodic stripping voltammetry	adsorptive stripping voltammetry
Bi^{3+}	Br^-	bilirubin
Cd^{2+}	Cl^-	codeine
Cu^{2+}	I^-	cocaine
Ga^{3+}	mercaptans (RSH)	digitoxin
In^{3+}	S^{2-}	dopamine
Pb^{2+}	SCN^-	heme
Tl^+		monensin
Sn^{2+}		testosterone
Zn^{2+}		

Source: Compiled from Peterson, W. M.; Wong, R. V. *Am. Lab.* November 1981, 116–128; Wang, J. *Am. Lab.* May 1985, 41–50.

The experimental design for cathodic stripping voltammetry is similar to anodic stripping voltammetry with two exceptions. First, the deposition step involves the oxidation of the Hg electrode to Hg_2^{2+}, which then reacts with the analyte to form an insoluble film at the surface of the electrode. For example, when Cl^- is the analyte the deposition step is

$$2\,Hg(l) + 2\,Cl^-(aq) \leftrightharpoons Hg_2Cl_2(s) + 2e^- \tag{11.4.12}$$

Second, stripping is accomplished by scanning cathodically toward a more negative potential, reducing Hg_2^{2+} back to Hg and returning the analyte to solution.

$$Hg_2Cl_2(s) + 2e^- \leftrightharpoons 2\,Hg(l) + 2\,Cl^-(aq) \tag{11.4.13}$$

Table 11.11 lists several analytes that have been analyzed successfully by cathodic stripping voltammetry.

In adsorptive stripping voltammetry the deposition step occurs without electrolysis. Instead, the analyte adsorbs to the electrode's surface. During deposition we maintain the electrode at a potential that enhances adsorption. For example, we can adsorb a neutral molecule on a Hg drop if we apply a potential of –0.4 V versus the SCE, a potential where the surface charge of mercury is approximately zero. When deposition is complete, we scan the potential in an anodic or a cathodic direction depending on whether we are oxidizing or reducing the analyte. Examples of compounds that have been analyzed by absorptive stripping voltammetry also are listed in Table 11.11.

Cyclic Voltammetry

In the voltammetric techniques we have consider to this point, we scan the potential in one direction, either to more positive potentials or to more negative potentials. In **cyclic voltammetry** we complete a scan in both directions. Figure 11.47a shows a typical potential-excitation signal. In this example, we first scan the potential to more positive values, resulting in the following oxidation reaction for the species R.

$$R \leftrightharpoons O + ne^- \tag{11.4.14}$$

When the potential reaches a predetermined switching potential, we reverse the direction of the scan toward more negative potentials. Because we generated the species O on the forward scan, during the reverse scan it is reduced back to R.

$$O + ne^- \leftrightharpoons R \tag{11.4.15}$$

Because we carry out cyclic voltammetry in an unstirred solution, the resulting cyclic voltammogram, as shown in Figure 11.47b, has peak currents instead of limiting currents. The voltammogram has separate peaks for the oxidation reaction and the reduction reaction, each characterized by a peak potential and a peak current.

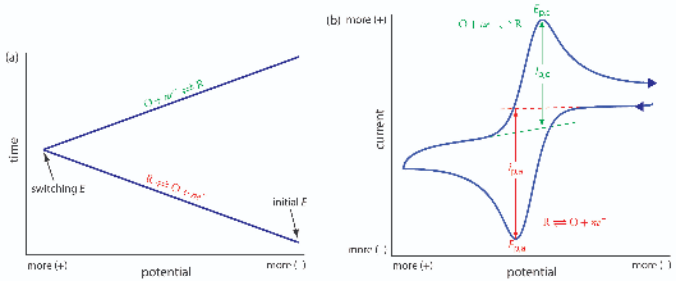


Figure 11.47 *Details for cyclic voltammetry. (a) One cycle of the triangular potential-excitation signal showing the initial potential and the switching potential. A cyclic voltammetry experiment can consist of one cycle or many cycles. Although the initial potential in this example is the negative switching potential, the cycle can begin with an intermediate initial potential and cycle between two limits. (b) The resulting cyclic voltammogram showing the measurement of the peak currents and peak potentials.*

The peak current in cyclic voltammetry is given by the Randles-Sevcik equation

$$i_p = (2.69 \times 10^5) n^{3/2} A D^{1/2} \nu^{1/2} C = KC \tag{11.4.16}$$

where n is the number of electrons in the redox reaction, A is the area of the working electrode, D is the diffusion coefficient for the electroactive species, ν is the scan rate, and C is the concentration of the electroactive species at the electrode. For a well-behaved system, the anodic and cathodic peak currents are equal, and the ratio $i_{p,a}/i_{p,c}$ is 1.00. The half-wave potential, $E_{1/2}$, is midway between the anodic and cathodic peak potentials.

$$E_{1/2} = \frac{E_{p,a} + E_{p,c}}{2} \tag{11.4.17}$$

Scanning the potential in both directions provides us with the opportunity to explore the electrochemical behavior of species generated at the electrode. This is a distinct advantage of cyclic voltammetry over other voltammetric techniques. Figure 11.48 shows the cyclic voltammogram for the same redox couple at both a faster and a slower scan rate. At the faster scan rate we see two peaks. At the slower scan rate in Figure 11.48b, however, the peak on the reverse scan disappears. One explanation for this is that the products from the reduction of R on the forward scan have sufficient time to participate in a chemical reaction whose products are not electroactive.

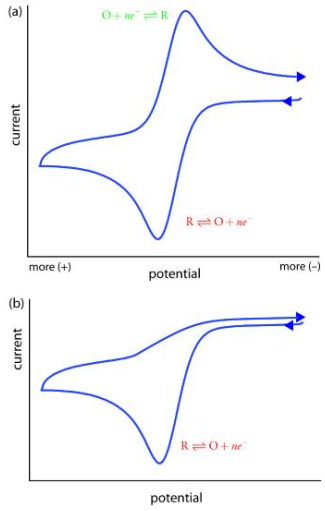


Figure 11.48 Cyclic voltammograms for R obtained at (a) a faster scan rate and (b) a slower scan rate. One of the principal uses of cyclic voltammetry is to study the chemical and electrochemical behavior of compounds. See this chapter's additional resources for further information.

Amperometry

The final voltammetric technique we will consider is **amperometry**, in which we apply a constant potential to the working electrode and measure current as a function of time. Because we do not vary the potential, amperometry does not result in a voltammogram.

One important application of amperometry is in the construction of chemical sensors. One of the first amperometric sensors was developed in 1956 by L. C. Clark to measure dissolved O_2 in blood. Figure 11.49 shows the sensor's design, which is similar to potentiometric membrane electrodes. A thin, gas-permeable membrane is stretched across the end of the sensor and is separated from the working electrode and the counter electrode by a thin solution of KCl. The working electrode is a Pt disk cathode, and a Ag ring anode serves as the counter electrode. Although several gases can diffuse across the membrane, including O_2, N_2, and CO_2, only oxygen undergoes reduction at the cathode

$$\mathrm{O_2}(aq) + 4\,\mathrm{H_3O^+}(aq) + 4e^- \leftrightharpoons 6\,\mathrm{H_2O}(l) \tag{11.4.18}$$

with its concentration at the electrode's surface quickly reaching zero. The concentration of O_2 at the membrane's inner surface is fixed by its diffusion through the membrane, creating a diffusion profile similar to that in Figure 11.41. The result is a steady-state current proportional to the concentration of dissolved oxygen. Because the electrode consumes oxygen, the sample must be stirred to prevent the depletion of O_2 at the membrane's outer surface.

> **Note**
>
> The oxidation of the Ag anode
>
> $$\mathrm{Ag}(s) + \mathrm{Cl^-}(aq) \leftrightharpoons \mathrm{AgCl}(s) + e^- \tag{11.4.19}$$
>
> is the other half-reaction.

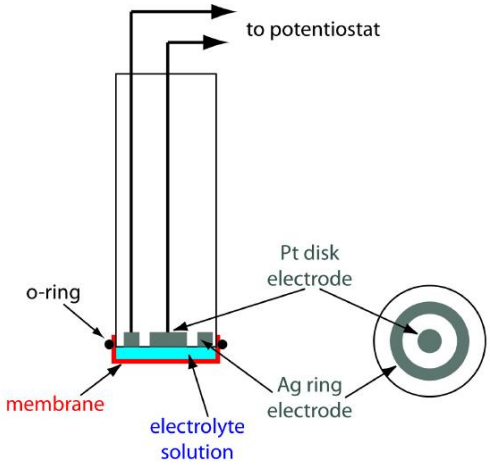


Figure 11.49 Clark amperometric sensor for determining dissolved O_2. The diagram on the right is a cross-section through the electrode, showing the Ag ring electrode and the Pt disk electrode.

Another example of an amperometric sensor is the glucose sensor. In this sensor the single membrane in Figure 11.49 is replaced with three membranes. The outermost membrane is of polycarbonate, which is permeable to glucose and O_2. The second membrane contains an immobilized preparation of glucose oxidase that catalyzes the oxidation of glucose to gluconolactone and hydrogen peroxide.

$$\text{β-D-glucose}(aq) + \mathrm{O_2}(aq) + \mathrm{H_2O}(l) \leftrightharpoons \text{gluconolactone}(aq) + \mathrm{H_2O_2}(aq) \tag{11.4.20}$$

The hydrogen peroxide diffuses through the innermost membrane of cellulose acetate where it undergoes oxidation at a Pt anode.

$$\mathrm{H_2O_2}(aq) + 2\,\mathrm{OH^-}(aq) \leftrightharpoons \mathrm{O_2}(aq) + 2\,\mathrm{H_2O}(l) + 2e^- \tag{11.4.21}$$

Figure 11.50 summarizes the reactions taking place in this amperometric sensor. FAD is the oxidized form of flavin adenine nucleotide—the active site of the enzyme glucose oxidase—and $FADH_2$ is the active site's reduced form. Note that O_2 serves a

mediator, carrying electrons to the electrode.

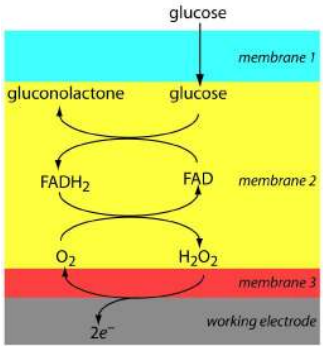


Figure 11.50 Schematic showing the reactions by which an amperometric biosensor responds to glucose.

By changing the enzyme and mediator, it is easy to extend to the amperometric sensor in Figure 11.50 to the analysis of other analytes. For example, a CO_2 sensor has been developed using an amperometric O_2 sensor with a two-layer membrane, one of which contains an immobilized preparation of autotrophic bacteria.[15] As CO_2 diffuses through the membranes it is converted to O_2 by the bacteria, increasing the concentration of O_2 at the Pt cathode.

11.4.6 Quantitative Applications

Voltammetry has been used for the quantitative analysis of a wide variety of samples, including environmental samples, clinical samples, pharmaceutical formulations, steels, gasoline, and oil.

Selecting the Voltammetric Technique

The choice of which voltammetric technique to use depends on the sample's characteristics, including the analyte's expected concentration and the sample's location. For example, amperometry is ideally suited for detecting analytes in flow systems, including the in vivo analysis of a patient's blood, or as a selective sensor for the rapid analysis of a single analyte. The portability of amperometric sensors, which are similar to potentiometric sensors, also make them ideal for field studies. Although cyclic voltammetry can be used to determine an analyte's concentration, other methods described in this chapter are better suited for quantitative work.

Pulse polarography and stripping voltammetry frequently are interchangeable. The choice of which technique to use often depends on the analyte's concentration, and the desired accuracy and precision. Detection limits for normal pulse polarography generally are on the order of 10^{-6} M to 10^{-7} M, and those for differential pulse polarography, staircase, and square wave polarography are between 10^{-7} M and 10^{-9} M. Because we concentrate the analyte in stripping voltammetry, the detection limit for many analytes is as little as 10^{-10} M to 10^{-12} M. On the other hand, the current in stripping voltammetry is much more sensitive than pulse polarography to changes in experimental conditions, which may lead to poorer precision and accuracy. We also can use pulse polarography to analyze a wider range of inorganic and organic analytes because there is no need to first deposit the analyte at the electrode surface.

Stripping voltammetry also suffers from occasional interferences when two metals, such as Cu and Zn, combine to form an intermetallic compound in the mercury amalgam. The deposition potential for Zn^{2+} is sufficiently negative that any Cu^{2+} in the sample also deposits into the mercury drop or film, leading to the formation of intermetallic compounds such as CuZn and $CuZn_2$. During the stripping step, zinc in the intermetallic compounds strips at potentials near that of copper, decreasing the current for zinc and increasing the apparent current for copper. It is often possible to overcome this problem by adding an element that forms a stronger intermetallic compound with the interfering metal. Thus, adding Ga^{3+} minimizes the interference of Cu when analyzing for Zn by forming an intermetallic compound of Cu and Ga.

Correcting for Residual Current

In any quantitative analysis we must correct the analyte's signal for signals arising from other sources. The total current, i_{tot}, in voltammetry consists of two parts: the current from the analyte's oxidation or reduction, i_a, and a background or residual current, i_r.

$$i_{tot} = i_a + i_r \tag{11.4.22}$$

The residual current, in turn, has two sources. One source is a faradaic current from the oxidation or reduction of trace impurities in the sample, i_{int}.The other source is the charging current, i_{ch}, that accompanies a change in the working electrode's potential.

$$i_r = i_{int} + i_{ch} \tag{11.4.23}$$

We can minimize the faradaic current due to impurities by carefully preparing the sample. For example, one important impurity is dissolved O_2, which undergoes a two-step reduction: first to H_2O_2 at a potential of –0.1 V versus the SCE, and then to H_2O at a potential of –0.9 V versus the SCE. Removing dissolved O_2 by bubbling an inert gas such as N_2 through the sample eliminates this interference. After removing the dissolved O_2, passing a blanket of N_2 over the top of the solution prevents O_2 from reentering the solution.

Note

The cell in Figure 11.37 shows a typical N_2 purge line.

There are two methods for compensating for the residual current. One method is to measure the total current at potentials where the analyte's faradaic current is zero and extrapolate it to other potentials. This is the method shown in Figure 11.42. One advantage of extrapolating is that we do not need to acquire additional data. An important disadvantage is that an extrapolation assumes that the change in the residual current with potential is predictable, which may not be the case. A second, and more rigorous approach, is to obtain a voltammogram for an appropriate blank. The blank's residual current is then subtracted from the sample's total current.

Analysis for Single Components

The analysis of a sample with a single analyte is straightforward. Any of the standardization methods discussed in Chapter 5 can be used to determine the relationship between the current and the analyte's concentration.

Example 11.12

The concentration of As(III) in water can be determined by differential pulse polarography in 1 M HCl. The initial potential is set to –0.1 V versus the SCE and is scanned toward more negative potentials at a rate of 5 mV/s. Reduction of As(III) to As(0) occurs at a potential of approximately –0.44 V versus the SCE. The peak currents for a set of standard solutions, which are corrected for the residual current, are shown in the following table.

[As(III)] (μM)	i_p (μA)
1.00	0.298
3.00	0.947
6.00	1.83
9.00	2.72

What is the concentration of As(III) in a sample of water if its peak current is 1.37 μA?

Solution

Linear regression gives the calibration curve shown in Figure 11.51, with an equation of

$$i_p(\mu A) = 0.0176 + 3.01 \times [As(III)](\mu M) \tag{11.4.24}$$

Substituting the sample's peak current into the regression equation gives the concentration of As(III) as 4.49×10^{-6} M.

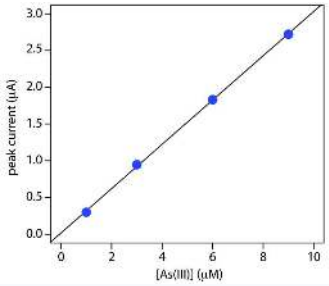


Figure 11.51 Calibration curve for the data in Example 11.12.

Exercise 11.8

The concentration of copper in a sample of sea water is determined by anodic stripping voltammetry using the method of standard additions. The analysis of a 50.0-mL sample gives a peak current of 0.886 μA. After adding a 5.00-μL spike of 10.0 mg/L Cu^{2+}, the peak current increases to 2.52 μA. Calculate the μg/L copper in the sample of sea water.

Click here to review your answer to this exercise.

Multicomponent Analysis

Voltammetry is a particularly attractive technique for the analysis of samples containing two or more analytes. Provided that the analytes behave independently, the voltammogram of a multicomponent mixture is a summation of each analyte's individual voltammograms. As shown in Figure 11.52, if the separation between the half-wave potentials or between the peak potentials is sufficient, we can independently determine each analyte as if it is the only analyte in the sample. The minimum separation between the half-wave potentials or peak potentials for two analytes depends on several factors, including the type of electrode and the potential-excitation signal. For normal polarography the separation must be at least ±0.2–0.3 V, and differential pulse voltammetry requires a minimum separation of ±0.04–0.05 V.

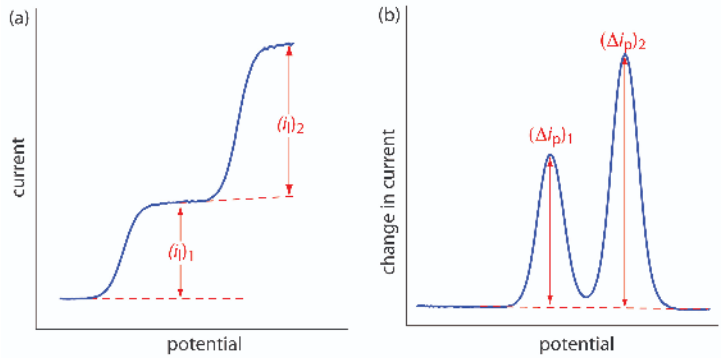


Figure 11.52 Voltammograms for a sample containing two analytes showing the measurement of (a) limiting currents, and (b) peak currents.

If the voltammograms for two analytes are not sufficiently separated, a simultaneous analysis may be possible. An example of this approach is outlined in Example 11.13.

Example 11.13

The differential pulse polarographic analysis of a mixture of indium and cadmium in 0.1 M HCl is complicated by the overlap of their respective voltammograms.[16] The peak potential for indium is at –0.557 V and that for cadmium is at –0.597 V. When a 0.800 ppm indium standard is analyzed, Δi_p (in arbitrary units) is 200.5 at –0.557 V and 87.5 at –0.597 V. A standard solution of 0.793 ppm cadmium has a Δi_p of 58.5 at –0.557 V and 128.5 at –0.597 V. What is the concentration of indium and cadmium in a sample if Δi_p is 167.0 at a potential of –0.557 V and 99.5 at a potential of –0.597V. Note: All potentials are relative to a saturated Ag/AgCl reference electrode.

Solution

The change in current, Δi_p, in differential pulse polarography is a linear function of the analyte's concentration

$$i_p = k_A C_A \tag{11.4.25}$$

where k_A is a constant that depends on the analyte and the applied potential, and C_A is the analyte's concentration. To determine the concentrations of indium and cadmium in the sample we must first find the value of k_A for each analyte at each potential. For simplicity we will identify the potential of –0.557 V as E_1, and that for –0.597 V as E_2. The values of k_A are

$$k_{In,E_1} = \frac{200.5}{0.800 \text{ ppm}} = 250.6 \text{ ppm}^{-1} \; k_{In,E_2} = \frac{87.5}{0.800 \text{ ppm}} = 109.4 \text{ ppm}^{-1} \tag{11.4.26}$$

$$k_{Cd,E_1} = \frac{58.5}{0.793 \text{ ppm}} = 73.8 \text{ ppm}^{-1} \; k_{Cd,E_2} = \frac{128.5}{0.793 \text{ ppm}} = 162.0 \text{ ppm}^{-1} \tag{11.4.27}$$

Next, we write simultaneous equations for the current at the two potentials.

$$i_{E_1} = 250.6 \text{ ppm}^{-1} \times C_{In} + 73.8 \text{ ppm}^{-1} \times C_{Cd} = 167.0 \tag{11.4.28}$$

$$i_{E_2} = 109.4 \text{ ppm}^{-1} \times C_{In} + 162.0 \text{ ppm}^{-1} \times C_{Cd} = 99.5 \tag{11.4.29}$$

Solving the simultaneous equations, which is left as an exercise, gives the concentration of indium as 0.606 ppm and the concentration of cadmium as 0.206 ppm.

Environmental Samples

Voltammetry is one of several important analytical techniques for the analysis of trace metals in environmental samples, including groundwater, lakes, rivers and streams, seawater, rain, and snow. Detection limits at the parts-per-billion level are routine for many trace metals using differential pulse polarography, with anodic stripping voltammetry providing parts-per-trillion detection limits for some trace metals.

Note

Other important techniques are atomic absorption spectroscopy (Chapter 10.4), atomic emission spectroscopy (Chapter 10.7), and ion-exchange chromatography (Chapter 12.6).

One interesting environmental application of anodic stripping voltammetry is the determination of a trace metal's chemical form within a water sample. Speciation is important because a trace metal's bioavailability, toxicity, and ease of transport through the environment often depend on its chemical form. For example, a trace metal strongly bound to colloidal particles generally is not toxic because it is not available to aquatic life-forms. Unfortunately, anodic stripping voltammetry can not distinguish a trace metal's exact chemical form because closely related species, such as Pb^{2+} and $PbCl^{+}$, produce a single stripping peak. Instead, trace metals are divided into "operationally defined" categories that have environmental significance.

Note

Operationally defined means that an analyte is divided into categories by the specific methods used to isolate it from the sample. There are many examples of operational definitions in the environmental literature. The distribution of trace metals in soils and sediments, for example, is often defined in terms of the reagents used to extract them; thus, you might find an operational definition for Zn^{2+} in a lake sediment as that extracted using 1.0 M sodium acetate, or that extracted using 1.0 M HCl.

Although there are many speciation schemes in the environmental literature, we will consider a speciation scheme proposed by Batley and Florence.[17] This scheme, which is outlined in Table 11.12, combines anodic stripping voltammetry with ion-exchange and UV irradiation, dividing soluble trace metals into seven groups. In the first step, anodic stripping voltammetry in a pH 4.8 acetic acid buffer differentiates between labile metals and nonlabile metals. Only labile metals—those present as hydrated ions, weakly bound complexes, or weakly adsorbed on colloidal surfaces—deposit at the electrode and give rise to a signal. Total metal concentration are determined by ASV after digesting the sample in 2 M HNO_3 for 5 min, which converts all metals into an ASV-labile form.

Table 11.12 Operational Speciation of Soluble Trace Metals

method	speciation of soluble metals

method	speciation of soluble metals						
ASV	labile metals			nonlabile or bound metals			
Ion-Exchange	removed	not removed		removed		not removed	
UV Irradiation		released	not released	released	not released	released	not released
Group	I	II	III	IV	V	VI	VII
Group I	free metal ions; weaker labile organic complexes and inorganic complexes						
Group II	stronger labile organic complexes; labile metals absorbed on organic solids						
Group III	stronger labile inorganic complexes; labile metals absorbed on inorganic solids						
Group IV	weaker nonlabile organic complexes						
Group V	weaker nonlabile inorganic complexes						
Group VI	stronger nonlabile organic complexes; nonlabile metals absorbed on organic solids						
Group VII	stronger nonlabile inorganic complexes; nonlabile metals absorbed on inorganic solids						

[a] As defined by (a) Batley, G. E.; Florence, T. M. *Anal. Lett.* **1976**, *9*, 379–388; (b) Batley, G. E.; Florence, T. M. *Talanta* **1977**, *24*, 151–158; (c) Batley, G. E.; Florence, T. M. *Anal. Chem.* **1980**, *52*, 1962–1963; (d) Florence, T. M., Batley, G. E.; *CRC Crit. Rev. Anal. Chem.* **1980**, *9*, 219–296.

A Chelex-100 ion-exchange resin further differentiates between strongly bound metals—usually those metals bound to inorganic and organic solids, but also those tightly bound to chelating ligands—and more loosely bound metals. Finally, UV radiation differentiates between metals bound to organic phases and inorganic phases. The analysis of seawater samples, for example, suggests that cadmium, copper, and lead are primarily present as labile organic complexes or as labile adsorbates on organic colloids (group II in Table 11.12).

> **Note**
>
> Problem 11.31 asks you to determine the speciation of trace metals in a sample of sea water.

Differential pulse polarography and stripping voltammetry also have been used to determine trace metals in airborne particulates, incinerator fly ash, rocks, minerals, and sediments. The trace metals, of course, are first brought into solution using a digestion or an extraction.

> **Note**
>
> See Chapter 7 for a discussion of digestions and extraction.

Amperometric sensors also are used to analyze environmental samples. For example, the dissolved O_2 sensor described earlier is used to determine the level of dissolved oxygen and the biochemical oxygen demand, or BOD, of waters and wastewaters. The latter test—which is a measure of the amount of oxygen required by aquatic bacteria when decomposing organic matter—is important when evaluating the efficiency of a wastewater treatment plant and for monitoring organic pollution in natural waters. A high BOD suggests that the water has a high concentration of organic matter. Decomposition of this organic matter may seriously deplete the level of dissolved oxygen in the water, adversely affecting aquatic life. Other amperometric sensors have been developed to monitor anionic surfactants in water, and CO_2, H_2SO_4, and NH_3 in atmospheric gases.

Clinical Samples

Differential pulse polarography and stripping voltammetry may be used to determine the concentration of trace metals in a variety of clinical samples, including blood, urine, and tissue. The determination of lead in blood is of considerable interest due to concerns about lead poisoning. Because the concentration of lead in blood is so small, anodic stripping voltammetry frequently is the more appropriate technique. The analysis is complicated, however, by the presence of proteins that may adsorb to the mercury electrode,

inhibiting either the deposition or stripping of lead. In addition, proteins may prevent the electrodeposition of lead through the formation of stable, nonlabile complexes. Digesting and ashing the blood sample minimizes this problem. Differential pulse polarography is useful for the routine quantitative analysis of drugs in biological fluids, at concentrations of less than 10^{-6} M.[18] Amperometric sensors using enzyme catalysts also have many clinical uses, several examples of which are shown in Table 11.13.

Table 11.13 Representative Amperometric Biosensors

analyte	enzyme	species detected
choline	choline oxidase	H_2O_2
ethanol	alcohol oxidase	H_2O_2
formaldehyde	formaldehyde dehydrogenase	NADH
glucose	glucose oxidase	H_2O_2
glutamine	glutaminase, glutamate oxidase	H_2O_2
glycerol	glycerol dehydrogenase	NADH, O_2
lactate	lactate oxidase	H_2O_2
phenol	polyphenol oxidase	quinone
inorganic phosphorous	nucleoside phosphorylase	O_2

Source: Cammann, K.; Lemke, U.; Rohen, A.; Sander, J.; Wilken, H.; Winter, B. *Angew. Chem. Int. Ed. Engl*. **1991**, *30*, 516–539.

Miscellaneous Samples

In addition to environmental samples and clinical samples, differential pulse polarography and stripping voltammetry have been used for the analysis of trace metals in other sample, including food, steels and other alloys, gasoline, gunpowder residues, and pharmaceuticals. Voltammetry is an important technique for the quantitative analysis of organics, particularly in the pharmaceutical industry where it is used to determine the concentration of drugs and vitamins in formulations. For example, voltammetric methods have been developed for the quantitative analysis of vitamin A, niacinamide, and riboflavin. When the compound of interest is not electroactive, it often can be derivatized to an electroactive form. One example is the differential pulse polarographic determination of sulfanilamide, which is converted into an electroactive azo dye by coupling with sulfamic acid and 1-napthol.

Note

The best way to appreciate the theoretical and practical details discussed in this section is to carefully examine a typical analytical method. Although each method is unique, the following description of the determination of chloropromazine in a pharmaceutical product provides an instructive example of a typical procedure. The description here is based on a method from Pungor, E. *A Practical Guide to Instrumental Analysis*, CRC Press: Boca Raton, FL, 1995, pp. 34–37.

Representative Method 11.3

Determination of Chlorpromazine in a Pharmaceutical Product

Description of Method

Chlorpromazine, which also is known by the trade name Thorazine, is an antipsychotic drug used in the treatment of schizophrenia. The amount of chlorpromazine in a pharmaceutical product is determined voltammetrically at a graphite working electrode in a unstirred solution, with calibration by the method of standard additions.

Procedure

Add 10.00 mL of an electrolyte solution consisting of 0.01 M HCl and 0.1 M KCl to the electrochemical cell. Place a graphite working electrode, a Pt auxiliary electrode, and a SCE reference electrode in the cell, and record the voltammogram from 0.2 V to 2.0 V at a scan rate of 50 mV/s. Weigh out an appropriate amount of the pharmaceutical product and dissolve it in a small amount of the electrolyte. Transfer the solution to a 100-mL volumetric flask and dilute to volume with the electrolyte. Filter a

small amount of the diluted solution and transfer 1.00 mL of the filtrate to the voltammetric cell. Mix the contents of the voltammetric cell and allow the solution to sit for 10 s before recording the voltammogram. Return the potential to 0.2 V, add 1.00 mL of a chlorpromazine standard and record the voltammogram. Report the %w/w chlorpromazine in the formulation.

Questions

1. Is chlorpromazine undergoing oxidation or reduction at the graphite working electrode?

Because we are scanning toward more positive potentials, we are oxidizing chlorpromazine.

2. Why does this procedure use a graphite electrode instead of a Hg electrode?

As shown in Figure 11.35, the potential window for a Hg electrode extends from approximately –0.3 V to between –1V and –2 V, depending upon the pH. Because we are scanning the potential from 0.2 V to 2.0 V, we cannot use a Hg electrode.

3. Many voltammetric procedures require that we first remove dissolved O_2 by bubbling N_2 through the solution. Why is this not necessary for this analysis?

Dissolved O_2 is a problem when we scan toward more negative potentials, because its reduction may produce a significant cathodic current. In this procedure we are scanning toward more positive potentials and generating anodic currents; thus, dissolved O_2 is not an interferent and does not need to be removed.

4. What is the purpose of recording a voltammogram in the absence of chlorpromazine?

This voltammogram serves as a blank, providing a measure of residual current due to the electrolyte. Because the potential window for a graphite working electrode (see Figure 11.35) does not extend to 2.0 V, there will be a measurable anodic residual current due to the solvent's oxidation. Having measured this residual current, we can subtract it from the total current in the presence of chlorpromazine.

5. Based on the description of this procedure, what is the shape of the resulting voltammogram. You may wish to review the three common shapes shown in Figure 11.42.

Because the solution is unstirred, the voltammogram will have a peak current similar to that shown in Figure 11.42b.

11.4.7 Characterization Applications

In the previous section we learned how to use voltammetry to determine an analyte's concentration in a variety of different samples. We also can use voltammetry to characterize an analyte's properties, including verifying its electrochemical reversibility, determining the number of electrons transferred during its oxidation or reduction, and determining its equilibrium constant in a coupled chemical reaction.

Electrochemical Reversibility and Determination of *n*

Earlier in this chapter we derived a relationship between $E_{1/2}$ and the standard-state potential for a redox couple (equation 11.44) noting that the redox reaction must be electrochemically reversible. How can we tell if a redox reaction is reversible by looking at its voltammogram? For a reversible redox reaction equation 11.43, which we repeat here, describes the relationship between potential and current for a voltammetric experiment with a limiting current.

$$E = E^\circ_{O/R} - \frac{0.05916}{n}\log\frac{K_O}{K_R} - \frac{0.05916}{n}\log\frac{i}{i_l - i} \qquad (11.4.30)$$

If a reaction is electrochemically reversible, a plot of E versus $\log(i/i_l - i)$ is a straight line with a slope of $-0.05916/n$. In addition, the slope should yield an integer value for n.

Example 11.14

The following data were obtained from a linear scan hydrodynamic voltammogram of a reversible reduction reaction.

E (V vs. SCE)	current (μA)
–0.358	0.37
–0.372	0.95
–0.382	1.71
–0.400	3.48
–0.410	4.20
–0.435	4.97

The limiting current was 5.15 μA. Show that the reduction reaction is reversible, and determine values for n and for $E_{1/2}$.

Solution

Figure 11.53 shows a plot of E_{cell} versus $\log(i/i_l - i)$. Because the result is a straight line, we know that the reaction is electrochemically reversible under the conditions of the experiment. A linear regression analysis gives the equation for the straight line as

$$E = -0.391\ \text{V} - 0.0300 \log \frac{i}{i_l - i} \tag{11.4.31}$$

From equation 11.43, the slope is equivalent to –0.05916/n; solving for n gives a value of 1.97, or 2 electrons. From equation 11.43 and equation 11.44, we know that $E_{1/2}$ is the y-intercept for a plot of E_{cell} versus $\log(i/i_l - i)$; thus, $E_{1/2}$ for the data in this example is –0.391 V versus the SCE.

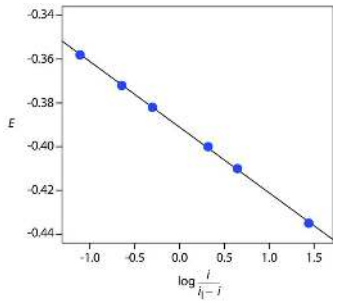


Figure 11.53 Determination of electrochemical reversibility for the data in Example 11.14.

We also can use cyclic voltammetry to evaluate electrochemical reversibility by looking at the difference between the peak potentials for the anodic and the cathodic scans. For an electrochemically reversible reaction, the following equation holds true.

$$E_p = E_{p,a} - E_{p,c} = \frac{0.05916\ \text{V}}{n} \tag{11.4.32}$$

For example, for a two-electron reduction, we expect a ΔE_p of approximately 29.6 mV. For an electrochemically irreversible reaction the value of ΔE_p will be larger than expected.

Determining Equilibrium Constants for Coupled Chemical Reactions

Another important application of voltammetry is determining the equilibrium constant for a solution reaction that is coupled to a redox reaction. The presence of the solution reaction affects the ease of electron transfer in the redox reaction, shifting $E_{1/2}$ to more negative or to more positive potentials. Consider, for example, the reduction of O to R

$$\text{O} + ne^- \leftrightharpoons \text{R} \tag{11.4.33}$$

the voltammogram for which is shown in Figure 11.54. If we introduce a ligand, L, that forms a strong complex with O, then we also must consider the reaction

$$\mathrm{O} + p\mathrm{L} \leftrightharpoons \mathrm{OL}_p \tag{11.4.34}$$

In the presence of the ligand, the overall redox reaction is

$$\mathrm{OL}_p + ne^- \leftrightharpoons \mathrm{R} + p\mathrm{L} \tag{11.4.35}$$

Because of its stability, the reduction of the OL_p complex is less favorable than the reduction of O. As shown in Figure 11.54, the resulting voltammogram shifts to a potential that is more negative than that for O. Furthermore, the shift in the voltammogram increases as we increase the ligand's concentration.

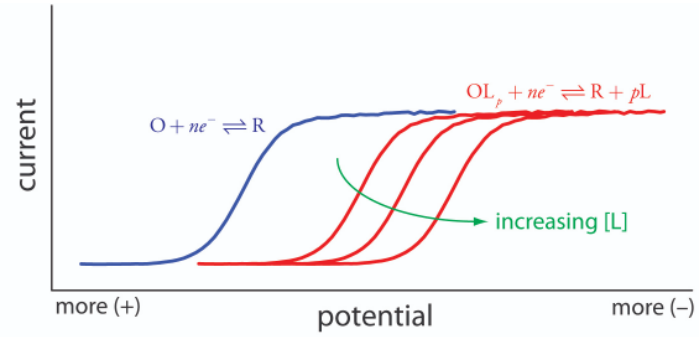


Figure 11.54 Effect of a metal-ligand complexation reaction on a voltammogram. The voltammogram in blue is for the reduction of O in the absence of ligand. Adding the ligand shifts the potentials to more negative potentials, as shown by the voltammograms in red.

We can use this shift in the value of $E_{1/2}$ to determine both the stoichiometry and the formation constant for a metal-ligand complex. To derive a relationship between the relevant variables we begin with two equations: the Nernst equation for the reduction of O

$$E = E^\circ_{\mathrm{O/R}} - \frac{0.05916}{n} \log \frac{[\mathrm{R}]_{x=0}}{[\mathrm{O}]_{x=0}} \tag{11.45}$$

and the stability constant, β_p for the metal-ligand complex at the electrode surface.

$$\beta_p = \frac{[\mathrm{OL}_p]_{x=0}}{[\mathrm{O}]_{x=0}[\mathrm{L}]^p_{x=0}} \tag{11.46}$$

Note

See Figure 3.5 to review the meaning of major, minor, and trace analytes.

In the absence of ligand the half-wave potential occurs when $[\mathrm{R}]_{\mathrm{x}\,=\,0}$ and $[\mathrm{O}]_{\mathrm{x}\,=\,0}$ are equal; thus, from the Nernst equation we have

$$(E_{1/2})_{\mathrm{nc}} = E^\circ_{\mathrm{O/R}} \tag{11.47}$$

where the subscript "nc" signifies that the complex is not present.

When ligand is present we must account for its effect on the concentration of O. Solving equation 11.46 for $[\mathrm{O}]_{\mathrm{x}\,=\,0}$ and substituting into the equation 11.45 gives

$$E = E^\circ_{\mathrm{O/R}} - \frac{0.05916}{n} \log \frac{[\mathrm{R}]_{x=0}[\mathrm{L}]^p_{x=0}\beta_p}{[\mathrm{OL}_p]_{x=0}} \tag{11.48}$$

If the formation constant is sufficiently large, such that essentially all of O is present as the complex, then $[\mathrm{R}]_{\mathrm{x}\,=\,0}$ and $[\mathrm{OL}_p]_{\mathrm{x}\,=\,0}$ are equal at the half-wave potential, and equation 11.48 simplifies to

$$(E_{1/2})_{\mathrm{c}} = E^\circ_{\mathrm{O/R}} - \frac{0.05916}{n} \log [\mathrm{L}]^p_{x=0}\beta_p \tag{11.49}$$

where the subscript "c" indicates that the complex is present. Defining $\Delta E_{1/2}$ as

$$\Delta E_{1/2} = (E_{1/2})_{\mathrm{c}} - (E_{1/2})_{\mathrm{nc}} \tag{11.50}$$

and substituting equation 11.47 and equation 11.49 and expanding the log term leaves us with the following equation.

$$\Delta E_{1/2} = -\frac{0.05916}{n}\log \beta_p - \frac{0.05916p}{n}\log[\text{L}] \tag{11.51}$$

A plot of $\Delta E_{1/2}$ versus log[L] is a straight line, with a slope of that is a function of the metal-ligand complex's stoichiometric coefficient, p, and a y-intercept that is a function of its formation constant β_p.

Example 11.15

A voltammogram for the two-electron reduction (n = 2) of a metal, M, has a half-wave potential of –0.226 V versus the SCE. In the presence of an excess of ligand, L, the following half-wave potentials are recorded.

[L] (M)	$(E_{1/2})_c$ (V vs. SCE)
0.020	–0.494
0.040	–0.512
0.060	–0.523
0.080	–0.530
0.100	–0.536

Determine the stoichiometry of the metal-ligand complex and its formation constant.

Solution

We begin by calculating values of $\Delta E_{1/2}$ using equation 11.50, obtaining the values in the following table.

[L] (M)	$\Delta(E_{1/2})_c$ (V vs. SCE)
0.020	–0.268
0.040	–0.286
0.060	–0.297
0.080	–0.304
0.100	–0.310

Figure 11.55 shows the resulting plot of $\Delta E_{1/2}$ as a function of log[L]. A linear regression analysis gives the equation for the straight line as

$$E_{1/2} = -0.370\ \text{V} - 0.0601\log[\text{L}] \tag{11.4.36}$$

From equation 11.51 we know that the slope is equal to .0.05916p/n. Using the slope and n = 2, we solve for p obtaining a value of 2.03 ≈ 2. The complexˆ's stoichiometry, therefore, is ML_2. We also know, from equation 11.51, that the y-intercept is equivalent to .(0.05916p/n)logβ_p. Solving for β_2 gives a formation constant of 3.5 ˆ× 10^{12}.

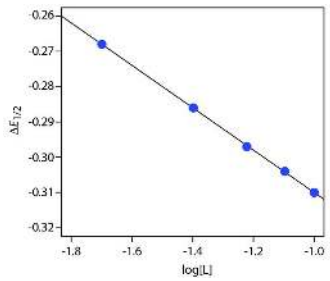


Figure 11.55 Determination of the stoichiometry and formation constant for a metal-ligand complex using the data in Example 11.15.

Practice Exercise 11.9

The voltammogram for 0.50 mM Cd^{2+} has an $E_{1/2}$ of –0.565 V versus an SCE. After making the solution 0.115 M in ethylenediamine, $E_{1/2}$ is –0.845 V, and $E_{1/2}$ is –0.873 V when the solution is 0.231 M in ethylenediamine. Determine the stoichiometry of the Cd^{2+}–ethylenediamine complex and its formation constant.

(The data in Practice Exercise 11.9 comes from Morinaga, K. "Polarographic Studies of Metal Complexes. V. Ethylenediamine Complexes of Cadmium, Nickel, and Zinc," *Bull. Chem. Soc. Japan* **1956**, *29*, 793–799.)

Click here to review your answer to this exercise.

As suggested by Figure 11.48, cyclic voltammetry is one of the most powerful electrochemical techniques for exploring the mechanism of coupled electrochemical and chemical reactions. The treatment of this aspect of cyclic voltammetry is beyond the level of this text, although you can consult this chapter's additional resources for additional information.

11.4.8 Evaluation

Scale of Operation

Detection levels at the parts-per-million level are routine. For some analytes and for some voltammetric techniques, lower detection limits are possible. Detection limits at the parts-per-billion and the part-per-trillion level are possible with stripping voltammetry. Although most analyses are carried out in conventional electrochemical cells using macro samples, the availability of microelectrodes, with diameters as small as 2 μm, allows for the analysis of samples with volumes under 50 μL. For example, the concentration of glucose in 200-μm pond snail neurons has been successfully monitored using an amperometric glucose electrode with a 2 μm tip.[19]

Note

See Figure 3.5 to review the meaning of major, minor, and and trace analytes.

Accuracy

The accuracy of a voltammetric analysis usually is limited by our ability to correct for residual currents, particularly those due to charging. For an analyte at the parts-per-million level, an accuracy of ±1–3% is routine. Accuracy decreases when analyzing samples with significantly smaller concentrations of analyte.

Precision

Precision is generally limited by the uncertainty in measuring the limiting current or the peak current. Under most conditions, a precision of ±1–3% is reasonable. One exception is the analysis of ultratrace analytes in complex matrices by stripping voltammetry, in which the precision may be as poor as ±25%.

Sensitivity

In many voltammetric experiments, we can improve the sensitivity by adjusting the experimental conditions. For example, in stripping voltammetry we can improve sensitivity by increasing the deposition time, by increasing the rate of the linear potential scan, or by using a differential-pulse technique. One reason that potential pulse techniques are popular is that they provide an improvement in current relative to a linear potential scan.

Selectivity

Selectivity in voltammetry is determined by the difference between half-wave potentials or peak potentials, with a minimum difference of ±0.2–0.3 V for a linear potential scan and ±0.04–0.05 V for differential pulse voltammetry. We often can improve selectivity by adjusting solution conditions. The addition of a complexing ligand, for example, can substantially shift the potential where a species is oxidized or reduced to a potential where it no longer interferes with the determination of an analyte. Other solution parameters, such as pH, also can be used to improve selectivity.

Time, Cost, and Equipment

Commercial instrumentation for voltammetry ranges from <$1000 for simple instruments, to >$20,000 for a more sophisticated instrument. In general, less expensive instrumentation is limited to linear potential scans. More expensive instruments provide for more complex potential-excitation signals using potential pulses. Except for stripping voltammetry, which needs a long deposition time, voltammetric analyses are relatively rapid.

Contributors

David Harvey (DePauw University)

11.4: Voltammetric Methods is shared under a CC BY-NC-SA 4.0 license and was authored, remixed, and/or curated by LibreTexts.

11.E: Electrochemical Methods (Exercises)

1. Identify the anode and cathode for the following electrochemical cells, and write the oxidation or reduction reaction at each electrode.

a. $\mathbf{Pt \mid FeCl_2}(aq, 0.015), \mathbf{FeCl_3}(aq, 0.045) \mid\mid \mathbf{AgNO_3}(aq, 0.1) \mid \mathbf{Ag}$

b. $\mathbf{Ag \mid AgBr}(s), \mathbf{NaBr}(aq, 1.0) \mid\mid \mathbf{CdCl_2}(aq, 0.05) \mid \mathbf{Cd}$

c. $\mathbf{Pb \mid PbSO_4}(s), \mathbf{H_2SO_4}(aq, 1.5) \mid\mid \mathbf{H_2SO_4}(aq, 2.0), \mathbf{PbSO_4}(s) \mid \mathbf{PbO_2}$

2. Calculate the potential for the electrochemical cells in problem 1. The values in parentheses are the activities of the associated species.

3. Calculate the activity of KI, *x*, in the following electrochemical cell if the potential is +0.294 V

$$\mathbf{Ag \mid AgCl}(s), \mathbf{NaCl}(aq, 0.1) \mid\mid \mathbf{KI}(aq, x), \mathbf{I_2}(s) \mid \mathbf{Pt}$$

4. What reaction prevents us from using Zn as an electrode of the first kind in acidic solutions? Which other electrodes of the first kind would you expect to behave in the same manner as Zn when immersed in an acidic solution?

5. Creager and colleagues designed a salicylate ion-selective electrode using a PVC membrane impregnated with tetraalkylammonium salicylate.[20] To determine the ion-selective electrode's selectivity coefficient for benzoate, they prepared a set of salicylate calibration standards in which the concentration of benzoate was held constant at 0.10 M. Using the following data, determine the value of the selectivity coefficient.

[salicylate] (M)	potential (mV)
1.0	20.2
1.0×10^{-1}	73.5
1.0×10^{-2}	126
1.0×10^{-3}	168
1.0×10^{-4}	182
1.0×10^{-5}	182
1.0×10^{-6}	177

What is the maximum acceptable concentration of benzoate if you plan to use this ion-selective electrode to analyze samples containing as little as 10^{-5} M salicylate with an accuracy of better than 1%?

6. Watanabe and co-workers described a new membrane electrode for the determination of cocaine, a weak base alkaloid with a pK_a of 8.64.[21] The electrode's response for a fixed concentration of cocaine is independent of pH in the range of 1–8, but decreases sharply above a pH of 8. Offer an explanation for this pH dependency.

7. Figure 11.20 shows a schematic diagram for an enzyme electrode that responds to urea by using a gas-sensing NH_3 electrode to measure the amount of ammonia released following the enzyme's reaction with urea. In turn, the NH_3 electrode uses a pH electrode to monitor the change in pH due to the ammonia. The response of the urea electrode is given by equation 11.14. Beginning with equation 11.11, which gives the potential of a pH electrode, show that equation 11.14 for the urea electrode is correct.

8. Explain why the response of an NH_3-based urea electrode (Figure 11.20 and equation 11.14) is different from the response of a urea electrode in which the enzyme is coated on the glass membrane of a pH electrode (Figure 11.21 and equation 11.15).

9. A potentiometric electrode for HCN uses a gas-permeable membrane, a buffered internal solution of 0.01 M $KAg(CN)_2$, and a Ag_2S ISE electrode that is immersed in the internal solution. Consider the equilibrium reactions taking place within the internal solution, and derive an equation relating the electrode's potential to the concentration of HCN in the sample.

10. Mifflin and associates described a membrane electrode for the quantitative analysis of penicillin in which the enzyme penicillinase is immobilized in a polyacrylamide gel coated on the glass membrane of a pH electrode.[22] The following data were collected using a set of penicillin standards.

[penicillin] (M)	potential (mV)
1.0×10^{-2}	220
2.0×10^{-3}	204
1.0×10^{-3}	190
2.0×10^{-4}	153
1.0×10^{-4}	135
1.0×10^{-5}	96
1.0×10^{-6}	80

(a) Over what range of concentrations is there a linear response?

(b) What is calibration curve's equation for this concentration range?

(c) What is the concentration of penicillin in a sample that yields a potential of 142 mV?

11. An ion-selective electrode can be placed in a flow cell into which we inject samples or standards. As the analyte passes through the cell, a potential spike is recorded instead of a steady-state potential. The concentration of K^+ in serum has been determined in this fashion using standards prepared in a matrix of 0.014 M NaCl.[23]

$[K^+]$ (mM)	potential (arb. units)
0.1	25.5
0.2	37.2
0.4	50.8
0.6	58.7
0.8	64.0
1.0	66.8

A 1.00-mL sample of serum is diluted to volume in a 10-mL volumetric flask and analyzed, giving a potential of 51.1 (arbitrary units). Report the concentration of K^+ in the sample of serum.

12. Wang and Taha described an interesting application of potentiometry, which they call batch injection.[24] As shown in Figure 11.56, an ionselective electrode is placed in an inverted position in a large volume tank, and a fixed volume of a sample or a standard solution is injected toward the electrode's surface using a micropipet. The response of the electrode is a spike in potential

that is proportional to the analyte's concentration. The following data were collected using a pH electrode and a set of pH standards.

pH	potential (mV)
2.0	+300
3.0	+240
4.0	+168
5.0	+81
6.0	+35
8.0	–92
9.0	–168
10.0	–235
11.0	–279

Determine the pH of the following samples given the recorded peak potentials: tomato juice, 167 mV; tap water, –27 mV; coffee, 122 mV.

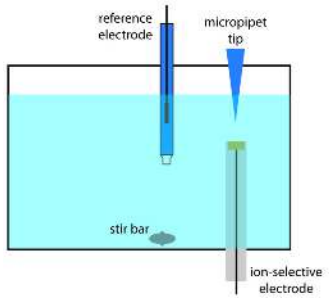


Figure 11.56 Schematic diagram for a batch injection analysis. See Problem 11.12 for more details.

13. The concentration of NO_3^- in a water sample is determined by a onepoint standard addition using a NO_3^- ion-selective electrode. A 25.00-mL sample is placed in a beaker and a potential of 0.102 V is measured. A 1.00-mL aliquot of a 200.0-mg/L standard solution of NO_3^- is added, after which the potential is 0.089 V. Report the mg NO_3^-/L in thewater sample.

14. In 1977, when I was an undergraduate student at Knox College, my lab partner and I did an experiment to determine the concentration of fluoride in tap water and the amount of fluoride in toothpaste. The data in this problem comes from my lab notebook.

(a) To analyze tap water, we took three 25.0-mL samples and added 25.0 mL of TISAB to each. We measured the potential of each solution using a F^- ISE and an SCE reference electrode. Next, we made five 1.00-mL additions of a standard solution of 100.0 ppm F^- to each sample, and measure the potential after each addition.

mL of standard added	potential (mV) sample 1	sample 2	sample 3
0.00	–79	–82	–81
1.00	–119	–119	–118
2.00	– 133	– 133	– 133
3.00	– 142	– 142	– 142
4.00	– 149	– 148	– 148
5.00	– 154	– 153	– 153

Report the parts-per-million of F^- in the tap water.

(b) To analyze the toothpaste, we measured 0.3619 g into a 100-mL volumetric flask, added 50.0 mL of TISAB, and diluted to volume with distilled water. After ensuring that the sample was thoroughly mixed, we transferred three 20.0-mL portions into separate beakers and measured the potential of each using a F^- ISE and an SCE reference electrode. Next, we made five 1.00-mL additions of a standard solution of 100.0 ppm F^- to each sample, and measured the potential after each addition.

Note

For a more thorough description of this analysis, see Representative Method 11.1.

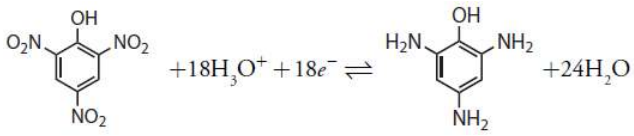
mL of standard added	potential (mV) sample 1	sample 2	sample 3
0.00	– 55	– 54	– 55
1.00	– 82	– 82	– 83
2.00	– 94	– 94	– 94
3.00	– 102	– 103	– 102
4.00	– 108	– 108	– 109
5.00	– 112	– 112	– 113

Report the parts-per-million F^- in the toothpaste.

15. You are responsible for determining the amount of KI in iodized salt and decide to use an I^- ion-selective electrode. Describe how you would perform this analysis using external standards and using the method of standard additions.

16. Explain why each of the following decreases the analysis time for controlled-potential coulometry: a larger surface area for the working electrode, a smaller volume of solution, and a faster stirring rate.

17. The purity of a sample of picric acid, $C_6H_3N_3O_7$, is determined by controlled-potential coulometry, converting the picric acid to triaminophenol, $C_6H_9N_3O$.



A 0.2917-g sample of picric acid is placed in a 1000-mL volumetric flask and diluted to volume. A 10.00-mL portion of this solution is transferred to a coulometric cell and sufficient water added so that the Pt cathode is immersed. The exhaustive electrolysis of the sample requires 21.67 C of charge. Report the purity of the picric acid.

18. The concentration of H_2S in the drainage from an abandoned mine can be determined by a coulometric titration using KI as a mediator and I_3^- as the titrant.

$$\mathrm{H_2S}(aq) + \mathrm{I_3^-}(aq) + 2\,\mathrm{H_2O}(l) \leftrightharpoons 2\,\mathrm{H_3O^+}(aq) + 3\,\mathrm{I^-}(aq) + \mathrm{S}(s) \tag{11.E.1}$$

A 50.00-mL sample of water is placed in a coulometric cell, along with an excess of KI and a small amount of starch as an indicator. Electrolysis is carried out at a constant current of 84.6 mA, requiring 386 s to reach the starch end point. Report the concentration of H_2S in the sample in parts-per-million.

19. One method for the determination of H_3AsO_3 is a coulometric titration using I_3^- as a titrant. The relevant standard-state reactions and potentials are summarized here.

$$\mathrm{H_3AsO_4}(aq) + 2\,\mathrm{H_3O^+}(aq) + 2e^- \leftrightharpoons \mathrm{H_3AsO_3}(aq) + 3\,\mathrm{H_2O}(l) \quad E^\circ = +0.559\ \mathrm{V} \tag{11.E.2}$$

$$\mathrm{I_3^-}(aq) + 2e^- \leftrightharpoons 3\mathrm{I^-}(aq) \quad E^\circ = +0.536\ \mathrm{V} \tag{11.E.3}$$

Explain why the coulometric titration must be carried out in a neutral solution (pH ≈ 7) instead of in a strongly acidic solution (pH < 0).

20. The production of adiponitrile, $NC(CH_2)_4CN$, from acrylonitrile, CH_2=CHCN, is an important industrial process. A 0.594-g sample of acrylonitrile is placed in a 1-L volumetric flask and diluted to volume. An exhaustive controlled-potential electrolysis of a 1.00-mL portion of the diluted acrylonitrile requires 1.080 C of charge. What is the value of *n* for the reduction of acrylonitrile to adiponitrile?

21. The linear-potential scan hydrodynamic voltammogram for a mixture of Fe^{2+} and Fe^{3+} is shown in Figure 11.57, where $i_{l,a}$ and $i_{l,c}$ are the anodic and cathodic limiting currents.

(a) Show that the potential is given by

$$E = E^\circ_{\mathrm{Fe^{3+}/Fe^{2+}}} - 0.05916 \log \frac{K_{\mathrm{Fe^{3+}}}}{K_{\mathrm{Fe^{2+}}}} - 0.05916 \log \frac{i - i_{\mathrm{l,a}}}{i_{\mathrm{l,c}} - i} \tag{11.E.4}$$

(b) What is the potential when i = 0 for a solution that is 0.1 mM Fe^{3+} and 0.05 mM Fe^{2+}? You may assume that $K_{Fe^{3+}} \approx K_{Fe^{2+}}$.

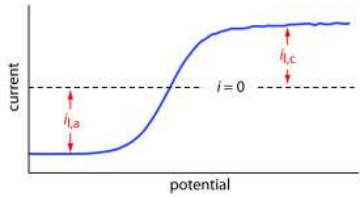


Figure 11.57 Linear-scan hydrodynamic voltammogram for a mixture of Fe^{2+} and Fe^{3+}. See Problem 11.21 for more details.

22. The amount of sulfur in aromatic monomers can be determined by differential pulse polarography. Standard solutions are prepared for analysis by dissolving 1.000 mL of the purified monomer in 25.00 mL of an electrolytic solvent, adding a known amount of S, deaerating, and measuring the peak current. The following results were obtained for a set of calibration standards.

μg S added	peak current (μA)
0	0.14
28	0.70
56	1.23
112	2.41
168	3.42

Analysis of a 1.000-mL sample, treated in the same manner as the standards, gives a peak current of 1.77 μA. Report the mg S/mL in the sample.

23. The purity of a sample of $K_3Fe(CN)_6$ was determined using linear-potential scan hydrodynamic voltammetry at a glassy carbon electrode. The following data were obtained for a set of external calibration standards.

$[K_3Fe(CN)_6]$ (mM)	limiting current (μA)
2.0	127
4.0	252
6.0	376
8.0	500
10.0	624

A sample of impure $K_3Fe(CN)_6$ was prepared for analysis by diluting a 0.246-g portion to volume in a 100-mL volumetric flask. The limiting current for the sample was found to be 444 μA. Report the purity of this sample of $K_3Fe(CN)_6$.

24. One method for determining whether an individual has recently fired a gun is to look for traces of antimony in the residue collected from the individual's hands. Anodic stripping voltammetry at a mercury film electrode is ideally suited for this analysis. In a typical analysis a sample is collected from a suspect with a cotton-tipped swab wetted with 5% v/v HNO_3. After returning to the lab, the swab is placed in a vial containing 5.0 mL of 4 M HCl that is 0.02 M in hydrazine sulfate. After allowing the swab to soak overnight, a 4.0-mL portion of the solution is transferred to an electrochemical cell along with 100 mL of 0.01 M HgCl2. After depositing the thin film of mercury and the antimony, the stripping step gives a peak current of 0.38 μA. After adding a standard addition of 100 μL of 5.00×10^2 ppb Sb, the peak current increases to 1.14 μA. How many nanograms of Sb were collected from the suspect's hand?

25. Zinc can be used as an internal standard in the analysis of thallium by differential pulse polarography. A standard solution containing 5.00×10^{-5} M Zn^{2+} and 2.50×10^{-5} M Tl^+ gave peak currents of 5.71 μA and 3.19 μA, respectively. An 8.713-g sample of an alloy known to be free of zinc was dissolved in acid, transferred to a 500-mL volumetric flask, and diluted to volume. A 25.0-mL portion of this solution was mixed with 25.0 mL of a 5.00×10^{-4} M solution of Zn^{2+}. Analysis of this solution gave a peak current for Zn^{2+} of 12.3 μA, and for Tl^+ of 20.2 μA. Report the %w/w Tl in the alloy.

26. Differential pulse voltammetry at a carbon working electrode can be used to determine the concentrations of ascorbic acid and caffeine in drug formulations.[25] In a typical analysis a 0.9183-g tablet is crushed and ground into a fine powder. A 0.5630-g sample of this powder is transferred to a 100-mL volumetric flask, brought into solution, and diluted to volume. A 0.500-mL portion is then transferred to a voltammetric cell containing 20.00 mL of a suitable supporting electrolyte. The resulting voltammogram gives peak currents of 1.40 μA and 3.88 μA for ascorbic acid and caffeine, respectively. A 0.500-mL aliquot of a standard solution containing 250.0 ppm ascorbic acid and 200.0 ppm caffeine is then added. A voltammogram of this solution gives peak currents of 2.80 μA and 8.02 μA for ascorbic acid and caffeine, respectively. Report the milligrams of ascorbic acid and milligrams of caffeine in the tablet.

27. Ratana-ohpas and co-workers described a stripping analysis method for determining the amount of tin in canned fruit juices.[26] Standards containing 50.0 ppb Sn^{4+}, 100.0 ppb Sn^{4+}, and 150.0 ppb Sn^{4+} were analyzed giving peak currents (arbitrary units) of 83.0, 171.6, and 260.2, respectively. A 2.00-mL sample of lychee juice was mixed with 20.00 mL of 1:1 HCl/HNO_3. A 0.500-mL portion of this mixture was added to 10 mL of 6 M HCl and the volume adjusted to 30.00 mL. Analysis of this diluted sample gave a signal of 128.2 (arbitrary units). Report the parts-per-million Sn^{4+} in the original sample of lychee juice.

28. Sittampalam and Wilson described the preparation and use of an amperometric sensor for glucose.[27] The sensor is calibrated by measuring the steady-state current when it is immersed in standard solutions of glucose. A typical set of calibration data is shown here.

[glucose] (mg/100 mL)	current (arb. units)
2.0	17.2
4.0	32.9
6.0	52.1
8.0	68.0
10.0	85.8

A 2.00-mL sample is diluted to 10 mL in a volumetric flask and a steady-state current of 23.6 (arbitrary units) is measured. What is the concentration of glucose in the sample in mg/100 mL?

29. Differential pulse polarography can be used to determine the concentrations of lead, thallium, and indium in a mixture. Because the peaks for lead and thallium, and for thallium and indium overlap, a simultaneous analysis is necessary. Peak currents (in arbitrary units) at –0.385 V, –0.455 V, and –0.557 V were measured for a single standard solution, and for a sample, giving the results shown in the following table.

standards		peak currents (arb. units) at		
analyte	μg/mL	–0.385 V	–0.455 V	–0.557 V
Pb^{2+}	1.0	26.1	2.9	0
Tl^{+}	2.0	7.8	23.5	3.2
In^{3+}	0.4	0	0	22.9
sample		60.6	28.8	54.1

Report the μg/mL of Pb^{2+}, Tl^{+} and In^{3+} in the sample.

30. Abass and co-workers developed an amperometric biosensor for NH_4^+ that uses the enzyme glutamate dehydrogenase to catalyze the following reaction

$$\begin{aligned}&\text{2-oxyglutarate}(aq) + \text{NH}_4^+(aq) + \text{NADH}(aq)\\ &\rightarrow \text{glutamate}(aq) + \text{NAD}^+(aq) + \text{H}_2\text{O}(l)\end{aligned} \qquad (11.E.5)$$

where NADH is the reduced form of nicotinamide adenine dinucleotide.[28] The biosensor actually responds to the concentration of NADH, however, the rate of the reaction depends on the concentration of NH_4^+. If the initial concentrations of 2-oxyglutarate and

NADH are the same for all samples and standards, then the signal is proportional to the concentration of NH_4^+. As shown in the following table, the sensitivity of the method is dependent on pH.

pH	sensitivity (nA s^{-1} M^{-1})
6.2	1.67×10^3
6.75	5.00×10^3
7.3	9.33×10^3
7.7	1.04×10^4
8.3	1.27×10^4
9.3	2.67×10^3

Two possible explanations for the effect of pH on the sensitivity of this analysis are the acid–base chemistry of NH_4^+, and the acid–base chemistry of the enzyme. Given that the pK_a for NH_4^+ is 9.244, explain the source of this pH-dependent sensitivity.

31. The speciation scheme for trace metals shown in Table 11.12 divides them into seven operationally defined groups by collecting and analyzing two samples following each of four treatments—a total of eight samples and eight measurements. After removing insoluble particulates by filtration (treatment 1), the solution is analyzed for the concentration of ASV labile metals and for the total concentration of metals. A portion of the filtered solution is passed through an ion-exchange column (treatment 2), and the concentrations of ASV metal and of total metal are determined. A second portion of the filtered solution is irradiated with UV light (treatment 3), and the concentrations of ASV metal and of total metal are measured. Finally, a third portion of the filtered solution is irradiated with UV light and passed through an ion-exchange column (treatment 4), and the concentrations of ASV labile metal and of total metal again are determined. The groups that are included in each measurement are summarized in the following table.

treatment	groups removed by treatment	groups contributing to ASV-labile metals	groups contributing to total metals
1	none	I, II, III	I, II, III, IV, V, VI, VII
2	I, IV, V	II, III	II, III, VI, VII
3	none	I, II, III, IV, VI	I, II, III, IV, V, VI, VII
4	I, II, IV, V, VI	III	III, VII

(a) Explain how you can use these eight measurements to determine the concentration of metals present in each of the seven groups identified in Table 11.12.

(b) Batley and Florence report the following results for the speciation of cadmium, lead, and copper in a sample of seawater.[29]

measurement (treatment: ASV-labile or total)	ppm Cd^{2+}	ppm Pb^{2+}	ppm Cu^{2+}
1: ASV-labile	0.24	0.39	0.26
1: total	0.28	0.50	0.40
2: ASV-labile	0.21	0.33	0.17
2: total	0.26	0.43	0.24
3: ASV-labile	0.26	0.37	0.33
3: total	0.28	0.50	0.43
4: ASV-labile	0.00	0.00	0.00
4: total	0.02	0.12	0.10

Determine the speciation of each metal in this sample of sea water.

32. The concentration of Cu^{2+} in seawater may be determined by anodic stripping voltammetry at a hanging mercury drop electrode after first releasing any copper bound to organic matter. To a 20.00-mL sample of seawater is added 1 mL of 0.05 M HNO_3 and 1 mL of 0.1% H_2O_2. The sample is irradiated with UV light for 8 hr and then diluted to volume in a 25-mL volumetric flask. Deposition of Cu^{2+} takes place at –0.3 V versus an SCE for 10 min, producing a peak current of 26.1 (arbitrary units). A second 20.00-mL sample of the seawater is treated identically, except that 0.1 mL of a 5.00 μM solution of Cu^{2+} is added, producing a peak current of 38.4 (arbitrary units). Report the concentration Cu^{2+} in the seawater in mg/L.

33. Thioamide drugs can be determined by cathodic stripping analysis.[30] Deposition occurs at +0.05 V versus an SCE. During the stripping step the potential is scanned cathodically, and a stripping peak is observed at –0.52 V. In a typical application a 2.00-mL sample of urine was mixed with 2.00 mL of a pH 4.78 buffer. Following a 2.00 min deposition, a peak current of 0.562 μA was measured. A 0.10-mL addition of a 5.00 μM solution of the drug was added to the same solution. A peak current of 0.837 mA was recorded using the same deposition and stripping conditions. Report the drug's molar concentration in the urine sample.

34. The concentration of vanadium (V) in sea water can be determined by adsorptive stripping voltammetry after forming a complex with catechol.[31] The catechol-V(V) complex is deposited on a hanging mercury drop electrode at a potential of –0.1 V versus a Ag/AgCl reference electrode. A cathodic potential scan gives a stripping peak that is proportional to the concentration of V(V). The following standard additions were used to analyze a sample of seawater.

$[V(V)]_{added}$ (M)	peak current (nA)
2.0×10^{-8}	24
4.0×10^{-8}	33
8.0×10^{-8}	52
1.2×10^{-7}	69
1.8×10^{-7}	97
2.8×10^{-7}	140

Determine the molar concentration of V (V) in the sample of sea water, assuming that the standard additions result in a negligible change in the sample's volume.

35. The standard-state reduction potential for Cu^{2+} to Cu is +0.342 V versus the SHE. Given that Cu^{2+} forms a very stable complex with the ligand EDTA, do you expect the standard-state reduction potential for $Cu(EDTA)^{2-}$ to be greater than +0.342 V, less than

+0.342 V, or equal to +0.342 V? Explain your reasoning.

36. The polarographic half-wave potentials (versus the SCE) for Pb^{2+} and Tl^{+} in 1 M HCl are, respectively, –0.44 V and –0.45 V. In an electrolyte of 1 M NaOH, however, the half-wave potentials are –0.76 V for Pb^{2+} and –0.48 V for Tl^{+}. Why does the change in electrolyte have such a significant effect on the half-wave potential for Pb^{2+}, but not on the half-wave potential for Tl^{+}?

37. The following data for the reduction of Pb^{2+} was collected by normal-pulse polarography.

potential (V vs. SCE)	current (μA)
–0.345	0.16
–0.370	0.98
–0.383	2.05
–0.393	3.13
–0.409	4.62
–0.420	5.16

The limiting current was 5.67 μA. Verify that the reduction reaction is reversible, and determine values for n and $E_{1/2}$. The half-wave potentials for the normal-pulse polarograms of Pb^{2+} in the presence of several different concentrations of OH^{-} are shown in the following table.

$[OH^{-}]$ (M)	$E_{1/2}$ (V vs. SCE)	$[OH^{-}]$ (M)	$E_{1/2}$ (V vs. SCE)
0.050	–0.646	0.150	–0.689
0.100	–0.673	0.300	–0.715

Determine the stoichiometry of the Pb-hydroxide complex and its formation constant.

38. In 1977, when I was an undergraduate student at Knox College, my lab partner and I did an experiment to study the voltammetric behavior of Cd^{2+} (in 0.1 M KNO_3) and Ni^{2+} (in 0.2 M KNO_3) at a dropping mercury electrode. The data in this problem comes from my lab notebook. All potentials are relative to an SCE reference electrode.

potential for Cd^{2+} (V)	current (μA)
–0.60	4.5
–0.58	3.4
–0.56	2.1
–0.54	0.6
–0.52	0.2

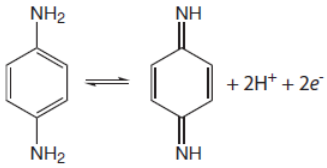
potential for Ni^{2+} (V)	current (μA)
–1.09	1.90
–1.05	1.75
–1.03	1.50
–1.02	1.25
–1.01	1.00

The limiting currents for Cd^{2+} was 4.8 μA and that for Ni^{2+} was 2.0 μA. Evaluate the electrochemical reversibility for each metal ion and comment on your results.

39. Baldwin and co-workers report the following data from a cyclic voltammetry study of the electrochemical behavior of *p*-phenylenediamine in a pH 7 buffer.[32] All potentials are measured relative to an SCE.

scan rate (mV/s)	$E_{p,a}$ (V)	$E_{p,c}$ (V)	$i_{p,a}$ (mA)	$i_{p,c}$ (mA)
2	0.148	0.104	0.34	0.30
5	0.149	0.098	0.56	0.53
10	0.152	0.095	1.00	0.94
20	0.161	0.095	1.44	1.44
50	0.167	0.082	2.12	1.81
100	0.180	0.063	2.50	2.19

The initial scan is toward more positive potentials, leading to the oxidation reaction shown here.



Use this data to show that the reaction is electrochemically irreversible. A reaction may show electrochemical irreversibility because of slow electron transfer kinetics or because the product of the oxidation reaction participates in a chemical reaction that produces an nonelectroactive species. Based on the data in this problem, what is the likely source of *p*-phenylenediamine's electrochemical irreversibility?

11.5.3 Solutions to Practice Exercises

Practice Exercise 11.1

The oxidation of H_2 to H^+ occurs at the anode

$$\mathrm{H_2}(g) \leftrightharpoons 2\,\mathrm{H^+}(aq) + 2e^- \tag{11.E.6}$$

and the reduction of Cu^{2+} to Cu occurs at the cathode.

$$\mathrm{Cu^{2+}}(aq) + 2e^- \leftrightharpoons \mathrm{Cu}(s) \tag{11.E.7}$$

The overall cell reaction, therefore, is

$$\mathrm{Cu^{2+}}(aq) + \mathrm{H_2}(g) \leftrightharpoons 2\,\mathrm{H^+}(aq) + \mathrm{Cu}(s) \tag{11.E.8}$$

Click here to return to the chapter.

Practice Exercise 11.2

Making appropriate substitutions into equation 11.3 and solving for E_{cell} gives its value as

$$E_{\text{cell}} = \left(E^\circ_{\mathrm{Cu^{2+}/Cu}} - \frac{0.05916}{2}\log\frac{1}{a_{\mathrm{Cu^{2+}}}}\right) - \left(E^\circ_{\mathrm{H^+/H_2}} - \frac{0.05916}{2}\log\frac{f_{\mathrm{H_2}}}{(a_{\mathrm{H^+}})^2}\right) \tag{11.E.9}$$

$$= \left(0.3419\ \mathrm{V} - \frac{0.05916}{2}\log\frac{1}{0.0500}\right) - \left(0.0000 - \frac{0.05916}{2}\log\frac{0.500}{(0.100)^2}\right) \tag{11.E.10}$$

$$= +0.2531\ \mathrm{V} \tag{11.E.11}$$

Click here to return to the chapter.

Practice Exercise 11.3

Making appropriate substitutions into equation 11.3

$$+0.257\ \text{V} = \left(0.3419\ \text{V} - \frac{0.05916}{2}\log\frac{1}{a_{\text{Cu}^{2+}}}\right) - \left(0.0000 - \frac{0.05916}{2}\log\frac{1.00}{(1.00)^2}\right) \tag{11.E.12}$$

and solving for $a_{Cu^{2+}}$ gives its activity as 1.35×10^{-3}.

Click here to return to the chapter.

Practice Exercise 11.4

When using a saturated calomel electrode, the potential of the electrochemical cell is

$$E_{\text{cell}} = E_{\text{UO}_2^+/\text{U}^{4+}} - E_{\text{SCE}} \tag{11.E.13}$$

Substituting in known values

$$-0.0190\ \text{V} = E_{\text{UO}_2^+/\text{U}^{4+}} - 0.2444\ \text{V} \tag{11.E.14}$$

and solving for $E_{UO2^+/U^{4+}}$ gives its value as +0.2254 V. The potential relative to the Ag/AgCl electrode is

$$E_{\text{cell}} = E_{\text{UO}_2^+/\text{U}^{4+}} - E_{\text{Ag/AgCl}} = 0.2254\ \text{V} - 0.197\ \text{V} = +0.028\ \text{V} \tag{11.E.15}$$

and the potential relative to the standard hydrogen electrode is

$$E_{\text{cell}} = E_{\text{UO}_2^+/\text{U}^{4+}} - E_{\text{SHE}} = 0.2254\ \text{V} - 0.0000\ \text{V} = +0.2254\ \text{V} \tag{11.E.16}$$

Click here to return to the chapter.

Practice Exercise 11.5

The larger the value of $K_{A,I}$ the more serious the interference. Larger values for $K_{A,I}$ correspond to more positive (less negative) values for $\log K_{A,I}$; thus, I^-, with a $K_{A,I}$ of 6.3×10^{-2}, is the most serious of these interferents.

To find the activity of I^- that gives a potential equivalent to a NO_2^- activity of 2.75×10^{-4}, we note that

$$a_{\text{NO}_2^-} = K_{\text{A.I}} \times a_{\text{I}^-} \tag{11.E.17}$$

Making appropriate substitutions

$$2.75\times10^{-4} = (6.3\times10^{-2}) \times a_{\text{I}^-} \tag{11.E.18}$$

and solving for a_{I^-} gives its activity as 4.4×10^{-3}.

Click here to return to the chapter.

Practice Exercise 11.6

In the presence of OH^- the cell potential is

$$E_{\text{cell}} = K - 0.05916\log\left\{a_{\text{NO}_2^-} + K_{\text{NO}_2^-/\text{OH}^-} \times a_{\text{OH}^-}\right\} \tag{11.E.19}$$

To achieve an error of less than 10%, the term $K_{NO2^-/OH^-} \times a_{OH^-}$ must be less than 1% of a_{NO2^-}; thus

$$K_{\text{NO}_2^-/\text{OH}^-} \times a_{\text{OH}^-} \le 0.10 \times a_{\text{NO}_2^-} \tag{11.E.20}$$

$$630 \times a_{\text{OH}^-} \le 0.10 \times (2.2\times10^{-4}) \tag{11.E.21}$$

Solving for a_{OH^-} gives its maximum allowable activity as 3.5×10^{-8}, which corresponds to a pH of less than 6.54.

The electrode does have a lower pH limit. Nitrite is the conjugate weak base of HNO_2, a species to which the ISE does not respond. As shown by the ladder diagram in Figure 11.58, at a pH of 4.15 approximately 10% of nitrite is present as HNO_2. A minimum pH of 4.5 is the usual recommendation when using a nitrite ISE. This corresponds to an NO_2^-/HNO_2 ratio of

$$\text{pH} = \text{p}K_\text{a} + \log \frac{[\text{NO}_2^-]}{[\text{HNO}_2]} \tag{11.E.22}$$

$$4.5 = 3.15 + \log \frac{[\text{NO}_2^-]}{[\text{HNO}_2]} \tag{11.E.23}$$

$$\frac{[NO2–]}{[HNO2]} \approx 22 \tag{11.E.24}$$

Thus, at a pH of 4.5 approximately 96% of nitrite is present as NO_2^-.

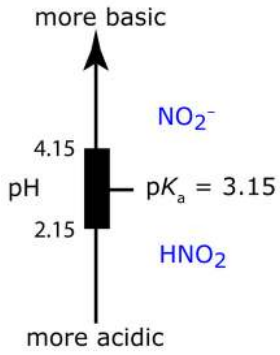


Figure 11.58 Ladder diagram for the weak base NO_2^-.

Click here to return to the chapter.

Practice Exercise 11.7

The reduction of Cu^{2+} to Cu requires two electrons per mole of Cu (n = 2). Using equation 11.25, we calculate the moles and the grams of Cu in the portion of sample being analyzed.

$$N_\text{Cu} = \frac{Q}{nF} = \frac{16.11\ \text{C}}{\frac{2\ \text{mol}\ e^-}{\text{mol Cu}} \times \frac{96487\ \text{C}}{\text{mol}\ e^-}} = 8.348 \times 10^{-5}\ \text{mol Cu} \tag{11.E.25}$$

$$8.348 \times 10^{-5}\ \text{mol Cu} \times \frac{63.55\ \text{g Cu}}{\text{mol Cu}} = 5.301 \times 10^{-3}\ \text{g Cu} \tag{11.E.26}$$

This is the Cu from a 10.00 mL portion of a 500.0 mL sample; thus, the %/w/w copper in the original sample of brass is

$$\frac{5.301 \times 10^{-3}\ \text{g Cu} \times \frac{500.0\ \text{mL}}{10.00\ \text{mL}}}{0.442\ \text{g sample}} \times 100 = 60.0\%\ \text{w/w Cu} \tag{11.E.27}$$

For lead, we follow the same process; thus

$$N_\text{Pb} = \frac{Q}{nF} = \frac{0.422\ \text{C}}{\frac{2\ \text{mol}\ e^-}{\text{mol Pb}} \times \frac{96487\ \text{C}}{\text{mol}\ e^-}} = 2.19 \times 10^{-6}\ \text{mol Pb} \tag{11.E.28}$$

$$2.19 \times 10^{-6}\ \text{mol Pb} \times \frac{207.2\ \text{g Pb}}{\text{mol Pb}} = 4.53 \times 10^{-4}\ \text{g Pb} \tag{11.E.29}$$

$$\frac{4.53 \times 10^{-4}\ \text{g Pb} \times \frac{500.0\ \text{mL}}{10.00\ \text{mL}}}{0.442\ \text{g sample}} \times 100 = 5.12\%\ \text{w/w Pb} \tag{11.E.30}$$

Click here to return to the chapter.

Practice Exercise 11.8

For anodic stripping voltammetry, the peak current, i_p, is a linear function of the analyte's concentration

$$i_\text{p} = KC_\text{Cu} \tag{11.E.31}$$

where K is a constant that accounts for experimental parameters such as the electrode's area, the diffusion coefficient for Cu^{2+}, the deposition time, and the rate of stirring. For the analysis of the sample before the standard addition we know that the current is

$$i_p = 0.886 \quad \text{A} = KC_{\text{Cu}} \tag{11.E.32}$$

and after the standard addition the current is

$$i_p = 2.52\ \mu\text{A} = K\left\{C_{\text{Cu}} \times \frac{50.00\ \text{mL}}{50.005\ \text{mL}} + \frac{10.00\ \text{mg Cu}}{\text{L}} \times \frac{0.005\ \text{mL}}{50.005\ \text{mL}}\right\} \tag{11.E.33}$$

where 50.005 mL is the total volume after adding the 5.00 µL spike. Solving each equation for K and combining leaves us with the following equation.

$$\frac{0.886\ \mu\text{A}}{C_{\text{Cu}}} = K = \frac{2.52\ \text{A}}{C_{\text{Cu}} \times \frac{50.00\ \text{mL}}{50.005\ \text{mL}} + \frac{10.00\ \text{mg Cu}}{\text{L}} \times \frac{0.005\ \text{mL}}{50.005\ \text{mL}}} \tag{11.E.34}$$

Solving this equation for C_{Cu} gives its value as 5.42×10^{-4} mg Cu^{2+}/L, or 0.542 µg Cu^{2+}/L.

Click here to return to the chapter.

Practice Exercise 11.9

From the three half-wave potentials we have a $\Delta E_{1/2}$ of –0.280 V for 0.115 M en and a $\Delta E_{1/2}$ of –0.308 V for 0.231 M en. Using equation 11.51 we write the following two equations.

$$-0.280 = -\frac{0.05916}{2}\log\beta_p - \frac{0.05916p}{2}\log(0.115) \tag{11.E.35}$$

$$-0.308 = -\frac{0.05916}{2}\log\beta_p - \frac{0.05916p}{2}\log(0.231) \tag{11.E.36}$$

To solve for the value of p, we first subtract the second equation from the first equation

$$0.028 = -\frac{0.05916p}{2}\log(0.115) - \left\{-\frac{0.05916p}{2}\log(0.231)\right\} \tag{11.E.37}$$

which eliminates the term with β_p. Next we solve this equation for p

$$0.028 = (2.778 \times 10^{-2})p - (1.882 \times 10^{-2})p \tag{11.E.38}$$

$$0.028 = (8.96 \times 10^{-3})p \tag{11.E.39}$$

obtaining a value of 3.1, or $p \approx 3$. Thus, the complex is $Cd(en)_3$. To find the formation complex, β_3, we return to equation 11.51, using our value for p. Using the data for an en concentration of 0.115 M

$$-0.280 = -\frac{0.05916}{2}\log\beta_p - \frac{0.05916 \times 3}{2}\log(0.115) \tag{11.E.40}$$

$$-0.363 = -0.059162\log\beta_p \tag{11.E.41}$$

gives a value for β_3 of 1.93×10^{12}. Using the data for an en concentration of 0.231 M gives a value of 2.10×10^{12}.

Click here to return to the chapter.

Contributors and Attributions

David Harvey (DePauw University)

11.E: Electrochemical Methods (Exercises) is shared under a CC BY-NC-SA 4.0 license and was authored, remixed, and/or curated by LibreTexts.

11.S: Electrochemical Methods (Summary)

In this chapter we introduced three electrochemical methods of analysis: potentiometry, coulometry, and voltammetry. In potentiometry we measure the potential of an indicator electrode without allowing any significant current to pass through the electrochemical cell. In principle we can use the Nernst equation to calculate the analyte's activity—junction potentials, however, require that we standardize the electrode.

There are two broad classes of potentiometric electrodes: metallic electrodes and membrane electrodes. The potential of a metallic electrode is the result of a redox reaction at the electrode's surface. An electrode of the first kind responds to the concentration of its cation in solution; thus, the potential of a Ag wire is determined by the activity of Ag^+ in solution. If another species is in equilibrium with the metal ion, the electrode's potential also responds to the concentration of that species. For example, the potential of a Ag wire in a solution of Cl^- responds to the concentration of Cl^- because the relative concentrations of Ag^+ and Cl^- are fixed by the solubility product for AgCl. We call this an electrode of the second kind.

The potential of a membrane electrode is determined by a difference in the composition of the solution on each side of the membrane. Electrodes using a glass membrane respond to ions that bind to negatively charged sites on the membrane's surface. A pH electrode is one example of a glass membrane electrode. Other kinds of membrane electrodes include those using insoluble crystalline solids or liquid ion-exchangers incorporated into a hydrophobic membrane. The F^- ion-selective electrode, which uses a single crystal of LaF_3 as the ion-selective membrane, is an example of a solid-state electrode. The Ca^{2+} ion-selective electrode, in which the chelating di-(*n*-decyl)phosphate is immobilized in a PVC membrane, is an example of a liquid-based ion-selective electrode.

Potentiometric electrodes can be designed to respond to molecules by using a chemical reaction that produces an ion whose concentration can be determined using a traditional ion-selective electrode. A gas-sensing electrode, for example, include a gas permeable membrane that isolates the ion-selective electrode from the gas. When the gas diffuses across the membrane it alters the composition of the inner solution, which is monitored with an ion-selective electrode. An enzyme electrodes operate in the same way.

Coulometric methods are based on Faraday's law that the total charge or current passed during an electrolysis is proportional to the amount of reactants and products in the redox reaction. If the electrolysis is 100% efficient—meaning that only the analyte is oxidized or reduced—then we can use the total charge or current to determine the amount of analyte in a sample. In controlled-potential coulometry we apply a constant potential and measure the resulting current as a function of time. In controlled-current coulometry the current is held constant and we measure the time required to completely oxidize or reduce the analyte.

In voltammetry we measure the current in an electrochemical cell as a function of the applied potential. There are several different voltammetric methods that differ in terms of the type of working electrode, how we apply the potential, and whether we include convection (stirring) as a means for transporting of material to the working electrode.

Polarography is a voltammetric technique that uses a mercury electrode and an unstirred solution. Normal polarography uses a dropping mercury electrode, or a static mercury drop electrode, and a linear potential scan. Other forms of polarography include normal pulse polarography, differential pulse polarography, staircase polarography, and square-wave polarography, all of which use a series of potential pulses.

In hydrodynamic voltammetry the solution is stirred using either a magnetic stir bar or by rotating the electrode. Because the solution is stirred a dropping mercury electrode can not be used; instead we use a solid electrode. Both linear potential scans and potential pulses can be applied.

In stripping voltammetry the analyte is first deposited on the electrode, usually as the result of an oxidation or reduction reaction. The potential is then scanned, either linearly or by using potential pulses, in a direction that removes the analyte by a reduction or oxidation reaction.

Amperometry is a voltammetric method in which we apply a constant potential to the electrode and measure the resulting current. Amperometry is most often used in the construction of chemical sensors for the quantitative analysis of single analytes. One important example is the Clark O_2 electrode, which responds to the concentration of dissolved O_2 in solutions such as blood and water.

11.5.1 Key Terms

amalgam	electrode of the first kind	nonfaradaic current
amperometry	electrode of the second kind	Ohm's law
anode	electrochemistry	overpotential
anodic current	electrogravimetry	peak current
asymmetry potential	enzyme electrodes	polarography
auxiliary electrode	faradaic current	potentiometer
cathode	Faraday's law	potentiostat
cathodic current	galvanostat	pulse polarography
charging current	gas-sensing electrode	redox electrode
controlled-current coulometry	glass electrode	reference electrode
controlled-potential coulometry	hanging mercury drop electrode	residual current
convection	hydrodynamic voltammetry	salt bridge
coulometric titrations	indicator electrode	saturated calomel electrode
coulometry	ionophore	selectivity coefficient
counter electrode	ion selective electrode	silver/silver chloride electrode
current efficiency	junction potential	solid-state ion-selective electrodes
cyclic voltammetry	limiting current	standard hydrogen electrode
diffusion	liquid-based ion-selective electrode	static mercury drop electrode
diffusion layer	mass transport	stripping voltammetry
dropping mercury electrode	mediator	total ionic strength adjustment buffer
electrical double layer	membrane potential	voltammetry
electrochemically irreversible	mercury film electrode	voltammogram
electrochemically reversible	migration	working electrode

References

1. Stork, J. T. *Anal. Chem.* **1993**, *65*, 344A–351A.
2. Sawyer, D. T.; Roberts, J. L., Jr. *Experimental Electrochemistry for Chemists*, Wiley-Interscience: New York, 1974, p. 22.
3. Sokalski, T.; Ceresa, A.; Zwicki, T.; Pretsch, E. *J. Am. Chem. Soc.* **1997**, *119*, 11347–11348.
4. (a) Papastathopoulos, D. S.; Rechnitz, G. A. *Anal. Chim. Acta* **1975**, *79*, 17–26; (b) Riechel, T. L. *J. Chem. Educ.* **1984**, *61*, 640–642.
5. Tor, R.; Freeman, A. *Anal. Chem.* **1986**, *58*, 1042–1046.
6. Kristensen, H. B.; Saloman, A.; Kokholm, G. *Anal. Chem.* **1991**, *63*, 885A–891A.
7. Hawkes, S. J. *J. Chem. Educ.* **1994**, *71*, 747–749.
8. Covington, A. K.; Bates, R. B.; Durst, R. A. *Pure & Appl. Chem.* **1985**, *57*, 531–542.
9. Bakker, E.; Pretsch, E. *Trends Anal. Chem.* **2008**, *27*, 612–618.
10. (a) Bakker, E.; Pretsch, E. *Anal. Chem.* **2002**, *74*, 420A–426A; (b) Bakker, E.; Pretsch, E. *Trends Anal. Chem.* **2005**, *24*, 199–207.
11. Tymecki, L.; Zwierkowska, E.; G^{31}b, S.; Koncki, R. *Sens. Actuators B* **2003**, *96*, 482–488.
12. Curran, D. J. "Constant-Current Coulometry," in Kissinger, P. T.; Heineman, W. R., eds., *Laboratory Techniques in Electroanalytical Chemistry*,Marcel Dekker Inc.: New York, 1984, pp. 539–568.
13. Maloy, J. T. *J. Chem. Educ.* **1983**, *60*, 285–289.
14. Osteryoung, J. *J. Chem. Educ.* **1983**, *60*, 296–298.
15. Karube, I.; Nomura, Y.; Arikawa, Y. *Trends in Anal. Chem.* **1995**, *14*, 295–299.
16. Lanza P. *J. Chem. Educ.* **1990**, *67*, 704–705.
17. (a) Batley, G. E.; Florence, T. M. *Anal. Lett.* **1976**, *9*, 379–388; (b) Batley, G. E.; Florence, T. M. *Talanta* **1977**, *24*, 151–158; (c) Batley, G. E.; Florence, T. M. *Anal. Chem.* **1980**, *52*, 1962–1963; (d) Florence, T. M., Batley, G. E.; *CRC Crit. Rev. Anal. Chem.* **1980**, *9*, 219–296.
18. Brooks, M. A. "Application of Electrochemistry to Pharmaceutical Analysis," Chapter 21 in Kissinger, P. T.; Heinemann, W. R., eds. *Laboratory Techniques in Electroanalytical Chemistry*, Marcel Dekker, Inc.: New York, 1984, pp 539–568.

19. Abe, T.; Lauw, L. L.; Ewing, A. G. *J. Am. Chem. Soc*. **1991**, *113*, 7421–7423.
20. Creager, S. E.; Lawrence, K. D.; Tibbets, C. R. *J. Chem. Educ.* **1995**, *72*, 274–276.
21. Watanabe, K.; Okada, K.; Oda, H.; Furuno, K.; Gomita, Y.; Katsu, T. *Anal. Chim. Acta* **1995**, *316*, 371–375.
22. Mifflin, T. E.; Andriano, K. M.; Robbins, W. B. J. Chem. Educ. 1984, 61, 638–639.
23. Meyerhoff, M. E.; Kovach, P. M. J. Chem. Educ. 1983, 9, 766–768.
24. Wang, J.; Taha, Z. *Anal. Chim. Acta* **1991**, *252*, 215–221.
25. Lau, O.; Luk, S.; Cheung, Y. *Analyst* **1989**, *114*, 1047–1051.
26. Ratana-ohpas, R.; Kanatharana, P.; Ratana-ohpas, W.; Kongsawasdi, W. *Anal. Chim. Acta* **1996**, *333*, 115–118.
27. Sittampalam, G.; Wilson, G. S. *J. Chem. Educ.* **1982**, *59*, 70–73.
28. Abass, A. K.; Hart, J. P.; Cowell, D. C.; Chapell, A. *Anal. Chim. Acta* **1988**, *373*, 1–8.
29. Batley, G. E.; Florence, T. M. *Anal. Lett.* **1976**, *9*, 379–388.
30. Davidson, I. E.; Smyth, W. F. Anal. Chem. 1977, 49, 1195–1198.
31. van der Berg, C. M. G.; Huang, Z. Q. *Anal. Chem.* **1984**, *56*, 2383–2386.
32. Baldwin, R. P.; Ravichandran, K.; Johnson, R. K. *J. Chem. Educ*. **1984**, *61*, 820–823.

Contributors

- David Harvey (DePauw University)

11.S: Electrochemical Methods (Summary) is shared under a CC BY-NC-SA 4.0 license and was authored, remixed, and/or curated by LibreTexts.

CHAPTER OVERVIEW

12: Chromatographic & Electrophoretic Methods

Drawing from an arsenal of analytical techniques—many of which were the subject of the preceding four chapters—analytical chemists design methods for the analysis of analytes at increasingly lower concentrations and in increasingly more complex matrices. Despite the power of these analytical techniques, they often suffer from a lack of selectivity. For this reason, many analytical procedures include a step to separate the analyte from potential interferents. Although effective, each additional step in an analytical procedure increases the analysis time and introduces uncertainty. In this chapter we consider two analytical techniques that avoid these limitations by combining the separation and analysis: chromatography and electrophoresis.

Topic hierarchy

12.1: Overview of Analytical Separations
12.2: General Theory of Column Chromatography
12.3: Optimizing Chromatographic Separations
12.4: Gas Chromatography
12.5: High-Performance Liquid Chromatography
12.6: Other Forms of Liquid Chromatography
12.7: Electrophoresis
12.E: Chromatographic and Electrophoretic Methods (Exercises)
12.S: Chromatographic and Electrophoretic Methods (Summary)
Index

Thumbnail: Separation of black ink on a thin layer chromatography plate. Image used with permission (CC BY-SA 3.0; Natrij)}

Contributors

- David Harvey (DePauw University)

12: Chromatographic & Electrophoretic Methods is shared under a CC BY-NC-SA 4.0 license and was authored, remixed, and/or curated by LibreTexts.

CHAPTER OVERVIEW

Front Matter

TitlePage
InfoPage

12: Chromatographic & Electrophoretic Methods

This text is disseminated via the Open Education Resource (OER) LibreTexts Project (https://LibreTexts.org) and like the thousands of other texts available within this powerful platform, it is freely available for reading, printing, and "consuming."

The LibreTexts mission is to bring together students, faculty, and scholars in a collaborative effort to provide an accessible, and comprehensive platform that empowers our community to develop, curate, adapt, and adopt openly licensed resources and technologies; through these efforts we can reduce the financial burden born from traditional educational resource costs, ensuring education is more accessible for students and communities worldwide.

Most, but not all, pages in the library have licenses that may allow individuals to make changes, save, and print this book. Carefully consult the applicable license(s) before pursuing such effects. Instructors can adopt existing LibreTexts texts or Remix them to quickly build course-specific resources to meet the needs of their students. Unlike traditional textbooks, LibreTexts' web based origins allow powerful integration of advanced features and new technologies to support learning.



LibreTexts is the adaptable, user-friendly non-profit open education resource platform that educators trust for creating, customizing, and sharing accessible, interactive textbooks, adaptive homework, and ancillary materials. We collaborate with individuals and organizations to champion open education initiatives, support institutional publishing programs, drive curriculum development projects, and more.

The LibreTexts libraries are Powered by NICE CXone Expert and was supported by the Department of Education Open Textbook Pilot Project, the California Education Learning Lab, the UC Davis Office of the Provost, the UC Davis Library, the California State University Affordable Learning Solutions Program, and Merlot. This material is based upon work supported by the National Science Foundation under Grant No. 1246120, 1525057, and 1413739.

Any opinions, findings, and conclusions or recommendations expressed in this material are those of the author(s) and do not necessarily reflect the views of the National Science Foundation nor the US Department of Education.

Have questions or comments? For information about adoptions or adaptions contact info@LibreTexts.org or visit our main website at https://LibreTexts.org.

This text was compiled on 01/12/2026

12.1: Overview of Analytical Separations

In Chapter 7 we examined several methods for separating an analyte from potential interferents. For example, in a liquid–liquid extraction the analyte and interferent are initially present in a single liquid phase. We add a second, immiscible liquid phase and mix them thoroughly by shaking. During this process the analyte and interferents partition themselves between the two phases to different extents, effecting their separation. After allowing the phases to separate, we draw off the phase enriched in analyte. Despite the power of liquid–liquid extractions, there are significant limitations.

12.1.1 Two Limitations of Liquid–Liquid Extractions

Suppose we have a sample containing an analyte in a matrix that is incompatible with our analytical method. To determine the analyte's concentration we first separate it from the matrix using a simple liquid–liquid extraction. If we have several analytes, we may need to complete a separate extraction for each analyte. For a complex mixture of analytes this quickly becomes a tedious process. This is one limitation to a liquid–liquid extraction.

A more significant limitation is that the extent of a separation depends on the distribution ratio of each species in the sample. If the analyte's distribution ratio is similar to that of another species, then their separation becomes impossible. For example, let's assume that an analyte, A, and an interferent, I, have distribution ratios of, respectively, 5 and 0.5. If we use a liquid–liquid extraction with equal volumes of sample and extractant, then it is easy to show that a single extraction removes approximately 83% of the analyte and 33% of the interferent. Although we can remove 99% of the analyte with three extractions, we also remove 70% of the interferent. In fact, there is no practical combination of number of extractions or volumes of sample and extractant that produce an acceptable separation.

Note

From Chapter 7 we know that the distribution ratio, D, for a solute, S, is

$$D = \frac{[\text{S}]_{\text{ext}}}{[\text{S}]_{\text{samp}}} \tag{12.1.1}$$

where $[\text{S}]_{\text{ext}}$ is its equilibrium concentration in the extracting phase and $[\text{S}]_{\text{samp}}$ is its equilibrium concentration in the sample.

We can use the distribution ratio to calculate the fraction of S that remains in the sample, q_{samp}, after an extraction

$$q_{\text{samp}} = \frac{V_{\text{samp}}}{DV_{\text{ext}} + V_{\text{samp}}} \tag{12.1.2}$$

where V_{samp} is the volume of sample and V_{ext} is the volume of the extracting phase. For example, if D = 10, V_{samp} = 20, and V_{ext} = 5, the fraction of S remaining in the sample after the extraction is

$$q_{\text{samp}} = \frac{20}{10 \times 5 + 20} = 0.29 \tag{12.1.3}$$

or 29%. The remaining 71% of the analyte is in the extracting phase.

12.1.2 A Better Way to Separate Mixtures

The problem with a liquid–liquid extraction is that the separation occurs in only one direction—from the sample to the extracting phase. Let's take a closer look at the liquid–liquid extraction of an analyte and an interferent with distribution ratios of, respectively, 5 and 0.5. Figure 12.1 shows that a single extraction using equal volumes of sample and extractant transfers 83% of the analyte and 33% of the interferent to the extracting phase. If the original concentrations of A and I are identical, then their concentration ratio in the extracting phase after one extraction is

$$\frac{[\text{A}]}{[\text{I}]} = \frac{0.83}{0.33} = 2.5 \tag{12.1.4}$$

A single extraction, therefore, enriches the analyte by a factor of 2.5×. After completing a second extraction (Figure 12.1) and combining the two extracting phases, the separation of the analyte and interferent is, surprisingly, less efficient.

$$\frac{[A]}{[I]} = \frac{0.97}{0.55} = 1.8 \tag{12.1.5}$$

Figure 12.1 makes it clear why the second extraction results in a poorer overall separation—the second extraction actually favors the interferent!

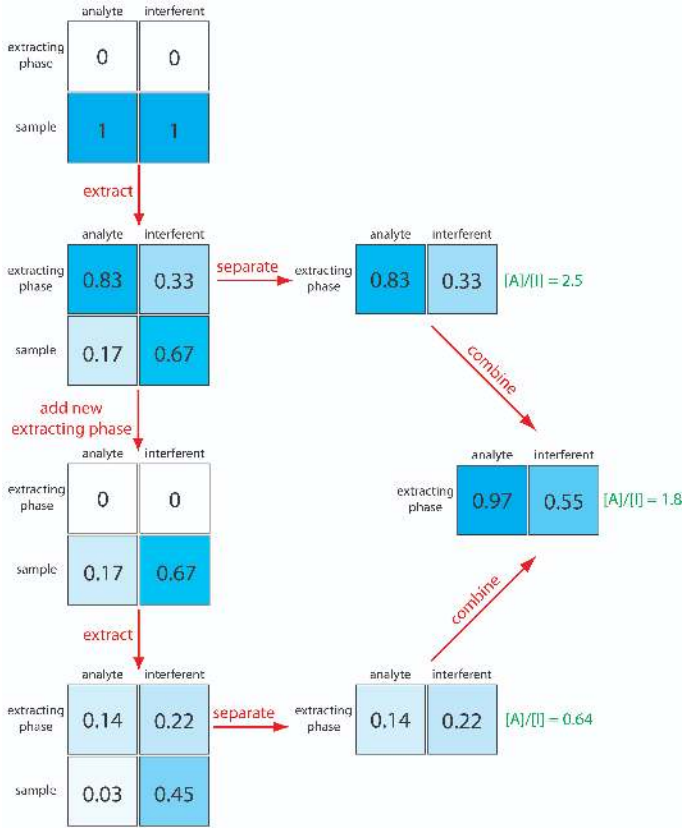


Figure 12.1: *Progress of a traditional liquid–liquid extraction using two identical extractions of a single sample with fresh portions of the extractant. The numbers give the fraction of analyte and interferent in each phase assuming equal volumes of sample and extractant and distribution ratios of 5 and 0.5 for the analyte and the interferent, respectively.*

We can improve the separation by first extracting the solutes from the sample into the extracting phase, and then extracting them back into a fresh portion of solvent that matches the sample's matrix (Figure 12.2). Because the analyte has the larger distribution ratio, more of it moves into the extractant during the first extraction, and less of it moves back to the sample phase during the second extraction. In this case the concentration ratio in the extracting phase after two extractions is significantly greater.

$$\frac{[A]}{[I]} = \frac{0.69}{0.11} = 6.3 \tag{12.1.6}$$

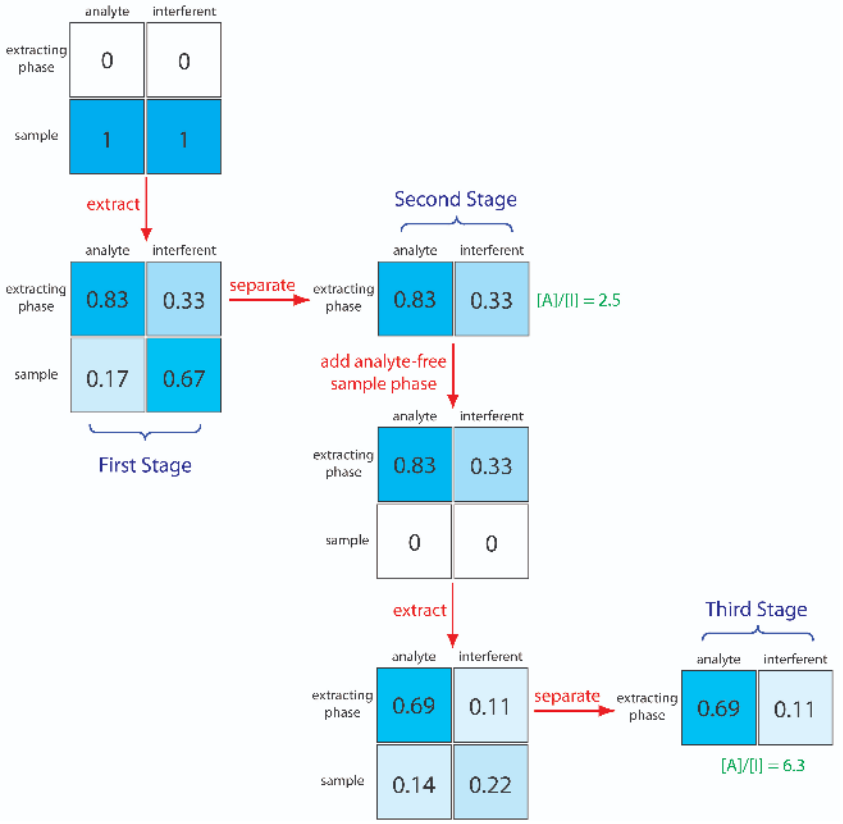


***Figure 12.2**: Progress of a liquid–liquid extraction in which we first extract the solutes into the extracting phase and then extract them back into an analyte-free portion of the sample's phase. The numbers give the fraction of analyte and interferent in each phase assuming equal volumes of sample and extractant and distribution ratios of 5 and 0.5 for the analyte and interferent, respectively.*

Not shown in Figure 12.2 is that we can add a fresh portion of the extracting phase to the sample that remains after the first extraction, beginning the process anew. As the number of extractions increases, the analyte and the interferent each spread out in space over a series of stages. Because the interferent's distribution ratio is smaller than that of the analyte, the interferent lags behind the analyte. With a sufficient number of extractions, a complete separation is possible. This process of extracting the solutes back and forth between fresh portions of the two phases, which we call a **countercurrent extraction**, was developed by Craig in the 1940s.[1] The same phenomenon forms the basis of modern chromatography.

> **Note**
>
> We can trace the history of chromatography to the turn of the century when the Russian botanist Mikhail Tswett used a column packed with calcium carbonate and a mobile phase of petroleum ether to separate colored pigments from plant extracts. As the sample moved through the column the plant's pigments separated into individual colored bands. After the pigments were adequately separated, the calcium carbonate was removed from the column, sectioned, and the pigments recovered by extraction. Tswett named the technique chromatography, combining the Greek words for "color" and "to write."
>
> There was little interest in Tswett's technique until Martin and Synge's pioneering development of a theory of chromatography (see Martin, A. J. P.; Synge, R. L. M. "A New Form of Chromatogram Employing Two Liquid Phases," *Biochem. J.* **1941**, *35*, 1358–1366). Martin and Synge were awarded the 1952 Nobel Prize in Chemistry for this work.

12.1.3 Chromatographic Separations

In **chromatography** we pass a sample-free phase, which we call the **mobile phase**, over a second sample-free **stationary phase** that remains fixed in space (Figure 12.3). We inject or place the sample into the mobile phase. As the sample moves with the mobile phase, its components partition themselves between the mobile phase and the stationary phase. A component whose

distribution ratio favors the stationary phase requires more time to pass through the system. Given sufficient time, and sufficient stationary and mobile phase, we can separate solutes even if they have similar distribution ratios.

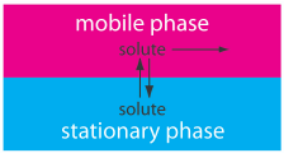


Figure 12.3: *In chromatography we pass a mobile phase over a stationary phase. When we inject a sample into the mobile phase, the sample's components both move with the mobile phase and partition into the stationary phase. The solute spending the most time in the stationary phase takes the longest time to move through the system.*

There are many ways in which we can identify a chromatographic separation: by describing the physical state of the mobile phase and the stationary phase; by describing how we bring the stationary phase and the mobile phase into contact with each other; or by describing the chemical or physical interactions between the solute and the stationary phase. Let's briefly consider how we might use each of these classifications.

Types of Mobile Phases and Stationary Phases

The mobile phase is a liquid or a gas, and the stationary phase is a solid or a liquid film coated on a solid substrate. We often name chromatographic techniques by listing the type of mobile phase followed by the type of stationary phase. In gas–liquid chromatography, for example, the mobile phase is a gas and the stationary phase is a liquid film coated on a solid substrate. If a technique's name includes only one phase, as in gas chromatography, it is the mobile phase.

Contact Between the Mobile Phase and the Stationary Phase

There are two common methods for bringing the mobile phase and the stationary phase into contact. In **column chromatography** we pack the stationary phase into a narrow column and pass the mobile phase through the column using gravity or by applying pressure. The stationary phase is a solid particle or a thin, liquid film coated on either a solid particulate packing material or on the column's walls. In **planar chromatography** the stationary phase is coated on a flat surface—typically, a glass, metal, or plastic plate. One end of the plate is placed in a reservoir containing the mobile phase, which moves through the stationary phase by capillary action. In paper chromatography, for example, paper is the stationary phase.

Interaction Between the Solute and the Stationary Phase

The interaction between the solute and the stationary phase provides a third method for describing a separation (Figure 12.4). In **adsorption chromatography**, solutes separate based on their ability to adsorb to a solid stationary phase. In **partition chromatography**, the stationary phase is thin, liquid film on a solid support. Separation occurs because of differences in the equilibrium partitioning of solutes between the stationary phase and the mobile phase. A stationary phase consisting of a solid support with covalently attached anionic (e.g., $–SO_3^–$) or cationic (e.g., $–N(CH_3)_3^+$) functional groups is the basis for ion-exchange chromatography. Ionic solutes are attracted to the stationary phase by electrostatic forces. In size-exclusion chromatography the stationary phase is a porous particle or gel, with separation based on the size of the solutes. Larger solutes, which are unable to penetrate as deeply into the porous stationary phase, move more quickly through the column.

> **Note**
>
> There are other interactions that can serve as the basis of a separation. In affinity chromatography the interaction between an antigen and an antibody, between an enzyme and a substrate, or between a receptor and a ligand can form the basis of a separation. See this chapter's additional resources for some suggested readings.

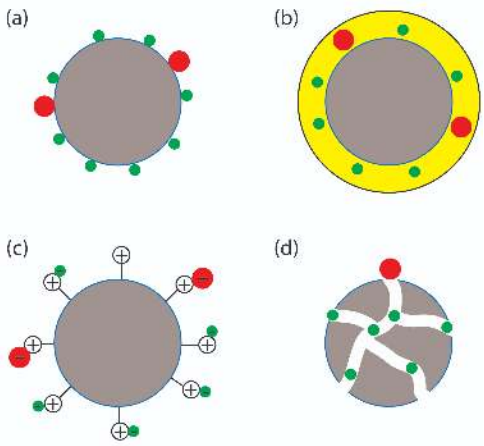


Figure 12.4: *Four examples of interactions between a solute and the stationary phase: (a) adsorption on a solid surface, (b) partitioning into a liquid phase, (c) ion-exchange, and (d) size exclusion. For each example, the smaller, green solute is more strongly retained than the larger, red solute.*

12.1.4 Electrophoretic Separations

In chromatography, a separation occurs because there is a difference in the equilibrium partitioning of solutes between the mobile phase and the stationary phase. Equilibrium partitioning, however, is not the only basis for effecting a separation. In an electrophoretic separation, for example, charged solutes migrate under the influence of an applied potential. Separation occurs because of differences in the charges and the sizes of the solutes (Figure 12.5).

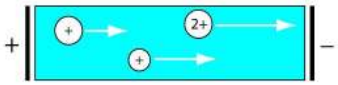


Figure 12.5*: Movement of charged solutes under the influence of an applied potential. The lengths of the arrows indicate the relative speed of the solutes. In general, a larger solute moves more slowly than a smaller solute of equal charge, and a solute with a larger charge move more quickly than a solute with a smaller charge.*

Contributors

David Harvey (DePauw University)

12.1: Overview of Analytical Separations is shared under a CC BY-NC-SA 4.0 license and was authored, remixed, and/or curated by LibreTexts.

12.2: General Theory of Column Chromatography

Of the two methods for bringing the stationary phase and the mobile phases into contact, the most important is column chromatography. In this section we develop a general theory that we may apply to any form of column chromatography.

Figure 12.6 provides a simple view of a liquid–solid column chromatography experiment. The sample is introduced at the top of the column as a narrow band. Ideally, the solute's initial concentration profile is rectangular (Figure 12.7a). As the sample moves down the column the solutes begin to separate (Figures 12.6b,c), and the individual solute bands begin to broaden and develop a Gaussian profile (Figures 12.7b,c). If the strength of each solute's interaction with the stationary phase is sufficiently different, then the solutes separate into individual bands (Figure 12.6d and Figure 12.7d).

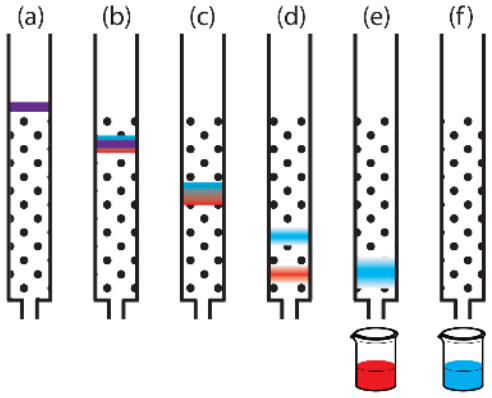


Figure 12.6 *Progress of a column chromatographic separation of a two-component mixture. In (a) the sample is layered on top of the stationary phase. As mobile phase passes through the column, the sample separates into two solute bands (b–d). In (e) and (f), we collect each solute as it elutes from the column.*

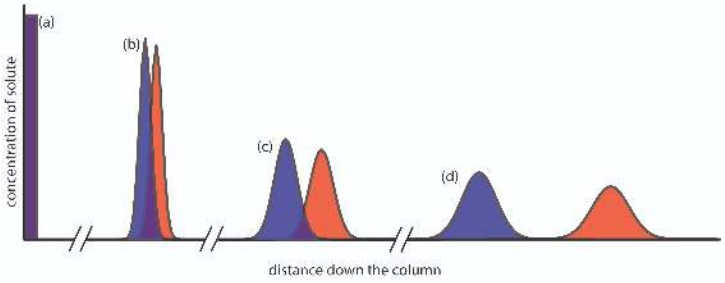


Figure 12.7 *An alternative view of the separation in Figure 12.6 showing the concentration of each solute as a function of distance down the column.*

We can follow the progress of the separation either by collecting fractions as they elute from the column (Figure 12.6e,f), or by placing a suitable detector at the end of the column. A plot of the detector's response as a function of elution time, or as a function of the volume of mobile phase, is known as a **chromatogram** (Figure 12.8), and consists of a peak for each solute.

> **Note**
>
> There are many possible detectors that we can use to monitor the separation. Later sections of this chapter describe some of the most popular.

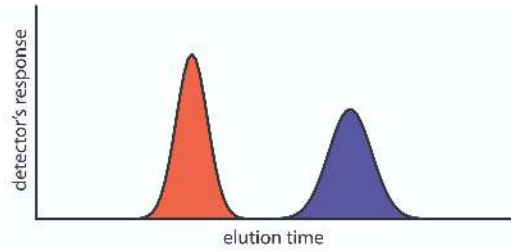


Figure 12.8 *Chromatogram for the separation shown in Figure 12.6 and Figure 12.7, showing the detector's response as a function of the elution time.*

A solute's chromatographic peak may be characterized in many ways, two of which are shown in Figure 12.9. **Retention time**, t_r, is the time between the sample's injection and the maximum response for the solute's peak. Another important parameter is the **baseline width**, w, which, as shown in Figure 12.9, is determined by extending tangent lines from the inflection points on either side of the chromatographic peak through the baseline. Although usually we report t_r and w using units of time, we can report them using units of volume by multiplying each by the mobile phase's velocity, or in linear units by measuring distances with a ruler.

For example, a solute's retention volume, V_r, is

$$V_r = t_r \times u \tag{12.2.1}$$

where u is the mobile phase's velocity through the column.

In addition to the peak for the solute, Figure 12.9 also shows a small peak that elutes shortly after injecting the sample into the mobile phase. This peak is for **nonretained solutes**. Because these solutes do not interact with the stationary phase, they move through the column at the same rate as the mobile phase. The time required to elute nonretained solutes is called the column's **void time**, t_m.

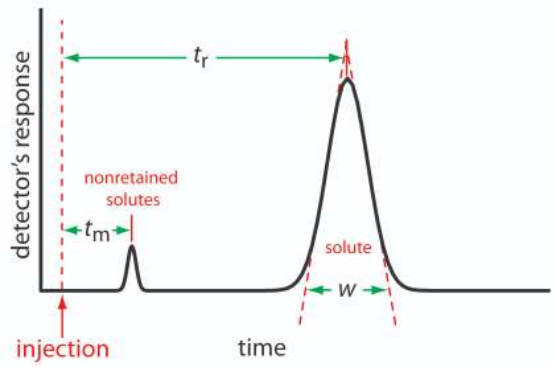


Figure 12.9: *Chromatogram showing a solute's retention time, t_r, and baseline width, w, and the column's void time, t_m, for nonretained solutes.*

12.2.1 Chromatographic Resolution

The goal of chromatography is to separate a mixture into a series of chromatographic peaks, each representing a single component of the mixture. The **resolution** between two chromatographic peaks, R_{AB}, is a quantitative measure of their separation, and is defined as

$$R_{AB} = \frac{t_{r,B} - t_{r,A}}{0.5(w_B + w_A)} = \frac{2\Delta t_r}{w_B + w_A} \tag{12.1}$$

where B is the later eluting of the two solutes. As shown in Figure 12.10, the separation of two chromatographic peaks improves with an increase in R_{AB}. If the areas under the two peaks are identical—as is the case in Figure 12.10—then a resolution of 1.50 corresponds to an overlap of only 0.13% for the two elution profiles. Because resolution is a quantitative measure of a separation's success, it is a useful way to determine if a change in experimental conditions leads to a better separation.

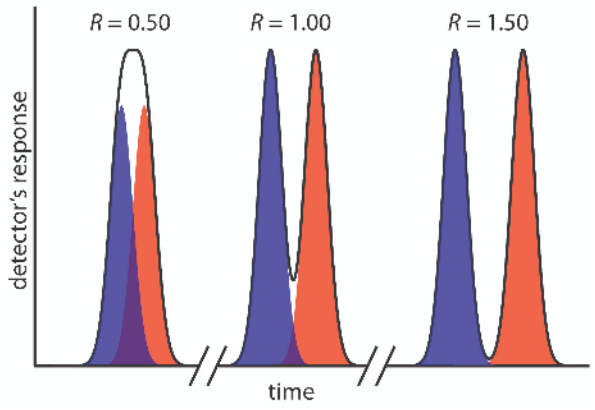


Figure 12.10 Three examples showing the relationship between resolution and the separation of a two component mixture. The blue and red peaks are the elution profiles for the two components. The chromatographic peak—which is the sum of the two elution profiles—is shown by the solid black line.

Example 12.1

In a chromatographic analysis of lemon oil a peak for limonene has a retention time of 8.36 min with a baseline width of 0.96 min. γ-Terpinene elutes at 9.54 min with a baseline width of 0.64 min. What is the resolution between the two peaks?

Solution

Using equation 12.1 we find that the resolution is

$$R_{AB} = \frac{2\Delta t_r}{w_B + w_A} = \frac{2(9.54\text{ min} - 8.36\text{ min})}{1.64\text{ min} + 0.96\text{ min}} = 1.48 \qquad (12.2.2)$$

Exercise 12.1

Figure 12.11 shows the separation of a two-component mixture. What is the resolution between the two components? Use a ruler to measure Δt_r,w_A, and w_B in millimeters.

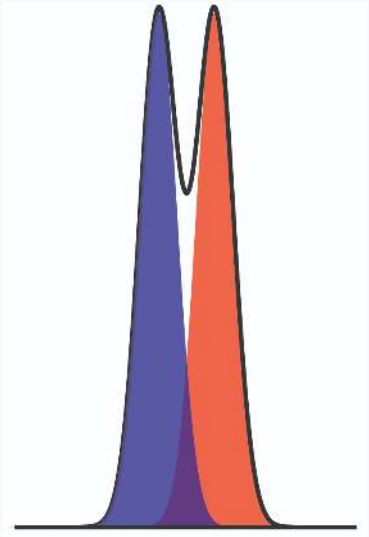


Figure 12.11 *Chromatogram for Practice Exercise 12.1.*

Click here to review your answer to this exercise.

Equation 12.1 suggests that we can improve resolution by increasing Δt_r, or by decreasing w_A and w_B (Figure 12.12). To increase Δt_r we can use one of two strategies. One approach is to adjust the separation conditions so that both solutes spend less time in the mobile phase—that is, we increase each *solute's retention factor*—which provides more time to effect a separation. A second

approach is to increase *selectivity* by adjusting conditions so that only one solute experiences a significant change in its retention time. The baseline width of a solute's peak depends on the solutes movement within and between the mobile phase and the stationary phase, and is governed by several factors that we collectively call *column efficiency*. We will consider each of these approaches for improving resolution in more detail, but first we must define some terms.

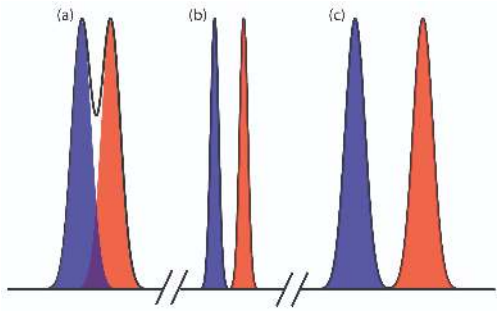


Figure 12.12: *Two method for improving chromatographic resolution: (a) original chromatogram; (b) chromatogram after decreasing w_A and w_B by 4×; (c) chromatogram after increasing Δt_r by 2×.*

12.2.2 Solute Retention Factor

Let's assume that we can describe a solute's distribution between the mobile phase and stationary phase using the following equilibrium reaction

$$\mathrm{S_m} \rightleftharpoons \mathrm{S_s} \tag{12.2.3}$$

where

- $\mathrm{S_m}$ is the solute in the mobile phase and
- $\mathrm{S_s}$ is the solute in the stationary phase.

> **Note**
>
> This is not a trivial assumption. In this section we are, in effect, treating the solute's equilibrium between the mobile phase and the stationary phase as if it is identical to the equilibrium in a liquid–liquid extraction. You might question whether this is a reasonable assumption.
>
> There is an important difference between the two experiments we need to consider. In a liquid–liquid extraction, which takes place in a separatory funnel, the two phases remain in contact with each other at all times, allowing for a true equilibrium. In chromatography, however, the mobile phase is in constant motion. A solute moving into the stationary phase from the mobile phase equilibrates back into a different portion of the mobile phase; this does not describe a true equilibrium.
>
> So, we ask again: Can we treat a solute's distribution between the mobile phase and the stationary phase as an equilibrium process? The answer is yes, if the mobile phase velocity is slow relative to the kinetics of the solute's moving back and forth between the two phase. In general, this is a reasonable assumption.

Following the same approach that we used in Section 7G.2 for liquid–liquid extractions, the equilibrium constant for this reaction is an equilibrium partition coefficient, K_D.

$$K_\mathrm{D} = \frac{[\mathrm{S_s}]}{[\mathrm{S_m}]} \tag{12.2.4}$$

In the absence of any additional equilibrium reactions in the mobile phase or stationary phase, K_D is equivalent to the distribution ratio, D,

$$D = \frac{[\mathrm{S_s}]}{[\mathrm{S_m}]} = \frac{(\mathrm{mol\ S})_\mathrm{s}/V_\mathrm{s}}{(\mathrm{mol\ S})_\mathrm{m}/V_\mathrm{m}} = K_\mathrm{D} \tag{12.2}$$

where V_s and V_m are the volumes of the stationary phase and the mobile phase, respectively.

A conservation of mass requires that the total moles of solute remain constant throughout the separation; thus, we know that the following equation is true.

$$(\text{mol S})_{\text{total}} = (\text{mol S})_{\text{m}} + (\text{mol S})_{\text{s}} \tag{12.3}$$

Solving equation 12.3 for the moles of solute in the stationary phase and substituting into equation 12.2 leaves us with

$$D = \frac{\{(\text{mol S})_{\text{total}} - (\text{mol S})_{\text{s}}\} / V_{\text{s}}}{(\text{mol S})_{\text{m}} / V_{\text{m}}} \tag{12.2.5}$$

Rearranging this equation and solving for the fraction of solute in the mobile phase, f_{m}, gives a result

$$f_m = \frac{(\text{mol S})_{\text{m}}}{(\text{mol S})_{\text{total}}} = \frac{V_{\text{m}}}{(DV_{\text{s}} + V_{\text{m}})} \tag{12.4}$$

that is identical to equation 7.26 for a liquid–liquid extraction. Because we may not know the exact volumes of the stationary phase and the mobile phase, we can simplify equation 12.4 by dividing both the numerator and the denominator by V_{m}; thus

$$f_m = \frac{V_{\text{m}}/V_{\text{m}}}{DV_{\text{s}}/V_{\text{m}} + V_{\text{m}}/V_{\text{m}}} = \frac{1}{DV_{\text{s}}/V_{\text{m}} + 1} = \frac{1}{1 + k} \tag{12.5}$$

where k

$$k = D \times \frac{V_{\text{s}}}{V_{\text{m}}} \tag{12.6}$$

is the solute's **retention factor**. Note that the larger the retention factor, the more the distribution ratio favors the stationary phase, leading to a more strongly retained solute and a longer retention time.

Note

The retention factor is also called the capacity factor, the capacity ratio, and the partition ratio, and is sometimes given the symbol k'. Keep this in mind if you are using other resources. Retention factor is the approved name from the IUPAC Gold Book.

We can determine a solute's retention factor from a chromatogram by measuring the column's void time, t_{m}, and the solute's retention time, t_{r} (see Figure 12.9). Solving equation 12.5 for k, we find that

$$k = \frac{1 - f_{\text{m}}}{f_{\text{m}}} \tag{12.7}$$

Earlier we defined f_{m} as the fraction of solute in the mobile phase. Assuming a constant mobile phase velocity, we also can define f_{m} as

$$f_{\text{m}} = \frac{\text{time spent in mobile phase}}{\text{total time spent on column}} = \frac{t_{\text{m}}}{t_{\text{r}}} \tag{12.2.6}$$

Substituting back into equation 12.7 and rearranging leaves us with

$$k = \frac{1 - \frac{t_{\text{m}}}{t_{\text{r}}}}{\frac{t_{\text{m}}}{t_{\text{r}}}} = \frac{t_{\text{r}} - t_{\text{m}}}{t_{\text{m}}} = \frac{t'_{\text{r}}}{t_{\text{m}}} \tag{12.8}$$

where t'_{r} is the **adjusted retention time**.

Example 12.2

In a chromatographic analysis of low molecular weight acids, butyric acid elutes with a retention time of 7.63 min. The column's void time is 0.31 min. Calculate the retention factor for butyric acid.

Solution

$$k_{\text{but}} = \frac{t_{\text{r}} - t_{\text{m}}}{t_{\text{m}}} = \frac{7.63\ \text{min} - 0.31\ \text{min}}{0.31\ \text{min}} = 23.6 \tag{12.2.7}$$

Practice Exercise 12.2

Figure 12.13 is the chromatogram for a two-component mixture. Determine the retention factor for each solute assuming the sample was injected at time $t = 0$.

Click here to review your answer to this exercise.

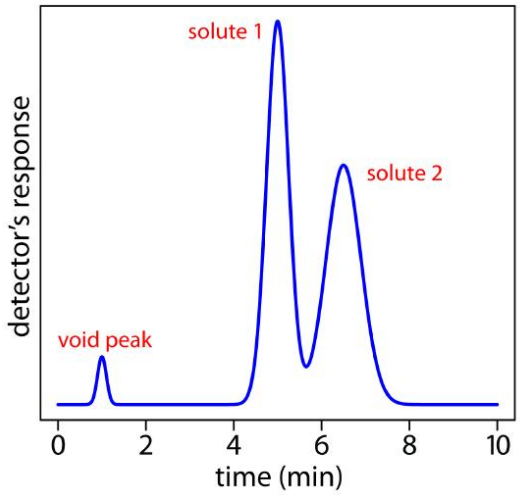


Figure 12.13 Chromatogram for Practice Exercise 12.2.

12.2.3 Selectivity

Selectivity is a relative measure of the retention of two solutes, which we define using a **selectivity factor**, α

$$\alpha = \frac{k_B}{k_A} = \frac{t_{r,B} - t_m}{t_{r,A} - t_m} \tag{12.9}$$

where solute A always has the smaller retention time. When two solutes elute with identical retention time, α = 1.00; for all other conditions α > 1.00.

Example 12.3

In the chromatographic analysis for low molecular weight acids described in Example 12.2, the retention time for isobutyric acid is 5.98 min. What is the selectivity factor for isobutyric acid and butyric acid?

Solution

First we must calculate the retention factor for isobutyric acid. Using the void time from Example 12.2.

$$k_{iso} = \frac{t_r - t_m}{t_m} = \frac{5.98\ \text{min} - 0.31\ \text{min}}{0.31\ \text{min}} = 18.3 \tag{12.2.8}$$

The selectivity factor, therefore, is

$$\alpha = \frac{k_{but}}{k_{iso}} = \frac{23.6}{18.3} = 1.29 \tag{12.2.9}$$

Practice Exercise 12.3

Determine the selectivity factor for the chromatogram in Practice Exercise 12.2.

Click here to review your answer to this exercise.

12.2.4 Column Efficiency

Suppose we inject a sample consisting of a single component. At the moment of injection the sample occupies a narrow band of finite width. As the sample passes through the column, the width of this band continually increases in a process we call **band**

broadening. Column efficiency provides a quantitative measure of the extent of band broadening.

> **Note**
>
> See Figure 12.6 and Figure 12.7. When we inject the sample it has a uniform, or rectangular concentration profile with respect to distance down the column. As it passes through the column, the band broadens and takes on a Gaussian concentration profile.

In their original theoretical model of chromatography, Martin and Synge divided the chromatographic column into discrete sections—what they called **theoretical plates**—in which there is an equilibrium partitioning of the solute between the stationary phase and the mobile phase.[2] They described column efficiency in terms of the number of theoretical plates, N,

$$N = \frac{L}{H} \tag{12.10}$$

where L is the column's length and H is the height of a theoretical plate. Column efficiency improves—and chromatographic peaks become narrower—when there are more theoretical plates.

If we assume that a chromatographic peak has a Gaussian profile, then the extent of band broadening is given by the peak's variance or standard deviation. The height of a theoretical plate is the variance per unit length of the column

$$H = \frac{\sigma^2}{L} \tag{12.11}$$

where the standard deviation, σ, has units of distance. Because retention times and peak widths are usually measured in seconds or minutes, it is more convenient to express the standard deviation in units of time, τ, by dividing σ by the solute's average linear velocity, $\overline{v}$.

$$\tau = \frac{\sigma}{\overline{v}} = \frac{\sigma t_r}{L} \tag{12.12}$$

> **Note**
>
> The solute's average linear velocity is the distance it travels, L, divided by its retention time, t_r.

For a Gaussian peak shape, the width at the baseline, w, is four times its standard deviation, τ.

$$w = 4\tau \tag{12.13}$$

Combining equation 12.11, equation 12.12, and equation 12.13 defines the height of a theoretical plate in terms of the easily measured chromatographic parameters t_r and w.

$$H = \frac{Lw^2}{16t_r^2} \tag{12.14}$$

> **Note**
>
> See Figure 12.9 for a review of how to determine values for t_r and w.

Combing equation 12.14 and equation 12.10 gives the number of theoretical plates.

$$N = 16\frac{t_r^2}{w^2} \tag{12.15}$$

> **Example 12.4**
>
> A chromatographic analysis for the chlorinated pesticide Dieldrin gives a peak with a retention time of 8.68 min and a baseline width of 0.29 min. What is the number of theoretical plates? Given that the column is 2.0 m long, what is the height of a theoretical plate in mm?
>
> ***Solution***
>
> Using equation 12.15, the number of theoretical plates is
>
> $$N = 16\frac{t_r^2}{w^2} = N = 16\frac{(8.68\text{ min})^2}{(0.29\text{ min})^2} = 14300\text{ plates} \tag{12.2.10}$$

Solving equation 12.10 for H gives the average height of a theoretical plate as

$$H = \frac{L}{N} = \frac{2.0\ \text{m}}{14300\ \text{plates}} \times \frac{1000\ \text{mm}}{\text{m}} = 0.14\ \text{mm/plate} \tag{12.2.11}$$

Practice Exercise 12.4

For each solute in the chromatogram for Practice Exercise 12.2, calculate the number of theoretical plates and the average height of a theoretical plate. The column is 0.5 m long.

Click here to review your answer to this exercise.

It is important to remember that a theoretical plate is an artificial construct and that a chromatographic column does not contain physical plates. In fact, the number of theoretical plates depends on both the properties of the column and the solute. As a result, the number of theoretical plates for a column may vary from solute to solute.

12.2.5 Peak Capacity

One advantage of improving column efficiency is that we can separate more solutes with baseline resolution. One estimate of the number of solutes that we can separate is

$$n_c = 1 + \frac{\sqrt{N}}{4} \ln \frac{V_{max}}{V_{min}} \tag{12.16}$$

where n_c is the column's **peak capacity**, and V_{min} and V_{max} are the smallest and the largest volumes of mobile phase in which we can elute and detect a solute.[3]

Note

The smallest volume we can use is the column's void volume. The largest volume is determined either by our patience—what is the maximum analysis time we can tolerate—or by our inability to detect solutes because there is too much band broadening.

A column with 10 000 theoretical plates, for example, can resolve no more than

$$n_c = 1 + \frac{\sqrt{10000}}{4} \ln \frac{30\ \text{mL}}{1\ \text{mL}} = 86\ \text{solutes} \tag{12.2.12}$$

if V_{min} and V_{max} are 1 mL and 30 mL, respectively. This estimate provides an upper bound on the number of solutes and may help us exclude from consideration a column that does not have enough theoretical plates to separate a complex mixture. Just because a column's theoretical peak capacity is larger than the number of solutes, however, does not mean that a separation is feasible. In most situations the practical peak capacity is less than the estimated value because the retention characteristics of some solutes are so similar that a separation is impossible. Nevertheless, columns with more theoretical plates, or with a greater range of possible elution volumes, are more likely to separate a complex mixture.

12.2.6 Asymmetric Peaks

Our treatment of chromatography in this section assumes that a solute elutes as a symmetrical Gaussian peak, such as that shown in Figure 12.9. This ideal behavior occurs when the solute's partition coefficient, K_D

$$K_D = \frac{[S_s]}{[S_m]} \tag{12.2.13}$$

is the same for all concentrations of solute. If this is not the case, then the chromatographic peak has an asymmetric peak shape similar to those shown in Figure 12.14. The chromatographic peak in Figure 12.14a is an example of peak **tailing**, which occurs when some sites on the stationary phase retain the solute more strongly than other sites. Figure 12.14b, which is an example of peak **fronting** is most often the result of overloading the column with sample.

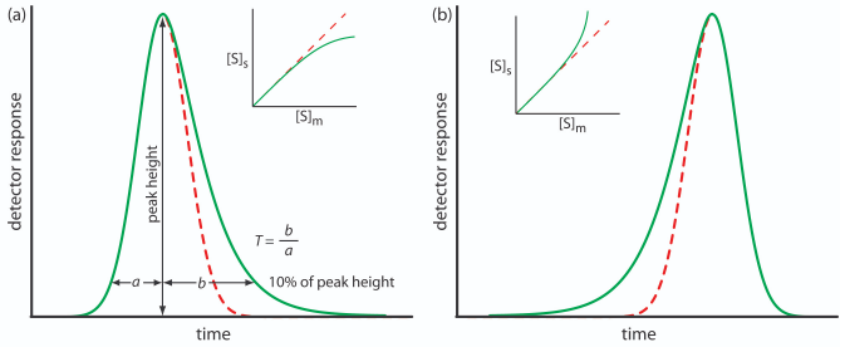


Figure 12.14 Examples of asymmetric chromatographic peaks showing (a) peak tailing and (b) peak fronting. For both (a) and (b) the green chromatogram is the asymmetric peak and the red dashed chromatogram shows the ideal, Gaussian peak shape. The insets show the relationship between the concentration of solute in the stationary phase, $[S]_s$, and its concentration in the mobile phase, $[S]_m$. The dashed red lines are for ideal behavior (K_D is constant for all conditions) and the green lines show nonideal behavior (K_D decreases or increases for higher total concentrations of solute). A quantitative measure of peak tailing, T, is shown in (a).

As shown in Figure 12.14a, we can report a peak's asymmetry by drawing a horizontal line at 10% of the peak's maximum height and measuring the distance from each side of the peak to a line drawn vertically through the peak's maximum. The asymmetry factor, T, is defined as

$$T = \frac{b}{a} \tag{12.2.14}$$

The number of theoretical plates for an asymmetric peak shape is approximately

$$N \approx \frac{41.7 \times \frac{t_r^2}{(w_{0.1})^2}}{T + 1.25} = \frac{41.7 \times \frac{t_r^2}{(a+b)^2}}{T + 1.25} \tag{12.2.15}$$

where $w_{0.1}$ is the width at 10% of the peak's height.[4]

Note

Asymmetric peaks have fewer theoretical plates, and the more asymmetric the peak the smaller the number of theoretical plates. For example, the following table gives values for N for a solute eluting with a retention time of 10.0 min and a peak width of 1.00 min.

b	a	T	N
0.5	0.5	1.00	1850
0.6	0.4	1.50	1520
0.7	0.3	2.33	1160
0.8	0.2	4.00	790
0.9	0.1	9.00	410

Contributors

David Harvey (DePauw University)

12.2: General Theory of Column Chromatography is shared under a CC BY-NC-SA 4.0 license and was authored, remixed, and/or curated by LibreTexts.

12.3: Optimizing Chromatographic Separations

Now that we have defined the solute retention factor, selectivity, and column efficiency we are able to consider how they affect the resolution of two closely eluting peaks. Because the two peaks have similar retention times, it is reasonable to assume that their peak widths are nearly identical. Equation 12.1, therefore, becomes

$$R_{AB} = \frac{t_{r,B} - t_{r,A}}{0.5(w_B + w_A)} \approx \frac{t_{r,B} - t_{r,A}}{0.5(2w_B)} = \frac{t_{r,B} - t_{r,A}}{w_B} \tag{12.17}$$

where B is the later eluting of the two solutes.

> **Note**
>
> If the number of theoretical plates is the same for all solutes—not strictly true, but not a bad assumption—then from equation 12.15, the ratio t_r/w is a constant. If two solutes have similar retention times, then their peak widths must be similar.

Solving equation 12.15 for w_B and substituting into equation 12.17 leaves us with the following result.

$$R_{AB} = \frac{\sqrt{N}}{4} \times \frac{t_{r,B} - t_{r,A}}{t_{r,B}} \tag{12.18}$$

Rearranging equation 12.8 provides us with the following equations for the retention times of solutes A and B.

$$t_{r,A} = k_A t_m + t_m \qquad t_{r,B} = k_B t_m + t_m \tag{12.3.1}$$

After substituting these equations into equation 12.18 and simplifying, we have

$$R_{AB} = \frac{\sqrt{N}}{4} \times \frac{k_B - k_A}{1 + k_B} \tag{12.3.2}$$

Finally, we can eliminate solute A's retention factor by substituting in equation 12.9. After rearranging, we end up with the following equation for the resolution between the chromatographic peaks for solutes A and B.

$$R_{AB} = \frac{\sqrt{N}}{4} \times \frac{\alpha - 1}{\alpha} \times \frac{k_B}{1 + k_B} \tag{12.19}$$

In addition to resolution, another important factor in chromatography is the amount of time needed to elute a pair of solutes, which we can approximate using the retention time for solute B.

$$t_{r,B} = \frac{16R_{AB}^2 H}{u} \times \left(\frac{\alpha}{\alpha - 1}\right)^2 \times \frac{(1 + k_B)^3}{k_B^2} \tag{12.20}$$

where u is the mobile phase's velocity.

Equation 12.19 and equation 12.20 contain terms corresponding to column efficiency, selectivity, and the solute retention factor. We can vary these terms, more or less independently, to improve resolution and analysis time. The first term, which is a function of the number of theoretical plates (for equation 12.19) or the height of a theoretical plate (for equation 12.20), accounts for the effect of column efficiency. The second term is a function of α and accounts for the influence of column selectivity. Finally, the third term in both equations is a function of k_B and accounts for the effect of solute B's retention factor. A discussion of how we can use these parameters to improve resolution is the subject of the remainder of this section.

12.3.1 Using the Retention factor to Optimize Resolution

One of the simplest ways to improve resolution is to adjust solute B's retention factor. If all other terms in equation 12.19 remain constant, increasing k_B improves resolution. As shown by the green curve in Figure 12.15, however, the improvement is greatest if the initial value of k_B is small. Once k_B exceeds a value of approximately 10, a further increase produces only a marginal improvement in resolution. For example, if the original value of k_B is 1, increasing its value to 10 gives an 82% improvement in resolution; a further increase to 15 provides a net improvement in resolution of only 87.5%.

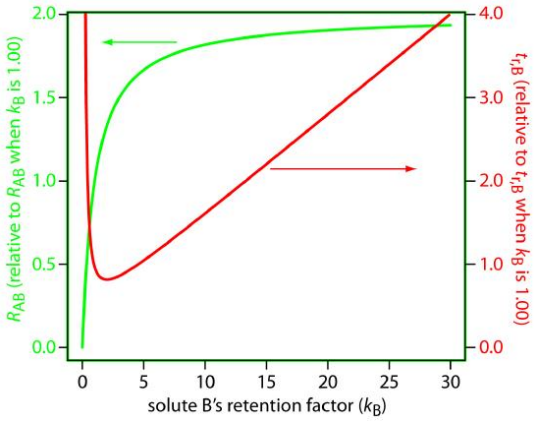


Figure 12.15: Effect of k_B on the resolution for a pair of solutes, R_{AB}, and the retention time for the later eluting solute, $t_{r,B}$. The *y*-axes display the resolution and retention time relative to their respective values when k_B is 1.00.

Any improvement in resolution by increasing the value of k_B generally comes at the cost of a longer analysis time. The red curve in Figure 12.15 shows the relative change in solute B's retention time as a function of its retention factor. Note that the minimum retention time is for $k_B = 2$. Increasing k_B from 2 to 10, for example, approximately doubles solute B's retention time.

> **Note**
>
> The relationship between retention factor and analysis time in Figure 12.15 works to our advantage if a separation produces an acceptable resolution with a large k_B. In this case we may be able to decrease k_B with little loss in resolution and with a significantly shorter analysis time.

To increase k_B without significantly changing the selectivity, α, any change to the chromatographic conditions must result in a general, nonselective increase in the retention factor for both solutes. In gas chromatography, we can accomplish this by decreasing the column's temperature. Because a solute's vapor pressure is smaller at lower temperatures, it spends more time in the stationary phase and takes longer to elute. In liquid chromatography, the easiest way to increase a solute's retention factor is to use a mobile phase that is a weaker solvent. When the mobile phase has a lower solvent strength, solutes spend proportionally more time in the stationary phase and take longer to elute.

Adjusting the retention factor to improve the resolution between one pair of solutes may lead to unacceptably long retention times for other solutes. For example, suppose we need to analyze a four-component mixture with baseline resolution and with a run-time of less than 20 min. Our initial choice of conditions gives the chromatogram in Figure 12.16a. Although we successfully separate components 3 and 4 within 15 min, we fail to separate components 1 and 2. Adjusting the conditions to improve the resolution for the first two components by increasing $k_{B,2}$ provides a good separation of all four components, but the run-time is now too long (Figure 12.16b). This problem of finding a single set of acceptable operating conditions is known as the **general elution problem**.

One solution to the general elution problem is to make incremental adjustments to the retention factor over time. Thus, we choose our initial chromatographic conditions to optimize the resolution for early eluting solutes. As the separation progresses, we adjust the chromatographic conditions to decrease k_B—and, therefore, decrease the retention time—for each of the later eluting solutes (Figure 12.16c). In gas chromatography this is accomplished by temperature programming. The column's initial temperature is selected such that the first solutes to elute are fully resolved. The temperature is then increased, either continuously or in steps, to bring off later eluting components with both an acceptable resolution and a reasonable analysis time. In liquid chromatography the same effect is obtained by increasing the solvent's eluting strength. This is known as a gradient elution. We will have more to say about each of these in later sections of this chapter.

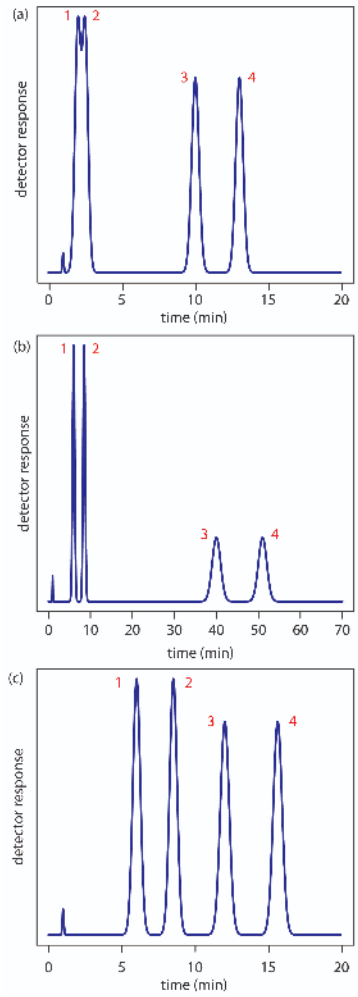


Figure 12.16: *Example showing the general elution problem in chromatography. See text for details.*

12.3.2 Using Selectivity to Optimize Resolution

A second approach to improving resolution is to adjust the selectivity, α. In fact, for α ≈ 1 it usually is not possible to improve resolution by adjusting the solute retention factor, k_B, or column efficiency, N. A change in α often has a more dramatic effect on resolution than a change in k_B. For example, changing α from 1.1 to 1.5, while holding all other terms constant, improves resolution by 267%. In gas chromatography, we usually adjust α by changing the stationary phase, and we usually change the composition of the mobile phase in liquid chromatography.

To change α we need to selectively adjust individual solute retention factors. Figure 12.17 shows one possible approach for the liquid chromatographic separation of a mixture of substituted benzoic acids. Because the components are weak acids, their retention times vary with the pH of the mobile phase, as shown in Figure 12.17a. The intersections of these curves show pH values where two solutes co-elute. For example, at a pH of 3.8 terephthalic acid and *p*-hydroxybenzoic acid elute as a single chromatographic peak.

Note

Let's use benzoic acid, C_6H_5COOH, to explain why pH can affect a solute's retention time. The separation uses an aqueous mobile phase and a nonpolar stationary phase. At lower pHs, benzoic acid is predominately in its weak acid form, C_6H_5COOH, and easily partitions into the nonpolar stationary phase. At more basic pHs, however, benzoic acid is in its weak base form, $C_6H_5COO^-$. Because it now carries a charge, its solubility in the mobile phase increases and its solubility in the nonpolar stationary phase decreases. As a result, it spends more time in the mobile phase and has a shorter retention time.

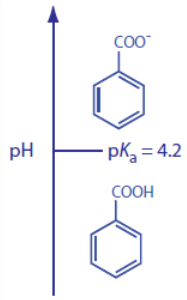


Figure 12.17a shows that there are many pH values where some separation is possible. To find the optimum separation, we plot α for each pair of solutes. The red, green, and orange curves in Figure 12.17b show the variation in a with pH for the three pairs of solutes that are hardest to separate (for all other pairs of solutes, α > 2 at all pH levels). The blue shading shows windows of pH values in which at least a partial separation is possible—this figure is sometimes called a window diagram—and the highest point in each window gives the optimum pH within that range. The best overall separation is the highest point in any window, which, for this example, is a pH of 3.5. Because the analysis time at this pH is more than 40 min (see Figure 12.17a), choosing a pH between 4.1–4.4 might produce an acceptable separation with a much shorter analysis time.

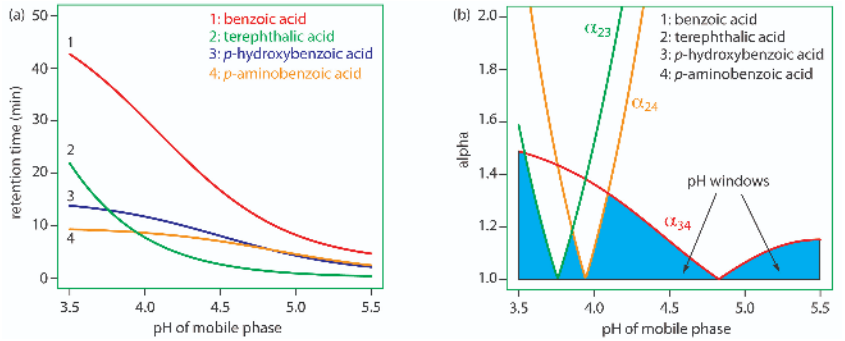


Figure 12.17: Example showing how the mobile phase pH in liquid chromatography affects selectivity: (a) retention times for four substituted benzoic acids as a function of the mobile phase's pH; (b) alpha values for three pairs of solutes that are difficult to separate. See text for details. The mobile phase is an acetic acid/sodium acetate buffer and the stationary phase is a nonpolar hydrocarbon. Data from Harvey, D. T.; Byerly, S.; Bowman, A.; Tomlin, J. "Optimization of HPLC and GC Separations Using Response Surfaces," *J. Chem. Educ.* **1991**, *68*, 162–168.

Table 12.1: Minimum Number of Theoretical Plates to Achieve Desired Resolution for Selected Values of k_B and α

	R_{AB} = 1.00		R_{AB} = 1.25		R_{AB} = 1.50	
k_B	α = 1.05	α = 1.10	α = 1.05	α = 1.10	α = 1.05	α = 1.10
0.5	63500	17400	99200	27200	143000	39200
1.0	28200	7740	44100	12100	63500	17400
1.5	19600	5380	30600	8400	44100	12100
2.0	15900	4360	24800	6810	35700	9800
3.0	12500	3440	19600	5380	28200	7740
5.0	10200	2790	15900	4360	22900	6270
10.0	8540	2340	13300	3660	19200	5270

12.3.3 Using Column Efficiency to Optimize Resolution

A third approach to improving resolution is to adjust the column's efficiency by increasing the number of theoretical plates, N. If we have values for k_B and α, then we can use equation 12.19 to calculate the number of theoretical plates for any resolution. Table 12.1 provides some representative values. For example, if α = 1.05 and k_B = 2.0, a resolution of 1.25 requires approximately 24 800 theoretical plates. If our column provides only 12 400 plates, half of what is needed, then a separation is not possible. How can we double the number of theoretical plates? The easiest way is to double the length of the column, although this also doubles the analysis time. A better approach is to cut the height of a theoretical plate, H, in half, providing the desired resolution without changing the analysis time. Even better, if we can decrease H by more than 50%, it may be possible to achieve the desired resolution with an even shorter analysis time by decreasing k_B or α.

To decrease the height of a theoretical plate we need to understand the experimental factors that affect band broadening. There are several theoretical treatments of band broadening. We will consider one approach that considers four contributions: variations in paths length, longitudinal diffusion, mass transfer in the stationary phase, and mass transfer in the mobile phase.

Multiple Paths: Variations in Path Length

As solute molecules pass through the column they travel paths that differ in length. Because of this difference in path length, solute molecules entering the column at the same time, exit the column at different times. The result, as shown in Figure 12.18, is band broadening. The contribution of **multiple paths** to the height of a theoretical plate, H_p, is

$$H_p = 2\lambda d_p \tag{12.21}$$

where d_p is the average diameter of the particulate packing material, and λ is a constant that accounts for the consistency of the packing. A smaller range of particle sizes and a more consistent packing produce a smaller value for λ. For a column without packing material, H_p is zero and there is no contribution to band broadening from multiple paths.

> **Note**
>
> Inconsistent packing can produces channels through the column that allow some solute molecules to travel quickly through the column. It also can lead to pockets that can temporarily trap some solute molecules, slowing their progress through the column. A more uniform packing minimizes these two problems.

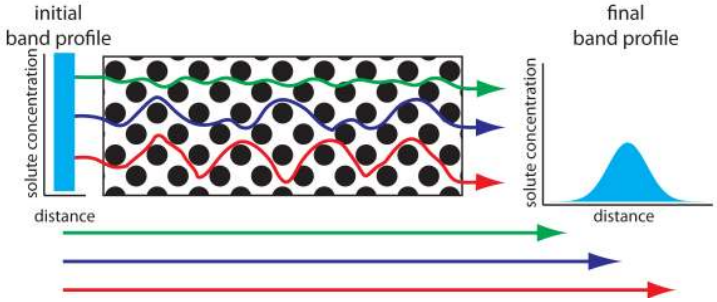


Figure 12.18: The effect of multiple paths on a solute's band broadening. The solute's initial band profile is rectangular. As this band travels through the column, individual solute molecules travel different paths, three of which are shown by the meandering colored paths (the actual lengths of these paths are shown by the straight arrows at the bottom of the figure). Most solute molecules travel paths with lengths similar to that shown in blue, with a few traveling much shorter paths (green) or much longer paths (red). As a result, the solute's band profile at the end of the column is broader and Gaussian in shape.

Longitudinal Diffusion

The second contribution to band broadening is the result of the solute's **longitudinal diffusion** in the mobile phase. Solute molecules are constantly in motion, diffusing from regions of higher solute concentration to regions where the concentration of solute is smaller. The result is an increase in the solute's band width (Figure 12.19). The contribution of longitudinal diffusion to the height of a theoretical plate, H_d, is

$$H_d = \frac{2\gamma D_m}{u} \tag{12.22}$$

where D_m is the solute's diffusion coefficient in the mobile phase, u is the mobile phase velocity, and γ is a constant related to the efficiency of column packing. Note that the effect of H_d on band broadening is inversely proportional to the mobile phase velocity—a higher velocity provides less time for longitudinal diffusion. Because a solute's diffusion coefficient is larger in the gas phase than in a liquid phase, longitudinal diffusion is a more serious problem in gas chromatography.

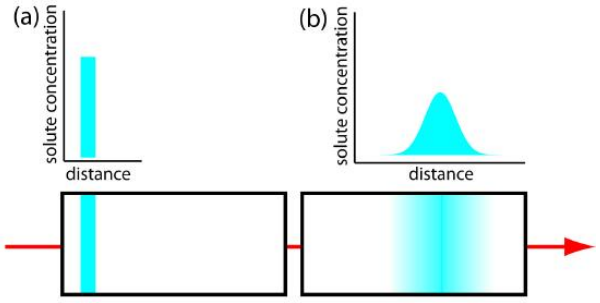


Figure 12.19: The effect of longitudinal diffusion on a solute's band broadening. Two horizontal crosssections through the column and the corresponding concentration versus distance profiles are shown, with (a) being earlier in time. The red arrow shows the direction in which the mobile phase is moving.

Mass Transfer

As the solute passes through the column it moves between the mobile phase and the stationary phase. We call this movement between phases **mass transfer**. As shown in Figure 12.20, band broadening occurs if the solute's movement within the mobile phase or within the stationary phase is not fast enough to maintain an equilibrium partitioning of solute between the two phases. On average, solute molecules in the mobile phase move further down the column before passing into the stationary phase. Solute molecules in the stationary phase, on the other hand, take longer than expected to move back into the mobile phase. The contributions of mass transfer in the stationary phase, H_s, and mass transfer in the mobile phase, H_m, are given by the following equations

$$H_s = \frac{qkd_f^2}{(1+k)^2 D_s} u \tag{12.23}$$

$$H_m = \frac{fn(d_p^2, d_c^2)}{D_m} u \tag{12.24}$$

where d_f is the thickness of the stationary phase, d_c is the column's diameter, D_s and D_m are the solute's diffusion coefficient in the stationary phase and the mobile phase, k is the solute's retention factor, and q is a constant related to the column packing material. Although the exact form of H_m is not known, it is a function of particle size and column diameter. Note that the effect of H_s and H_m on band broadening is directly proportional to the mobile phase velocity—smaller velocities provide more time for mass transfer.

> **Note**
>
> The abbreviation *fn* in equation 12.24 means "function of."

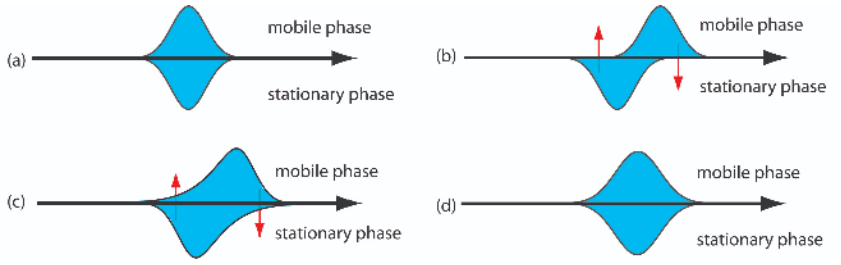


Figure 12.20 Effect of mass transfer on band broadening: (a) Ideal equilibrium Gaussian profiles for the solute in the mobile phase and in the stationary phase. (b, c) If we allow the solute's band to move a small distance down the column, an equilibrium between the two phases no longer exits. The red arrows show the movement of solute—what we call the mass transfer of solute—from the

stationary phase to the mobile phase, and from the mobile phase to the stationary phase. (d) Once equilibrium is reestablished, the solute's band is now broader.

Putting it All Together

The height of a theoretical plate is a summation of the contributions from each of the terms affecting band broadening.

$$H = H_p + H_d + H_s + H_m \tag{12.25}$$

An alternative form of this equation is the **van Deemter equation**

$$H = A + \frac{B}{u} + Cu \tag{12.26}$$

which emphasizes the importance of the mobile phase's velocity. In the van Deemter equation,

- The A term accounts for the contribution of multiple paths (H_p),
- The B/u term accounts for the contribution of longitudinal diffusion (H_d), and
- The Cu term accounts for the combined contribution of mass transfer in the stationary phase and mobile phase (H_s and H_m).

There is some disagreement on the best equation for describing the relationship between plate height and mobile phase velocity.[5] In addition to the van Deemter equation, other equations include

$$H = \frac{B}{u} + (C_s + C_m)u \tag{12.3.3}$$

where C_s and C_m are the mass transfer terms for the stationary phase and the mobile phase and

$$H = Au^{1/3} + \frac{B}{u} + Cu \tag{12.3.4}$$

All three equations, and others, have been used to characterize chromatographic systems, with no single equation providing the best explanation in every case.[6]

To increase the number of theoretical plates without increasing the length of the column we need to decrease one or more of the terms in equation 12.25. The easiest way to decrease H is by adjusting the velocity of the mobile phase. For smaller mobile phase velocities, column efficiency is limited by longitudinal diffusion, and at higher velocities efficiency is limited by the two mass transfer terms. As shown in Figure 12.21—which uses the van Deemter equation—the optimum mobile phase velocity is the minimum in a plot of H as a function of u.

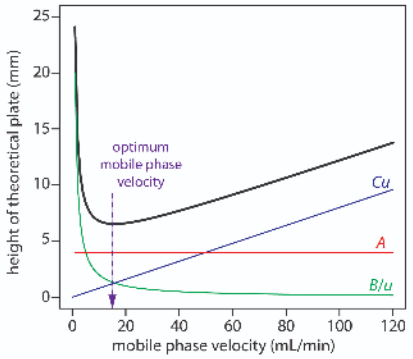


Figure 12.21: Plot showing the relationship between the height of a theoretical plate, H, and the mobile phase's velocity, u, based on the van Deemter equation.

The remaining parameters affecting the terms in equation 12.25 are functions of the column's properties and suggest other possible approaches to improving column efficiency. For example, both H_p and H_m are a function of the size of the particles used for packing the column. Decreasing particle size, therefore, is another useful method for improving efficiency.

https://chem.libretexts.org/@go/page/70718

> **Note**
>
> The smaller the particles, the more pressure is needed to push the mobile phase through the column. As a result, for any form of chromatography there is a practical limit to particle size.

Perhaps the most important advancement in chromatography columns is the development of open-tubular, or **capillary columns**. These columns have very small diameters ($d_c \approx 50–500$ μm) and contain no packing material ($d_p = 0$). Instead, the interior wall of a capillary column is coated with a thin film of the stationary phase. Plate height is reduced because the contribution to H from H_p (equation 12.21) disappears and the contribution from H_m (equation 12.24) becomes smaller. Because the column does not contain any solid packing material, it takes less pressure to move the mobile phase through the column, allowing for much longer columns. The combination of a longer column and a smaller height for a theoretical plate increases the number of theoretical plates by approximately 100ˆ~. Capillary columns are not without disadvantages. Because they are much narrower than packed columns, they require a significantly smaller amount of sample, which may be difficult to inject reproducibly. Another approach to improving resolution is to use thin films of stationary phase, which decreases the contribution to H from H_s (equation 12.23).

Contributors

David Harvey (DePauw University)

12.3: Optimizing Chromatographic Separations is shared under a CC BY-NC-SA 4.0 license and was authored, remixed, and/or curated by LibreTexts.

12.4: Gas Chromatography

In **gas chromatography** (GC) we inject the sample, which may be a gas or a liquid, into an gaseous mobile phase (often called the carrier gas). The mobile phase carries the sample through a packed or capillary column that separates the sample's components based on their ability to partition between the mobile phase and the stationary phase. Figure 12.22 shows an example of a typical gas chromatograph, which consists of several key components: a supply of compressed gas for the mobile phase; a heated injector, which rapidly volatilizes the components in a liquid sample; a column, which is placed within an oven whose temperature we can control during the separation; and a detector for monitoring the eluent as it comes off the column. Let's consider each of these components.

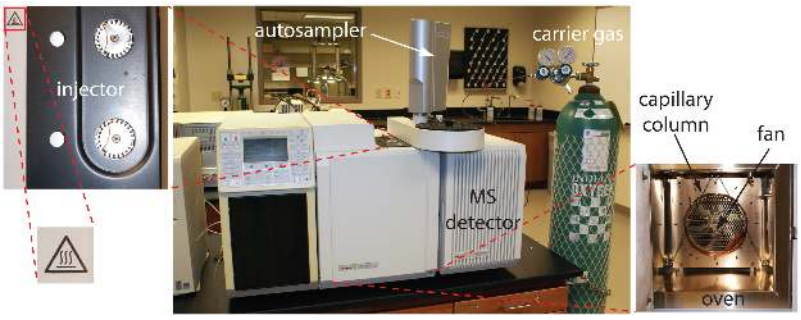


Figure 12.22 *Example of a typical gas chromatograph with insets showing the heated injection ports—note the symbol indicating that it is hot—and the oven containing the column. This particular instrument is equipped with an autosampler for injecting samples, a capillary column, and a mass spectrometer (MS) as the detector. Note that the carrier gas is supplied by a tank of compressed gas.*

12.4.1 Mobile Phase

The most common mobile phases for gas chromatography are He, Ar, and N_2, which have the advantage of being chemically inert toward both the sample and the stationary phase. The choice of carrier gas is often determined by the instrument's detector. For a packed column the mobile phase velocity is usually 25–150 mL/min. The typical flow rate for a capillary column is 1–25 mL/min.

12.4.2 Chromatographic Columns

There are two broad classes of chromatographic columns: packed columns and capillary columns. In general, a packed column can handle larger samples and a capillary column can separate more complex mixtures.

Packed Columns

Packed columns are constructed from glass, stainless steel, copper, or aluminum, and are typically 2–6 m in length with internal diameters of 2–4 mm. The column is filled with a particulate solid support, with particle diameters ranging from 37–44 μm to 250–354 μm. Figure 12.23 shows a typical example of a packed column.

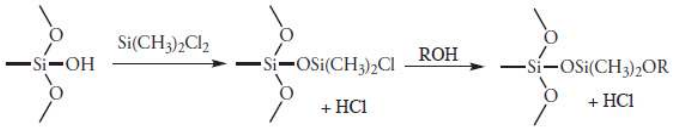


Figure 12.23 *Typical example of a packed column for gas chromatography. This column is made from stainless steel and is 2 m long with an internal diameter of 3.2 mm. The packing material in this column has a particle diameter of 149–177 μm. To put this in perspective, beach sand has a typical diameter of 700 μm and the diameter of fine grained sand is 250 μm.*

The most widely used particulate support is diatomaceous earth, which is composed of the silica skeletons of diatoms. These particles are very porous, with surface areas ranging from 0.5–7.5 m^2/g, providing ample contact between the mobile phase and the

stationary phase. When hydrolyzed, the surface of a diatomaceous earth contains silanol groups (–SiOH), which serve as active sites for absorbing solute molecules in **gas-solid chromatography** (GSC).

In **gas-liquid chromatography** (GLC), we coat the packing material with a liquid mobile phase. To prevent any uncoated packing material from adsorbing solutes, which degrades the quality of the separation, the surface silanols are deactivated by reacting them with dimethyldichlorosilane and rinsing with an alcohol—typically methanol—before coating the particles with stationary phase.



Other types of solid supports include glass beads and fluorocarbon polymers, which have the advantage of being more inert than diatomaceous earth.

To minimize the effect on plate height from multiple path and mass transfer, the diameter of the packing material should be as small as possible (see equation 12.21 and 12.25) and loaded with a thin film of stationary phase (see equation 12.23). Compared to capillary columns, which are discussed below, a packed column can handle larger sample volumes, typically 0.1–10 μL. Column efficiencies range from several hundred to 2000 plates/m, with a typical column having 3000–10 000 theoretical plates. The column in Figure 12.23, for example, has approximately 1800 plates/m, or a total of approximately 3600 theoretical plates. If we assume a $V_{max}/V_{min} \approx 50$, then it has a peak capacity of

$$n_c = 1 + \frac{\sqrt{3600}}{4}\ln(50) \approx 60 \tag{12.4.1}$$

> **Note**
>
> You can use equation 12.16 to estimate a column's peak capacity.

Capillary Columns

A capillary, or **open tubular column** is constructed from fused silica and is coated with a protective polymer coating. Columns range from 15–100 m in length with an internal diameter of approximately 150–300 μm. Figure 12.24 shows a typical example of a capillary column.



Figure 12.24 *Typical example of a capillary column for gas chromatography. This column is 30 m long with an internal diameter of 247 μm. The interior surface of the capillary has a 0.25 μm coating of the liquid phase.*

Capillary columns are of three principle types. In a **wall-coated open tubular column** (WCOT) a thin layer of stationary phase, typically 0.25 μm thick, is coated on the capillary's inner wall. In a **porous-layer open tubular column** (PLOT), a porous solid support—alumina, silica gel, and molecular sieves are typical examples—is attached to the capillary's inner wall. A **support-coated open tubular column** (SCOT) is a PLOT column that includes a liquid stationary phase. Figure 12.25 shows the differences between these types of capillary columns.

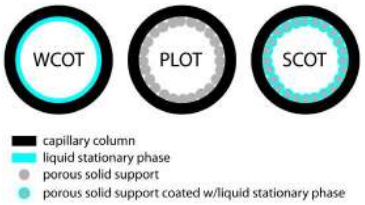


Figure 12.25 Cross-sections through the three types of capillary columns.

A capillary column provides a significant improvement in separation efficiency because it has more theoretical plates per meter and is longer than a packed column. For example, the capillary column in Figure 12.24 has almost 4300 plates/m, or a total of 129 000 theoretical plates. If we assume a $V_{max}/V_{min} \approx 50$, then it has a peak capacity of approximately 350. On the other hand, a packed column can handle a larger sample. Because of its smaller diameter, a capillary column requires a smaller sample, typically less than 10^{-2} μL.

Stationary Phases for Gas–Liquid Chromatography

Elution order in gas–liquid chromatography depends on two factors: the boiling point of the solutes, and the interaction between the solutes and the stationary phase. If a mixture's components have significantly different boiling points, then the choice of stationary phase is less critical. If two solutes have similar boiling points, however, then a separation is possible only if the stationary phase selectively interacts with one of the solutes. As a general rule, nonpolar solutes are more easily separated with a nonpolar stationary phase, and polar solutes are easier to separate when using a polar stationary phase.

There are several important criteria for choosing a stationary phase: it must not react chemically with the solutes, it must be thermally stable, it must have a low volatility, and it must have a polarity that is appropriate for the sample's components. Table 12.2 summarizes the properties of several popular stationary phases.

***Table 12.2**: Selected Examples of Stationary Phases for Gas–Liquid Chromatography*

stationary phase	polarity	trade name	temperature limit (°C)	representative applications
squalane	nonpolar	Squalane	150	low-boiling aliphatics hydrocarbons
Apezion L	nonpolar	Apezion L	300	amides, fatty acid methyl esters, terpenoids
polydimethyl siloxane	slightly polar	SE-30	300–350	alkaloids, amino acid derivatives, drugs, pesticides, phenols, steroids
phenylmethyl polysiloxane (50% phenyl, 50% methyl)	moderately polar	OV-17	375	alkaloids, drugs, pesticides, polyaromatic hydrocarbons, polychlorinated biphenyls
trifluoropropylmethyl polysiloxane (50% trifluoropropyl, 50% methyl)	moderately polar	OV-210	275	alkaloids, amino acid derivatives, drugs, halogenated compounds, ketones
cyanopropylphenylmethyl polysiloxane (50% cyanopropyl, 50% phenylmethyl)	polar	OV-225	275	nitriles, pesticides, steroids
polyethylene glycol	polar	Carbowax 20M	225	aldehydes, esters, ethers, phenols

Many stationary phases have the general structure shown in Figure 12.26a. A stationary phase of polydimethyl siloxane, in which all the –R groups are methyl groups, $–CH_3$, is nonpolar and often makes a good first choice for a new separation. The order of elution when using polydimethyl siloxane usually follows the boiling points of the solutes, with lower boiling solutes eluting first. Replacing some of the methyl groups with other substituents increases the stationary phase's polarity and provides greater selectivity. For example, replacing 50% of the $–CH_3$ groups with phenyl groups, $–C_6H_5$, produces a slightly polar stationary phase. Increasing polarity is provided by substituting trifluoropropyl, $–C_3H_6CF$, and cyanopropyl, $–C_3H_6CN$, functional groups, or by using a stationary phase of polyethylene glycol (Figure 12.26b).

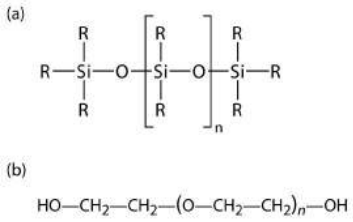


Figure 12.26: *General structures of common stationary phases: (a) substituted polysiloxane; (b) polyethylene glycol.*

An important problem with all liquid stationary phases is their tendency to elute, or **bleed** from the column when it is heated. The temperature limits in Table 12.2 minimize this loss of stationary phase. Capillary columns with bonded or cross-linked stationary phases provide superior stability. A bonded stationary phase is chemically attached to the capillary's silica surface. Cross-linking, which is done after the stationary phase is in the capillary column, links together separate polymer chains, providing greater stability.

Another important consideration is the thickness of the stationary phase. From equation 12.23 we know that separation efficiency improves with thinner films of stationary phase. The most common thickness is 0.25 μm, although a thicker films may be used for highly volatile solutes, such as gases, because it has a greater capacity for retaining such solutes. Thinner films are used when separating low volatility solutes, such as steroids.

A few stationary phases take advantage of chemical selectivity. The most notable are stationary phases containing chiral functional groups, which can be used for separating enantiomers.[7]

12.4.3 Sample Introduction

Three considerations determine how we introduce a sample to the gas chromatograph. First, all of the sample's constituents must be volatile. Second, the analytes must be present at an appropriate concentration. Finally, the physical process of injecting the sample must not degrade the separation.

Preparing a Volatile Sample

Not every sample can be injected directly into a gas chromatograph. To move through the column, the sample's constituents must be volatile. A solute of low volatility may be retained by the column and continue to elute during the analysis of subsequent samples. A nonvolatile solute will condense at the top of the column, degrading the column's performance.

We can separate a sample's volatile analytes from its nonvolatile components using any of the extraction techniques described in Chapter 7. A liquid–liquid extraction of analytes from an aqueous matrix into methylene chloride or another organic solvent is a common choice. Solid-phase extractions also are used to remove a sample's nonvolatile components.

An attractive approach to isolating analytes is a **solid-phase microextraction** (SPME). In one approach, which is illustrated in Figure 12.27, a fused-silica fiber is placed inside a syringe needle. The fiber, which is coated with a thin film of an adsorbent, such as polydimethyl siloxane, is lowered into the sample by depressing a plunger and is exposed to the sample for a predetermined time. After withdrawing the fiber into the needle, it is transferred to the gas chromatograph for analysis.

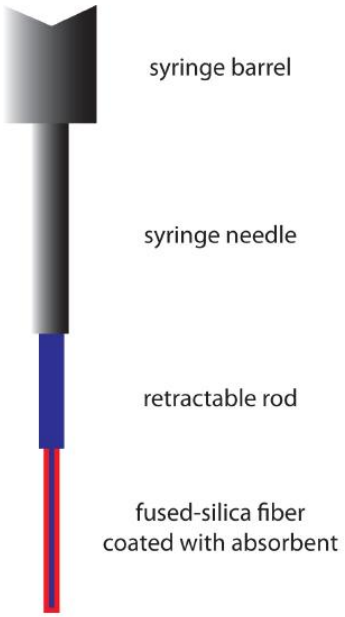


Figure 12.27 Schematic diagram of a solid-phase microextraction device.

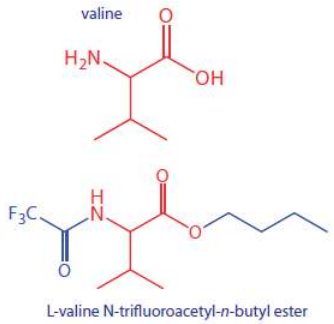
Two additional methods for isolating volatile analytes are a purge-and-trap and headspace sampling. In a **purge-and-trap** (see Figure 7.25 in Chapter 7), we bubble an inert gas, such as He or N_2, through the sample, releasing—or purging—the volatile compounds. These compounds are carried by the purge gas through a trap containing an absorbent material, such as Tenax, where they are retained. Heating the trap and back-flushing with carrier gas transfers the volatile compounds to the gas chromatograph. In **headspace sampling** we place the sample in a closed vial with an overlying air space. After allowing time for the volatile analytes

to equilibrate between the sample and the overlying air, we use a syringe to extract a portion of the vapor phase and inject it into the gas chromatograph. Alternatively, we can sample the headspace with an SPME.

Thermal desorption is a useful method for releasing volatile analytes from solids. We place a portion of the solid in a glass-lined, stainless steel tube. After purging with carrier gas to remove any O_2 that might be present, we heat the sample. Volatile analytes are swept from the tube by an inert gas and carried to the GC. Because volatilization is not a rapid process, the volatile analytes are often concentrated at the top of the column by cooling the column inlet below room temperature, a process known as **cryogenic focusing**. Once the volatilization is complete, the column inlet is rapidly heated, releasing the analytes to travel through the column.

> **Note**
>
> The reason for removing O_2 is to prevent the sample from undergoing an oxidation reaction when it is heated.

To analyze a nonvolatile analyte we must chemically convert it to a volatile form. For example, amino acids are not sufficiently volatile to analyze directly by gas chromatography. Reacting an amino acid with 1-butanol and acetyl chloride produces an esterfied amino acid. Subsequent treatment with trifluoroacetic acid gives the amino acid's volatile N-trifluoroacetyl-*n*-butyl ester derivative.



L-valine N-trifluoroacetyl-*n*-butyl ester

Adjusting the Analyte's Concentration

In an analyte's concentration is too small to give an adequate signal, then it needs to be concentrated before injecting the sample into the gas chromatograph. A side benefit of many extraction methods is that they often concentrate the analytes. Volatile organic materials isolated from an aqueous sample by a purge-and-trap, for example, may be concentrated by as much as 1000×.

If an analyte is too concentrated it is easy to overload the column, resulting in peak fronting (see Figure 12.14) and a poor separation. In addition, the analyte's concentration may exceed the detector's linear response. Injecting less sample or diluting the sample with a volatile solvent, such as methylene chloride, are two possible solutions to this problem.

Injecting the Sample

In Section 12.3.3 we examined several explanations for why a solute's band increases in width as it passes through the column, a process we called band broadening. We also introduce an additional source of band broadening if we fail to inject the sample into the minimum possible volume of mobile phase. There are two principal sources of this precolumn band broadening: injecting the sample into a moving stream of mobile phase and injecting a liquid sample instead of a gaseous sample. The design of a gas chromatograph's injector helps minimize these problems.

An example of a simple injection port for a packed column is shown in Figure 12.28. The top of the column fits within a heated injector block, with carrier gas entering from the bottom. The sample is injected through a rubber septum using a microliter syringe such as the one shown in Figure 12.29. Injecting the sample directly into the column minimizes band broadening by mixing the sample with the smallest possible amount of carrier gas. The injector block is heated to a temperature that is at least 50°C above the sample component with the highest boiling point, ensuring a rapid vaporization of the sample's components.

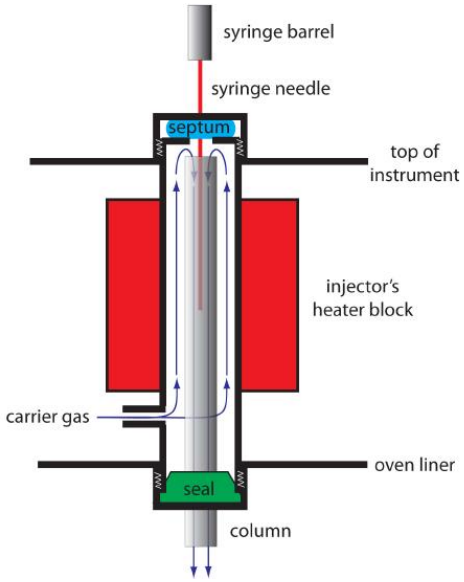


Figure 12.28 Schematic diagram showing a heated GC injector port for use with packed columns. The needle pierces a rubber septum and enters into the top of the column, which is located within a heater block.



Figure 12.29 Example of a syringe for injecting samples into a gas chromatograph. This syringe has a maximum capacity of 10 µL with graduations every 0.1 µL.

Because a capillary column's volume is significantly smaller than that for a packed column, it requires a different style of injector to avoid over-loading the column with sample. Figure 12.30 shows a schematic diagram of a typical split/splitless injector for use with capillary columns.

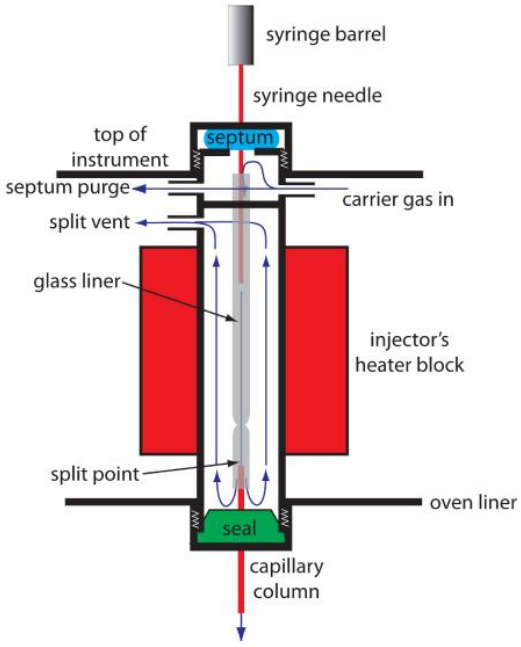


Figure 12.30 Schematic diagram showing a split/splitless injection port for use with capillary columns. The needle pierces a rubber septum and enters into a glass liner, which is located within a heater block. In a split injection the split vent is open; the split vent is closed for a splitless injection.

In a **split injection** we inject the sample through a rubber septum using a microliter syringe. Instead of injecting the sample directly into the column, it is injected into a glass liner where it mixes with the carrier gas. At the split point, a small fraction of the carrier gas and sample enters the capillary column with the remainder exiting through the split vent. By controlling the flow rate of the carrier gas entering the injector, and the flow rates through the septum purge and the split vent, we can control what fraction of the sample enters the capillary column, typically 0.1–10%.

> **Note**
>
> For example, if the carrier gas flow rate is 50 mL/min, and the flow rates for the septum purge and the split vent are 2 mL/min and 47 mL/min, respectively, then the flow rate through the column is 1 mL/min (= 50 – 2 – 46). The ratio of sample entering the column is 1/50, or 2%.

In a **splitless injection**, which is useful for trace analysis, we close the split vent and allow all the carrier gas passing through the glass liner to enter the column—this allows virtually all the sample to enters the column. Because the flow rate through the injector is low, significant precolumn band broadening is a problem. Holding the column's temperature approximately 20–25°C below the solvent's boiling point allows the solvent to condense at the entry to the capillary column, forming a barrier that traps the solutes. After allowing the solutes to concentrate, the column's temperature is increased and the separation begins.

For samples that decompose easily, an **on-column injection** may be necessary. In this method the sample is injected directly into the column without heating. The column temperature is then increased, volatilizing the sample with as low a temperature as is practical.

12.4.4 Temperature Control

Control of the column's temperature is critical to attaining a good separation in gas chromatography. For this reason the column is placed inside a thermostated oven (see Figure 12.22). In an **isothermal** separation we maintain the column at a constant temperature. To increase the interaction between the solutes and the stationary phase, the temperature usually is set slightly below that of the lowest-boiling solute.

One difficulty with an isothermal separation is that a temperature favoring the separation of a low-boiling solute may lead to an unacceptably long retention time for a higher-boiling solute. **Temperature programming** provide a solution to this problem. At the

beginning of the analysis we set the column's initial temperature below that for the lowest-boiling solute. As the separation progresses, we slowly increase the temperature at either a uniform rate or in a series of steps.

> **Note**
>
> You may recall that we called this the general elution problem (see Figure 12.16).

12.4.5 Detectors for Gas Chromatography

The final part of a gas chromatograph is the detector. The ideal detector has several desirable features, including: a low detection limit, a linear response over a wide range of solute concentrations (which makes quantitative work easier), sensitivity for all solutes or selectivity for a specific class of solutes, and an insensitivity to a change in flow rate or temperature.

Thermal Conductivity Detector (TCD)

One of the earliest gas chromatography detectors takes advantage of the mobile phase's thermal conductivity. As the mobile phase exits the column it passes over a tungsten-rhenium wire filament (see Figure 12.31). The filament's electrical resistance depends on its temperature, which, in turn, depends on the thermal conductivity of the mobile phase. Because of its high thermal conductivity, helium is the mobile phase of choice when using a **thermal conductivity detector** (TCD).

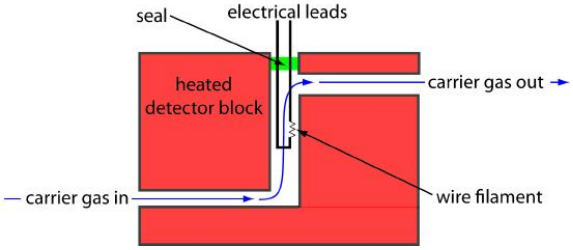


Figure 12.31 Schematic diagram showing a thermal conductivity detector. This is one cell of a matched pair. The sample cell takes the carrier gas as it elutes from the column. A source of carrier gas that bypasses the column passes through a reference cell.

When a solute elutes from the column, the thermal conductivity of the mobile phase in the TCD cell decreases and the temperature of the wire filament, and thus it resistance, increases. A reference cell, through which only the mobile phase passes, corrects for any time-dependent variations in flow rate, pressure, or electrical power, all of which may lead to a change in the filament's resistance.

Because all solutes affect the mobile phase's thermal conductivity, the thermal conductivity detector is a universal detector. Another advantage is the TCD's linear response over a concentration range spanning 10^4–10^5 orders of magnitude. The detector also is non-destructive, allowing us to isolate analytes using a postdetector cold trap. One significant disadvantage of the TCD detector is its poor detection limit for most analytes.

Flame Ionization Detector (FID)

The combustion of an organic compound in an H_2/air flame results in a flame containing electrons and organic cations, presumably CHO^+. Applying a potential of approximately 300 volts across the flame creates a small current of roughly 10^{-9} to 10^{-12} amps. When amplified, this current provides a useful analytical signal. This is the basis of the popular **flame ionization detector**, a schematic diagram of which is shown in Figure 12.32.

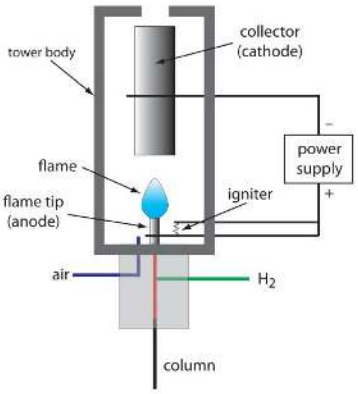


Figure 12.32 Schematic diagram showing a flame ionization detector. The eluent from the column mixes with H_2 and is burned in the presence of excess air. Combustion produces a flame containing electrons and the cation CHO^+. Applying a potential between the flame tip and the collector, a current that is proportional to the concentration of cations in the flame.

Most carbon atoms—except those in carbonyl and carboxylic groups—generate a signal, which makes the FID an almost universal detector for organic compounds. Most inorganic compounds and many gases, such as H_2O and CO_2, are not detected, which makes the FID detector a useful detector for the analysis of atmospheric and aqueous environmental samples. Advantages of the FID include a detection limit that is approximately two to three orders of magnitude smaller than that for a thermal conductivity detector, and a linear response over 10^6–10^7 orders of magnitude in the amount of analyte injected. The sample, of course, is destroyed when using a flame ionization detector.

Electron Capture Detector (ECD)

The **electron capture detector** is an example of a selective detector. As shown in Figure 12.33, the detector consists of a β-emitter, such as ^{63}Ni. The emitted electrons ionize the mobile phase, which is usually N_2, generating a standing current between a pair of electrodes. When a solute with a high affinity for capturing electrons elutes from the column, the current decreases. This decrease in current serves as the signal. The ECD is highly selective toward solutes with electronegative functional groups, such as halogens and nitro groups, and is relatively insensitive to amines, alcohols, and hydrocarbons. Although its detection limit is excellent, its linear range extends over only about two orders of magnitude.

> **Note**
>
> A β-particle is an electron.

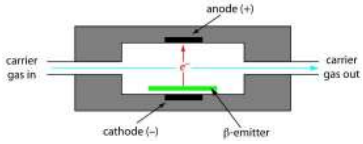


Figure 12.33 Schematic diagram showing an electron capture detector.

Mass Spectrometer (MS)

A **mass spectrometer** is an instrument that ionizes a gaseous molecule using enough energy that the resulting ion breaks apart into smaller ions. Because these ions have different mass-to-charge ratios, it is possible to separate them using a magnetic field or an electrical field. The resulting **mass spectrum** contains both quantitative and qualitative information about the analyte. Figure 12.34 shows a mass spectrum for toluene.

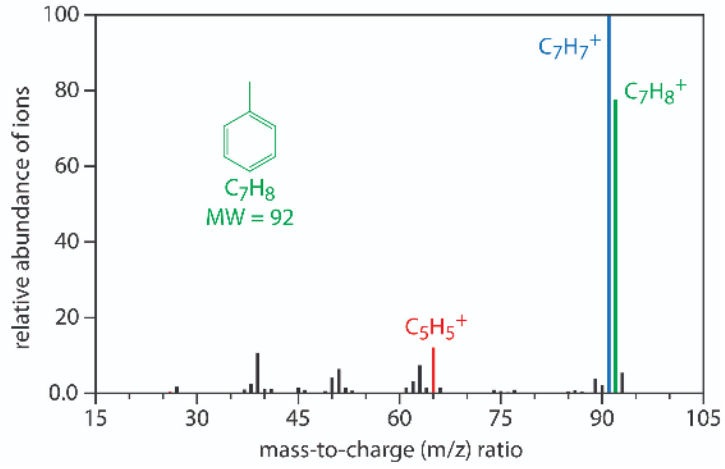


Figure 12.34 Mass spectrum for toluene highlighting the molecular ion in green (m/z = 92), and two fragment ions in blue (m/z = 91) and in red (m/z = 65). A mass spectrum provides both quantitative and qualitative information: the height of any peak is proportional to the amount of toluene in the mass spectrometer and the fragmentation pattern is unique to toluene.

Figure 12.35 shows a block diagram of a typical gas chromatography-mass spectrometer (GC–MS) instrument. The effluent from the column enters the mass spectrometer's ion source in a manner that eliminates the majority of the carrier gas. In the ionization chamber the remaining molecules—a mixture of carrier gas, solvent, and solutes—undergo ionization and fragmentation. The mass spectrometer's mass analyzer separates the ions by their mass-to-charge ratio. A detector counts the ions and displays the mass spectrum.

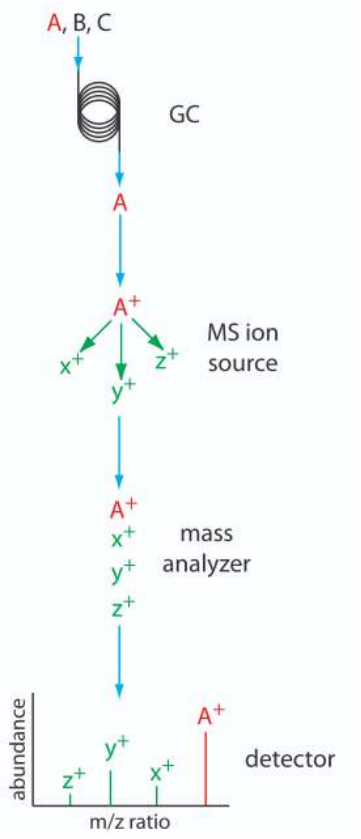


Figure 12.35 Block diagram of GC–MS. A three component mixture enters the GC. When component A elutes from the column, it enters the MS ion source and ionizes to form the parent ion and several fragment ions. The ions enter the mass analyzer, which separates them by their mass-tocharge ratio, providing the mass spectrum shown at the detector.

https://chem.libretexts.org/@go/page/70719

There are several options for monitoring the chromatogram when using a mass spectrometer as the detector. The most common method is to continuously scan the entire mass spectrum and report the total signal for all ions reaching the detector during each scan. This total ion scan provides universal detection for all analytes. We can achieve some degree of selectivity by monitoring only specific mass-to-charge ratios, a process called selective-ion monitoring. A mass spectrometer provides excellent detection limits, typically 25 fg to 100 pg, with a linear range of 10^5 orders of magnitude. Because we are continuously recording the mass spectrum of the column's eluent, we can go back and examine the mass spectrum for any time increment. This is a distinct advantage for GC–MS because we can use the mass spectrum to help identify a mixture's components.

Other Detectors

Two additional detectors are similar in design to a flame ionization detector. In the flame photometric detector optical emission from phosphorous and sulfur provides a detector selective for compounds containing these elements. The thermionic detector responds to compounds containing nitrogen or phosphorous.

A Fourier transform infrared spectrophotometer (FT–IR) also can serve as a detector. In GC–FT–IR, effluent from the column flows through an optical cell constructed from a 10–40 cm Pyrex tube with an internal diameter of 1–3 mm. The cell's interior surface is coated with a reflecting layer of gold. Multiple reflections of the source radiation as it is transmitted through the cell increase the optical path length through the sample. As is the case with GC–MS, an FT–IR detector continuously records the column eluent's spectrum, which allows us to examine the IR spectrum for any time increment.

> **Note**
>
> See Chapter 10.3 for a discussion of FT-IR spectroscopy and instrumentation.

12.4.6 Quantitative Applications

Gas chromatography is widely used for the analysis of a diverse array of samples in environmental, clinical, pharmaceutical, biochemical, forensic, food science and petrochemical laboratories. Table 12.3 provides some representative examples of applications.

Table 12.3 Representative Applications of Gas Chromatography

area	applications
environmental analysis	green house gases (CO_2, CH_4, NO_x) in air pesticides in water, wastewater, and soil vehicle emissions trihalomethanes in drinking water
clinical analysis	drugs blood alcohols
forensic analysis	analysis of arson accelerants detection of explosives
consumer products	volatile organics in spices and fragrances trace organics in whiskey monomers in latex paint
petroleum and chemical industry	purity of solvents refinery gas composition of gasoline

Quantitative Calculations

In a GC analysis the area under the peak is proportional to the amount of analyte injected onto the column. The peak's area is determined by integration, which usually is handled by the instrument's computer or by an electronic integrating recorder. If two peak are fully resolved, the determination of their respective areas is straightforward. Overlapping peaks, however, require a choice

between one of several options for dividing up the area shared by the two peaks (Figure 12.36). Which method to use depends on the relative size of the two peaks and their resolution. In some cases, the use of peak heights provides more accurate results.[8]

Note

Before electronic integrating recorders and computers, two methods were used to find the area under a curve. One method used a manual planimeter; as you use the planimeter to trace an object's perimeter, it records the area. A second approach for finding the area is the cut-and-weigh method. The chromatogram is recorded on a piece of paper. Each peak of interest is cut out and weighed. Assuming the paper is uniform in thickness and density of fibers, the ratio of weights for two peaks is the same as the ratio of areas. Of course, this approach destroys your chromatogram.

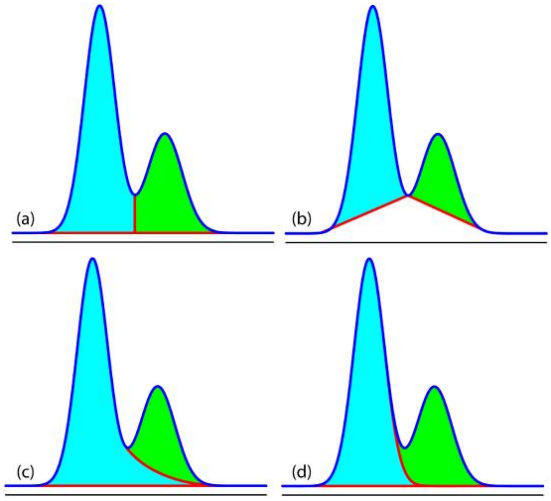


Figure 12.36 Four methods for determining the areas under two overlapping chromatographic peaks: (a) the drop method; (b) the valley method; (c) the exponential skim method; and (d) the Gaussian skim method. Other methods for determining areas also are available.

For quantitative work we need to establish a calibration curve that relates the detector's response to the concentration of analyte. If the injection volume is identical for every standard and sample, then an external standardization provides both accurate and precise results. Unfortunately, even under the best conditions the relative precision for replicate injections may differ by 5%—often it is substantially worse. For quantitative work requiring high accuracy and precision, the use of internal standards is recommended.

Note

To review the method of internal standards, see Section 5.3.4.

Example 12.5

Marriott and Carpenter report the following data for five replicate injections of a mixture consisting of 1% v/v

methylisobutylketone and 1% v/v *p*-xylene in dichloromethane.[9]

injection	peak	peak area (arb. units)
I	1	49075
	2	78112
II	1	85829
	2	135404
III	1	84136
	2	132332
IV	1	71681
	2	112889
V	1	58054
	2	91287

Assume that *p*-xylene (peak 2) is the analyte, and that methylisobutylketone (peak 1) is the internal standard. Determine the 95% confidence interval for a single-point standardization, with and without using the internal standard.

Solution

For a single-point external standardization we ignore the internal standard and determine the relationship between the peak area for *p*-xylene, A_2, and the concentration, C_2, of *p*-xylene.

$$A_2 = kC_2 \tag{12.4.2}$$

Substituting the known concentration for *p*-xylene and the appropriate peak areas, gives the following values for the constant *k*.

78 112 135 404 132 332 112 889 91 287

The average value for *k* is 110 000 with a standard deviation of 25 100 (a relative standard deviation of 22.8%). The 95% confidence interval is

$$\mu = \overline{X} \pm \frac{ts}{\sqrt{n}} = 111000 \pm \frac{(2.78)(25100)}{\sqrt{5}} = 111000 \pm 31200 \tag{12.4.3}$$

For an internal standardization, the relationship between the analyte's peak area, A_2, the peak area for the internal standard, A_1, and their respective concentrations, C_2 and C_1, is

$$\frac{A_2}{A_1} = k\frac{C_2}{C_1} \tag{12.4.4}$$

Substituting the known concentrations and the appropriate peak areas gives the following values for the constant *k*.

1.5917 1.5776 1.5728 1.5749 1.5724

The average value for *k* is 1.5779 with a standard deviation of 0.0080 (a relative standard deviation of 0.507%). The 95% confidence interval is

$$\mu = \overline{X} \pm \frac{ts}{\sqrt{n}} = 1.5779 \pm \frac{(2.78)(0.0080)}{\sqrt{5}} = 1.5779 \pm 0.0099 \tag{12.4.5}$$

Although there is a substantial variation in the individual peak areas for this set of replicate injections, the internal standard compensates for these variations, providing a more accurate and precise calibration.

Practice Exercise 12.5

Figure 12.37 shows chromatograms for five standards and one sample. Each standard and the sample contains the same concentration of an internal standard, which is 2.50 mg/mL. For the five standards, the concentrations of analyte are 0.20 mg/mL, 0.40 mg/mL, 0.60 mg/mL, 0.80 mg/mL, and 1.00 mg/mL, respectively. Determine the concentration of analyte in the sample by (a) ignoring the internal standards and creating an external standards calibration curve, and (b) creating an internal standard calibration curve. For each approach, report the analyte's concentration and the 95% confidence interval. Use peak heights instead of peak areas.

(You may wish to review our earlier coverage of linear regression in Chapter 5.4.)

Click here to review your answer to this exercise.

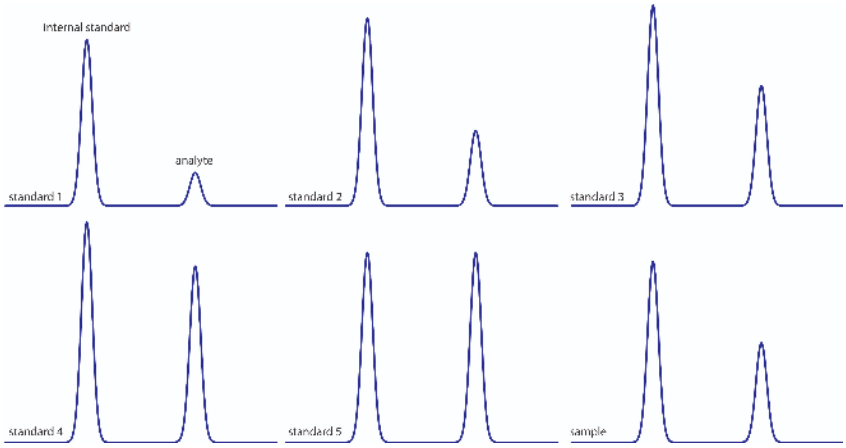


Figure 12.37 Chromatograms for Practice Exercise 12.5.

12.4.7 Qualitative Applications

In addition to a quantitative analysis, we also can use chromatography to identify the components of a mixture. As noted earlier, when using an FT–IR or a mass spectrometer as the detector we have access to the eluent's full spectrum for any retention time. By interpreting the spectrum or by searching against a library of spectra, we can identify the analyte responsible for each chromatographic peak.

Note

In addition to identifying the component responsible for a particular chromatographic peak, we also can use the saved spectra to evaluate peak purity. If only one component is responsible for a chromatographic peak, then the spectra should be identical throughout the peak's elution. If a spectrum at the beginning of the peak's elution is different from a spectrum taken near the end of the peak's elution, then there must be at least two components that are co-eluting.

When using a nonspectroscopic detector, such as a flame ionization detector, we must find another approach if we need to identify the components of a mixture. One approach is to spike the sample the suspected compound and looking for an increase in peak height. We also can compare a peak's retention time to the retention time for a known compound if we use identical operating conditions.

Because a compound's retention times on two identical columns are not likely to be the same—differences in packing efficiency, for example, will affect a solute's retention time on a packed column—a table of standard retention times is not useful. **Kovat's retention index** provides one solution to the problem of matching retention times. Under isothermal conditions, the adjusted retention times for normal alkanes increase logarithmically. Kovat defined the retention index, I, for a normal alkane as 100 times the number of carbon atoms. For example, the retention index is 400 for butane, C_4H_{10}, and 500 for pentane, C_5H_{12}. To determine the a compound's retention index, I_{cpd}, we use the following formula

$$I_{cpd} = 100 \times \frac{\log t'_{r,cpd} - \log t'_{r,x}}{\log t'_{r,x+1} - \log t'_{r,x}} + I_x \tag{12.27}$$

where $t'_{r,cpd}$ is the compound's adjusted retention time, $t'_{x,r}$ and $t'_{x,r+1}$ are the adjusted retention times for the normal alkanes that elute immediately before the compound and after the compound, respectively, and I_x is the retention index for the normal alkane eluting immediately before the compound. A compound's retention index for a particular set of chromatographic conditions—stationary phase, mobile phase, column type, column length, temperature, etc.—should be reasonably consistent from day to day and between different columns and instruments.

Note

Tables of Kovat's retention indices are available; see, for example, the NIST Chemistry Webbook. A search for toluene returns 341 values of *I* for over 20 different stationary phases, and for both packed columns and capillary columns.

Example 12.6

In a separation of a mixture of hydrocarbons the following adjusted retention times were measured: 2.23 min for propane, 5.71 min for isobutane, and 6.67 min for butane. What is the Kovat's retention index for each of these hydrocarbons?

Solution

Kovat's retention index for a normal alkane is 100 times the number of carbons; thus, for propane, I = 300 and for butane, I = 400. To find Kovat's retention index for isobutane we use equation 12.27.

$$I_{cpd} = 100 \times \frac{\log(5.71) - \log(2.23)}{\log(6.67) - \log(2.23)} + 300 = 386 \qquad (12.4.6)$$

Practice Exercise 12.6

When using a column with the same stationary phase as in Example 12.6, you find that the retention times for propane and butane are 4.78 min and 6.86 min, respectively. What is the expected retention time for isobutane?

Click here to review your answer to this exercise.

Note

The best way to appreciate the theoretical and practical details discussed in this section is to carefully examine a typical analytical method. Although each method is unique, the following description of the determination of trihalomethanes in drinking water provides an instructive example of a typical procedure. The description here is based on a Method 6232B in *Standard Methods for the Examination of Water and Wastewater*, 20th Ed., American Public Health Association: Washington, DC, 1998.

Representative Method 12.1

Determination of Trihalomethanes in Drinking Water

Description of Method

Trihalomethanes, such as chloroform, $CHCl_3$, and bromoform, $CHBr_3$, are found in most chlorinated waters. Because chloroform is a suspected carcinogen, the determination of trihalomethanes in public drinking water supplies is of considerable importance. In this method the trihalomethanes $CHCl_3$, $CHBrCl_2$, $CHBr_2Cl$, and $CHBr_3$ are isolated using a liquid–liquid extraction with pentane and determined using a gas chromatograph equipped with an electron capture detector.

Procedure

Collect the sample in a 40-mL glass vial with a screw-cap lined with a TFE-faced septum. Fill the vial to overflowing, ensuring that there are no air bubbles. Add 25 mg of ascorbic acid as a reducing agent to quench the further production of trihalomethanes. Seal the vial and store the sample at 4°C for no longer than 14 days.

(TFE is tetrafluoroethylene. Teflon is a polymer formed from TFE.)

Prepare a standard stock solution for each trihalomethane by placing 9.8 mL of methanol in a 10-mL volumetric flask. Let the flask stand for 10 min, or until all surfaces wetted with methanol are dry. Weigh the flask to the nearest ±0.1 mg. Using a 100-µL syringe, add 2 or more drops of trihalomethane to the volumetric flask, allowing each drop to fall directly into the methanol.

Reweigh the flask before diluting to volume and mixing. Transfer the solution to a 40-mL glass vial with a TFE-lined screw-top and report the concentration in μg/mL. Store the stock solutions at –10 to –20°C and away from the light.

Prepare a multicomponent working standard from the stock standards by making appropriate dilutions of the stock solution with methanol in a volumetric flask. Choose concentrations so that calibration standards (see below) require no more than 20 μL of working standard per 100 mL of water.

Using the multicomponent working standard, prepare at least three, but preferably 5–7 calibration standards. At least one standard must be near the detection limit and the standards must bracket the expected concentration of trihalomethanes in the samples. Using an appropriate volumetric flask, prepare the standards by injecting at least 10 μL of the working standard below the surface of the water and dilute to volume. Mix each standard gently three times only. Discard the solution in the neck of the volumetric flask and then transfer the remaining solution to a 40-mL glass vial with a TFE-lined screw-top. If the standard has a headspace, it must be analyzed within 1 hr; standards without any headspace may be held for up to 24 hr.

Prepare an internal standard by dissolving 1,2-dibromopentane in hexane. Add a sufficient amount of this solution to pentane to give a final concentration of 30 μg 1,2-dibromopentane/L.

To prepare the calibration standards and samples for analysis, open the screw top vial and remove 5 mL of the solution. Recap the vial and weigh to the nearest ±0.1 mg. Add 2.00 mL of pentane (with the internal standard) to each vial and shake vigorously for 1 min. Allow the two phases to separate for 2 min and then use a glass pipet to transfer at least 1 mL of the pentane (the upper phase) to a 1.8-mL screw top sample vial with a TFE septum, and store at 4°C until you are ready to inject them into the GC. After emptying, rinsing, and drying the sample's original vial, weigh it to the nearest ±0.1 mg and calculate the sample's weight to ±0.1 g. If the density is 1.0 g/mL, then the sample's weight is equivalent to its volume.

Inject a 1–5 μL aliquot of the pentane extracts into a GC equipped with a 2-mm ID, 2-m long glass column packed with a stationary phase of 10% squalane on a packing material of 80/100 mesh Chromosorb WAW. Operate the column at 67°C and a flow rate of 25 mL/min.

(A variety of other columns can be used. Another option, for example, is a 30-m fused silica column with an internal diameter of 0.32 mm and a 1 μm coating of the stationary phase DB-1. A linear flow rate of 20 cm/s is used with the following temperature program: hold for 5 min at 35°C; increase to 70°C at 10°C/min; increase to 200°C at 20°C.)

Questions

1. A simple liquid–liquid extraction rarely extracts 100% of the analyte. How does this method account for incomplete extractions?

Because the extraction procedure for the samples and the standards are identical, the ratio of analyte between any two samples or standards is unaffected by an incomplete extraction.

2. Water samples are likely to contain trace amounts of other organic compounds, many of which will extract into pentane along with the trihalomethanes. A short, packed column, such as the one used in this method, generally does not do a particularly good job of resolving chromatographic peaks. Why do we not need to worry about these other compounds?

An electron capture detector responds only to compounds, such as the trihalomethanes, that have electronegative functional groups. Because an electron capture detector will not respond to most of the potential interfering compounds, the chromatogram will have relatively few peaks other than those for the trihalomethanes and the internal standard.

3. Predict the order in which the four analytes elute from the GC column.

Retention time should follow the compound's boiling points, eluting from the lowest boiling point to the highest boiling points. The elution order is $CHCl_3$ (61.2°C), $CHCl_2Br$ (90°C), $CHClBr_2$ (119°C), and $CHBr_3$ (149.1°C).

4. Although chloroform is an analyte, it also is an interferent because it is present at trace levels in the air. Any chloroform present in the laboratory air, for example, may enter the sample by diffusing through the sample vial's silicon septum. How can we determine whether samples have been contaminated in this manner?

A sample blank of trihalomethane-free water can be kept with the samples at all times. If the sample blank shows no evidence for chloroform, then we can safely assume that the samples also are free from contamination.

5. Why is it necessary to collect samples without any headspace (a layer of air overlying the liquid) in the sample vial?

Because trihalomethanes are volatile, the presence of a headspace allows for the possible loss of analyte.

6. In preparing the stock solution for each trihalomethane, the procedure specifies that we can add the two or more drops of the pure compound by dropping them into the volumetric flask containing methanol. When preparing the calibration standards, however, the working standard must be injected below the surface of the water. Explain the reason for this difference.

When preparing a stock solution, the potential loss of the volatile trihalomethane is unimportant because we determine its concentration by weight after adding it to the water. When we prepare the calibration standard, however, we must ensure that the addition of trihalomethane is quantitative.

12.4.8 Evaluation

Scale of Operation

Gas chromatography is used to analyze analytes present at levels ranging from major to ultratrace components. Depending on the detector, samples with major and minor analytes may need to be diluted before analysis. The thermal conductivity and flame ionization detectors can handle larger amounts of analyte; other detectors, such as an electron capture detector or a mass spectrometer, require substantially smaller amounts of analyte. Although the injection volume for gas chromatography is quite small—typically about a microliter—the amount of available sample must be sufficient that the injection is a representative subsample. For a trace analyte, the actual amount of injected analyte is often in the picogram range. Using Representative Method 12.1 as an example, a 3.0-μL injection of 1 μg/L $CHCl_3$ is equivalent to 15 pg of $CHCl_3$, assuming a 100% extraction efficiency.

Note

See Figure 3.5 to review the meaning of major, minor, and ultratrace analytes.

Accuracy

The accuracy of a gas chromatographic method varies substantially from sample to sample. For routine samples, accuracies of 1–5% are common. For analytes present at very low concentration levels, samples with complex matrices, or samples requiring significant processing before analysis, accuracy may be substantially poorer. In the analysis for trihalomethanes described in Representative Method 12.1, for example, determinate errors as large as ±25% are possible.

Precision

The precision of a gas chromatographic analysis includes contributions from sampling, sample preparation, and the instrument. The relative standard deviation due to the instrument is typically 1–5%, although it can be significantly higher. The principle limitations are detector noise, which affects the determination of peak area, and the reproducibility of injection volumes. In quantitative work, the use of an internal standard compensates for any variability in injection volumes.

Sensitivity

In a gas chromatographic analysis, sensitivity is determined by the detector's characteristics. Of particular importance for quantitative work is the detector's linear range; that is, the range of concentrations over which a calibration curve is linear. Detectors with a wide linear range, such as the thermal conductivity detector and the flame ionization detector, can be used to analyze samples over a wide range of concentrations without adjusting operating conditions. Other detectors, such as the electron capture detector, have a much narrower linear range.

Selectivity

Because it combines separation with analysis, chromatographic methods provide excellent selectivity. By adjusting conditions it is usually possible to design a separation so that the analytes elute by themselves, even when the mixture is complex. Additional selectivity is obtained by using a detector, such as the electron capture detector, that does not respond to all compounds.

Time, Cost, and Equipment

Analysis time can vary from several minutes for samples containing only a few constituents, to more than an hour for more complex samples. Preliminary sample preparation may substantially increase the analysis time. Instrumentation for gas

chromatography ranges in price from inexpensive (a few thousand dollars) to expensive (>$50,000). The more expensive models are equipped for capillary columns, include a variety of injection options and more sophisticated detectors, such as a mass spectrometer. Packed columns typically cost <$200, and the cost of a capillary column is typically $300–$1000.

Contributors

David Harvey (DePauw University)

12.4: Gas Chromatography is shared under a CC BY-NC-SA 4.0 license and was authored, remixed, and/or curated by LibreTexts.

12.5: High-Performance Liquid Chromatography

In **high-performance liquid chromatography** (HPLC) we inject the sample, which is in solution form, into a liquid mobile phase. The mobile phase carries the sample through a packed or capillary column that separates the sample's components based on their ability to partition between the mobile phase and the stationary phase. Figure 12.38 shows an example of a typical HPLC instrument, which consists of several key components: reservoirs containing the mobile phase; a pump for pushing the mobile phase through the system; an injector for introducing the sample; a column; and a detector for monitoring the eluent as it comes off the column. Let's consider each of these components.

> **Note**
>
> A solute's retention time in HPLC is determined by its interaction with the stationary phase and the mobile phase. There are a several different types of solute/stationary phase interactions, including liquid–solid adsorption, liquid–liquid partitioning, ion-exchange, and size-exclusion (see Figure 12.4). Section 12.5 deals exclusively with HPLC separations based on liquid–liquid partitioning. Other forms of liquid chromatography receive consideration in Section 12.6.

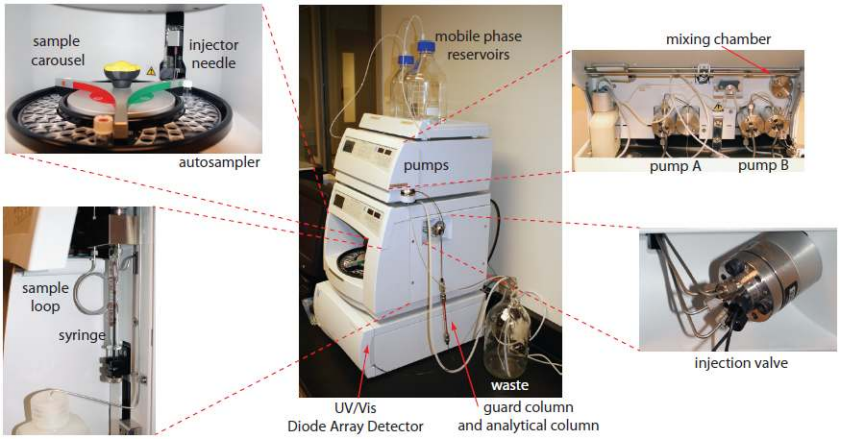


Figure 12.38 Example of a typical high-performance liquid chromatograph with insets showing the pumps that move the mobile phase through the system, and the plumbing used to inject the sample into the mobile phase. This particular instrument includes an autosampler. An instrument in which samples are injected manually does not include the features shown in the two left-most insets, and has a different style of loop injector (see Figure 12.45).

12.5.1 HPLC Columns

An HPLC typically includes two columns: an analytical column responsible for the separation and a guard column. The guard column is placed before the analytical column, protecting it from contamination.

Analytical Columns

The most common type of HPLC column is a stainless steel tube with an internal diameter between 2.1 mm and 4.6 mm and a length between 30 mm and 300 mm (Figure 12.39). The column is packed with 3–10 μm porous silica particles with either an irregular or a spherical shape. Typical column efficiencies are 40 000–60 000 theoretical plates/m. Assuming a V_{max}/V_{min} of approximately 50, a 25-cm column with 50 000 plates/m has 12 500 theoretical plates and a peak capacity of 110.

> **Note**
>
> You can use equation 12.16 to estimate a column's peak capacity.



Figure 12.39 Typical packed column for HPLC. This particular column has an internal diameter of 4.6 mm and a length of 150 mm, and is packed with 5 μm particles coated with stationary phase.

Capillary columns use less solvent and, because the sample is diluted to a lesser extent, produce larger signals at the detector. These columns are made from fused silica capillaries with internal diameters from 44–200 μm and lengths of 50–250 mm. Capillary columns packed with 3–5 μm particles have been prepared with column efficiencies of up to 250 000 theoretical plates.[10]

One limitation to a packed capillary column is the back pressure that develops when trying to move the mobile phase through the small interstitial spaces between the particulate micron-sized packing material (Figure 12.40). Because the tubing and fittings that carry the mobile phase have pressure limits, a higher back pressure requires a lower flow rate and a longer analysis time. **Monolithic columns**, in which the solid support is a single, porous rod, offer column efficiencies equivalent to a packed capillary column while allowing for faster flow rates. A monolithic column—which usually is similar in size to a conventional packed column, although smaller, capillary columns also are available—is prepared by forming the monolithic rod in a mold and covering it with PTFE tubing or a polymer resin. Monolithic rods made of a silica-gel polymer typically have macropores with diameters of approximately 2 μm and mesopores—pores within the macropores—with diameters of approximately 13 nm.[11]

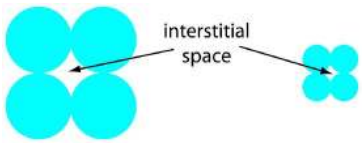


Figure 12.40 The packing of smaller particles creates smaller interstitial spaces than the packing of larger particles. Although reducing particle size by 2× increases efficiency by a factor of 1.4, it also produces a 4-fold increase in back pressure.

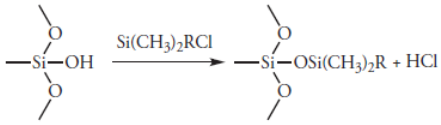
Guard Columns

Two problems tend to shorten the lifetime of an analytical column. First, solutes binding irreversibly to the stationary phase degrade the column's performance by decreasing the available stationary phase. Second, particulate material injected with the sample may clog the analytical column. To minimize these problems we place a guard column before the analytical column. **Guard columns** usually contain the same particulate packing material and stationary phase as the analytical column, but are significantly shorter and less expensive—a length of 7.5 mm and a cost one-tenth of that for the corresponding analytical column is typical. Because they are intended to be sacrificial, guard columns are replaced regularly.

> **Note**
>
> If you look closely at Figure 12.39, you will see the small guard column just above the analytical column.

Stationary Phases for Gas–Liquid Chromatography

In liquid–liquid chromatography the stationary phase is a liquid film coated on a packing material, typically 3–10 μm porous silica particles. Because the stationary phase may be partially soluble in the mobile phase, it may elute, or bleed from the column over time. To prevent the loss of stationary phase, which shortens the column's lifetime, it is covalently bound to the silica particles. **Bonded stationary phases** are created by reacting the silica particles with an organochlorosilane of the general form $Si(CH_3)_2RCl$, where R is an alkyl, or substituted alkyl group.



To prevent unwanted interactions between the solutes and any remaining –SiOH groups, $Si(CH_3)_3Cl$ is added, converting the unreacted sites to $–SiOSi(CH_3)_3$; such columns are designated as end-capped.

The properties of a stationary phase depend on the organosilane's alkyl group. If R is a polar functional group, then the stationary phase is polar. Examples of polar stationary phases include those where R contains a cyano ($–C_2H_4CN$), a diol ($–C_3H_6OCH_2CHOHCH_2OH$), or an amino ($–C_3H_6NH_2$) functional group. Because the stationary phase is polar, the mobile phase is a nonpolar or moderately polar solvent. The combination of a polar stationary phase and a nonpolar mobile phase is called **normal-phase chromatography**.

In **reversed-phase chromatography**, which is the more common form of HPLC, the stationary phase is nonpolar and the mobile phase is polar. The most common nonpolar stationary phases use an organochlorosilane where the R group is an *n*-octyl (C_8) or *n*-octyldecyl (C_{18}) hydrocarbon chain. Most reversed-phase separations are carried out using a buffered aqueous solution as a polar mobile phase, or with other polar solvents, such as methanol and acetonitrile. Because the silica substrate may undergo hydrolysis in basic solutions, the pH of the mobile phase must be less than 7.5.

> **Note**
>
> It might strike you as odd that the less common form of liquid chromatography is identified as normal-phase. You might recall that one of the earliest examples of chromatography was Mikhail Tswett's separation of plant pigments using a polar column of calcium carbonate and a nonpolar mobile phase of petroleum ether. The assignment of normal and reversed, therefore, is all about precedence.

12.5.2 Mobile Phases

The elution order of solutes in HPLC is governed by polarity. For a normal-phase separation, solutes of lower polarity spend proportionally less time in the polar stationary phase and are the first solutes to elute from the column. Given a particular stationary phase, retention times in normal-phase HPLC are controlled by adjusting the mobile phase's properties. For example, if the resolution between two solutes is poor, switching to a less polar mobile phase keeps the solutes on the column for a longer time and provides more opportunity for their separation. In reversed-phase HPLC the order of elution is the opposite of that in a normal-phase separation, with more polar solutes eluting first. Increasing the polarity of the mobile phase leads to longer retention times. Shorter retention times require a mobile phase of lower polarity.

Choosing a Mobile Phase–Using the Polarity Index

There are several indices that help in choosing a mobile phase, one of which is the **polarity index**.[12] Table 12.4 provides values of the polarity index, P', for several common mobile phases, where larger values of P' correspond to more polar solvents. Mixing together two or more mobile phases.assuming they are miscible.creates a mobile phase of intermediate polarity. For example, a binary mobile phase made by combining solvents A and B has a polarity index, P'_{AB}, of

$$P'_{AB} = \Phi_A P'_A + \Phi_B P'_B \tag{12.28}$$

where P'_A and P'_B are the polarity indices for solvents A and B, and Φ_A and Φ_B are the volume fractions for the two solvents.

> **Example 12.7**
>
> A reversed-phase HPLC separation is carried out using a mobile phase of 60% v/v water and 40% v/v methanol. What is the mobile phase's polarity index?
>
> ***Solution***
>
> Using equation 12.28 and the values in Table 12.4, the polarity index for a 60:40 water–methanol mixture is
>
> $$P'_{AB} = \Phi_{H_2O} P'_{H_2O} + \Phi_{CH_3OH} P'_{CH_3OH} \tag{12.5.1}$$
>
> $$P'_{AB} = 0.60 \times 10.2 + 0.40 \times 5.1 = 8.2 \tag{12.5.2}$$

Table 12.4 Properties of HPLC Mobile Phases

mobile phase	polarity index (***P′***)	UV cutoff (nm)
cyclohexane	0.04	210
n-hexane	0.1	210
carbon tetrachloride	1.6	265
i-propyl ether	2.4	220
toluene	2.4	286
diethyl ether	2.8	218
tetrahydrofuran	4.0	220
ethanol	4.3	210
ethyl acetate	4.4	255
dioxane	4.8	215
methanol	5.1	210
acetonitrile	5.8	190
water	10.2	—

Practice Exercise 12.7

Suppose you need a mobile phase with a polarity index of 7.5. Explain how you can prepare this mobile phase using methanol and water?

Click here to review your answer to this exercise.

As a general rule, a two unit change in the polarity index corresponds to approximately a 10-fold change in a solute's retention factor. Here is a simple example. If a solute's retention factor, k, is 22 when using water as a mobile phase (P' = 10.2), then switching to a mobile phase of 60:40 water–methanol (P' = 8.2) decreases k to approximately 2.2. Note that the retention factor becomes smaller because we are switching from a more polar mobile phase to a less polar mobile phase in a reversed-phase separation.

Choosing a Mobile Phase–Adjusting Selectivity

Changing the mobile phase's polarity index changes a solute's retention factor. As we learned in Section 12C.1, however, a change in k is not an effective method for improving resolution when its initial value is greater than 10. To effect a better separation between two solutes we must improve the selectivity factor, α. There are two commonly used approaches for increasing α: add a reagent to the mobile phase that reacts with the solutes in a secondary equilibrium reaction, or try a different mobile phase.

Taking advantage of a secondary equilibrium reaction is a useful strategy for improving a separation.[13] Figure 12.17, which we considered earlier in this chapter, shows the reversed-phase separation of four weak acids—benzoic acid, terephthalic acid, *p*-aminobenzoic acid, and *p*-hydroxybenzoic acid—on a nonpolar C_{18} column using a aqueous mobile phase that includes a buffer of acetic acid and sodium acetate. Retention times are shorter for less acidic mobile phases because each solute is present in an anionic, weak base form that is less soluble in the nonpolar stationary phase. If the mobile phase's pH is sufficiently acidic, the solutes are present as neutral weak acids that partition into the stationary phase and take longer to elute. Because these solutes do not have identical pK_a values, the pH of the mobile phase affects each solute's retention time differently, allowing us to find the optimum pH for effecting a complete separation of the four solutes.

Note

Acid–base chemistry is not the only example of a secondary equilibrium reaction. Other examples include ion-pairing, complexation, and the interaction of solutes with micelles. We will consider the last of these in Section 12.7.3 when we discuss

micellar electrokinetic capillary chromatography.

In Example 12.7 we learned how to adjust the mobile phase's polarity by blending together two solvents. A polarity index, however, is just a guide, and binary mobile phase mixtures with identical polarity indices may not equally resolve a pair of solutes. Table 12.5, for example, shows retention times for four weak acids in two mobile phases with nearly identical values for P'. Although the order of elution is the same for both mobile phases, each solute's retention time is affected differently by the choice of organic solvent. If we switch from using acetonitrile to tetrahydrofuran, for example, benzoic acid elutes more quickly and *p*-hydroxybenzoic acid elutes more slowly. Although we can resolve these two solutes using a mobile phase that is 16% v/v acetonitrile, we cannot resolve them if the mobile phase is 10% tetrahydrofuran.

Table 12.5 Retention Times for Four Weak Acids in Mobile Phases With Similar Polarity Indexes

retention time (min)	16% acetonitrile (CH_3CN) 84% pH 4.11 aqueous buffer ($\boldsymbol{P'}$ = 9.5)	10% tetrahydrofuran (THF) 90% pH 4.11 aqueous buffer ($\boldsymbol{P'}$ = 9.6)
$t_{r,BA}$	5.18	4.01
$t_{r,PH}$	1.67	2.91
$t_{r,PA}$	1.21	1.05
$t_{r,TP}$	0.23	0.54

Key: BA is benzoic acid; PH is *p*-hydroxybenzoic acid; PA is *p*-aminobenzoic acid; TP is terephthalic acid
Source: Harvey, D. T.; Byerly, S.; Bowman, A.; Tomlin, J. "Optimization of HPLC and GC Separations Using Response Surfaces," *J. Chem. Educ.* **1991**, *68*, 162–168.

One strategy for finding the best mobile phase is to use the solvent triangle shown in Figure 12.41, which allows us to explore a broad range of mobile phases with only seven experiments. We begin by adjusting the amount of acetonitrile in the mobile phase, producing the best possible separation within the desired analysis time. Next, we use Table 12.6 to estimate the composition of methanol/H_2O and tetrahydrofuran/H_2O mobile phases that will produce similar analysis times. Four additional mobile phases are prepared using the binary and ternary mobile phases shown in Figure 12.41. By evaluating the chromatograms from these seven mobile phases, we may find that one or more provides an adequate separation, or identify a region within the solvent triangle where a separation if feasible. Figure 12.42 shows results for the reversed-phase separation of benzoic acid, terephthalic acid, *p*-aminobenzoic acid, and *p*-hydroxybenzoic acid on a nonpolar C_{18} column in which the maximum analysis time is set to 6 min.[14] The areas in blue, green, and red show mobile phase compositions that do not provide baseline resolution. The unshaded area represents mobile phase compositions where a separation is possible.

Note

The choice to start with acetonitrile is arbitrary—we can just as easily choose to begin with methanol or with tetrahydrofuran.

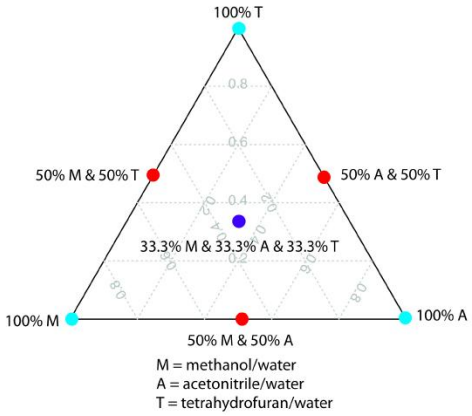


Figure 12.41 Solvent triangle for optimizing a reversed-phase HPLC separation. The three blue circles show mobile phases consisting of an organic solvent and water. The three red circles are binary mobile phases created by combining equal volumes of the pure mobile phases. The ternary mobile phase shown by the purple circle contains all three of the pure mobile phases.

Table 12.6 Compositions of Mobile Phases with Approximately Equal Solvent Strengths

%v/v CH_3OH	%v/v CH_3CN	%v/v THF
0	0	0
10	6	4
20	14	10
30	22	16
40	32	24
50	40	30
60	50	36
70	60	44
80	72	52
90	87	62
100	99	71

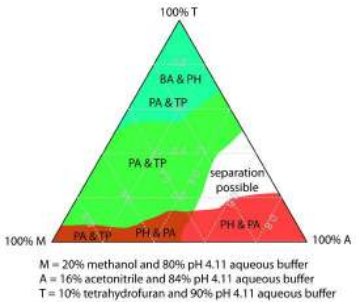


Figure 12.42 Resolution map for the separation of benzoic acid (BA), terephthalic acid (TP), *p*-aminobenzoic acid (PA), and *p*-hydroxybenzoic acid (PH) on a nonpolar C_{18} column subject to a maximum analysis time of 6 min. The shaded areas represent regions where a separation is not possible, with the unresolved solutes identified. A separation is possible in the unshaded area. See Chapter 14 for a discussion of how we can develop a mathematical model for optimizing separations.

Choosing a Mobile Phase–Isocratic and Gradient Elutions

A separation using a mobile phase that has a fixed composition is an **isocratic elution**. One difficulty with an isocratic elution is that an appropriate mobile phase strength for early eluting solutes may lead to unacceptably long retention times for later eluting solutes. Optimizing the mobile phase for late eluting solutes, on the other hand, may provide an inadequate separation of early eluting solutes. Changing the mobile phase's composition as the separation progresses is one solution to this problem. For a reversed-phase separation we use an initial mobile phase that is more polar. As the separation progresses, we adjust the composition of mobile phase so that it becomes less polar (see Figure 12.43). Such separations are called **gradient elutions**.

> **Note**
>
> You may recall that we called this the general elution problem (see Figure 12.16).

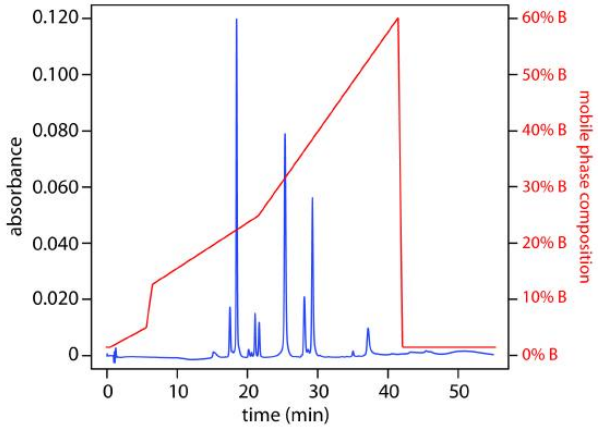


Figure 12.43 Gradient elution separation of a mixture of flavonoids. Mobile phase A is an aqueous solution of 0.1% formic acid and mobile phase B is 0.1% formic acid in acetonitrile. The initial mobile phase is 98% A and 2% B. The percentage of mobile phase B increases in four steps: from 2% to 5% over 5 min, beginning at 0.5 min; from 5% to 12% over 1 min, beginning at 5.5 min; from 12% to 25% over 15 min, beginning at 6.5 min; and from 25% to 60% over 20 min, beginning at 21.5 min. Data provided by Chistopher Schardon, Kyle Meinhardt, and Michelle Bushey, Department of Chemistry, Trinty University.

12.5.3 HPLC Plumbing

In a gas chromatograph the pressure of the compressed gas cylinder containing the mobile phase is sufficient to push it through the column. Pushing a liquid mobile phase through a column takes a great deal more effort, generating pressures in excess of several hundred atmospheres. In this section we consider the basic plumbing needed to move the mobile phase through the column and to inject the sample into the mobile phase.

Moving the Mobile Phase

A typical HPLC includes between 1–4 reservoirs for storing mobile phase solvents. The instrument in Figure 12.38, for example, has two mobile phase reservoirs that can be used for an isocratic or a gradient elution by drawing solvents from one or both reservoirs.

Before using a mobile phase solvent we must remove dissolved gases, such as N_2 and O_2, and small particulate matter, such as dust. Because there is a large drop in pressure across the column—the pressure at the column's entrance may be several hundred atmospheres, but it is atmospheric pressure at its exit—any dissolved gases in the mobile phase are released as gas bubbles that may interfere with the detector's response. Degassing is accomplished in several ways, but the most common are the use of a vacuum pump or sparging with an inert gas, such as He, which has a low solubility in the mobile phase. Particulate material, which may clog the HPLC tubing or column, is removed by filtering the solvents.

> **Note**
>
> Bubbling an inert gas through the mobile phase releases volatile dissolved gases. This process is called sparging.

The mobile phase solvents are pulled from their reservoirs by the action of one or more pumps. Figure 12.44 shows a close-up view of the pumps for the instrument in Figure 12.38. The working pump and equilibrating pump each have a piston whose back and forth movement is capable both of maintaining a constant flow rate of up to several mL/min and of obtaining the high output pressure needed to push the mobile phase through the chromatographic column. In this particular instrument, each pump sends its mobile phase to a mixing chamber where they combine to form the final mobile phase. The relative speed of the two pumps determines the mobile phase's final composition.

> **Note**
>
> There are other possible ways to control the mobile phase's composition and flow rate. For example, instead of the two pumps in Figure 12.45, we can place a solvent proportioning valve before a single pump. The solvent proportioning value connects two or more solvent reservoirs to the pump and determines how much of each solvent is pulled during each of the pump's cycles.
>
> Another approach for eliminating a pulsed flow is to include a pulse damper between the pump and the column. A pulse damper is a chamber filled with an easily compressed fluid and a flexible diaphragm. During the piston's forward stroke the fluid in the pulse damper is compressed. When the piston withdraws to refill the pump, pressure from the expanding fluid in the pulse damper maintains the flow rate.

The back and forth movement of a reciprocating pump creates a pulsed flow that contributes noise to the chromatogram. To minimize these pulses, each pump in Figure 12.44 has two cylinders. During the working cylinder's forward stoke it fills the equilibrating cylinder and establishes flow through the column. When the working cylinder is on its reverse stroke, the flow is maintained by the piston in the equilibrating cylinder. The result is a pulse-free flow.

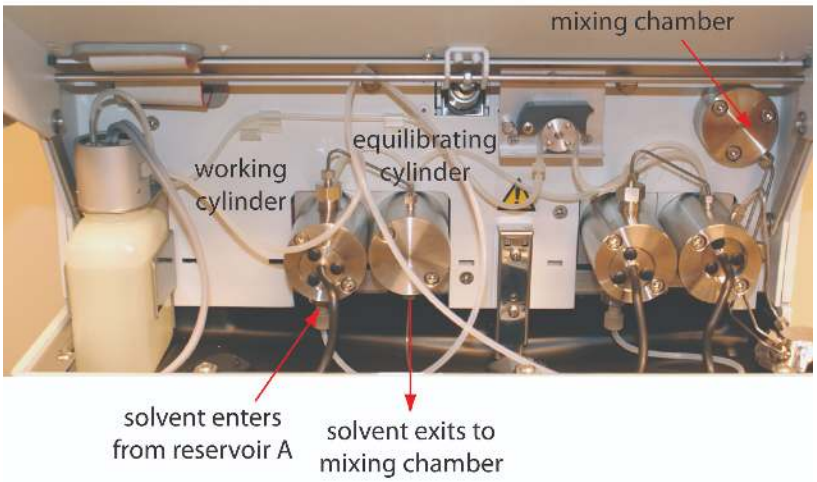


Figure 12.44 Close-up view of the pumps for the instrument shown in Figure 12.38. The working cylinder and equilibrating cylinder for the pump on the left take solvent from reservoir A and send it to the mixing chamber. The pump on the right moves solvent from reservoir B to the mixing chamber. The mobile phase's flow rate is determined by the combined speeds of the two pumps. By changing the relative speeds of the two pumps, different binary mobile phases can be prepared.

Injecting the Sample

The operating pressure within an HPLC is sufficiently high that we cannot inject the sample into the mobile phase by inserting a syringe through a septum. Instead, we inject the sample using a **loop injector**, a diagram of which is shown in Figure 12.45.

In the load position a sample loop—which is available in a variety of sizes ranging from 0.5 μL to 5 mL—is isolated from the mobile phase and open to the atmosphere. The sample loop is filled using a syringe with a capacity several times that of the sample loop, with the excess sample exiting through the waste line. After loading the sample, the injector is turned to the inject position, directing the mobile phase through the sample loop and onto the column.

> **Note**
>
> The instrument in Figure 12.39 uses an autosampler to inject samples. Instead of using a syringe to push the sample into the

sample loop, the syringe draws sample into the sample loop.

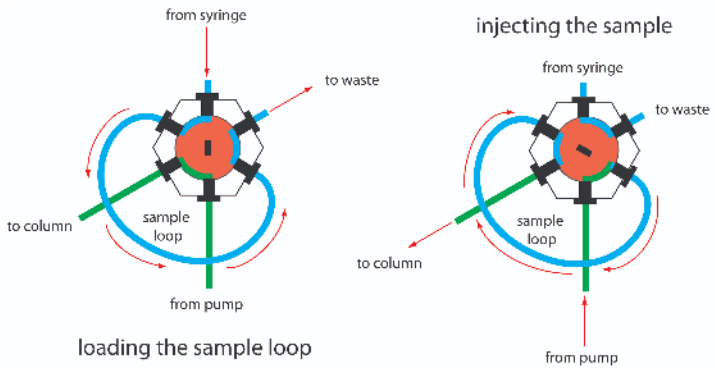


Figure 12.45 Schematic diagram showing a manual loop injector. In the load position the flow of mobile phase from the pump to the column (shown in green) is isolated from the sample loop, which is filled using a syringe (shown in blue). Rotating the inner valve (shown in red) to the inject position directs the mobile phase through the sample loop and onto the column.

12.5.4 Detectors for HPLC

Many different types of detectors have been use to monitor HPLC separations, most of which use the spectroscopic techniques from Chapter 10 or the electrochemical techniques from Chapter 11.

Spectroscopic Detectors

The most popular HPLC detectors take advantage of an analyte's UV/Vis absorption spectrum. These detectors range from simple designs, in which the analytical wavelength is selected using appropriate filters, to a modified spectrophotometer in which the sample compartment includes a flow cell. Figure 12.46 shows the design of a typical flow cell for a detector using a diode array spectrometer. The flow cell has a volume of 1–10 μL and a path length of 0.2–1 cm.

> **Note**
>
> To review the details of how we measure absorbance, see Chapter 10.2. More information about different types of instruments, including the diode array spectrometer, is in Chapter 10.3.

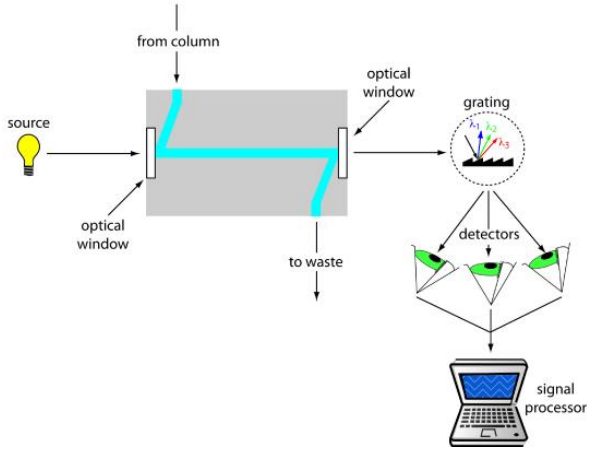


Figure 12.46 Schematic diagram showing a flow cell for a detector using a diode array spectrometer.

When using a UV/Vis detector the resulting chromatogram is a plot of absorbance as a function of elution time (see Figure 12.47). If the detector is a diode array spectrometer, then we also can display the result as a three-dimensional chromatogram showing absorbance as a function of wavelength and elution time. One limitation to using absorbance is that the mobile phase cannot absorb at the wavelengths we wish to monitor. Table 12.4 lists the minimum useful UV wavelength for several common HPLC solvents. Absorbance detectors provide detection limits of as little as 100 pg–1 ng of injected analyte.

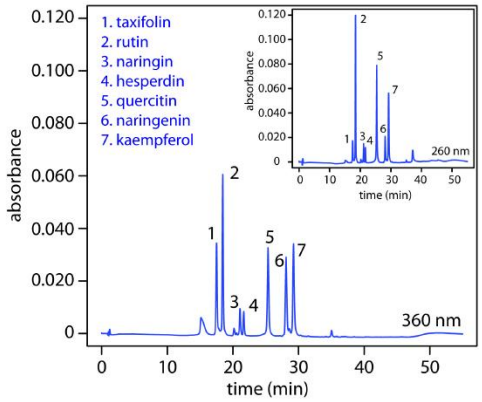


Figure 12.47 HPLC separation of a mixture of flavonoids with UV/Vis detection at 360 nm and 260 nm. The choice of wavelength affects each analyte's signal. By carefully choosing the wavelength, we can enhance the signal for the analytes of greatest interest. Data provided by Chistopher Schardon, Kyle Meinhardt, and Michelle Bushey, Department of Chemistry, Trinty University.

If an analyte is fluorescent, we can place the flow cell in a spectrofluorimeter. As shown in Figure 12.48, a fluorescence detector provides additional selectivity because only a few of a sample's components are fluorescent. Detection limits are as little as 1–10 pg of injected analyte.

> **Note**
>
> See Chapter 10.6 for a review of fluorescence spectroscopy and spectrofluorimeters.

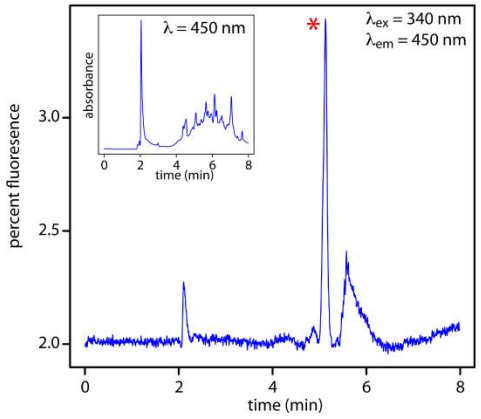


Figure 12.48 HPLC chromatogram for the determination of riboflavin in urine using fluorescence detection with excitation at a wavelength of 340 nm and detection at 450 nm. The peak corresponding to riboflavin is marked with a red asterisk (*). The inset shows the same chromatogram when using a less-selective UV/Vis detector at a wavelength of 450 nm. Data provided by Jason Schultz, Jonna Berry, Kaelene Lundstrom, and Dwight Stoll, Department of Chemistry, Gustavus Adolphus College.

Electrochemical Detectors

Another common group of HPLC detectors are those based on electrochemical measurements such as amperometry, voltammetry, coulometry, and conductivity. Figure 12.49, for example, shows an amperometric flow cell. Effluent from the column passes over the working electrode, which is held at a constant potential—relative to a downstream reference electrode—that completely oxidizes or reduces the analytes. The current flowing between the working electrode and the auxiliary electrode serves as the analytical signal. Detection limits for amperometric electrochemical detection are from 10 pg–1 ng of injected analyte.

> **Note**
>
> See Chapter 11.4.5 for a review of amperometry.

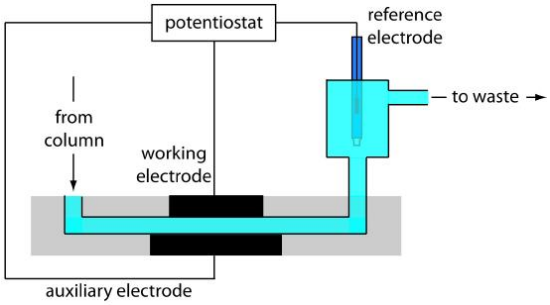


Figure 12.49 Schematic diagram showing a flow cell for an amperometric electrochemical detector.

Other Detectors

Several other detectors have been used in HPLC. Measuring a change in the mobile phase's refractive index is analogous to monitoring the mobile phase's thermal conductivity in gas chromatography. A refractive index detector is nearly universal, responding to almost all compounds, but has a relatively poor detection limit of 100 ng–1 µg of injected analyte. An additional limitation of a refractive index detector is that it cannot be used for gradient elution unless the mobile phase components have identical refractive indexes.

Another useful detector is a mass spectrometer. Figure 12.50 shows a block diagram of a typical HPLC–MS instrument. The effluent from the column enters the mass spectrometer's ion source using an interface the removes most of the mobile phase, an essential need because of the incompatibility between the liquid mobile phase and the mass spectrometer's high vacuum environment. In the ionization chamber the remaining molecules—a mixture of carrier gas, solvent, and solutes—undergo ionization and fragmentation. The mass spectrometer's mass analyzer separates the ions by their mass-to-charge ratio (m/z). A detector counts the ions and displays the mass spectrum.

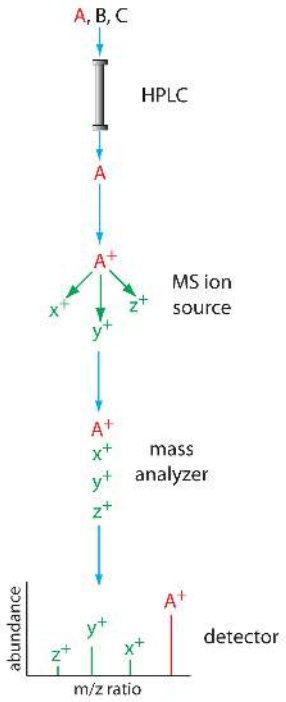


Figure 12.50 Block diagram of an HPLC–MS. A three component mixture enters the HPLC. When component A elutes from the column, it enters the MS ion source and ionizes to form the parent ion (A+) and several fragment ions. The ions enter the mass analyzer, which separates them by their mass-to-charge ratio, providing the mass spectrum shown at the detector.

There are several options for monitoring the chromatogram when using a mass spectrometer as the detector. The most common method is to continuously scan the entire mass spectrum and report the total signal for all ions reaching the detector during each

scan. This total ion scan provides universal detection for all analytes. As seen in Figure 12.51, we can achieve some degree of selectivity by monitoring only specific mass-to-charge ratios, a process called selective-ion monitoring).

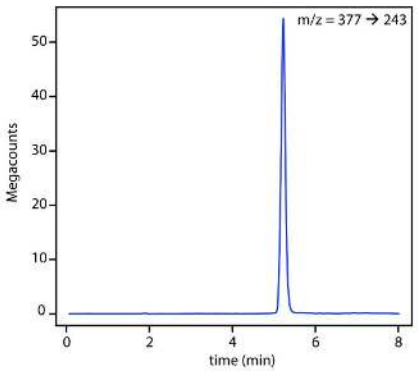


Figure 12.51 HPLC–MS/MS chromatogram for the determination of riboflavin in urine. An initial parent ion with an m/z ratio of 377 enters a second mass spectrometer where it undergoes additional ionization; the fragment ion with an m/z ratio of 243 provides the signal. The selectivity of this detector is evident when you compare this chromatogram to the one in Figure 12.48, which uses fluoresence deterction. Data provided by Jason Schultz, Jonna Berry, Kaelene Lundstrom, and Dwight Stoll, Department of Chemistry, Gustavus Adolphus College.

The advantages of using a mass spectrometer in HPLC are the same as for gas chromatography. Detection limits are very good, typically 100 pg–1 ng of injected analyte, with values as low as 1–10 pg for some samples. In addition, a mass spectrometer provides qualitative, structural information that can help in identifying the analytes. The interface between the HPLC and mass spectrometer is technically more difficult than that in a GC–MS because of the incompatibility of a liquid mobile phase with the mass spectrometer's high vacuum requirement.

12.5.5 Quantitative Applications

High-performance liquid chromatography is routinely used for both qualitative and quantitative analyses of environmental, pharmaceutical, industrial, forensic, clinical, and consumer product samples.

Preparing Samples for Analysis

Samples in liquid form are injected into the HPLC after a suitable clean-up to remove any particulate materials, or after a suitable extraction to remove matrix interferents. In determining polyaromatic hydrocarbons (PAH) in wastewater, for example, an extraction with CH_2Cl_2 serves the dual purpose of concentrating the analytes and isolating them from matrix interferents. Solid samples are first dissolved in a suitable solvent, or the analytes of interest brought into solution by extraction. For example, an HPLC analysis for the active ingredients and degradation products in a pharmaceutical tablet often begins by extracting the powdered tablet with a portion of mobile phase. Gas samples are collected by bubbling them through a trap containing a suitable solvent. Organic isocyanates in industrial atmospheres are collected by bubbling the air through a solution of 1-(2-methoxyphenyl)piperazine in toluene. The reaction between the isocyanates and 1-(2-methoxyphenyl)piperazine both stabilizes them against degradation before the HPLC analysis and converts them to a chemical form that can be monitored by UV absorption.

Quantitative Calculations

A quantitative HPLC analysis is often easier than a quantitative GC analysis because a fixed volume sample loop provides a more precise and accurate injection. As a result, most quantitative HPLC methods do not need an internal standard and, instead, use external standards and a normal calibration curve.

> **Note**
>
> An internal standard is necessary when using HPLC–MS because the interface between the HPLC and the mass spectrometer does not allow for a reproducible transfer of the column's eluent into the MS's ionization chamber.

Example 12.8

The concentration of polynuclear aromatic hydrocarbons (PAH) in soil are determined by first extracting the PAHs with methylene chloride. The extract is diluted, if necessary, and the PAHs separated by HPLC using a UV/Vis or fluorescence detector. Calibration is achieved using one or more external standards. In a typical analysis a 2.013-g sample of dried soil is extracted with 20.00 mL of methylene chloride. After filtering to remove the soil, a 1.00-mL portion of the extract is removed and diluted to 10.00 mL with acetonitrile. Injecting 5 µL of the diluted extract into an HPLC gives a signal of 0.217 (arbitrary units) for the PAH fluoranthene. When 5 µL of a 20.0-ppm fluoranthene standard is analyzed using the same conditions, a signal of 0.258 is measured. Report the parts per million of fluoranthene in the soil.

Solution

For a single-point external standard, the relationship between the signal, *S*, and the concentration, *C*, of fluoranthene is

$$S = kC \tag{12.5.3}$$

Substituting in values for the standard's signal and concentration gives the value of *k* as

$$k = \frac{S}{C} = \frac{0.258}{20.0\ \text{ppm}} = 0.0129\ \text{ppm}^{-1} \tag{12.5.4}$$

Using this value for *k* and the sample's HPLC signal gives a fluoranthene concentration of

$$C = \frac{S}{k} = \frac{0.217}{0.0129\ \text{ppm}^{-1}} = 16.8\ \text{ppm} \tag{12.5.5}$$

for the extracted and diluted soil sample. The concentration of fluoranthene in the soil is

$$\frac{16.8\ \text{g/mL} \times \frac{10.00\ \text{mL}}{1.00\ \text{mL}} \times 20.00\ \text{mL}}{2.013\ \text{g sample}} = 1670\ \text{ppm fluoranthene} \tag{12.5.6}$$

Practice Exercise 12.8

The concentration of caffeine in beverages can be determined by a reversed-phase HPLC separation using a mobile phase of 20% acetonitrile and 80% water and a nonpolar C_8 column. Results for a series of 10-µL injections of caffeine standards are in the following table.

[caffeine] (mg/L)	peak area (arb. units)
50.0	226 724
100.0	453 762
125.0	559 443
250.0	1 093 637

What is the concentration of caffeine in a sample if a 10-µL injection gives a peak area of 424 195?

(The data in this problem comes from Kusch, P.; Knupp, G. "Simultaneous Determination of Caffeine in Cola Drinks and Other Beverages by Reversed-Phase HPTLC and Reversed-Phase HPLC," *Chem. Educator*, **2003**, *8*, 201–205.)

Click here to review your answer to this exercise.

Note

The best way to appreciate the theoretical and practical details discussed in this section is to carefully examine a typical analytical method. Although each method is unique, the following description of the determination of fluoxetine in serum provides an instructive example of a typical procedure. The description here is based on Smyth, W. F. *Analytical Chemistry of Complex Matricies*, Wiley Teubner: Chichester, England, 1996, pp. 187–189.

Representative Method 12.2

Determination of Fluoxetine in Serum

Description of Method

Fluoxetine is another name for the antidepressant drug Prozac. The determination of fluoxetine in serum is an important part of monitoring its therapeutic use. The analysis is complicated by the complex matrix of serum samples. A solid-phase extraction followed by an HPLC analysis using a fluorescence detector provides the necessary selectivity and detection limits.

Procedure

Add a known amount of the antidepressant protriptyline, which serves as an internal standard, to each serum sample and to each external standard. To remove matrix interferents, pass a 0.5-mL aliquot of each serum sample or standard through a C18 solid-phase extraction cartridge. After washing the cartridge to remove the interferents, elute the remaining constituents, including the analyte and the internal standard, by washing the cartridge with 0.25 mL of a 25:75 v/v mixture of 0.1 M $HClO_4$ and acetonitrile. Inject a 20-µL aliquot onto a 15-cm × 4.6-mm column packed with a 5 µm C8-bonded stationary phase. The isocratic mobile phase is 37.5:62.5 v/v acetonitrile and water (containing 1.5 g of tetramethylammonium perchlorate and 0.1 mL of 70% v/v $HClO_4$). Monitor the chromatogram using a fluorescence detector set to an excitation wavelength of 235 nm and an emission wavelength of 310 nm.

(For a review of solid-phase extraction (SPE), see Section 7.6.5. Table 7.8 describes the properties of several different types of SPE cartridges. Figure 7.22 shows a photo of SPE cartridges, and Figure 7.23 illustrates the steps in completing a solid-phase extraction.)

Questions

1. The solid-phase extraction is important because it removes constitutions in the serum that might interfere with the analysis. What types of interferences are possible?

Blood serum, which is a complex mixture of compounds, is approximately 92% water, 6–8% soluble proteins, and less than 1% each of various salts, lipids, and glucose. A direct injection of serum is not advisable for three reasons. First, any particulate materials in the serum will clog the column and restrict the flow of mobile phase. Second, some of the compounds in the serum may absorb too strongly to the stationary phase, degrading the column's performance. Finally, although an HPLC is capable of separating and analyzing complex mixtures, an analysis may still be difficult if the number of constituents exceeds the column's peak capacity.

2. One advantage of an HPLC analysis is that a loop injector often eliminates the need for an internal standard. Why is an internal standard used in this analysis? What assumption(s) must we make when using the internal standard?

An internal standard is necessary because of uncertainties introduced during the solid-phase extraction. For example, the volume of serum transferred to the solid-phase extraction cartridge, 0.5 mL, and the volume of solvent used to remove the analyte and internal standard, 0.25 mL, are very small. The precision and accuracy with which we can measure these volumes is not as good as when using larger volumes. In addition, the concentration of eluted analytes may vary from trial to trial due to variations in the amount of solution held up by the cartridge. Using an internal standard compensates for these variation. To be useful we must assume that the analyte and the internal standard are completely retained during the initial loading, that they are not lost when the cartridge is washed, and that they are completely extracted during the final elution.

(Note: If we extract all of the analyte into a volume of 0.24 mL instead of 025 mL, the concentration of the analyte increases by slightly more than 4%.)

3. Why does the procedure monitor fluorescence instead of monitoring UV absorption?

Fluorescence is a more selective technique for detecting analytes. Many other commonly prescribed antidepressants (and their metabolites) elute with retention times similar to that of fluoxetine. These compounds, however, either do not fluoresce or are only weakly fluorescent.

4. If the peaks for fluoxetine and protriptyline are insufficiently resolved, how might you alter the mobile phase to improve their separation?

Decreasing the amount of acetonitrile and increasing the amount of water in the mobile will increase retention times, providing a better resolution.

12.5.6 Evaluation

With a few exceptions, the scale of operation, accuracy, precision, sensitivity, selectivity, analysis time, and cost for an HPLC method are similar to GC methods. Injection volumes for an HPLC method are usually larger than for a GC method because HPLC columns have a greater capacity. Because it uses a loop injection, the precision of an HPLC method is often better. HPLC is not limited to volatile analytes, which means that we can analyze a broader range of compounds. Capillary GC columns, on the other hand, have more theoretical plates, and can separate more complex mixtures.

> **Note**
>
> See Section 12.4.8 for an evaluation of GC methods.

Contributors

David Harvey (DePauw University)

12.5: High-Performance Liquid Chromatography is shared under a CC BY-NC-SA 4.0 license and was authored, remixed, and/or curated by LibreTexts.

12.6: Other Forms of Liquid Chromatography

At the beginning of Section 12.5, we noted that there are several different types of solute/stationary phase interactions in liquid chromatography. In Section 12.5 we limited our discussion to liquid–liquid chromatography. In this section we turn our attention to liquid chromatography techniques in which partitioning occurs by liquid–solid adsorption, ion-exchange, and size exclusion.

12.6.1 Liquid-Solid Adsorption Chromatography

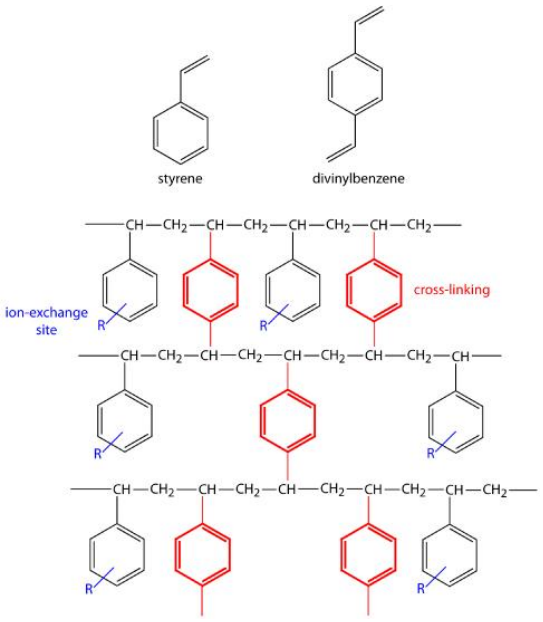
In **liquid–solid adsorption chromatography** (LSC) the column packing also serves as the stationary phase. In Tswett's original work the stationary phase was finely divided $CaCO_3$, but modern columns employ porous 3–10 μm particles of silica or alumina. Because the stationary phase is polar, the mobile phase is usually a nonpolar or moderately polar solvent. Typical mobile phases include hexane, isooctane, and methylene chloride. The usual order of elution—from shorter to longer retention times—is

olefins < aromatic hydrocarbons < ethers < esters, aldehydes, ketones < alcohols, amines < amide < carboxylic acids

Nonpolar stationary phases, such as charcoal-based absorbents, also may be used. For most samples, liquid–solid chromatography does not offer any special advantages over liquid–liquid chromatography. One exception is the analysis of isomers, where LLC excels.

12.6.2 Ion-Exchange Chromatography

In **ion-exchange chromatography** (IEC) the stationary phase is a cross-linked polymer resin, usually divinylbenzene cross-linked polystyrene, with covalently attached ionic functional groups (see Figure 12.52 and Table 12.7). The counterions to these fixed charges are mobile and can be displaced by ions that compete more favorably for the exchange sites. Ion-exchange resins are divided into four categories: strong acid cation exchangers; weak acid cation exchangers; strong base anion exchangers; and weak base anion exchangers.



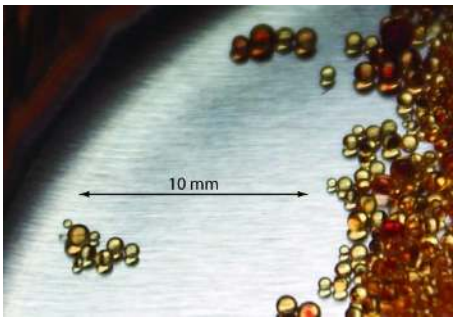


Figure 12.52 Structures of styrene, divinylbenzene, and a styrene–divinylbenzene co-polymer modified for use as an ion-exchange resin. The ion-exchange sites, indicated by R and shown in blue, are mostly in the *para* position and are not necessarily bound to all styrene units. The cross-linking is shown in red. The photo shows an example of the polymer beads. These beads are approximately 0.30–0.85 mm in diameter. Resins for use in ion-exchange chromatography are typically 5–11 μm in diameter.

Table 12.7 Examples of Common Ion-Exchange Resins

Type	Functional group (R)	Examples
strong acid cation exchanger	sulfonic acid	$-SO_3^-$ $-CH_2CH_2SO_3^-$
weak acid cation exchanger	carboxylic acid	$-COO^-$ $-CH_2COO^-$
strong base anion exchanger	quaternary amine	$-CH_2N(CH_3)_3^+$ $-CH_2CH_2N(CH_2CH_3)_3^+$
weak base anion exchanger	amine	$-NH_3^+$ $-CH_2CH_2NH(CH_2CH_3)_2^+$

Strong acid cation exchangers include a sulfonic acid functional group that retains it anionic form—and thus its capacity for ion-exchange—in strongly acidic solutions. The functional groups for a weak acid cation exchanger, however, become fully protonated at pH levels less then 4 and lose their exchange capacity. The strong base anion exchangers include a quaternary amine, which retains a positive charge even in strongly basic solutions. Weak base anion exchangers remain protonated only at pH levels that are moderately basic. Under more basic conditions a weak base anion exchanger loses a proton and its exchange capacity.

The ion-exchange reaction of a monovalent cation, M^+, at a strong acid exchange site is

$$-SO_3-H^+(s) + M^+(aq) \rightleftharpoons -SO_3-M^+(s) + H^+(aq) \tag{12.6.1}$$

The equilibrium constant for this ion-exchange reaction, which we call the selectivity coefficient, K, is

$$K = \frac{\{-SO_3-M^+\}\,[H^+]}{\{-SO_3-H^+\}\,[M^+]} \tag{12.29}$$

where we use brackets { } to indicate a surface concentration instead of a solution concentration.

> We don't usually think about a solid's concentration. There is a good reason for this. In most cases, a solid's concentration is a constant. If you break a piece of chalk into two parts, for example, the mass and the volume retain the same proportion. When we consider an ion binding to a reactive site on the solid's surface, however, the fraction of sites that are bound, and thus the concentration of bound sites, can take on any value between 0 and some maximum value that is proportional to the density of reactive sites.

Rearranging equation 12.29 shows us that the distribution ratio, *D*, for the exchange reaction

$$D = \frac{\text{amount of } M^+ \text{ in the stationary phase}}{\text{amount of } M^+ \text{ in the mobile phase}} \tag{12.6.2}$$

$$D = \frac{\{-SO_3-M^+\}}{[M^+]} = K \times \frac{\{-SO_3-H^+\}}{[H^+]} \tag{12.30}$$

is a function of the concentration of H^+ and, therefore, the pH of the mobile phase.

An ion-exchange resin's selectivity is somewhat dependent on whether it includes strong or weak exchange sites and on the extent of cross-linking. The latter is particularly important as it controls the resin's permeability, and, therefore, the accessibility of exchange sites. An approximate order of selectivity for a typical strong acid cation exchange resin, in order of decreasing *D*, is

$$Al^{3+} > Ba^{2+} > Pb^{2+} > Ca^{2+} > Ni^{2+} > Cd^{2+} > Cu^{2+} > Co^{2+} > Zn^{2+} > Mg^{2+} > Ag^+ > K^+ > NH_4^+ > Na^+ > H^+ > Li^+$$

Note that highly charged ions bind more strongly than ions of lower charge, and that for ions of similar charge, those with a smaller hydrated radius (see Table 6.2 in Chapter 6), or that are more polarizable, bind more strongly. For a strong base anion exchanger the general elution order is

$$SO_4^{2-} > I^- > HSO_4^- > NO_3^- > > Br^- > NO_2^- > Cl^- > HCO_3^- > CH_3COO^- > OH^- > F^-$$

Again, ions of higher charge and of smaller hydrated radius bind more strongly than ions with a lower charge and a larger hydrated radius.

The mobile phase in IEC is usually an aqueous buffer, the pH and ionic composition of which determines a solute's retention time. Gradient elutions are possible in which the mobile phase's ionic strength or pH is changed with time. For example, an IEC separation of cations might use a dilute solution of HCl as the mobile phase. Increasing the concentration of HCl speeds the elution rate for more strongly retained cations because the higher concentration of H^+ allows it to compete more successfully for the ion-exchange sites.

> **Note**
>
> From equation 12.30, a cation's distribution ratio, *D*, becomes smaller when the concentration of H^+ in the mobile phase increases.

An ion-exchange resin is incorporated into an HPLC column either as 5–11 μm porous polymer beads or by coating the resin on porous silica particles. Columns typically are 250 mm in length with internal diameters ranging from 2–5 mm.

Measuring the conductivity of the mobile phase as it elutes from the column is a universal detector for cationic and anionic analytes. Because the mobile phase contains a high concentration of ions—a mobile phase of dilute HCl, for example, contains significant concentrations of H^+ and Cl^-—we need a method for detecting the analytes in the presence of a significant background conductivity.

To minimize the mobile phase's contribution to conductivity an **ion-suppressor column** is placed between the analytical column and the detector. This column selectively removes mobile phase ions without removing solute ions. For example, in cation-exchange chromatography using a dilute solution of HCl as the mobile phase, the suppressor column contains a strong base anion-exchange resin. The exchange reaction

$$H^+(aq) + Cl^-(aq) + \text{Resin}^+OH^-(s) \rightleftharpoons \text{Resin}^+Cl^-(s) + H_2O(l) \tag{12.6.3}$$

replaces the mobile phase ions H^+ and Cl^- with H_2O. A similar process is used in anion-exchange chromatography where the suppressor column contains a cation-exchange resin. If the mobile phase is a solution of Na_2CO_3, the exchange reaction

$$2\,Na^+(aq) + CO_3^{2-}(aq) + 2\,\text{Resin}^-\ H^+(s) \rightleftharpoons 2\,\text{Resin}^-\ Na^+(s) + H_2CO_3(aq) \tag{12.6.4}$$

replaces a strong electrolyte, Na_2CO_3, with a weak electrolyte, H_2CO_3.

Ion-suppression is necessary when the mobile phase contains a high concentration of ions. **Single-column ion chromatography**, in which an ion-suppressor column is not needed, is possible if the concentration of ions in the mobile phase is small. Typically the stationary phase is a resin with a low capacity for ion-exchange and the mobile phase is a very dilute solution of methane sulfonic acid for cationic analytes, or potassium benzoate or potassium hydrogen phthalate for anionic analytes. Because the background conductivity is sufficiently small, it is possible to monitor a change in conductivity as the analytes elute from the column.

A UV/Vis absorbance detector can also be used if the analytes absorb ultraviolet or visible radiation. Alternatively, we can detect indirectly analytes that do not absorb in the UV/Vis if the mobile phase contains a UV/Vis absorbing species. In this case, when a solute band passes through the detector, a decrease in absorbance is measured at the detector.

Ion-exchange chromatography is an important technique for the analysis of anions and cations in water. For example, an ion-exchange chromatographic analysis for the anions F^-, Cl^-, Br^-, NO_2^-, NO_3^-, PO_4^{3-}, and SO_4^{2-} takes approximately 15 minutes (Figure 12.53). A complete analysis of the same set of anions by a combination of potentiometry and spectrophotometry requires 1–2 days. Ion-exchange chromatography also has been used for the analysis of proteins, amino acids, sugars, nucleotides, pharmaceuticals, consumer products, and clinical samples.

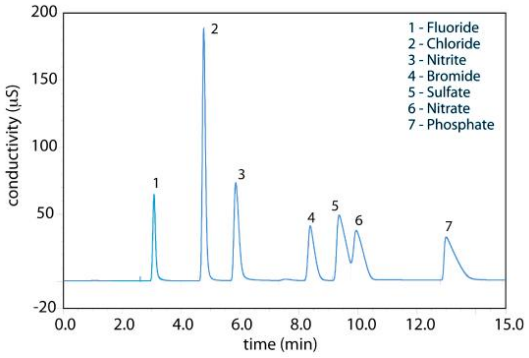


Figure 12.53 *Ion-exchange chromatographic analysis of water from Big Walnut Creek in Putnam County, Indiana. Data provided by Jeanette Pope, Department of Geosciences, DePauw University.*

12.6.3 Size-Exclusion Chromatography

We have considered two classes of micron-sized stationary phases in this section: silica particles and cross-linked polymer resin beads. Both materials are porous, with pore sizes ranging from approximately 5–400 nm for silica particles, and from 5 nm to 100 µm for divinylbenzene cross-linked polystyrene resins. In **size-exclusion chromatography**—which also is known by the terms molecular-exclusion or gel permeation chromatography—the separation of solutes depends upon their ability to enter into the pores of the stationary phase. Smaller solutes spend proportionally more time within the pores and take longer to elute from the column.

A stationary phase's size selectivity extends over a finite range. All solutes significantly smaller than the pores move through the column's entire volume and elute simultaneously, with a retention volume, V_r, of

$$V_r = V_i + V_o \tag{12.31}$$

where V_i is the volume of mobile phase occupying the stationary phase's pore space, and V_o is volume of mobile phase in the remainder of the column. The largest solute for which equation 12.31 holds is the column's **inclusion limit**, or permeation limit. Those solutes that are too large to enter the pores elute simultaneously with an retention volume of

$$V_r = V_o \tag{12.32}$$

Equation 12.32 defines the column's **exclusion limit**.

For a solute whose size is between the inclusion limit and the exclusion limit, the amount of time it spends in the stationary phase's pore space is proportional to its size. The retention volume for these solutes is

$$V_r = V_o + DV_i \tag{12.33}$$

where D is the solute's distribution ratio, which ranges from 0 at the exclusion limit, to 1 at the inclusion limit. Equation 12.33 assumes that size-exclusion is the only interaction between the solute and the stationary phase that affects the separation. For this reason, stationary phases using silica particles are deactivated as described earlier, and polymer resins are synthesized without exchange sites.

Size-exclusion chromatography provides a rapid means for separating larger molecules, including polymers and biomolecules. A stationary phase for proteins consisting of particles with 30 nm pores has an inclusion limit of 7500 g/mol and an exclusion limit of 1.2×10^6 g/mol. Mixtures containing proteins spanning a wider range of molecular weights can be separated by joining together in series several columns with different inclusion and exclusion limits.

Another important application of size-exclusion chromatography is the estimation of a solute's molecular weight (MW). Calibration curves are prepared using a series of standards of known molecular weight and measuring each standard's retention volume. As shown in Figure 12.54, a plot of log(MW) versus V_r is roughly linear between the exclusion limit and the inclusion limit. Because a solute's retention volume is influenced by both its size and its shape, a reasonably accurate estimation of molecular weight is possible only if the standards are carefully chosen to minimize the effect of shape.

Size-exclusion chromatography can be carried out using conventional HPLC instrumentation, replacing the HPLC column with an appropriate size-exclusion column. A UV/Vis detector is the most common means for obtaining the chromatogram.

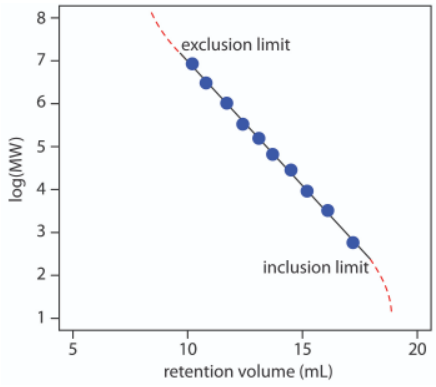


Figure 12.54 *Calibration curve for the determination of molecular weight by size-exclusion chromatography. The data shown here are adapted from Rouessac, F.; Rouessac, A. Chemical Analysis: Modern Instrumentation Methods and Techniques, Wiley: Chichester, England, 2004, p 141.*

12.6.4 Supercritical Fluid Chromatography

Although there are many analytical applications of gas chromatography and liquid chromatography, they can not separate and analyze all types of samples. Capillary column GC can separate complex mixtures with excellent resolution and short analysis times. Its application is limited, however, to volatile analytes or to analytes made volatile by a suitable derivatization reaction. Liquid chromatography can separate a wider range of solutes than GC, but the most commonly used detectors—UV, fluorescence, and electrochemical—have poorer detection limits and smaller linear ranges than GC detectors, and are not as nearly universal in their selectivity.

For some samples, **supercritical fluid chromatography** (SFC) provides a useful alternative to gas chromatography and liquid chromatography. The mobile phase in supercritical fluid chromatography is a gas held at a temperature and pressure that exceeds its critical point (Figure 12.55). Under these conditions the mobile phase is neither a gas nor a liquid. Instead, the mobile phase is a supercritical fluid.

> **Note**
>
> Click here to see an interesting video demonstration of supercritical fluids from Nottingham Science City at the University of Nottingham.

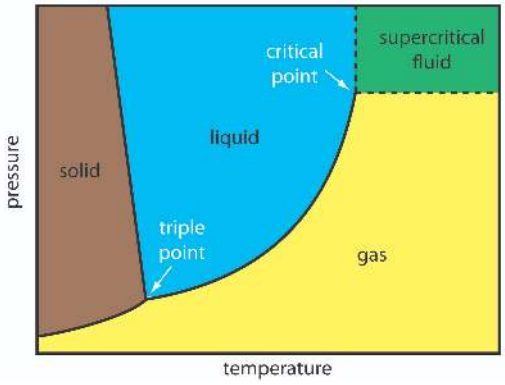


Figure 12.55 *Phase diagram showing the combinations of temperature and pressure for which a compound is in its solid state, its liquid state, and its gas state. For pressures and temperatures above the compound's critical point, the compound is a supercritical fluid with properties intermediate between a gas and a liquid.*

The properties of a supercritical fluid, as shown in Table 12.8, are intermediate between those of a gas and a liquid. Specifically, the viscosity of a supercritical fluid is similar to that for a gas, which means we can move a supercritical fluid can move through a capillary or a packed column without the high pressures needed in HPLC. Analysis time and resolution, although not as good as in GC, are usually better than in conventional HPLC. The density of a supercritical fluid is much closer to that of a liquid, which

explains why supercritical fluids are good solvents. The mobile phase in SFC, therefore, behaves more like the liquid mobile phase in HPLC than the gaseous mobile phase in GC.

Table 12.8 Typical Properties of Gases, Liquids, and Supercritical Fluids

phase	density ($g\ cm^{-3}$)	viscosity ($g\ cm^{-1}\ s^{-1}$)	diffusion coefficient ($cm^2\ s^{-1}$)
gas	$\approx 10^{-3}$	$\approx 10^{-4}$	≈ 0.1
supercritical fluid	$\approx 0.1–1$	$\approx 10^{-4}–10^{-3}$	$\approx 10^{-4}–10^{-3}$
liquid	≈ 1	$\approx 10^{-2}$	$< 10^{-5}$

The most common mobile phase for supercritical fluid chromatography is CO_2. Its low critical temperature, 3°C, and critical pressure, 72.9 atm, are relatively easy to achieve and maintain. Although supercritical CO_2 is a good solvent for nonpolar organics, it is less useful for polar solutes. The addition of an organic modifier, such as methanol, improves the mobile phase's elution strength. Other common mobile phases and their critical temperatures and pressures are listed in Table 12.9.

Table 12.9 Critical Points for Selected Supercritical Fluids

compound	critical temperature (°C)	critical pressure (atm)
carbon dioxide	31.3	72.9
ethane	32.4	48.3
nitrous oxide	36.5	71.4
ammonia	132.3	111.3
diethyl ether	193.6	36.3
isopropanol	235.3	47.0
methanol	240.5	78.9
ethanol	243.4	63.0
water	374.4	226.8

The instrumentation for supercritical fluid chromatography is essentially the same as that for a standard HPLC. The only important additions are a heated oven for the column and a pressure restrictor downstream from the column to maintain the critical pressure. Gradient elutions are accomplished by changing the applied pressure over time. The resulting change in the mobile phase's density affects its solvent strength. Detection can be accomplished using standard GC detectors or HPLC detectors. Supercritical fluid chromatography has found many applications in the analysis of polymers, fossil fuels, waxes, drugs, and food products.

Contributors

- David Harvey (DePauw University)

12.6: Other Forms of Liquid Chromatography is shared under a CC BY-NC-SA 4.0 license and was authored, remixed, and/or curated by LibreTexts.

12.7: Electrophoresis

Electrophoresis is a class of separation techniques in which we separate analytes by their ability to move through a conductive medium—usually an aqueous buffer—in response to an applied electric field. In the absence of other effects, cations migrate toward the electric field's negatively charged cathode. Cations with larger charge-to-size ratios—which favors ions of larger charge and of smaller size—migrate at a faster rate than larger cations with smaller charges. Anions migrate toward the positively charged anode and neutral species do not experience the electrical field and remain stationary.

There are several forms of electrophoresis. In slab gel electrophoresis the conducting buffer is retained within a porous gel of agarose or polyacrylamide. Slabs are formed by pouring the gel between two glass plates separated by spacers. Typical thicknesses are 0.25–1 mm. Gel electrophoresis is an important technique in biochemistry where it is frequently used for separating DNA fragments and proteins. Although it is a powerful tool for the qualitative analysis of complex mixtures, it is less useful for quantitative work.

In **capillary electrophoresis**, the conducting buffer is retained within a capillary tube whose inner diameter is typically 25–75 μm. Samples are injected into one end of the capillary tube. As the sample migrates through the capillary its components separate and elute from the column at different times. The resulting **electropherogram** looks similar to a GC or an HPLC chromatogram, providing both qualitative and quantitative information. Only capillary electrophoretic methods receive further consideration in this section.

> **Note**
>
> As we will see shortly, under normal conditions even neutral species and anions migrate toward the cathode.

12.7.1 Theory of Capillary Electrophoresis

In capillary electrophoresis we inject the sample into a buffered solution retained within a capillary tube. When an electric field is applied across the capillary tube, the sample's components migrate as the result of two types of action: electrophoretic mobility and electroosmotic mobility. **Electrophoretic mobility** is the solute's response to the applied electrical field. As described earlier, cations move toward the negatively charged cathode, anions move toward the positively charged anode, and neutral species remain stationary. The other contribution to a solute's migration is **electroosmotic flow**, which occurs when the buffer moves through the capillary in response to the applied electrical field. Under normal conditions the buffer moves toward the cathode, sweeping most solutes, including the anions and neutral species, toward the negatively charged cathode.

Electrophoretic Mobility

The velocity with which a solute moves in response to the applied electric field is called its **electrophoretic velocity**, ν_{ep}; it is defined as

$$\nu_{ep} = \mu_{ep} E \tag{12.43}$$

where μ_{ep} is the solute's electrophoretic mobility, and E is the magnitude of the applied electrical field. A solute's electrophoretic mobility is defined as

$$\mu_{ep} = \frac{q}{6\pi\eta r} \tag{12.35}$$

where

- q is the solute's charge,
- η is the buffer viscosity, and
- r is the solute's radius.

Using equation 12.34 and equation 12.35 we can make several important conclusions about a solute's electrophoretic velocity. Electrophoretic mobility and, therefore, electrophoretic velocity, increases for more highly charged solutes and for solutes of smaller size. Because q is positive for a cation and negative for an anion, these species migrate in opposite directions. Neutral species, for which q is zero, have an electrophoretic velocity of zero.

Electroosmotic Mobility

When an electrical field is applied to a capillary filled with an aqueous buffer we expect the buffer's ions to migrate in response to their electrophoretic mobility. Because the solvent, H_2O, is neutral we might reasonably expect it to remain stationary. What we observe under normal conditions, however, is that the buffer solution moves towards the cathode. This phenomenon is called the electroosmotic flow.

Electroosmotic flow occurs because the walls of the capillary tubing are electrically charged. The surface of a silica capillary contains large numbers of silanol groups (–SiOH). At pH levels greater than approximately 2 or 3, the silanol groups ionize to form negatively charged silanate ions ($–SiO^–$). Cations from the buffer are attracted to the silanate ions. As shown in Figure 12.56, some of these cations bind tightly to the silanate ions, forming a fixed layer. Because the cations in the fixed layer only partially neutralize the negative charge on the capillary walls, the solution adjacent to the fixed layer—what we call the diffuse layer—contains more cations than anions. Together these two layers are known as the double layer. Cations in the diffuse layer migrate toward the cathode. Because these cations are solvated, the solution is also pulled along, producing the electroosmotic flow.

> **Note**
>
> The anions in the diffuse layer, which also are solvated, try to move toward the anode. Because there are more cations than anions, however, the cations win out and the electroosmotic flow moves in the direction of the cathode.

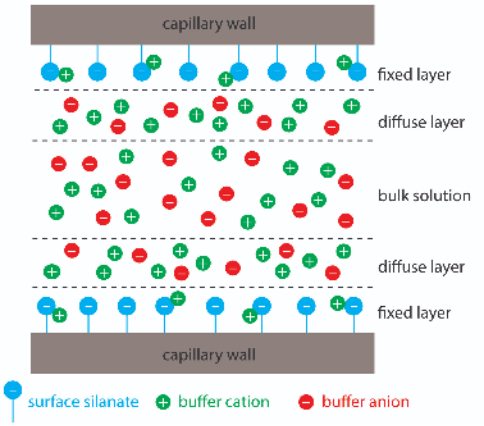


Figure 12.56: *Schematic diagram showing the origin of the double layer within a capillary tube. Although the net charge within the capillary is zero, the distribution of charge is not. The walls of the capillary have an excess of negative charge, which decreases across the fixed layer and the diffuse layer, reaching a value of zero in bulk solution.*

The rate at which the buffer moves through the capillary, what we call its **electroosmotic flow velocity**, ν_{eof}, is a function of the applied electric field, E, and the buffer's electroosmotic mobility, μ_{eof}.

$$\nu_{eof} = \mu_{eof} E \tag{12.36}$$

Electroosmotic mobility is defined as

$$\mu_{eof} = \frac{\varepsilon \zeta}{4\pi\eta} \tag{12.37}$$

where

- ε is the buffer dielectric constant,
- ζ is the zeta potential, and
- η is the buffer viscosity.

The **zeta potential**—the potential of the diffuse layer at a finite distance from the capillary wall—plays an important role in determining the electroosmotic flow velocity. Two factors determine the zeta potential's value. First, the zeta potential is directly proportional to the charge on the capillary walls, with a greater density of silanate ions corresponding to a larger zeta potential. Below a pH of 2 there are few silanate ions, and the zeta potential and electroosmotic flow velocity are zero. As the pH increases, both the zeta potential and the electroosmotic flow velocity increase. Second, the zeta potential is directly proportional to the

thickness of the double layer. Increasing the buffer's ionic strength provides a higher concentration of cations, decreasing the thickness of the double layer and decreasing the electroosmotic flow.

Note: Zeta Potential

The definition of zeta potential given here is admittedly a bit fuzzy. For a much more technical explanation see Delgado, A. V.; González-Caballero, F.; Hunter, R. J.; Koopal, L. K.; Lyklema, J. "Measurement and Interpretation of Electrokinetic Phenomena," Pure. Appl. Chem. 2005, 77, 1753–1805. Although this a very technical report, Sections 1.3–1.5 provide a good introduction to the difficulty of defining the zeta potential and measuring its value.

The electroosmotic flow profile is very different from that of a fluid moving under forced pressure. Figure 12.57 compares the electroosmotic flow profile with that the hydrodynamic flow profile in gas chromatography and liquid chromatography. The uniform, flat profile for electroosmosis helps minimize band broadening in capillary electrophoresis, improving separation efficiency.

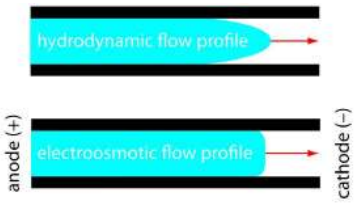


Figure 12.57: *Comparison of hydrodynamic flow and electroosmotic flow. The nearly uniform electroosmotic flow profile means that the electroosmotic flow velocity is nearly constant across the capillary.*

Total Mobility

A solute's total velocity, v_{tot}, as it moves through the capillary is the sum of its electrophoretic velocity and the electroosmotic flow velocity.

$$\nu_{\text{tot}} = \nu_{\text{ep}} + \nu_{\text{eof}} \tag{12.7.1}$$

As shown in Figure 12.58, under normal conditions the following general relationships hold true.

$$(\nu_{\text{tot}})_{\text{cations}} > \nu_{\text{eof}} \tag{12.7.2}$$

$$(\nu_{\text{tot}})_{\text{neutrals}} = \nu_{\text{eof}} \tag{12.7.3}$$

$$(\nu_{\text{tot}})_{\text{anions}} < \nu_{\text{eof}} \tag{12.7.4}$$

Cations elute first in an order corresponding to their electrophoretic mobilities, with small, highly charged cations eluting before larger cations of lower charge. Neutral species elute as a single band with an elution rate equal to the electroosmotic flow velocity. Finally, anions are the last components to elute, with smaller, highly charged anions having the longest elution time.

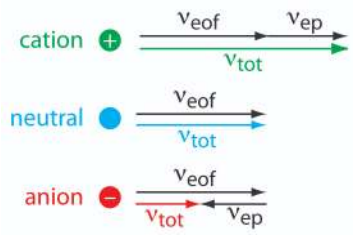


Figure 12.58: *Visual explanation for the general elution order in capillary electrophoresis. Each species has the same electroosmotic flow, v_{eof}. Cations elute first because they have a positive electrophoretic velocity, v_{ep}. Anions elute last because their negative electrophoretic velocity partially offsets the electroosmotic flow velocity. Neutrals elute with a velocity equal to the electroosmotic flow.*

Migration Time

Another way to express a solute's velocity is to divide the distance it travels by the elapsed time

$$\nu_{tot} = \frac{l}{t_m} \tag{12.38}$$

where l is the distance between the point of injection and the detector, and t_m is the solute's migration time. To understand the experimental variables affecting migration time, we begin by noting that

$$\nu_{tot} = \mu_{tot} E = (\mu_{ep} + \mu_{eof}) E \tag{12.39}$$

Combining equation 12.38 and equation 12.39 and solving for t_m leaves us with

$$t_m = \frac{l}{(\mu_{ep} + \mu_{eof}) E} \tag{12.40}$$

Finally, the magnitude of the electrical field is

$$E = \frac{V}{L} \tag{12.41}$$

where V is the applied potential and L is the length of the capillary tube. Finally, substituting equation 12.41 into equation 12.40 leaves us with the following equation for a solute's migration time.

$$t_m = \frac{lL}{(\mu_{ep} + \mu_{eof}) V} \tag{12.42}$$

To decrease a solute's migration time—and shorten the analysis time—we can apply a higher voltage or use a shorter capillary tube. We can also shorten the migration time by increasing the electroosmotic flow, although this decreases resolution.

Efficiency

As we learned in Section 12.2.4, the efficiency of a separation is given by the number of theoretical plates, N. In capillary electrophoresis the number of theoretic plates is

$$N = \frac{l^2}{2Dt_m} = \frac{(\mu_{ep} + \mu_{eof}) Vl}{2DL} \tag{12.43}$$

where D is the solute's diffusion coefficient.

> **Note**
>
> From equation 12.10 and equation 12.11, we know that the number of theoretical plates for a solute is
>
> $$N = \frac{l^2}{\sigma^2} \tag{12.7.5}$$
>
> where l is the distance the solute travels and σ is the standard deviation for the solute's band broadening. For capillary electrophoresis band broadening is due to longitudinal diffusion and is equivalent to $2Dt_m$, where t_m is the migration time.

From equation 12.43, the efficiency of a capillary electrophoretic separation increases with higher voltages. Increasing the electroosmotic flow velocity improves efficiency, but at the expense of resolution. Two additional observations deserve comment. First, solutes with larger electrophoretic mobilities—in the same direction as the electroosmotic flow—have greater efficiencies; thus, smaller, more highly charged cations are not only the first solutes to elute, but do so with greater efficiency. Second, efficiency in capillary electrophoresis is independent of the capillary's length. Theoretical plate counts of approximately 100,000–200,000 are not unusual.

> **Note**
>
> It is possible to design an electrophoretic experiment so that anions elute before cations—more about this later—in which smaller, more highly charged anions elute with greater efficiencies.

Selectivity

In chromatography we defined the selectivity between two solutes as the ratio of their retention factors (see equation 12.9). In capillary electrophoresis the analogous expression for selectivity is

$$\alpha = \frac{\mu_{ep,1}}{\mu_{ep,2}} \tag{12.7.6}$$

where $\mu_{ep,1}$ and $\mu_{ep,2}$ are the electrophoretic mobilities for the two solutes, chosen such that $\alpha \geq 1$. We can often improve selectivity by adjusting the pH of the buffer solution. For example, NH_4^+ is a weak acid with a pK_a of 9.75. At a pH of 9.75 the concentrations of NH_4^+ and NH_3 are equal. Decreasing the pH below 9.75 increases its electrophoretic mobility because a greater fraction of the solute is present as the cation NH_4^+. On the other hand, raising the pH above 9.75 increases the proportion of the neutral NH_3, decreasing its electrophoretic mobility.

Resolution

The resolution between two solutes is

$$R = \frac{0.177(\mu_{ep,1} - \mu_{ep,2})\sqrt{V}}{\sqrt{D(\mu_{avg} - \mu_{eof})}} \tag{12.44}$$

where μ_{avg} is the average electrophoretic mobility for the two solutes. Increasing the applied voltage and decreasing the electroosmotic flow velocity improves resolution. The latter effect is particularly important. Although increasing electroosmotic flow improves analysis time and efficiency, it decreases resolution.

12.7.2 Instrumentation

The basic instrumentation for capillary electrophoresis is shown in Figure 12.59 and includes a power supply for applying the electric field, anode and cathode compartments containing reservoirs of the buffer solution, a sample vial containing the sample, the capillary tube, and a detector. Each part of the instrument receives further consideration in this section.

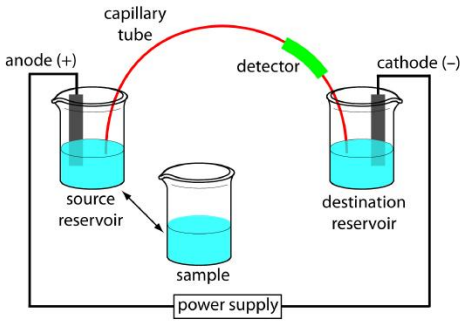
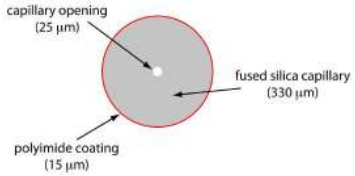


Figure 12.59 *Schematic diagram of the basic instrumentation for capillary electrophoresis. The sample and the source reservoir are switched when making injections.*

Capillary Tubes

Figure 12.60 shows a cross-section of a typical capillary tube. Most capillary tubes are made from fused silica coated with a 15–35 μm layer of polyimide to give it mechanical strength. The inner diameter is typically 25–75 μm—smaller than the internal diameter of a capillary GC column—with an outer diameter of 200–375 μm.



https://chem.libretexts.org/@go/page/70722

Figure 12.60 Cross section of a capillary column for capillary electrophoresis. The dimensions shown here are typical and are scaled proportionally.

The capillary column's narrow opening and the thickness of its walls are important. When an electric field is applied to the buffer solution within the capillary, current flows through the capillary. This current leads to the release of heat—what we call **Joule heating**. The amount of heat released is proportional to the capillary's radius and the magnitude of the electrical field. Joule heating is a problem because it changes the buffer solution's viscosity, with the solution at the center of the capillary being less viscous than that near the capillary walls. Because a solute's electrophoretic mobility depends on viscosity (see equation 12.35), solute species in the center of the capillary migrate at a faster rate than those near the capillary walls. The result is an additional source of band broadening that degrades the separation. Capillaries with smaller inner diameters generate less Joule heating, and capillaries with larger outer diameters are more effective at dissipating the heat. Placing the capillary tube inside a thermostated jacket is another method for minimizing the effect of Joule heating; in this case a smaller outer diameter allows for a more rapid dissipation of thermal energy.

Injecting the Sample

There are two commonly used method for injecting a sample into a capillary electrophoresis column: hydrodynamic injection and electrokinetic injection. In both methods the capillary tube is filled with the buffer solution. One end of the capillary tube is placed in the destination reservoir and the other end is placed in the sample vial.

Hydrodynamic injection uses pressure to force a small portion of sample into the capillary tubing. A difference in pressure is applied across the capillary by either pressurizing the sample vial or by applying a vacuum to the destination reservoir. The volume of sample injected, in liters, is given by the following equation

$$V_{\text{inj}} = \frac{Pd^4\pi t}{128\eta L} \times 10^3 \tag{12.45}$$

where ΔP is the difference in pressure across the capillary in pascals, d is the capillary's inner diameter in meters, t is the amount of time that the pressure is applied in seconds, η is the buffer's viscosity in kg m^{-1} s^{-1}, and L is the length of the capillary tubing in meters. The factor of 10^3 changes the units from cubic meters to liters.

Note

For a hydrodynamic injection we move the capillary from the source reservoir to the sample. The anode remains in the source reservoir.

A hydrodynamic injection is also possible by raising the sample vial above the destination reservoir and briefly inserting the filled capillary.

If you want to verify the units in equation 12.45, recall from Table 2.2 that 1 Pa is equivalent to 1 kg m^{-1} s^{-2}.

Example 12.9

In a hydrodynamic injection we apply a pressure difference of 2.5×10^3 Pa (a $\Delta P \approx 0.02$ atm) for 2 s to a 75-cm long capillary tube with an internal diameter of 50 μm. Assuming that the buffer's viscosity is 10^{-3} kg m^{-1} s^{-1}, what volume and length of sample did we inject?

Solution

Making appropriate substitutions into equation 12.45 gives the sample's volume as

$$V_{\text{inj}} = \frac{(2.5 \times 10^3\ \text{kg m}^{-1}\ \text{s}^{-2})(50 \times 10^{-6}\ \text{m})^4(3.14)(2\ \text{s})}{(128)(0.001\ \text{kg m}^{-1}\ \text{s}^{-1})(0.75\ \text{m})} \times 10^3\ \text{L/m}^3 \tag{12.7.7}$$

$$V_{\text{inj}} = 1 \times 10^{-9}\ \text{L} = 1\ \text{nL} \tag{12.7.8}$$

Because the interior of the capillary is cylindrical, the length of the sample, l, is easy to calculate using the equation for the volume of a cylinder; thus

$$l = \frac{V_{\text{inj}}}{\pi r^2} = \frac{(1.0 \times 10^{-9}\ \text{L})(10^{-3}\ \text{m}^3/\text{L})}{(3.14)(25 \times 10^{-6}\ \text{m})^2} = 5 \times 10^{-4}\ \text{m} = 0.5\ \text{mm} \tag{12.7.9}$$

Exercise 12.9

Suppose that you need to limit your injection to less than 0.20% of the capillary's length. Using the information from Example 12.9, what is the maximum injection time for a hydrodynamic injection?

Click here to review your answer to this exercise.

In an **electrokinetic injection** we place both the capillary and the anode into the sample and briefly apply an potential. The volume of injected sample is the product of the capillary's cross sectional area and the length of the capillary occupied by the sample. In turn, this length is the product of the solute's velocity (see equation 12.39) and time; thus

$$l = \frac{V_{inj}}{\pi r^2} = \frac{(1.0 \times 10^{-9}\ \text{L})(10^{-3}\ \text{m}^3/\text{L})}{(3.14)(25 \times 10^{-6}\ \text{m})^2} = 5 \times 10^{-4}\ \text{m} = 0.5\ \text{mm} \tag{12.7.10}$$

where

- r is the capillary's radius,
- L is the length of the capillary, and
- E' is effective electric field in the sample.

An important consequence of equation 12.46 is that an electrokinetic injection is inherently biased toward solutes with larger electrophoretic mobilities. If two solutes have equal concentrations in a sample, we inject a larger volume—and thus more moles—of the solute with the larger μ_{ep}.

Note

The electric field in the sample is different that the electric field in the rest of the capillary because the sample and the buffer have different ionic compositions. In general, the sample's ionic strength is smaller, which makes its conductivity smaller. The effective electric field is

$$E' = E \times \frac{\kappa_{buf}}{\kappa_{sam}} \tag{12.7.11}$$

where κ_{buf} and κ_{sam} are the conductivities of the buffer and the sample, respectively.

When an analyte's concentration is too small to detect reliably, it may be possible to inject it in a manner that increases its concentration in the capillary tube. This method of injection is called **stacking**. Stacking is accomplished by placing the sample in a solution whose ionic strength is significantly less than that of the buffer in the capillary tube. Because the sample plug has a lower concentration of buffer ions, the effective field strength across the sample plug, E' is larger than that in the rest of the capillary.

We know from equation 12.34 that electrophoretic velocity is directly proportional to the electrical field. As a result, the cations in the sample plug migrate toward the cathode with a greater velocity, and the anions migrate more slowly—neutral species are unaffected and move with the electroosmotic flow. When the ions reach their respective boundaries between the sample plug and the buffering solution, the electrical field decreases and the electrophoretic velocity of cations decreases and that for anions increases. As shown in Figure 12.61, the result is a stacking of cations and anions into separate, smaller sampling zones. Over time, the buffer within the capillary becomes more homogeneous and the separation proceeds without additional stacking.

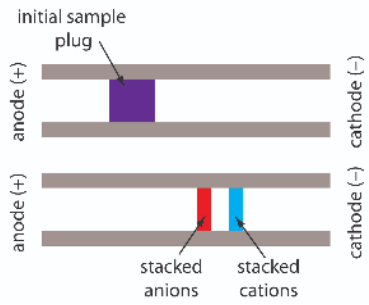


Figure 12.61 *The stacking of cations and anions. The top diagram shows the initial sample plug and the bottom diagram shows how the cations and anions become concentrated at opposite sides of the sample plug.*

Applying the Electrical Field

Migration in electrophoresis occurs in response to an applied electrical field. The ability to apply a large electrical field is important because higher voltages lead to shorter analysis times (see equation 12.42), more efficient separations (equation 12.43), and better resolution (equation 12.44). Because narrow bored capillary tubes dissipate Joule heating so efficiently, voltages of up to 40 kV are possible.

> **Note**
>
> Because of the high voltages, be sure to follow your instrument's safety guidelines.

Detectors

Most of the detectors used in HPLC also find use in capillary electrophoresis. Among the more common detectors are those based on the absorption of UV/Vis radiation, fluorescence, conductivity, amperometry, and mass spectrometry. Whenever possible, detection is done "on-column" before the solutes elute from the capillary tube and additional band broadening occurs.

UV/Vis detectors are among the most popular. Because absorbance is directly proportional to path length, the capillary tubing's small diameter leads to signals that are smaller than those obtained in HPLC. Several approaches have been used to increase the pathlength, including a Z-shaped sample cell and multiple reflections (see Figure 12.62). Detection limits are about 10^{-7} M.

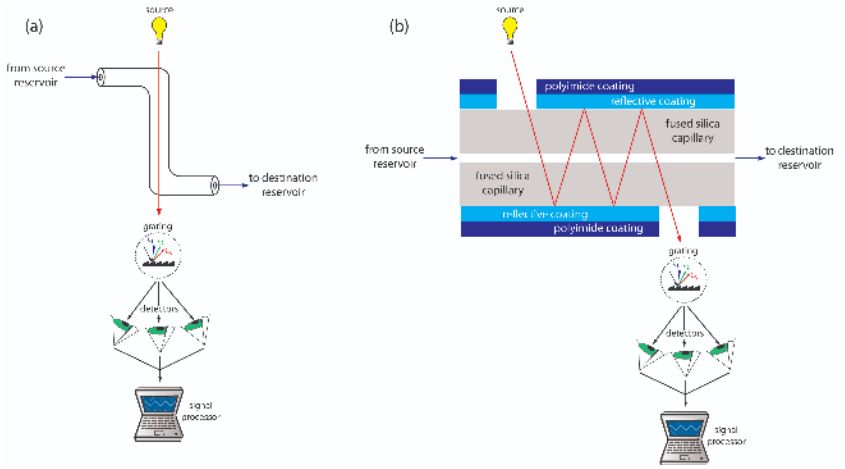


Figure 12.62 Two approaches to on-column detection in capillary electrophoresis using a UV/Vis diode array spectrometer: (a) Z-shaped bend in capillary, and (b) multiple reflections.

Better detection limits are obtained using fluorescence, particularly when using a laser as an excitation source. When using fluorescence detection a small portion of the capillary's protective coating is removed and the laser beam is focused on the inner portion of the capillary tubing. Emission is measured at an angle of 90° to the laser. Because the laser provides an intense source of radiation that can be focused to a narrow spot, detection limits are as low as 10^{-16} M.

Solutes that do not absorb UV/Vis radiation or that do not undergo fluorescence can be detected by other detectors. Table 12.10 provides a list of detectors for capillary electrophoresis along with some of their important characteristics.

Table 12.10 Characteristics of Detectors for Capillary Electrophoresis

		detection limit		
detector	selectivity universal or analyte must...	moles injected	molarity	on-column detection?
UV/Vis absorbance	have a UV/Vis chromophore	10^{-13}–10^{-16}	10^{-5}–10^{-7}	yes
indirect absorbance	universal	10^{-12}–10^{-15}	10^{-4}–10^{-6}	yes
fluorescence	have a favorable quantum yield	10^{-15}–10^{-17}	10^{-7}–10^{-9}	yes
laser fluorescence	have a favorable quantum yield	10^{-18}–10^{-20}	10^{-13}–10^{-16}	yes
mass spectrometer	universal (total ion) selective (single ion)	10^{-16}–10^{-17}	10^{-8}–10^{-10}	no
amperometry	undergo oxidation or reduction	10^{-18}–10^{-19}	10^{-7}–10^{-10}	no
conductivity	universal	10^{-15}–10^{-16}	10^{-7}–10^{-9}	no
radiometric	be radioactive	10^{-17}–10^{-19}	10^{-10}–10^{-12}	yes

Source: Baker, D. R. *Capillary Electrophoresis*, Wiley-Interscience: New York, 1995.

12.7.3 Capillary Electrophoresis Methods

There are several different forms of capillary electrophoresis, each of which has its particular advantages. Four of these methods are briefly described in this section.

Capillary Zone Electrophoresis (CZE)

The simplest form of capillary electrophoresis is **capillary zone electrophoresis**. In CZE we fill the capillary tube with a buffer solution and, after loading the sample, place the ends of the capillary tube in reservoirs containing additional buffer solution. Usually the end of the capillary containing the sample is the anode and solutes migrate toward the cathode at a velocity determined by their electrophoretic mobility and the electroosmotic flow. Cations elute first, with smaller, more highly charged cations eluting before larger cations with smaller charges. Neutral species elute as a single band. Anions are the last species to elute, with smaller, more negatively charged anions being the last to elute.

We can reverse the direction of electroosmotic flow by adding an alkylammonium salt to the buffer solution. As shown in Figure 12.63, the positively charged end of the alkyl ammonium ions bind to the negatively charged silanate ions on the capillary's walls. The tail of the alkyl ammonium ion is hydrophobic and associates with the tail of another alkyl ammonium ion. The result is a layer of positive charges that attract anions in the buffer solution. The migration of these solvated anions toward the anode reverses the electroosmotic flow's direction. The order of elution is exactly opposite of that observed under normal conditions.

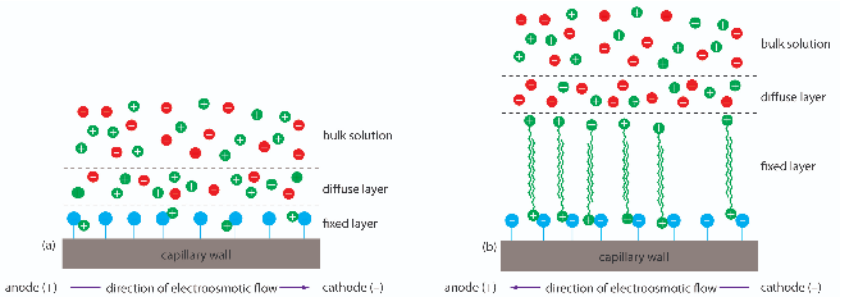


Figure 12.63 Two modes of capillary zone electrophoresis showing (a) normal migration with electroosmotic flow toward the cathode and (b) reversed migration in which the electroosmotic flow is toward the anode.

Coating the capillary's walls with a nonionic reagent eliminates the electroosmotic flow. In this form of CZE the cations migrate from the anode to the cathode. Anions elute into the source reservoir and neutral species remain stationary.

Capillary zone electrophoresis provides effective separations of charged species, including inorganic anions and cations, organic acids and amines, and large biomolecules such as proteins. For example, CZE has been used to separate a mixture of 36 inorganic and organic ions in less than three minutes.[15] A mixture of neutral species, of course, can not be resolved.

Micellar Electrokinetic Capillary Chromatography (MEKC)

One limitation to CZE is its inability to separate neutral species. **Micellar electrokinetic capillary chromatography** overcomes this limitation by adding a surfactant, such as sodium dodecylsulfate (Figure 12.64a) to the buffer solution. Sodium dodecylsulfate, or SDS, has a long-chain hydrophobic tail and a negatively charged ionic functional group at its head. When the concentration of SDS is sufficiently large a micelle forms. A **micelle** consists of a spherical agglomeration of 40–100 surfactant molecules in which the hydrocarbon tails point inward and the negatively charged heads point outward (Figure 12.64b).

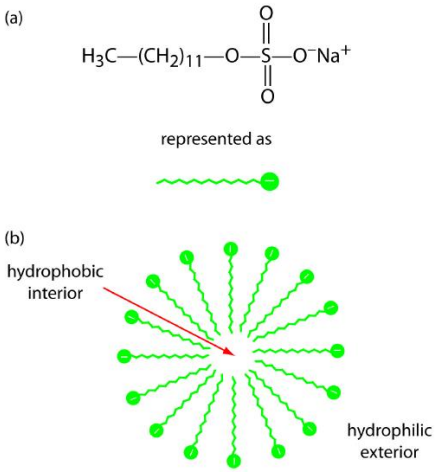


***Figure 12.64**: (a) Structure of sodium dodecylsulfate and its representation, and (b) cross section through a micelle showing its hydrophobic interior and its hydrophilic exterior.*

Because micelles have a negative charge, they migrate toward the cathode with a velocity less than the electroosmotic flow velocity. Neutral species partition themselves between the micelles and the buffer solution in a manner similar to the partitioning of solutes between the two liquid phases in HPLC. Because there is a partitioning between two phases, we include the descriptive term chromatography in the techniques name. Note that in MEKC both phases are mobile.

The elution order for neutral species in MEKC depends on the extent to which each partitions into the micelles. Hydrophilic neutrals are insoluble in the micelle's hydrophobic inner environment and elute as a single band, as they would in CZE. Neutral solutes that are extremely hydrophobic are completely soluble in the micelle, eluting with the micelles as a single band. Those neutral species that exist in a partition equilibrium between the buffer solution and the micelles elute between the completely hydrophilic and completely hydrophobic neutral species. Those neutral species favoring the buffer solution elute before those favoring the micelles. Micellar electrokinetic chromatography has been used to separate a wide variety of samples, including mixtures of pharmaceutical compounds, vitamins, and explosives.

Capillary Gel Electrophoresis (CGE)

In **capillary gel electrophoresis** the capillary tubing is filled with a polymeric gel. Because the gel is porous, a solute migrates through the gel with a velocity determined both by its electrophoretic mobility and by its size. The ability to effect a separation using size is helpful when the solutes have similar electrophoretic mobilities. For example, fragments of DNA of varying length have similar charge-to-size ratios, making their separation by CZE difficult. Because the DNA fragments are of different size, a CGE separation is possible.

The capillary used for CGE is usually treated to eliminate electroosmotic flow, preventing the gel's extrusion from the capillary tubing. Samples are injected electrokinetically because the gel provides too much resistance for hydrodynamic sampling. The primary application of CGE is the separation of large biomolecules, including DNA fragments, proteins, and oligonucleotides.

Capillary Electrochromatography (CEC)

Another approach to separating neutral species is **capillary electrochromatography**. In CEC the capillary tubing is packed with 1.5–3 μm particles coated with a bonded stationary phase. Neutral species separate based on their ability to partition between the stationary phase and the buffer, which is moving as a result of the electroosmotic flow; Figure 12.65 provides a representative example for the separation of a mixture of hydrocarbons. A CEC separation is similar to the analogous HPLC separation, but without the need for high pressure pumps. Efficiency in CEC is better than in HPLC, and analysis times are shorter.

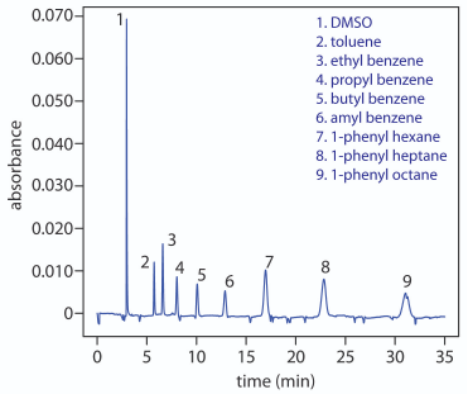


Figure 12.65 *Capillary electrochromatographic separation of a mixture of hydrocarbons in DMSO. The column contains a porous polymer of butyl methacrylate and lauryl acrylate (25%:75% mol:mol) with butane dioldacrylate as a crosslinker. Data provided by Zoe LaPier and Michelle Bushey, Department of Chemistry, Trinity University.*

Note

The best way to appreciate the theoretical and practical details discussed in this section is to carefully examine a typical analytical method. Although each method is unique, the following description of the determination of a vitamin B complex by capillary zone electrophoresis or by micellar electrokinetic capillary chromatography provides an instructive example of a typical procedure. The description here is based on Smyth, W. F. *Analytical Chemistry of Complex Matrices*, Wiley Teubner: Chichester, England, 1996, pp. 154–156.

Representative Method 12.3

Determination of a Vitamin B Complex by CZE or MEKC

Description of Method

The water soluble vitamins B_1 (thiamine hydrochloride), B_2 (riboflavin), B_3 (niacinamide), and B_6 (pyridoxine hydrochloride) are determined by CZE using a pH 9 sodium tetraborate-sodium dihydrogen phosphate buffer or by MEKC using the same buffer with the addition of sodium dodecyl sulfate. Detection is by UV absorption at 200 nm. An internal standard of *o*-ethoxybenzamide is used to standardize the method.

Procedure

Crush a vitamin B complex tablet and place it in a beaker with 20.00 mL of a 50 % v/v methanol solution that is 20 mM in sodium tetraborate and 100.0 ppm in *o*-ethoxybenzamide. After mixing for 2 min to ensure that the B vitamins are dissolved, pass a 5.00-mL portion through a 0.45-μm filter to remove insoluble binders. Load an approximately 4 nL sample into a capillary column with an inner diameter of a 50 μm. For CZE the capillary column contains a 20 mM pH 9 sodium tetraborate-sodium dihydrogen phosphate buffer. For MEKC the buffer is also 150 mM in sodium dodecyl sulfate. Apply a 40 kV/m electrical field to effect both the CZE and MEKC separations.

Questions

1. Methanol, which elutes at 4.69 min, is included as a neutral species to indicate the electroosmotic flow. When using standard solutions of each vitamin, CZE peaks are found at 3.41 min, 4.69 min, 6.31 min, and 8.31 min. Examine the structures and pK_a information in Figure 12.66 and identify the order in which the four B vitamins elute.

Vitamin B_1 is a cation and elutes before the neutral species methanol; thus it is the compound that elutes at 3.41 min. Vitamin B_3 is a neutral species and elutes with methanol at 4.69 min. The remaining two B vitamins are weak acids that partially ionize to weak base anions in the pH 9 buffer. Of the two, vitamin B_6 is the stronger acid (a pK_a of 9.0 versus a pK_a of 9.7) and is present to a greater extent in its anionic form. Vitamin B_6, therefore, is the last of the vitamins to elute.

2. The order of elution when using MEKC is vitamin B_3 (5.58 min), vitamin B_6 (6.59 min), vitamin B_2 (8.81 min), and vitamin B_1 (11.21 min). What conclusions can you make about the solubility of the B vitamins in the sodium dodecylsulfate micelles? The micelles elute at 17.7 min.

The elution time for vitamin B_1 shows the greatest change, increasing from 3.41 min to 11.21 minutes. Clearly vitamin B_1 has the greatest solubility in the micelles. Vitamin B_2 and vitamin B_3 have a more limited solubility in the micelles, showing only slightly longer elution times in the presence of the micelles. Interestingly, the elution time for vitamin B_6 decreases in the presence of the micelles.

3. For quantitative work an internal standard of o-ethoxybenzamide is added to all samples and standards. Why is an internal standard necessary?

Although the method of injection is not specified, neither a hydrodynamic injection nor an electrokinetic injection is particularly reproducible. The use of an internal standard compensates for this limitation.

(You can read more about the use of internal standards in capillary electrophoresis in the following paper: Altria, K. D. "Improved Performance in Capillary Electrophoresis Using Internal Standards," LC.GC Europe, September 2002.)

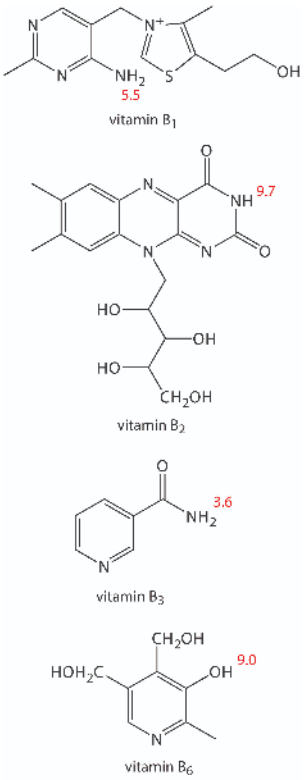


Figure 12.66: *Structures of the four water soluble B vitamins in their predominate forms at a pH of 9; pK_a values are shown in red.*

12.7.4 Evaluation

When compared to GC and HPLC, capillary electrophoresis provides similar levels of accuracy, precision, and sensitivity, and a comparable degree of selectivity. The amount of material injected into a capillary electrophoretic column is significantly smaller than that for GC and HPLC—typically 1 nL versus 0.1 µL for capillary GC and 1–100 µL for HPLC. Detection limits for capillary electrophoresis, however, are 100–1000 times poorer than that for GC and HPLC. The most significant advantages of capillary electrophoresis are improvements in separation efficiency, time, and cost. Capillary electrophoretic columns contain substantially more theoretical plates ($\approx 10^6$ plates/m) than that found in HPLC ($\approx 10^5$ plates/m) and capillary GC columns ($\approx 10^3$ plates/m), providing unparalleled resolution and peak capacity. Separations in capillary electrophoresis are fast and efficient. Furthermore, the capillary column's small volume means that a capillary electrophoresis separation requires only a few microliters of buffer solution, compared to 20–30 mL of mobile phase for a typical HPLC separation.

> **Note**
>
> See Section 12.4.8 for an evaluation of gas chromatography, and Section 12.5.6 for an evaluation of high-performance liquid chromatography.

Contributors

David Harvey (DePauw University)

12.7: Electrophoresis is shared under a CC BY-NC-SA 4.0 license and was authored, remixed, and/or curated by LibreTexts.

12.E: Chromatographic and Electrophoretic Methods (Exercises)

1. The following data were obtained for four compounds separated on a 20-m capillary column.

compound	t_r (min)	w (min)
A	8.04	0.15
B	8.26	0.15
C	8.43	0.16

a. Calculate the number of theoretical plates for each compound and the average number of theoretical plates for the column.
b. Calculate the average height of a theoretical plate.
c. Explain why it is possible for each compound to have a different number of theoretical plates.

2. Using the data from Problem 1, calculate the resolution and the selectivity factors for each pair of adjacent compounds. For resolution, use both equation 12.1 and equation 12.19, and compare your results. Discuss how you might improve the resolution between compounds B and C. The retention time for an nonretained solute is 1.19 min.

3. Using the chromatogram in Figure 12.67, obtained using a 2-m column, determine values for t_r, w, t_r', k, N, and H.

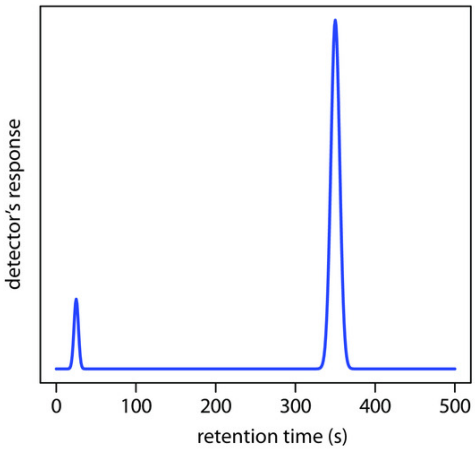


Figure 12.67 Chromatogram for Problem 12.3.

4. Using the partial chromatogram in Figure 12.68, determine the resolution between the two solute bands.

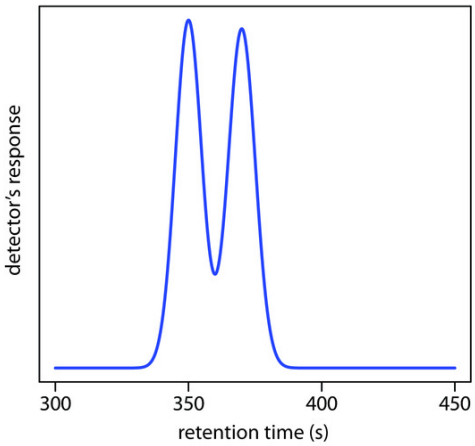


Figure 12.68 Chromatogram for Problem 12.4.

5. The chromatogram in Problem 4 was obtained on a 2-m column with a column dead time of 50 s. Suppose you want to increase the resolution between the two components to 1.5. Without changing the height of a theoretical plate, what length column do you need? What height of a theoretical plate do you need to achieve a resolution of 1.5 without increasing the column's length?

6. Complete the following table.

N_B	α	k_B	R
100000	1.05	0.50	
10000	1.10		1.50
10000		4.0	1.00
	1.05	3.0	1.75

7. Moody studied the efficiency of a GC separation of 2-butanone on a dinonyl phthalate column.[16] Evaluating plate height as a function of flow rate gave a van Deemter equation for which A is 1.65 mm, B is 25.8 mm•mL min^{-1}, and C is 0.0236 mm•min mL^{-1}.

a. Prepare a graph of H versus u for flow rates in the range of 5–120 mL/min.
b. For what range of flow rates does each term in the Van Deemter equation have the greatest effect?
c. What is the optimum flow rate and the corresponding height of a theoretical plate?
d. For open-tubular columns the A term is no longer needed. If the B and C terms remain unchanged, what is the optimum flow rate and the corresponding height of a theoretical plate?
e. Compared to the packed column, how many more theoretical plates are there in the open-tubular column?

8. Hsieh and Jorgenson prepared 12–33-μm inner diameter HPLC columns packed with 5.44-μm spherical stationary phase particles. To evaluate these columns they measured reduced plate height, h, as a function of reduced flow rate, v,

$$h = \frac{H}{d_p} \quad v = \frac{ud_p}{D_m} \tag{12.E.1}$$

where d_p is the particle diameter and D_m is the solute's diffusion coefficient in the mobile phase.

Note

When comparing columns, chromatographers often use dimensionless, reduced parameters. By including particle size and the solute's diffusion coefficient, the reduced plate height and reduced flow rate correct for differences between the packing material, the solute, and the mobile phase.

The data were analyzed using van Deemter plots. The following table contains a portion of their results for norepinephrine.

internal diameter (μm)	A	B	C
33	0.63	1.32	0.10
33	0.67	1.30	0.08
23	0.40	1.34	0.09
23	0.58	1.11	0.09
17	0.31	1.47	0.11
17	0.40	1.41	0.11
12	0.22	1.53	0.11
12	0.19	1.27	0.12

a. Construct separate van Deemter plots using the data in the first row and the last row for flow rates in the range 0.7–15. Determine the optimum flow rate and plate height for each case given d_p = 5.44 μm and $D_m = 6.23 \times 10^{-6}$ cm^2 s^{-1}.
b. The *A* term in the van Deemter equation appears to be strongly correlated with the column's inner diameter, with smaller diameter columns providing smaller values of *A*. Offer an explanation for this observation. *Hint: consider how many particles can fit across a capillary of each diameter.*

9. A mixture of *n*-heptane, tetrahydrofuran, 2-butanone, and *n*-propanol elutes in this order when using a polar stationary phase such as Carbowax. The elution order is exactly the opposite when using a nonpolar stationary phase such as polydimethyl siloxane. Explain the order of elution in each case.

10. The analysis of trihalomethanes in drinking water is described in Representative Method 12.1. A single standard containing all four trihalomethanes gives the following results.

compound	concentration (ppb)	peak area
$CHCl_3$	1.30	1.35×10^4
$CHCl_2Br$	0.90	6.12×10^4
$CHClBr_2$	4.00	1.71×10^4
$CHBr_3$	1.20	1.52×10^4

Analysis of water from a drinking fountain gives areas of 1.56×10^4, 5.13×10^4, 1.49×10^4, and 1.76×10^4 for $CHCl_3$ $CHCl_2Br$, $CHClBr_2$, and $CHBr_3$, respectively. All peak areas have been corrected for variations in injection volumes using an internal standard of 1,2-dibromopentane. Determine the concentration of each of the trihalomethanes in the sample of water.

11. Zhou and colleagues determined the %w/w H_2O in methanol by capillary column GC using a nonpolar stationary phase and a thermal conductivity detector.[17] A series of calibration standards gave the following results.

%w/w H_2O	peak height (arb. units)
0.00	1.15
0.0145	2.74
0.0472	6.33
0.0951	11.58
0.1757	20.43
0.2901	32.97

a. What is the %w/w H_2O in a sample giving a peak height of 8.63?
b. The %w/w H_2O in a freeze-dried antibiotic is determined in the following manner. A 0.175-g sample is placed in a vial along with 4.489 g of methanol. Water in the vial extracts into the methanol. Analysis of the sample gave a peak height of 13.66. What is the %w/w H_2O in the antibiotic?

12. Loconto and co-workers describe a method for determining trace levels of water in soil.[18] The method takes advantage of the reaction of water with calcium carbide, CaC_2, to produce acetylene gas, C_2H_2. By carrying out the reaction in a sealed vial, the amount of acetylene produced may be determined by sampling the headspace. In a typical analysis a sample of soil is placed in a sealed vial with CaC_2. Analysis of the headspace gave a blank corrected signal of 2.70×10^5. A second sample is prepared in the same manner except that a standard addition of 5.0 mg H_2O/g solid is added, giving a blank-corrected signal of 1.06×10^6. Determine the milligrams H_2O/g soil in the soil sample.

13. Van Atta and Van Atta used gas chromatography to determine the %v/v methyl salicylate in rubbing alcohol.[19] A set of standard additions was prepared by transferring 20.00 mL of rubbing alcohol to separate 25-mL volumetric flasks and pipeting 0.00 mL, 0.20 mL, and 0.50 mL of methyl salicylate to the flasks. All three flasks were then diluted to volume using isopropanol. Analysis of

the three samples gave peak heights for methyl salicylate of 57.00 mm, 88.5 mm, and 132.5 mm, respectively. Determine the %v/v methyl salicylate in the rubbing alcohol.

14. The amount of camphor in an analgesic ointment can be determined by GC using the method of internal standards.[20] A standard sample was prepared by placing 45.2 mg of camphor and 2.00 mL of a 6.00 mg/mL internal standard solution of terpene hydrate in a 25-mL volumetric flask and diluting to volume with CCl_4. When an approximately 2-µL sample of the standard was injected, the FID signals for the two components were measured (in arbitrary units) as 67.3 for camphor and 19.8 for terpene hydrate. A 53.6-mg sample of an analgesic ointment was prepared for analysis by placing it in a 50-mL Erlenmeyer flask along with 10 mL of CCl_4. After heating to 50°C in a water bath, the sample was cooled to below room temperature and filtered. The residue was washed with two 5-mL portions of CCl_4 and the combined filtrates were collected in a 25-mL volumetric flask. After adding 2.00 mL of the internal standard solution, the contents of the flask were diluted to volume with CCl_4. Analysis of an approximately 2-µL sample gave FID signals of 13.5 for the terpene hydrate and 24.9 for the camphor. Report the %w/w camphor in the analgesic ointment.

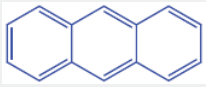
15. The concentration of pesticide residues on agricultural products, such as oranges, may be determined by GC-MS.[21] Pesticide residues are extracted from the sample using methylene chloride and concentrated by evaporating the methylene chloride to a smaller volume. Calibration is accomplished using anthracene-d_{10} as an internal standard. In a study to determine the parts per billion heptachlor epoxide on oranges, a 50.0-g sample of orange rinds was chopped and extracted with 50.00 mL of methylene chloride. After removing any insoluble material by filtration, the methylene chloride was reduced in volume, spiked with a known amount of the internal standard and diluted to 10 mL in a volumetric flask. Analysis of the sample gives a peak–area ratio ($A_{analyte}/A_{int\ std}$) of 0.108. A series of calibration standards, each containing the same amount of anthracene-d_{10} as the sample, gave the following results.

ppb heptachlor epoxide	$A_{analyte}/A_{int\ std}$
20.0	0.065
60.0	0.153
200.0	0.637
500.0	1.554
1000.0	3.198

Report the nanograms per gram of heptachlor epoxide residue on the oranges.

Note

Anthracene consists of three fused aromatic rings and has the formula $C_{14}H_{10}$.



In anthracene-d_{10} all ten hydrogens are replaced with deuteriems.

16. The adjusted retention times for octane, toluene, and nonane on a particular GC column are 15.98 min, 17.73 min, and 20.42 min, respectively. What is the retention index for each compound?

17. The following data were collected for a series of normal alkanes using a stationary phase of Carbowax 20M.

alkane	t_r' (min)
pentane	0.79
hexane	1.99
heptane	4.47
octane	14.12
nonane	33.11

What is the retention index for a compound whose adjusted retention time is 9.36 min?

18. The following data have been reported for the gas chromatographic analysis of *p*-xylene and methylisobutylketone (MIBK) on a capillary column.[9]

injection mode	compound	t_r (min)	peak area (arb. units)	peak width (min)
split	MIBK	1.878	54 285	0.028
	p-xylene	5.234	123 483	0.044
splitless	MIBK	3.420	2 493 005	1.057
	p-xylene	5.795	3 396 656	1.051

Explain the difference in the retention times, the peak areas, and the peak widths when switching from a split injection to a splitless injection.

19. Otto and Wegscheider report the following retention factors for the reversed-phase separation of 2-aminobenzoic acid on a C_{18} column when using 10% v/v methanol as a mobile phase.[22]

pH	*k*
2.0	10.5
3.0	16.7
4.0	15.8
5.0	8.0
6.0	2.2
7.0	1.8

Explain why pH affects the retention factor's value.

20. Haddad and associates report the following retention factors for the reversed-phase separation of salicylamide and caffeine.

%v/v methanol	30%	35%	40%	45%	50%	55%
k_{sal}	2.4	1.6	1.6	1.0	0.7	0.7
k_{caff}	4.3	2.8	2.3	1.4	1.1	0.9

a. Explain the trends in the retention factors for these compounds.
b. What is the advantage of using a mobile phase with a smaller %v/v methanol? Are there any disadvantages?

21. Suppose you need to separate a mixture of benzoic acid, aspartame, and caffeine in a diet soda. The following information is available.

	t_r in aqueous mobile phase of pH			
compound	3.0	3.5	4.0	4.5
benzoic acid	7.4	7.0	6.9	4.4
aspartame	5.9	6.0	7.1	8.1
caffeine	3.6	3.7	4.1	4.4

(a) Explain the change in retention time for each compound.

(b) Prepare a single graph showing the retention time versus pH for each compound. Using your plot, identify a pH level that will yield an acceptable separation.

22. The composition of a multivitamin tablet is conveniently determined using an HPLC with a diode array UV/Vis detector. A 5-µL standard sample containing 170 ppm vitamin C, 130 ppm niacin, 120 ppm niacinamide, 150 ppm pyridoxine, 60 ppm thiamine, 15 ppm folic acid, and 10 ppm riboflavin is injected into the HPLC, giving signals (in arbitrary units) of, respectively, 0.22, 1.35, 0.90, 1.37, 0.82, 0.36, and 0.29. The multivitamin tablet is prepared for analysis by grinding into a powder and transferring to a 125-mL Erlenmeyer flask containing 10 mL of 1% v/v NH_3 in dimethyl sulfoxide. After sonicating in an ultrasonic bath for 2 min, 90 mL of 2% acetic acid is added and the mixture is stirred for 1 min and sonicated at 40ºC for 5 min. The extract is then filtered through a 0.45-µm membrane filter. Injection of a 5-µL sample into the HPLC gives signals of 0.87 for vitamin C, 0.00 for niacin, 1.40 for niacinamide, 0.22 for pyridoxine, 0.19 for thiamine, 0.11 for folic acid, and 0.44 for riboflavin. Report the milligrams of each vitamin present in the tablet.

23. The amount of caffeine in an analgesic tablet was determined by HPLC using a normal calibration curve. Standard solutions of caffeine were prepared and analyzed using a 10-µL fixed-volume injection loop. Results for the standards are summarized in the following table.

concentration (ppm)	signal (arb. units)
50.0	8354
100.0	16925
150.0	25218
200.0	33584
250.0	42002

The sample was prepared by placing a single analgesic tablet in a small beaker and adding 10 mL of methanol. After allowing the sample to dissolve, the contents of the beaker, including the insoluble binder, were quantitatively transferred to a 25-mL volumetric flask and diluted to volume with methanol. The sample was then filtered, and a 1.00-mL aliquot was transferred to a 10-mL volumetric flask and diluted to volume with methanol. When analyzed by HPLC, the signal for caffeine was found to be 21 469. Report the milligrams of caffeine in the analgesic tablet.

24. Kagel and Farwell report a reversed-phase HPLC method for determining the concentration of acetylsalicylic acid (ASA) and caffeine (CAF) in analgesic tablets using salicylic acid (SA) as an internal standard.[23] A series of standards was prepared by adding known amounts of acetylsalicylic acid and caffeine to 250-mL Erlenmeyer flasks and adding 100 mL of methanol. A 10.00-mL

aliquot of a standard solution of salicylic acid was then added to each. The following results are obtained for a typical set of standard solutions.

	milligrams of		peak height ratios for	
standard	ASA	CAF	ASA/SA	CAF/SA
1	200.0	20.0	20.5	10.6
2	250.0	40.0	25.1	23.0
3	300.0	60.0	30.9	36.8

A sample of an analgesic tablet was placed in a 250-mL Erlenmeyer flask and dissolved in 100 mL of methanol. After adding a 10.00-mL portion of the internal standard, the solution was filtered. Analysis of the sample gave a peak height ratio of 23.2 for ASA and of 17.9 for CAF.

a. Determine the milligrams of ASA and CAF in the tablet.
b. Why was it necessary to filter the sample?
c. The directions indicate that approximately 100 mL of methanol is used to dissolve the standards and samples. Why is it not necessary to measure this volume more precisely?
d. In the presence of moisture, ASA decomposes to SA and acetic acid. What complication might this present for this analysis? How might you evaluate whether this is a problem?

25. Bohman and colleagues described a reversed-phase HPLC method for the quantitative analysis of vitamin A in food using the method of standard additions.[24] In a typical example, a 10.067-g sample of cereal is placed in a 250-mL Erlenmeyer flask along with 1 g of sodium ascorbate, 40 mL of ethanol, and 10 mL of 50% w/v KOH. After refluxing for 30 min, 60 mL of ethanol is added and the solution cooled to room temperature. Vitamin A is extracted using three 100-mL portions of hexane. The combined portions of hexane are evaporated and the residue containing vitamin A transferred to a 5-mL volumetric flask and diluted to volume with methanol. A standard addition is prepared in a similar manner using a 10.093-g sample of the cereal and spiking with 0.0200 mg of vitamin A. Injecting the sample and standard addition into the HPLC gives peak areas of, respectively, 6.77×10^3 and 1.32×10^4. Report the vitamin A content of the sample in milligrams/100 g cereal.

26. Ohta and Tanaka reported an ion-exchange chromatographic method for the simultaneous analysis of several inorganic anions and the cations Mg^{2+} and Ca^{2+} in water.[25] The mobile phase includes 1,2,4-benzenetricarboxylate, which absorbs strongly at 270 nm. Indirect detection of the analytes is possible because their presence in the detector leads to a decrease in absorbance. Unfortunately, Ca^{2+} and Mg^{2+}, which are present at high concentrations in many environmental waters, form stable complexes with 1,2,4-benzenetricarboxylate that interfere with their analysis.

(a) The procedure calls for adding EDTA to the mobile phase. What role does the EDTA play in this analysis?

(b) A standard solution containing 1.0 M $NaHCO_3$, 0.2 mM $NaNO_2$, 0.2 mM $MgSO_4$, 0.1 mM $CaCl_2$, and 0.1 mM $Ca(NO_3)_2$ gives the following peak areas (arbitrary units).

ion	HCO_3^-	Cl^-	NO_2^-	NO_3^-
peak area	373.5	322.5	264.8	262.7
ion	Ca^{2+}	Mg^{2+}	SO_4^{2-}	
peak area	458.9	352.0	341.3	

Analysis of a river water sample (pH of 7.49) gives the following results.

ion	HCO_3^-	Cl^-	NO_2^-	NO_3^-
peak area	310.0	403.1	3.97	157.6
ion	Ca^{2+}	Mg^{2+}	SO_4^{2-}	
peak area	734.3	193.6	324.3	

Determine the concentration of each ion in the sample.

(c) The detection of HCO_3^- actually gives the total concentration of carbonate in solution ($[CO_3^{2-}] + [HCO_3^-] + [H_2CO_3]$). Given that the pH of the water is 7.49, what is the actual concentration of HCO_3^-?

(d) An independent analysis gives the following additional concentrations for ions in the sample: $[Na^+]$ = 0.60 mM; $[NH_4^+]$ = 0.014 mM; and $[K^+]$ = 0.046 mM. A solution's ion balance is defined as the ratio of the total cation charge to the total anion charge. Determine the ion balance for this sample of water and comment on whether the result is reasonable.

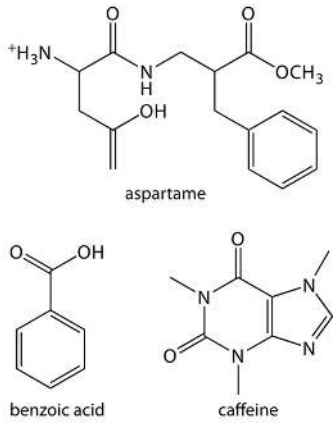
27. The concentrations of Cl^-, NO_3^-, and SO_4^{2-} may be determined by ion chromatography. A 50-μL standard sample of 10.0 ppm Cl^-, 2.00 ppm NO_3^-, and 5.00 ppm SO_4^{2-} gave signals (in arbitrary units) of 59.3, 16.1, and 6.08 respectively. A sample of effluent from a wastewater treatment plant was diluted tenfold, and a 50 μL portion gave signals of 44.2 for Cl^-, 2.73 for NO_3^-, and 5.04 for SO_4^{2-}. Report the parts per million for each anion in the effluent sample.

28. A series of polyvinylpyridine standards of different molecular weight were analyzed by size-exclusion chromatography, yielding the following results.

formula weight	retention volume (mL)
600000	6.42
100000	7.98
20000	9.30
3000	10.94

When a preparation of polyvinylpyridine of unknown formula weight is analyzed, the retention volume is 8.45 mL. Report the average formula weight for the preparation.

29. Diet soft drinks contain appreciable quantities of aspartame, benzoic acid, and caffeine. What is the expected order of elution for these compounds in a capillary zone electrophoresis separation using a pH 9.4 buffer solution given that aspartame has pK_a values of 2.964 and 7.37, benzoic acid has a pK_a of 4.2, and the pK_a for caffeine is less than 0. Figure 12.69 provides the structures of these compounds.



https://chem.libretexts.org/@go/page/70723

Figure 12.69 Structures for the compounds in Problem 12.29.

30. Janusa and coworkers describe the determination of chloride by CZE.[26] Analysis of a series of external standards gives the following calibration curve.

$$\text{area} = -883 + 5590 \times \text{ppm } Cl^- \tag{12.E.2}$$

A standard sample of 57.22% w/w Cl^- was analyzed by placing 0.1011-g portions in separate 100-mL volumetric flasks and diluting to volume. Three unknowns were prepared by pipeting 0.250 mL, 0.500 mL, and 0.750 mL of the bulk unknown in separate 50-mL volumetric flasks and diluting to volume. Analysis of the three unknowns gave areas of 15 310, 31 546, and 47 582, respectively. Evaluate the accuracy of this analysis.

31. The analysis of NO_3^- in aquarium water was carried out by CZE using IO_4^- as an internal standard. A standard solution of 15.0 ppm NO_3^- and 10.0 ppm IO_4^- gives peak heights (arbitrary units) of 95.0 and 100.1, respectively. A sample of water from an aquarium is diluted 1:100, and sufficient internal standard added to make its concentration 10.0 ppm. Analysis gives signals of 29.2 and 105.8 for NO_3^- and IO_4^-, respectively. Report the ppm NO_3^- in the sample of aquarium water.

32. Suggest conditions for separating a mixture of 2-aminobenzoic acid (pK_{a1} = 2.08, pK_{a2} = 4.96), benzylamine (pK_a = 9.35), and 4-methylphenol (pK_{a2} = 10.26) by capillary zone electrophoresis. Figure 12.70 provides the structures of these compounds.

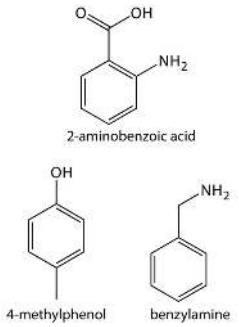


Figure 12.70 Structures for the compounds in Problem 12.32.

33. McKillop and associates examined the electrophoretic separation of some alkylpyridines by CZE.[27] Separations were carried out using either 50-µm or 75-µm inner diameter capillaries, with a total length of 57 cm and a length of 50 cm from the point of injection to the detector. The run buffer was a pH 2.5 lithium phosphate buffer. Separations were achieved using an applied voltage of 15 kV. The electroosmotic flow velocity, as measured using a neutral marker, was found to be 6.398×10^{-5} $cm^2\ V^{-1}\ s^{-1}$.

(a) Calculate the electrophoretic mobility for 2-ethylpyridine given that its elution time is 8.20 min.

(b) How many theoretical plates are there for 2-ethylpyridine?

(c) The electrophoretic mobilities for 3-ethylpyridine and 4-ethylpyridine are 3.366×10^{-4} $cm^2\ V^{-1}\ s^{-1}$ and 3.397 x $\times 10^{-4}$ $cm^2\ V^{-1}\ s^{-1}$, respectively. What is the expected resolution between these two alkylpyridines?

(d) Explain the trends in electrophoretic mobility shown in the following table.

alkylpyridine	μ_{ep} ($cm^2\ V^{-1}\ s^{-1}$)
2-methylpyridine	3.581×10^{-4}
2-ethylpyridine	3.222×10^{-4}
2-propylpyridine	2.923×10^{-4}
2-pentylpyridine	2.534×10^{-4}
2-hexylpyridine	2.391×10^{-4}

(e) Explain the trends in electrophoretic mobility shown in the following table.

alkylpyridine	μ_{ep} ($cm^2\ V^{-1}\ s^{-1}$)
2-ethylpyridine	3.222×10^{-4}
3-ethylpyridine	3.366×10^{-4}
4-ethylpyridine	3.397×10^{-4}

(f) The pK_a for pyridine is 5.229. At a pH of 2.5 the electrophoretic mobility of pyridine is 4.176×10^{-4} $cm^2\ V^{-1}\ s^{-1}$. What is the expected electrophoretic mobility if the run buffer's pH is 7.5?

12.8.3 Solutions to Practice Exercises

Practice Exercise 12.1

Because the relationship between elution time and distance is proportional, we can measure Δt_r, w_A, and w_B using a ruler. My measurements are 8.5 mm for Δt_r, and 12.0 mm each for w_A and w_B. Using these values, the resolution is

$$R_{AB} = \frac{2\Delta t_r}{w_A + w_B} = \frac{2(8.5\ \text{mm})}{12.0\ \text{mm} + 12.0\ \text{mm}} = 0.70 \tag{12.E.3}$$

Note

The data for this exercise were created so that the actual resolution is 0.75. Given the resolution of my ruler's scale, my answer is a pretty reasonable. Your measurements may be slightly different, but your answer should be close to the actual value.

Click here to return to the chapter.

Practice Exercise 12.2

Because the relationship between elution time and distance is proportional, we can measure t_m, $t_{r,1}$, and $t_{r,2}$ using a ruler. My measurements are 7.8 mm, 40.2 mm, and 51.5 mm, respectively. Using these values, the retention factors for solute A and solute B are

$$k_1 = \frac{t_r - t_m}{t_m} = \frac{40.2\ \text{mm} - 7.8\ \text{mm}}{7.8\ \text{mm}} = 4.15 \tag{12.E.4}$$

$$k_2 = \frac{t_r - t_m}{t_m} = \frac{51.5\ \text{mm} - 7.8\ \text{mm}}{7.8\ \text{mm}} = 5.60 \tag{12.E.5}$$

Note

The data for this exercise were created so that the actual retention factors are 4 for solute 1 and 5.5 for solute 2. Given the resolution of my ruler's scale, my answers are pretty reasonable. Your measurements may be slightly different, but your answers should be close to the actual values.

Click here to return to the chapter.

Practice Exercise 12.3

Using the results from Practice Exercise 12.2, the selectivity factor is

$$\alpha = \frac{k_2}{k_1} = \frac{5.60}{4.15} = 1.35 \tag{12.E.6}$$

Your answer may differ slightly due to differences in your values for the two retention factors.

Note

The data for this exercise were created so that the actual selectivity factor is 1.375. Given the resolution of my ruler's scale, my answer is pretty reasonable. Your measurements may be slightly different, but your answer should be close to the actual values.

Click here to return to the chapter.

Practice Exercise 12.4

Because the relationship between elution time and distance is proportional, we can measure $t_{r,1}$, $t_{r,2}$, w_1, and w_2 using a ruler. My measurements are 40.2 mm, 51.5 mm, 8.0 mm, and 13.5 mm, respectively. Using these values, the number of theoretical plates for each solute is

$$N_1 = 16\frac{t_{r,1}^2}{w_1^2} = 16\frac{(40.2\text{ mm})^2}{(8.0\text{ mm})^2} = 400\text{ theoretical plates} \tag{12.E.7}$$

$$N_2 = 16\frac{t_{r,2}^2}{w_2^2} = 16\frac{(51.5\text{ mm})^2}{(13.5\text{ mm})^2} = 233\text{ theoretical plates} \tag{12.E.8}$$

Note

The data for this exercise were created so that the actual number of theoretical plates is 400 for solute 1 and 264 for solute 2. Given the resolution of my ruler's scale, my answer is pretty reasonable. Your measurements may be slightly different, but your answers should be close to the actual values.

The height of a theoretical plate for each solute is

$$H_1 = \frac{L}{N_1} = \frac{0.500\text{ m}}{400\text{ plates}} \times \frac{1000\text{ mm}}{\text{m}} = 1.2\text{ mm/plate} \tag{12.E.9}$$

$$H_2 = \frac{L}{N_2} = \frac{0.500\text{ m}}{233\text{ plates}} \times \frac{1000\text{ mm}}{\text{m}} = 2.15\text{ mm/plate} \tag{12.E.10}$$

Click here to return to the chapter.

Practice Exercise 12.5

The following table summarizes my measurements of the peak heights for each standard and the sample.

	peak heights (mm)		
[standard] (mg/mL)	internal standard	analyte	peak height ratio
0.20	35	7	0.20
0.40	41	16	0.39
0.60	44	27	0.61
0.80	48	39	0.81
1.00	41	41	1.00
sample	39	21	0.54

Figure 12.71a shows the calibration curve and calibration equation when we ignore the internal standard. Substituting the sample's peak height into the calibration equation gives the analyte's concentration in the sample as 0.49 mg/mL. The 95% confidence interval is ±0.24 mg/mL. The calibration curve shows quite a bit of scatter in the data because of uncertainty in the injection volumes.

Figure 12.71b shows the calibration curve and calibration equation when we include the internal standard. Substituting the sample's peak height ratio into the calibration equation gives the analyte's concentration in the sample as 0.54 mg/mL. The 95% confidence interval is ±0.04 mg/mL.

Note

The data for Practice Exercise 12.5 were created so that the analyte's actual concentration is 0.55 mg/mL. Given the resolution of my ruler's scale, my answer is pretty reasonable. Your measurements may be slightly different, but your answers should be close to the actual values.

To review the use of Excel or R for regression calculations and confidence intervals, see Chapter 5.5.

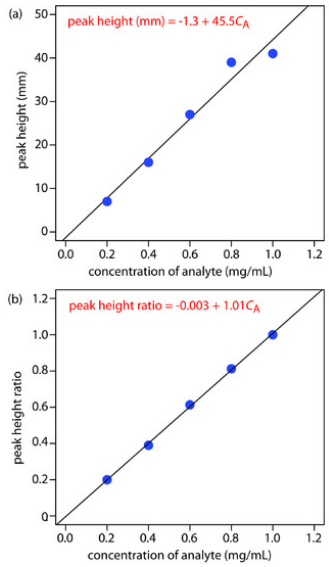


Figure 12.71 Calibration curves for the data in Practice Exercise 12.5.

Click here to return to the chapter.

Practice Exercise 12.6

Because we are using the same column we can assume that isobutane's retention index of 386 remains unchanged. Using equation 12.27, we have

$$386 = 100 \times \frac{\log x - \log(4.78)}{\log(6.86) - \log(4.78)} + 300 \tag{12.E.11}$$

where x is the retention time for isobutane. Solving for x, we find that

$$0.86 = \frac{\log x - 0.679}{0.836 - 0.679} \tag{12.E.12}$$

$$0.135 = \log x - 0.679 \tag{12.E.13}$$

$$0.814 = \log x \tag{12.E.14}$$

$$x = 6.52 \tag{12.E.15}$$

the retention time for isobutane is 6.52 min.

Click here to return to the chapter.

Practice Exercise 12.7

If we let x be the fraction of water in the mobile phase, then 1 – x is the fraction of methanol. Substituting these values into equation 12.28 and solving for x

$$7.5 = 10.2x + 5.1 \times (1 - x) \tag{12.E.16}$$

$$7.5 = 10.2x + 5.1 - 5.1x \tag{12.E.17}$$

$$2.4 = 5.1x \tag{12.E.18}$$

gives x as 0.47. The mobile phase is 47% v/v water and 53% v/v methanol.

Click here to return to the chapter.

Practice Exercise 12.8

Figure 12.72 shows the calibration curve and calibration equation for the set of external standards. Substituting the sample's peak area into the calibration equation gives the concentration of caffeine in the sample as 94.4 mg/L.

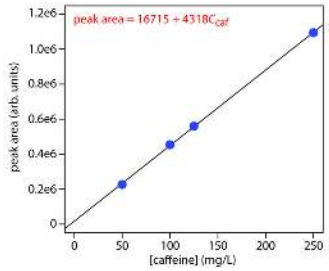


Figure 12.72 Calibration curves for the data in Practice Exercise 12.8.

Click here to return to the chapter.

Practice Exercise 12.9

The capillary is 75 cm long, which means that 0.20% of that sample's maximum length is 0.15 cm. To convert this to the maximum volume of sample we use the equation for the volume of a cylinder.

$$V_{inj} = l\pi r^2 = (0.15\text{ cm})(3.14)(25 \times 10^{-4}\text{ cm})^2 = 2.94 \times 10^{-6}\text{ cm}^3 \tag{12.E.19}$$

Given that 1 cm^3 is equivalent to 1 mL, the maximum volume is 2.94 × 10^{-6} mL of 2.94× 10^{-9} L. To find the maximum injection time, we first solve equation 12.45 for t

$$t = \frac{128 V_{inj} \eta L}{P d^4 \pi} \times 10^{-3}\text{ m}^3/\text{L} \tag{12.E.20}$$

and then make appropriate substitutions.

$$t = \frac{(128)(2.94 \times 10^{-9}\text{ L})(0.001\text{ kg m}^{-1}\text{ s}^{-1})(0.75\text{ m})}{2.5 \times 10^3\text{ kg m}^{-1}\text{ s}^{-2})(50 \times 10^{-6}\text{ m})^4(3.14)} \times \frac{10^{-3}\text{ m}^3}{\text{L}} = 5.8\text{ s} \tag{12.E.21}$$

The maximum injection time, therefore, is 5.8 s.

Click here to return to the chapter.

Contributors and Attributions

- David Harvey (DePauw University)

12.E: Chromatographic and Electrophoretic Methods (Exercises) is shared under a CC BY-NC-SA 4.0 license and was authored, remixed, and/or curated by LibreTexts.

12.S: Chromatographic and Electrophoretic Methods (Summary)

Chromatography and electrophoresis are powerful analytical techniques that both separate a sample into its components and provide a means for determining each component's concentration. Chromatographic separations utilize the selective partitioning of the sample's components between a stationary phase that is immobilized within a column and a mobile phase that passes through the column.

The effectiveness of a separation is described by the resolution between two chromatographic bands and is a function of each component's retention factor, the column's efficiency, and the column's selectivity. A solute's retention factor is a measure of its partitioning into the stationary phase, with larger retention factors corresponding to more strongly retained solutes. The column's selectivity for two solutes is the ratio of the their retention factors, providing a relative measure of the column's ability to retain the two solutes. Column efficiency accounts for those factors that cause a solute's chromatographic band to increase in width during the separation. Column efficiency is defined in terms of the number of theoretical plates and the height of a theoretical plate, the later of which is a function of a number of parameters, most notably the mobile phases' flow rate. Chromatographic separations are optimized by either increasing the number of theoretical plates, by increasing the column's selectivity, or by increasing the solute retention factor.

In gas chromatography the mobile phase is an inert gas and the stationary phase is a nonpolar or polar organic liquid that is either coated on a particulate material and packed into a wide-bore column, or coated on the walls of a narrow-bore capillary column. Gas chromatography is useful for the analysis of volatile components.

In high-performance liquid chromatography the mobile phase is either a nonpolar solvent (normal phase) or a polar solvent (reversed-phase). A stationary phase of opposite polarity, which is bonded to a particulate material, is packed into a wide-bore column. HPLC can be applied to a wider range of samples than GC; however, the separation efficiency for HPLC is not as good as that for GC.

Together, GC and HPLC account for the largest number of chromatographic separations. Other separation techniques, however, find specialized applications. Of particular importance are: ion-exchange chromatography for separating anions and cations; size-exclusion chromatography for separating large molecules; and supercritical fluid chromatography for the analysis of samples that are not easily analyzed by GC or HPLC.

In capillary zone electrophoresis a sample's components are separated based on their ability to move through a conductive medium under the influence of an applied electric field. Positively charged solutes elute first, with smaller, more highly charged cationic solutes eluting before larger cations of lower charge. Neutral species elute without undergoing further separation. Finally, anions elute last, with smaller, more negatively charged anions being the last to elute. By adding a surfactant, neutral species can be separated by micellar electrokinetic capillary chromatography. Electrophoretic separations also can take advantage of the ability of polymeric gels to separate solutes by size (capillary gel electrophoresis), and the ability of solutes to partition into a stationary phase (capillary electrochromatography). In comparison to GC and HPLC, capillary electrophoresis provides faster and more efficient separations.

12.8.1 Key Terms

adjusted retention time
adsorption chromatography
band broadening
baseline width
bleed
bonded stationary phase
capillary column
capillary electrochromatography
capillary electrophoresis
capillary gel electrophoresis
capillary zone electrophoresis
chromatogram
chromatography
column chromatography
counter-current extraction
cryogenic focusing
electrokinetic injection
electroosmotic flow
electroosmotic flow velocity
electron capture detector
electropherogram
electrophoresis
electrophoretic mobility
electrophoretic velocity
exclusion limit
flame ionization detector
fronting
gas chromatography
gas–liquid chromatography
gas–solid chromatography
general elution problem
guard column
gradient elution
headspace sampling
high-performance liquid chromatography
hydrodynamic injection
inclusion limit
ion-exchange chromatography
ion suppressor column
isocratic elution
isothermal
Joule heating
Kovat's retention index
liquid–solid adsorption chromatography
longitudinal diffusion
loop injector
mass spectrometer
mass spectrum
mass transfer
micelle
micellar electrokinetic capillary chromatography
mobile phase
monolithic column
multiple paths
nonretained solutes
normal-phase chromatography
on-column injection
open tubular column
packed columns
partition chromatography
peak capacity
planar chromatography
polarity index
porous-layer open tubular column
purge-and-trap
resolution
retention factor
retention time
reversed-phase chromatography
selectivity factor
single-column ion chromatography
solid-phase microextraction
split injection
splitless injection
stacking
stationary phase
supercritical fluid chromatography
support-coated open tubular column
tailing
temperature programming
theoretical plate
thermal conductivity detector
van Deemter equation
void time
wall-coated open-tubular column
zeta potential

References

1. Craig, L. C. *J. Biol. Chem.* **1944**, *155*, 519–534.
2. Martin, A. J. P.; Synge, R. L. M. *Biochem. J.* **1941**, *35*, 1358–1366.
3. Giddings, J. C. *Unified Separation Science*, Wiley-Interscience: New York, 1991.
4. Foley, J. P.; Dorsey, J. G. *Anal. Chem.* **1983**, *55*, 730–737.
5. Hawkes, S. J. *J. Chem. Educ.* **1983**, *60*, 393–398.
6. Kennedy, R. T.; Jorgenson, J. W. *Anal. Chem.* **1989**, *61*, 1128–1135.
7. Hinshaw, J. V.*LC·GC* **1993**, *11*, 644–648.
8. (a) Bicking, M. K. L. Chromatography Online, April 2006; (b) Bicking, M. K. L. Chromatography Online, June 2006.
9. Marriott, P. J.; Carpenter, P. D. *J. Chem. Educ.* **1996**, *73*, 96–99.
10. Novotony, M. *Science*, **1989**, *246*, 51–57.
11. Cabrera, K. Chromatography Online, April 1, 2008.
12. Snyder, L. R.; Glajch, J. L.; Kirkland, J. J. *Practical HPLC Method Development*, Wiley-Interscience: New York, 1988.
13. (a) Foley, J. P. *Chromatography*, **1987**, *7*, 118–128; (b) Foley, J. P.; May, W. E. Anal. Chem. 1987, 59, 102–109; (c) Foley, J. P.; May, W. E. Anal. Chem. 1987, 59, 110–115.
14. Harvey, D. T.; Byerly, S.; Bowman, A.; Tomlin, J. *J. Chem. Educ.* **1991**, *68*, 162–168
15. Jones, W. R.; Jandik, P. *J. Chromatog.* **1992**, *608*, 385–393.
16. Moody, H. W. *J. Chem. Educ.* **1982**, *59*, 218–219.
17. Zhou, X.; Hines, P. A.; White, K. C.; Borer, M. W. *Anal. Chem.* **1998**, *70*, 390–394.

18. Loconto, P. R.; Pan, Y. L.; Voice, T. C. *LC•GC* **1996**, *14*, 128–132.
19. Van Atta, R. E.; Van Atta, R. L. *J. Chem. Educ.* **1980**, *57*, 230–231.
20. Pant, S. K.; Gupta, P. N.; Thomas, K. M.; Maitin, B. K.; Jain, C. L. *LC•GC* **1990**, *8*, 322–325.
21. Feigel, C. *Varian GC/MS Application Note*, Number 52.
22. Otto, M.; Wegscheider, W. *J. Chromatog.* **1983**, *258*, 11–22.
23. Kagel, R. A.; Farwell, S. O. *J. Chem. Educ.* **1983**, *60*, 163–166.
24. Bohman, O.; Engdahl, K. A.; Johnsson, H. *J. Chem. Educ.* **1982**, *59*, 251–252.
25. Ohta, K.; Tanaka, K. *Anal. Chim. Acta* **1998**, *373*, 189–195.
26. Janusa, M. A.; Andermann, L. J.; Kliebert, N. M.; Nannie, M. H. *J. Chem. Educ.* **1998**, *75*, 1463–1465.
27. McKillop, A. G.; Smith, R. M.; Rowe, R. C.; Wren, S. A. C. *Anal. Chem.* **1999**, *71*, 497–503.

Contributors

David Harvey (DePauw University)

12.S: Chromatographic and Electrophoretic Methods (Summary) is shared under a CC BY-NC-SA 4.0 license and was authored, remixed, and/or curated by LibreTexts.

CHAPTER OVERVIEW

Back Matter

Index

Index

D

dire

CHAPTER OVERVIEW

13: Kinetic Methods

There are many ways to categorize analytical techniques, several of which we introduced in earlier chapters. In Chapter 3 we classified techniques by whether the signal is proportional to the absolute amount or the relative amount of analyte. For example, precipitation gravimetry is a total analysis technique because the precipitate's mass is proportional to the absolute amount, or moles, of analyte. UV/Vis absorption spectroscopy, on the other hand, is a concentration technique because absorbance is proportional to the relative amount, or concentration, of analyte.

A second method for classifying analytical techniques is to consider the source of the analytical signal. For example, gravimetry encompasses all techniques in which the analytical signal is a measurement of mass or a change in mass. Spectroscopy, on the other hand, includes those techniques in which we probe a sample with an energetic particle, such as the absorption of a photon. This is the classification scheme used in organizing Chapters 8–11.

Another way to classify analytical techniques is by whether the analyte's concentration is determined by an equilibrium reaction or by the kinetics of a chemical reaction or a physical process. The analytical methods described in Chapter 8–11 mostly involve measurements made on systems in which the analyte is always at equilibrium. In this chapter we turn our attention to measurements made under non-equilibrium conditions.

Topic hierarchy

13.1: Kinetic Methods Versus Equilibrium Methods
13.2: Chemical Kinetics
13.3: Radiochemistry
13.4: Flow Injection Analysis
13.E: Kinetic Methods (Exercises)
13.S: Kinetic Methods (Summary)

Thumbnail: Determination of a reaction's intermediate rate from the slope of a line tangent to a curve showing the change in the analyte's concentration as a function of time.

Contributors

- David Harvey (DePauw University)

13: Kinetic Methods is shared under a CC BY-NC-SA 4.0 license and was authored, remixed, and/or curated by LibreTexts.

13.1: Kinetic Methods Versus Equilibrium Methods

In an **equilibrium method** the analytical signal is determined by an equilibrium reaction involving the analyte or by a steady-state process that maintains the analyte's concentration. When we determine the concentration of iron in water by measuring the absorbance of the orange-red $Fe(phen)_3^{2+}$ complex (see Representative Method 10.1), the signal depends upon the concentration of $Fe(phen)_3^{2+}$, which, in turn, is determined by the complex's formation constant. In the flame atomic absorption determination of Cu and Zn in tissue samples (see Representative Method 10.2), the concentration of each metal in the flame remains constant because each step in the process of atomizing the sample is in a steady-state. In a **kinetic method** the analytical signal is determined by the rate of a reaction involving the analyte, or by a nonsteady-state process. As a result, the analyte's concentration changes during the time in which we are monitoring the signal.

In many cases, we can complete an analysis using either an equilibrium method or a kinetic method by simply changing the time at which we choose to measure the analytical signal. For example, one method for determining the concentration of nitrite, NO_2^-, in groundwater utilizes the two-step diazotization reaction shown in Figure 13.1.[1] The final product, which is a reddish-purple azo dye, absorbs visible light at a wavelength of 543 nm. Because neither reaction in Figure 13.1 is rapid, the absorbance—which is directly proportional to the concentration of NO_2^-—is measured 10 min after adding the last reagent, ensuring that it reaches the steady-state value required of an equilibrium method.

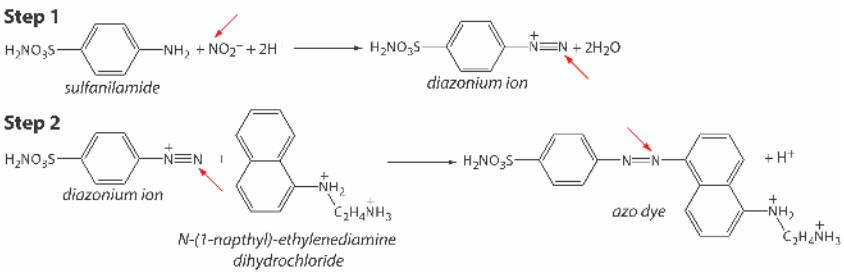


Figure 13.1 Analytical scheme for the analysis of NO_2^- in groundwater. The red arrow highlights the nitrogen in NO_2^- that becomes part of the azo dye.

We can use the same set of reactions as the basis for a kinetic method by measuring the absorbance during the 10-min development period, obtaining information about the reaction's rate. If the rate is a function of the concentration of NO_2^-, then we can use the rate to determine its concentration in the sample.[2]

There are many potential advantages to kinetic methods of analysis, perhaps the most important of which is the ability to use chemical reactions and systems that are slow to reach equilibrium. In this chapter we examine three techniques that rely on measurements made while the analytical system is under kinetic control: chemical kinetic techniques, in which we measure the rate of a chemical reaction; radiochemical techniques, in which we measure the decay of a radioactive element; and flow injection analysis, in which we inject the analyte into a continuously flowing carrier stream, where its mixing with and reaction with reagents in the stream are controlled by the kinetic processes of convection and diffusion.

Contributors

David Harvey (DePauw University)

13.1: Kinetic Methods Versus Equilibrium Methods is shared under a CC BY-NC-SA 4.0 license and was authored, remixed, and/or curated by LibreTexts.

13.2: Chemical Kinetics

The earliest analytical methods based on chemical kinetics—which first appear in the late nineteenth century—took advantage of the catalytic activity of enzymes. In a typical method of that era, an enzyme was added to a solution containing a suitable substrate and their reaction monitored for a fixed time. The enzyme's activity was determined by the change in the substrate's concentration. Enzymes also were used for the quantitative analysis of hydrogen peroxide and carbohydrates. The development of chemical kinetic methods continued in the first half of the twentieth century with the introduction of nonenzymatic catalysts and noncatalytic reactions.

Despite the diversity of chemical kinetic methods, by 1960 they were no longer in common use. The principal limitation to their broader acceptance was a susceptibility to significant errors from uncontrolled or poorly controlled variables—temperature and pH are two examples—and the presence of interferents that activate or inhibit catalytic reactions. By the 1980s, improvements in instrumentation and data analysis methods compensated for these limitations, ensuring the further development of chemical kinetic methods of analysis.[3]

13.2.1 Theory and Practice

Every chemical reaction occurs at a finite rate, making it a potential candidate for a chemical kinetic method of analysis. To be effective, however, the chemical reaction must meet three necessary conditions: the reaction must not occur too quickly or too slowly; we must know the reaction's rate law; and we must be able to monitor the change in concentration for at least one species. Let's take a closer look at each of these needs.

The material in this section assumes some familiarity with chemical kinetics, which is part of most courses in general chemistry. For a review of reaction rates, rate laws, and integrated rate laws, see the material in Appendix 17.

Reaction Rate

The **rate** of the chemical reaction—how quickly the concentrations of reactants and products change during the reaction—must be fast enough that we can complete the analysis in a reasonable time, but also slow enough that the reaction does not reach equilibrium while the reagents are mixing. As a practical limit, it is not easy to study a reaction that reaches equilibrium within several seconds without the aid of special equipment for rapidly mixing the reactants. We will discuss two examples of instrumentation for studying reactions with fast kinetics in Section 13.2.3.

Rate Law

The second requirement is that we must know the reaction's **rate law**—the mathematical equation describing how the concentrations of reagents affect the rate—for the period in which we are making measurements. For example, the rate law for a reaction that is first order in the concentration of an analyte, A, is

$$\text{rate} = -\frac{d[\text{A}]}{dt} = k[\text{A}] \tag{13.2.1}$$

where k is the reaction's **rate constant**.

> Because the concentration of A decreases during the reactions, d[A] is negative. The minus sign in Equation 13.2.1 makes the rate positive. If we choose to follow a product, P, then d[P] is positive because the product's concentration increases throughout the reaction. In this case we omit the minus sign; see Equation 13.2.45 for an example.

An **integrated rate law** often is a more useful form of the rate law because it is a function of the analyte's initial concentration. For example, the integrated rate law for Equation 13.2.1 is

$$\ln [\text{A}]_t = \ln [\text{A}]_0 - kt \tag{13.2.2}$$

or

$$[\text{A}]_t = [\text{A}]_0 e^{-kt} \tag{13.2.3}$$

where $[\text{A}]_0$ is the analyte's initial concentration and $[\text{A}]_t$ is the analyte's concentration at time t.

Unfortunately, most reactions of analytical interest do not follow a simple rate law. Consider, for example, the following reaction between an analyte, A, and a reagent, R, to form a single product, P

$$\mathrm{A} + \mathrm{R} \underset{k_b}{\overset{k_f}{\rightleftharpoons}} \mathrm{P} \tag{13.2.4}$$

where k_f is the rate constant for the forward reaction, and k_b is the rate constant for the reverse reaction. If the forward and reverse reactions occur as single steps, then the rate law is

$$\text{rate} = -\frac{d[\mathrm{A}]}{dt} = k_f[\mathrm{A}][\mathrm{R}] - k_b[\mathrm{P}] \tag{13.2.5}$$

The first term of Equation 13.2.5, $k_f[\mathrm{A}][\mathrm{R}]$ accounts for the loss of A as it reacts with R to make P, and the second term, $k_b[\mathrm{P}]$ accounts for the formation of A as P converts back to A and R.

Although we know the reaction's rate law, there is no simple integrated form that we can use to determine the analyte's initial concentration. We can simplify Equation 13.2.5 by restricting our measurements to the beginning of the reaction when the product's concentration is negligible. Under these conditions we can ignore the second term in Equation 13.2.5, which simplifies to

$$\text{rate} = -\frac{d[\mathrm{A}]}{dt} = k_f[\mathrm{A}][\mathrm{R}] \tag{13.2.6}$$

The integrated rate law for Equation 13.2.6, however, is still too complicated to be analytically useful. We can further simplify the kinetics by carefully adjusting the reaction conditions.[4] For example, we can ensure pseudo-first-order kinetics by using a large excess of R so that its concentration remains essentially constant during the time we are monitoring the reaction. Under these conditions Equation 13.2.6 simplifies to

$$\text{rate} = -\frac{d[\mathrm{A}]}{dt} = k_f[\mathrm{A}][\mathrm{R}]_0 = k'[\mathrm{A}] \tag{13.2.7}$$

where $k' = k_f[\mathrm{R}]_0$.

> To say that the reaction is pseudo-first-order in A means that the reaction behaves as if it is first order in A and zero order in R even though the underlying kinetics are more complicated. We call k' **the pseudo-first-order rate constant.**

The integrated rate laws for Equation 13.2.7 are

$$\ln [\mathrm{A}]_t = \ln [\mathrm{A}]_0 - k't \tag{13.2.8}$$

or

$$[\mathrm{A}]_t = [\mathrm{A}]_0 e^{-k't} \tag{13.2.9}$$

It may even be possible to adjust the conditions so that we use the reaction under pseudo-zero-order conditions.

$$\text{rate} = -\frac{d[\mathrm{A}]}{dt} = k_f[\mathrm{A}]_0[\mathrm{R}]_0 = k'' \tag{13.2.10}$$

$$[\mathrm{A}]_t = [\mathrm{A}]_0 - k''t \tag{13.2.11}$$

where $k'' = k_f[\mathrm{A}]_0[\mathrm{R}]_0$.

> To say that a reaction is pseudo-zero-order means that the reaction behaves as if it is zero order in A and zero order in R even though the underlying kinetics are more complicated. We call k'' the **pseudo-zero-order rate constant**.

Equation 13.2.11 is the integrated rate law for Equation 13.2.10.

Monitoring the Reaction

The final requirement is that we must be able to monitor the reaction^'s progress by following the change in concentration for at least one of its species. Which species we choose to monitor is not important. It can be the analyte, a reagent reacting with the

analyte, or a product. For example, we can determine concentration of phosphate in a sample by first reacting it with Mo(VI) to form 12.molybdophosphoric acid (12-MPA).

$$H_3PO_{4(aq)} + 6\,Mo(VI)^{+}_{(aq)} \rightarrow 12\text{-}MPA_{(aq)} + 9\,H^{+}_{(aq)} \tag{13.2.12}$$

Next, we reduce **12-MPA** to form heteropolyphosphomolybdenum blue, **PMB**. The rate of formation of PMB is measured spectrophotometrically, and is proportional to the concentration of 12-MPA. The concentration of 12-MPA, in turn, is proportional to the concentration of phosphate.[5] We also can follow reaction 13.11 spectrophotometrically by monitoring the formation of the yellow-colored 12-MPA.[6]

13.2.2 Classifying Chemical Kinetic Methods

Figure 13.2 provides one useful scheme for classifying chemical kinetic methods of analysis. Methods are divided into two main categories: direct-computation methods and curve-fitting methods. In a direct-computation method we calculate the analyte's initial concentration, $[A]_0$, using the appropriate rate law. For example, if the reaction is first-order in analyte, we can use Equation 13.2.2 to determine $[A]_0$ if we have values for k, t, and $[A]_t$. With a curve-fitting method, we use regression to find the best fit between the data—for example, $[A]_t$ as a function of time—and the known mathematical model for the rate law. If the reaction is first-order in analyte, then we fit Equation 13.2.2 to the data using k and $[A]_0$ as adjustable parameters.

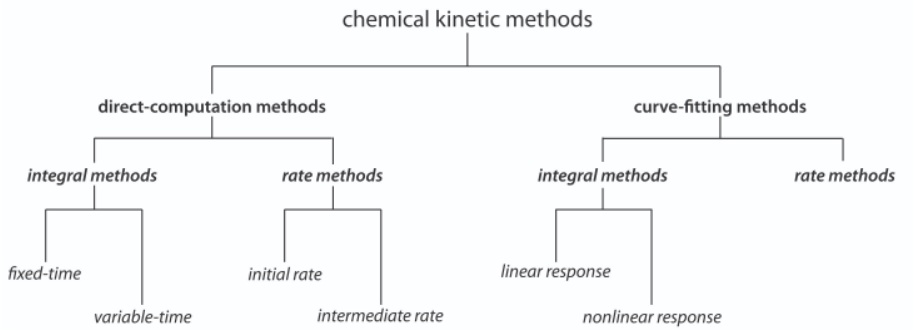


Figure 13.2: *Classification of chemical kinetic methods of analysis adapted from Pardue, H. L. "Kinetic Aspects of Analytical Chemistry," Anal. Chim. Acta* ***1989****, 216, 69–107.*

Direct-Computation Fixed-Time Integral Methods

A direct-computation integral method uses the integrated form of the rate law. In a **one-point fixed-time integral method**, for example, we determine the analyte's concentration at a single time and calculate the analyte's initial concentration, $[A]_0$, using the appropriate integrated rate law. To determine the reaction's rate constant, k, we run a separate experiment using a standard solution of analyte. Alternatively, we can determine the analyte's initial concentration by measuring $[A]_t$ for several standards containing known concentrations of analyte and constructing a calibration curve.

Example 13.1

The concentration of nitromethane, CH_3NO_2, can be determined from the kinetics of its decomposition reaction. In the presence of excess base the reaction is pseudo-first-order in nitromethane. For a standard solution of 0.0100 M nitromethane, the concentration of nitromethane after 2.00 s is 4.24×10^{-4} M. When a sample containing an unknown amount of nitromethane is analyzed, the concentration of nitromethane remaining after 2.00 s is 5.35×10^{-4} M. What is the initial concentration of nitromethane in the sample?

Solution

First, we determine the value for the pseudo-first-order rate constant, k'. Using Equation 13.2.8 and the result for the standard, we find its value is

$$k' = \frac{\ln [A]_0 - \ln [A]_t}{t} = \frac{\ln(0.0100) - \ln(4.24 \times 10^{-4})}{2.00\ s} = 1.58\ s^{-1} \tag{13.2.13}$$

Next we use Equation 13.2.9 to calculate the initial concentration of nitromethane in the sample.

$$[A]_0 = \frac{[A]_t}{e^{-k't}} = \frac{5.34 \times 10^{-4}\ M}{e^{-(1.58\ s^{-1})(2.00\ s)}} = 0.0126\ M \tag{13.2.14}$$

Note: Equation 13.2.8 and Equation 13.2.9 are equally appropriate integrated rate laws for a pseudo-first-order reaction. The decision to use Equation 13.2.8 to calculate k' and Equation 13.2.9 to calculate $[A]_0$ is a matter of convenience.

Exercise 13.1

In a separate determination for nitromethane, a series of external standards gives the following concentrations of nitromethane after a 2.00 s decomposition under pseudo-first-order conditions.

$[CH_3NO_2]_0$ (M)	$[CH_3NO_2]$ (M) at t = 2.00 s
0.0100	3.82×10^{-4}
0.0200	8.19×10^{-4}
0.0300	1.15×10^{-3}
0.0400	1.65×10^{-3}
0.0500	2.14×10^{-3}
0.0600	2.53×10^{-3}
0.0700	3.21×10^{-3}
0.0800	3.35×10^{-3}
0.0900	3.99×10^{-3}
0.100	4.15×10^{-3}

Analysis of a sample under the same conditions gives a nitromethane concentration of 2.21×10^{-3} M after 2 s. What is the initial concentration of nitromethane in the sample?

Click here to review your answer to this exercise.

In Example 13.1 we determined the initial concentration of analyte by measuring the amount of unreacted analyte. Sometimes it is more convenient to measure the concentration of a reagent that reacts with the analyte, or to measure the concentration of one of the reaction's products. We can still use a one-point fixed-time integral method if we know the reaction's stoichiometry. For example, if we measure the concentration of the product, P, in the reaction

$$A + R \rightarrow P \tag{13.2.15}$$

then the concentration of the analyte at time t is

$$[A]_t = [A]_0 - [P]_t \tag{13.2.16}$$

because the stoichiometry between the analyte and product is 1:1. If the reaction is pseudo-first-order in A, then substituting equation 13.2.16 into equation 13.2.8 gives

$$\ln([A]_0 - [P]_t) = \ln [A]_0 - k't \tag{13.2.17}$$

which we simplify by writing in exponential form.

$$[A]_0 - [P]_t = [A]_0 e^{-kt} \tag{13.2.18}$$

Finally, solving equation 13.2.18 for $[A]_0$ gives the following equation.

$$[A]_0 = \frac{[P]_t}{1 - e^{-kt}} \tag{13.2.19}$$

The kinetic method for phosphate described earlier is an example of a method in which we monitor the product. Because the phosphate ion does not absorb visible light, we incorporate it into a reaction that produces a colored product. That product, in turn, is converted into a different product that is even more strongly absorbing.

Example 13.2

The concentration of thiocyanate, SCN^-, can be determined from the pseudo-first-order kinetics of its reaction with excess Fe^{3+} to form a reddish colored complex of $Fe(SCN)^{2+}$. The reaction's progress is monitored by measuring the absorbance of $Fe(SCN)^{2+}$ at a wavelength of 480 nm. When using a standard solution of 0.100 M SCN^-, the concentration of $Fe(SCN)^{2+}$ after 10 s is 0.0516 M. The concentration of $Fe(SCN)^{2+}$ in a sample containing an unknown amount of SCN^- is 0.0420 M after 10 s. What is the initial concentration of SCN^- in the sample?

Figure 6.15 shows the color of a solution containing the $Fe(SCN)^{2+}$ complex.

Solution

First, we must determine a value for the pseudo-first-order rate constant, k'. Using equation 13.2.17, we find that its value is

$$k' = \frac{\ln [A]_0 - \ln([A]_0 - [P]_t)}{t} = \frac{\ln(0.100) - \ln(0.100 - 0.0516)}{10.0\ \text{s}} = 0.0726\ \text{s}^{-1} \tag{13.2.20}$$

Next, we use equation 13.15 to determine the initial concentration of SCN^- in the sample.

$$[A]_0 = \frac{[P]_t}{1 - e^{-k't}} = \frac{0.0420\ \text{M}}{1 - e^{-(0.0726\ \text{s}^{-1})(10.0\ \text{s})}} = 0.0814\ \text{M} \tag{13.2.21}$$

Exercise 13.2

In a separate determination for SCN^-, a series of external standards gives the following concentrations of $Fe(SCN)^{2+}$ after a 10.0 s reaction with excess Fe^{3+} under pseudo-first-order conditions.

$[SCN^-]_0$ (M)	$[Fe(SCN)^{2+}]$ (M) at t = 10.0 s
5.00×10^{-3}	1.79×10^{-3}
1.50×10^{-2}	8.24×10^{-3}
2.50×10^{-2}	1.28×10^{-2}
3.50×10^{-2}	1.85×10^{-2}
4.50×10^{-2}	2.21×10^{-2}
5.50×10^{-2}	2.81×10^{-2}
6.50×10^{-2}	3.27×10^{-2}
7.50×10^{-2}	3.91×10^{-2}
8.50×10^{-2}	4.34×10^{-2}
9.50×10^{-2}	4.89×10^{-2}

Analysis of a sample under the same conditions gives a $Fe(SCN)^{2+}$ concentration of 3.52×10^{-2} M after 10 s. What is the initial concentration of SCN^- in the sample?

Click here to review your answer to this exercise.

A one-point fixed-time integral method has the advantage of simplicity because we need only a single measurement to determine the analyte's initial concentration. As with any method that relies on a single determination, a one-point fixed-time integral method can not compensate for a constant determinate error. In a **two-point fixed-time integral method** we correct for constant determinate errors by making measurements at two points in time and using the difference between the measurements to determine

the analyte's initial concentration. Because it affects both measurements equally, the difference between the measurements is independent of a constant determinate error.

> See Chapter 4 for a review of constant determinate errors and how they differ from proportional determinate errors.

For a pseudo-first-order reaction in which we measure the analyte's concentration at times t_1 and t_2, we can write the following two equations.

$$[\mathrm{A}]_{t_1} = [\mathrm{A}]_0 e^{-k't_1} \tag{13.2.22}$$

$$[\mathrm{A}]_{t_2} = [\mathrm{A}]_0 e^{-k't_2} \tag{13.2.23}$$

Subtracting Equation 13.2.23 from Equation 13.2.22 and solving for $[A]_0$ leaves us with

$$[\mathrm{A}]_0 = \frac{[\mathrm{A}]_{t_1} - [\mathrm{A}]_{t_2}}{e^{-k't_1} - e^{-k't_2}} \tag{13.2.24}$$

To determine the rate constant, k', we measure $[\mathrm{A}]_{t1}$ and $[\mathrm{A}]_{t2}$ for a standard solution of analyte. Having obtained a value for k', we can determine $[\mathrm{A}]_0$ by measuring the analyte^'s concentration at t_1 and t_2. We can also determine the analyte^'s initial concentration using a calibration curve consisting of a plot of $([\mathrm{A}]_{t1} - [\mathrm{A}]_{t2})$ versus $[\mathrm{A}]_0$.

A fixed-time integral method is particularly useful when the signal is a linear function of concentration because we can replace the reactant's concentration terms with the corresponding signal. For example, if we follow a reaction spectrophotometrically under conditions where the analyte's concentration obeys Beer's law

$$(Abs)_t = \varepsilon b[\mathrm{A}]_t \tag{13.2.25}$$

then we can rewrite equation 13.2.9 and equation 13.2.24 as

$$(Abs)_t = [\mathrm{A}]_0 e^{-k't} \varepsilon b = c[\mathrm{A}]_0 \tag{13.2.26}$$

$$[\mathrm{A}]_0 = \frac{(Abs)_{t_1} - (Abs)_{t_2}}{e^{-k't_1} - e^{-k't_2}} \times (\varepsilon b)^{-1} = c'[(Abs)_{t_1} - (Abs)_{t_2}] \tag{13.2.27}$$

where $(Abs)_t$ is the absorbance at time t, and c and c^' are constants.

Note

$$c = e^{-k't} \varepsilon b \tag{13.2.28}$$

$$c' = \frac{1}{(\varepsilon b)\left(e^{-k't_1} - e^{-k't_2}\right)} \tag{13.2.29}$$

Direct-Computation Variable-Time Integral Methods

In a **variable-time integral method** we measure the total time, Δt, needed to effect a specific change in concentration for one species in the chemical reaction. One important application is for the quantitative analysis of catalysts, which takes advantage of the catalyst's ability to increase the rate of reaction. As the concentration of catalyst increase, Δt decreases. For many catalytic systems the relationship between Δ_t and the catalyst's concentration is

$$\frac{1}{\Delta t} = F_{\text{cat}}[A]_0 + F_{\text{uncat}} \tag{13.2.30}$$

where $[\mathrm{A}]_0$ is the catalyst's concentration, and F_{cat} and F_{uncat} are constants accounting for the rate of the catalyzed and uncatalyzed reactions.[7]

Example 13.3

Sandell and Kolthoff developed a quantitative method for iodide based on its ability to catalyze the following redox reaction.[8]

$$\mathrm{As}^{3+}(aq) + 2\,\mathrm{Ce}^{4+}(aq) \rightarrow \mathrm{As}^{5+}(aq) + 2\,\mathrm{Ce}^{3+}(aq) \tag{13.2.31}$$

An external standards calibration curve was prepared by adding 1 mL of a KI standard to a mixture consisting of 2 mL of 0.05 M As^{3+}, 1 mL of 0.1 M Ce^{4+}, and 1 mL of 3 M H_2SO_4, and measuring the time for the yellow color of Ce^{4+} to disappear. The following table summarizes the results for one analysis.

$[I^-]$ (µg/mL)	Δt (min)
5.0	0.9
2.5	1.8
1.0	4.5

What is the concentration of I^- in a sample Δt is 3.2 min?

Solution

Figure 13.3 shows the calibration curve and calibration equation for the external standards based on equation 13.19. Substituting 3.2 min for Δt gives the concentration of I^- in the sample as 1.4 µg/mL.

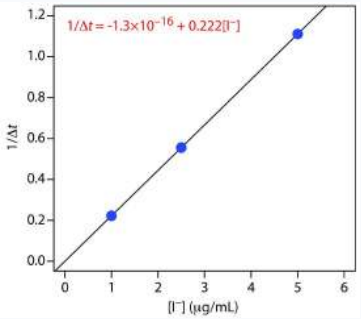


Figure 13.3 *Calibration curve and calibration equation for Example 13.3.*

Direct-Computation Rate Methods

In a **rate method** we use the differential form of the rate law—Equation 13.2.1 is one example of a differential rate law—to determine the analyte's concentration. As shown in Figure 13.4, the rate of a reaction at time t, $(rate)_t$, is the slope of a line tangent to a curve showing the change in concentration as a function of time. For a reaction that is first-order in analyte, the rate at time t is

$$(\text{rate})_t = k[\text{A}]_t \tag{13.2.32}$$

Substituting in Equation 13.2.3 leaves us with the following equation relating the rate at time t to the analyte's initial concentration.

$$(\text{rate})_t = k[\text{A}]_0 e^{-kt} \tag{13.2.33}$$

If we measure the rate at a fixed time, then both k and e^{-kt} are constant and we can use a calibration curve of $(\text{rate})_t$ versus $[\text{A}]_0$ for the quantitative analysis of the analyte.

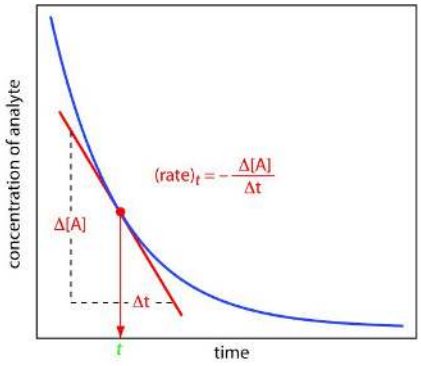


Figure 13.4: Determination of a reaction's intermediate rate from the slope of a line tangent to a curve showing the change in the analyte's concentration as a function of time.

There are several advantages to using the reaction's **initial rate** (t = 0). First, because the reaction's rate decreases over time, the initial rate provides the greatest sensitivity. Second, because the initial rate is measured under nearly pseudo-zero-order conditions, in which the change in concentration with time is effectively linear, the determination of slope is easier. Finally, as the reaction of interest progresses competing reactions may develop, complicating the kinetics—using the initial rate eliminates these complications. One disadvantage of the initial rate method is that there may be insufficient time for completely mixing the reactants. This problem is avoided by using an **intermediate rate** measured at a later time (t > 0).

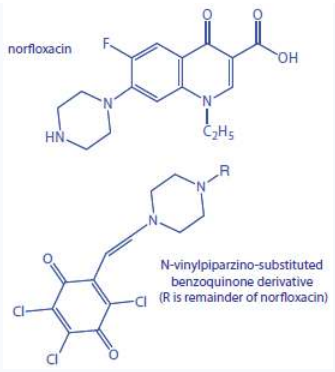
As a general rule (see Mottola, H. A. "Kinetic Determinations of Reactants Utilizing Uncatalyzed Reactions," *Anal. Chim. Acta* **1993**, *280*, 279–287), the time for measuring a reaction's initial rate should result in the consumption of no more than 2% of the reactants. The smaller this percentage, the more linear the change in concentration as a function of time.

Example 13.4

The concentration of norfloxacin, a commonly prescribed antibacterial agent, is determined using the initial rate method. Norfloxacin is converted to an N-vinylpiperazine derivative and reacted with 2,3,5,6-tetrachloro-1,4-benzoquinone to form an N-vinylpiperazino-substituted benzoquinone derivative that absorbs strongly at 625 nm.[9] The initial rate of the reaction—as measured by the change in absorbance as a function of time (AU/min)—is pseudo-first order in norfloxacin. The following data were obtained for a series of external norfloxacin standards.

[norfloxacin] (μg/mL)	initial rate (AU/min)
63	0.0139
125	0.0355
188	0.0491
251	0.0656
313	0.0859

To analyze a sample of prescription eye drops, a 10.00-mL portion was extracted with dichloromethane. The extract was dried and the norfloxacin reconstituted in methanol and diluted to 10 mL in a volumetric flask. A 5.00-mL portion of this solution was diluted to volume in a 100-mL volumetric flask. Analysis of this sample gave an initial rate of 0.0394 AU/min. What is the concentration of norfloxacin in the eye drops? AU stands for absorbance unit.



Solution

Figure 13.5 shows the calibration curve and calibration equation for the external standards. Substituting 0.0394 AU/min for the initial rate and solving for the concentration of norfloxacin gives a result of 152 mg/mL. This is the concentration in a diluted sample of the extract. The concentration in the extract before dilution is

$$\frac{152\ \text{g}}{\text{mL}} \times \frac{100.0\ \text{mL}}{5.00\ \text{mL}} \times \frac{1\ \text{g}}{1000\ \text{mg}} = 3.04\ \text{mg/mL} \tag{13.2.34}$$

Because the dried extract was reconstituted using a volume identical to that of the original sample, the concentration of norfloxacin in the eye drops is 3.04 mg/mL.

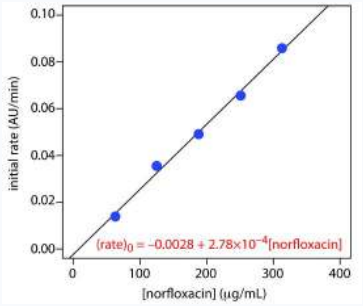


***Figure 13.5**: Calibration curve and calibration equation for Example 13.4.*

Curve-Fitting Methods

In direct-computation methods we determine the analyte's concentration by solving the appropriate rate equation at one or two discrete times. The relationship between the analyte's concentration and the measured response is a function of the rate constant, which we determine in a separate experiment using a single external standard (see Example 13.1 or Example 13.2), or a calibration curve (see Example 13.3 or Example 13.4).

In a **curve-fitting method** we continuously monitor the concentration of a reactant or a product as a function of time and use a regression analysis to fit the data to an appropriate differential rate law or integrated rate law. For example, if we are monitoring the concentration of a product for a reaction that is pseudo-first-order in the analyte, then we can fit the data to the following rearranged form of Equation 13.2.19

$$[\text{P}]_t = [\text{A}]_0(1 - e^{-k't}) \tag{13.2.35}$$

using $[\text{A}]_0$ and k' as adjustable parameters. Because we are using data from more than one or two discrete times, a curve-fitting method is capable of producing more reliable results.

Example 13.5

The data shown in the following table were collected for a reaction that is known to be pseudo-zero-order in analyte.

time (s)	$[A]_t$ (mM)	time (s)	$[A]_t$ (mM)
3	0.0731	8	0.0448
4	0.0728	9	0.0404
5	0.0681	10	0.0339
6	0.0582	11	0.0217
7	0.0511	12	0.0143

What is the initial concentration of analyte in the sample and the rate constant for the reaction?

Solution

From equation 13.10 we know that for a pseudo-zero-order reaction a plot of $[A]_t$ versus time is linear with a slope of $-k''$, and a y-intercept of $[A]_0$. Figure 13.6 shows a plot of the kinetic data and the result of a linear regression analysis. The initial concentration of analyte is 0.0986 mM and the rate constant is 0.00677 M^{-1} s^{-1}.

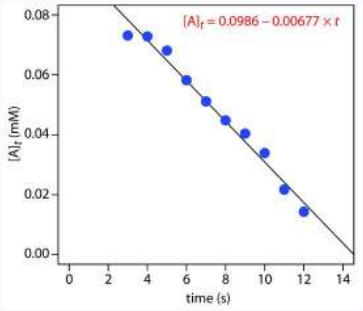


Figure 13.6 *Result of fitting equation 13.10 to the data in Example 13.5.*

The best way to appreciate the theoretical and practical details discussed in this section is to carefully examine a typical analytical method. Although each method is unique, the following description of the determination of creatinine in urine provides an instructive example of a typical procedure. The description here is based on Diamandis, E. P.; Koupparis, M. A.; Hadjiioannou, T. P. "Kinetic Studies with Ion Selective Electrodes: Determination of Creatinine in Urine with a Picrate Ion Selective Electrode," *J. Chem. Educ.* **1983**, *60*, 74–76.

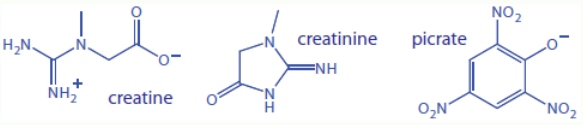
Representative Method 13.1: **Determination of Creatinine in Urine**

Description of Method

Creatine is an organic acid found in muscle tissue that supplies energy for muscle contractions. One of its metabolic products is creatinine, which is excreted in urine. Because the concentration of creatinine in urine and serum is an important indication of renal function, rapid methods for its analysis are clinically important. In this method the rate of reaction between creatinine and picrate in an alkaline medium is used to determine the concentration of creatinine in urine. Under the conditions of the analysis the reaction is first order in picrate, creatinine, and hydroxide.

$$\text{rate} = k[\text{picrate}][\text{creatinine}][\text{OH}^-] \qquad (13.2.36)$$

The reaction is monitored using a picrate ion selective electrode.



Procedure

Prepare a set of external standards containing 0.5–3.0 g/L creatinine using a stock solution of 10.00 g/L creatinine in 5 mM H_2SO_4, diluting each to volume using 5 mM H_2SO_4. Prepare a solution of 1.00×10^{-2} M sodium picrate. Pipet 25.00 mL of 0.20

M NaOH, adjusted to an ionic strength of 1.00 M using Na_2SO_4, into a thermostated reaction cell at 25°C. Add 0.500 mL of the 1.00×10^{-2} M picrate solution to the reaction cell. Suspend a picrate ion selective in the solution and monitor the potential until it stabilizes. When the potential is stable, add 2.00 mL of a creatinine external standard and record the potential as a function of time. Repeat this procedure using the remaining external standards. Construct a calibration curve of $\Delta E/\Delta t$ versus the initial concentration of creatinine. Use the same procedure to analyze samples, using 2.00 mL of urine in place of the external standard. Determine the concentration of creatinine in the sample using the calibration curve.

Questions

1. The analysis is carried out under conditions that are pseudo-first order in picrate. Show that under these conditions the change in potential as a function of time is linear.

The potential, E, of the picrate ion selective electrode is given by the Nernst equation

$$E = K - \frac{RT}{F}\ln[\text{picrate}] \tag{13.2.37}$$

where K is a constant that accounts for the reference electrodes, junction potentials, and the ion selective electrode's asymmetry potential, R is the gas constant, T is the temperature, and F is Faraday's constant.

(For a review of the Nernst equation for ion selective electrodes, see Section 11.2.3 in Chapter 11.)

We know from equation 13.7 that for a pseudo-first-order reaction, the concentration of picrate at time t is

$$\ln[\text{picrate}]_t = \ln[\text{picrate}]_0 - k't \tag{13.2.38}$$

where k' is the pseudo-first-order rate constant. Substituting this integrated rate law into the ion selective electrode's Nernst equation leave us with the following result.

$$E_t = K - \frac{RT}{F}(\ln[\text{picrate}]_0 - k't) \tag{13.2.39}$$

$$E_t = K - \frac{RT}{F}\ln[\text{picrate}]_0 + \frac{RT}{F}k't \tag{13.2.40}$$

Because K and $(RT/F)\ln[\text{picrate}]_0$ are constants, a plot of E_t versus t is a straight line with a slope of RTk'/F.

2. Under the conditions of the analysis the rate of the reaction is pseudo-first-order in picrate and pseudo-zero-order in creatinine and OH^-. Explain why it is possible to prepare a calibration curve of $\Delta E/\Delta t$ versus the concentration of creatinine.

The slope of a plot of E_t versus t is $\Delta E/\Delta t = RTk'/F$ (see the previous question). Because the reaction is carried out under conditions where it is pseudo-zero-order in creatinine and OH^-, the rate law is

$$\text{rate} = k[\text{picrate}]\ [\text{creatinine}]_0[OH^-]_0 = k'[\text{picrate}] \tag{13.2.41}$$

The pseudo-first-order rate constant, k', is

$$k' = k[\text{creatinine}]_0[OH^-]_0 = c[\text{creatinine}]_0 \tag{13.2.42}$$

where c is a constant. The slope of a plot of E_t versus t, therefore, is linear function of creatinine's initial concentration

$$\frac{E}{t} = \frac{RTk'}{F} = \frac{RTc}{F}[\text{creatinine}]_0 \tag{13.2.43}$$

and a plot of $\Delta E/\Delta t$ versus the concentration of creatinine can serve as a calibration curve.

3. Why is it necessary to thermostat the reaction cell?

The rate of a reaction is temperature-dependent. To avoid a determinate error resulting from a systematic change in temperature, or to minimize indeterminate errors due to fluctuations in temperature, the reaction cell is thermostated to maintain a constant temperature.

4. Why is it necessary to prepare the NaOH solution so that it has an ionic strength of 1.00 M?

The potential of the picrate ion selective electrode actually responds to the activity of the picrate anion in solution. By adjusting the NaOH solution to a high ionic strength we maintain a constant ionic strength in all standards and samples. Because the

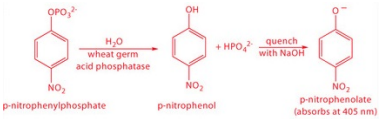
relationship between activity and concentration is a function of ionic strength, the use of a constant ionic strength allows us to write the Nernst equation in terms of picrate's concentration instead of its activity.

For a review of the relationship between concentration, activity, and ionic strength, see Chapter 6.9.

13.2.3 Making Kinetic Measurements

When using Representative Method 13.1 to determine the concentration of creatinine in urine, we follow the reactions kinetics using an ion selective electrode. In principle, we can use any of the analytical techniques in Chapters 8–12 to follow a reaction's kinetics provided that the reaction does not proceed to any appreciable extent during the time it takes to make a measurement. As you might expect, this requirement places a serious limitation on kinetic methods of analysis. If the reaction's kinetics are slow relative to the analysis time, then we can make our measurements without the analyte undergoing a significant change in concentration. When the reaction's rate is too fast—which often is the case—then we introduce a significant error if our analysis time is too long.

One solution to this problem is to stop, or **quench** the reaction by adjusting experimental conditions. For example, many reactions show a strong pH dependency, and may be quenched by adding a strong acid or a strong base. Figure 13.7 shows a typical example for the enzymatic analysis of *p*-nitrophenylphosphate using the enzyme wheat germ acid phosphatase to hydrolyze the analyte to *p*-nitrophenol.



The reaction has a maximum rate at a pH of 5. Increasing the pH by adding NaOH quenches the reaction and converts the colorless *p*-nitrophenol to the yellow-colored *p*-nitrophenolate, which absorbs at 405 nm.

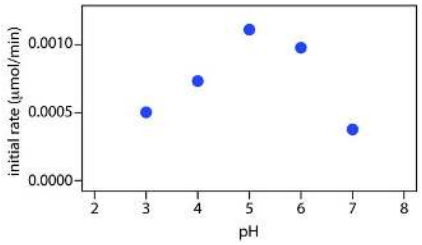


Figure 13.7: *Initial rate for the enzymatic hydrolysis of p-nitrophenylphosphate using wheat germ acid phosphatase. Increasing the pH quenches the reaction and coverts colorless p-nitrophenol to the yellow-colored p-nitrophenolate, which absorbs at 405 nm. The data are adapted from socrates.hunter.cuny.edu.*

An additional experimental problem when the reaction's kinetics are fast is ensuring that we rapidly and reproducibly mix the sample and the reagents. For a fast reaction we need to make measurements in a few seconds, or even a few milliseconds. This presents us with both a problem and an important advantage. The problem is that rapidly and reproducibly mixing the sample and the reagent requires a dedicated instrument, which adds an additional expense to the analysis. The advantage is that a rapid, automated analysis allows for a high throughput of samples. Instrumentation for the automated kinetic analysis of phosphate using reaction 13.11, for example, have sampling rates of approximately 3000 determinations per hour.

A variety of instruments have been developed to automate the kinetic analysis of fast reactions. One example, which is shown in Figure 13.8, is the **stopped-flow analyzer**. The sample and reagents are loaded into separate syringes and precisely measured volumes are dispensed into a mixing chamber by the action of a syringe drive. The continued action of the syringe drive pushes the mixture through an observation cell and into a stopping syringe. The back pressure generated when the stopping syringe hits the stopping block completes the mixing, after which the reaction's progress is monitored spectrophotometrically. With a stopped-flow analyzer it is possible to complete the mixing of sample and reagent, and initiate the kinetic measurements in approximately 0.5 ms. By attaching an autosampler to the sample syringe it is possible to analyze up to several hundred samples per hour.

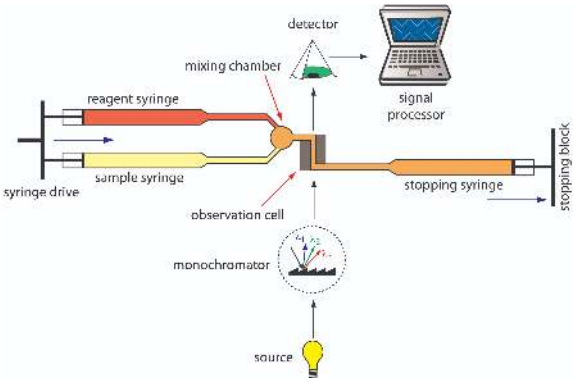


Figure 13.8: *Schematic diagram of a stopped-flow analyzer. The blue arrows show the direction in which the syringes are moving.*

Another instrumental design is the **centrifugal analyzer**, a partial cross section of which is shown in Figure 13.9. The sample and the reagents are placed in separate wells, which are oriented radially around a circular transfer disk. As the centrifuge spins, the centrifugal force pulls the sample and the reagents into the cuvette where mixing occurs. A single optical source and detector, located below and above the transfer disk's outer edge, measures the absorbance each time the cuvette passes through the optical beam. When using a transfer disk with 30 cuvettes and rotating at 600 rpm, we can collect 10 data points per second for each sample.

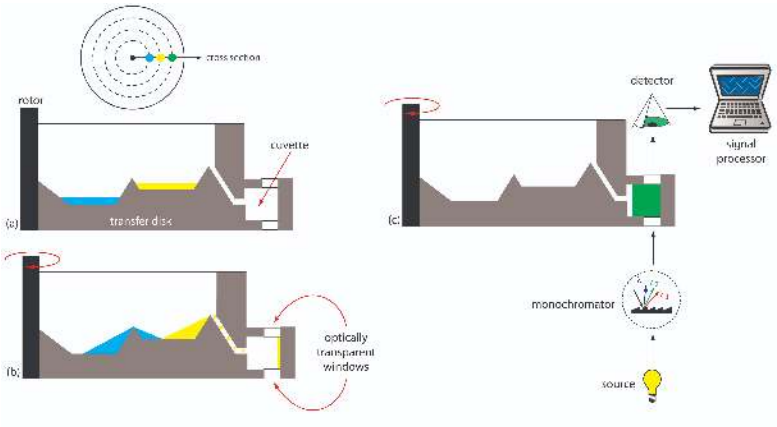


Figure 13.9: *Cross sections through a centrifugal analyzer showing (a) the wells holding the sample and the reagents, (b) the mixing of the sample and the reagents, and (c) the configuration of the spectrophotometric detector.*

The ability to collect lots of data and to collect it quickly requires appropriate hardware and software. Not surprisingly, automated kinetic analyzers developed in parallel with advances in analog and digital circuitry—the hardware—and computer software for smoothing, integrating, and differentiating the analytical signal. For an early discussion of the importance of hardware and software, see Malmstadt, H. V.; Delaney, C. J.; Cordos, E. A. "Instruments for Rate Determinations," *Anal. Chem.* **1972**, *44(12)*, 79A–89A.

13.2.4 Quantitative Applications

Chemical kinetic methods of analysis continue to find use for the analysis of a variety of analytes, most notably in clinical laboratories where automated methods aid in handling the large volume of samples. In this section we consider several general quantitative applications.

Enzyme-Catalyzed Reactions

Enzymes are highly specific catalysts for biochemical reactions, with each enzyme showing a selectivity for a single reactant, or **substrate**. For example, the enzyme acetylcholinesterase catalyzes the decomposition of the neurotransmitter acetylcholine to choline and acetic acid. Many enzyme–substrate reactions follow a simple mechanism that consists of the initial formation of an enzyme–substrate complex, ***ES***, which subsequently decomposes to form product, releasing the enzyme to react again.

$$\mathrm{E} + \mathrm{S} \underset{k_{-1}}{\overset{k_1}{\rightleftharpoons}} \mathrm{ES} \underset{k_{-2}}{\overset{k_2}{\rightleftharpoons}} \mathrm{E} + \mathrm{P} \tag{13.2.44}$$

where k_1, k_{-1}, k_2, and k_{-2} are rate constants. If we make measurement early in the reaction, the concentration of products is negligible and we can ignore the step described by the rate constant k_{-2}. Under these conditions the reaction's rate is

$$\text{rate} = \frac{d[\mathrm{P}]}{dt} = k_2[\mathrm{ES}] \tag{13.2.45}$$

To be analytically useful we need to write Equation 13.2.45 in terms of the concentrations of enzyme and substrate. To do this we use the **steady-state approximation**, in which we assume that the concentration of ES remains essentially constant. Following an initial period, during which the enzyme–substrate complex first forms, the rate at which ES forms

$$\frac{d[\mathrm{ES}]}{dt} = k_1[\mathrm{E}][\mathrm{S}] = k_1([\mathrm{E}]_0 - [\mathrm{ES}])[\mathrm{S}] \tag{13.2.46}$$

is equal to the rate at which it disappears

$$-\frac{d[\mathrm{ES}]}{dt} = k_{-1}[\mathrm{ES}] + k_2[\mathrm{ES}] \tag{13.2.47}$$

where $[E]_0$ is the enzyme's original concentration. Combining Equations 13.2.46 and 13.2.47 gives

$$k_1([\mathrm{E}]_0 - [\mathrm{ES}])[\mathrm{S}] = k_{-1}[\mathrm{ES}] + k_2[\mathrm{ES}] \tag{13.2.48}$$

which we solve for the concentration of the enzyme–substrate complex

$$[ES] = \frac{[\mathrm{E}]_0[\mathrm{S}]}{\frac{k_{-1} + k_2}{k_1} + [S]} = \frac{[\mathrm{E}]_0[\mathrm{S}]}{K_\mathrm{m} + [S]} \tag{13.2.49}$$

where K_m is the **Michaelis constant**. Substituting Equation 13.2.49 into Equation 13.2.45 leaves us with our final rate equation.

$$\frac{d[\mathrm{P}]}{dt} = \frac{k_2[\mathrm{E}]_0[\mathrm{S}]}{K_\mathrm{m} + [S]} \tag{13.2.50}$$

A plot of Equation 13.2.50, as shown in Figure 13.10, is instructive for defining conditions where we can use the rate of an enzymatic reaction for the quantitative analysis of an enzyme or substrate. For high substrate concentrations, where $[\mathrm{S}] >> K_\mathrm{m}$, Equation 13.2.50 simplifies to

$$\frac{d[\mathrm{P}]}{dt} = \frac{k_2[\mathrm{E}]_0[\mathrm{S}]}{K_\mathrm{m} + [S]} \approx \frac{k_2[\mathrm{E}]_0[\mathrm{S}]}{[S]} = k_2[\mathrm{E}]_0 = V_\mathrm{max} \tag{13.2.51}$$

where V_max is the maximum rate for the catalyzed reaction. Under these conditions the reaction is pseudo-zero-order in substrate, and we can use V_max to calculate the enzyme's concentration, typically using a variable-time method. At lower substrate concentrations, where $[\mathrm{S}] << K_\mathrm{m}$, Equation 13.2.50 becomes

$$\frac{d[\mathrm{P}]}{dt} = \frac{k_2[\mathrm{E}]_0[\mathrm{S}]}{K_\mathrm{m} + [S]} \approx \frac{k_2[\mathrm{E}]_0[\mathrm{S}]}{K_\mathrm{m}} = \frac{V_\mathrm{max}[\mathrm{S}]}{K_\mathrm{m}} \tag{13.2.52}$$

The reaction is now first-order in substrate, and we can use the rate of the reaction to determine the substrate's concentration by a fixed-time method.

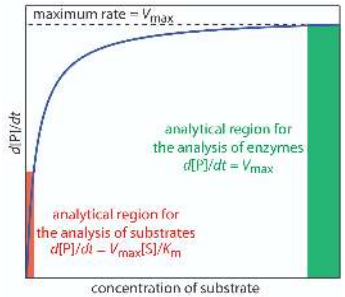


Figure 13.10: *Plot of Equation 13.2.50 showing limits for the analysis of substrates and enzymes in an enzyme-catalyzed chemical kinetic method of analysis. The curve in the region highlighted in red obeys Equation 13.2.52 and the curve in the area highlighted in green follows Equation 13.2.51.*

Chemical kinetic methods have been applied to the quantitative analysis of a number of enzymes and substrates.[10] One example, is the determination of glucose based on its oxidation by the enzyme glucose oxidase

$$\text{glucose}_{(aq)} + \text{H}_2\text{O}_{(l)} + \text{O}_{2(aq)} \overset{\text{glucose oxidase}}{\rightarrow} \text{gluconolactone}_{(aq)} + \text{H}_2\text{O}_{2(aq)} \tag{13.2.53}$$

under conditions where Equation 13.2.44 is valid. The reaction is monitored by following the rate of change in the concentration of dissolved O_2 using an appropriate voltammetric technique.

One method for measuring the concentration of dissolved O_2 is the Clark amperometric sensor described in Chapter 11.

Nonenzyme-Catalyzed Reactions

The variable-time method has also been used to determine the concentration of nonenzymatic catalysts. One of the most commonly used reactions is the reduction of H_2O_2 by reducing agents such as thiosulfate, iodide, and hydroquinone. These reactions are catalyzed by trace amounts of selected metal ions. For example the reduction of H_2O_2 by I^-

$$2\,\text{I}^-_{(aq)} + \text{H}_2\text{O}_{2(aq)} + 2\,\text{H}_3\text{O}^+_{(aq)} \rightarrow 4\,\text{H}_2\text{O}_{(l)} + \text{I}_{2(aq)} \tag{13.2.54}$$

is catalyzed by Mo(VI), W(VI), and Zr(IV). A variable-time analysis is conducted by adding a small, fixed amount of ascorbic acid to each solution. As I_2 is produced it rapidly oxidizes the ascorbic acid, and is reduced back to I^-. Once all the ascorbic acid is consumed, the presence of excess I_2 provides a visual endpoint.

Noncatalytic Reactions

Chemical kinetic methods are not as common for the quantitative analysis of analytes in noncatalytic reactions. Because they lack the enhancement of reaction rate that a catalyst affords, noncatalytic methods generally are not useful for determining small concentrations of analytes. Noncatalytic methods for inorganic analytes are usually based on a complexation reaction. One example is the determination of aluminum in serum by measuring the initial rate for the formation of its complex with 2-hydroxy-1-napthaldehyde *p*-methoxybenzoyl-hydrazone.[11] The greatest number of noncatalytic methods, however, are for the quantitative analysis of organic analytes. For example, the insecticide methyl parathion has been determined by measuring its rate of hydrolysis in alkaline solutions.[12]

13.2.5 Characterization Applications

Chemical kinetic methods also find use in determining rate constants and in elucidating reaction mechanisms. Two examples from the kinetic analysis of enzymes illustrate these applications.

Determining V_{max} and K_m for Enzyme-Catalyzed Reactions

The value of V_{max} and K_m for an enzymatic reaction are of significant interest in the study of cellular chemistry. For an enzyme following the mechanism in reaction 13.2.44, V_{max} is equivalent to $k_2[\text{E}]_0$, where $[\text{E}]_0$ is the enzyme's concentration and k_2 is the enzyme's turnover number. The turnover number is the maximum number of substrate molecules converted to product by a single active site on the enzyme, per unit time. A turnover number, therefore, provides a direct indication of the active site's catalytic efficiency. The Michaelis constant, K_m, is significant because it provides an estimate of the substrate's intracellular concentration.[13]

Turnover Rate

An enzyme's turnover number also is know as k_{cat} and is equal to $V_{max}/[\text{E}]_0$. For the mechanism in reaction 13.2.44, k_{cat} is equivalent to k_2. For more complicated mechanisms, k_{cat} is a function of additional rate constants.

As shown in Figure 13.10, we can find values for V_{max} and K_m by measuring the reaction's rate for small and for large concentrations of the substrate. Unfortunately, this is not always practical as the substrate's limited solubility may prevent us from using the large substrate concentrations needed to determine V_{max}. Another approach is to rewrite Equation 13.2.50 by taking its reciprocal

$$\frac{1}{d[\mathrm{P}]/dt} = \frac{1}{v} = \frac{K_\mathrm{m}}{V_\mathrm{max}} \times \frac{1}{[\mathrm{S}]} + \frac{1}{V_\mathrm{max}} \tag{13.2.55}$$

where v is the reaction's rate. As shown in Figure 13.11, a plot of $\frac{1}{v}$ versus $\frac{1}{[\mathrm{S}]}$, which is called a double reciprocal or **Lineweaver–Burk plot**, is a straight line with a slope of $\frac{K_\mathrm{m}}{V_\mathrm{max}}$, a y-intercept of $1/V_\mathrm{max}$, and an x-intercept of $-\frac{1}{K_\mathrm{m}}$.

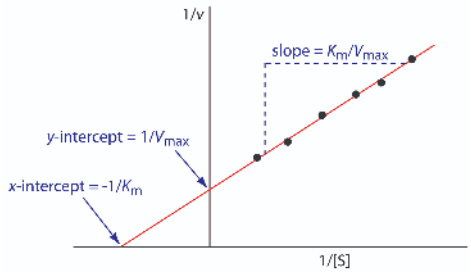


Figure 13.11: *Lineweaver–Burk plot of Equation 13.2.50 using Equation 13.2.55.*

In Chapter 5 we noted that when faced with a nonlinear model—and Equation 13.2.50 is one example of a nonlinear model—it may be possible to rewrite the equation in a linear form. This is the strategy used here. Linearizing a nonlinear model is not without limitations, two of which deserve a brief mention. First, because we are unlikely to have data for large substrate concentrations, we will not have many data points for small values of 1/[S]. As a result, our determination of the y-intercept's value relies on a significant extrapolation. Second, taking the reciprocal of the rate distorts the experimental error in a way that may invalidate the assumptions of a linear regression. Nonlinear regression provides a more rigorous method for fitting Equation 13.2.50 to experimental data. The details are beyond the level of this textbook, but you may consult Massart, D. L.; Vandeginste, B. G. M.; Buydens, L. M. C. De Jong, S.; Lewi, P. J.; Smeyers-Verbeke, J. "Nonlinear Regression," Chapter 11 in *Handbook of Chemometrics and Qualimetrics: Part A*, Elsevier: Amsterdam, 1997 for additional details. The simplex algorithm described in Chapter 14 also can be used to fit a nonlinear equation to experimental data.

Example 13.6

The reaction between nicotineamide mononucleotide and ATP to form nicotineamide–adenine dinucleotide and pyrophosphate is catalyzed by the enzyme nicotinamide mononucleotide adenylyltransferase.[14] The following table provides typical data obtained at a pH of 4.95. The substrate, S, is nicotinamide mononucleotide and the initial rate, v, is the μmol of nicotinamide–adenine dinucleotide formed in a 3-min reaction period.

[S] (mM)	v (μmol)	[S] (mM)	v (μmol)
0.138	0.148	0.560	0.324
0.220	0.171	0.766	0.390
0.291	0.234	1.460	0.493

Determine values for V_max and K_m.

Solution

Figure 13.12 shows the Lineweaver–Burk plot for this data and the resulting regression equation. Using the y-intercept, we calculate V_max as

$$V_\mathrm{max} = \frac{1}{y\text{–intercept}} = \frac{1}{1.708\ \mathrm{mol}} = 0.585\ \mathrm{mol} \tag{13.2.56}$$

and using the slope we find that K_m is

$$K_\mathrm{m} = \text{slope} \times V_\mathrm{max} = 0.7528\ \mathrm{mol^{\circ}mM} \times 0.585\ \mathrm{mol} = 0.440\ \mathrm{mM} \tag{13.2.57}$$

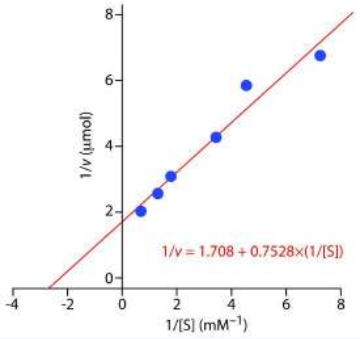
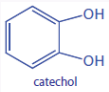
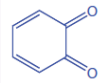


Figure 13.12 Linweaver–Burk plot and regression equation for the data in Example 13.6.

Exercise 13.3



catechol



o-quinone

The following data are for the oxidation of catechol (the substrate) to *o*-quinone by the enzyme *o*-diphenyl oxidase. The reaction is followed by monitoring the change in absorbance at 540 nm. The data in this exercise are adapted from jkimball.

[catechol] (mM)	0.3	0.6	1.2	4.8
rate (ΔAU/min)	0.020	0.035	0.048	0.081

Determine values for V_{max} and K_m.

Click here to review your answer to this exercise.

Elucidating Mechanisms for the Inhibition of Enzyme Catalysis

When an **inhibitor** interacts with an enzyme it decreases the enzyme's catalytic efficiency. An irreversible inhibitor covalently binds to the enzyme's active site, producing a permanent loss in catalytic efficiency even if we decrease the inhibitor's concentration. A reversible inhibitor forms a noncovalent complex with the enzyme, resulting in a temporary decrease in catalytic efficiency. If we remove the inhibitor, the enzyme's catalytic efficiency returns to its normal level.

There are several pathways for the reversible binding of an inhibitor to an enzyme, as shown in Figure 13.13. In **competitive inhibition** the substrate and the inhibitor compete for the same active site on the enzyme. Because the substrate cannot bind to an enzyme–inhibitor complex, EI, the enzyme's catalytic efficiency for the substrate decreases. With **noncompetitive inhibition** the substrate and the inhibitor bind to different active sites on the enzyme, forming an enzyme–substrate–inhibitor, or ESI complex. The formation of an ESI complex decreases catalytic efficiency because only the enzyme–substrate complex reacts to form the product. Finally, in **uncompetitive inhibition** the inhibitor binds to the enzyme–substrate complex, forming an inactive ESI complex.

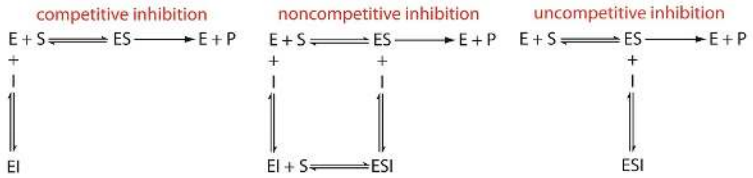


***Figure 13.13**: Mechanisms for the reversible inhibition of enzyme catalysis. E: enzyme, S: substrate, P: product, I: inhibitor, ES: enzyme–substrate complex, EI: enzyme–inhibitor complex, ESI: enzyme–substrate–inhibitor complex.*

We can identify the type of reversible inhibition by observing how a change in the inhibitor's concentration affects the relationship between the rate of reaction and the substrate's concentration. As shown in Figure 13.14, when we display kinetic data using as a Lineweaver-Burk plot it is easy to determine which mechanism is in effect. For example, an increase in slope, a decrease in the *x*-intercept, and no change in the *y*-intercept indicates competitive inhibition. Because the inhibitor's binding is reversible, we can still obtain the same maximum velocity—thus the constant value for the *y*-intercept—by adding enough substrate to completely displace the inhibitor. Because it takes more substrate, the value of K_m increases, which explains the increase in the slope and the decrease in the *x*-intercept's value.

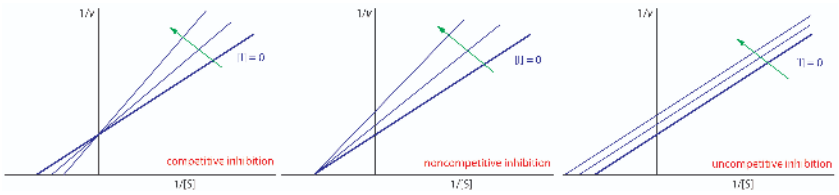


***Figure 13.14** Linweaver–Burk plots for competitive inhibition, noncompetitive inhibition, and uncompetitive inhibition. The thick blue line in each plot shows the kinetic behavior in the absence of inhibitor, and the thin blue lines in each plot show the change in behavior for increasing concentrations of the inhibitor. In each plot, the inhibitor's concentration increases in the direction of the green arrow.*

Example 13.7

Practice Exercise 13.3 provides kinetic data for the oxidation of catechol (the substrate) to *o*-quinone by the enzyme *o*-diphenyl oxidase in the absence of an inhibitor. The following additional data are available when the reaction is run in the presence of *p*-hydroxybenzoic acid, PBHA. Is PBHA an inhibitor for this reaction and, if so, what type of inhibitor is it? The data in this exercise are adapted from jkimball.

[catechol] (mM)	0.3	0.6	1.2	4.8
rate (ΔAU/min)	0.011	0.019	0.022	0.060

Solution

Figure 13.15 shows the resulting Lineweaver–Burk plot for the data in Practice Exercise 13.3 and Example 13.7. Although the *y*-intercepts are not identical in value—the result of uncertainty in measuring the rates—the plot suggests that PBHA is a competitive inhibitor for the enzyme's reaction with catechol.

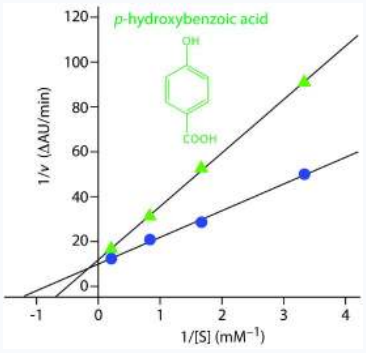


Figure 13.15 Lineweaver–Burk plots for the data in Practice Exercise 13.3 and Example 13.7.

Exercise 13.4

Practice Exercise 13.3 provides kinetic data for the oxidation of catechol (the substrate) to *o*-quinone by the enzyme *o*-diphenyl oxidase in the absence of an inhibitor. The following additional data are available when the reaction is run in the presence of

phenylthiourea. Is phenylthiourea an inhibitor for this reaction and, if so, what type of inhibitor is it? The data in this exercise are adapted from jkimball.

[catechol] (mM)	0.3	0.6	1.2	4.8
rate (ΔAU/min)	0.010	0.016	0.024	0.040

Click here to review your answer to this exercise.

13.2.6 Evaluation of Chemical Kinetic Methods

Scale of Operation

The detection limit for chemical kinetic methods ranges from minor components to ultratrace components, and is principally determined by two factors: the rate of the reaction and the instrumental technique used to monitor the rate. Because the signal is directly proportional to the reaction rate, faster reactions generally result in lower detection limits. All other factors being equal, detection limits are smaller for catalytic reactions than for noncatalytic reactions. Not surprisingly, some of the earliest chemical kinetic methods took advantage of catalytic reactions. For example, ultratrace levels of Cu (<1 ppb) can be determined by measuring its catalytic effect on the redox reaction between hydroquinone and H_2O_2.

See Figure 3.5 to review the meaning of minor, trace, and ultratrace components.

In the absence of a catalyst, most chemical kinetic methods for organic compounds involve reactions with relatively slow rates, limiting the method to minor and higher concentration trace analytes. Noncatalytic chemical kinetic methods for inorganic compounds involving metal–ligand complexation may be fast or slow, with detection limits ranging from trace to minor analyte.

The second factor influencing a method's detection limit is the instrumental technique used to monitor the reaction's progress. Most reactions are monitored spectrophotometrically or electrochemically. The scale of operation for these techniques are discussed in Chapter 10 and Chapter 11.

Accuracy

As noted earlier, a chemical kinetic method is potentially subject to larger errors than an equilibrium method due to the effect of uncontrolled or poorly controlled variables, such as temperature or pH. Although a direct-computation chemical kinetic method can achieve moderately accurate results (a relative error of 1–5%), the accuracy often is much worse. Curve-fitting methods may provide significant improvements in accuracy because they use more data. In one study, for example, accuracy was improved by two orders of magnitude—from errors of 500% to 5%—by replacing a direct-computation analysis with a curve-fitting analysis.[15] Although not discussed in this chapter, data analysis methods that include the ability to compensate for experimental errors can lead to a significant improvement in accuracy.[16]

Precision

The precision of a chemical kinetic method is limited by the signal-to-noise ratio of the instrumental technique used to monitor the reaction's progress. When using an integral method, a precision of 1–2% is routinely possible. The precision for a differential method may be somewhat poorer, particularly when the signal is noisy.

Sensitivity

We can improve the sensitivity of a one-point fixed-time integral method by making measurements under conditions where the concentration of the species we are monitoring is as large as possible. When monitoring the analyte's concentration—or the concentration of any other reactant—we want to take measurements early in the reaction before its concentration decreases. On the other hand, if we choose to monitor one of the reaction's products, then it is better to take measurements at longer times. For a two-point fixed-time integral method, we can improve sensitivity by increasing the difference between times t_1 and t_2. As discussed earlier, the sensitivity of a rate method improves when we choose to measure the initial rate.

Selectivity

The analysis of closely related compounds, as we have seen in earlier chapters, is often complicated by their tendency to interfere with each other. To overcome this problem we usually need to separate the analyte and the interferent before completing the analysis. One advantage of a chemical kinetic method is that we often can adjust the reaction conditions so that the analyte and the interferent have different reaction rates. If the difference in their respective rates is large enough, then one species reacts completely before the other species has a chance to react.

> The need to analyze multiple analytes in complex mixtures is, of course, one of the advantages of the separation techniques covered in Chapter 12. Kinetic techniques provide an alternative approach for simple mixtures.

We can use the appropriate integrated rate laws to find the conditions necessary to separate a faster reacting species from a more slowly reacting species. Let's consider a system consisting of an analyte, A, and an interferent, B, both of which show first-order kinetics with a common reagent. To avoid an interference, the relative magnitudes of their rate constants must be sufficiently different. The fractions, *f*, of A and B remaining at any point in time, *t*, are defined by the following equations

$$(f_A)_t = \frac{[A]_t}{[A]_0} \tag{13.2.58}$$

$$(f_B)_t = \frac{[B]_t}{[B]_0} \tag{13.2.59}$$

where $[A]_0$ and $[B]_0$ are the initial concentrations of A and B, respectively. Rearranging Equation 13.2.2 and substituting in Equation 13.2.58 or Equation 13.2.59 leaves use with the following two equations.

$$\ln \frac{[A]_t}{[A]_0} = \ln (f_A)_t = -k_A t \tag{13.2.60}$$

$$\ln \frac{[B]_t}{[B]_0} = \ln (f_B)_t = -k_B t \tag{13.2.61}$$

where k_A and k_B are the rate constants for A and B. Dividing Equation 13.2.60 by Equation 13.2.61 leave us with

$$\frac{k_A}{k_B} = \frac{\ln (f_A)_t}{\ln (f_B)_t} \tag{13.2.62}$$

Suppose we want 99% of A react before 1% of B reacts. The fraction of A that remains is 0.01 and the fraction of B remaining is 0.99, which requires that

$$\frac{k_A}{k_B} = \frac{\ln (f_A)_t}{\ln (f_B)_t} = \frac{\ln(0.01)}{\ln(0.99)} = 460 \tag{13.2.63}$$

the rate constant for A be at least 460 times larger than that for B. Under these conditions we can determine the analyte's concentration before the interferent begins to react. If the analyte has the slower reaction, then we can determine its concentration after allowing the interferent to react to completion.

This method of adjusting reaction rates is useful if we need to analyze for an analyte in the presence of an interferent, but impractical if both A and B are analytes because conditions favoring the analysis of A will not favor the analysis of B. For example, if we adjust our conditions so that 99% of A reacts in 5 s, then 99% of B must react within 0.01 s if it has the faster kinetics, or in 2300 s if it has the slower kinetics. The reaction of B is too fast or too slow to make this a useful analytical method.

What do we do if the difference in the rate constants for A and B are not significantly different? We can still complete an analysis if we can simultaneously monitor both species. Because both A and B react at the same time, the integrated form of the first-order rate law becomes

$$C_t = [A]_t + [B]_t = [A]_0 e^{-k_A t} + [B]_0 e^{-k_B t} \tag{13.2.64}$$

where C_t is the total concentration of A and B at time, *t*. If we measure C_t at times t_1 and t_2, we can solve the resulting pair of simultaneous equations to determine values $[A]_0$ and $[B]_0$. The rate constants k_A and k_B are determined in separate experiments using standard solutions of A and B.

Equation 13.2.64 can also serve as the basis for a curve-fitting method. As shown in Figure 13.16, a plot of $\ln(C_t)$ as a function of time consists of two regions. At shorter times the plot is curved because A and B are reacting simultaneously. At later times, however, the concentration of the faster reacting component, A, decreases to zero, and Equation 13.2.64 simplifies to

$$C_t \approx [\mathrm{B}]_t = [\mathrm{B}]_0 e^{-k_B t} \tag{13.2.65}$$

Under these conditions a plot of $\ln(C_t)$ versus time is linear. Extrapolating the linear portion to $t = 0$ gives $[\mathrm{B}]_0$, with $[\mathrm{A}]_0$ determined by difference.

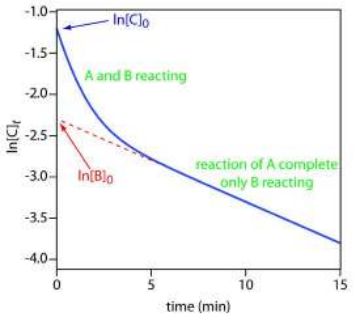


Figure 13.16: Kinetic determination of a slower reacting analyte, B, in the presence of a faster reacting analyte, A. The rate constants for the two analytes are: $k_A = 1\ \mathrm{min}^{-1}$ and $k_B = 0.1\ \mathrm{min}^{-1}$. Example 13.8 asks you to use this data to determine the concentrations of A and B in the original sample.

Example 13.8

Use the data in Figure 13.16 to determine the concentrations of A and B in the original sample.

Solution

Extrapolating the linear part of the curve back to $t = 0$ gives $\ln[\mathrm{B}]_0$ as –2.3, or a $[\mathrm{B}]_0$ of 0.10 M. At $t = 0$, $\ln[\mathrm{C}]_0$ is –1.2, corresponding to a $[\mathrm{C}]_0$ of 0.30 M. Because $[\mathrm{C}]_0 = [\mathrm{A}]_0 + [\mathrm{B}]_0$, the concentration of A in the original sample is 0.20 M.

Time, Cost, and Equipment

An automated chemical kinetic method of analysis provides a rapid means for analyzing samples, with throughputs ranging from several hundred to several thousand determinations per hour. The initial start-up costs may be fairly high because an automated analysis requires a dedicated instrument designed to meet the specific needs of the analysis. When measurements are handled manually, a chemical kinetic method requires routinely available equipment and instrumentation, although the sample throughput is much lower than with an automated method.

Contributors

David Harvey (DePauw University)

13.2: Chemical Kinetics is shared under a CC BY-NC-SA 4.0 license and was authored, remixed, and/or curated by LibreTexts.

13.3: Radiochemistry

Atoms having the same number of protons but a different number of neutrons are **isotopes**. To identify an isotope we use the notation ${}^{A}_{Z}E$, where E is the element's atomic symbol, Z is the element's atomic number, and A is the element's atomic mass number. Although an element's different isotopes have the same chemical properties, their nuclear properties are different. The most important difference between isotopes is their stability. The nuclear configuration of a stable isotope remains constant with time. Unstable isotopes, however, spontaneously disintegrate, emitting radioactive particles as they transform into a more stable form.

An element's atomic number is equal to the number of protons and its atomic mass is equal to the sum of the number of protons and neutrons. We represent an isotope of carbon-13 as

$${}^{13}_{6}\mathrm{C}$$

because carbon has 6 protons and 7 neutrons. Sometimes we omit Z from this notation—identifying the element and the atomic number is repetitive because all isotopes of carbon have 6 protons and any atom having 6 protons is an isotope of carbon. Thus, ^{13}C and C–13 are alternative notations for this isotope of carbon.

The most important types of radioactive particles are alpha particles, beta particles, gamma rays, and X-rays. An **alpha particle**, α, is equivalent to a helium nucleus, ${}^{4}_{2}\mathrm{He}$. When an atom emits an alpha particle, the product in a new atom whose atomic number and atomic mass number are, respectively, 2 and 4 less than its unstable parent. The decay of uranium to thorium is one example of alpha emission.

$${}^{238}_{92}\mathrm{U} \longrightarrow {}^{234}_{90}\mathrm{Th} + \alpha \tag{13.3.1}$$

A **beta particle**, β, comes in one of two forms. A **negatron**, ${}^{0}_{-1}\beta$, is produced when a neutron changes into a proton, increasing the atomic number by one, as shown here for lead.

$${}^{214}_{82}\mathrm{Pb} \longrightarrow {}^{214}_{83}\mathrm{Bi} + {}^{0}_{-1}\beta \tag{13.3.2}$$

Negatrons

A negatron, which is the more common type of beta particle, is equivalent to an electron. You may recall from Section 12.4.5 that the electron capture detector for gas chromatography uses ^{63}Ni as a beta emitter.

The conversion of a proton to a neutron results in the emission of a **positron**, ${}^{0}_{1}\beta$.

$${}^{30}_{15}\mathrm{P} \longrightarrow {}^{30}_{14}\mathrm{Si} + {}^{0}_{1}\beta \tag{13.3.3}$$

The emission of an alpha or a beta particle often produces an isotope in an unstable, high energy state. This excess energy is released as a **gamma ray**, γ, or as an X-ray. Gamma ray and X-ray emission may also occur without the release of an alpha particle or a beta particle.

13.3.1 Theory and Practice

A radioactive isotope's rate of decay, or activity, follows first-order kinetics

$$A = -\frac{dN}{dt} = \lambda N \tag{13.3.4}$$

where A is the activity, N is the number of radioactive atoms present in the sample at time t, and λ is the isotope's decay constant. Activity is expressed as the number of disintegrations per unit time.

Note the similarity between Equation 13.3.4 and Equation 13.1

$$\text{rate} = -\frac{d[\mathrm{A}]}{dt} = k[\mathrm{A}]$$

where activity is equivalent to rate, N is equivalent to [A], and l is equivalent to k.

As with any first-order process, we can rewrite Equation ??? in an integrated form.

$$N_t = N_0 e^{-\lambda t} \tag{13.3.5}$$

Substituting Equation 13.3.5 into Equation 13.3.4 gives

$$A = \lambda N_0 e^{-\lambda t} = A_0 e^{-\lambda t} \tag{13.3.6}$$

If we measure a sample's activity at time t we can determine the sample's initial activity, A_0, or the number of radioactive atoms originally present in the sample, N_0.

An important characteristic property of a radioactive isotope is its **half-life**, $t_{1/2}$, which is the amount of time required for half of the radioactive atoms to disintegrate. For first-order kinetics the half-life is

$$t_{1/2} = \frac{0.693}{\lambda} \tag{13.3.7}$$

Because the half-life is independent of the number of radioactive atoms, it remains constant throughout the decay process. For example, if 50% of the radioactive atoms remain after one half-life, then 25% remain after two half-lives, and 12.5% remain after three half-lives.

> Suppose we begin with an N_0 of 1200 atoms During the first half-life, 600 atoms disintegrate and 600 remain. During the second half-life, 300 of the 600 remaining atoms disintegrate, leaving 300 atoms or 25% of the original 1200 atoms. Of the 300 remaining atoms, only 150 remain after the third half-life, or 12.5% of the original 1200 atoms.

Kinetic information about a radioactive isotope is usually given in terms of its half-life because it provides a more intuitive sense of the isotope's stability. Knowing, for example, that the decay constant for $^{90}_{38}\text{Sr}$ is 0.0247 yr^{-1} does not give an immediate sense of how fast it disintegrates. On the other hand, knowing that its half-life is 28.1 y makes it clear that the concentration of $^{90}_{38}\text{Sr}$ in a sample remains essentially constant over a short period of time.

13.3.2 Instrumentation

Alpha particles, beta particles, gamma rays, and X-rays are measured by using the particle's energy to produce an amplified pulse of electrical current in a detector. These pulses are counted to give the rate of disintegration. Three types of detectors commonly are encountered: gas-filled detectors, scintillation counters, and semiconductor detectors. A gas-filled detector consists of a tube containing an inert gas, such as Ar. When a radioactive particle enters the tube it ionizes the inert gas, producing an Ar^+/e^- ion-pair. Movement of the electron toward the anode and the Ar^+ toward the cathode generates a measurable electrical current. A **Geiger counter** is one example of a gas-filled detector. A **scintillation counter** uses a fluorescent material to convert radioactive particles into easily measurable photons. For example, a solid-state scintillation counter consisting of a NaI crystal containing 0.2% TlI produces several thousand photons for each radioactive particle. Finally, in a semiconductor detector, adsorption of a single radioactive particle promotes thousands of electrons to the semiconductor's conduction band, increasing conductivity.

> You can learn more about these radiation detectors and the signal processors used to count particles by consulting this chapter's additional resources.

13.3.3 Quantitative Applications

In this section we consider three common quantitative radiochemical methods of analysis: the direct analysis of a radioactive isotope by measuring its rate of disintegration, neutron activation, and isotope dilution.

Direct Analysis of Radioactive Analytes

The concentration of a long-lived radioactive isotope remains essentially constant during the period of analysis. As shown in Example 13.9, we can use the sample's activity to calculate the number of radioactive particles in the sample.

Example 13.9

The activity in a 10.00-mL sample of wastewater containing $^{90}_{38}\text{Sr}$ is 9.07×10^6 disintegrations/s. What is the molar concentration of $^{90}_{38}\text{Sr}$ in the sample? The half-life for $^{90}_{38}\text{Sr}$ is 28.1 yr.

Solution

Solving equation 13.37 for λ, substituting into Equation 13.3.4, and solving for N gives

$$N = \frac{A \times t_{1/2}}{0.693} \tag{13.3.8}$$

Before we can determine the number of atoms of $^{90}_{38}\text{Sr}$ in the sample we must express its activity and its half-life using the same units. Converting the half-life to seconds gives $t_{1/2}$ as 8.86×10^8 s; thus, there are

$$\frac{(9.07 \times 10^6 \text{ disintergrations/s})(8.86 \times 10^8 \text{ s})}{0.693} = 1.16 \times 10^{16} \text{ atoms } ^{90}_{38}\text{Sr} \tag{13.3.9}$$

The concentration of $^{90}_{38}\text{Sr}$ in the sample is

$$\frac{1.16 \times 10^{16} \text{ atoms } ^{90}_{38}\text{Sr}}{(6.022 \times 10^{23} \text{ atom/mol})(0.01000 \text{ L})} = 1.93 \times 10^{-6} \text{ M } ^{90}_{38}\text{Sr} \tag{13.3.10}$$

The direct analysis of a short-lived radioactive isotope using the method outlined in Example 13.9 is less useful because it provides only a transient measure of the isotope's concentration. Instead, we can measure its activity after an elapsed time, t, and use Equation 13.3.6 to calculate N_0.

Neutron Activation Analysis

Few analytes are naturally radioactive. For many analytes, however, we can induce radioactivity by irradiating the sample with neutrons in a process called neutron activation analysis (NAA). The radioactive element formed by **neutron activation** decays to a stable isotope by emitting a gamma ray, and, possibly, other nuclear particles. The rate of gamma-ray emission is proportional to the analyte's initial concentration in the sample. For example, if we place a sample containing non-radioactive $^{27}_{13}\text{Al}$ in a nuclear reactor and irradiate it with neutrons, the following nuclear reaction takes place.

$$^{27}_{13}\text{Al} + ^{1}_{0}\text{n} \longrightarrow ^{28}_{13}\text{Al} \tag{13.3.11}$$

The radioactive isotope of $^{28}_{13}\text{Al}$ has a characteristic decay process that includes the release of a beta particle and a gamma ray.

$$^{28}_{13}\text{Al} \longrightarrow ^{28}_{14}\text{Si} + ^{0}_{-1}\beta + \gamma \tag{13.3.12}$$

When irradiation is complete, we remove the sample from the nuclear reactor, allow any short-lived radioactive interferences to decay into the background, and measure the rate of gamma-ray emission.

The initial activity at the end of irradiation depends on the number of atoms that are present. This, in turn, is a equal to the difference between the rate of formation for $^{28}_{13}\text{Al}$ and its rate of disintegration

$$\frac{dN_{^{28}_{13}\text{Al}}}{dt} = \Phi\sigma N_{^{27}_{13}\text{Al}} - \lambda N_{^{28}_{13}\text{Al}} \tag{13.3.13}$$

where Φ is the neutron flux and σ is the reaction cross-section, or probability that a $^{27}_{13}\text{Al}$ nucleus captures a neutron. Integrating equation 13.38 over the time of irradiation, t_i, and multiplying by λ gives the initial activity, A_0, at the end of irradiation as

$$A_0 = \lambda N_{^{28}_{13}\text{Al}} = \Phi\sigma N_{^{28}_{13}\text{Al}}(1 - e^{-\lambda t_i}) \tag{13.3.14}$$

If we know the values for A_0, Φ, σ, λ, and t_i, then we can calculate the number of atoms of $^{27}_{13}\text{Al}$ initially present in the sample.

A simpler approach is to use one or more external standards. Letting $(A_0)_x$ and $(A_0)_s$ represent the initial activity for the analyte in an unknown and in an external standard, and letting w_x and w_s represent the analyte's weight in the unknown and in the external standard, we obtain the following pair of equations

$$(A_0)_x = kw_x \tag{13.3.15}$$

$$(A_0)_s = kw_s \tag{13.3.16}$$

that we can solve to determine the analyte's mass in the sample.

As noted earlier, gamma ray emission is measured following a period during which we allow short-lived interferents to decay into the background. As shown in Figure 13.17, we determine the sample's and the standard's initial activity by extrapolating a curve of activity versus time back to $t = 0$. Alternatively, if we irradiate the sample and the standard simultaneously, and if we measure their activities at the same time, then we can substitute these activities for $(A_0)_x$ and $(A_0)_s$. This is the strategy used in the following example.

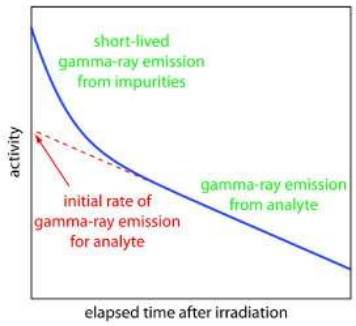


Figure 13.17 *Plot of gamma-ray emission as a function of time showing how the analyte's initial activity is determined.*

Example 13.10

The concentration of Mn in steel can be determined by a neutron activation analysis using the method of external standards. A 1.000-g sample of an unknown steel sample and a 0.950-g sample of a standard steel known to contain 0.463% w/w Mn are irradiated with neutrons in a nuclear reactor for 10 h. After a 40-min delay the gamma ray emission is 2542 cpm (counts per minute) for the unknown and 1984 cpm for the external standard. What is the %w/w Mn in the unknown steel sample?

Solution

Combining equation 13.39 and equation 13.40 gives

$$w_x = \frac{A_x}{A_s} \times w_s \tag{13.3.17}$$

The weight of Mn in the external standard is

$$w_s = \frac{0.00463 \text{ g Mn}}{\text{g steel}} \times 0.950 \text{ g steel} = 0.00440 \text{ g Mn} \tag{13.3.18}$$

Substituting into the above equation gives

$$w_x = \frac{2542 \text{ cpm}}{1984 \text{ cpm}} \times 0.00440 \text{ g Mn} = 0.00564 \text{ g Mn} \tag{13.3.19}$$

Because the original mass of steel is 1.000 g, the %w/w Mn is 0.564%.

Among the advantages of neutron activation are its applicability to almost all elements in the periodic table and that it is nondestructive to the sample. Consequently, NAA is an important technique for analyzing archeological and forensic samples, as well as works of art.

Isotope Dilution

Another important radiochemical method for the analysis of nonradioactive analytes is **isotope dilution**. An external source of analyte is prepared in a radioactive form with a known activity, A_T, for its radioactive decay—we call this form of the analyte a **tracer**. To prepare a sample for analysis we add a known mass of the tracer, w_T, to a portion of sample containing an unknown mass, w_x, of analyte. After homogenizing the sample and tracer, we isolate w_A grams of analyte by using a series of appropriate chemical and physical treatments. Because our processing techniques cannot distinguish between radioactive and nonradioactive forms of the analyte, the isolated material contains both. Finally, we measure the activity of the isolated sample, A_A. If we recover all the analyte—both the radioactive tracer and the nonradioactive analyte—then A_A and A_T are equal and $w_x = w_A - w_T$. Normally, we fail to recover all the analyte. In this case A_A is less than A_T, and

$$A_A = A_T \times \frac{w_A}{w_x + w_T} \tag{13.3.20}$$

The ratio of weights in Equation 13.3.20 accounts for the loss of the activity resulting from our failure to recover all the analyte. Solving equation 13.41 for w_x gives

$$w_x = \frac{A_T}{A_A} w_A - w_T \tag{13.3.21}$$

How we process the sample depends on the analyte and the sample's matrix. We might, for example, digest the sample to bring the analyte into solution. After filtering the sample to remove the residual solids, we might precipitate the analyte, isolate it by filtration, dry it in an oven, and obtain its weight.

Given that the goal of an analysis is to determine the amount of nonradioactive analyte in our sample, the thought that we might not recover all the analyte might strike you as unsettling. Recall from Chapter 7.7, that a single liquid–liquid extraction rarely has an extraction efficiency of 100%. One advantage of isotope dilution is that the extraction efficiency for the nonradioactive analyte and the tracer are the same. If we recover 50% of the tracer, then we also recover 50% of the nonradioactive analyte. Because we know how much tracer we added to the sample, we can determine how much of the nonradioactive analyte is in the sample.

Example 13.11

The concentration of insulin in a production vat is determined by isotope dilution. A 1.00-mg sample of insulin labeled with ^{14}C having an activity of 549 cpm is added to a 10.0-mL sample taken from the production vat. After homogenizing the sample, a portion of the insulin is separated and purified, yielding 18.3 mg of pure insulin. The activity for the isolated insulin is measured at 148 cpm. How many mg of insulin are in the original sample?

Solution

Substituting known values into Equation 13.3.21 gives

$$w_x = \frac{549 \text{ cpm}}{148 \text{ cpm}} \times 18.3 \text{ mg} - 1.00 \text{ mg} = 66.9 \text{ mg insulin} \tag{13.3.22}$$

Equation 13.3.20 and Equation 13.3.21 are valid only if the tracer's half-life is considerably longer than the time it takes to conduct the analysis. If this is not the case, then the decrease in activity is due both to the incomplete recovery and the natural decrease in the tracer's activity. Table 13.1 provides a list of several common tracers for isotope dilution.

Table 13.1: Common Tracers for Isotope Dilution

isotope	half-life
^{3}H	12.5 years
^{14}C	5730 years
^{32}P	14.3 days
^{35}S	87.1 days
^{45}Ca	152 days
^{55}Fe	2.91 years
^{60}Co	5.3 years
^{131}I	8 days

An important feature of isotope dilution is that it is not necessary to recover all the analyte to determine the amount of analyte present in the original sample. Isotope dilution, therefore, is useful for the analysis of samples with complex matrices, where a complete recovery of the analyte is difficult.

13.3.4 Characterization Applications

One example of a characterization application is the determination of a sample's age based on the decay of a radioactive isotope naturally present in the sample. The most common example is carbon-14 dating, which is used to determine the age of natural organic materials.

As cosmic rays pass through the upper atmosphere, some of the $^{14}_{7}\text{N}$ atoms in the atmosphere capture high energy neutrons, converting into $^{14}_{6}\text{C}$. The $^{14}_{6}\text{C}$ then migrates into the lower atmosphere where it oxidizes to form C-14 labeled CO_2. Animals and plants subsequently incorporate this labeled CO_2 into their tissues. Because this is a steady-state process, all plants and animals have the same ratio of $^{14}_{6}\text{C}$ to $^{12}_{6}\text{C}$ in their tissues. When an organism dies, the radioactive decay of $^{14}_{6}\text{C}$ to $^{14}_{7}\text{N}$ by $^{0}_{-1}\beta$ emission ($t_{1/2}$ = 5730 years) leads to predictable reduction in the $^{14}_{6}\text{C}$ to $^{12}_{6}\text{C}$ ratio. We can use the change in this ratio to date samples that are as much as 30 000 years old, although the precision of the analysis is best when the sample's age is less than 7000 years. The accuracy of carbon-14 dating depends upon our assumption that the $^{14}_{6}\text{C}$ to $^{12}_{6}\text{C}$ ratio is constant over time. Some variation in the ratio has occurred as the result of the increased consumption of fossil fuels and the production of $^{14}_{6}\text{C}$ during the testing of nuclear weapons. A calibration curve prepared using samples of known age—these include tree rings, deep ocean sediments, coral samples, and cave deposits—limits this source of uncertainty.

There is no need to prepare a calibration curve for each analysis. Instead, there is a universal calibration curve known as IntCal. The most recent such curve, IntCal04 is described in the following paper: Reimer, P. J., et. al. "IntCal04 Terrestrial Radiocarbon Age Calibration, 0–26 Cal Kyr BP," *Radiocarbon* **2004**, *46*, 1029–1058. This calibration spans 26 000 years (Cal Kyr) before the present (BP).

Example 13.12

To determine the age of a fabric sample the relative ratio of $^{14}_{6}\text{C}$ to $^{12}_{6}\text{C}$ was measured yielding a result of 80.9% of that found in modern fibers. How old is the fabric?

Solution

Equations 13.36 and 13.37 provide us with a method for converting a change in the ratio of $^{14}_{6}\text{C}$ to $^{12}_{6}\text{C}$ to the fabric's age. Letting A_0 be the ratio of $^{14}_{6}\text{C}$ to $^{12}_{6}\text{C}$ in modern fibers, we assign it a value of 1.00. The ratio of $^{14}_{6}\text{C}$ to $^{12}_{6}\text{C}$ in the sample, A, is 0.809. Solving gives

$$t = \ln \frac{A_0}{A} \times \frac{t_{1/2}}{0.693} = \ln \frac{1.00}{0.809} \times \frac{5730\ \text{yr}}{0.693} = 1750\ \text{yr} \tag{13.3.23}$$

Other isotopes can be used to determine a sample's age. The age of rocks, for example, has been determined from the ratio of the number of radioactive $^{238}_{92}\text{U}$ atoms to the number of stable $^{206}_{82}\text{Pb}$ atoms produced by radioactive decay. For rocks that do not contain uranium, dating is accomplished by comparing the ratio of radioactive $^{40}_{19}\text{K}$ to the stable $^{40}_{18}\text{Ar}$. Another example is the dating of sediments collected from lakes by measuring the amount of $^{210}_{82}\text{Pb}$ that is present.

13.3.5 Evaluation

Radiochemical methods are routinely used for the analysis of trace analytes in macro and meso samples. The accuracy and precision of radiochemical methods are generally within the range of 1.5%. We can improve the precision.which is limited by the random nature of radioactive decay.by counting the emission of radioactive particles for as long a time as is practical. If the number of counts, M, is reasonably large (M . 100), and the counting period is significantly less than the isotopeˆ's half-life, then the percent relative standard deviation for the activity, $(\sigma_A)_{rel}$, is approximately

$$(\sigma_A)_{rel} = \frac{1}{\sqrt{M}} \times 100 \tag{13.3.24}$$

See Figure 3.5 to review the meaning of macro and meso samples.

For example, if we determine the activity by counting 10 000 radioactive particles, then the relative standard deviation is 1%. A radiochemical method's sensitivity is inversely proportional to $(\sigma_A)_{rel}$, which means we can improve the sensitivity by counting more particles. Selectivity rarely is of concern when using a radiochemical method because most samples have only a single

radioactive isotope. When several radioactive isotopes are present, we can determine each isotope's activity by taking advantage of differences in the energies of their respective radioactive particles or differences in their respective decay rates. In comparison to most other analytical techniques, radiochemical methods are usually more expensive and require more time to complete an analysis. Radiochemical methods also are subject to significant safety concerns due to the analyst's potential exposure to high energy radiation and the need to safely dispose of radioactive waste.

Contributors

- David Harvey (DePauw University)

13.3: Radiochemistry is shared under a CC BY-NC-SA 4.0 license and was authored, remixed, and/or curated by LibreTexts.

13.4: Flow Injection Analysis

The focus of this chapter is on methods in which we measure a time-dependent signal. Chemical kinetic methods and radiochemical methods are two examples. In this section we consider the technique of flow injection analysis in which we inject the sample into a flowing carrier stream that gives rise to a transient signal at the detector. Because the shape of this transient signal depends on the physical and chemical kinetic processes occurring in the carrier stream during the time between injection and detection, we include flow injection analysis in this chapter.

13.4.1 Theory and Practice

Flow injection analysis (FIA) was developed in the mid-1970s as a highly efficient technique for the automated analyses of samples.[17] Unlike the centrifugal analyzer described earlier in this chapter, in which the number of samples is limited by the transfer disk's size, FIA allows for the rapid, sequential analysis of an unlimited number of samples. FIA is one example of a continuous-flow analyzer, in which we sequentially introduce samples at regular intervals into a liquid carrier stream that transports them to the detector.

A schematic diagram detailing the basic components of a flow injection analyzer is shown in Figure 13.18. The reagent serving as the carrier is stored in a reservoir, and a propelling unit maintains a constant flow of the carrier through a system of tubing that comprises the transport system. We inject the sample directly into the flowing carrier stream, where it travels through one or more mixing and reaction zones before reaching the detector's flow-cell. Figure 13.18 is the simplest design for a flow injection analyzer, consisting of a single channel and one reagent reservoir. Multiple channel instruments that merge together separate channels, each introducing a new reagent into the carrier stream, also are possible. A more detailed discussion of FIA instrumentation is found in the next section.

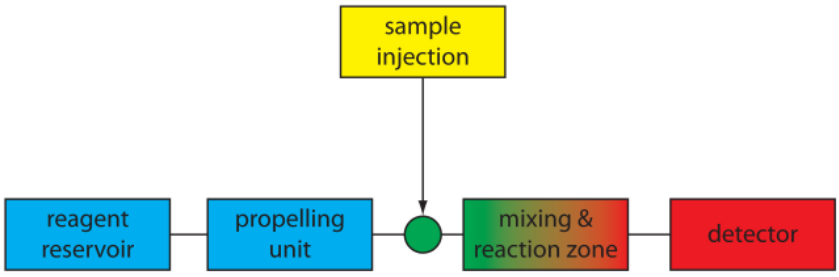


Figure 13.18 Schematic diagram of a simple flow injection analyzer showing its basic components. After its injection into the carrier stream the samples mixes and reacts with the carrier stream's reagents before reaching the detector.

When we first inject a sample into the carrier stream it has the rectangular flow profile of width *w* as shown in Figure 13.19a. As the sample moves through the mixing and reaction zone, the width of its flow profile increases as the sample disperses into the carrier stream. Dispersion results from two processes: convection due to the flow of the carrier stream and diffusion due to the concentration gradient between the sample and the carrier stream. Convection occurs by laminar flow. The linear velocity of the sample at the tube's walls is zero, but the sample at the center of the tube moves with a linear velocity twice that of the carrier stream. The result is the parabolic flow profile shown in Figure 13.19b. Convection is the primary means of dispersion in the first 100 ms following the sample's injection.

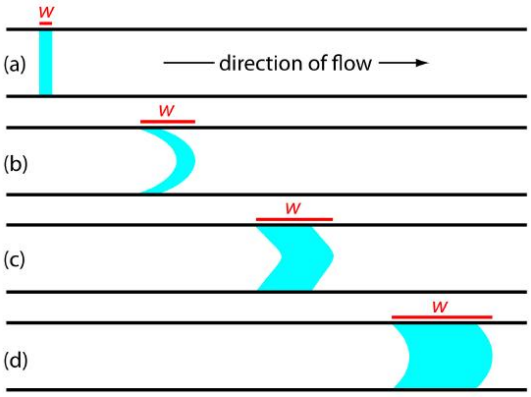


Figure 13.19 Effect of dispersion on the shape of a sample's flow profile at different times during a flow injection analysis: (a) at injection; (b) when convection dominates dispersion; (c) when convection and diffusion contribute to dispersion; and (d) when diffusion dominates dispersion. The red line shows the width, *w*, of the samples flow profile.

The second contribution to the sample's dispersion is diffusion due to the concentration gradient between the sample and the carrier stream. As shown in Figure 13.20, diffusion occurs parallel (axially) and perpendicular (radially) to the direction in which the carrier stream is moving. Only radial diffusion is important in flow injection analysis. Radial diffusion decreases the sample's linear velocity at the center of the tubing, while the sample at the edge of the tubing experiences an increase in its linear velocity. Diffusion helps to maintain the integrity of the sample's flow profile (Figure 13.19c), preventing samples in the carrier stream from dispersing into one another. Both convection and diffusion make significant contributions to dispersion from approximately 3–20 s after the sample's injection. This is the normal time scale for a flow injection analysis. After approximately 25 s, diffusion is the only significant contributor to dispersion, resulting in a flow profile similar to that shown in Figure 13.19d.

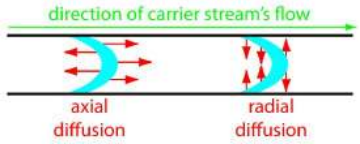


Figure 13.20 Illustration showing axial and radial diffusion. The blue band is the sample's flow profile and the red arrows indicate the direction of diffusion.

An FIA curve, or **fiagram**, is a plot of the detector^'s signal as a function of time. Figure 13.21 shows a typical fiagram for conditions in which both convection and diffusion contribute to the sample^'s dispersion. Also shown on the figure are several parameters for characterizing a sample^'s fiagram. Two parameters define the time for a sample to move from the injector to the detector. Travel time, t_a, is the time between the sample^'s injection and the arrival of its leading edge at the detector. Residence time, *T*, on the other hand, is the time required to obtain the maximum signal. The difference between the residence time and travel time is $t^{\prime}$, which approaches zero when convection is the primary means of dispersion, and increases in value as the contribution from diffusion becomes more important.

https://chem.libretexts.org/@go/page/70729

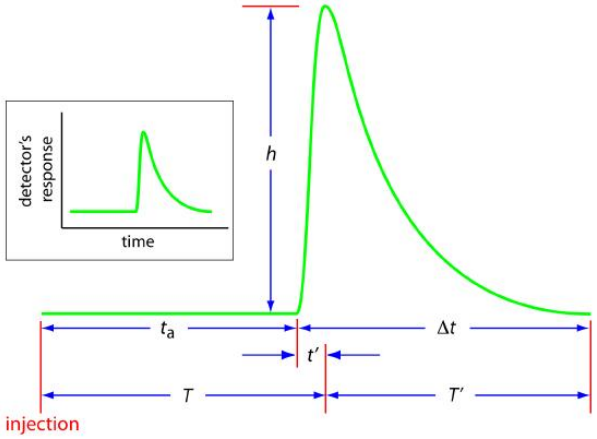


Figure 13.21 Typical fiagram for flow injection analysis showing the detectorˆ's response as a function of time. See the text for an explanation of the parameters t_a, t', Δt, T, T', and h.

The time required for the sample to pass through the detectorˆ's flow cell.and for the signal to return to the baseline.is also described by two parameters. The baseline-to-baseline time, Δt, is the time between the arrival of the sampleˆ's leading edge to the departure of its trailing edge. The elapsed time between the maximum signal and its return to the baseline is the return time, T'. The final characteristic parameter of a fiagram is the sampleˆ's peak height, h.

Of the six parameters shown in Figure 13.21, the most important are peak height and return time. Peak height is important because it is directly or indirectly related to the analyteˆ's concentration. The sensitivity of an FIA method, therefore, is determined by the peak height. The return time is important because it determines the frequency with which we may inject samples. Figure 13.22 shows that if we inject a second sample at a time T' after injecting the first sample, there is little overlap of the two FIA curves. By injecting samples at intervals of T', we obtain the maximum possible sampling rate.

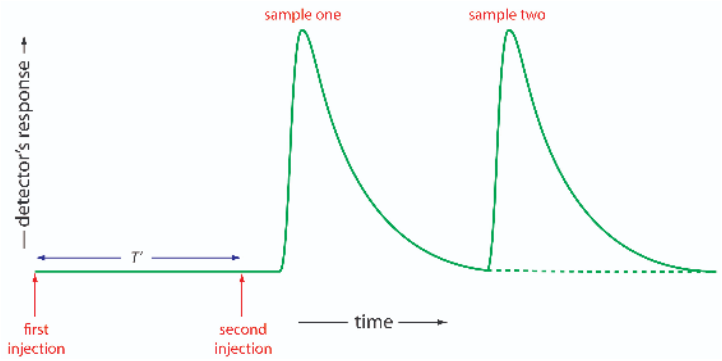


Figure 13.22 Effect of return time, T', on sampling frequency.

Peak heights and return times are influenced by the dispersion of the sampleˆ's flow profile and by the physical and chemical properties of the flow injection system. Physical parameters affecting h and T' include the volume of sample we inject, the flow rate, the length, diameter and geometry of the mixing and reaction zones, and the presence of mixing points where separate channels merge together. The kinetics of any chemical reactions between the sample and the reagents in the carrier stream also influence the peak height and return time.

Unfortunately, there is no good theory that we can use to consistently predict the peak height and return time for a given set of physical and chemical parameters. The design of a flow injection analyzer for a particular analytical problem still occurs largely by a process of experimentation. Nevertheless, we can make some general observations about the effects of physical and chemical parameters. In the absence of chemical effects, we can improve sensitivity—that is, obtain larger peak heights—by injecting larger samples, increasing the flow rate, decreasing the length and diameter of the tubing in the mixing and reaction zone, and merging separate channels before the point where the sample is injected. With the exception of sample volume, we can increase the sampling rate—that is, decrease the return time—using by the same combination of physical parameters. Larger sample volumes,

however, lead to longer return times and a decrease in sample throughput. The effect of chemical reactivity depends on whether the species we are monitoring is a reactant or a product. For example, if we are monitoring a reactant, we can improve sensitivity by choosing conditions that decrease the residence time, *T*, or by adjusting the carrier stream's composition so that the reaction occurs more slowly.

13.4.2 Instrumentation

The basic components of a flow injection analyzer are shown in Figure 13.23 and include a pump for propelling the carrier stream and reagent streams, a means for injecting the sample into the carrier stream, and a detector for monitoring the composition of the carrier stream. Connecting these units is a transport system that brings together separate channels and provides time for the sample to mix with the carrier stream and to react with the reagent streams. We also can incorporate separation modules into the transport system. Each of these components is considered in greater detail in this section.

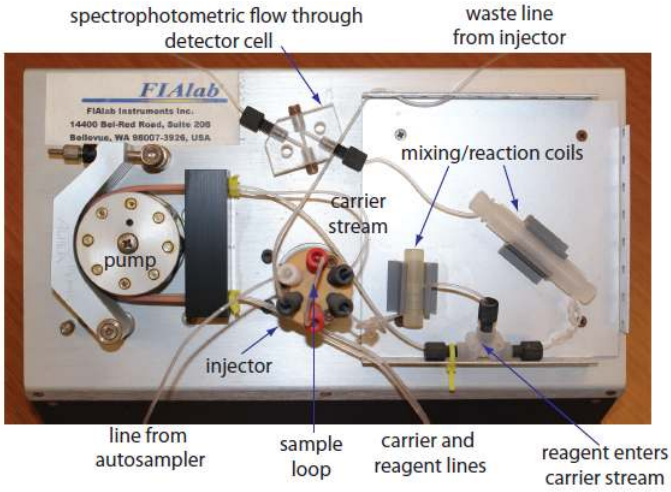


Figure 13.23 Example of a typical flow injection analyzer showing the pump, the injector, the transport system consisting of mixing/reaction coils and junctions, and the detector (minus the spectrophotometer). This particular configuration has two channels: the carrier stream and a reagent line.

Propelling Unit

The propelling unit moves the carrier stream through the flow injection analyzer. Although several different propelling units have been used, the most common is a **peristaltic pump**. A peristaltic pump consists of a set of rollers attached to the outside of a rotating drum, as shown in Figure 13.24. Tubing from the reagent reservoirs fits between the rollers and a fixed plate. As the drum rotates the rollers squeeze the tubing, forcing the contents of the tubing to move in the direction of the rotation. Peristaltic pumps provide a constant flow rate, which is controlled by the drum's speed of rotation and the inner diameter of the tubing. Flow rates from 0.0005–40 mL/min are possible, which is more than adequate to meet the needs of FIA where flow rates of 0.5–2.5 mL/min are common. One limitation to a peristaltic pump is that it produces a pulsed flow—particularly at higher flow rates—that may lead to oscillations in the signal.

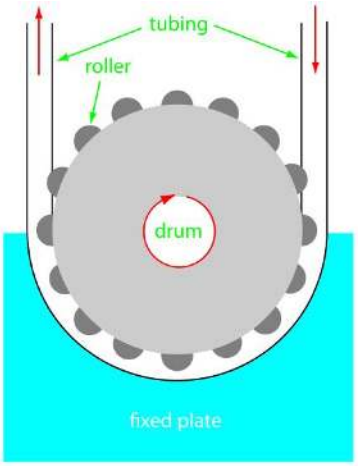


Figure 13.24 Schematic diagram of a peristaltic pump.

Injector

The sample, typically 5–200 μL, is injected into the carrier stream. Although syringe injections through a rubber septum are possible, the more common method—as seen in Figure 13.23—is to use a rotary, or loop injector similar to that used in an HPLC. This type of injector provides for a reproducible sample volume and is easily adaptable to automation, an important feature when high sampling rates are needed.

> **Note**
>
> Figure 12.39 and Figure 12.45 show examples of an HPLC loop injector.

Detector

The most commonly used detectors for flow injection analysis are the electrochemical and optical detectors used in HPLC. These detectors are discussed in Chapter 12 and are not considered further in this section. FIA detectors also have been designed around the use of ion selective electrodes and atomic absorption spectroscopy.

Transport System

The heart of a flow injection analyzer is the transport system that brings together the carrier stream, the sample, and any reagents that react with the sample. Each reagent stream is considered a separate channel, and all channels must merge before the carrier stream reaches the detector. The complete transport system is called a **manifold**.

The simplest manifold includes only a single channel, the basic outline of which is shown in Figure 13.25. This type of manifold is commonly used for direct analyses that do not require a chemical reaction. In this case the carrier stream serves only as a means for rapidly and reproducibly transporting the sample to the detector. For example, this manifold design has been used for sample introduction in atomic absorption spectroscopy, achieving sampling rates as high as 700 samples/h. A single-channel manifold also is used for determining a sample's pH or determining the concentration of metal ions using an ion selective electrode.

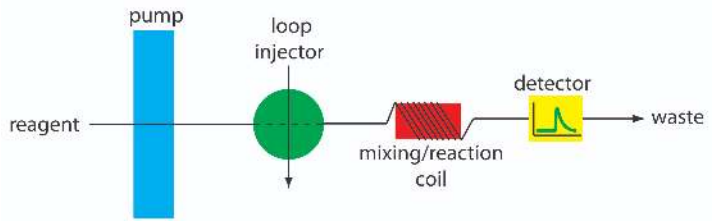


Figure 13.25 Example of a single-channel manifold in which the reagent serves as the carrier stream and as a species that reacts with the sample. The mixing/reaction coil is wrapped around a plastic cylinder.

We can also use the single-channel manifold in Figure 13.25 for systems in which we monitor the product of a chemical reaction between the sample and a reactant. In this case the carrier stream both transports the sample to the detector and reacts with the

sample. Because the sample must mix with the carrier stream, a lower flow rate is used. One example is the determination of chloride in water, which is based on the following sequence of reactions.

$$Hg(SCN)_2(aq) + 2\,Cl^-(aq) \leftrightharpoons HgCl_2(aq) + 2\,SCN^-(aq) \quad (13.4.1)$$

$$Fe^{3+}(aq) + SCN^-(aq) \leftrightharpoons Fe(SCN)^{2+}(aq) \quad (13.4.2)$$

The carrier stream consists of an acidic solution of $Hg(SCN)_2$ and Fe^{3+}. Injecting a sample containing chloride into the carrier stream displaces thiocyanate from $Hg(SCN)_2$. The displaced thiocyanate then reacts with Fe^{3+} to form the red-colored $Fe(SCN)^{2+}$ complex, the absorbance of which is monitored at a wavelength of 480 nm. Sampling rates of approximately 120 samples per hour have been achieved with this system.[18]

Most flow injection analyses that include a chemical reaction use a manifold with two or more channels. Including additional channels provides more control over the mixing of reagents and the interaction between the reagents and the sample. Two configurations are possible for a dual-channel system. A dual-channel manifold, such as the one shown in Figure 13.26a, is used when the reagents cannot be premixed because of their reactivity. For example, in acidic solutions phosphate reacts with molybdate to form the heteropoly acid $H_3P(Mo_{12}O_{40})$. In the presence of ascorbic acid the molybdenum in the heteropoly acid is reduced from Mo(VI) to Mo(V), forming a blue-colored complex that is monitored spectrophotometrically at 660 nm.[18] Because ascorbic acid reduces molybdate, the two reagents are placed in separate channels that merge just before injecting the sample.

A dual-channel manifold can also be used to add a second reagent after injecting the sample into a carrier stream, as shown in Figure 13.26b. This style of manifold is used for the quantitative analysis of many analytes, including the determination of a wastewater's chemical oxygen demand (COD).[19] Chemical oxygen demand is a measure of the amount organic matter in the wastewater sample. In the conventional method of analysis, COD is determined by refluxing the sample for 2 h in the presence of acid and a strong oxidizing agent, such as $K_2Cr_2O_7$ or $KMnO_4$. When refluxing is complete, the amount of oxidant consumed in the reaction is determined by a redox titration. In the flow injection version of this analysis, the sample is injected into a carrier stream of aqueous H_2SO_4, which merges with a solution of the oxidant from a secondary channel. The oxidation reaction is kinetically slow. As a result, the mixing and reaction coils are very long, typically 40 m, and submerged in a thermostated bath. The sampling rate is lower than that for most flow injection analyses, but at 10–30 samples/h it is substantially greater than the redox titrimetric method.

> **Note**
>
> You will find a more detailed description of the redox titrimetric method for COD in Chapter 9.

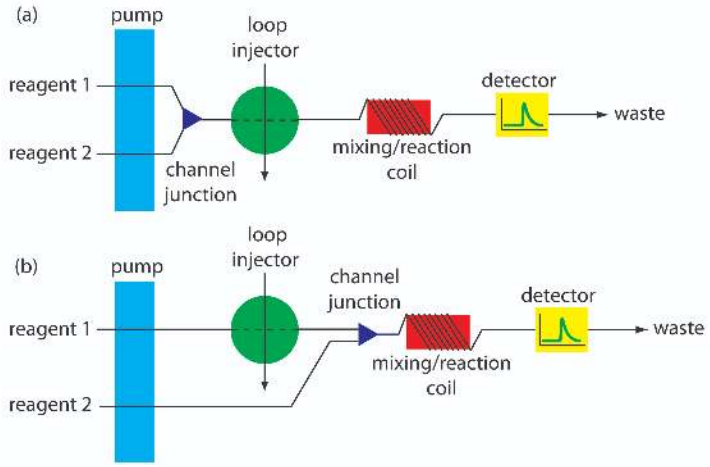


Figure 13.26 Two examples of a dual-channel manifold for flow injection analysis. In (a) the two channels merge before the loop injector, and in (b) the two channels merge after the loop injector.

More complex manifolds involving three or more channels are common, but the possible combination of designs is too numerous to discuss. One example of a four-channel manifold is shown in Figure 13.27.

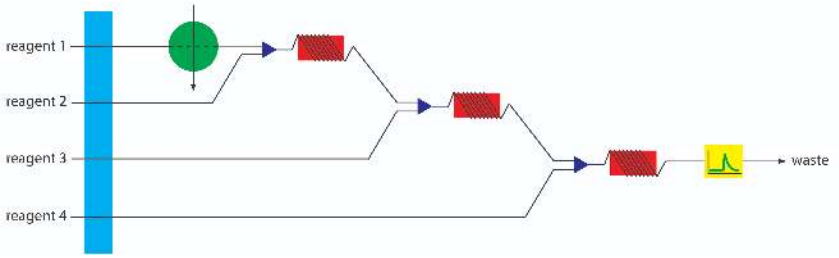


Figure 13.27 Example of a four-channel manifold for a flow injection analysis.

Separation Modules

By incorporating a separation module in the flow injection manifold we can include a separation—dialysis, gaseous diffusion and liquid-liquid extractions are examples—into a flow injection analysis. Although these separations are never complete, they are reproducible if we carefully control the experimental conditions.

Dialysis and gaseous diffusion are accomplished by placing a semipermeable membrane between the carrier stream containing the sample and an acceptor stream, as shown in Figure 13.28. As the sample stream passes through the separation module, a portion of those species capable of crossing the semipermeable membrane do so, entering the acceptor stream. This type of separation module is common for the analysis of clinical samples, such as serum and urine, where a dialysis membrane separates the analyte from its complex matrix. Semipermeable gaseous diffusion membranes have been used for the determination of ammonia and carbon dioxide in blood. For example, ammonia is determined by injecting the sample into a carrier stream of aqueous NaOH. Ammonia diffuses across the semipermeable membrane into an acceptor stream containing an acid–base indicator. The resulting acid–base reaction between ammonia and the indicator is monitored spectrophotometrically.

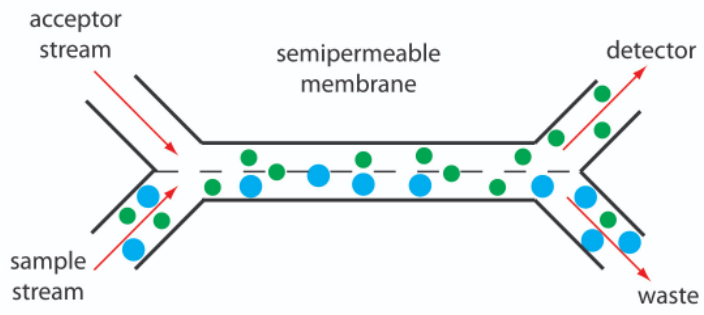


Figure 13.28 Separation module for a flow injection analysis using a semipermeable membrane. The smaller green solutes can pass through the semipermeable membrane and enter the acceptor stream, but the larger blue solutes cannot. Although the separation is not complete—note that some of the green solute remains in the sample stream and exits as waste—it is reproducible if we do not change the experimental conditions.

Liquid–liquid extractions are accomplished by merging together two immiscible fluids, each carried in a separate channel. The result is a segmented flow through the separation module, consisting of alternating portions of the two phases. At the outlet of the separation module the two fluids are separated by taking advantage of the difference in their densities. Figure 13.29 shows a typical configuration for a separation module in which the sample is injected into an aqueous phase and extracted into a less dense organic phase that passes through the detector.

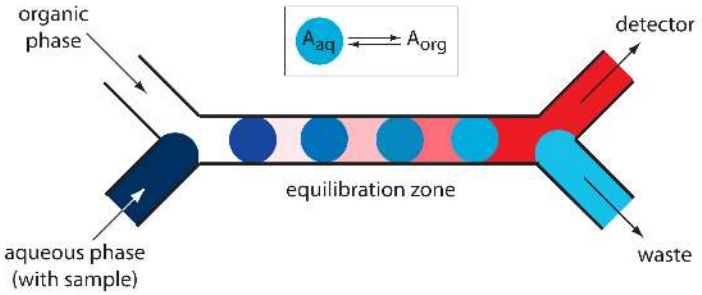


Figure 13.29 Separation module for flow injection analysis using a liquid–liquid extraction. The inset shows the equilibrium reaction. As the sample moves through the equilibration zone, the analyte extracts into the organic phase.

13.4.3 Quantitative Applications

In a quantitative flow injection method a calibration curve is determined by injecting a series of external standards containing known concentrations of analyte. The calibration curve's format—examples include plots of absorbance versus concentration and potential versus concentration—depends on the method of detection. Calibration curves for standard spectroscopic and electrochemical methods are discussed in Chapters 10 and 11 and are not considered further in this chapter.

> **Note**
>
> Example 13.13 shows a typical example of a calibration curve for a flow injection analysis.

Flow injection analysis has been used to analyze a wide variety of samples, including environmental, clinical, agricultural, industrial, and pharmaceutical samples. The majority of analyses involve environmental and clinical samples, which is the focus of this section.

Quantitative analytical flow injection analytical methods have been developed for cationic, anionic, and molecular pollutants in wastewater, freshwaters, groundwaters, and marine waters, three examples of which we described in the previous section. Table 13.2 provides a partial listing of other analytes that have been determined using FIA, many of which are modifications of standard spectrophotometric and potentiometric methods. An additional advantage of FIA for environmental analysis is the ability to provide for the continuous, in situ monitoring of pollutants in the field.[20]

> **Note**
>
> The three examples are: the determination of chloride, the determination of phosphate, and the determination of chemical oxygen demand.

Table 13.2 Selected Flow Injection Analysis Methods for Environmental Samples

analyte	sample	sample volume (µL)	concentration range	sampling frequency (h^{-1})
Ca^{2+}	freshwater	20	0.8–7.2 ppm	80
Cu^{2+}	groundwater	70–700	100–400 ppb	20
Pb^{2+}	groundwater	70–700	0–40 ppb	20
Zn^{2+}	sea water	1000	1–100 ppb	30-60
NH_4^+	sea water	60	0.18–18.1 ppb	288
NO_3^-	rain water	1000	1–10 ppm	40
SO_4^{2-}	fresh water	400	4–140 ppm	180
CN^-	industrial	10	0.3–100 ppm	40

Source: Adapted from Valcárcel, M.; Luque de Castro, M. D. *Flow-Injection Analysis: Principles and Practice*, Ellis Horwood: Chichester, England, 1987.

As noted in Chapter 9, several standard methods for the analysis of water involve an acid–base, complexation, or redox titration. It is easy to adapt these titrations to FIA using a single-channel manifold similar to that shown in Figure 13.25.[21] The titrant—whose concentration must be stoichiometrically less than that of the analyte—and a visual indicator are placed in the reagent reservoir and continuously pumped through the manifold. When we inject the sample it thoroughly mixes with the titrant in the carrier stream. The reaction between the analyte, which is in excess, and the titrant produces a relatively broad rectangular flow profile for the sample. As the sample moves toward the detector, additional mixing occurs and the width of its flow profile decreases. When the sample passes through the detector, we determine the width of its flow profile, Δt, by monitoring the indicator's absorbance. A calibration curve of Δt versus log[analyte] is prepared using standard solutions of analyte.

Flow injection analysis has also found numerous applications in the analysis of clinical samples, using both enzymatic and nonenzymatic methods. Table 13.3 summarizes several examples.

Table 13.3 Selected Flow Injection Analysis Methods for Clinical Samples

analyte	sample	sample volume (µL)	concentration range	sampling frequency (h^{-1})
nonenzymatic methods				
Cu^{2+}	serum	20	0.7–1.5 ppm	70
Cl^-	serum	60	50–150 meq/L	125
PO_4^{3-}	serum	200	10–60 ppm	130
total CO_2	serum	50	10–50 mM	70
chloropromazine	blood plasma	200	1.5–9 µM	24
enzymatic methods				
glucose	blood serum	26.5	0.5–15 mM	60
urea	blood serum	30	4–20 mM	60
ethanol	blood	30	5–30 ppm	50

Source: Adapted from Valcárcel, M.; Luque de Castro, M. D. *Flow-Injection Analysis: Principles and Practice*, Ellis Horwood: Chichester, England, 1987.

Note

The best way to appreciate the theoretical and practical details discussed in this section is to carefully examine a typical analytical method. Although each method is unique, the following description of the determination of phosphate provides an instructive example of a typical procedure. The description here is based on Guy, R. D.; Ramaley, L.; Wentzell, P. D. "An Experiment in the Sampling of Solids for Chemical Analysis," *J. Chem. Educ.* **1998**, *75*, 1028–1033. As the title suggests, the primary focus of this chapter is on sampling. A flow injection analysis, however, is used to analyze samples.

Representative Method 13.2

Determination of Phosphate by FIA

Description of Method

The FIA determination of phosphate is an adaptation of a standard spectrophotometric analysis for phosphate. In the presence of acid, phosphate reacts with ammonium molybdate to form a yellow-colored complex in which molybdenum is present as Mo(VI).

$$H_3PO_4(aq) + 12\,H_2MoO_4(aq) \rightleftharpoons H_3P(Mo_{12}O_{40})(aq) + 12\,H_2O(l) \qquad (13.4.3)$$

In the presence of a reducing agent, such as ascorbic acid, the yellow-colored complex is reduced to a blue-colored complex of Mo(V).

Procedure

Prepare the following three solutions: (a) 5.0 mM ammonium molybdate in 0.40 M HNO_3; (b) 0.7% w/v ascorbic acid in 1% v/v glycerin; and (c) 100.0 ppm phosphate standard using KH_2PO_4. Using the phosphate standard, prepare a set of external standards with phosphate concentrations of 10, 20, 30, 40, 50 and 60 ppm. Use a manifold similar to that shown in Figure 13.26a, placing a 50-cm mixing coil between the pump and the loop injector and a 50-cm reaction coil between the loop injector and the detector. For both coils, use PTFE tubing with an internal diameter of 0.8 mm. Set the flow rate to 0.5 mL/min. Prepare a calibration curve by injecting 50 µL of each standard, measuring the absorbance at 650 nm. Samples are analyzed in the same manner.

Questions

1. How long does it take a sample to move from the loop injector to the detector?

The reaction coil is 50-cm long with an internal diameter of 0.8 mm. The volume of this tubing is

$$V = l \times \pi r^2 = 50\ \text{cm} \times \left(\frac{0.08\ \text{cm}}{2}\right)^2 \times \pi = 0.25\ \text{cm}^3 = 0.25\ \text{mL} \tag{13.4.4}$$

With a flow rate of 0.5 mL/min, it takes about 30 s for a sample to pass through the system.

2. The instructions for the standard spectrophotometric method indicate that the absorbance should be measured 5–10 min after adding the ascorbic acid. Why is this waiting period necessary in the spectrophotometric method, but not necessary in the FIA method?

The reduction of the yellow-colored Mo(VI) complex to the blue-colored Mo(V) complex is a slow reaction. In the standard spectrophotometric method it is difficult to reproducibly control the time between adding the reagents to the sample and measuring the sample's absorbance. To achieve good precision we allow the reaction to proceed to completion before we measure the absorbance. As seen by the answer to the previous question, in the FIA method the flow rate and the dimensions of the reaction coil determine the reaction time. Because this time is precisely controlled, the reaction occurs to the same extent for all standards and samples. A shorter reaction time has the advantage of allowing for a higher throughput of samples.

3. The spectrophotometric method recommends using phosphate standards of 2–10 ppm. Explain why the FIA method uses a different range of standards.

In the FIA method we measure the absorbance before the formation of the blue-colored Mo(V) complex is complete. Because the absorbance for any standard solution of phosphate is always smaller when using the FIA method, the FIA method is less sensitive and higher concentrations of phosphate are necessary.

4. How would you incorporate a reagent blank into the FIA analysis?

A reagent blank can be obtained by injecting a sample of distilled water in place of the external standard or sample. The reagent blank's absorbance is subtracted from the absorbances obtained for the standards and samples.

Example 13.13

The following data were obtained for a set of external standards when using Representative Method 13.2 to analyze phosphate in a wastewater sample.

$[PO_4^{3-}]$ (ppm)	absorbance
10.00	0.079
20.00	0.160
30.00	0.233
40.00	0.316
50.00	0.482

What is the concentration of phosphate in a sample if it gives an absorbance of 0.287?

Solution

Figure 13.30 shows the external standards calibration curve and equation. Substituting in the sample's absorbance gives the concentration of phosphate in the sample as 36.1 ppm.

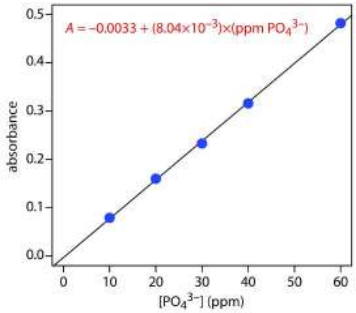


Figure 13.30 Calibration curve and equation for the data in Example 13.13.

13.4.4 Evaluation

The majority of flow injection analysis applications are modifications of conventional titrimetric, spectrophotometric, and electrochemical methods of analysis; thus, it is appropriate to compare FIA methods to conventional methods. The scale of operations for FIA allows for the routine analysis of minor and trace analytes, and for macro, meso, and micro samples. The ability to work with microliter injection volumes is useful when the sample is scarce. Conventional methods of analysis usually have smaller detection limits.

> **Note**
>
> See Figure 3.5 to review the meaning minor and trace analytes, and the meaning of macro, meso and micro samples.

The accuracy and precision of FIA methods are comparable to conventional methods of analysis. The precision of a flow injection analysis is influenced by several variables that do not affect conventional methods, including the stability of the flow rate and the reproducibility of the sample's injection. In addition, results from FIA may be more susceptible to temperature variations.

In general, the sensitivity of FIA is less than that for conventional methods of analysis for at least two reasons. First, as with chemical kinetic methods, measurements in FIA are made under nonequilibrium conditions when the signal has yet to reach its maximum value. Second, dispersion dilutes the sample as it moves through the manifold. Because the variables that affect sensitivity are known, we can design the FIA manifold to optimize the method's sensitivity.

Selectivity for an FIA method is often better than that for the corresponding conventional method of analysis. In many cases this is due to the kinetic nature of the measurement process, in which potential interferents may react more slowly than the analyte. Contamination from external sources also is less of a problem because reagents are stored in closed reservoirs and are pumped through a system of transport tubing that is closed to the environment.

Finally, FIA is an attractive technique when considering time, cost, and equipment. When using an autosampler, a flow injection method can achieve very high sampling rates. A sampling rate of 20–120 samples/h is not unusual and sampling rates as high as 1700 samples/h are possible. Because the volume of the flow injection manifold is small, typically less than 2 mL, the consumption of reagents is substantially smaller than that for a conventional method. This can lead to a significant decrease in the cost per analysis. Flow injection analysis does require the need for additional equipment—a pump, a loop injector, and a manifold—which adds to the cost of an analysis.

Contributors

David Harvey (DePauw University)

13.4: Flow Injection Analysis is shared under a CC BY-NC-SA 4.0 license and was authored, remixed, and/or curated by LibreTexts.

13.E: Kinetic Methods (Exercises)

1. Equation 13.18 shows how $[A]_0$ is determined using a two-point fixed-time integral method in which the concentration of A for the pseudo-first-order reaction

$$\mathbf{A + R \rightarrow P} \tag{13.E.1}$$

is measured at times t_1 and t_2. Derive a similar equation for the case where the product is monitored under pseudo-first order conditions.

2. The concentration of phenylacetate can be determined from the kinetics of its pseudo-first order hydrolysis reaction in an ethylamine buffer. When a standard solution of 0.55 mM phenylacetate is analyzed, the concentration of phenylacetate after 60 s is 0.17 mM. When an sample is analyzed the concentration of phenylacetate remaining after 60 s is 0.23 mM. What is the initial concentration of phenylacetate in the sample?

3. In the presence of acid, solutions of iodide are oxidized by hydrogen peroxide

$$\mathbf{2\,I^-(\mathit{aq}) + H_2O_2(\mathit{aq}) + 2\,H_3O^+(\mathit{aq}) \rightarrow 4\,H_2O(\mathit{l}) + I_2(\mathit{aq})} \tag{13.E.2}$$

When I^- and H_3O^+ are present in excess we can use the kinetics of the reaction—which is pseudo-first order in H_2O_2—to determine the concentration of H_2O_2 by following the production of I_2 with time. In one analysis the absorbance of the solution was measured after 240 s at 348 nm. Analysis of a set of standard solutions of H_2O_2 gives the results shown in the following table.

$[H_2O_2]$ (μM)	absorbance
100.0	0.236
200.0	0.471
400.0	0.933
800.0	1.872

What is the concentration of H_2O_2 in a sample if its absorbance is 0.669 after 240 s?

4. The concentration of chromic acid can be determined by reducing it with an alcohol under conditions that are pseudo-first order in analyte. One approach is to monitor the reaction mixture's absorbance at a wavelength of 355 nm. A standard of 5.1×10^{-4} M chromic acid yields absorbances of 0.855 and 0.709 at 100 s and 300 s after the reaction's initiation. When a sample with an unknown amount of chromic acid is analyzed under identical conditions, the absorbances are 0.883 and 0.706. What is the concentration of chromic acid in the sample?

5. Malmstadt and Pardue developed a variable time method for the determination of glucose based on its oxidation by the enzyme glucose oxidase.[22] To monitor the reaction's progress, iodide is added to the samples and standards. The H_2O_2 produced by the oxidation of glucose reacts with I^-, forming I_2 as a product. The time required to produce a fixed amount of I_2 is determined spectrophotometrically. The following data was reported for a set of calibration standards

[glucose] (ppm)	time (s)		
5.0	146.5	150.0	149.6
10.0	69.2	67.1	66.0
20.0	34.8	35.0	34.0
30.0	22.3	22.7	22.6
40.0	16.7	16.5	17.0
50.0	13.3	13.3	13.8

To verify the method a 1.00-mL aliquot of a standard solution of 40.0 ppm glucose was added to 1.00 mL of the combined reagents, requiring 34.6 s to produce the same extent of reaction. Determine the concentration of glucose in the standard and the percent error for the analysis.

6. Deming and Pardue studied the kinetics for the hydrolysis of *p*-nitrophenyl phosphate by the enzyme alkaline phosphatase.[23] The reaction's progress was monitored by measuring the absorbance of *p*-nitrophenol, which is one of the reaction's products. A plot of the reaction's rate (with units of μmol mL^{-1} sec^{-1}) versus the volume, *V*, in milliliters of a serum calibration standard containing the enzyme, yielded a straight line with the following equation.

$$\text{rate} = 2.7 \times 10^{-7} + 3.485 \times 10^{-5}\, V \tag{13.E.3}$$

A 10.00-mL sample of serum is analyzed, yielding a rate of 6.84×10^{-5} μmol mL^{-1} sec^{-1}. How much more dilute is the enzyme in the serum sample than in the serum calibration standard?

7. The following data were collected for a reaction known to be pseudo-first order in analyte, A, during the time in which the reaction is monitored.

time (s)	$[A]_t$ (mM)
2	1.36
4	1.24
6	1.12
8	1.02
10	0.924
12	0.838
14	0.760
16	0.690
18	0.626
20	0.568

What are the rate constant and the initial concentration of analyte in the sample?

8. The enzyme acetylcholinesterase catalyzes the decomposition of acetylcholine to choline and acetic acid. Under a given set of conditions the enzyme has a K_m of 9×10^{-5} M and a k_2 of 1.4×10^4 s^{-1}. What is the concentration of acetylcholine in a sample if the rate of reaction in the presence of 6.61×10^{-7} M enzyme is 12.33 μM s^{-1}? You may assume that the concentration of acetylcholine is significantly smaller than K_m.

9. The enzyme fumarase catalyzes the stereospecific addition of water to fumarate to form l-malate. A standard 0.150 μM solution of fumarase has a rate of reaction of 2.00 μM min^{-1} under conditions in which the substrate's concentration is significantly greater than K_m. The rate of reaction for a sample under identical condition is 1.15 μM min^{-1}. What is the concentration of fumarase in the sample?

10. The enzyme urease catalyzes the hydrolysis of urea. The rate of this reaction was determined for a series of solutions in which the concentration of urea was changed while maintaining a fixed urease concentration of 5.0 μM. The following data were obtained.

[urea] (mM)	rate (mM s^{-1})
0.100	6.25
0.200	12.5
0.300	18.8
0.400	25.0
0.500	31.2
0.600	37.5
0.700	43.7
0.800	50.0
0.900	56.2
1.00	62.5

Determine the values of V_{max}, k_2, and K_m for urease.

11. To study the effect of an enzyme inhibitor V_{max} and K_m are measured for several concentrations of inhibitor. As the concentration of the inhibitor increases V_{max} remains essentially constant, but the value of K_m increases. Which mechanism for enzyme inhibition is in effect?

12. In the case of competitive inhibition, the equilibrium between the enzyme, E, the inhibitor, I, and the enzyme–inhibitor complex, EI, is described by the equilibrium constant K_I. Show that for competitive inhibition the equation for the rate of reaction is

$$\frac{d[\mathrm{P}]}{dt} = \frac{V_{\max}[\mathrm{S}]}{K_m\{1 + ([\mathrm{I}]/K_I)\} + [\mathrm{S}]} \tag{13.E.4}$$

where K_I is the formation constant for the EI complex

$$\mathrm{E} + \mathrm{I} \leftrightharpoons \mathrm{EI} \tag{13.E.5}$$

You may assume that $k_2 << k_{-1}$.

13. Analytes A and B react with a common reagent R with first-order kinetics. If 99.9% of A must react before 0.1% of B has reacted, what is the minimum acceptable ratio for their respective rate constants?

14. A mixture of two analytes, A and B, is analyzed simultaneously by monitoring their combined concentration, C = [A] + [B], as a function of time when they react with a common reagent. Both A and B are known to follow first-order kinetics with the reagent,

and A is known to react faster than B. Given the data in the following table, determine the initial concentrations of A and B, and the first-order rate constants, k_A and k_B.

time (min)	[C] (mM)
1	0.313
6	0.200
11	0.136
16	0.098
21	0.074
26	0.058
31	0.047
36	0.038
41	0.032
46	0.027
51	0.023
56	0.019
61	0.016
66	0.014
71	0.012

15. Table 13.1 provides a list of several isotopes commonly used as tracers. The half-lives for these isotopes also are listed. What is the rate constant for the radioactive decay of each isotope?

16. ^{60}Co is a long-lived isotope ($t_{1/2}$ = 5.3 yr) frequently used as a radiotracer. The activity in a 5.00-mL sample of a solution of ^{60}Co is 2.1×10^7 disintegrations/sec. What is the molar concentration of ^{60}Co in the sample?

17. The concentration of Ni a new alloy is determined by a neutron activation analysis. A 0.500-g sample of the alloy and a 1.000-g sample of a standard alloy that is 5.93% w/w Ni are irradiated with neutrons in a nuclear reactor. When irradiation is complete, the sample and standard are allowed to cool and the gamma ray activities measured. Given that the activity is 1020 cpm for the sample and 3540 cpm for the standard, determine the %w/w Ni in the alloy.

18. The vitamin B_{12} content of a multivitamin tablet is determined by the following procedure. A sample of 10 tablets is dissolved in water and diluted to volume in a 100-mL volumetric flask. A 50.00-mL portion is removed and treated with 0.500 mg of radioactive vitamin B_{12} having an activity of 572 cpm. After homogenization, the vitamin B_{12} in the sample is isolated and purified, producing 18.6 mg with an activity of 361 cpm. Calculate the milligrams of vitamin B_{12} in a multivitamin tablet.

19. The oldest sample that can be dated by ^{14}C is approximately 30 000 years. What percentage of the ^{14}C still remains after this time span?

20. Potassium–argon dating is based on the nuclear decay of ^{40}K to ^{40}Ar ($t_{1/2}$ = 1.3 × yr). If no ^{40}Ar is originally present in the rock, and if ^{40}Ar can not escape to the atmosphere, then the relative amounts of 40K and 40Ar can be used to determine the age of the rock. When a 100.0-mg rock sample was analyzed it contains 4.63×10^{-6} mol of ^{40}K and 2.09×10^{-6} mol ^{40}Ar. How old is the rock sample?

21. The steady state activity for ^{14}C is 15 cpm of carbon. If counting is limited to 1 hr, what mass of carbon is needed to give a percent relative standard deviation of 1% for the sample's activity? How long must we monitor the radioactive decay from a 0.50-gram sample of carbon to give a percent relative standard deviation of 1% for the activity?

22. To improve the sensitivity of a FIA analysis you might do any of the following: inject a larger volume of sample, increase the flow rate, decrease the length and the diameter of the manifold's tubing, or merge separate channels before injecting the sample. For each action, explain why it leads to an improvement in sensitivity.

23. Figure 13.31 shows a fiagram for a solution of 50.0-ppm PO_4^{3-} using the method in Representative Method 13.2. Determine values for h, t_a, T, t', Δt, and T'. What is the sensitivity of this FIA method, assuming a linear relationship between absorbance and concentration? How many samples can be analyzed per hour?

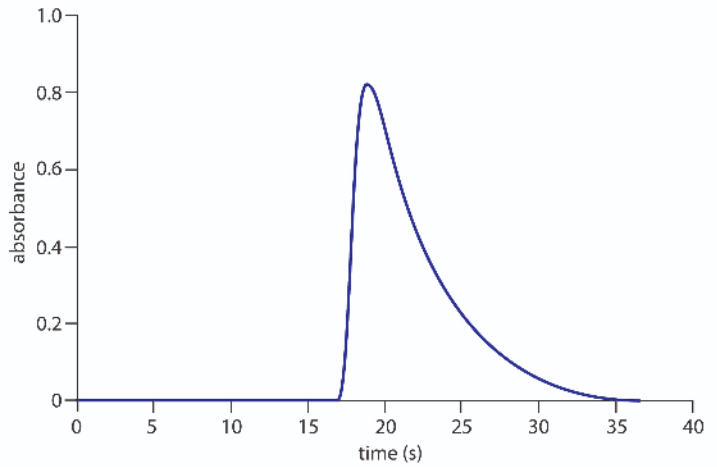


Figure 13.31 Diagram for Problem 13.23.

23. A sensitive method for the flow injection analysis of Cu^{2+} is based on its ability to catalyze the oxidation of di-2-pyridyl ketone hydrazone (DPKH).[24] The product of the reaction is fluorescent and can be used to generate a signal when using a fluorimeter as a detector. The yield of the reaction is at a maximum when the solution is made basic with NaOH. The fluorescence, however, is greatest in the presence of HCl. Sketch an appropriate FIA manifold for this analysis.

24. The concentration of chloride in seawater can be determined by a flow injection analysis. The analysis of a set of calibration standards gives the following results.

$[Cl^-]$ (ppm)	absorbance
5.00	0.057
10.00	0.099
20.00	0.230
30.00	0.354
40.00	0.478
50.00	0.594
75.00	0.840

A 1.00-mL sample of seawater is placed in a 500-mL volumetric flask and diluted to volume with distilled water. When injected into the flow injection analyzer an absorbance of 0.317 is measured. What is the concentration of Cl^- in the sample?

https://chem.libretexts.org/@go/page/70730

25. Ramsing and co-workers developed an FIA method for acid–base titrations using a carrier stream consisting of 2.0×10^{-3} M NaOH and the acid–base indicator bromothymol blue.[25] Standard solutions of HCl were injected, and the following values of Δt were measured from the resulting fiagrams.

[HCl] (M)	Δt (s)	[HCl] (M)	Δt (s)
0.008	3.13	0.080	7.71
0.010	3.59	0.100	8.13
0.020	5.11	0.200	9.27
0.040	6.39	0.400	10.45
0.060	7.06	0.600	11.40

A sample with an unknown concentration of HCl is analyzed five times, giving values of 7.43, 7.28, 7.41, 7.37, and 7.33 s for Δt. Determine the concentration of HCl in the sample and its 95% confidence interval.

26. Milardovíc and colleagues used a flow injection analysis method with an amperometric biosensor to determine the concentration of glucose in blood.[26] Given that a blood sample that is 6.93 mM in glucose has a signal of 7.13 nA, what is the concentration of glucose in a sample of blood if its signal is 11.50 nA?

27. Fernández-Abedul and Costa-García developed an FIA method for detecting cocaine in samples using an amperometric detector.[27] The following signals (arbitrary units) were collected for 12 replicate injections of a 6.2×10^{-6} M sample of cocaine.

24.5	24.1	24.1
23.8	23.9	25.1
23.9	24.8	23.7
23.3	23.2	23.2

(a) What is the relative standard deviation for this sample?

(b) If it took 10.5 min to obtain these replicate analyses, what is the expected sample throughput in samples per hour?

(c) The following calibration data are available

[cocaine] (μM)	signal (arb. units)
0.18	0.8
0.36	2.1
0.60	2.4
0.81	3.2
1.0	4.5
2.0	8.1
4.0	14.4
6.0	21.6
8.0	27.1
10.0	32.9

In a typical analysis a 10.0-mg sample is dissolved in water and diluted to volume in a 25-mL volumetric flask. A 125-µL aliquot is transferred to a 25-mL volumetric flask and diluted to volume with a pH 9 buffer. When injected into the flow injection apparatus a signal of 21.4 (arb. units) is obtained. What is the %w/w cocaine in the sample?

28. Holman, Christian, and Ruzicka described an FIA method for determining the concentration of H_2SO_4 in nonaqueous solvents.[28] Agarose beads (22–45 µm diameter) with a bonded acid–base indicator are soaked in NaOH and immobilized in the detector's flow cell. Samples of H_2SO_4 in *n*-butanol are injected into the carrier stream. As a sample passes through the flow cell, an acid–base reaction takes place between H_2SO_4 and NaOH. The endpoint of the neutralization reaction is signaled by a change in the bound indicator's color and is detected spectrophotometrically. The elution volume needed to reach the titration's endpoint is inversely proportional to the concentration of H_2SO_4; thus, a plot of endpoint volume versus $[H_2SO_4]^{-1}$ is linear. The following data is typical of that obtained using a set of external standards.

$[H_2SO_4]$ (mM)	end point volume (mL)
0.358	0.266
0.436	0.227
0.560	0.176
0.752	0.136
1.38	0.075
2.98	0.037
5.62	0.017

What is the concentration of H_2SO_4 in a sample if its endpoint volume is 0.157 mL?

13.5.3 Solutions to Practice Exercises

Practice Exercise 13.1

Figure 13.32 shows the calibration curve and calibration equation for the external standards. Substituting 2.21×10^{-3} M for $[CH_3NO_2]_{t=2s}$ gives $[CH_3NO_2]_0$ as 5.21×10^{-2} M.

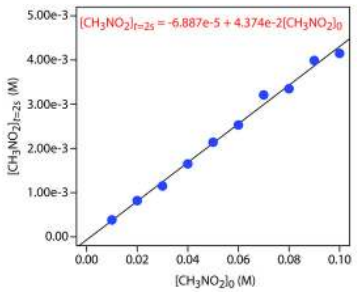


Figure 13.32 Calibration curve and calibration equation for Practice Exercise 13.1.

Click here to return to the chapter.

Practice Exercise 13.2

Figure 13.33 shows the calibration curve and calibration equation for the external standards. Substituting 3.52×10^{-2} M for $[Fe(SCN)^{2+}]_{t=10s}$ gives $[SCN^-]_0$ as 6.87×10^{-2} M.

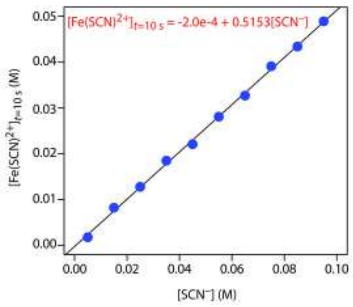


Figure 13.33 Calibration curve and calibration equation for Practice Exercise 13.2.

Click here to return to the chapter.

Practice Exercise 13.3

Figure 13.34 shows the Lineweaver–Burk plot and equation for the data in Practice Exercise 13.3. The *y*-intercept of 9.974 min/ΔAU is equivalent to $1/V_{max}$; thus, V_{max} is 0.10 ΔAU/min. The slope of 11.89 min/ΔAU•mM is equivalent to K_m/V_{max}; thus, K_m is 1.2 mM.

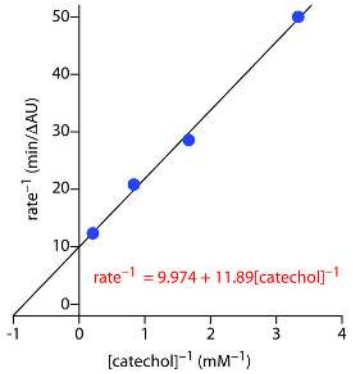


Figure 13.34 Lineweaver–Burk plot and equation for Practice Exercise 13.3.

Click here to return to the chapter.

Practice Exercise 13.4

Figure 13.35 shows the Lineweaver–Burk plots for the two sets of data in Practice Exercise 13.4. The nearly identical *x*-intercepts suggests that phenylthiourea is a noncompetitive inhibitor.

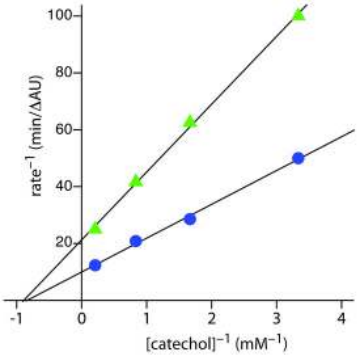


Figure 13.35 Lineweaver–Burk plots for Practice Exercise 13.4.

Click here to return to the chapter.

Contributors and Attributions

David Harvey (DePauw University)

13.E: Kinetic Methods (Exercises) is shared under a CC BY-NC-SA 4.0 license and was authored, remixed, and/or curated by LibreTexts.

13.S: Kinetic Methods (Summary)

Kinetic methods of analysis use the rate of a chemical or physical process to determine an analyte's concentration. Three types of kinetic methods are discussed in this chapter: chemical kinetic methods, radiochemical methods, and flow injection methods.

Chemical kinetic methods use the rate of a chemical reaction and either its integrated or differential rate law. For an integral method, we determine the concentration of analyte—or the concentration of a reactant or product stoichiometrically related to the analyte—at one or more points in time following the reaction's initiation. The initial concentration of analyte is then determined using the integral form of the reaction's rate law. Alternatively, we can measure the time required to effect a given change in concentration. In a differential kinetic method we measure the rate of the reaction at a time *t*, and use the differential form of the rate law to determine the analyte's concentration.

Chemical kinetic methods are particularly useful for reactions that are too slow for other analytical methods. For reactions with fast kinetics, automation allows for sampling rates of more than 100 samples/h. Another important application of chemical kinetic methods is the quantitative analysis of enzymes and their substrates, and the characterization of enzyme catalysis.

Radiochemical methods of analysis take advantage of the decay of radioactive isotopes. A direct measurement of the rate at which a radioactive isotope decays may be used to determine its concentration in a sample. For an analyte that is not naturally radioactive, neutron activation often can be used to induce radioactivity. Isotope dilution, in which we spike a radioactively-labeled form of analyte into the sample, can be used as an internal standard for quantitative work.

In flow injection analysis we inject the sample into a flowing carrier stream that often merges with additional streams of reagents. As the sample moves with the carrier stream it both reacts with the contents of the carrier stream and any additional reagent streams, and undergoes dispersion. The resulting fiagram of signal versus time bears some resemblance to a chromatogram. Unlike chromatography, however, flow injection analysis is not a separation technique. Because all components in a sample move with the carrier stream's flow rate, it is possible to introduce a second sample before the first sample reaches the detector. As a result, flow injection analysis is ideally suited for the rapid throughput of samples.

13.5.1 Key Terms

alpha particle	integrated rate law	quench
beta particle	intermediate rate	rate
centrifugal analyzer	isotope	rate constant
competitive inhibitor	isotope dilution	rate law
curve-fitting method	kinetic method	rate method
enzyme	Lineweaver-Burk plot	scintillation counter
equilibrium method	manifold	steady-state approximation
fiagram	Michaelis constant	stopped-flow analyzer
flow injection analysis	negatron	substrate
gamma ray	neutron activation	tracer
Geiger counter	noncompetitive inhibitor	two-point fixed-time integral method
half-life	one-point fixed-time integral method	uncompetitive inhibitor
inhibitor	peristaltic pump	variable time integral method
initial rate	positron	

References

1. Method 4500-NO_2^- B in *Standard Methods for the Analysis of Waters and Wastewaters*, American Public Health Association: Washington, DC, 20th Ed., 1998.
2. Karayannis, M. I.; Piperaki, E. A.; Maniadaki, M. M. *Anal. Lett.* **1986**, *19*, 13–23.
3. Pardue, H. L. *Anal. Chim. Acta* **1989**, *216*, 69–107.
4. Mottola, H. A. *Anal. Chim. Acta* **1993**, *280*, 279–287.
5. (a) Crouch, S. R.; Malmstadt, H. V. *Anal. Chem.* **1967**, *39*, 1084–1089; (b) Crouch, S. R.; Malmstadt, H. V. *Anal. Chem.* **1967**, *39*, 1090–1093; (c) Malmstadt, H. V.; Cordos, E. A.; Delaney, C. J. *Anal. Chem.* **1972**, *44(12)*, 26A–41A.

6. Javier, A. C.; Crouch, S. R.; Malmstadt, H. V. *Anal. Chem.* **1969**, *41*, 239–243.
7. Mark, H. B.; Rechnitz, G. A. *Kinetics in Analytical Chemistry*, Interscience: New York, 1968.
8. Sandell, E. B.; Kolthoff, I. M. *J. Am. Chem. Soc.* **1934**, *56*, 1426.
9. Darwish, I. A.; Sultan, M. A.; Al-Arfaj, H. A. *Talanta* **2009**, *78*, 1383–1388.
10. Guilbault, G. G. Handbook of Enzymatic Methods of Analysis, Marcel Dekker: New York, 1976.
11. Ioannou. P. C.; Piperaki, E. A. *Clin. Chem.* **1986**, *32*, 1481–1483.
12. Cruces Blanco, C.; Garcia Sanchez, F. *Int. J. Environ. Anal. Chem.* **1990**, *38*, 513–523.
13. (a) Northup, D. B. *J. Chem. Educ.* **1998**, *75*, 1153–1157; (b) Zubay, G. *Biochemistry*, Macmillan Publishing Co.: New York, 2nd Ed., p 269.
14. (a) Atkinson, M. R.; Jackson, J. F.; Morton, R. K. *Biochem. J.* **1961**, *80*, 318–323; (b) Wilkinson, G. N. *Biochem. J.* **1961**, *80*, 324–332.
15. Pauch, J. B.; Margerum, D. W. *Anal. Chem.* **1969**, *41*, 226–232.
16. (a) Holler, F. J.; Calhoun, R. K.; MClanahan, S. F. *Anal. Chem.* **1982**, *54*, 755–761; (b) Wentzel, P. D.; Crouch, S. R. *Anal. Chem.* **1986**, *58*, 2851–2855; (c) Wentzel, P. D.; Crouch, S. R. *Anal. Chem.* **1986**, *58*, 2855–2858.
17. (a) Ruzicka, J.; Hansen, E. H. *Anal. Chim. Acta* **1975**, *78*, 145–157; (b) Stewart, K. K.; Beecher, G. R.; Hare, P. E. *Anal. Biochem*. **1976**, *70*, 167–173; (c) Valcárcel, M.; Luque de Castro, M. D. *Flow Injection Analysis: Principles and Applications*, Ellis Horwood: Chichester, England, 1987.
18. Hansen, E. H.; Ruzicka, J. *J. Chem. Educ.* **1979**, *56*, 677–680.
19. Korenaga, T.; Ikatsu, H. *Anal. Chim. Acta* **1982**, *141*, 301–309.
20. Andrew, K. N.; Blundell, N. J.; Price, D.; Worsfold, P. J. *Anal. Chem.* **1994**, *66*, 916A–922A.
21. Ramsing, A. U.; Ruzicka, J.; Hansen, E. H. *Anal. Chim. Acta* **1981**, *129*, 1–17.
22. Malmstadt, H. V.; Pardue, H. L. *Anal. Chem.* **1961** *33*, 1040–1047.
23. Deming, S. N.; Pardue, H. L. *Anal. Chem.* **1971**, *43*, 192–200.
24. Lazaro, F.; Luque de Castro, M. D.; Valcárcel, M. Analyst, 1984, 109, 333–337.
25. Ramsing, A. U.; Ruzicka, J.; Hansen, E. H. *Anal. Chim. Acta* **1981**, *129*, 1–17.
26. Milardović, S.; Kruhak, I.; Iveković, D.; Rumenjak, V.; Tkalčec, M.; Grabarić, B. S. *Anal. Chim. Acta* **1997**, *350*, 91–96.
27. Fernández-Abedul, M; Costa-García, A. *Anal. Chim. Acta* **1996**, *328*, 67–71.
28. Holman, D. A.; Christian, G. D.; Ruzicka, J. *Anal. Chem.* **1997**, *69*, 1763–1765.

Contributors

David Harvey (DePauw University)

13.S: Kinetic Methods (Summary) is shared under a CC BY-NC-SA 4.0 license and was authored, remixed, and/or curated by LibreTexts.

CHAPTER OVERVIEW

14: Developing a Standard Method

In Chapter 1 we made a distinction between analytical chemistry and chemical analysis. Among the goals of analytical chemistry are improving established methods of analysis, extending existing methods of analysis to new types of samples, and developing new analytical methods. Once we develop a new method, its routine application is best described as chemical analysis. We recognize the status of these methods by calling them standard methods. Numerous examples of standard methods are presented and discussed in Chapters 8–13. What we have not yet considered is what constitutes a standard method. In this chapter we discuss how we develop a standard method, including optimizing the experimental procedure, verifying that the method produces acceptable precision and accuracy in the hands of a single analyst, and validating the method for general use.

Topic hierarchy

14.1: Optimizing the Experimental Procedure
14.2: Verifying the Method
14.3: Validating the Method as a Standard Method
14.4: Using Excel and R for an Analysis of Variance
14.E: Developing a Standard Method (Exercises)
14.S: Developing a Standard Method (Summary)

Contributors

- David Harvey (DePauw University)

14: Developing a Standard Method is shared under a CC BY-NC-SA 4.0 license and was authored, remixed, and/or curated by LibreTexts.

14.1: Optimizing the Experimental Procedure

In the presence of H_2O_2 and H_2SO_4, a solution of vanadium forms a reddish brown color that is believed to be a compound with the general formula $(VO)_2(SO_4)_3$. The intensity of the solution's color depends on the concentration of vanadium, which means we can use its absorbance at a wavelength of 450 nm to develop a quantitative method for vanadium.

The intensity of the solution's color also depends on the amounts of H_2O_2 and H_2SO_4 that we add to the sample—in particular, a large excess of H_2O_2 decreases the solution's absorbance as it changes from a reddish brown color to a yellowish color.[1] Developing a **standard method** for vanadium based on this reaction requires that we optimize the additions of H_2O_2 and H_2SO_4 to maximize the absorbance at 450 nm. Using the terminology of statisticians, we call the solution's absorbance the system's **response**. Hydrogen peroxide and sulfuric acid are **factors** whose concentrations, or **factor levels**, determine the system's response. To optimize the method we need to find the best combination of factor levels. Usually we seek a maximum response, as is the case for the quantitative analysis of vanadium as $(VO)_2(SO_4)_3$. In other situations, such as minimizing an analysis's percent error, we are looking for a minimum response.

> **Note**
>
> We will return to this analytical method for vanadium in Example 14.4 and in Problem 14.11.

14.1.1 Response Surfaces

One of the most effective ways to think about an optimization is to visualize how a system's response changes when we increase or decrease the levels of one or more of its factors. We call a plot of the system's response as a function of the factor levels a **response surface**. The simplest response surface has only one factor and is displayed graphically in two dimensions by placing the response on the *y*-axis and the factor's levels on the *x*-axis. The calibration curve in Figure 14.1 is an example of a one-factor response surface. We also can define the response surface mathematically. The response surface in Figure 14.1, for example, is

$$A = 0.008 + 0.0896C_A \tag{14.1.1}$$

where A is the absorbance and C_A is the analyte's concentration in ppm.

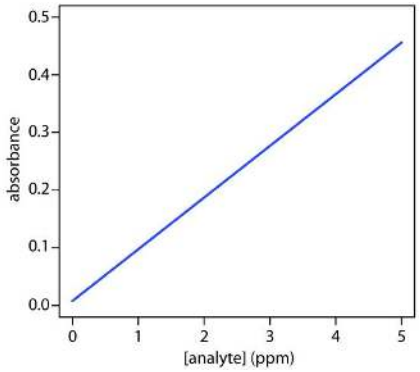


Figure 14.1 A calibration curve is an example of a one-factor response surface. The response (absorbance) is plotted on the *y*-axis and the factor levels (concentration of analyte) is plotted on the *x*-axis.

For a two-factor system, such as the quantitative analysis for vanadium described earlier, the response surface is a flat or curved plane in three dimensions. As shown in Figure 14.2a, we place the response on the *z*-axis and the factor levels on the *x*-axis and the *y*-axis. Figure 14.2a shows a pseudo-three dimensional wireframe plot for a system obeying the equation

$$R = 3.0 - 0.30A + 0.020AB \tag{14.1.2}$$

where R is the response, and A and B are the factors. We can also represent a two-factor response surface using the two-dimensional level plot in Figure 12.4b, which uses a color gradient to show the response on a two-dimensional grid, or using the two-dimensional contour plot in Figure 14.2c, which uses contour lines to display the response surface.

> **Note**
>
> We also can overlay a level plot and a contour plot. See Figure 14.7b for a typical example.

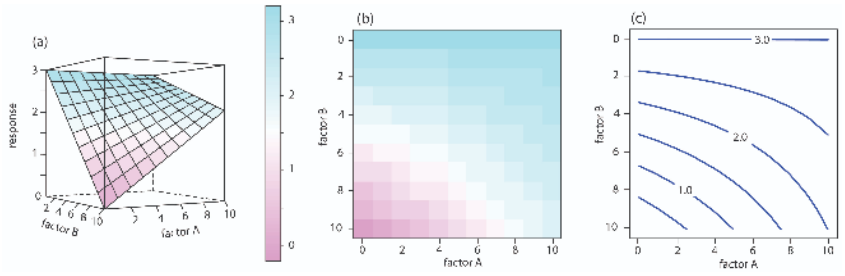


Figure 14.2 Three examples of a two-factor response surface displayed as (a) a pseudo-three-dimensional wireframe plot, (b) a two-dimensional level plot, and (c) a two-dimensional contour plot. We call the display in (a) a pseudo-three dimensional response surface because we show the presence of three dimensions on the page's flat, two-dimensional surface.

The response surfaces in Figure 14.2 cover a limited range of factor levels ($0 \le A \le 10$, $0 \le B \le 10$), but we can extend each to more positive or more negative values because there are no constraints on the factors. Most response surfaces of interest to an analytical chemist have natural constraints imposed by the factors or have practical limits set by the analyst. The response surface in Figure 14.1, for example, has a natural constraint on its factor because the analyte's concentration cannot be smaller than zero.

> **Note**
>
> We express this constraint as $C_A \ge 0$.

If we have an equation for the response surface, then it is relatively easy to find the optimum response. Unfortunately, we rarely know any useful details about the response surface. Instead, we must determine the response surface's shape and locate the optimum response by running appropriate experiments. The focus of this section is on useful experimental designs for characterizing response surfaces. These experimental designs are divided into two broad categories: searching methods, in which an algorithm guides a systematic search for the optimum response, and modeling methods, in which we use a theoretical or empirical model of the response surface to predict the optimum response.

14.1.2 Searching Algorithms for Response Surfaces

Figure 14.3 shows a portion of the South Dakota Badlands, a landscape that includes many narrow ridges formed through erosion. Suppose you wish to climb to the highest point of this ridge. Because the shortest path to the summit is not obvious, you might adopt the following simple rule—look around you and take a step in the direction that has the greatest change in elevation. The route you follow is the result of a systematic search using a **searching algorithm**. Of course there are as many possible routes as there are starting points, three examples of which are shown in Figure 14.3. Note that some routes do not reach the highest point—what we call the **global optimum**. Instead, many routes reach a **local optimum** from which further movement is impossible.

> **Note**
>
> Searching algorithms have names—the one described here is the method of steepest ascent.

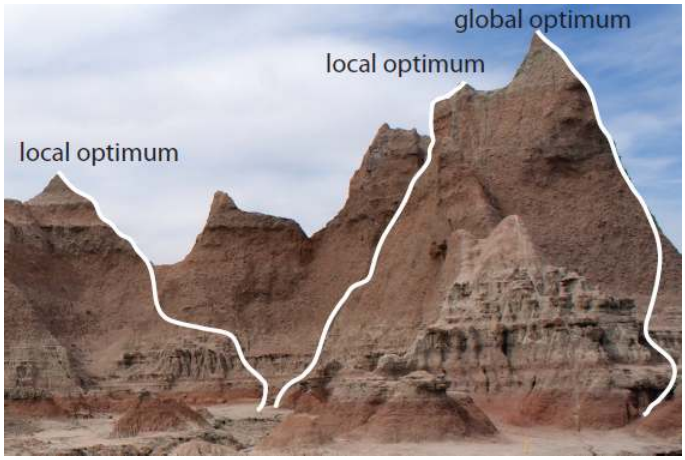


Figure 14.3 Finding the highest point on a ridge using a searching algorithm is one useful model for finding the optimum on a response surface. The path on the far right reaches the highest point, or the global optimum. The other two paths reach local optima. This ridge is part of the South Dakota Badlands National Park. You can read about the geology of the park as www.nps.gov/badl/.

We can use a systematic searching algorithm to locate the optimum response for an analytical method. We begin by selecting an initial set of factor levels and measure the response. Next, we apply the rules of our searching algorithm to determine a new set of factor levels, continuing this process until we reach an optimum response. Before we consider two common searching algorithms, let's consider how we evaluate a searching algorithm.

Effectiveness and Efficiency

A searching algorithm is characterized by its effectiveness and its efficiency. To be effective, a searching algorithm must find the response surface's global optimum, or at least reach a point near the global optimum. A searching algorithm may fail to find the global optimum for several reasons, including a poorly designed algorithm, uncertainty in measuring the response, and the presence of local optima. Let's consider each of these potential problems.

A poorly designed algorithm may prematurely end the search before it reaches the response surface's global optimum. As shown in Figure 14.4, an algorithm for climbing a ridge that slopes to the northeast is likely to fail if it allows you to take steps only to the north, south, east, or west. An algorithm must be that responds to a change in the direction of steepest ascent is **effective**.

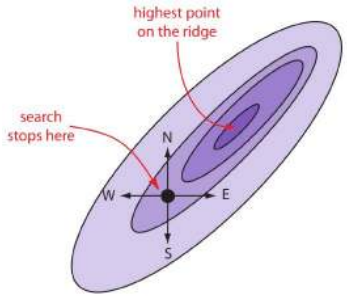


Figure 14.4 Example showing how a poorly designed searching algorithm can fail to find a response surface's global optimum.

All measurements contain uncertainty, or noise, that affects our ability to characterize the underlying signal. When the noise is greater than the local change in the signal, then a searching algorithm is likely to end before it reaches the global optimum. Figure 14.5 provides a different view of Figure 14.3, showing us that the relatively flat terrain leading up to the ridge is heavily weathered and uneven. Because the variation in local height exceeds the slope, our searching algorithm stops the first time we step up onto a less weathered surface.



Figure 14.5 Another view of the ridge in Figure 14.3 showing the weathered terrain leading up to the ridge. The yellow rod at the bottom of the figure, which marks a trail, is about 18 in high.

Finally, a response surface may contain several local optima, only one of which is the global optimum. If we begin the search near a local optimum, our searching algorithm may not be capable of reaching the global optimum. The ridge in Figure 14.3, for example, has many peaks. Only those searches beginning at the far right reach the highest point on the ridge. Ideally, a searching algorithm should reach the global optimum regardless of where it starts.

A searching algorithm always reaches an optimum. Our problem, of course, is that we do not know if it is the global optimum. One method for evaluating a searching algorithm's effectiveness is to use several sets of initial factor levels, finding the optimum response for each, and comparing the results. If we arrive at the same optimum response after starting from very different locations on the response surface, then we are more confident that is it the global optimum.

Efficiency is the second desirable characteristic for a searching algorithm. An efficient algorithm moves from the initial set of factor levels to the optimum response in as few steps as possible. We can increase the rate at which we approach the optimum by taking larger steps. If the step size is too large, however, the difference between the experimental optimum and the true optimum may be unacceptably large. One solution is to adjust the step size during the search, using larger steps at the beginning and smaller steps as we approach the global optimum.

One-Factor-at-a-Time Optimization

A simple algorithm for optimizing the quantitative method for vanadium described earlier is to select initial concentrations for H_2O_2 and H_2SO_4 and measure the absorbance. Next, we optimize one reagent by increasing or decreasing its concentration—holding constant the second reagent's concentration—until the absorbance decreases. We then vary the concentration of the second reagent—maintaining the first reagent's optimum concentration—until we observe a decrease in absorbance. We can stop this process, which we call a **one-factor-at-a-time optimization**, after one cycle or repeat it until the absorbance reaches a maximum value or it exceeds an acceptable threshold value.

A one-factor-at-a-time optimization is consistent with a notion that to determine the influence of one factor we must hold constant all other factors. This is an effective, although not necessarily an efficient experimental design when the factors are independent.[2] Two factors are **independent** when changing the level of one factor does not influence the effect of changing the other factor's level. Table 14.1 provides an example of two independent factors. If we hold factor B at level B_1, changing factor A from level A_1 to level A_2 increases the response from 40 to 80, or a change in response, ΔR, of

$$R = 80 - 40 = 40 \tag{14.1.3}$$

If we hold factor B at level B_2, we find that we have the same change in response when the level of factor A changes from A_1 to A_2.

$$R = 100 - 60 = 40 \tag{14.1.4}$$

We can see this independence graphically by plotting the response versus factor A's level, as shown in Figure 14.6. The parallel lines show that the level of factor B does not influence factor A's effect on the response.

Table 14.1 Example of Two Independent Factors

factor A	factor B	response
A_1	B_1	40
A_2	B_1	80
A_1	B_2	60
A_2	B_2	100

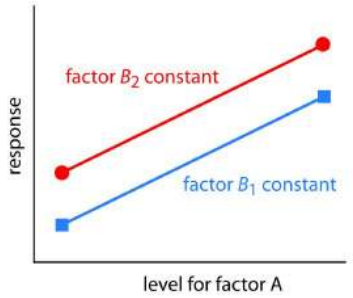


Figure 14.6 Factor effect plot for two independent factors. Note that the two lines are parallel, indicating that the level for factor B does not influence how factor A's level affects the response.

Practice Exercise 14.1

Using the data in Table 14.1, show that factor B's affect on the response is independent of factor A.

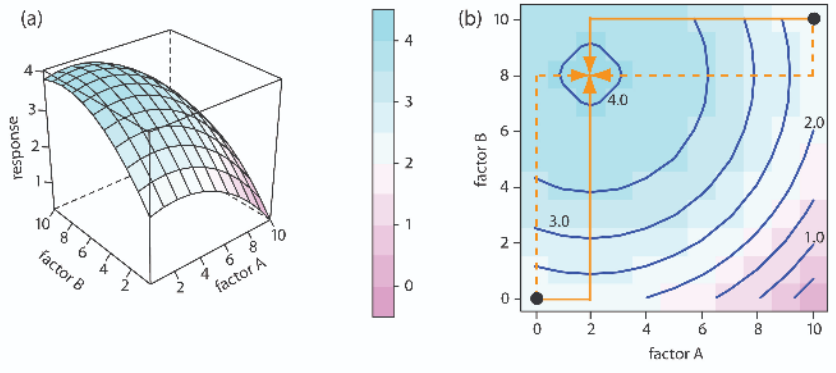
Click here to review your answer to this exercise.

Mathematically, two factors are independent if they do not appear in the same term in the equation describing the response surface. Equation 14.1, for example, describes a response surface with independent factors because no term in the equation includes both factor A and factor B.

$$R = 2.0 + 0.12A + 0.48B - 0.03A^2 - 0.03B^2 \tag{14.1}$$

Figure 14.7 shows the resulting pseudo-three-dimensional surface and a contour map for equation 14.1.

The easiest way to follow the progress of a searching algorithm is to map its path on a contour plot of the response surface. Positions on the response surface are identified as (a, b) where a and b are the levels for factors A and B. The contour plot in Figure 14.7b, for example, shows four one-factor-at-a-time optimizations of the response surface for equation 14.1. The effectiveness and efficiency of this algorithm when optimizing independent factors is clear—each trial reaches the optimum response at (2, 8) in a single cycle.



https://chem.libretexts.org/@go/page/70733

Figure 14.7 The response surface for two independent factors based on equation 14.1, displayed as (a) a wireframe, and (b) an overlaid contour plot and level plot. The orange lines in (b) show the progress of one-factor-at-a-time optimizations beginning from two starting points (•) and optimizing factor A first (solid line) or factor B first (dashed line). All four trials reach the optimum response of (2,8) in a single cycle.

Unfortunately, factors usually do not behave independently. Consider, for example, the data in Table 14.2. Changing the level of factor B from level B_1 to level B_2 has a significant effect on the response when factor A is at level A_1

$$R = 60 - 20 = 40 \tag{14.1.5}$$

but no effect when factor A is at level A_2.

$$R = 80 - 80 = 0 \tag{14.1.6}$$

Table 14.2 Example of Two Dependent Factors

factor A	factor B	response
A_1	B_1	20
A_2	B_1	80
A_1	B_2	60
A_2	B_2	80

Figure 14.8 shows this **dependent** relationship between the two factors. Factors that are dependent are said to interact and the response surface's equation includes an interaction term containing both factors A and B. The final term in equation 14.2, for example, accounts for the interaction between the factors A and B.

$$R = 5.5 + 1.5A + 0.6B - 0.15A^2 - 0.0245B^2 - 0.0857AB \tag{14.2}$$

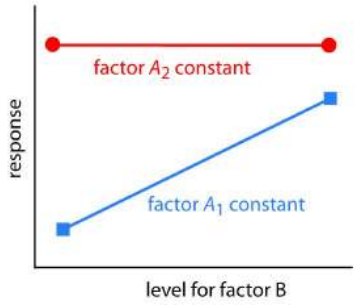


Figure 14.8 Factor effect plot for two dependent factors. Note that the two lines are not parallel, indicating that the level for factor A influences how factor B's level affects the response.

Figure 14.9 shows the resulting pseudo-three-dimensional surface and a contour map for equation 14.2.

The progress of a one-factor-at-a-time optimization for equation 14.2 is shown in Figure 14.9b. Although the optimization for dependent factors is effective, it is less efficient than that for independent factors. In this case it takes four cycles to reach the optimum response of (3, 7) if we begin at (0, 0).

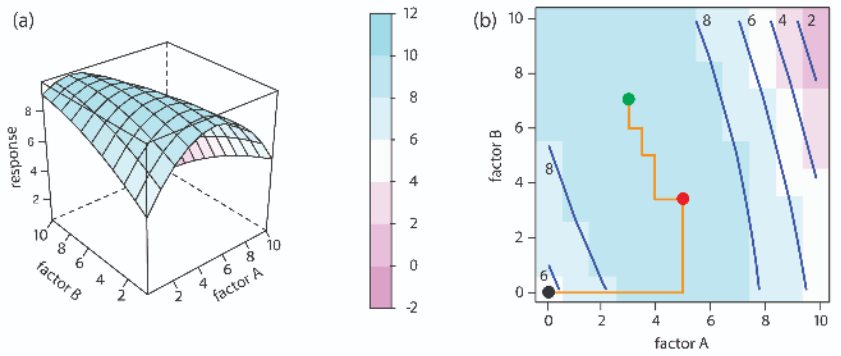


Figure 14.9 The response surface for two dependent factors based on equation 14.2, displayed as (a) a wireframe, and (b) an overlaid contour plot and level plot. The orange lines in (b) show the progress of one-factor-at-a-time optimization beginning from the starting point (•) and optimizing factor A first. The red dot (•) marks the end of the first cycle. It takes four cycles to reach the optimum response of (3, 7) as shown by the green dot (•).

Practice Exercise 14.2

Using the data in Table 14.2, show that factor A's affect on the response is independent of factor B.

Click here to review your answer to this exercise.

Simplex Optimization

One strategy for improving the efficiency of a searching algorithm is to change more than one factor at a time. A convenient way to accomplish this when there are two factors is to begin with three sets of initial factor levels, which form the vertices of a triangle. After measuring the response for each set of factor levels, we identify the combination giving the worst response and replace it with a new set of factor levels using a set of rules (Figure 14.10). This process continues until we reach the global optimum or until no further optimization is possible. The set of factor levels is called a **simplex**. In general, for k factors a simplex is a $k + 1$ dimensional geometric figure.[3]

Note

Thus, for two factors the simplex is a triangle. For three factors the simplex is a tetrahedron.

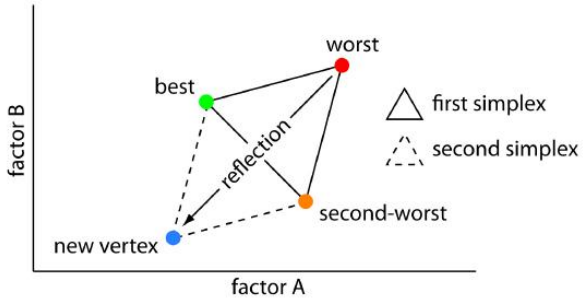


Figure 14.10 Example of a two-factor simplex. The original simplex is formed by the green, orange, and red vertices. Replacing the worst vertex with a new vertex moves the simplex into a new position on the response surface.

To place the initial two-factor simplex on the response surface, we choose a starting point (a, b) for the first vertex and place the remaining two vertices at ($a + s_a$, b) and ($a + 0.5s_a$, $b + 0.87s_b$) where s_a and s_b are step sizes for factors A and B.[4] The following set of rules moves the simplex across the response surface in search of the optimum response:

Rule 1. Rank the vertices from best (v_b) to worst (v_w).

Rule 2. Reject the worst vertex (v_w) and replace it with a new vertex (v_n) by reflecting the worst vertex through the midpoint of the remaining vertices. The new vertex's factor levels are twice the average factor levels for the retained vertices minus the factor levels for the worst vertex. For a two-factor optimization, the equations are shown here where v_s is the third vertex.

$$a_{v_n} = 2\left(\frac{a_{v_b} + a_{v_s}}{2}\right) - a_{v_w} \tag{14.3}$$

$$b_{v_n} = 2\left(\frac{b_{v_b} + b_{v_s}}{2}\right) - b_{v_w} \tag{14.4}$$

Note

The variables a and b in equation 14.3 and equation 14.4 are the factor levels for factors A and B, respectively. Problem 14.3 in the end-of-chapter problems asks you to derive these equations.

Rule 3. If the new vertex has the worst response, then return to the previous vertex and reject the vertex with the second worst response, (v_s) calculating the new vertex's factor levels using rule 2. This rule ensures that the simplex does not return to the previous simplex.

Rule 4. Boundary conditions are a useful way to limit the range of possible factor levels. For example, it may be necessary to limit a factor's concentration for solubility reasons, or to limit the temperature because a reagent is thermally unstable. If the new vertex exceeds a boundary condition, then assign it the worst response and follow rule 3.

Because the size of the simplex remains constant during the search, this algorithm is called a **fixed-sized simplex optimization**. Example 14.1 illustrates the application of these rules.

Example 14.1

Find the optimum response for the response surface in Figure 14.9 using the fixed-sized simplex searching algorithm. Use (0, 0) for the initial factor levels and set each factor's step size to 1.00.

Solution

Letting $a = 0$, $b = 0$, $s_a = 1$, and $s_b = 1$ gives the vertices for the initial simplex as

Vertex 1: $(a, b) = (0, 0)$

Vertex 2: $(a + s_a, b) = (1.00, 0)$

Vertex 3: $(a + 0.50s_a, b + 0.87s_b) = (0.50, 0.87)$

The responses, from equation 14.2, for the three vertices are shown in the following table

vertex	a	b	response
v_1	0	0	5.50
v_2	1.00	0	6.85
v_3	0.50	0.87	6.68

with v_1 giving the worst response and v_3 the best response. Following Rule 1, we reject v_1 and replace it with a new vertex using equation 14.3 and equation 14.4; thus

$$a_{v_4} = 2 \times \frac{1.00 + 0.50}{2} - 0 = 1.50 \quad b_{v_4} = 2 \times \frac{0 + 0.87}{2} - 0 = 0.87 \tag{14.1.7}$$

The following table gives the vertices of the second simplex.

vertex	a	b	response
v_2	1.50	0	6.85
v_3	0.50	0.87	6.68
v_4	1.50	0.87	7.80

with v_3 giving the worst response and v_4 the best response. Following Rule 1, we reject v_3 and replace it with a new vertex using equation 14.3 and equation 14.4; thus

$$a_{v_5} = 2 \times \frac{1.00 + 1.50}{2} - 0.50 = 2.00 \quad b_{v_5} = 2 \times \frac{0 + 0.87}{2} - 0.87 = 0 \tag{14.1.8}$$

The following table gives the vertices of the third simplex.

vertex	a	b	response
v_2	1.50	0	6.85
v_4	1.50	0.87	7.80
v_5	2.00	0	7.90

The calculation of the remaining vertices is left as an exercise. Figure 14.11 shows the progress of the complete optimization. After 29 steps the simplex begins to repeat itself, circling around the optimum response of (3, 7).

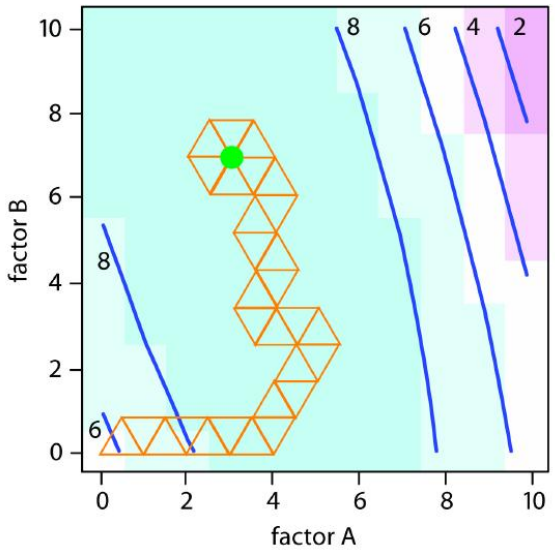


Figure 14.11 Progress of the fixed-size simplex optimization in Example 14.1. The green dot marks the optimum response of (3, 7). Optimization ends when the simplexes begin to circle around a single vertex.

Practice Exercise 14.3

The following exercise will help you evaluate the efficiency and effectiveness of three common searching algorithms: one-factor-at-a-time, fixed-size simplex, and variable-sized simplex (see the following side comment for a brief description and a link to additional information). Click on this link, which opens a java applet. Scroll down to read the applet's instructions and then experiment with the controls. When you are comfortable with the applet's interface, answer the following questions: (a) How sensitive is each algorithm to its initial starting point and to the size of the initial simplex or step? In your answer, consider both effectiveness and efficiency. (b) Are the optimizations for some response surfaces particularly sensitive to the initial position? If so, what are the characteristics of these response surfaces?

Click here to review your answer to this exercise.

Note

The size of the initial simplex ultimately limits the effectiveness and the efficiency of a fixed-size simplex searching algorithm. We can increase its efficiency by allowing the size of the simplex to expand or contract in response to the rate at which we are approaching the optimum. For example, if we find that a new vertex is better than any of the vertices in the preceding simplex, then we expand the simplex further in this direction on the assumption that we are moving directly toward the optimum. Other

conditions cause us to contract the simplex—making it smaller—to encourage the optimization to move in a different direction. We call this a **variable-sized simplex optimization**.

Consult this chapter's additional resources for further details of the variable-sized simplex optimization.

14.1.3 Mathematical Models of Response Surfaces

A response surface is described mathematically by an equation relating the response to its factors. Equation 14.1 and equation 14.2 provide two examples. If we measure the response for several combinations of factor levels, then we can model the response surface by using a linear regression analysis to fit an appropriate equation to the data. There are two broad categories of models that we can use in a regression analysis: theoretical models and empirical models.

Theoretical Models of the Response Surface

A **theoretical model** is derived from the known chemical and physical relationships between the response and its factors. In spectrophotometry, for example, Beer's law is a theoretical model that relates a substance's absorbance, A, to its concentration, C_A

$$A = \varepsilon b C_A \tag{14.1.9}$$

where ε is the molar absorptivity and b is the pathlength of the electromagnetic radiation passing through the sample. A Beer's law calibration curve, therefore, is a theoretical model of a response surface.

> **Note**
>
> For a review of Beer's law, see Section 10.2.3 in Chapter 10. Figure 14.1 is an example of a Beer's law calibration curve.

Empirical Models of the Response Surface

In many cases the underlying theoretical relationship between the response and its factors is unknown. We can still develop a model of the response surface if we make some reasonable assumptions about the underlying relationship between the factors and the response. For example, if we believe that the factors A and B are independent and that each has only a first-order effect on the response, then the following equation is a suitable model.

$$R = \beta_0 + \beta_a A + \beta_b B \tag{14.1.10}$$

where R is the response, A and B are the factor levels, and β_0, β_a, and β_b are adjustable parameters whose values are determined by a linear regression analysis. Other examples of equations include those for dependent factors

$$R = \beta_0 + \beta_a A + \beta_b B + \beta_{ab} AB \tag{14.1.11}$$

and those with higher-order terms.

$$R = \beta_0 + \beta_a A + \beta_b B + \beta_{aa} A^2 + \beta_{bb} B^2 \tag{14.1.12}$$

Each of these equations provides an **empirical model** of the response surface because it has no basis in a theoretical understanding of the relationship between the response and its factors. Although an empirical model may provide an excellent description of the response surface over a limited range of factor levels, it has no basis in theory and cannot be extended to unexplored parts of the response surface.

> **Note**
>
> The calculations for a linear regression when the model is first-order in one factor (a straight line) is described in Chapter 5.4. A complete mathematical treatment of linear regression for models that are second-order in one factor or which contain more than one factor is beyond the scope of this text. The computations for a few special cases, however, are straightforward and are considered in this section. A more comprehensive treatment of linear regression can be found in several of this chapter's additional resources.

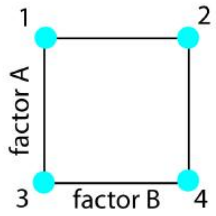
Factorial Designs

To build an empirical model we measure the response for at least two levels for each factor. For convenience we label these levels as high, H_f, and low, L_f, where f is the factor; thus H_A is the high level for factor A and L_B is the low level for factor B. If our

empirical model contains more than one factor, then each factor's high level is paired with both the high level and the low level for all other factors. In the same way, the low level for each factor is paired with the high level and the low level for all other factors. As shown in Figure 14.12, this requires 2^k experiments where k is the number of factors. This experimental design is known as a **2^k factorial design**.

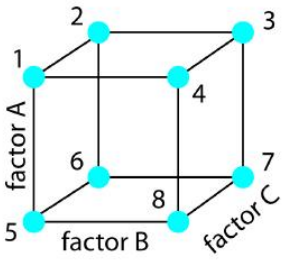
Note

Another system of notation is to use a plus sign (+) to indicate a factor's high level and a minus sign (–) to indicate its low level. We will use *H* or *L* when writing an equation and a plus sign or a minus sign in tables.



factor levels

trial	A	B
1	+	–
2	+	+
3	–	–
4	–	+



factor levels

trial	A	B	C
1	+	–	–
2	+	–	+
3	+	+	+
4	+	+	–
5	–	–	–
6	–	–	+
7	–	+	+
8	–	+	–

Figure 14.12 2^k factorial designs for (top) $k = 2$, and (bottom) $k = 3$. A 2^2 factorial design requires four experiments and a 2^3 factorial design requires eight experiments.

Coded Factor Levels

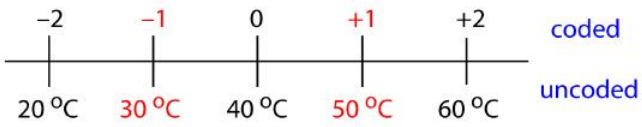
The calculations for a 2^k factorial design are straightforward and easy to complete with a calculator or spreadsheet. To simplify the calculations, we code the factor levels using +1 for a high level and –1 for a low level. Coding has two additional advantages: scaling the factors to the same magnitude makes it easier to evaluate each factor's relative importance, and it places the model's intercept, β_0, at the center of the experimental design. As shown in Example 14.2, it is easy to convert between coded and uncoded factor levels.

Example 14.2

To explore the effect of temperature on a reaction, we assign 30°C to a coded factor level of –1, and assign a coded level +1 to a temperature of 50°C. What temperature corresponds to a coded level of –0.5 and what is the coded level for a temperature of 60°C?

Solution

The difference between –1 and +1 is 2, and the difference between 30°C and 50°C is 20°C; thus, each unit in coded form is equivalent to 10°C in uncoded form. With this information, it is easy to create a simple scale between the coded and the uncoded values, as shown in Figure 14.13. A temperature of 35°C corresponding to a coded level of –0.5 and a coded level of +2 corresponds to a temperature of 60°C.



https://chem.libretexts.org/@go/page/70733

Figure 14.13 The relationship between the coded factor levels and the uncoded factor levels for Example 14.2. The numbers in red are the values defined in the 2^2 factorial design.

Determining the Empirical Model

Let's begin by considering a simple example involving two factors, A and B, and the following empirical model.

$$R = \beta_0 + \beta_a A + \beta_b B + \beta_{ab} AB \tag{14.5}$$

A 2^k factorial design with two factors requires four runs. Table 14.3 provides the uncoded levels (A and B), the coded levels (A* and B*), and the responses (*R*) for these experiments. The terms β_0, β_a, β_b, and β_{ab} in equation 14.5 account for, respectively, the mean effect (which is the average response), first-order effects due to factors A and B, and the interaction between the two factors.

Table 14.3 Example of Uncoded and Coded Factor Levels and Responses for a 2^2 Factorial Design

run	*A*	*B*	*A**	*B**	*R*
1	15	30	+1	+1	22.5
2	15	10	+1	–1	11.5
3	5	30	–1	+1	17.5
4	5	10	–1	–1	8.5

Equation 14.5 has four unknowns—the four beta terms—and Table 14.3 describes four experiments. We have just enough information to calculate values for β_0, β_a, β_b, and β_{ab}. When working with the coded factor levels, the values of these parameters are easy to calculate using the following equations, where *n* is the number of runs.

$$\beta_0 \approx b_0 = \frac{1}{n}\sum_i R_i \tag{14.6}$$

$$\beta_a \approx b_a = \frac{1}{n}\sum_i A_i^* R_i \tag{14.7}$$

$$\beta_b \approx b_b = \frac{1}{n}\sum_i B_i^* R_i \tag{14.8}$$

$$\beta_{ab} \approx b_{ab} = \frac{1}{n}\sum_i A_i^* B_i^* R_i \tag{14.9}$$

> **Note**
>
> Recall that we introduced coded factor levels with the promise that they simplify calculations.
>
> In Section 5.4.1 of Chapter 5 we introduced the convention of using β to indicate the true value of a regression's model's parameter's and *b* to indicate its calculated value. We estimate β from *b*.

Solving for the estimated parameters using the data in Table 14.3

$$b_0 = \frac{22.5 + 11.5 + 17.5 + 8.5}{4} = 15.0 \tag{14.1.13}$$

$$b_a = \frac{22.5 + 11.5 - 17.5 - 8.5}{4} = 2.0 \tag{14.1.14}$$

$$b_b = \frac{22.5 - 11.5 + 17.5 - 8.5}{4} = 5.0 \tag{14.1.15}$$

$$b_{ab} = \frac{22.5 - 11.5 - 17.5 + 8.5}{4} = 0.5 \tag{14.1.16}$$

leaves us with the following coded empirical model for the response surface.

$$R = 15.0 + 2.0A^* + 5.0B^* + 0.5A^*B^* \tag{14.10}$$

Note

Although we can convert this coded model into its uncoded form, there is no need to do so. If we need to know the response for a new set of factor levels, we just convert them into coded form and calculate the response. For example, if *A* is 10 and *B* is 15, then *A** is 0 and *B** is –0.5. Substituting these values into equation 14.10 gives a response of 12.5.

We can extend this approach to any number of factors. For a system with three factors—A, B, and C—we can use a 2^3 factorial design to determine the parameters in the following empirical model

$$R = \beta_0 + \beta_a A + \beta_b B + \beta_c C + \beta_{ab} AB + \beta_{ac} AC + \beta_{bc} BC + \beta_{abc} ABC \tag{14.11}$$

where *A*, *B*, and *C* are the factor levels. The terms β_0, β_a, β_b, and β_{ab} are estimated using equation 14.6, equation 14.7, equation 14.8, and equation 14.9, respectively. To find estimates for the remaining parameters we use the following equations.

$$\beta_c = b_c = \frac{1}{n} \sum C_i^* R_i \tag{14.12}$$

$$\beta_{ac} = b_{ac} = \frac{1}{n} \sum A_i^* C_i^* R_i \tag{14.13}$$

$$\beta_{bc} = b_{bc} = \frac{1}{n} \sum B_i^* C_i^* R_i \tag{14.14}$$

$$\beta_{abc} = b_{abc} = \frac{1}{n} \sum A_i^* B_i^* C_i^* R_i \tag{14.15}$$

Example 14.3

Table 14.4 lists the uncoded factor levels, the coded factor levels, and the responses for a 2^3 factorial design. Determine the coded empirical model for the response surface based on equation 14.11. What is the expected response when *A* is 10, *B* is 15, and *C* is 50?

Solution

Equation 14.5 has eight unknowns—the eight beta terms—and Table 14.4 describes eight experiments. We have just enough information to calculate values for β_0, β_a, β_b, β_c, β_{ab}, β_{ac}, β_{bc}, and β_{abc}; these values are

$$b_0 = \frac{1}{8}(137.25 + 54.75 + 73.75 + 30.25 + 61.75 + 30.25 + 41.25 + 18.75) = 56.0 \tag{14.1.17}$$

(See equation 14.6.)

$$b_a = \frac{1}{8}(137.25 + 54.75 + 73.75 + 30.25 - 61.75 - 30.25 - 41.25 - 18.75) = 18.0 \tag{14.1.18}$$

(See equation 14.7.)

$$b_b = \frac{1}{8}(137.25 + 54.75 - 73.75 - 30.25 + 61.75 + 30.25 - 41.25 - 18.75) = 15.0 \tag{14.1.19}$$

(See equation 14.8.)

$$b_c = \frac{1}{8}(137.25 - 54.75 + 73.75 - 30.25 + 61.75 - 30.25 + 41.25 - 18.75) = 22.5 \tag{14.1.20}$$

(See equation 14.9.)

$$b_{ab} = \frac{1}{8}(137.25 + 54.75 - 73.75 - 30.25 - 61.75 - 30.25 + 41.25 + 18.75) = 7.0 \quad (14.1.21)$$

(See equation 14.12.)

$$b_{ac} = \frac{1}{8}(137.25 - 54.75 + 73.75 - 30.25 - 61.75 + 30.25 - 41.25 + 18.75) = 9.0 \quad (14.1.22)$$

(See equation 14.13.)

$$b_{bc} = \frac{1}{8}(137.25 - 54.75 - 73.75 + 30.25 + 61.75 - 30.25 - 41.25 + 18.75) = 6.0 \quad (14.1.23)$$

(See equation 14.14.)

$$b_{abc} = \frac{1}{8}(137.25 - 54.75 - 73.75 + 30.25 - 61.75 + 30.25 + 41.25 - 18.75) = 3.75 \quad (14.1.24)$$

(See equation 14.15.)

The coded empirical model, therefore, is

$$R = 56.0 + 18.0A^* + 15.0B^* + 22.5C^* + 7.0A^*B^* + 9.0A^*C^* + 6.0B^*C^* + 3.75A^*B^*C^* \quad (14.1.25)$$

To find the response when A is 10, B is 15, and C is 50, we first convert these values into their coded form. Figure 14.14 helps us make the appropriate conversions; thus, A* is 0, B* is –0.5, and C* is +1.33. Substituting back into the empirical model gives a response of

$$R = 56.0 + 18.0(0) + 15.0(-0.5) + 22.5(1.33) + 7.0(0)(-0.5) + 9.0(0)(1.33) + 6.0(-0.5)(1.33) + 3.75(0)(-0.5)(1.33) = 74.435 \quad (14.1.26)$$

Table 14.4 Example of Uncoded and Coded Factor Levels and Responses for the 2^3 Factorial Design in Example 14.3

run	*A*	*B*	*C*	*A**	*B**	*C**	*R*
1	15	30	45	+1	+1	+1	137.25
2	15	30	15	+1	+1	–1	54.75
3	15	10	45	+1	–1	+1	73.75
4	15	10	15	+1	–1	–1	30.25
5	5	30	45	–1	+1	+1	61.75
6	5	30	15	–1	+1	–1	30.25
7	5	10	45	–1	–1	+1	41.25
8	5	10	15	–1	–1	–1	18.75

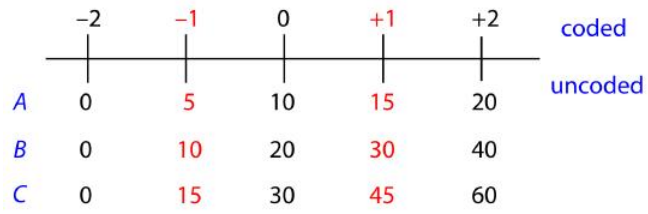


Figure 14.14 The relationship between the coded factor levels and the uncoded factor levels for Example 14.3. The numbers in red are the values defined in the 2^3 factorial design.

A 2^k factorial design can model only a factor's first-order effect on the response. A 2^2 factorial design, for example, includes each factor's first-order effect (β_a and β_b) and a first-order interaction between the factors (β_{ab}). A 2^k factorial design cannot model higher-order effects because there is insufficient information. Here is simple example that illustrates the problem. Suppose we need to model a system in which the response is a function of a single factor. Figure 14.15a shows the result of an experiment using a 2^1 factorial design. The only empirical model we can fit to the data is a straight line.

$$R = \beta_0 + \beta_a A \tag{14.1.27}$$

If the actual response is a curve instead of a straight-line, then the empirical model is in error. To see evidence of curvature we must measure the response for at least three levels for each factor. We can fit the 3^1 factorial design in Figure 14.15b to an empirical model that includes second-order factor effects.

$$R = \beta_0 + \beta_a A + \beta_{aa} A^2 \tag{14.1.28}$$

In general, an *n*-level factorial design can model single-factor and interaction terms up to the $(n - 1)$th order.

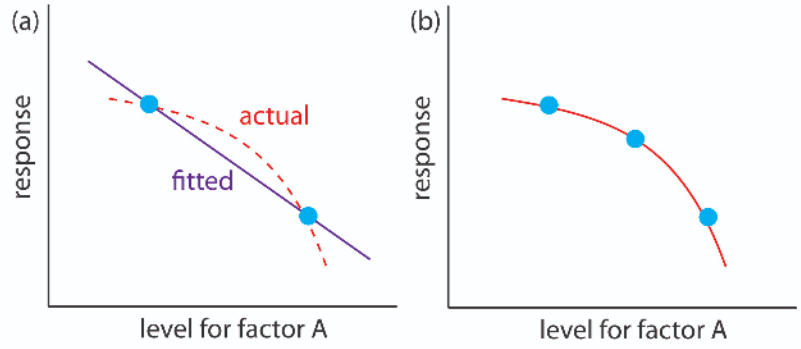


Figure 14.15 A curved one-factor response surface, in red, showing (a) the limitation of using a 2^1 factorial design, which can only fit a straight-line to the data, and (b) the application of a 3^1 factorial design that takes into account second-order effects.

We can judge the effectiveness of a first-order empirical model by measuring the response at the center of the factorial design. If there are no higher-order effects, the average response of the trials in a 2^k factorial design should equal the measured response at the center of the factorial design. To account for influence of random error we make several determinations of the response at the center of the factorial design and establish a suitable confidence interval. If the difference between the two responses is significant, then a first-order empirical model is probably inappropriate.

Note

One of the advantages of working with a coded empirical model is that b_0 is the average response of the $2 \times k$ trials in a 2^k factorial design.

Example 14.4

One method for the quantitative analysis of vanadium is to acidify the solution by adding H_2SO_4 and oxidizing the vanadium with H_2O_2 to form a red-brown soluble compound with the general formula $(VO)_2(SO_4)_3$. Palasota and Deming studied the effect of the relative amounts of H_2SO_4 and H_2O_2 on the solution's absorbance, reporting the following results for a 2^2 factorial design.[5]

H_2SO_4	H_2O_2	absorbance
+1	+1	0.330
+1	–1	0.359
–1	+1	0.293
–1	–1	0.420

Four replicate measurements at the center of the factorial design give absorbances of 0.334, 0.336, 0.346, and 0.323. Determine if a first-order empirical model is appropriate for this system. Use a 90% confidence interval when accounting for the effect of random error.

Solution

We begin by determining the confidence interval for the response at the center of the factorial design. The mean response is 0.335 with a standard deviation of 0.0094, which gives a 90% confidence interval of

$$= \bar{X} \pm \frac{ts}{\sqrt{n}} = 0.335 \frac{(2.35)(0.0094)}{\sqrt{4}} = 0.335 \pm 0.011 \tag{14.1.29}$$

The average response, $\overline{R}$, from the factorial design is

$$\bar{R} = \frac{0.330 + 0.359 + 0.293 + 0.420}{4} = 0.350 \tag{14.1.30}$$

Because $\overline{R}$ exceeds the confidence interval's upper limit of 0.346, we can reasonably assume that a 2^2 factorial design and a first-order empirical model are inappropriate for this system at the 95% confidence level.

(Problem 14.11 in the end-of-chapter problems provides a complete empirical model for this system.)

If we cannot fit a first-order empirical model to our data, we may be able to model it using a full second-order polynomial equation, such as that shown here for a two factors.

$$R = \beta_0 + \beta_a A + \beta_b B + \beta_{aa} A^2 + \beta_{bb} B^2 + \beta_{ab} AB \tag{14.1.31}$$

Because we must measure each factor for at least three levels if we are to detect curvature (see Figure 14.15b), a convenient experimental design is a 3^k factorial design. A 3^2 factorial design for two factors, for example, is shown in Figure 14.16. The computations for 3^k factorial designs are not as easy to generalize as those for a 2^k factorial design and are not considered in this text. See this chapter's additional resources for details about the calculations.

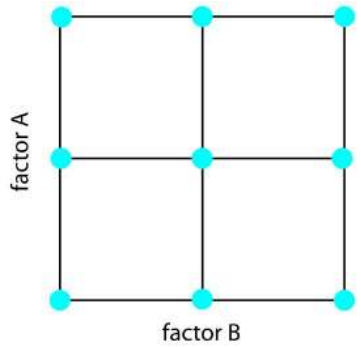


Figure 14.16 A 3^k factorial design for $k = 2$.

Central Composite Designs

One limitation to a 3^k factorial design is the number of trials we need to run. As shown in Figure 14.16, a 3^2 factorial design requires 9 trials. This number increases to 27 for three factors and to 81 for 4 factors. A more efficient experimental design for systems containing more than two factors is a **central composite design**, two examples of which are shown in Figure 14.17. The central composite design consists of a 2^k factorial design, which provides data for estimating each factor's first-order effect and interactions between the factors, and a star design consisting of $2k + 1$ points, which provides data for estimating second-order effects. Although a central composite design for two factors requires the same number of trials, 9, as a 3^2 factorial design, it requires only 15 trials and 25 trials for systems involving three factors or four factors. See this chapter's additional resources for details about the central composite designs.

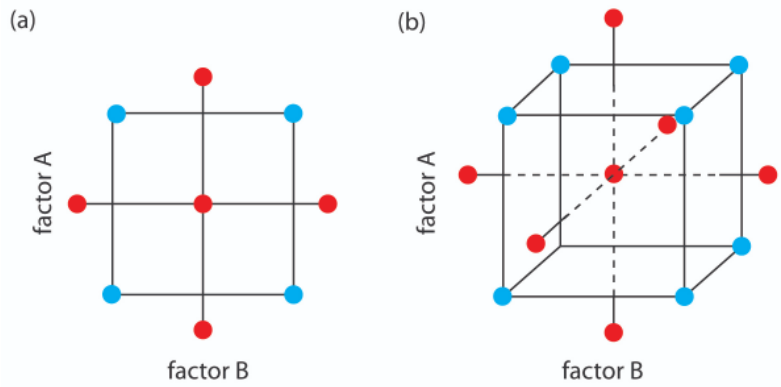


Figure 14.17 Two examples of a central composite design for (a) $k = 2$ and (b) $k = 3$. The points in blue are a 2^k factorial design, and the points in red are a star design.

Contributors

David Harvey (DePauw University)

14.1: Optimizing the Experimental Procedure is shared under a CC BY-NC-SA 4.0 license and was authored, remixed, and/or curated by LibreTexts.

14.2: Verifying the Method

After developing and optimizing a method, the next step is to determine how well it works in the hands of a single analyst. Three steps make up this process: determining single-operator characteristics, completing a blind analysis of standards, and determining the method's ruggedness. If another standard method is available, then we can analyze the same sample using both the standard method and the new method, and compare the results. If the result for any single test is unacceptable, then the method is not a suitable standard method.

14.2.1 Single Operator Characteristics

The first step in verifying a method is to determine the precision, accuracy, and detection limit when a single analyst uses the method to analyze a standard sample. The detection limit is determined by analyzing an appropriate reagent blank. Precision is determined by analyzing replicate portions of the sample, preferably more than ten. Accuracy is evaluated using a *t*-test comparing the experimental results to the known amount of analyte in the standard. Precision and accuracy are evaluated for several different concentrations of analyte, including at least one concentration near the detection limit, and for each different sample matrix. Including different concentrations of analyte helps identify constant sources of determinate error and establishes the range of concentrations for which the method is applicable.

> **Note**
>
> See Chapter 4.8 for a discussion of detection limits. Pay particular attention to the difference between a detection limit, a limit of identification, and a limit of quantitation.
>
> See Section 4.6.1 for a review of the *t*-test.
>
> See Chapter 4.2 for a review of constant determinate errors. Figure 4.3 illustrates how we can detect a constant determinate error by analyzing samples containing different amounts of analyte.

14.2.2 Blind Analysis of Standard Samples

Single-operator characteristics are determined by analyzing a standard sample that has a concentration of analyte known to the analyst. The second step in verifying a method is a **blind analysis** of standard samples. Although the concentration of analyte in the standard is known to a supervisor, the information is withheld from the analyst. After analyzing the standard sample several times, the analyte's average concentration is reported to the test's supervisor. To be accepted, the experimental mean should be within three standard deviations—as determined from the single-operator characteristics—of the analyte's known concentration.

> **Note**
>
> An even more stringent requirement is to require that the experimental mean be within two standard deviations of the analyte's known concentration.

14.2.3 Ruggedness Testing

An optimized method may produce excellent results in the laboratory that develops a method, but poor results in other laboratories. This is not particularly surprising because a method typically is optimized by a single analyst using the same reagents, equipment, and instrumentation for each trial. Any variability introduced by the analysts, the reagents, the equipment, and the instrumentation is not included in the single-operator characteristics. Other less obvious factors may affect an analysis, including environmental factors, such as the temperature or relative humidity in the laboratory. If the procedure does not require their control, then they may contribute to variability. Finally, the analyst optimizing usually takes particular care to perform the analysis in exactly the same way during every trial, which may minimize the run to run variability.

An important step in developing a standard method is to determine which factors have a pronounced effect on the quality of the results. Once we identify these factors, we can write into the procedure instructions that specify how these factors must be controlled. A procedure that, when carefully followed, produces results of high quality in different laboratories is considered rugged. The method by which the critical factors are discovered is called **ruggedness testing**.[6]

> **Note**
>
> For example, if temperature is a concern, we might specify that it be held at 25 ± 2°C.

Ruggedness testing usually is performed by the laboratory developing the standard method. After identifying potential factors, their effects are evaluated by performing the analysis at two levels for each factor. Normally one level is that specified in the procedure, and the other is a level likely to be encountered when the procedure is used by other laboratories.

This approach to ruggedness testing can be time consuming. If there are seven potential factors, for example, a 2^7 factorial design can evaluate each factor's first-order effect. Unfortunately, this requires a total of 128 trials—too many trials to be a practical solution. A simpler experimental design is shown in Table 14.5, in which the two factor levels are identified by upper case and lower case letters. This design, which is similar to a 2^3 factorial design, is called a fractional factorial design. Because it includes only eight runs, the design provides information about only the eight first-order factor effects. It does not provide sufficient information to evaluate higher-order effects or interactions between factors, both of which are probably less important than the first-order effects.

> **Note**
>
> Why does this model estimate the seven first-order factor effects and not seven of the 20 possible first-order interactions? With eight experiments, we can only choose to calculate seven parameters (plus the average response). The calculation of E_D, for example, also gives the value for E_{AB}. You can convince yourself of this by replacing each upper case letter with a +1 and each lower case letter with a –1 and noting that A × B = D. We choose to report the first-order factor effects because they are likely to be more important than interactions between factors.

Table 14.5 Experimental Design for a Ruggedness Test Involving Seven Factors

	factors							
run	A	B	C	D	E	F	G	response
1	*A*	*B*	*C*	*D*	*E*	*F*	*G*	R_1
2	*A*	*B*	*c*	*D*	*e*	*f*	*g*	R_2
3	*A*	*b*	*C*	*d*	*E*	*f*	*g*	R_3
4	*A*	*b*	*c*	*d*	*e*	*F*	*G*	R_4
5	*a*	*B*	*C*	*d*	*e*	*F*	*g*	R_5
6	*a*	*B*	*c*	*d*	*E*	*f*	*G*	R_6
7	*a*	*b*	*C*	*D*	*e*	*f*	*G*	R_7
8	*a*	*b*	*c*	*D*	*E*	*F*	*g*	R_8

The experimental design in Table 14.5 is balanced in that each of a factor's two levels is paired an equal number of times with the upper case and lower case levels for every other factor. To determine the effect, E_f, of changing a factor's level, we subtract the average response when the factor is at its upper case level from the average value when it is at its lower case level.

$$E_f = \frac{(\sum R_i)_{\text{upper case}}}{4} - \frac{(\sum R_i)_{\text{lower case}}}{4} \tag{14.16}$$

Because the design is balanced, the levels for the remaining factors appear an equal number of times in both summation terms, canceling their effect on E_f. For example, to determine the effect of factor A, E_A, we subtract the average response for runs 5–8 from the average response for runs 1–4. Factor B does not affect E_A because its upper case levels in runs 1 and 2 are canceled by the upper case levels in runs 5 and 6, and its lower case levels in runs 3 and 4 are canceled by the lower case levels in runs 7 and 8. After calculating each of the factor effects we rank them from largest to smallest without regard to sign, identifying those factors whose effects are substantially larger than the other factors.

Note

To see that this is design is balanced, look closely at the last four runs. Factor A is present at its level *a* for all four of these runs. For each of the remaining factors, two levels are upper case and two levels are lower case. Runs 5–8 provide information about the effect of *a* on the response, but do not provide information about the effect of any other factor. Runs 1, 2, 5, and 6 provide information about the effect of *B*, but not of the remaining factors. Try a few other examples to convince yourself that this relationship is general.

We also can use this experimental design to estimate the method's expected standard deviation due to the effects of small changes in uncontrolled or poorly controlled factors.[7]

$$s = \sqrt{\frac{2}{7}\sum E_f^2} \tag{14.17}$$

If this standard deviation is unacceptably large, then the procedure is modified to bring under greater control those factors having the greatest effect on the response.

Example 14.5

The concentration of trace metals in sediment samples collected from rivers and lakes can be determined by extracting with acid and analyzing the extract by atomic absorption spectrophotometry. One procedure calls for an overnight extraction using dilute HCl or HNO_3. The samples are placed in plastic bottles with 25 mL of acid and placed on a shaker operated at a moderate speed and at ambient temperature. To determine the method's ruggedness, the effect of the following factors was studied using the experimental design in Table 14.5.

Factor A: extraction time	*A* = 24 h	*a* = 12 h
Factor B: shaking speed	*B* = medium	*b* = high
Factor C: acid type	*C* = HCl	*c* = HNO_3
Factor D: acid concentration	*D* = 0.1 M	*d* = 0.05 M
Factor E: volume of acid	*E* = 25 mL	*e* = 35 mL
Factor F: type of container	*F* = plastic	*f* = glass
Factor G: temperature	*G* = ambient	*g* = 25°C

Eight replicates of a standard sample containing a known amount of analyte were carried through the procedure. The analyte's recovery in the samples, given as a percentage, are shown here.

R_1 = 98.9 R_5 = 97.4	R_2 = 99.0 R_6 = 97.3	R_3 = 97.5 R_7 = 98.6	R_4 = 97.7 R_8 = 98.6

Determine which factors appear to have a significant effect on the response and estimate the method's expected standard deviation.

Solution

To calculate the effect of changing each factor's level we use equation 14.16 and substitute in appropriate values. For example, E_A is

$$E_A = \frac{98.9 + 99.0 + 97.5 + 97.7}{4} - \frac{97.4 + 97.3 + 98.6 + 98.6}{4} = 0.30 \quad (14.2.1)$$

and E_G is

$$E_A = \frac{98.9 + 97.7 + 97.3 + 98.6}{4} - \frac{99.0 + 97.5 + 97.4 + 98.6}{4} = 0.00 \quad (14.2.2)$$

Completing the remaining calculations and ordering the factors by the absolute values of their effects

Factor D	1.30
Factor A	0.35
Factor E	-0.10
Factor B	0.05
Factor C	-0.05
Factor F	0.05
Factor G	0.00

shows us that the concentration of acid (Factor D) has a substantial effect on the response, with a concentration of 0.05 M providing a much lower percent recovery. The extraction time (Factor A) also appears significant, but its effect is not as important as the acid's concentration. All other factors appear insignificant. The method's estimated standard deviation, from equation 14.27, is

$$s = \sqrt{\frac{2}{7}\{(1.30)^2 + (0.35)^2 + (-0.10)^2 + (0.05)^2 + (-0.05)^2 + (0.05)^2 + (0.00)^2\}} = 0.72 \quad (14.2.3)$$

which, for an average recovery of 98.1% gives a relative standard deviation of approximately 0.7%. If we control the acid's concentration so that its effect approaches that for factors B, C, and F, then the relative standard deviation becomes 0.18, or approximately 0.2%.

14.2.4 Equivalency Testing

If an approved standard method is available, then the new method should be evaluated by comparing results to those obtained with the standard method. Normally this comparison is made at a minimum of three concentrations of analyte to evaluate the new method over a wide dynamic range. Alternatively, we can plot the results using the new method against the results using the approved standard method. A slope of 1.00 and a *y*-intercept of 0.0 provides evidence that the two methods are equivalent.

Contributors

David Harvey (DePauw University)

14.2: Verifying the Method is shared under a CC BY-NC-SA 4.0 license and was authored, remixed, and/or curated by LibreTexts.

14.3: Validating the Method as a Standard Method

For an analytical method to be useful, an analyst must be able to achieve results of acceptable accuracy and precision. Verifying a method, as described in the previous section, establishes this goal for a single analyst. Another requirement for a useful analytical method is that an analyst should obtain the same result from day to day, and different labs should obtain the same result when analyzing the same sample. The process by which we approve method for general use is known as **validation** and it involves a collaborative test of the method by analysts in several laboratories. Collaborative testing is used routinely by regulatory agencies and professional organizations, such as the U. S. Environmental Protection Agency, the American Society for Testing and Materials, the Association of Official Analytical Chemists, and the American Public Health Association. Many of the representative methods in earlier chapters are identified by these agencies as validated methods.

> **Note**
>
> Representative Method 10.1 for the determination of iron in water and wastewater, and Representative Method 10.5 for the determination of sulfate in water, are two examples of standard methods validated through collaborative testing.

When an analyst performs a single analysis on a sample the difference between the experimentally determined value and the expected value is influenced by three sources of error: random errors, systematic errors inherent to the method, and systematic errors unique to the analyst. If the analyst performs enough replicate analyses, then we can plot a distribution of results, as shown in Figure 14.18a. The width of this distribution is described by a standard deviation, providing an estimate of the random errors effecting the analysis. The position of the distribution's mean, $\overline{X}$, relative to the sample's true value, μ, is determined both by systematic errors inherent to the method and those systematic errors unique to the analyst. For a single analyst there is no way to separate the total systematic error into its component parts.

The goal of a **collaborative test** is to determine the magnitude of all three sources of error. If several analysts each analyze the same sample one time, the variation in their collective results, as shown in Figure 14.18b, includes contributions from random errors and those systematic errors (biases) unique to the analysts. Without additional information, we cannot separate the standard deviation for this pooled data into the precision of the analysis and the systematic errors introduced by the analysts. We can use the position of the distribution, to detect the presence of a systematic error in the method.

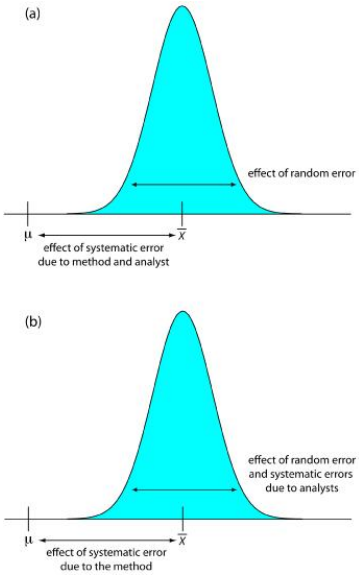


Figure 14.18 Partitioning of random errors, systematic errors due to the analyst, and systematic errors due to the method for (a) replicate analyses performed by a single analyst, and (b) single determinations performed by several analysts.

14.3.1 Two-Sample Collaborative Testing

The design of a collaborative test must provide the additional information we need to separate random errors from the systematic errors introduced by the analysts. One simple approach—accepted by the Association of Official Analytical Chemists—is to have

each analyst analyze two samples that are similar in both their matrix and in their concentration of analyte. To analyze their results we represent each analyst as a single point on a two-sample chart, using the result for one sample as the *x*-coordinate and the result for the other sample as the *y*-coordinate.[8]

As shown in Figure 14.19, a two-sample chart divides the results into four quadrants, which we identify as (+, +), (–, +), (–, –) and (+, –), where a plus sign indicates that the analyst's result exceeds the mean for all analysts and a minus sign indicates that the analyst's result is smaller than the mean for all analysts. The quadrant (+, –), for example, contains results for analysts that exceeded the mean for sample X and that undershot the mean for sample Y. If the variation in results is dominated by random errors, then we expect the points to be distributed randomly in all four quadrants, with an equal number of points in each quadrant. Furthermore, as shown in Figure 14.19a, the points will cluster in a circular pattern whose center is the mean values for the two samples. When systematic errors are significantly larger than random errors, then the points occur primarily in the (+, +) and the (–, –) quadrants, forming an elliptical pattern around a line bisecting these quadrants at a 45° angle, as seen in Figure 14.19b.

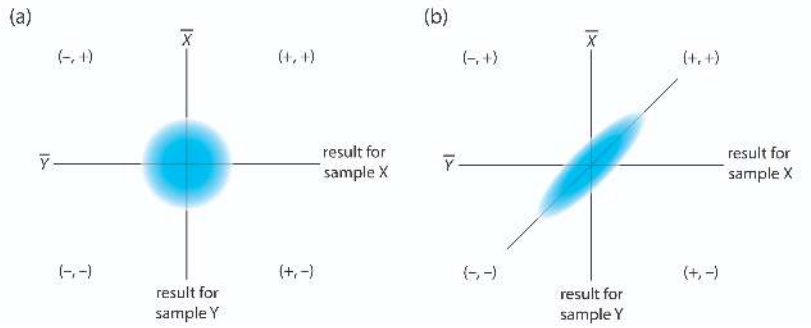


Figure 14.19 Typical two-sample plots when (a) random errors are significantly larger than systematic errors due to the analysts, and (b) when systematic errors due to the analysts are significantly larger than the random errors.

A visual inspection of a two-sample chart is an effective method for qualitatively evaluating the results of analysts and the capabilities of a proposed standard method. If random errors are insignificant, then the points fall on the 45° line. The length of a perpendicular line from any point to the 45° line, therefore, is proportional to the effect of random error on that analyst's results. The distance from the intersection of the axes—corresponding to the mean values for samples X and Y—to the perpendicular projection of a point on the 45° line is proportional to the analyst's systematic error. Figure 14.20 illustrates these relationships. An ideal standard method has small random errors and small systematic errors due to the analysts, and has a compact clustering of points that is more circular than elliptical.

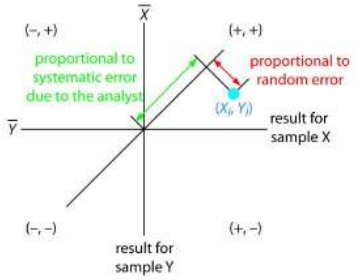


Figure 14.20 Relationship between the result for a single analyst (in blue) and the contribution of random error (red arrow) and the contribution from the analyst's systematic error (green arrow).

We also can use the data in a two-sample chart to separate the total variation in the data, σ_{tot}, into contributions from random error, σ_{rand}, and systematic errors due to the analysts, σ_{syst}.[9] Because an analyst's systematic errors are present in his or her analysis of both samples, the difference, *D*, between the results

$$D_i = X_i - Y_i \tag{14.3.1}$$

is the result of random error. To estimate the total contribution from random error we use the standard deviation of these differences, s_D, for all analysts

https://chem.libretexts.org/@go/page/70735

$$s_D = \sqrt{\frac{\sum (D_i - \overline{D})^2}{2(n-1)}} = s_{rand} \approx \sigma_{rand} \tag{14.18}$$

where n is the number of analysts. The factor of 2 in the denominator of equation 14.18 is the result of using two values to determine D_i. The total, T, of each analyst's results

$$T_i = X_i + Y_i \tag{14.3.2}$$

contains contributions from both random error and twice the analyst's systematic error.

$$\sigma^2_{tot} = \sigma^2_{rand} + 2\sigma^2_{syst} \tag{14.19}$$

Note

We double the analyst's systematic error in equation 14.19 because it is the same in each analysis.

The standard deviation of the totals, s_T, provides an estimate for σ_{tot}.

$$s_T = \sqrt{\frac{\sum (T_i - \overline{T})^2}{2(n-1)}} = s_{tot} \approx \sigma_{tot} \tag{14.20}$$

Again, the factor of 2 in the denominator is the result of using two values to determine T_i.

If the systematic errors are significantly larger than the random errors, then s_T is larger than s_D, a hypothesis we can evaluate using a one-tailed F-test

$$F = \frac{s^2_T}{s^2_D} \tag{14.3.3}$$

where the degrees of freedom for both the numerator and the denominator are n – 1. As shown in the following example, if s_T is significantly larger than s_D we can use equation 14.19 to separate σ_{tot}^2 into components representing random error and systematic error.

Note

For a review of the *F*-test, see Section 4.6.2 and Section 4.6.3. Example 4.18 illustrates a typical application.

Example 14.6

As part of a collaborative study of a new method for determining the amount of total cholesterol in blood, you send two samples to 10 analysts with instructions to analyze each sample one time. The following results, in mg total cholesterol per 100 mL of serum, are returned to you.

analyst	sample 1	sample 2
1	245.0	229.4
2	247.4	249.7
3	246.0	240.4
4	244.9	235.5
5	255.7	261.7
6	248.0	239.4
7	249.2	255.5
8	255.1	224.3
9	255.0	246.3
10	243.1	253.1

Use this data estimate σ_{rand} and σ_{syst} for the method.

Solution

Figure 14.21 provides a two-sample plot of the results. The clustering of points suggests that the systematic errors of the analysts are significant. The vertical line at 245.9 mg/100 mL is the average value for sample 1 and the average value for sample 2 is shown by the horizontal line at 243.5 mg/100 mL. To estimate σ_{rand} and σ_{syst} we first calculate values for D_i and T_i.

analyst	D_i	T_i
1	15.6	474.4
2	-2.3	497.1
3	5.6	486.4
4	9.4	480.4
5	-6.0	517.4
6	8.6	487.4
7	-6.3	504.7
8	0.8	449.4
9	8.7	501.3
10	-10.0	496.2

Next, we calculate the standard deviations for the differences, s_D, and the totals, s_T, using equations 14.18 and 14.20, giving s_D = 5.95 and s_T = 13.3. To determine if the systematic errors between the analysts are significant, we use an *F*-test to compare s_T and s_D.

$$F = \frac{s_T^2}{s_D^2} = \frac{(13.3)^2}{(5.95)^2} = 5.00 \tag{14.3.4}$$

Because the *F*-ratio is larger than *F*(0.05, 9, 9), which is 3.179, we conclude that the systematic errors between the analysts are significant at the 95% confidence level. The estimated precision for a single analyst is

$$\sigma_{rand} \approx s_D = 5.95 \tag{14.3.5}$$

(Critical values for the *F*-test are in Appendix 5.)

The estimated standard deviation due to systematic errors between analysts is calculated from equation 14.18.

$$\sigma_{syst} \approx \sqrt{\frac{\sigma_{tot}^2 - \sigma_{rand}^2}{2}} \approx \sqrt{\frac{s_T^2 - s_D^2}{2}} = \sqrt{\frac{(13.3)^2 - (5.95)^2}{2}} = 8.41 \tag{14.3.6}$$

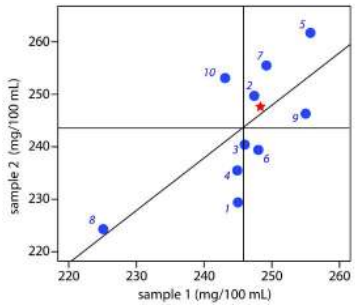


Figure 14.21 Two-sample plot for the data in Example 14.6. The number by each blue point indicates the analyst. The true values for each sample (see Example 14.7) are indicated by the red star.

If the true values for the two samples are known, we also can test for the presence of a systematic error in the method. If there are no systematic method errors, then the sum of the true values, μ_{tot}, for samples X and Y

$$\mu_{tot} = \mu_X + \mu_Y \tag{14.3.7}$$

should fall within the confidence interval around $\overline{T}$. We can use a two-tailed *t*-test of the following null and alternate hypotheses

$$H_0 : \overline{T} = \mu_{tot} \qquad H_A : \overline{T} \neq \mu_{tot} \tag{14.3.8}$$

to determine if there is evidence for a systematic error in the method. The test statistic, t_{exp}, is

$$t_{exp} = \frac{|\overline{T} - \mu_{tot}|\sqrt{n}}{s_T\sqrt{2}} \tag{14.21}$$

with $n - 1$ degrees of freedom. We include the $\sqrt{2}$ in the denominator because s_T (see equation 14.20) underestimates the standard deviation when comparing $\overline{T}$ to μ_{tot}.

> **Note**
>
> For a review of the *t*-test of an experimental mean to a known mean, see Section 4.6.1. Example 4.16 illustrates a typical application.

> **Example 14.7**
>
> The two samples analyzed in Example 14.6 are known to contain the following concentrations of cholesterol
>
> $$\mu_{samp\ 1} = 248.3\ mg/100\ mL \qquad \mu_{samp\ 2} = 247.6\ mg/100\ mL \tag{14.3.9}$$
>
> Determine if there is any evidence for a systematic error in the method at the 95% confidence level.
>
> ***Solution***
>
> Using the data from Example 14.6 and the true values for the samples, we know that s_T is 13.3, and that
>
> $$\overline{T} = \overline{X}_{samp\ 1} + \overline{X}_{samp\ 2} = 245.9 + 243.5 = 489.4\ mg/100\ mL \tag{14.3.10}$$
>
> $$\mu_{tot} = \mu_{samp\ 1} + \mu_{samp\ 2} = 248.3 + 247.6 = 495.9\ mg/100\ mL \tag{14.3.11}$$
>
> Substituting these values into equation 14.21 gives
>
> $$t_{exp} = \frac{|489.4 - 495.9|\sqrt{10}}{13.3\sqrt{2}} = 1.09 \tag{14.3.12}$$
>
> Because this value for t_{exp} is smaller than the critical value of 2.26 for $t(0.05, 9)$, there is no evidence for a systematic error in the method at the 95% confidence level.
>
> (Critical values for the *t*-test are in Appendix 4.)

Example 14.6 and Example 14.7 illustrate how we can use a pair of similar samples in a collaborative test of a new method. Ideally, a collaborative test involves several pairs of samples that span the range of analyte concentrations for which we plan to use the method. In doing so, we evaluate the method for constant sources of error and establish the expected relative standard deviation and bias for different levels of analyte.

14.3.2 Collaborative Testing and Analysis of Variance

In a two-sample collaborative test we ask each analyst to perform a single determination on each of two separate samples. After reducing the data to a set of differences, *D*, and a set of totals, *T*, each characterized by a mean and a standard deviation, we extract values for the random errors affecting precision and the systematic differences between then analysts. The calculations are relatively simple and straightforward.

An alternative approach for completing a collaborative test is to have each analyst perform several replicate determinations on a single, common sample. This approach generates a separate data set for each analyst, requiring a different statistical treatment to arrive at estimates for σ_{rand} and σ_{syst}.

There are several statistical methods for comparing three or more sets of data. The approach we consider in this section is an **analysis of variance** (ANOVA). In its simplest form, a one-way ANOVA allows us to explore the importance of a single variable—the identity of the analyst is one example—on the total variance. To evaluate the importance of this variable, we compare its variance to the variance explained by indeterminate sources of error.

We first introduced variance in Chapter 4 as one measure of a data set's spread around its central tendency. In the context of an analysis of variance, it is useful for us to understand that variance is simply a ratio of two terms: a sum of squares for the differences between individual values and their mean, and the available degrees of freedom. For example, the variance, s^2, of a data set consisting of n measurements is

$$s^2 = \frac{\sum (X_i - \overline{X})^2}{n-1} = \frac{\text{sum of squares}}{\text{degrees of freedom}} \tag{14.3.13}$$

where X_i is the value of a single measurement and $\overline{X}$ is the mean. The ability to partition the variance into a sum of squares and the degrees of freedom greatly simplifies the calculations in a one-way ANOVA.

Let's use a simple example to develop the rationale behind a one-way ANOVA calculation. The data in Table 14.6 are from four analysts, each asked to determine the purity of a single pharmaceutical preparation of sulfanilamide. Each column in Table 14.6 provides the results for an individual analyst. To help us keep track of this data, we will represent each result as X_{ij}, where i identifies the analyst and j indicates the replicate. For example, $X_{3,5}$ is the fifth replicate for the third analyst, or 94.24%.

Table 14.6 Determination of the %Purity of a Sulfanilamide Preparation by Four Analysts

replicate	analyst A	analyst B	analyst C	analyst D
1	94.09	99.55	95.14	93.88
2	94.64	98.24	94.62	94.23
3	95.08	101.1	95.28	96.05
4	94.54	100.4	94.59	93.89
5	95.38	100.1	94.24	94.95
6	93.62			95.49
$\overline{X}$	94.56	99.88	95.86	94.77
s	0.630	1.073	0.428	0.899

The data in Table 14.6 show variability, both in the results obtained by each analyst and in the difference in the results between the analysts. There are two sources for this variability: indeterminate errors associated with the analytical procedure experienced equally by each analyst, and systematic or determinate errors introduced by individual analysts.

One way to view the data in Table 14.6 is to treat it as a single large sample, characterized by a global mean and a global variance

$$\overline{\overline{X}} = \frac{\sum_{i=1}^{h} \sum_{j=1}^{n_i} X_{ij}}{N} \tag{14.22}$$

$$\overline{\overline{s^2}} = \frac{\sum_{i=1}^{h} \sum_{j=1}^{n_i} (X_{ij} - \overline{\overline{X}})^2}{N-1} \tag{14.23}$$

where h is the total number of samples (in this case the number of analysts), n_i is the number of replicates for the ith sample (in this case the ith analyst), and N is the total number of data points (in this case 22). The global variance—which includes all sources of variability affecting the data—provides an estimate of the combined influence of indeterminate errors and systematic errors.

A second way to work with the data in Table 14.6 is to treat the results for each analyst separately. If we assume that each analyst experiences the same indeterminate errors, then the variance, s^2, for each analyst provides a separate estimate of σ_{rand}^2. To pool

these individual variances, which we call the **within-sample variance**, s_w^2, we square the difference between each replicate and its corresponding mean, add them up, and divide by the degrees of freedom.

$$\sigma_{\text{rand}}^2 \approx s_w^2 = \frac{\sum_{i=1}^{h}\sum_{j=1}^{n_i}(X_{ij} - \overline{X}_i)^2}{N - h} \tag{14.24}$$

Note

Carefully compare our description of equation 14.24 to the equation itself. It is important that you understand why equation 14.24 provides our best estimate of the indeterminate errors affecting the data in Table 14.6. Note that we lose one degree of freedom for each of the *h* means included in the calculation.

Equation 14.24 provides an estimate for σ_{rand}^2. To estimate the systematic errors, σ_{syst}^2, affecting the results in Table 14.6 we need to consider the differences between the analysts. The variance of the individual mean values about the global mean, which we call the **between-sample variance**, s_b^2, provides this estimate.

$$\sigma_{\text{syst}}^2 \approx s_b^2 = \frac{\sum_{i=1}^{h} n_i(\overline{X}_i - \overline{\overline{X}})^2}{h - 1} \tag{14.25}$$

Note

We lose one degree of freedom for the global mean.

The between-sample variance includes contributions from both indeterminate errors and systematic errors

$$s_b^2 = \sigma_{\text{rand}}^2 + \bar{n}\sigma_{\text{syst}}^2 \tag{14.26}$$

where $\bar{n}$ is the average number of replicates per analyst.

$$\bar{n} = \frac{\sum_{i=1}^{h} n_i}{h} \tag{14.3.14}$$

Note

Note the similarity between equation 14.26 and equation 14.19. The analysis of the data in a two-sample plot is the same as a one-way analysis of variance with $h = 2$.

In a one-way ANOVA of the data in Table 14.6 we make the null hypothesis that there are no significant differences between the mean values for each analyst. The alternative hypothesis is that at least one of the means is significantly different. If the null hypothesis is true, then σ_{syst}^2 must be zero, and s_w^2 and s_b^2 should have similar values. If s_b^2 is significantly greater than s_w^2, then σ_{syst}^2 is greater than zero. In this case we must accept the alternative hypothesis that there is a significant difference between the means for the analysts. The test statistic is the *F*-ratio

$$F_{\text{exp}} = \frac{s_b^2}{s_w^2} \tag{14.3.15}$$

which is compared to the critical value $F(\alpha, h - 1, N - h)$. This is a one-tailed significance test because we are only interested in whether s_b^2 is significantly greater than s_w^2.

Both s_b^2 and s_w^2 are easy to calculate for small data sets. For larger data sets, calculating s_w^2 is tedious. We can simplify the calculations by taking advantage of the relationship between the sum-of-squares terms for the global variance (equation 14.23), the within-sample variance (equation 14.24), and the between-sample variance (equation 14.25). We can split the numerator of equation 14.23, which is the total sum-of-squares, SS_t, into two terms

$$SS_t = SS_w + SS_b \tag{14.3.16}$$

where SS_w is the sum-of-squares for the within-sample variance and SS_b is the sum-of-squares for the between-sample variance. Calculating SS_t and SS_b gives SS_w by difference. Finally, dividing SS_w and SS_b by their respective degrees of freedom gives s_w^2 and s_b^2. Table 14.7 summarizes the equations for a one-way ANOVA calculation. Example 14.8 walks you through the calculations, using the data in Table 14.6. Section 14D provides instructions on using Excel and R to complete a one-way analysis of variance.

Note

Problem 14.17 in the end of chapter problems asks you to verify this relationship between the sum-of-squares.

Table 14.7 Summary of Calculations for a One-Way Analysis of Variance

source	sum-of-squares	degrees of freedom	variance	expected variance	F-ratio
between samples	$SS_b = \sum_{i=1}^{h} n_i(\overline{X}_i - \overline{\overline{X}})^2$	$h-1$	$s_b^2 = \frac{SS_b}{h-1}$	$s_b^2 = \sigma_{rand}^2 + \bar{n}\sigma_{syst}^2$	$F_{exp} = \frac{s_b^2}{s_w^2}$
within samples	$SS_t = SS_w + SS_b$	$N-h$	$s_w^2 = \frac{SS_w}{N-h}$	$s_w^2 = \sigma_{rand}^2$	
total	$SS_t = \sum_{i=1}^{h}\sum_{j=1}^{n_i}(X_{ij} - \overline{\overline{X}})^2 = \overline{\overline{s^2}}(N-1)$ (14.3.18)	$N-1$			

Example 14.8

The data in Table 14.6 are from four analysts, each asked to determine the purity of a single pharmaceutical preparation of sulfanilamide. Determine if the difference in their results is significant at α = 0.05. If such a difference exists, estimate values for σ_{rand}^2 and σ_{syst}^2.

Solution

To begin we calculate the global mean (equation 14.22) and the global variance (equation 14.23) for the pooled data, and the means for each analyst; these values are summarized here.

$$\overline{\overline{X}} = 95.87 \quad \overline{\overline{s^2}} = 5.506 \tag{14.3.19}$$

$$\overline{X}_A = 94.56 \quad \overline{X}_B = 99.88 \quad \overline{X}_C = 94.77 \quad \overline{X}_S = 94.75 \tag{14.3.20}$$

Using these values we calculate the total sum of squares

$$SS_t = \overline{\overline{s^2}}(N-1) = (5.506)(22-1) \tag{14.3.21}$$

the between sample sum of squares

$$SS_b = \sum_{i=1}^{h} n_i(\overline{X}_i - \overline{\overline{X}}) = 6(94.56-95.87)^2 + 5(99.88-95.87)^2 + 5(94.77-95.87)^2 + 6(94.75-95.87)^2 = 104.27 \tag{14.3.22}$$

and the within sample sum of squares

$$SS_w = SS_t - SS_b = 115.63 - 104.27 = 11.36 \tag{14.3.23}$$

The remainder of the necessary calculations are summarized in the following table.

source	sum-of-squares	degrees of freedom	variance
between samples	104.27	h – 1 = 4 – 1 = 3	34.76
within samples	11.36	N – h = 22 – 4 = 8	0.631

Comparing the variances we find that

$$F_{exp} = \frac{s_b^2}{s_w^2} = \frac{34.76}{0.631} = 55.08 \tag{14.3.24}$$

Because F_{exp} is greater than $F(0.05, 3, 18)$, which is 3.16, we reject the null hypothesis and accept the alternative hypothesis that the work of at least one analyst is significantly different from the remaining analysts. Our best estimate of the within sample variance is

$$\sigma^2_{rand} \approx s^2_w = 0.631 \tag{14.3.25}$$

and our best estimate of the between sample variance is

$$\sigma^2_{syst} \approx \frac{s^2_b - s^2_w}{\bar{n}} = \frac{34.76 - 0.631}{22/4} = 6.205 \tag{14.3.26}$$

In this example the variance due to systematic differences between the analysts is almost an order of magnitude greater than the variance due to the method's precision.

Having demonstrated that there is significant difference between the analysts, we can use a modified version of the *t*-test, known as **Fisher's least significant difference**, to determine which analyst or analysts are responsible for the difference. The test statistic for comparing two mean values is the *t*-test given in equation 4.21 in Chapter 4, except we replace the pooled standard deviation, s_{pool}, by the square root of the within-sample variance from the analysis of variance.

$$t_{exp} = \frac{|\overline{X}_1 - \overline{X}_2|}{\sqrt{s^2_w}\sqrt{\frac{1}{n_A} + \frac{1}{n_B}}} = \frac{|\overline{X}_1 - \overline{X}_2|}{\sqrt{s^2_w}} \times \sqrt{\frac{n_A n_B}{n_A + n_B}} \tag{14.27}$$

We compare t_{exp} to its critical value $t(\alpha, \nu)$ using the same significance level as the ANOVA calculation. The degrees of freedom are the same as that for the within sample variance. Since we are interested in whether the larger of the two means is significantly greater than the other mean, the value of $t(\alpha, \nu)$ is that for a one-tailed significance test.

Note

You might ask why we bother with the analysis of variance if we are planning to use a *t*-test to compare pairs of analysts. Each *t*-test carries a probability, α, of claiming that a difference is significant even though it is not (a type 1 error). If we set α to 0.05 and complete six *t*-tests, the probability of a type 1 error increases to 0.265. Knowing that there is a significant difference within a data set—what we gain from the analysis of variance—protects the *t*-test.

Example 14.9

In Example 14.8 we showed that there is a significant difference between the work of the four analysts in Table 14.6. Determine the source of this significant difference.

Solution

Individual comparisons using Fisher's least significant difference test are based on the following null hypothesis and the appropriate one-tailed alternative hypothesis.

$$H_0 : \overline{X}_i = \overline{X}_j \quad H_A : \text{ one of the following } \overline{X}_i > \overline{X}_j \text{ or } \overline{X}_i < \overline{X}_j \tag{14.3.27}$$

Using equation 14.27 we calculate values of t_{exp} for each possible comparison and compare them to the one-tailed critical value of 1.73 for $t(0.05, 18)$. For example, t_{exp} for analysts A and B is

$$(t_{exp})_{A,B} = \frac{|\overline{X}_1 - \overline{X}_2|}{\sqrt{s^2_w}} \times \sqrt{\frac{n_A n_B}{n_A + n_B}} = \frac{|94.56 - 99.88|}{\sqrt{0.631}} \times \sqrt{\frac{6 \times 5}{6 + 5}} = 11.06 \tag{14.3.28}$$

Because $(t_{exp})_{A,B}$ is greater than $t(0.05, 18)$ we reject the null hypothesis and accept the alternative hypothesis that the results for analyst B are significantly greater than those for analyst A. Continuing with the other pairs it is easy to show that $(t_{exp})_{A,C}$ is 0.437, $(t_{exp})_{A,D}$ is 0.414, $(t_{exp})_{B,C}$ is 10.17, $(t_{exp})_{B,D}$ is 10.67, and $(t_{exp})_{C,D}$ is 0.04. Collectively, these results suggest that there is a significant systematic difference between the work of analyst B and the work of the other analysts. There is no way to decide whether any of the four analysts has done accurate work.

(We know that analyst B's result is significantly different than the results for analysts A, C, and D, and that we have no evidence that there is any significant difference between the results of analysts A, C, and D. We do not know if analyst B's results is

accurate, or if the results of analysts A, C, and D are accurate. In fact, it is possible that none of the results in Table 14.6 are accurate.)

We can extend an analysis of variance to systems involving more than a single variable. For example, we can use a two-way ANOVA to determine the effect on an analytical method of both the analyst and the instrumentation. The treatment of multivariate ANOVA is beyond the scope of this text, but is covered in several of the texts listed in this chapter's additional resources.

14.3.3 What is a Reasonable Result for a Collaborative Study?

Collaborative testing provides us with a method for estimating the variability (or reproducibility) between analysts in different labs. If the variability is significant, we can determine what portion is due to indeterminate method errors (σ_{rand}^2) and what portion is due to systematic differences between the analysts (σ_{syst}^2). What we have left unanswered is the following important question: What is a reasonable value for a method's reproducibility?

An analysis of nearly 10 000 collaborative studies suggests that a reasonable estimate for a method's reproducibility is

$$R = 2^{(1-0.5 \log C)} \tag{14.28}$$

where R is the percent relative standard deviation for the results included in the collaborative study and C is the fractional amount of analyte in the sample on a weight-to-weight basis.[10] Equation 14.28 appears to be independent of the type of analyte, the type of matrix, and the method of analysis. For example, when a sample in a collaborative study contains 1 microgram of analyte per gram of sample, C is 10^{-6} and the estimated relative standard deviation is

$$R = 2^{(1-0.5 \log 10^{-6})} = 16\% \tag{14.3.29}$$

Note

For a discussion of the limitations of equation 14.28, see Linsinger, T. P. J.; Josephs, R. D. "Limitations of the Application of the Horwitz Equation," *Trends Anal. Chem.* **2006**, *25*, 1125–1130, as well as a rebuttal (Thompson, M. "Limitations of the Application of the Horwitz Equation: A Rebuttal," *Trends Anal. Chem.* **2007**, *26*, 659–661) and response (Linsinger, T. P. J.; Josephs, R. D. "Reply to Professor Michael Thompson's Rebuttal," *Trends Anal. Chem.* **2007**, *26*, 662–663.

Example 14.10

What is the estimated relative standard deviation for the results of a collaborative study when the sample is pure analyte (100% w/w analyte)? Repeat for the case where the analyte's concentration is 0.1% w/w.

Solution

When the sample is 100% w/w analyte (C = 1) the estimated relative standard deviation is

$$R = 2^{(1-0.5 \log 1)} = 2\% \tag{14.3.30}$$

We expect that approximately 67% of the participants in the collaborative study (±1σ) will report the analyte's concentration within the range of 98% w/w to 102% w/w. If the analyte's concentration is 0.1% w/w (C = 0.001), the estimated relative standard deviation is

$$R = 2^{(1-0.5 \log 0.001)} = 5.7\% \tag{14.3.31}$$

and we expect that 67% of the analysts will report the analyte's concentration within the range of 0.094% w/w to 0.106% w/w.

(For a normal distribution, 68.26% of the results fall within ±1s of the population's mean (see Table 4.12).)

Of course, equation 14.28 only estimates the expected relative standard. If the method's relative standard deviation falls with a range of one-half to twice the estimated value, then it is acceptable for use by analysts in different laboratories. The percent relative standard deviation for a single analyst should be one-half to two-thirds of that for the variability between analysts.

Contributors

David Harvey (DePauw University)

14.3: Validating the Method as a Standard Method is shared under a CC BY-NC-SA 4.0 license and was authored, remixed, and/or curated by LibreTexts.

14.4: Using Excel and R for an Analysis of Variance

Although the calculations for an analysis of variance are relatively straightforward, they can be tedious for large data sets. Both Excel and R include functions for completing an analysis of variance. In addition, R provides a function for identifying the source(s) of significant differences within the data set.

14.4.1 Excel

Excel's Analysis ToolPak includes a tool to help you complete an analysis of variance. Let's use the ToolPak to complete an analysis of variance on the data in Table 14.6. Enter the data from Table 14.6 into a spreadsheet as shown in Figure 14.22. To complete the analysis of variance select **Data Analysis...** from the **Tools** menu, which opens a window entitled "*Data Analysis*." Scroll through the window, select **Analysis: Single Factor** from the available options, and click **OK**. Place the cursor in the box for the "*Input range*" and then click and drag over the cells B1:E7. Select the radio button for "*Grouped by: columns*" and check the box for "*Labels in the first row*." In the box for "*Alpha*" enter 0.05 for α. Select the radio button for "*Output range*," place the cursor in the box and click on an empty cell; this is where Excel will place the results. Clicking **OK** generates the information shown in Figure 14.23. The small value of 3.05×10^{-9} for falsely rejecting the null hypothesis indicates that there is a significant source of variation between the analysts.

	A	B	C	D	E
1	replicate	analyst A	analyst B	analyst C	analyst D
2	1	94.09	99.55	95.14	93.88
3	2	94.64	98.24	94.62	94.23
4	3	95.08	101.1	95.28	96.05
5	4	94.54	100.4	94.59	93.89
6	5	95.38	100.1	94.24	94.59
7	6	93.62			95.49

Figure 14.22 Portion of a spreadsheet containing the data from Table 14.6.

Anova: Single Factor

SUMMARY

Groups	*Count*	*Sum*	*Average*	*Variance*
analyst A	6	567.35	94.5583333	0.41081667
analyst B	5	499.39	99.878	1.15142
analyst C	5	473.87	94.774	0.18318
analyst D	6	568.49	94.7483333	0.80889667

ANOVA

Source of Variation	*SS*	*df*	*MS*	*F*	*P-value*	*F crit*
Between Groups	104.197961	3	34.7326535	54.6637742	3.0463E-09	3.1599076
Within Groups	11.4369667	18	0.63538704			
Total	115.634927	21				

Figure 14.23 Output from Excel's one-way analysis of variance of the data in Table 14.6. The summary table provides the mean and variance for each analyst. The ANOVA table summarizes the sum-of-squares terms (*SS*), the degrees of freedom (*df*), the variances (*MS* for mean square), the value of F_{exp} and the critical value of *F*, and the probability of incorrectly rejecting the null hypothesis that there is no significant difference between the analysts.

14.4.2 R

To complete an analysis of variance for the data in Table 14.6 using R, we first need to create several objects. The first object contains each result from Table 14.6.

```
> results=c(94.090, 94.640, 95.008, 94.540, 95.380, 93.620, 99.550, 98.240, 101.100, 100.400, 100.100, 95.140, 94.620, 95.280, 94.590, 94.240, 93.880, 94.230, 96.050, 93.890, 94.950, 95.490)
```

> **Note**
>
> You can arrange the results in any order. In creating this object, I choose to list the results for analyst A, followed by the results for analyst B, C, and D.

The second object contains labels to identify the source of each entry in the first object. The following code creates this object.

```
> analyst = c(rep("a",6), rep("b",5), rep("c",5), rep("d",6))
```

> **Note**
>
> The command **rep** (for repeat) has two variables: the item to repeat and the number of times it is repeated. The object analyst is the vector ("a","a","a","a","a","a", "b","b","b","b","b", "c", "c","c","c","c","d", "d", "d", "d", "d", "d").

Next, we combine the two objects into a table with two columns, one containing the data (*results*) and one containing the labels (*analyst*).

```
> df = data.frame(results, labels = factor(analyst))
```

> **Note**
>
> We call this table a data frame. Many functions in R work on the columns in a data frame.

The command **factor** indicates that the object *analyst* contains the categorical factors for the analysis of variance. The command for an analysis of variance takes the following form

anova(lm(*data* ~ *factors*), data = *data.frame*)

where *data* and *factors* are the columns containing the data and the categorical factors, and *data.frame* is the name we assigned to the data table. Figure 14.24 shows the output for an analysis of variance of the data in Table 14.6. The small value of 3.04×10^{-9} for falsely rejecting the null hypothesis indicates that there is a significant source of variation between the analysts.

> **Note**
>
> The command **lm** stands for linear model. See Section 5.6.2 in Chapter 5 for a discussion of linear models in R.

```
> anova(lm(results ~ labels, data = df))

Analysis of Variance Table

Response: results
           Df  Sum Sq Mean Sq F value    Pr(>F)
labels      3 104.198  34.733  54.664 3.04e-09 ***
Residuals 18  11.366   0.631
---
Signif. codes:  0 '***' 0.001 '**' 0.01 '*' 0.05 '.' 0.1 ' ' 1
```

Figure 14.24 Output of an R session for an analysis of variance for the data in Table 14.6. In the table, "labels" is the between-sample variance and "residuals" is the within-sample variance. The p-value of 3.04e-09 is the probability of incorrectly rejecting the null hypothesis that the within-sample and between-sample variances are the same.

Having found a significant difference between the analysts, we want to identify the source of this difference. R does not include Fisher's least significant difference test, but it does include a function for a related method called Tukey's honest significant difference test. The command for this test takes the following form

> TukeyHSD(aov(lm(*data* ~ *factors*), data = *data.frame*), conf.level = 0.95)

where *data* and *factors* are the columns containing the data and the categorical factors, and *data.frame* is the name we assigned to the data table.

> **Note**
>
> You may recall that an underlined command is the default value. If you are using an α of 0.05 (a 95% confidence level), then you do not need to include the entry for conf.level. If you wish to use an α of 0.10, then enter conf.level = 0.90.

Figure 14.25 shows the output of this command and its interpretation. The small probability values when comparing analyst B to each of the other analysts indicates that this is the source of the significant difference identified in the analysis of variance.

> **Note**
>
> Note that *p* value is small when the confidence interval for the difference includes zero.

```
> TukeyHSD(aov(results ~ labels, data = df))

Tukey multiple comparisons of means
  95% family-wise confidence level

Fit: aov(formula = results ~ labels, data = df)

$labels
         diff       lwr       upr     p adj
b-a  5.31966667  3.928277  6.711057 0.0000000
c-a  0.21566667 -1.175723  1.607057 0.9710635
d-a  0.28000000 -1.046638  1.606638 0.9318110
c-b -5.10400000 -6.557260 -3.650740 0.0000001
d-b -5.03966667 -6.431057 -3.648277 0.0000000
d-c  0.06433333 -1.327057  1.455723 0.9991718
```

Figure 14.25 Output of an R session for a Tukey honest significance difference test for the data in Table 14.6. For each possible comparison of analysts, the table gives the actual difference between the analysts, "diff," and the smallest, "lwr," and the largest, "upr," differences for a 95% confidence interval. The "p adj" is the probability that a difference of zero falls within this confidence interval. The smaller the p-value, the greater the probability that the difference between the analysts is significant.

Contributors

David Harvey (DePauw University)

14.4: Using Excel and R for an Analysis of Variance is shared under a CC BY-NC-SA 4.0 license and was authored, remixed, and/or curated by LibreTexts.

14.E: Developing a Standard Method (Exercises)

14.1

For each of the following equations determine the optimum response using the one-factor-at-a-time searching algorithm. Begin the search at (0,0) by first changing factor A, using a step-size of 1 for both factors. The boundary conditions for each response surface are 0 ≤ A ≤ 10 and 0 ≤ B ≤ 10. Continue the search through as many cycles as necessary until you find the optimum response. Compare your optimum response for each equation to the true optimum.

a. $R = 1.68 + 0.24A + 0.56B - 0.04A^2 - 0.04B^2 \quad \mu_{opt} = (3, 7)$
b. $R = 4.0 - 0.4A + 0.08B \quad \mu_{opt} = (10, 10)$
c. $R = 3.264 + 1.537A + 0.5664B - 0.1505A^2 - 0.02734B^2 - 0.05785AB \quad \mu_{opt} = (391, 6.22)$

> Note: These equations are from Deming, S. N.; Morgan, S. L. *Experimental Design: A Chemometric Approach*, Elsevier: Amsterdam, 1987, and pseudo-three dimensional plots of the response surfaces can be found in their Figures 11.4, 11.5 and 11.14.

14.2.

Determine the optimum response for the equation in Problem 14.1c, using the fixed-sized simplex searching algorithm. Compare your optimum response to the true optimum.

14.3

Show that equation 14.3 and equation 14.4 are correct.

14.4

A 2^k factorial design was used to determine the equation for the response surface in Problem 1b. The uncoded levels, coded levels, and the responses are shown in the following table.

A	*B*	*A**	*B**	response
8	8	+1	+1	5.92
8	2	+1	–1	2.08
2	8	–1	+1	4.48
2	2	–1	–1	3.52

Determine the uncoded equation for the response surface.

14.5

Koscielniak and Parczewski investigated the influence of Al on the determination of Ca by atomic absorption spectrophotometry using the 2^k factorial design shown in the following table.[11]

Ca^{2+} (ppm)	Al^{3+} (ppm)	*Ca**	*Al**	response
10	160	+1	+1	54.92
10	0	+1	–1	98.44
4	160	–1	+1	19.18
4	0	–1	–1	38.52

a. Determine the uncoded equation for the response surface

a. Determine the uncoded equation for the response surface.
b. If you wish to analyze a sample that is 6.0 ppm Ca^{2+}, what is the maximum concentration of Al^{3+} that can be present if the error in the response must be less than 5.0%?

14.6

Strange reports the following information for a 2^3 factorial design used to investigate the yield of a chemical process.[12]

factor	high (+1) level	low (–1) level
X: temperature	140°C	120°C
Y: catalyst	type B	type A
Z: [reactant]	0.50 M	0.25 M

run	*X**	*Y**	*Z**	% yield
1	–1	–1	–1	28
2	+1	–1	–1	17
3	–1	+1	–1	41
4	+1	+1	–1	34
5	–1	–1	+1	56
6	+1	–1	+1	51
7	–1	+1	+1	42
8	+1	+1	+1	36

a. Determine the coded equation for this data.
b. If β terms of less than ±1 are insignificant, what main effects and interaction terms in the coded equation are important? Write down this simpler form for the coded equation.
c. Explain why the coded equation for this data can not be transformed into an uncoded form.
d. Which is the better catalyst, A or B?
e. What is the yield using this catalyst if the temperature is set to 125°C and the concentration of the reactant is 0.45 M?

14.7

Pharmaceutical tablets coated with lactose often develop a brown discoloration. The primary factors affecting the discoloration are temperature, relative humidity, and the presence of a base acting as a catalyst. The following data have been reported for a 2^3 factorial design.[13]

factor	high (+1) level	low (–1) level
X: benzocaine	present	absent
Y: temperature	40°C	25°C
Z: relative humidity	75%	50%

run	*X**	*Y**	*Z**	color (arb. units)
1	–1	–1	–1	1.55
2	+1	–1	–1	5.40
3	–1	+1	–1	3.50
4	+1	+1	–1	6.75
5	–1	–1	+1	2.45
6	+1	–1	+1	3.60
7	–1	+1	+1	3.05
8	+1	+1	+1	7.10

a. Determine the coded equation for this data.
b. If β terms of less than 0.5 are insignificant, what main effects and interaction terms in the coded equation are important? Write down this simpler form for the coded equation.

14.8

The following data for a 2^3 factorial design were collected during a study of the effect of temperature, pressure, and residence time on the % yield of a reaction.[14]

factor	high (+1) level	low (–1) level
X: temperature	200°C	100°C
Y: pressure	0.6 MPa	0.2 MPa
Z: residence time	20 min	10 min

run	*X**	*Y**	*Z**	percent yield
1	–1	–1	–1	2
2	+1	–1	–1	6
3	–1	+1	–1	4
4	+1	+1	–1	8
5	–1	–1	+1	10
6	+1	–1	+1	18
7	–1	+1	+1	8
8	+1	+1	+1	12

a. Determine the coded equation for this data.
b. If β terms of less than 0.5 are insignificant, what main effects and interaction terms in the coded equation are important? Write down this simpler form for the coded equation.
c. Three runs at the center of the factorial design—a temperature of 150°C, a pressure of 0.4 MPa, and a residence time of 15 min—give percent yields of 12%, 8%, 9%, and 8.8%. Determine if a first-order empirical model is appropriate for this system at α = 0.05.

14.9

Duarte and colleagues used a factorial design to optimize a flow-injection analysis method for determining penicillin.[15] Three factors were studied: reactor length, carrier flow rate, and sample volume, with the high and low values summarized in the following table.

factor	high (+1) level	low (–1) level
X: reactor length	1.5 cm	2.0 cm
Y: carrier flow rate	1.6 mL/min	2.2 mL/min
Z: sample volume	100 µL	150 µL

The authors determined the optimum response using two criteria: the greatest sensitivity, as determined by the change in potential for the potentiometric detector, and the largest sampling rate. The following table summarizes their optimization results.

run	*X**	*Y**	*Z**	Δ*E*(mV)	samples/h
1	–1	–1	–1	37.45	21.5
2	+1	–1	–1	31.70	26.0
3	–1	+1	–1	32.10	30.0
4	+1	+1	–1	27.20	33.0
5	–1	–1	+1	39.85	21.0
6	+1	–1	+1	32.85	19.5
7	–1	+1	+1	35.00	30.0
8	+1	+1	+1	32.15	34.0

a. Determine the coded equation for the response surface where Δ*E* is the response.
b. Determine the coded equation for the response surface where sample/h is the response.
c. Based on the coded equations, do conditions favoring sensitivity also improve the sampling rate?
d. What conditions would you choose if your goal is to optimize both sensitivity and sampling rate?

14.10

Here is a challenge! McMinn, Eatherton, and Hill investigated the effect of five factors for optimizing an H_2-atmosphere flame ionization detector using a 2^5 factorial design.[16] The factors and their levels were

factor	**high (+1) level**	**low (–1) level**
A: H_2 flow rate	1460 mL/min	1382 mL/min
B: SiH_4	20.0 ppm	12.2 ppm
C: O_2 + N_2 flow rate	255 mL/min	210 mL/min
D: O_2/N_2	1.36	1.19
E: electrode height	75 (arb. unit)	55 (arb. unit)

The coded ("+" = +1, "–" = –1) factor levels and responses, *R*, for the 32 experiments are shown in the following table

run	*A**	*B**	*C**	*D**	*E**	run	*A**	*B**	*C**	*D**	*E**
1	–	–	–	–	–	17	–	–	–	–	+
2	+	–	–	–	–	18	+	–	–	–	+
3	–	+	–	–	–	19	–	+	–	–	+
4	+	+	–	–	–	20	+	+	–	–	+
5	–	–	+	–	–	21	–	–	+	–	+
6	+	–	+	–	–	22	+	–	+	–	+
7	–	+	+	–	–	23	–	+	+	–	+
8	+	+	+	–	–	24	+	+	+	–	+
9	–	–	–	+	–	25	–	–	–	+	+
10	+	–	–	+	–	26	+	–	–	+	+
11	–	+	–	+	–	27	–	+	–	+	+
12	+	+	–	+	–	28	+	+	–	+	+
13	–	+	+	+	–	29	–	–	+	+	+
14	+	–	+	+	–	30	+	–	+	+	+
15	–	+	+	+	–	31	–	+	+	+	+
16	+	+	+	+	–	32	+	+	+	+	+

a. Determine the coded equation for this response surface, ignoring β terms less than ±0.03.

b. A simplex optimization of this system finds optimal values for the factors of A = 2278 mL/min, B = 9.90 ppm, C = 260.6 mL/min, and D = 1.71. The value of E was maintained at its high level. Are these values consistent with your analysis of the factorial design?

14.11

A good empirical model provides an accurate picture of the response surface over the range of factor levels within the experimental design. The same model, however, may yield an inaccurate prediction for the response at other factor levels. For this reason, an empirical model, is tested before extrapolating to conditions other than those used in determining the model. For example, Palasota and Deming studied the effect of the relative amounts of H_2SO_4 and H_2O_2 on the absorbance of solutions of vanadium using the following central composite design.[17]

https://chem.libretexts.org/@go/page/70737

run	drops 1% H_2SO_4	drops 20% H_2O_2
1	15	22
2	10	20
3	20	20
4	8	15
5	15	15
6	15	15
7	15	15
8	15	15
9	22	15
10	10	10
11	20	10
12	15	8

The reaction of H_2SO_4 and H_2O_2 generates a red-brown solution whose absorbance is measured at a wavelength of 450 nm. A regression analysis on their data yielded the following uncoded equation for the response (absorbance × 1000).

$$R = 835.90 - 36.82X_1 - 21.34X_2 + 0.52(X_1)^2 + 0.15(X_2)^2 + 0.98X_1X_2 \quad (14.E.1)$$

where X_1 is the drops of H_2O_2, and X_2 is the drops of H_2SO_4. Calculate the predicted absorbances for 10 drops of H_2O_2 and 0 drops of H_2SO_4, 0 drops of H_2O_2 and 10 drops of H_2SO_4, and for 0 drops of each reagent. Are these results reasonable? Explain. What does your answer tell you about this empirical model?

14.12

A newly proposed method is to be tested for its single-operator characteristics. To be competitive with the standard method, the new method must have a relative standard deviation of less than 10%, with a bias of less than 10%. To test the method, an analyst performs 10 replicate analyses on a standard sample known to contain 1.30 ppm of analyte. The results for the 10 trials are

1.25 1.26 1.29 1.56 1.46 1.23 1.49 1.27 1.31 1.43

Are the single-operator characteristics for this method acceptable?

14.13

A proposed gravimetric method was evaluated for its ruggedness by varying the following factors.

Factor A: sample size	A = 1 g	a = 1.1 g
Factr B: pH	B = 6.5	b = 6.0
Factor C: digestion time	C = 3 h	c = 1 h
Factor D: number rinses	D = 3	d = 5
Factor E: precipitant	E = reagent 1	e = reagent 2
Factor F: digestion temperature	F = 50°C	f = 60°C
Factor G: drying temperature	G = 110°C	g = 140°C

A standard sample containing a known amount of analyte was carried through the procedure using the experimental design in Table 14.5. The percentage of analyte actually found in the eight trials were found to be

R_1 = 98.9 R_5 = 98.8	R_2 = 98.5 R_6 = 98.5	R_3 = 97.7 R_7 = 97.7	R_4 = 97.0 R_8 = 97.3

Determine which factors, if any, appear to have a significant affect on the response, and estimate the expected standard deviation for the method.

14.14

The two-sample plot for the data in Example 14.6 is shown in Figure 14.21. Identify the analyst whose work is (a) the most accurate, (b) the most precise, (c) the least accurate, and (d) the least precise.

14.15

Chichilo reports the following data for the determination of the %w/w Al in two samples of limestone.[18]

analyst	sample 1	sample 2
1	1.35	1.57
2	1.35	1.33
3	1.34	1.47
4	1.50	1.60
5	1.52	1.62
6	1.39	1.52
7	1.30	1.36
8	1.32	1.53

Construct a two-sample plot for this data and estimate values for σ_{rand} and σ_{syst}.

14.16

The importance of between-laboratory variability on the results of an analytical method can be determined by having several laboratories analyze the same sample. In one such study, seven laboratories analyzed a sample of homogenized milk for a selected alfatoxin.[19] The results, in ppb, are summarized below.

lab A	lab B	lab C	lab D	lab E	lab F	lab G
1.6	4.6	1.2	1/5	6.0	6.2	3.3
2.9	2.8	1.9	2.17	3.9	3.8	3.8
3.5	3.0	2.9	3.4	4.3	5.5	5.5
1.8	4.5	1.1	2.0	5.8	4.2	4.9
2.2	3.1	2.9	3.4	4.0	5.3	4.5

a. Determine if the between-laboratory variability is significantly greater than the within-laboratory variability at $\alpha = 0.05$. If the between-laboratory variability is significant, then determine the source(s) of that variability.
b. Estimate values for σ_{rand}^2 and σ_{syst}^2.

14.17

Show that the total sum-of-squares (SS_t) is the sum of the within-sample sum-of-squares (SS_w) and the between-sample sum-of-squares (SS_b). See Table 14.7 for the relevant equations.

14.18

Eighteen analytical students are asked to determine the %w/w Mn in a sample of steel, with the results shown here.

0.26%	0.28%	0.27%	0.24%	0.26%	0.25%
0.26%	0.28%	0.25%	0.24%	0.26%	0.25%
0.29%	0.24%	0.27%	0.23%	0.26%	0.24%

(a) Given that the steel sample is 0.26% w/w Mn, estimate the expected relative standard deviation for the class' results.

(b) The actual results obtained by the students are shown here. Are these results consistent with the estimated relative standard deviation?

14.5.3 Solutions to Practice Exercises

Practice Exercise 14.1

If we hold factor A at level A_1, changing factor B from level B_1 to level B_2 increases the response from 40 to 60, or a change ΔR, of

$$R = 60 - 40 = 20 \tag{14.E.2}$$

If we hold factor A at level A_2, we find that we have the same change in response when the level of factor B changes from B_1 to B_2.

$$R = 100 - 80 = 20 \tag{14.E.3}$$

Click here to return to the chapter.

Practice Exercise 14.2

If we hold factor B at level B_1, changing factor A from level A_1 to level A_2 increases the response from 20 to 80, or a change ΔR, of

$$R = 80 - 20 = 60 \tag{14.E.4}$$

If we hold factor B at level B_2, we find that the change in response when the level of factor A changes from A_1 to A_2 is now 20.

$$R = 80 - 20 = 60 \tag{14.E.5}$$

Click here to return to the chapter.

Practice Exercise 14.3

Answers will vary here depending on the options you decided to explore. The last response surface is an interesting one to explore. Figure 14.26 shows the response surface as a level plot and a contour plot. The interesting feature of this surface is the saddle point on a ridge connecting a local optimum (maximum response of 4.45) and the global optimum (maximum response of 10.0). All three optimization strategies are very sensitive to the initial position and the step-size.

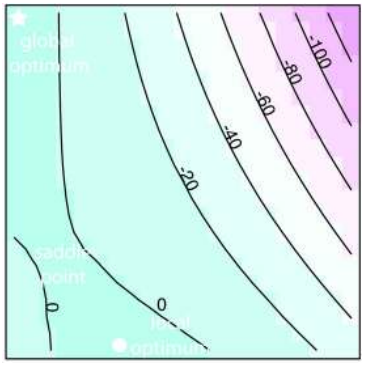


Figure 14.26 Level plot and contour plot for the fifth response surface in Practice Exercise 14.3.

Click here to return to the chapter.

Contributors and Attributions

- David Harvey (DePauw University)

14.E: Developing a Standard Method (Exercises) is shared under a CC BY-NC-SA 4.0 license and was authored, remixed, and/or curated by LibreTexts.

14.S: Developing a Standard Method (Summary)

One of the goals of analytical chemistry is to develop new analytical methods that are accepted as standard methods. In this chapter we have considered how a standard method is developed, including finding the optimum experimental conditions, verifying that the method produces acceptable precision and accuracy, and validating the method for general use.

To optimize a method we try to find the combination of experimental parameters producing the best result or response. We can visualize this process as being similar to finding the highest point on a mountain. In this analogy, the mountain's topography corresponds to a response surface, which is a plot of the system's response as a function of the factors under our control.

One method for finding the optimum response is to use a searching algorithm. In a one-factor-at-a-time optimization, we change one factor, while holding constant all other factors until there is no further improvement in the response. The process continues with the next factor, cycling through the factors until there is no further improvement in the response. This approach to finding the optimum response is often effective, but not efficient. A searching algorithm that is both effective and efficient is a simplex optimization, the rules of which allow us to change the levels of all factors simultaneously.

Another approach to optimizing a method is to develop a mathematical model of the response surface. Such models can be theoretical, in that they are derived from a known chemical and physical relationship between the response and its factors. Alternatively, we can develop an empirical model, which does not have a firm theoretical basis, by fitting an empirical equation to our experimental data. One approach is to use a 2^k factorial design in which each factor is tested at both a high level and a low level, and paired with the high level and the low level for all other factors.

After optimizing a method it is necessary to demonstrate that it can produce acceptable results. Verifying a method usually includes establishing single-operator characteristics, the blind analysis of standard samples, and determining the method's ruggedness. Single-operator characteristics include the method's precision, accuracy, and detection limit when used by a single analyst. To test against possible bias on the part of the analyst, he or she analyzes a set of blind samples in which the analyst does not know the concentration of analyte. Finally, we use ruggedness testing to determine which experimental factors must be carefully controlled to avoid unexpectedly large determinate or indeterminate sources of error.

The last step in establishing a standard method is to validate its transferability to other laboratories. An important step in the process of validating a method is collaborative testing, in which a common set of samples is analyzed by different laboratories. In a well-designed collaborative test it is possible to establish limits for the method's precision and accuracy.

14.5.1 Key Terms

2^k factorial design	factor	response surface
analysis of variance	factor level	ruggedness testing
between-sample variance	Fisher's least significant difference	searching algorithm
blind analysis	fixed-size simplex optimization	simplex
central composite design	global optimum	standard method
collaborative testing	independent	theoretical model
dependent	local optimum	validation
effective	one-factor-at-a-time optimization	variable-sized simplex optimization
efficiency	response	within-sample variance
empirical model		

References

1. *Vogel's Textbook of Quantitative Inorganic Analysis*, Longman: London, 1978, p. 752.
2. Sharaf, M. A.; Illman, D. L.; Kowalski, B. R. *Chemometrics*, Wiley-Interscience: New York, 1986.
3. (a) Spendley, W.; Hext, G. R.; Himsworth, F. R. *Technometrics* **1962**, *4*, 441–461; (b) Deming, S. N.; Parker, L. R. *CRC Crit. Rev. Anal. Chem.* **1978** *7(3)*, 187–202.
4. Long, D. E. *Anal. Chim. Acta* **1969**, *46*, 193–206.
5. Palasota, J. A.; Deming, S. N. *J. Chem. Educ.* **1992**, *62*, 560–563.
6. Youden, W. J. *Anal. Chem.* **1960**, *32(13)*, 23A–37A.

7. Youden, W. J. “Statistical Techniques for Collaborative Tests,” in *Statistical Manual of the Association of Official Analytical Chemists*, Association of Official Analytical Chemists: Washington, D. C., 1975, p. 35.
8. Youden, W. J. “Statistical Techniques for Collaborative Tests,” in *Statistical Manual of the Association of Official Analytical Chemists*, Association of Official Analytical Chemists: Washington, D. C., 1975, pp 10–11.
9. Youden, W. J. “Statistical Techniques for Collaborative Tests,” in *Statistical Manual of the Association of Official Analytical Chemists*, Association of Official Analytical Chemists: Washington, D. C., 1975, pp 22–24.
10. (a) Horwitz, W. *Anal. Chem.* **1982**, *54*, 67A–76A; (b) Hall, P.; Selinger, B. *Anal. Chem.* **1989**, *61*, 1465–1466; (c) Albert, R.; Horwitz, W. *Anal. Chem.* **1997**, *69*, 789–790, (d) “The Amazing Horowitz Function,” AMC Technical Brief 17, July 2004; (e) Lingser, T. P. J. Trends Anal. Chem. 2006, 25, 1125 Link: page not found?
11. Koscielniak, P.; Parczewski, A. *Anal. Chim. Acta* **1983**, *153*, 111–119.
12. Strange, R. S. *J. Chem. Educ.* **1990**, *67*, 113–115.
13. Armstrong, N. A.; James, K. C. *Pharmaceutical Experimental Design and Interpretation*, Taylor and Francis: London, 1996 as cited in Gonzalez, A. G. *Anal. Chim. Acta* **1998**, *360*, 227–241.
14. Akhnazarova, S.; Kafarov, V. *Experimental Optimization in Chemistry and Chemical Engineering*, MIR Publishers: Moscow, 1982 as cited in Gonzalez, A. G. *Anal. Chim. Acta* **1998**, *360*, 227–241.
15. Duarte, M. M. M. B.; de O. Netro, G.; Kubota, L. T.; Filho, J. L. L.; Pimentel, M. F.; Lima, F.; Lins, V. *Anal. Chim. Acta* **1997**, *350*, 353–357.
16. McMinn, D. G.; Eatherton, R. L.; Hill, H. H. *Anal. Chem.* **1984**, *56*, 1293–1298.
17. Palasota, J. A.; Deming, S. N. *J. Chem. Educ.* **1992**, *62*, 560–563.
18. Chichilo, P. J. *J. Assoc. Offc. Agr. Chemists* **1964**, *47*, 1019 as reported in Youden, W. J. “Statistical Techniques for Collaborative Tests,” in *Statistical Manual of the Association of Official Analytical Chemists*, Association of Official Analytical Chemists: Washington, D. C., 1975
19. Massart, D. L.; Vandeginste, B. G. M; Deming, S. N.; Michotte, Y.; Kaufman, L. *Chemometrics: A Textbook*, Elsevier: Amsterdam, 1988.

Contributors

- David Harvey (DePauw University)

14.S: Developing a Standard Method (Summary) is shared under a CC BY-NC-SA 4.0 license and was authored, remixed, and/or curated by LibreTexts.

CHAPTER OVERVIEW

15: Quality Assurance

In Chapter 14 we discussed the process of developing a standard method, including optimizing the experimental procedure, verifying that the method produces acceptable precision and accuracy in the hands of a signal analyst, and validating the method for general use by the broader analytical community. Knowing that a method meets suitable standards is important if we are to have confidence in our results. Even so, using a standard method does not guarantee that the result of an analysis is acceptable. In this chapter we introduce the quality assurance procedures used in industry and government labs for monitoring routine chemical analyses.

Topic hierarchy

15.1: The Analytical Perspective—Revisited

15.2: Quality Control

15.3: Quality Assessment

15.4: Evaluating Quality Assurance Data

15.E: Quality Assurance (Exercises)

Thumbnail: Examples of property control charts that show a sequence of results.

Contributors

- David Harvey (DePauw University)

15: Quality Assurance is shared under a CC BY-NC-SA 4.0 license and was authored, remixed, and/or curated by LibreTexts.

15.1: The Analytical Perspective—Revisited

As we noted in Chapter 1, each area of chemistry brings a unique perspective to the broader discipline of chemistry. For analytical chemistry this perspective is as an approach to solving problem, one representation of which is shown in Figure 15.1.

Figure 15.1 is the same as Figure 1.3. You may wish to review our earlier discussion of this figure and of the analytical approach to solving problems.

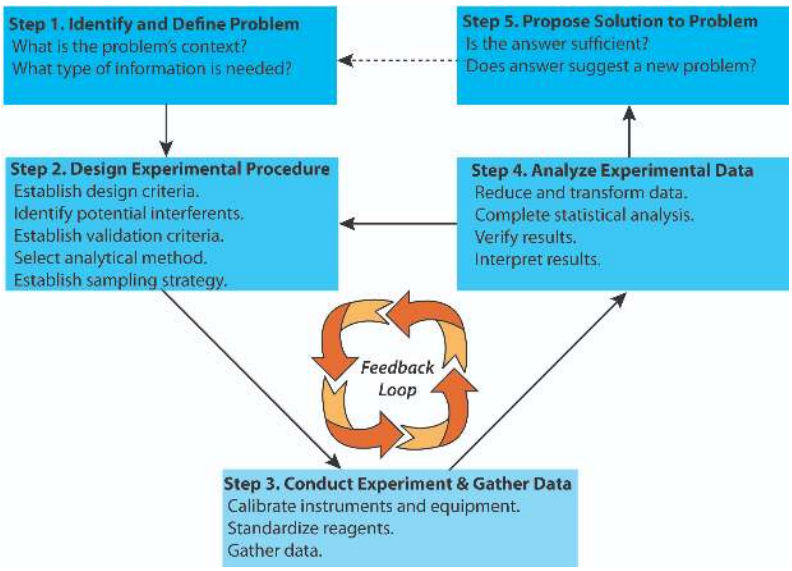


Figure 15.1 *Flow diagram showing one view of the analytical approach to solving problems. This diagram is modified after Atkinson, G. F. J. Chem. Educ.* ***1982****, 59, 201–202.*

If you examine the procedure for a standard method it appears, it often seems that its development was a straightforward process of moving from a problem to a solution. Unfortunately—or, perhaps, fortunately for those who consider themselves to be analytical chemists!—developing a standard method is seldom routine. Even a well-established standard method, carefully followed, can yield poor data.

An important feature of the analytical approach outlined in Figure 15.1 is the feedback loop involving steps 2, 3, and 4, in which the outcome of one step may lead us to reevaluate the other steps. For example, after standardizing a spectrophotometric method for the analysis of iron (step 3), we may find that its sensitivity does not meet the original design criteria (step 2). In response, we might choose a different method, change the original design criteria, or improve the sensitivity.

The feedback loop in Figure 15.1 is maintained by a quality assurance program, whose objective is to control systematic and random sources of error.[1] The underlying assumption of a quality assurance program is that results obtained when an analysis is under **statistical control** are free of bias and are characterized by well-defined confidence intervals. When used properly, a quality assurance program identifies the practices necessary to bring a system into statistical control, allows us to determine if the system remains in statistical control, and suggests a course of corrective action if the system falls out of statistical control.

An analysis is in a state of statistical control when it is reproducible and free from bias.

The focus of this chapter is on the two principal components of a **quality assurance program**: quality control and quality assessment. In addition, considerable attention is given to the use of control charts for routinely monitoring the quality of analytical data.

Contributors

- David Harvey (DePauw University)

Template:HideTOC

15.1: The Analytical Perspective—Revisited is shared under a CC BY-NC-SA 4.0 license and was authored, remixed, and/or curated by LibreTexts.

15.2: Quality Control

Quality control encompasses all activities that bring an analysis into statistical control. The most important facet of quality control is a set of written directives describing the relevant laboratory-specific, technique-specific, sample-specific, method-specific, and protocol-specific operations. **Good laboratory practices** (GLPs) describe the general laboratory operations that we must follow in any analysis. These practices include properly recording data and maintaining records, using chain-of-custody forms for samples, specifying and purifying chemical reagents, preparing commonly used reagents, cleaning and calibrating glassware, training laboratory personnel, and maintaining the laboratory facilities and general laboratory equipment.

For one example of quality control, see Keith, L. H.; Crummett, W.; Deegan, J., Jr.; Libby, R. A.; Taylor, J. K.; Wentler, G. "Principles of Environmental Analysis," *Anal. Chem.* **1983**, *55*, 2210–2218. This article describes guidelines developed by the Subcommittee on Environmental Analytical Chemistry, a subcommittee of the American Chemical Society's Committee on Environmental Improvement.

Good measurement practices (GMPs) describe operations specific to a technique. In general, GMPs provide instructions for maintaining, calibrating, and using equipment and instrumentation. For example, a GMP for a titration describes how to calibrate the buret (if required), how to fill the buret with titrant, the correct way to read the volume of titrant in the buret, and the correct way to dispense the titrant.

The directions for analyzing a specific analyte in a specific matrix are described by a **standard operations procedure** (SOP). The SOP indicates how we process the sample in the laboratory, how we separate the analyte from potential interferents, how we standardize the method, how we measure the analytical signal, how we transform the data into the desired result, and how we use the quality assessment tools to maintain quality control. If the laboratory is responsible for sampling, then the SOP will also states how we are to collect, process, and preserve the sample in the field. An SOP may be developed and used by a single laboratory, or it may be a standard procedure approved by an organization such as the American Society for Testing Materials or the Federal Food and Drug Administration. A typical SOP is provided in the following example.

Example 15.1

Provide an SOP for the determination of cadmium in lake sediments using atomic absorption spectroscopy and a normal calibration curve.

Solution

Collect sediment samples using a bottom grab sampler and store them at 4°C in acid-washed polyethylene bottles during transportation to the laboratory. Dry the samples to constant weight at 105°C and grind them to a uniform particle size. Extract the cadmium in a 1-g sample of sediment by adding the sediment and 25 mL of 0.5 M HCl to an acid-washed 100-mL polyethylene bottle and shaking for 24 h. After filtering, analyze the sample is analyzed by atomic absorption spectroscopy using an air–acetylene flame, a wavelength of 228.8 nm, and a slit width of 0.5 nm. Prepare a normal calibration curve using five standards with nominal concentrations of 0.20, 0.50, 1.00, 2.00, and 3.00 ppm. Periodically check the accuracy of the calibration curve by analyzing the 1.00-ppm standard. An accuracy of ±10% is considered acceptable.

Figure 7.7 in Chapter 7 shows an example of a bottom grab sampler.

Although an SOP provides a written procedure, it is not necessary to follow the procedure exactly as long as we are careful to identify any modifications. On the other hand, we must follow all instructions in a **protocol for a specific purpose** (PSP)—the most detailed of the written quality control directives—before agencies or clients will accept our results. In many cases the required elements of a PSP are established by the agency sponsoring the analysis. For example, labs working under contract with the Environmental Protection Agency must develop a PSP that addresses such items as sampling and sample custody, frequency of calibration, schedules for the preventive maintenance of equipment and instrumentation, and management of the quality assurance program.

Two additional aspects of a quality control program deserve mention. The first is that the individuals responsible for collecting and analyzing the samples can critically examine and reject individual samples, measurements, and results. For example, when analyzing sediments for cadmium (see the SOP in Example 15.1) we might choose to screen sediment samples, discarding those

containing foreign objects—such as rocks, twigs, or trash—replacing them with additional samples. If we observe a sudden change in the performance of the atomic absorption spectrometer, we may choose to reanalyze the affected samples. We may also decide to reanalyze a sample if the result of its analysis is clearly unreasonable. By identifying those samples, measurements, and results subject to gross systematic errors, inspection helps control the quality of an analysis.

The second additional consideration is the certification of an analyst's competence to perform the analysis for which he or she is responsible. Before an analyst is allowed to perform a new analytical method, he or she may be required to successfully analyze an independent check sample with acceptable accuracy and precision. The check sample is similar in composition to samples that the analyst will routinely encounter, with a concentration that is 5 to 50 times that of the method's detection limit.

Contributors

David Harvey (DePauw University)

Template:HideTOC

15.2: Quality Control is shared under a CC BY-NC-SA 4.0 license and was authored, remixed, and/or curated by LibreTexts.

15.3: Quality Assessment

The written directives of a quality control program are a necessary, but not a sufficient, condition for obtaining and maintaining a state of statistical control. Although quality control directives explain how we are to conduct an analysis, they do not indicate whether the system is under statistical control. This is the role of **quality assessment**, the second component of a quality assurance program.

The goals of quality assessment are to determine when an analysis has reached a state of statistical control, to detect when an analysis falls out of statistical control, and to suggest the reason(s) for this loss of statistical control. For convenience, we divide quality assessment into two categories: internal methods coordinated within the laboratory, and external methods organized and maintained by an outside agency.

15.3.1 Internal Methods of Quality Assessment

The most useful methods for quality assessment are those coordinated by the laboratory, providing immediate feedback about the analytical method's state of statistical control. Internal methods of quality assessment include the analysis of duplicate samples, the analysis of blanks, the analysis of standard samples, and spike recoveries.

Analysis of Duplicate Samples

An effective method for determining the precision of an analysis is to analyze **duplicate samples**. Duplicate samples are obtained by dividing a single gross sample into two parts, although in some cases the duplicate samples are independently collected gross samples.

> **Note**
>
> A split sample is another name for duplicate samples created from a single gross sample.

We report the results for the duplicate samples, X_1 and X_2, by determining the difference, d, or the relative difference, $(d)_r$, between the two samples

$$d = X_1 - X_2 \tag{15.3.1}$$

$$(d)_r = \frac{d}{(X_1 + X_2)/2} \times 100 \tag{15.3.2}$$

and comparing to accepted values, such as those shown in Table 15.1 for the analysis of waters and wastewaters. Alternatively, we can estimate the standard deviation using the results for a set of n duplicates

$$s = \sqrt{\frac{\sum d_i^2}{2n}} \tag{15.3.3}$$

where d_i is the difference between the ith pair of duplicates. The degrees of freedom for the standard deviation is the same as the number of duplicate samples. If we combine duplicate samples from several sources, then the precision of the measurement process must be approximately the same for each.

Table 15.1: *Quality Assessment Limits for the Analysis of Waters and Wastewaters*

analyte	$(d)_r$ when [analyte] < 20×MDL (±%)	$(d)_r$ when [analyte] > 20×MDL (±%)	spike recovery limit (%)
acids	40	20	60–140
anions	25	10	80–120
bases or neutrals	40	20	70–130
carbamate pesticides	40	20	50–150
herbicides	40	20	40–160
metals	25	10	80–120
other inorganics	25	10	80–120
volatile organics	40	20	70–130

Abbreviation: MDL = method's detection limit

Source: Table 1020.I in *Standard Methods for the Analysis of Water and Wastewater*, American Public Health Association: Washington, D. C., 18th Ed., 1992.

Example 15.2

To evaluate the precision for the determination of potassium in blood serum, duplicate analyses were performed on six samples, yielding the following results in mg K/L.

duplicate	X_1	X_2
1	160	147
2	196	202
3	207	196
4	185	193
5	172	188
6	133	119

Estimate the standard deviation for the analysis.

Solution

To estimate the standard deviation we first calculate the difference, d, and the squared difference, d^2, for each duplicate. The results of these calculations are summarized in the following table.

duplicate	$d = X_1 - X_2$	d^2
1	13	169
2	–6	36
3	11	121
4	–8	64
5	–16	256
6	14	196

Finally, we calculate the standard deviation.

$$s = \sqrt{\frac{169 + 36 + 121 + 64 + 256 + 196}{2 \times 6}} = 8.4 \quad (15.3.4)$$

Practice Exercise 15.1

To evaluate the precision of a glucometer—a device a patient uses at home to monitor his or her blood glucose level—duplicate analyses were performed on samples from five individuals, yielding the following results in mg glucose/100 mL.

duplicate	X_1	X_2
1	148.5	149.1
2	96.5	98.8
3	174.9	174.5
4	118.1	118.9
5	72.7	70.4

Estimate the standard deviation for the analysis.

Click here to review your answer to this exercise.

The Analysis of Blanks

We introduced the use of a blank in Chapter 3 as a way to correct the signal for contributions from sources other than the analyte. The most common blank is a **method blank** in which we take an analyte free sample through the analysis using the same reagents, glassware, and instrumentation. A method blank allows us to identify and correct systematic errors due to impurities in the reagents, contaminated glassware, and poorly calibrated instrumentation. At a minimum, a method blank is analyzed whenever we prepare a new reagent. Even better, the regular analysis of method blanks provides an ongoing monitoring for potential systematic errors. A new method blank is run whenever we analyze a sample with a high concentration of the analyte, because any residual carryover of analyte produces a positive determinate error.

The contamination of reagents over time is a significant concern. The regular use of a method blank compensates for this contamination. A method blank also is called a **reagent blank**.

When we collect samples in the field, additional blanks are needed to correct for potential sampling errors.[2] A **field blank** is an analyte-free sample carried from the laboratory to the sampling site. At the sampling site the blank is transferred to a clean sample container, exposing it to the local environment in the process. The field blank is then preserved and transported back to the laboratory for analysis. A field blank helps identify systematic errors due to sampling, transport, and analysis. A **trip blank** is an analyte-free sample carried from the laboratory to the sampling site and back to the laboratory without being opened. A trip blank helps to identify systematic errors due to cross-contamination of volatile organic compounds during transport, handling, storage, and analysis.

Analysis of Standards

Another tool for monitoring an analytical method's state of statistical control is to analyze a standard containing a known concentration of analyte. A standard reference material (SRM) is the ideal choice, provided that the SRM's matrix is similar to that of our samples. A variety of SRMs are available from the National Institute of Standards and Technology (NIST). If a suitable SRM is not available, then we can use an independently prepared synthetic sample if it is prepared from reagents of known purity. In all cases, the analyte's experimentally determined concentration in the standard must fall within predetermined limits before the analysis is considered under statistical control.

Table 4.7 in Chapter 4 provides a summary of SRM 2346, a standard sample of Gingko biloba leaves with certified values for

the concentrations of flavonoids, terpene ketones, and toxic elements, such as mercury and lead.

Spike Recoveries

One of the most important quality assessment tools is the recovery of a known addition, or spike, of analyte to a method blank, a field blank, or a sample. To determine a **spike recovery**, the blank or sample is split into two portions and a known amount of a standard solution of analyte is added to one portion. The concentration of the analyte is determined for both the spiked, F, and unspiked portions, I, and the percent recovery, $\%R$, is calculated as

$$\%R = \frac{F - I}{A} \times 100 \tag{15.3.5}$$

where A is the concentration of analyte added to the spiked portion.

Example 15.3

A spike recovery for the analysis of chloride in well water was performed by adding 5.00 mL of a 25 000 ppm solution of Cl^- to a 50-mL volumetric flask and diluting to volume with the sample. An unspiked sample was prepared by adding 5.00 mL of distilled water to a separate 50-mL volumetric flask and diluting to volume with the sample. Analysis of the sample and the spiked sample return chloride concentrations of 18.3 ppm and 40.9 ppm, respectively. Determine the spike recovery.

Solution

To calculate the concentration of the analyte added in the spike, we take into account the effect of dilution.

$$A = 250.0 \text{ ppm} \times \frac{5.00 \text{ mL}}{50.00 \text{ mL}} = 25.0 \text{ ppm} \tag{15.3.6}$$

Thus, the spike recovery is

$$\%R = \frac{40.9 - 18.3}{25.0} \times 100 = \frac{22.6}{25.0} \times 100 = 90.4\% \tag{15.3.7}$$

Exercise 15.2

To test a glucometer, a spike recovery is carried out by measuring the amount of glucose in a sample of a patient's blood before and after spiking it with a standard solution of glucose. Before spiking the sample the glucose level is 86.7 mg/100 mL and after spiking the sample it is 110.3 mg/100 mL. The spike is prepared by adding 10.0 µL of a 25 000 mg/100mL standard to a 10.0-mL portion of the blood. What is the spike recovery for this sample.

Click here to review your answer to this exercise.

We can use spike recoveries on method blanks and field blanks to evaluate the general performance of an analytical procedure. A known concentration of analyte is added to the blank that is 5 to 50 times the method's detection limit. A systematic error during sampling and transport results in an unacceptable recovery for the field blank, but not for the method blank. A systematic error in the laboratory, however, affects the recoveries for both the field blank and the method blank.

Figure 15.2, which we will discuss in Section 15.4, illustrates the use of spike recoveries as part of a quality assessment program.

Spike recoveries on samples are used to detect systematic errors due to the sample matrix, or to evaluate the stability of a sample after its collection. Ideally, samples are spiked in the field at a concentration that is 1 to 10 times the analyte's expected concentration or 5 to 50 times the method's detection limit, whichever is larger. If the recovery for a field spike is unacceptable, then a sample is spiked in the laboratory and analyzed immediately. If the laboratory spike's recovery is acceptable, then the poor recovery for the field spike may be the result of the sample's deterioration during storage. If the recovery for the laboratory spike also is unacceptable, the most probable cause is a matrix-dependent relationship between the analytical signal and the analyte's concentration. In this case the sample is analyzed by the method of standard additions. Typical limits for acceptable spike recoveries for the analysis of waters and wastewaters are shown in Table 15.1.

15.3.2 External Methods of Quality Assessment

Internal methods of quality assessment always carry some level of suspicion because there is a potential for bias in their execution and interpretation. For this reason, external methods of quality assessment also play an important role in quality assurance programs. One external method of quality assessment is the certification of a laboratory by a sponsoring agency. Certification is based on the successful analysis of a set of **proficiency standards** prepared by the sponsoring agency. For example, laboratories involved in environmental analyses may be required to analyze standard samples prepared by the Environmental Protection Agency. A second example of an external method of quality assessment is a laboratory's voluntary participation in a collaborative test sponsored by a professional organization such as the Association of Official Analytical Chemists. Finally, an individual contracting with a laboratory can perform his or her own external quality assessment by submitting blind duplicate samples and blind standards to the laboratory for analysis. If the results for the quality assessment samples are unacceptable, then there is good reason to question the laboratory's results for other samples.

See Chapter 14 for a more detailed description of collaborative testing.

Contributors

David Harvey (DePauw University)

15.3: Quality Assessment is shared under a CC BY-NC-SA 4.0 license and was authored, remixed, and/or curated by LibreTexts.

15.4: Evaluating Quality Assurance Data

In the previous section we described several internal methods of quality assessment that provide quantitative estimates of the systematic errors and the random errors in an analytical method. Now we turn our attention to how we incorporate this quality assessment data into a complete quality assurance program. There are two general approaches to developing a quality assurance program: a prescriptive approach, in which we prescribe an exact method of quality assessment, and a performance-based approach in which we can use any form of quality assessment, provided that we can demonstrate an acceptable level of statistical control.[3]

15.4.1 Prescriptive Approach

With a prescriptive approach to quality assessment, duplicate samples, blanks, standards, and spike recoveries are measured following a specific protocol. We compare the result for each analysis to a single predetermined limit, taking an appropriate corrective action if the limit is exceeded. Prescriptive approaches to quality assurance are common for programs and laboratories subject to federal regulation. For example, the Food and Drug Administration (FDA) specifies quality assurance practices that must be followed by laboratories analyzing products regulated by the FDA.

Figure 15.2 provides a typical example of a prescriptive approach to quality assessment. Two samples, A and B, are collected at the sample site. Sample A is split into two equal-volume samples, A_1 and A_2. Sample B is also split into two equal-volume samples, one of which, B_{SF}, is spiked in the field with a known amount of analyte. A field blank, D_F, also is spiked with the same amount of analyte. All five samples (A_1, A_2, B, B_{SF}, and D_F) are preserved if necessary and transported to the laboratory for analysis.

After returning to the lab, the first sample that is analyzed is the field blank. If its spike recovery is unacceptable—an indication of a systematic error in the field or in the lab—then a laboratory method blank, D_L, is prepared and analyzed. If the spike recovery for the method blank is unsatisfactory, then the systematic error originated in the laboratory; this is something we can find and correct before proceeding with the analysis. An acceptable spike recovery for the method blank, however, indicates that the systematic error occurred in the field or during transport to the laboratory, casting uncertainty on the quality of the samples. The only recourse is to discard the samples and return to the field to collect new samples.

If the field blank is satisfactory, then sample B is analyzed. If the result for B is above the method's detection limit, or if it is within the range of 0.1 to 10 times the amount of analyte spiked into B_{SF}, then a spike recovery for B_{SF} is determined. An unacceptable spike recovery for B_{SF} indicates the presence of a systematic error involving the sample. To determine the source of the systematic error, a laboratory spike, B_{SL}, is prepared using sample B, and analyzed. If the spike recovery for B_{SL} is acceptable, then the systematic error requires a long time to have a noticeable effect on the spike recovery. One possible explanation is that the analyte has not been properly preserved or it has been held beyond the acceptable holding time. An unacceptable spike recovery for B_{SL} suggests an immediate systematic error, such as that due to the influence of the sample's matrix. In either case the systematic errors are fatal and must be corrected before the sample is reanalyzed.

> *This is one reason that environmental testing is so expensive.*

If the spike recovery for B_{SF} is acceptable, or if the result for sample B is below the method's detection limit, or outside the range of 0.1 to 10 times the amount of analyte spiked in B_{SF}, then the duplicate samples A_1 and A_2 are analyzed. The results for A_1 and A_2 are discarded if the difference between their values is excessive. If the difference between the results for A_1 and A_2 is within the accepted limits, then the results for samples A_1 and B are compared. Because samples collected from the same sampling site at the same time should be identical in composition, the results are discarded if the difference between their values is unsatisfactory, and accepted if the difference is satisfactory.

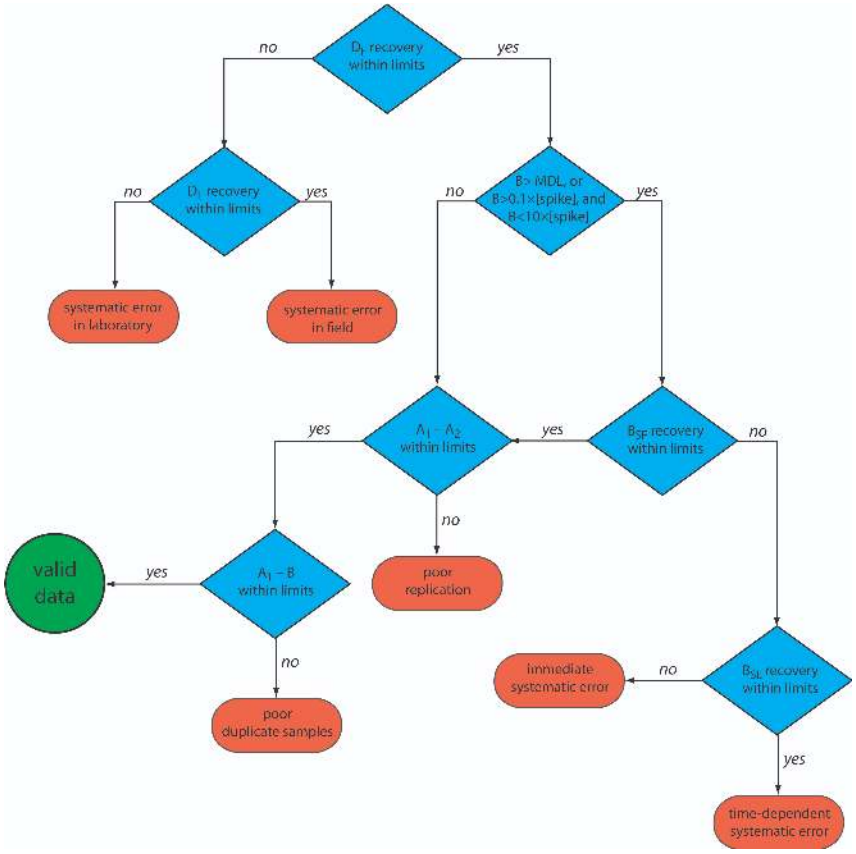


Figure 15.2: *Example of a prescriptive approach to quality assurance for laboratories monitoring waters and wastewaters. Adapted from Environmental Monitoring and Support Laboratory, U. S. Environmental Protection Agency, "Handbook for Analytical Quality Control in Water and Wastewater Laboratories," March 1979.*

The protocol in Figure 15.2 requires four to five evaluations of quality assessment data before the result for a single sample is accepted, a process that we must repeat for each analyte and for each sample. Other prescriptive protocols are equally demanding. For example, Figure 3.7 in Chapter 3 shows a portion of a quality assurance protocol for the graphite furnace atomic absorption analysis of trace metals in aqueous solutions. This protocol involves the analysis of an initial calibration verification standard and an initial calibration blank, followed by the analysis of samples in groups of ten. Each group of samples is preceded and followed by continuing calibration verification (CCV) and continuing calibration blank (CCB) quality assessment samples. Results for each group of ten samples are accepted only if both sets of CCV and CCB quality assessment samples are acceptable.

The advantage of a prescriptive approach to quality assurance is that all laboratories use a single consistent set of guideline. A significant disadvantage is that it does not take into account a laboratory's ability to produce quality results when determining the frequency of collecting and analyzing quality assessment data. A laboratory with a record of producing high quality results is forced to spend more time and money on quality assessment than is perhaps necessary. At the same time, the frequency of quality assessment may be insufficient for a laboratory with a history of producing results of poor quality.

15.4.2 Performance-Based Approach

In a performance-based approach to quality assurance, a laboratory is free to use its experience to determine the best way to gather and monitor quality assessment data. The quality assessment methods remain the same—duplicate samples, blanks, standards, and spike recoveries—because they provide the necessary information about precision and bias. What a laboratory can control is the frequency with which it analyzes quality assessment samples and the conditions it chooses to identify when an analysis falls out of a state of statistical control.

The principal tool for performance-based quality assessment is a **control chart**, which provides a continuous record of quality assessment results. Our fundamental assumption is that if an analysis is under statistical control, individual quality assessment

results are randomly distributed around a known mean with a known standard deviation. When an analysis moves out of statistical control, the quality assessment data is influenced by additional sources of error, increasing the standard deviation or changing the mean value.

Control charts were originally developed in the 1920s as a quality assurance tool for the control of manufactured products.[4] Although there are many types of control charts, two are common in quality assessment programs: a property control chart, in which we record single measurements or the means for several replicate measurements, and a precision control chart, in which we record ranges or standard deviations. In either case, the control chart consists of a line representing the mean value for the measured property or the precision, and two or more boundary lines whose positions are determined by the precision of the measurement process. The position of the data points about the boundary lines determines whether the analysis is in statistical control.

Constructing a Property Control Chart

The simplest property control chart is a sequence of points, each representing a single determination of the property we are monitoring. To construct the control chart, we analyze a minimum of 7–15 samples while the system is under statistical control. The center line (*CL*) of the control chart is the average of these *n* samples.

$$CL = \overline{X} = \frac{\sum X_i}{n} \tag{15.4.1}$$

The more samples in the original control chart, the easier it is to detect when an analysis is beginning to drift out of statistical control. Building a control chart with an initial run of 30 or more samples is not an unusual choice.

Boundary lines around the center line are determined by the standard deviation, *S*, of the *n* points

$$S = \sqrt{\frac{\sum (X_i - \overline{X})^2}{n-1}} \tag{15.4.2}$$

The upper and lower warning limits (*UWL* and *LWL*) and the upper and lower control limits (*UCL* and *LCL*) are given by the following equations.

$$UWL = CL + 2S \quad LWL = CL - 2S \tag{15.4.3}$$

$$UCL = CL + 3S \quad LCL = CL - 3S \tag{15.4.4}$$

Why these limits? Examine Table 4.12 in Chapter 4 and consider your answer to this question. We will return to this point later in this chapter when we consider how to use a control chart.

Example 15.4

Construct a property control chart using the following spike recovery data (all values are for percentage of spike recovered).

sample:	1	2	3	4	5
result:	97.3	98.1	100.3	99.5	100.9
sample:	6	7	8	9	10
result:	98.6	96.9	99.6	101.1	100.4
sample:	11	12	13	14	15
result:	100.0	95.9	98.3	99.2	102.1
sample:	16	17	18	19	20
result:	98.5	101.7	100.4	99.1	100.3

Solution

The mean and the standard deviation for the 20 data points are 99.4% and 1.6%, respectively. Using these values, we find that the *UCL* is 104.2%, the *UWL* is 102.6%, the *LWL* is 96.2%, and the *LCL* is 94.6%. To construct the control chart, we plot the data points sequentially and draw horizontal lines for the center line and the four boundary lines. The resulting property control chart is shown in Figure 15.3.

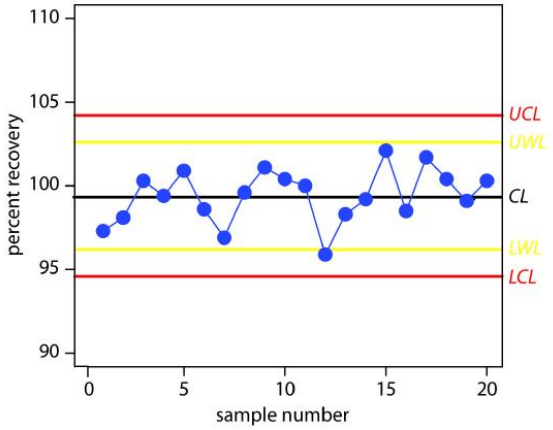


Figure 15.3 *Property control chart for Example 15.4. The warning limits are shown in yellow and the control limits in red.*

Practice Exercise 15.3

A control chart is a useful method for monitoring a glucometer's performance over time. One approach is to use the glucometer to measure the glucose level of a standard solution. An initial analysis of the standard yields a mean value of 249.4 mg/100 mL and a standard deviation of 2.5 mg/100 mL. An analysis of the standard over 20 consecutive days gives the following results.

day:	1	2	3	4	5	6	7	8	9	10
result:	248.1	246.0	247.9	249.4	250.9	249.7	250.2	250.3	247.3	245.6
day:	11	12	13	14	15	16	17	18	19	20
result:	246.2	250.8	249.0	254.3	246.1	250.8	248.1	246.7	253.5	251.0

Construct a control chart and evaluate the glucometer's performance.

Click here to review your answer to this exercise.

We also can construct a control chart using the means for a set of replicate determinations on each sample. The mean for the *i*th sample is

$$\overline{X}_i = \frac{\sum_j X_{ij}}{n_{\text{rep}}} \tag{15.4.5}$$

where X_{ij} is the *j*th replicate and n_{rep} is the number of replicate determinations for each sample.

> *When using means to construct a property control chart, all samples must have the same number of replicates.*

The control chart's center line is

$$CL = \frac{\sum \overline{X}_i}{n} \tag{15.4.6}$$

where *n* is the number of samples used in constructing the control chart. To determine the standard deviation for the warning limits and the control limits, we first calculate the variance for each sample.

$$s_i^2 = \frac{\sum_j (X_{ij} - \overline{X}_i)^2}{n_{\text{rep}} - 1} \tag{15.4.7}$$

The overall standard deviation, S, is the square root of the average variance for the samples used in constructing the control plot.

$$S = \sqrt{\frac{\sum s_i^2}{n}} \tag{15.4.8}$$

The resulting warning and control limits are given by the following four equations.

$$UWL = CL + \frac{2S}{\sqrt{n_{\text{rep}}}} \quad LWL = CL - \frac{2S}{\sqrt{n_{\text{rep}}}} \tag{15.4.9}$$

$$UCL = CL + \frac{3S}{\sqrt{n_{\text{rep}}}} \quad LCL = CL - \frac{3S}{\sqrt{n_{\text{rep}}}} \tag{15.4.10}$$

Constructing a Precision Control Chart

A precision control chart shows how the precision of an analysis changes over time. The most common measure of precision is the range, R, between the largest and the smallest results for n_{rep} analyses on a sample.

$$R = X_{\text{largest}} - X_{\text{smallest}} \tag{15.4.11}$$

To construct the control chart, we analyze a minimum of 15–20 samples while the system is under statistical control. The center line (CL) of the control chart is the average range of these n samples.

$$\overline{R} = \frac{\sum R_i}{n} \tag{15.4.12}$$

> The more samples in the original control chart, the easier it is to detect when an analysis is beginning to drift our of statistical control. Building a control chart with an initial run of 30 or more samples is not an unusual choice.

The upper warning line and the upper control line are given by the following equations

$$UWL = f_{\text{UWL}} \times \overline{R} \tag{15.4.13}$$

$$UCL = f_{\text{UCL}} \times \overline{R} \tag{15.4.14}$$

where f_{UWL} and f_{UCL} are statistical factors determined by the number of replicates used in determining the range. Table 15.2 provides representative values for f_{UWL} and f_{UCL}. Because the range is greater than or equal to zero, there is no lower control limit or lower warning limit.

Table 15.2: Statistical Factors for the Upper Warning Limit and the Upper Control Limit of a Precision Control Chart

replicates	f_{UWL}	f_{UCL}
2	2.512	3.267
3	2.050	2.575
4	1.855	2.282
5	1.743	2.115
6	1.669	2.004

Example 15.5

Construct a precision control chart using the following ranges, each determined from a duplicate analysis of a 10.0-ppm calibration standard.

sample:	1	2	3	4	5
result:	0.36	0.09	0.11	0.06	0.25
sample:	6	7	8	9	10
result:	0.15	0.28	0.27	0.03	0.28
sample:	11	12	13	14	15
result:	0.21	0.19	0.06	0.13	0.37
sample:	16	17	18	19	20
result:	0.01	0.19	0.39	0.05	0.05

Solution

The average range for the duplicate samples is 0.177. Because two replicates were used for each point the *UWL* and *UCL* are

$$UWL = 2.512 \times 0.177 = 0.44 \quad (15.4.15)$$

$$UCL = 3.267 \times 0.177 = 0.58 \quad (15.4.16)$$

The resulting property control chart is shown in Figure 15.4.

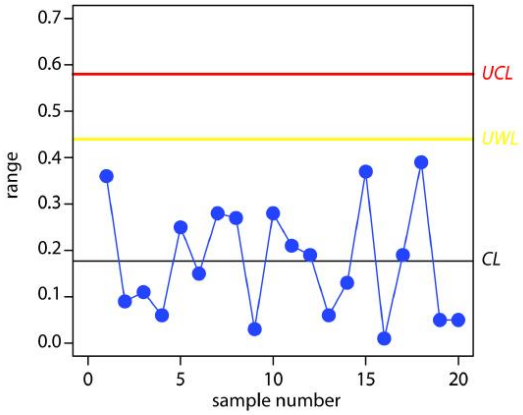


Figure 15.4 Precision control chart for Example 15.5. The warning limits are shown in yellow and the control limits in red.

The precision control chart in Figure 15.4 is strictly valid only for the replicate analysis of identical samples, such as a calibration standard or a standard reference material. Its use for the analysis of nonidentical samples—as often is the case in clinical analyses and environmental analyses—is complicated by the fact that the range usually is not independent of the magnitude of the measurements. For example, Table 15.3 shows the relationship between the average range and the concentration of chromium in 91 water samples. The significant difference in the average range for different concentrations of chromium makes a single precision control chart impossible. As shown in figure 15.5, one solution is to prepare separate precision control charts, each of which covers a range of concentrations for which $\overline{R}$ is approximately constant.

Table 15.3 Average Range for the Concentration of Chromium in Duplicate Water Samples

[Cr] (ppb)	number of duplicate samples	$\overline{R}$
5 to < 10	32	0.32
10 to < 25	15	0.57
25 to < 50	16	1.12
50 to < 150	15	3.80
150 to < 500	8	5.25
> 500	5	76.0

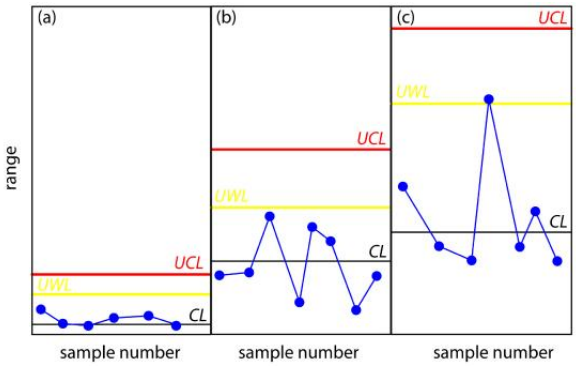


Figure 15.5 *Example showing the use of a precision control chart for samples that span a range of analyte concentrations. The precision control charts are for (a) low concentrations of analyte; (b) intermediate concentrations of analyte; and (c) high concentrations of analyte.*

Interpreting Control Charts

The purpose of a control chart is to determine if an analysis is in a state of statistical control. We make this determination by examining the location of individual results relative to the warning limits and the control limits, and by examining the distribution of results around the central line. If we assume that the individual results are normally distributed, then the probability of finding a point at any distance from the control limit is determined by the properties of a normal distribution.[5] We set the upper and lower control limits for a property control chart to $CL \pm 3S$ because 99.74% of a normally distributed population is within three standard deviations of the population's mean. This means that there is only a 0.26% probability of obtaining a result larger than the *UCL* or smaller than the *LCL*. When a result exceeds a control limit, the most likely explanation is a systematic error in the analysis or a loss of precision. In either case, we assume that the analysis no longer is in a state of statistical control.

Rule 1. An analysis is no longer under statistical control if any single point exceeds either the *UCL* or the *LCL*.

By setting the upper and lower warning limits to $CL \pm 2S$, we expect that no more than 5% of the results will exceed one of these limits; thus

Rule 2. An analysis is no longer under statistical control if two out of three consecutive points are between the *UWL* and the *UCL* or between the *LWL* and the *LCL*.

If an analysis is under statistical control, then we expect a random distribution of results about the center line. The presence of an unlikely pattern in the data is another indication that the analysis is no longer under statistical control.

Rule 3. An analysis is no longer under statistical control if seven consecutive results fall completely above or completely below the center line.

Rule 4. An analysis is no longer under statistical control if six consecutive results increase or decrease in value.

Rule 5. An analysis is no longer under statistical control if 14 consecutive alternate up and down in value.

Rule 6. An analysis is no longer under statistical control if there is any obvious nonrandom patter to the results.

Figure 15.6 shows three examples of control charts in which the results show an analysis that has fallen out of statistical control. The same rules apply to precision control charts with the exception that there are no lower warning limits and lower control limits.

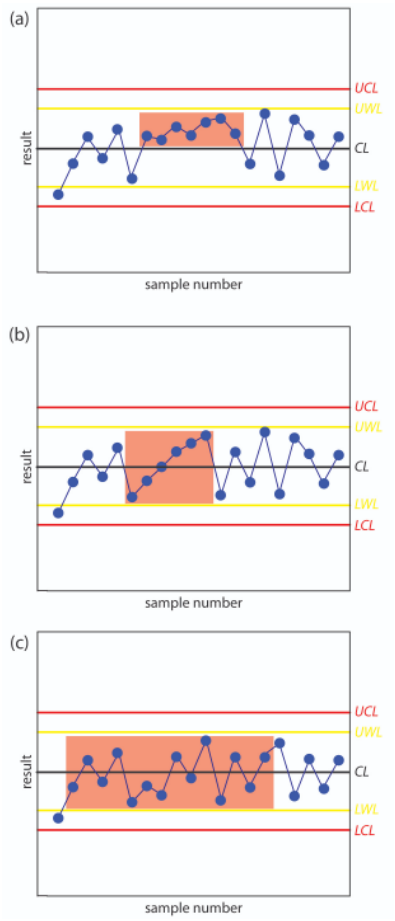


Figure 15.6 Examples of property control charts that show a sequence of results—indicated by the highlighting—that violate (a) rule 3; (b) rule 4; and (c) rule 5.

Exercise 15.4

In Practice Exercise 15.3 you created a property control chart for a glucometer. Examine your property control chart and evaluate the glucometer's performance. Does your conclusion change if the next three results are 255.6, 253.9, and 255.8 mg/100 mL?

Click here to review your answer to this exercise.

Using Control Charts for Quality Assurance

Control charts play an important role in a performance-based program of quality assurance because they provide an easily interpreted picture of the statistical state of an analysis. Quality assessment samples such as blanks, standards, and spike recoveries are monitored with property control charts. A precision control chart is used to monitor duplicate samples.

The first step in using a control chart is to determine the mean value and the standard deviation (or range) for the property being measured while the analysis is under statistical control. These values must be established using the same conditions that will be present during subsequent analyses. Preliminary data is collected both throughout the day and over several days to account for short-term and long-term variability. An initial control chart is prepared using this preliminary data and discrepant points identified using the rules discussed in the previous section. After eliminating questionable points, the control chart is replotted. Once the control chart is in use, the original limits may be adjusted if the number of new data points is at least equivalent to the amount of data used to construct the original control chart. For example, if the original control chart includes 15 points, new limits can be calculated after collecting 15 additional points. The 30 points are pooled together to calculate the new limits. A second modification can be made after collecting an addition 30 points. Another indication that a control chart needs to be modified is when points rarely exceed the warning limits. In this case the new limits can be recalculated using the last 20 points.

Once a control chart is in use, new quality assessment data is added at a rate sufficient to ensure that the analysis remains in statistical control. As with prescriptive approaches to quality assurance, when the analysis falls out of statistical control, all samples analyzed since the last successful verification of statistical control must be reanalyzed. The advantage of a performance-based approach to quality assurance is that a laboratory may use its experience, guided by control charts, to determine the frequency for collecting quality assessment samples. When the system is stable, quality assessment samples can be acquired less frequently.

Contributors

- David Harvey (DePauw University)

15.4: Evaluating Quality Assurance Data is shared under a CC BY-NC-SA 4.0 license and was authored, remixed, and/or curated by LibreTexts.

15.E: Quality Assurance (Exercises)

1. Make a list of good laboratory practices for the lab accompanying this course, or another lab if this course does not have an associated laboratory. Explain the rationale for each item on your list.

2. Write directives outlining good measurement practices for a buret, a pH meter, and a spectrophotometer.

3. A atomic absorption method for the analysis of lead in an industrial wastewater has a method detection limit of 10 ppb. The relationship between the absorbance and the concentration of lead, as determined from a calibration curve, is

$$A = 0.349 \times (\text{ppm Pb}) \tag{15.E.1}$$

Analysis of a sample in duplicate gives absorbance values of 0.554 and 0.516. Is the precision between these two duplicates acceptable based on the limits in Table 15.1?

4. The following data were obtained for the duplicate analysis of a 5.00 ppm NO_3^- standard.

sample	X1 (ppm)	X2 (ppm)
1	5.02	4.90
2	5.10	5.18
3	5.07	4.95
4	4.96	5.01
5	4.88	4.98
6	5.04	4.97

Calculate the standard deviation for these duplicate samples. If the maximum limit for the relative standard deviation is 1.5%, are these results acceptable?

5. Gonzalez and colleagues developed a voltammetric method for the determination of *tert*-butylhydroxyanisole (BHA) in chewing gum.[6] Analysis of a commercial chewing gum gave results of 0.20 mg/g. To evaluate the accuracy of their results, they performed five spike recoveries, adding an amount of BHA equivalent to 0.135 mg/g to each sample. The experimentally determined concentrations of BHA in these samples were reported as 0.342, 0.340, 0.340, 0.324, and 0.322 mg/g. Determine the percent recovery for each sample and the average percent recovery.

6. A sample is analyzed following the protocol shown in Figure 15.2, using a method with a detection limit of 0.05 ppm. The relationship between the analytical signal, S_{meas}, and the concentration of the analyte, C_A, as determined from a calibration curve, is

$$S_{meas} = 0.273 \times (\text{ppm analyte}) \tag{15.E.2}$$

Answer the following questions if the limit for a successful spike recovery is ±10%.

(a) A field blank is spiked with the analyte to a concentration of 2.00 ppm and returned to the lab. Analysis of the spiked field blank gives a signal of 0.573. Is the spike recovery for the field blank acceptable?

(b) The analysis of a spiked field blank is unacceptable. To determine the source of the problem, a spiked method blank is prepared by spiking distilled water with the analyte to a concentration of 2.00 ppm. Analysis of the spiked method blank gives a signal of 0.464. Is the source of the problem in the laboratory or in the field?

(c) The analysis for a spiked field sample, B_{SF}, is unacceptable. To determine the source of the problem, the sample was spiked in the laboratory by adding sufficient analyte to increase the concentration by 2.00 ppm. Analysis of the sample before and after the spike gives signals of 0.456 for B and 1.03 for B_{SL}. Considering this data, what is the most likely source of the systematic error?

7. The following data were obtained for the repetitive analysis of a stable standard.[7]

sample	X_i (ppm)	sample	X_i (ppm)	sample	X_i (ppm)
1	35.1	10	35.0	18	36.4
2	33.2	11	31.4	19	32.1
3	33.7	12	35.6	20	38.2
4	35.9	13	30.2	21	33.1
5	34.5	14	31.1	22	36.2
6	34.5	15	31.1	23	36.2
7	34.4	16	34.8	24	34.0
8	34.3	17	34.3	25	33.8
9	31.8				

Construct a property control chart for these data and evaluate the state of statistical control.

8. The following data were obtained for the repetitive spike recoveries of field samples.[8]

sample	% recovery	sample	% recovery	sample	% recovery
1	94.6	10	104.6	18	104.6
2	93.1	11	123.8	19	91.5
3	100.0	12	93.8	20	83.1
4	122.3	13	80.0	21	100.8
5	120.8	14	99.2	22	123.1
6	93.1	15	101.5	23	96.2
7	117.7	16	74.6	24	96.9
8	96.2	17	108.5	25	102.3
9	73.8				

Construct a property control chart for these data and evaluate the state of statistical control.

9. The following data were obtained for the duplicate analysis of a stable standard.[9]

sample	X_1 (ppm)	X_2 (ppm)	sample	X_1 (ppm)	X_2 (ppm)
1	50	46	14	36	36
2	37	36	15	47	45
3	22	19	16	16	20
4	17	20	17	18	21
5	32	34	18	26	22
6	46	46	19	35	36
7	26	28	20	26	25
8	26	30	21	49	51
9	61	58	22	33	32
10	44	45	23	40	38
11	40	44	24	16	13
12	36	35	25	39	42
13	29	31			

Construct a precision control chart for these data and evaluate the state of statistical control.

15.5.3 Solutions to Practice Exercises

Practice Exercise 15.1

To estimate the standard deviation we first calculate the difference, d, and the squared difference, d^2, for each duplicate. The results of these calculations are summarized in the following table.

duplicate	$d = X_1 - X_2$	d^2
1	–0.6	0.36
2	–2.3	5.29
3	0.4	0.16
4	–0.8	0.64
5	2.3	5.29

Finally, we calculate the standard deviation.

$$s = \sqrt{\frac{0.36 + 5.29 + 0.16 + 0.64 + 5.29}{2 \times 5}} = 1.08 \tag{15.E.3}$$

Click here to return to the chapter.

Practice Exercise 15.2

Adding a 10.0-µL spike to a 10.0-mL sample is a 1000-fold dilution; thus, the concentration of added glucose is 25.0 mg/100 mL and the spike recovery is

$$\%R = \frac{110.3 - 86.7}{25.0} \times 100 = \frac{23.6}{25.0} \times 100 = 94.4\% \tag{15.E.4}$$

Click here to return to the chapter.

Practice Exercise 15.3

The *UCL* is 256.9, the *UWL* is 254.4, the *CL* is 249.4, the *LWL* is 244.4, and the *LCL* is 241.9 mg glucose/100 mL. Figure 15.7 shows the resulting property control plot.

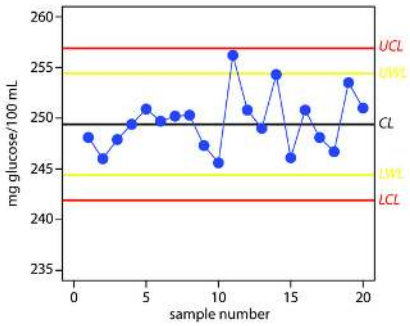


Figure 15.7 *Property control plot for Practice Exercise 15.3.*

Click here to return to the chapter.

Practice Exercise 15.4

Although the variation in the results appears to be greater for the second 10 samples, the results do not violate any of the six rules. There is no evidence in Figure 15.7 that the analysis is out of statistical control. The next three results, in which two of the three results are between the *UWL* and the *UCL*, violates the second rule. Because the analysis is no longer under statistical control, we must stop using the glucometer until we determine the source of the problem.

Click here to return to the chapter.

Contributors and Attributions

- David Harvey (DePauw University)

15.E: Quality Assurance (Exercises) is shared under a CC BY-NC-SA 4.0 license and was authored, remixed, and/or curated by LibreTexts.

Additional Resources

Gathered here are three types of resources: suggested experiments, mostly from the *Journal of Chemical Education* and *The Chemical Educator*, that provide practical examples of concepts in the textbook; additional readings from the analytical literature that extend and supplement topics covered in the textbook; and electronic resources, many of which are cataloged in the Analytical Sciences Digital Library, that help illustrate concepts from the textbook. Although primarily intended for the use of instructors, these resources also will benefit students who wish to pursue a topic at more depth.

The following experiments provide useful introductions to the statistical analysis of data in the analytical chemistry laboratory.

- Bularzik, J. "The Penny Experiment Revisited: An Illustration of Significant Figures, Accuracy, Precision, and Data Analysis," *J. Chem. Educ.* **2007**, *84*, 1456–1458.
- Columbia, M. R. "The Statistics of Coffee: 1. Evaluation of Trace Metals for Establishing a Coffee's Country of Origin Based on a Means Comparison," *Chem. Educator* **2007**, *12*, 260–262.
- Cunningham, C. C.; Brown, G. R.; St Pierre, L. E. "Evaluation of Experimental Data," *J. Chem. Educ.* **1981**, *58*, 509–511.
- Edminston, P. L.; Williams, T. R. "An Analytical Laboratory Experiment in Error Analysis: Repeated Determination of Glucose Using Commercial Glucometers," *J. Chem. Educ.* **2000**, *77*, 377–379.
- Gordus, A. A. "Statistical Evaluation of Class Data for Two Buret Readings," *J. Chem. Educ.* **1987**, *64*, 376–377.
- Harvey, D. T. "Statistical Evaluation of Acid/Base Indicators," *J. Chem. Educ.* **1991**, *68*, 329–331.
- Hibbert, D. B. "Teaching modern data analysis with The Royal Austrian Chemical Institute's titration competition," *Aust. J. Ed. Chem.* **2006**, *66*, 5–11.
- Johll, M. E.; Poister, D.; Ferguson, J. "Statistical Comparison of Multiple Methods for the Determination of Dissolved Oxygen Levels in Natural Water," *Chem. Educator* **2002**, *7*, 146–148.
- Jordon, A. D. "Which Method is Most Precise; Which is Most Accurate?," *J. Chem. Educ.* **2007**, *84*, 1459–1460.
- Olsen, R. J. "Using Pooled Data and Data Visualization To Introduce Statistical Concepts in the General Chemistry Laboratory," *J. Chem. Educ.* **2008**, *85*, 544–545.
- O'Reilley, J. E. "The Length of a Pestle," *J. Chem. Educ.* **1986**, *63*, 894–896.
- Paselk, R. A. "An Experiment for Introducing Statistics to Students of Analytical and Clinical Chemistry," *J. Chem. Educ.* **1985**, *62*, 536.
- Puignou, L.; Llauradó, M. "An Experimental Introduction to Interlaboratory Exercises in Analytical Chemistry," *J. Chem. Educ.* **2005**, *82*, 1079–1081.
- Quintar, S. E.; Santagata, J. P.; Villegas, O. I.; Cortinez, V. A. "Detection of Method Effects on Quality of Analytical Data," *J. Chem. Educ.* **2003**, *80*, 326–329.
- Richardson, T. H. "Reproducible Bad Data for Instruction in Statistical Methods," *J. Chem. Educ.* **1991**, *68*, 310–311.
- Salzsieder, J. C. "Statistical Analysis Experiment for Freshman Chemistry Lab," *J. Chem. Educ.* **1995**, *72*, 623.
- Samide, M. J. "Statistical Comparison of Data in the Analytical Laboratory," *J. Chem. Educ.* **2004**, *81*, 1641–1643.
- Sheeran, D. "Copper Content in Synthetic Copper Carbonate: A Statistical Comparison of Experimental and Expected Results," *J. Chem. Educ.* **1998**, *75*, 453–456.
- Spencer, R. D. "The Dependence of Strength in Plastics upon Polymer Chain Length and Chain Orientation," *J. Chem. Educ.* **1984**, *61*, 555–563.
- Stolzberg, R. J. "Do New Pennies Lose Their Shells? Hypothesis Testing in the Sophomore Analytical Chemistry Laboratory," *J. Chem. Educ.* **1998**, *75*, 1453–1455.
- Stone, C. A.; Mumaw, L. D. "Practical Experiments in Statistics," *J. Chem. Educ.* **1995**, *72*, 518–524.
- Thomasson, K.; Lofthus-Merschman, S.; Humbert, M.; Kulevsky, N. "Applying Statistics in the Undergraduate Chemistry Laboratory: Experiments with Food Dyes," *J. Chem. Educ.* **1998**, *75*, 231–233.
- Vitha, M. F.; Carr, P. W. "A Laboratory Exercise in Statistical Analysis of Data," *J. Chem. Educ.* **1997**, *74*, 998–1000.

A more comprehensive discussion of the analysis of data, covering all topics considered in this chapter as well as additional material, can be found in any textbook on statistics or data analysis; several such texts are listed here.

- Anderson, R. L. *Practical Statistics for Analytical Chemists*, Van Nostrand Reinhold: New York; 1987.

- Graham, R. C. *Data Analysis for the Chemical Sciences*, VCH Publishers: New York; 1993.
- Mark, H.; Workman, J. *Statistics in Spectroscopy*, Academic Press: Boston; 1991.
- Mason, R. L.; Gunst, R. F.; Hess, J. L. *Statistical Design and Analysis of Experiments*; Wiley: New York, 1989.
- Massart, D. L.; Vandeginste, B. G. M.; Buydens, L. M. C.; De Jong, S.; Lewi, P. J.; Smeyers-Verbeke, J. *Handbook of Chemometrics and Qualimetrics*, Elsevier: Amsterdam, 1997.
- Miller, J. C.; Miller, J. N. *Statistics for Analytical Chemistry*, Ellis Horwood PTR Prentice-Hall: New York; 3rd Edition, 1993.
- *NIST/SEMATECH e-Handbook of Statistical Methods*, http://www.itl.nist.gov/div898/handbook/, 2006.
- Sharaf, M. H.; Illman, D. L.; Kowalski, B. R. *Chemometrics*, Wiley-Interscience: New York; 1986.

The importance of defining statistical terms is covered in the following papers.

- Analytical Methods Committee "Terminology—the key to understanding analytical science. Part 1: Accuracy, precision and uncertainty," AMC Technical Brief No. 13, Sept. 2003 (http://www.rsc.org/lap/rsccom/amc/amc_index.htm).
- Goedart, M. J.; Verdonk, A. H. "The Development of Statistical Concepts in a Design-Oriented Laboratory Course in Scientific Measuring," *J. Chem. Educ.* **1991**, *68*, 1005–1009.
- Sánchez, J. M. "Teaching Basic Applied Statistics in University Chemistry Courses: Students' Misconceptions," *Chem. Educator* **2006**, *11*, 1–4.
- Thompson, M. "Towards a unified model of errors in analytical measurements," *Analyst* **2000**, *125*, 2020–2025.
- Treptow, R. S. "Precision and Accuracy in Measurements," *J. Chem. Educ.* **1998**, *75*, 992–995.

The detection of outliers, particularly when working with a small number of samples, is discussed in the following papers.

- Analytical Methods Committee "Robust Statistics—How Not To Reject Outliers Part 1. Basic Concepts," *Analyst* **1989**, *114*, 1693–1697.
- Analytical Methods Committee "Robust Statistics—How Not to Reject Outliers Part 2. Inter-laboratory Trials," *Analyst* **1989**, *114*, 1699–1702.
- Analytical Methods Committee "Robust statistics: a method of coping with outliers," AMC Technical Brief No. 6, April 2001 (http://www.rsc.org/lap/rsccom/amc/amc_index.htm).
- Efstathiou, C. "Stochastic Calculation of Critical Q-Test Values for the Detection of Outliers in Measurements," *J. Chem. Educ.* **1992**, *69*, 773–736.
- Efstathiou, C. "Estimation of type 1 error probability from experimental Dixon's Q parameter on testing for outliers within small data sets," *Talanta* **2006**, *69*, 1068–1071.
- Kelly, P. C. "Outlier Detection in Collaborative Studies," *Anal. Chem.* **1990**, *73*, 58–64.
- Mitschele, J. "Small Sample Statistics," *J. Chem. Educ.* **1991**, *68*, 470–473.

The following papers provide additional information on error and uncertainty, including the propagation of uncertainty.

- Andraos, J. "On the Propagation of Statistical Errors for a Function of Several Variables," *J. Chem. Educ.* **1996**, *73*, 150–154.
- Donato, H.; Metz, C. "A Direct Method for the Propagation of Error Using a Personal Computer Spreadsheet Program," *J. Chem. Educ.* **1988**, *65*, 867–868.
- Gordon, R.; Pickering, M.; Bisson, D. "Uncertainty Analysis by the 'Worst Case' Method," *J. Chem. Educ.* **1984**, *61*, 780–781.
- Guare, C. J. "Error, Precision and Uncertainty," *J. Chem. Educ.* **1991**, *68*, 649–652.
- Guedens, W. J.; Yperman, J.; Mullens, J.; Van Poucke, L. C.; Pauwels, E. J. "Statistical Analysis of Errors: A Practical Approach for an Undergraduate Chemistry Lab Part 1. The Concept," *J. Chem. Educ.* **1993**, *70*, 776–779
- Guedens, W. J.; Yperman, J.; Mullens, J.; Van Poucke, L. C.; Pauwels, E. J. "Statistical Analysis of Errors: A Practical Approach for an Undergraduate Chemistry Lab Part 2. Some Worked Examples," *J. Chem. Educ.* **1993**, *70*, 838–841.
- Heydorn, K. "Detecting Errors in Micro and Trace Analysis by Using Statistics," *Anal. Chim. Acta* **1993**, *283*, 494–499.
- Hund, E.; Massart, D. L.; Smeyers-Verbeke, J. "Operational definitions of uncertainty," *Trends Anal. Chem.* **2001**, *20*, 394–406.
- Kragten, J. "Calculating Standard Deviations and Confidence Intervals with a Universally Applicable Spreadsheet Technique," *Analyst* **1994**, *119*, 2161–2165.
- Taylor, B. N.; Kuyatt, C. E. "Guidelines for Evaluating and Expressing the Uncertainty of NIST Measurement Results," NIST Technical Note 1297, 1994.
- Yates, P. C. "A Simple Method for Illustrating Uncertainty Analysis," *J. Chem. Educ.* **2001**, *78*, 770–771.

Consult the following resources for a further discussion of detection limits.

- Boumans, P. W. J. M. “Detection Limits and Spectral Interferences in Atomic Emission Spectrometry,” *Anal. Chem.* **1984**, *66*, 459A–467A.
- Currie, L. A. “Limits for Qualitative Detection and Quantitative Determination: Application to Radiochemistry,” *Anal. Chem.* **1968**, *40*, 586–593.
- Currie, L. A. (ed.) *Detection in Analytical Chemistry: Importance, Theory and Practice*, American Chemical Society: Washington, D. C., 1988.
- Ferrus, R.; Egea, M. R. “Limit of discrimination, limit of detection and sensitivity in analytical systems,” *Anal. Chim. Acta* **1994**, *287*, 119–145.
- Glaser, J. A.; Foerst, D. L.; McKee, G. D.; Quave, S. A.; Budde, W. L. “Trace analyses for wastewaters,” *Environ. Sci. Technol.* **1981**, *15*, 1426–1435.
- Kimbrough, D. E.; Wakakuwa, J. “Quality Control Level: An Introduction to Detection Levels,” *Environ. Sci. Technol.* **1994**, *28*, 338–345.

The following resources provide additional information on using Excel, including reports of errors in its handling of some statistical procedures.

- McCollough, B. D.; Wilson, B. “On the accuracy of statistical procedures in Microsoft Excel 2000 and Excel XP,” *Comput. Statist. Data Anal.* **2002**, *40*, 713–721.
- Morgon, S. L.; Deming, S. N. “Guide to Microsoft *Excel* for calculations, statistics, and plotting data,” (http://www.chem.sc.edu/faculty/morgan/resources/Excel/Excel_Guide_Morgan.pdf).
- Pottel, H. “Statistical flaws in Excel,” (http://www.coventry.ac.uk/ec/~nhunt/pottel.pdf).

To learn more about using R, consult the following resources.

- Chambers, J. M. *Software for Data Analysis: Programming with R*, Springer: New York, 2008.
- Maindonald, J.; Braun, J. *Data Analysis and Graphics Using R*, Cambridge University Press: Cambridge, UK, 2003.
- Sarkar, D. *Lattice: Multivariate Data Visualization With R*, Springer: New York, 2008.

The following papers provide insight into visualizing data.

- Analytical Methods Committee “Representing data distributions with kernel density estimates,” AMC Technical Brief, March 2006 (http://www.rsc.org/lap/rsccom/amc/amc_index.htm).
- Frigge, M.; Hoaglin, D. C.; Iglewicz, B. “Some Implementations of the Boxplot,” *The American Statistician* **1989**, *43*, 50–54.

Gathered here are links to on-line computational tools, simulations, and tutorials, many of which are found on the Analytical Sciences Digital Library.

- Applets for Statistics (link).
- GraphPad QuickCalcs: Free On-Line Calculators (link).
- Introduction to Data Analysis (link).
- Introduction to Probability and Statistics (link).
- Overway, K. “Population versus Sampling Statistics: A Spreadsheet Exercise,” *J. Chem. Educ.* **2008** *85*, 749 (link).
- Van Bramer, S. E. “A Brief Introduction to the Gaussian Distribution, Sample Statistics, and the Student’s t Statistic,” *J. Chem. Educ.* **2007**, *84*, 1231 (link).
- Web Tutorials in Chemistry—Statistics (link).

Chapter 5

Although there are many experiments in the literature that incorporate external standards, the method of standard additions, or internal standards, the issue of choosing a method standardization is not the experiment’s focus. One experiment designed to consider the issue of selecting a method of standardization is given here.

- Harvey, D. T. “External Standards or Standard Additions? Selecting and Validating a Method of Standardization,” *J. Chem. Educ.* **2002**, *79*, 613–615.

In addition to the texts listed as suggested readings in Chapter 4, the following text provide additional details on linear regression.

- Draper, N. R.; Smith, H. *Applied Regression Analysis*, 2nd. ed.; Wiley: New York, 1981.

The following articles providing more details about linear regression.

- Analytical Methods Committee "Is my calibration linear?" AMC Technical Brief, December 2005 (http://www.rsc.org/pdf/amc/brief3.pdf).
- Badertscher, M.; Pretsch, E. "Bad results from good data," *Trends Anal. Chem.* **2006**, *25*, 1131–1138.
- Boqué, R.; Rius, F. X.; Massart, D. L. "Straight Line Calibration: Something More Than Slopes, In• tercepts, and Correlation Coefficients," *J. Chem. Educ.* **1993**, *70*, 230–232.
- Danzer, K.; Currie, L. A. "Guidelines for Calibration in Analytical Chemistry. Part 1. Fundamentals and Single Component Calibration," *Pure Appl. Chem.* **1998**, *70*, 993–1014.
- Henderson, G. "Lecture Graphic Aids for Least-Squares Analysis," *J. Chem. Educ.* **1988**, *65*, 1001–1003.
- Logan, S. R. "How to Determine the Best Straight Line," *J. Chem. Educ.* **1995**, *72*, 896–898.
- Miller, J. N. "Basic Statistical Methods for Analytical Chemistry. Part 2. Calibration and Regression Methods," *Analyst* **1991**, *116*, 3–14.
- Renman, L., Jagner, D. "Asymmetric Distribution of Results in Calibration Curve and Standard Addition Evaluations," *Anal. Chim. Acta* **1997**, *357*, 157–166.
- Rodriguez, L. C.; Gamiz-Gracia; Almansa-Lopez, E. M.; Bosque-Sendra, J. M. "Calibration in chemical measurement processes. II. A methodological approach," *Trends Anal. Chem.* **2001**, *20*, 620–636.

Useful papers providing additional details on the method of standard additions are gathered here.

- Bader, M. "A Systematic Approach to Standard Addition Methods in Instrumental Analysis," *J. Chem. Educ.* **1980**, *57*, 703–706.
- Brown, R. J. C.; Roberts, M. R.; Milton, M. J. T. "Systematic error arising form 'Sequential' Standard Addition Calibrations. 2. Determination of Analyte Mass Fraction in Blank Solutions," *Anal. Chim. Acta* **2009**, *648*, 153–156.
- Brown, R. J. C.; Roberts, M. R.; Milton, M. J. T. "Systematic error arising form 'Sequential' Standard Addition Calibrations: Quantification and correction," *Anal. Chim. Acta* **2007**, *587*, 158–163.
- Bruce, G. R.; Gill, P. S. "Estimates of Precision in a Standard Additions Analysis," *J. Chem. Educ.* **1999**, *76*, 805–807.
- Kelly, W. R.; MacDonald, B. S.; Guthrie "Gravimetric Approach to the Standard Addition Method in Instrumental Analysis. 1." *Anal. Chem.* **2008**, *80*, 6154–6158.
- Nimura, Y.; Carr, M. R. "Reduction of the Relative Error in the Standard Additions Method," *Analyst* **1990**, *115*, 1589–1595.

The following papers discusses the importance of weighting experimental data when use linear regression.

- Analytical Methods Committee "Why are we weighting?" AMC Technical Brief, June 2007 (http://www.rsc.org/images/brief27_tcm18-92066.pdf)
- Karolczak, M. "To Weight or Not to Weight? An Analyst's Dilemma," *Current Separations* **1995**, *13*, 98–104.

Algorithms for performing a linear regression with errors in both *X* and *Y* are discussed in the following papers. Also included here are papers that address the difficulty of using linear regression to compare two analytical methods.

- Irvin, J. A.; Quickenden, T. L. "Linear Least Squares Treatment When There are Errors in Both x and y," *J. Chem. Educ.* **1983**, *60*, 711–712.
- Kalantar, A. H. "Kerrich's Method for y = αx Data When Both y and x Are Uncertain," *J. Chem. Educ.* **1991**, *68*, 368–370.
- Macdonald, J. R.; Thompson, W. J. "Least-Squares Fitting When Both Variables Contain Errors: Pitfalls and Possibilities," *Am. J. Phys.* **1992**, *60*, 66–73.
- Martin, R. F. "General Deming Regression for Estimating Systematic Bias and Its Confidence Interval in Method-Comparison Studies," *Clin. Chem.* **2000**, *46*, 100–104.
- Ogren, P. J.; Norton, J. R. "Applying a Simple Linear Least-Squares Algorithm to Data with Uncertainties in Both Variables," *J. Chem. Educ.* **1992**, *69*, A130–A131.
- Ripley, B. D.; Thompson, M. "Regression Techniques for the Detection of Analytical Bias," *Analyst* **1987**, *112*, 377–383.

Outliers present a problem for a linear regression analysis. The following papers discuss the use of robust linear regression techniques.

- Glaister, P. "Robust Linear Regression Using Thiel's Method," *J. Chem. Educ.* **2005**, *82*, 1472–1473.
- Glasser, L. "Dealing with Outliers: Robust, Resistant Regression," *J. Chem. Educ.* **2007**, *84*, 533–534.
- Ortiz, M. C.; Sarabia, L. A.; Herrero, A. "Robust regression techniques. A useful alternative for the detection of outlier data in chemical analysis," *Talanta* **2006**, *70*, 499–512.

The following papers discusses some of the problems with using linear regression to analyze data that has been mathematically transformed into a linear form, as well as alternative methods of evaluating curvilinear data.

- Chong, D. P. "On the Use of Least Squares to Fit Data in Linear Form," *J. Chem. Educ.* **1994**, *71*, 489–490.
- Hinshaw, J. V. "Nonlinear Calibration," *LCGC* **2002**, *20*, 350–355.
- Lieb, S. G. "Simplex Method of Nonlinear Least-Squares - A Logical Complementary Method to Linear Least-Squares Analysis of Data," *J. Chem. Educ.* **1997**, *74*, 1008–1011.
- Zielinski, T. J.; Allendoerfer, R. D. "Least Squares Fitting of Nonlinear Data in the Undergraduate Laboratory," *J. Chem. Educ.* **1997**, *74*, 1001–1007.

More information on multivariate and multiple regression can be found in the following papers.

- Danzer, K.; Otto, M.; Currie, L. A. "Guidelines for Calibration in Analytical Chemistry. Part 2. Multispecies Calibration," Pure Appl. Chem. 2004, 76, 1215–1225.
- Escandar, G. M.; Faber, N. M.; Goicoechea, H. C.; de la Pena, A. M.; Olivieri, A.; Poppi, R. J. "Second- and third-order multivariate calibration: data, algorithms and applications," *Trends Anal. Chem.* **2007**, *26*, 752–765.
- Kowalski, B. R.; Seasholtz, M. B. "Recent Developments in Multivariate Calibration," *J. Chemometrics* **1991**, *5*, 129–145.
- Lang, P. M.; Kalivas, J. H. "A Global Perspective on Multivariate Calibration Methods," *J. Chemometrics* **1993**, *7*, 153–164.
- Madden, S. P.; Wilson, W.; Dong, A.; Geiger, L.; Mecklin, C. J. "Multiple Linear Regression Using a Graphing Calculator," J. Chem. Educ. 2004, 81, 903–907.
- Olivieri, A. C.; Faber, N. M.; Ferré, J.; Boqué, R.; Kalivas, J. H.; Mark, H. "Uncertainty Estimation and Figures of Merit for Multivariate Calibration," *Pure Appl. Chem.* **2006**, *78*, 633–661.

An additional discussion on method blanks, including the use of the total Youden blank, is found in the following papers.

- Cardone, M. J. "Detection and Determination of Error in Analytical Methodology. Part II. Correction for Corrigible Systematic Error in the Course of Real Sample Analysis," *J. Assoc. Off. Anal. Chem.* **1983**, *66*, 1283–1294.
- Cardone, M. J. "Detection and Determination of Error in Analytical Methodology. Part IIB. Direct Calculational Technique for Making Corrigible Systematic Error Corrections," *J. Assoc. Off. Anal. Chem.* **1985**, *68*, 199-202.
- Ferrus, R.; Torrades, F. "Bias-Free Adjustment of Analytical Methods to Laboratory Samples in Routine Analytical Procedures," *Anal. Chem.* **1988**, *60*, 1281–1285.
- Vitha, M. F.; Carr, P. W.; Mabbott, G. A. "Appropriate Use of Blanks, Standards, and Controls in Chemical Measurements," *J. Chem. Educ.* **2005**, *82*, 901–902.

There are a variety of computational packages for completing linear regression analyses. These papers provide details on there use in a variety of contexts.

- Espinosa-Mansilla, A.; de la Peña, A. M.; González-Gómez, D. "Using Univariate Linear Regression Calibration Software in the MATLAB Environment. Application to Chemistry Laboratory Practices," *Chem. Educator* **2005**, *10*, 1–9.
- Harris, D. C. "Nonlinear Least-Squares Curve Fitting with Microsoft Excel Solver," *J. Chem. Educ.* **1998**, *75*, 119–121.
- Kim, M. S.; Bukart, M.; Kim, M. H. "A Method Visual Interactive Regression," *J. Chem. Educ.* **2006**, *83*, 1884.
- Machuca-Herrera, J. G. "Nonlinear Curve Fitting with Spreadsheets," *J. Chem. Educ.* **1997**, *74*, 448–449.
- Smith, E. T.; Belogay, E. A.; Hõim "Linear Regression and Error Analysis for Calibration Curves and Standard Additions: An Excel Spreadsheet Exercise for Undergraduates," Chem. Educator 2010, 15, 100–102.
- Smith, E. T.; Belogay, E. A.; Hõim "Using Multiple Linear Regression to Analyze Mixtures: An Excel Spreadsheet Exercise for Undergraduates," Chem. Educator 2010, 15, 103–107.

- Young, S. H.; Wierzbicki, A. “Mathcad in the Chemistry Curriculum. Linear Least-Squares Regression,” *J. Chem. Educ.* **2000**, *77*, 669.
- Young, S. H.; Wierzbicki, A. “Mathcad in the Chemistry Curriculum. Non-Linear Least-Squares Regression,” *J. Chem. Educ.* **2000**, *77*, 669.

Gathered here are links to on-line computational tools, simulations, and tutorials, many of which are found on the Analytical Sciences Digital Library.

- Multiple Regression (link).
- Non-Parametric Regression with Errors in X and Y (link).
- Linear Regression Tutorial (link).
- Modeling Data Tutorial (link).

Chapter 6

The following experiments involve the experimental determination of equilibrium constants, the characterization of buffers, and, in some cases, demonstrate the importance of activity effects.

- “The Effect of Ionic Strength on an Equilibrium Constant (A Class Study)” in *Chemical Principles in Practice*, J. A. Bell, Ed., Addison-Wesley: Reading, MA, 1967.
- “Equilibrium Constants for Calcium Iodate Solubility and Iodic Acid Dissociation” in *Chemical Principles in Practice*, J. A. Bell, Ed., Addison-Wesley: Reading, MA, 1967.
- “The Solubility of Silver Acetate” in *Chemical Principles in Practice*, J. A. Bell, Ed., Addison-Wesley: Reading, MA, 1967.
- Cobb, C. L.; Love, G. A. “Iron(III) Thiocyanate Revisited: A Physical Chemistry Equilibrium Lab Incorporating Ionic Strength Effects,” *J. Chem. Educ.* **1998**, *75*, 90–92.
- Green, D. B.; Rechtsteiner, G.; Honodel, A. “Determination of the Thermodynamic Solubility Product, K_{sp}, of PbI_2 Assuming Nonideal Behavior,” *J. Chem. Educ.* **1996**, *73*, 789–792.
- Russo, S. O.; Hanania, I. H. “Buffer Capacity,” *J. Chem. Educ.* **1987**, *64*, 817–819.
- Stolzberg, R. J. “Discovering a Change in Equilibrium Constant with Change in Ionic Strength,” *J. Chem. Educ.* **1999**, *76*, 640–641.
- Wiley, J. D. “The Effect of Ionic Strength on the Solubility of an Electrolyte,” *J. Chem. Educ.* **2004**, *81*, 1644–1646.

A nice discussion of Berthollet’s discovery of the reversibility of reactions is found in

- Roots-Bernstein, R. S. *Discovering*, Harvard University Press: Cambridge, MA, 1989.

The following texts provide additional coverage of equilibrium chemistry.

- Butler, J. N. *Ionic Equilibria: A Mathematical Approach*; Addison-Wesley: Reading, MA, 1964.
- Butler, J. N. *Solubility and pH Calculations*; Addison-Wesley: Reading, MA, 1973.
- Fernando, Q.; Ryan, M. D. *Calculations in Analytical Chemistry*, Harcourt Brace Jovanovich: New York, 1982.
- Freiser, H.; Fernando, Q. *Ionic Equilibria in Analytical Chemistry*, Wiley: New York, 1963.
- Freiser, H. *Concepts and Calculations in Analytical Chemistry*, CRC Press: Boca Raton, 1992.
- Gordus, A. A. *Schaum’s Outline of Analytical Chemistry*; McGraw-Hill: New York, 1985.
- Ramette, R. W. *Chemical Equilibrium and Analysis*, Addison-Wesley: Reading, MA, 1981.

The following papers discuss a variety of general aspects of equilibrium chemistry.

- Gordus, A. A. “Chemical Equilibrium I. The Thermodynamic Equilibrium Concept,” *J. Chem. Educ.* **1991**, *68*, 138–140.
- Gordus, A. A. “Chemical Equilibrium II. Deriving an Exact Equilibrium Equation,” *J. Chem. Educ.* **1991**, *68*, 215–217.
- Gordus, A. A. “Chemical Equilibrium III. A Few Math Tricks,” *J. Chem. Educ.* **1991**, *68*, 291–293.
- Gordus, A. A. “Chemical Equilibrium IV. Weak Acids and Bases,” *J. Chem. Educ.* **1991**, *68*, 397–399.
- Gordus, A. A. “Chemical Equilibrium VI. Buffer Solutions,” *J. Chem. Educ.* **1991**, *68*, 656–658.
- Gordus, A. A. “Chemical Equilibrium VII. Precipitates, “*J. Chem. Educ.* **1991**, *68*, 927–930.
- Thomson, B. M.; Kessick, M. A. “On the Preparation of Buffer Solutions,” *J. Chem. Educ.* **1981**, *58*, 743-746.

- Weltin, E. “Are the Equilibrium Concentrations for a Chemical Reaction Always Uniquely Determined by the Initial Concentrations?” *J. Chem. Educ.* **1990**, *67*, 548.
- Weltin, E. “Are the Equilibrium Compositions Uniquely Determined by the Initial Compositions? Properties of the Gibbs Free Energy Function,” J. Chem. Educ. 1995, 72, 508–511.

Collected here are a papers discussing a variety of approaches to solving equilibrium problems.

- Ault, A. “Do pH in Your Head,” *J. Chem. Educ.* **1999**, *76*, 936–938.
- Chaston, S. “Calculating Complex Equilibrium Concentrations by a Next Guess Factor Method,” *J. Chem. Educ.* **1993**, *70*, 622–624.
- Donato, H. “Graphing Calculator Strategies for Solving Chemical Equilibrium Problems,” J. Chem. Educ. 1999, 76, 632–634.
- Olivieri, A. C. “Solution of Acid-Base Equilibria by Successive Approximations,” *J. Chem. Educ.* **1990**, *67*, 229–231.
- Weltin, E. “A Numerical Method to Calculate Equilibrium Concentrations for Single-Equation Systems,” *J. Chem. Educ.* **1991**, *68*, 486–487.
- Weltin, E. “Calculating Equilibrium Concentrations,” *J. Chem. Educ.* **1992**, *69*, 393–396.
- Weltin, E. “Calculating Equilibrium Concentrations for Stepwise Binding of Ligands and Polyprotic Acid-Base Systems,” J. *Chem. Educ.* **1993**, *70*, 568–571.
- Weltin, E. “Equilibrium Calculations are Easier Than You Think - But You do Have to Think!” *J. Chem. Educ.* **1993**, *70*, 571–573.
- Weltin, E. “Calculating Equilibrium Concentrations by Iteration: Recycle Your Approximations,” J. Chem. Educ. 1995, 72, 36–38.

Additional historical background on the development of the Henderson-Hasselbalch equation is provided by the following papers.

- de Levie, R. “The Henderson Approximation and the Mass Action Law of Guldberg and Waage,” *Chem. Educator* **2002**, *7*, 132–135.
- de Levie, R. “The Henderson-Hasselbalch Equation: Its History and Limitations,” *J. Chem. Educ.* **2003**, *80*, 146.

A simulation is a useful tool for helping students gain an intuitive understanding of a topic. Gathered here are some simulations for teaching equilibrium chemistry.

- Edmonson, L. J.; Lewis, D. L. “Equilibrium Principles: A Game for Students,” *J. Chem. Educ.* **1999**, *76*, 502.
- Huddle, P. A.; White, M. W.; Rogers, F. “Simulations for Teaching Chemical Equilibrium,” *J. Chem. Educ.* **2000**, *77*, 920–926.

The following papers provide additional resources on ionic strength, activity, and the effect of ionic strength and activity on equilibrium reactions and pH.

- Clark, R. W.; Bonicamp, J. M. “The Ksp-Solubility Conundrum,” *J. Chem. Educ.* **1998**, *75*, 1182–1185.
- de Levie, R. “On Teaching Ionic Activity Effects: What, When, and Where?” *J. Chem. Educ.* **2005**, *82*, 878–884.
- McCarty, C. G.; Vitz, E. “pH Paradoxes: Demonstrating That It Is Not True That pH = –log[H^+],” *J. Chem. Educ.* **2006**, *83*, 752–757.
- Ramshaw, J. D. “Fugacity and Activity in a Nutshell,” *J. Chem. Educ.* **1995**, *72*, 601–603.
- Sastre de Vicente, M. E. “The Concept of Ionic Strength Eighty Years After Its Introduction,” *J. Chem. Educ.* **2004**, *81*, 750–753.
- Solomon, T. “The Definition and Unit of Ionic Strength,” *J. Chem. Educ.* **2001**, *78*, 1691–1692.

For a contrarian’s view of equilibrium chemistry, please see the following papers.

- Hawkes, S. J. “Buffer Calculations Deceive and Obscure,” *Chem. Educator*, **1996**, *1*, 1–8.
- Hawkes, S. J. “What Should We Teach Beginners About Solubility and Solubility Products?” *J. Chem. Educ.* **1998**, *75*, 1179–1181.
- Hawkes, S. J. “Complexation Calculations are Worse Than Useless,” *J. Chem. Educ.* **1999**, *76*, 1099–1100.
- Hawkes, S. J. “Easy Deviation of pH ≈ (pK_{a1} + pK_{a2})/2 Using Autoprotolysis of HA^-: Doubtful Value of the Supposedly More Rigorous Equation,” *J. Chem. Educ.* **2000**, *77*, 1183–1184. See, also, an exchange of letters between J. J. Roberts and S. J. Hawkes, *J. Chem. Educ.* **2002**, *79*, 161–162.

Chapter 7

The following set of experiments and class exercises introduce students to the importance of sampling on the quality of analytical results.

- Bauer, C. F. “Sampling Error Lecture Demonstration,” *J. Chem. Educ.* **1985**, *62*, 253.
- Canaes, L. S.; Brancalion, M. L.; Rossi, A. V.; Rath, S. “Using Candy Samples to Learn About Sampling Techniques and Statistical Evaluation of Data,” *J. Chem. Educ.* **2008**, *85*, 1083–1088.
- Clement, R. E. “Environmental Sampling for Trace Analysis,” *Anal. Chem.* **1992**, *64*, 1076A–1081A.
- Dunn, J. G.; Phillips, D. N.; van Bronswijk, W. “An Exercise to Illustrate the Importance of Sample Preparation in Chemical Analysis,” *J. Chem. Educ.* **1997**, *74*, 1188–1191.
- Fritz, M. D. “A Demonstration of Sample Segregation,” *J. Chem. Educ.* **2005**, *82*, 255–256.
- Guy, R. D.; Ramaley, L.; Wentzell, P. D. “An Experiment in the Sampling of Solids for Chemical Analysis”, J. Chem. Educ. 1998, 75, 1028-1033.
- Hartman, J. R. “An In-Class Experiment to Illustrate the Importance of Sampling Techniques and Statistical Analysis of Data to Quantitative Analysis Students,” *J. Chem. Educ.* **2000**, *77*, 1017–1018.
- Harvey, D. T. “Two Experiments Illustrating the Importance of Sampling in a Quantitative Chemical Analysis,” *J. Chem. Educ.* **2002**, *79*, 360–363.
- Herrington, B. L. “A Demonstration of the Necessity for Care in Sampling,” *J. Chem. Educ.* **1937**, *14*, 544.
- Kratochvil, B.; Reid, R. S.; Harris, W. E. “Sampling Error in a Particulate Mixture”, *J. Chem. Educ.* **1980**, *57*, 518–520.
- Ross, M. R. “A Classroom Exercise in Sampling Technique,” *J. Chem. Educ.* **2000**, *77*, 1015–1016.
- Settle, F. A.; Pleva, M. “The Weakest Link Exercise,” *Anal. Chem.* **1999**, *71*, 538A–540A.
- Vitt, J. E.; Engstrom, R. C. “Effect of Sample Size on Sampling Error,” *J. Chem. Educ.* **1999**, *76*, 99–100.

The following experiments describe homemade sampling devices for collecting samples in the field.

- Delumyea, R. D.; McCleary, D. L. “A Device to Collect Sediment Cores,” *J. Chem. Educ.* **1993**, *70*, 172–173.
- Rockwell, D. M.; Hansen, T. “Sampling and Analyzing Air Pollution,” *J. Chem. Educ.* **1994**, *71*, 318–322.
- Saxena, S., Upadhyay, R.; Upadhyay, P. “A Simple and Low-Cost Air Sampler,” *J. Chem. Educ.* **1996**, *73*, 787–788.
- Shooter, D. “Nitrogen Dioxide and Its Determination in the Atmosphere,” *J. Chem. Educ.* **1993**, *70*, A133–A140.

The following experiments introduce students to methods for extracting analytes from their matrix.

- “Extract-Clean™ SPE Sample Preparation Guide Volume 1”, Bulletin No. 83, Alltech Associates, Inc. Deerfield, IL.
- Freeman, R. G.; McCurdy, D. L. “Using Microwave Sample Decomposition in Undergraduate Analytical Chemistry,” *J. Chem. Educ.* **1998**, *75*, 1033–1032.
- Snow, N. H.; Dunn, M.; Patel, S. “Determination of Crude Fat in Food Products by Supercritical Fluid Extraction and Gravimetric Analysis,” *J. Chem. Educ.* **1997**, *74*, 1108–1111.
- Yang, M. J.; Orton, M. L.; Pawliszyn, J. “Quantitative Determination of Caffeine in Beverages Using a Combined SPME-GC/MS Method,” *J. Chem. Educ.* **1997**, *74*, 1130–1132.

The following paper provides a general introduction to the terminology used in describing sampling.

- “Terminology—The key to understanding analytical science. Part 2: Sampling and sample preparation,” AMC Technical Brief No. 19, March 2005 (link).
- Majors, R. E. “Nomenclature for Sampling in Analytical Chemistry” *LC•GC* **1992**, *10*, 500–506.

Further information on the statistics of sampling is covered in the following papers and textbooks.

- “What is uncertainty from sampling, and why is it important?” AMC Technical Brief No. 16A, June 2004 (link).
- “Analytical and sampling strategy, fitness for purpose, and computer games,” AMC Technical Brief No. 20, August 2005 (link).
- “Measurement uncertainty arising from sampling: the new Eurachem Guide,” AMC Technical Brief No. 31, July 2008 (link).
- *Sampling for Analytical Purpose*, Gy, P. ed., Wiley: NY, 1998.
- Baiulescu, G. E.; Dumitrescu, P.; Zuaravescu, P. G. *Sampling*, Ellis Horwood: NY, 1991.

- Cohen, R. D. “How the Size of a Random Sample Affects How Accurately It Represents a Population,” *J. Chem. Educ.* **1992**, *74*, 1130–1132.
- Efstathiou, C. E. “On the sampling variance of ultra-dilute solutions,” *Talanta* **2000**, *52*, 711–715.
- Gerlach, R. W.; Dobb, D. E.; Raab, G. A.; Nocerino, J. M. *J. Chemom.* **2002**, *16*, 321–328.
- Gy, P. M. *Sampling of Particulate Materials: Theory and Practice*; Elsevier: Amsterdam, 1979.
- Gy, P. M. *Sampling of Heterogeneous and Dynamic Materials: Theories of Heterogeneity, Sampling and Homogenizing*; Elsevier: Amsterdam, 1992.
- Kratochvil, B.; Taylor, J. K. “Sampling for Chemical Analysis,” *Anal. Chem.* **1981**, *53*, 924A–938A.
- Kratochvil, B.; Goewie, C. E.; Taylor, J. K. “Sampling Theory for Environmental Analysis,” *Trends Anal. Chem.* **1986**, *5*, 253–256.
- Meyer, V. R. *LC•GC* **2002**, *20*, 106–112.
- Rohlf, F. J.; Akçakaya, H. R.; Ferraro, S. P. “Optimizing Composite Sampling Protocols,” *Environ. Sci. Technol.* **1996**, *30*, 2899–2905.
- Smith, R.; James, G. V. *The Sampling of Bulk Materials*; Royal Society of Chemistry: London, 1981.

The process of collecting a sample presents a variety of difficulties, particularly with respect to the analyte’s integrity. The following papers provide representative examples of sampling problems.

- Barceló, D.; Hennion, M. C. “Sampling of Polar Pesticides from Water Matrices,” *Anal. Chim. Acta* **1997**, *338*, 3–18.
- Batley, G. E.; Gardner, D. “Sampling and Storage of Natural Waters for Trace Metal Analysis,” *Wat. Res.* **1977**, *11*, 745–756.
- Benoit, G.; Hunter, K. S.; Rozan, T. F. “Sources of Trace Metal Contamination Artifacts during Collection, Handling, and Analysis of Freshwaters,” *Anal. Chem.* **1997**, *69*, 1006–1011
- Brittain, H. G. “Particle-Size Distribution II: The Problem of Sampling Powdered Solids,” *Pharm. Technol.* July **2002**, 67–73.
- Ramsey, M. H. “Measurement Uncertainty Arising from Sampling: Implications for the Objectives of Geoanalysis,” *Analyst*, **1997**, *122*, 1255–1260.
- Seiler, T-B; Schulze, T.; Hollert, H. “The risk of altering soil and sediment samples upon extract preparation for analytical and bio-analytical investigations—a review,” *Anal. Bioanal. Chem.* **2008**, 390, 1975–1985.

The following texts and articles provide additional information on methods for separating analytes and interferents.

- “Guide to Solid Phase Extraction,” Bulletin 910, Sigma-Aldrich, 1998.
- “Solid Phase Microextraction: Theory and Optimization of Conditions,” Bulletin 923, Sigma-Aldrich, 1998.
- *Microwave-Enhanced Chemistry: Fundamentals, Sample Preparation, and Applications*, Kingston, H. M.; Haswell, S. J., eds.; American Chemical Society: Washington, D.C., 1997.
- Anderson, R. *Sample Pretreatment and Separation*, Wiley: Chichester, 1987.
- Bettiol, C.; Stievano, L.; Bertelle, M.; Delfino, F.; Argese, E. “Evaluation of microwave-assisted acid extraction procedures for the determination of metal content and potential bioavailability in sediments,” Appl. Geochem. 2008, 23, 1140–1151.
- Compton, T. R. *Direct Preconcentration Techniques*, Oxford Science Publications: Oxford, 1993.
- Compton, T. R. *Complex-Formation Preconcentration Techniques*, Oxford Science Publications: Oxford, 1993.
- Hinshaw, J. V. “Solid-Phase Microextraction,” *LC•GC Europe* **2003**, *December*, 2–5.
- Karger, B. L.; Snyder, L. R.; Harvath, C. *An Introduction to Separation Science*, Wiley-Interscience: N. Y.; 1973.
- Majors, R. E.; Raynie, D. E. “Sample Preparation and Solid-Phase Extraction”, *LC•GC* **1997**, *15*, 1106–1117.
- Luque de Castro, M. D.; Priego-Capote, F.; Sánchez-Ávila, N. “Is dialysis alive as a membrane-based separation technique?” *Trends Anal. Chem.* **2008**, *27*, 315–326.
- Mary, P.; Studer, V.; Tabeling, P. “Microfluidic Droplet-Based Liquid–Liquid Extraction,” *Anal. Chem.* **2008**, *80*, 2680–2687.
- Miller, J. M. *Separation Methods in Chemical Analysis*, Wiley-Interscience: N. Y.; 1975.
- Morrison, G. H.; Freiser, H. *Solvent Extraction in Analytical Chemistry*, John Wiley and Sons: N. Y.; 1957.
- Pawliszyn, J. *Solid-Phase Microextraction: Theory and Practice*, Wiley: NY, 1997.
- Pawliszyn, J. “Sample Preparation: Quo Vadis?” *Anal. Chem.* **2003**, *75*, 2543–2558.
- Sulcek, Z.; Povondra, P. *Methods of Decomposition in Inorganic Analysis*; CRC Press: Boca Raton, FL, 1989.
- Theis, A. L.; Waldack, A. J.; Hansen, S. M.; Jeannot, M. A. “Headspace Solvent Microextraction,” *Anal. Chem.* **2001**, *73*, 5651–5654.

- Thurman, E. M.; Mills, M. S. *Solid-Phase Extraction: Principles and Practice*, Wiley: NY, 1998.
- Zhang, Z.; Yang, M.; Pawliszyn, J. "Solid-Phase Microextraction," *Anal. Chem.* **1994**, *66*, 844A–853A.

Chapter 8

The following set of experiments introduce students to the applications of gravimetry.

- Burrows, H. D.; Ellis, H. A.; Odilora, C. A. "The Dehydrochlorination of PVC," *J. Chem. Educ.* **1995**, *72*, 448–450.
- Carmosini, N.; Ghoreshy, S. Koether, M. C. "The Gravimetric Analysis of Nickel Using a Microwave Oven," *J. Chem. Educ.* **1997**, *74*, 986–987.
- Harris, T. M. "Revitalizing the Gravimetric Determination in Quantitative Analysis Laboratory," *J. Chem. Educ.* **1995**, *72*, 355–356.
- Henrickson, C. H.; Robinson, P. R. "Gravimetric Determination of Calcium as $CaC_2O_4 \cdot H_2O$," *J. Chem. Educ.* **1979**, *56*, 341–342.
- Shaver, L. A. "Determination of Phosphates by the Gravimetric Quimociac Technique," *J. Chem. Educ.* **2008**, *85*, 1097–1098.
- Snow, N. H.; Dunn, M.; Patel, S. "Determination of Crude Fat in Food Products by Supercritical Fluid Extraction and Gravimetric Analysis," *J. Chem. Educ.* **1997**, *74*, 1108–1111.
- Thompson, R. Q.; Ghadiali, M. "Microwave Drying of Precipitates for Gravimetric Analysis," *J. Chem. Educ.* **1993**, *70*, 170–171.
- Wynne, A. M. "The Thermal Decomposition of Urea," *J. Chem. Educ.* **1987**, *64*, 180–182.

The following resources provide a general history of gravimetry.

- A History of Analytical Chemistry; Laitinen, H. A.; Ewing, G. W., Eds.; The Division of Analytical Chemistry of the American Chemical Society: Washington, D. C., 1977, pp. 10-24.
- Beck, C. M. "Classical Analysis: A Look at the Past, Present, and Future," *Anal. Chem.* **1991**, *63*, 993A–1003A; *Anal. Chem.* **1994**, *66*, 224A–239A

Consult the following texts for additional examples of inorganic and organic gravimetric methods include the following texts.

- Bassett, J.; Denney, R. C.; Jeffery, G. H.; Mendham, J. *Vogel's Textbook of Quantitative Inorganic Analysis*, Longman: London, 4th Ed., 1981.
- Erdey, L. *Gravimetric Analysis*, Pergamon: Oxford, 1965.
- Steymark, A. *Quantitative Organic Microanalysis*, The Blakiston Co.: NY, 1951.
- Wendlandt, W. W. *Thermal Methods of Analysis*, 2nd Ed. Wiley: NY. 1986.

For a review of isotope dilution mass spectrometry see the following article.

- Fassett, J. D.; Paulsen, P. J. "Isotope Dilution Mass Spectrometry for Accurate Elemental Analysis," *Anal. Chem.* **1989**, *61*, 643A–649A.

Chapter 9

The following set of experiments introduce students to the applications of titrimetry. Experiments are grouped into four categories based on the type of reaction (acid–base, complexation, redox, and precipitation). Additional experiments emphasizing potentiometric electrodes are found in Chapter 11.

Acid–base titrimetry

- Boiani, J. A. "The Gran Plot Analysis of an Acid Mixture," *J. Chem. Educ.* **1986**, *63*, 724–726.
- Castillo, C. A.; Jaramillo, A. "An Alternative Procedure for Titration Curves of a Mixture of Acids of Different Strengths," *J. Chem. Educ.* **1989**, *66*, 341.
- Clark, R. W.; White, G. D.; Bonicamp, J. M.; Watts, E. D. "From Titration Data to Buffer Capacities: A Compter Experiment for the Chemistry Lab or Lecture," *J. Chem. Educ.* **1995**, *72*, 746–750.
- Clay, J. T.; Walters, E. A.; Brabson, G. D. "A Dibasic Acid Titration for the Physical Chemistry Laboratory" *J. Chem. Educ.* **1995**, *72*, 665–667.

- Crossno, S. K; Kalbus, L. H.; Kalbus, G. E. “Determinations of Carbon Dioxide by Titration,” *J. Chem. Educ.* **1996**, *73*, 175–176.
- Flowers, P. A. “Potentiometric Measurement of Transition Ranges and Titration Errors for Acid/Base Indicators,” *J. Chem. Educ.* **1997**, *74*, 846–847.
- Fuchsam, W. H.; Garg, Sandhya “Acid Content of Beverages,” *J. Chem. Educ.* **1990**, *67*, 67–68
- Graham. R.C.; DePew, S. “Determination of Ammonia in Household Cleaners,” *J. Chem. Educ.* **1983**, *60*, 765–766.
- Kalbus, L. H.; Petrucci, R. H.; Forman, J. E.; Kalbus, G. E. “Titration of Chromate-Dichromate Mixtures,” *J. Chem. Educ.* **1991**, *68*, 677–678.
- Kooser, A. S.; Jenkins, J. L.; Welch, L. E. “Acid–Base Indicators: A New Look at an Old Topic,” *J. Chem. Educ.* **2001**, *78*, 1504–1506.
- Kraft, A. “The Determination of the pK_a of Multiprotic, Weak Acids by Analyzing Potentiometric Acid–Base Titration Data with Difference Plots,” *J. Chem. Educ.* **2003**, *80*, 554–559.
- Murphy, J. “Determination of Phosphoric Acid in Cola Beverages,” *J. Chem. Educ.* **1983**, *60*, 420–421.
- Nyasulu, F.; Barlag, R.; Macklin, J. *Chem. Educator* **2008**, *13*, 289–294.
- Ophardt, C. E. “Acid Rain Analysis by Standard Addition Titration,” *J. Chem. Educ.* **1985**, *62*, 257–258.
- Partanen, J. I.; Kärki, M. H. “Determination of the Thermodynamic Dissociation Constant of a Weak Acid by Potentiometric Acid-Base Titration,” *J. Chem. Educ.* **1994**, *71*, A120–A122.
- Thompson, R. Q. “Identification of Weak Acids and Bases by Titration with Primary Standards,” *J. Chem. Educ.* **1988**, *65*, 179–180.
- Tucker, S. A.; Amszi, V. L.; Acree, Jr. W. E. “Studying Acid-Base Equilibria in Two-Phase Solvent Media,” *J. Chem. Educ.* **1993**, *70*, 80–82.
- Tucker, S. A.; Acree, Jr., W. E. “A Student-Designed Analytical Laboratory Method,” *J. Chem. Educ.* **1994**, *71*, 71–74.
- Werner, J. A.; Werner, T. C. “Multifunctional Base Unknowns in the Introductory Analytical Chemistry Lab,” *J. Chem. Educ.* **1991**, *68*, 600–601.

Complexation Titrimetry

- Ceretti, H.; Hughes, E. A.; Zalts, A. “The Softening of Hard Water and Complexometric Titrations,” *J. Chem. Educ.* **1999**, *76*, 1420–1421.
- Fulton, R.; Ross, M.; Schroeder, K. “Spectrophotometric Titration of a Mixture of Calcium and Magnesium,” *J. Chem. Educ.* **1986**, *63*, 721–723.
- Novick, S. G. “Complexometric Titration of Zinc,” *J. Chem. Educ.* **1997**, *74*, 1463.
- Olsen, K. G.; Ulicny, L. J. “Reduction of Calcium Concentrations by the Brita Water Filtration System: A Practical Experiment in Titrimetry and Atomic Absorption Spectroscopy,” *J. Chem. Educ.* **2001**, *78*, 941.
- Smith, R. L.; Popham, R. E. “The Quantitative Resolution of a Mixture of Group II Metal Ions by Thermometric Titration with EDTA,” *J. Chem. Educ.* **1983**, *60*, 1076–1077.
- Yappert, M. C.; DuPré, D. B. “Complexometric Titrations: Competition of Complexing Agents in the Determination of Water Hardness with EDTA,” *J. Chem. Educ.* **1997**, *74*, 1422–1423.

Redox Titrimetry

- Guenther, W. B. “Supertitrations: High-Precision Methods,” *J. Chem. Educ.* **1988**, *65*, 1097–1098.
- Haddad, P. “Vitamin C Content of Commercial Orange Juices,” *J. Chem. Educ.* **1977**, *54*, 192–193.
- Harris, D. C.; Hills, M. E.; Hewston, T. A. “Preparation, Iodometric Analysis and Classroom Demonstration of Superconductivity in $YBa_2Cu_3O_{8-x}$,” *J. Chem. Educ.* **1987**, *64*, 847–850.
- Lau, O.-W.; Luk, S.-F.; Cheng, N. L. N.; Woo, H.-O. “Determination of Free Lime in Clinker and Cement by Iodometry,” *J. Chem. Educ.* **2001**, *78*, 1671–1673.
- Phinyocheep, P.; Tang, I. M. “Determination of the Hole Concentration (Copper Valency) in the High Tc Superconductors,” *J. Chem. Educ.* **1994**, *71*, A115–A118.
- Powell, J. R.; Tucker, S. A.; Acree, Jr., W. E.; Sees, J. A.; Hall, L. M. “A Student-Designed Potentiometric Titration: Quantitative Determination of Iron(II) by Caro’s Acid Titration,” *J. Chem. Educ.* **1996**, *73*, 984–986.

Precipitation Titrimetry

- Ueno, K.; Kina, K. “Colloid Titration - A Rapid Method for the Determination of Charged Colloid,” *J. Chem. Educ.* **1985**, *62*, 627–629.

For a general history of titrimetry, see the following sources.

- *A History of Analytical Chemistry*; Laitinen, H. A.; Ewing, G. W., Eds.; The Division of Analytical Chemistry of the American Chemical Society: Washington, D. C., 1977, pp. 52–93.
- Kolthoff, I. M. “Analytical Chemistry in the USA in the First Quarter of This Century,” *Anal. Chem.* **1994**, *66*, 241A–249A.

The use of weight instead of volume as a signal for titrimetry is reviewed in the following paper.

- Kratochvil, B.; Maitra, C. “Weight Titrations: Past and Present,” *Am. Lab.* **1983**, January, 22–29.

A more thorough discussion of non-aqueous titrations, with numerous practical examples, is provided in the following text.

- Fritz, J. S. *Acid-Base Titrations in Nonaqueous Solvents*; Allyn and Bacon, Boston; 1973.

The sources listed below provides more details on the how potentiometric titration data may be used to calculate equilibrium constants.

- Babić, S.; Horvat, A. J. M.; Pavlović, D. M.; Kaštelan-Macan, M. “Determination of pKa values of active pharmaceutical ingredients,” *Trends Anal. Chem.* **2007**, *26*, 1043–1061.
- Meloun, M.; Havel, J.; Högfeldt, E. *Computation of Solution Equilibria*, Ellis Horwood Limited: Chichester, England; 1988.

The following provides additional information about Gran plots.

- Michalowski, T.; Kupiec, K.; Rymanowski, M. *Anal. Chim. Acta* **2008**, *606*, 172–183.
- Schwartz, L. M. “Advances in Acid-Base Gran Plot Methodology,” *J. Chem. Educ.* **1987**, *64*, 947–950.
- Schwartz, L. M. “Uncertainty of a Titration Equivalence Point,” *J. Chem. Educ.* **1992**, *69*, 879–883.

The following provide additional information about calculating or sketching titration curves.

- Barnum, D. “Predicting Acid–Base Titration Curves without Calculations,” *J. Chem. Educ.* **1999**, *76*, 938–942.
- de Levie, R. “A simple expression for the redox titration curve,” *J. Electroanal. Chem.* **1992**, *323*, 347–355.
- King, D. W. “A General Approach for Calculating Speciation and Posing Capacity of Redox Systems with Multiple Oxidation States: Application to Redox Titrations and the Generation of pε–pH,” *J. Chem. Educ.* **2002**, *79*, 1135–1140.

For a complete discussion of the application of complexation titrimetry see the texts listed below.

- Pribil, R. *Applied Complexometry*, Pergamon Press: Oxford, 1982.
- Ringbom, A. *Complexation in Analytical Chemistry*, John Wiley and Sons, Inc.: New York, 1963.
- Schwarzenbach, G. *Complexometric Titrations*, Methuen & Co. Ltd: London, 1957.

A good source for additional examples of the application of all forms of titrimetry is

- *Vogel’s Textbook of Quantitative Inorganic Analysis*, Longman: London, 4th Ed., 1981.

Chapter 10

The following set of experiments introduce students to the applications of spectroscopy. Experiments are grouped into five categories: UV/Vis spectroscopy, IR spectroscopy, atomic absorption and atomic emission, fluorescence and phosphorescence, and signal averaging.

UV/Vis Spectroscopy

- Abney, J. R.; Scalettar, B. A. “Saving Your Students’ Skin. Undergraduate Experiments That Probe UV Protection by Sunscreens and Sunglasses,” *J. Chem. Educ.* **1998**, *75*, 757–760.
- Ainscough, E. W.; Brodie, A. M. “The Determination of Vanillin in Vanilla Extract,” *J. Chem. Educ.* **1990**, *67*, 1070–1071.
- Allen, H. C.; Brauers, T.; Finlayson-Pitts, B. J. “Illustrating Deviations in the Beer-Lambert Law in an Instrumental Analysis Laboratory: Measuring Atmospheric Pollutants by Differential Optical Absorption Spectrometry,” *J. Chem. Educ.* **1997**, *74*, 1459–1462.

- Blanco, M.; Iturriaga, H.; Maspoch, S.; Tarîn, P. “A Simple Method for Spectrophotometric Determination of Two-Components with Overlapped Spectra,” *J. Chem. Educ.* **1989**, *66*, 178–180.
- Bonicamp, J. M.; Martin, K. L.; McBride, G. R.; Clark, R. W. “Beer’s Law is Not a Straight Line: Amplification of Errors by Transformation,” *Chem. Educator* **1999**, *4*, 81–88.
- Bruneau, E.; Lavabre, D.; Levy, G.; Micheau, J. C. “Quantitative Analysis of Continuous-Variation Plots with a Comparison of Several Methods,” *J. Chem. Educ.* **1992**, *69*, 833–837.
- Cappas, C.; Hoffman, N.; Jones, J.; Young, S. “Determination of Concentrations of Species Whose Absorption Bands Overlap Extensively,” *J. Chem. Educ.* **1991**, *68*, 300–303.
- Crisp, P. T.; Eckert, J. M.; Gibson, N. A. “The Determination of Anionic Surfactants in Natural and Waste Waters,” *J. Chem. Educ.* **1983**, *60*, 236–238.
- Dilbeck, C. W.; Ganske, J. A. “Detection of NOx in Automobile Exhaust: An Applied Experiment in Atmospheric/Environmental Chemistry for the General Chemistry Laboratory,” *Chem. Educator* **2008**, *13*, 1–5.
- Domínguez, A., Fernández, A.; González, N.; Iglesias, E.; Montenegro, L. “Determination of Critical Micelle Concentration of Some Surfactants by Three Techniques,” *J. Chem. Educ.* **1997**, *74*, 1227–1231.
- Gilbert, D. D. “Determining Optimum Spectral Bandwidth,” *J. Chem. Educ.* **1991**, *68*, A278–A281.
- Han, J.; Story, T.; Han, G. “A Spectrophotometric Method for Quantitative Determination of Bromine Using Tris(2-carboxyethyl)phophine,” *J. Chem. Educ.* **1999**, *76*, 976–977.
- Higginbotham, C.; Pike, C. F.; Rice, J, K. “Spectroscopy in Sol-Gel Matricies,” *J. Chem. Educ.* **1998**, *75*, 461–464.
- Hill, Z. D.; MacCarthy, P. “Novel Approach to Job’s Method,” *J. Chem. Educ.* **1986**, *63*, 162–167.
- Ibañez, G. A.; Olivieri, A. C.; Escandar, G. M. “Determination of Equilibrium Constants of Metal Complexes from Spectrophotometric Measurements,” *J. Chem. Educ.* **1999**, *76*, 1277–1281.
- Long, J. R.; Drago, R. S. “The Rigorous Evaluation of Spectrophotometric Data to Obtain an Equilibrium Constant,” *J. Chem. Educ.* **1982**, *59*, 1037–1039.
- Lozano-Calero; D.; Martin-Palomeque, P. “Determination of Phosphorous in Cola Drinks,” *J. Chem. Educ.* **1996**, *73*, 1173–1174.
- Maloney, K. M.; Quiazon, E. M.; Indralingam, R. “Measurement of Iron in Egg Yolk: An Instrumental Analysis Measurement Using Biochemical Principles,” *J. Chem. Educ.* **2008**, *85*, 399–400.
- Mascotti, D. P.; Waner, M. J. “Complementary Spectroscopic Assays for Investigation Protein-Ligand Binding Activity: A Project for the Advanced Chemistry Laboratory,” *J. Chem. Educ.* **2010**, *87*, 735–738.
- McDevitt, V. L.; Rodriquez, A.; Williams, K. R. “Analysis of Soft Drinks: UV Spectrophotometry, Liquid Chromatography, and Capillary Electrophoresis,” *J. Chem. Educ.* **1998**, *75*, 625–629.
- Mehra, M. C.; Rioux, J. “An Analytical Chemistry Experiment in Simultaneous Spectrophotometric Determination of Fe(III) and Cu(II) with Hexacyanoruthenate(II) Reagent,” *J. Chem. Educ.* **1982**, *59*, 688–689.
- Mitchell-Koch, J. T.; Reid, K. R.; Meyerhoff, M. E. “Salicylate Detection by Complexation with Iron(III) and Optical Absorbance Spectroscopy,” *J. Chem. Educ.* **2008**, *85*, 1658–1659.
- Msimanga, H. Z.; Wiese, J. “Determination of Acetaminophen in Analgesics by the Standard Addition Method: A Quantitative Analytical Chemistry Laboratory,” *Chem. Educator* **2005**, *10*, 1–7.
- Örstan, A.; Wojcik, J. F. “Spectroscopic Determination of Protein-Ligand Binding Constants,” *J. Chem. Educ.* **1987**, *64*, 814–816.
- Pandey, S.; Powell, J. R.; McHale, M. E. R.; Acree Jr., W. E. “Quantitative Determination of Cr(III) and Co(II) Using a Spectroscopic H-Point Standard Addition,” *J. Chem. Educ.* **1997**, *74*, 848–850.
- Parody-Morreale, A.; Cámara-Artigas, A.; Sánchez-Ruiz, J. M. “Spectrophotometric Determination of the Binding Constants of Succinate and Chloride to Glutamic Oxalacetic Transaminase,” *J. Chem. Educ.* **1990**, *67*, 988–990.
- Ravelo-Perez, L. M.; Hernández-Borges, J.; Rodríguez-Delgado, M. A.; Borges-Miquel, T. “Spectrophotometric Analysis of Lycopene in Tomatoes and Watermelons: A Practical Class,” *Chem. Educator* **2008**, *13*, 1–3.
- Russell, D. D.; Potts, J.; Russell, R. M.; Olson, C.; Schimpf, M. “Spectroscopic and Potentiometric Investigation of a Diprotic Acid: An Experimental Approach to Understanding Alpha Functions,” *Chem. Educator* **1999**, *4*, 68–72.
- Smith, E. T.; Matachek, J. R. “A Colorful Investigation of a Diprotic Acid: A General Chemistry Laboratory Exercise,” *Chem. Educator* **2002**, *7*, 359–363

- Tello-Solis, S. R. “Thermal Unfolding of Lysozyme Studied by UV Difference Spectroscopy,” *Chem. Educator* **2008**, *13*, 16–18.
- Tucker, S.; Robinson, R.; Keane, C.; Boff, M.; Zenko, M.; Batish, S.; Street, Jr., K. W. “Colorimetric Determination of pH,” *J. Chem. Educ.* **1989**, *66*, 769–771.
- Vitt, J. E. “Troubleshooting 101: An Instrumental Analysis Experiment,” *J. Chem. Educ.* **2008**, *85*, 1660–1662.
- Williams, K. R.; Cole, S. R.; Boyette, S. E.; Schulman, S. G. “The Use of Dristan Nasal Spray as the Unknown for Simultaneous Spectrophotometric Analysis of a Mixture,” *J. Chem. Educ.* **1990**, *67*, 535.
- Walmsley, F. “Aggregation in Dyes: A Spectrophotometric Study,” *J. Chem. Educ.* **1992**, *69*, 583.
- Wells, T. A. “Construction of a Simple Myoglobin-Based Optical Biosensor,” *Chem. Educator* **2007**, *12*, 1–3.
- Yarnelle, M. K.; West, K. J. “Modification of an Ultraviolet Spectrophotometric Determination of the • Active Ingredients in APC Tablets,” *J. Chem. Educ.* **1989**, *66*, 601–602.

IR Spectroscopy

- Dragon, S.; Fitch, A. “Infrared Spectroscopy Determination of Lead Binding to Ethylenediaminetetraacetic Acid,” *J. Chem. Educ.* **1998**, *75*, 1018–1021.
- Frohlich, H. “Using Infrared Spectroscopy Measurements to Study Intermolecular Hydrogen Bonding,” *J. Chem. Educ.* **1993**, *70*, A3–A6.
- Garizi, N.; Macias, A.; Furch, T.; Fan, R.; Wagenknecht, P.; Singmaster, K. A. “Cigarette Smoke Analysis Using an Inexpensive Gas-Phase IR Cell,” *J. Chem. Educ.* **2001**, *78*, 1665–1666.
- Indralingam, R.; Nepomuceno, A. I. “The Use of Disposable IR Cards for Quantitative Analysis Using an Internal Standard,” *J. Chem. Educ.* **2001**, *78*, 958–960.
- Mathias, L. J.; Hankins, M. G.; Bertolucci, C. M.; Grubb, T. L.; Muthiah, J. “Quantitative Analysis by FTIR: Thin Films of Copolymers of Ethylene and Vinyl Acetate,” *J. Chem. Educ.* **1992**, *69*, A217–A219.
- Schuttlefield, J. D.; Grassian, V. H. “ATR-FTIR Spectroscopy in the Undergraduate Chemistry Laboratory. Part I: Fundamentals and Examples,” *J. Chem. Educ.* **2008**, *85*, 279–281.
- Schuttlefield, J. D.; Larsen, S. C.; Grassian, V. H. “ATR-FTIR Spectroscopy in the Undergraduate Chemistry Laboratory. Part II: A Physical Chemistry Laboratory Experiment on Surface Adsorption,” *J. Chem. Educ.* **2008**, *85*, 282–284.
- Seasholtz, M. B.; Pence, L. E.; Moe Jr., O. A. “Determination of Carbon Monoxide in Automobile Exhaust by FTIR Spectroscopy,” *J. Chem. Educ.* **1988**, *65*, 820–823.

Atomic Absorption and Atomic Emission Spectroscopy

- Amarasiriwardena, D. “Teaching analytical atomic spectroscopy advances in an environmental chemistry class using a project-based laboratory approach: investigation of lead and arsenic distributions in a lead arsenate contaminated apple orchard,” *Anal. Bioanal. Chem.* **2007**, *388*, 307–314.
- Buffen, B. P. “Removal of Heavy Metals from Water: An Environmentally Significant Atomic Absorption Spectrometry Experiment,” *J. Chem. Educ.* **1999**, *76*, 1678–1679.
- Dockery, C. R.; Blew, M. J.; Goode, S. R. “Visualizing the Solute Vaporization Interference in Flame Atomic Absorption Spectroscopy,” *J. Chem. Educ.* **2008**, *85*, 854–858.
- Donas, M. K.; Whissel, G.; Dumas, A.; Golden, K. “Analyzing Lead Content in Ancient Bronze Coins by Flame Atomic Absorption Spectroscopy,” *J. Chem. Educ.* **2009**, *86*, 343–346.
- Gilles de Pelichy, L. D.; Adams, C.; Smith, E. T. “Analysis of the Essential Nutrient Strontium in Marine Aquariums by Atomic Absorption Spectroscopy,” *J. Chem. Educ.* **1997**, *74*, 1192–1194.
- Hoskins, L. C.; Reichardt, P. B.; Stolzberg, R. J. “Determination of the Extraction Constant for Zinc Pyrrolidinecarbodithioate,” *J. Chem. Educ.* **1981**, *58*, 580–581.
- Kooser, A. S.; Jenkins, J. L.; Welch, L. E. “Inductively Coupled Plasma-Atomic Emission Spectroscopy: Two Laboratory Activities for the Undergraduate Instrumental Analysis Course,” *J. Chem. Educ.* **2003**, *80*, 86–88.
- Kostecka, K. S. “Atomic Absorption Spectroscopy of Calcium in Foodstuffs in Non-Science-Major Courses,” *J. Chem. Educ.* **2000**, *77*, 1321–1323.
- Lehman, T. A.; Everett, W. W. “Solubility of Lead Sulfate in Water and in Sodium Sulfate Solutions,” *J. Chem. Educ.* **1982**, *59*, 797.

- Markow, P. G. “Determining the Lead Content of Paint Chips,” *J. Chem. Educ.* **1996**, *73*, 178–179.
- Masina, M. R.; Nkosi, P. A.; Rasmussen, P. W.; Shelembe, J. S.; Tyobeka, T. E. “Determination of Metal Ions in Pineapple Juice and Effluent of a Fruit Canning Industry,” *J. Chem. Educ.* **1989**, *66*, 342–343.
- Quigley, M. N. “Determination of Calcium in Analgesic Tablets using Atomic Absorption Spectrophotometry,” *J. Chem. Educ.* **1994**, *71*, 800.
- Quigley, M. N.; Vernon, F. “Determination of Trace Metal Ion Concentrations in Seawater,” *J. Chem. Educ.* **1996**, *73*, 671–675.
- Quigley, M. N.; Vernon, F. “A Matrix Modification Experiment for Use in Electrothermal Atomic Absorption Spectrophotometry,” *J. Chem. Educ.* **1996**, *73*, 980–981.
- Rheingold, A. L.; Hues, S.; Cohen, M. N. “Strontium and Zinc Content in Bones as an Indication of Diet,” *J. Chem. Educ.* **1983**, *60*, 233–234.
- Rocha, F. R. P.; Nóbrega, J. A. “Effects of Solution Physical Properties on Copper and Chromium Signals in Flame Atomic Absorption Spectrometry,” *J. Chem. Educ.* **1996**, *73*, 982–984.

Fluorescence and Phosphorescence Spectroscopy

- Buccigross, J. M.; Bedell, C. M.; Suding-Moster, H. L. “Fluorescent Measurement of TNS Binding to Calmodulin,” *J. Chem. Educ.* **1996**, *73*, 275–278.
- Henderleiter, J. A.; Hyslopo, R. M. “The Analysis of Riboflavin in Urine by Fluorescence,” *J. Chem. Educ.* **1996**, *73*, 563–564.
- Lagoria, M. G.; Román, E. S. “How Does Light Scattering Affect Luminescence? Fluorescence Spectra and Quantum Yields in the Solid Form,” *J. Chem. Educ.* **2002**, *79*, 1362–1367.
- Richardson, D. P.; Chang, R. “Lecture Demonstrations of Fluorescence and Phosphorescence,” *Chem. Educator* **2007**, *12*, 272–274.
- Seixas de Melo, J. S.; Cabral, C.; Burrows, H. D. “Photochemistry and Photophysics in the Laboratory. Showing the Role of Radiationless and Radiative Decay of Excited States,” *Chem. Educator* **2007**, *12*, 1–6.
- Sheffield, M. C.; Nahir, T. M. “Analysis of Selenium in Brazil Nuts by Microwave Digestion and Fluorescence Detection,” *J. Chem. Educ.* **2002**, *79*, 1345–1347.

Signal Averaging

- Blitz, J. P.; Klarup, D. G. “Signal-to-Noise Ratio, Signal Processing, and Spectral Information in the Instrumental Analysis Laboratory,” *J. Chem. Educ.* **2002**, *79*, 1358–1360.
- Stolzberg, R. J. “Introduction to Signals and Noise in an Instrumental Method Course,” *J. Chem. Educ.* **1983**, *60*, 171–172.
- Tardy, D. C. “Signal Averaging. A Signal-to-Noise Enhancement Experiment for the Advanced Chemistry Laboratory,” *J. Chem. Educ.* **1986**, *63*, 648–650.

The following sources provide additional information on spectroscopy in the following areas: general spectroscopy, Beer’s law, instrumentation, Fourier transforms, , IR spectroscopy, atomic absorption and emission, luminescence, and applications.

General Spectroscopy

- Ball, D. W. “Units! Units! Units!” *Spectroscopy* **1995**, *10(8)*, 44–47.
- *A History of Analytical Chemistry*, Laitinen, H. A.; Ewing, G. W, Eds. The Division of Analytical Chemistry of the American Chemical Society: Washington, D. C., 1977, p103–243.
- Ingle, J. D.; Crouch, S. R. *Spectrochemical Analysis*, Prentice Hall, Englewood Cliffs, N. J.; 1988.
- Macomber, R. S. “A Unifying Approach to Absorption Spectroscopy at the Undergraduate Level,” *J. Chem. Educ.* **1997**, *74*, 65–67.
- Orchin, M.; Jaffe, H. H. *Symmetry, Orbitals and Spectra*, Wiley-Interscience: New York, 1971.
- Thomas, N. C. “The Early History of Spectroscopy,” *J. Chem. Educ.* **1991**, *68*, 631–633.

Beer’s Law

- Lykos, P. “The Beer-Lambert Law Revisited: A Development without Calculus,” *J. Chem. Educ.* **1992**, *69*, 730–732.
- Ricci, R. W.; Ditzler, M. A.; Nestor, L. P. “Discovering the Beer-Lambert Law,” *J. Chem. Educ.* **1994**, *71*, 983–985.

Instrumentation

- Altermose, I. R. “Evolution of Instrumentation for UV-Visible Spectrophotometry: Part I,” *J. Chem. Educ.* **1986**, *63*, A216–A223.
- Altermose, I. R. “Evolution of Instrumentation for UV-Visible Spectrophotometry: Part II,” *J. Chem. Educ.* **1986**, *63*, A262–A266.
- Grossman, W. E. L. “The Optical Characteristics and Production of Diffraction Gratings,” *J. Chem. Educ.* **1993**, *70*, 741–748.
- Jones, D. G. “Photodiode Array Detectors in UV-Vis Spectroscopy: Part I,” *Anal. Chem.* **1985**, *57*, 1057A–1073A.
- Jones, D. G. “Photodiode Array Detectors in UV-Vis Spectroscopy: Part II,” *Anal. Chem.* **1985**, 11, 1207A–1214A.
- Palmer, C. “Diffraction Gratings,” *Spectroscopy*, **1995**, *10(2)*, 14–15.

Fourier Transforms

- Bracewell, R. N. “The Fourier Transform,” *Sci. American* **1989**, *260(6)*, 85–95.
- Glasser, L. “Fourier Transforms for Chemists: Part I. Introduction to the Fourier Transform,” *J. Chem. Educ.* **1987**, *64*, A228–A233.
- Glasser, L. “Fourier Transforms for Chemists: Part II. Fourier Transforms in Chemistry and Spectroscopy,” *J. Chem. Educ.* **1987**, *64*, A260–A266.
- Glasser, L. “Fourier Transforms for Chemists: Part III. Fourier Transforms in Data Treatment,” *J. Chem. Educ.* **1987**, *64*, A306–A313.
- Graff, D. K. “Fourier and Hadamard: Transforms in Spectroscopy,” *J. Chem. Educ.* **1995**, *72*, 304–309.
- Griffiths, P. R. *Chemical Fourier Transform Spectroscopy*, Wiley-Interscience: New York, 1975.
- *Transform Techniques in Chemistry*, Griffiths, P. R. Ed., Plenum Press: New York, 1978.
- Perkins, W. E. “Fourier Transform Infrared Spectroscopy: Part I. Instrumentation,” *J. Chem. Educ.* **1986**, *63*, A5–A10.
- Perkins, W. E. “Fourier Transform Infrared Spectroscopy: Part II. Advantages of FT-IR,” *J. Chem. Educ.* **1987**, *64*, A269–A271.
- Perkins, W. E. “Fourier Transform Infrared Spectroscopy: Part III. Applications,” *J. Chem. Educ.* **1987**, *64*, A296–A305.
- Strong III, F. C. “How the Fourier Transform Infrared Spectrophotometer Works,” *J. Chem. Educ.* **1979**, *56*, 681–684.

IR Spectroscopy

- *Optical Spectroscopy: Sampling Techniques Manual*, Harrick Scientific Corporation: Ossining, N. Y., 1987.
- Leyden, D. E.; Shreedhara Murthy, R. S. “Surface-Selective Sampling Techniques in Fourier Transform Infrared Spectroscopy,” *Spectroscopy* **1987**, *2(2)*, 28–36.
- Porro, T. J.; Pattacini, S. C. “Sample Handling for Mid-Infrared Spectroscopy, Part I: Solid and Liquid Sampling,” *Spectroscopy* **1993**, *8(7)*, 40–47.
- Porro, T. J.; Pattacini, S. C. “Sample Handling for Mid-Infrared Spectroscopy, Part II: Specialized Techniques,” *Spectroscopy* **1993**, *8(8)*, 39–44.

Atomic Absorption and Emission

- Blades, M. W.; Weir, D. G. “Fundamental Studies of the Inductively Coupled Plasma,” *Spectroscopy* **1994**, *9*, 14–21.
- Greenfield, S. “Invention of the Annular Inductively Coupled Plasma as a Spectroscopic Source,” *J. Chem. Educ.* **2000**, *77*, 584–591.
- Hieftje, G. M. “Atomic Absorption Spectrometry - Has it Gone or Where is it Going?” *J. Anal. At. Spectrom.* **1989**, *4*, 117–122.
- Jarrell, R. F. “A Brief History of Atomic Emission Spectrochemical Analysis, 1666-1950,” *J. Chem. Educ.* **2000**, *77*, 573–576
- Koirtyohann, S. R. “A History of Atomic Absorption Spectrometry From an Academic Perspective,” *Anal. Chem.* **1991**, *63*, 1024A–1031A.
- L’Vov, B. V. “Graphite Furnace Atomic Absorption Spectrometry,” *Anal. Chem.* **1991**, *63*, 924A–931A.
- Slavin, W. “A Comparison of Atomic Spectroscopic Analytical Techniques,” *Spectroscopy*, **1991**, *6*, 16–21.
- Van Loon, J. C. *Analytical Atomic Absorption Spectroscopy*, Academic Press: New York, 1980.
- Walsh, A. “The Development of Atomic Absorption Methods of Elemental Analysis 1952-1962,” *Anal. Chem.* **1991**, *63*, 933A–941A.
- Welz, B. *Atomic Absorption Spectroscopy*, VCH: Deerfield Beach, FL, 1985.

Luminescence Spectroscopy

- Guilbault, G. G. *Practical Fluorescence*, Decker: New York, 1990.

- Schenk, G. “Historical Overview of Fluorescence Analysis to 1980,” *Spectroscopy* **1997**, *12*, 47–56.
- Vo-Dinh, T. *Room-Temperature Phosphorimetry for Chemical Analysis*, Wiley-Interscience: New York, 1984.
- Winefordner, J. D.; Schulman, S. G.; O’Haver, T. C. *Luminescence Spectroscopy in Analytical Chemistry*, Wiley-Interscience: New York, 1969.

Applications

- *Trace Analysis and Spectroscopic Methods for Molecules*, Christian, G. D.; Callis, J. B. Eds., Wiley-Interscience: New York, 1986.
- Vandecasteele, C.; Block, C. B. *Modern Methods for Trace Element Determination*, Wiley: Chichester, England, 1994.
- Skoog, D. A.; Holler, F. J.; Nieman, T. A. *Principles of Instrumental Analysis*, Saunders: Philadelphia, 1998.
- Van Loon, J. C. *Selected Methods of Trace Metal Analysis: Biological and Environmental Samples*, Wiley-Interscience: New York, 1985.

Gathered here are resources and experiments for analyzing multicomponent samples using mathematical techniques not covered in this textbook.

- Aberasturi, F.; Jimenez, A. I.; Jimenez, F.; Arias, J. J. “UV-Visible First-Derivative Spectrophotometry Applied to an Analysis of a Vitamin Mixture,” *J. Chem. Educ.* **2001**, *78*, 793–795.
- Afkhami, A.; Abbasi-Tarighat, M.; Bahram, M.; Abdollahi, H. “A new strategy for solving matrix effect in multivariate calibration standard addition data using combination of H-point curve isolation and H-point standard addition methods,” *Anal. Chim. Acta* **2008**, *613*, 144–151.
- Brown, C. W.; Obremski, R. J. “Multicomponent Quantitative Analysis,” *Appl. Spectrosc. Rev.* **1984**, *20*, 373–418.
- Charles, M. J.; Martin, N. W.; Msimanga, H. Z. “Simultaneous Determination of Aspirin, Salicylamide, and Caffeine in Pain Relievers by Target Factor Analysis,” *J. Chem. Educ.* **1997**, *74*, 1114–1117.
- Dado, G.; Rosenthal, J. “Simultaneous Determination of Cobalt, Copper, and Nickel by Multivariate Linear Regression,” *J. Chem. Educ.* **1990**, *67*, 797–800.
- DiTusa, M. R.; Schilt, A. A. “Selection of Wavelengths for Optimum Precision in Simultaneous Spectrophotometric Determinations,” *J. Chem. Educ.* **1985**, *62*, 541–542.
- Gómez, D. G.; de la Peña, A. M.; Mansilla, A. E.; Olivieri, A. C. “Spectrophotometric Analysis of Mixtures by Classical Least-Squares Calibration: An Advanced Experiment Introducing MATLAB,” *Chem. Educator* **2003**, *8*, 187–191.
- Harvey, D. T.; Bowman, A. “Factor Analysis of Multicomponent Samples,” *J. Chem. Educ.* **1990**, *67*, 470–472.
- Lucio-Gutierrez, J. R.; Salazar-Cavazos, M. L.; de Torres, N. W. “Chemometrics in the Teaching Lab. Quantification of a Ternary Mixture of Common Pharmaceuticals by First- and Second-Derivative IR Spectroscopy,” *Chem. Educator* **2004**, *9*, 234–238.
- Padney, S.; McHale, M. E. R.; Coym, K. S.; Acree Jr., W. E. “Bilinear Regression Analysis as a Means to Reduce Matrix Effects in Simultaneous Spectrophotometric Determination of Cr(III) and Co(II),” *J. Chem. Educ.* **1998**, *75*, 878–880.
- Raymond, M.; Jochum, C.; Kowalski, B. R. “Optimal Multicomponent Analysis Using the Generalized Standard Addition Method,” *J. Chem. Educ.* **1983**, *60*, 1072–1073.
- Ribone, M. E.; Pagani, A. P.; Olivieri, A. C.; Goicoechea, H. C. “Determination of the Active Principle in a Spectrophotometry and Principal Component Regression Analysis,” *J. Chem. Educ.* **2000**, *77*, 1330–1333.
- Rojas, F. S.; Ojeda, C. B. “Recent developments in derivative ultraviolet/visible absorption spectrophotometry: 2004-2008,” *Anal. Chim. Acta* **2009**, *635*, 22–44.

Chapter 11

The following set of experiments introduce students to the applications of electrochemistry. Experiments are grouped into four categories: general electrochemistry, preparation of electrodes, potentiometry, coulometry, and voltammetry and amperometry.

General Electrochemistry

- Mills, K. V.; Herrick, R. S.; Guilmette, L. W.; Nestor, L. P.; Shafer, H.; Ditzler, M. A. “Introducing Undergraduate Students to Electrochemistry: A Two-Week Discovery Chemistry Experiment,” J. Chem. Educ. 2008, 85, 1116–119.

Preparation of Electrodes

- Christopoulos, T. K.; Diamandis, E. P. “Use of a Sintered Glass Crucible for Easy Construction of Liquid-Membrane Ion-Selective Electrodes,” *J. Chem. Educ.* **1988**, *65*, 648.
- Fricke, G. H.; Kuntz, M. J. “Inexpensive Solid-State Ion-Selective Electrodes for Student Use,” *J. Chem. Educ.* **1977**, *54*, 517–520.
- Inamdar, S. N.; Bhat, M. A.; Haram, S. K. “Construction of Ag/AgCl Reference Electrode form Used Felt-Tipped Pen Barrel for Undergraduate Laboratory,” *J. Chem. Educ.* **2009**, *86*, 355–356.
- Lloyd, B. W.; O’Brien, F. L.; Wilson, W. D. “Student Preparation and Analysis of Chloride and Calcium Ion Selective Electrodes,” *J. Chem. Educ.* **1976**, *53*, 328–330.
- Mifflin, T. E.; Andriano, K. M.; Robbins, W. B. “Determination of Penicillin Using an Immobilized Enzyme Electrode,” *J. Chem. Educ.* **1984**, *61*, 638–639.
- Palanivel, A.; Riyazuddin, P. “Fabrication of an Inexpensive Ion-Selective Electrode,” *J. Chem. Educ.* **1984**, *61*, 290.
- Ramaley, L; Wedge, P. J.; Crain, S. M. “Inexpensive Instrumental Analysis: Part 1. Ion-Selective Electrodes,” *J. Chem. Educ.* **1994**, *71*, 164–167.
- Selig, W. S. “Potentiometric Titrations Using Pencil and Graphite Sensors,” *J. Chem. Educ.* **1984**, *61*, 80–81.

Potentiometry

- Chan, W. H; Wong, M. S.; Yip, C. W. “Ion-Selective Electrode in Organic Analysis: A Salicylate Electrode,” *J. Chem. Educ.* **1986**, *63*, 915–916.
- Harris, T. M. “Potentiometric Measurement in a Freshwater Aquarium,” *J. Chem. Educ.* **1993**, *70*, 340–341.
- Kauffman, C. A.; Muza, A. L.; Porambo, M. W.; Marsh, A. L. “Use of a Commercial Silver-Silver Chloride Electrode for the Measurement of Cell Potentials to Determine Mean Ionic Activity Coefficients,” *Chem. Educator* **2010**, *15*, 178–180.
- Martínez-Fàbregas, E.; Alegret, S. “A Practical Approach to Chemical Sensors through Potentiometric Transducers: Determination of Urea in Serum by Means of a Biosensor,” *J. Chem. Educ.* **1994**, *71*, A67–A70.
- Moresco, H.; Sansón, P.; Seoane, G. “Simple Potentiometric Determination of Reducing Sugars,” *J. Chem. Educ.* **2008**, *85*, 1091–1093.
- Radic, N.; Komijenovic, J. “Potentiometric Determination of an Overall Formation Constant Using an Ion-Selective Membrane Electrode,” *J. Chem. Educ.* **1993**, *70*, 509–511.
- Riyazuddin, P.; Devika, D. “Potentiometric Acid–Base Titrations with Activated Graphite Electrodes,” *J. Chem. Educ.* **1997**, *74*, 1198–1199.

Coulometry

- Bertotti, M.; Vaz, J. M.; Telles, R. “Ascorbic Acid Determination in Natural Orange Juice,” *J. Chem. Educ.* **1995**, *72*, 445–447.
- Kalbus, G. E.; Lieu, V. T. “Dietary Fat and Health: An Experiment on the Determination of Iodine Number of Fats and Oils by Coulometric Titration,” *J. Chem. Educ.* **1991**, *68*, 64–65.
- Lötz, A. “A Variety of Electrochemical Methods in a Coulometric Titration Experiment,” *J. Chem. Educ.* **1998**, *75*, 775–777.
- Swim, J.; Earps, E.; Reed, L. M.; Paul, D. “Constant-Current Coulometric Titration of Hydrochloric Acid,” *J. Chem. Educ.* **1996**, *73*, 679–683.

Voltammetry and Amperometry

- Blanco-López, M. C.; Lobo-Castañón, M. J.; Miranda-Ordieres, A. J. “Homemade Bienzymatic-Amperometric Biosensor for Beverages Analysis,” *J. Chem. Educ.* **2007**, *84*, 677–680.
- García-Armada, P.; Losada, J.; de Vicente-Pérez, S. “Cation Analysis Scheme by Differential Pulse Polarography,” *J. Chem. Educ.* **1996**, *73*, 544–547.
- Herrera-Melián, J. A.; Doña-Rodríguez, J. M.; Hernández-Brito, J.; Pérez-Peña, J. “Voltammetric Determination of Ni and Co in Water Samples,” *J. Chem. Educ.* **1997**, *74*, 1444–1445.
- King, D.; Friend, J.; Kariuki, J. “Measuring Vitamin C Content of Commercial Orange Juice Using a Pencil Lead Electrode,” *J. Chem. Educ.* **2010**, *87*, 507–509.
- Marin, D.; Mendicuti, F. “Polarographic Determination of Composition and Thermodynamic Stability Constant of a Complex Metal Ion,” *J. Chem. Educ.* **1988**, *65*, 916–918.
- Sadik, O. A.; Brenda, S.; Joasil, P.; Lord, J. “Electropolymerized Conducting Polymers as Glucose Sensors,” *J. Chem. Educ.* **1999**, *76*, 967–970.

- Sittampalam, G.; Wilson, G. S. “Amperometric Determination of Glucose at Parts Per Million Levels with Immobilized Glucose Oxidase,” *J. Chem. Educ.* **1982**, *59*, 70–73.
- Town, J. L.; MacLaren, F.; Dewald, H. D. “Rotating Disk Voltammetry Experiment,” *J. Chem. Educ.* **1991**, *68*, 352–354.
- Wang, J. “Sensitive Electroanalysis Using Solid Electrodes,” *J. Chem. Educ.* **1982**, *59*, 691–692.
- Wang, J. “Anodic Stripping Voltammetry,” *J. Chem. Educ.* **1983**, *60*, 1074–1075.
- Wang, J.; Maccà, C. “Use of Blood-Glucose Test Strips for Introducing Enzyme Electrodes and Modern Biosensors,” *J. Chem. Educ.* **1996**, *73*, 797–800.
- Wang, Q.; Geiger, A.; Frias, R; Golden, T. D. “An Introduction to Electrochemistry for Undergraduates: Detection of Vitamin C (Ascorbic Acid) by Inexpensive Electrode Sensors,” *Chem. Educator* **2000**, *5*, 58–60.

The following general references providing a broad introduction to electrochemistry.

- Adams, R. N. *Electrochemistry at Solid Surfaces*, Marcel Dekker: New York, 1969.
- Bard, A. J.; Faulkner, L. R. *Electrochemical Methods*, Wiley: New York, 1980.
- Faulkner, L. R. “Electrochemical Characterization of Chemical Systems” in Kuwana, T. E., ed. *Physical Methods in Modern Chemical Analysis*, Vol. 3, Academic Press: New York, 1983, pp. 137–248.
- Kissinger, P. T.; Heineman, W. R. *Laboratory Techniques in Electroanalytical Chemistry*, Marcel Dekker: New York, 1984.
- Lingane, J. J. *Electroanalytical Chemistry*, 2nd Ed., Interscience: New York, 1958.
- Sawyer, D. T.; Roberts, J. L., Jr. *Experimental Electrochemistry for Chemists*, Wiley-Interscience: New York, 1974.
- Vassos, B. H.; Ewing, G. W. *Electroanalytical Chemistry*, Wiley-Interscience: New York, 1983.

These short articles provide a good introduction to important principles of electrochemistry.

- Faulkner, L. R. “Understanding Electrochemistry: Some Distinctive Concepts,” *J. Chem. Educ.* **1983**, *60*, 262–264.
- Huddle, P. A.; White, M. D.; Rogers, F. “Using a Teaching Model to Correct Known Misconceptions in Electrochemistry,” *J. Chem. Educ.* **2000**, *77*, 104–110.
- Maloy, J. T. “Factors Affecting the Shape of Current-Potential Curves,” *J. Chem. Educ.* **1983**, *60*, 285–289.
- Thompson, R. Q.; Craig, N. C. “Unified Electroanalytical Chemistry: Application of the Concept of Equilibrium,” *J. Chem. Educ.* **2001**, *78*, 928–934.
- Zoski, C. G. “Charging Current Discrimination in Analytical Voltammetry,” *J. Chem. Educ.* **1986**, *63*, 910–914.

Additional information on potentiometry and ion-selective electrodes can be found in the following sources.

- Bakker, E.; Diamond, D.; Lewenstam, A.; Pretsch, E. “Ions Sensors: Current Limits and New Trends,” *Anal. Chim. Acta* **1999**, *393*, 11–18.
- Bates, R. G. *Determination of pH: Theory and Practice*, 2nd ed., Wiley: New York, 1973.
- Buck, R. P. “Potentiometry: pH Measurements and Ion Selective Electrodes” in Weissberger, A., ed. *Physical Methods of Organic Chemistry*, Vol. 1, Part IIA, Wiley: New York, 1971, pp. 61–162.
- Cammann, K. *Working With Ion-Selective Electrodes*, Springer-Verlag: Berlin, 1977.
- Evans, A. *Potentiometry and Ion-Selective Electrodes*, Wiley: New York, 1987.
- Frant, M. S. “Where Did Ion Selective Electrodes Come From?” *J. Chem. Educ.* **1997**, *74*, 159–166.
- Light, T. S. “Industrial Use and Application of Ion-Selective Electrodes,” *J. Chem. Educ.* **1997**, *74*, 171–177.
- Rechnitz, G. A. “Ion and Bio-Selective Membrane Electrodes,” *J. Chem. Educ.* **1983**, *60*, 282–284.
- Ruzicka, J. “The Seventies—Golden Age for Ion-Selective Electrodes,” *J. Chem. Educ.* **1997**, *74*, 167–170.
- Young, C. C. “Evolution of Blood Chemistry Analyzers Based on Ion Selective Electrodes,” *J. Chem. Educ.* **1997**, *74*, 177–182.

The following sources provide additional information on electrochemical biosensors.

- Alvarez-Icasa, M.; Bilitewski, U. “Mass Production of Biosensors,” *Anal. Chem.* **1993**, *65*, 525A–533A.
- Meyerhoff, M. E.; Fu, B.; Bakker, E. Yun, J-H; Yang, V. C. “Polyion-Sensititve Membrane Electrodes for Biomedical Analysis,” *Anal. Chem.* **1996**, *68*, 168A–175A.
- Nicolini, C.; Adami, M; Antolini, F.; Beltram, F.; Sartore, M.; Vakula, S. “Biosensors: A Step to Bioelectronics,” *Phys. World*, May 1992, 30–34.
- Rogers, K. R.; Williams. L. R. “Biosensors for Environmental Monitoring: A Regulatory Perspective,” *Trends Anal. Chem.* **1995**, *14*, 289–294.

- Schultz, J. S. “Biosensors,” *Sci. Am.* August 1991, 64–69.
- Thompson, M.; Krull, U. “Biosensors and the Transduction of Molecular Recognition,” *Anal. Chem.* **1991**, *63*, 393A–405A.
- Vadgama, P. “Designing Biosensors,” *Chem. Brit.* **1992**, *28*, 249–252.

A good source covering the clinical application of electrochemistry is listed below.

- Wang, J. *Electroanalytical Techniques in Clinical Chemistry and Laboratory Medicine*, VCH: New York, 1998.

Coulometry is covered in the following texts.

- Rechnitz, G. A. *Controlled-Potential Analysis*, Macmillan: New York, 1963.
- Milner, G. W. C.; Philips, G. *Coulometry in Analytical Chemistry*, Pergamon: New York, 1967.

For a description of electrogravimetry, see the following resource.

- Tanaka, N. “Electrodeposition”, in Kolthoff, I. M.; Elving, P. J., eds. *Treatise on Analytical Chemistry, Part I: Theory and Practice*, Vol. 4, Interscience: New York, 1963.

The following sources provide additional information on polarography and pulse polarography.

- Flato, J. B. “The Renaissance in Polarographic and Voltammetric Analysis,” *Anal. Chem.* **1972**, *44(11)*, 75A–87A.
- Kolthoff, I. M.; Lingane, J. J. *Polarography*, Interscience: New York, 1952.
- Osteryoung, J. “Pulse Voltammetry,” *J. Chem. Educ.* **1983**, *60*, 296–298.

Additional Information on stripping voltammetry is available in the following text.

- Wang, J. *Stripping Analysis*, VCH Publishers: Deerfield Beach, FL, 1985.

The following papers discuss the numerical simulation of voltammetry.

- Bozzini, B. “A Simple Numerical Procedure for the Simulation of “Lifelike” Linear-Sweep Voltammograms,” *J. Chem. Educ.* **2000**, *77*, 100–103.
- Howard, E.; Cassidy, J. “Analysis with Microelectrodes Using Microsoft Excel Solver,” *J. Chem. Educ.* **2000**, *77*, 409–411.

Gathered together here are many useful resources for cyclic voltammetry, including experiments.

- Carriedo, G. A. “The Use of Cyclic Voltammetry in the Study of the Chemistry of Metal–Carbonyls,” *J. Chem. Educ.* **1988**, *65*, 1020–1022.
- García-Jareño, J. J.; Benito, D.; Navarro-Laboulais, J.; Vicente, F. “Electrochemical Behavior of Electrodeposited Prussian Blue Films on ITO Electrodes,” *J. Chem. Educ.* **1998**, *75*, 881–884.
- Gilles de Pelichy, L. D.; Smith, E. T. “A Study of the Oxidation Pathway of Adrenaline by Cyclic Voltammetry,” *Chem. Educator* **1997**, *2(2)*, 1–13.
- Gomez, M. E.; Kaifer, A. E. “Voltammetric Behavior of a Ferrocene Derivative,” *J. Chem. Educ.* **1992**, *69*, 502–505.
- Heffner, J. E.; Raber, J. C.; Moe, O. A.; Wigal, C. T. “Using Cyclic Voltammetry and Molecular Modeling to Determine Substituent Effects in the One-Electron Reduction of Benzoquinones,” *J. Chem. Educ.* **1998**, *75*, 365–367.
- Heinze, J. “Cyclic Voltammetry—Electrochemical Spectroscopy,” *Angew. Chem, Int. Ed. Eng.* **1984**, *23*, 831–918.
- Holder, G. N.; Farrar, D. G.; McClure, L. L. “Voltammetric Reductions of Ring-Substituted Acetophenones. 1. Determination of an Electron-Transfer Mechanism Using Cyclic Voltammetry and Computer Modeling: The Formation and Fate of a Radical Anion,” *Chem. Educator* **2001**, *6*, 343–349.
- Ibanez, J. G.; Gonzalez, I.; Cardenas, M. A. “The Effect of Complex Formation Upon the Redox Potentials of Metal Ions: Cyclic Voltammetry Experiments,” *J. Chem. Educ.* **1988**, *65*, 173–175.
- Ito, T.; Perara, D. M. N. T.; Nagasaka, S. “Gold Electrodes Modified with Self-Assembled Monolayers for Measuring L-Ascobric acid,” *J. Chem. Educ.* **2008**, *85*, 1112–1115.
- Kissinger, P. T.; Heineman, W. R. “Cyclic Voltammetry,” *J. Chem. Educ.* **1983**, *60*, 702–706.
- Mabbott, G. A. “An Introduction to Cyclic Voltammetry,” *J. Chem. Educ.* **1983**, *60*, 697–702.
- Petrovic, S. “Cyclic Voltammetry of Hexachloroiridate (IV): An Alternative to the Electrochemical Study of the Ferricyanide Ion,” *Chem. Educator* **2000**, *5*, 231–235.

- Toma, H. E.; Araki, K.; Dovidauskas, S. “A Cyclic Voltammetry Experiment Illustrating Redox Potentials, Equilibrium Constants and Substitution Reaction in Coordination Chemistry,” *J. Chem. Educ.* **2000**, *77*, 1351–1353.
- Walczak, M. W.; Dryer, D. A.; Jacobson, D. D,; Foss, M. G.; Flynn, N. T. “pH-Dependent Redox Couple: Illustrating the Nernst Equation Using Cyclic Voltammetry,” *J. Chem. Educ.* **1997**, *74*, 1195–1197.

Chapter 12

The following set of experiments introduce students to the applications of chromatography and electrophoresis. Experiments are grouped into five categories: gas chromatography, high-performance liquid chromatography, ion-exchange chromatography, size-exclusion chromatography, and electrophoresis.

Gas Chromatography

- Bishop, R. D., Jr. “Using GC–MS to Determine Relative Reactivity Ratios,” *J. Chem. Educ.* **1995**, *72*, 743–745.
- Elderd, D. M.; Kildahl, N. K.; Berka, L. H. “Experiments for Modern Introductory Chemistry: Identification of Arson Accelerants by Gas Chromatography,” *J. Chem. Educ.* **1996**, *73*, 675–677.
- Fleurat-Lessard, P.; Pointet, K.; Renou-Gonnord, M.-F. “Quantitative Determination of PAHs in Diesel Engine Exhausts by GC–MS,” *J. Chem. Educ.* **1999**, *76*, 962–965.
- Galipo, R. C.; Canhoto, A. J.; Walla, M. D.; Morgan, S. L. “Analysis of Volatile Fragrance and Flavor Compounds by Headspace Solid Phase Microextraction and GC–MS,” *J. Chem. Educ.* **1999**, *76*, 245–248.
- Graham, R. C.; Robertson, J. K. “Analysis of Trihalomethanes in Soft Drinks,” *J. Chem. Educ.* **1988**, *65*, 735–737.
- Heinzen, H.; Moyan, P.; Grompone, A. “Gas Chromatographic Determination of Fatty Acid Compositions,” *J. Chem. Educ.* **1985**, *62*, 449–450.
- Kegley, S. E.; Hansen, K. J.; Cunningham, K. L. “Determination of Polychlorinated Biphenyls (PCBs) in River and Bay Sediments,” *J. Chem. Educ.* **1996**, *73*, 558–562.
- Kostecka, K. S.; Rabah, A.; Palmer, C. F., Jr. “GC/MS Analysis of the Aromatic Composition of Gasoline,” *J. Chem. Educ.* **1995**, *72*, 853–854.
- Quach, D. T.; Ciszkowski, N. A.; Finlayson-Pitts, B. J. “A New GC-MS Experiment for the Undergraduate Instrumental Analysis Laboratory in Environmental Chemistry: Methyl-t-butyl Ether and Benzene in Gasoline,” *J. Chem. Educ.* **1998**, *75*, 1595–1598.
- Ramachandran, B. R.; Allen, J. M.; Halpern, A. M. “Air–Water Partitioning of Environmentally Important Organic Compounds,” *J. Chem. Educ.* **1996**, *73*, 1058–1061.
- Rice, G. W. “Determination of Impurities in Whiskey Using Internal Standard Techniques,” *J. Chem. Educ.* **1987**, *64*, 1055–1056.
- Rubinson, J. F.; Neyer-Hilvert, J. “Integration of GC-MS Instrumentation into the Undergraduate Laboratory: Separation and Identification of Fatty Acids in Commercial Fats and Oils,” *J. Chem. Educ.* **1997**, *74*, 1106–1108.
- Rudzinski, W. E.; Beu, S. “Gas Chromatographic Determination of Environmentally Significant Pesticides,” *J. Chem. Educ.* **1982**, *59*, 614–615.
- Sobel, R. M.; Ballantine, D. S.; Ryzhov, V. “Quantitation of Phenol Levels in Oil of Wintergreen Using Gas Chromatography–Mass Spectrometry with Selected Ion Monitoring,” *J. Chem. Educ.* **2005**, *82*, 601–603.
- Welch, W. C.; Greco, T. G. “An Experiment in Manual Multiple Headspace Extraction for Gas Chromatography,” *J. Chem. Educ.* **1993**, *70*, 333–335.
- Williams, K. R.; Pierce, R. E. “The Analysis of Orange Oil and the Aqueous Solubility of d-Limone,” *J. Chem. Educ.* **1998**, *75*, 223–226.
- Wong, J. W.; Ngim, K. K.; Shibamoto, T.; Mabury, S. A.; Eiserich, J. P.; Yeo, H. C. H. “Determination of Formaldehyde in Cigarette Smoke,” *J. Chem. Educ.* **1997**, *74*, 1100–1103.
- Yang, M. J.; Orton, M. L., Pawliszyn, J. “Quantitative Determination of Caffeine in Beverages Using a Combined SPME-GC/MS Method,” *J. Chem. Educ.* **1997**, *74*, 1130–1132.

High-Performance Liquid Chromatography

- Batchelor, J. D.; Jones, B. T. “Determination of the Scoville Heat Value for Hot Sauces and Chilies: An HPLC Experiment,” *J. Chem. Educ.* **2000**, *77*, 266–267.

- Beckers, J. L. “The Determination of Caffeine in Coffee: Sense or Nonsense?” *J. Chem. Educ*. **2004**, *81*, 90–93.
- Betts, T. A. “Pungency Quantitation of Hot Pepper Sauces Using HPLC,” *J. Chem. Educ.* **1999**, *76*, 240–244.
- Bidlingmeyer, B. A.; Schmitz, S. “The Analysis of Artificial Sweeteners and Additives in Beverages by HPLC,” *J. Chem. Educ.* **1991**, *68*, A195–A200.
- Bohman, O.; Engdahl, K.-A.; Johnsson, H. “High Performance Liquid Chromatography of Vitamin A: A Quantitative Determination,” *J. Chem. Educ.* **1982**, *59*, 251–252.
- Brenneman, C. A.; Ebeler, S. E. “Chromatographic Separations Using Solid-Phase Extraction Cartridges: Separation of Wine Phenolics,” *J. Chem. Educ.* **1999**, *76*, 1710–1711.
- Cantwell, F. F.; Brown, D. W. “Liquid Chromatographic Determination of Nitroanilines,” *J. Chem. Educ.* **1981**, *58*, 820–823.
- DiNunzio, J. E. “Determination of Caffeine in Beverages by High Performance Liquid Chromatography,” *J. Chem. Educ.* **1985**, *62*, 446–447.
- Ferguson, G. K. “Quantitative HPLC Analysis of an Analgesic/Caffeine Formulation: Determination of Caffeine,” *J. Chem. Educ.* **1998**, *75*, 467–469.
- Ferguson, G. K. “Quantitative HPLC Analysis of a Psychotherapeutic Medication: Simultaneous Determination of Amitriptyline Hydrochloride and Perphenazine,” *J. Chem. Educ.* **1998**, *75*, 1615–1618.
- Goodney, D. E. “Analysis of Vitamin C by High-Pressure Liquid Chromatography,” *J. Chem. Educ.* **1987**, *64*, 187–188.
- Guevremont, R.; Quigley, M. N. “Determination of Paralytic Shellfish Poisons Using Liquid Chromatography,” *J. Chem. Educ.* **1994**, *71*, 80–81.
- Haddad, P.; Hutchins, S.; Tuffy, M. “High Performance Liquid Chromatography of Some Analgesic Compounds,” *J. Chem. Educ.* **1983**, *60*, 166–168.
- Huang, J.; Mabury, S. A.; Sagebiel, J. C. “Hot Chili Peppers: Extraction, Cleanup, and Measurement of Capscaicin,” *J. Chem. Educ.* **2000**, *77*, 1630–1631.
- Joeseph, S. M.; Palasota, J. A. “The Combined Effect of pH and Percent Methanol on the HPLC Separation of Benzoic Acid and Phenol,” *J. Chem. Educ.* **2001**, *78*, 1381–1383.
- Lehame, S. “The Separation of Copper, Iron, and Cobalt Tetramethylene Dithiocarbamates by HPLC,” *J. Chem. Educ.* **1986**, *63*, 727–728.
- Luo, P.; Luo, M. Z.; Baldwin, R. P. “Determination of Sugars in Food Products,” *J. Chem. Educ*. **1993**, *70*, 679–681.
- Mueller, B. L.; Potts, L. W. “HPLC Analysis of an Asthma Medication,” *J. Chem. Educ.* **1988**, *65*, 905–906.
- Munari, M.; Miurin, M.; Goi, G. “Didactic Application to Riboflavin HPLC Analysis,” *J. Chem. Educ.* **1991**, *68*, 78–79.
- Orth, D. L. “HPLC Determination of Taurine in Sports Drinks,” *J. Chem. Educ.* **2001**, *78*, 791–792.
- Remcho, V. T.; McNair, H. M.; Rasmussen, H. T. “HPLC Method Development with the Photodiode Array Detector,” *J. Chem. Educ.* **1992**, *69*, A117–A119.
- Richardson, W. W., III; Burns, L. “HPLC of the Polypeptides in a Hydrolyzate of Egg-White Lysozyme,” *J. Chem. Educ.* **1988**, *65*, 162–163.
- Silveira, A., Jr.; Koehler, J. A.; Beadel, E. F., Jr.; Monore, P. A. “HPLC Analysis of Chlorophyll a, Chlorophyll b, and β-Carotene in Collard Greens,” *J. Chem. Educ.* **1984**, *61*, 264–265.
- Siturmorang, M.; Lee, M. T. B.; Witzeman, L. K.; Heineman, W. R. “Liquid Chromatography with Electrochemical Detection (LC-EC): An Experiment Using 4-Aminophenol,” *J. Chem. Educ.* **1998**, *75*, 1035–1038.
- Sottofattori, E.; Raggio, R.; Bruno, O. “Milk as a Drug Analysis Medium: HPLC Determination of Isoniazid,” *J. Chem. Educ.* **2003**, *80*, 547–549.
- Strohl, A. N. “A Study of Colas: An HPLC Experiment,” *J. Chem. Educ.* **1985**, *62*, 447–448.
- Tran, C. D.; Dotlich, M. “Enantiomeric Separation of Beta-Blockers by High Performance Liquid Chromatography,” *J. Chem. Educ.* **1995**, *72*, 71–73.
- Van Arman, S. A.; Thomsen, M. W. “HPLC for Undergraduate Introductory Laboratories,” *J. Chem. Educ.* **1997**, *74*, 49–50.
- Wingen, L. M.; Low, J. C.; Finlayson-Pitts, B. J. “Chromatography, Absorption, and Fluorescence: A New Instrumental Analysis Experiment on the Measurement of Polycyclic Aromatic Hydrocarbons in Cigarette Smoke,” *J. Chem. Educ.* **1998**, *75*, 1599–1603.

Ion-Exchange Chromatography

- Bello, M. A.; Gustavo González, A. “Determination of Phosphate in Cola Beverages Using Nonsuppressed Ion Chromatography,” *J. Chem. Educ.* **1996**, *73*, 1174–1176.
- Kieber, R. J.; Jones, S. B. “An Undergraduate Laboratory for the Determination of Sodium, Potassium, and Chloride,” *J. Chem. Educ.* **1994**, *71*, A218–A222.
- Koubek, E.; Stewart, A. E. “The Analysis of Sulfur in Coal,” *J. Chem. Educ.* **1992**, *69*, A146–A148.
- Sinniah, K.; Piers, K. “Ion Chromatography: Analysis of Ions in Pond Water,” *J. Chem. Educ.* **2001**, *78*, 358–362.
- Xia, K.; Pierzynski, G. “Competitive Sorption between Oxalate and Phosphate in Soil: An Environmental Chemistry Laboratory Using Ion Chromatography,” *J. Chem. Educ.* **2003**, *80*, 71–75.

Size-Exchange Chromatography

- Brunauer, L. S.; Davis, K. K. “Size Exclusion Chromatography: An Experiment for High School and Community College Chemistry and Biotechnology Laboratory Programs,” *J. Chem. Educ.* **2008**, *85*, 683–685.
- Saiz, E.; Tarazona, M. P. “Size-Exclusion Chromatography Using Dual Detection,” *Chem. Educator* **2000**, *5*, 324–328.

Electrophoresis

- Almarez, R. T.; Kochis, M. “Microscale Capillary Electrophoresis: A Complete Instrumentation Experiment for Chemistry Students at the Undergraduate Junior or Senior Level,” *J. Chem. Educ.* **2003**, *80*, 316–319.
- Beckers, J. L. “The Determination of Caffeine in Coffee: Sense or Nonsense?” *J. Chem. Educ.* **2004**, *81*, 90–93.
- Beckers, J. L. “The Determination of Vanillin in a Vanilla Extract,” *J. Chem. Educ.* **2005**, *82*, 604–606.
- Boyce, M. “Separation and Quantification of Simple Ions by Capillary Zone Electrophoresis,” *J. Chem. Educ.* **1999**, *76*, 815–819.
- Conradi, S.; Vogt, C.; Rohde, E. “Separation of Enatiomeric Barbiturates by Capillary Electrophoresis Using a Cyclodextrin-Containing Run Buffer,” *J. Chem. Educ.* **1997**, *74*, 1122–1125.
- Conte, E. D.; Barry, E. F.; Rubinstein, H. “Determination of Caffeine in Beverages by Capillary Zone Electrophoresis,” *J. Chem. Educ.* **1996**, *73*, 1169–1170.
- Demay, S.; Martin-Girardeau, A.; Gonnord, M.-F. “Capillary Electrophoretic Quantitative Analysis of Anions in Drinking Water,” *J. Chem. Educ.* **1999**, *76*, 812–815.
- Emry, R.; Cutright, R. D.; Wright, J.; Markwell, J. “Candies to Dye for: Cooperative, Open-Ended Student Activities to Promote Understanding of Electrophoretic Fractionation,” *J. Chem. Educ.* **2000**, *77*, 1323–1324.
- Gardner, W. P.; Girard, J. E. “Analysis of Common Household Cleaner-Disinfectants by Capillary Electrophoresis,” *J. Chem. Educ.* **2000**, *77*, 1335–1338.
- Gruenhagen, J. A.; Delaware, D.; Ma, Y. “Quantitative Analysis of Non-UV-Absorbing Cations in Soil Samples by High-Performance Capillary Electrophoresis,” *J. Chem. Educ.* **2000**, *77*, 1613–1616.
- Hage, D. S.; Chattopadhyay, A.; Wolfe, C. A. C.; Grundman, J.; Kelter, P. B. “Determination of Nitrate and Nitrite in Water by Capillary Electrophoresis,” *J. Chem. Educ.* **1998**, *75*, 1588–1590.
- Herman, H. B.; Jezorek, J. R.; Tang, Z. “Analysis of Diet Tonic Water Using Capillary Electrophoresis,” *J. Chem. Educ.* **2000**, *77*, 743–744.
- Janusa, M. A.; Andermann, L. J.; Kliebert, N. M.; Nannie, M. H. “Determination of Chloride Concentration Using Capillary Electrophoresis,” *J. Chem. Educ.* **1998**, *75*, 1463–1465.
- McDevitt, V. L.; Rodríguez, A.; Williams, K. R. “Analysis of Soft Drinks: UV Spectrophotometry, Liquid Chromatography, and Capillary Electrophoresis,” *J. Chem. Educ.* **1998**, *75*, 625–629.
- Palmer, C. P. “Demonstrating Chemical and Analytical Concepts in the Undergraduate Laboratory Using Capillary Electrophoresis and Micellar Electrokinetic Chromatography,” *J. Chem. Educ.* **1999**, *76*, 1542–1543.
- Pursell, C. J.; Chandler, B.; Bushey, M. M. “Capillary Electrophoresis Analysis of Cations in Water Samples,” *J. Chem. Educ.* **2004**, *81*, 1783–1786.
- Solow, M. “Weak Acid pK_a Determination Using Capillary Zone Electrophoresis,” *J. Chem. Educ.* **2006**, *83*, 1194–1195.
- Thompson, L.; Veening, H.; Strain, T. G. “Capillary Electrophoresis in the Undergraduate Instrumental Analysis Laboratory: Determination of Common Analgesic Formulations,” *J. Chem. Educ.* **1997**, *74*, 1117–1121.
- Vogt, C.; Conradi, S.; Rhode, E. “Determination of Caffeine and Other Purine Compounds in Food and Pharmaceuticals by Micellar Electrokinetic Chromatography” *J. Chem. Educ.* **1997**, *74*, 1126–1130.

- Weber, P. L.; Buck, D. R. “Capillary Electrophoresis: A Fast and Simple Method for the Determination of the Amino Acid Composition of Proteins,” *J. Chem. Educ.* **1994**, *71*, 609–612.
- Welder, F.; Colyer, C. L. “Using Capillary Electrophoresis to Determine the Purity of Acetylsalicylic Acid Synthesized in the Undergraduate Laboratory,” *J. Chem. Educ.* **2001**, *78*, 1525–1527.
- Williams, K. R.; Adhyaru, B.; German, I.; Russell, T. “Determination of a Diffusion Coefficient by Capillary Electrophoresis,” *J. Chem. Educ.* **2002**, *79*, 1475–1476.

The following texts provide a good introduction to the broad field of separations, including chromatography and electrophoresis.

- Giddings, J. C. *Unified Separation Science*, Wiley-Interscience: New York 1991.
- Karger, B. L.; Snyder, L. R.; Harvath, C. *An Introduction to Separation Science*, Wiley-Interscience: New York, 1973
- Miller, J. M. *Separation Methods in Chemical Analysis*, Wiley-Interscience: New York, 1975.
- Poole, C. F. *The Essence of Chromatography*, Elsevier: Amsterdam, 2003.

A more recent discussion of peak capacity is presented in the following paper.

- Davis, J. M.; Stoll, D. R.; Carr, P. W. “Dependence of Effective Peak Capacity in Comprehensive Two-Dimensional Separations on the Distribution of Peak Capacity between the Two Dimensions,” *Anal. Chem.* **2008**, *80*, 8122–8134.
- Li, X.; Stoll, D. R.; Carr, P. W. “Equation for Peak Capacity Estimation in Two-Dimensional Liquid Chromatography,” *Anal. Chem.* **2009**, *81*, 845–850.
- Shen, Y.; Lee, M. “General Equation for Peak Capacity in Column Chromatography,” *Anal. Chem.* **1998**, *70*, 3853–3856.

The following references may be consulted for more information on gas chromatography.

- Grob, R. L., ed, *Modern Practice of Gas Chromatography*, Wiley-Interscience: New York, 1972.
- Hinshaw, J. V. “A Compendium of GC Terms and Techniques,” *LC•GC* **1992**, *10*, 516–522.
- Ioffe, B. V.; Vitenberg, A. G. *Head-Space Analysis and Related Methods in Gas Chromatography*, Wiley-Interscience: New York, 1982.
- Kitson, F. G.; Larsen, B. S.; McEwen, C. N. *Gas Chromatography and Mass Spectrometry: A Practical Guide*, Academic Press: San Diego, 1996.
- McMaster, M. C. *GC/MS: A Practical User’s Guide*, Wiley-Interscience: Hoboken, NJ, 2008.

The following references provide more information on high-performance liquid chromatography.

- Dorschel, C. A.; Ekmanis, J. L.; Oberholtzer, J. E.; Warren, Jr. F. V.; Bidlingmeyer, B. A. “LC Detectors,” *Anal. Chem.* **1989**, *61*, 951A–968A.
- Ehlert, S.; Tallarek, U. “High-pressure liquid chromatography in lab-on-a-chip devices,” *Anal. Bioanal. Chem.* **2007**, *388*, 517–520.
- Francois, I.; Sandra, K.; Sandra, P. “Comprehensive liquid chromatography: Fundamental aspects and practical considerations—A review,” *Anal. Chim. Acta* **2009**, *641*, 14–31.
- Harris, C. M. “Shrinking the LC Landscape,” *Anal. Chem.* **2003**, *75*, 64A–69A.
- Meyer, V. R. *Pitfalls and Errors of HPLC in Pictures*, Wiley-VCH: Weinheim, Germany, 2006.
- Pozo, O. J.; Van Eenoo, P.; Deventer, K.; Delbeke, F. T. “Detection and characterization of anabolic steroids in doping analysis by LC–MS,” *Trends Anal. Chem.* **2008**, *27*, 657–671.
- Scott, R. P. W. “Modern Liquid Chromatography,” *Chem. Soc. Rev.* **1992**, *21*, 137–145.
- Simpson, C. F., ed. *Techniques in Liquid Chromatography*, Wiley-Hayden: Chichester, England; 1982.
- Snyder, L. R.; Glajch, J. L.; Kirkland, J. J. *Practical HPLC Method Development*, Wiley-Interscience: New York,1988.
- van de Merbel, N. C. “Quantitative determination of endogenous compounds in biological samples using chromatographic techniques,” *Trends Anal. Chem.* **2008**, *27*, 924–933.
- Yeung, E. S. “Chromatographic Detectors: Current Status and Future Prospects,” *LC•GC* **1989**, *7*, 118–128.

The following references may be consulted for more information on ion chromatography.

- Shpigun, O. A.; Zolotov, Y. A. *Ion Chromatography in Water Analysis*, Ellis Horwood: Chichester, England, 1988.
- Smith, F. C. Jr.; Chang, R. C. *The Practice of Ion Chromatography*, Wiley-Interscience: New York, 1983.

The following references may be consulted for more information on supercritical fluid chromatography.

- Palmieri, M. D. “An Introduction to Supercritical Fluid Chromatography. Part I: Principles and Applications,” *J. Chem. Educ.* **1988**, *65*, A254–A259.
- Palmieri, M. D. “An Introduction to Supercritical Fluid Chromatography. Part II: Applications and Future Trends,” *J. Chem. Educ.* **1989**, *66*, A141–A147.

The following references may be consulted for more information on capillary electrophoresis.

- Baker, D. R. *Capillary Electrophoresis*, Wiley-Interscience: New York, 1995.
- Copper, C. L. “Capillary Electrophoresis: Part I. Theoretical and Experimental Background,” *J. Chem. Educ.* **1998**, *75*, 343–347.
- Copper, C. L.; Whitaker, K. W. “Capillary Electrophoresis: Part II. Applications,” *J. Chem. Educ.* **1998**, *75*, 347–351.
- DeFrancesco, L. “Capillary Electrophoresis: Finding a Niche,” *Today’s Chemist at Work*, February 2002, 59–64.
- Ekins, R. P. “Immunoassay, DNA Analysis, and Other Ligand Binding Assay Techniques: From Electropherograms to Multiplexed, Ultrasensative Microarrays on a Chip,” *J. Chem. Educ.* **1999**, *76*, 769–780.
- Revermann, T.; Götz, S.; Künnemeyer, J.; Karst, U. “Quantitative analysis by microchip capillary electrophoresis—current limitations and problem-solving strategies,” *Analyst* **2008**, *133*, 167–174.
- Timerbaev, A. R. “Capillary electrophoresis coupled to mass spectrometry for biospeciation analysis: critical evaluation,” *Trends Anal. Chem.* **2009**, *28*, 416–425.
- Unger, K. K.; Huber, M.; Hennessy, T. P.; Hearn, M. T. W.; Walhagen, K. “A Critical Appraisal of Capillary Electrochromatography,” *Anal. Chem.* **2002**, *74*, 200A–207A.
- Varenne, A.; Descroix, S. “Recent strategies to improve resolution in capillary electrophoresis—A review,” *Anal. Chim. Acta* **2008**, *628*, 9–23.
- Vetter, A. J.; McGowan, G. J. “The Escalator—An Analogy for Explaining Electroosmotic Flow,” J. Chem. Educ. 2001, 78, 209–211.
- Xu, Y. “Tutorial: Capillary Electrophoresis,” *Chem. Educator*, **1996**, *1(2)*, 1–14.

The application of spreadsheets and computer programs for modeling chromatography is described in the following papers.

- Abbay, G. N.; Barry, E. F.; Leepipatpiboon, S.; Ramstad, T.; Roman, M. C.; Siergiej, R. W.; Snyder, L. R.; Winniford, W. L. “Practical Applications of Computer Simulation for Gas Chromatography Method Development,” *LC•GC* **1991**, *9*, 100–114.
- Drouen, A.; Dolan, J. W.; Snyder, L. R.; Poile, A.; Schoenmakers, P. J. “Software for Chromatographic Method Development,” *LC•GC* **1991**, *9*, 714–724.
- Kevra, S. A.; Bergman, D. L.; Maloy, J. T. “A Computational Introduction to Chromatographic Bandshape Analysis,” *J. Chem. Educ.* **1994**, *71*, 1023–1028.
- Rittenhouse, R. C. “HPLC for Windows: A Computer Simulation of High-Performance Liquid Chromatography,” *J. Chem. Educ.* **1995**, *72*, 1086–1087.
- Shalliker, R. A.; Kayillo, S.; Dennis, G. R. “Optimizing Chromatographic Separations: An Experiment Using an HPLC Simulator,” *J. Chem. Educ.* **2008**, *85*, 1265–1268.
- Sundheim, B. R. “Column Operations: A Spreadsheet Model,” *J. Chem. Educ.* **1992**, *69*, 1003–1005.

The following papers discuss column efficiency, peak shapes, and overlapping chromatographic peaks.

- Bildingmeyer, B. A.; Warren, F. V., Jr. “Column Efficiency Measurement,” *Anal. Chem.* **1984**, *56*, 1583A–1596A.
- Hawkes, S. J. “Distorted Chromatographic Peaks,” *J. Chem. Educ.* **1994**, *71*, 1032–1033.
- Hinshaw, J. “Pinning Down Tailing Peaks,” *LC•GC* **1992**, *10*, 516–522.
- Meyer, V. K. “Chromatographic Integration Errors: A Closer Look at a Small Peak,” *LC•GC North* America **2009**, *27*, 232–244.
- Reid, V. R.; Synovec, R. E. “High-speed gas chromatography: The importance of instrumentation optimization and the elimination of extra-column band broadening,” *Talanta***2008**, *76*, 703–717.

Chapter 13

The following set of experiments introduce students to the applications of chemical kinetic methods, including enzyme kinetic methods, and flow injection analysis.

Chemical Kinetic Methods

- Abramovitch, D. A.; Cunningham, L. K.; Litwer, M. R. "Decomposition Kinetics of Hydrogen Perox- ide: Novel Lab Experiments Employing Computer Technology," *J. Chem. Educ.* **2003**, *80*, 790–792.
- Bateman, Jr. R. C.; Evans, J. A. "Using the Glucose Oxidase/Peroxidase Systems in Enzyme Kinetics," *J. Chem. Educ.* **1995**, *72*, A240–A241.
- Bendinskas, K.; DiJacomo, C.; Krill, A.; Vitz, E. "Kinetics of Alcohol Dehydrogenase-Catalyzed Oxidation of Ethanol Followed by Visible Spectroscopy," *J. Chem. Educ.* **1068**, *82*, 1068–1070.
- Clark, C. R. "A Stopped-Flow Kinetics Experiment for Advanced Undergraduate Laboratories: Formation of Iron(III) Thiocyanate," *J. Chem. Educ.* **1997**, *74*, 1214–1217.
- Diamandis, E. P.; Koupparis, M. A.; Hadjiionnou, T. P. "Kinetic Studies with Ion-Selective Electrodes: Determination of Creatinine in Urine with a Picrate Ion-Selective Electrode," *J. Chem. Educ.* **1983**, *60*, 74–76.
- Frey, M. W.; Frey, S. T.; Soltau, S. R. "Exploring the pH Dependence of L-leucine-*p*-nitroanilide Cleavage by Aminopeptidase Aeromonas Proteolytica: A Combined Buffer-Enzyme Kinetics Experiment for the General Chemistry Laboratory," *Chem. Educator* **2010**, *15*, 117-120.
- Gooding, J. J.; Yang, W.; Situmorang, M. "Bioanalytical Experiments for the Undergraduate Laboratory: Monitoring Glucose in Sport Drinks," *J. Chem. Educ.* **2001**, *78*, 788–790.
- Hamilton, T. M.; Dobie-Galuska, A. A.; Wietstock, S. M. "The *o*-Phenylenediamine-Horseradish Peroxidase System: Enzyme Kinetics in the General Chemistry Lab," *J. Chem. Educ.* **1999**, *76*, 642– 644.
- Johnson, K. A. "Factors Affecting Reaction Kinetics of Glucose Oxidase," *J. Chem. Educ.* **2002**, *79*,74–76.
- Mowry, S.; Ogren, P. J. "Kinetics of Methylene Blue Reduction by Ascorbic Acid," *J. Chem. Educ.* **1999**, *76*, 970–974.
- Nyasulu, F. W.; Barlag, R. "Gas Pressure Sensor Monitored Iodide-Catalyzed Decomposition Kinetics of Hydrogen Peroxide: An Initial Rate Approach," *Chem. Educator* **2008**, *13*, 227–230.
- Nyasulu, F. W.; Barlag, R. "Thermokinetics: Iodide-Catalyzed Decomposition Kinetics of Hydrogen Peroxide; An Integrated Rate Approach," *Chem. Educator* **2010**, *15*, 168–170.
- Pandey, S.; McHale, M. E. R.; Horton, A. M.; Padilla, S. A.; Trufant, A. L.; De La Sancha, N. U.; Vela, E.; Acree, Jr., W. E. "Kinetics-Based Indirect Spectrophotometric Method for the Simultaneous Determination of $MnO^{4-}$and $Cr_2O_7^{2-}$," *J. Chem. Educ.* **1998**, *75*, 450–452.
- Stock, E.; Morgan, M. "A Spectroscopic Analysis of the Kinetics of the Iodine Clock Reaction without Starch," *Chem. Educator* **2010**, *15*, 158–161.
- Vasilarou, A.-M. G.; Georgiou, C. A. "Enzymatic Spectrophotometric Reaction Rate Determination of Glucose in Fruit Drinks and Carbonated Beverages," *J. Chem. Educ*. **2000**, *77*, 1327–1329.
- Williams, K. R.; Adhyaru, B.; Timofeev, J.; Blankenship, M. K. "Decomposition of Aspartame. A Kinetics Experiment for Upper-Level Chemistry Laboratories," *J. Chem. Educ.* **2005**, *82*, 924–925.

Flow Injection Methods

- Carroll, M. K.; Tyson, J. F. "An Experiment Using Time-Based Detection in Flow Injection Analysis," *J. Chem. Educ.* **1993**, *70*, A210–A216.
- Conceição, A. C. L.; Minas da Piedade, M. E. "Determination of Acidity Constants by Gradient Flow-Injection Titration," *J. Chem. Educ.* **2006**, *83*, 1853–1856.
- Hansen, E. H.; Ruzicka, J. "The Principles of Flow Injection Analysis as Demonstrated by Three Lab Exercises," *J. Chem. Educ.* **1979**, *56*, 677–680.
- McKelvie, I. D.; Cardwell, T. J.; Cattrall, R. W. "A Microconduit Flow Injection Analysis Demonstration using a 35-mm Slide Projector," *J. Chem. Educ.* **1990**, *67*, 262–263.
- Meyerhoff, M. E.; Kovach, P. M. "An Ion-Selective Electrode/Flow Injection Analysis Experiment: Determination of Potassium in Serum," *J. Chem. Educ.* **1983**, *60*, 766–768.
- Nóbrega, J. A.; Rocha, F. R. P. "Ionic Strength Effect on the Rate of Reduction of Hexacyanoferrate(II) by Ascorbic Acid," *J. Chem. Educ.* **1997**, *74*, 560–562.

- Ríos, A.; Luque de Castro, M.; Valcárcel, M. "Determination of Reaction Stoichiometries by Flow Injection Analysis," *J. Chem. Educ.* **1986**, *63*, 552–553.
- Stults, C. L. M.; Wade, A. P.; Crouch, S. R. "Investigation of Temperature Effects on Dispersion in a Flow Injection Analyzer," *J. Chem. Educ.* **1988**, *65*, 645–647.
- Wolfe, C. A. C.; Oates, M. R.; Hage, D. S. "Automated Protein Assay Using Flow Injection Analysis," *J. Chem. Educ.* **1998**, *75*, 1025–1028.

The following sources provides a general review of the importance of chemical kinetics in analytical chemistry.

- Bergmyer, H. U.; Grassl, M. *Methods of Enzymatic Analysis*, Verlag Chemie: Deerfield Beach, FL, 3rd Ed., 1983.
- Laitinen, H. A.; Ewing, G. W., eds., *A History of Analytical Chemistry*, The Division of Analytical Chemistry of the American Chemical Society: Washington, D. C., 1977, pp. 97–102.
- Malmstadt, H. V.; Delaney, C. J.; Cordos, E. A. "Reaction-Rate Methods of Chemical Analysis," *Crit. Rev. Anal. Chem.* **1972**, *2*, *559–619.*
- Mark, H. B.; Rechnitz, G. A. *Kinetics in Analytical Chemistry*, Wiley: New York, 1968.
- Mottola, H. A. "Catalytic and Differential Reaction-Rate Methods of Chemical Analysis," *Crit. Rev. Anal. Chem.* ***1974***, *4*, *229–280*.
- Mottola, H. A. "Some Kinetic Aspects Relevant to Contemporary Analytical Chemistry," *J. Chem. Educ.* **1981**, *58*, 399–403.
- Mottola, H. A. *Kinetic Aspects of Analytical Chemistry*, Wiley: New York, 1988.
- Pardue, H. L. "A Comprehensive Classification of Kinetic Methods of Analysis Used in Clinical Chemistry," Clin. Chem. 1977, 23, 2189–2201.
- Pardue, H. L. "Kinetic Aspects of Analytical Chemistry," *Anal. Chim. Acta*, **1989**, *216*, 69–107.
- Perez-Bendito, D.; Silva, M. *Kinetic Methods in Analytical Chemistry*, Ellis Horwood: Chichester, 1988.
- Pisakiewicz, D. *Kinetics of Chemical and Enzyme-Catalyzed Reactions*, Oxford University Press: New York, 1977.

The following instrumental analysis textbooks may be consulted for further information on the detectors and signal analyzers used in radiochemical methods of analysis.

- Skoog, D. A.; Holler, F. J.; Nieman, T. A. *Principles of Instrumental Analysis*, 5th Ed., Saunders College Publishing/Harcourt Brace and Co.: Philadelphia., 1998, Chapter 32.
- Strobel, H. A.; Heineman, W. R. *Chemical Instrumentation: A Systematic Approach*, 3rd Ed., Wiley-Interscience: New York, 1989.

The following resources provide additional information on the theory and application of flow injection analysis.

- Andrew, K. N.; Blundell, N. J.; Price, D.; Worsfold, P. J. "Flow Injection Techniques for Water Monitoring," *Anal. Chem.* **1994**, *66*, 916A–922A.
- Betteridge, D. "Flow Injection Analysis," *Anal. Chem.* **1978**, *50*, 832A–846A.
- Kowalski, B. R.; Ruzicka, J. Christian, G. D. "Flow Chemography - The Future of Chemical Education," *Trends Anal. Chem.* **1990**, *9*, 8–13.
- Mottola, H. A. "Continuous Flow Analysis Revisited," *Anal. Chem.* **1981**, *53*, 1312A–1316A.
- Ruzicka, J. "Flow Injection Analysis: From Test Tube to Integrated Microconduits," *Anal. Chem.* **1983**, *55*, 1040A–1053A.
- Ruzicka, J.; Hansen, E. H. *Flow-Injection Analysis*, Wiley-Interscience: New York, 1989.
- Ruzicka, J.; Hansen, E. H. "Retro-Review of Flow-Injection Analysis," *Trends Anal. Chem.* **2008**, *27*,390–393.
- Silvestre, C. I. C.; Santos, J. L. M.; Lima, J. L. F. C.; Zagatto, E. A. G. "Liquid-Liquid Extraction in Flow Analysis: A Critical Review," *Anal. Chim. Acta* **2009**, *652*, 54–65.
- Stewart, K. K. "Flow Injection Analysis: New Tools for Old Assays, New Approaches to Analytical Measurements," *Anal. Chem.* **1983**, *55*, 931A–940A.
- Tyson, J. F. "Atomic Spectrometry and Flow Injection Analysis: A Synergic Combination," *Anal. Chim. Acta*, **1988**, *214*, *57–75*.
- Valcarcel, M.; Luque de Castro, M. D. *Flow-Injection Analysis: Principles and Applications*, Ellis Horwood: Chichester, England, 1987.

Chapter 14

The following set of experiments provide practical examples of the optimization of experimental conditions. Examples include simplex optimization, factorial designs for developing empirical models of response surfaces, and fitting experimental data to theoretical models of the response surface.

- Amenta, D. S.; Lamb, C. E.; Leary, J. J. "Simplex Optimization of Yield of *sec*-Butylbenzene in a Friedel-Crafts Alkylation," *J. Chem. Educ.* **1979**, *56*, 557–558.
- Harvey, D. T.; Byerly, S.; Bowman, A.; Tomlin, J. "Optimization of HPLC and GC Separations Using Response Surfaces," *J. Chem. Educ.* **1991**, *68*, 162–168.
- Leggett, D. L. "Instrumental Simplex Optimization," *J. Chem. Educ.* **1983**, *60*, 707–710.
- Oles, P. J. "Fractional Factorial Experimental Design as a Teaching Tool for Quantitative Analysis," *J. Chem. Educ.* **1998**, *75*, 357–359.
- Palasota, J. A.; Deming, S.N. "Central Composite Experimental Design," *J. Chem. Educ.* **1992**, *69*, 560–561.
- Sangsila, S.; Labinaz, G.; Poland, J. S.; vanLoon, G. W. "An Experiment on Sequential Simplex Optimization of an Atomic Absorption Analysis Procedure," *J. Chem. Educ.* **1989**, *66*, 351–353.
- Santos-Delgado, M. J.; Larrea-Tarruella, L. "A Didactic Experience of Statistical Analysis for the Determination of Glycine in a Nonaqueous Medium using ANOVA and a Computer Program," *J. Chem. Educ.* **2004**, *81*, 97–99.
- Shavers, C. L.; Parsons, M. L.; Deming, S. N. "Simplex Optimization of Chemical Systems," *J. Chem Educ.* **1979**, *56*, 307–309.
- Stieg, S. "A Low-Noise Simplex Optimization Experiment," *J. Chem. Educ.* **1986**, *63*, 547–548.
- Stolzberg, R. J. "Screening and Sequential Experimentation: Simulations and Flame Atomic Absorption Spectrometry Experiments," *J. Chem. Educ.* **1997**, *74*, 216–220.
- Van Ryswyk, H.; Van Hecke, G. R. "Attaining Optimal Conditions," *J. Chem. Educ.* **1991**, *66*, 878–882.

The following texts and articles provide an excellent discussion of optimization methods based on searching algorithms and mathematical modeling use factorial designs, including a discussion of the relevant calculations. A few of these sources discuss other types of experimental designs.

- Bayne, C. K.; Rubin, I. B. *Practical Experimental Designs and Optimization Methods for Chemists*, VCH Publishers: Deerfield Beach, FL; 1986.
- Box, G. E. P. "Statistical Design in the Study of Analytical Methods," *Analyst* **1952**, *77*, 879–891.
- Deming, S. N.; Morgan, S. L. *Experimental Design: A Chemometric Approach*, Elsevier: Amsterdam, 1987.
- Ferreira, S. L. C.; dos Santos, W. N. L.; Quintella, C. M.; Neto, B. B.; Bosque-Sendra, J. M. "Doehlert • Matrix: A Chemometric Tool for Analytical Chemistry—Review," *Talanta* **2004**, *63*, 1061–1067.
- Ferreira, S. L. C.; Bruns, R. E.; Ferreira, H. S.; Matos, G. D.; David, J. M.; Brandão, G. C.; da Silva, E. G. P.; Portugal, L. A.; dos Reis, P. S.; Souza, A. S.; dos Santos, W. N. L. "Box-Behnken Design: An Alternative for the Optimization of Analytical Methods," *Anal. Chim. Acta* **2007**, *597*, 179–186.
- Gonzalez, A. G. "Two Level Factorial Experimental Designs Based on Multiple Linear Regression Models: A Tutorial Digest Illustrated by Case Studies," *Anal. Chim. Acta* **1998**, *360*, 227–241.
- Goupy, J. "What Kind of Experimental Design for Finding and Checking Robustness of Analytical Methods?" *Anal. Chim. Acta* **2005**, *544*, 184–190.
- Hendrix, C. D. "What Every Technologist Should Know About Experimental Design," *Chemtech* **1979**, *9*, 167–174.
- Hendrix, C. D. "Through the Response Surface with Test Tube and Pipe Wrench," *Chemtech* **1980**, *10*, 488–497.
- Leardi, R. "Experimental Design: A Tutorial," *Anal. Chim. Acta* **2009**, *652*, 161–172.
- Liang, Y. "Comparison of Optimization Methods," *Chromatography Review* **1985**, *12(2)*, 6–9.
- Morgan, E. *Chemometrics: Experimental Design*, John Wiley and Sons: Chichester, 1991.
- Thompson, M., ed. "Experimental Design and Optimization (1): An Introduction to Some Basic Concepts," AMC Technical Brief 24, June 2006.
- Thompson, M., ed. "Experimental Design and Optimization (2): Handling Uncontrolled Factors" AMC Technical Brief 26, December 2006.

- Thompson, M., ed. “Experimental Design and Optimization (3): Some Fractional Factorial Designs,” AMC Technical Brief 36, January 2009.
- Walters, F. H.; Morgan, S. L.; Parker, L. P., Jr.; Deming, S. N. *Sequential Simplex Optimization*, CRC Press: Boca Raton, FL, 1991. (an electronic version of this text is freely available from Multisimplex AB and is available here.)

The following texts provide additional information about ANOVA calculations, including discussions of two-way analysis of variance.

- Graham, R. C. *Data Analysis for the Chemical Sciences*, VCH Publishers: New York, 1993.
- Miller, J. C.; Miller, J. N. *Statistics for Analytical Chemistry*, Ellis Horwood Limited: Chichester, 1988.

The following resources provide additional information on the validation of analytical methods.

- Gonzalez, A. G.; Herrador, M. A. “A Practical Guide to Analytical Method Validation, Including Measurement Uncertainty and Accuracy Profiles,” *Trends Anal. Chem.* **2007**, *26*, 227–238.
- Thompson, M.; Ellison, S. L. R.; Wood, R. “Harmonized Guidelines for Single-Laboratory Validation of Analytical Methods,” *Pure Appl. Chem.* **2002**, *74*, 835–855.

Chapter 15

The following three experiments introduce aspects of quality assurance and quality control.

- Bell, S. C.; Moore, J. “Integration of Quality Assurance/Quality Control into Quantitative Analysis,” *J. Chem. Educ.* **1998**, *75*, 874–877.
- Cancilla, D. A. “Integration of Environmental Analytical Chemistry with Environmental Law: The Development of a Problem-Based Laboratory,” *J. Chem. Educ.* **2001**, *78*, 1652–1660.
- Laquer, F. C. “Quality Control Charts in the Quantitative Analysis Laboratory Using Conductance Measurement,” *J. Chem. Educ.* **1990**, *67*, 900–902.
- Marcos, J.; Ríos, A.; Valcárcel, M. “Practicing Quality Control in a Bioanalytical Experiment,” *J. Chem. Educ.* **1995**, *72*, 947–949.

The following texts and articles may be consulted for an additional discussion of quality assurance and quality control.

- Amore, F. “Good Analytical Practices,” *Anal. Chem.* **1979**, *51*, 1105A–1110A.
- Barnard, Jr. A. J.; Mitchell, R. M.; Wolf, G. E. “Good Analytical Practices in Quality Control,” *Anal. Chem.* **1978**, *50*, 1079A–1086A.
- Cairns, T.; Rogers, W. M. “Acceptable Analytical Data for Trace Analysis,” *Anal. Chem.* **1993**, *55*, 54A–57A.
- Taylor, J. K. *Quality Assurance of Chemical Measurements*, Lewis Publishers: Chelsa, MI, 1987.

Additional information about the construction and use of control charts may be found in the following sources.

- Miller, J. C.; Miller, J. N. Statistics for Analytical Chemistry, 2nd Ed., Ellis Horwood Limited: Chichester, 1988.
- Ouchi, G. I. “Creating Control Charts with a Spreadsheet Program,” *LC•GC* **1993**, *11*, 416–423.
- Ouchi, G. I. “Creating Control Charts with a Spreadsheet Program,” *LC•GC* **1997**, *15*, 336–344.
- Simpson, J. M. “Spreadsheet Statistics,” *J. Chem. Educ.* **1994**, *71*, A88–A89.

Contributors

- David Harvey (DePauw University)

Additional Resources is shared under a CC BY-NC-SA 4.0 license and was authored, remixed, and/or curated by LibreTexts.

Index

D

dire

Glossary

Sample Word 1 | Sample Definition 1

Detailed Licensing

Overview

Title: CHEM 1000: General Chemistry

Webpages: 155

Applicable Restrictions: Noncommercial

All licenses found:

- CC BY-NC-SA 4.0: 87.7% (136 pages)
- Undeclared: 12.3% (19 pages)

By Page

- CHEM 1000: General Chemistry - *CC BY-NC-SA 4.0*
  - Front Matter - *Undeclared*
    - TitlePage - *Undeclared*
    - InfoPage - *Undeclared*
    - Table of Contents - *Undeclared*
    - Licensing - *Undeclared*
  - 1: Introduction to Analytical Chemistry - *CC BY-NC-SA 4.0*
    - 1.1: What is Analytical Chemistry? - *CC BY-NC-SA 4.0*
    - 1.2: The Analytical Perspective - *CC BY-NC-SA 4.0*
    - 1.3: Common Analytical Problems - *CC BY-NC-SA 4.0*
    - 1.E: Introduction to Analytical Chemistry (Exercises) - *CC BY-NC-SA 4.0*
    - 1.S: Introduction to Analytical Chemistry (Summary) - *CC BY-NC-SA 4.0*
  - 2: Basic Tools of Analytical Chemistry - *CC BY-NC-SA 4.0*
    - 2.1: Measurements in Analytical Chemistry - *CC BY-NC-SA 4.0*
    - 2.2: Concentration - *CC BY-NC-SA 4.0*
    - 2.3: Stoichiometric Calculations - *CC BY-NC-SA 4.0*
    - 2.4: Basic Equipment - *CC BY-NC-SA 4.0*
    - 2.5: Preparing Solutions - *CC BY-NC-SA 4.0*
    - 2.6: Spreadsheets and Computational Software - *CC BY-NC-SA 4.0*
    - 2.7: The Laboratory Notebook - *CC BY-NC-SA 4.0*
    - 2.E: Basic Tools of Analytical Chemistry (Exercises) - *CC BY-NC-SA 4.0*
    - 2.S: Basic Tools of Analytical Chemistry (Summary) - *CC BY-NC-SA 4.0*
  - 3: The Vocabulary of Analytical Chemistry - *CC BY-NC-SA 4.0*
    - Front Matter - *Undeclared*
      - TitlePage - *Undeclared*
      - InfoPage - *Undeclared*
    - 3.1: Analysis, Determination, and Measurement - *CC BY-NC-SA 4.0*
    - 3.2: Techniques, Methods, Procedures, and Protocols - *CC BY-NC-SA 4.0*
    - 3.3: Classifying Analytical Techniques - *CC BY-NC-SA 4.0*
    - 3.4: Selecting an Analytical Method - *CC BY-NC-SA 4.0*
    - 3.5: Developing the Procedure - *CC BY-NC-SA 4.0*
    - 3.6: Protocols - *CC BY-NC-SA 4.0*
    - 3.7: The Importance of Analytical Methodology - *CC BY-NC-SA 4.0*
    - 3.E: The Vocabulary of Analytical Chemistry (Exercises) - *CC BY-NC-SA 4.0*
    - 3.S: The Vocabulary of Analytical Chemistry (Summary) - *CC BY-NC-SA 4.0*
    - Back Matter - *Undeclared*
      - Index - *Undeclared*
  - 4: Evaluating Analytical Data - *CC BY-NC-SA 4.0*
    - 4.1: Characterizing Measurements and Results - *CC BY-NC-SA 4.0*
    - 4.2: Characterizing Experimental Errors - *CC BY-NC-SA 4.0*
    - 4.3: Propagation of Uncertainty - *CC BY-NC-SA 4.0*
    - 4.4: The Distribution of Measurements and Results - *CC BY-NC-SA 4.0*
    - 4.5: Statistical Analysis of Data - *CC BY-NC-SA 4.0*
    - 4.6: Statistical Methods for Normal Distributions - *CC BY-NC-SA 4.0*
    - 4.7: Detection Limits - *CC BY-NC-SA 4.0*
    - 4.8: Using Excel and R to Analyze Data - *CC BY-NC-SA 4.0*
    - 4.E: Evaluating Analytical Data (Exercises) - *CC BY-NC-SA 4.0*

- 4.S: Evaluating Analytical Data (Summary) - *CC BY-NC-SA 4.0*

- 5: Standardizing Analytical Methods - *CC BY-NC-SA 4.0*
  - 5.1: Analytical Standards - *CC BY-NC-SA 4.0*
  - 5.2: Calibrating the Signal - *CC BY-NC-SA 4.0*
  - 5.3: Determining the Sensitivity - *CC BY-NC-SA 4.0*
  - 5.4: Linear Regression and Calibration Curves - *CC BY-NC-SA 4.0*
  - 5.5: Blank Corrections - *CC BY-NC-SA 4.0*
  - 5.6: Using Excel and R for a Regression Analysis - *CC BY-NC-SA 4.0*
  - 5.E: Standardizing Analytical Methods (Exercises) - *CC BY-NC-SA 4.0*
  - 5.S: Standardizing Analytical Methods (Summary) - *CC BY-NC-SA 4.0*
- 6: Equilibrium Chemistry - *CC BY-NC-SA 4.0*
  - 6.1: Reversible Reactions and Chemical Equilibria - *CC BY-NC-SA 4.0*
  - 6.2: Thermodynamics and Equilibrium Chemistry - *CC BY-NC-SA 4.0*
  - 6.3: Manipulating Equilibrium Constants - *CC BY-NC-SA 4.0*
  - 6.4: Equilibrium Constants for Chemical Reactions - *CC BY-NC-SA 4.0*
  - 6.5: Le Châtelier's Principle - *CC BY-NC-SA 4.0*
  - 6.6: Ladder Diagrams - *CC BY-NC-SA 4.0*
  - 6.7: Solving Equilibrium Problems - *CC BY-NC-SA 4.0*
  - 6.8: Buffer Solutions - *CC BY-NC-SA 4.0*
  - 6.9: Activity Effects - *CC BY-NC-SA 4.0*
  - 6.10: Using Excel and R to Solve Equilibrium Problems - *CC BY-NC-SA 4.0*
  - 6.11: Some Final Thoughts on Equilibrium Calculations - *CC BY-NC-SA 4.0*
  - 6.E: Equilibrium Chemistry (Exercises) - *CC BY-NC-SA 4.0*
  - 6.S: Equilibrium Chemistry (Summary) - *CC BY-NC-SA 4.0*
- 7: Collecting and Preparing Samples - *CC BY-NC-SA 4.0*
  - 7.1: The Importance of Sampling - *CC BY-NC-SA 4.0*
  - 7.2: Designing a Sampling Plan - *CC BY-NC-SA 4.0*
  - 7.3: Implementing the Sampling Plan - *CC BY-NC-SA 4.0*
  - 7.4: Separating the Analyte from Interferents - *CC BY-NC-SA 4.0*
  - 7.5: General Theory of Separation Efficiency - *CC BY-NC-SA 4.0*
  - 7.6: Classifying Separation Techniques - *CC BY-NC-SA 4.0*
  - 7.7: Liquid–Liquid Extractions - *CC BY-NC-SA 4.0*
  - 7.8: Separation Versus Preconcentration - *CC BY-NC-SA 4.0*
  - 7.E: Collecting and Preparing Samples (Exercises) - *CC BY-NC-SA 4.0*
  - 7.S: Collecting and Preparing Samples (Summary) - *CC BY-NC-SA 4.0*
- 8: Gravimetric Methods - *CC BY-NC-SA 4.0*
  - 8.1: Overview of Gravimetric Methods - *CC BY-NC-SA 4.0*
  - 8.2: Precipitation Gravimetry - *CC BY-NC-SA 4.0*
  - 8.3: Volatilization Gravimetry - *CC BY-NC-SA 4.0*
  - 8.4: Particulate Gravimetry - *CC BY-NC-SA 4.0*
  - 8.E: Gravimetric Methods (Exercises) - *CC BY-NC-SA 4.0*
  - 8.S: Gravimetric Methods (Summary) - *CC BY-NC-SA 4.0*
- 9: Titrimetric Methods - *CC BY-NC-SA 4.0*
  - 9.1: Overview of Titrimetry - *CC BY-NC-SA 4.0*
  - 9.2: Acid–Base Titrations - *CC BY-NC-SA 4.0*
  - 9.3: Complexation Titrations - *CC BY-NC-SA 4.0*
  - 9.4: Redox Titrations - *CC BY-NC-SA 4.0*
  - 9.5: Precipitation Titrations - *CC BY-NC-SA 4.0*
  - 9.E: Titrimetric Methods (Exercises) - *CC BY-NC-SA 4.0*
  - 9.S: Titrimetric Methods (Summary) - *CC BY-NC-SA 4.0*
- 10: Spectroscopic Methods - *CC BY-NC-SA 4.0*
  - 10.1: Overview of Spectroscopy - *CC BY-NC-SA 4.0*
  - 10.2: Spectroscopy Based on Absorption - *CC BY-NC-SA 4.0*
  - 10.3: UV/Vis and IR Spectroscopy - *CC BY-NC-SA 4.0*
  - 10.4: Atomic Absorption Spectroscopy - *CC BY-NC-SA 4.0*
  - 10.5: Emission Spectroscopy - *CC BY-NC-SA 4.0*
  - 10.6: Photoluminescence Spectroscopy - *CC BY-NC-SA 4.0*
  - 10.7: Atomic Emission Spectroscopy - *CC BY-NC-SA 4.0*
  - 10.8: Spectroscopy Based on Scattering - *CC BY-NC-SA 4.0*
  - 10.E: Spectroscopic Methods (Exercises) - *CC BY-NC-SA 4.0*
  - 10.S: Spectroscopic Methods (Summary) - *CC BY-NC-SA 4.0*
- 11: Electrochemical Methods - *CC BY-NC-SA 4.0*

- 11.1: Overview of Electrochemistry - *CC BY-NC-SA 4.0*
- 11.2: Potentiometric Methods - *CC BY-NC-SA 4.0*
- 11.3: Coulometric Methods - *CC BY-NC-SA 4.0*
- 11.4: Voltammetric Methods - *CC BY-NC-SA 4.0*
- 11.E: Electrochemical Methods (Exercises) - *CC BY-NC-SA 4.0*
- 11.S: Electrochemical Methods (Summary) - *CC BY-NC-SA 4.0*

12: Chromatographic & Electrophoretic Methods - *CC BY-NC-SA 4.0*

- Front Matter - *Undeclared*
  - TitlePage - *Undeclared*
  - InfoPage - *Undeclared*
- 12.1: Overview of Analytical Separations - *CC BY-NC-SA 4.0*
- 12.2: General Theory of Column Chromatography - *CC BY-NC-SA 4.0*
- 12.3: Optimizing Chromatographic Separations - *CC BY-NC-SA 4.0*
- 12.4: Gas Chromatography - *CC BY-NC-SA 4.0*
- 12.5: High-Performance Liquid Chromatography - *CC BY-NC-SA 4.0*
- 12.6: Other Forms of Liquid Chromatography - *CC BY-NC-SA 4.0*
- 12.7: Electrophoresis - *CC BY-NC-SA 4.0*
- 12.E: Chromatographic and Electrophoretic Methods (Exercises) - *CC BY-NC-SA 4.0*
- 12.S: Chromatographic and Electrophoretic Methods (Summary) - *CC BY-NC-SA 4.0*
- Back Matter - *Undeclared*
  - Index - *Undeclared*

13: Kinetic Methods - *CC BY-NC-SA 4.0*

- 13.1: Kinetic Methods Versus Equilibrium Methods - *CC BY-NC-SA 4.0*
- 13.2: Chemical Kinetics - *CC BY-NC-SA 4.0*
- 13.3: Radiochemistry - *CC BY-NC-SA 4.0*
- 13.4: Flow Injection Analysis - *CC BY-NC-SA 4.0*
- 13.E: Kinetic Methods (Exercises) - *CC BY-NC-SA 4.0*
- 13.S: Kinetic Methods (Summary) - *CC BY-NC-SA 4.0*

14: Developing a Standard Method - *CC BY-NC-SA 4.0*

- 14.1: Optimizing the Experimental Procedure - *CC BY-NC-SA 4.0*
- 14.2: Verifying the Method - *CC BY-NC-SA 4.0*
- 14.3: Validating the Method as a Standard Method - *CC BY-NC-SA 4.0*
- 14.4: Using Excel and R for an Analysis of Variance - *CC BY-NC-SA 4.0*
- 14.E: Developing a Standard Method (Exercises) - *CC BY-NC-SA 4.0*
- 14.S: Developing a Standard Method (Summary) - *CC BY-NC-SA 4.0*

15: Quality Assurance - *CC BY-NC-SA 4.0*

- 15.1: The Analytical Perspective—Revisited - *CC BY-NC-SA 4.0*
- 15.2: Quality Control - *CC BY-NC-SA 4.0*
- 15.3: Quality Assessment - *CC BY-NC-SA 4.0*
- 15.4: Evaluating Quality Assurance Data - *CC BY-NC-SA 4.0*
- 15.E: Quality Assurance (Exercises) - *CC BY-NC-SA 4.0*

Additional Resources - *CC BY-NC-SA 4.0*

Back Matter - *Undeclared*

- Index - *Undeclared*
- Glossary - *Undeclared*
- Detailed Licensing - *Undeclared*